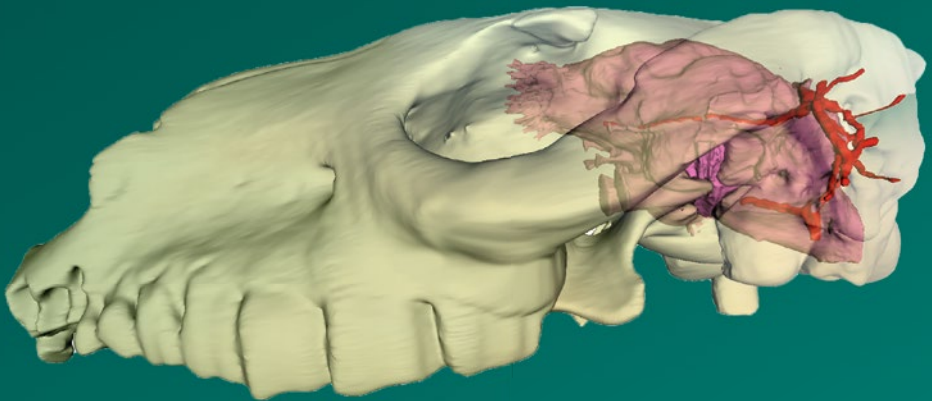


María Teresa Dozo
Ariana Paulina-Carabajal
Thomas E. Macrini
Stig Walsh *Editors*

Paleoneurology of Amniotes

New Directions in the Study
of Fossil Endocasts



 Springer

Paleoneurology of Amniotes

María Teresa Dozo
Ariana Paulina-Carabajal
Thomas E. Macrini • Stig Walsh
Editors

Paleoneurology of Amniotes

New Directions in the Study of Fossil
Endocasts

 Springer

Editors

María Teresa Dozo
Instituto Patagónico de Geología y
Paleontología
CCT CONICET-CENPAT
Puerto Madryn, Argentina

Thomas E. Macrini 
Department of Biological Sciences
St. Mary's University
San Antonio, TX, USA

Ariana Paulina-Carabajal
Instituto de Investigaciones en
Biodiversidad y Medioambiente
CONICET-Universidad Nacional
del Comahue
San Carlos de Bariloche, Argentina

Stig Walsh 
National Museum of Scotland
Edinburgh, Midlothian, UK

ISBN 978-3-031-13982-6 ISBN 978-3-031-13983-3 (eBook)
<https://doi.org/10.1007/978-3-031-13983-3>

© Springer Nature Switzerland AG 2023

This work is subject to copyright. All rights are reserved by the Publisher, whether the whole or part of the material is concerned, specifically the rights of translation, reprinting, reuse of illustrations, recitation, broadcasting, reproduction on microfilms or in any other physical way, and transmission or information storage and retrieval, electronic adaptation, computer software, or by similar or dissimilar methodology now known or hereafter developed.

The use of general descriptive names, registered names, trademarks, service marks, etc. in this publication does not imply, even in the absence of a specific statement, that such names are exempt from the relevant protective laws and regulations and therefore free for general use.

The publisher, the authors, and the editors are safe to assume that the advice and information in this book are believed to be true and accurate at the date of publication. Neither the publisher nor the authors or the editors give a warranty, expressed or implied, with respect to the material contained herein or for any errors or omissions that may have been made. The publisher remains neutral with regard to jurisdictional claims in published maps and institutional affiliations.

This Springer imprint is published by the registered company Springer Nature Switzerland AG
The registered company address is: Gewerbestrasse 11, 6330 Cham, Switzerland

Otilie (“Tilly”) Edinger
(1897–1967)

in memoriam

“Dr. Tilly Edinger’s first published paper dealt with a brain cast of Nothosaurus, a Triassic relative of the plesiosaurs. With this she embarked on a working lifetime of devotion to paleoneurology, a field of study that she was to transform.”

Bryan Patterson

List of Reviewers

- Heather Ahrens**, Center for Functional Anatomy and Evolution, Johns Hopkins University School of Medicine, Baltimore, USA.
- Kari Allen**, Department of Neuroscience, Washington University School of Medicine, USA
- Amy Balanoff**, Center for Functional Anatomy & Evolution, Johns Hopkins University School of Medicine, USA
- Ana Balcarcel**, Palaeontological Institute and Museum, University of Zurich, Zurich, Switzerland
- Julien Benoit**, Evolutionary Studies Institute (ESI), University of the Witwatersrand, Johannesburg, South Africa
- Ornella C. Bertrand**, School of GeoSciences, University of Edinburgh, Scotland, UK
- Gabriel Bever**, Center for Functional Anatomy & Evolution, Johns Hopkins University School of Medicine, USA
- Guillaume Billet**, Département de Histoire de la Terre, Museum national d’Histoire naturelle, Paris, France
- Adhil Bhagwandin**, School of Anatomical Sciences, University of the Witwatersrand, Johannesburg, South Africa
- Andrej Černansky**, Department of Ecology, Laboratory of Evolutionary Biology, Faculty of Natural Sciences, Comenius University in Bratislava, Slovakia
- Juan Carlos Cisneros**, Universidade Federal do Piauí, Museu de Arqueologia e Paleontologia, Teresina, Brasil
- Loic Costeur**, Department of Geosciences, Natural History Museum Basel, Basel, Switzerland
- Darin Croft**, Department of Anatomy, Case Western Reserve University School of Medicine, Cleveland, OH, USA
- Carlos de Miguel Chaves**, Grupo de Biología Evolutiva, Facultad de Ciencias, UNED, Madrid, España
- Hans Dieter Sues**, Department of Paleobiology, National Museum of Natural History, Smithsonian Institution, Washington, DC, USA
- Eric Ekdale**, Department of Biology, San Diego State University, San Diego, USA

- Serjoscha Evers**, Department of Geosciences, University of Fribourg, Fribourg, Switzerland
- Martín Ezcurra**, Sección Paleontología de Vertebrados CONICET–Museo Argentino de Ciencias Naturales Bernardino Rivadavia, Buenos Aires, Argentina
- Marcos Fernández Moncillo**, Museo de Paleontología, Facultad de Ciencias Exactas, Físicas y Naturales, Universidad Nacional de Córdoba, Córdoba, Argentina
- Adan Garcia-Pérez**, Facultad de Ciencias, Universidad Nacional de Educación a Distancia, Madrid, Spain
- Timothy Gaudin**, Department of Biology, Geology & Environmental Science, University of Tennessee at Chattanooga, TN, USA
- Georgios L. Georgalis**, Institute of Systematics and Evolution of Animals Polish Academy of Sciences, Kraków, Poland
- Yanina Herrera**, División Paleontología Vertebrados, Museo de La Plata, Universidad Nacional de La Plata, La Plata, Argentina
- Dmitry Ivanoff**, Department of Palaeontology, National Museum of Natural History, National Academy of Sciences of Ukraine, Kiev, Ukraine
- Walter Joyce**, Department of Geosciences, University of Fribourg, Fribourg, Switzerland
- Soichiro Kawabe**, Institute of Dinosaur Research, Fukui Prefectural University, Fukui, Japan
- E. Christopher Kirk**, Department of Anthropology, Center for Perceptual Systems, University of Texas, Austin, USA
- Daniel Ksepka**, Bruce Museum, Greenwich, Connecticut, USA
- Greg McDonald**, Bureau of Land Management, Colorado State Office, Colorado, USA
- Felipe Montefeltro**, Departamento de Biologia e Zootecnia, Faculdade de Engenharia de Ilha Solteira, Universidade Estadual Paulista, Sao Paulo, Brazil
- Maeva Orliac**, Institut des Sciences de l'Evolution, Université de Montpellier, France
- Marcelo Sánchez-Villagra**, Palaeontological Institute and Museum, University of Zurich, Zurich, Switzerland
- Raffaele Sardella**, Dipartimento di Scienze della Terra, Sapienza Università di Roma, Rome, Italy
- Torsten Scheyer**, Paläontologisches Institut und Museum, Universität Zürich, Zürich, Switzerland
- Julia Schwab**, School of GeoSciences, University of Edinburgh, Edinburgh, Scotland, UK
- Gabriela Sobral**, Staatliches Museum für Naturkunde Stuttgart, Stuttgart, Germany
- Leonardo Souza Lobo**, Departamento de Geologia e Paleontologia, Universidade Federal do Rio de Janeiro (UFRJ), Museu Nacional (MN), (DGP), Rio de Janeiro, Brasil
- Luciano Varela**, Departamento de Paleontología, Facultad de Ciencias, Universidad de la República, Montevideo, Uruguay
- Stig Walsh**, National Museum of Scotland and University of Edinburgh, Scotland, UK

Contents

1	Introduction	1
	María Teresa Dozo, Ariana Paulina-Carabajal, Thomas E. Macrini, and Stig Walsh	
2	The Paleoneurology of Early Reptiles	9
	Gabriela Sobral	
3	The Paleoneurology of Ichthyopterygia and Sauropterygia: Diverse Endocranial Anatomies of Secondarily Aquatic Diapsids . . .	29
	Rémi Allemand, Benjamin C. Moon, and Dennis F. A. E. Voeten	
4	Contrasting Brains and Bones: Neuroanatomical Evolution of Turtles (Testudinata)	79
	Gabriel S. Ferreira, Ingmar Werneburg, Stephan Lautenschlager, and Serjoscha W. Evers	
5	A Look in to the Neurocranium of Living and Extinct Lepidosauria	123
	Ariana Paulina-Carabajal, Paulina Jiménez-Huidobro, Laura Natalia Triviño, Edward L. Stanley, Hussam Zaher, and Juan D. Daza	
6	Paleoneurology of the Early Diversification of Triassic Archosauriforms and Pseudosuchians	179
	M. Belén von Baczko, Julia B. Desojo, M. Jimena Trotteyn, and Michelle R. Stocker	
7	An Overview on the Crocodylomorpha Cranial Neuroanatomy: Variability, Morphological Patterns and Paleobiological Implications	213
	Francisco Barrios, Paula Bona, Ariana Paulina-Carabajal, Juan Martín Leardi, Casey M. Holliday, and Emily J. Lessner	

8	Paleoneurology of Non-avian Dinosaurs: An Overview	267
	Ariana Paulina-Carabajal, Mario Bronzati, and Penélope Cruzado-Caballero	
9	Anatomy and Evolution of Avian Brain and Senses: What Endocasts Can Tell Us	333
	Federico J. Degrange, Julieta Carril, Ricardo S. De Mendoza, María M. Demmel Ferreira, and Claudia P. Tambussi	
10	Evolution of the Mammalian Neurosensory System: Fossil Evidence and Major Events	365
	Timothy B. Rowe	
11	Evolution of the Brain and Sensory Structures in Metatherians	423
	Thomas E. Macrini, Michael Leary, and Vera Weisbecker	
12	Early Evolution of the Brain in Primates and Their Close Kin	457
	Mary T. Silcox, Ornella C. Bertrand, Arianna R. Harrington, Madlen M. Lang, Gabriela A. San Martin-Flores, and Sergi López-Torres	
13	Paleoneurology of Artiodactyla, an Overview of the Evolution of the Artiodactyl Brain	507
	Maeva J. Orliac, Jacob Maugoust, Ana Balcarcel, and Emmanuel Gilissen	
14	Evolution of the Brain and Sensory Structures in Sirenia	557
	Thomas E. Macrini and Johanset Orihuela	
15	Paleoneurology of the Proboscidea (Mammalia, Afrotheria): Insights from Their Brain Endocast and Labyrinth	579
	Julien Benoit, George A. Lyras, Arnaud Schmitt, Mpilo Nxumalo, Rodolphe Tabuce, Teodor Obada, Vladislav Mararsecul, and Paul Manger	
16	Brain Evolution in Fossil Rodents: A Starting Point	645
	Ornella C. Bertrand and Mary T. Silcox	
17	Paleoneurology of Carnivora	681
	George A. Lyras, Alexandra A. E. van der Geer, and Lars Werdelin	
18	Paleoneurology of Extinct Cingulates and Insights into Their Inner Ear Anatomy	711
	P. Sebastián Tambusso, Flávio Góis, Jorge Felipe Moura, Chiara Villa, and Roberta Veronese do Amaral	
19	The Endocranial Cavities of Sloths (Xenarthra, Folivora): Insights from the Brain Endocast, Bony Labyrinth, and Cranial Sinuses	737
	Alberto Boscaini, Dawid A. Iurino, Raffaele Sardella, Timothy J. Gaudin, and François Pujos	

20 Endocranial Morphology and Paleoneurology in Notoungulates: Braincast, Auditory Region and Adjacent Intracranial Spaces 761
Gastón Martínez, Thomas E. Macrini, María Teresa Dozo, Bárbara Vera, and Javier N. Gelfo

21 Paleoneurology of Litopterna: Digital and Natural Endocranial Casts of Macraucheniiidae 809
María Teresa Dozo, Gastón Martínez, and Javier N. Gelfo

Index 837

About the Editors

María Teresa Dozo holds a PhD in natural sciences from Universidad Nacional de La Plata and is a researcher at CONICET (National Scientific and Technical Research Council) in Argentina. In the field of paleoneurology, her research has focused on brain evolution of Cenozoic continental mammals of South America. With traditional approaches and advanced methods of virtual reconstruction, she conducts studies of the endocranial cavities of marsupials, edentates, notoungulates, litopterns, rodents, and carnivores, in order to understand their neuromorphologies in the systematic, paleobiological, and evolutionary history of each group and their implications on brain evolution of mammals. Her research also includes general studies on Oligocene and Miocene mammals and paleoenvironments from central Patagonia to understand the evolutionary history of extinct South American mammals. Dr. Dozo is currently co-director of Instituto Patagónico de Geología y Paleontología (IPGP), CCT CONICET-CENPAT, in Puerto Madryn, Chubut Province, Patagonia, Argentina.

Ariana Paulina-Carabajal is a dinosaur paleontologist at Instituto de Investigaciones en Biodiversidad y Medioambiente (INIBIOMA) and a researcher at the National Scientific and Technical Research Council (CONICET) in S.C. de Bariloche, Argentina. She received a doctorate in natural sciences from Universidad Nacional de La Plata in 2009. Her paleoneurology studies center on the braincase and endocranial morphology of dinosaurs and other extinct reptiles, looking to better understand the paleobiological implications of certain anatomical regions (like those associated to sense organs) as well as their impact on the evolution of each group. These were pioneer studies in South America. Dr. Paulina-Carabajal is currently director of the Museo Paleontológico Bariloche in Rio Negro Province, Argentina.

Thomas E. Macrini has a PhD in geological sciences from the University of Texas at Austin. Subsequently, he was a postdoctoral researcher at the American Museum of Natural History in New York, NY, in the Departments of Mammalogy and Vertebrate Paleontology. He currently holds the rank of Department Chair and

Professor of Biological Sciences at St. Mary's University. His research focuses on the evolution of the brain and sensory structures in mammals and utilizes high-resolution X-ray computed tomography and traditional histological serial sections to study the endocranial cavity, internal nasal cavity skeleton (turbinals) and associated epithelia, and inner ear of fossil and extant mammals. This research has laid the groundwork for incorporation of anatomical characters from these regions of the mammalian skull into phylogenetic analyses.

Stig Walsh is Senior Curator of Vertebrate Palaeobiology at the National Museum of Scotland in the United Kingdom. His research centers on neurosensory evolution in archosauromorph reptiles, especially within the paraavian lineage, but he maintains an active interest in overarching evolutionary questions about the evolution of the brain and senses across all vertebrate clades, including fishes, stem tetrapods, and synapsid-line tetrapods. Walsh has been using μ CT methods to investigate external brain shape since 2003, and has published both descriptive and quantitative experimental work and reviews of the field of paleoneurology.

Contributors

Rémi Allemand Department of Anthropology, University of Toronto Scarborough, Toronto, ON, Canada

Ana Balcarcel Palaeontological Institute and Museum, Zurich, Switzerland

Francisco Barrios Departamento de Paleontología, Museo Provincial de Ciencias Naturales “Prof. Juan Olsacher”, Neuquén, Argentina

Julien Benoit Evolutionary Studies Institute (ESI), University of the Witwatersrand, Johannesburg, South Africa

Ornella C. Bertrand School of Geosciences, Grant Institute, University of Edinburgh, Edinburgh, Scotland

Paula Bona Facultad de Ciencias Naturales y Museo, División Paleontología de Vertebrados, Anexo Laboratorios, Buenos Aires, Argentina

CONICET, Consejo Nacional de Investigaciones Científicas y Técnicas, Buenos Aires, Argentina

Alberto Boscaini Instituto de Ecología, Genética y Evolución de Buenos Aires (IEGEB – CONICET), Departamento de Ecología, Genética y Evolución, Facultad de Ciencias Exactas y Naturales, Universidad de Buenos Aires, Ciudad Autónoma de Buenos Aires, Argentina

Mario Bronzati Department of Biology, Faculty of Philosophy, Sciences and Letters at Ribeirão Preto, University of São Paulo, São Paulo, Brazil

Julieta Carril Consejo Nacional de Investigaciones Científicas y Técnicas (CONICET), Buenos Aires, Argentina

Laboratorio de Histología y Embriología Descriptiva, Experimental y Comparada (LHYEDEC), Facultad de Ciencias Veterinarias, Universidad Nacional de La Plata, La Plata, Argentina

Penélope Cruzado-Caballero Paleontology Area, Department of Animal Biology, Edaphology and Geology, University of La Laguna, Santa Cruz de Tenerife, Spain

Juan D. Daza Department of Biological Sciences, Sam Houston State University, Huntsville, TX, USA

Federico J. Degrange Centro de Investigaciones en Ciencias de la Tierra (CICTERRA), UNC, CONICET, Córdoba, Argentina

Consejo Nacional de Investigaciones Científicas y Técnicas (CONICET), Buenos Aires, Argentina

Ricardo S. De Mendoza Consejo Nacional de Investigaciones Científicas y Técnicas (CONICET), Buenos Aires, Argentina

Laboratorio de Histología y Embriología Descriptiva, Experimental y Comparada (LHYEDEC), Facultad de Ciencias Veterinarias, Universidad Nacional de La Plata, La Plata, Argentina

María M. Demmel Ferreira Centro de Investigaciones en Ciencias de la Tierra (CICTERRA), UNC, CONICET, Córdoba, Argentina

Consejo Nacional de Investigaciones Científicas y Técnicas (CONICET), Buenos Aires, Argentina

Julia B. Desojo Consejo Nacional de Investigaciones Científicas y Técnicas (CONICET), Ciudad Autónoma de Buenos Aires, Argentina

División Paleontología Vertebrados, Facultad de Ciencias Naturales y Museo, Universidad Nacional de La Plata, La Plata, Argentina

Roberta Veronese do Amaral Departamento de Geologia e Paleontologia, Setor de Paleovertebrados, Museu Nacional/Universidade Federal do Rio de Janeiro, Rio de Janeiro, Brazil

María Teresa Dozo Instituto Patagónico de Geología y Paleontología, CCT CONICET-CENPAT, Puerto Madryn, Argentina

Consejo Nacional de Investigaciones Científicas y Técnicas (CONICET), CABA, Argentina

Serjoscha W. Evers Department of Geosciences, University of Fribourg, Fribourg, Switzerland

Gabriel S. Ferreira Fachbereich Geowissenschaften, Senckenberg Centre for Human Evolution and Palaeoenvironment at the Eberhard Karls Universität Tübingen, Tübingen, Germany

Timothy J. Gaudin Department of Biology, Geology, and Environmental Sciences, University of Tennessee at Chattanooga, Chattanooga, TN, USA

Javier N. Gelfo Consejo Nacional de Investigaciones Científicas y Técnicas (CONICET), CABA, Argentina

División Paleontología Vertebrados, Museo de La Plata, Facultad de Ciencias Naturales y Museo, Universidad Nacional de La Plata, La Plata, Argentina

Emmanuel Gilissen Department of African Zoology, Royal Museum for Central Africa, Tervuren, Belgium

Flávio Góis Laboratorio de Paleontología de Vertebrados, Centro de Investigación Científica y de Transferencia Tecnológica a la Producción, Diamante, Entre Ríos, Argentina

Arianna R. Harrington Department of Biology, Dixie State University, St. George, UT, USA

Casey M. Holliday Department of Pathology and Anatomical Sciences, School of Medicine, University of Missouri, Columbia, MO, USA

Paulina Jiménez Huidobro Division of Paleontology, Institute of Geosciences, Bonn, Germany

Dawid A. Iurino PaleoFactory, Sapienza Università di Roma, Rome, Italy

Madlen M. Lang Department of Anthropology, University of Toronto Scarborough, Toronto, ON, Canada

Stephan Lautenschlager School of Geography, Earth and Environmental Sciences, University of Birmingham, Birmingham, UK

Juan Martín Leardi CONICET, Consejo Nacional de Investigaciones Científicas y Técnicas, Buenos Aires, Argentina

Facultad de Ciencias Exactas y Naturales, Departamento de Ciencias Geológicas, Instituto de Estudios Andinos “Don Pablo Groeber” (IDEAN), Universidad de Buenos Aires, Buenos Aires, Argentina

Departamento de Biodiversidad y Biología Experimental, Facultad de Ciencias Exactas y Naturales, Universidad de Buenos Aires, Buenos Aires, Argentina

Michael Leary Department of Biological Sciences, St. Mary’s University, San Antonio, TX, USA

Emily J. Lessner Department of Pathology and Anatomical Sciences, School of Medicine, University of Missouri, Columbia, MO, USA

Sergi López-Torres Institute of Evolutionary Biology, Biological and Chemical Research Centre, Faculty of Biology, University of Warsaw, Warsaw, Poland

George A. Lyras Department of Geology and Geoenvironment, National and Kapodistrian University of Athens, Athens, Greece

Thomas E. Macrini Department of Biological Sciences, St. Mary’s University, San Antonio, TX, USA

Paul Manger School of Anatomical Sciences, Faculty of Health Sciences, University of the Witwatersrand, Johannesburg, South Africa

Vladislav Mararsecul Institute of Zoology, National Museum of Ethnography and Natural History of Moldova, Chişinău, Moldova

Gastón Martínez Museo de Paleontología, Facultad de Ciencias Exactas, Físicas y Naturales, Universidad Nacional de Córdoba, Córdoba, Argentina

Jacob Mougoust Institut Des Sciences de L'Évolution de Montpellier, Université de Montpellier, Montpellier, France

Benjamin C. Moon Palaeobiology Research Group, School of Earth Sciences, University of Bristol, Bristol, UK

Jorge Felipe Moura Laboratório de Paleocologia e Paleoicnologia, Departamento de Ecologia e Biologia Evolutiva (DEBE), Universidade Federal de São Carlos (UFSCar), São Carlos, SP, Brazil

Mpilo Nxumalo Evolutionary Studies Institute (ESI), University of the Witwatersrand, Johannesburg, South Africa

Teodor Obada Institute of Zoology, National Museum of Ethnography and Natural History of Moldova, Chişinău, Moldova

Johanset Orihuela Department of Earth and Environment (Geosciences), Florida International University, Miami, FL, USA

Maeva J. Orliac Institut Des Sciences de L'Évolution de Montpellier, Université de Montpellier, Montpellier, France

Ariana Paulina-Carabajal Instituto de Investigaciones en Biodiversidad y Medioambiente, CONICET-Universidad Nacional del Comahue, San Carlos de Bariloche, Argentina

CONICET, Consejo Nacional de Investigaciones Científicas y Técnicas, Buenos Aires, Argentina

François Pujos Instituto Argentino de Nivología, Glaciología y Ciencias Ambientales (IANIGLA), CCT-CONICET-Mendoza, Mendoza, Argentina

Timothy B. Rowe Jackson School of Geological Sciences, University of Texas at Austin, Austin, TX, USA

Gabriela A. San Martín-Flores Department of Anthropology, University of Toronto Scarborough, Toronto, ON, Canada

Raffaele Sardella PaleoFactory, Sapienza Università di Roma, Rome, Italy
Dipartimento di Scienze della Terra, Sapienza Università di Roma, Rome, Italy

Arnaud Schmitt Centre de Recherche en Paléontologie, Museum National d'Histoire Naturelle, Paris, France

Mary T. Silcox Department of Anthropology, University of Toronto Scarborough, Toronto, ON, Canada

Gabriela Sobral Staatliches Museum für Naturkunde Stuttgart, Stuttgart, Germany

Edward L. Stanley Department of Natural History, Florida Museum of Natural History, Gainesville, FL, USA

Michelle R. Stocker Department of Geosciences, Virginia Tech, Blacksburg, VA, USA

Rodolphe Tabuce Institut des Sciences de l'Évolution (UM, CNRS, IRD, EPHE), Université Montpellier, Montpellier, France

Claudia P. Tambussi Centro de Investigaciones en Ciencias de la Tierra (CICTERRA), UNC, CONICET, Córdoba, Argentina

Consejo Nacional de Investigaciones Científicas y Técnicas (CONICET), Buenos Aires, Argentina

P. Sebastián Tambusso Departamento de Paleontología, Facultad de Ciencias, Universidad de la República, Montevideo, Uruguay

Servicio Académico Universitario y Centro de Estudio Paleontológicos (SAUCE-P), Departamento de Canelones, Universidad de la República, Montevideo, Uruguay

Laura Natalia Triviño CONICET- Departamento de Herpetología, Museo de La Plata, La Plata, Argentina

M. Jimena Trotteyn Consejo Nacional de Investigaciones Científicas y Técnicas (CONICET), Ciudad Autónoma de Buenos Aires, Argentina

INGEO, Departamento de Biología, Departamento de Geología, Facultad de Ciencias Exactas, Físicas y Naturales, Universidad Nacional de San Juan, San Juan, Argentina

Alexandra A. E. van der Geer Naturalis Biodiversity Center, Leiden, The Netherlands

Bárbara Vera Consejo Nacional de Investigaciones Científicas y Técnicas (CONICET), CABA, Argentina

Centro de Investigación Esquel de Montaña y Estepa Patagónica, CONICET–Universidad Nacional de la Patagonia ‘San Juan Bosco’, Esquel, Argentina

Chiara Villa Laboratory of Advanced Imaging and 3D Modeling, Section of Forensic Pathology, Department of Forensic Medicine, University of Copenhagen, Copenhagen, Denmark

Dennis F. A. E. Voeten Department of Organismal Biology, Subdepartment of Evolution and Development, Uppsala University, Uppsala, Sweden

European Synchrotron Radiation Facility, Grenoble cedex 09, France

Naturalis Biodiversity Center, CR, Leiden, The Netherlands

M. Belén von Baczko Sección Paleontología de Vertebrados, Museo Argentino de Ciencias Naturales “Bernardino Rivadavia”, Ciudad Autónoma de Buenos Aires, Argentina

Consejo Nacional de Investigaciones Científicas y Técnicas (CONICET), Ciudad Autónoma de Buenos Aires, Argentina

Stig Walsh National Museum of Scotland, Edinburgh, Midlothian, UK

Vera Weisbecker College of Science and Engineering, Flinders University, Bedford Park, Australia

Lars Werdelin Department of Palaeobiology, Swedish Museum of Natural History, Stockholm, Sweden

Ingmar Werneburg Fachbereich Geowissenschaften, Senckenberg Centre for Human Evolution and Palaeoenvironment at the Eberhard Karls Universität Tübingen, Tübingen, Germany

Hussam Zaher Museu de Zoologia, Universidade de São Paulo, São Paulo, SP, Brazil

Chapter 1

Introduction



**María Teresa Dozo, Ariana Paulina-Carabajal, Thomas E. Macrini,
and Stig Walsh**

Paleoneurology is a branch of paleontology that is dedicated to the study of the anatomy and evolution of the nervous system of extinct animals. You are reading the introduction to this book about paleoneurology because you are a descendent of a long line of primate ancestors that had evolved progressively larger brains, and that were eventually able to communicate using symbolic written language. However, humans are not the only animals to have evolved relatively large brains. Trends towards brain enlargement have long been known in other vertebrate lineages, such as other mammals, and also in reptiles. Furthermore, throughout the evolution of amniotes there has been a brain size increase that corresponded, mainly, to an increase of the cerebrum with the highest encephalization observed in avian dinosaurs (birds) and mammals (e.g. Bruce 2007; Balanoff et al. 2014; Güntürkün et al. 2020; Smaers et al. 2021). Investigating patterns of brain evolution in other vertebrates offers a window on how human intelligence may have evolved, but the evolution of the brain and senses in those groups is fascinating in its own right. Primate and hominid brain evolution have been the subject of many previous volumes, and this book focuses on the state of knowledge of the paleoneurology in those other amniote groups (Fig. 1.1).

M. T. Dozo (✉)

Consejo Nacional de Investigaciones Científicas y Técnicas (CONICET), CABA, Argentina

Instituto Patagónico de Geología y Paleontología, CCT CONICET-CENPAT, Puerto Madryn, Argentina

e-mail: dozo@cenpat-conicet.gob.ar

A. Paulina-Carabajal

Instituto de Investigaciones en Biodiversidad y Medioambiente, CONICET-Universidad Nacional del Comahue, San Carlos de Bariloche, Argentina

e-mail: a.paulinacarabajal@conicet.gov.ar

T. E. Macrini

Department of Biological Sciences, St. Mary's University, San Antonio, TX, USA

e-mail: tmacrini@stmarytx.edu

S. Walsh

National Museum of Scotland, Edinburgh, Midlothian, UK

e-mail: s.walsh@nms.ac.uk

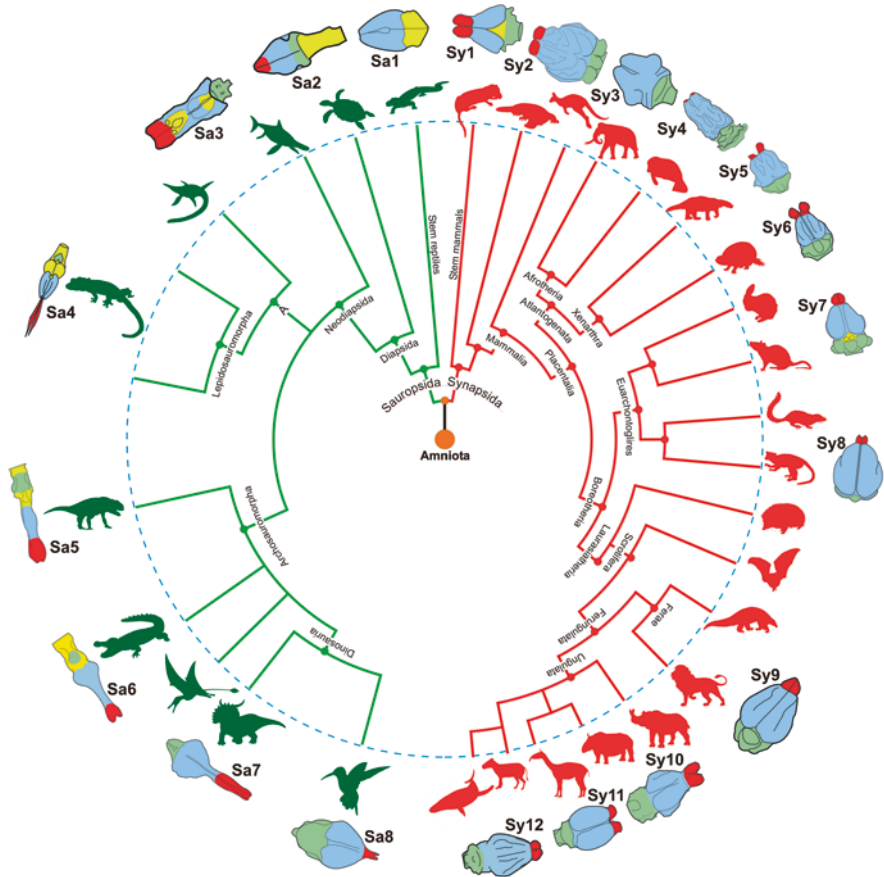


Fig. 1.1 Simplified phylogenetic hypothesis for the main amniote clades covered in this book, including dorsal views of endocrasts of taxa representative of those clades. Since the paleoneurology of some higher clades is still poorly known, those clades are not covered in this book. **Sa1.** *Avicranium* (basal diapsid (sensu Pritchard and Nesbitt 2017); Chap. 2) redrawn from Sobral (Chap. 2); **Sa2.** *Plesiochelys* (Testudinata; Chap. 4) redrawn from Paulina-Carabajal et al. (2013); **Sa3.** *Ichthyosaurus* (Ichthyopterygia; Chap. 3) redrawn from Allemand et al. (Chap. 3); **Sa4.** *Platecarpus* (Lepidosauromorpha; Chap. 5) redrawn from Camp (1942); **Sa5.** *Parringtonia* (Archosauromorpha; Chap. 6) redrawn from Nesbitt et al. (2017); **Sa6.** *Rukwasuchus* (Crocodylomorpha; Chap. 7) redrawn from Barrios et al. (Chap. 7); **Sa7.** *Latenivenatrix* (non-avian Dinosauria; Chap. 8) redrawn from Paulina-Carabajal et al. (Chap. 8); **Sa8.** *Archaeopteryx* (Avialae/Aves; Chap. 9) redrawn from Degrange et al. (Chap. 9); **Sy1.** *Hadrocodium* (stem mammals; Chap. 10) redrawn from Rowe et al. (2011); **Sy2.** *Thylacoleo* (Metatheria; Chap. 11) redrawn from Macrini et al. (Chap. 11); **Sy3.** *Palaeoloxodon* (Proboscidea) redrawn from Benoit et al. (Chap. 15); **Sy4.** *Prorastomus* (Sirenia; Chap. 14) redrawn from Macrini and Orihuela (Chap. 14); **Sy5.** *Glossotherium* (Pilosa; Chap. 19) redrawn from Boscaini et al. (Chap. 19); **Sy6.** *Glyptodon* (Cingulata; Chap. 18) redrawn from Tambusso et al. (Chap. 18); **Sy7.** *Reithroparamys* (Rodentia; Chap. 16) redrawn from Bertrand and Silcox (Chap. 16); **Sy8.** *Rooneyia* (Primates; Chap. 12) redrawn from Kirk et al. (2014); **Sy9.** *Hesperocyon* (Carnivora; Chap. 17) redrawn from Lyras et al. (Chap. 17); **Sy10.** *Notostylops* (Notoungulata; Chap. 20) redrawn from Perini et al. (2022); **Sy11.** *Macrauchenia* (Liptoptera; Chap. 21) redrawn from Dozo et al. (Chap. 21); **Sy12.** *Bathygenys* (Artiodactyla; Chap. 13) redrawn from Macrini (2009). Endocast color key: red represents olfactory bulbs, blue represents cerebrum, green represents cerebellum, yellow represents brain stem (medulla, midbrain etc.). **A.** Diapsid reptiles closer to lizards than to birds

Paleoneurology holds the key to unlock these secrets from Deep Time, but those secrets are not easily uncovered because brains and nerves do not fossilize directly. The brain, nerves, and associated soft tissues, such as the meninges and venous sinuses, degrade very rapidly after an animal dies, making the study of the neuroanatomy of extinct species extremely difficult. There are practically no fossils for which this type of soft tissue has been preserved in the fossil record of vertebrates. There are a few exceptions scattered throughout the Phanerozoic rock record from most higher vertebrate clades, such as Pleistocene mammals (Farrand 1961; Guthrie 1990), Cenozoic amphibians (Báez and Púgener 2003), Mesozoic reptiles (Brasier et al. 2016; Armitage 2021) and Paleozoic fishes (Pradel et al. 2009; Davidson and Trewin 2005). Beyond these very particular and extremely rare examples in nature, the available source of data for paleontologists is indirect and corresponds to the impressions or marks left by the soft tissues inside bones that held these structures in life. These marks, known as ‘osteological correlates’ can be studied using three-dimensional volumetric copies, created either through a casting material (e.g. Hopson 1979) or, more commonly in recent years, digital models created from computed tomographic data (e.g. Witmer et al. 2008).

Neurological structures of the central nervous system (CNS) such as the brain, cranial nerves, and sensory organs such as the eyes, inner ear and olfactory apparatus in the cranium, have been the focus of a great deal of attention for over 200 years. However, some groups are much better known than others, partly because of the variability in the fossil record of braincase material, but also because of other factors such as the size of the specimens, with smaller body-sized groups (e.g. lepidosaurs) among the most poorly known. The wealth of information available in the endocranium has meant that research in paleoneurology has historically focused on the anatomy of the CNS (particularly biased towards brain studies rather than spinal), and the peripheral nervous system (PNS) has been the subject of far fewer studies despite what the PNS can reveal about innervation to muscles and other soft tissues that rarely fossilize. Parts of the CNS and PNS are observable through casts of the vertebral neural canal, and of foramina in vertebrae through which motor and sensory nerves passed to connect to muscles and other soft tissues, respectively.

Paleoneurology has a long history of research. The earliest mention of what we now refer to as an endocast in the scientific literature appears to have been right at the start of the nineteenth century, when the French naturalist Georges Cuvier briefly described a mammalian endocast from Montmartre, Paris (Cuvier 1804 in Knoll and Kawabe 2020). There are also other mentions of endocasts in the early part of that century (e.g. Oken 1819), but credit for the realization that information from endocasts and the endocranial surface could demonstrate brain form through time arguably belongs to Cuvier (1822). Other authors followed, many of them leading scientists of their day. These include the English paleontologist and coiner of the term ‘Dinosauria’, Richard Owen (Owen 1842), the French paleontologist Paul Gervais (Gervais 1869, 1870) and the American paleontologist, Othniel Marsh (e.g. Marsh 1874, 1878, 1880) (see Edinger 1975 for a detailed review). Advances in paleoneurology at this time were aided by new discoveries in comparative neuroscience, but hampered by the availability of material, which was only available

through fortuitous discoveries of fossils (natural endocasts), and which sometimes required the partial destruction of skulls in order to view the endocranial anatomy.

At the end of the nineteenth century, ‘laws’ of mammalian brain evolution were proposed by Marsh (1884) based on the study of natural endocast material. Marsh’s ‘laws’ are listed below:

1. All Tertiary mammals had small brains.
2. There was a gradual increase in the size of the brain during this period.
3. This increase was confined mainly to the cerebral hemispheres, or higher portion of the brain.
4. In some groups, the convolutions of the brain have gradually become more complex.
5. In some, the cerebellum and the olfactory lobes have even diminished in size.
6. There is some evidence that the same general law of brain growth holds good for birds and reptiles from the Cretaceous to the present time.

These ‘laws’ of brain evolution dominated the science of paleoneurology through the early part of the twentieth century until they were mostly rejected by the work of Edinger (1951) and later Jerison (1973).

During the first half of the twentieth century, a number of significant descriptions of natural endocasts from a variety of extinct amniotes were being made. Some of these included important new information about brain evolution in early mammals such as the Jurassic triconodontid *Triconodon* (Simpson 1927, 1928), and the early Paleocene multituberculate *Ptilodus* (Simpson 1937), which show some lateral expansion in the cerebral region. During this period, artificial endocasts were widely incorporated in paleoneurological studies for the first time, following the work of the German-born scientist “Tilly” Edinger (Buchholtz and Seyfarth 2001). Despite the work that had gone before, Edinger has been regarded as the true founder of paleoneurology-proper due to the volume and detail of her work, which included some of the first comparative studies of the paleoneuroanatomy within different amniote lineages (e.g. Edinger 1941, 1948, 1949, 1955, 1964). One of the most prominent of these studies was on horses (Edinger 1948).

The taxonomic scope of Edinger’s work was truly broad, but ultimately was restricted to qualitative assessment of endocast shape. In the period ranging from the 1950s to the early 1970s, quantitative approaches were beginning to be used. In particular, two measures of relative brain size in mammals were presented, one based on relative body size (i.e., encephalization; Jerison 1955, 1973) and the other relating the endocranial cavity volume to foramen magnum area (Radinsky 1967). The former of these two comparisons utilizes encephalization quotients (EQs; Jerison 1955, 1973), which are the ratios of actual to expected brain sizes for particular taxa, and have a wide application to all vertebrate clades. These ratios are determined using plots of body size versus brain size among a number of closely related taxa. The EQ approach remains in use today, although with some modification for some groups such as reptiles (e.g. the REQ; Hurlburt 1996) and for the effects of relatedness (e.g. PEQs; Ni et al. 2019; Perini et al. 2022). The endurance

of Jerison's EQ approach is reflected in the longevity of the man himself; at time of writing, Harry Jerison is still alive and working.

Arguably, the real game-changer in paleoneurology was the advent of X-ray computed tomography toward the end of the 1990s. For the first time it was possible to extract information about brain shape, nerve pathways and indeed any endocranial structure without having to damage the fossil skull at all. This allowed endocasts for many more species to be known, including evolutionary pivotal taxa such as *Archaeopteryx*, the earliest-known avialan (Dominguez et al. 2004), and *Hadrocodium wui*, the sister taxon to crown Mammalia (Rowe et al. 2011). It also allows large 3D morphological libraries of endocasts to be collected from extant taxa, in which known behavior can be correlated with patterns of endocast shape and brain regional volume variation using multivariate statistics (e.g. Witmer et al. 2008; Balanoff et al. 2013; Kawabe et al. 2013; Walsh et al. 2013; Balanoff and Bever 2017; Weisbecker et al. 2021).

This book provides a detailed examination of paleoneurology in the second decade of the twenty-first century, and its advances through new technologies, focusing on recent studies in the main amniote clades (reptiles, birds, and mammals; Fig. 1.1). The volume provides a general picture of the great diversity of brain morphologies in different groups (stem and crown), the evolutionary history of brain structures and future directions of this field, testing old hypotheses with new methods. It brings together the most complete compilation of paleontological studies of non-preserved neuroanatomical structures, based on osteological correlates within the brain cavity and osseous labyrinth morphology in a wide taxonomic spread.

The book is organized into 21 chapters (including this introduction) that are interrelated and organized in order to be read separately, and include references and key terms within each chapter. Chapters 2, 3, 4, 5, 6, 7 and 8 update paleoneurological studies in sauropsid amniotes. They include a broad overview from stem Sauropsida/basal Diapsida (Chap. 2) to Aves (Chap. 9), through Sauropterygia and Ichthyopterygia (Chap. 3), Testudines (Chap. 4), Lepidosauria (Chap. 5), basal Archosauropomorpha (Chap. 6), Crocodylomorpha (Chap. 7) and Dinosauria (Chap. 8). Chapters 10, 11, 12, 13, 14, 15, 16, 17, 18, 19, 20 and 21 update the paleoneurology studies of synapsid amniotes, from early events in the evolution of the group (Chap. 10), Metatheria (Chap. 11), Primates (Chap. 12), Artiodactyla (Chap. 13), Sirenia (Chap. 14), Proboscidea (Chap. 15), Rodentia (Chap. 16), Carnivora (Chap. 17), Cingulata (Chap. 18), Pilosa (Chap. 19), Notoungulata (Chap. 20) and Litopterna (Chap. 21).

This book is the result of the collective effort of 70 authors and 39 reviewers to whom we editors are extremely grateful, not only for their effort and dedication, but also for their motivation and patience. The book was assembled during the COVID-19 global pandemic, which certainly imposed many difficulties on all of our personal and professional lives.

Finally, our particular and special thanks to João Pildervasser, Editor Life Science and Neuroscience (Springer Brazil) for his invitation to carry out this editorial project, and for his professional support and pertinent suggestions along the way.

References

- Armitage MH (2021) First report of peripheral nerves in bone from *triceratops horridus* occipital condyle. *MTO* 29(2):20–25
- Báez AM, Púgener LA (2003) Ontogeny of a new Paleogene pipid frog from southern South America and xenopodinomorph evolution. *Z J Linn Soc* 139:439–476
- Balanoff AM, Bever GS (2017) The role of endocasts in the study of brain evolution. In: Kaas JH (ed) *Evolution of nervous systems*, vol 1. Academic, Oxford, pp 223–241
- Balanoff AM, Bever GS, Rowe TB et al (2013) Evolutionary origins of the avian brain. *Nature* 501(7465):93–96
- Balanoff AM, Bever GS, Norell MA (2014) Reconsidering the avian nature of the Oviraptorosaur brain (Dinosauria: Theropoda). *PLoS One* 9(12):e113559
- Brasier MD, Norman DB, Liu AG et al (2016) Remarkable preservation of brain tissues in an Early Cretaceous iguanodon dinosaur. *Geol Soc Publ* 448:383–398
- Bruce LL (2007) Evolution of the nervous system in reptiles. In: Kaas JH (ed) *Evolution of nervous systems*, vol 2. Academic, Oxford, pp 125–156
- Buchholtz E, Seyfarth E-A (2001) The study of “fossil brains”: tilly Edinger (1897–1967) and the beginnings of Paleoneurology. *Bioscience* 51:674–682
- Camp CL (1942) *California mosasaurs*. University of California Press, Berkeley
- Cuvier G (1822) *Recherches sur les ossements fossiles*, vol 3, 2nd edn. E D’Ocagne E, Paris
- Davidson RG, Trewin NH (2005) Unusual preservation of the internal organs of acanthodian and actinopterygian fish in the middle Devonian of Scotland. *Scot J Geol* 41:129–134
- Dominguez P et al (2004) The avian nature of the brain and inner ear of *Archaeopteryx*. *Nature* 430:666–669
- Edinger T (1941) The brain of *Pterodactylus*. *Am J Sci* 239:665–662
- Edinger T (1948) Evolution of the horse brain. *Mem Geol Soc Am* 25:1–177
- Edinger T (1949) Paleoneurology versus comparative brain anatomy. *Confin Neurol* 9:5–24
- Edinger T (1951) The brains of the Odontognathae. *Evolution* 5:6–24
- Edinger T (1955) Hearing and smell in cetacean history. *Monatsschr Psychiatr Neurol* 129:37–58
- Edinger T (1964) Midbrain exposure and overlap in mammals. *Am Zool* 4:5–19
- Edinger T (1975) *Paleoneurology 1804–1966: an annotated bibliography*. Springer, Berlin
- Farrand WR (1961) Frozen mammoths and modern geology. *Science* 133:729–735
- Gervais P (1869) *Mémoire sur les formes cerebrales propes aux marsupiaux*. *Nouv Arch Mus Hist Nat Paris* 5:229–251
- Gervais P (1870) *Mémoire sur les formes cerebrales a differents groupes de Mammiferes*. *J Zool* I:425–469
- Güntürkün O, Stacho M, Strökens F (2020) The brains of reptiles and birds. In: Kaas JH (ed) *Evolutionary neuroscience*. Elsevier, pp 159–212
- Guthrie RD (1990) *Frozen Fauna of the mammoth steppe: the story of blue babe*. The University of Chicago Press, Chicago/London
- Hopson JA (1979) *Paleoneurology*. In: Gans C, Northcutt R, Ulinski P (eds) *Biology of the reptilia*. Academic, New York, pp 39–146
- Hurlburt GR (1996) *Relative brain size in recent and fossil amniotes: determination and interpretation*. Dissertation, University of Toronto
- Jerison HJ (1955) Brain to body ratios and the evolution of intelligence. *Science* 121:447–449
- Jerison HJ (1973) *Evolution of the brain and intelligence*. Academic, New York
- Kawabe S et al (2013) Variation in avian brain shape: relationship with size and orbital shape. *J Anat* 223:495–508
- Kirk EC, Daghighi P, Macrini TE et al (2014) Cranial anatomy of the Duchesnean primate *Rooneyia viejaensis*: new insights from high resolution computed tomography. *J Hum Evol* 74:82–95
- Knoll F, Kawabe S (2020) Avian palaeoneurology: reflections on the eve of its 200th anniversary. *J Anat* 236:965–979

- Macrini TE (2009) Description of a digital cranial endocast of *Bathygenys reevesi* (Merycoidodontidae; Oreodontioidea) and implications for apomorphy-based diagnosis of isolated, natural endocasts. *J Vertebr Paleontol* 29:1199–1211
- Marsh OC (1874) Small size of the brain in Tertiary mammals. *Am J Sci* 8:66–67
- Marsh OC (1878) Brain of a fossil mammal. *Nature* 17:340
- Marsh OC (1880) *Odontornithes: a monograph on the extinct toothed birds of North America*. U.S. Geol Expl 40th Parallel 7:1–20
- Marsh OC (1884) *Dinocerata. A monograph of an extinct order of gigantic mammals*. US Geol Surv 10:1–237
- Nesbitt SJ, Stocker MR, Parker WG et al (2017) The braincase and endocast of *Parringtonia gracilis*, a Middle Triassic suchian (Archosaur: Pseudosuchia). *J Vert Paleontol* 37(suppl1):122–141. <https://doi.org/10.1080/02724634.2017.1393431>
- Ni X, Flynn JJ, Wyss AR et al (2019) Cranial endocast of a stem platyrrhine primate and ancestral brain conditions in anthropoids. *Sci Adv* 5:eaav7913
- Oken L (1819) *Isis, oder encyclopädische Zeitung von Oken*. Expedition der Isis, Jena, pp 1817–1819
- Owen R (1842) Report on British fossil reptiles. Pt II. *Rep British Assoc Adv Sci* 11:60–204
- Paulina-Carabajal A, Sterli J, Müller J et al (2013) Neuroanatomy of the marine Jurassic turtle *Plesiochelys etalloni* (Testudinata, Plesiochelyidae). *PLoS One* 8:e69264. <https://doi.org/10.1371/journal.pone.0069264>
- Perini FA, Macrini TE, Flynn JJ et al (2022) Comparative endocranial anatomy, encephalization, and phylogeny of Notoungulata (Placentalia, Mammalia). *J Mamm Evol* 29:369–394
- Pradel A et al (2009) Skull and brain of a 300-million-year-old chimaeroid fish revealed by synchrotron holotomography. *PNAS* 106:5224–5228
- Prichard AC, Nesbitt SJ (2017) A bird-like skull in a Triassic diapsid reptile increases heterogeneity of the morphological and phylogenetic radiation of Diapsida. *R Soc Open Sci* 4:170499. <https://doi.org/10.1098/rsos.170499>
- Radinsky L (1967) Relative brain size: a new measure. *Science* 155:836–838
- Rowe TB, Macrini TE, Luo Z-X (2011) Fossil evidence on origin of the mammalian brain. *Science* 332:955–957
- Simpson GG (1927) *Mesozoic Mammalia. IX. The brain of Jurassic mammals*. *Am J Sci* 214:259–268
- Simpson GG (1928) *A catalogue of the Mesozoic Mammalia in the Geological Department of the British Museum*. William Clowes and Sons, London
- Simpson GG (1937) Skull structure of the Multituberculata. *Bull Am Mus Nat Hist* 73:727–763
- Smaers JB, Rothman RS, Hudson DR et al (2021) The evolution of mammalian brain size. *Sci Adv* 7(18):eabe2101. <https://doi.org/10.1126/sciadv.abe2101>
- Walsh SA, Iwaniuk AN, Knoll MA et al (2013) Avian cerebellar floccular fossa size is not a proxy for flying ability in birds. *PLoS One* 8(6):e67176
- Weisbecker V, Rowe T, Wroe S et al (2021) Global elongation and high shape flexibility as an evolutionary hypothesis of accommodating mammalian brains into skulls. *Evolution* 75:625–640
- Witmer LM, Ridgely RC, Dufeu DL, Semones MC (2008) Using CT to peer into the past: 3D visualization of the brain and ear regions of birds, crocodiles, and nonavian dinosaurs. In: Endo H, Frey R (eds) *Anatomical imaging: towards a new morphology*. Springer, Tokyo, pp 67–87

Chapter 2

The Paleoneurology of Early Reptiles



Gabriela Sobral

2.1 Early Evolutionary History and Diversity of Reptiles

Reptiles, including birds, comprise the most diverse group of present-day tetrapods. With over 20,000 species, they occupy a vast number of niches and display a wide range of locomotory modes, from flying birds to marine turtles and fossorial snakes (Sues 2019). Reptiles first appeared in the Late Carboniferous, at about 320 million years ago, but the composition of early reptile groups remains disputed. For instance, recent phylogenetic analyses have placed traditional non-amniote, “lepospondyl” groups like Lysorophia and Rhynchonkidae among early-diverging reptilian clades (Pardo et al. 2017) and varanopids, traditionally considered as synapsids, among early-diverging diapsids (Ford and Benson 2020). Still, Mesosauria and Parareptilia are traditionally considered the earliest diverging groups, respectively (Laurin and Reisz 1995), although this too has been revisited, with either the former within the latter (Fig. 2.1; MacDougall et al. 2019) or parareptiles considered as more derived than some of the earliest diapsids instead (Laurin and Piñero 2017). This is a field of study that has recently attracted renewed interest and it is likely to change in the future. In any case, the ecological and morphological diversity of early reptiles mirrors, or even surpasses, that of extant groups.

Mesosaurs were the first reptiles completely adapted to an aquatic lifestyle, with early Permian fossils found around the borders of the Irati-Whitehill inner sea, an early sea covering parts of South America and Africa (Laurin and Piñero 2017). On the other hand, derived groups of parareptiles such as bolosaurids and pareiasaurs, were fully terrestrial and included some of the first herbivorous reptiles. They may have also been the first to develop terrestrial specializations in hearing which later appeared convergently in diapsids (Müller and Tsuji 2007), the main reptile radiation. Other anatomical features of parareptiles, such as the temporal emargination,

G. Sobral (✉)
Staatliches Museum für Naturkunde Stuttgart, Stuttgart, Germany
e-mail: gabriela.sobral@smns-bw.de

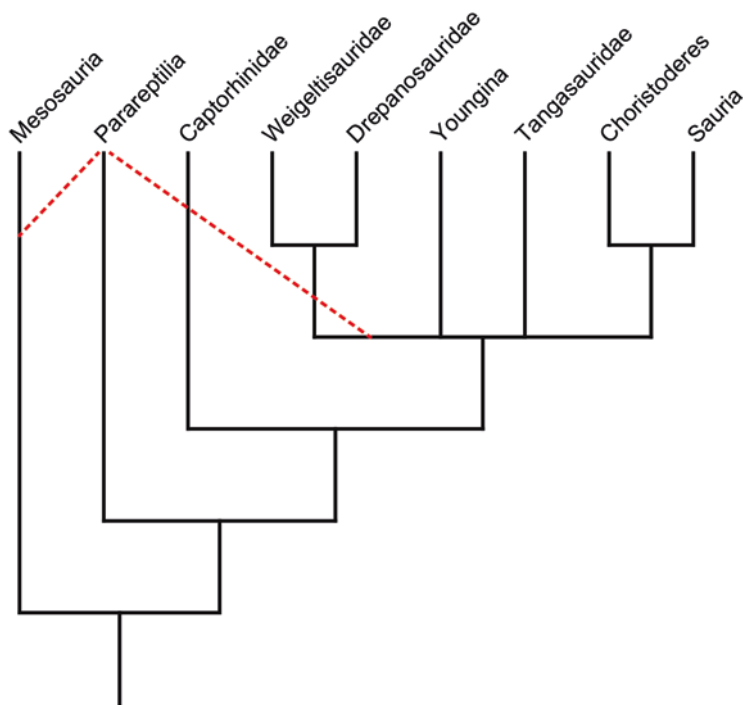


Fig. 2.1 Phylogenetic relationships of the main reptile groups discussed here based on Laurin and Reisz (1995) and Pritchard et al. (2021). The red lines indicate alternative placements of Parareptilia based on Ford and Benson (2020), Laurin and Piñero (2017), and MacDougall et al. (2019)

are also similar to those of diapsids, indicating further potential convergences between the two groups. Another early-diverging branch is represented by captorhinids (Fig. 2.1). They were small to medium-sized reptiles known from many complete, often exquisitely preserved fossils. Captorhinids are sometimes found in sites with a great aquatic influence from where amphibious tetrapods are known, such as embolomeres and temnospondyls (Lucas et al. 2005). *Captorhinus* has been interpreted as semi-aquatic (Canoville and Laurin 2010), although this remains contentious as this taxon and closely related forms are very common in clearly terrestrial deposits.

Diapsida represents the main reptilian radiation, to which all extant reptiles belong. Despite this, the fossil record is poor for most of the stem clades, especially for terrestrial groups such as younginids. The latter were small lizard-like animals that include the well-known *Youngina* (Fig. 2.1). The morphological diversity, in contrast, was high among these groups. One example is Drepanosauridae, a strange group of arboreal, chameleon-like reptiles with prehensile tails and modified front limbs that were also used for digging in some species (Pritchard and Nesbitt 2017). Stem-diapsids also include groups that took to the air millions of years before pterosaurs or birds did, although they did not employ active flight. They are the

weigeltisaurids and kuehneosaurids (Evans 1982; Robinson 1962), gliding reptiles similar to the Flying Dragon of Southeast Asia. Once again, controversies regarding classification exist and the latter have alternatively been included in the lepidosauromorph or archosauromorph lineages (Ezcurra 2016; Pritchard et al. 2021; Simões et al. 2018).

The remaining reptile groups represent fully aquatic radiations with significant ecological and anatomical diversity, such as tangasaurids, thalattosaurs, ichthyosauroid forms, sauropterygians, and choristoderans. Little is still known about their early evolution, and their phylogenetic relationships remain poorly understood. Some analyses considered them stem-diapsids (Scheyer et al. 2017, 2020), but others found them as part of the diapsid crown (Sauria; Fig. 2.1), either in the lepidosaur or in the archosaur radiation (Chen et al. 2014; Li et al. 2014). One reason for these conflicting interpretations of their evolutionary history is the highly modified nature of their body plans for an aquatic mode of life, which makes the traditional members of these groups look very different from their putative terrestrial ancestors. Anatomical convergence and the limited number of transitional fossils complicates further our understanding of their evolution. Secondarily aquatic reptiles will be discussed in a subsequent chapter, except for choristoderans, which will be covered here.

2.2 Historical Background

2.2.1 *The Fossil Record*

Paleoneurology has largely been a neglected area of study for early reptiles. Apart from sauropterygians, natural and artificial casts of the inner ear and endocranial cavity of early reptiles are extremely scarce. For this reason, most of the early accounts do not rely on endocasts, but rather on osteological correlates to infer the size and position of neurological structures instead. These studies consider parts of the central nervous system, such as the pineal organ, the pituitary, cranial nerves, and general brain cavity size and shape (Boonstra 1934; Edinger 1955; Nopcsa 1923; Reich 1927; Watson 1914, 1916), covering pareiasaurian parareptiles and captorhinids. More recently, osteological correlates such as the patterns of carotid circulation in various groups, including parareptiles, were used to inform on the phylogenetic affinities of turtles (Müller et al. 2011). With the development and subsequent wide use of computed tomography (CT) scanning techniques, virtual endocasts of the encephalon and inner ear have now been produced, such as for the captorhinid *Labidosaurus* (Klembara et al. 2020a), the early diapsid *Youngina* (Gardner et al. 2010; Fabbri et al. 2017), the choristoderan *Champsosaurus* (Dudgeon et al. 2020a), and the drepanosaurid *Avicranium* (Pritchard and Nesbitt 2017).

A further difficulty when studying fossil endocasts is the fact that in many adult living reptiles, the brain does not entirely fill in the endocranial cavity as it does in mammals (Hopson 1979), and so the question arises as to how precise the fossil record is when assessing the brain shape and size of extinct groups. Early studies showed that the brain can correspond to as little as 50% (Hopson 1979) to the endocast volume, and while modern approaches to the issue show that this may be in fact the case, they also show that the correspondence between brain and endocast volume is in fact very high, at least among archosaurs (Watanabe et al. 2019). Variation in this relationship may occur depending on the ontogenetic stage, brain region, and taxonomic group. The higher correspondence between brain size and endocranial cavity in archosaurs, however, had already been recognized (Hopson 1979), but the relationship between these variables in other reptile groups remain to be tested in a more modern approach. One interesting finding of these early studies is that brain-cases which are partly cartilaginous in life may show a different correspondence when only the bony parts are considered (Jerison 1973), which could have interesting implications for taphonomy more broadly, and for early reptiles in particular.

2.2.2 Unresolved Issues

Recently, paleoneurology has seen a resurgence with modern technologies becoming more affordable, and most studies in the area are now done using CT scanning. However, despite becoming an accessible tool, CT scans are still not universally available nor can all specimens can be CT scanned, owing to their size or composition of the matrix and/or fossil. However, anatomical analyses of the materials and identification of osteological correlates can be used to assess the morphology of the brain and ears in fossils without CT scans. This anatomical approach has been used in some studies, but still comparatively much less than in crown diapsids, especially archosaurs (e.g. Walker 1990).

An additional challenge is posed by the post-mortem crushing of many stem-diapsid fossils. Assessing the brain and inner ear of 2D preserved specimens still remains a challenge, but recent studies on tanystropheid archosauromorphs (Miadema et al. 2020; Spiekman et al. 2020) have proved that may be possible. However, the fossil record of early reptiles is rich with examples of three-dimensional preserved specimens that could be used to understand the early evolution of the nervous system in the group (e.g. Gardner et al. 2010), but there are still very few number of such studies. Much of the scarce data that exists for early-diverging reptile groups is often superficial and/or used in a comparative context for understanding the paleoneurology of other, usually late-diverging groups (Ezcurra 2016; Fabbri et al. 2017; Klembara et al. 2020a; Müller et al. 2011; Pritchard and Nesbitt 2017) with little focus on their evolutionary histories. This hampers our understanding of the early evolution of the nervous system and its role in the subsequent ecological and anatomical diversification of reptiles.

2.3 Anatomical Overview

2.3.1 *Characterization of Cranial Endocast Morphology*

With a lack of such studies, it is very difficult to characterize the early reptilian brain. Judging by the anatomy of the braincase, the brain of pareiasaurian parareptiles was low and long, with moderate cephalic and pontine flexures (Boonstra 1934), and with a moderate-sized pineal organ (Watson 1914). The medial wall of the braincase appears smooth, possibly indicating a likewise moderately-sized cerebellum and floccular lobe (Watson 1914). This may be in contrast with some procolophonid parareptiles, who have more compact braincases such as *Procolophon* (Carroll and Lindsay 1985) and *Leptopleuron* (Spencer 2000), but not others like *Eomurrina* (Hamley et al. 2021). The relatively early-diverging position of the latter in relation to the formers may be indicative of a generalized, plesiomorphic state for the group.

A streamlined brain also seems to have been present in the diapsid *Youngina* (Fabbri et al. 2017; Fig. 2.2a). This contrasts with the apparent high and short braincase of the early diverging reptile *Captorhinus* (Watson 1916), although the pineal organ was also moderately developed (Edinger 1955). The optic lobes of *Captorhinus* appear to have been round and were located posterior to the pineal region (Heaton 1979). A very high and short braincase is also found in the drepanosaurid *Avicranium* (Pritchard and Nesbitt 2017; Fig. 2.2b), although to a more extreme extent, suggesting a highly sigmoidal encephalon like those of pterosaurs and birds (Witmer et al. 2003). Given the arboreal habits of *Avicranium*, it has been postulated that its brain regions were also arranged similarly, but a more complete study of its endocast is still missing. It is unclear to which extent such high and short braincases imply a rearrangement of the brain regions as there appears to be some intraspecific variation. The endocasts of two specimens of the choristodere *Champsosaurus* show that a long, streamlined brain and a larger encephalon with more evident cephalic and pontine flexures can be found within the same species (Dudgeon et al. 2020b; Fig. 2.2c, d). It is also unclear if these differences can be traced back to different ontogenetic stages, like what is seen in the extant crocodile *Alligator* (Hu et al. 2020).

2.3.2 *Spaces Associated with Cranial Blood Supply*

There is not much known about the patterns of vasculature in the braincase of early reptiles, except for the internal carotid artery. The pattern in these groups is extremely conserved, in which division into palatal and cerebral branches take place outside the braincase, with the foramina for the entrance of the cerebral branch located on the ventral surface of the parasphenoid, medial to the basiptyergoid processes such as in the captorhinids *Labidosaurus* and *Captorhinus* (Müller et al. 2011). In parareptiles, however, this division happens within the parasphenoid and

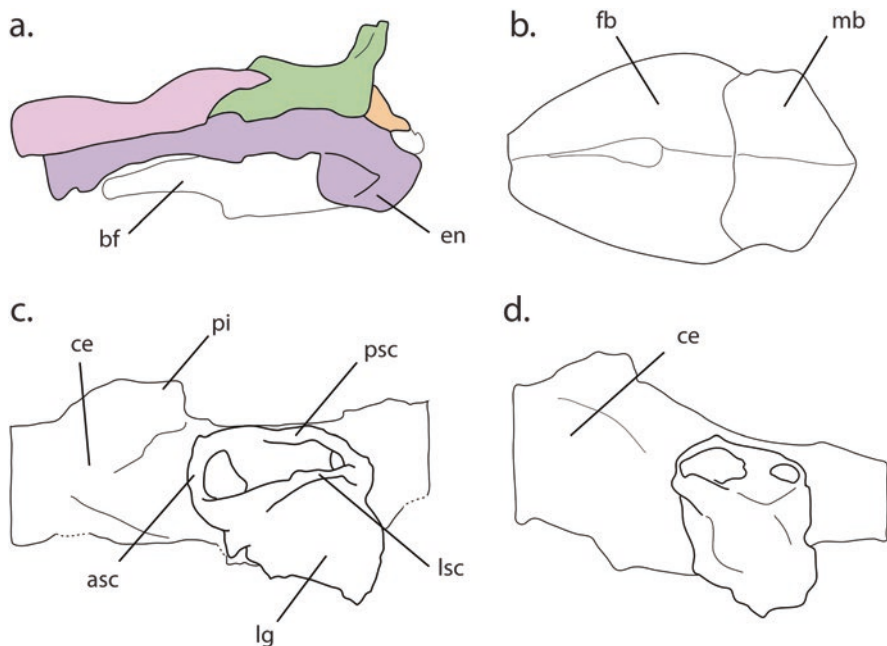


Fig. 2.2 Available virtual endocasts of stem-reptiles. (a), the early diapsid *Youngina* in oblique dorso-lateral view. (Modified from Fabbri et al. 2017); (b), the drepanosaurid *Avicranium* in dorsal view. (Modified from Pritchard and Nesbitt 2017); (c) and (d), different specimens of the choristodere *Champsosaurus* in left lateral view. (Modified from Dudgeon et al. 2020b). Anterior to the left. Abbreviations: *asc* anterior semicircular canal, *bf* braincase floor, *ce* cerebellum, *en* encephalon, *fb* fore-brain, *lg* lagena, *lsc* lateral semicircular canal, *mb* mid-brain, *pi* pineal gland, *psc* posterior semicircular canal

the entrance foramina of the internal carotid artery are positioned laterally, dorsal to the basiptyergoid process. There is some variation on the exit foramina of the carotid branches. The varying patterns found in parareptiles are similar to those seen in squamates, dinosaurs (including birds), late-diverging turtles, and some sauropterygians. This appears to result largely from the increased degree of ossification of the pterygoid, which results in a reduction or closure of the interptyergoid vacuity and the concealment of the braincase floor in ventral view.

Similarly, parareptiles seem to show a pattern for the exit of the posterior cerebral vein (=jugular vein) from the braincase that is different from other early reptiles but similar to that in crown lepidosaurs and archosaurs. In early reptiles in general, such as *Youngina* (Gardner et al. 2010), the posterior cerebral vein, together with cranial nerves IX-XI, exits the brain cavity through the metotic foramen, which also accommodates the perilymphatic sac (Sobral et al. 2016a). In crown groups, like in the ornithomimid dinosaur *Dysalotosaurus* (Sobral et al. 2012), the metotic foramen becomes subdivided into an anterior fenestra pseudorotunda and a posterior vagus foramen. The latter is sometimes termed jugular foramen, but the exit path of the posterior cerebral vein is known to vary in some taxa (Sobral et al. 2012), whereas

the nervous path is more conserved. Parareptiles may also have had a separate foramen for the posterior cerebral vein and the vagus nerve, although more careful analyses are needed (Sobral et al. 2016b).

2.4 Brain Evolution and Paleobiological Inferences

The extant diversity of reptiles is represented by the variety of niches that they occupy. This diversity is closely mirrored, and even surpassed, by its fossil history, where even more diverse body plans and modes of life can be found. The fossil record can provide us unique information on the evolution of reptiles, enabling us to understand how this diversity originated and flourished. However, given this immense diversity, and the disproportionate lack of data, it is difficult to establish a general trend between brain shape and the evolution and paleobiology of the group.

Reptiles are usually regarded as a primarily terrestrial group. In fact, one of the key ecological features for amniotes is the full conquest of terrestrial environments. The reptile fossil record, however, shows us many instances where they went back to water, which may complicate the history of their sensory systems. The fundamentally different media of water and air pose great challenges to neurosensory perception, especially to hearing (Müller et al. 2018). The lack of data on brain and inner ear morphology and the confusing relationships of early reptiles hinder our understanding of the evolution of the nervous system and sensory perception in the group. Renewed interest on the phylogeny of early reptile groups is an important step forward but our understanding of their neuroanatomy and associated sensory systems is still lagging behind.

2.4.1 Morphological Brain Diversity

To understand the reptilian brain within the context of its evolution, it is important to compare anatomical features of early diverging reptiles with closely related groups such as non-amniote tetrapods like diadectomorphs (although their phylogenetic relationships has been recently challenged – Klembara et al. 2020a). The endocast of *Diadectes* (Hopson 1979) shows a pronounced dural peak, indicating the presence of a well-developed pineal organ. The pituitary fossa is also well-developed and is located slightly anterior to the level of the pineal organ. The cephalic and pontine flexures of *Diadectes* have moderate angles. The fore- and mid-brain are narrow and the cerebrum is visible on the endocast. The cerebellum is slightly developed but the medulla is narrow. In parareptiles, the dural peak is also distinct and well developed dorsally, but positioned more anteriorly (Hopson 1979). The general outline of the brain is, however, different. It is more horizontal, with much less marked flexures and the medulla is long and low (Hopson 1979). In the early eureptile however, the braincase indicates the brain was rather high and short

(Watson 1916), with a moderate-sized pineal organ (Edinger 1955). The optic lobes of *Captorhinus* mark the ventral surface of the parietals and seem to have been round (Heaton 1979). They were located posterior to the level of the pineal organ.

The endocast of the choristodere *Champsosaurus* is also flat (Dudgeon et al. 2020b) like that of pareiasaurs, with a prominent pineal organ (Fig. 2.2c, d). The pituitary fossa, in contrast, is shallow and shows no striations, indicating the hypophysis would not have filled it entirely. The optic lobes and flocculus are not apparent in the endocast. A partial endocast for the drepanosaurid *Avicranium* (Pritchard and Nesbitt 2017) shows enlarged cerebral hemispheres and optic lobes (Fig. 2.2b). The pituitary fossa is deep, indicating the presence of a well-developed hypophysis.

As previously noted, the lack of endocasts poses a constraint on paleoneurological studies of early reptiles, but the identification of osteological correlates to infer brain morphology can be used to partially fill in this gap. For instance, the position and size of the pineal organ can be inferred from the pineal foramen and from the depth of the fossa on the ventral side of the parietal. Likewise, the hypophysis can be studied from the size of the pituitary fossa on the basisphenoid. Other regions of the brain can be inferred from braincase morphology. The narrow nature of the fore- and mid-brains of *Diadectes* relative to the hind-brain are indicated by the narrow sphenethmoid and basisphenoid in comparison to the basioccipital (Klembara et al. 2020b). Unfortunately, the braincase in stem-reptiles is often not ossified in the sphenoid region anterior to the prootic, and the absence of such ossifications limits our understanding of the shape of the fore- and mid-brains. However, the suture between the frontal and parietal bones can provide good estimates for the limit between these regions (Fabbri et al. 2017). Another potential correlation that could be explored is the relative contributions of the para- and basisphenoid and the basioccipital to the braincase floor and their relationship with the mid- and hind-brains. In the braincase of *Diadectes*, the proportion between both bones is very similar (Klembara et al. 2020b), which seems to be preserved in *Captorhinus* (Heaton 1979). However, this relationship appears to change in *Araeoscelis* (Vaughn 1955) and *Youngina* (Evans 1987; Gardner et al. 2010), where the basioccipital increases its participation in the braincase floor.

The relationship between the parasphenoid and basioccipital also changes as the diapsid braincase verticalises. The posterior region of the braincase floor may become more dorsally positioned than the anterior one, resulting in the occipital condyle lying dorsal to both the basal tubera and the basipterygoid processes in lateral view. The braincase of *Captorhinus* (Heaton 1979) is rather flat, with the occipital condyle, basal tubera, and basipterygoid processes lying roughly in the same horizontal plane. This appears to change in *Youngina* (Gardner et al. 2010), where the condyle lies more dorsal than the other structures (Fig. 2.3a). This trend becomes stronger in at least some archosauriforms, with a marked difference between the dorsal position of the tubera in relation to the basipterygoid process (Sobral et al. 2016a; Sobral and Müller 2019) – but not in proterosuchids and erythrosuchids (Ezcurra 2016). Verticalisation of the braincase is also apparent in the

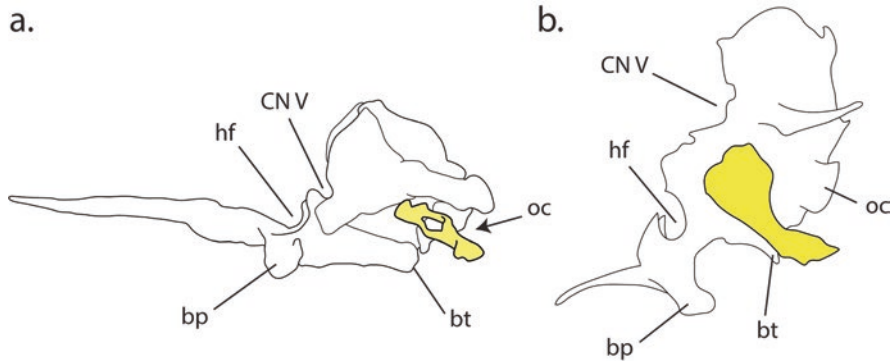


Fig. 2.3 Brainscases of the stem-diapsids *Youngina* (a) and *Avicranium* (b). (Modified from Gardner et al. 2010; Pritchard and Nesbitt 2017). Stapes in yellow. Abbreviations: *bt* basal tubera, *CN V* trigeminal cranial nerve, *hf* hypophyseal fossa, *oc* occipital condyle

dorsoventral expansion of its lateral elements, i.e. the prootic, opisthotic, and exoccipital. The prootic seems to expand dorsoventrally through incorporation of part of the embryonic pila antotica during its ossification (Evans 2008). Ventral to the exit of the trigeminal nerve, the prootic assimilates the pila as its anteroventral process, resulting in decreased participation of the parasphenoid in the lateral wall of the brainscase, as in the archosauromorph *Euparkeria* (Sobral et al. 2016a). In *Diadectes*, the prootic is very low barely shows any trace of a trigeminal notch (Klembara et al. 2020b). In contrast, the prootic increasingly encloses the trigeminal nerve in reptiles, appearing as an open notch in *Captorhinus* (Heaton 1979). In parareptiles, brainscase patterns similar to diapsids can be found. A flat brainscase with a rather dorsoventrally low prootic is found in *Milleretta*, which has also a basioccipital with a limited contribution to the brainscase floor in relation to the parasphenoid (Gow 1972). However, in derived procolophonians such as *Procolophon* (Carroll and Lindsay 1985) and *Macroleter* (Müller and Tsuji 2007), the contribution of both bones becomes more equal. The brainscases of these latter two taxa are also more verticalised, although verticalisation of the brainscase floor in *Macroleter* is less evident than that of the lateral wall.

It is unclear why verticalisation of the brainscase occurs. Verticalised brainscases are present in taxa with highly sigmoidal brains, such as birds and pterosaurs (Balanoff et al. 2014; Bennet 2001), but also in non-avian theropods with a more linear endocast (Witmer and Ridgely 2009). Brains with a sigmoidal shape take their form from inflation and re-arrangement of brain regions in relation to each other, with the cerebral hemispheres becoming more dorsally positioned in relation to the optic lobes and the enlargement of both areas (Balanoff et al. 2014). Determining the processes through which these changes took place is less simple, and powered flight, miniaturization, heterochrony, and progenetic developments have been proposed (Balanoff et al. 2014; Shimizu et al. 2017; Beyrand et al. 2019).

As in birds and pterosaurs, the partial endocast of the drepanosaurid *Avicranium* shows enlarged cerebral hemispheres and optic lobes (Fig. 2.2a; Pritchard and

Nesbitt 2017). The braincase floor is strongly vertical, with the occipital condyle, basal tubera, and basipterygoid processes lying in successive more dorsal planes in lateral view (Fig. 2.3b). However, dorsoventral expansion of the prootic seems to result from the development of the anterior semicircular canal (Witmer et al. 2003) rather than incorporation of large portions of the pila antotica. The dorsal portion of the alar process of the bone, which houses the canal, is prominently developed, in contrast with the portion of the prootic ventral to the trigeminal foramen. The anteroventral process of the prootic is quite modest, and the parasphenoid still seems to contribute a good portion to the lateral braincase wall. The enlarged cerebral hemispheres and optic lobes of *Avicranium* suggest that the brain regions could have been arranged in a manner similar to those in birds (Pritchard and Nesbitt 2017). Brain enlargement seems to be correlated to the enhancement of stereoscopic vision and development of flight in birds, so that the arboreal habits of *Avicranium* likely offered a similar path of brain evolution (Pritchard and Nesbitt 2017).

In contrast, the braincase of the probable semi-aquatic/aquatic *Champsosaurus* is not verticalised (Dudgeon et al. 2020b). The prootic shows no sign of incorporation of the pila antotica and the parasphenoid has a strong participation in the lateral braincase wall, forming the ventral rim of the trigeminal foramen. As a result, the endocast of *Champsosaurus* is very linear, similar to other aquatic taxa – although intraspecific variation exists. Choristoderes have a particularly flat skull, and so it remains unclear whether this brain and braincase anatomies are related to aquatic habits or to the strongly flattened skull.

2.4.2 *Brain-Size Evolution and Encephalization Quotient*

The encephalization quotient (EQ) is better understood in mammals and birds than in extinct or extant non-avian reptiles. The recognition that some reptilian species such as the Nile crocodile (*Crocodylus niloticus*) grows continuously, as well as other relationships to body size and weight to the brain, may affect our understanding of the EQ in at least these reptiles (Güntürkün et al. 2020).

As mentioned in Sect. 2.2.1, the fact that the brain volume does not always have a close correspondence with the endocranial cavity in extant reptiles makes it difficult to understand EQ in extinct groups. The correspondence may vary according to ontogenetic stage, region of the brain, and taxonomic group (Hopson 1979; Watanabe et al. 2019), so that to have a clear understanding how EQ changes during the early evolution of reptiles, much more data is needed than is currently available. Early studies on the EQ of fossil amniotes basically consider relatively derived therapsids and archosaurs (Hopson 1979; Jerison 1973), and to date there are still no studies on EQ that include early reptiles. Difficulties in determining body size in extinct taxa, especially when considering aquatic reptile groups (e.g. Campione and Evans 2012) pose an extra challenge to the issue.

2.4.3 Sensory Perception

There is a wide range of information on sensory perception in fossil groups that can be assessed through anatomical analyses of the skull. Studies on the topic are done mostly in the context of cranial nerves, nasal capsule, and orbit size. The evolutionary history of sensory perception in amniotes, including early reptiles, has been recently summarised in Müller et al. (2018), but it is interesting to provide here a few updates.

Hearing and Balance

These are senses related mostly to the inner ear, although balance has also strong connections to the floccular lobe of the cerebellum. The inner ear and the floccular lobe are involved in the vestibulo-ocular and vestibulocollic reflexes, intricate neuronal circuitries that connect and coordinate muscle movements of the eyes, head, and neck (Voogd and Wylie 2004). Features of the semicircular canals like thickness, length, radius of curvature, and orthogonality, as well as size and depth of the floccular fossa have been used to assess locomotor abilities and niche occupation in fossils (Bronzati et al. 2021; Schwab et al. 2020). Likewise, there is an intricate relationship between the length of the cochlea, anatomy of the stapes, degree of ossification of the otic capsule, presence of pressure-relief mechanisms, and hearing range (Sobral et al. 2016a), but this topic has been comparatively less explored (e.g. Evans 1986). The inner ear is an organ separate from, but closely associated with, the brain. Although it is considered as part of the field of paleoneurology, it is sometimes treated separately, and the inner ear of tetrapods has been covered in its own volume of the SHAR book series (Clack et al. 2016). Early reptiles were reviewed in that volume (Sobral et al. 2016b) and therefore will not be covered in depth here. However, a short summary will be given, especially in the light of recent discoveries made after the publication of the book.

The inner ear of the captorhinid *Labidosaurus* has been studied recently (Klembara et al. 2020a). Its common crus is markedly short, associated with the small radii of curvature of the anterior and posterior semicircular canals (Fig. 2.4). The vestibule is located ventral to the lateral semicircular canal, giving the labyrinth an unusual antero-posteriorly elongate outline. The lagena is short, not extending further than the fenestra ovalis. The morphology of the inner ear of *Labidosaurus* conforms to the hypothesis proposed by Sobral et al. (2016a, b), in which a gradual transition to terrestrial environments took place in the early evolutionary history of reptiles and that the so-called tympanic hearing appeared in a stepwise fashion. The anatomy of the otic region in captorhinids indicates their hearing range likely remained very sensitive to low frequencies, as indicated by the relatively short lagena when compared to later-diverging taxa such as *Youngina* (Gardner et al. 2010). The lagena of *Labidosaurus* is proportionately longer than that of the stem-amniote *Seymouria* (Klembara et al. 2020a), but it is surprisingly different from that

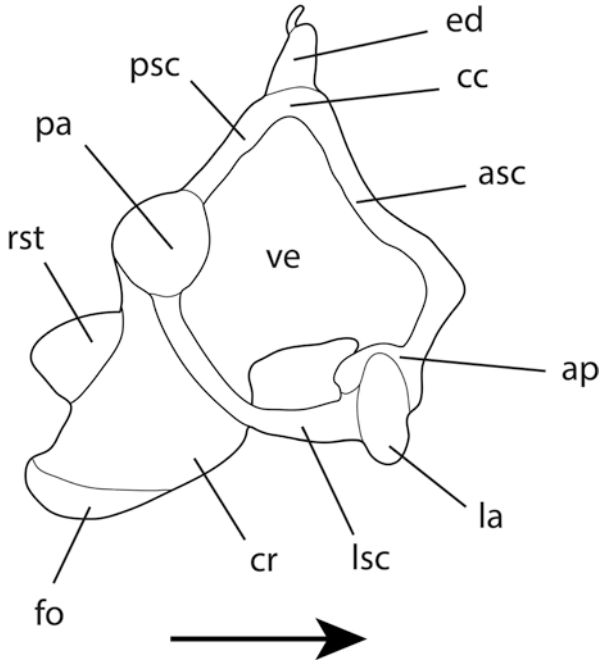


Fig. 2.4 Inner ear of the captorhinid reptile *Labidosaurus*. (Modified from Klembara et al. 2020a). Arrow indicates anterior direction. Abbreviations: *ap* anterior ampulla, *asc* anterior semicircular canal, *cc* common crus, *cr* cochlear recess, *ed* endolymphatic duct, *fo* fenestra ovalis region, *la* lateral ampulla, *lsc* lateral semicircular canal, *pa* posterior ampulla, *psc* posterior semicircular canal, *rst* recessus scala tympani, *ve* vestibule

of *Carrollia* (Maddin et al. 2011), which has a more globose shape. Even in scenarios where brachystelechids like *Carrollia* are considered crown-amniotes, they are still retrieved as more basal than captorhinids (Pardo et al. 2017), and it remains unknown whether the short lagena and common crus of *Labidosaurus* may be apomorphically related to other variables like ecology, rather than showing the plesiomorphic condition of reptiles.

Another important addition has been the description of the skull of the drepanosaur *Avicranium* (Pritchard and Nesbitt 2017). Unfortunately, the braincase is not well-preserved and a cast of the inner ear has not been provided, but the anatomy of the stapes and of the quadrate suggest similar hearing abilities to other basal diapsids. The lack of an otic conch and the stout stapes with an enlarged footplate filling most, if not all, of the fenestra ovalis indicate intra-bone conduction of low-frequency sounds played an important role in hearing, conforming to the general evolutionary trends of early diapsids (Sobral et al. 2016b). What does not conform is the anatomy of the semicircular canals. Although a digital cast of the semicircular canals is missing, the external anatomy of some braincase bones can provide important information on the likely morphology of the inner ear. Since the anterior semicircular canal extends partially in the prootic, the outline of the dorsal portion of the

alar process provides an approximation of the radius of curvature of this element, just as the crista prootica can provide information on the lateral canal (Evans 2008; Sobral and Müller 2019). The general outline of the prootic in *Avicranium* indicates that the anterior semicircular canal was likely elongate whereas the lateral canal was short. It would differ to what has been described for *Youngina* (Gardner et al. 2010), but it would correspond to the proposed highly-specialised arboreal lifestyle of *Avicranium* (Pritchard and Nesbitt 2017). The canalicular portion of the inner ear of *Avicranium* is thus likely not representative of a general early diapsid trend.

The most recent addition to the diapsid stem is the choristodere *Champsosaurus* (Dudgeon et al. 2020a, b). The cochlea is quite short and the semicircular canals are short and thick, all being roughly similar in length. The semicircular canals suggest limited sensitivity to angular movement (Dudgeon et al. 2020a, but see Bronzati et al. 2021) and the short cochlea indicates preferential detection of low-frequency sounds, matching the morphotype of other aquatic diapsids (Dudgeon et al. 2020a). Other anatomical features that corroborate this hypothesis are the lack of an otic conch on the posterior region of the skull and the potential lack of the stapes. A stapes is so far unknown in the group – except for a possible fragment in the basal choristodere *Coelurodraco* (Matsumoto et al. 2019). On the other hand, choristoderes have a unique bone in the suspensorium called the neomorph, which contacts the otic capsule medially and the quadrate laterally. It has been suggested that the neomorph may be homologous to the stapes (Dudgeon et al. 2020b). The neomorph would thus have a plesiomorphic, structural role, similar to stapes of stem-amniotes and early tetrapodomorphs (Clack et al. 2016). The inner ear of *Champsosaurus* is probably also not representative of a general trend for diapsids, and must be considered in a “return to water” scenario. However, without information on early-diverging choristoderes, the details of this transition are currently obscure.

As demonstrated by the above examples, much of the early evolutionary history of hearing and balance in reptiles remains unknown. The anatomical analysis conducted by Sobral et al. (2016b) was far from extensive, although the new information on the inner ear of *Labidosaurus* supports the suggested hypothesis. *Avicranium* and *Champsosaurus* are much needed additions to the diversity of the early reptilian ear that open new roads for exploration of niche specialization. However, detailed morphological analyses of the ear are almost entirely missing for early reptiles, implying a lack of tools to understand important transitions in their evolutionary history, such as terrestrialization and the appearance of tympanic hearing. Classical approaches on tympanic hearing basically consider only the morphology of the stapes and the presence of an otic notch. However, this latter osteological correlate is based entirely on the anatomy of lizards and it remains to be established whether the same applies to other reptile groups. It is possible that the tympanum appeared independently the archosaur and lepidosaur lineages (Sobral et al. 2016a), and that taxa that lack an otic notch could nonetheless support a tympanic membrane (Sobral and Müller 2019). A very important study for understanding this relationship between post-temporal anatomy and the tympanic membrane has been made by Montefeltro et al. (2016), in which homologies are proposed for several external ear structures

in the crocodylian line of archosaurs, but similar homology tests for stem-groups remain to be made.

Olfaction

Detailed analyses of the nasal cavity of early reptiles are also mostly lacking from the literature, the exception being some acleistorhinid parareptiles, *Captorhinus*, and some accounts for choritoderes, including the recently published endocast of *Champsosaurus*. The nasal capsules of the parareptiles *Delorhynchus* (Reisz et al. 2014) and *Karutia* (Cisneros et al. 2021) are prominent, suggesting at least moderate olfactory capabilities. The same is true for *Captorhinus* (Heaton 1979), which shows a rather elongate nasal chamber on the dorsal surface of the vomer. The premaxilla and the vomer are separated by a short distance, which indicates the presence of a small vomeronasal organ.

A virtual endocast is only available for the choristodere *Champsosaurus* (Dudgeon et al. 2020b), although *Ikechosaurus* has also been CT-scanned (Lu et al. 1999). The olfactory chambers are well-developed, implying a high level of olfactory acuity. While olfaction in totally aquatic taxa is typically poorly developed (Pihlström 2008), semi-aquatic groups may still rely on airborne odors for mating and other types of intraspecific communication (Cummins and Bowie 2012). The nasal passages are smooth and thus devoid of turbinates (Dudgeon et al. 2020b), but they might have been present in *Ikechosaurus* (Lu et al. 1999).

2.5 Outstanding Questions and Perspectives

There are a number of obstacles still to be overcome in order for us to better understand the early evolution of sensory perception and brain anatomy in reptiles. The poor fossil record of stem-diapsids hampers our understanding of the phylogenetic relationships of major groups and makes it challenging to approach evolutionary questions from a quantitative perspective. This knowledge gap is even present in non-diapsid groups with a more complete record, namely parareptiles and captorhinids. Recent reassessments on the phylogenetic relationships of early reptiles can partially fill in those gaps, but the lack of understanding on brain anatomy and sensory perception has yet to be addressed as no extensive studies on the paleoneurology of these groups have been published. Likewise, old evolutionary conceptions are still present in many comparative studies. The general idea that the brains of present-day reptiles represent the plesiomorphic condition for mammals still persists (Güntürkün et al. 2020), even though these groups diverged from each other approximately 320 million years ago – just as the idea that the brain of extant reptiles are good representations of the brain of early reptiles. How the reptilian brain originated, which evolutionary paths it took, and what the implications of these

trajectories were for the evolution of major extant and extinct groups remain to be assessed.

It is not only a general trend that is unavailable for early reptiles, but we also do not understand particular processes in specific groups. Parareptiles for instance were important faunal components of the Permian. Some (pareiasaurs) achieved large body sizes and were among the first reptiles specialized for an herbivorous diet (Boitsova et al. 2019). If their placement within Diapsida is not confirmed, then they developed several convergent features with diapsids, including sensory specializations for the terrestrial environment like impedance-matching hearing (Sobral et al. 2016b). Still, we know little about how these processes took place. It would be interesting, for instance, to compare the brain anatomy of derived parareptiles with that of later diapsids to evaluate if convergences also include major brain patterns. Once we understand how the reptilian brain and sensory mechanisms appeared, we will more fully comprehend major transitions that enabled the flourishing of the current reptile diversity.

2.6 Conclusions

The brain of early reptiles is virtually unknown, despite the relatively good record of braincase material in several groups. Early accounts considered parts of the brain like the pineal organ and the hypophysis, and the general brain cavity shape (Boonstra 1934; Edinger 1955; Watson 1914, 1916), but they did not include analyses of particular brain regions, like the optic lobe or cerebrum, and rarely considered the data in a broader evolutionary context. Likewise, recent approaches remain few in number and are either superficial or focused on serving as a comparative basis for understanding other, usually later-diverging groups (Fabbri et al. 2017; Müller et al. 2011). The addition of the drepanosaurid *Avicranium* (Pritchard and Nesbitt 2017) and the choristodere *Champsosaurus* (Dudgeon et al. 2020a) to the literature, although important, cannot be considered representative of a general reptile trend. Choristoderes were aquatic or semi-aquatic animals with an unusually flattened skull, whereas drepanosaurids were, at least in part, arboreal animals, and the endocasts of these taxa seem to be apomorphically related to their inferred specialized habits.

CT scanning has been widely used to assess the brain anatomy in some extinct tetrapod clades, but such studies are still largely missing for early reptiles. However, brain evolution and sensory perception can also be inferred from direct anatomical analyses of fossils, but so far only hearing has been relatively more explored in this manner. The identification of osteological correlates can provide interesting starting points such as the suture between parietals and frontals, which indicate the limit between fore- and mid-brain (Fabbri et al. 2017). The data on the paleoneurology of early reptiles, albeit scarce, seems to indicate a stepwise adaptation to the terrestrial environment, but subsequent changes, like the transitions back to aquatic environments, remain obscure. Without proper information on early diverging reptile

clades, not only is our understanding of the paleobiology of these groups limited, but it also hampers our comprehension on the flourishing of the reptile diversity.

Acknowledgments I would like to thank Stig Walsh (National Museums Scotland, UK), Amy Balanoff (Johns Hopkins University, USA), Felipe Pinheiro (Universidade Federal do Pampa, Brazil) and Lucas Camargos (Staatliches Museum für Naturkunde Stuttgart, Germany) for comments on early versions of the manuscript. I also thank Martin Ezcurra (Museo Argentino de Ciencias Naturales “Bernardino Rivadavia”, Argentina), Hans-Dieter Sues (Smithsonian National Museums, USA), and Juan Cisneros (Universidade Federal do Piauí, Brazil) for their constructive reviews.

References

- Balanoff AM, Bever GS, Norell MA (2014) Reconsidering the avian nature of the oviraptorosaur brain (Dinosauria: Theropoda). *PLoS One* 9:e113559
- Bennet SC (2001) The osteology and functional morphology of the late cretaceous pterosaur *Pteranodon*. *Palaeontogr Abt A* 260:1–112
- Beyrand V, Voeten DFAE, Bureš S et al (2019) Multiphase progenetic development shaped the brain of flying archosaurs. *Sci Rep* 9:10807
- Boitsova EA, Skutschas PP, Sennikov AG et al (2019) Bone histology of two pareiasaurs from Russia (*Deltavjatia rossica* and *Scutosaurus karpinskii*) with implications for pareiasaurian palaeobiology. *Biol J Linn Soc* 128:289–310
- Boonstra LD (1934) Pareiasaurian studies, part IX: the cranial osteology. *Ann S Afr Mus* 31:1–38
- Bronzati M, Benson RBJ, Evers SW et al (2021) Deep evolutionary diversification of semicircular canals in archosaurs. *Curr Biol* 31:2520–2529. <https://doi.org/10.1016/j.cub.2021.03.086>
- Campione NE, Evans DC (2012) A universal scaling relationship between body mass and proximal limb bone dimensions in quadrupedal terrestrial tetrapods. *BMC Biol* 10:60. <https://doi.org/10.1186/1741-7007-10-60>
- Canoville A, Laurin M (2010) Evolution of humeral microanatomy and lifestyle in amniotes, and some comments on palaeobiological inferences. *Biol J Linn Soc* 100:384–406
- Carroll RL, Lindsay W (1985) Cranial anatomy of the primitive reptile *Procolophon*. *Can J Earth Sci* 22:1571–1587
- Chen X-H, Motani R, Cheng L et al (2014) The enigmatic marine reptile *Nanchangosaurus* from the Lower Triassic of Hubei, China and the phylogenetic affinities of Hupehsuchia. *PLoS One* 9:e102361
- Cisneros JC, Kammerer CF, Angielczyk KD et al (2021) A new reptile from the lower Permian of Brazil (*Karutia fortunate* gen. et sp. nov.) and the interrelationships of Parareptilia. *J Syst Palaeontol*. <https://doi.org/10.1080/14772019.2020.1863487>
- Clack JA, Fay RR, Popper AN (2016) Evolution of the vertebrate ear – evidence from the fossil record, Springer handbook of auditory research, vol 59. Springer, Cham
- Cummins SF, Bowie JH (2012) Pheromones, attractants and other chemical cues of aquatic organisms and amphibians. *Nat Prod Rep* 29:642–658
- Dudgeon TW, Maddin HC, Evans DC et al (2020a) Computed tomography analysis of the cranium of *Champsosaurus lindoei* and implications for the choristoderan neomorphic ossification. *J Anat* 236:630–659
- Dudgeon TW, Maddin HC, Evans DC et al (2020b) The internal cranial anatomy of *Champsosaurus* (Choristodera: Champsosauridae): implications for neurosensory function. *Sci Rep* 10:7122
- Edinger T (1955) The size of parietal foramen and organ in reptiles. A rectification. *Bull Mus Comp Zool* 114:1–34
- Evans SE (1982) The gliding reptiles of the Upper Permian. *Zool J Linnean Soc* 76:97–123

- Evans SE (1986) The braincase of *Prolacerta broomi* (Reptilia, Triassic). *Neues Jahrb Geol Palaontol Abh* 173:181–200
- Evans SE (1987) The braincase of *Youngina capensis* (Reptilia: Diapsida; Permian). *Neues Jahrb Geol Palaontol Monatsh* 1987:193–203
- Evans SE (2008) The skull of lizards and tuatara. In: Gans C, Gaunt AS, Adler K (eds) *Biology of the reptilia: the skull of Lepidosauria*, volume 20, morphology H. Society for the Study of Amphibians and Reptiles, London, pp 1–347
- Ezcurra MD (2016) The phylogenetic relationships of basal archosauromorphs, with an emphasis on the systematics of proterosuchian archosauriforms. *Peer J* 4:e1778
- Fabbri M, Koch NM, Pritchard AC et al (2017) The skull roof tracks the brain during the evolution and development of reptiles including birds. *Nat Ecol Evol* 1:1543–1550
- Ford PD, Benson RBJ (2020) The phylogeny of early amniotes and the affinities of Parareptilia and Varanopidae. *Nature Ecology & Evolution* 4:57–65. <https://doi.org/10.1038/s41559-019-1047-3>
- Gardner NM, Holliday CM, O’Keefe FR (2010) The braincase of *Youngina capensis* (Reptilia, Diapsida): new insights from high-resolution CT scanning of the holotype. *Palaeontol Electron* 13:19A
- Gow CE (1972) The osteology and relationships of the Millerettidae (Reptilia: Cotylosauria). *J Zool* 167:219–264
- Güntürkün O, Stacho M, Ströckens F (2020) The brains of reptiles and birds. In: Kaas JH (ed) *Evolutionary neuroscience*, 2nd edn. Academic Press, London, pp 159–212
- Hamley T, Cisneros JC, Damiani R (2021) A procolophonid reptile from the Lower Triassic of Australia. *Zool J Linnean Soc* 192:554–609
- Heaton MJ (1979) Cranial anatomy of primitive captorhinid reptiles from the Late Pennsylvanian and Early Permian Oklahoma and Texas. *Oklahoma Geol Surv Bull* 127:1–81
- Hopson JA (1979) Paleoneurology. In: Gans C, Northcutt R, Ulinski P (eds) *Biology of the reptilia*, vol 9. Society for the Study of Amphibians and Reptiles, London, pp 39–146
- Hu K, King JL, Romick CA et al (2020) Ontogenetic endocranial shape change in alligators and ostriches and implications for the development of the non-avian dinosaur endocranium. *Anat Rec* 304:1759–1775
- Jerison HJ (1973) *Evolution of the brain and intelligence*. Academic, London
- Klembara J, Hain M, Ruta M et al (2020a) Inner ear morphology of diadectomorphs and seymouriamorphs (Tetrapoda) uncovered by high-resolution X-ray microcomputed tomography, and the origin of the amniote crown group. *Palaeontology* 63:131–154
- Klembara J, Hain M, Čerňanský A et al (2020b) Anatomy of the neural endocranium, parasphenoid and stapes of *Diadectes absitus* (Diadectomorpha) from the Early Permian of Germany based on the high-resolution X-ray microcomputed tomography. *Anat Rec* 303:2977–2999
- Laurin M, Piñero GH (2017) A reassessment of the taxonomic position of mesosaurs, and a surprising phylogeny of early amniotes. *Front Earth Sci* 5(88):1–13
- Laurin M, Reisz RR (1995) A reevaluation of early amniote phylogeny. *Zool J Linnean Soc* 113:165–223
- Li C, Jiang D-Y, Cheng L (2014) A new species of *Largocephalosaurus* (Diapsida: Saurosphargidae), with implications for the morphological diversity and phylogeny of the group. *Geol Mag* 151:100–120
- Lu J, Zhu Q, Cheng X et al (1999) Computed tomography (CT) of nasal cavity of *Ikechosaurus sunailinae* (Reptilia: Choristodera). *Chin Sci Bull* 44:2277–2281
- Lucas SG, Harris SK, Spielmann JA et al (2005) Early Permian vertebrate assemblage and its biostratigraphic significance, 56th field conference guidebook. New Mexico Geological Society, Arroyo del Agua, pp 288–296
- MacDougall MJ, Winge A, Ponstein J, Jansen M, Reisz RR, Fröbisch J (2019) New information on the early Permian lanthanosuchoid *_Feeserpeton oklahomensis_* based on computed tomography. *PeerJ*:e7753 <https://doi.org/10.7717/peerj.7753>

- Maddin HC, Olori JC, Anderson JS (2011) A redescription of *Carrolla craddocki* (Lepospondyli: Brachystelechidae) based on high-resolution CT, and the impacts of miniaturization and fossoriality on morphology. *J Morphol* 272:722–743
- Matsumoto R, Dong L, Wang Y et al (2019) The first record of a nearly complete choristodere (Reptilia: Diapsida) from the Upper Jurassic of Hebei Province, People's Republic of China. *J Syst Palaeontol* 17:1031–1048
- Miadema F, Spiekman SNF, Fernandez V, Reumer JWF, Scheyer TM (2020) cranial morphology of the tanystropheid *Macrocnemus bassanii* unveiled using synchrotron microtomography. *Sci Rep* 10,12412. <https://doi.org/10.1038/s41598-020-68912-4>
- Montefeltro FC, Andrade DV, Larsson HCE (2016) The evolution of the meatal chamber in crocodyliforms. *Journal of Anatomy* 228(5):838–863 <https://doi.org/10.1111/joa.12439>
- Müller J, Tsuji LA (2007) Impedance-matching hearing in Paleozoic reptiles: evidence of advanced sensory perception at an early stage of amniote evolution. *PLoS One* 2:e889
- Müller J, Sterli J, Anquetin J (2011) Carotid circulation in amniotes and its implications for turtle relationships. *Neues Jahrb Geol Palaontol Abh* 261:289–297
- Müller J, Bickelmann C, Sobral G (2018) The evolution and fossil history of sensory perception in amniote vertebrates. *Annu Rev Earth Planet Sci* 46:495–519
- Nopcsa F (1923) Die Familien der Reptilien. In: Soergel W (ed) Fortschritte der Geologie und Paläontologie, Heft 2. Verlag von Gebrüder Borntraeger, Berlin
- Pardo JD, Szostakiwskyj M, Ahlberg PE et al (2017) Hidden morphological diversity among early tetrapods. *Nature* 546:642–645
- Pihlström H (2008) Comparative anatomy and physiology of chemical senses in aquatic mammals. In: JGM T, Nummela S (eds) Sensory evolution on the threshold: adaptations in secondarily aquatic vertebrates. University of California Press, Berkeley, pp 95–109
- Pritchard AC, Nesbitt SJ (2017) A bird-like skull in a Triassic diapsid reptile increases heterogeneity of the morphological and phylogenetic radiation of Diapsida. *R Soc Open Sci* 4:170499. <https://doi.org/10.1098/rsos.170499>
- Pritchard AC, Sues H-D, Scott D et al (2021) Osteology, relationships and functional morphology of *Weigeltisaurus jaekeli* (Diapsida, Weigeltisauridae) based on a complete skeleton from the Upper Permian Kupferschiefer of Germany. *Peer J* 9:e11413. <https://doi.org/10.7717/peerj.11413>
- Reich HW (1927) Studie über die Lage von Epiphyse und Hypophyse. *Z gesamt Neurol Psychiatr* 109:1–14
- Reisz RR, Macdougall MJ, Modesto SP (2014) A new species of the parareptile genus *Delorhynchus*, based on articulated skeletal remains from Richards spur, lower Permian of Oklahoma. *J Vert Paleontol* 34:1033–1043
- Robinson PL (1962) Gliding lizards from the upper Keuper of Great Britain. *Proc Geol Soc Lond* 1601:137–146
- Scheyer TM, Neenan JM, Bogodan T et al (2017) A new, exceptionally preserved juvenile specimen of *Eusauropsphargis dalsassoi* (Diapsida) and implications for Mesozoic marine diapsid phylogeny. *Sci Rep* 7:4406
- Scheyer TM, Spiekman SNF, Sues H-D et al (2020) Colobops: a juvenile rhynchocephalian reptile (Lepidosauromorpha), not a diminutive archosauromorph with an unusually strong bite. *R Soc Open Sci* 7:192179
- Schwab JA, Young MT, Neenan JM et al (2020) Inner ear sensory system changes as extinct crocodylomorphs transitioned from land to water. *PNAS* 117:10422–10428
- Shimizu T, Shinozuka K, Uysal AK et al (2017) The origins of the bird brain: multiple pulses of cerebral expansion in evolution. In: Watanabe S, Hofman M, Shimizu T (eds) Evolution of the brain, cognition, and emotion in vertebrates, Brain science. Springer, Tokyo, pp 35–57
- Simões TR, Caldwell MW, Talandá M et al (2018) The origin of squamates revealed by a Middle Triassic lizard from the Italian Alps. *Nature* 557:706–709
- Sobral G, Müller J (2019) The braincase of *Mesosuchus browni* (Reptilia, Archosauromorpha) with information on the inner ear and description of a pneumatic sinus. *Peer J* 7:e6798

- Sobral G, Hipsley CA, Müller J (2012) Braincase redescription of *Dysalotosaurus lettowvorbecki* (Dinosauria, Ornithomimidae) based on computed tomography. *J Vert Paleontol* 32:1090–1102
- Sobral G, Sookias RB, Bhullar B-AS et al (2016a) New information on the braincase and inner ear of *Euparkeria capensis* Broom: implications for diapsid and archosaur evolution. *R Soc Open Sci* 3:160072
- Sobral G, Reisz R, Neenan JM et al (2016b) Basal reptilians, marine diapsids, and turtles: the flowering of reptile diversity. In: Clack JA, Fay RR, Popper AN (eds) *Evolution of the vertebrate ear – evidence from the fossil record*, Springer handbook of auditory research, vol 59, pp 207–243
- Spencer PS (2000) The braincase structure of *Leptopleuron lacertinum* Owen (Parareptilia: Procolophonidae). *J Vert Paleontol* 20:21–30
- Spiekman SNF, Neenan JM, Fraser NC, Fernandez V, Rieppel O, Nosotti S, Scheyer TM (2020) The cranial morphology of *Tanystropheus hydroides* (Tanystropheidae, Archosauromorpha) as revealed by synchrotron microtomography. *PeerJ* 8:e10299 <https://doi.org/10.7717/peerj.10299>
- Sues H-D (2019) *The rise of reptiles: 320 million years of evolution*. Johns Hopkins University Press, Baltimore
- Vaughn PP (1955) The Permian reptile *Araeoscelis* restudied. *Bull Mus Comp Zool* 113:305–467
- Voogd J, Wylie DRW (2004) Functional and anatomical organization of floccular zones: a preserved feature in vertebrates. *J Comp Neurol* 470:107–112
- Walker AD (1990) A revision of *Sphenosuchus acutus* Houghton, a crocodylomorph reptile from the Elliot Formation (late Triassic or early Jurassic) of South Africa. *Philos Trans R Soc B* 330:1–120
- Watanabe A, Gignac PM, Balanoff AM et al (2019) Are endocasts good proxies for brain size and shape in archosaurs throughout ontogeny? *J Anat* 234:291–305
- Watson DMS (1914) On the skull of a pareiasaurian reptile, and on the relationship of that type. *J Zool* 1914:155–180
- Watson DMS (1916) On the structure of the brain-case in certain lower Permian tetrapods. *Bull Am Mus Nat Hist* 35:611–636
- Witmer LM, Ridgely RC (2009) New insights into the brain, braincase, and ear region of tyrannosaurs (Dinosauria, Theropoda), with implications for sensory organization and behavior. *Anat Rec* 292:1266–1296
- Witmer LM, Chatterjee S, Franzosa J et al (2003) Neuroanatomy of flying reptiles and implications for flight, posture and behavior. *Nature* 425:950–953

Chapter 3

The Paleoneurology of Ichthyopterygia and Sauropterygia: Diverse Endocranial Anatomies of Secondarily Aquatic Diapsids



Rémi Allemand, Benjamin C. Moon, and Dennis F. A. E. Voeten

Institutional Abbreviations

BRLSI	Bath Royal Literary and Scientific Institute, Bath, UK
D	Musée de Rhinopolis, Gannat, France
LEICT	New Walk Museum, Leicester, UK
MB.R	Museum für Paläontologie der Alexander von Humboldt-Universität, Berlin, Germany
MNHN	Musée National d'Histoire Naturelle, Paris, France
MUPA-ATZ	El Atance collection, Museo de Paleontología de Castilla-La Mancha, Cuenca, Spain
NHMUK	Natural History Museum, London, UK
NME	Naturkundemuseum Erfurt, Erfurt, Germany
SGU	Saratov State University, Saratov, Russia
SM	Senckenberg Museum, Frankfurt, Germany
SMNS	Staatliches Museum für Naturkunde, Stuttgart, Germany
SMUSMP	Shuler Museum of Paleontology, Southern Methodist University, Dallas, USA
TW	Museum TwentseWelle Enschede, The Netherlands

R. Allemand (✉)

Department of Anthropology, University of Toronto Scarborough, Toronto, ON, Canada
e-mail: remi.allemand@utoronto.ca

B. C. Moon

Bristol Palaeobiology Group, School of Earth Sciences, University of Bristol, Bristol, UK
e-mail: ben@bcmoon.uk

Dennis F. A. E. Voeten

Department of Organismal Biology, Subdepartment of Evolution and Development, Uppsala University, Uppsala, Sweden

European Synchrotron Radiation Facility, Grenoble cedex 09, France

Naturalis Biodiversity Center, CR, Leiden, The Netherlands

e-mail: dennis.voeten01@upol.cz

UMO Urwelt-Museum, Bayreuth, Germany
 UN-DG Universidad Nacional de Colombia, Departamento de Geología,
 Bogotá, Colombia

3.1 Systematics and Phylogenetic Context

Ichthyopterygia and Sauropterygia are the two dominant clades of secondarily aquatic marine reptiles that diversified in the aftermath of the Permian–Triassic mass extinction approximately 252 million years ago (Figs. 3.1 and 3.2). Although both clades are considered monophyletic (e.g. Motani 1999a; Maisch and Matzke 2000a), their systematic positions among Neodiapsida remain debated (e.g. Scheyer et al. 2017; Simões et al. 2022). The paucity of known intermediate forms and their generally derived morphologies have inspired numerous hypotheses on their origins and affinities (e.g. Romer 1968; Sues 1987; de Braga and Rieppel 1997; Motani et al. 1998; Rieppel and Reisz 1999; Maisch and Matzke 2000b; Müller 2003; Maisch 2010; Neenan et al. 2013; Chen et al. 2014; Schoch and Sues 2015; Scheyer et al. 2017). Both Ichthyopterygia and Sauropterygia seem to first appear in the Early Triassic, with body plans of their earliest known representatives already adapted to aquatic life to variable degrees (Motani 2005a, 2009). The two lineages thrived throughout most of the Mesozoic and only went extinct at the beginning

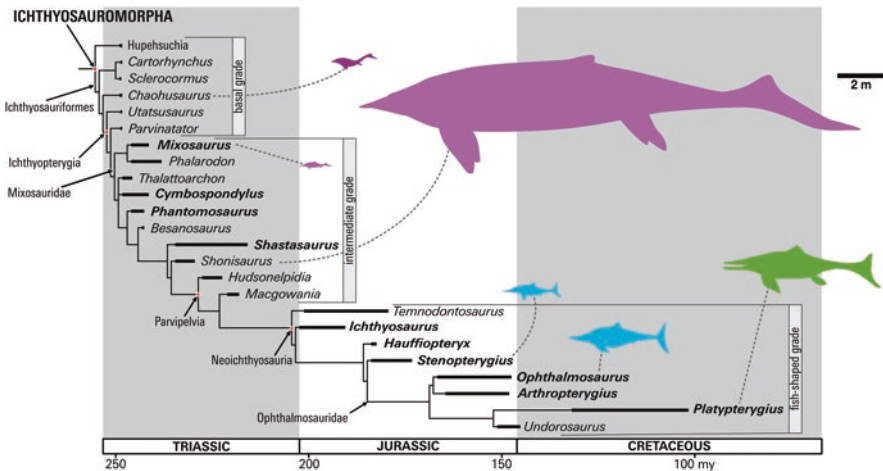


Fig. 3.1 Simplified phylogeny of Ichthyosauromorpha showing the positions of major named clades and examples, and occurrence ranges of the best-known taxa. Topology based on Moon (2019) and Zverkov and Jacobs (2020). Taxa discussed in the main text are indicated in boldface. Silhouettes, taken from PhyloPic and used under the CC-BY 3.0 license, are at approximate scale relative to each other (Credits: *Grippia longirostris* [D. Bogdanov, vectorized by M. Keesey], *Mixosaurus cornalianus* [G. Monger], *Ophthalmosaurus icenicus* [G. Monger], *Platypterygius sachicarum* [Zimices], *Shonisaurus sikkaniensis* [G. Monger], and *Stenopterygius quadriscissus* [G. Monger]; <https://creativecommons.org/licenses/by/3.0/>). Silhouette colors: Triassic = purple, Jurassic = blue, Cretaceous = green

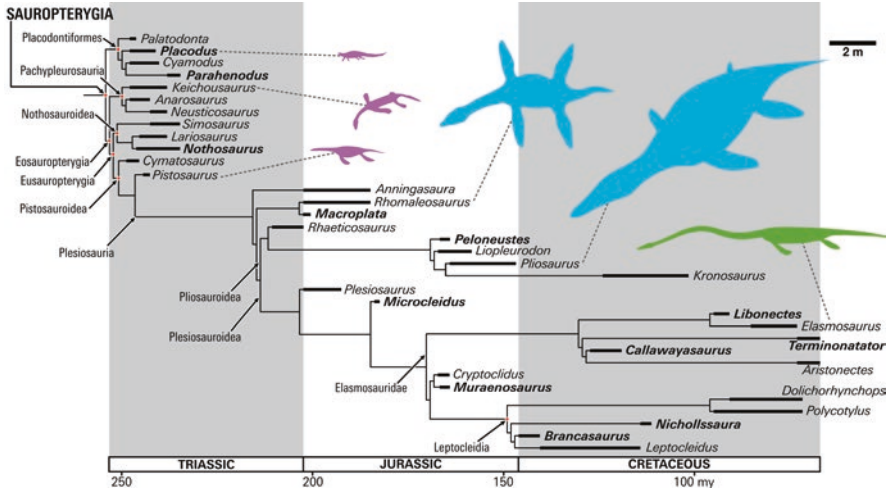


Fig. 3.2 Simplified phylogeny of Sauropterygia showing the positions of major named clades, and examples and occurrence ranges of key taxa. Topology based on Liu et al. (2011, 2014), Benson et al. (2013), and Wintrich et al. (2017). Taxa discussed in the main text are indicated in boldface. Silhouettes, taken from PhyloPic and used under the CC-BY 3.0 license, are at approximate scale relative to each other (Credits: *Elamosaurus platyrurus* [E.D. Cope, vectorized by M. Keesey], *Keichousaurus hui* [G. Monger], *Peloneustes philarchus* [N. Tamura, vectorized by M. Keesey], *Pistosaurus longaeus* [N. Tamura, vectorized by M. Keesey], *Placodus gigas* [N. Tamura, vectorized by M. Keesey], and *Rhomaleosaurus cramptoni* [G. Monger]; <https://creativecommons.org/licenses/by/3.0/>). Silhouette colors: Triassic = purple, Jurassic = blue, Cretaceous = green

(Ichthyopterygia) or the end (Sauropterygia) of the Late Cretaceous (Bardet et al. 2014; Motani et al. 2014; Fischer et al. 2016).

3.1.1 Ichthyopterygia Owen, 1860

Ichthyopterygia represent a diverse and well-studied group of predatory reptiles that feature among the most substantial aquatic adaptations of any marine tetrapod clade, including a streamlined body shape, reduced hydrodynamic limbs, tail fluke, and viviparity (Motani 2005a, 2009; Moon 2019; Moon and Stubbs 2020). Ichthyopterygia are placed within the more inclusive clade Ichthyosauriformes, all members of which are generally referred to as “ichthyosaurs” (Motani 1999a; Ji et al. 2016; Moon 2019). Ichthyosauriformes are the sister clade to Hupehsuchia within Ichthyosauromorpha (Fig. 3.1; Chen et al. 2014; Motani et al. 2015a; Ji et al. 2016; Moon 2019). Although the broader relationships among ichthyosaurs are relatively well resolved, many interrelationships remain debated because the positions of some taxa are highly mobile across phylogenetic hypotheses, which produces topological instability and weak support at finer-scale resolutions (Motani 1999a; Sander 2000; Maisch and Matzke 2000a; Fröbisch et al. 2013; Ji et al. 2016; Moon 2019; Bindellini et al. 2021).

Ichthyosaurs are divided into three main evolutionary grades that form relatively distinct morphological, and potentially ecological, groups (Fig. 3.1; Motani 2005a; Moon and Stubbs 2020; Reeves et al. 2020). The basal grade of ichthyosaurs encompasses the most plesiomorphic ichthyosauriforms (Fig. 3.1; Moon 2019) that constitute a paraphyletic assemblage across a wide range of habitats along the northern coast of Pangea (i.e. China, Japan, and Canada; Motani 2005a; Bardet et al. 2014). While early ichthyosaurs already featured a caudal peak, homologous with the tail bend of later taxa, and somewhat paddle-like limbs, they also retained characters of ancestral terrestrial diapsids, such as a robust articulation of the pelvic girdle with the axial skeleton (Motani 2005a). These relatively small-bodied taxa (0.4–3 m; Motani et al. 1998, 2015a) were moderately adept swimmers using anguilliform locomotion to ambush prey in shallow waters (Massare 1987, 1994; Sander et al. 2011; Thorne et al. 2011; Motani et al. 2014; Dick and Maxwell 2015; Reeves et al. 2020) or in the pelagic realm (e.g. *Utatsusaurus*; Nakajima et al. 2014; Gutarra et al. 2019).

During the Middle and Late Triassic, ichthyosaurs gradually acquired more fish-like morphological attributes, including more strongly modified paddle-like limbs and a pronounced tail bend (McGowan and Motani 2003; Moon 2019). Intermediate-grade ichthyosaurs have a worldwide distribution across shallow-marine habitats and into the pelagic realm, and account for the early ichthyosaurian colonization of oceanic ecologies before their demise towards the end of the Late Triassic (Fig. 3.1; Motani 2009; Bardet et al. 2014; Moon 2019; Moon and Stubbs 2020). Intermediate-grade ichthyosaurs span an extreme size range from the small durophagous Mixosauridae (0.5–2 m in body length; e.g. Jiang et al. 2008) to the colossal apex predators representing the largest marine reptiles to have ever evolved (>15 m; e.g. *Shonisaurus*; Nicholls and Manabe 2004).

During the Late Triassic, a third grade of distinctly “fish-shaped” ichthyosaurs emerged that would become the only group to survive into the Jurassic and up to the extinction of ichthyosaurs at the Cenomanian–Turonian boundary (Fig. 3.1; Motani 2009; Bardet et al. 2014). Although the exact phylogenetic context for the appearance of the fish-shaped body plan among ichthyosaurs remains controversial (Moon 2019), this grade is almost entirely represented by the large clade Neoichthyosauria (Motani 2005a; Moon 2019). Neoichthyosauria are characterized by a thunniform body shape, a demarcated caudal fin, and a reduced pelvis relative to more basal forms (Motani 2005a). This body plan was optimized for open water cruising and reflects a shift to oscillatory swimming using a tail fluke (Motani et al. 2014; Gutarra et al. 2019). Neoichthyosaurians were likely fast-moving and active marine predators capable of maintaining elevated body temperatures, rendering them well adapted to life in the pelagic realm (Motani et al. 1999; Motani 2002, 2010; Bernard et al. 2010; Dick and Maxwell 2015; Reeves et al. 2020).

3.1.2 *Sauropterygia* Owen, 1860

Sauropterygia constitute a highly diversified and geographically widespread group that acquired various adaptations to aquatic life in diverse habitats and ecological niches (Fig. 3.2; Rieppel 2000; Bardet et al. 2014). Although the exact relationships

among and within groups are still debated (e.g. Neenan et al. 2013; de Miguel Chaves et al. 2018a; Li and Liu 2020), Sauropterygia are traditionally separated into Placodontia and Eosauropterygia (Fig. 3.2; e.g. Rieppel 2000). The latter clade represents a diverse assemblage that includes pachypleurosaurs, nothosaurs, pistosaurs, and plesiosaurs (e.g. Rieppel 2000; O’Keefe 2002; Benson et al. 2012; Neenan et al. 2015; Wintrich et al. 2017).

Placodontia (or placodonts) are basal medium-sized (approximately 0.6–2 m; Motani 2009) sauropterygians that appeared at the beginning of the Middle Triassic across both the Western and the Eastern Tethyan realm and went extinct at the end of the Late Triassic (Scheyer 2007; Bardet et al. 2014; Neenan et al. 2019a). They were short-necked animals with short and robust skulls that inhabited shallow aquatic environments (Motani 2009; Klein et al. 2015a) and show variable degrees of durophagy (e.g. Rieppel 2002; Motani 2009; Scheyer et al. 2012; de Miguel Chaves et al. 2018b; Neenan et al. 2019a; Pommery et al. 2021). Placodontia are traditionally divided into two presumably paraphyletic groups: Placodontoidea and Cyamodontoidea, which can be discerned through the respective absence or presence of extensive body armour (e.g. Rieppel 2000, 2002; Motani 2009; Scheyer 2010; Neenan et al. 2019a; Wang et al. 2019a, b). All placodonts had proportionately short and unmodified limbs and were interpreted as slow swimmers also capable of foraging by “bottom walking” (Scheyer et al. 2012; Renesto and Dalla Vecchia 2018; Reeves et al. 2020). Placodonts relied on either undulations of the tail (placodontoids) or alternating strokes of the robust hind limbs (cyamodontoids) as their primary means of propulsion (Renesto and Tintori 1995; Renesto and Dalla Vecchia 2018).

Pachypleurosaurs were relatively small-bodied (~50–120 cm long) eosauropterygians that diversified along the Tethyan shores in epicontinental seas and intraplateform basins during the Middle Triassic (Rieppel 2000; Klein 2009; Bardet et al. 2014). Although Pachypleurosauria were traditionally recovered as the monophyletic sister clade to Eosauropterygia (Fig. 3.2; e.g. Rieppel 2000; Liu et al. 2011), the exact relationships between these groups are still discussed (e.g. Neenan et al. 2013; de Miguel Chaves et al. 2018a; Li and Liu 2020). Recent analyses have proposed that pachypleurosaurs constitute a paraphyletic evolutionary grade (e.g. Ma et al. 2015; Shang et al. 2017; Klein and Sander 2019). Pachypleurosaurs shared a lizard-like appearance with a moderately elongate neck, a proportionally small skull, loose attachment of the pectoral and pelvic girdles to the vertebral spine, and a long tail (Rieppel 2000; Renesto and Dalla Vecchia 2018). They are interpreted as anguilliform swimmers with poor diving capabilities that were confined to coastal and shallow marine environments (Rieppel 1989; Čerňanský et al. 2018). Most of them likely predated upon small invertebrates (e.g. arthropods; Čerňanský et al. 2018), although some of them may have preyed on small-shelled mollusks (Houssaye 2009; Klein 2009, 2012).

Nothosauroida (Fig. 3.2) include some of the largest predators to have roamed the Middle and Late Triassic seas and are known from across Europe, the Middle East, North America, and China (Rieppel 2000; Scheyer et al. 2019; Voeten et al.

2019a, b). Nothosauroida include the two clades Simosauridae and Nothosauria (Rieppel 2000; Voeten et al. 2019a) with debated ingroup relationships (e.g. Lin et al. 2017, 2021; Scheyer et al. 2019; Li and Liu 2020; Shang et al. 2020). Both clades exhibit elongate body shapes with dorsoventrally flattened skulls and long necks and tails (Voeten et al. 2019a). The medium-sized (3–4 m in length) simosaurids encompass littoral predators feeding on relatively hard prey (Rieppel 1994a, 2002; de Miguel Chaves et al. 2018a) as well as highly pachyostotic filter-feeders (de Miguel Chaves et al. 2018c). Nothosauria include small to large forms (<1 m to 5–7 m length; e.g. Klein and Albers 2009; Liu et al. 2014) that shared an active predatory lifestyle (Rieppel 2002; Voeten et al. 2019a). Simosaurids may have used anguilliform locomotion for foraging in shallow open water (Rieppel 1994a). Nothosaurians, however, were efficient paraxial swimmers (Klein and Griebeler 2016) that actively employed their robust forelimbs for propulsion (Carroll and Gaskill 1985; Rieppel 2000; Klein et al. 2016; Lin et al. 2017; Voeten et al. 2019a). All nothosaurians were adapted to free-swimming ecologies in near-shore and shallow marine habitats, although large-bodied taxa may have colonized more pelagic environments (Klein et al. 2016; Voeten et al. 2019a).

The best known Pistosauroida are its derived representatives: Plesiosauria – the only sauropterygians to survive the Triassic–Jurassic mass extinction (Fig. 3.2; e.g. Rieppel 2000; Benson et al. 2012). However, prior to this plesiosaurian radiation, pistosauroids developed a modest diversity of basal forms found in Europe, China, and the United States. They exhibit a mosaic of plesiomorphic (i.e. shared with basal sauropterygians) and derived (i.e. more plesiosaurian) features illustrating a gradual shift to offshore life during the Middle Triassic (e.g. Sato et al. 2010; Krahl et al. 2013; Ma et al. 2015). Among Sauropterygia, plesiosaurians exhibit the most advanced adaptations to marine life that culminated in a short and stiff trunk, a short tail, and four enlarged hydrofoil-shaped propulsive flippers optimized for swimming (e.g. Massare 1994; O’Keefe 2002; Motani 2009; Carpenter et al. 2010; Liu et al. 2015; Muscutt et al. 2017). Plesiosauria acquired a large range of body proportions (i.e. skull, neck, tail, and flipper length relative to the trunk length and width) that converged on the “plesiosauromorph” and “pliosauromorph” morphotypes. These blueprints evolved independently across different clades (e.g. Carpenter 1997, O’Keefe 2002; O’Keefe and Carrano 2005; Benson et al. 2012) and recorded diverse swimming performances, as well as the colonization of numerous habitats and feeding guilds (e.g. Massare 1987; Clarke and Etches 1992; Sato and Tanabe 1998; McHenry et al. 2005; Bardet et al. 2014; Campbell et al. 2021). The ecological flexibility of plesiosaurs, aided by active body temperature regulation (e.g. Rothschild and Storrs 2003; Bernard et al. 2010; O’Keefe and Chiappe 2011; Vincent et al. 2017), facilitated their successful global dispersal in the aquatic realm up to their disappearance at the end of the Cretaceous (Bardet et al. 2014; Reeves et al. 2020).

3.2 Historical Background

3.2.1 *The Record of Endocranial Morphologies and Other Paleoneurological Features in Ichthyopterygia and Sauropterygia*

Towards the end of the nineteenth century, Koken described the braincase of *Nothosaurus marchicus* and unlocked insight into the position and size of several cranial nerves and the “*foramen eustachii*” (Koken 1890, 1893). This work constitutes the earliest documentation of paleoneurological features in Sauropterygia. However, the first report of a sauropterygian cranial endocast was the first publication of Tilly Edinger (1921; Buchholtz and Seyfarth 1999, 2001). While preparing her doctoral dissertation on the palate of *Nothosaurus*, Edinger encountered and described a natural cranial endocast (i.e., internal cast of the braincase) in a skull of *Nothosaurus mirabilis*, which would prove foundational for her future career (Buchholtz and Seyfarth 1999, 2001). Several years later, Edinger described an artificial endocast and partially preserved natural cranial molds from two specimens of *Placodus gigas* (Edinger 1925) and illustrated an endocast of the plesiosaurian *Brancaosaurus brancai* modeled from isolated cranial elements (Edinger 1928; see Hopson 1979 and Sachs et al. 2016a). Since these pioneering efforts, research into sauropterygian paleoneurology largely stagnated and mainly resorted to indirect osteological inferences made from braincases (e.g. Haas 1981; Sues 1987; Rieppel 1989, 1994b, 2001; Evans 1999; Nosotti and Rieppel 2002; Sato 2003). Two notable exceptions are the descriptions of latex plesiosaurian endocasts of *Libonectes morgani* and *Aristonectes quiriquinensis* (Carpenter 1997; Otero et al. 2018).

The study of ichthyosaur paleoneurology only took off after the mid-twentieth century. Following early work by Sollas (1916), who employed serial sectioning that only allowed for the reconstruction of some internal cranial features in three-dimensionally-preserved specimens, the first latex endocast of *Ichthyosaurus* cf. *communis* was described by McGowan (1973). Kirton (1983) and Maisch (1997) provided indirect descriptions of the endocast in *Ophthalmosaurus* through imprints left by structures on the ventral surfaces of the skull roof.

The last two decades have seen a gradual revival of the field thanks to the advances in computed tomography (CT). These non-destructive tools allowed researchers to expand on indirect observations of endocranial anatomies through osteological studies of the internal braincase (e.g. Kear 2005; Sato et al. 2011; Zverkov et al. 2017; Lomax et al. 2019). This enabled the first digital endocasts of the pliosaurid *Acostasaurus pavachoquensis* (Gómez Pérez 2008; Gómez-Pérez and Noè 2017), the basal sauropterygian *Placodus gigas* (Neenan and Scheyer 2012), and a juvenile specimen of the ichthyosaur *Hauffiopteryx typicus* (Marek et al. 2015) to be reconstructed. More recently, Neenan et al. (2017) provided a comparative study of sauropterygian endosseous labyrinth morphologies, and digital endocasts were reconstructed for the placodont *Parahenodus atancensis* (de

Miguel Chaves et al. 2020), the nothosaur *Nothosaurus marchicus* (Voeten et al. 2018a), and three plesiosaurs: *Libonectes morgani* and an indeterminate Polycotylidae (Allemand et al. 2019); and *Alexandronectes zealandiensis* (O’Gorman et al. 2021). These recent contributions have substantially improved our understanding of sauropterygian paleoneurology.

3.2.2 Problematics

Ichthyopterygian and sauropterygian adaptations to the aquatic realm have been extensively studied through skeletal (e.g. O’Keefe 2002; Araújo et al. 2015a), microanatomical and histological (e.g. Krahl et al. 2013; Nakajima et al. 2014; Klein et al. 2016; Wintrich et al. 2017), and physiological features (i.e. diet, reproduction, and thermoregulation; e.g. Massare 1987, 1988; Maxwell and Caldwell 2003; Bernard et al. 2010; O’Keefe and Chiappe 2011; Motani et al. 2014; Klein et al. 2015b). However, little remains known about the neuroanatomical and neurosensory changes that accompanied these clades along their evolutionary history and during their successful colonization of aquatic environments. Modest inferences have been made from endocranial and osteological studies, but these have only considered the limited number of taxa for which exceptionally preserved remains are available.

The feasibility of endocranial explorations mainly hinges on the availability of suitable fossil crania. Although Ichthyopterygia and Sauropterygia are both represented by a rich fossil record including a wealth of well-preserved specimens (e.g. Druckenmiller and Russell 2008; Maisch 2008; O’Keefe 2008; Cleary et al. 2015; Lin et al. 2017; Flannery Sutherland et al. 2019; Wang et al. 2020), the associated skulls tend to be crushed or compressed. This often renders the braincase inaccessible and precludes extensive three-dimensional reconstruction. Advances in CT techniques importantly grant non-destructive access to internal structures, yet these methods have mainly facilitated visualization of isolated skull regions (e.g. Kear 2005; Sato et al. 2011; Zverkov et al. 2017; Lomax et al. 2019), partially because many specimens are too large to fit in conventional tomographic setups or achieve adequate X-ray penetration. A compounding problem stems from the ossification patterns of ichthyopterygian and sauropterygian skulls. As portions of these braincases remain cartilaginous, many endocranial boundaries are not preserved, permitting reliable reconstruction of only the dorsal endocast surface (e.g. Marek et al. 2015; Voeten et al. 2018a; Allemand et al. 2019).

Despite these challenges, our understanding of ichthyopterygian and sauropterygian paleoneurology has considerably improved over the past decade. Here, we provide an overview of the present knowledge by highlighting the endocranial modifications and sensory adaptations that accompanied their evolution and colonization of aquatic realms.

3.3 Overview of General and Comparative Anatomy

3.3.1 Characterization of Cranial Endocast Morphology

Ichthyopterygia

Endocasts To date, the study of ichthyosaur paleoneurology remains largely limited to Neoichthyosauria. The following description is based on the endocasts reconstructed for a juvenile specimen of *Hauffiopteryx typicus* (Fig. 3.3a, b, d; Marek et al. 2015) and an adult *Ichthyosaurus* cf. *communis* (Fig. 3.3c, e; McGowan 1973), as well as information provided by osteological investigations of the braincase in *Ophthalmosaurus icenicus* (Kirton 1983; Maisch 1997; Moon and Kirton 2016) and *Platypterygius australis* (Kear 2005).

Neoichthyosaurian endocasts are proportionally large, measuring about one-third of the cranial length (Fig. 3.3a; McGowan 1973; Marek et al. 2015). The endocast in the juvenile *Hauffiopteryx typicus* gradually arches dorsally along its anteroposterior endocranial course, as it follows the curvature of the cranial roof, and shows pronounced cephalic and pontine flexures (Fig. 3.3a, b; Marek et al. 2015). Such flexures are not observed in the adult *Ichthyosaurus* cf. *communis* (Fig. 3.3c; McGowan 1973). As the skull shape of *Ichthyosaurus* is flatter, but still rather curved dorsally, the absence of flexure on its endocast could be due to the cast-making method (CT scan versus latex). The neoichthyosaurian endocast maintains a constant width along its length, although there is some evidence for anterior widening, at the olfactory bulbs, and posterior widening at the optic lobes. The ventral extent of the endocast in Neoichthyosauria, however, remains unknown due to the limited ossification and the capacious nature of the ventral braincase (McGowan 1973; Marek et al. 2015). At the anterior end of the endocast, the elongated olfactory region involves olfactory bulbs that proceed undifferentiated into the olfactory tracts (e.g. Marek et al. 2015). These tracts form two long and medially separated ridges that are anteriorly delimited by impressions in the ventral nasal slightly posterior to the external naris, and dorsally by two broad grooves in the ventral surface of the posterior nasal and anterior frontal (Fig. 3.3d, e; Marek et al. 2015; Moon and Kirton 2016). Although the lack of ventral limits renders its exact extent unknown, the ichthyosaur olfactory region appears proportionally large compared to the rest of the endocast (Kirton 1983; Marek et al. 2015). Posteriorly, the narrow cerebrum appears as wide as the posterior part of the olfactory region and is only known through elongate and shallow depressions in the ventral parietal (McGowan 1973; Kirton 1983; Kear 2005). The pineal complex (referred as “pineal organ” in Marek et al. 2015) forms a pronounced dorsomedial bulge, granting the cerebrum a triangular appearance with strongly curved lateral margins (Marek et al. 2015). Posterior to the pineal complex and ventral to the parietal, two bilaterally symmetrical bulges that account for the dorsalmost features on the endocast were interpreted as the optic lobes (see fig. 11 in Marek et al. 2015). However, we suggest these bulges may alternatively correspond to the posterior part of the cerebrum. The

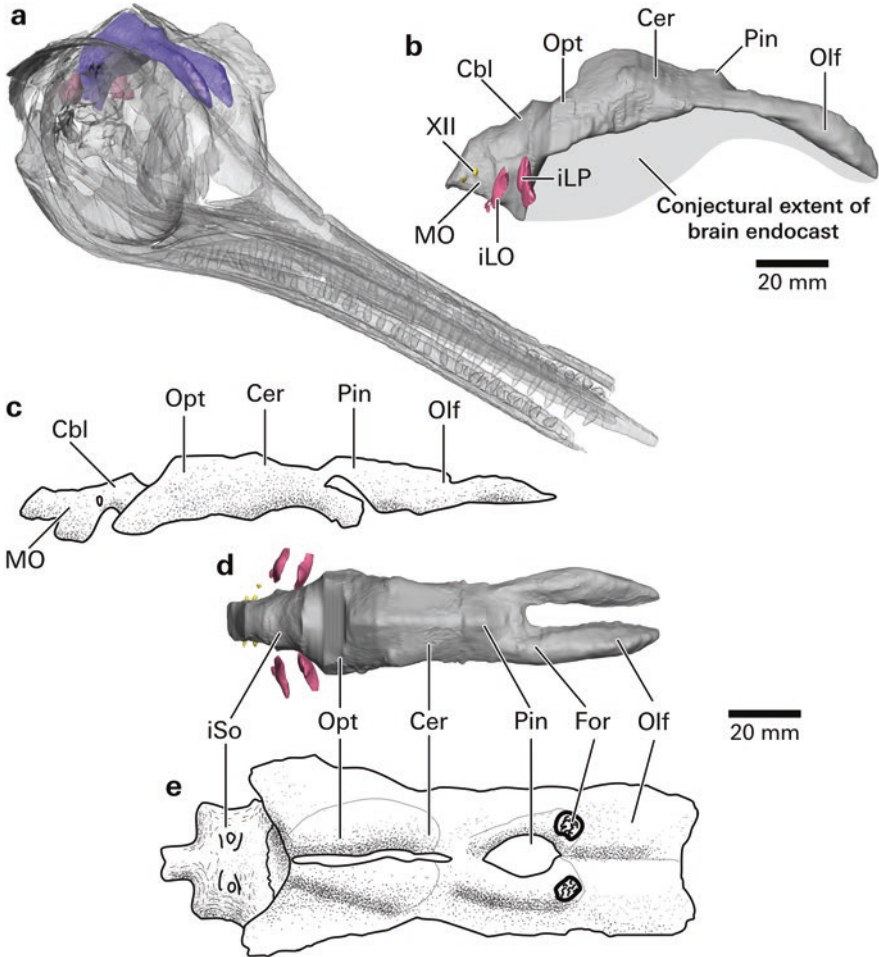


Fig. 3.3 Reconstructions of the endocranial cavity in two Early Jurassic ichthyosaurs. (a, b, d) Three-dimensional CT reconstruction of a juvenile *Hauffiopteryx typicus* endocranium (BRLSI M1399 after Marek et al. 2015) within the skull (a), in right lateral (b), and dorsal (d) views. (c, e) Latex surface cast of *Ichthyosaurus* cf. *communis* (NHMUK PV R8177, redrawn from McGowan 1973) in right lateral (c) and dorsal (e) views. Abbreviations: *Cbl* cerebellum, *Cer* cerebrum, *For* foraminous region, *iLO* impression of the labyrinth on the opisthotic, *iLP* impression of the labyrinth on the prootic, *iSo* impression of the supraoccipital, *MO* medulla oblongata, *Olf* olfactory bulb, *Opt* optic lobe, *Pin* pineal complex, *XII* branches of the hypoglossal (XII) nerve

optic lobes are potentially located more posteroventrally, restricted to the posterior one-third of the ventral parietal (Kirton 1983; Moon and Kirton 2016), and represented by the lateral bulges just anterior to the impression of the supraoccipital (Fig. 3.3b–e). Following our novel interpretation, the cerebellum would be located dorsal to the endosseous labyrinth (Fig. 3.3b) and more posteriorly than in the initial interpretation (see Fig. 11 in Marek et al. 2015). This solution would be more

consistent with the spatial relationships between the cerebellum and the endosseous labyrinth in turtles and alligators (e.g. Evers et al. 2019; Lessner and Holliday 2020). Because of the gap between the posteroventral surfaces of the parietals and the supraoccipital, the true dorsal extent of the cerebellum remains unknown (Kirton 1983; Marek et al. 2015). Posteroventrally, the narrow *medulla oblongata* is laterally constricted by the exoccipitals and rapidly narrows posteriorly into the spinal cord.

Endosseous Labyrinth The morphology and structure of the ichthyopterygian endosseous labyrinth remains largely unknown. In Triassic taxa, the endosseous labyrinths completely reside inside the otic capsules that are mainly formed by the prootic, supraoccipital, and opisthotic, which are surrounded by other braincase elements (Maisch and Matzke 2006; Maisch et al. 2006). Although such structures have been outlined in *Mixosaurus* cf. *cornalianus* and *Phantomosaurus neubigi*, ossification and constriction of the otic capsule prevent direct access to the endosseous labyrinth with traditional osteological approaches (Maisch and Matzke 2006; Maisch et al. 2006). Computed tomographic explorations have so far only considered post-Triassic ichthyosaurs, none of which feature fully articulated crania (Kear 2005; Marek et al. 2015).

Unlike in Triassic ichthyosaurs, the otic capsule in neoichthyosaurians remains largely cartilaginous (e.g. McGowan 1973; Fischer et al. 2012, 2014; Moon and Kirton 2016) and permits limited assessment of endosseous labyrinth morphology. The semicircular canal imprints preserved in the juvenile *Hauffiopteryx typicus* appear to indicate that its labyrinth was dorsoventrally extended and anteroposteriorly short (Fig. 3.3b; Marek et al. 2015). Since labyrinth geometry does not change much during ontogeny (e.g. in sauropodomorphs; Neenan et al. 2019b), the overall labyrinth geometry reconstructed for *Hauffiopteryx* is likely to be relatively representative for those in mature ichthyosaurs. Nevertheless, changes in absolute labyrinth dimensions are expected during ichthyosaurian ontogeny. A growth series of *Stenopterygius* prootics revealed that, from embryo to adult and associated with a fourfold increase in jaw length, canal impression widths increased from about 0.5 mm to 4 mm while the prootic expands as it ossifies (Miedema and Maxwell 2019).

The lateral semicircular canal extends laterally between the opisthotic and prootic, the anterior semicircular canal rises through the prootic and supraoccipital, and the posterior semicircular canal rises through the opisthotic and supraoccipital (Fig. 3.4a–f, i; McGowan 1973; Moon and Kirton 2016). The otic capsule impressions on the prootic and the opisthotic are somewhat V- or T-shaped (e.g. Kear 2005; Fischer et al. 2011, 2012; Moon and Kirton 2016) and indicate that the lateral canal meets both the anterior and posterior canals at angles of roughly 90° (Fig. 3.4a–d). The triangular impression of the labyrinth on the supraoccipital suggests that the anterior and posterior semicircular canals meet at an angle of nearly 180° in the Triassic ichthyosaur *Shonisaurus popularis* (Camp 1980) as well as in Jurassic ophthalmosaurids (Fig. 3.4e, f; Kear 2005; Fischer et al. 2012). Such impressions on the supraoccipital are tilted anterodorsally/posteroventrally (Fig. 3.4e, f; Kear 2005;

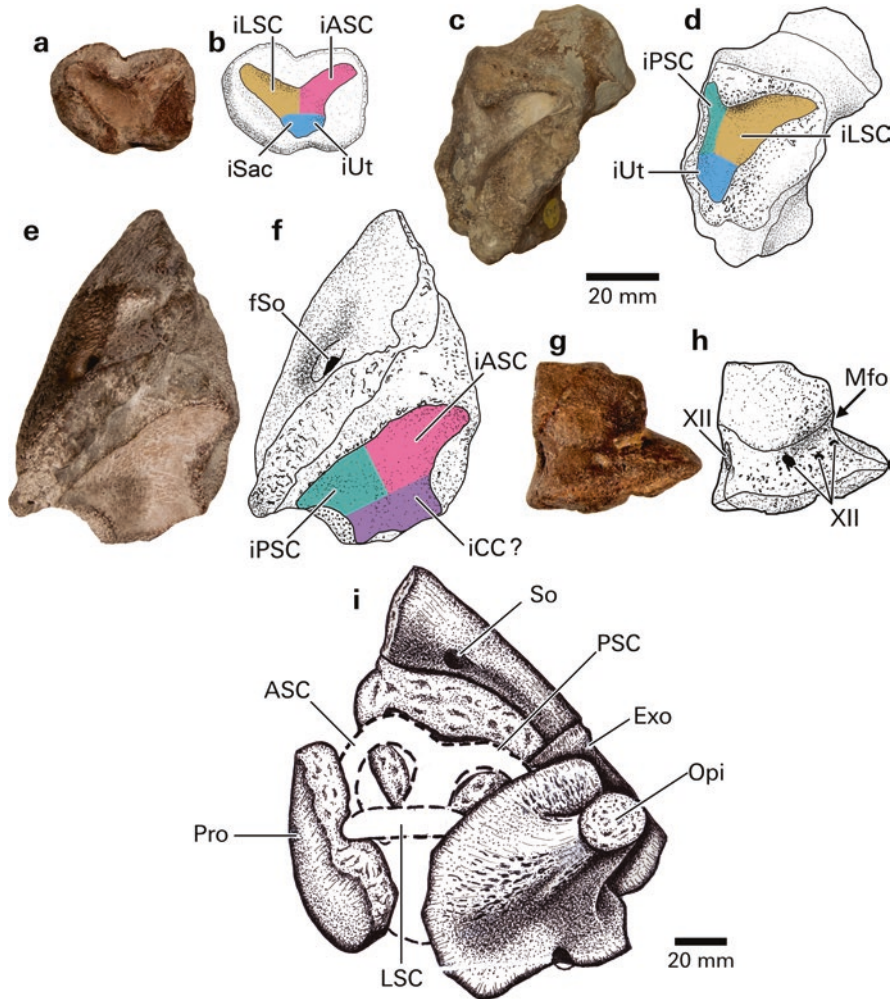


Fig. 3.4 Otic capsule and labyrinth in the Jurassic ichthyosaur *Ophthalmosaurus icenicus*. (a–h) Disarticulated elements of *Ophthalmosaurus icenicus* showing impressions of the endosseous labyrinth (after Moon and Kirton 2016) on a left prootic in posterior view (a, b; LEICT 100'1949–43), left opisthotic in medial view (c, d; NHMUK PV R2133), supraoccipital in right lateral view (e, f; LEICT 100'1949–43), and right exoccipital in lateral view (g, h; LEICT 100'1949–64). Impressions of the endosseous labyrinths are indicated in the same colors throughout. (i) reconstruction of the left osseous labyrinth of *Ophthalmosaurus icenicus* (image by A. Kirton, used with permission). Abbreviations: ASC anterior semicircular canal, Exo exoccipital, fSo foramen in the supraoccipital for passage of a vein, iASC impression of the anterior vertical semicircular canal, iCC impression common crus, iLSC impressions of the lateral semicircular canal, iPSC impression of the posterior vertical semicircular canal, iSac impression of the saccule, iUt impression of the utricule, LSC lateral semicircular canal, Mfo metotic foramen, PSC posterior semicircular canal, Opi opisthotic, Pro prootic, So supraoccipital, XII foramina for passage of the hypoglossal (XII) nerve

Fischer et al. 2012; Moon and Kirton 2016), which could reflect a higher and longer anterior semicircular canal relative to the posterior semicircular canal.

Although the absolute widths of the canals remain uncertain, the lateral semicircular canal may have been wider than the anterior (e.g. Kear 2005; Fischer et al. 2011) or the posterior semicircular canal (e.g. Bindellini et al. 2021). Additionally, impressions of the otic capsule in the intermediate-grade *Shonisaurus popularis* show that the semicircular canals are relatively narrower than in Neoiichthyosauria (Camp 1980; Fischer et al. 2012; Moon and Kirton 2016), suggesting a trend towards thicker canals during ichthyosaur evolution. Ventral to the labyrinth, large and rounded impressions on the prootic, opisthotic, and supraoccipital may correspond to the locations of the sacculle, utricule, and common crus (Fig. 3.4a–f; McGowan 1973; Moon and Kirton 2016). Although these regions are weakly demarcated, the sizes of the impressions are clearly variable, potentially quite large, and offset from the canals in *Arthropterygius hoybergeti* and *Acamptonectes densus* (Fischer et al. 2012; Zverkov and Prilepskaya 2019).

Cranial Nerves Our understanding of ichthyopterygian cranial nerves is extremely limited and mainly inferred from the foramina or grooves observed on bone surfaces. Their identity is often still uncertain (Moon and Kirton 2016) and cranial nerves I–VI remain undocumented. Accordingly, the trajectory of the palatine ramus of the facial (VII) nerve in ichthyosaurs is only indicated by two shallow grooves on the dorsal surface of the parabasisphenoid (e.g. Kirton 1983; Moon and Kirton 2016). A groove in the stapedial facet of the opisthotic is interpreted to have accommodated the glossopharyngeal (IX) nerve (Andrews 1910; Appleby 1961). However, Kirton (1983) alternatively proposed that this groove may carry the hyomandibular branch of the facial (VII) nerve (Kear 2005; Moon and Kirton 2016). This would imply that the glossopharyngeal (IX) nerve, together with the jugular vein, the vagus (X) and possibly the accessory (XI) nerves, exit through the undivided metotic foramen located between the exoccipital and the opisthotic (Fig. 3.4g, h; *sensu* Rieppel 1985 and Maisch et al. 2006; reported as “vagus foramen” or “jugular foramen” in Kirton 1983; Kear 2005; Moon and Kirton 2016). The presence or absence of an accessory nerve in ichthyopterygians is unclear and no direct osteological correlates have been identified. As variable configurations across extant non-avian reptiles prevent more informed recognition of this nerve (e.g. Auen and Langebartel 1977; Evers et al. 2019; Lessner and Holliday 2020), we suggest that (?XI) is the most likely candidate for the accessory nerve in ichthyosaurs. Finally, a variable number of foramina piercing the exoccipital (Fig. 3.4g, h) are consistently associated with the pathways of the hypoglossal (XII) nerves (e.g. Maisch 1997; Marek et al. 2015; Moon and Kirton 2016).

Sauropterygia

Endocasts Sauropterygian paleoneurology is much better documented than that of Ichthyopterygia, with most of the major groups represented. The placodont endocast is known from the placodontoid *Placodus gigas* (Fig. 3.5a–d; Edinger 1925; Hopson 1979; Neenan and Scheyer 2012) and the cyamodontoid *Parahenodus atancensis* (Fig. 3.5e, f; de Miguel Chaves et al. 2020). The nothosauroid endocast is thus far known through two species of the genus *Nothosaurus* (Edinger 1921; Hopson 1979; Voeten et al. 2018a) that are represented by an immature early Middle Triassic specimen of the relatively small *N. marchicus* (body length of circa 0.5–1.5 m; following Voeten et al. 2015; Fig. 3.6), and a larger middle to late Middle Triassic individual of *N. mirabilis* (estimated body length of 3 m; following Westheide et al. 2003). Information regarding the plesiosaurian endocast is mainly based on the reconstructions realized for the elasmosaurid *Libonectes morgani* (Fig. 3.7b–e; Carpenter 1997; Allemand et al. 2019) and the pliosaurid *Acostasaurus pavachoquensis* (Fig. 3.7g; Gómez Pérez 2008). Additionally, the reliable but less complete endocranial information extracted from the leptocleidid *Brancaesaurus brancai* (Edinger 1928; Hopson 1979; Sachs et al. 2016a), the elasmosaurids *Terminatorator ponteixensis* (Sato 2003), *Aristonectes quiriquinensis* (Otero et al. 2018), and *Alexandronectes zealandiensis* (O’Gorman et al. 2021), as well as the indeterminate polycotyloid MNHN F-GOU14 (Allemand et al. 2019), were considered to describe the plesiosaurian endocast.

Endocasts of Placodontia The known endocasts of both *Placodus gigas* and *Parahenodus atancensis* are incomplete, missing the olfactory region (olfactory bulbs and olfactory tracts), the pituitary organ, and the anterior forebrain (Fig. 3.5; Edinger 1925; Neenan and Scheyer 2012; de Miguel Chaves et al. 2020). Correlated with the deep and relatively short braincase (Fig. 3.5a), the endocast in *Placodus* has an overall sigmoidal shape with a pronounced cephalic flexure and a subtle pontine flexure (Fig. 3.5b, d). The endocast in *Parahenodus*; however, is long and straight as a result of its more dorsoventrally compressed skull (Fig. 3.5f; de Miguel Chaves et al. 2020). Although information regarding the cerebrum in *Placodus* is lacking, the structure projects dorsally into an elongate oval impression on the ventral cranial roof (Hopson 1979) and differs from the flat dorsal surface reported for the endocast of *Parahenodus* (de Miguel Chaves et al. 2020). Dorsal to the cerebrum, a large pineal complex is observed in *Placodus* (Fig. 3.4b–d; “parietal foramen” in Edinger 1925; Hopson 1979; Neenan and Scheyer 2012), whereas the structure in *Parahenodus* appears very narrow and laterally compressed (Fig. 3.5e, f; “pineal organ or system” in de Miguel Chaves et al. 2020). Although the endocast in both species offer no (*Placodus*) to little (*Parahenodus*) information regarding the pituitary organ (or hypophysis), the shape and size of the *sella turcica* suggest that this structure was large and dorsoventrally elongated in *Placodus* (Hopson 1979). This contrasts with the poorly developed *sella turcica* in *Parahenodus* (Fig. 3.5f), also reported in other cyamodontoids (*Placochelys placodonta* and *Psephoderma alpinum*; de Miguel Chaves et al. 2020), which indicates weak

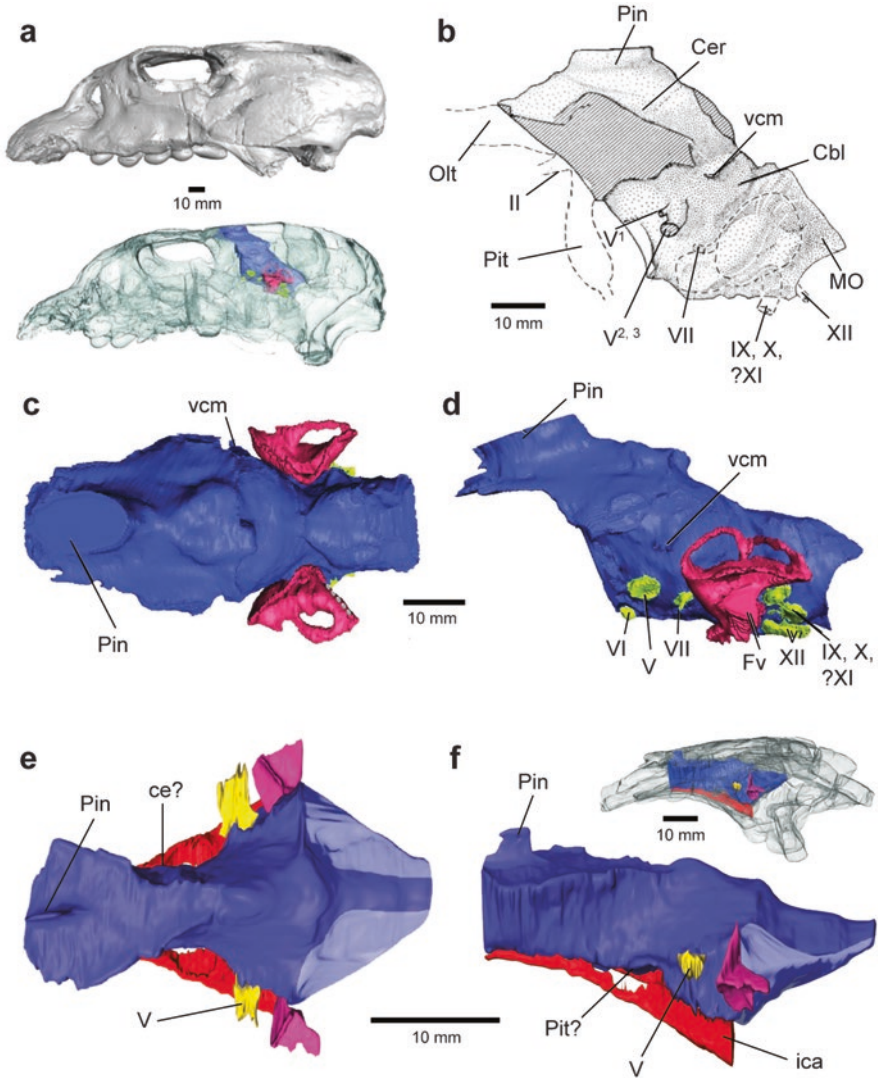


Fig. 3.5 Endocranial anatomy in Placodontia. (a) Virtual reconstruction of the skull of *Placodus gigas* (UMO BT 13) in lateral view, associated with the endocast projection in cranial model. (Modified from Neenan and Scheyer 2012). (b) Composite endocranial endocast of *Placodus gigas* based on an artificial endocranial endocast (SM R359) and a partial natural endocranial endocast (SM R4038) in lateral view, with missing parts indicated by broken lines and damaged surfaces indicated by diagonal lines. (Modified from Hopson 1979). (c, d) Virtual cranial endocast and endosseous labyrinth of *Placodus gigas* (UMO BT 13) in dorsal (c) and lateral (d) views. (Modified from Neenan and Scheyer 2012). (e, f) Virtual cranial endocast of *Parahenodus atancensis* (MUPA ATZ0104) in dorsal (e) and lateral (f) views, associated with the endocast projection in cranial model (de Miguel Chaves et al. 2020). Abbreviations: *Cbl* cerebellum, *ce* cavum epiptericum, *Cer* cerebrum, *Fv* fenestra vestibuli, *ica* internal carotid artery, *MO* medulla oblongata, *Olt* restored olfactory tract, *Pin* pineal complex, *Pit* pituitary fossa, *vcm* vena cerebri media, *II* restored optic nerve, *V* trigeminal nerve canal, *V¹* ophthalmic branch of the trigeminal nerve, *V^{2,3}* maxillary and mandibular branches of the trigeminal nerve, *VI* abducens nerve canal, *VII* facial nerve canal, *IX, X, ?XI* foramen for glossopharyngeal vagus and potentially accessory nerves, *XII* hypoglossal nerve canal

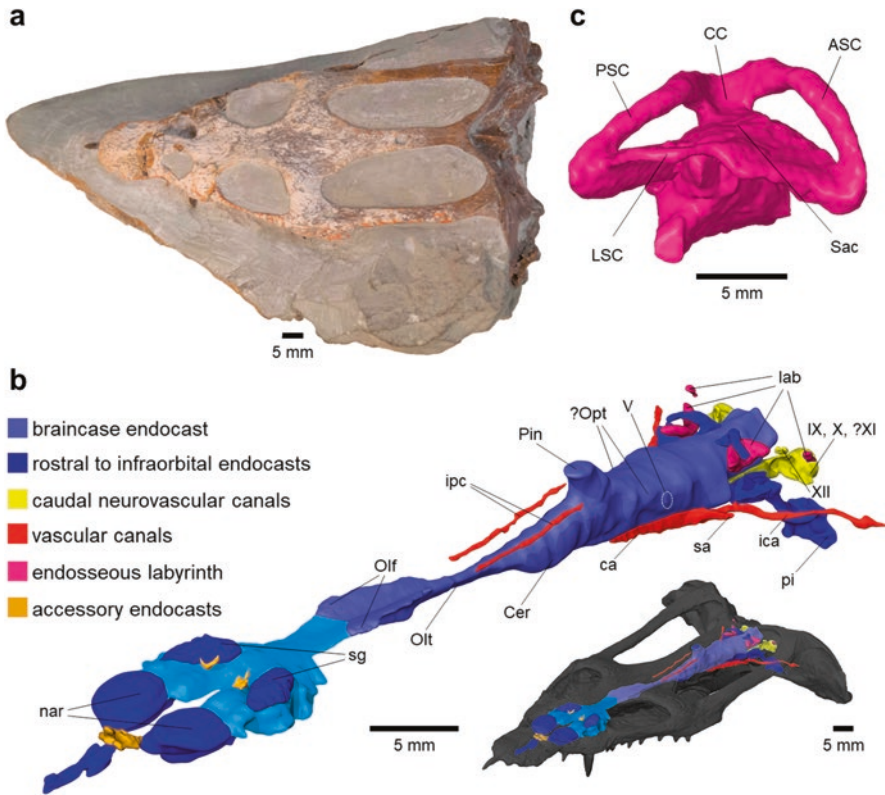


Fig. 3.6 Endocranial anatomy of *Nothosaurus*. (a) Specimen TW480000375 in dorsal view – De Museumfabriek, Enschede, the Netherlands. (b) Cranial endocast and other endocranial voids of *Nothosaurus marchicus* (TW480000375) in angled anterodorsal view associated with the endocast projection in cranial model. (Modified from Voeten et al. 2018a). (c) Right endosseous labyrinth of *Nothosaurus* sp. NME 16/4 in lateral view (Neenan et al. 2017; sourced from MorphoMuseum under M3#326_NME 16/4: <https://morphomuseum.com/specimenfiles/view/326>). Abbreviations: ASC anterior semicircular canal, ca cerebral artery, CC common crus, Cer cerebrum, ica internal carotid artery, ipc infraparietal canals, lab portions endosseous labyrinth, LSC lateral semicircular canal, nar narial passages, Olf olfactory bulb, Olt olfactory tract, Opt optic lobes, pi paracondylar interstice, Pin pineal complex, PSC posterior semicircular canal, sa stapedia artery, Sac saccule, sg salt glands, V foramen for trigeminal nerve, IX X?XI foramen for the glossopharyngeal vagus and possible accessory nerves, XII root of hypoglossal nerve

development of the pituitary. Posterior to the pineal complex, the dorsal surface of the endocast in *Placodus* slopes posteroventrally and a distinct swelling may mark the location of the optic tectum (Edinger 1925; Hopson 1979). However, this tentative structure is challenging to delimit and could not be resolved by Neenan and Scheyer (2012). Although the mesencephalic cast in *Parahenodus* could be identified as a symmetrical pair of lateral constrictions that may correspond to the *cava epiptERICA* (Fig. 3.4e; de Miguel Chaves et al. 2020), the optic tectum could not be distinguished. The short hindbrain in *Placodus* features a low swelling above and

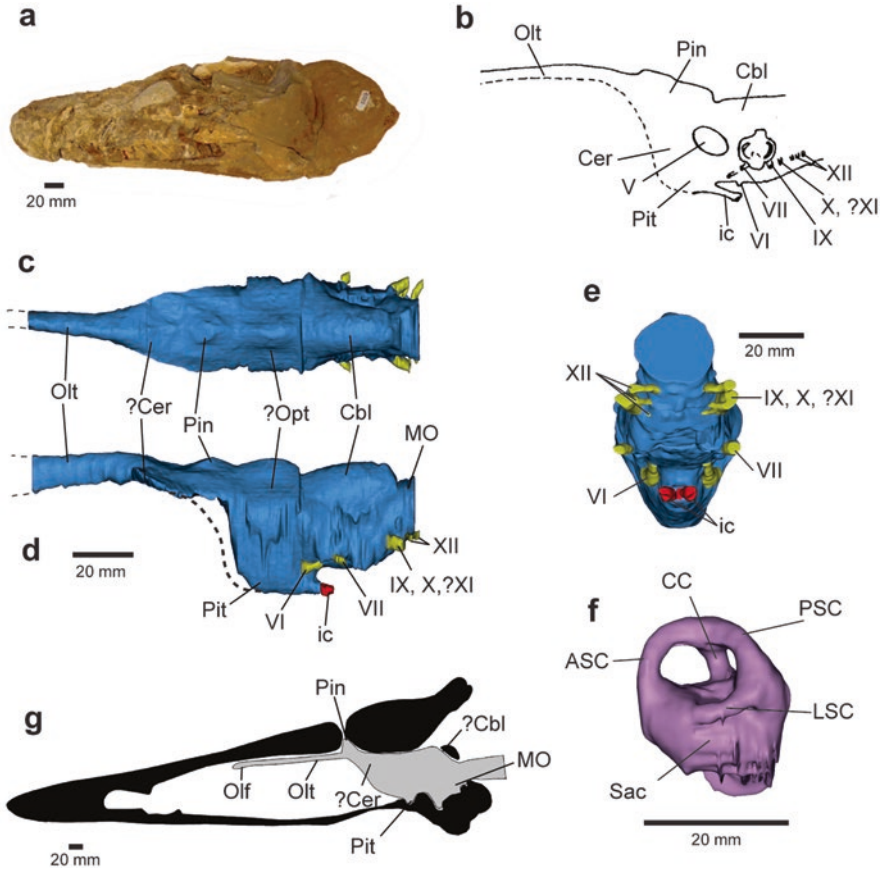


Fig. 3.7 Endocranial anatomy in Plesiosauria. (a) Specimen SMNS 81783 in lateral view – Staatliches Museum für Naturkunde Stuttgart, Germany. (b) Latex endocast of *Libonectes morgani* (SMUSMP 69120) in lateral view (Modified from Carpenter 1997). (c–e) Virtual endocast of *Libonectes morgani* (D1–8213) in dorsal (c), lateral (d) and posteroventral (e) views. (Modified from Allemand et al. 2019). The dotted lines indicate the missing parts. (f) Left endosseous labyrinth of *Libonectes morgani* (D1–8213) in lateral view. (Modified from Allemand et al. 2019). (g) Diagrammatic representation of the endocast of *Acostasaurus pavachoquensis* (UN-DG-R-1000) along the midline of the cranium based on partial digital endocasts. (Modified from Gómez Pérez 2008). Abbreviations: ASC anterior semicircular canal, Cbl cerebellum, CC common crus, Cer cerebrum, ic internal carotid, LSC lateral semicircular canal, MO medulla oblongata, Olf olfactory bulbs, Olt olfactory tract, Opt optic lobe, Pin pineal complex, Pit pituitary fossa, PSC posterior semicircular canal, Sac sacculle, V foramen for trigeminal nerve, VI foramen for abducens nerve, VII foramen for facial nerve, IX foramen for glossopharyngeal nerve, X?XI foramen for the vagus and potentially the accessory nerves, XII foramen for hypoglossal nerve

behind the trigeminal root that had been tentatively identified as the cerebellum (Fig. 3.5b) by Edinger (1925) but remained unrecognized by Neenan and Scheyer (2012). The cast of the medulla in *Placodus* is slightly higher than wide and is dorso-laterally constricted by elements housing the inner ear cavities (Fig. 3.5b, d).

Although the trigeminal root was also reconstructed in *Parahenodus* (Fig. 3.5e, f), the morphology of the hindbrain provides insufficient information to delimit the cerebellum and the medulla (de Miguel Chaves et al. 2020).

Endocasts of Nothosauria Associated with profound dorsoventral flattening, postorbital elongation, and lateral constriction of the skull and braincase, the endocasts of *Nothosaurus marchicus* and *N. mirabilis* are anteroposteriorly elongated and remarkably straight without noticeable flexures (Fig. 3.6b; Edinger 1921; Voeten et al. 2018a). The dorsal impressions of the ovoid olfactory bulbs invade the ventral surface of the frontals (Edinger 1921; Voeten et al. 2018a), although the limited osseous expression of these structures and lack of ventral delimitation prevent a confident reconstruction of their size (Fig. 3.6b; Voeten et al. 2018a). Posteriorly, the casts of the olfactory tracts are very elongate, thin, and deeper than wide (Fig. 3.6b). In *N. marchicus*, the olfactory tracts are bilaterally divided up to their mid-length by the sagittal ventral projection of the interfrontal suture (Fig. 3.6b; Voeten et al. 2018a). This differs from *N. mirabilis*, in which the olfactory tracts, oval in cross section, are undivided along their entire length (Edinger 1921; Hopson 1979). In both species, the olfactory tracts gradually widen posteriorly to merge into the very narrow cerebrum, which is marked only by a lateral divergence of the osseous walls resulting in pronounced bilateral bulging of the endocast surface (Fig. 3.6b; Hopson 1979; Voeten et al. 2018a). Posterior to the cerebrum, a large pineal complex forms an elliptic cone rising dorsally from the brain endocast up into the parietal foramen (Fig. 3.6b; Edinger 1921; Hopson 1979; Voeten et al. 2018a). Posterior to the pineal complex, the *cava epiptERICA*, resulting from lateral constriction by the epipterygoids, may indicate the transition from the forebrain to the midbrain (Fig. 3.6b; Voeten et al. 2018a). Posterior to this structure, a subtle bilateral dorso-lateral swelling invading the ventral surface of the parietal may correspond to the optic lobes (Fig. 3.6b; Voeten et al. 2018a). This structure constitutes the broadest cephalic domain in *N. marchicus* (Voeten et al. 2018a) but was not reported in *N. mirabilis* (Edinger 1921; Hopson 1979). Ventral to the potential optic lobes, the absence of a well-differentiated pituitary on the ventral surface of the endocast (Edinger 1921; Voeten et al. 2018a) indicates that this structure may have been underdeveloped, which agrees with the flattened and shallow *sella turcica* generalized for nothosaurians (Gorce 1960; Rieppel 1994b). In the posterior part of the endocast, the transition from the midbrain to the hindbrain is unpronounced. The roof of the hindbrain region is flat and horizontally oriented, offering no indications for the position or size of the cerebellum (Edinger 1921; Voeten et al. 2018a). The separation between the pons and medulla is marked by a faint flexure resulting from constriction associated with the parietal-supraoccipital suture (Fig. 3.6b; Voeten et al. 2018a). Between this constriction and the *foramen magnum*, the *medulla oblongata* tapers posteriorly, covered dorsally by the supraoccipital and ventrally by the basioccipital (Voeten et al. 2018a). Lateral to the occipital condyle, the open space between the basioccipital and pterygoids described as “eustachian foramina” by Koken (1893:p 353) were reinterpreted as “paracondylar interstices,” which may represent representing non-functional byproducts of nothosauroid cranial

development rather than true foramina (Fig. 3.6b; Rieppel 1994b; Voeten et al. 2018a).

Endocasts of Plesiosauria The plesiosaurian endocast is anteroposteriorly elongated and straight, with only a slight ventral flexure at the level of the contact between the olfactory tract and the cerebrum (Fig. 3.7b, d, g; Carpenter 1997; Gómez Pérez 2008; Allemand et al. 2019). In the anterior part of the endocast, the kite-shaped olfactory bulbs reconstructed in *Acostasaurus pavachoquensis* and *Libonectes morgani* are located at the level of the external nares (Gómez Pérez 2008; Allemand et al. 2019). In both species, the ventral delimitation of the olfactory bulbs could not be reconstructed. The olfactory bulbs connect to the cerebrum through long olfactory tracts that are joined along their entire length and account for about one-half of the brain cast length (Fig. 3.7b–d, g; Gómez Pérez 2008; Allemand et al. 2019). The olfactory tracts are projected in the ventral wall of the frontal, which reveals maximum mediolateral compression at their mid-length and subsequent widening towards their contact with the cerebrum (Fig. 3.7c; Gómez Pérez 2008; Allemand et al. 2019). In both *Acostasaurus* and *Libonectes*, the exact shape of the cerebrum is unknown, as the open condition of the plesiosaurian braincase prevents the reconstruction of its ventral and lateral extent (Fig. 3.7b–d, g; Gómez Pérez 2008; Allemand et al. 2019). The pineal complex in *Acostasaurus* forms a large oval prominence (“pineal gland” in Gómez Pérez 2008), whereas in *Libonectes*, it appears to form a small bulge on the dorsal surface of the endocast (Fig. 3.7b–d, g; “pineal and dura” in Carpenter 1997; “pineal organ” in Allemand et al. 2019). In *Libonectes*, the optic lobes are potentially situated posterior to the pineal complex at the level of a more pronounced dorsal bulge on the endocast (Fig. 3.7c, d; Allemand et al. 2019). However, their exact location and delimitation remains unknown in plesiosaurians. At the anteroposterior level of the potentially resolved optic lobes, a distinct bulge on the ventral surface of the plesiosaurian endocast appears to represent the pituitary cast (Fig. 3.7b–d, g; Carpenter 1997; Gómez Pérez 2008; Otero et al. 2018; Allemand et al. 2019; O’Gorman et al. 2021). This well-defined structure, associated with the proportionally large and long *sella turcica* reported in plesiosaurians (e.g. Gómez Pérez 2008; Zverkov et al. 2017; Otero et al. 2018), is consistent with a well-developed pituitary organ. The posterior part of the endocast carries an anteroposteriorly developed bulge on its dorsal surface that is interpreted to represent the cerebellum (Fig. 3.7b–d, g; Gómez Pérez 2008; Allemand et al. 2019; O’Gorman et al. 2021). Casts of the floccular recesses are reported at this level in the pliosaurid *Acostasaurus* and the elasmosaurid *Alexandronectes zealandiensis* (Gómez Pérez 2008; O’Gorman et al. 2021) in the form of small processes that project laterally through the anterior semicircular canals. However, this floccular recess was not recorded in the leptocleidid *Brancaesaurus brancai* (Sachs et al. 2016a) and in the elasmosaurids *Libonectes* (Carpenter 1997; Allemand et al. 2019) and *Aristonectes quiriquinensis* (Otero et al. 2018). The ventral delimitations of the casts representing the *medulla oblongata* in *Acostasaurus*, *Aristonectes*, and *Alexandronectes* (Gómez Pérez 2008; Otero et al. 2018; O’Gorman et al. 2021) are unknown. In *Libonectes*, this region is slightly

offset ventrally relative to the anterior endocast domain and rises dorsally on its posterior part to reach the foramen magnum (Fig. 3.7b, d; Allemand et al. 2019).

Endosseous Labyrinth Endosseous labyrinth morphologies are documented for most major sauropterygian groups. In placodonts, the endosseous labyrinth is mainly known from *Placodus gigas* (Fig. 3.5c, d; Neenan and Scheyer 2012), as only small parts of the anterior semicircular canal and vestibule could be reconstructed in *Parahenodus atancensis* (Fig. 3.5e, f; de Miguel Chaves et al. 2020). The geometry of nothosauroid endosseous labyrinths are known through *Simosaurus gaillardoti* and *Nothosaurus* sp. (Fig. 3.6c; Neenan et al. 2017). Pistosaurid endosseous labyrinths were reconstructed for the basal pistosaur *Augustasaurus hagdorni* (Neenan et al. 2017) and several plesiosaurian taxa: the pliosaurids *Acostasaurus pavachoquensis*, *Peloneustes philarchus*, and *Hauffiosaurus tomistomimus* (Gómez Pérez 2008; Neenan et al. 2017); the rhomaleosaurid *Macroplata tenuiceps* (Neenan et al. 2017); the cryptocleidids *Microcleidus homalospondylus*, *M. macropterus*, *Muraenosaurus leedsii*, and *Picrocleidus beloclis* (Evans 1999; Neenan et al. 2017); the leptocleidids *Brancaesaurus brancai* and *Nichollsaura borealis* (Sachs et al. 2016a; Neenan et al. 2017); and the elasmosaurids *Callawayasaurus colombiensis* (Neenan et al. 2017), *Libonectes morgani* (Fig. 3.7f; Allemand et al. 2019), *Cardiocorax mukulu* (Marx et al. 2021), and *Alexandronectes zealandiensis* (O’Gorman et al. 2021).

The endosseous labyrinths in placodonts, nothosauroids, and the basal pistosaur *Augustasaurus hagdorni* exhibits a “generalized reptilian morphology” (Figs. 3.5d and 3.6c; Neenan et al. 2017; Voeten et al. 2018a; de Miguel Chaves et al. 2020). Triassic sauropterygians are characterized by an anteroposteriorly elongate labyrinth with gracile semicircular canals, a narrow common crus, and a short and uncoiled lagena (Neenan and Scheyer 2012; Neenan et al. 2017). The medial portions of the anterior and posterior canals form a distinct M-shape, with the anterior canal longer and reaching higher dorsally than the posterior canal (Neenan et al. 2017). The lateral semicircular canal is relatively straight with a small lateral extension (Neenan et al. 2017). The endosseous labyrinth in placodonts and nothosauroids is more dorsoventrally compressed than that of the basal pistosaur *A. hagdorni*, (Neenan et al. 2017). The generalized architecture of the plesiosaurian endosseous labyrinth is characterized by a compact, bulbous morphology involving a wider common crus (Fig. 3.7f; Evans 1999; Neenan et al. 2017; Allemand et al. 2019). In most taxa, the endosseous labyrinths are square shaped in lateral view, robust, low, and lack sinusoidal curvature, although some variability exists. The elasmosaurid *Callawayasaurus colombiensis*, for example, features a taller endosseous labyrinth than other plesiosaurians (Neenan et al. 2017), which results in dorsal extension of both the posterior and anterior semicircular canals and a longer common crus (Neenan et al. 2017). Although the true ventral extent of the lagena is unknown for all plesiosaurians, it appears to be relatively short, robust, and uncoiled (Neenan et al. 2017; Allemand et al. 2019).

Cranial Nerves As the anteroventral part of the skull surrounding the sauropterygian endocast remains unossified, cranial nerves I–IV and VIII are generally undocumented. Although the oculomotor (III) and trochlear (IV) nerves were reported in *Aristonectes quiriquinensis* (Otero et al. 2018), these features may also represent *haemal sulci*, rendering their identity inconclusive.

The large passage for the trigeminal (V) nerve is completely enclosed by the prootic fenestra in *Placodus gigas* (Neenan and Scheyer 2012). In cyamodontoids, nothosauroids and plesiosaurians, this foramen (i.e. trigeminal foramen *sensu* Rieppel 2001; *cavum epiptericum sensu* Brown et al. 2013; prootic foramen *sensu* Neenan and Scheyer 2014) is delimited by the epipterygoid anteriorly and the prootic posteriorly (e.g. Rieppel 1994b, 2001; Neenan and Scheyer 2014; Brown et al. 2013; de Miguel Chaves et al. 2020). In all sauropterygians, the trigeminal nerve emerges on the lateral surface of the endocast (Figs. 3.5d, f and 3.7b; Carpenter 1997; Neenan and Scheyer, 2012; de Miguel Chaves et al. 2020). Although the nerve itself was not identified in *Nothosaurus marchicus* due to the absence of prootics in the studied specimen (Voeten et al. 2018a), the approximate position of its eruption (Fig. 3.6b) is inferred to be well posterior to the epipterygoid (Rieppel 1994b, fig. 5b). The separation of the trigeminal nerve into its three main branches remains unknown in Sauropterygia. Nevertheless, the *maxillaris* and *ophthalmicus* rami of the trigeminal nerve in plesiosaurians were recognized to form an extensive neurovascular plexus in the premaxilla and maxillae (e.g. Smith and Vincent 2010; O’Gorman and Gasparini 2013; Foffa et al. 2014; Sachs et al. 2017). In the cyamodontoid placodont *Psephoderma alpinum*, the cutaneous branches of the superior alveolar nerve (i.e. the terminal branches of the *maxillaris* rami) innervate the tooth plates (Neenan and Scheyer 2014). Peripheral canals in the rostral region of *Nothosaurus marchicus* have been argued to potentially contribute to a dermal sensor innervated by the trigeminal nerve, although their identity could not be conclusively established due to the unique rostral configuration of the taxon (Voeten et al. 2018a).

Anteroventrally to the trigeminal nerve, a small abducens (VI) nerve in *Placodus gigas* is associated with the foramen located in the *dorsum sellae* (Fig. 3.5d; Neenan and Scheyer 2012). In plesiosaurians, the abducens nerve is located ventral to the trigeminal nerve and posterolateral to the pituitary organ (Fig. 3.7b, d, e; Carpenter 1997; Allemand et al. 2019). It pierces the dorsal surface of the *dorsum sellae* and exits on the anterior margin of the clinoid processes (upper cylindrical processes *sensu* Carpenter 1997) of the parabasisphenoid (e.g. Sato et al. 2011; Zverkov et al. 2017; Marx et al. 2021). Similar passage through the *dorsum sellae* and the clinoid processes was reported in nothosauroids (Rieppel 1994b).

The facial (VII) nerve, visualized in *Placodus gigas* and *Libonectes morgani* (Figs. 3.5b, d and 3.7b, d, e; Neenan and Scheyer 2012; Allemand et al. 2019), emerges on the lateral surface of the endocast, posteroventral to the trigeminal nerve and just anterior to the endosseous labyrinth. Although the nothosauroid facial nerve was reported in *Nothosaurus marchicus* (Edinger 1921; Hopson 1979), that structure later was considered an artefact (Voeten et al. 2018a), leaving the pathway of this nerve only inferred from the foramina or grooves observed on bone surfaces

(Rieppel 1994b). The facial nerve foramen in nothosauroids is located on the ventral part of the prootic in proximity to the basisphenoid (Rieppel 1994b). The subdivision of the facial nerve into the hyomandibular and palatine branches occurs after its passage through the prootic in *Nothosaurus* sp. but remains unclear in *Simosaurus gaillardoti* (Rieppel 1994b). Anteriorly, the palatine branch of the facial nerve may have traveled through the vidian canal together with the sphenopalatine artery (Rieppel 1994b; Voeten et al. 2018a). In both placodonts and plesiosaurians, the pathway of the facial nerve and the subdivision between the hyomandibular and palatine branches of the nerve remain unknown.

Posterior to the endosseous labyrinth, the glossopharyngeal (IX), vagus (X), and hypoglossal (XII) nerves merge on the lateral surface of the sauropterygian endocast (Figs. 3.5b, d; 3.6b and 3.7b, d, e). As for ichthyopterygians, the possible presence and passage of the accessory (XI) nerve in Sauropterygia are not conclusively established, which is why we propose the use of (?XI) to indicate this putative structure for now. In both *Placodus gigas* and *Nothosaurus marchicus* (Figs. 3.5b and 2.6b), the glossopharyngeal, vagus, and possible accessory nerves form a single plexus that pass through the undivided metotic foramen (*sensu* Rieppel 1985, but also “jugular foramen” *sensu* Neenan and Scheyer 2012 and Voeten et al. 2018a, or “vagus foramen” *sensu* Wang et al. 2019a) located between the opisthotic and the exoccipital. In both taxa, two distinct roots for the hypoglossal nerves are identified (Rieppel 1994b; Neenan and Scheyer 2012; Voeten et al. 2018a) that may exit through a distinct foramen located between the exoccipital and basioccipital (*Placodus*) or through the metotic foramen with the cranial nerves IX, X, and XI (*Nothosaurus*). In plesiosaurians, different interpretations have been suggested for the identification and passages of the glossopharyngeal, vagus, and possible accessory nerves. Carpenter (1997) labelled two distinct canals on the endocast of *Libonectes morgani* (Fig. 3.7b), one for the glossopharyngeal nerve and a second one accommodating the vagus nerve and potentially the accessory nerve. This differs from the endocasts of *Acostasaurus pavachoquensis* (Gómez Pérez 2008), two other specimens of *L. morgani* (Allemand et al. 2019 reinterpreted here), and *Alexandronectes zealandiensis* (O’Gorman et al. 2021), in which the glossopharyngeal and vagus nerves (including the possible accessory nerve) merge into a single canal (Fig. 3.7d, e). Because both interpretations are consistent with osteological inferences (e.g. Druckenmiller and Russell 2008; Sachs et al. 2016b; Zverkov et al. 2017 for two distinct canals; Druckenmiller 2002; Sato et al. 2011; Evans 2012; Brown et al. 2013; Marx et al. 2021 for a single canal), conclusive establishment of this condition remains challenging. Posteroventrally, the medial surface of the plesiosaurian exoccipital is pierced by one (e.g. Ketchum and Benson 2010; Benson et al. 2015), two (e.g. reinterpretation of fig. 4C in Benson et al. 2011; Sato et al. 2011), or three (e.g. Chatterjee and Small 1989; Carpenter 1997) foramina that correspond to the roots of hypoglossal nerves. Laterally, all these canals may merge with the foramen that also accommodates the glossopharyngeal and vagus nerves (e.g. Benson et al. 2013, 2015), or depart through one (e.g. Maisch 1998; Brown et al. 2013), or two (e.g. Druckenmiller 2002; Evans 2012) other distinct foramina. Although the branching pattern of the hypoglossal nerves might be of phylogenetic

and taxonomic significance (Zverkov et al. 2017), the presence of a possible right-left asymmetry (Chatterjee and Small 1989), as well as potential misidentification of vascular or nutritive foramina (e.g. Evans 2012) may challenge the recognition of the hypoglossal foramina. This requires reassessing the identity of the cranial nerves (IX to XII) and the affinities of these foramina. Additionally, consistent usage of nomenclature (e.g. metotic foramen *sensu* Rieppel 1985; Evans 2012; but generally referred as the “vagus”, “jugular” or “anterior jugular” foramen, e.g. Carpenter 1997; Noe et al. 2003; Benson et al. 2015; Marx et al. 2021) would help to resolve the ambiguities induced by the variable number of foramina.

3.3.2 Voids Associated with Cranial Blood Supply

The reconstructed pattern of cranial blood supply in both Ichthyopterygia and Sauropterygia is not completely understood and mainly informed by foramina revealing the pathways of the internal carotids through the posterior braincase (e.g. Zverkov et al. 2017).

Ichthyopterygia

In most ichthyosaurs, the internal carotid artery enters the cranium ventrally through a singular foramen in the basisphenoid (Fig. 3.8; e.g. McGowan and Motani 2003; Kear 2005; Maxwell and Caldwell 2006; Maxwell 2010). Nevertheless, this condition is not shared across the entire clade, as a more posterior entry has been hypothesized in several taxa. This interpretation is inspired by either posteriorly extending parasphenoids in *Cymbospondylus petrinus*, *Shastasaurus alexandrae*, and *Arthropterygius chrisorum* (Maisch and Matzke 2000a; Fernández and Maxwell 2012), or through the presence of a large foramen at the posterior end of the basioccipital in *Cymbospondylus nichollsi* (Fröbisch et al. 2006). Since *Cymbospondylus*, *Shastasaurus*, and *Arthropterygius* are not closely related, it appears that a posteriorly directed foramen for the internal carotid artery evolved multiple times in ichthyosaurs (Maxwell 2010). In addition, the internal carotid artery departs the basisphenoid via a single large posteroventral foramen in most taxa (Fig. 3.8a–c; e.g. Marek et al. 2015; Lomax et al. 2019), but through paired ventral foramina piercing the posterior parasphenoid in *Temnodontosaurus* cf. *trigonodon* (Fig. 3.8d; Maisch 2002).

Sauropterygia

In sauropterygians, the internal carotid arteries enter the posterior cranium through either the cranioquadrate passage in placodonts and derived plesiosaurians (Fig. 3.9a, d), or through the quadrate ramus of the pterygoid in nothosauroids,

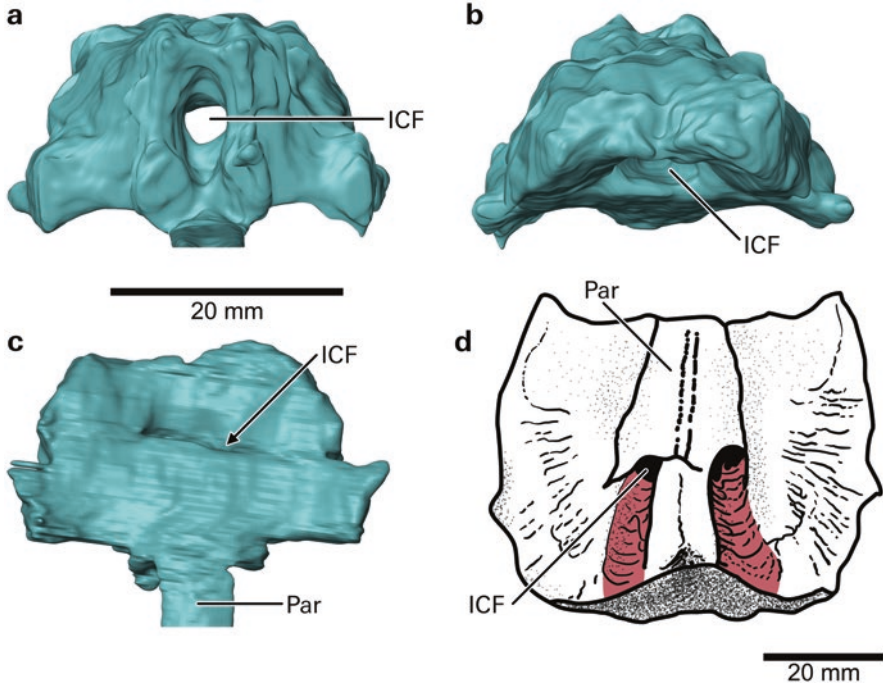


Fig. 3.8 Passage of the internal carotid arteries through two Early Jurassic ichthyosaur parabasi-sphenoids. (a–c) Three-dimensional CT reconstruction of a juvenile *Hauffiopteryx typicus* (BRLSI M1399 after Marek et al. 2015) in anterior (a), posterior (b), and ventral (c) views. (d) Separation of the carotid arteries by the parasphenoid in a juvenile *Temnodontosaurus cf. trigonodon* (MB.R.2878.3) in ventral view, redrawn from Maisch 2002. Abbreviations: ICF internal carotid foramen, Par parasphenoidal portion of the parabasi-sphenoid

non-plesiosaurian pistosauroids, and basal plesiosaurians (Fig. 3.9b, c; Zverkov et al. 2017). In placodonts, the anterior course of the internal carotid artery is unclear, and a potential split between the cerebral and palatine branches inside the bones surrounding the otic capsule remains uncertain (Müller et al. 2011). In nothosauroids, the internal carotid artery continues its anterior course into a groove along the dorsolateral suture between the basioccipital and basisphenoid and passes through the medioventral aspect of the *cavum vestibuli* of the otic capsule to pierce the basisphenoid in which it divides into a cerebral and a palatine branch (Fig. 3.9g; Rieppel 1994b; Müller et al. 2011; Voeten et al. 2018a). This differs from plesiosaurians in which the internal carotid artery continues its anterior course in a ventrolateral sulcus on the basisphenoid and divides into a cerebral and palatal branch outside the bone (Fig 3.9e, f; Zverkov et al. 2017). Although the departure of the palatine branch laterally to the *crista trabecularis* appears conservative among sauropterygians, this may not be the case for the departure of the cerebral artery. The cerebral artery erupts in the *sella turcica* through a pair of closely spaced medial openings in placodonts (Neenan and Scheyer 2012), whereas these foramina are more widely spaced in nothosauroids (e.g. Rieppel 1994b; Voeten et al. 2018a). In plesiosaurians,

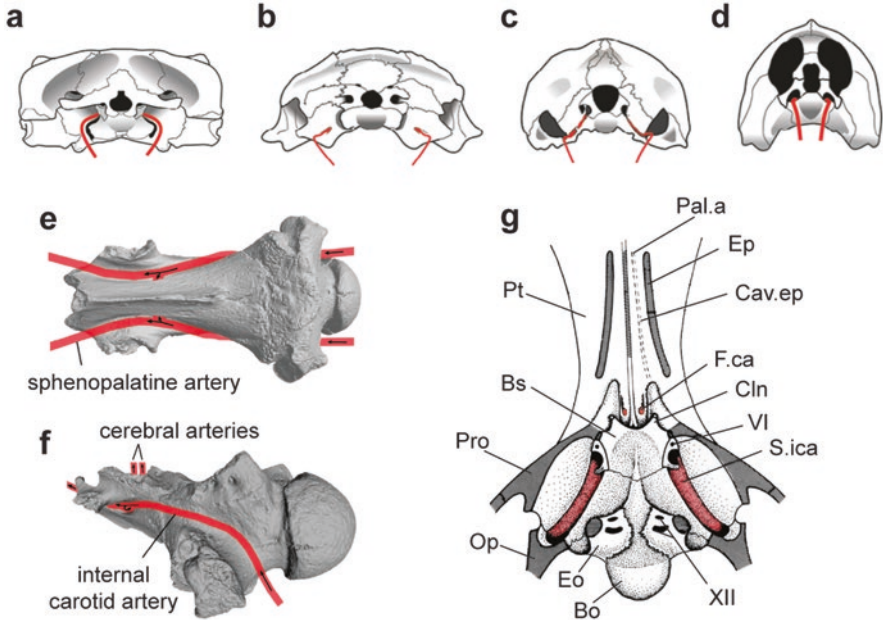


Fig. 3.9 Sauropterygian carotid arteries. (a–d) Occipital views showing the position of the internal carotid artery entrance in *Placodus* (a), *Nothosaurus* (b), *Wangosaurus* (c), and *Libonectes* (d). (Modified from Zverkov et al. 2017). Reconstruction of carotid arteries circulation in the elasmosaurid plesiosaur (SGU 251/1) in ventral (e) and posterolateral (f) views. (Modified from Zverkov et al. 2017). Schematic horizontal section through the braincase of *Nothosaurus* exposing the dorsal view of the basicranium (g; Modified from Rieppel 1994b). Abbreviations: *Bo* basioccipital, *Bs* basisphenoid, *Cav.ep* cavum epiptericum, *Cln* clinoid process of basisphenoid, *Eo* exoccipital, *Ep* epipterygoid, *F.ca* foramen for cerebral artery, *Op* opisthotic, *Pal.a* foramen (canal) for the palatine artery, *Pro* prootic, *Pt* pterygoid, *S.ica* sulcus for the internal carotid artery, *VI* abducens nerve, *XII* hypoglossal nerve

both unpaired and paired foramina for the cerebral artery have been reported across different taxa (Otero et al. 2016; Allemand et al. 2017a; O’Gorman et al. 2017; Zverkov et al. 2017), which casts doubt on a potentially conservative phylogenetic distribution of this structure.

3.4 Brain Evolution and Paleobiologic Inferences Based on Endocast Morphology

3.4.1 Morphological Brain Diversity

Ichthyopterygia

Knowledge of ichthyopterygian paleoneurology remains restricted to derived neoichthyosaurians, rendering evolutionary changes in endocranial morphologies along ichthyopterygian evolutionary history partially obscured. Currently available ichthyosaur endocrania span about 100 Myr, from the Toarcian *Hauffiopteryx typicus* to the Albian *Platypterygius australis*, during which they appear to have remained remarkably consistent. The only appreciable variability in ichthyopterygian endocast geometry is expressed in the cephalic and pontine flexures, which appear pronounced in *H. typicus* (Marek et al. 2015) but are relatively less evident in *Ichthyosaurus* cf. *communis* (McGowan 1973). Although this difference could be due to the distinct cast-making method employed in the reconstruction of the two endocasts, it may also result from the different ontogenetic stages of these specimens. The flexed endocast in the juvenile *H. typicus* is consistent with the early ontogenetic stage of brain development reported in extant archosaurs (e.g. Jirak and Janacek 2017; Beyrand et al. 2019; Lessner and Holliday 2020), in which strongly flexed brains become more tubular and straight during ontogeny. Additionally, retaining the curved endocast in adult ichthyopterygian could be indicative of paedomorphism within the evolution of their skulls, associated with the enlarged orbit and reduced cranial ossification seen in, for example, *Ophthalmosaurus icenicus* (Moon and Kirton 2016).

Sauropterygia

Comparison of sauropterygian endocasts reveals that the pronounced sigmoidal shape characterizing the endocast of the placodontoid *Placodus gigas* (Neenan and Scheyer 2012) is markedly less expressed in the cyamodontoid *Parahenodus atan-censis* (de Miguel Chaves et al. 2020) or in nothosaurs and plesiosaurs (Edinger 1921; Carpenter 1997; Gómez Pérez 2008; Voeten et al. 2018a; Allemand et al. 2019). As pronounced brain flexure generally characterizes the early ontogenetic stages of brain development (e.g. crocodylians, Jirak and Janacek 2017; Beyrand et al. 2019; Lessner and Holliday 2020), differences in the degrees of flexure across sauropterygian endocasts may capture the influence of heterochronic evolution. Nevertheless, the highly flexed brain in *Placodus* may also reflect specific spatial constraints imposed by its specialized skull morphology. As such, the pronounced cephalic flexure observed in *Placodus* is accommodated in a particularly high, short, and stocky skull that facilitated feeding on hard-shelled mollusks. The subsequent reduction of cephalic flexure in *Parahenodus*, which is less durophagous than

Placodus (e.g. Pommery et al. 2021), as well as in eosauropterygians, appears to relate to their relative cranial elongation and associated cranial flattening (e.g. Voeten et al. 2018a).

Although the exact delimitation of endocranial components is somewhat uncertain in Sauropterygia, several changes in the relative size and the presence or absence of endocranial components are noticeable. The relative size of the pineal complex shows considerable variability, being very large in the placodontoid *Placodus gigas*, very small in the cyamodontoid *Parahenodus atancensis* and the plesiosaur *Libonectes morgani*, and of intermediate size in the nothosaurs *Nothosaurus marchicus* and *N. mirabilis* as well as the pliosaur *Acostasaurus pavachoquensis*. Similarly, the sauropterygian pituitary cast may exhibit variable relative sizes. Based on the size of the *sella turcica*, the pituitary was interpreted as large in *Placodus gigas* (Neenan and Scheyer 2012). In plesiosaurians, a distinct pituitary protrudes from the ventral surface of the endocast (Gómez Pérez 2008; Otero et al. 2018; Allemand et al. 2019; O’Gorman et al. 2021) and the proportionally large and long *sella turcica* associated with this structure is also consistent with a well-developed pituitary organ. However, the absence of a well-differentiated pituitary lobe on the endocasts of *Parahenodus atancensis* and *Nothosaurus marchicus* (Voeten et al. 2018a; de Miguel Chaves et al. 2020) potentially indicates that this structure was underdeveloped in these taxa. On the posterior part of the endocast, the cerebellum is not differentiated in placodonts and nothosauroids (Neenan and Scheyer 2012; Voeten et al. 2018a; de Miguel Chaves et al. 2020), whereas it forms a prominent structure in the elasmosaurids *Libonectes morgani* (Allemand et al. 2019) and *Alexandronectes zealandiensis* (O’Gorman et al. 2021). As this region is only described as “a moderate expansion” in the pliosaurid *Acostasaurus pavachoquensis* (Gómez Pérez 2008:p 90), it is unclear if a large cerebellum is shared by all plesiosaurians or only characterizes the family Elasmosauridae. Furthermore, the presence of a floccular recess is reported in the pliosauriid *Acostasaurus* and the elasmosaurid *Alexandronectes* (Gómez Pérez 2008; O’Gorman et al. 2021), whereas such a structure was not detected in the elasmosaurid plesiosaurian *Libonectes* (Carpenter 1997; Allemand et al. 2019), the placodonts *Placodus* and *Parahenodus* (Neenan and Scheyer 2012; de Miguel Chaves et al. 2020), and the nothosauroids *N. marchicus* and *N. mirabilis* (Edinger 1921; Voeten et al. 2018a). Although these modifications do not converge on a unidirectional trend along sauropterygian evolutionary history, they do capture endocast diversity across in the clade.

3.4.2 Brain-Size Evolution and Encephalization Quotient

In non-avian reptiles, the brain does not completely fill the endocranial cavity (e.g. Starck 1979; Jirak and Janacek 2017; Evers et al. 2019). Therefore, the cranial endocast does not capture the morphology of exclusively the brain but rather the superficial contours of all associated tissues in direct contact with the internal surface of the braincase, including the meninges, blood vessels, and cerebrospinal

fluids (Hopson 1979; Witmer and Ridgely 2009). These structures may account for a significant proportion of the endocranial space, importantly governing the degree to which the cranial endocast reflects the external brain shape (Witmer et al. 2008). A wide range of proportions between brain and endocranial space occur that depend on phylogeny (e.g. Kim and Evans 2014) and ontogenetic stage (e.g. Jirak and Janacek 2017). The absence of extant ichthyopterygian and sauropterygian representatives as well as the uncertain phylogenetic placement and anatomical idiosyncrasies of these groups may explain why reliable information on encephalization quotient (EQ) is virtually unavailable for these clades.

The only relevant EQ calculated so far has been proposed for *Nothosaurus marchicus* by Voeten et al. (2018a). If the studied specimen featured a body length (about 650 mm) to body mass ratio comparable with those of *Varanus keithhornei* or a juvenile alligator, its total body mass was estimated to range between 270 and 306 g (Voeten et al. 2018a). The volume of the complete endocranial cavity, excluding the poorly defined olfactory tract and olfactory lobes, was inferred to be circa 810 mm³, which corresponds with a brain mass between 0.4 and 0.8 g, depending on whether the brain fills 50% or 100% of the endocranial space. These relations converge on a reptilian encephalization quotient (REQ; Hurlburt 1996) between 0.15 and 0.35, which places *Nothosaurus marchicus* in the typical range of the relation between body weight and brain weight followed by extant reptilian taxa (Voeten et al. 2018a).

3.4.3 Sensory Evolution in Ichthyopterygia and Sauropterygia

Secondary invasions of the aquatic realm by amniotes are generally accompanied by profound reorganizations of their sensory systems (Thewissen and Nummela 2008). Recent studies into the sensory abilities of extinct taxa mostly employ computed tomography to facilitate non-destructive access to cranial endocasts and endosseous labyrinths. Based on the Principal of Proper Mass formulated by Jerison (1973), the relative size of different endocast regions inform on the animal's relative reliance on corresponding sensory capabilities. Nevertheless, because delimitations between endocranial regions are often lacking, such sensory inferences remain scarce for both Ichthyopterygia and Sauropterygia. This complicates the use of size as an indicator for the relative importance of a sensor. In addition, the degree to which the endocast captures the shape and size of the brain remains unknown for both groups but would strongly influence the extent to which endocast proportions truly reflect sensory dependencies. The lack of extant ichthyopterygians and sauropterygians, as well as their ambiguous phylogenetic bracketing, prevent objective corroboration of the morphometric relations between endocranium and brain. Although ichthyopterygian and sauropterygian endocasts may provide valuable clues towards inferring functional hypotheses, such biological interpretations therefore require due caution.

Ichthyopterygia

The limited information on ichthyopterygian endocranial anatomies prevents in-depth discussion on the evolution of their sensory abilities. Based on the potential large size of the olfactory region and optic lobes, McGowan (1973), Kirton (1983), and Marek et al. (2015) suggested that both olfaction and vision were well developed and important senses. Such inferences remain preliminary due to the poor delimitation of both brain regions (e.g. position and size of the olfactory bulbs relative to the olfactory tracts). However, as ichthyosaurs possess the proportionally and absolutely largest eyeballs of any vertebrate (Motani et al. 1999), the presence of enlarged optic lobes support the primacy of vision in these taxa. Ichthyosaur sensory capabilities and feeding strategies have been inferred from the orbit diameter of *Ophthalmosaurus* by comparing metrics of sensitivity, specifically using the f -number (ratio of focal length to aperture diameter; Motani et al. 1999), and resolving power (ratio of focal length to spacing of receptors in the retina; Humphries and Ruxton 2002), in concert with gastric contents. While it has been noted that *Ophthalmosaurus* represents an outlier even among ichthyosaurs regarding its extremely large eyes, cooperative adaptation to enable superb light sensitivity and visual acuity appears to generally govern the size and morphology of neoichthyosaurian eyes (Humphries and Ruxton 2002; Fernández et al. 2005).

The possibly enlarged olfactory system and the inferred enhanced sense of smell in ichthyosaurs, however, is somewhat unexpected, as it differs from most secondarily aquatic mammals and reptiles (e.g. Pihlström 2008). Nevertheless, it is not unique as similar enhanced olfaction was also reported in baleen whales (Thewissen et al. 2011). McGowan (1973) and Kirton (1983) both hypothesized that, without a secondary palate, the narial canals in ichthyosaurs were in direct contact with the buccal cavity rather than with the lungs. The external nares must therefore have been closed when the animal was submerged, as in crocodylians and cetaceans. Bony struts in the narial chamber that may have supported soft tissues used in olfaction have been reported in, for example, *Ichthyosaurus*, *Ophthalmosaurus*, and *Platypterygius* (McGowan 1973; Kear 2005; Moon and Kirton 2016). This arrangement could have allowed ichthyosaurs to employ their olfactory system when underwater (McGowan 1973), possibly through retained air volumes, for recognizing conspecifics (such as potential mates), tracking prey, or when evading predators (Marek et al. 2015). Additionally, the increasing complexity of the external narial opening in Ophthalmosauridae suggests some selective pressure to facilitate respiration as well as salt excretion (Fischer et al. 2014; Campos et al. 2020).

The dorsal surface of the endocast in both *Hauffiopteryx typicus* and *Ichthyosaurus cf. communis* exhibits a distinct bulge connected to the parietal foramen (also referred as pineal foramen; e.g. Chen et al. 2013; Lomax 2017) that is identified as the pineal complex. Across vertebrates, this term refers to the parapineal organ (also named parietal or pineal eye) and pineal organ (also termed posterior parietal organ, pineal gland or epiphysis; e.g. Quay 1979). As these organs may be variably associated with the parietal foramen (e.g. Smith et al. 2018), the exact internal organization of this structure in ichthyosaurs remains unknown. Therefore, the morphological

term “pineal complex” is preferred to designate this pineal-parapineal association. The parapineal and pineal organs both originated as photosensory organs. During vertebrate evolution, the pineal organ transformed into a photosensitive neuroendocrine gland (e.g. Quay 1979; Concha and Wilson 2001; Benoit et al. 2016; Smith et al. 2018). The vertebrate pineal complex is known to variably influence behavior, body temperature regulation, seasonal cycles, regulation of the circadian rhythm, and spatial orientation (e.g. Quay 1979; Tosini 1997). The structural persistence of a parietal foramen throughout ichthyopterygian evolutionary history advocates sustained dependence on photosensitive functions associated with the pineal complex. Both location and morphology of the parietal foramen vary substantially across ichthyosaurian diversity, with a general trend from exclusive perforation of the parietals in Early and Middle Triassic ichthyosaurs to a more anterior position situated between the parietals and frontals, or only in the frontals, in Euichthyosauria (e.g. Massare and Callaway 1990; Druckenmiller and Maxwell 2010; Fischer 2012; Lomax et al. 2019). However, the functional and sensory implications of this variability remain unknown and additional study is required to resolve their coupled physiological roles.

Comparisons of ichthyosaur labyrinths across Jurassic and Cretaceous taxa resolve surprisingly little modification over 100 million years of evolution (McGowan 1973; Kear 2005; Moon and Kirton 2016). Their morphologies, as interpreted here, present similarities with other pelagic reptiles such as sea turtles, plesiosaurs, and metriorhynchids (Georgi and Sipla 2008; Neenan et al. 2017; Evers et al. 2019; Schwab et al. 2020). For example, the thick semicircular canals observed in all these taxa seem to indicate shared physical constraints. Conversely, the possibly dorsoventrally tall and anteroposteriorly short ichthyosaur labyrinth differs from the typical morphology hypothesized for aquatic reptiles (Georgi and Sipla 2008), but require additional verification to further explore its divergent function from those generally reported in pelagic taxa (Neenan et al. 2017).

Sauropterygia

Among sauropterygians, the indistinct optic lobes in *Placodus gigas* and *Parahenodus atancensis* have been interpreted as indicative for limited dependence on visual acuity (de Miguel Chaves et al. 2020), while their olfactory capacities remain unknown. In both *Nothosaurus marchicus* and *Libonectes morgani*, the hard-to-resolve but potentially large-sized optic lobes coupled with the absence of indications for a pronounced development of the vomeronasal, olfactory, or mechanosensitive senses suggest that vision may have formed their primary contactless sensor (Voeten et al. 2018a; Allemand et al. 2019). Such relative reliance on vision in Eosauropterygia is corroborated by the large size of their dorsally positioned and somewhat anteriorly directed orbits, as well as by the potential presence of sclerotic rings throughout the entire clade. However, as the mesencephalic cast is known to be a poor proxy for the geometry of the corresponding brain region in adult non-avian reptiles (e.g. Jirak and Janacek 2017; Evers et al. 2019; Perez-Martinez and

Leal 2021), optic lobe sizes in both *Nothosaurus* and *Libonectes* may very well be over-estimated. Although their preserved geometries may still inform on proportional reliance relative to other sensory systems, direct inferences of visual acuities remain challenging.

Based on the length of the olfactory system in *Acostasaurus pavachoquensis*, Gómez Pérez (2008) suggested that both the olfactory and mechanosensitive senses were substantially developed in plesiosaurians. Despite previous assertions that underwater olfaction and contact-sensory perception optimized for prey detection were present in plesiosaurians (Cruickshank et al. 1991; Foffa et al. 2014), such inferences remain circumstantial. Comparisons with non-avian reptiles sharing a similar organization of the olfactory system (e.g. crocodylians; Jirak and Janacek 2017) show that the plesiosaurian olfactory system is characterized by exceptionally long and thin olfactory tracts coupled with proportionally small olfactory bulbs. Furthermore, the plesiosaurian rostral chamber suggested to accommodate an olfactory epithelium (Cruickshank et al. 1991) was later proposed to house salt glands (Voeten et al. 2018a). These inferences suggest a diminished sense of olfaction. In addition, no supportive neurosensory indications for a mechanosensor have yet surfaced beyond the intricate neurovascular infrastructure resolved in a plesiosaurian rostrum (Foffa et al. 2014). The similar endocasts of *A. pavachoquensis* and *L. morgani* provide ambiguous clues that highlight the challenges towards inferring olfaction and visual capacities from endocranial regions that are incomplete, poorly defined, or highly derived in Sauropterygia.

Contrary to ichthyosaurs, the sauropterygian pineal complex displays a distinct variability in relative size through their evolution. In non-avian reptiles, relative pineal size ranges have been correlated with latitude (e.g. Gundy et al. 1975; Ralph 1975) and thermoregulatory strategy (e.g. Hutchison and Kosh 1974; Ralph et al. 1979; Labra et al. 2010). However, these correlations are not consistently expressed across all studied taxa (see Labra et al. 2010; Connolly 2016), rendering pineal size an ambiguous proxy for physiological or ecological affinity. Cretaceous plesiosaurs recovered from high paleolatitudes may or may not feature a well-developed pineal foramen (Kear et al. 2006; O’Keefe et al. 2017), which challenges a straightforward relation between size and function of the pineal complex and latitudinal distribution. Furthermore, as both *Placodus* and pistosauroids (including plesiosaurs) preserve osteohistological indicators for elevated growth rate and metabolic performance (de Buffrénil and Mazin 1992; Krahl et al. 2013; Klein et al. 2015a; Fleischle et al. 2018), relative size reduction of the sauropterygian pineal complex cannot be unambiguously correlated with an increase in metabolic rate. Changes in the size of the pineal complex in Sauropterygia remain poorly understood. Although these likely capture shifts in photoreceptive strategies, additional study of morphology and physiological function of the reptilian pineal complex is required to conclusively interpret such diversity.

The relative size of the pituitary organ, as inferred directly from endocasts and *sellae turcicae*, is highly variable among Sauropterygia. The pituitary organ is an endocrine gland associated with the production of multiple hormones serving various purposes in reproductive cycles, growth, fluid balance, skin pigmentation, and

secondary gland control (e.g. Edinger 1942; Heller 1942, 1950; Saint Girons 1970; Butler and Hodos 2005). The size of the pituitary organ has been correlated with gigantism in sauropods (e.g. Edinger 1942; Balanoff et al. 2010), whereas in crocodylomorphs, enlargement and increased activity of the structure may aid in preventing dehydration in marine environments (e.g. Pierce et al. 2017; Schwab et al. 2021). Among studied Sauropterygia, such correlations remain inconclusive and incapable of explaining why the proportionally largest pituitary organ is encountered in *Placodus gigas*. In crocodylians and turtles, the *sella turcica* houses an enlarged venous sinus (“cavernous sinus;” of Saint Girons 1970; Porter et al. 2016), whereas in lepidosaurs, the lateral periphery of the *sella turcica* around the *crista trabecularis* can serve as the origin for important oculomotor musculature (Säve-Söderbergh 1946). As the *sella turcica* in *Placodus* may not exclusively enclose the pituitary organ, its apparent large size may not reflect the size of the pituitary organ.

The cerebellar casts of both *Libonectes morgani* and *Alexandronectes zealandiensis* constitute conspicuous components of their respective endocasts (Allemand et al. 2019; O’Gorman et al. 2021). The cerebellar domain forms a prominent and well-differentiated bulge in the two elasmosaurid plesiosaurians, notwithstanding that cerebellar dimensions, as reconstructed from endocasts, may also (partially) involve the venous system overlying the cerebellum (e.g. Aurboonyawat et al. 2008). Since the cerebellum is understood to play a significant role in maintaining postural equilibrium and controlling locomotory behavior (Thach and Bastian 2004; Butler and Hodos 2005), its large size in *Libonectes* and *Alexandronectes* may reflect the substantial cognitive requirements associated with extreme neck elongation in certain plesiosauromorph morphotypes and/or with plesiosaurian modes of paraxial locomotion (e.g. Carpenter et al. 2010; Liu et al. 2015). Such hypotheses require further testing against cerebellar morphologies of short-necked pliosaurids, such as that of *Acostasaurus pavachoquensis*, which remains mostly unknown.

A floccular recess (or fossa) is reported in both the pliosaurid *Acostasaurus pavachoquensis* and the elasmosaurid *Alexandronectes zealandiensis* (Gómez Pérez 2008; O’Gorman et al. 2021). The floccular recess houses the floccular lobe of the cerebellum that, via the vestibulocular and vestibulocollic reflexes, aids in coordination of extrinsic muscles of the eyes, retinal adjustment and coordination of eye-neck movements for image stabilization (e.g. Walsh et al. 2013). Although the general functions of the floccular lobe are well established, the relation between the size of the floccular recess and ecology and behavior across vertebrates is not clear (Walsh et al. 2013) and correlations were found in birds only (feeding categories and activity pattern; Ferreira-Cardoso et al. 2017). Irrespective of their size, the endocast expressions of the floccular recesses in *Acostasaurus* and *Alexandronectes* endocasts may nevertheless correlate with elevated visual processing capacity, oculomotor performance, and higher reliance on image stabilization. Such correlations are intuitively consistent with the active, agile and high-speed predation inferred for the short-neck pliosaurid *Acostasaurus*. Conversely, such correlations appear less consistent with the ecomorphology of the long-neck elasmosaurid *Alexandronectes* suggested to have been an ambush-predator specialized for cruising at low to intermediate speeds (Carpenter et al. 2010). Although vision likely also represents a

crucial sense in ambush predation (e.g. Shine 2005; Nagloo et al. 2016) and may explain the presence of a distinct floccular recess in *Alexandronectes*, the absence of such a structure in the endocast of the elasmosaurid *Libonectes morgani* (Carpenter 1997; Allemand et al. 2019) questions casts doubt on its distribution and this interpretation.

The bony labyrinth of Sauropterygia experienced distinct transformations along its evolutionary history. Placodonts, pachypleurosaurs, nothosaurs, and basal pistosaurs have dorsoventrally compact, anteroposteriorly elongate labyrinths with gracile semicircular canals, resembling the generalized reptilian morphology, whereas plesiosaurs feature compact, bulbous labyrinths with stout semicircular canals (Neenan et al. 2017). Neenan et al. (2017) concluded that this shift in labyrinth shape coincides with the transition from nearshore to pelagic environments and the acquisition of the unique four-flipped underwater flight locomotion that characterizes plesiosaurs. However, similarly compact and bulbous labyrinths have been observed in aquatic taxa that do not feature plesiosaur-like locomotory strategies (e.g. metriorhynchids; Schwab et al. 2020) and even in highly terrestrial testudines (e.g. *Indotestudo elongata*; Evers et al. 2019), which confuses such ecological correlations. Neenan et al. (2017) also reported differences in the relative anteroposterior length of the sauropterygian labyrinth. Bottom-walking placodonts feature proportionally longer labyrinths than actively swimming eosauroptrygians, and short-necked plesiosaurians (i.e. pliosauromorphs) have particularly small labyrinths relative to head size. Contrary to labyrinth shape, changes in relative labyrinth length appear to not conservatively capture the transition from nearshore to pelagic environments, as corresponding shifts have not been documented between nothosaurs, basal pistosaurs, and long-necked plesiosaurians (Neenan et al. 2017). This proxy may, however, have recorded transitions in aquatic foraging strategy, for example, from habitual piscivory across early plesiosaurs to obligate megacarnivory in derived pliosauromorphs. As important components of the equilibrioceptive system, bony labyrinths contribute to gaze stabilization by detecting angular accelerations of the head and driving vestibuloocular and vestibulocollic reflexes (Spoor and Zonneveld 1998). Pliosauromorphs were adapted for high-speed maneuverability while pursuing and capturing large prey, which was likely subdued and processed using forceful agitation or twist-rolling movements (e.g. Taylor and Cruickshank 1993; McHenry 2009; Carpenter et al. 2010). Their reduced labyrinth sizes may reflect attenuated sensory sensitivity to prevent sensory overstimulation during vigorous head movements that cannot be stabilized with their short necks.

3.5 Future Directions: Outstanding Questions and Perspectives

The recent embracement of computed tomography in paleoneurology has considerably improved accessibility to, and the availability of, endocranial anatomies of Ichthyopterygia and Sauropterygia. Nevertheless, this is limited to only a few

species and therefore hardly captures their full diversity. Since extensive endocranial explorations of Ichthyosauromorpha have thus far remained restricted to Neoiichthyosauria, comparative information from Triassic ichthyosaurs is virtually absent. Well-preserved specimens from Early and Middle Triassic representatives, such as *Chaohusaurus*, *Mixosaurus*, and *Guizhouichthyosaurus* (Motani 1999b; Shang et al. 2012; Zhou et al. 2017), would be suitable candidates for CT visualization towards resolving endocranial morphologies associated with both basal- and intermediate-grade body plans. Additionally, as different ecologies have been suggested for the large, ram-feeder *Guizhouichthyosaurus* (Motani et al. 2013; Jiang et al. 2020) and the smaller, (diversely) durophagous *Chaohusaurus* and *Mixosaurus* (Motani 2005b; Zhou et al. 2017), the consideration of such taxa would grant insight into endocranial heterogeneity across this niche disparity.

The presently known endocranial diversity of Sauropterygia discontinuously samples the ecological gradient from near-shore bottom foraging to a gamut of agile pelagic lifestyles. Evaluation of additional taxa along this ecomorphological range, for example through the nothosauroids *Simosaurus gaillardoti* (de Miguel Chaves et al. 2018a) and *Lariosaurus xingyiensis* (Lin et al. 2017), the basal pistosaur *Yunguisaurus liae* (Zhao et al. 2008) and the pliosaur *Rhomaleosaurus cramptoni* (Smith and Dyke 2008), would produce a valuable comparative library to facilitate exploration of key sauropterygian endocranial modifications. This evolutionary gradient appropriately spans gradual colonization of increasingly pelagic environments, the progressive acquisition of the “four-limb paddling” mode of locomotion, and shifts towards predation on larger and more mobile prey. The endocasts in some of these key fossil taxa are notoriously challenging to access with conventional computed tomographic techniques because specimens remain embedded in lithologies with comparable radiodensities to the contained skeletal elements, are permeated with abundant metallic inclusions, or are crushed flat. However, solutions tailored to imaging flat fossils (e.g. Voeten et al. 2018b) and post-processing protocols for alleviating the adverse effects of metallic inclusions (e.g. Cau et al. 2017) may aid in overcoming these challenges. Finally, the use of synchrotron microtomography could help in improving data contrast and resolve fine-scaled features (e.g. Voeten et al. 2018a; Miedema et al. 2020).

Ecological associations including ichthyopterygians alongside sauropterygians and other marine reptile groups are regularly reported (e.g. Kear et al. 2018; Lazo et al. 2018; Vincent et al. 2020), with some even involving members of both their respective apex predator guilds (e.g. Bardet et al. 2016). The coexistence of such presumed ecological competitors raises questions on their mutual interactions regarding niche partitioning versus competitive exclusion. Investigations of these exchanges have thus far focused on paleoecological inferences from external morphological characters, most notably dentition (e.g. Massare 1987; Foffa et al. 2018; Reeves et al. 2020). However, neurosensory specializations identified through comparative endocranial mapping could importantly supplement the insights gained from skeletal morphology (e.g. Schwab et al. 2020), functional analysis (e.g. Ballell et al. 2019), and habitat distribution towards reconstructing extinct ecological communities and, ultimately, ecosystems (e.g. Reeves et al. 2020). Sensory inferences

for both Ichthyopterygia and Sauropterygia remain challenging because the delimitation of endocranial components is often ambiguous. It is therefore crucial to understand the spatial relationships between the brain, its subregions, and the skull of extant non-avian reptiles in detail. In addition, the position, size, and shape of the different structures surrounding the brain in the cranial cavity of these taxa (such as the venous sinus and endolymphatic sac) need to be mapped and examined to better resolve their impact on endocast morphology (e.g. Werneburg et al. 2021). Establishing standardized landmarks that optimally capture the location and extent of each individual brain compartment could shed more light on the functional and comparative significance of ichthyopterygian and sauropterygian endocasts. Insights gleaned from additional studies correlating endocranial morphologies in extant non-avian reptiles with their functions to functional and ecological implications will aid in calibrating the endocast interpretations of these fossil taxa.

In-depth assessment of the phylogenetic signals contained in endocranial morphology (e.g. Macrini et al. 2006, 2007; Corfield et al. 2015; Allemand et al. 2017b) may prove instrumental in resolving uncertain relationships within Ichthyopterygia and Sauropterygia (e.g. Benson et al. 2012; Neenan et al. 2015; Moon 2019; Zverkov and Jacobs 2020). Although endocranial characters are still underrepresented in phylogenetic studies, such markers may serve to expand or refine character state matrices. Secondly aquatic adaptation of Mesozoic reptiles often involves skeletal paedomorphism (e.g. Araújo et al. 2015b; Motani et al. 2015b; Moon and Kirton 2016) and may contribute a puzzling interplay of heterochronic effects (e.g. the skull of *Nothosaurus marchicus*; Voeten et al. 2018a) that render the unambiguous recognition of skeletal maturity and reliable phylogenetic indicators particularly challenging. Better insight into the influence of ontogeny on endocast morphologies is therefore imperative to reliably discern ontogeny-dependent and taxon-specific endocranial characters. Furthermore, because the relations of Ichthyopterygia and Sauropterygia within Diapsida remain to be conclusively resolved, the assessment of early representatives (such as the ichthyosauromorph *Hupehsuchus* [Wu et al. 2016] and the placodontiform *Palatodonta* [Neenan et al. 2013]), relative to candidate outgroups presumably conserving their ancestral condition (e.g., *Eusauropsphargis* [Scheyer et al. 2017] or *Claudiosaurus* [Carroll 1981] for Sauropterygia) could help to resolve their deeper Paleozoic origins and changes in endocranial anatomy associated with the broader transition from terrestrial to aquatic life.

3.6 Conclusions

Secondary adaptation to the aquatic realm involves some of the most remarkable transformations in tetrapod evolution. As historical recorders of neuroanatomical evolution, cranial endocasts disclose valuable information about the central nervous systems during these eye-catching chapters in the history of life. Although Sauropterygia played an integral role during the establishment and early

development of paleoneurology as a field, the potential of in-depth assessment and comparison of ichthyopterygian and sauropterygian endocranial features has only recently begun to be realized and remains overshadowed by the wealth of neurosensory research into other extinct diapsids.

We reviewed the present knowledge on endocranial configurations of both Ichthyopterygia and Sauropterygia with an emphasis on the anatomical and neurosensory modifications associated with their return to, and subsequent colonization of, aquatic environments. While the paucity of insight across the paleoneurology of ichthyosaurs has thus far prevented detailed reconstruction of gradual endocranial changes along their evolutionary history, comparisons with plesiosaurs nevertheless inform on their distinctive endocranial organizations in broadly comparable pelagic ecologies. The diverse endocranial arrangements observed in Sauropterygia reflect the ecomorphological flexibility of the clade that ranges from near-shore bottom foraging to agile pelagic cruising. Particular ecological innovations and developments that drove trophic, locomotory, and metabolic diversification in Sauropterygia can be traced through progressive modifications of the relative size, shape, and proportions of the endocranial vault, endosseous labyrinths, and peripheral neurosensory infrastructures.

The endocranial anatomy observed in ichthyopterygians and sauropterygians suggests that their colonization of the aquatic realm was facilitated by distinct sensory adaptations. Although neurosensory inferences informed by endocranial architectures should continue to reserve an appropriate degree of caution, further exploration and contextualization of this neurosensory diversity will help to: (1) identify conservative structures that recorded evolutionary ancestries; (2) recognize the trophic, locomotory, and sensory adaptations that accompanied rapid invasion of aquatic niches; and (3) resolve the key specializations that drove progressive habitat partitioning.

Acknowledgments We thank the editors María Teresa Dozo, Ariana Paulina-Carabajal, Thomas E. Macrini and Stig Walsh, for inviting us to contribute to this special volume. We are grateful to Serjoscha W. Evers, Carlos de Miguel Chaves, and Torsten M. Scheyer for offering feedback that helped to improve this contribution. Henk Wim van Dorssen (then Museum TwentseWelle, Enschede, the Netherlands) graciously provided the picture of the *Nothosaurus* cranium included as Fig. 2.6. We thank Matt Williams (Bath Royal Literary and Scientific Institute), Sandra Chapman (Natural History Museum, London), Erin Maxwell (Staatliches Museum für Naturkunde Stuttgart), Mark Evans (New Walk Museum, Leicester), Mark Mavrogordato (μ -Vis, University of Southampton), and Rhinopolis Museum (Ganat, France) for access to specimens. We acknowledge the Naturkundemuseum Erfurt (Erfurt, Germany) for curating specimen NME 16/4 of which the endosseous labyrinth was here visualized through data created by Neenan et al. (2017) and made available through MorphoMuseum (<https://morphomuseum.com/specimenfiles/view/326>). We also thank all contributors to PhyloPic for making the silhouettes presented in Figs. 3.1 and 3.2 freely available. BCM is funded by NERC BETR Project grant NE/P013724/1 and ERC grant 788203 (INNOVATION).

References

- Allemand R, Bardet N, Houssaye A et al (2017a) Virtual reexamination of a plesiosaurian specimen (Reptilia, Plesiosauria) from the late cretaceous (Turonian) of Goulmima, Morocco, using computed tomography. *J Vertebr Paleontol* 37. <https://doi.org/10.1080/02724634.2017.1325894>
- Allemand R, Boistel R, Daghfous G et al (2017b) Comparative morphology of snake (Squamata) endocasts: evidence of phylogenetical and ecological signals. *J Anat* 231:849–868
- Allemand R, Houssaye A, Bardet N et al (2019) Endocranial anatomy of plesiosaurians (Reptilia, Plesiosauria) from the Late Cretaceous (Turonian) of Goulmima (southern Morocco). *J Vertebr Paleontol* 39. <https://doi.org/10.1080/02724634.2019.1595636>
- Andrews CW (1910) A descriptive catalogue of the marine reptiles of the Oxford clay. Part I. British Museum (Nat Hist). <https://doi.org/10.5962/bhl.title.61785>
- Appleby RM (1961) On the cranial morphology of ichthyosaurs. *Proc Zool Soc Lond* 137:333–370
- Araújo R, Polcyn MJ, Schulp AS et al (2015a) A new elasmosaurid from the early Maastrichtian of Angola and the implications of girdle morphology on swimming style in plesiosaurs. *Neth J Geosci* 94:109–120
- Araújo R, Polcyn MJ, Lindgren J et al (2015b) New aristonecine elasmosaurid plesiosaur specimens from the Early Maastrichtian of Angola and comments on paedomorphism in plesiosaurs. *Neth J Geosci* 94:93–108
- Auen EL, Langebartel DA (1977) The cranial nerves of the colubrid snakes *Elaphe* and *Thamnophis*. *J Morphol* 154:205–222
- Aurboonyawat T, Pereira V, Kring T et al (2008) Patterns of the cranial venous system from the comparative anatomy in vertebrates: part II. The lateral-ventral venous system. *Interv Neuroradiol* 14:21–31
- Balanoff AM, Bever GS, Ikejiri T (2010) The braincase of *Apatosaurus* (Dinosauria: Sauropoda) based on computed tomography of a new specimen with comments on variation and evolution in sauropod neuroanatomy. *Am Mus Novit* 2010:1–32
- Ballell A, Moon BC, Porro LB et al (2019) Convergence and functional evolution of longirostry in crocodylomorphs. *Palaeontology* 62:867–887
- Bardet N, Falconnet J, Fischer V et al (2014) Mesozoic marine reptile palaeobiogeography in response to drifting plates. *Gondwana Res* 26:869–887
- Bardet N, Fischer V, Machalski M (2016) Large predatory marine reptiles from the Albian–Cenomanian of Annopol, Poland. *Geol Mag* 153:1–16
- Benoit J, Abdala F, Manger PR et al (2016) The sixth sense in mammalian forerunners: variability of the parietal foramen and the evolution of the pineal eye in South African Permo-Triassic eutheriodont therapsids. *Acta Palaeontol Pol* 61:777–789
- Benson RBJ, Bates KT, Johnson MR et al (2011) Cranial anatomy of *Thalassiodracon hawkinsii* (Reptilia, Plesiosauria) from the Early Jurassic of Somerset, United Kingdom. *J Vertebr Paleontol* 31:562–574
- Benson RBJ, Evans M, Druckenmiller PS (2012) High diversity, low disparity and small body size in plesiosaurs (Reptilia, Sauropterygia) from the Triassic–Jurassic boundary. *PLoS One* 7. <https://doi.org/10.1371/journal.pone.0031838>
- Benson RB, Ketchum HF, Naish D et al (2013) A new leptocleidid (Sauropterygia, Plesiosauria) from the Vectis Formation (Early Barremian–early Aptian; Early Cretaceous) of the Isle of Wight and the evolution of Leptocleididae, a controversial clade. *J Syst Palaeontol* 11:233–250
- Benson RBJ, Evans M, Taylor MA (2015) The anatomy of *Stratesaurus* (Reptilia, Plesiosauria) from the lowermost Jurassic of Somerset, United Kingdom. *J Vertebr Paleontol* 35:e933739. <https://doi.org/10.1080/02724634.2014.933739>
- Bernard A, Lécuyer C, Vincent P et al (2010) Regulation of body temperature by some Mesozoic marine reptiles. *Science* 328:1379–1382
- Beyrand V, Voeten DFAE, Bureš S et al (2019) Multiphase progenetic development shaped the brain of flying archosaurs. *SciRep* 9:10807. <https://doi.org/10.1038/s41598-019-46959-2>

- Bindellini G, Wolniewicz A, Miedema F et al (2021) Cranial anatomy of *Besanosaurus leptorhynchus* Dal Sasso & Pinna, 1996 (Reptilia: Ichthyosauria) from the Middle Triassic Besano Formation of Monte San Giorgio, Italy/Switzerland: taxonomic and palaeobiological implications. Peer J 9:e11179. <https://doi.org/10.7717/peerj.11179>
- Brown D, Vincent P, Bardet N (2013) Osteological redescription of the skull of *Microcleidus homalospondylus* (Sauropterygia, Plesiosauria) from the lower Jurassic of England. J Paleontol 87:537–549
- Buchholtz EA, Seyfarth EA (1999) The gospel of the fossil brain: Tilly Edinger and the science of paleoneurology. Brain Res Bull 48:351–361
- Buchholtz EA, Seyfarth EA (2001) The study of “fossil brains”: Tilly Edinger (1897–1967) and the beginnings of paleoneurology. Bioscience 51:674–682
- Butler AB, Hodos W (eds) (2005) Comparative vertebrate neuroanatomy: evolution and adaptation. Wiley, Hoboken
- Camp CL (1980) Large ichthyosaurs from the upper triassic of Nevada. Palaeontogr Abt A 170:139–200
- Campbell JA, Mitchell MT, Ryan MJ et al (2021) A new elasmosaurid (Sauropterygia: Plesiosauria) from the non-marine to paralic Dinosaur Park Formation of southern Alberta, Canada. Peer J 9:e10720. <https://doi.org/10.7717/peerj.10720>
- Campos L, Fernández MS, Herrera Y (2020) A new ichthyosaur from the Late Jurassic of north-west Patagonia (Argentina) and its significance for the evolution of the narial complex of the ophthalmosaurids. Zool J Linn Soc 188:180–201
- Carpenter K (1997) Comparative cranial anatomy of two North American Cretaceous plesiosaurs. In: Callaway JM, Nicholls EL (eds) Ancient marine reptiles. Academic Press, San Diego, pp 191–216
- Carpenter K, Sanders F, Reed B et al (2010) Plesiosaur swimming as interpreted from skeletal analysis and experimental results. Trans Kans Acad Sci 113:1–34
- Carroll RL (1981) Plesiosaur ancestors from the Upper Permian of Madagascar. Philos T R Soc Lond B Biol Sci 293:315–383
- Carroll RL, Gaskill P (1985) The nothosaur *Pachypleurosaurus* and the origin of plesiosaurs. Philos T R Soc Lond B Biol Sci 309:343–393
- Cau A, Beyrand V, Voeten DFAE et al (2017) Synchrotron scanning reveals amphibious ecomorphology in a new clade of bird-like dinosaurs. Nature 552:395–399
- Čerňanský A, Klein N, Soták J et al (2018) A Middle Triassic pachypleurosaur (Diapsida: Eosauropterygia) from a restricted carbonate ramp in the Western Carpathians (Gutenstein Formation, Fatric Unit): paleogeographic implications. Geol Carpath 69:3–16
- Chatterjee S, Small BJ (1989) New plesiosaurs from the Upper Cretaceous of Antarctica. Geol Soc Spec Publ 47:197–215
- Chen X, Sander PM, Cheng L et al (2013) A new Triassic primitive ichthyosaur from Yuanan, South China. Acta Geol Sin (English Edition) 87:672–677
- Chen X, Motani R, Cheng L et al (2014) The enigmatic marine reptile *Nanchangosaurus* from the lower Triassic of Hubei, China and the phylogenetic affinities of Hupehsuchidae. PLoS One 9. <https://doi.org/10.1371/journal.pone.0102361>
- Clarke J, Etches S (1992) Predation among Jurassic reptiles. Proc Dorset Nat Hist Archaeol Soc 113:202–205
- Cleary TJ, Moon BC, Dunhill AM et al (2015) The fossil record of ichthyosaurs, completeness metrics and sampling biases. Palaeontology 58:521–536
- Concha ML, Wilson SW (2001) Asymmetry in the epithalamus of vertebrates. J Anat 199:63–84
- Connolly A (2016) Exploring the relationship between paleobiogeography, deep-diving behavior, and size variation of the parietal eye in mosasaurs. PhD dissertation, University of Kansas
- Corfield JR, Price K, Iwaniuk AN et al (2015) Diversity in olfactory bulb size in birds reflects allometry, ecology and phylogeny. Front Neuroanat 9. <https://doi.org/10.3389/fnana.2015.00102>
- Cruikshank ARI, Small PG, Taylor MA (1991) Dorsal nostrils and hydrodynamically driven underwater olfaction in plesiosaurs. Nature 352:62–64

- de Braga M, Rieppel O (1997) Reptile phylogeny and the interrelationships of turtles. *Zool J Linnean Soc* 120:281–354
- de Buffrénil V, Mazin JM (1992) Contribution de l'histologie osseuse à l'interprétation paléobiologique du genre *Placodus* Agassiz, 1883 (Reptilia, Placodontia). *Rev Paléobiol* 11:397–407
- de Miguel Chaves C, Ortega F, Pérez-García A (2018a) Cranial variability of the European Middle Triassic sauropterygian *Simosaurus gaillardoti*. *Acta Palaeontol Pol* 63:315–326
- de Miguel Chaves C, Ortega F, Pérez-García A (2018b) A new placodont from the Upper Triassic of Spain provides new insights on the acquisition of the specialized skull of Henodontidae. *Pap Palaeontol* 4:567–576
- de Miguel Chaves C, Ortega F, Pérez-García A (2018c) New highly pachyostotic nothosauroid interpreted as a filter-feeding Triassic marine reptile. *Biol Lett* 14:20180130
- de Miguel Chaves C, Serrano A, Ortega F et al (2020) Braincase and endocranium of the Placodont *Parahenodus atancensis* de Miguel Chaves, Ortega & Pérez-García, 2018, a representative of the highly specialized clade Henodontidae. *C R Palevol* 19:173–186
- Dick DG, Maxwell EE (2015) The evolution and extinction of the ichthyosaurs from the perspective of quantitative ecospace modelling. *Biol Lett* 11:20150339. <https://doi.org/10.1098/rsbl.2015.0339>
- Druckenmiller PS (2002) Osteology of a new plesiosaur from the Lower Cretaceous (Albian) Thermopolis Shale of Montana. *J Vertebr Paleontol* 22:29–42
- Druckenmiller PS, Russell AP (2008) Skeletal anatomy of an exceptionally complete specimen of a new genus of plesiosaur from the Early Cretaceous (Early Albian) of northeastern Alberta, Canada. *Palaeontogr Abt A* 283:1–33
- Druckenmiller PS, Maxwell EE (2010) A new lower Cretaceous (lower Albian) ichthyosaur genus from the Clearwater Formation, Alberta, Canada. *Can J Earth Sci* 47:1037–1053
- Edinger T (1921) Über *Nothosaurus*. I. Ein Steinkern der Schädelhöhle. *Senckenb* 3:121–129
- Edinger T (1925) Das Zentralnervensystem von *Placodus gigas*. *Abh Senckenb Naturforsch Ges* 88:311–318
- Edinger T (1928) Über einige fossile Gehirne. *Pal Z* 9:379–402
- Edinger T (1942) The pituitary body in giant animals fossil and living: a survey and a suggestion. *Q Rev Biol* 17:31–45
- Evans M (1999) A new reconstruction of the skull of the Callovian elasmosaurid plesiosaur *Muraenosaurus leedsii* Seeley. *Mercian Geol* 14:191–198
- Evans M (2012) A new genus of plesiosaur (Reptilia: Sauropterygia) from the Pliensbachian (Early Jurassic) of England, and a phylogeny of the Plesiosauria. PhD Dissertation, University of Leicester
- Evers SW, Neenan JM, Ferreira GS et al (2019) Neurovascular anatomy of the protostegid turtle *Rhinochelys pulchriceps* and comparisons of membranous and endosseous labyrinth shape in an extant turtle. *Zool J Linnean Soc* 187:800–828
- Fernández MS, Maxwell EE (2012) The genus *Arthropterygius* Maxwell (Ichthyosauria: Ophthalmosauridae) in the Late Jurassic of the Neuquén Basin, Argentina. *Geobios* 45:535–540
- Fernández MS, Archuby F, Talevi M et al (2005) Ichthyosaurian eyes: paleobiological information content in the sclerotic ring of *Caypullisaurus* (Ichthyosauria, Ophthalmosauria). *J Vertebr Paleontol* 25:330–337
- Ferreira-Cardoso S, Araújo R, Martins NE et al (2017) Floccular fossa size is not a reliable proxy of ecology and behaviour in vertebrates. *Sci Rep* 7:1–11
- Fischer V (2012) New data on the ichthyosaur *Platypterygius hercynicus* and its implications for the validity of the genus. *Acta Palaeontol Pol* 57:123–134
- Fischer V, Masure E, Arkhangelsky MS et al (2011) A new Barremian (Early Cretaceous) ichthyosaur from western Russia. *J Vertebr Paleontol* 31:1010–1025
- Fischer V, Maisch MW, Naish D et al (2012) New ophthalmosaurid ichthyosaurs from the European lower cretaceous demonstrate extensive ichthyosaur survival across the Jurassic–cretaceous boundary. *PLoS One* 7. <https://doi.org/10.1371/journal.pone.0029234>

- Fischer V, Arkhangelsky MS, Naish D et al (2014) *Simbirskiasaurus* and *Pervushovisaurus* reassessed: implications for the taxonomy and cranial osteology of Cretaceous platypterygiine ichthyosaurs. *Zool J Linnean Soc* 171:822–841
- Fischer V, Bardet N, Benson RBJ et al (2016) Extinction of fish-shaped marine reptiles associated with reduced evolutionary rates and global environmental volatility. *Nat Commun*:7. <https://doi.org/10.1038/ncomms10825>
- Flannery Sutherland JT, Moon BC, Stubbs TL et al (2019) Does exceptional preservation distort our view of disparity in the fossil record? *Proc R Soc B* 286. <https://doi.org/10.1098/rspb.2019.0091>
- Fleischle CV, Wintrich T, Sander PM (2018) Quantitative histological models suggest endothermy in plesiosaurs. *Peer J* 6. <https://doi.org/10.7717/peerj.4955>
- Foffa D, Sassoon J, Cuff AR et al (2014) Complex rostral neurovascular system in a giant plesiosaur. *Naturwissenschaften* 101:453–456
- Foffa D, Young MT, Stubbs TL et al (2018) The long-term ecology and evolution of marine reptiles in a Jurassic seaway. *Nat Ecol Evol* 2:1548–1555
- Fröbisch NB, Sander PM, Rieppel O (2006) A new species of *Cymbospondylus* (Diapsida, Ichthyosauria) from the Middle Triassic of Nevada and a re-evaluation of the skull osteology of the genus. *Zool J Linnean Soc* 147:515–538
- Fröbisch NB, Fröbisch J, Sander PM et al (2013) Macropredatory ichthyosaur from the Middle Triassic and the origin of modern trophic networks. *Proc Natl Acad Sci* 110:1393–1397
- Georgi JA, Sipla JS (2008) Comparative and functional anatomy of balance in aquatic reptiles and birds. In: Thewissen JGM, Nummela S (eds) *Sensory evolution on the threshold: adaptations in secondarily aquatic vertebrates*. University of California Press, Berkeley, pp 233–256
- Gómez Pérez M (2008) The palaeobiology of an exceptionally preserved Colombian plesiosaur (Sauropterygia: Plesiosauria). PhD Dissertation, University of Cambridge
- Gómez-Pérez M, Noè LF (2017) Cranial anatomy of a new plesiosaurid *Acostasaurus pavachoquensis* from the Lower Cretaceous of Colombia, South America. *Palaeontogr. Abt A* 2017:5–42
- Gorce F (1960) Etude de quelques vertébrés du Muschelkalk du Djebel Rehach (Sud tunisien). *Mém Soc géol Fr* 88:1–33
- Gundy GC, Ralph CL, Wurst GZ (1975) Parietal eyes in lizards: zoogeographical correlates. *Science* 190:671–673
- Gutarra S, Moon BC, Rahman IA et al (2019) Effects of body plan evolution on the hydrodynamic drag and energy requirements of swimming in ichthyosaurs. *Proc R Soc B* 286. <https://doi.org/10.1098/rspb.2018.2786>
- Haas G (1981) A fragmentary skull of *Simosaurus* (Reptilia: Sauropterygia) from the Middle Triassic of the Makhtesh Ramon, Israel. *Israel J Zool* 30:30–34
- Heller H (1942) The posterior pituitary principles of a species of reptile (*Tropidonotus natrix*) with some remarks on the comparative physiology of the posterior pituitary gland generally. *J Physiol* 101:317–326
- Heller H (1950) The comparative physiology of the neurohypophysis. *Cell Mol Life Sci* 6:368–376
- Hopson JA (1979) Paleoneurology. In: Gans C, Northcutt RG, Ulinski P (eds) *Biology of the reptilia (Neurology A)* vol 9. Academic, New York, pp 39–146
- Houssaye A (2009) “Pachyostosis” in aquatic amniotes: a review. *Integr Zool* 4:325–340
- Humphries S, Ruxton GD (2002) Why did some ichthyosaurs have such large eyes? *J Exp Biol* 205:439–441
- Hurlburt GR (1996) Relative brain size in recent and fossil amniotes: determination and interpretation. University of Toronto, PhD Dissertation
- Hutchison VH, Kosh RJ (1974) Thermoregulatory function of the parietal eye in the lizard *Anolis carolinensis*. *Oecologia* 16:173–177
- Jerison H (1973) *Evolution of the brain and intelligence*. Academic, New York
- Ji C, Jiang D, Motani R et al (2016) Phylogeny of the Ichthyopterygia incorporating recent discoveries from South China. *J Vertebr Paleontol* 36. <https://doi.org/10.1080/02724634.2015.1025956>

- Jiang D, Motani R, Hao W et al (2008) New primitive ichthyosaurian (Reptilia, Diapsida) from the Middle Triassic of Panxian, Guizhou, southwestern China and its position in the Triassic biotic recovery. *Prog Nat Sci* 18:1315–1319
- Jiang D, Motani R, Tintori A et al (2020) Evidence supporting predation of 4-m marine reptile by Triassic megapredator. *iScience* 23:101347. <https://doi.org/10.1016/j.isci.2020.101347>
- Jirak D, Janacek J (2017) Volume of the crocodylian brain and endocast during ontogeny. *PLoS One* 12. <https://doi.org/10.1371/journal.pone.0178491>
- Kear BP (2005) Cranial morphology of *Platypterygius longmani* Wade, 1990 (Reptilia: Ichthyosauria) from the Lower Cretaceous of Australia. *Zool J Linnean Soc* 145:583–622
- Kear BP, Schroeder NI, Lee MS (2006) An archaic crested plesiosaur in opal from the Lower Cretaceous high-latitude deposits of Australia. *Biol Lett* 2:615–619
- Kear BP, Fordyce RE, Hiller N et al (2018) A palaeobiogeographical synthesis of Australasian Mesozoic marine tetrapods. *Alcheringa* 42:461–486
- Ketchum HF, Benson RB (2010) Global interrelationships of Plesiosauria (Reptilia, Sauropterygia) and the pivotal role of taxon sampling in determining the outcome of phylogenetic analyses. *Biol Rev* 85:361–392
- Klein N (2009) Skull morphology of *Anarosaurus heterodontus* (Reptilia: Sauropterygia: Pachypleurosauria) from the Lower Muschelkalk of the Germanic Basin (Winterswijk, The Netherlands). *J Vertebr Paleontol* 29:665–676
- Klein N (2012) Postcranial morphology and growth of the pachypleurosaur *Anarosaurus heterodontus* (Sauropterygia) from the Lower Muschelkalk of Winterswijk, The Netherlands. *Pal Z* 86:389–408
- Klein N, Albers PCH (2009) A new species of the sauropsid reptile *Nothosaurus* from the Lower Muschelkalk of the western Germanic Basin, Winterswijk, The Netherlands. *Acta Palaeontol Pol* 54:589–598
- Klein N, Griebeler EM (2016) Bone histology, microanatomy, and growth of the nothosauroid *Simosaurus gaillardoti* (Sauropterygia) from the Upper Muschelkalk of southern Germany/Baden-Württemberg. *C R Palevol* 15:142–162
- Klein N, Sander PM (2019) *Anarosaurus heterodontus* – the least aquatic pachypleurosaur. *Star* 16:226–233
- Klein N, Houssaye A, Neenan JM et al (2015a) Long bone histology and microanatomy of Placodontia (Diapsida: Sauropterygia). *Contrib Zool* 84:59–84
- Klein N, Voeten DFAE, Lankamp J et al (2015b) Postcranial material of *Nothosaurus marchicus* from the Lower Muschelkalk (Anisian) of Winterswijk, The Netherlands, with remarks on swimming styles and taphonomy. *Pal Z* 89:961–981
- Klein N, Sander PM, Krahl A et al (2016) Diverse aquatic adaptations in *Nothosaurus* spp. (Sauropterygia)—inferences from humeral histology and microanatomy. *PLoS ONE* 11. <https://doi.org/10.1371/journal.pone.0158448>
- Kim R, Evans D (2014) Relationships among brain, endocranial cavity, and body sizes in reptiles. In: Maxwell E, Miller-Camp J (eds) Society of Vertebrate Paleontology 74th Annual Meeting, Berlin, Germany, 5–8 November 2014
- Kirton AM (1983) A review of British Upper Jurassic Ichthyosaurs. PhD Dissertation, University of New-castle-upon-Tyne
- Koken E (1890) Über die Bildung des Schädels, der Gehirnhöhle und des Gehörorgans bei der Gattung *Nothosaurus*. *Sitzungber Ges Naturf Freunde Berl* 1890:108–111
- Koken E (1893) Beiträge zur Kenntnis der Gattung *Nothosaurus*. *Z Dtsch Geol Ges* 45:337–377
- Krahl A, Klein N, Sander PM (2013) Evolutionary implications of the divergent long bone histologies of *Nothosaurus* and *Pistosaurus* (Sauropterygia, Triassic). *BMC Evol Biol* 13. <https://doi.org/10.1186/1471-2148-13-123>
- Labra A, Voje KL, Seligmann H et al (2010) Evolution of the third eye: a phylogenetic comparative study of parietal-eye size as an ecophysiological adaptation in *Liolaemus* lizards. *Biol J Linn Soc* 101:870–883

- Lazo DG, Talevi M, Cataldo CS et al (2018) Description of ichthyosaur remains from the Lower Cretaceous Agrio Formation (Neuquén Basin, west-central Argentina) and their paleobiological implications. *Cretac Res* 89:8–21
- Lessner EJ, Holliday CM (2020) A 3D ontogenetic atlas of *Alligator mississippiensis* cranial nerves and their significance for comparative neurology of reptiles. *Anat Rec*. <https://doi.org/10.1002/ar.24550>
- Li Q, Liu J (2020) An early Triassic sauropterygian and associated fauna from South China provide insights into Triassic ecosystem health. *Commun Biol* 3:1–11
- Lin WB, Jiang DY, Rieppel O et al (2017) A new specimen of *Lariosaurus xingyiensis* (Reptilia, Sauropterygia) from the Ladinian (Middle Triassic) Zhuganpo Member, Falang Formation, Guizhou, China. *J Vertebr Paleontol* 37:e12787. <https://doi.org/10.1080/02724634.2017.1278703>
- Lin WB, Jiang DY, Rieppel O et al (2021) Panzhousaurus rotundirostris Jiang et al., 2019 (Diapsida: Sauropterygia) and the recovery of the monophyly of Pachypleurosauridae. *J Vertebr Paleontol*:e1901730. <https://doi.org/10.1080/02724634.2021.1901730>
- Liu J, Rieppel O, Jiang DY et al (2011) A new pachypleurosaur (Reptilia: Sauropterygia) from the lower Middle Triassic of southwestern China and the phylogenetic relationships of Chinese pachypleurosaur. *J Vertebr Paleontol* 31:292–302
- Liu J, Hu SX, Rieppel O et al (2014) A gigantic nothosaur (Reptilia: Sauropterygia) from the Middle Triassic of SW China and its implication for the Triassic biotic recovery. *Sci Rep* 4:1–9. <https://doi.org/10.1038/srep07142>
- Liu S, Smith AS, Gu Y et al (2015) Computer simulations imply forelimb-dominated underwater flight in plesiosaurs. *PLoS Comput Biol*:11. <https://doi.org/10.1371/journal.pcbi.1004605>
- Lomax DR (2017) A new leptonectid ichthyosaur from the Lower Jurassic (Hettangian) of Nottinghamshire, England, UK, and the taxonomic usefulness of the ichthyosaurian coracoid. *J Syst Palaeontol* 15:387–401
- Lomax DR, Porro LB, Larkin NR (2019) Descriptive anatomy of the largest known specimen of *Protoichthyosaurus prostaialis* (Reptilia: Ichthyosauria) including computed tomography and digital reconstruction of a three-dimensional skull. *Peer J* 7. <https://doi.org/10.7717/peerj.6112>
- Ma LT, Jiang DY, Rieppel O et al (2015) A new pistosauroid (Reptilia, Sauropterygia) from the late Ladinian Xingyi marine reptile level, southwestern China. *J Vertebr Paleontol* 35. <https://doi.org/10.1080/02724634.2014.881832>
- Macrini TE, Rowe T, Archer M (2006) Description of a cranial endocast from a fossil platypus, *Obdurodon dicksoni* (Monotremata, Ornithorhynchidae), and the relevance of endocranial characters to monotreme monophyly. *J Morphol* 267:1000–1015
- Macrini TE, Rowe T, VandeBerg JL (2007) Cranial endocasts from a growth series of *Monodelphis domestica* (Didelphidae, Marsupialia): a study of individual and ontogenetic variation. *J Morphol* 268:844–865
- Maisch MW (1997) Variationen im Verlauf der Gehirnnerven bei *Ophthalmosaurus* (Ichthyosauria, Jura). *Neues Jahrb Geol Paläontol Monatsh* 7:425–433
- Maisch MW (1998) Notes on the cranial osteology of *Muraenosaurus* Seeley, 1874 (Sauropterygia, Jurassic), with special reference to the neurocranium and its implications for sauropterygian phylogeny. *Neues Jahrb Geol Palaeontol Abh* 207:207–253
- Maisch MW (2002) A braincase of *Temnodontosaurus* cf. *trigonodon* (von Theodori, 1843) (Ichthyosauria) from the lower Jurassic of Germany. *Geol Palaeontol* 36:115–122
- Maisch MW (2008) Revision der Gattung *Stenopterygius* Jaekel, 1904 emend. von Huene, 1922 (Reptilia: Ichthyosauria) aus dem unteren Jura Westeuropas. *Palaeodiversity* 1:227–271
- Maisch MW (2010) Phylogeny, systematics, and origin of the Ichthyosauria, the state of the art. *Palaeodiversity* 3:151–214
- Maisch MW, Matzke AT (2000a) The Ichthyosauria. *Stutt Beitr Naturkd B* 298:1–159
- Maisch MW, Matzke AT (2000b) New data on the cranial osteology of *Ichthyosaurus communis* Conybeare, 1822 (Ichthyosauria, Lower Jurassic). *Geol Palaeontol* 34:137–143

- Maisch MW, Matzke AT (2006) The braincase of *Phantomosaurus neubigi* (Sander, 1997) an unusual ichthyosaur from the Middle Triassic of Germany. *J Vertebr Paleontol* 26:598–607
- Maisch MW, Matzke AT, Brinkmann W (2006) The otic capsule of the Middle Triassic ichthyosaur *Mixosaurus* from Monte San Giorgio (Switzerland): New evidence on the braincase structure of basal ichthyosaurs. *Eclogae Geol Helv* 99:205–210
- Marek RD, Moon BC, Williams M et al (2015) The skull and endocranium of a Lower Jurassic ichthyosaur based on digital reconstructions. *Palaeontology* 58:723–742
- Marx MP, Mateus O, Polcyn MJ et al (2021) The cranial anatomy and relationships of *Cardiocorax mukulu* (Plesiosauria: Elasmosauridae) from Bentiaba, Angola. *PLoS ONE* 16. <https://doi.org/10.1371/journal.pone.0255773>
- Massare JA (1987) Tooth morphology and prey preference of Mesozoic marine reptiles. *J Vertebr Paleontol* 7:121–137
- Massare JA (1988) Swimming capabilities of Mesozoic marine reptiles: implications for method of predation. *Paleobiology* 14:187–205
- Massare JA (1994) Swimming capabilities of Mesozoic marine reptiles: a review. In: Maddock L, Bone Q, Rayner JMV (eds) *Mechanics and physiology of animal swimming*. Cambridge University Press, Cambridge, pp 133–150
- Massare JA, Callaway JM (1990) The affinities and ecology of Triassic ichthyosaurs. *Geol Soc Am Bull* 102:409–416
- Maxwell EE (2010) Generic reassignment of an ichthyosaur from the Queen Elizabeth Islands, Northwest Territories, Canada. *J Vertebr Paleontol* 30:403–415
- Maxwell EE, Caldwell MW (2003) First record of live birth in Cretaceous ichthyosaurs: closing an 80 million year gap. *Proc R Soc Lond B* 270:S104–S107
- Maxwell EE, Caldwell MW (2006) A new genus of ichthyosaur from the Lower Cretaceous of Western Canada. *Palaeontology* 49:1043–1052
- McGowan C (1973) The cranial morphology of the Lower Liassic latipinnate ichthyosaurs of England. *Bull Br Mus Nat Hist Geol* 24:1–109
- McGowan C, Motani R (2003) Ichthyopterygia. In: Sues HD (ed) *Handbook of Paleoherpitology*, Verlag Dr, vol 8. Friedrich Pfeil, Munich, pp 1–175
- McHenry CR (2009) *Devourer of gods: the palaeoecology of the Cretaceous pliosaur Kronosaurus queenslandicus*. PhD Dissertation, University of Newcastle
- McHenry CR, Cook AG, Wroe S (2005) Bottom-feeding plesiosaurs. *Science* 310. <https://doi.org/10.1126/science.1117241>
- Miedema F, Maxwell EE (2019) Ontogeny of the braincase in *Stenopterygius* (Reptilia, Ichthyosauria) from the Lower Jurassic of Germany. *J Vertebr Paleontol* 39:e1675164. <https://doi.org/10.1080/02724634.2019.1675164>
- Miedema F, Spiekman SN, Fernandez V et al (2020) Cranial morphology of the tanystropheid *Macrocnemus bassanii* unveiled using synchrotron microtomography. *Sci Rep*:10. <https://doi.org/10.1038/s41598-020-68912-4>
- Moon BC (2019) A new phylogeny of ichthyosaurs (Reptilia: Diapsida). *J Syst Palaeontol* 17:129–155
- Moon BC, Kirton AM (2016) Ichthyosaurs of the British Middle and Upper Jurassic. Part 1, *Ophthalmosaurus*. *Palaeontogr Soc Monogr* 170:1–84
- Moon BC, Stubbs TL (2020) Early high rates and disparity in the evolution of ichthyosaurs. *Commun Biol* 3. <https://doi.org/10.1038/s42003-020-0779-6>
- Motani R (1999a) Phylogeny of the Ichthyopterygia. *J Vertebr Paleontol* 19:473–496
- Motani R (1999b) The skull and taxonomy of *Mixosaurus* (Ichthyopterygia). *J Paleontol* 73:924–935
- Motani R (2002) Scaling effects in caudal fin propulsion and the speed of ichthyosaurs. *Nature* 415:309–312
- Motani R (2005a) Evolution of fish-shaped reptiles (Reptilia: Ichthyopterygia) in their physical environments and constraints. *Annu Rev Earth Planet Sci* 33:395–420

- Motani R (2005b) Detailed tooth morphology in a durophagous ichthyosaur captured by 3D laser scanner. *J Vertebr Paleontol* 25:462–465
- Motani R (2009) The evolution of marine reptiles. *Evo Edu Outreach* 2:224–235
- Motani R (2010) Warm-blooded “sea dragons”? *Science* 328:1361–1362
- Motani R, Minoura N, Ando T (1998) Ichthyosaurian relationships illuminated by new primitive skeletons from Japan. *Nature* 393:255–257
- Motani R, Rothschild BM, Wahl WR (1999) Large eyeballs in diving ichthyosaurs. *Nature* 202:747
- Motani R, Ji C, Tomita T et al (2013) Absence of suction feeding ichthyosaurs and its implications for Triassic mesopelagic paleoecology. *PLoS One* 8. <https://doi.org/10.1371/journal.pone.0066075>
- Motani R, Jiang DY, Tintori A et al (2014) Terrestrial origin of viviparity in Mesozoic marine reptiles indicated by Early Triassic embryonic fossils. *PLoS ONE*:9. <https://doi.org/10.1371/journal.pone.0088640>
- Motani R, Jiang DY, Chen GB et al (2015a) A basal ichthyosauriform with a short snout from the lower Triassic of China. *Nature* 517:485–488
- Motani R, Jiang DY, Tintori A et al (2015b) First evidence of centralia in Ichthyopterygia reiterating bias from paedomorphic characters on marine reptile phylogenetic reconstruction. *J Vertebr Paleontol* 35. <https://doi.org/10.1080/02724634.2014.948547>
- Müller J (2003) Early loss and multiple return of the lower temporal arcade in diapsid reptiles. *Naturwissenschaften* 90:473–476
- Müller J, Sterli J, Anquetin J (2011) Carotid circulation in amniotes and its implications for turtle relationships. *Neues Jahrb Geol Palaontol Abh* 261:289–297
- Muscutt LE, Dyke G, Weymouth GD et al (2017) The four-flipper swimming method of plesiosaurs enabled efficient and effective locomotion. *Proc R Soc B*:284. <https://doi.org/10.1098/rspb.2017.0951>
- Nagloo N, Collin SP, Hemmi JM et al (2016) Spatial resolving power and spectral sensitivity of the saltwater crocodile, *Crocodylus porosus*, and the freshwater crocodile, *Crocodylus johnstoni*. *J Exp Biol* 219:1394–1404
- Nakajima Y, Houssaye A, Endo H (2014) Osteohistology of *Utatusaurus hataii* (Reptilia: Ichthyopterygia): implications for early ichthyosaur biology. *Acta Palaeontol Pol* 59:343–352
- Neenan JM, Scheyer TM (2012) The braincase and inner ear of *Placodus gigas* (Sauropterygia, Placodontia)—a new reconstruction based on micro-computed tomographic data. *J Vertebr Paleontol* 32:1350–1357
- Neenan JM, Scheyer TM (2014) New specimen of *Psephoderma alpinum* (Sauropterygia, Placodontia) from the Late Triassic of Schesaplana Mountain, Graubünden, Switzerland *Swiss J Geosci* 107:349–357
- Neenan JM, Klein N, Scheyer TM (2013) European origin of placodont marine reptiles and the evolution of crushing dentition in Placodontia. *Nat Commun* 4:1–8
- Neenan JM, Li C, Rieppel O et al (2015) The cranial anatomy of Chinese placodonts and the phylogeny of Placodontia (Diapsida: Sauropterygia). *Zool J Linnean Soc* 175:415–428
- Neenan JM, Reich T, Evers SW et al (2017) Evolution of the sauropterygian labyrinth with increasingly pelagic lifestyles. *Curr Biol* 27:3852–3858
- Neenan JM, During MA, Scheyer TM (2019a) The importance of Winterswijk for understanding placodontiform evolution. *Star* 73:222–225
- Neenan JM, Chapelle KE, Fernandez V et al (2019b) Ontogeny of the *Massospondylus* labyrinth: implications for locomotory shifts in a basal sauropodomorph dinosaur. *Palaeontology* 62:255–265
- Nicholls EL, Manabe M (2004) Giant ichthyosaurs of the Triassic: a new species of *Shonisaurus* from the Pardonet Formation (Norian: Late Triassic) of British Columbia. *J Vertebr Paleontol* 24:838–849
- Noe LF, Liston J, Evans M (2003) The first relatively complete exoccipital-opisthotic from the braincase of the Callovian pliosaur, *Liopleurodon*. *Geol Mag* 140:479–486

- Nosotti S, Rieppel O (2002) The braincase of *Placodus* Agassiz, 1833 (Reptilia, Placodontia). *Memoire della Società Italiana di Scienze Naturali e del Museo Civico di Storia Naturale di Milano* 31:3–18
- O’Gorman JP, Gasparini Z (2013) Revision of *Sulcusuchus erraini* (Sauropterygia, Polycotylidae) from the Upper Cretaceous of Patagonia, Argentina. *Alcheringa* 37:163–176
- O’Gorman JP, Otero RA, Hiller N et al (2017) Redescription of *Tuarangisaurus keyesi* (Sauropterygia; Elasmosauridae), a key species from the uppermost Cretaceous of the Weddellian Province: internal skull anatomy and phylogenetic position. *Cretac Res* 71:118–136
- O’Gorman JP, Otero RA, Hiller N et al (2021) CT-scan description of *Alexandronectes zealandiensis* (Elasmosauridae, Aristonectinae), with comments on the elasmosaurid internal cranial features. *J Vertebr Paleontol*. <https://doi.org/10.1080/02724634.2017.1408638>
- O’Keefe FR (2002) The evolution of plesiosaur and pliosaur morphotypes in the Plesiosauria (Reptilia: Sauropterygia). *Paleobiology* 28:101–112
- O’Keefe FR (2008) Cranial anatomy and taxonomy of *Dolichorhynchops bonneri* new combination, a polycotylid (Sauropterygia: Plesiosauria) from the Pierre Shale of Wyoming and South Dakota. *J Vertebr Paleontol* 28:664–676
- O’Keefe FR, Carrano MT (2005) Correlated trends in the evolution of the plesiosaur locomotor system. *Paleobiology* 31:656–675
- O’Keefe FR, Chiappe LM (2011) Viviparity and K-selected life history in a Mesozoic marine plesiosaur (Reptilia, Sauropterygia). *Science* 333:870–873
- O’Keefe FR, Otero RA, Soto-Acuña S et al (2017) Cranial anatomy of *Morturneria seymourensis* from Antarctica, and the evolution of filter feeding in plesiosaurs of the Austral Late Cretaceous. *J Vertebr Paleontol* 37. <https://doi.org/10.1080/02724634.2017.1347570>
- Otero RA, O’Gorman JP, Hiller N et al (2016) *Alexandronectes zealandiensis* gen. et sp. nov., a new aristonectine plesiosaur from the lower Maastrichtian of New Zealand. *J Vertebr Paleontol* 36. <https://doi.org/10.1080/02724634.2015.1054494>
- Otero RA, Soto-Acuña S, O’Keefe FR (2018) Osteology of *Aristonectes quiriquinensis* (Elasmosauridae, Aristonectinae) from the upper Maastrichtian of Central Chile. *J Vertebr Paleontol* 38. <https://doi.org/10.1080/02724634.2017.1408638>
- Owen R (1860) On the orders of fossil and recent Reptilia, and their distribution in time. *Rep Br Ass Advmt Sci* 29:153–166
- Perez-Martinez CA, Leal M (2021) Contribution to the special issue on reptile cognition: lizards as models to explore the ecological and neuroanatomical correlates of miniaturization. *Behaviour* 158:1121–1168
- Pierce SE, Williams M, Benson RBJ (2017) Virtual reconstruction of the endocranial anatomy of the early Jurassic marine crocodylomorph *Pelagosaurus typus* (Thalattosuchia). *Peer J* 5:e3225. <https://doi.org/10.7717/peerj.3225>
- Pihlström H (2008) Comparative anatomy and physiology of chemical senses in aquatic mammals. In: Thewissen JGM, Nummela S (eds) *Sensory evolution on the threshold: adaptations in secondarily aquatic vertebrates*, Berkeley, University of California Press, p 95–109
- Pommery Y, Scheyer TM, Neenan JM et al (2021) Dentition and feeding in Placodontia: tooth replacement in *Henodus chelyops*. *BMC Ecol Evo* 21:136. <https://doi.org/10.1186/s12862-021-01835-4>
- Porter WR, Sedlmayr JC, Witmer LM (2016) Vascular patterns in the heads of crocodylians: blood vessels and sites of thermal exchange. *J Anat* 229:800–824
- Quay WB (1979) The parietal eye-pineal complex. In: Gans C, Northcutt RG, Ulinski P (eds) *Biology of the reptilia (Neurology A)* vol 9. Academic, New York, pp 245–406
- Ralph CL (1975) The pineal gland and geographical distribution of animals. *Int J Biometeorol* 19:289–303
- Ralph CL, Firth BT, Turner JS (1979) The role of the pineal body in ectotherm thermoregulation. *Am Zool* 19:273–293
- Reeves JC, Moon BC, Benton MJ et al (2020) Evolution of ecospace occupancy by Mesozoic marine tetrapods. *Palaeontology*:1–18

- Renesto S, Tintori A (1995) Functional morphology and mode of life of the Late Triassic placodont *Psephoderma alpinum* Meyer from the Calcare di Zorzino (Lombardy, N Italy). *Riv Ital Paleontol S* 101:37–48
- Renesto S, Dalla Vecchia FM (2018) Late Triassic marine reptiles. In: Tanner LH (ed) *The late Triassic world*. Springer, Cham, pp 26–313
- Rieppel O (1985) The recessus scalae tympani and its bearing on the classification of reptiles. *J Herpetol* 19:373–384
- Rieppel O (1989) A new pachypleurosaur (Reptilia: Sauropterygia) from the Middle Triassic of Monte San Giorgio, Switzerland. *Philos T R Soc Lond B* 323:1–73
- Rieppel O (1994a) Osteology of *Simosaurus gaillardoti* and the relationships of stem-group Sauropterygia. *Fieldiana, Geol* 28:1–85
- Rieppel O (1994b) The braincases of *Simosaurus* and *Nothosaurus*: Monophyly of the Nothosauridae (Reptilia: Sauropterygia). *J Vertebr Paleontol* 14:9–23
- Rieppel O (2000) Sauropterygia I: placodontia, pachypleurosauria, nothosauroida, pistosauroida. In: Wellnhofer P (ed) *Encyclopedia of paleoherpétology*, vol 12A. Verlag Dr. Friedrich Pfeil, Munich, pp 1–134
- Rieppel O (2001) Cranial anatomy of *Placochelys placodonta* Jaekel, 1902, and a review of the Cyamodontoidea (Reptilia, Placodonta). *Fieldiana Geol* 45:1–101
- Rieppel O (2002) Feeding mechanics in Triassic stem-group sauropterygians: the anatomy of a successful invasion of Mesozoic seas. *Zool J Linnean Soc* 135:33–63
- Rieppel O, Reisz RR (1999) The origin and early evolution of turtles. *Annu Rev Ecol Evol Syst* 30:1–22. <https://doi.org/10.1146/annurev.ecolsys.30.1.1>
- Romer AS (1968) An ichthyosaur skull from the Cretaceous of Wyoming. *Contrib Geol Univ Wyoming* 7:27–41
- Rothschild BM, Storrs GW (2003) Decompression syndrome in plesiosaurs (Sauropterygia: Reptilia). *J Vertebr Paleontol* 23:324–328
- Sachs S, Hornung JJ, Kear BP (2016a) Reappraisal of Europe’s most complete Early Cretaceous plesiosaurian: *Brancaesaurus brancai* Wegner, 1914 from the “Wealden facies” of Germany. *Peer J* 4. <https://doi.org/10.7717/peerj.2813>
- Sachs S, Lindgren J, Siversson M (2016b) A partial plesiosaurian braincase from the Upper Cretaceous of Sweden. *Geol Soc Spec Publ* 434:293–301
- Sachs S, Hornung JJ, Kear BP (2017) A new basal elasmosaurid (Sauropterygia: Plesiosauria) from the Lower Cretaceous of Germany. *J Vertebr Paleontol* 37:e1301945
- Saint Girons H (1970) The pituitary gland. In: Gans C, Northcutt RG, Ulinski P (eds) *Biology of the reptilia (Morphology C)* vol 3. Academic, New York, pp 245–406
- Sander PM (2000) Ichthyosauria: their diversity, distribution, and phylogeny. *Pal Z* 74:1–35
- Sander PM, Chen X, Cheng L et al (2011) Short-snouted toothless ichthyosaur from China suggests Late Triassic diversification of suction feeding ichthyosaurs. *PLoS ONE*:6. <https://doi.org/10.1371/journal.pone.0019480>
- Sato T (2003) *Terminonator ponteixensis*, a new elasmosaur (Reptilia: Sauropterygia) from the Upper Cretaceous of Saskatchewan. *J Vertebr Paleontol* 23:89–103
- Sato T, Tanabe K (1998) Cretaceous plesiosaurs ate ammonites. *Nature* 394:629–630
- Sato T, Cheng YN, Wu XC et al (2010) Osteology of *Yunguisaurus* Cheng et al., 2006 (Reptilia: Sauropterygia), a Triassic pistosauroid from China. *Paleontol Res* 14:179–195
- Sato T, Wu XC, Tirabasso A et al (2011) Braincase of a polycotyloid plesiosaur (Reptilia: Sauropterygia) from the Upper Cretaceous of Manitoba, Canada. *J Vertebr Paleontol* 31:313–329
- Säve-Söderbergh G (1946) On the fossa hypophyseos and the attachment of the retractor bulbi group in *Sphenodon*, *Varanus*, and *Lacerta*. *Ark Zool* 38:1–24
- Scheyer TM (2007) Skeletal histology of the dermal armor of Placodontia: the occurrence of ‘postcranial fibro-cartilaginous bone’ and its developmental implications. *J Anat* 211:737–753

- Scheyer TM (2010) New interpretation of the postcranial skeleton and overall body shape of the placodont *Cyamodus hildegardis* Peyer, 1931 (Reptilia, Sauropterygia). *Palaeontol Electron* 13. Available at http://palaeo-electronica.org/2010_2/232/index.html. Accessed 3 Aug 2020
- Scheyer TM, Neenan JM, Renesto S et al (2012) Revised paleoecology of placodonts with a comment on 'The shallow marine placodont *Cyamodus* of the central European Germanic Basin: its evolution, paleobiogeography and paleoecology' by CG Diedrich. *Hist Biol* 24:257–267
- Scheyer TM, Neenan JM, Bodogan T et al (2017) A new, exceptionally preserved juvenile specimen of *Eusaurosphargis dalsassoi* (Diapsida) and implications for Mesozoic marine diapsid phylogeny. *Sci Rep* 7:1–22
- Scheyer TM, Neuman AG, Brinkman DB (2019) A large marine eosauroptrygian reptile with affinities to nothosauroid diapsids from the Early Triassic of British Columbia, Canada. *Acta Palaeontol Pol* 64:745–755
- Schoch RR, Sues HD (2015) A Middle Triassic stem-turtle and the evolution of the turtle body plan. *Nature* 523:584–587
- Schwab JA, Young MT, Neenan JM et al (2020) Inner ear sensory system changes as extinct crocodylomorphs transitioned from land to water. *Proc Natl Acad Sci* 117:10422–10428
- Schwab JA, Young MT, Herrera Y et al (2021) The braincase and inner ear of '*Metriorhynchus*' cf. '*M. brachyrhynchus* – implications for aquatic sensory adaptations in crocodylomorphs. *J Vertebr Paleontol* 41:e1912062. <https://doi.org/10.1080/02724634.2021.1912062>
- Shang QH, Di ZW, Li C (2012) New observations on the cranial osteology of the late Triassic *Shastasaurus tangae* and their evolutionary trend. *Sci Sin Terrae* 42:773–783
- Shang QH, Li C, Wu XC (2017) New information on *Dianmeisaurus gracilis* Shang and Li, 2015. *Vert Pal As* 55:145–161
- Shang QH, Wu XC, Li C (2020) A New Ladinian Nothosauroid (Sauropterygia) from Fuyuan, Yunnan Province, China. *J Vertebr Paleontol* 40:e1789651. <https://doi.org/10.1080/02724634.2020.1789651>
- Shine R (2005) All at sea: aquatic life modifies mate-recognition modalities in sea snakes (*Emydocephalus annulatus*, Hydrophiidae). *Behav Ecol Sociobiol* 57:591–598
- Simões TR, Kammerer CF, Caldwell MW, Pierce SE (2022) Successive climate crises in the deep past drove the early evolution and radiation of reptiles. *Sci Adv* 8:eabq1898. <https://doi.org/10.1126/sciadv.abq1898>
- Smith AS, Dyke GJ (2008) The skull of the giant predatory pliosaur *Rhomaleosaurus cramptoni*: implications for plesiosaur phylogenetics. *Naturwissenschaften* 95:975–980
- Smith AS, Vincent P (2010) A new genus of pliosaur (Reptilia: Sauropterygia) from the Lower Jurassic of Holzmaden, Germany. *Palaeontology* 53:1049–1063
- Smith KT, Bhullar BAS, Köhler G et al (2018) The only known jawed vertebrate with four eyes and the Bauplan of the pineal complex. *Curr Biol* 28:1101–1107
- Sollas WJ (1916) The skull of *ichthyosaurus*, studied in serial sections. *Philos T R Soc Lond B* 208:63–126
- Spoor F, Zonneveld F (1998) Comparative review of the human bony labyrinth. *Am J Phys Anthropol* 107:211–251
- Stark D (1979) Cranio-cerebral relations in recent reptiles. In: Gans C, Northcutt RG, Ulinski P (eds) *Biology of the reptilia (Neurology A)* vol 9. Academic, New York, pp 1–39
- Sues HD (1987) On the skull of *Placodus gigas* and the relationships of the Placodontia. *J Vertebr Paleontol* 7:138–144
- Taylor MA, Cruickshank ARI (1993) Cranial anatomy and functional morphology of *Pliosaurus brachyspondylus* (Reptilia: Plesiosauria) from the Upper Jurassic of Westbury, Wiltshire. *Phil T R Soc Lond B* 341:399–418
- Thach WT, Bastian AJ (2004) Role of the cerebellum in the control and adaptation of gait in health and disease. *Prog Brain Res* 143:353–366
- Thewissen JGM, Nummela S (eds) (2008) *Sensory evolution on the threshold: adaptations in secondarily aquatic vertebrates*. University of California Press, Berkeley

- Thewissen JGM, George J, Rosa C et al (2011) Olfaction and brain size in the bowhead whale (*Balaena mysticetus*). *Mar Mam Sci* 27:282–294
- Thorne PM, Ruta M, Benton MJ (2011) Resetting the evolution of marine reptiles at the Triassic–Jurassic boundary. *Proc Natl Acad Sci* 108:8339–8344
- Tosini G (1997) The pineal complex of reptiles: physiological and behavioral roles. *Ethol Ecol Evol* 9:313–333
- Vincent P, Allemand R, Taylor PD et al (2017) New insights on the systematics, palaeoecology and palaeobiology of a plesiosaurian with soft tissue preservation from the Toarcian of Holzmaden, Germany *Sci Nat* 104. <https://doi.org/10.1007/s00114-017-1472-6>
- Vincent P, Grosjean AS, Bert D et al (2020) Paleoenvironmental context and significance of a partial elasmosaurid skeleton from the Albian of Haute-Provence, France *Cretac Res* 108. <https://doi.org/10.1016/j.cretres.2019.104293>
- Voeten DFAE, Sander PM, Klein N (2015) Skeletal material from larger Eusauroptrygia (Reptilia: Eosauroptrygia) with nothosaurian and cymatosaurian affinities from the Lower Muschelkalk of Winterswijk, The Netherlands. *Pal Z* 89:943–960
- Voeten DFAE, Reich T, Araujo R et al (2018a) Synchrotron microtomography of a *Nothosaurus marchicus* skull informs on nothosaurian physiology and neurosensory adaptations in early Sauroptrygia. *PLoS One* 13. <https://doi.org/10.1371/journal.pone.0188509>
- Voeten DFAE, Cubo J, De Margerie E et al (2018b) Wing bone geometry reveals active flight in *archaeopteryx*. *Nat Commun* 9. <https://doi.org/10.1038/s41467-018-03296-8>
- Voeten DFAE, Albers PCH, Klein N (2019a) Nothosauroida from the Vossenveld Formation and their relatives. *Staringia* 16:23–244
- Voeten DFAE, During MAD, Lankamp J et al (eds) (2019b) *Staringia 16—the middle Triassic Vossenveld formation in Winterswijk*. Dutch Geological Association, Winterswijk
- Walsh SA, Iwaniuk AN, Knoll MA et al (2013) Avian cerebellar floccular fossa size is not a proxy for flying ability in birds. *PLoS One* 8:e67176. <https://doi.org/10.1371/journal.pone.0067176>
- Wang W, Li C, Scheyer TM et al (2019a) A new species of *Cyamodus* (Placodontia, Sauroptrygia) from the early Late Triassic of south-west China. *J Syst Palaeontol* 17:1457–1476
- Wang W, Li C, Wu XC (2019b) An adult specimen of *Sinocyamodus xinpuensis* (Sauroptrygia: Placodontia) from Guanling, Guizhou, China. *Zool J Linnean Soc* 185:910–924
- Wang X, Lu H, Jiang DY et al (2020) A new specimen of *Yunguisaurus* (Reptilia; Sauroptrygia) from the Ladinian (Middle Triassic) Zhuganpo Member, Falang Formation, Guizhou, China and the restudy of *Dingxiaosaurus*. *Palaeoworld* 29:137–150
- Werneburg I, Evers SW, Ferreira GS (2021) On the “cartilaginous rider” in the endocasts of turtle brain cavities. *Vertebr Zool* 71:403–418
- Westheide W, Rieger R, Goldschmid A (2003) *Spezielle Zoologie Teil II: Wirbeloder Schädeltiere*. Spektrum Akademischer Verlag, Heidelberg/Berlin
- Wintrich T, Hayashi S, Houssaye A et al (2017) A Triassic plesiosaurian skeleton and bone histology inform on evolution of a unique body plan. *Sci Adv* 3. <https://doi.org/10.1126/sciadv.1701144>
- Witmer LM, Ridgely RC (2009) New insights into the brain, braincase, and ear region of tyrannosaurs (Dinosauria, Theropoda), with implications for sensory organization and behavior. *Anat Rec* 292:1266–1296
- Witmer LM, Ridgely RC, Dufeau DL et al (2008) Using CT to peer into the past: 3D visualization of the brain and ear regions of birds, crocodiles, and non-avian dinosaurs. In: Frey R, Endo H (eds) *Anatomical imaging: towards a new morphology*. Springer, Tokyo, pp 67–87
- Wu XC, Zhao LJ, Sato T et al (2016) A new specimen of *Hupehsuchus nanchangensis* Young, 1972 (Diapsida, Hupehsuchia) from the Triassic of Hubei, China. *Hist Biol* 28:43–52
- Zhao LJ, Sato T, Li C (2008) The most complete pistosauroid skeleton from the Triassic of Yunnan, China. *Acta Geol Sin-Engl* 82:283–286
- Zhou M, Jiang D, Motani R et al (2017) The cranial osteology revealed by three-dimensionally preserved skulls of the Early Triassic ichthyosauriform *Chaohusaurus chaoxianensis* (Reptilia: Ichthyosauromorpha) from Anhui, China. *J Vertebr Paleontol* 37. <https://doi.org/10.1080/002724634.2017.1343831>

- Zverkov NG, Averianov AO, Popov EV (2017) Basicranium of an elasmosaurid plesiosaur from the Campanian of European Russia. *Alcheringa* 42:528–542
- Zverkov NG, Prilepskaya NE (2019) A prevalence of *Arthropterygius* (Ichthyosauria: Ophthalmosauridae) in the Late Jurassic–Earliest Cretaceous of the Boreal Realm. *Peer J* 7:e6799. <https://doi.org/10.7717/peerj.6799>
- Zverkov NG, Jacobs ML (2020) Revision of *Nannopterygius* (Ichthyosauria: Ophthalmosauridae): reappraisal of the ‘inaccessibile’ holotype resolves a taxonomic tangle and reveals an obscure ophthalmosaurid lineage with a wide distribution. *Zool J Linnean Soc.* <https://doi.org/10.1093/zoolinnean/zlaa028>

Chapter 4

Contrasting Brains and Bones: Neuroanatomical Evolution of Turtles (Testudinata)



Gabriel S. Ferreira, Ingmar Werneburg, Stephan Lautenschlager,
and Serjoscha W. Evers

4.1 Systematic and Phylogenetic Context

The phylogenetic position of turtles among amniotes has been a contentious matter for the past century. Molecular data almost entirely point to an archosaur affinity (e.g. Crawford et al. 2012; Wang et al. 2013), whereas morphology-based phylogenetic analyses including fossil material yield conflicting results. Many earlier studies recovered Testudinata (sensu Joyce et al. 2021a; i.e. all extant turtles plus their relatives with a fully developed shell) in various positions within Amniota (see Sues 2019 for a summary). However, recent analyses find support for a diapsid affinity of turtles (Laurin and Piñeiro 2017; Li et al. 2018; Schoch and Sues 2018). Independent of the position of Testudinata within Amniota, turtle in-group relations based on molecular data are stabilizing (e.g. Pereira et al. 2017; Thomson et al. 2021). All analyses agree upon a basal dichotomy between Pleurodira (side-necked turtles) and Cryptodira (hidden-necked turtles). Crown-pleurodiran turtles are divided into Chelidae and Pelomedusoides (which includes Pelomedusidae, Podocnemididae

Supplementary Information The online version contains supplementary material available at https://doi.org/10.1007/978-3-031-13983-3_4.

G. S. Ferreira (✉) · I. Werneburg
Fachbereich Geowissenschaften, Senckenberg Centre for Human Evolution and
Palaeoenvironment at the Eberhard Karls Universität Tübingen, Tübingen, Germany
e-mail: gabriel.ferreira@senckenberg.de; ingmar.werneburg@senckenberg.de

S. Lautenschlager
School of Geography, Earth and Environmental Sciences, University of Birmingham,
Birmingham, UK
e-mail: s.lautenschlager@bham.ac.uk

S. W. Evers
Department of Geosciences, University of Fribourg, Fribourg, Switzerland
e-mail: serjoscha.evers@unifr.ch

and extinct clades; Gaffney et al. 2006; Ferreira et al. 2018a). The relationship among crown-cryptodiran lineages has been subjected to incongruences, particularly regarding the position of Trionychia (summarized by Crawford et al. 2015). However, all recent studies (Crawford et al. 2015; Pereira et al. 2017; Thomson et al. 2021) find Trionychia as the sister to Durocryptodira (all other cryptodires), which itself is formed by Americhelydia (Chelonioida and Chelydridae+Kinosternoidea) and Testudinoidea (Emydidae+*Platysternon megacephalum*, and Geoemydidae+Testudinidae) (Fig. 4.1).

In contrast, the position of some extinct lineages is still highly disputed. Recent analyses agree regarding the stem-ward shift of some extinct species and clades previously classified as stem-pleurodires (e.g. *Proterochersis robusta*) or stem-cryptodires (e.g. *Kayentachelys aprix*, Paracryptodira, Meiolaniformes), which expanded the stem-lineage diversity prior to the divergence of Testudines (Joyce 2007). Likewise, most recent studies generally agree on the position of those fossils, with some exceptions (summarized by Evers and Benson 2019). Those include most notably Thalassochelydia, Protostegidae, Xinjiangchelyidae, Macrobaenidae and Sinemydidae, which float around the stem or crown of Testudines and/or Cryptodira. Here, we adopt one of the latest and most comprehensive phylogenetic analyses of the group (Sterli et al. 2018) as the framework (Fig. 4.1) for the analyses and discussions developed below. Throughout the text, we refer to non-Testudines testudinates as “early-diverging” taxa (see Fig. 4.1).

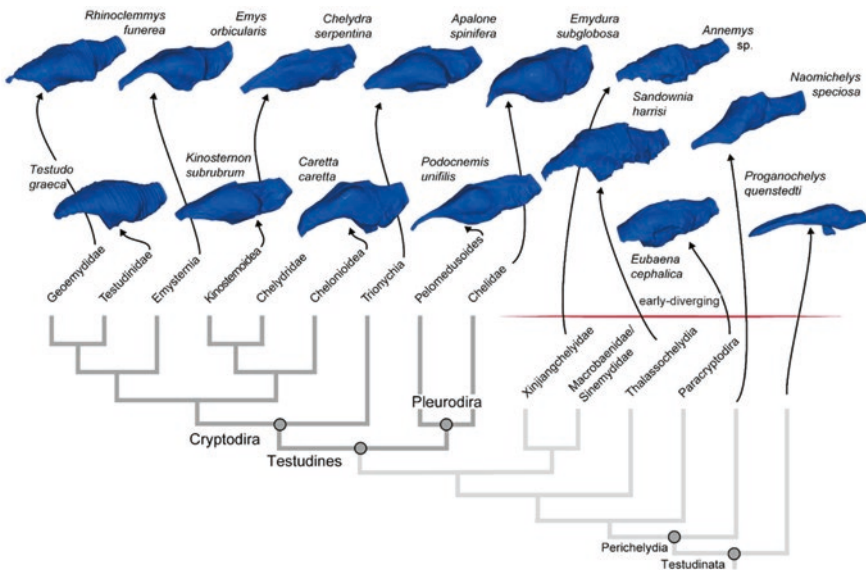


Fig. 4.1 A simplified phylogenetic tree representing the relations between the turtle lineages addressed in this chapter and digitally rendered braincase endocasts of representative taxa. “Early-diverging taxa” are herein defined as all Testudinata clades not belonging to Testudines, unless specifically noted

4.2 Historical Background

4.2.1 Summary of Neuroanatomical Research History

Turtles are extant animals in which neurological structures and blood vessels can be studied directly by means of wet dissection (e.g. neurological structures *sensu stricto*: Shiino 1912; Soliman 1964; Wyneken 2001; blood vessels: Shindo 1914; McDowell et al. 1961; Albrecht 1967, 1976), and often neurological and circulatory details were provided in monographic treatments of single species (e.g. Bojanus 1819–21; Nick 1912; Ogushi 1913). More recently, digital dissection of stained tomographic data can document neuroanatomy and blood vessels in 3D (e.g. Evers et al. 2019b). Studies on the soft tissues of extant turtles provide a framework for understanding related paleontological data, i.e. the endocasts of braincases, nerve passages, and blood canals—a framework that is lacking for many fossil reptile groups (see Chap. 2 and 3 of this volume). On the other hand, neurological structures and particularly blood vessels even of extant turtles are often studied in the context of their cranial cavities and digital endocasts produced from them (e.g. Hermanson et al. 2020; Rollot et al. 2021a; Martín-Jiménez and Pérez-García 2021). This is partly because endocasts enable direct comparisons with fossil data, and partly because the methodological procedure of scanning dry skulls is easier than both the digital or traditional dissection of wet specimens. As the evolution of neurological structures can only be truly understood when integrating fossils, the following historical section summarizes the research history of endocasts or endocast-soft tissue comparisons for turtles. Although a clear distinction between ‘neuroanatomical’ data (meaning actual soft tissues) and ‘endocranial anatomy of the neurocranium’ (including information from endocasts) could be made for turtles, we use the term ‘neuroanatomy’ more fluently as an umbrella term throughout this contribution (for example including blood circulation structures, and pertaining to endocast as well as soft tissue features), as is commonly done in the palaeontological literature.

The first endocranial study to include a turtle coincides with the earliest investigations in paleoneuroanatomy: Tilly Edinger’s (1929) “*Die fossilen Gehirne*”, which figures and discusses an endocranial cast of a turtle (*Chelonia mydas*: Chelonioidae). However, only six additional publications from 1929 to 2013—based either on latex endocasts (Zangerl 1960), on fossilized natural casts (Gaffney and Zangerl 1968; Gaffney 1977, 1982), or on dissections and comparisons of the bones surrounding the endocranial cavity (Edinger 1934; Wyneken 2001)—provided but a glimpse into the general patterns of neuroanatomical variation in the group.

The past decade, influenced by access to computed tomography, saw a renewed interest in turtle neuroanatomy, including more comprehensive studies (e.g. Paulina-Carabajal et al. 2017; Lautenschlager et al. 2018; Werneburg et al. 2021a, b), which tripled the number of studied taxa. Although species level coverage for neuroanatomical data in turtles is still low, most of the main clades of Testudines are

represented by endocranial studies. Extinct taxa, on the other hand, are less well-sampled, but the increased interest in this topic is leading to a growing number of analyses on crown turtles (Gaffney and Zangerl 1968; Gaffney 1977, 1982; Paulina-Carabajal et al. 2013, 2017, 2019; Ferreira et al. 2018b; Evers et al. 2019b; Hermanson et al. 2020; Martín-Jiménez and Pérez-García 2021) and fossil stem turtles (Lautenschlager et al. 2018; Martín-Jiménez et al. 2021; Pérez-García et al. 2021).

Besides brain endocasts, the inner ear is the sensory organ that received most research attention. Some anatomical dissections of related structures exist (e.g. Zangerl 1960; Baird 1974; Gaffney 1979, 1982; Brichta et al. 1988), and digital endosseous labyrinths of individual species are frequently reported in the literature (Paulina-Carabajal et al. 2013, 2019; Mautner et al. 2017; Ferreira et al. 2018b; Lautenschlager et al. 2018; Evers et al. 2020, 2021; Hermanson et al. 2020; Joyce et al. 2021b; Martín-Jiménez et al. 2021; Martín-Jiménez and Pérez-García 2021; Pérez-García et al. 2021). Comparative assessments or shape analyses are rare and with limited taxon sampling (Georgi and Sipla 2008; Walsh et al. 2009; Neenan et al. 2017; Paulina-Carabajal et al. 2017; Evers et al. 2019b). Those studies mostly focused on the vestibular part of the labyrinth, specifically labyrinth size or semicircular canal shape. Only one publication broadly analyzed morphological aspects related to middle ear structures which likely affect hearing (Foth et al. 2019). A handful of publications analyzed and discussed the olfactory structures in turtles (e.g. Parsons 1959a, 1970; Paulina-Carabajal et al. 2013, 2017, 2019; Lautenschlager et al. 2018; Yamaguchi et al. 2021).

4.2.2 *Problematics*

The general observation that the brains of reptiles do not completely fill the endocranial cavity (Hopson 1979) questions the accuracy of endocasts as representatives of soft tissue neuroanatomy, and thus as adequate proxies for sensory evolution. Despite this, only a couple of taxon-specific analyses have assessed this issue in turtles (Evers et al. 2019b). In addition, no information has so far been published on the ontogeny of turtle brains and endocasts. Although aspects of comparative neuroanatomy were assessed in a few studies (e.g. brain endocasts: Lautenschlager et al. 2018; labyrinth endocasts: Evers et al. 2019b), analytical studies performing statistical hypothesis tests on form-function relationships of neuroanatomical structures are conspicuously absent for turtles. For example, the habitat diversity of Testudinata provides research opportunities to study how sensory structures adapt to different environments, but few analyses ventured toward this direction (e.g. Willis et al. 2013; Foth et al. 2019). Fossil neuroanatomy coverage is greatly uneven, even though turtle skulls are common in the fossil record. Some studies (Evers et al. 2019a; Hermanson et al. 2020) used characters about brain and/or inner ear endocasts in phylogenetic analyses, but their impact has not yet been addressed in detail.

Although the scope of this contribution does not allow addressing all of these issues, we provide some novel data and analyses herein to inspire future work on the outstanding research questions on turtle neuroanatomy. We briefly outline our sampling and methodology below, but analytical details are given in the respective sections that discuss the results. Specimen data and general measurements on which our analyses are based are given in Table 4.1.

We expanded the segmentation models for *Trachemys scripta* (Emystrernia) of Evers et al. (2019b) and use this taxon as our model species to illustrate brain shape, nerve passages, blood circulation, and labyrinth shape of turtles. The respective 3D models are available on MorphoSource (Supplementary Table 4.S1; Ferreira 2021), and scan details are given in Evers et al. (2019b). In addition, we segmented 3D model pairs of the brains and endocasts of twelve turtle species (Table 4.1), as well as four additional pairs of endosseous and membranous labyrinths, from stained micro-CT scans. Phosphotungstic acid (PTA) staining of specimens followed the procedure of Metscher (2009), and tomography data were acquired using a SkyScan/Bruker 1173 at the Department of Paleontology in Vienna. Scans were checked for signs of soft tissue shrinkage, and only those with low degrees of shrinkage were processed. Digital models and respective CT scans with scanning parameters are deposited on MorphoSource or MorphoMuseuM (for detailed information on data availability see Supplementary Table 4.S1 at the GitHub repository: Ferreira 2021). We assess brain tissue–endocast shape correspondence over our sample with linear measurements (detailed below; Sect. 4.3.1.3). Eight of our twelve brain-endocast pair specimens are identified as juveniles (Table 4.1) based on considerable differences in skull length in comparison to known adult skull sizes. Although our PTA data do not represent true ontogenetic series, brain-endocast pairs of juvenile turtles show systematic differences to those of adults across taxonomy, which allowed us to propose gross ontogenetic shape trends for turtle brains and braincases (Sect. 4.3.1.4). These trends can be verified for endocasts based on differently sized specimens of the same species and/or sister species (Table 4.1). The phylogenetically closely related emydid turtles *Emys orbicularis* (juvenile specimen) and *Trachemys scripta* (adult specimen) were additionally contrasted for a tentative ontogenetic assessment of brain tissue. This is justified if ontogenetic trends among turtle brain development are similar among closely related species, a reasonable assumption we made herein. Juvenile–adult endocast comparisons provide morphological cues for rough ontogenetic assessments (juvenile vs. adult) also for fossils. To assess endocast shape disparity (Sect. 4.3.1.5), we combined our novel model data with previously published turtle endocasts (including fossils) to produce a geometric morphometric dataset (deposited at GitHub repository: Ferreira 2021), whereby shape was quantified using 300 equally spaced semilandmarks outlining endocasts in dorsal view in tpsDIG2 (Rohlf 2006). We conducted Generalized Procrustes Analysis (GPA; Gower 1975) followed by Principal Component Analysis (PCA) in R using the package geomorph (Adams et al. 2021) on a dataset of 47 endocasts including juveniles (Sect. 4.3.1.4), and a reduced dataset of 39 specimens excluding our eight juveniles (Sect. 4.3.1.5). In addition to these analyses that largely explore shape aspects of brains and endocasts, we also used phylogenetic regressions of

Table 4.1 New specimens with volumetric measurements and ratios discussed in the text

Taxon	Specimen	Box [cm ³]	Ecv [cm ³]	Brv [cm ³]	Br/ Ec	OR	
Early-diverging	<i>Annemys</i> sp.	IVPP-V-18106	25.10	1.15	–	–	0.73
	<i>Eubaena cephalica</i>	DMNH-96004	110.85	3.22	–	–	0.73
	<i>Naomichelys speciosa</i>	FMNH-PR-273	767.64	9.81	–	–	0.76
	<i>Proganochelys quenstedtii</i>	MB-1910452	1096.20	8.17	–	–	1.02
		SMNS-16980	244.44	3.79	–	–	0.83
	<i>Xinjiangchelys radiplicatoides</i>	IVPP-V-9539	51.30	1.51	–	–	0.82
Chelidae	<i>Chelodina reimanni</i>	ZMB-49659	12.96	0.76	–	–	0.51
	<i>Emydura subglobosa</i>	PIMUZ-2009.37	13.13	1.56	–	–	0.50
Chelonioidae	<i>Caretta caretta</i>	NHMUK-19403151	50.03	2.59	–	–	0.73
		GPIT-PV-122905**	2.11	0.18	0.13	0.71	0.59
	<i>Chelonia mydas</i>	ZMB-37416MS	611.52	7.08	–	–	0.75
	<i>Rhinochelys pulchriceps</i>	CAMSMB-55775	4.71	0.23	–	–	0.84
	Chelydroidea	<i>Chelydra serpentina</i>	UFRVP-1	271.24	7.35	–	–
YPM VZ-14442**			1.52	0.16	0.06	0.38	0.57
<i>Kinosternon subrubrum</i>		FMNH-211711	7.53	0.38	–	–	0.54
		YPM VZ-10089*	2.76	0.25	0.14	0.55	0.51
<i>Macrochelys temminckii</i>		GPITRE-10801	631.68	9.58	–	–	0.46
Pelomedusoides	<i>Pelusios niger</i>	SMNS-4625**	3.49	1.12	0.71	0.64	0.52
	<i>Podocnemis erythrocephala</i>	SMNS-6063**	0.71	0.15	0.11	0.74	0.40
	<i>Podocnemis unifilis</i>	SMF-55470	47.84	1.73	–	–	0.69
Testudinoidea	<i>Emys orbicularis</i>	SMF-1987	8.34	1.46	–	–	0.51
		SMNS-11390**	0.88	0.15	0.11	0.76	0.61
	<i>Cuora amboinensis</i>	NHMUK-69421454	11.33	0.80	–	–	0.43
		SMNS-48672**	0.65	0.11	0.09	0.79	0.38
	<i>Gopherus berlandieri</i>	AMNH-73816	13.27	0.97	–	–	0.68
	<i>Kinixys belliana</i>	AMNH-10028	6.84	0.62	–	–	0.60
	<i>Malacochersus tornieri</i>	SMF-58702	11.76	1.36	–	–	0.60
	<i>Platysternon megacephalum</i>	YPM VZ-12559*	13.94	0.58	0.25	0.43	0.50
		SMF-69684	69.30	0.90	–	–	0.61
	<i>Trachemys scripta</i>	MS 000376944		1.43	0.74	0.52	
	<i>Rhinoclemmys funerea</i>	YPM-12174	11.45	1.06	–	–	0.42
	<i>Testudo graeca</i>	YPM-14342	5.85	0.54	–	–	0.69
<i>Testudo hermanni</i>	AMNH-134518			–	–	0.71	

(continued)

Table 4.1 (continued)

Taxon	Specimen	Box [cm ³]	Ecv [cm ³]	Brv [cm ³]	Br/ Ec	OR	
Thalassochelydia	<i>Sandownia harrisi</i>	MIWG-3480	97.06	3.52	–	–	0.90
Trionychia	<i>Apalone spinifera</i>	FMNH-22178	75.36	3.03	–	–	0.50
		YPM VZ-12970**	4.44	0.61	0.36	0.59	0.48
	<i>Carettochelys insculpta</i>	USNM-327690*	20.12	2.00	0.65	0.32	0.56
	<i>Pelodiscus sinensis</i>	GPIT-PV-122907	31.86	0.71	–	–	0.39

Specimens marked with a * are considered juveniles (i.e., very small or hatchling), and with a × were stained with contrast enhancement prior to CT scan (see Ferreira et al. 2020)

Measurements abbreviations: *Box* box volume, *Ecv* braincase endocast volume, *Brv* brain tissue volume, *Br/Ec* brain/endocast volume ratio, *OR* olfactory ratio

Institutional abbreviations: *AMNH* American Museum of Natural History, USA, *CAMSMB* Sedgwick Museum of Earth Sciences, UK, *DMNH* Denver Museum of Nature and Science, USA, *FMNH* Field Museum of Natural History, USA, *GPIT* Paläontologische Sammlung der Universität Tübingen, Germany, *IVPP* Institute of Vertebrate Paleontology and Paleoanthropology, China, *MB* Museum für Naturkunde Berlin, Germany, *MIWG* Museum of Isle of Wight Geology, UK, *MS* MorphoSource digital collection, <http://morphosource.org>, *NHMUK* Natural History Museum, UK, *PIMUZ* Laboratory collection of Paläontologisches Institut und Museum der Universität Zürich, Switzerland, *SMF* Senckenberg Museum Frankfurt, Germany, *SMNS* Staatliches Museum für Naturkunde Stuttgart, Germany, *USNM* United States National Museum, USA, *YPM* Yale Peabody Museum, USA, *ZMB* Zoologisches Museum Berlin, Germany, *UFRVP* Université de Fribourg, Switzerland, *YPM* Yale Peabody Museum of Natural History, New Haven, USA

volumetric brain–endocast pairs using *gls* function of *nlme* R package (Pinheiro et al. 2021), to show that endocast size is a sufficiently good proxy for brain size in turtles (Sect. 4.4.1). This justifies our evolutionary analysis of relative brain size using 27 endocast volumes of extant and extinct fossils and ancestral state reconstructions (*fastAnc* function of R package *phytools*; Revell 2012) presented in Sect. 4.4.1.

4.3 Overview of General and Comparative Anatomy

4.3.1 Characterization of Neuroanatomical Structures

Brain Morphology of Turtles

Turtle brain shape has been described for only a few species based on dissections (e.g. Bojanus 1819–21; Shiino 1912; Ogushi 1913; Wyneken 2001), or digital brain models (Evers et al. 2019b). Here, we present additional digital brain models of four adult or subadult cryptodiran turtles to give a gross assessment of variation in brain shape across clades (Fig. 4.2). The general brain morphology of the pond turtle

Trachemys scripta (Fig. 4.2a) was described previously (Evers et al. 2019b), so that we limit ourselves to comparative statements.

The adult turtle brain is tubular and similar in structure and morphology to brains of other non-avian reptiles, although our (albeit small) sample suggests less brain shape variation for at least cryptodiran turtles than is seen in squamates (Macrì et al. 2019). Unlike crocodylians (Lessner and Holliday 2020) or squamates (Macrì et al. 2019), turtles have virtually no olfactory tracts, and the olfactory bulbs are located immediately anterior to the cerebrum (Fig. 4.2). However, an elongate olfactory nerve can be traced anteriorly through the sulcus olfactorius underlying the frontals, extending into the nasal cavity (Fig. 4.2). The anteroventral parts of the olfactory bulbs anteriorly extend beyond the ossified (secondary) braincase walls formed by the parietals mainly, as the anterior neurocranium remains unossified in turtles (ossified orbitosphenoids and laterosphenoids are absent). However, our stained micro-MRI scan of *Trachemys scripta* (see Evers et al. 2019b for scan details) shows that some of the cartilaginous chondrocranium is retained into adulthood (Fig. 4.3). The chondrocranial cartilage of *T. scripta* includes the planum suprasetale, which caps the sulcus olfactorius ventrally. Ventrally confluent with it is a median, vertical interorbital septum. Posteroventrally, the pila metoptica forms the posterior margin of the optic (CN II) foramen. More posterior chondrocranial elements, such as the taenia medialis or the pila antotica are not formed as cartilage but seem to have been replaced by dural membrane.

The large ovoid cerebral hemispheres of turtles show the greatest amount of variation in our sample. In *Platysternon megacephalum* (Emysternia), the cerebral hemispheres are relatively small and diverge little from the midline with their posterior section (Fig. 4.2d). This divergence is much larger in *Trachemys scripta* (Fig. 4.2a). *Apalone spinifera* (Trionychia) shows extremely enlarged cerebral hemispheres in comparison to the other turtles for which we have data (Fig. 4.2c). This is coincident with it being a small specimen (26.3 mm skull length) and probably the relatively youngest of the adults in our sample (see section 4.3.1.4 for a discussion on ontogenetic changes). The pineal gland ascends dorsally from the midline and between the cerebrum anteriorly, and the optic lobes posteriorly (Fig. 4.2b). Although the pineal gland is present in all turtles, its weak contrast did not allow consistent segmentation across our sample. The optic lobes of turtles are well rounded, tightly spaced across the midline, smaller than in most squamates (Macrì et al. 2019), but generally comparable to those of crocodylians (Lessner and Holliday 2020). Pontine and cephalic flexures, as well as the morphology of the cerebellum or medulla oblongata show little variation among adult turtles, even in taxa whose endocasts possess more marked flexures (e.g. cheloniids; Wyneken 2001). All turtles have prominent optic stalks on the anteroventral side of the fore-brain, which give off the optic nerves (CN II) anteriorly and which are connected to the hypophysis (=pituitary) via the infundibulum (Fig. 4.2).

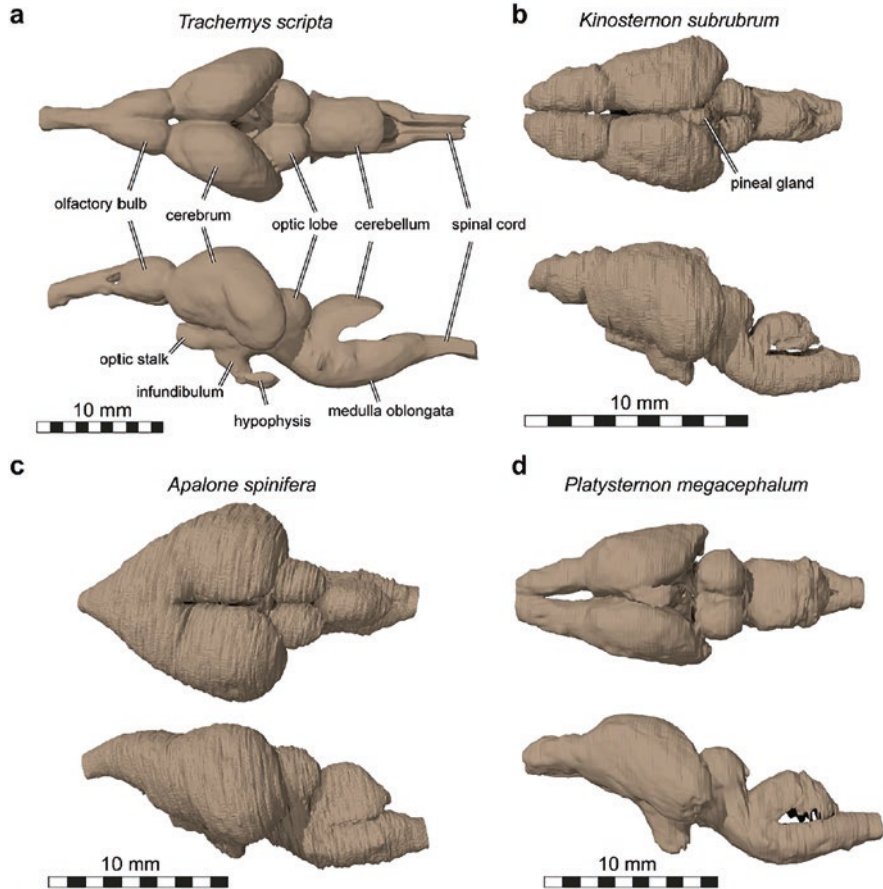


Fig. 4.2 Comparison of adult/subadult brain shapes of four turtle species in dorsal (top) and left lateral (bottom) view in each panel, respectively. (a), the emydid *Trachemys scripta* (MS 000376944); (b), the kinosternid *Kinosternon subrubrum* (YPM VZ-10089); (c), the trionychid *Apalone spinifera* (YPM VZ-12970); (d), the platysternid *Platysternon megacephalum* (YPM VZ-12559)

Cranial Nerves of Turtles

Although several pieces of historical literature discuss individual cranial nerves of turtles, comprehensive descriptions and illustrations are rare. The best available resources are the dissection-based studies of cranial nerves of *Emys orbicularis* (Emystrernia) by Bojanus (1819-21), *Clemmys guttata* (Emystrernia) by Shiino (1912), *Pelodisucs sinensis* (*Trionyx japonicus*; Trionychia) by Ogushi (1913), *Eretmochelys imbricata* (Chelonioida) and *Chelydra serpentina* (Chelydridae) by Soliman (1964), and the digitally dissected cranial nerves of *Trachemys scripta* (Emydidae) by Evers et al. (2019b). Here, we expand the digital segmentations of

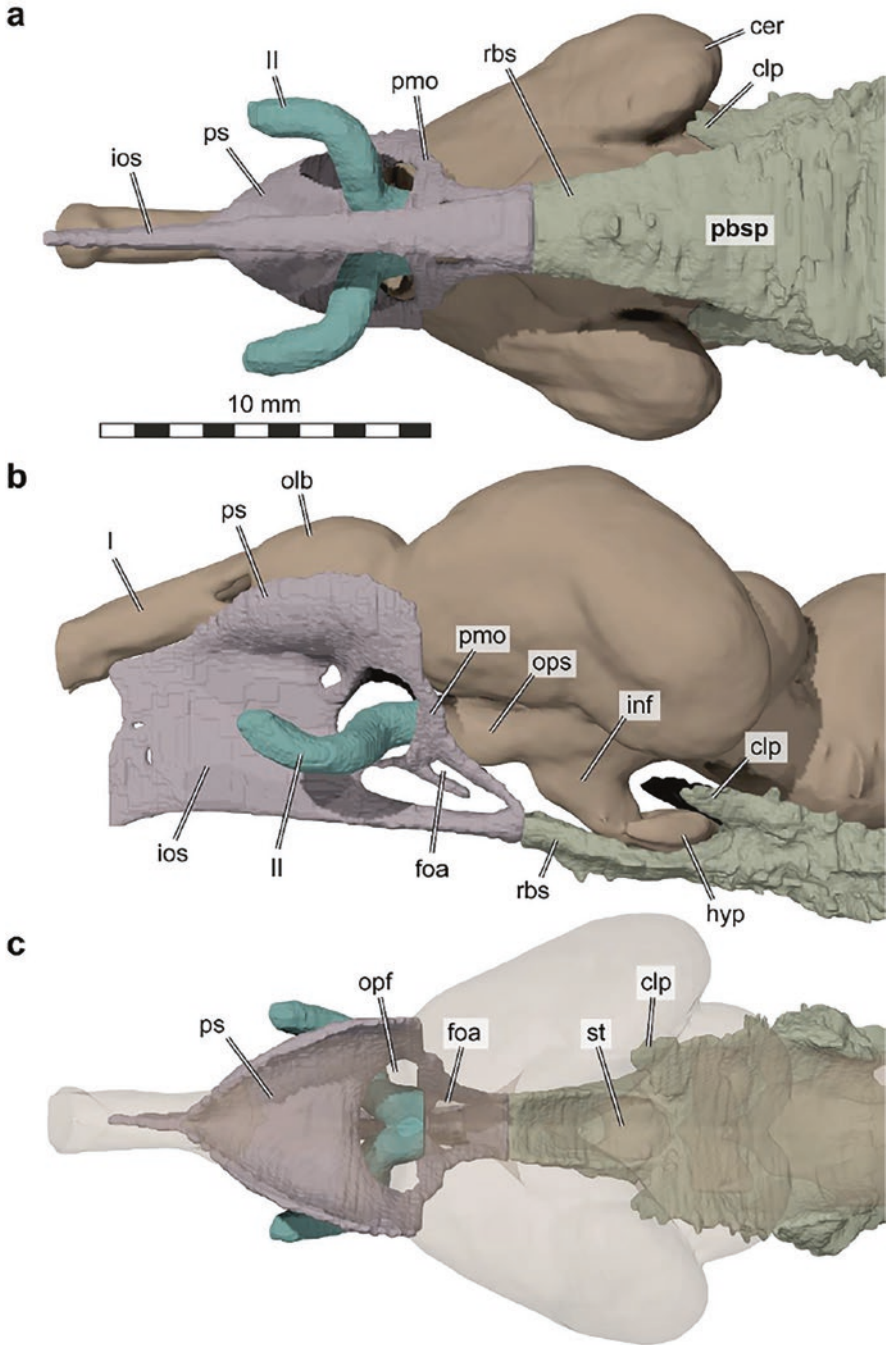


Fig. 4.3 Anterior brain region, chondrocranial sphenoid cartilage, parabasisphenoid, and optic nerve of *Trachemys scripta* (MS 000376944). (a), ventral view. (b), left lateral view. (c), dorsal view, with brain tissue rendered semi-transparent. Abbreviations: *cer* cerebral hemisphere, *clp* clinoid process, *foa* foramen for a small ophthalmic artery, *hyp* hypophysis, *I* olfactory nerve, *II* optic nerve, *inf* infundibulum, *ios* interorbital septum, *olb* olfactory bulb, *opf* optic nerve foramen, *ops* optic stalk, *pbsp* parabasisphenoid, *pmo* pila metoptica, *ps* planum suprasedale, *rbs* rostrum basisphenoidale, *st* sella turcica

Evers et al. (2019b) by including details of the facial nerve and separating each cranial nerve for a better individual appreciation of these structures (Fig. 4.4). Our observations for *T. scripta* and literature comparisons (Shiino 1912; Ogushi 1913; Soliman 1964) suggest that there is overall little variation in the proximal sections (herein: closer to the brain than to innervated structures) of the cranial nerves of turtles (as observed also from endocasts and/or osteology; Gaffney 1979; Lautenschlager et al. 2018); but that more variation is apparent along the more distal portions of the nerves, particularly for CN V₂ (maxillary branch of the trigeminal nerve) related to differing jaw adductor musculature anatomy (Poglayen-Neuwall 1953, Werneburg 2011).

The olfactory nerve (CN I) of *Trachemys scripta* originates anteriorly from the olfactory bulbs (Fig. 4.4). The right and left nerves lie against one another in the median sulcus olfactorius, which is always formed by the frontal bones but may have contributions from the parietals or prefrontals among different turtle species. The sulcus olfactorius of *T. scripta* is ventrally closed by the cartilaginous planum suprasetale (Fig. 4.3). As in other turtles, the optic nerve (CN II) is the thickest among the cranial nerves in *T. scripta* (Fig. 4.4). It emerges from the optic stalk of the anteroventral brain surface dorsal to the infundibulum, takes a sharp lateral turn through the optic foramen, which is encased in chondrocranial cartilage, and then continues forward to the eyeball. The oculomotor nerve (CN III) originates on the ventral surface of the midbrain near the midline (Fig. 4.4a), from where it diverges laterally to the internal surface of the dura mater that surrounds the brain. From there, it extends anteriorly in close association with the ophthalmic nerve (see below), which lies against the outer surface of the dura but within the bony braincase. Although the optic nerve (CN II) exits the brain cavity through the sphenoid cartilages, no such cartilaginous foramen for the oculomotor nerve (CN III) is evident in *T. scripta*. Instead, the oculomotor nerve (CN III) exits through openings in the membranous dura which surrounds the brain and is attached to the sphenoid cartilages. Both types of ‘foramina’ (i.e. CN II in cartilage and CN III in dura mater) cannot be reconstructed from macerated specimens or fossils (with the noteworthy exception of *Proganochelys*, which ancestrally retains the laterosphenoid Bhullar and Bever 2009; Werneburg and Yaryhin 2019). The trochlear nerve (CN IV) emerges from the lateral brain surface between the optic lobe anteriorly and cerebellum posteriorly (Fig. 4.4b). It extends anteroventrally into the cavum epiptericum, i.e. the space between the basisphenoid and secondary braincase wall in which the trigeminal ganglion is positioned. Evers et al. (2019b) reported the trochlear nerve to extend anteriorly with the ophthalmic and oculomotor nerves, but the course of the trochlear nerve lies slightly dorsally to the aforementioned (Fig. 4.4b, c). The trigeminal nerve (CN V; Fig. 4.4) has a short and thick stem that extends from the lateral brain surface in the pons-medulla oblongata region anterolaterally into the cavum epiptericum, where it forms the trigeminal ganglion. The anteriorly directed ophthalmic nerve (CN V₁) lies intracranially, i.e. medial to the external wall of the braincase as formed by the descending process of the parietal, as also reported for other turtles (Ogushi 1913; Soliman 1964), and extends along the outer dura surface forward. The ophthalmic nerve has several anterior divisions and subbranches, but

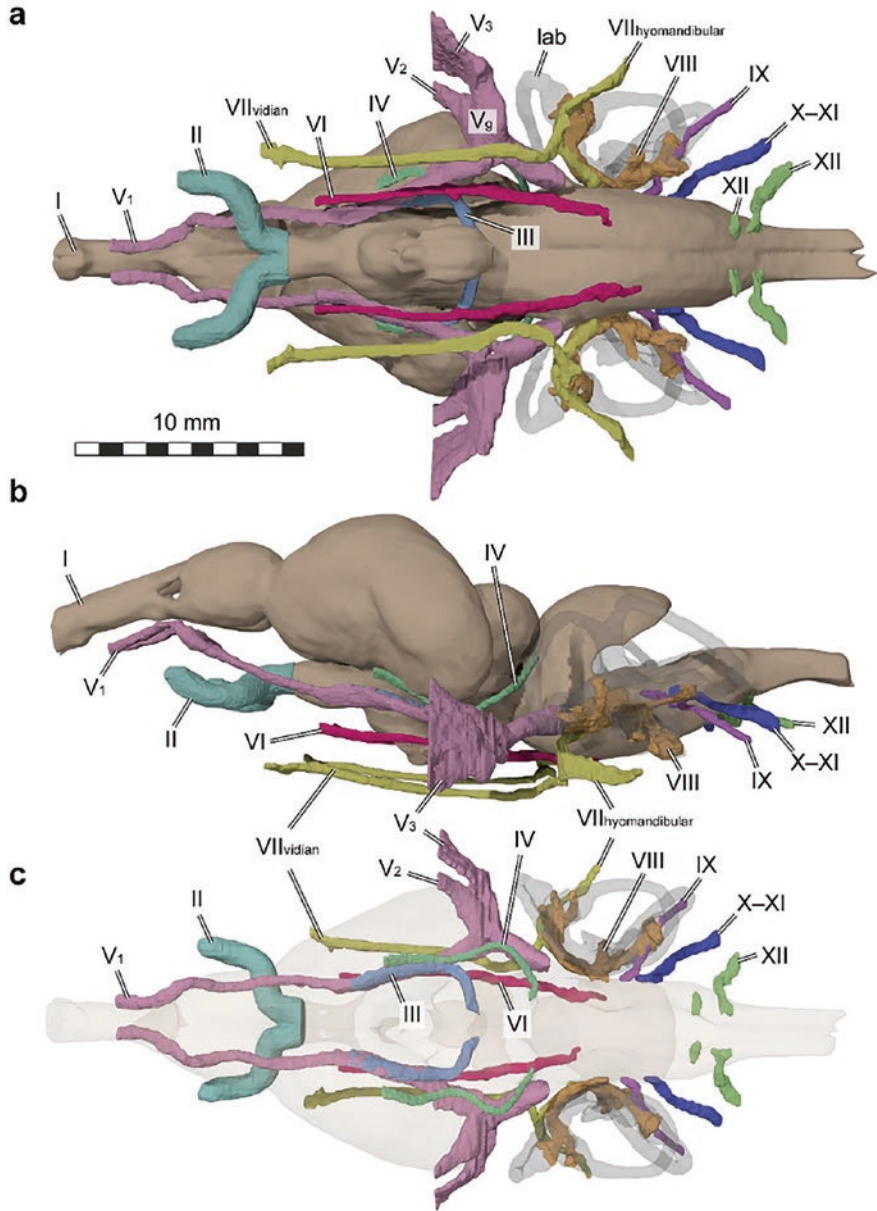


Fig. 4.4 3D renderings of the brain and major cranial nerves in *Trachemys scripta* (MS 000376944). (a), ventral view. (b), left lateral view. (c), dorsal view with brain mass rendered semi-transparent. Abbreviations: *I* olfactory nerve, *II* optic nerve, *III* oculomotor nerve, *IV*, trochlear nerve, *V*₁ ophthalmic branch of trigeminal nerve, *V*₂ maxillary branch of trigeminal nerve, *V*₃ mandibular branch of trigeminal nerve, *VI* abducens nerve, *VII*_{hyomandibular} hyomandibular branch of facial nerve, *VII*_{vidian} vidian branch of facial nerve, *VIII* vestibulochoclear nerve, *IX* glossopharyngeal nerve, *X–XI* accessorio-vagus nerve (see text), *XII* hypoglossal nerve, *lab* membranous labyrinth

only the thickest branch leading to the nasal cavity is shown here (Fig. 4.4). The other two principal rami of the trigeminal nerve, the maxillary (CN V₂) and mandibular (CN V₃) nerves exit the cavum epiptericum laterally through the trigeminal foramen (in turtles formed principally by the parietal and pterygoid), which can be readily identified in the crania of most extant and fossil turtles (see Evers et al. 2019b for further discussions on the trigeminal nerve). The abducens nerve (CN VI) of *T. scripta* originates on the ventral surface of the medulla oblongata in a more medial position than the trigeminal nerve (CN V) but more laterally than the oculomotor nerve (CN III) (Fig. 4.4a). Abducens foramina and canals are easily identified in the basisphenoids of turtles. The facial nerve (CN VII) and vestibulocochlear nerve (CN VIII) of *T. scripta* emerge together from the lateral brain surface at the same level but slightly posterior to the trigeminal nerve (Fig. 4.4a, c). In turtle brain-cases, this origin is usually documented by a large fossa on the medial surface of the prootic bone, the fossa acustico-facialis (Gaffney 1979). Whereas the vestibulocochlear nerve forms a ganglion in this fossa from which its separate rami emerge (see Evers et al. 2019b, for details of labyrinth innervation), the facial nerve of *T. scripta* extends laterally through a canal in the prootic that drains into the canalis cavernosus. Here, the facial nerve enters a small geniculate ganglion from which two prominent rami emerge (Fig. 4.4a). Posteriorly, the hyomandibular branch of the facial nerve extends along the lateral head vein before it gives off further branches (not shown in Fig. 4.4). The anterior, vidian branch of the facial nerve exits the canalis cavernosus ventrally through a small canal that leads to the carotid arterial canal system at the level of the bifurcation of the internal carotid artery. The vidian nerve extends shortly alongside the palatine artery, before entering its own vidian canal that extends anterolaterally and opens near the foramen palatinum posterius, through which the vidian nerve passes. Rollot et al. (2021a) recently described variation regarding the facial nerve canal system, which, particularly for the vidian branch, shows higher variation than canals associated with other nerves in turtles. The glossopharyngeal nerve (CN IX) of *T. scripta* originates just posterior to the facial and vestibulocochlear nerves (Fig. 4.4a) and takes the path apomorphic for turtles (Rieppel 1985) through the cavum labyrinthicum via a series of foramina in the opisthotic (Gaffney 1972, 1979). Its subordinate branches that diverge in the cavum acustico-jugulare were not segmented here for *T. scripta*. As reported for other turtles (Shiino 1912; Ogushi 1913; Soliman 1964), the vagus nerve (CN X) and accessory nerves (CN XI) of *T. scripta* form a tightly intertwined unit (i.e. accessorio-vagus nerve of Shiino 1912), which could not be separated digitally (see Evers et al. 2019a, b). These nerves originate on the same level of the CN VII–IX, but somewhat posterior to the glossopharyngeal nerve (Fig. 4.4). CN X–XI pass through a large aperture, the embryonic metotic fissure of reptiles (Rieppel 1985), which in turtles is usually called the anterior jugular foramen in adults (as the jugular vein also passes through this opening; Gaffney 1972, 1979). As already reported by Evers et al. (2019b) and in agreement with other turtles (e.g. Soliman 1964), *T. scripta* has two separate rami of the hypoglossal nerve (CN XII), which pass from the ventral surface of the posterior interface between medulla oblongata and spinal cord through canals in the exoccipital into the cervical region (Fig. 4.4a).

Braincase Endocast Morphology of Turtles and Correspondence of Brain and Endocast Shape

The endocast of the braincase of turtles is difficult to segment coherently because the anterior chondrocranial cartilages do not ossify (see above, and Fig. 4.3), leaving no clear anterior delimitation for the braincase endocast (e.g. Paulina-Carabajal et al. 2013; Evers et al. 2019b). This is important to note, because differences in interpreting this anterior region may affect volumetric assessments of turtle endocasts. Turtle braincase endocasts are characterized by a narrow anterior portion representing the endocast of the sulcus olfactorius, a transversely broad cerebral region, and a transversely constricted optic and cerebellar region that makes room for the semicircular canal system laterally (Fig. 4.5) (Edinger 1929; Zangerl 1960; Gaffney and Zangerl 1968; Gaffney 1977, 1982; Paulina-Carabajal et al. 2013; Lautenschlager et al. 2018; Martín-Jiménez and Pérez-García 2021; Werneburg et al. 2021a). Cranial flexures differ between species, whereby taxa with high-domed, macrocephalic skulls seem to have stronger cranial flexures (e.g. Ferreira et al. 2018b). However, flexures are generally moderate to weak, contributing to a relatively tubular endocast shape (Fig. 4.5). Ventrally, the endocast of the pituitary fossa is usually clear in endocasts, but most other specific brain regions are poorly demarcated in turtle endocasts (Fig. 4.5).

Even though the endocasts of mammals and birds are good predictors of brain shape (Balanoff et al. 2016), it is generally believed that reptile brains fill only about 50% of the cavity (Hopson 1979), with the rest occupied by dural venous sinuses and cerebrospinal fluid (Witmer et al. 2008). However, this assertion has been poorly evaluated empirically. The correspondence between brain tissue and endocast in reptiles varies extensively between taxa and over ontogeny (Allemant et al. 2017 and references therein). Among squamates the brain can occupy 35–97% of the endocast volume (Kim and Evans 2014). This evaluation is important because if the braincase of reptiles is indeed a poor predictor of neuroanatomy, then there is only weak support for ecological and behavioral inferences derived from endocasts.

Our comparisons of adult brain-tissue-to-braincase-endocasts largely confirm previous observations (Edinger 1929; Zangerl 1960; Wyneken 2001; Paulina-Carabajal et al. 2013; Mautner et al. 2017; Evers et al. 2019b) that endocast shape poorly reflects brain shape in turtles (Fig. 4.5). Large sub- and epidural spaces surround the turtle brain (Fig. 4.5b, d), and most brain regions are poorly demarcated in the endocasts (Lautenschlager et al. 2018; Evers et al. 2019b; Fig. 4.5a, c). The best correspondence is seen in the cerebral hemispheres: the extent of the cerebrum can be approximated from dorsal and lateral views of braincase endocasts. The olfactory bulbs are also relatively well represented in the endocasts. On the other hand, the mid- and hindbrain are inadequately reflected. Large gaps surround the optic lobes and the cerebellum, notably on their dorsal and ventral aspects. The width of the optic lobes is not well imprinted in the endocast either, similarly to the medulla oblongata and cerebellar regions. A curious morphological feature that is often identified in the braincase endocasts of extant and fossil turtles is a small central protuberance or ridge posterior to the cerebral area of the endocast, called the

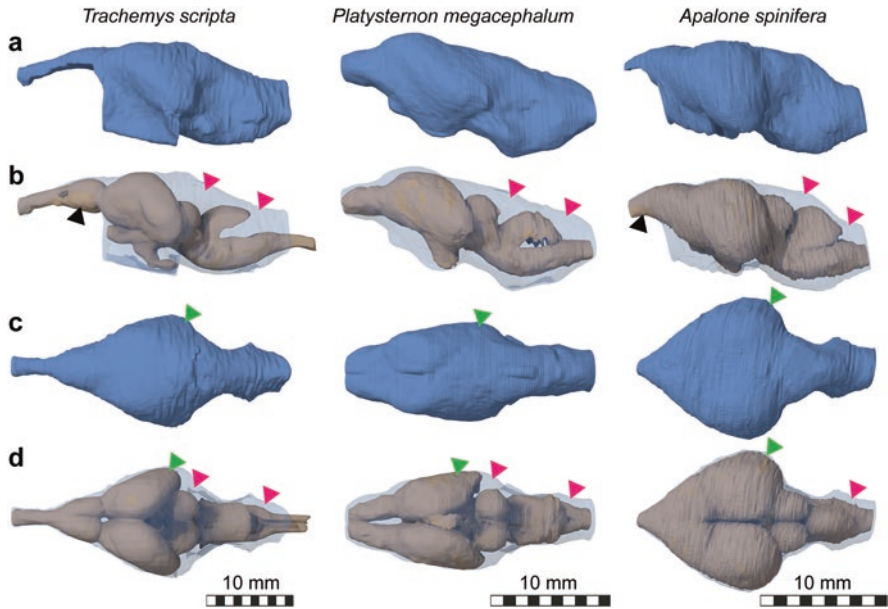


Fig. 4.5 Comparison of braincase endocast shape for three turtles (adult *Trachemys scripta*: MS 000376944; adult *Platysternon megacephalum*: YPM VZ-12559; subadult *Apalone spinifera*: YPM VZ-12970) for which we had brain and braincase data. **(a)**, endocasts in left lateral view. **(b)**, brains and transparent endocasts in left lateral view, showing dural spaces surrounding brain. **(c)**, endocasts in dorsal view. **(d)**, brains in dorsal view. Red arrow heads show regions of particularly poor brain-braincase shape correspondence. Green arrow heads show regions of close correspondence. Black arrows show brain tissue that extends out of the space commonly segmented in turtle endocasts, highlighting the poor endocast-brain correspondence along the anterior, unossified surfaces of the braincase

“cartilaginous rider” (Gaffney and Zangerl 1968). Our soft tissue segmentations confirm recent assessments (Werneburg et al. 2021a) that the rider has no neurovascular correlate (contra, for instance, Paulina-Carabajal et al. 2013; Deantoni et al. 2015), and that this feature is an endocast of the cartilaginous anterior imprint of the chondrocranial tectum synoticum, which posteriorly ossifies as the supraoccipital.

To (a) test if brain tissue and braincase endocasts correspond well for a taxonomically broad sample of turtles, and to (b) test the influence of ontogeny on this correspondence, we compared brain tissues and endocasts from eleven turtles (see Supplementary Table 4.S2 on the GitHub repository: Ferreira 2021) in multiple ways. The visual comparisons of two adult and one subadult turtle presented above (Fig. 4.5) indicate a mixed correspondence depending on brain/endocast region, as well as a possible ontogenetic trend to poorer correspondence with increasing maturity. We furthermore scrutinized overall correspondence by volumetric comparisons, and specific correspondence with linear measurements (explained graphically in Fig. 4.6) for three adult and eight juvenile turtles. Volumetric correspondence is particularly relevant for inferring overall brain sizes from endocasts, a common

endeavor in the literature for researching brain size evolution. Specific linear measurement comparisons on the other hand may provide additional insights, particularly when correspondence levels vary across brain/endocast regions. Although our specimens represent different species, we interpret size-dependent discrepancies as an ontogenetic trend across our observations. This is justified in two ways: the trends that we interpret from cross-species brain–endocast pairs mirror ‘true’ ontogenetic trends for endocasts of differently sized turtles of the same species (see Sect. 4.4.1); and comparisons with different amniote groups show that our identified shape and size trends for turtles reflect the strong ontogenetic endocast and brain changes occurring in squamates (Kim and Evans 2014) and crocodiles (Jirak and Janacek 2017).

Our volumetric comparisons indicate that brain to endocast size correspondence is weaker among adult turtles (43–55%; Table 4.1, Fig. 4.6) than in juveniles (59%–79%) with the exception of a juvenile *Chelydra serpentina* (YPM VZ-14442; Table 4.1, taxon 3 in Fig. 4.6), in which the brain fills only 38% of the endocranial cavity (but this is not mirrored in linear measurements, see below). Volumetric data for turtle endocasts are tricky due to the poor bony constraints on the anterior braincase side, which can easily cause volumetric deviations and which could explain the unexpected low values retrieved for *C. serpentina* here. Thus, we only interpret these data in the sense of a gross trend that with increasing ontogenetic maturity, the braincase becomes a poorer reflection of brain volumes. Despite this weak allometric trend (slope = 0.91, isometry expectation of 1; see Sect. 4.4.1), there is a clear correlation between brain volume and endocast volume across different species ($R^2 = 0.97$; $p < 0.001$; see Sect. 4.4.1), which may justify the use of endocast volumetric data as a proxy for brain size in turtles.

Our linear measurement comparisons (Supplementary Table 4.S2 on the GitHub repository: Ferreira 2021 and Fig. 4.6) confirm the notion that brain–endocast correspondence is higher in juveniles, but also demonstrate that tissue–bone correspondence varies according to brain region. Across most measurements, the adult specimens of our sample, *Platysternon megacephalum*, *Kinosternon subrubrum* (Kinosternoidea) and *Trachemys scripta*, show the highest dissimilarity between brain tissue and braincase endocast: their endocast measurements consistently overestimate brain size (Fig. 4.6a), confirming our observations from volumetric data. Figure 4.6 also shows that the orbital region and the height of the olfactory bulbs have a stronger ontogenetic discrepancy than measurements from anterior brain regions: adult brains (blue circles to the left of the graph’s x-axis) fill a considerably smaller proportion of the endocast than in juveniles (red diamonds to the right). Measurements for the cerebral hemispheres as well as the width of the olfactory bulbs conversely show less spread in values, and adult turtles do not perform considerably worse than juvenile turtles. Although *Chelydra serpentina* (YPM VZ-14442) was an outlier in terms of extremely poor volumetric brain–endocast correspondence for a juvenile specimen, linear measurement comparisons of this specimen do not support this observation (taxon number 3 in Fig. 4.6). This indicates that the volumetric discrepancies result from areas of the brain/endocast not sampled by measurements (including the possibility of inconsistently segmented

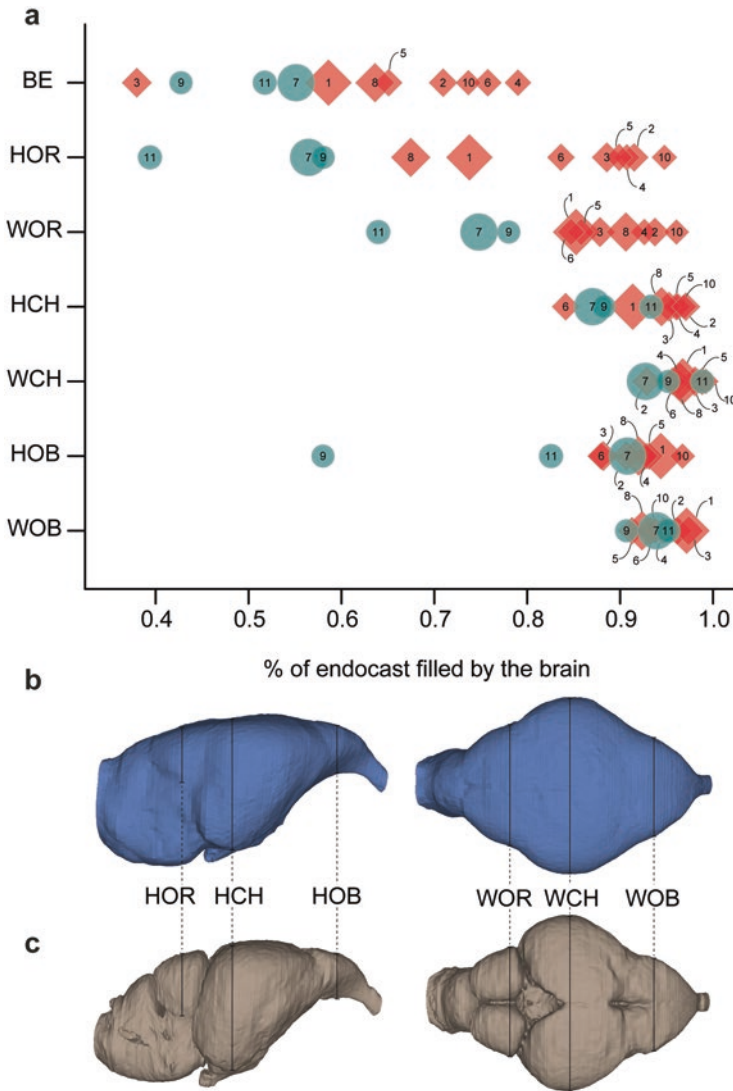


Fig. 4.6 Quantitative brain tissue and braincase endocast comparison based on volumetric and linear measurements. Graph (a) shows proportion of braincase filled by the brain (x-axis) for each measurement (y-axis) and eleven specimens indicated by numbers, with juvenile specimens indicated by red diamonds and adult specimens indicated by blue circles. The size of the points indicate their absolute size. 3D models of *Emydura subglobosa* (GPIT-PV-122906) braincase endocast (b) and brain tissue (c) shows the position of each linear measurement. Abbreviations: *H*- height, *W*- width, *-CH* cerebral hemispheres, *-OB* olfactory bulbs, *-OR* optic region. Specimen key for graph: (1) *Apalone spinifera* (YPM VZ-12970); (2) *Caretta caretta* (GPIT-PV-122905); (3) *Chelydra serpentina* (YPM VZ-14442); (4) *Cuora amboinensis* (SMNS 4867-2); (5) *Emydura subglobosa* (GPIT-PV-122906); (6) *Emys orbicularis* (SMNS 11390); (7) *Kinosternon subrubrum* (YPM VZ-10089); (8) *Pelusios niger* (SMNS 4625); (9) *Platysternon megacephalum* (YPM R-12559); (10) *Podocnemis erythrocephala* (SMNS 6063); (11) *Trachemys scripta* (MS 000376944)

endocast models along the poorly delimited anterior side) and highlights the merits of using different metrics for brain–endocast comparisons.

In summary, we propose that the endocasts of juvenile or young adult turtles are acceptable predictors of brain anatomy, but those of older individuals are not. Thus, the current evidence does not give much support for correlations of endocast shape and ecological/behavioral traits in adult turtles, except for the forebrain, i.e. olfactory bulbs and cerebral hemispheres, which are relatively well represented in the models. We suggest future studies should use paleoneuroanatomical evidence cautiously in conjunction with other sources of data (e.g. nasal cavity volume, endosseous labyrinth morphology) to infer paleobiology.

Ontogeny of the Turtle Brain and Endocast

There are few published accounts on the juvenile brain morphology of turtles, or on ontogenetic changes in brain morphology (Werneburg and Maier 2019). Here, we examined brains of eight juvenile turtles using digital dissections of stained micro-CT scans, and show models for a hatchling *Emys orbicularis* as an example. A comprehensive assessment of anatomical variation among juvenile brains of a large sample of species is beyond the scope of this contribution, and we focus our brief description on features that appear to be ubiquitous for juvenile turtle brains. Although we do not have data for an ontogenetic series of brains of a single species, we contrast the juvenile brain morphology of *E. orbicularis* with that of an adult emydid *Trachemys scripta* (Fig. 4.7), the phylogenetically nearest adult turtle for which we have data available, highlighting several features that appear to undergo ontogenetic change.

The brain of the juvenile *Emys orbicularis* is anteroposteriorly short, mediolaterally broad, and dorsoventrally high in comparison to adult turtle brains, including *Trachemys scripta* (Fig. 4.7). The midbrain of juvenile turtles is strongly vertically oriented, leading to strongly angled pontine flexure (4 in Fig. 4.7a) and strongly ventrally convex pons–medulla elongata area (3 in Fig. 4.7a). Ontogenetic elongation of the brain leads to a more horizontal orientation of the midbrain, a reduction of the embryonic brain flexures, and an overall more tube-like brain shape (Fig. 4.7b). In the midbrain, the optic lobes are proportionally large in juvenile turtles (2 in Fig. 4.7a) but become ventrally retracted and anterolaterally covered by the cerebral hemisphere in adults (Fig. 4.7b), presumably as a consequence of both cerebrum growth and brain elongation. In the forebrain, olfactory bulbs and cerebral hemispheres are originally not well differentiated from one another (1 in Fig. 4.7a) but become clearly demarcated by a coronal groove that circumscribes their boundary in adults (Fig. 4.7b).

These general ontogenetic shape changes are also reflected in the endocasts of the braincase (Figs. 4.7b, d and 4.8). When endocasts of juvenile turtles are included in our geometric morphometric dataset of (dorsal) brain outlines (N = 47, of which eight are juveniles and 39 are adults) and analyzed with GPA and PCA, juveniles and adults are separated along the first PC axis (accounting for 68.5% of total

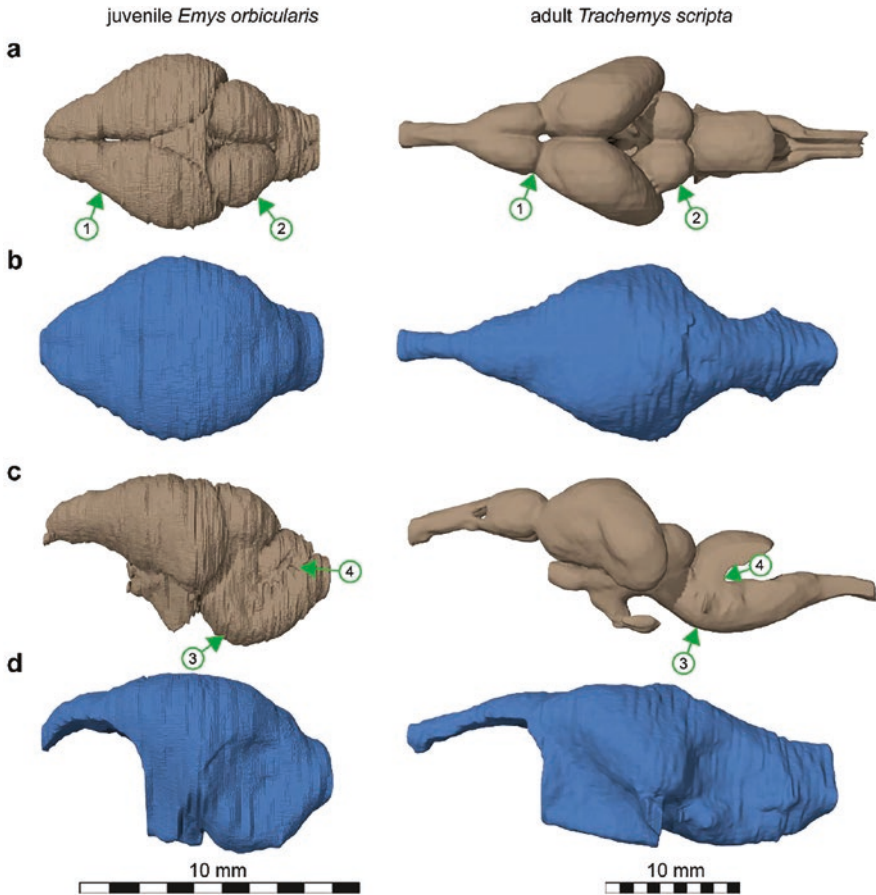


Fig. 4.7 Gross ontogenetic trends in postnatal turtle brain ontogeny. Early juvenile (hatchling) brain and braincase endocast of *Emys orbicularis* (SMNS 11390) in left column, adult brain and braincase endocast of *Trachemys scripta* (MS 000376944) in right column. (a), dorsal view of brains; (b), dorsal view of endocasts; (c), left lateral view of brains; (d), left lateral view of endocasts. 1–4 denote major areas of ontogenetic shape change as described in the text. (1), delimitation of olfactory lobe and cerebral hemisphere; (2), relative size of optic lobe; (3), pons-medulla oblongata area; (4), pontine flexure. Note 1:2 scale between left and right column

variation) (Fig. 4.8a). All juvenile specimens have extreme positive PC1 values and are characterized by more compact and rounder endocasts, with well-developed cerebral hemispheres and olfactory bulbs relative to the hindbrain regions. The adult specimens have much lower PC1 values, with more elongated endocasts. These ontogenetic changes (relative volume reduction, relative braincase elongation and decreased width along cerebrum) are particularly evident from juvenile-adult specimen-pairs of the same species (or closely related, e.g., *Podocnemis erythrocephala* and *P. unifilis*, Pelomedusoides; Fig. 4.8a). PC2 accounts for much less of total shape variation (9.5%), highlighting the relative importance of ontogeny

displayed along PC1. PC2 is associated with the relative position of the cerebral hemispheres and olfactory bulbs, either more anteriorly (positive values) or posteriorly (negative values) on the endocast.

Variation in Adult Braincase Endocast Morphology

To examine possible shape differences between phylogenetic groups we conducted a GPA and PCA on our dorsal outline landmark dataset excluding juveniles ($N = 39$). The results show a less predominant PC1 (49.1% of total variation)—although accounting for similar shape variation to that of the PCA including juveniles—and a more important PC2 (15.3%), which mostly explains changes on the olfactory bulb and nerve width and on the relative elongation of the mid- and hindbrain regions (Fig. 4.8b). Similar to the results by Lautenschlager et al. (2018) based on lateral outlines of endocasts, we found no significant morphospace separation between distinct clades or ecological groups and instead extensive overlap between groups. Nevertheless, early diverging taxa (Fig. 4.1) are more predominant on positive PC2 values, consistent with their less differentiated cerebral hemispheres and near-equal width along the entire endocast (Lautenschlager et al. 2018), but they overlap with a significant portion of the morphospace of crown-clades (Fig. 4.8b). Still, no Testudines extend into extremely positive PC2 values, indicating that a change to more defined and enlarged cerebral hemispheres and overall less elongated endocasts might have occurred on the transition to Testudines. This is reminiscent of the ontogenetic changes discussed above, suggesting a possible

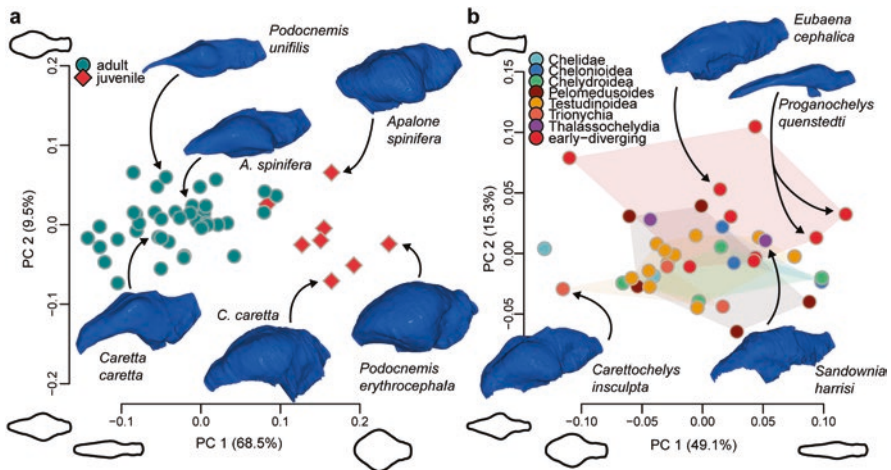


Fig. 4.8 (a), first PCA morphospace of braincase endocast shape (300 Procrustes-aligned evenly spaced landmarks on the dorsal view) on all complete dataset ($N = 47$), with datapoints colored by age class. (b), second PCA morphospace of braincase endocast shape based on the reduced dataset ($N = 39$), excluding juvenile specimens. Datapoints and convex hulls are colored by taxonomy

paedomorphic change in this region of the turtle skull. Although our analyses supplement those of Lautenschlager et al. (2018), future studies should analyze more complete ontogenetic series of extant taxa, a larger sample of early-diverging fossil turtles, and 3D shapes of endocasts. Especially 3D geometric morphometric approaches may capture variational features that are not included in our dataset. For example, our shape dataset includes no information about the nasal capsules, the endocasts of which also show variation in turtles. Paulina-Carabajal et al. (2017) computed relative olfactory bulb diameter (= OR, olfactory ratio) and nasal cavity volumes for three meiolaniid turtles, five testudinids and one geoemydid, and suggested that terrestrial turtles tend to have higher ORs and larger nasal cavities in comparison to aquatic species. Nasal cavity volume relative to total endocast volume has also been used to support interpretations of ecological adaptations for *Proganochelys quenstedtii* (Lautenschlager et al. 2018) and *Naomichelys speciosa* (Perichelydia; Paulina-Carabajal et al. 2019) as terrestrial turtles (see sect. 4.4.2.4), but these hypotheses require testing in a comparative statistical framework.

4.3.2 Spaces Associated with Cranial Blood Supply

A characteristic feature of the anatomically modern skull of crown turtles is a tight fusion between the palatoquadrate and the basicranium primitively along the pterygoid and basisphenoid, with various contributions from other bones such as the quadrate or prootic in some crown turtles, particularly pleurodires (Gaffney 1979; Werneburg and Maier 2019). This region of the skull is traversed by major blood vessels in amniotes (Müller et al. 2011), which become encased in bony canals during the evolution of the akinetic turtle cranium (e.g. Gaffney 1979). The carotid canals and their respective foramina have been intensely studied primarily for phylogenetic purposes (Gaffney 1975; Gaffney and Meylan 1988; Jamniczky 2008; Sterli and de la Fuente 2010; Rabi et al. 2013; Evers and Benson 2019; Hermanson et al. 2020; Rollot et al. 2021a). We direct the reader to Rollot et al. (2021a) for the latest revision of nomenclature and discussion of canals, foramina and associated structures.

Evolution of the Blood Canal System in Turtles

Early stem turtles such as *Proganochelys quenstedtii*, in which the basicranial joint, the cranioquadrate space, and the interpterygoid vacuity are retained (Gaffney 1990), show that the plesiomorphic condition of turtles is similar to that of other amniotes (Müller et al. 2011), in that they lack distinct canals for the cranial arteries and veins except for a canal for the cerebral artery, which traverses the basisphenoid (Gaffney 1990). The subsequent evolutionary encasing of blood vessels in bone is documented by fossil turtles. The lateral head vein is encased in the canalis cavernosus even in early diverging turtles more crownwards than *Proganochelys*, such as

the mesochelyids *Kayentachelys aprix* (Sterli and Joyce 2007), *Condorchelys antiqua* (Sterli and de la Fuente 2010) and *Eileanchelys waldmanni* (Anquetin 2010). These turtles also show an ossified canalis stapedio-temporalis for the stapedia artery. With the closure of the interpterygoid vacuity in perichelydians (Joyce 2017), the palatine artery becomes encased in a bony canal, which is for instance documented in *Mongolochelys efremovi* and *Kallokibotion bajazidi* (Sterli et al. 2010; Rabi et al. 2013; Martín-Jiménez et al. 2021). Subsequently, the course of the internal carotid artery, as well as its splitting point into cerebral and palatine arteries becomes encased in bone. However, the exact sequence of this closure is not well understood, primarily due to phylogenetic uncertainties (e.g. Joyce 2007; Evers and Benson 2019), and requires further research. Most fossil turtle clades which are frequently (but not consistently) found along the upper part of the turtle stem, such as sinemydids, xinjiangchelyids, and thalassochelydians (Fig. 4.1) have their posterior section of the internal carotid artery embedded in bone (Rabi et al. 2013; Evers and Joyce 2021), whereas the arterial split into palatine and cerebral artery is exposed in a fenestra caroticus (sensu Rabi et al. 2013). This possibly indicates that the closure followed a “posterior-section-first” pattern according to which the posterior section of the internal carotid artery closes before more anterior sections became encased (Rollot et al. 2021a). The arterial pattern of several clades, for instance in thalassochelydians (Raselli and Anquetin 2019; Evers and Joyce 2021) and paracryptodires (Rollot et al. 2018; Evers et al. 2020; Rollot et al. 2021b), shows considerable variation, which further complicates understanding the evolution of the carotid canal system. Some paracryptodires seem to have secondarily lost the palatine artery (Lipka et al. 2006; Rollot et al. 2018; Evers et al. 2020), and the repeated reduction of this artery has also been demonstrated for extant clades (Albrecht 1967; Rollot et al. 2021a). Notably, a palatine artery loss is observed in pleurodires, carettochelyids and testudinids (Joyce et al. 2018; Rollot et al. 2021a). The tight spatial association of parts of the vidian branch of the facial nerve with the internal carotid artery have sometimes led researchers to incorrect canal identifications (e.g. Sterli et al. 2010; Hermanson et al. 2020). Besides using dissection data (e.g. Albrecht 1967, 1976), digital segmentation of contrast-enhancing stained CT or MRI scans allow the unequivocal identification of canals of extant turtles based on tracing the neurovascular tissue through their canals.

Digital Dissection of Major Cranial Blood Vessels in *Trachemys scripta*

We use the *Trachemys scripta* scan to show the main arteries, the facial nerve, and the lateral head vein (Fig. 4.9). Despite variation in the blood supply system of extant turtles (see Albrecht 1967, 1976; Rollot et al. 2021a), particularly regarding the reduction of the palatine artery, the relative importance of the stapedia vs. palatine vs. cerebral arteries for supplying the facial region of the skull, and the origin of the mandibular artery, the carotid system of *T. scripta* serves as a good exemplar species for the generalized pattern described for turtles in the literature (e.g. Gaffney 1979).

In *Trachemys scripta*, the common carotid artery splits extracranially into the internal carotid and the stapediaal arteries (Fig. 4.9b). The stapediaal artery enters the skull via the fenestra postotica, joins the course of the lateral head vein in the cavum acustico-jugulare, where it gives off the mandibular artery before entering the stapediaal canal dorsally (Fig. 4.9a). The stapediaal artery exits dorsally into the upper temporal fossa via the foramen stapedio-temporale, where it bifurcates into the posteriorly directed cervical artery, and the anteriorly directed orbital branch of the stapediaal artery (Fig. 4.9a). In *T. scripta*, this anterior branch lies against the outer wall of the braincase and bifurcates upon entering the orbital fossa into a supra- and infraorbital artery. The mandibular artery follows the course of the lateral head vein through the canalis cavernosus and exits the skull laterally through the trigeminal foramen (Fig. 4.9a, b), together with the maxillomandibular branches of the trigeminal nerve. The internal carotid artery enters the skull via the foramen posterius canalis carotici interni and splits intracranially into the laterally directed palatine artery and the medially directed cerebral artery (Fig. 4.9b). Within the sella turcica, the cerebral artery develops a medial branch that anastomoses with the respective branch of the artery of the opposite skull side. From this network, a central branch supplies the hypophysis of the brain (Fig. 4.9b). Another, more lateral branch of the cerebral artery traverses around the hypophysis, where it splits into several subordinate branches that supply various regions of the brain. The palatine artery is antero-medially directed, and right and left arteries converge medially and anteriorly to the basisphenoid after exiting their anterior foramina (Fig. 4.9b).

4.4 Brain Evolution and Paleobiologic Inferences Based on Endocast Morphology

4.4.1 Brain-Size Evolution

The shape of the braincase endocast is not a good predictor of brain shape in turtles (see above), but its volume might still be informative on brain size. Despite the variation in the filling of the endocranial cavity by the brain (Table 4.1), the total volume of the endocast is highly correlated to the volume of the brain tissue in turtles as indicated by phylogenetic generalized least squares (pGLS; Grafen 1989) regression analysis of brain volume ~ endocast volume ($R^2 = 0.97$, $p = <0.001$, $\lambda = -0.56$). This result provides support for analyses of brain size evolution in turtles using endocast volumetric measurements as a reliable proxy. The slope of the regression (slope = 0.92; SE = 0.08) indicates weak negative allometry (i.e., larger turtles have proportionally smaller brains in comparison to braincases) based on an isometric expectation of 1. However, as our data includes juveniles and adults of several species, further data is required to disentangle ontogenetic and evolutionary allometry for turtle brain-endocast relationships. In addition, a pGLS regression between endocast and box volumes (the smallest virtual digital cube to contain the

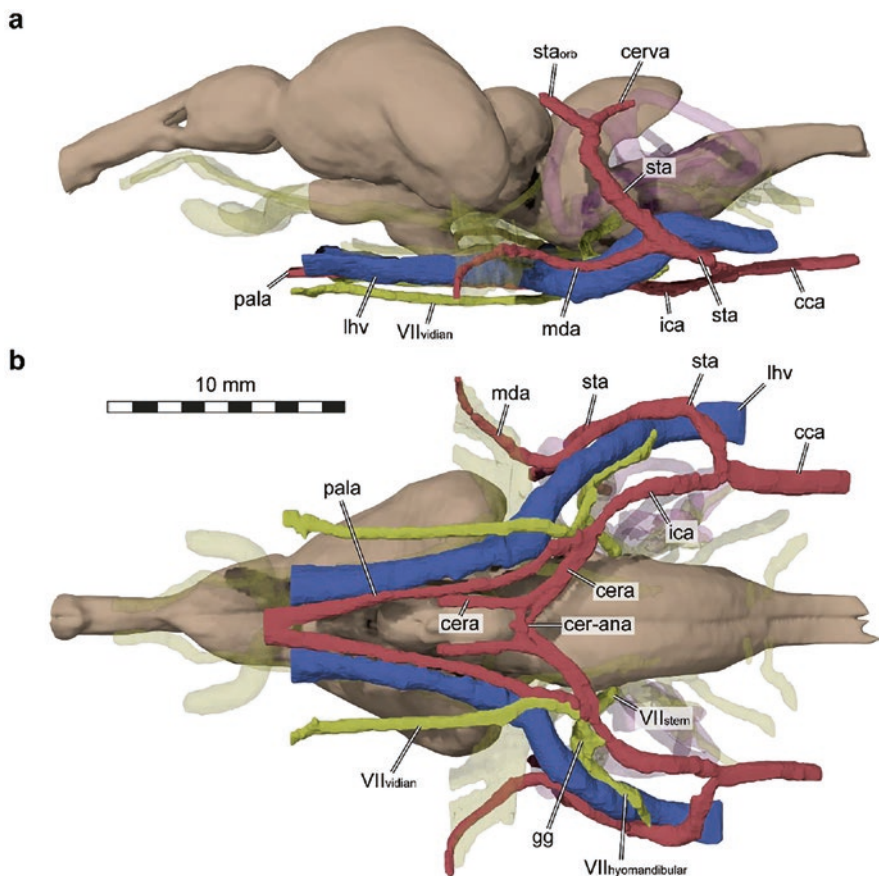


Fig. 4.9 3D rendering of brain, major cranial arteries, lateral head vein and the facial nerve (CN VII) of *Trachemys scripta* (MS 000376944). (a), left lateral view. (b), ventral view. Abbreviations: *cca* common carotid artery, *cer-ana* anastomosing region of cerebral artery, *cera* cerebral artery, *cerva* cervical artery, *gg* geniculate ganglion of the facial nerve, *ica* internal carotid artery, *lhv* lateral head vein, *mda* mandibular artery, *pala* palatine artery, *sta* stapedial artery, *sta_orb* orbital branch of stapedial artery (subdivides anteriorly into infra- and supraorbital arteries), *VII_{hyomandibular}* hyomandibular branch of the facial nerve, *VII_{stem}* nerve stem of facial nerve, *VII_{vidian}* vidian branch of facial nerve

whole skull) shows a high correlation between endocast volume and skull size (slope = 0.64, SE = 0.05, $p < 0.001$, $R^2 = 0.83$, lambda = 0.46), suggesting that braincase size has a negative allometric relationship with skull size (i.e. turtles with larger skulls have proportionally smaller endocast volumes).

There is currently no published encephalization quotient (EQ) data specifically for turtles (although it has been done for reptiles; Jerison 1973; Hurlburt 1996) and only a few studies examined broad patterns of brain size evolution in turtles. Van Dongen (1998) and Northcutt (2013) used regressions of brain to total body weight to explore relative brain size in various reptiles, and turtles were shown to have the

lowest values in the group (together with snakes; Van Dongen 1998). This has been explained by the “simple locomotion, and a passive protection against predators” characteristic of turtles, thought to be correlated with smaller brains (Van Dongen 1998). However, those early studies included small samples—only seven species, all cryptodires—and turtles in fact engage in a greater array of locomotion and feeding behaviors than commonly appreciated (see, for instance, Bonin et al. 2006 or Pritchard 1984).

Paulina-Carabajal et al. (2017) investigated the evolution of volumetric measurements obtained from digital endocasts of turtles, nasal capsule size and the olfactory ratio. Lautenschlager et al. (2018) compared the endocast volume relative to body size of eleven turtles, in a first attempt to analyze relative brain size evolution. Here, we present an expanded analysis to explore this trait in turtles, using a larger sample and ancestral state reconstructions (fastAnc function of R package phytools; Revell 2012). We extracted endocast volumes of 27 (19 extant and eight extinct) taxa spanning the whole Testudinata tree, only using adult specimens (Fig. 4.1). The log-transformed endocast volume was divided by the log-transformed skull box volume (length x width x height) to estimate the brain size relative to body size. We chose box volume to avoid introducing errors deriving from distinct dimensionalities. We then performed a Maximum Likelihood ancestral states estimate using the endocast/box volume ratio and a large Testudinata tree (from B. Farina, unpublished results) pruned to our taxon sample.

The earliest nodes and taxa (e.g., *Proganochelys quenstedtii* and *Naomichelys speciosa*) have the smallest relative brain sizes in our sample (Fig. 4.10, Testudinata node). Relative brain size then successively increases until reaching larger ancestral values at the Testudines node (in agreement with Lautenschlager et al. 2018). Stem-turtles close to the crown, such as *Annemys* sp. (Xinjiangchelyidae) and *Plesiochelys etalloni* (Thalassochelydia), already possess moderate relative brain sizes, with similar values to those estimated for the Cryptodira and Pleurodira nodes, showing relative brain size increases predated the origin of crown turtles. When these results are paired with shape evolution from PCA analyses (Fig. 4.8b), this suggests that turtle brains evolved larger sizes relative to their skulls in conjunction with shape changes towards rounder and less elongated endocasts with more prominent cerebral hemispheres. As evolutionary brain shape changes mirror those happening during ontogeny (Figs. 4.7 and 4.8a), it is possible that such paedomorphic (shape) changes resulted in relative brain size increases, given that paedomorphic changes have also been proposed to be related to larger brains in other groups (e.g. Bhullar et al. 2016). This also supports the hypothesis of Sterli et al. (2018) that paedomorphic changes may have played a major role during the early evolution of turtles.

For crown turtles (Testudines), our results suggest at least three episodes of relative brain size increase: in Chelidae, Carettochelyidae and Testudinoidea; and four decreasing episodes: in Chelydridae, Cheloniidae, Trionychidae, and the branch leading to *Platysternon megacephalum* (Fig. 4.10). Although these episodes could be an artifact of our small sample size and non-random selection of taxa, we do not think this is the case in Testudinoidea, which was relatively well-sampled and in which taxa consistently presented high values (Fig. 4.10). It is unknown how (and

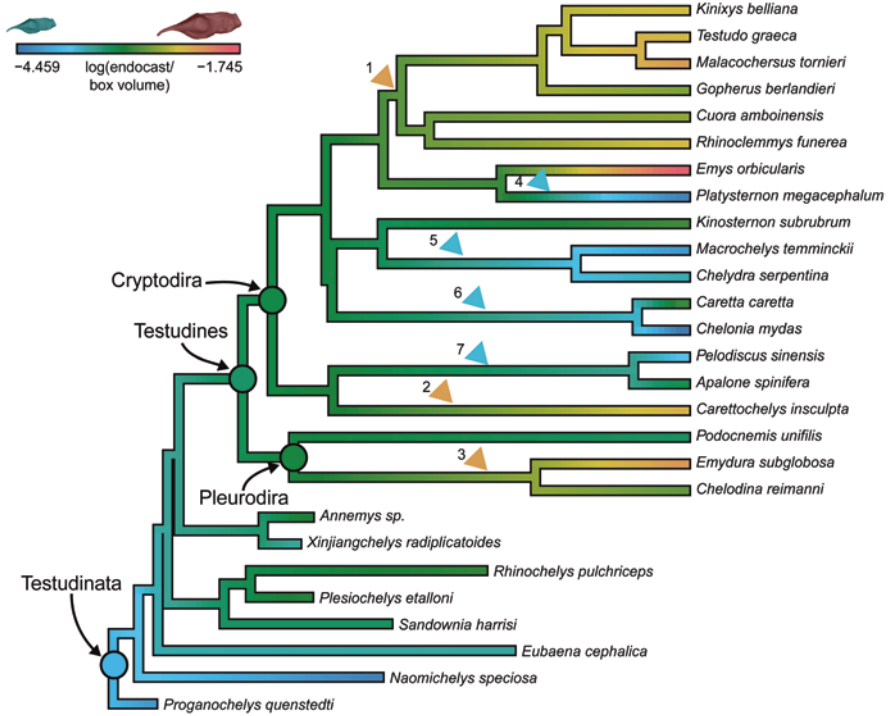


Fig. 4.10 Relative brain size evolution in Testudinata. Maximum-likelihood ancestral estimate mapping of log-transformed endocast/box volume ratio for a sample of adult crown and stem-turtles. Warmer and colder colors indicate, larger and smaller relative brain sizes, respectively. Colored triangles highlight potential episodes of significant brain size changes numbered accordingly: (1), Testudinoidea; (2), Carettochelyinae; (3), Chelidae; (4), Platysternidae; (5), Chelydridae; (6), Cheloniidae; (7), Trionychia

if) relative brain size is correlated with general or specific ecological and behavioral characters in turtles, but it is noteworthy that relatively high levels of social cognition have been identified for tortoises (Wilkinson et al. 2010). Shifts to relatively smaller brains in our data are associated with larger heads—Trionychia being the exception: chelydrids, cheloniids and *Pl. megacephalum* are all macrocephalic turtles with short necks, with limited or no ability of head retraction (Werneburg et al. 2015). This might reflect the choice of head box volume as an allometric correction variable, biasing the results in macrocephalic turtles, but it is reasonable to assume the brain size is proportional to body size and not simply to head size. Future studies should consider this and use a different variable, for example a proxy for total body size (e.g. carapace length).

4.4.2 Sensory Evolution

Vestibular Sense

The membranous ducts of the vestibular organ are contained in bony canals and cavities—the endosseous labyrinth—that can be studied from skeletal remains, including fossils. In all turtles, the prootic, opisthotic, and supraoccipital jointly form the endosseous labyrinth (Gaffney 1979). The endosseous labyrinths of turtles are known from a variety of different extant species (Georgi and Sipla 2008; Paulina-Carabajal et al. 2017; Lautenschlager et al. 2018; Evers et al. 2019b), which have primarily been documented as comparative data in studies of fossil turtles. Labyrinths are known for many extinct turtle groups, including Triassic stem-turtles (Lautenschlager et al. 2018), meiolaniforms (Paulina-Carabajal et al. 2017), thalassochelydians (Paulina-Carabajal et al. 2013; Evers et al. 2020), paracryptodires, helochelydrids and *Kallokibotion* (Paulina-Carabajal et al. 2019; Martín-Jiménez et al. 2021; Evers et al. 2021), protostegids (Evers et al. 2019b), and various fossil pelomedusoids (Ferreira et al. 2018b; Hermanson et al. 2020; Joyce et al. 2021b; Martín-Jiménez and Pérez-García 2021).

All turtles share a similar endosseous labyrinth morphology (Fig. 4.11). Turtle labyrinths are low dorsoventrally and broad anteroposteriorly in comparison with mammals (e.g. Ekdale 2013) or birds (e.g. Benson et al. 2017) and closer in their aspect ratio to labyrinths of crocodylians and lepidosaurs (e.g. Walsh et al. 2009). However, at least for the crocodylian labyrinth, shape similarities to other reptiles including turtles are the result of convergence rather than plesiomorphic retention of a ‘reptilian’ labyrinth shape (Bronzati et al. 2021). As in crocodylians and rhychocephalians, the anterior and posterior semicircular canals of turtles are roughly symmetrical, giving a low pyramidal outline of the labyrinth in lateral view (Fig. 4.11b). The semicircular canals of turtles are generally thick and robust, and very unlike the delicate canals seen in most mammals, birds, or squamates. All turtles have a secondary common crus (Fig. 4.11c), which masks parts of the course of the lateral and posterior semicircular ducts as can be seen from membranous to endosseous labyrinth comparison of *Trachemys scripta* (Evers et al. 2019b), and which we confirm here with additional comparisons in *Apalone spinifera* and *Platysternon megacephalum* (Fig. 4.11h–m). The ampullae of the semicircular canals are rarely discernible from turtle endosseous labyrinths, and there is no osteologically traceable cochlear duct (Fig. 4.11), unlike in most other vertebrates (e.g. Walsh et al. 2009).

In general, the morphology of the endosseous labyrinth of turtles is a particularly poor representation of the membranous labyrinth in comparison to most other gnathostomes (Evers et al. 2019b). As it is the membranous labyrinth that determines the functionality and sensitivity of the vestibular organ (e.g. Wilson and Melvill Jones 1979; Rabbitt et al. 2004), it is difficult to make functional predictions or paleoecological inferences based on the shape of the endosseous labyrinth from single taxon studies. Evers et al. (2019b) suggested using a landmarking protocol that reconstructs the approximate endolymph flow path of turtle inner ears to

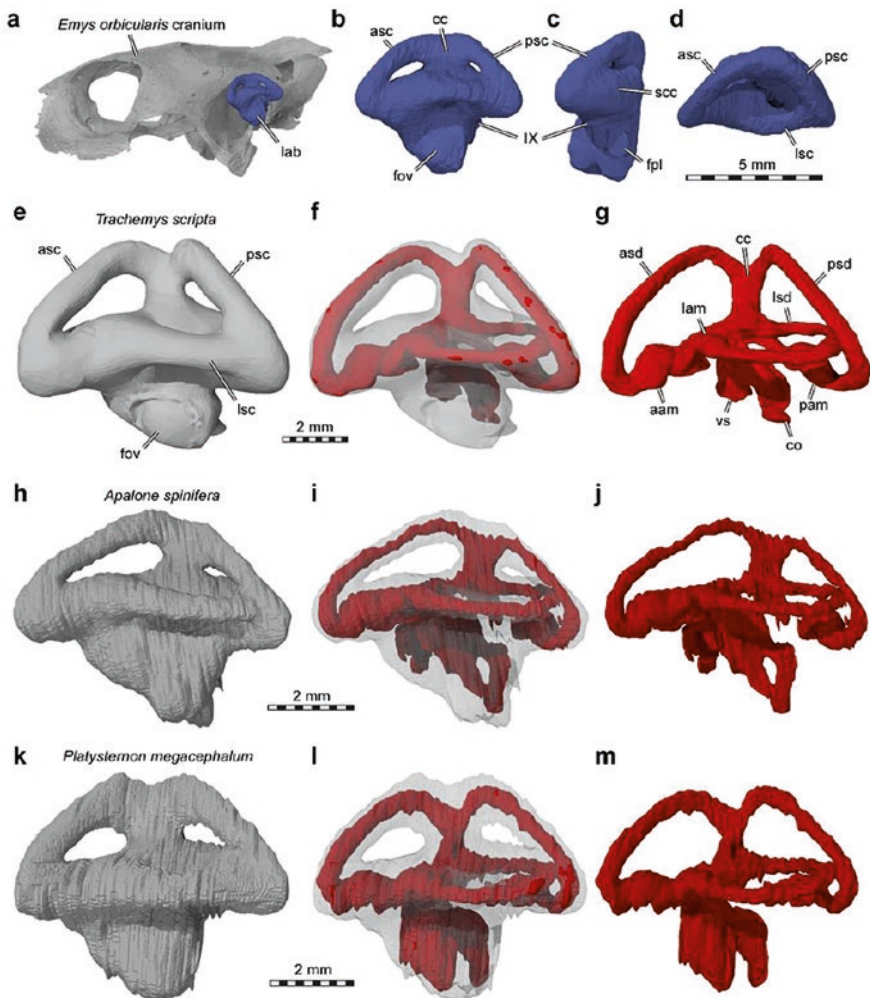


Fig. 4.11 (a), digital transparent rendering of the cranium of *Emys orbicularis* (SMF 1987a) and endosseous labyrinth to scale in left lateral view. (b–d), details of endosseous labyrinth morphology of *Emys orbicularis* (SMF 1987a) in lateral (b), posterior (c), and dorsal (d) views. (e–m), comparisons of endosseous (e, h, k) and membranous (g, j, m) left labyrinths and spatial associations between both (f, i, l) in lateral view. (e–g), *Trachemys scripta* (MS 000376944). (h–j), *Apalone spinifera* (YPM VZ-12970). (k–m), *Platysternon megacephalum* (YPM VZ-12559). Abbreviations: *aam/lam/pam* anterior/lateral/posterior ampulla, *asc/lsc/psc* anterior/lateral/posterior semicircular canal, *asd/lsd/psd* anterior/lateral/posterior semicircular duct, *cc* common crus, *co* cochlear duct, *fpl* fenestra perilymphatica, *fov* fenestra ovalis, *IX* glossopharyngeal nerve, *lab* endosseous labyrinth, *scc* secondary common crus, *vs* vestibule

mitigate the weak shape correspondence of endosseous labyrinths with the membranous ducts. Contrary to protocols landmarking external features of the endosseous labyrinth endocasts (e.g. Hanson et al. 2021), such a concept captures shape aspects

related to the functionality of the labyrinth organ more directly, and was recently implemented by Bronzati et al. (2021). Although turtle labyrinth shape has not yet been quantitatively analyzed in an ecomorphological context, some possible functional signal has been identified qualitatively. Particularly, Neenan et al. (2017) noticed that chelonoid sea turtles and pelagic sauropterygians have increased thickness of the semicircular canals, which has since also been observed for metriorhynchosaurs (Schwab et al. 2020). Evers et al. (2019b) corroborated the principal observations of Neenan et al. (2017) for chelonoids, finding extreme canal thickness in the leatherback sea turtle *Dermochelys coriacea* (Chelonioida), but noticed that some non-marine turtle clades also show thicker semicircular canals, e.g. the exclusively terrestrial Testudinidae. Thus, a marine lifestyle cannot be the only explanation for increased canal thickness. Given that the ecomorphological signal of the labyrinth is surprisingly low for archosaurs (Bronzati et al. 2021) and birds (Benson et al. 2017), turtle labyrinth shape should be interpreted with caution until comparative ecomorphological studies have been conducted for the group.

Hearing

Hearing is thought to be a less important sense than vision or chemoreception in turtles (Thewissen and Nummela 2008), once thought to be “the silent group” (Campbell and Evans 1972). Until recently little was known about the role of sound production and perception in the group, although some studies investigated vocalization in terrestrial turtles (reviewed in Giles et al. 2009). Varied types and degrees of vocalization have now been reported in sea (e.g. Mrosovsky 1972; Ferrara et al. 2014a, b) and freshwater turtles (e.g. Ferrara et al. 2017). Even pleurodires, once thought not to vocalize at all (Galeotti et al. 2005), are now known to exhibit incredibly rich vocalization repertoires (Giles et al. 2009; Ferrara et al. 2013, 2014c). Vocalization capacity does not necessarily equate to similar ranges of hearing sensibility, as has been shown for birds (Konishi 1970), but if a variety of calls and sounds are used in association with social behaviors (Ferrara et al. 2014b, c), it is expected that hearing plays a more relevant role in turtles than previously thought.

The turtle middle and inner ears have been described in great detail elsewhere (e.g. Hetherington 2008; Foth et al. 2019), hence we will simply outline their most important morphological features here. Impedance-matching hearing in turtles evolved independently from other amniotes (Sobral et al. 2016), but it displays its common features: a tympanum, an air-filled middle ear cavity and an osseous element (columella) that transfers vibrations to the inner ear. In all extant turtles, the middle ear cavity is compartmentalized to a lateral, funnel-shaped cavum tympani of the quadrate that embraces the tympanic membrane, and a medial pericapsular recess. This space functions as a re-entrant fluid system and constitutes the pressure relief mechanism in turtles, which lack a fenestra pseudorotunda (Sobral et al. 2016; Foth et al. 2019). The ossicular chain consists of a thin, rod-like bony columella and a cartilaginous extracolumella. The columella broadens medially forming the stapedial footplate, which articulates with the oval window. Laterally it passes into the

cavum tympani through the incisura columella auris (Gaffney 1979) and contacts the extracolumella that, in turn, contacts the tympanic membrane. The membrane is covered by layers of connective tissue and skin in turtles (Wever 1978), being much thicker in comparison to most tetrapods (Hetherington 2008). Inside the inner ear, the hair cells of the basilar papilla are also distributed on the limbic cells in turtles, instead of exclusively on the basilar membrane as in other reptiles (Wever 1978). This condition is similar to that of amphibians, in which it has been hypothesized to be related to underwater hearing (Hetherington 2008).

Some adaptations in the hearing system of turtles have been recognized for some time, such as the presence of fatty tissue in the middle ear of sea turtles (Ridgway et al. 1969; Lenhardt et al. 1985) and the variation in the convergence ratio of the tympanic membrane and oval window areas, as well as the presence of otoliths in the inner ears of the fossorial gopher tortoises (Bramble 1982), as well as many other species of various clades (SWE, personal observation). Also, the volume of the middle ear cavity correlates with a gradient of strongly aquatic-terrestrial habits in turtles (Foth et al. 2019). Chelonoids, for example, have a reduced antrum postoticum (even more reduced by the presence of fatty tissue) in comparison to most less aquatic turtles (Gaffney 1979). Moreover, aquatic turtles can vocalize both in air and underwater (e.g. Ferrara et al. 2013) and recent studies even suggest turtles overall hear slightly better in air than under water (e.g. Zeyl and Johnston 2015). The earliest stem turtles likely did not possess a complete impedance-matching ear and it is unclear in which environment this innovation has evolved in the lineage. The columella of *Proganochelys quenstedtii* is stout and articulated with the quadrate instead of a tympanic membrane (Gaffney 1990; Lautenschlager et al. 2018). The earliest turtle to show all osteological traits of the modern turtle ear is the Middle Jurassic *Eileanchelys waldmani* (Foth et al. 2019). Finally, physiological data on turtle hearing are currently insufficient to derive strong correlations between function and middle ear morphology in the group (Foth et al. 2019).

Vision

Turtles are in general diurnal reptiles that are thought to heavily rely on their visual senses (Northmore and Granda 1991; Schuyler et al. 2014). Experiments on sea turtles have shown that they are relatively limited in using chemical cues to find food and always prefer visual signs instead (Constantino and Salmon 2003; Southwood et al. 2007). Turtles, in general, possess a well-developed visual apparatus, having tetrachromatic vision (except in trionychids; Emerling 2017), with three types of photopigments aided by four classes of oil droplets, which act as cut-off filters enhancing discrimination of colors (Vorobyev 2003). Indeed, the most complex cone system ever studied in vertebrates is that of *Trachemys scripta* (Loew and Govardovskii 2001). Sea turtles are also able to select prey based on their color (usually avoiding blueish objects; Schuyler et al. 2014) and detect transparent plankton using UV sensitive photoreceptors (Wyneken et al. 2013).

Although most extant turtles inhabit aquatic environments, Northmore and Granda (1991) showed that both the freshwater *Trachemys scripta* and the marine *Chelonia mydas* possess emmetropic (i.e. no refractive error or de-focus) eyes in aerial medium, becoming hyperopic underwater. As such, they need to accommodate their eyes underwater to focus on images. This is usually accomplished by deforming the lens using ciliary body and iris muscles (but Brudenall et al. 2008 suggested a different mechanism for *Dermochelys coriacea*; Wyneken et al. 2013). The overall shape of the eye and lenses also seem to differ among freshwater and sea turtles: in the freshwater *Pseudemys scripta* the lenses are flat and the cornea rounded, the cornea being the refraction structure, whereas in sea turtles, the lenses are spherical and possess refractive power and the straighter corneas work more as a barrier from the external environment (Northmore and Granda, 1991; Wyneken et al. 2013). Marine turtles also present a shift towards shorter wavelengths (blue), accomplished by chromophores derived from vitamin A1 (instead of A2; Emerling 2017). All those observations were done on a rather small sample of turtles, restricted to sea turtles, the emydid *Pseudemys scripta* and two trionychid species (Northmore and Granda 1991; Wyneken et al. 2013; Emerling 2017). To our knowledge, the vision system of pleurodires and most cryptodiran lineages has never been analyzed, so generalizations made from the previously cited studies should be considered with caution.

The parietal (or pineal) eye, a portion of the epithalamus commonly exposed dorsally on the skull roof of reptiles, is absent in turtles. It is a conspicuous trait in squamates, and functions as a photoreceptive organ aiding in thermoregulation through the modulation of melatonin secretion (Eakin 1973). Turtles have lost the pineal eye early in their evolution, considering that it is absent in all candidate proto-turtles (Li et al. 2008, 2018; Schoch and Sues 2018), except *Eunotosaurus africanus* (Bever et al. 2015). The visual system can be studied in fossils, for example by assessing orbit size and diverticula evolution. Turtles—as most reptiles—possess small eyes relative to body size (Howland et al. 2004), but there is extensive variation in orbit sizes in the group, with early turtles (such as *Proganochelys quenstedtii*) and chelonioids seemingly having larger orbits than most freshwater taxa. Further, pockets in the postorbital septum found in some marine pleurodires (Gaffney et al. 2006, 2011) have been associated with salt glands (Ferreira et al. 2015), as have reduced descending processes of the parietal in protostegids (Hirayama 1998). Such glands are found in modern sea turtles (Wyneken 2001), which also show reduced ossification of the interorbital region. However, short anterior braincase walls also exist in some terrestrial species (Joyce 2007), so that this condition should perhaps not be seen as an unambiguous indication for the presence of salt glands.

Olfaction

The nasal cavity of turtles, as in other tetrapods, is roughly subdivided into three main areas (Parsons 1959a): the anterior vestibulum, which connects the remainder of the nasal cavity to the external nares (= apertura narium externa; Gaffney 1979); the cavum nasi proprium, the intermediate main chamber; and the posterior connection to the choanae, the nasopharyngeal duct. The borders between those regions are usually not well defined externally, but the epithelia in each of them show clear specializations (Parsons 1959b).

The vestibulum and the nasopharyngeal duct of turtles are simple tubular structures connecting the external nares and the choanae, respectively, to the proper nasal cavity (Parsons 1959a, 1970). They are not sensorial organs as they are covered only by epidermal-like epithelium (Parsons 1959a, 1967), thus mainly functioning as air passages through the nasal organ. In some turtles, such as trionychians and the chelid *Chelus fimbriatus*, the vestibulum forms an anterior projection of soft-tissue that extends beyond the bony nostrils. In some of those this proboscis functions as a snorkel (e.g. *Chelus fimbriatus* and *Dogania subplana*; Bonin et al. 2006), but in most species, its function is unclear. It seems, however, that in all these taxa the ventral margin of the apertura narium externa is considerably projected in relation to its dorsal edges (Gaffney 1979), providing support for the elongation of the soft-tissue structure. The elongation of the vestibulum can thus be inferred from this osteological correlate. The anterior elongation of the vestibulum can also be achieved by expansion of both its floor and roof, as is the case of the extinct turtles *Naomichelys speciosa* and meiolaniids, and in some testudinids, such as *Gopherus berlandieri* (Paulina-Carabajal et al. 2017, 2019), as well as in *Macrochelys temminckii* and *Platysternon megacephalum* (Lautenschlager et al. 2018). In these taxa, the vestibulum is easily distinguishable from the cavum nasi proprium by a constriction on the endocast (Paulina-Carabajal et al. 2017, 2019; Lautenschlager et al. 2018), but a proboscis is not present. In either case, expanded vestibula might relate to enlarged external nasal glands, which develop on the posterior portion of this region (Parsons 1970); alternatively, they can represent an adaptation to life in arid conditions, restricting sand particles from reaching the inner nasal cavity (Parsons 1959a). The nasopharyngeal duct also varies considerably in length, depending on the position of the choanae. It is particularly long in taxa which develop a hard secondary palate, e.g., *Caretta caretta* (Jones et al. 2012; Yamaguchi et al. 2021). The endocast of the nasopharyngeal duct might exhibit laterally divergent or convergent chambers (Lautenschlager et al. 2018).

The cavum nasi proprium is the olfactory sensitive region in the nasal organ. The entire inner surface of the cavum is covered by sensorial epithelium (Parsons 1959b). Its dorsal portion, which is coated by Bowman's glands, is the olfactory region sensu stricto (Parsons 1967). The olfactory region in turtles usually develops two (Cheloniodea; Parsons 1967; Yamaguchi et al. 2021) or one (all other known turtles; Parsons 1967) sac-like chambers, but, unlike amphibians (except Caudata; Parsons 1959a) and all other amniotes, they never develop conchae, i.e. wall infoldings (Parsons 1959a, 1967). In some turtles, especially in trionychids, some

ridges—named “Muschelwulst”—develop on the walls of the olfactory region, however those are typically low and not as elaborate as the conchae in other amniotes (Parsons 1967). A particularly well-developed ridge partially separates the olfactory and the intermediate region, i.e. the ventral half of the *cavum nasi proprium*, whose epithelium, called vomeronasal epithelium, lacks Bowman’s glands. When the vomeronasal epithelium is restricted to ventromedial pockets, it is called Jacobson’s or vomeronasal organ, found in many other amniotes (Parsons 1959b, 1967). The vomeronasal epithelium is always present in turtles, but they generally lack any ventromedial pockets, with the curious exception of cheloniids in which a single or a pair of pockets forms (Parsons 1959a, 1967; Yamaguchi et al. 2021). However, since the vomeronasal epithelium is not restricted to those pockets in sea turtles (Saito et al. 2000), they are not termed vomeronasal organs. Similar ventral pockets have been identified and tentatively associated with the vomeronasal system in some fossil turtles, notably protostegids (Evers et al. 2019a). How similar these pockets in sea turtles are to the true vomeronasal organs of other amniotes is currently unclear.

Two metrics have been used to investigate quantitatively the olfactory sense in turtles (and in other taxa; Zelenitsky et al. 2009, 2011) using endocasts: the olfactory ratio (OR) i.e. the ratio between olfactory bulb and cerebral hemisphere maximum diameters (Bang and Cobb 1968; Bang and Wenzel 1985), and the volume of the nasal cavity relative to total (nasal cavity and brain) endocast volume (Paulina-Carabajal et al. 2013, 2017; Lautenschlager et al. 2018). Among extant taxa, the terrestrial testudinids have the largest relative nasal cavities and highest ORs, while the early diverging *Proganochelys quenstedtii* (Lautenschlager et al. 2018) and meiolaniids (Paulina-Carabajal et al. 2017) show the highest values among all Testudinata. These data point to a greater reliance on olfaction in testudinids in comparison to other modern turtles, and suggests a more terrestrial lifestyle in those fossils, agreeing with previous paleobiological inferences (Sterli 2015; Joyce 2017). It is important to note, though, that there are no available data supporting a correlation between the size of the nasal cavity and olfactory acuity, contrary to the well-established relation with OR values (Zelenitsky et al. 2009). Nevertheless, considering that sensory epithelium covers the *cavum nasi proprium*, larger cavities will surely result in larger sensorial surfaces. Hence, we agree with Paulina-Carabajal et al. (2017) that the size of the nasal cavity can be used together with OR values to indicate olfactory acuity.

Both the OR and the relative size of the nasal cavity carry methodological and biological caveats. First, as recognized by Lautenschlager et al. (2018), the high OR value found in *P. quenstedtii* is likely not entirely related to larger olfactory bulbs, but also to its underdeveloped cerebral hemispheres. The nasal cavity volume might as a ratio reflect proportional changes in the brain endocasts instead of actual larger nasal cavities. Further, even though the *cavum nasi proprium* is the actual chemical sensory organ (Parsons 1959a), in many animals it serves additional functions, such as thermoregulation and sound production (Parsons 1959a, 1970; Bourke et al. 2014). Thus, nasal cavity volume alone might be misleading when investigating paleobiology. Nevertheless, because turtles lack nasal conchae (Parsons 1959a,

1967), expanding the total volume of the nasal cavity might be the best strategy for increasing the area of olfactory acuity. Future studies should tackle the relation between the size of this structure and both life habits and olfactory capabilities in turtles to explore potential ecomorphological trends.

4.5 Future Directions

Our summary of turtle neuroanatomical information highlights numerous knowledge gaps and areas requiring further investigations. There is a lack of physiological studies on sensory perception and such studies are necessary as they form the basis for morphofunctional inferences. Using contrast-enhancing stained CT or MRI protocols to analyze extant species and increase documentation of fossils over the entire tree should be one focus for turtle anatomy specialists. Overinterpretation of individual morphology should be avoided and based on rigorous form-function analyses in a statistical framework including large sample sizes, which are currently rare. Turtles present a great case-study of ecomorphology due to their uncommonly rich fossil record and multiple habitat transitions during their evolution. Our functional understanding of morphological structures related to sensory evolution, such as the relative size of the nasal cavity and olfactory bulb, and the structures of the middle and inner ear, can greatly benefit from future studies using an ecomorphological approach. Even though endosseous endocasts do not seem like good predictors of soft tissue anatomy in the group, potential correlations between those and the varied ecologies of turtles might yield valuable evolutionary conclusions. On the other hand, our positive results for the relation between the relative volume of endocasts and soft tissue structures should stimulate further research on size evolution of neuroanatomical structures. Particularly interesting are the great changes observed between juvenile and adult turtles. More data on ontogenetic series are also needed to further explore potential heterochronic and allometric relations of neurological structures and the skull in turtles.

4.6 Concluding Remarks

Although the increased availability of digital tools and methods fuels progress in neuroanatomical research on turtles, the topic remains underexplored. Most studies on turtle neuroanatomy are reports of fossil or extant neuroanatomical structures of individual species, and taxonomically more comprehensive studies often lack an explicit phylogenetic comparative framework in which ecomorphological hypotheses could be tested – instead, most ecological inferences that are drawn from turtle neuroanatomical structures are based on anecdotal correlations of form and ecology. For instance, the relationships between specific semicircular canal diameters and degrees of aquatic ecology including untested correlations of thick canals with

diving ecology are sometimes invoked – to name but one example. In addition, most studies have so far relatively uncritically assumed that the endosseous cavities of dry skulls or fossils are faithful representations of the organs they hold. With this contribution, we have specifically highlighted caveats regarding this practice, and found mixed results for brain-braincase and membranous-endosseous labyrinth comparisons. Turtles as extant reptiles offer the chance to more regularly use actual soft tissue anatomy to inform paleoneurological studies, even if only to be cautious about overinterpreting structures from braincases that may not be mirrored in soft tissue organs. In this regard, turtles may even be insightful for distantly related reptile groups that lack extant representatives, including ichthyosauriforms, sauropterygians, or even clades of early archosauriforms. What is also needed is a good understanding of the ecology and biology of extant turtles, without which paleontologists cannot establish a solid framework for understanding extinct animals. Exciting findings have emerged recently, showing for example that vocalization (and probably hearing as well) is far more important to turtle biology than previously thought. Currently, the evolution of neuroanatomical structures including the arterial circulation system are better understood than their ecomorphology. Neuroanatomical characters are increasingly used in phylogenies, but character construction is difficult due to the necessity to discretize often continuous observations. The use of continuous characters as well as assessing the impact of current approaches to neuroanatomical characters could be research topics worth exploring. Our novel data reveal extensive ontogenetic changes on the brains and endocasts of extant turtles and suggest that similar transformations may have occurred during the evolutionary transitions of Testudines, indicating that evo-devo approaches may provide interesting insights in the future.

A critical point for the future of the field is the deposition of scan and model data in online repositories. Currently, the practice for this varies between research groups, but the wide availability of data will be instrumental for future ‘big data’ approaches and comparative anatomical analyses. In addition to the hesitation of individual researchers to deposit data, the matter is complicated by a spectrum of institutional policies varying from the requirement of online deposition of data without download restrictions to the physical retention of data at museums without the possibility of online deposition or the permission to share data directly. For old scans that have been passed on through several researchers, permissions are sometimes unclear, further complicating the issue. Whenever possible, we ask and recommend colleagues to deposit the data for open use, as the community tremendously benefits from this practice.

Acknowledgments We thank Bruna Farina, Guilherme Hermanson and Pedro Godoy for advice and insights on the analyses; we further acknowledge Bruna Farina for sharing the supertree we used here. Cathrin Pfaff and Jürgen Kriwet are thanked for scanning specimens at the University of Vienna. We also thank Gilles Laurent for sharing the *Trachemys scripta* scan with us, as well as James Neenan for organizing the scan for our previous paper. The reviewers Walter Joyce and Adan Pérez-García, and the editors María Teresa Dozo, Ariana Paulina-Carabajal, Thomas Macrini and Stig Walsh are thanked for their insightful comments and suggestions. IW acknowledges DFG for financial support (grant WE 5440/6-1).

References

- Adams D, Collyer M, Kaliontzopoulou A, Baken E (2021) Geomorph: software for geometric morphometric analyses. R package version 4.0. <https://cran.r-project.org/package=geomorph>. Accessed 12 Aug 2021
- Albrecht PW (1967) The cranial arteries and cranial arterial foramina of the turtle genera *Chrysemys*, *Sternotherus*, and *Trionyx*: a comparative study with analysis of possible evolutionary implications. *Tulane Stud Zool* 14:191–216
- Albrecht PW (1976) The cranial arteries of turtles and their evolutionary significance. *J Morphol* 149:159–182
- Allemand R, Boistel R, Daghfous G et al (2017) Comparative morphology of snake (Squamata) endocasts: evidence of phylogenetic and ecological signals. *J Anat* 231:849–868. <https://doi.org/10.1111/joa.12692>
- Anquetin J (2010) The anatomy of the basal turtle *Eileanchelys waldmani* from the Middle Jurassic of the Isle of Skye, Scotland. *Earth Environ Sci Trans R Soc Edinburgh* 101:67–96. <https://doi.org/10.1017/S1755691010009217>
- Baird IL (1974) Anatomical features of the inner ear in submammalian vertebrates. In: Keidel WD, Neff WD (eds) *Handbook of sensory physiology, volume V/1: auditory system: anatomy physiology (ear)*. Springer, Berlin, pp 159–212
- Balanoff AM, Bever GS, Colbert MW et al (2016) Best practices for digitally constructing endocranial casts: examples from birds and their dinosaurian relatives. *J Anat* 229:173–190. <https://doi.org/10.1111/joa.12378>
- Bang B, Cobb S (1968) The size of the olfactory bulb in 108 species of birds. *Auk* 85:55–61
- Bang B, Wenzel B (1985) Nasal cavity and olfactory system. In: King A, McLelland J (eds) *Form and function in birds*. Academic, New York, pp 195–225
- Benson RBJ, Starmer-Jones E, Close RA, Walsh SA (2017) Comparative analysis of vestibular ecomorphology in birds. *J Anat* 231:990–1018. <https://doi.org/10.1111/joa.12726>
- Bever GS, Lyson TR, Field DJ, Bhullar B-AS (2015) Evolutionary origin of the turtle skull. *Nature* 525:239–242. <https://doi.org/10.1038/nature14900>
- Bhullar B-AS, Bever GS (2009) An archosaur-like laterosphenoid in early turtles (Reptilia: Pantestudines). *Breviora* 518:1–11. <https://doi.org/10.3099/0006-9698-518.1.1>
- Bhullar B-AS, Hanson M, Fabbri M et al (2016) How to make a bird skull: major transitions in the evolution of the avian cranium, paedomorphosis, and the beak as a surrogate hand. *Integr Comp Biol* 56:389–403. <https://doi.org/10.1093/icb/icw069>
- Bojanus LH (1819–21) *Anatome testudinis europaeae*. *ISIS* 11:1766–1769
- Bonin F, Devaux B, Dupré A (2006) *Turtles of the world*. The Johns Hopkins University Press, Baltimore
- Bourke JM, Porter WM, Ridgely RC et al (2014) Breathing life into dinosaurs: tackling challenges of soft-tissue restoration and nasal airflow in extinct species. *Anat Rec* 297:2148–2186. <https://doi.org/10.1002/ar.23046>
- Bramble DM (1982) *Scaptochelys*: generic revision and evolution of Gopher tortoises. *Copeia* 4:852–867
- Brichta AM, Acuña DL, Peterson EH (1988) Planal relations of semicircular canals in awake, resting turtles, *Pseudemys scripta*. *Brain Behav Evol* 32:236–245
- Bronzati M, Benson RBJ, Evers SW et al (2021) Deep evolutionary diversification of semicircular canals in archosaurs. *Curr Biol* 31(12):2520–2529. <https://doi.org/10.1016/j.cub.2021.03.086>
- Brudenell DK, Schwab IR, Fritsches KA (2008) Ocular morphology of the Leatherback Sea turtle (*Dermochelys coriacea*). *Vet Ophthalmol* 11:99–110. <https://doi.org/10.1111/j.1463-5224.2008.00607.x>
- Campbell H, Evans W (1972) Observations on the vocal behavior of chelonians. *Herpetologica* 28:277–280

- Constantino MA, Salmon M (2003) Role of chemical and visual cues in food recognition by leatherback posthatchlings (*Dermochelys coriacea* L). *Zoology* 106:173–181. <https://doi.org/10.1078/0944-2006-00114>
- Crawford NG, Faircloth BC, McCormack JE et al (2012) More than 1000 ultraconserved elements provide evidence that turtles are the sister group of archosaurs. *Biol Lett* 8:783–786. <https://doi.org/10.1098/rsbl.2012.0331>
- Crawford NG, Parham JF, Sellas AB et al (2015) A phylogenomic analysis of turtles. *Mol Phylogenet Evol* 83:250–257. <https://doi.org/10.1016/j.ympev.2014.10.021>
- Deantoni FO, Romano PS, Azevedo SA (2015) Analysis of internal structure of the skull of Pelomedusoides (Testudines, Pleurodira) based on three-dimensional helical tomography. In: Symposium on Turtle Evolution. Tübingen, Germany, p 17
- Eakin R (1973) *The third eye*, 1st edn. University of California Press, Berkeley/Los Angeles
- Edinger T (1929) *Die fossilen Gehirne*. Julius Springer Verlag, Berlin
- Edinger T (1934) Anton Fritsch's "Grosshirn von *Polyptychodon*" ist der Steinkern eines Schildkrötenschadels. *Psychiatr en Neurol BI* 3–4:396–404
- Ekdale EG (2013) Comparative anatomy of the bony labyrinth (inner ear) of placental mammals. *PLoS One* 8:e66624. <https://doi.org/10.1371/journal.pone.0066624>
- Emerling CA (2017) Archelosaurian color vision, parietal eye loss, and the crocodylian nocturnal bottleneck. *Mol Biol Evol* 34:666–676. <https://doi.org/10.1093/molbev/msw265>
- Evers SW, Benson RBJ (2019) A new phylogenetic hypothesis of turtles with implications for the timing and number of evolutionary transitions to marine lifestyles in the group. *Palaeontology* 62:93–134. <https://doi.org/10.1111/pala.12384>
- Evers SW, Joyce WG (2021) A re-description of *Sandownia harrisi* (Testudinata: Sandownidae) from the Aptian of the Isle of Wight based on computed tomography scans. *R Soc Open Sci* 7:191936. <https://doi.org/10.1098/rsos.191936>
- Evers SW, Barrett PM, Benson RBJ (2019a) Anatomy of *Rhinochelys pulchriceps* (Protostegidae) and marine adaptation during the early evolution of chelonoids. *Peer J* 7:e6811. <https://doi.org/10.7717/peerj.6811>
- Evers SW, Neenan JM, Ferreira GS et al (2019b) Neurovascular anatomy of the protostegid turtle *Rhinochelys pulchriceps* and comparisons of membranous and endosseous labyrinth shape in an extant turtle. *Zool J Linnean Soc* 187:800–828. <https://doi.org/10.1093/zoolinnean/zlz063>
- Evers SW, Rollot Y, Joyce WG (2020) Cranial osteology of the Early Cretaceous turtle *Pleurosternon bullockii* (Paracryptodira: Pleurosternidae). *Peer J* 8:e9454. <https://doi.org/10.7717/peerj.9454>
- Evers SW, Rollot Y, Joyce WG (2021) New interpretation of the cranial osteology of the Early Cretaceous turtle *Arundelemys dardeni* (Paracryptodira) based on a CT-based re-evaluation of the holotype. *Peer J* 9:e11495. <https://doi.org/10.7717/peerj.11495>
- Ferrara CR, Vogt RC, Sousa-Lima RS (2013) Turtle vocalizations as the first evidence of post-hatching parental care in chelonians. *J Comp Psychol* 127:24–32
- Ferrara CR, Mortimer JA, Vogt RC (2014a) First evidence that hatchlings of *Chelonia mydas* emit sounds. *Copeia* 2014:245–247. <https://doi.org/10.1643/CE-13-087>
- Ferrara CR, Vogt RC, Harfush MR et al (2014b) First evidence of leatherback turtle (*Dermochelys coriacea*) embryos and hatchlings emitting sounds. *Chelonian Conserv Biol* 13:110–114. <https://doi.org/10.2744/CCB-1045.1>
- Ferrara CR, Vogt RC, Sousa-Lima RS et al (2014c) Sound communication and social behavior in an Amazonian River Turtle (*Podocnemis expansa*). *Herpetologica* 70:149–156. <https://doi.org/10.1655/HERPETOLOGICA-D-13-00050R2>
- Ferrara CR, Vogt RC, Eisemberg CC et al (2017) First evidence of the Pig-nosed Turtle (*Carettochelys insculpta*) vocalizing underwater. *Copeia* 105:29–32. <https://doi.org/10.1643/CE-16-407>
- Ferreira GS, Lautenschlager S, Evers SW, Pfaff C, Kriwet J, Raselli I, Werneburg I (2020) Feeding biomechanics suggests progressive correlation of skull architecture and neck evolution in turtles. *Sci Rep* 10:5505. <https://doi.org/10.1038/s41598-020-62179-5>

- Ferreira GS (2021) Paleoneurology. <https://github.com/gsferreirabio/paleoneurology>. Accessed 09 Sep 2022
- Ferreira GS, Rincón AD, Solórzano A et al (2015) The last marine pelomedusoids (Testudines: Pleurodira): a new species of *Bairdemys* and the paleoecology of Stereogenyina. *Peer J* 3:e1063. <https://doi.org/10.7717/peerj.1063>
- Ferreira GS, Bronzati M, Langer MC et al (2018a) Phylogeny, biogeography and diversification patterns of side-necked turtles (Testudines: Pleurodira). *R Soc Open Sci* 5:17171773. <https://doi.org/10.1098/rsos.171773>
- Ferreira GS, Iori FV, Hermanson G et al (2018b) New turtle remains from the Late Cretaceous of Monte Alto-SP, Brazil, including cranial osteology, neuroanatomy and phylogenetic position of a new taxon. *PalZ* 92:481–498. <https://doi.org/10.1007/s12542-017-0397-x>
- Foth C, Evers SW, Joyce WG et al (2019) Comparative analysis of the shape and size of the middle ear cavity of turtles reveals no correlation with habitat ecology. *J Anat* 235:1078–1097. <https://doi.org/10.1111/joa.13071>
- Gaffney ES (1972) An illustrated glossary of turtle skull nomenclature. *Am Museum Novit*:1–33
- Gaffney ES (1975) A phylogeny and classification of the higher categories of turtles. *Bull Am Museum Nat Hist* 155:387–436
- Gaffney ES (1977) An endocranial cast of the side-necked turtle, *Bothremys*, with a new reconstruction of the palate. *Am Museum Novit*:1–12
- Gaffney ES (1979) Comparative cranial morphology of recent and fossil turtles. *Bull Am Museum Nat Hist* 164:65–376
- Gaffney ES (1982) Cranial morphology of Baenid turtles. *Am Museum Novit*:1–22
- Gaffney ES (1990) The comparative osteology of the Triassic turtle *Proganochelys*. *Bull Am Museum Nat Hist*:1–263
- Gaffney ES, Meylan PA (1988) A phylogeny of turtles. In: Benton MJ (ed) *The phylogeny and classification of the Tetrapods, Amphibians, reptiles, birds, systematic*, vol 1. Clarendon Press, Oxford, pp 157–219
- Gaffney ES, Zangerl R (1968) A revision of the chelonian genus *Bothremys*: (Pleurodira: Pelomedusidae). *Fieldiana Geol* 16:193–239
- Gaffney ES, Tong H, Meylan PA (2006) Evolution of the side-necked turtles: the families Bothremyidae, Euraxemyidae, and Araripemyidae. *Bull Am Museum Nat Hist* 2006:1–698. [https://doi.org/10.1206/0003-0090\(2006\)300\[1:EOTSTT\]2.0.CO;2](https://doi.org/10.1206/0003-0090(2006)300[1:EOTSTT]2.0.CO;2)
- Gaffney ES, Meylan PA, Wood RC et al (2011) Evolution of the side-necked turtles: the family Podocnemididae. *Bull Am Museum Nat Hist*:1–237
- Galeotti P, Sacchi R, Fasola M, Ballasina D (2005) Do mounting vocalizations in tortoises have a communication function? A comparative analysis. *Herpetol J* 15:61–71
- Georgi JA, Sipla JS (2008) Comparative and functional anatomy of balance in aquatic reptiles and birds. In: Thewissen JGM, Nummela S (eds) *Sensory evolution on the threshold: adaptations in secondarily aquatic vertebrates*. University of California Press, Berkeley, pp 233–256
- Giles JC, Davis JA, McCauley RD et al (2009) Voice of the turtle: the underwater acoustic repertoire of the long-necked freshwater turtle, *Chelodina oblonga*. *J Acoust Soc Am* 126:434–443. <https://doi.org/10.1121/1.3148209>
- Gower JC (1975) Generalized procrustes analysis. *Psychometrika* 40:33–51
- Grafan A (1989) The phylogenetic regression. *Philos Trans R Soc London B Biol Sci* 326:119–157. <https://doi.org/10.1098/rstb.1989.0106>
- Hanson M, Hoffman EA, Norell MA et al (2021) The early origin of a birdlike inner ear and the evolution of dinosaurian movement and vocalization. *Science* 372:601–609. <https://doi.org/10.1126/science.abb4305>
- Hermanson G, Iori FV, Evers SW et al (2020) A small podocnemidoid (Pleurodira, Pelomedusoides) from the Late Cretaceous of Brazil, and the innervation and carotid circulation of side-necked turtles. *Pap Palaeontol* 6:329–347. <https://doi.org/10.1002/spp2.1300>
- Hetherington T (2008) Comparative anatomy and function of hearing in aquatic amphibians, reptiles, and birds. In: Thewissen JGM, Nummela S (eds) *Sensory evolution on the threshold:*

- adaptations in secondarily aquatic vertebrates. University of California Press, Berkeley/Los Angeles/London, pp 183–209
- Hirayama R (1998) Oldest known sea turtle. *Nature* 392:705–708
- Hopson J (1979) Paleoneurology. In: Gans C, Northcutt R, Ulinski P (eds) *Biology of the Reptilia*, Academic Press, vol 9. London, New York/San Francisco, pp 39–146
- Howland HC, Merola S, Basarab JR (2004) The allometry and scaling of the size of vertebrate eyes. *Vis Res* 44:2043–2065. <https://doi.org/10.1016/j.visres.2004.03.023>
- Hurlburt GR (1996) *Relative brain size in recent and fossil amniotes: determination and interpretation*. University of Toronto
- Jamniczky HA (2008) Turtle carotid circulation: a character analysis case study. *Biol J Linn Soc* 93:239–256. <https://doi.org/10.1111/j.1095-8312.2007.00923.x>
- Jerison H (1973) *Evolution of the brain and intelligence*. Academic, New York
- Jirak D, Janacek J (2017) Volume of the crocodylian brain and endocast during ontogeny. *PLoS One* 12:e0178491. <https://doi.org/10.1371/journal.pone.0178491>
- Jones MEH, Werneburg I, Curtis N et al (2012) The head and neck anatomy of sea turtles (Cryptodira: Chelonioidae) and skull shape in Testudines. *PLoS One* 7:e47852. <https://doi.org/10.1371/journal.pone.0047852>
- Joyce WG (2007) Phylogenetic relationships of Mesozoic turtles. *Bull Peabody Museum Nat Hist* 48:3–102. [https://doi.org/10.3374/0079-032X\(2007\)48\[3:PROMT\]2.0.CO;2](https://doi.org/10.3374/0079-032X(2007)48[3:PROMT]2.0.CO;2)
- Joyce WG (2017) A review of the fossil record of basal Mesozoic turtles. *Bull Peabody Museum Nat Hist* 58:65–113. <https://doi.org/10.3374/014.058.0105>
- Joyce WG, Volpato VS, Rollot Y (2018) The skull of the carettochelyid turtle *Anosteira pulchra* from the Eocene (Uintan) of Wyoming and the carotid canal system of carettochelyid turtles. *Foss Rec* 21:301–310. <https://doi.org/10.5194/fr-21-301-2018>
- Joyce WG, Anquetin J, Cadena E-A et al (2021a) A nomenclature for fossil and living turtles using phylogenetically defined clade names. *Swiss J Palaeontol* 140:5. <https://doi.org/10.1186/s13358-020-00211-x>
- Joyce WG, Rollot Y, Evers SW et al (2021b) A new pelomedusoid turtle, *Sahonachelys mailakavava*, from the Late Cretaceous of Madagascar provides evidence for convergent evolution of specialized suction feeding among pleurodires. *R Soc Open Sci* 8:210098. <https://doi.org/10.1098/rsos-210098>
- Kim R, Evans D (2014) Relationships among brain, endocranial cavity, and body sizes in reptiles. In: *Society of Vertebrate Paleontology 74th Annual Meeting*, Berlin
- Konishi M (1970) Comparative neurophysiological studies of hearing and vocalizations in song-birds. *Z Vgl Physiol* 66:257–272
- Laurin M, Piñeiro GH (2017) A reassessment of the taxonomic position of mesosaurs, and a surprising phylogeny of early amniotes. *Front Earth Sci* 5:88. <https://doi.org/10.3389/feart.2017.00088>
- Lautenschlager S, Ferreira GS, Werneburg I (2018) Sensory evolution and ecology of early turtles revealed by digital endocranial reconstructions. *Front Ecol Evol* 6:7. <https://doi.org/10.3389/fevo.2018.00007>
- Lenhardt M, Klinger R, Musick J (1985) Middle ear anatomy of the marine turtle. *J Aud Res* 25:66–72
- Lessner EJ, Holliday CM (2020) A 3D ontogenetic atlas of *Alligator mississippiensis* cranial nerves and their significance for comparative neurology of reptiles. *Anat Rec*. <https://doi.org/10.1002/ar.24550>
- Li C, Wu X-C, Rieppel O et al (2008) An ancestral turtle from the Late Triassic of southwestern China. *Nature* 456:497–501. <https://doi.org/10.1038/nature07533>
- Li C, Fraser NC, Rieppel O et al (2018) A Triassic stem turtle with an edentulous beak. *Nature* 560:476–479. <https://doi.org/10.1038/s41586-018-0419-1>
- Lipka TR, Therrien F, Weishampel DB et al (2006) A new turtle from the Arundel Clay facies (Potomac Formation, Early Cretaceous) of Maryland, U.S.A. *J Vertebr Paleontol* 26:300–307. [https://doi.org/10.1671/0272-4634\(2006\)26\[300:ANTFTA\]2.0.CO;2](https://doi.org/10.1671/0272-4634(2006)26[300:ANTFTA]2.0.CO;2)

- Loew E, Govardovskii V (2001) Photoreceptors and visual pigments in the red eared turtle, *Trachemys scripta elegans*. *Vis Neurosci* 18:753–757
- Macrì S, Savriama Y, Khan I et al (2019) Comparative analysis of squamate brains unveils multi-level variation in cerebellar architecture associated with locomotor specialization. *Nat Commun* 10:5560. <https://doi.org/10.1038/s41467-019-13405-w>
- Martín-Jiménez M, Pérez-García A (2021) Neuroanatomical study and three-dimensional reconstruction of the skull of the bothremydid turtle (Pleurodira) based on the European Eocene *Tartaruscola teodorii*. *Diversity* 13:298. <https://doi.org/10.3390/d13070298>
- Martín-Jiménez M, Codrea V, Pérez-García A (2021) Neuroanatomy of the European uppermost Cretaceous stem turtle *Kallokibotion bajazidi*. *Cretac Res* 120:104720. <https://doi.org/10.1016/j.cretres.2020.104720>
- Mautner A-K, Latimer AE, Fritz U et al (2017) An updated description of the osteology of the pancake tortoise *Malacochersus tornieri* (Testudines: Testudinidae) with special focus on intraspecific variation. *J Morphol* 278:321–333. <https://doi.org/10.1002/jmor.20640>
- McDowell FH, Potes J, Groch S (1961) The natural history of internal carotid and vertebral-basilar artery occlusion. *Neurology* 11:153–157
- Metscher BD (2009) MicroCT for comparative morphology: simple staining methods allow high-contrast 3D imaging of diverse non-mineralized animal tissues. *BMC Physiol* 9:11. <https://doi.org/10.1186/1472-6793-9-1>
- Mrosovsky N (1972) Spectrographs of the sounds of Leatherback Turtles. *Herpetologica* 28:256–258
- Müller J, Sterli J, Anquetin J (2011) Carotid circulation in amniotes and its implications for turtle relationships. *Neues Jahrb Geol Palaontol Abh* 261:289–297. <https://doi.org/10.1127/0077-7749/2011/0157>
- Neenan JM, Reich T, Evers SW et al (2017) Evolution of the sauropterygian labyrinth with increasingly pelagic lifestyles. *Curr Biol* 27:3852–3858.e3. <https://doi.org/10.1016/j.cub.2017.10.069>
- Nick L (1912) Das Kopfskelett von *Dermochelys coriacea* L. *Zool Jb Abt f Anat* 33:1–238
- Northcutt RG (2013) Variation in reptilian brains and cognition. *Brain Behav Evol* 82:45–54. <https://doi.org/10.1159/000351996>
- Northmore DPM, Granda AM (1991) Ocular dimensions and schematic eyes of freshwater and sea turtles. *Vis Neurosci* 7:627–635. <https://doi.org/10.1017/S0952523800010415>
- Ogushi K (1913) Zur Anatomie der Hirnnerven und des Kopf-Sympathicus von *Trionyx japonicus* nebst einigen kritischen Bemerkungen. *Morphol Jahrb* 45:441–480
- Parsons TS (1959a) Nasal anatomy and the phylogeny of reptiles. *Evolution (N Y)* 13:175–187
- Parsons TS (1959b) Studies on the comparative embryology of the reptilian nose. *Bull Museum Comp Zool* 120:103–277
- Parsons TS (1967) Evolution of the nasal structure in the lower tetrapods. *Am Zool* 7:397–413. <https://doi.org/10.1093/icb/7.3.397>
- Parsons TS (1970) The nose and Jacobson's organ. In: Gans C, Parsons TS (eds) *Biology of the Reptilia*, vol 2. Academic Press, London, New York
- Paulina-Carabajal A, Sterli J, Müller J et al (2013) Neuroanatomy of the Marine Jurassic Turtle *Plesiochelys etalloni* (Testudinata, Plesiochelyidae). *PLoS One* 8:e69264. <https://doi.org/10.1371/journal.pone.0069264>
- Paulina-Carabajal A, Sterli J, Georgi J et al (2017) Comparative neuroanatomy of extinct horned turtles (Meiolaniidae) and extant terrestrial turtles (Testudinidae), with comments on the palaeobiological implications of selected endocranial features. *Zool J Linnean Soc* 180:930–950. <https://doi.org/10.1093/zoolinnean/zw024>
- Paulina-Carabajal A, Sterli J, Werneburg I (2019) The endocranial anatomy of the stem turtle *Naomichelys speciosa* from the Early Cretaceous of North America. *Acta Palaeontol Pol* 64:711–716. <https://doi.org/10.4202/app.00606.2019>
- Pereira AG, Sterli J, Moreira FRR, Schrago CG (2017) Multilocus phylogeny and statistical biogeography clarify the evolutionary history of major lineages of turtles. *Mol Phylogenet Evol* 113:59–66. <https://doi.org/10.1016/j.ympev.2017.05.008>

- Pérez-García A, Martín-Jiménez M, Aurell M et al (2021) A new Iberian pleurosternid (Jurassic-Cretaceous transition, Spain) and first neuroanatomical study of this clade of stem turtles. *Hist Biol*. <https://doi.org/10.1080/08912963.2021.1910818>
- Pinheiro J, Bates D, DebRoy S, Sarkar D, R Core Team (2021) Nlme: linear and nonlinear mixed effects models. R package version 3.1-152, <https://CRAN.R-project.org/package=nlme>. Accessed 12 Aug 2021
- Poglayen-Neuwall I (1953) Untersuchungen der Kiefermuskulatur und deren Innervation bei Schildkröten. *Acta Zool* 34:241–292
- Pritchard PCH (1984) Piscivory in turtles, and evolution of the long-necked Chelidae. *Symp Zool Soc Lond* 52:87–110
- Rabbitt RD, Edward R, Grant J (2004) Biomechanics of the semicircular canals and otolith organs. In: Highstein SM, Fay RR, Popper AN (eds) *The vestibular system*. Springer, New York, pp 153–201
- Rabi M, Zhou C-F, Wings O et al (2013) A new xinjiangchelyid turtle from the Middle Jurassic of Xinjiang, China and the evolution of the basiptyergoid process in Mesozoic turtles. *BMC Evol Biol* 13:203. <https://doi.org/10.1186/1471-2148-13-203>
- Raselli I, Anquetin J (2019) Novel insights into the morphology of *Plesiochelys bigleri* from the early Kimmeridgian of northwestern Switzerland. *PLoS One* 14:e0214629. <https://doi.org/10.1371/journal.pone.0214629>
- Revell LJ (2012) Phytools: an R package for phylogenetic comparative biology (and other things). *Methods Ecol Evol* 3:217–223. <https://doi.org/10.1111/j.2041-210X.2011.00169.x>
- Ridgway S, Wever E, McCormick J et al (1969) Hearing in the giant sea turtle, *Chelonia mydas*. *Proc Natl Acad Sci* 64:884–890
- Rieppel O (1985) The recessus scalae tympani and its bearing on the classification of reptiles. *J Herpetol* 19:373–384
- Rohlf FJ (2006) tpsDig, digitize landmarks and outlines v 2.05. Department of Ecology and Evolution, State University of New York, Stony Brook
- Rollot Y, Lyson TR, Joyce WG (2018) A description of the skull of *Eubaena cephalica* (Hay, 1904) and new insights into the cranial circulation and innervation of Baenid turtles. *J Vertebr Paleontol* 38:e1474886. <https://doi.org/10.1080/02724634.2018.1474886>
- Rollot Y, Evers SW, Joyce WG (2021a) A review of the carotid artery and facial nerve canal systems in extant turtles. *Peer J* 8:e10475. <https://doi.org/10.7717/peerj.10475>
- Rollot Y, Evers SW, Joyce WG (2021b) A redescription of the Late Jurassic (Tithonian) turtle *Uluops uluops* and a new phylogenetic hypothesis of Paracryptodira. *Swiss Journal of Paleontology*
- Saito K, Shoji T, Uchida I et al (2000) Structure of the olfactory and vomeronasal epithelia in the loggerhead turtle *Caretta caretta*. *Fish Sci* 66:409–411
- Schoch RR, Sues H-D (2018) Osteology of the Middle Triassic stem-turtle *Pappochelys rosinae* and the early evolution of the turtle skeleton. *J Syst Palaeontol* 16:927–965. <https://doi.org/10.1080/14772019.2017.1354936>
- Schuyler QA, Wilcox C, Townsend K et al (2014) Mistaken identity? Visual similarities of marine debris to natural prey items of sea turtles. *BMC Ecol* 14:14. <https://doi.org/10.1186/1472-6785-14-14>
- Schwab JA, Young MT, Neenan JM et al (2020) Inner ear sensory system changes as extinct crocodylomorphs transitioned from land to water. *Proc Natl Acad Sci* 117:10422 LP – 10428. <https://doi.org/10.1073/pnas.2002146117>
- Shiino K (1912) Beitrag zur Kenntnis der Gehirnnerven der Schildkröten. *Anat Hefte I Abteilung* 47:1–34
- Shindo T (1914) Zur vergleichenden Anatomie der arteriellen Kopfgefäße der Reptilien. *Anatomie Hefte* 51:267–356
- Sobral G, Reisz R, Neenan JM et al (2016) Basal reptilians, marine diapsids, and turtles: the flowering of reptile diversity. In: Clack JA, Fay RR, Popper AN (eds) *Evolution of the vertebrate ear : evidence from the fossil record*. Springer International Publishing, Cham, pp 207–243

- Soliman M (1964) Die Kopfnerven der Schildkröten. *Zeitschrift für Wissenschaftliche Zool* 169:216–312
- Southwood A, Higgins B, Brill R et al (2007) Chemoreception in loggerhead sea turtles: an assessment of the feasibility of using chemical deterrents to prevent sea turtle interactions with long-line fishing gear. Honolulu
- Sterli J (2015) A review of the fossil record of Gondwanan turtles of the clade Meiolaniformes. *Bull Peabody Museum Nat Hist* 56:21–45. <https://doi.org/10.3374/014.056.0102>
- Sterli J, de la Fuente MS (2010) Anatomy of *Condorchelys antiqua* Sterli, 2008, and the origin of the modern jaw closure mechanism in turtles. *J Vertebr Paleontol* 30:351–366. <https://doi.org/10.1080/02724631003617597>
- Sterli J, Joyce WG (2007) The cranial anatomy of the Early Jurassic turtle *Kayentachelys aprix*. *Acta Palaeontol Pol* 52:675–694
- Sterli J, Müller J, Anquetin J et al (2010) The parabasisphenoid complex in Mesozoic turtles and the evolution of the testudinate basicranium. *Can J Earth Sci* 47:1337–1346. <https://doi.org/10.1139/E10-061>
- Sterli J, de la Fuente MS, Rougier GW (2018) New remains of *Condorchelys antiqua* (Testudinata) from the Early-Middle Jurassic of Patagonia: anatomy, phylogeny, and paedomorphosis in the early evolution of turtles. *J Vertebr Paleontol* 38:1–17. <https://doi.org/10.1080/02724634.2018.1480112>
- Sues H-D (2019) The rise of reptiles. John Hopkins University Press, Baltimore
- Thewissen JGM, Nummela S (2008) Sensory evolution on the threshold: adaptations in secondarily aquatic vertebrates. University of California Press, Berkeley/Los Angeles/London
- Thomson RC, Spinks PQ, Shaffer HB (2021) A global phylogeny of turtles reveals a burst of climate-associated diversification on continental margins. *Proc Natl Acad Sci* 118:e2012215118. <https://doi.org/10.1073/pnas.2012215118>
- Van Dongen P (1998) Brain Size in Vertebrates. In: Nieuwenhuys R, ten Donkelaar H, Nicholson C (eds) The central nervous system of vertebrates. Springer, Berlin/Heidelberg, pp 2099–2134
- Vorobyev M (2003) Coloured oil droplets enhance colour discrimination. *Proc R Soc London Ser B Biol Sci* 270:1255–1261. <https://doi.org/10.1098/rspb.2003.2381>
- Walsh SA, Barrett PM, Milner AC et al (2009) Inner ear anatomy is a proxy for deducing auditory capability and behaviour in reptiles and birds. *Proc R Soc B Biol Sci* 276:1355–1360. <https://doi.org/10.1098/rspb.2008.1390>
- Wang Z, Pascual-Anaya J, Zadissa A et al (2013) The draft genomes of soft-shell turtle and green sea turtle yield insights into the development and evolution of the turtle-specific body plan. *Nat Genet* 45:701–706. <https://doi.org/10.1038/ng.2615>
- Werneburg I (2011) The cranial musculature of turtles. *Palaeontologia Electronica* 14(2):15A, 1–99. palaeo-electronica.org/2011_2/254/index.html
- Werneburg I, Maier W (2019) Diverging development of akinetic skulls in cryptodire and pleurodire turtles: an ontogenetic and phylogenetic study. *Vertebr Zool* 69:113–143. <https://doi.org/10.26049/VZ69-2-2019-01>
- Werneburg I, Yaryhin O (2019) Character definition and tempus optimum in comparative chondrocranial research. *Acta Zool* 100:376–388. <https://doi.org/10.1111/azo.12260>
- Werneburg I, Wilson LAB, Parr WCH, Joyce WG (2015) Evolution of neck vertebral shape and neck retraction at the transition to modern turtles: an integrated geometric morphometric approach. *Syst Biol* 64:187–204. <https://doi.org/10.1093/sysbio/syu072>
- Werneburg I, Evers SW, Ferreira GS (2021a) On the “cartilaginous rider” in the endocast of turtle brain cavities. *Vertebr Zool* 71:403–418. <https://doi.org/10.3897/vz.71.e66756>
- Werneburg I, Evers SW, Ferreira GS (2021b) 3D models related to the publication: On the “cartilaginous rider” in the endocasts of turtle brain cavities. *MorphoMuseum* 7(3):e146. <https://doi.org/10.18563/journal.m3.146>
- Wever E (1978) The reptile ear. Princeton University Press, Princeton
- Wilkinson A, Kuenstner K, Mueller J et al (2010) Social learning in a non-social reptile (*Geochelone carbonaria*). *Biol Lett* 6:614–616. <https://doi.org/10.1098/rsbl.2010.0092>

- Willis KL, Christensen-Dalsgaard J, Ketten DR et al (2013) Middle ear cavity morphology is consistent with an aquatic origin for Testudines. *PLoS One* 8:e54086. <https://doi.org/10.1371/journal.pone.0054086>
- Wilson V, Melvill Jones G (1979) *Mammalian vestibular physiology*. Plenum Press, New York
- Witmer LM, Ridgely RC, Dufeu D et al (2008) Using CT to peer into the past: 3D visualization of the brain and ear regions of birds, crocodiles, and nonavian dinosaurs. In: Endo H, Frey R (eds) *Anatomical Imaging*. Springer, Tokyo, pp 67–87
- Wyneken J (2001) *The anatomy of sea turtles*. US Department of Commerce Miami, USA
- Wyneken J, Lohmann K, Musick J (2013) *The biology of sea turtles*. CRC Press, Boca Raton/London/New York
- Yamaguchi Y, Kitayama C, Tanaka S et al (2021) Computed tomographic analysis of internal structures within the nasal cavities of green, loggerhead and leatherback sea turtles. *Anat Rec* 304:584–590. <https://doi.org/10.1002/ar.24469>
- Zangerl R (1960) The vertebrate fauna of the Selma Formation of Alabama. Part 5. An advanced cheloniid sea turtle. *Fieldiana. Geol Mem* 3:281–312
- Zelenitsky DK, Therrien F, Kobayashi Y (2009) Olfactory acuity in theropods: palaeobiological and evolutionary implications. *Proc R Soc B Biol Sci* 276:667–673. <https://doi.org/10.1098/rspb.2008.1075>
- Zelenitsky DK, Therrien F, Ridgely RC et al (2011) Evolution of olfaction in non-avian theropod dinosaurs and birds. *Proc R Soc B Biol Sci* 278:3625–3634. <https://doi.org/10.1098/rspb.2011.0238>
- Zeyl JN, Johnston CE (2015) Amphibious auditory evoked potentials in four North American Testudines genera spanning the aquatic–terrestrial spectrum. *J Comp Physiol A* 201:1011–1018. <https://doi.org/10.1007/s00359-015-1031-6>

Chapter 5

A Look in to the Neurocranium of Living and Extinct Lepidosauria



Ariana Paulina-Carabajal, Paulina Jiménez-Huidobro,
Laura Natalia Triviño, Edward L. Stanley, Hussam Zaher, and Juan D. Daza

5.1 Introduction

Lepidosauria Haeckel, 1866 is traditionally defined as the crown-clade comprising the most recent common ancestor of *Sphenodon* and Squamata and all its descendants. This includes the extant orders Rhynchocephalia (including Sphenodontia) and Squamata and their extinct forms (Gauthier et al. 1988). Lepidosaurians are very contrasting in terms of diversity and biogeography (Evans 1984; Evans and Jones 2010) and include reptiles commonly known as tuatara, lizards, amphisbaenians, and snakes (Fig. 5.1). Lepidosauria diversified through the Mesozoic, and many groups survived the K-Pg extinction event. Estimates of molecular divergence place

A. Paulina-Carabajal (✉)

Instituto de Investigaciones en Biodiversidad y Medioambiente, CONICET-Universidad Nacional del Comahue, San Carlos de Bariloche, Argentina
e-mail: a.paulinacarabajal@conicet.gov.ar

P. Jiménez-Huidobro

Division of Paleontology, Institute of Geosciences, University of Bonn, Bonn, Germany
e-mail: jimenezh@uni-bonn.de

L. N. Triviño

CONICET- Departamento de Herpetología, Museo de La Plata, La Plata, Argentina
e-mail: lauratrivinio@fcnym.unlp.edu.ar

E. L. Stanley

Department of Natural History, Florida Museum of Natural History, Gainesville, FL, USA
e-mail: elstanley@flmnh.ufl.edu

H. Zaher

Museu de Zoologia, Universidade de São Paulo, São Paulo, SP, Brazil
e-mail: hzaher@usp.br

J. D. Daza

Department of Biological Sciences, Sam Houston State University, Huntsville, TX, USA
e-mail: daza@shsu.edu

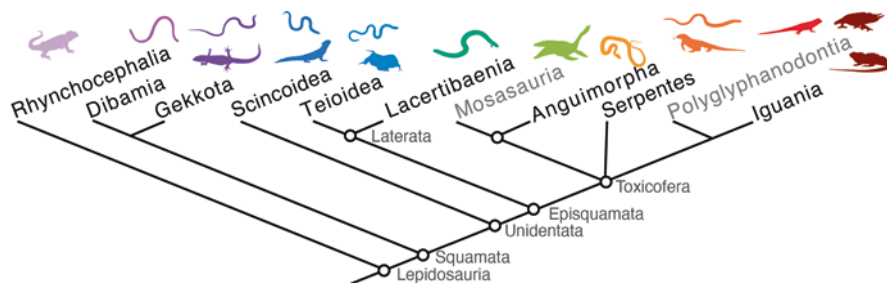


Fig. 5.1 Simplified phylogeny of lepidosaurs based on morphological and molecular data. The topology is highly congruent with several published combined analyses (Wiens et al. 2010; Longrich et al. 2012; Wiens et al. 2012; Reeder et al. 2015; Burbrink et al. 2020; Zaher and Smith 2020). Main differences between studies rely on the position of wildcard fossil groups, and the way that characters are treated (See also Bolet et al. 2021). Only the position of mosasaurs and polyglyphanodonts among fossil groups are indicated. For some major clades, a silhouette of a limbed and limbless representative is included

the most common ancestor of crown-Lepidosauria during the Early Triassic, at approximately 242 Mya, whereas the divergence of the clade Squamata would have been during the Early Jurassic, finding the most recent common ancestor of crown-Squamates around 193 Mya (Longrich et al. 2012; Jones et al. 2013; but see Simões et al. 2018 for older dates). These two groups show different evolutionary rates through their history, which has been suggested to account for their current diversification (Hay et al. 2008; Herrera-Flores et al. 2021).

The braincase anatomy and particularly the endocranial morphology of both extant and extinct representatives of Lepidosauria have been in general poorly explored. Most fossil forms –as the living ones– are small sized, and the preservation of delicate skull remains such as the braincase, is rare, except in special conditions (i.e. Fossil Lagerstätte, amber embedded). Thus, the endocranial morphology and its diversification within the group remains poorly known when compared to other sauropsids. In fact, there are only a few studies based on natural or artificial cranial endocasts of representatives of Lepidosauria.

5.1.1 The Osseous Braincase

The skull of living lepidosaur representatives has been largely studied in terms of hard and soft tissue anatomy and functional morphology (e.g. Schwenk 2000; Evans 2008; Cundall and Irish 2008). However, our knowledge on the osteology of the skull, particularly the braincase proper (*sensu* Säve-Söderbergh 1947), is still poorly documented. Here, we follow the definition of Säve-Söderbergh (1947) and recognize the braincase proper as the part of the orbito-temporal region that is mostly ossified to enclose mainly the hindbrain, the middle and inner ear, but not the septum interorbitale and pituitary region (except in snakes where the septum is absent and the pituitary organ is completely enclosed in the braincase, see below). The

braincase is typically formed ventrally by the unpaired parasphenoid, basisphenoid, and basioccipital, laterally by the paired prootics, opisthotics, and exoccipitals, and dorsally by the unpaired supraoccipital. In derived alethinophidian snakes, a membrane bone – the ophidiosphenoid (laterosphenoid of older authors) – fuses to the lateral surface of the prootic, separating the maxillary and mandibular branches of the trigeminal nerve (CN V).

The braincase has been described in detail in Sphenodontidae (e.g. Wyeth 1924; Säve-Söderbergh 1947; Pratt 1948; Evans 2008; Jones 2008), Dibamidae (Rieppel 1984a), and in a limited number of representatives of the higher groups Gekkota (Kluge 1962; Rieppel 1984b; Conrad and Norell 2006; Daza et al. 2008; Daza and Bauer 2015; Bauer et al. 2018), Scinciformata (Rieppel 1981; Paluh and Bauer 2017; Stepanova and Bauer 2021), Laterata (Jollie 1960; Montero and Gans 1999; Hernández Morales et al. 2018; Holovacs et al. 2019), and Toxicofera (e.g. Säve-Söderbergh 1947; McDowell and Bogert 1954; Oelrich 1956; Rieppel and Zaher 2000; Bever et al. 2005; Conrad and Norell 2008; Cundall and Irish 2008; Conrad and Daza 2015; Paluh and Bauer 2017). Within that latter group, special attention was traditionally given to the highly specialized braincase of snakes (Rieppel 1979a, b; Zaher et al. 2009, 2022a, b; Olori 2010; Olori and Bell 2012; Yi and Norell 2015; Garberoglio et al. 2019), while broader detailed comparative studies among squamates remain sparse (e.g. McDowell and Bogert 1954; Evans 2008).

5.1.2 *The Brain and Cranial Nerves*

The anatomy of the brain in Squamata has been studied in several groups. In fact, there is a complete volume dedicated to “behavior and neurology of lizards” (Greenberg and MacLean 1978), in addition to three complete volumes of Neurology that reviewed the anatomy of reptiles, including many squamates (Gans et al. 1979a, b, 1992). Detailed anatomical preparations and histological sections are available for many groups, including the tuatara and lizards (Versluys 1898; Wyeth 1924; Shute and Bellairs 1953; Underwood 1957; Northcutt 1978), blind snakes (Haas 1964), and in some cases using modern approaches, models of the brain have been generated in living species (Hoops et al. 2018; Hoops et al. 2021; Perez-Martinez and Leal 2021), and even in early embryological sequences (Griffing et al. 2019).

In this chapter, an overview of the knowledge on the poorly explored lepidosaur paleoneurology is provided, together with the braincase and brain morphology of living representatives studied using Micro-CT and diceCT data, which are novel technologies that are facilitating the study of internal structures. Descriptions and comparisons include key fossil taxa as well as living representatives of all major groups. This revision, however, is not intended to be exhaustive, as some early reviews have done a more detailed evaluation of the skull of lepidosaurs (e.g. McDowell and Bogert 1954; Estes 1983; Cundall and Irish 2008; Evans 2008). Instead, an overview of the osteological and neuroanatomical characters that are diagnosable on both fossil and extant groups is presented, showing the relationship

between the soft tissues and the endocranial cavity. The authors hope that researchers interested in the field of comparative neuroanatomy in both living and extinct species, will find in this chapter a basic and useful read.

5.2 Phylogeny and Diversity of Lepidosauria

5.2.1 Early Diverging Lepidosaurian Lineages

Lepidosaur stem lineages are represented by a few Triassic and Jurassic forms, including *Paliguana whitei*, *Marmoretta oxoniensis*, *Sophineta cracoviensis*, and *Fraxinisaura rozynekae*, which preserve braincase elements (Renesto and Bernardi 2014; Schoch and Sues 2018; Sobral et al. 2020; Ford et al. 2021; Griffiths et al. 2021). Some of these early diverging lepidosaurs are alternatively recovered as stem-squamates (e.g. *Megachirella wachtleri*), illustrating our limited knowledge on the early diversification of the group (Simões et al. 2018; Sobral et al. 2020; Ford et al. 2021). With some exceptions, known stem-lepidosaurs are mainly small-sized animals, which probably narrowed down their chances of fossilization, resulting in a poor documentation of the earliest stages of lepidosaurian history.

5.2.2 Rhynchocephalia Günter, 1867

Rhynchocephalia, the sister-group to Squamata, represents a lineage of lepidosaurian lizard-like reptiles with a long-standing and diversified fossil record, but represented nowadays by only one surviving species: *Sphenodon punctatus* (commonly known as the tuatara) (Fig. 5.1). The fossil record of rhynchocephalians has a deep evolutionary history and can be traced back to the Middle Triassic, around 240 Mya (Jones et al. 2013). Rhynchocephalian diversity expanded considerably along the Mesozoic, particularly during the Late Triassic and Early Jurassic. During the Cretaceous, squamate diversification began to overtake rhynchocephalian species richness (Sues and Reisz 1995; Apesteguía 2008; Albino 2011; Meloro and Jones 2012; Jones et al. 2013; Herrera-Flores et al. 2021). The Early Jurassic *Gephyrosaurus bridensis* and Late Triassic *Diphydontosaurus avonis* represent the earliest diverging definitive rhynchocephalians (Evans 1980; Whiteside 1986; Bever and Norell 2017).

5.2.3 Squamata Opperl, 1811

Squamata is a diverse group of reptiles commonly known as lizards (amphisbaenians included) and snakes. Today, this group is the most morphologically and ecologically diverse reptile clade, being represented by more than 11,431 living species

(Uetz et al. 2022), which occupy a vast array of ecological niches and exhibit unique behavioral features (Greene 1997; Pianka and Vitt 2003; Vitt and Caldwell 2013; Pough et al. 2016; Hoops et al. 2018; Sues 2019).

Recent large-scale phylogenetic hypotheses for Squamata that combined morphological and molecular datasets (Pyrón 2017; Reeder et al. 2015) resulted in very similar general topologies with four, mainly molecular, major clades (Vidal and Hedges 2005; Burbrink et al. 2020) – Gekkota, Scincomorpha, Laterata, and Toxicofera – encompassing all known extant families, except for the enigmatic legless Dibamidae that was either retrieved as the sister-group of the Gekkota or as the sister-group of the larger clade Unidentata (composed by scincomorphs, lateratans, and toxicoferans; Vidal and Hedges 2005) along the base of the squamate tree. Another region of instability in the total-evidence squamate tree remains between toxicoferan main clades, which include crown anguiformes, iguanians, snakes, and the extinct mosasaurians (Pyrón 2017; Reeder et al. 2015; Zaher and Smith 2020; Zaher et al. 2022a). Additionally, polyglyphanodontids were alternatively retrieved as lateratans or nested within toxicoferans as the sister-group of iguanians (Reeder et al. 2015). The phylogenetic affinities of dibamids, snakes, mosasaurians, and polyglyphanodontids remain, understandably, as major standing problems to be solved in squamate phylogenetics (Simões and Pyron 2021). For the sake of simplicity in this chapter, we synthesized these conflicting points in a tree topology that is largely congruent with recent large-scale combined analyses (Fig. 5.1).

The first undisputed squamates are from the Middle Jurassic, but are known only from fragmentary skull elements (Evans 1998). A number of Triassic to Early and Middle Cretaceous forms, including here the genera *Eichstaettisaurus*, *Hongshanxi*, *Hoyalacerta*, *Huehuecuetzpali*, *Liushusaurus*, *Megachirella*, *Oculudentavis*, *Scandensia*, and *Yabeinosaurus*, have been assigned to both stem- and crown-squamatan positions, and are considered of uncertain phylogenetic affinities within Lepidosauria (Evans and Jones 2010, 2022; Simões et al. 2018; Ford et al. 2021; Griffiths et al. 2021). Among these, the Early Triassic *Megachirella wachtleri*, Early Jurassic *Eichstaettisaurus schroederi*, and Early Cretaceous *Huehuecuetzpali mixtecus* are more commonly retrieved as stem-squamates in recent phylogenetic analyses (e.g., Simões et al. 2018; Sobral et al. 2020; Ford et al. 2021). All three species exhibit partially preserved braincases.

Contrary to the scarcity of stem-squamate lineages, the fossil record of crown-squamates is abundant and diversified, with a substantial global expansion occurring throughout the Early and Middle Cretaceous, when the first modern families are recorded (Evans and Jones 2010; Evans 2022). Although the fossil record of squamates improves in the Cretaceous and Cenozoic, delicate structures like the braincase complex are often poorly preserved. However, a significant number of exceptions are known in most of the major lineages (e.g. *Dorsetisaurus purbeckensis*, *Gobiderma pulchrum*, several species of mosasaurs). Additionally, at least three localities in the world (Myanmar: Mid-Cretaceous, European Baltic Region: Eocene, and Dominican Republic: Miocene) have squamates preserved in amber, which includes several three dimensional, and fully articulated skeletons, including in some cases soft tissue (Daza et al. 2016; Chou and Xing 2020). However, in some

of the most complete studies, despite the quality of the preservation, the braincase is rarely depicted in detail or illustrated separately (Estes 1983; Gao and Norell 2000). Up to date, there are few studies where the braincase has been described or illustrated (e.g. Borsuk-Białynicka 1990; Conrad and Norell 2006). On the other hand, endocasts of the inner ear of a variety of fossil squamates have recently become common practice with the application of CT scan data (e.g. Conrad and Daza 2015; Yi and Norell 2015; Palci et al. 2017; Čerňanský et al. 2022).

The Extinct Mosasauria

This clade includes dolichosaurs and mosasauroids, but since there is no paleoneurological studies in dolichosaurs so far, this chapter will refer only to the latter. Mosasauroida sensu Bell Jr (1997) includes the small to medium size Aigialosauridae and the derived Mosasauridae divided into 6 subfamilies from which only Halisaurinae, Plioplatecarpinae, and Tylosaurinae were described as fully aquatic forms (Bardet et al. 2003; Bell and Polcyn 2005; Polcyn and Bell Jr 2005; Makádi et al. 2012; Palci et al. 2013, Polcyn et al. 2014). The extinct Mosasauroida was a diverse and globally distributed clade of squamates that invaded aquatic environments during the Late Cretaceous, becoming extinct during the K-Pg mass extinction (Russell 1967; Bell Jr 1997; Grigoriev et al. 2009; Caldwell 1999, 2012; Bardet et al. 2014). Mosasauroid lizards were a highly evolved and specialized group becoming fully aquatic in terms of anatomy, ecology, and life history (Motani 2009; Caldwell 2012; Jiménez-Huidobro 2016; Jiménez-Huidobro et al. 2017). Historically they have been considered derived varanoids (Camp 1923; Russell 1967; Carroll and deBraga 1992; deBraga and Carroll 1993; Conrad 2008; Wiens et al. 2010), recently Gauthier et al. (2012) recovered them as the sister group of Scleroglossa, whereas new phylogenies based on large-scale combined morphological and molecular data recovered mosasauroids either as the sister group of Serpentes (Reeder et al. 2015; Simões et al. 2018, 2020) or nested within stem clade Anguimorpha (Zaher and Smith 2020; Zaher et al. 2022a). The earliest analysis of the mosasauroid neurology was made for *Platecarpus tympaniticus* and *Clidastes "tortor"* by Camp (1942), followed by a description of the braincase of North American mosasauroids and the analysis of their sensory functions published by Russell (1967), and subsequently the description of the braincase of *Platecarpus* and the skull roof of *Tylosaurus* (Rieppel and Zaher 2000). More recently, the use of CT scans provided the first three-dimensional casts of the endosseous labyrinths of *Plioplatecarpus peckensis* and *Tethysaurus nopcsai* (Cuthbertson et al. 2015; Allemand 2017).

5.3 Lepidosaur Braincase Diversity and the Fossil Record

5.3.1 Braincase of Stem-Lepidosaurians

The skull of *Paliguana whitei*, from the Early Triassic of South Africa (Broom 1903), preserves only the left prootic and right exoccipital (Ford et al. 2021: fig. S10). The prootic lacks a crista prootica and alar process, and has a shallow incisura prootica, resembling the plesiomorphic condition present in the Late Permian diapsid *Youngina* (Evans 1987; Gardner et al. 2010; Ford et al. 2021). According to Ford et al. (2021) the exoccipital was not fused to the opisthotic or the basioccipital, and contributed along with the supraoccipital and basioccipital to the margin of the foramen magnum. *Marmoretta oxoniensis*, known from the Middle Jurassic of England (Evans 1991), is represented by several specimens that together preserve the epipterygoid, parabasisphenoid, basioccipital, and exoccipital (Evans 1991; Griffiths et al. 2021).

The fossil lepidosaur *Taytalura alcoberi* from the Triassic has been described as a basal lepidosauromorph (Martínez et al. 2021), and despite the fragmentary nature of this fossil, several important features are discernable including a left stapes articulated on the fenestra ovalis, paroccipital process, basipterygoid process, cultriform process, hypophyseal fossa, dorsum sella, clinoid process, sphenoccipital tubercle, a possible orbitosphenoid with a clear foramen (CN IV?), and the two epipterygoids, and a deep incisura prootica for CN V (Martínez et al. 2021). It is unclear if the metotic fissure is divided, although there seems to be no indication of the lateral aperture of the recessus scalae tympani (LARST).

5.3.2 Braincase of Rhynchocephalia

Basal lepidosaurs and *Sphenodon* share a primitive braincase condition characterized by an undivided metotic fissure (Figs. 5.2 and 5.3), therefore the lateral compensatory window seen in Squamates as a discrete opening (the LARST), corresponds to the lower part of the metotic fissure (Susan Evans, personal communication), which remains as an unossified vestibular eminence (that allows compensatory movement in the perilymph, and closes after the establishment of the compensatory window), and an internal carotid artery and palatine nerve running in an open groove (the vidian canal is closed in squamates) (Evans 2008). Few other fossil lepidosaurian braincases have been described in detail, including illustrations of cranial nerve foramina and endocranial cavities.

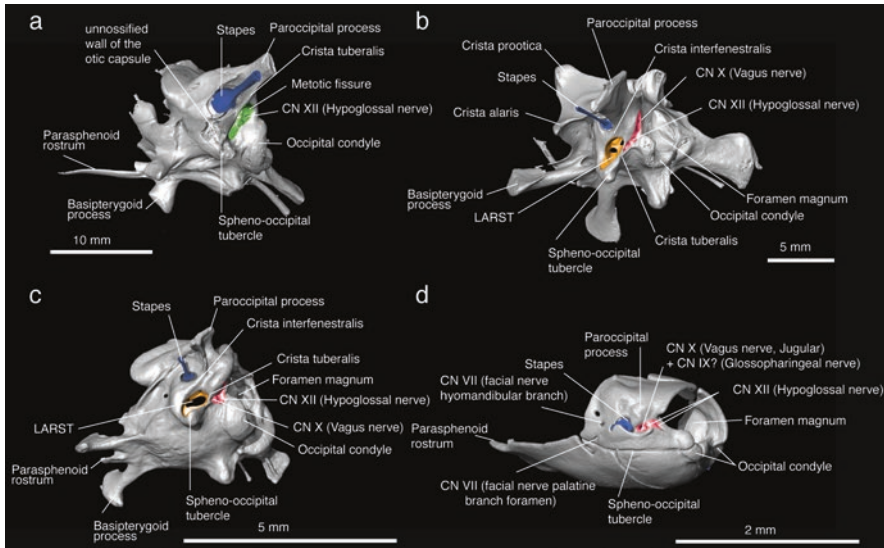


Fig. 5.2 Lepidosaurian braincase proper in posterolateral view: **(a)** *Sphenodon punctatus* (UF Herp 11978) presents undivided metotic fissure (green area); **(b)** *Gekko gecko* (UF Herp 72672), and **(c)** *Anolis olssoni* (YPM HERR.003101) both exhibiting divided condition of the metotic fissure with a superior portion for the CNs X and XII (red), and a ventral portion for the lateral aperture of the recessus scalae tympani (yellow); and **(d)** the blindsnake *Liotyphlops bondensis armandoi* (CPZ-UV 7289) showing a modified braincase, where the lateral aperture of the recessus scalae tympani is closed

Endocranial Features of Stem-Rhynchocephalia

There are no published studies on the paleoneurology of any extinct rhynchocephalian so far. Partial regions of the braincase, and/or cranial neurovascular foramina have been described or illustrated for a few number of taxa, including the early rhynchocephalian *Gephyrosaurus bridensis*, and the sphenodontians *Clevosaurus* sp., *Diphydontosaurus avonis*, *Planocephalosaurus robinsonae*, and *Kaikaifilusaurus calvoi* (Evans 1980; Fraser 1982; Whiteside 1986; Apesteguía 2008).

In extinct sphenodontian taxa, a pineal foramen is present in the skull roof (the foramen is completely bounded by the parietal in basal forms, Apesteguía 2008), while orbitosphenoids and laterosphenoids do not ossify. In *Diphydontosaurus avonis* an olfactory tract space on the ventral surface is bounded by a well-developed crista cranii, and in *Gephyrosaurus* the ventral aspect of the frontals indicates slightly laterally projected cerebral hemispheres, wide transverse space for the olfactory tracts and divergent olfactory bulbs. As in *Sphenodon* (e.g. Gower and Weber 1998), in *Diphydontosaurus* there is a large metotic foramen (probably for the glossopharyngeal nerve) and two foramina for CN XII (also two foramina in the exoccipital of *Gephyrosaurus*). There is a medullary eminence (a median ridge) on the floor of the endocranial cavity of *Diphydontosaurus*, a trait that is also present in the basicrania of *Gephyrosaurus* and *Kaikaifilusaurus*. In *Diphydontosaurus* the

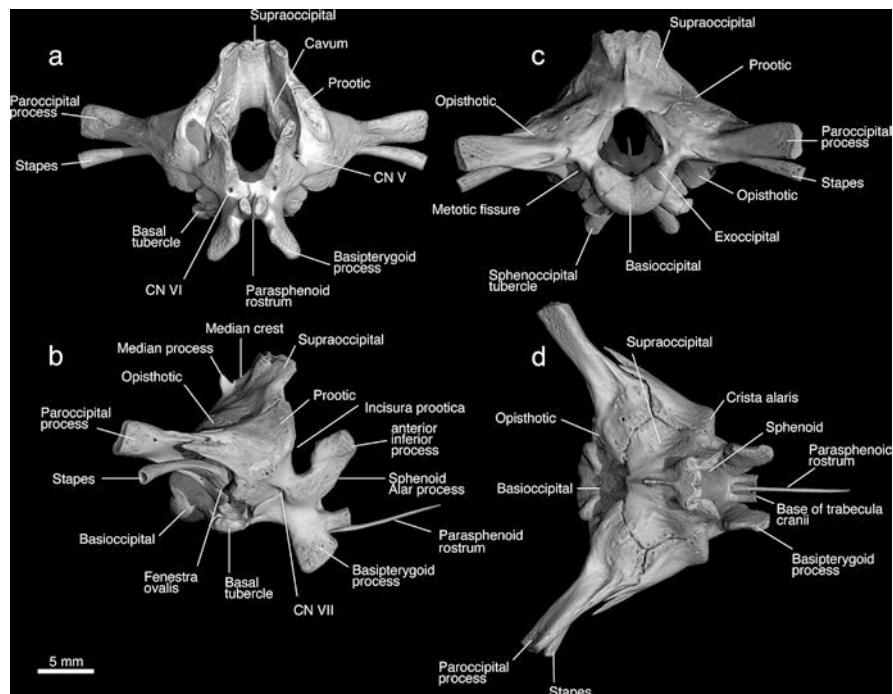


Fig. 5.3 Brainscase of *Sphenodon punctatus* (FMNH-R11115) in anterior (a), lateral (b), posterior (c), and dorsal (d) views. Anatomical parts follow largely Evans (2008), but in some cases the names have been changed

paired internal carotid foramina are noticeable and there are no vidian canals on the parasphenoid. Only CNs V and VII were described for *Clevosaurus* sp., together with the internal carotid arteries that enter separately in the pituitary fossa. In a recent study, the brainscase of a specimen from the Late Triassic of Britain was virtually reconstructed using CT scans, but no endocranial traits nor cranial nerves were described (Chambi-Trowell et al. 2019).

Based on this available brainscase information, a hypothetical rhynchocephalian endocast would not have accurately reflected the surface morphology of the brain, as in the living relative *Sphenodon*. The dorsal surface of the endocast would probably show evidence of the presence of a pineal foramen, together with the dorsal surface of the forebrain (olfactory bulbs and tracts), although there are no clear impressions on the ventral surface of parietals and frontals in *Kaikaifilusaurus* (Apesteguía 2008) and *Sphenodon*. There would be a single large passage for all branches of CN V, as they leave the endocranial cavity through a single foramen, and also for CNs IX–XI, which leave the endocranial cavity through the metotic foramen. There is a variable number of branches of CN XII as Ross et al. (1999) described three hypoglossal foramina in the brainscase of *Sphenodon*, whereas Gower and Weber (1998) described two. The floor of the endocranial cavity bears a median medullar eminence that turns in a ventral longitudinal cleft on the medulla

oblongata. This trait is observed in living *Sphenodon* (Ross et al. 1999), the Triassic *Diphydontosaurus*, and the Cretaceous *Kaikaifilusaurus*, being probably a synapomorphy of Rhynchocephalia. Interestingly, the dorsal surface of the basisphenoid in *Kaikaifilusaurus* is wrinkled (Apesteguíá 2008), a character not described in other related taxa, that may reflect some aspect related to the ventral longitudinal venous sinus.

5.3.3 Squamata

The embryonic squamate braincase can be diagnosed by the fusion of the exoccipital and opisthotic, forming a composite otooccipital at hatchling, and the presence of a metotic fissure subdivided into the lateral aperture of the recessus scalae tympani anteroventrally (occipital recess in Oelrich 1956) and posterodorsally by a space where the foramen for the vagus nerve (CN X) and the foramina for the hypoglossal nerve (CN XII) are located (Säve-Söderbergh 1947; Kamal 1971; Bellairs and Kamal 1981; Rieppel 1993; Montero et al. 1999; Fig. 5.2). An otooccipital is present in all squamates, except in dibamids where the exoccipital and opisthotic bones remain separate in the juveniles, eventually fusing in later stages (Greer 1985; Rieppel 1984a, b). Similarly, the opisthotic and exoccipital are separate in the juveniles of *Sphenodon*, fusing posteriorly in the adults (Sienbenrock 1893; Evans 2008). A fully divided metotic fissure is present in the earliest known squamate braincase remains from the Early Cretaceous, but is absent in *Sphenodon* and all fossil rhynchocephalians (Evans 2016; Ross et al. 1999). Although similarly subdivided with an anterior recessus scalae tympani separated from the vagus and hypoglossal nerves, developmental observations show that the divided metotic fissure in lizards and snakes follows different developmental pathways (Kamal 1971; Bellairs and Kamal 1981; Rieppel 1993). Paleoneurological studies on non-marine lizards are limited to a few publications involving a highly fragmentary braincase (Cruzado-Caballero et al. 2019), and an unpublished preliminary study (García 2021). In this regard, detailed descriptions of braincases –and particularly endocranial cavities– in extinct (and also extant) forms are scarce. There are a few studies of cranial endocasts of fossils, including the enigmatic lizard *Oculudentavis* (Xing et al. 2020), Cretaceous mosasauroids (Camp 1942; Russell 1967; Rieppel and Zaher 2000; Georgi and Sipla 2008; Cuthbertson et al. 2015; Allemand 2017), a Cretaceous snake (Zaher and Scanferla 2012; Yi and Norell 2015; Triviño et al. 2018), and two Cenozoic lizards (Cruzado-Caballero et al. 2019; García et al. 2021), the two latter corresponding to highly fragmented or preliminarily studied specimens. In recent publications, aspects of the inner ear anatomy within a sample of extinct and living snakes were analyzed through digital 3D reconstructions based on CT scans (Yi and Norell 2013, 2015; Conrad and Daza 2015; Palci et al. 2017; Čerňanský et al. 2022). Study of cranial endocasts have the potential to produce new sources of information, which can be relevant for highly debated topics such as the origin of snakes (Allemand et al. 2017). All squamates share a braincase character, the metotic

fissure subdivided by the contact of the basal plate and otic capsule (Gauthier et al. 2012).

Braincase of Stem-Squamata

Megachirella wachleri preserves the braincase, but in both the photographs and the 3D model of the skull, there is not enough detail to describe the foramina and fenestrations, or the individual elements, however the braincase was described as having a well-developed alar process of the prootic (Simões et al. 2018). Additionally, on the published 3D models this fossil had a large paroccipital process, a single (undivided) occipital condyle, short basiptyergoid processes, and a ventral ridge in the basioccipital.

The fossil *Huehuecuetzpalli mixtecus* is also frequently recovered as a stem squamate, unfortunately the preservation of the braincase is limited, and not many details are available in the description. However, it has been described as having a short supraoccipital, well developed paroccipital processes (lateral process of the opisthotic), a small “C” shaped exoccipital, a robust stapes similar to that of *Sphenodon* and differing from the slender condition in Squamata (although this structure is highly variable among squamates; Weber 1978; Sánchez-Martínez et al. 2021), and an alar process of the prootic contacting the columnar epiptyergoid (Reynoso 1998).

The enigmatic fossil *Oculudentavis*, known by two fully articulated and three dimensional specimens embedded in amber has been recovered in a basal position, either as sister to *Scandensia ciervensis*, sister to Dibamia, or mosasaurs (Bolet et al. 2021). Although this fossil is very complete, its affinities are still uncertain, possibly caused by its unique morphology. However, several features are known from its braincase, and serve to diagnose this taxon, including a vaulted braincase, well-developed crista prootica, short alar process, slender basiptyergoid processes (not expanded distally in a *O. khaungrae*), short basisphenoid, enclosed vidian canals opening posteriorly within the basisphenoid, robust parasphenoid rostrum, short supraoccipital, visible processus ascendens, and short paroccipital processes (Bolet et al. 2021). In its original description as a dinosaur, a model of the endocast was included where the authors inferred a prominent cerebrum (although not a clear optic lobe as in birds) and part of the olfactory tracts (Xing et al. 2020).

Braincase of Dibamidae

Dibamids (Fig. 5.4) have been consistently recovered as an early branching squamate group, or as sister to Gekkota. They have some distinctive characters of the braincase such as the lack of an optic foramen and crista prootica (the latter shared with amphisbaenians), and the presence of ophidiosphenoid (= laterosphenoid or pleurosphenoid) a character shared with amphisbaenians and snakes (Gauthier et al. 2012) that seems to be convergent among those groups.

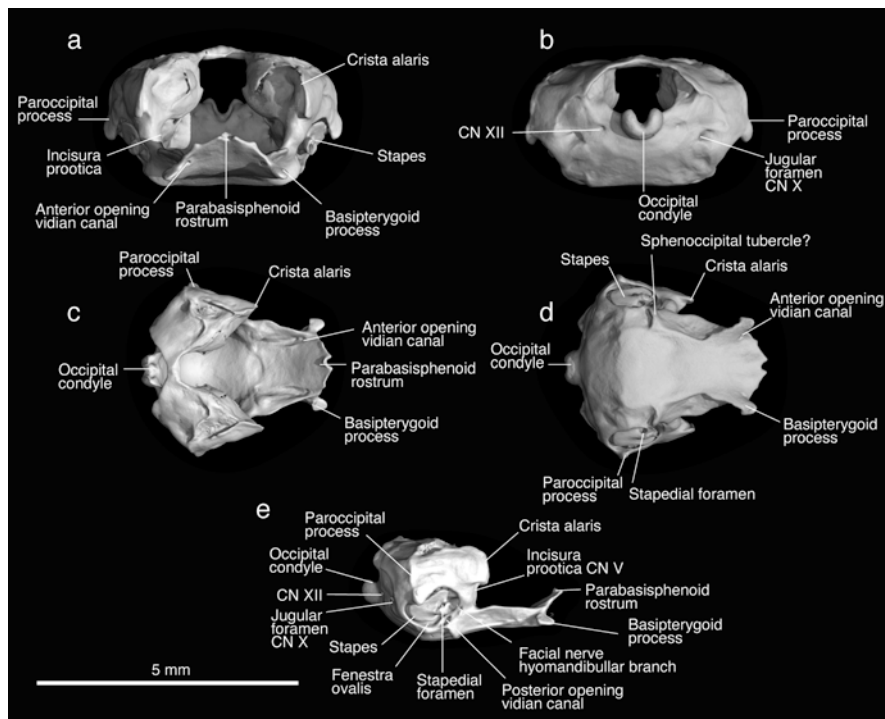


Fig. 5.4 Brainscase of *Dibamus novaeguineae* (CAS-SU-26872) in anterior (a), posterior (b), dorsal (c), ventral (d), and lateral (e) views. Anatomical parts follow largely Rieppel (1984a, b), but in some cases the names have been changed

Brainscase of Gekkonomorpha

The brainscase of gekkonomorph lizards has two main contrasting morphologies: in limbed gekkotans the brainscase is wide, while in limb-attenuated pygopods the brainscase becomes narrow and elongated (Kluge 1976) (Fig. 5.5). Virtually, all limbed crown gekkotans have the incisura prootica (CN V) medially closed into a bony canal (Evans 2008), also called foramen prootico (Daza et al. 2013). The foramen prootico forms a bony enclosure of the trigeminal nerve, and it is lost only in some members of the Indopacific gecko group (e.g. *Gekko*, *Luperosaurus*, *Ptychozoon*), although the distribution of this character is uncertain since the taxonomy of *Gekko* s.l. is under major changes (Wood et al. 2020a, b). Some species of the genus *Gekko* might have the enclosure (e.g. *G. vittatus*), and some not (e.g. *G. gecko*) (See also Daza et al. 2015). The bony enclosure is also lost in the Pygopodidae (reversed to the widespread condition of squamates, considering the current hypothesis of relationships). Limbed gekkonomorphs are also distinct by having a well-developed crista prootica, this trait is very reduced in pygopodids, probably due to their narrowed skull when compared with limbed gekkotans.

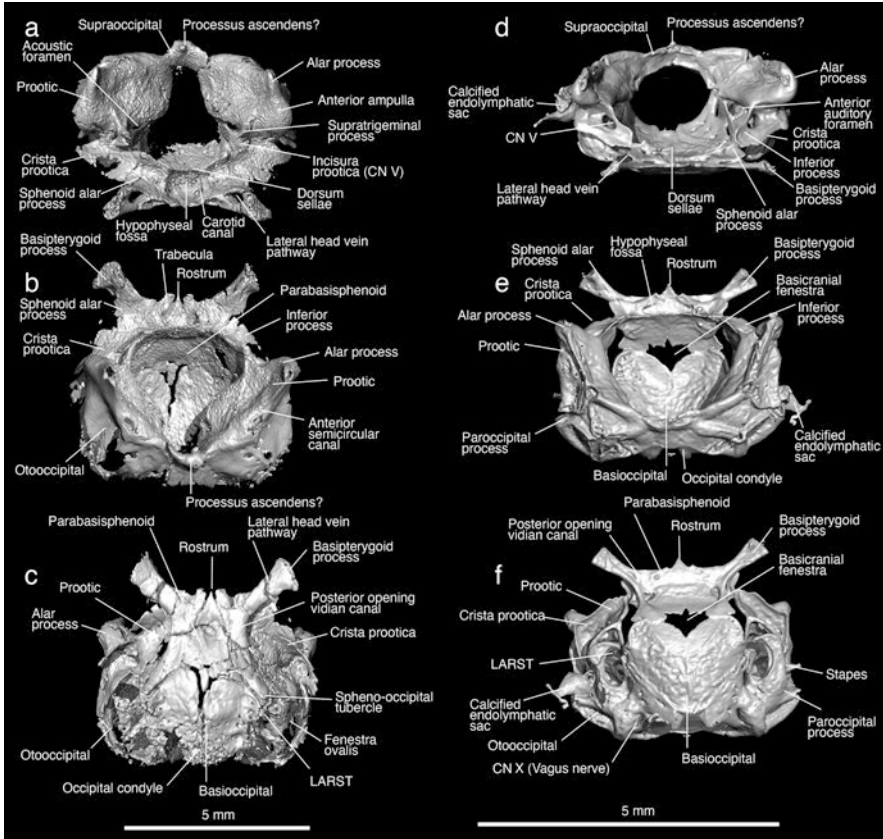


Fig. 5.5 Brainscases of two fossil gekkonormorphs: (a–c) *Norellius nyctisaurops* (AMNH FR 21444); and (d–f) an undescribed fossil embedded in Burmese amber (JZC Bu1802). Notice the different enclosure for the trigeminal nerve, and the low processus ascendens

One clear distinct feature of gekkotans from early gekkonormorphs is the lack of a pineal foramen, visible in *Norellius* and in *Eichstaettisaurus* but absent in the crown group and *Gobekko* (Borsuk-Białynicka 1990; Daza et al. 2013). Another character is the lack of the processus ascendens of the supratemporal (Bellairs and Kamal 1981; Rieppel 1984b; Estes et al. 1988; Daza et al. 2013). Gekkotans and some iguanians also develop extracranial calcified endolymphatic sacs (Kluge 1967; Bauer 1989; Gamble et al. 2012; Laver et al. 2020). These structures, although hard to preserve in fossils, are visible in amber inclusions (Fig. 5.3).

Perhaps the best preserved brainscases in any fossil geckos are the gekkonormorph *Norellius nyctisaurops* (Conrad and Norell 2006; Conrad and Daza 2015; Fig. 5.3a–c), and the brainscase of an undescribed gecko in amber from Myanmar (Daza et al. 2016; Fig. 5.3d–f). In all gekkotans, the orbitosphenoid is cartilaginous.

There are four brainscase characters that differentiate geckos from other lepidosaurs, including: a crista prootica present and sometimes prominent and extending

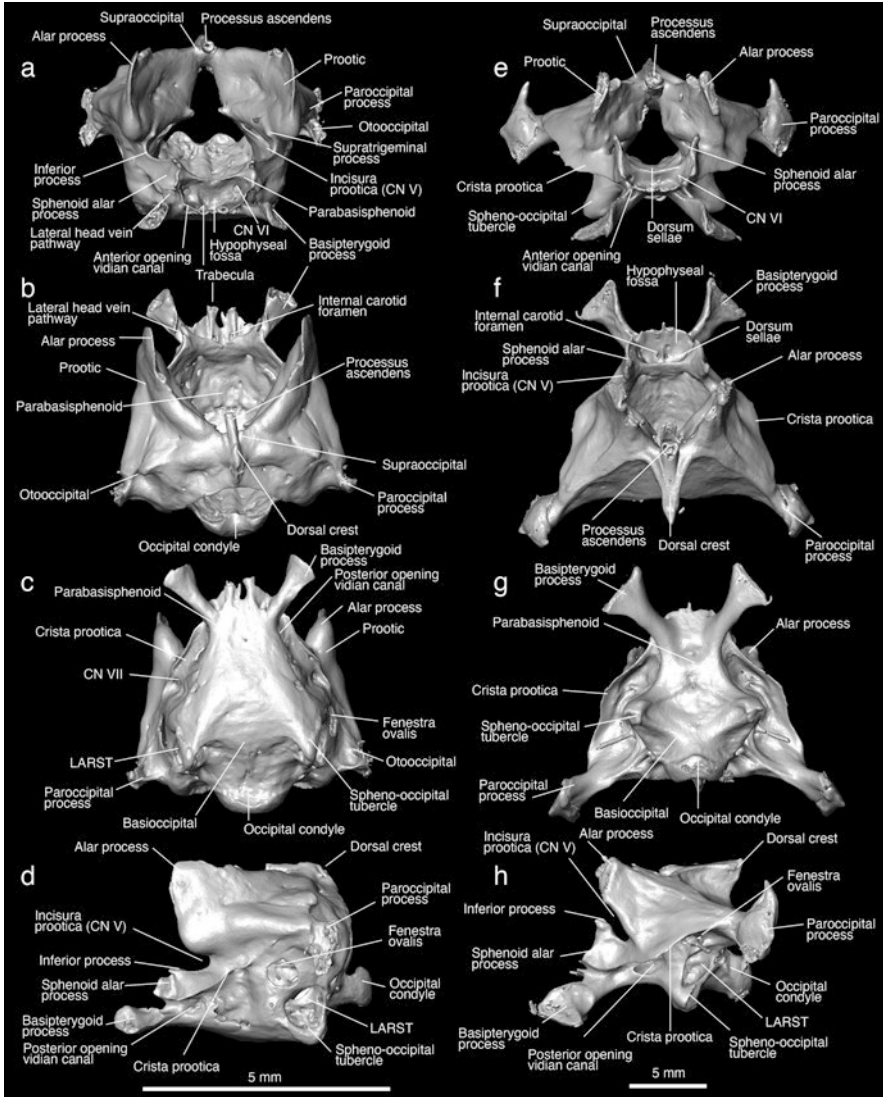


Fig. 5.6 Brainscape of two extant scincoideans (cordylids): (a–d) *Chamaesaura anguina* (UF-H-27589); and (e–h) *Smaug giganteus* (UF-119459). Notice the deep flanges on the hypophyseal fossa, large dorsal crest, sphenoccipital tubercle and LARST opening

onto basipterygoid process and forming an open or closed canal (similar in some iguanians), a trigeminal foramen enclosed by bone (foramen prootico, lost in some forms), and medial aperture of the recessus scalae tympani divided into anterior and posterior openings (not present in some genera, e.g. *Gonatodes*) (Gauthier et al. 2012).

Braincase of Scinciformata

Scinciformata includes the families Scincidae, Gerrhosauridae, Cordylidae, and Xantusiidae. The braincase morphology is modified in limb-reduced and first head burrowing species (Fig. 5.6), where the braincase is narrowed to the point that in some species the medial wall of the otic capsule contact each other in the midline (as in *Typhlacontias gracilis*, Stepanova and Bauer 2021). The braincase also develops a lateral closure by an increased contact between the parietal ventrolateral flange and the alar process of the prootic (Rieppel 1981). Several characters from the braincase have been used to diagnose each one of the scinciformatan clades (Evans 2008); however, these show a large amount of variation, making it difficult to characterize their braincase. Scinciformatans in general have ossified orbitosphe-noids, well-developed alar process and crista prootica, a prominent sphenoccipital tubercle, the paroccipital process with a recess for the quadrate, a large lateral opening for the recessus scalae tympani, sometimes a small supratrigeminal process, and sometimes a well-defined processus ascendens and a dorsal crest on the supraoccipital (Evans 2008; Fig. 5.4). The clinoid process, also known as the alar process of the sphenoid, is enlarged and it contacts the inferior process of the prootic. One character in some scinciformatans, such as cordylids and xantusiids, is the presence of a supraoccipital crest (Gauthier et al. 2012).

Several fossils have been recovered as stem-scinciformatan, including *Parmeosaurus*, *Paramacellodus*, *Myrmecodaptria*, *Carusia*, *Eoxanta*, *Hymenosaurus*, *Globaura*, *Ardeosaurus*, and *Retinosaurus*. Some of these preserve braincase remains, such as *Paramacellodus* presenting a short and broad braincase, with short and thick paroccipital process and a kidney-shaped occipital condyle (Evans and Chure 1998). The braincase of *Myrmecodaptria* (IMG 3/95) has a poorly preserved braincase, limited to a portion of the parabasisphenoid including the basipterygoid processes, part of the basioccipital, and the occipital condyle. The braincase floor is narrow and elongated, and although originally discussed as possibly related to Gekkota (Gao and Norell 2000), the authors pointed out that the occipital condyle was not bipartite as in limbed geckos (Gardiner 1982). The prootic is also described as extending onto the basipterygoids to cover the recessus vena jugularis, perhaps describing the clinoid process and the lateral head vein below. Additionally, a prominent processus ascendens was also described. The braincase of *Carusia* is preserved in several specimens (Borsuk-Białynicka 1985; Borsuk-Białynicka 1987; Gao and Norell 1998), exhibiting a hexagonal supraoccipital, a prominent processus ascendens, a well-developed recess for the lateral head vein, well developed crista prootica, and two foramina open into the recessus vena jugularis: one posterior to the vidian canal, and the facial foramen. A prominent sphenoccipital tubercle, and a small hypoglossal foramen, opening close to the LARST. Perhaps one of the best-preserved articulated skulls and braincases is the one of the amber embedded scinciformatan *Retinosaurus*, which has been found to be a stem-xantusiid (Čerňanský et al. 2022). The preservation of this delicate structure allowed also to produce an endocast of the inner ear. *Retinosaurus* has a well-developed alar process, crista prootica, a marked groove for the lateral head vein on

Braincase of Laterata

Laterata is also a diverse clade (Fig. 5.7), containing the Teioidea (Teiidae, Gymnophthalmidae, and Alopoglossidae) and Lacertibaenia (Lacertidae, and the amphisbaenians, Bipedidae, Rhineuridae, Blanidae, Cadeidae, Trogonophidae, and Amphisbaenidae). There are detailed descriptions of the skull of many of their members, including extant species (Jollie 1960; Bell et al. 2003; Montero et al. 2004; Montero and Gans 2008; Guerra and Montero 2009; Roscito and Rodrigues 2010; Hernández Morales et al. 2018; Holovacs et al. 2019). Laterata has experienced limb reduction and first head burrowers in both main groups, resulting in very contrasting morphologies, e.g. the lateral closure of the skull in sand swimmers such as *Calyptommatius* (Gymnophthalmide, Roscito and Rodrigues 2010; Holovacs et al. 2019) and the Amphisbaenia (Montero and Gans 1999, 2008), where the skull is closed by an enlarged descensus parietalis process in the former, and by an extended contact between the parietal and the anterior part of the braincase in the latter. Given the morphological disparity in this group, it is hard to characterize their braincase, to the point that comparisons with amphisbaenians become complicated. This is also exacerbated by the terminology used for some elements that are likely to be homologous or largely equivalent, but that when proposed, amphisbaenians were considered a separate group of reptiles, and these terms have been traditionally maintained (Fig. 5.7). A good example is the element that caps the sphenoccipital tubercle reinterpreted as the basicranial sesamoid (Montero et al. 2017), or the tabulosphenoid of amphisbaenians, which includes the orbitosphenoid and other elements of dermal origin (Montero and Gans 1999; Montero pers. comm.). Likewise, the anterolateral process of the fused otico-occipital complex of amphisbaenians corresponds, or at least, closes the braincase laterally in a similar way to the prootic alar process. Considering how extremely modified are amphisbaenians, it is difficult to describe a putative synapomorphy from the braincase, for example all the limbed members of Laterata have an orbitosphenoid that is either bi or tri-radiated, but in Amphisbaenia the element that includes the orbitosphenoid (i.e. tabulosphenoid) is unpaired and has a unique flattened morphology. Likewise, all limbed forms have an alar process, and a crista prootica. Likewise, the crista tuberalis is strong and located behind the LARST. Evans (2008) described an interesting basicranial character referring to a pit in front of the posterior ampullary prominence, where the epibranchial 2 will meet the skull. Such character deserves a more detailed revision, although present in all revised gymnophthalmids, alopoglossids, and in small teiids, and it seems to be affected by size (Evans, personal communication). Another braincase character described for gymnophthalmids and teiids (and most likely alopoglossids as well) is the participation of the prootic in the margin of the medial aperture of the recessus scalae tympani (Bell et al. 2003; Gauthier et al. 2012).

Despite the extreme transformation of amphisbaenians, shared characters with most of the limbed forms are: the presence of a prominent sphenoccipital tubercle (capped or not by the basicranial sesamoid), a tendency to reduce the size, or at least the thickness of the basiptyergoid process, and a parabasisphenoid rostrum with a broad base. Many members also show very globular braincases in the occipital area,

especially in small forms (e.g. gymnophthalmids, alopoglossids and amphisbaenians). Unique amphisbaenian characters include the origin of temporal muscles spread onto braincase dorsally (an homoplastic condition also present in snakes), optic foramen enclosed entirely within the tabulosphenoid, and perilymphatic foramen facing posteriorly (Gauthier et al. 2012).

Some of the most remarkable Laterata fossils with well-preserved braincases include the teiids *Dracaena uruguaiensis* (Hsiou 2007; Quadros et al. 2018) and *Callopietes bicuspidatus* (Brizuela and Albino 2017), several rhineurid amphisbaenians (Berman 1973, 1976, 1977; Kearney et al. 2005; Stocker and Kirk 2016), a blanid amphisbaenian (Bolet et al. 2014), and a number of transitional fossils that have been proposed as early stages in the evolution of amphisbaenians (Wu et al. 1993; Müller et al. 2011), although the phylogenetic placement of one of them has been challenged (i.e. *Sineoamphisbaena*; Kearney 2003; Conrad 2008).

The braincase of amphisbaenians is completely ossified, as in snakes, providing a complete cast of the endocranial cavity. However, in the fossil record there is a lack of detailed knowledge of the braincase anatomy of this clade in general, and although certain taxa have complete skulls (e.g. Berman 1976), the cranial neurovascular foramina have never been described nor illustrated, neither are the endocranial aspects. The amphisbaenians *Spathorhynchus fossorium* and *Rhineura hatcherii* from the early Cenozoic of USA are some of the few fossil taxa studied using micro-CT scans (Kearney et al. 2005; Muller et al. 2016). However, skull descriptions do not include the braincase. On the other hand, studies by Maisano et al. (2005) that were also based on micro-CT scans, provided detailed descriptions of the braincase and cranial foramina of the extant species *Diplometopon zarudnyi*. The endocranial cavity is in general anteriorly heart-shaped (indicating that the cerebral hemispheres are well differentiated, at least laterally), and almost completely enclosed by the frontals, whereas posteriorly the shape of the cranial cavity becomes more circular. The gasserian foramen (for CN V) opens between the parietal temporal lamina and the parabasisphenoid, followed by CN VII, which is bounded by the prootic. The fenestra ovalis opens ventrolateral into the jugular recess. The vestibular eminence on each side protrudes well into the endocranial cavity. The bony labyrinth (inner ear) has an ovoid statolith mass that extends posteriorly to fill roughly half of the vestibule (Maisano et al. 2005).

Some aspects of sensory biology were made regarding the sculpturing on the snout of *R. hatcherii* formed by perforating canals, which responds to an unprecedented degree of cutaneous peripheral innervation (by means of the trigeminal nerve), not observed in living representatives (Maisano et al. 2005). In turn, *S. fossorium* has a reinforced orbital rim that suggests selection against the loss of a functional eye, indicating an ecology potentially different from modern taxa and a more complex history for the cranial traits traditionally linked to fossoriality.

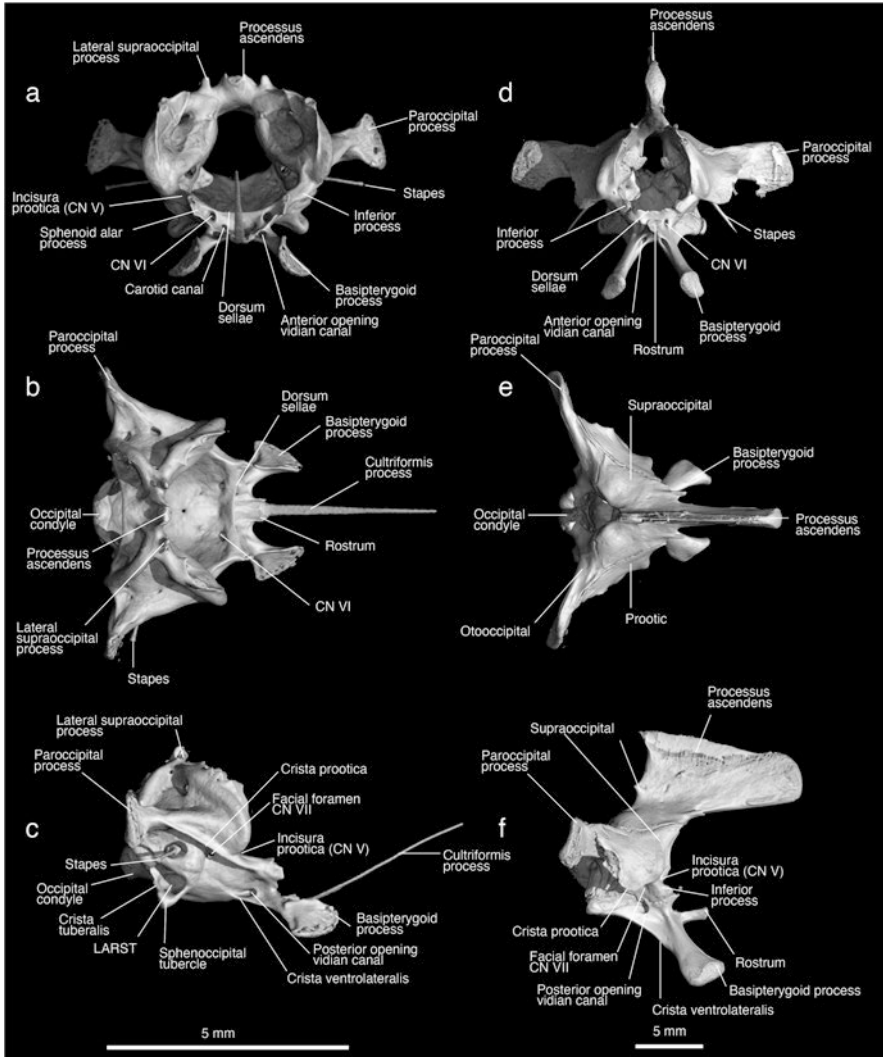


Fig. 5.8 Brainscase of two extant toxicoferans: (a–c) the dactyloid *Anolis carolinensis* (UF-H-102367); and (d–f) the chameleonic *Chameleo calypratus* (UF-H-191369)

Brainscase of Toxicofera

This group comprises a large diversity of forms, including the extant clades Anguimorpha (Anguidae, Helodermatidae, Lanthanotidae, Shinisauridae, Varanidae, Xenosauridae, plus certain extinct forms [e.g. Palaeovaranidae]), Iguania (Acrodonta: Agamidae, Chamaeleonidae; Pleurodonta: Corytophanidae, Crotaphytidae, Dactyloidae, Hoplocercidae, Iguanidae, Leiocephalidae, Leiosauridae, Liolaemidae, Opluridae, Phrynosomatidae, Polychrotidae,

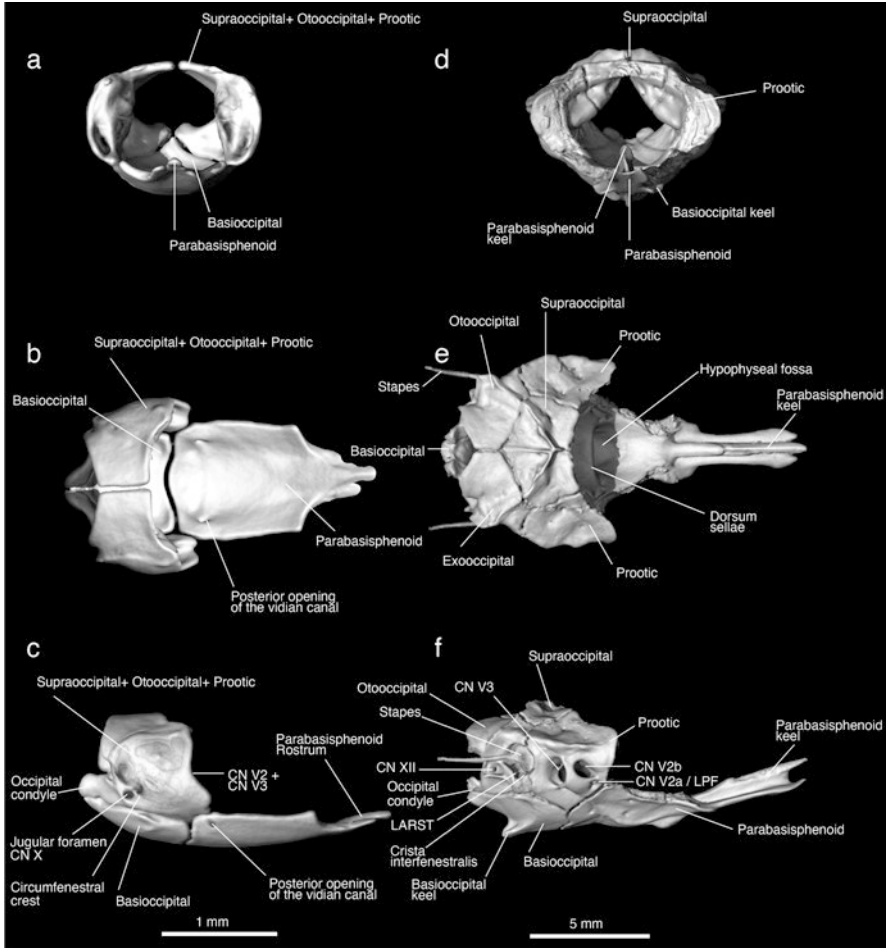


Fig. 5.9 Brainscapes of two extant toxicoferans: (a–c) the typhlopod *Indotyphlops braminus* (UF-Herp-29433); and (d–f) the colubrid *Nerodia sipedon* (UF-Herp-177819)

Tropiduridae), Serpentes, and the extinct Mosasauroida and Polyglyphanodonta (Figs. 5.8 and 5.9). Comparisons in brainscape anatomy are difficult because of highly divergent forms such as chameleons and snakes. Brainscape characters unique to this group are hard to identify, however, the limbed forms usually have a well-developed sphenoccipital tubercle, and occipital recess – the occipital recess is reduced in Anguinae and Varanidae, and sometimes associated with an enlarged fenestra ovalis; a well-developed inferior process, a deep incisura prootica, and an enlarged crista tuberalis that makes the vagus foramen shift to the posterior part of the skull (Rieppel 1980; Conrad and Norell 2008; Evans 2008; Conrad et al. 2011). There are highly detailed descriptions of the brainscape in toxicoferans, including isolated bones of living groups: Anguinae (Conrad and Norell 2008), Iguanidae

(Oelrich 1956; Evans 2008), Lanthonothidae (McDowell and Bogert 1954), Shinisauridae (Bever et al. 2005), and Varanidae (Säve-Söderbergh 1947; Conrad et al. 2008), among others. Studies of fossil taxa include the polyglyphanodontid *Macrocephalosaurus chulsanensis* (Sulimski 1975), the monstersaurian *Gobiderma pulchrum*, the anguids *Melanosaurus maximus*, *Helodermoides tuberculatus*, and *Pseudopus laurillardi* (Range and Bailon 2005; Conrad and Norell 2008; Klembara et al. 2010), the varanid *Saniwa ensidens* and *Varanus marathonensis* (Conrad et al. 2012; Smith et al. 2018; Villa et al. 2018), the palaeovaranid *Paranecrosaurus feisti* (Smith and Habersetzer 2021), and the iguanian *Geiseltaliellus maarius* (Smith 2009).

Braincase of Extinct Snakes and Available Endocranial Features

The braincase morphology of snakes departs from other toxicoferans by their highly specialized nature (Bellairs and Kamal 1981; McDowell 2008; Cundall and Irish 2008). Additionally, snakes are also characterized by having elongated and mainly limbless bodies, but several limbed forms were recovered from Cretaceous rocks, including the four-limbed Early Cretaceous *Tetrapodophis amplectus* (Martill et al. 2015; Zaher and Smith 2020; Zaher et al. 2022a) and the hind-limbed Late Cretaceous *Najash rionegrina*, *Pachyrhachis problematicus*, *Haasiophis terrasanctus*, and *Eupodophis descouensi* (Haas 1979, 1980a, b; Rage and Escuillié 2000; Tchernov et al. 2000; Apesteguía and Zaher 2006). Although not preserved in any of the known specimens so far, similarly well-developed hindlimbs were most likely present in the Late Cretaceous *Dinilysia patagonica* and *Sanajeh indicus*. Including snakes, limb reduction and body elongation has occurred in all major squamate groups except in the Iguania – squamate reptiles show a large spectrum of serpentine-form groups ranging from fully limbed to complete limblessness (Camaiti et al. 2021).

Snakes probably diverged from their closest lizard ancestors at some point in the Jurassic (Zheng and Wiens 2016; Pyron 2017; Burbrink et al. 2020). The earliest informative articulated specimens are only known from the latest Early Cretaceous (Cuny et al. 1990). Despite their strongly ossified braincase, only a few Cretaceous snakes preserved their skull and braincase anatomy, the group being predominantly represented by isolated vertebrae throughout the Mesozoic. Well-preserved braincases are known in the stem snakes *Tetrapodophis amplectus* from the Early Cretaceous of Brazil, *Dinilysia patagonica* and *Najash rionegrina* from the Late Cretaceous of Argentina, and *Sanajeh indicus* from the Late Cretaceous of India (Estes et al. 1970; Apesteguía and Zaher 2006; Zaher et al. 2009; Wilson et al. 2010; Zaher and Scanferla 2012; Martill et al. 2015; Garberoglio et al. 2019; Zaher et al. 2022a), and in the more derived crown alethinophidians *Pachyrhachis problematicus*, *Haasiophis terrasanctus*, and *Eupodophis descouensi* from the Cenomanian of the Middle East (Haas 1979, 1980a, b; Rage and Escuillié 2000; Tchernov et al. 2000; Rieppel and head 2004; Garberoglio et al. 2019; Zaher et al. 2022b). Recently, a small number of poorly preserved Middle Jurassic and Early Cretaceous

squamates collectively referred to as ‘parviraptorids’ were re-interpreted as stem snakes (Caldwell et al. 2015). Although ‘parviraptorids’ would appear to fill a significant gap in the fossil record of snakes, their affinities and complex taxonomic history are still in dispute (Conrad 2008; Panciroli et al. 2020).

Among the known Cenozoic snakes with a well-preserved braincase, the Australian “madtsooids” *Wonambi naracoortensis* and *Yurlunggur camfieldensis* gained relevance in the debate on the origin of snakes (Scanlon and Lee 2000; Rieppel et al. 2002; Scanlon 2003, 2005, 2006). Their phylogenetic position as early diverging snakes has been controversial (Rieppel et al. 2002), and recent studies are supporting a more derived position as stem alethinophidians (Zaher and Smith 2020; Zaher et al. 2022a). Other relevant Cenozoic fossil snakes with described and figured braincases include the alethinophidians *Kataria anisodonta*, *Archaeophis proavus*, *Archaeophis turkmenicus*, *Crythosaurus mongoliensis* (Janensch 1906; Gilmore 1943; Tatarinov 1988; Scanferla et al. 2013), the constrictores *Messelophis variatus*, *Rieppelophis ermannorum*, *Boavus idelmanni*, *Eoconstrictor fischeri*, *Messelopython freyi*, *Palaeopython schaali* (Hoffstetter and Rage 1977; Scanferla et al. 2016; Scanferla and Smith 2020a, b; Georgalis et al. 2021; Smith and Scanferla 2021), and a small number of colubroideans (Szyndlar 1985, 1988, 1991; Szyndlar and Zarova 1990; Rage 1976).

In contrast to fossil snakes, the braincase of extant snakes have been studied extensively, including a wealth of available embryological and anatomical works that offer a robust body of evidence (see Underwood 1967; Bellairs and Kamal 1981; McDowell 2008; Cundall and Irish 2008; Werneburg and Sánchez-Villagra 2015 for a detailed review of the literature). Several braincase characters are unique to extant snakes, including a nuchal crest of the supraoccipital extending laterally, alar process short or absent, crista tuberalis and crista prootica prominent and combined to surround the stapedia footplate and the LARST, crista interfenestralis reduced, maxillary branch of the trigeminal nerve passing between the palatine and the prefrontal, parietal roofing the vidian canal, trabeculae cranii platybasic, sella turcica recessed below a high dorsum sellae posteriorly, basiptyergoid process (when present) lacking a synovial palatobasal articulation, CN IX exits posteriorly via the vagus (=jugular) foramen, the LARST is small, and the exoccipital parts of the otooccipital contact each other above the foramen magnum (Gauthier et al. 2012).

Tetrapodophis and *Sanajeh* retain a complete rod-like and gracile upper temporal bar formed by the postorbital and squamosal, absent in all other known snakes (Zaher et al. 2022a). *Sanajeh* also retains a multipartite suspensorium that is intermediate between lizards and snakes, with an otooccipital contacting the quadrate laterally and below the expanded supratemporal. Within crown Serpentes, the suspensorium reduces independently in scolecophidians and alethinophidians, being lost independently in scolecophidians and uropeltids (with the quadrate articulating directly with the braincase wall) or reducing significantly in alethinophidians where the supratemporal takes the role as the only suspensorial element of the braincase (Zaher et al. 2022a). The stapedia footplate in stem snakes *Dinilyisia*, *Najash*, and *Sanajeh* is expanded, being much larger than the condition known to occur in crown Serpentes, including *Yurlunggur*, *Wonambi*, and pachyophiids (Zaher et al. 2022b).

The crista circum fenestralis is also characteristically reduced (low) in these snakes with an expanded stapedia footplate. A shallow sella turcica with a low dorsum sellae characterizes *Dinilyisia*, *Najash*, scolecophidians, *Yurlunggur*, *Wonambi*, *Anilius*, and uropeltoids, while a deep sella turcica recessed below a well-defined dorsum sellae is uniformly present in pachyophiids and all other crown alethinophidians (Rieppel 1979a, b; Rieppel et al. 2009; Zaher et al. 2022b). In *Dinilyisia*, *Najash*, and *Sanajeh*, the basiptyergoid process fits into a socket or deep recess in the pterygoid, suggesting that a synovial palatobasal articulation was present in these forms. In all other snakes (including pachyophiids, *Wonambi* and *Yurlunggur*) this synovial joint is absent and the basiptyergoid process, when present, contacts a flat surface on the pterygoid where it attaches via tendinous tissues (Zaher et al. 2022a). The trigeminal foramen is markedly larger than other cranial foramina in *Dinilyisia*, *Najash*, *Sanajeh*, *Wonambi*, *Yurlunggur*, and pachyophiids, resulting from the anteroposterior extension of the braincase and lateral enclosure of the braincase wall by the parietal and frontals. Scolecophidians also have a single opening for the trigeminal nerve, but it is much smaller and fails to form a deep notch on the prootic. In crown alethinophidians, the maxillary (CN V₂) and mandibular (CN V₃) branches are separated by the presence of an ophidiosphenoid (=laterosphenoid), which forms as a membrane bone.

As for other lepidosaurian groups, the paleoneurology of snakes has been poorly explored. The endocranial anatomy of *Dinilyisia patagonica* was described by Zaher and Scanferla (2012) as part of a more inclusive analysis of the skull, but the first paleoneurological study for an extinct snake was made by Triviño et al. (2018), based on a natural endocast. More recently, the inner ear morphology of *Yurlunggur* and *Wonambi* were analyzed based on CT-scan data (Palci et al. 2017, 2018). According to Evans (2016) the ear region of both madtsoiids shows a derived condition when compared to *Dinilyisia*. Differently from *Dinilyisia* and *Najash*, both *Wonambi* and *Yurlunggur* possess a distinct juxtastapedial recess delimited by a well-developed crista circumfenestralis (Zaher et al. 2009; Zaher and Scanferla 2012; Evans 2016).

In *Dinilyisia* the basioccipital extends ventrally to the accessory process of the crista interfenestralis to form a well-developed lizard-like spheno-occipital tubercle. An expanded spheno-occipital tubercle is absent in pachyophiids, *Wonambi* and all extant snakes. It is not preserved in *Sanajeh* and *Najash*. In *Wonambi*, the internal (posterior) opening for CN VI is posterior to the pituitary pit, whereas the external (anterior) opening is just dorsal to the anterior vidian canal, being the latter probably the case in *Dinilyisia* as well (Scanlon 2005). There is a single foramen for CN VII, whereas in living snakes the two branches of the facial nerve either exit through separate foramina or one of the branches penetrates the interior of the vidian canal as probably in *Dinilyisia* (Estes et al. 1970; Zaher and Scanferla 2012). In *Wonambi* the fenestra ovalis is observed on the lateral side of the braincase, and the jugular foramen (for CN X) opens anterolateral to the two hypoglossal (CN XII) foramina. Apart from the largest and most conservative features, identification of vascular and nervous foramina in fossil snakes must be somewhat speculative due to the lack of direct evidence of soft tissues (osteological correlates).

5.4 Overview of General Comparative Neuroanatomy

5.4.1 *Characterization of the Reptilian Central Nervous System*

The reptilian central nervous system is in general relatively simple anatomically and most living lepidosaurians have “tubular brain”, meaning that the forebrain, mid-brain, and hindbrain are linearly or horizontally aligned. Cerebral hemispheres are in general relatively small and have smooth surfaces (Goldby and Gamble 1957; Wyneken 2007). The forebrain or procerebrum is the most anterior part of the brain, related mainly with the senses of smell and taste, and to sensory-motor integration. It subdivides in telencephalon and diencephalon, comprising the olfactory apparatus (olfactory bulbs and tracts), cerebral hemispheres, pineal complex and pituitary. The midbrain or mesencephalon relates with visual processing and neuroendocrine regulation, and this region of the brain is formed by the Tectum (optic lobes). The hindbrain or rhombencephalon relates with hearing and balance, and is subdivided in metencephalon and myelencephalon, comprising the cerebellum and medulla oblongata (Romer 1956; Nieuwenhuys 1998; Butler and Hodos 2005; Wyneken 2007; Bruce 2009). Compared to the forebrain regions, the mid-brain and hindbrain leave less osteological correlates on the endocranial cavity. Plus, in many cases there are large longitudinal venous sinuses obscuring the brain surfaces (e.g. Porter and Witmer 2015). Regarding the evolutionary pattern, the brain size increment along the evolution of amniotes is not uniform for all the regions of the brain and responds, mainly, to a forebrain increment. The pallium of the telencephalon experiences hypertrophy particularly in snakes and some lizards (Bruce 2006; Güntürkün et al. 2020).

The cranial nerves (CNs) are highly conservative among Lepidosauria, in terms of their topography, origins, and endings (Diaz and Trainor 2019). They have been largely studied particularly in lizards, but also in snakes, and in the single representative of the Rhynchocephalia whose CNs were first illustrated by Dendy in 1909 (Watkinson 1906; Willard 1915; Oelrich 1956; Barbas-Henry 1988; Islam and Ashiq 1972; Auen and Langebartel 1977; Dakrory 2011a, b). *Sphenodon* and lizards have 12 pairs of cranial nerves besides the terminal nerve (CN 0), although in the former, CNs VI and VIII share the same root (Dendy 1909). Snake nerves are in general similar to those of lizards, but exhibit the following modifications: the olfactory nerve (and epithelium) is more extensive, there is a pterygoid division of the trigeminal nerve (V_4) (innervating the muscles of the upper jaw series of bones), the spinal accessory (CN XI) is absent (due the cucullaris muscle is not present in this group) and CNs III, IV, V₁, and VI combine forming the ocular trunk, whereas CNs IX-XII form a common cervical trunk (Auen and Langebartel 1977; Young 1987; Diaz and Trainor 2019). Further cranial nerve specializations among some families of snakes include sensory pits innervated by CN V that can detect infrared radiation (Güntürkün et al. 2020). In this regard, Scanferla and Smith (2020a, b) provided the

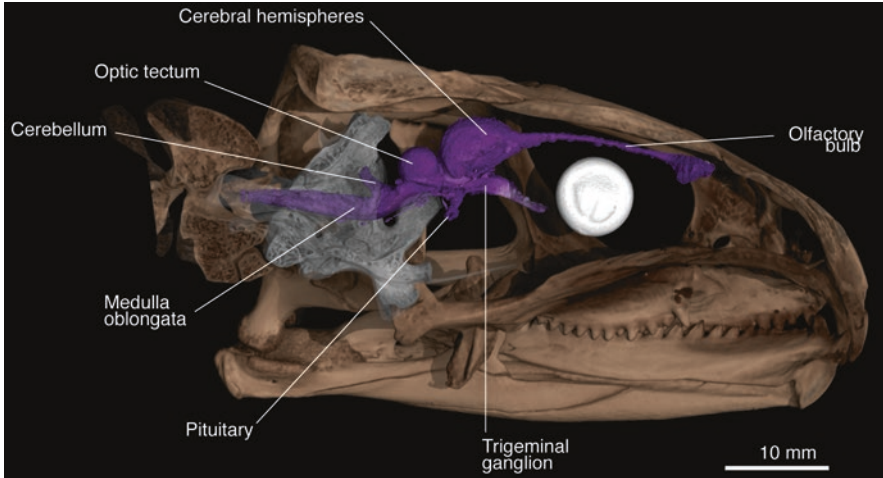


Fig. 5.10 *Sphenodon punctatus* (FMNH-R11115), sagittal cutaway of the brain *in situ* based on diceCT specimen. The region of the braincase proper that covers the brain was rendered as transparent to indicate the spatial position of the brain with respect to the endocranial cavity. Although the small size of the brain can be result of shrinkage due to formaline fixation and ethanol storage, the position of the brain is particularly different to squamates, the optic tectum and is completely anterior to the prootic and the position of trigeminal ganglion is very anterior to the incisura prootica. The pituitary gland also is placed very anterior to the braincase. Olfactory bulbs are very long and narrow, keeping a constant width along its way

first evidence for the early presence of specialized organs to detect infrared radiation in the Paleogene Messel fossil booids.

5.4.2 Brain Morphology of *Sphenodon*

The braincase anatomy and neural soft tissues of *Sphenodon punctatus* had been largely explored, indicating a relatively modest pallial specialization for this taxon (e.g., Gisi 1808; Dendy 1909, 1910; O'Donoghue 1920; Christensen 1927; Platel 1976, 1989; Bruce 2009; Jones et al. 2011; among many others). Although not described, illustrations of the brain anatomy were made by Dendy (1909) accompanying his work on intracranial vascular descriptions and re-drawn by Diaz and Trainor (2019). The brain of *Sphenodon* is simple and tubular, and the olfactory tracts are anteroposteriorly elongated as in most lizards (Starck 1979; Fig. 5.10). The cerebral hemispheres are oval, and the optic lobes are rounded and pronounced. Between cerebral hemispheres and optic lobes, a well-defined pineal complex projects dorsally, with the infundibular stalk projecting posteroventrally and ending in a slightly swallowed pituitary. These studies allowed to determine that there is a substantial space between the brain and the endocranial walls of the braincases. The BEC index is of 0.5, and opposite to that observed in most lacertids, the

encephalization index in the Tuatara is low (Dendy 1910; Platel 1989; Wyneken 2007; Balanoff and Bever 2017).

5.4.3 Brain Morphology of the Squamata

Brain Morphology of Lizards

The generalized lizard brain is also simple and tubular, and relatively small in proportion to the body size. The olfactory structure (olfactory lobes) is well-differentiated into relatively large olfactory bulbs and tracts. These structures are however relatively small, and even some lizards are microsmatic, i.e. a poorly developed sense of smell. The cerebral hemispheres are oval and smooth, and are separated medially from each other by an interhemispheric fissure. The diencephalon is a small protuberance between the cerebrum and the midbrain (optic tectum), and the optic lobes are oval and dorsally located. The epiphysial apparatus possess an anterior parietal body and a posterior pineal body, and the pineal eye is present. The cerebellum is poorly developed, and particularly the legless condition among lizards is expressed by a reduction of cerebellar volume (Platel 1976). The medulla oblongata is not overlapped by the cerebellum, and its roof is thin and vascular.

In most lizards the anteroventral part of the braincase remains cartilaginous preventing a complete cast of the endocranial cavity. There are both early and recent studies focused on the external surface morphology of the lizard brain in certain taxa (e.g. Shanklin 1930; Goldby 1934; Armstrong et al. 1953; Butler and Northcutt 1973; Northcutt 1978; Smeets et al. 1986; Hoops et al. 2018, 2021). However, only recently the lizard and amphisbaenid brain-to-endocranial cavity relationship has been studied, hand in hand with the use of micro-CT scans (Starck 1979; Allemand 2017; Allemand et al. 2017; Macri et al. 2019; Güntürkün et al. 2020).

The Dibamid Brain In the dibamid *Dibamus novaeguineae* (CAS-SU-26872, Fig. 5.11a), the brain shows the typical modified morphology of the head first burrowers, where this structure is wedge shaped and occupies most of the endocranial cavity. The medulla oblongata is sigmoidal in shape, and together with the optic tectum reduces the space for the cerebellum into a narrow space where this organ is squeezed. The braincase proper encloses for the most part the hindbrain (medulla oblongata, a very reduced cerebellum, and the optic tectum). The trigeminal ganglion lies entirely outside of the braincase and branches into the mandibular and the maxillary branches. The parietal bones enclose most of the cerebral hemispheres, while the frontals enclose both olfactory tract and bulb. The braincase extends anteriorly to reach almost the same level of the anterior border of the parietals, and provides an osseous ventral support for the medulla, optic tectum and cerebral hemispheres.

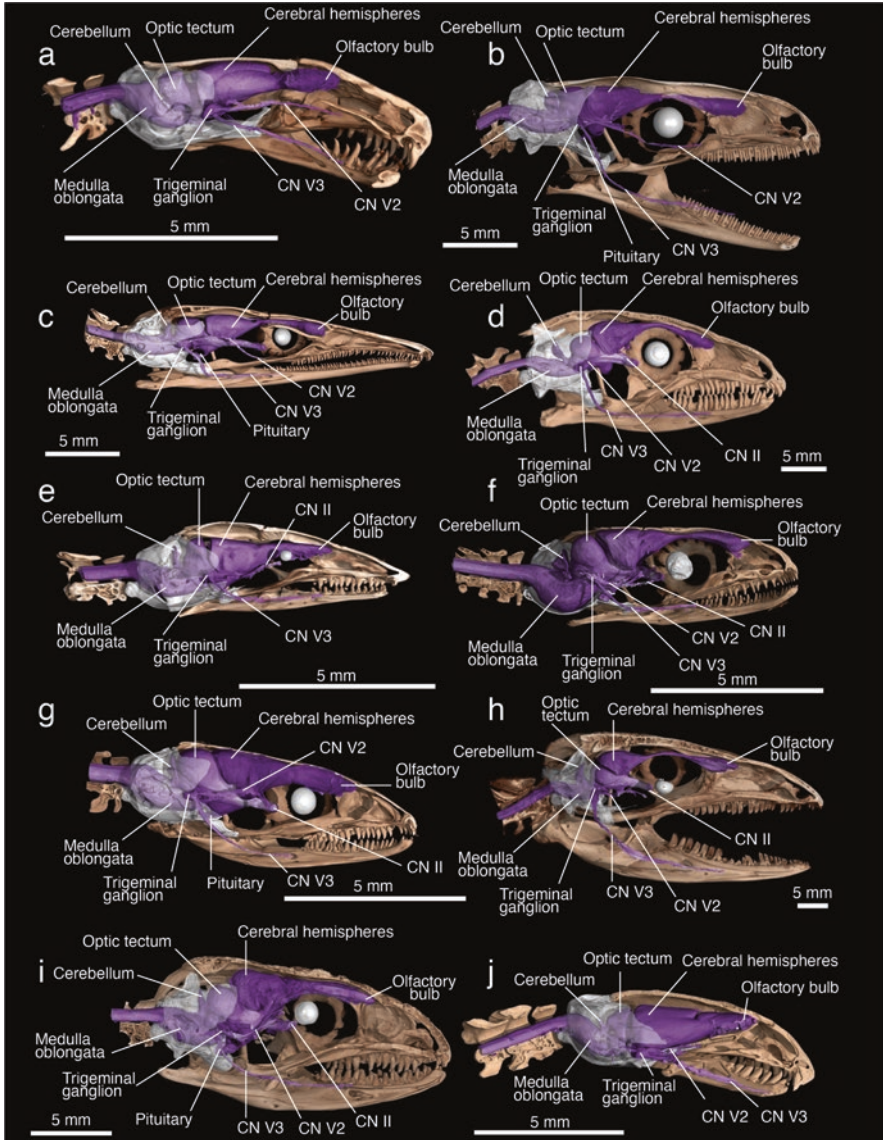


Fig. 5.11 Sagittal cutaway of the brain *in situ* based on diceCT specimens of representatives of Dibamidae (a–c), Scinciformata (d–f), Laterata (g–j). **Dibamidae:** (a) *Dibamus novaeguineae* (CAS-SU-26872); Gekkota: (b) the eublepharid *Coleonyx elegans* (UF-Herp-11258); (c) the pygopod *Lialis buronsis* (UF-Herp-43419 2). **Scinciformata:** (d) the gerrhosaurid *Gerrhosaurus flavigularis* (UF-Herp-63112); (e) the scincids *Plestiodon reynaldsi* (UF-Herp-14628-1), and f, *Scincella lateralis* (UF-Herp-189710). **Laterata:** (g) the gymnophthalmid *Gymnophthalmus speciosus* (UF-Herp-188822); (h) the teiid *Ameiva ameiva*; (i) the lacertid *Lacerta agilis* (UF-Herp-91747); and (j) the amphisbaenian *Amphisbaena manni* (UF-Herp-66308)

The Gekkotan Brain In gekkotans, the hindbrain is organized in a very straight fashion, leaving an ampler space for the cerebellum; in the two gekkotans illustrated here (Fig. 5.11b–c), the brain doesn't occupy the entire endocranial space of the braincase proper (although this is seen in extremely modified forms such as *Sphaerodactylus* (Perez-Martinez and Leal 2021)). The olfactory tracts become narrowed in both gekkotans, being transformed into two stalks along the frontal bone. This is clearly an effect of the interorbital constriction, influenced by the large size of the eye. In gekkotans the braincase does not extend anteriorly to the level of the frontal or the anterior border of the parietals (except in some *Aprasia* and *Ophidiocephalus*), therefore, the osseous ventral support ends at the level of the pituitary. In both gekkotans, the lateral closure of the braincase reaches the level of the optic tectum by an anterior extension of the crista alaris. The trigeminal ganglion is located more medially in the braincase than in *Dibamus*, being just outside of the foramen prootico in *Coleonyx*, and at the incisura prootica in *Lialis*.

The Scinciformatan Brain In scinciformatans (Fig. 5.11d–f), we see the same contrasting pattern between a limbed form such as *Gerrhosaurus flavigularis*, compared to a limb reduced, body elongated form, such as the sand swimmer *Plestiodon reynoldsi*. In the limbed form, the eyes are prominent, causing a constriction of the olfactory tracts at the interorbital area along the frontal bone, just as in gekkotans, although in the gekkotan *Lialis* which is also limb reduced and body elongated, the eyes are not reduced with the constriction also present. In *Lialis*, the lack of eye reduction is due to their terrestrial habitat preferences and foraging activities as predators. Despite the similar wedge shaped brain in both *Plestiodon* and *Dibamus*, there are still differences, such as a flat dorsal surface of the brain and a wider braincase space for the cerebellum in the former compared to the latter. As a comparison, in the limbed *Scincella lateralis*, the braincase proper is proportionally larger than in *Gerrhosaurus flavigularis*, creating more space to fit a larger brain as it has been demonstrated for geckos (Perez-Martinez and Leal 2021).

The Lateratan Brain In lateratans the brain exhibits a great variation, even though the dorsal surface of the brain is usually flat (as in *Plestiodon*) and the brain tends to be wedge shaped (Fig. 5.11g–j). However, in larger forms such as *Ameiva*, the olfactory tracts are constricted along the interorbital section of the frontal, preventing the wedge shape of the forebrain. On the other hand, even in small lateratans such as *Gymnophthalmus*, the eye socket medial wall is marked onto the lateral sides of the olfactory tracts without constricting it. In *Gymnophthalmus* the eyes are relatively large, where the lack of constriction of the olfactory tract can be inferred by the position of the orbits. Another noticeable variation in *Ameiva* is the position of the cerebral hemispheres, almost completely covering the optic tectum, placing the cerebral hemisphere/ optic tectum fissure into a nearly horizontal orientation. The braincase proper is also shortened in *Ameiva*, leaving the optic tectum completely outside the bony enclosure. The extremely modified brain of *Amphisbaena*, has the most wedge shaped among the species illustrated. The *Amphisbaena* brain is similar to *Dibamus*, although the transition from the cerebral hemispheres to the olfactory

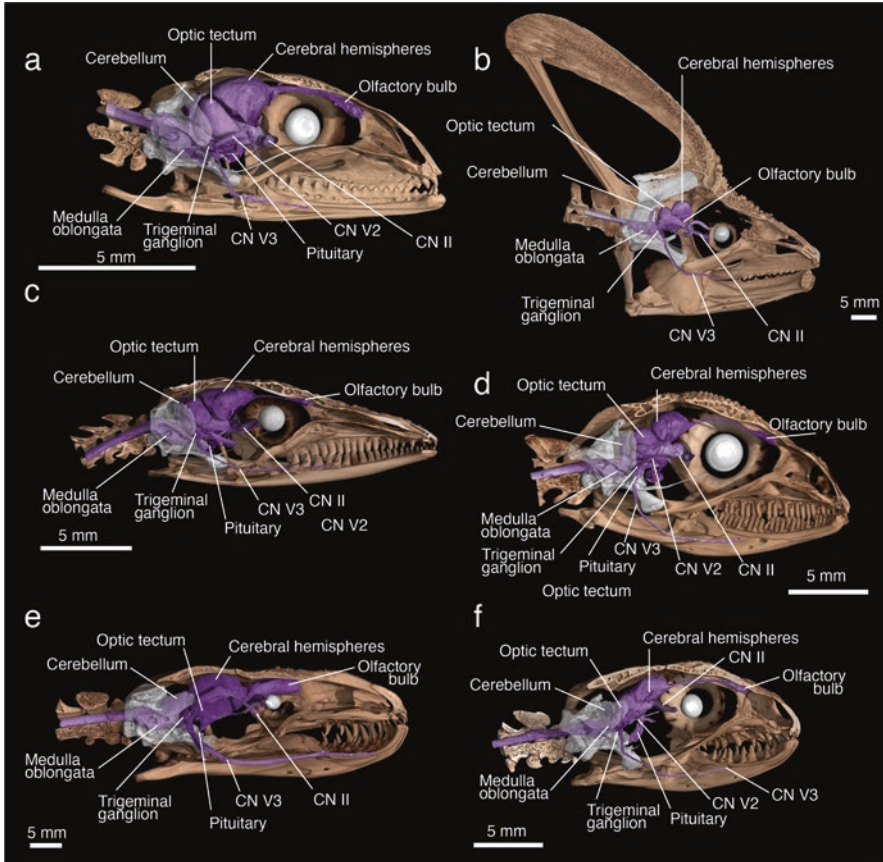


Fig. 5.12 Sagittal cutaway of the brain *in situ* based on diceCT specimens representatives of Toxicofera: (a) the agamid *Agama agama* (UF-Herp-180711); (b) the chamaeleonid (UF-Herp-191369); (c) the dactyloid *Anolis carolinensis* (UF-Herp-102367); (d) the hoplocercid *Enyalioides oshaugnessy* (UF-Herp-191439); (e) the helodermatid *Heloderma horridum* (UF-Herp-42033); and (f) the shinisaurid *Shinosaurus crocodilurus* (UF-Herp-45615). The region of the braincase proper that covers the brain was rendered as transparent to indicate the spatial position of the brain within the endocranial cavity

lobe is more gradual in *Amphisbaena*. Both *Dibamus* and *Amphisbaena* show some trend towards the reduction of the cerebellum, in part due to the sigmoidal shape of the medulla oblongata.

The Toxicoferan Brain The brain in toxicoferans is highly variable (Fig. 5.12 and 5.13). The olfactory tracts are very reduced in Iguanians (Fig. 5.12a–d), which is correlated with their reduced vomeronasal organ. Chameleons show the extreme of variation, with a very reduced brain, and almost nonexistent olfactory bulbs. The olfactory bulb is more developed in toxicoferans that rely more on chemoreception (e.g. anguimorphs and snakes).

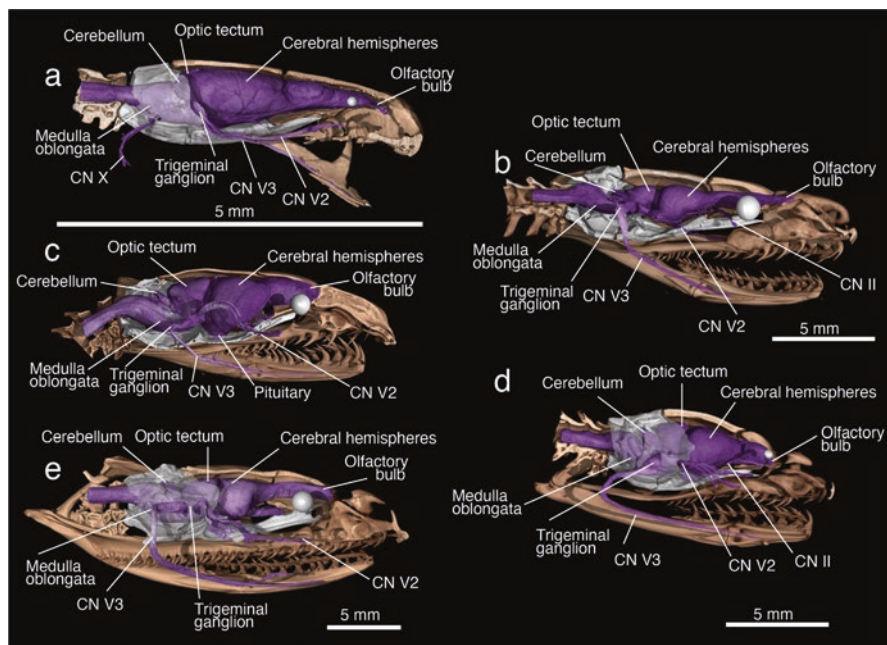


Fig. 5.13 Sagittal cutaway of the brain *in situ* based on diceCT specimens representatives of Serpentes: (a) the typhlopid *Indotyphlops braminus* (UF-Herp-29433); (b) the tropidophiid *Tropidophus haetianus* (UF-Herp-59679); (c) the boid *Eryx conicus* (UF-Herp-66735); (d) the acrochordid *Acrochordus granulatus* (UF-Herp-87078); (e) the colubrid *Nerodia sipedon* (UF-Herp-177819). The region of the braincase proper that covers the brain was rendered as transparent to indicate the spatial in position of the brain within the endocranial cavity

Endocranial Casts in Lizards

The only cranial endocasts of living lizards were made for varanid species by Allemand (2017). In those, the distinction between the olfactory bulbs and the olfactory tracts is difficult to establish, and the length of the olfactory structure (olfactory bulbs and tracts) is about two thirds of the endocast. Although all lizards share a basic pattern of brain organization, the morphological variation is associated with changes in the length and curvature of both olfactory tracts and medulla oblongata, and the arrangement and relative development of cerebral hemispheres, optic tectum, and cerebellum (Macri et al. 2019). This morphological brain divergence between species has been related not only to morphology, but to differences in ecology and behavior. For example, in diurnal lizards the optic tectum is larger, whereas the size of the cerebellum relates to the type of locomotion, being larger in quadrupedal lizards and smaller in limbless ones (Hoops et al. 2018; and references therein). Also, quadrupedal lizards exhibit thin and elongated olfactory tracts and bulbs (except for two species of chameleons with stunted olfactory tracts), and antero-posteriorly compressed and laterally expanded cerebral hemispheres (Macri et al. 2019).

Brain Morphology of Snakes

The anatomy of the snake brain is relatively simple, with its elements (or regions) disposed linearly. In dorsal view, the lobes are consecutive and have a decreasing size, whereas in lateral view they are located one behind another, except for the anterior part of the hindbrain that is ventral to the midbrain. Snakes are less different among themselves than lizards, having a brain with laterally compressed optic tectum and compact forebrain showing stout olfactory bulbs and tracts, as well as ventro-laterally expanded cerebral hemispheres, being the derived Caenophidia the most telencephalized clade within snakes (Platel 1975; Macri et al. 2019). Blindsnakes (Fig. 5.13a–e) show a notable reduction of the optic tectum, with a brain dominated by the cerebral hemispheres. Although blindsnakes develop a similar wedge shaped brain as in other head first burrowers (e.g. amphisbaenians, dibamids), in other groups the optic tectum is more prominent.

Although compared to other lepidosaurs the brain of living snakes occupies most of the endocranial space, the endocranial cavity can still have small empty spaces (subdural and epidural spaces) between the bones and the brain (Wyneken 2007). As a result, the endocranial cavity of snakes offers a faithful copy of the surface of the brain, similar to that obtained in mammals, providing more accurate information about their sensory abilities (Starck 1979; Nieuwenhuys 1998; Olori 2010; Olori and Bell 2012; Allemand et al. 2017). For example, studies on the main olfactory path and vomeronasal system suggest that snakes live in an olfactory world, as the olfactory system constitutes a major part of the brain (Güntürkün et al. 2017; and references therein).

Recent works focusing on the brain-to-endocranial cavity relationship in living snakes are a useful comparative tool for paleoneurology because they allow to determine how closely the soft tissues are reflected in an endocast. In the snake cranial endocast there are well developed olfactory bulbs separated medially by a longitudinal groove, cerebral hemispheres that comprise the widest region of the endocast (exhibiting sometimes an interhemispheric fissure, and often not differentiated posteriorly from the optic tectum), the pituitary is a small bulge on the ventral side of the endocast, and the medulla oblongata narrows lateromedially at the inner ear region (the cerebellum is not observed in the endocast). The venous system may obscure some regions, particularly the hindbrain. Although the relationship between the brain and the endocast is currently being tested in living snakes, the link between sensory abilities and endocasts has not been investigated in detail (Allemand et al. 2017).

5.5 Paleoneurology

5.5.1 Sources of Data for Paleoneurology and Limitation for the Study

The paleoneurological studies in reptiles have a long history. Early studies started at the end of 1800s with the discovery of natural endocasts and/or the confection of physical artificial endocasts of certain taxa (pterosaurs, dinosaurs, and crocodylians). More recently, digital cranial endocasts based on non-invasive techniques such as Computed Tomography (CT) are now widely used in the field of comparative neuroanatomy, providing a useful tool for the approximation of the morphology of the brain and associated soft tissues.

Considering the caveat of different size between the hindbrain and forebrain in relation with the proportions of the endocast (Watanabe et al. 2019), the latter offers an approximation to the overall shape of the brain in extinct forms. Osteological correlations of brain tissues and endocranial vascular elements are the main sources of data for paleoneurological studies, together with a knowledge of the gross anatomy of living related forms. Under the lack of such studies in many representatives of Lepidosauria, information from braincase descriptions, and particularly of the endocranial cavity, may provide useful data. Particularly useful are impressions left on the ventral surface of the skull roof (commonly found isolated in the fossil record) and the floor of the endocranial cavity (basicranium, also commonly found isolated), and the preserved cranial nerve foramina. Thus, impressions of the olfactory tracts, olfactory bulbs and cerebral hemispheres may be found on the ventral side of frontals and parietals, whereas impressions of cerebellum, medulla oblongata and roots of CNs V-XII can be observed in the remaining ossified regions of the braincase. The osteological correlates are the base-line to work in the field of paleoneurology. All available information about the non-preserved brains relies then on surface information provided by the endocasts. Furthermore, differential development of brain regions, insights on senses, behavior, and lifestyle can be gained through anatomical comparisons with extant relatives, and using methods of inference, such as the Extant Phylogenetic Bracketing (Witmer 1995).

Limitations in the Study of Endocranial Casts One limitation is that in many lepidosaurs, large part of the braincase (the anterior region) remains cartilaginous (Starck 1979), thus preventing the complete cast of the endocranial cavity because the physical boundaries are difficult to determine, except in snakes, amphisbaenians, and some fossorial forms which have completely ossified braincases. The available information on brain morphology relies on surface information provided by the cranial endocasts. But, how reliable an endocast can be? In terms of brain size, there are striking differences among vertebrates. In average, reptiles have relative brain sizes 6-10 times smaller than in birds and mammals, ranging from 0.03 g in small lizards, more than 0.5 g in *Sphenodon*, and 1.1 g in varanid species (Northcutt 2002, 2013; Güntürkün et al. 2017). The brain size alone may not be

enough data to predict cognitive capabilities of a given taxon, but the analysis of this measure allows insights in the evolution of the nervous system through comparative anatomy studies, and estimates of Encephalization Quotient (a measure of the “intelligence” of the animal based on the ratio between brain and body size; Jerison 1973), among others. However, one of the main problems facing the study of endocranial casts is that in many reptiles the brain does not completely fill the endocranial cavity. The differential relationship between the brain and the occupied space within the endocranial cavity was named brain-to-endocranial cavity index (BEC) by Balanoff et al. (2016). This index varies among vertebrates with direct implications for the study of endocasts, where high values indicate endocasts that reflect brain volume and morphology with higher fidelity, while low values are associated with more cylindrical endocasts with less resemblance to the actual brain (Hopson 1979; Witmer et al. 2008; Balanoff and Bever 2020).

Cranial Endocast and the Brain-to-Endocranial Ratio in Living Forms In the field of paleoneurology, it has been historically assumed by specialists on different groups that in most adult non-avian sauropsids (except snakes, amphisbaenians and some other head first burrower lizards) the brains did not fill the endocranial cavity (e.g. Hopson 1979; Starck 1979; Nieuwenhuys 1998). This hypothesis was based on early studies of two living taxa, *Sphenodon* and *Iguana*, which exhibited a 50% filling (or a 0.5 BEC index) of the endocranial cavity (Dendy 1910; Allemand et al. 2017). However, more recent comparative studies on extant squamates showed that living lizards exhibit a wider range of brain-to-endocranial cavity proportions than previously thought (Hurlburt et al. 2013; Kim and Evans 2014; Allemand et al. 2017; Macri et al. 2019). The lowest BEC index reported was found in *Gekko gekko* (0.35), whereas the brain nearly fills the endocranial cavity in *Callopiastes maculatus* (0.97), suggesting that in some squamates the cranial endocasts may approximately reflect the surface morphology of the brain with certain degree of accuracy (Allemand et al. 2017). These estimates have to be considered carefully, for example, in archosaurs it has been demonstrated that the size of certain regions of the brain (e.g. hindbrain) are considerably smaller than the potential braincase space, therefore this has to be considered in paleoneurological studies (Watanabe et al. 2019). It has also been noted that the differences in BEC index may be affected by size, being higher in extremely miniaturized species of geckos when compared with non-miniaturized species (Perez-Martinez and Leal 2021).

Fortunately for paleontologists, cranial endocasts of living snakes have been made and analyzed comparatively (e.g. Olori 2010; Allemand et al. 2017). These cranial endocasts, performed in a wide number of living snakes (43 species), indicate that snake endocasts show size variability in olfactory bulb, optic tectum, and pituitary gland (Allemand 2017; Allemand et al. 2017). The general snake cranial endocast morphology recognizes the forebrain (olfactory bulbs, olfactory tracts, cerebral hemispheres, and pituitary gland), midbrain (optic tectum), and hindbrain (medulla oblongata). There is a wide range of cranial endocast shapes (characterized by different relative proportions of visible structures) from stout to elongated

and gracile, or elongate and wide cranial endocasts, which are associated with the different niches occupied by the group. For example, ecological trends related to certain snake cranial endocast morphologies include reduced optic tectum and pituitary gland in fossorial species, cerebral hemispheres poorly projected laterally in both marine and fossorial species, and well developed cerebral hemispheres and optic tectum in arboreal and terrestrial species (Allemand et al. 2017).

Although studies on brain endocasts of living lepidosaurs are yet rare, CT scans and Magnetic Resonance Imaging have been used to visualize soft tissues (brain, inner ear, blood vessels, early ontogenetic stages) of several lizard and snake species (e.g. Anderson et al. 2000; Porter and Witmer 2015; Hoops et al. 2018; Macri et al. 2019; Strong et al. 2020). Everything points to the fact that in the absence of early paleoneurology studies in most extinct lepidosaurian groups, the future of the paleoneurology of this group will be highly improved by the use of CT scans and particularly micro-CT scans. Another technique involves the use of iodine as a contrast reagent combined with CT scans of diceCT. This technique allows the visualization of brains in situ, which here we use to demonstrate the high morphological disparity among squamates. In this chapter we show several examples of lepidosaur brains (Figs. 5.11, 5.12 and 5.13), but this variation needs to be assessed elsewhere in more detail. Just looking at the few forms illustrated in this chapter indicates that this is a promising field in anatomical and systematic studies.

5.5.2 *Paleoneurology of Snakes and Mosasauroids: Cranial Endocasts and Other Sources of Information*

Paleoneuroanatomy of *Dinilysia patagonica*

The specimen MLP 79-II-27-1 (Fig. 5.14a–c) corresponds to a partial skull that preserves a natural cranial endocast, described in detail by Triviño et al. (2018). The fractured skull bones reveal part of the cerebral hemispheres and optic lobes dorsally, and the pituitary and part of the medulla oblongata ventrally.

The posterior region of the cerebral hemispheres is poorly expanded laterally, and there is no visible fissura interhemispherica to medially divide them. Posteromedially, there are paired median protuberances identified here as the optic lobes, whereas the cerebellum remained covered by bone (contra Triviño et al. 2018). Ventrally, the only observed structure of the forebrain is the pituitary, a relatively large and oval protuberance, ventrally aligned to the trigeminal nerve. The anterior body of this gland is covered by vascular vessels of small diameter, whereas larger diameter cerebral branches of the internal carotid artery are observed posteriorly, entering the pituitary fossa. At the anterior region of the hindbrain, the vestibular eminences are large and strongly protrude into the endocranial cavity, reaching the midline and practically excluding the dorsal surface of the endocast.

Cranial Nerves The trigeminal ganglion is external and the nerve is composed by four branches with motor and sensitive components: the ophthalmic branch (CN V₁)

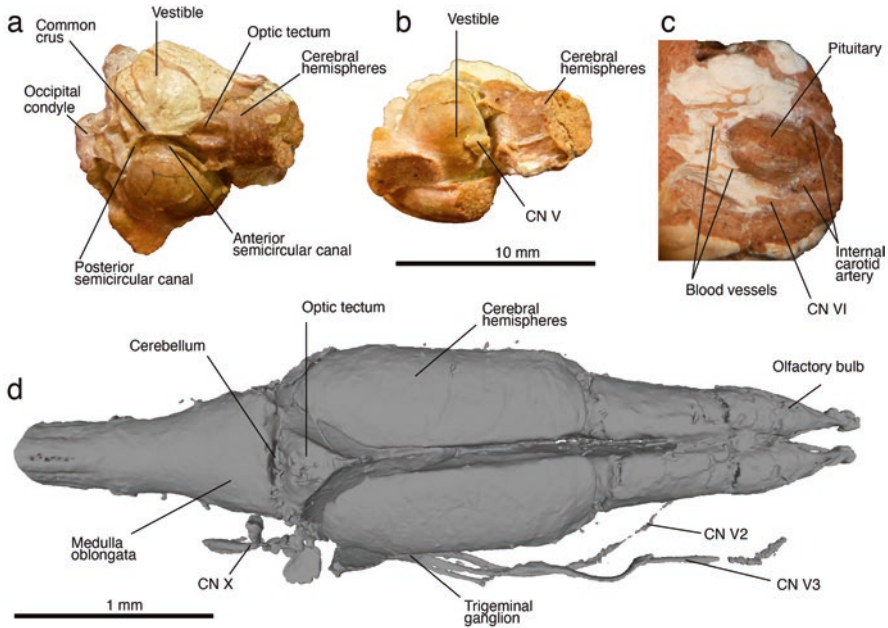


Fig. 5.14 Natural cranial endocast of *Dinilyisia patagonica* (MLP 79-II-27-1) in dorsal (a), right lateral (b) views. (c), detail of pituitary gland in ventral views. (d), dorsal view of the brain of the blind snake *Indotyphlops braminus* (UF-Herp-29433) showing comparable structures to *Dinilyisia*

that runs towards the anterior part of the skull passing above the eye; the maxillary branch (CN V₂) that runs anteriorly through the superior mandible innervating the skin, teeth and thermoreceptor structures (as in *Boidae* and *Viperidae*); the mandibular branch (CN V₃) that descends from the ganglion to the inferior mandible innervating the abductor musculature; and lastly the pterygoid branch (CN V₄, only described by Auen and Langebartel 1977 as a motor component innervating the muscles of the upper jaw) that exits the ganglion ventrally to enter –together with the palatine branch of the facial nerve–to the posterior foramen of the vidian canal. The abducens nerve (CN VI) runs near the pituitary, and the facial nerve (CN VII) has a dorsal branch (hyomandibular, CN VII_y) that runs lateroventrally to the external side of the cast, and a ventral branch (CN VII_p) that runs towards the posterior foramen of the vidian canal innervating the ventral region of the mandible (gustative glands). From the medulla oblongata emerge the roots of the CNs V-VII and the posterior CNs IX, X and XII (see Triviño et al. 2018).

Blood Vessels The endocranial cast of *D. patagonica* also preserves casts of the vasculature. The blood vessels run along the dorsal surface of the brain, along the midline (dorsal longitudinal sinus) and splits into posterior cerebral veins, which leave the braincase through the jugular foramen. Above the inner ear (vestibule) there are small canals that run towards the median region of the brain. Such vessels converge into the dorsal longitudinal venous sinus. The internal carotid artery

reaches the pituitary. The blood vessels related to the ventral circulatory system are behind the pituitary gland. The cast of the internal carotid arteries are confluent with the most anterior part of the pituitary gland.

Burrowing or Not? The lifestyle of *D. patagonica* has been a subject of debate since its discovery (e.g. Albino and Caldwell 2003; Triviño et al. 2018; Palci et al. 2017). Endocranial traits such as poorly developed optic lobes (yet visible in the endocast) and markedly expanded vestibule in the inner ear, plus the relative large size of the skull, suggest a fossorial or semifossorial mode of life for this snake. This, meaning *Dinilysia* was partly a surface-active snake that spent some time below non-consolidate ground. Although the morphology of the inner ear (markedly expanded vestibule and slender semicircular canals) is present in extreme living fossorial snakes (Yi and Norell 2015), it has been found also in subfossorial and semi-aquatic snakes (Palci et al. 2017). Recent integrative analysis of the relationship between the sensory ecology and endocranial shape in living snakes have demonstrated that size is the main driver of endocranial shape, and that endocranial morphology alone is not sufficient to predict activity period without a phylogenetic context (Segall et al. 2021).

Paleoneuroanatomy of Mosasauroida

Almost all formal studies on paleoneurology of mosasauroids have been made for Plioplatecarpinae and Tethysaurinae taxa (Georgi and Sipla 2008; Cuthbertson et al. 2015; Allemand 2017; Yi and Norell 2018). Most of the data of mosasauroid endocasts refer to derived fully aquatic mosasauroids, such as *Clidastes*, *Platecarpus*, and *Plioplatecarpus*, with the exception of *Tethysaurus nopcsai*, considered basal within “Russellosaurina” (Bardet et al. 2003; Houssaye and Bardet 2013). Therefore, there is no information on how the neuroanatomy varies phylogenetically at the level of Mosasauroida (mosasaurids + aigialosaurids) nor Mosasauria (Mosasauroida + dolichosaurs).

Cranial endocasts are known for *Platecarpus*, *Clidastes* and *Tethysaurus* (Camp 1942; Allemand 2017). Different regions of the brain are nearly horizontally aligned, although a slight curvature gives a soft S-shape to the endocast in lateral view (Fig. 5.15). The olfactory bulbs are elongated, oval and poorly divergent from the midline, whereas the olfactory tract is markedly narrow and long. In the basal mosasauroid *Tethysaurus nopcsai* and in *Platecarpus* the olfactory bulbs are almost the same length as the olfactory tracts, whereas in *Clidastes* the olfactory bulbs are longer than the olfactory tracts. As noticed by Allemand (2017), the olfactory bulbs and tracts in *Tethysaurus* are similar in length to the mosasaurine *Clidastes* figured by Camp (1942), while in *Platecarpus* they seem to be relatively shorter. Impressions of the olfactory bulbs, olfactory tracts and cerebrum are in general visible in the ventral surface of the isolated frontals, although there is no clear delimitation for the cerebrum (Russell 1967 contra Camp’s statement, 1942). The cerebral hemispheres are laterally expanded; however, there is not a clear differentiation from the

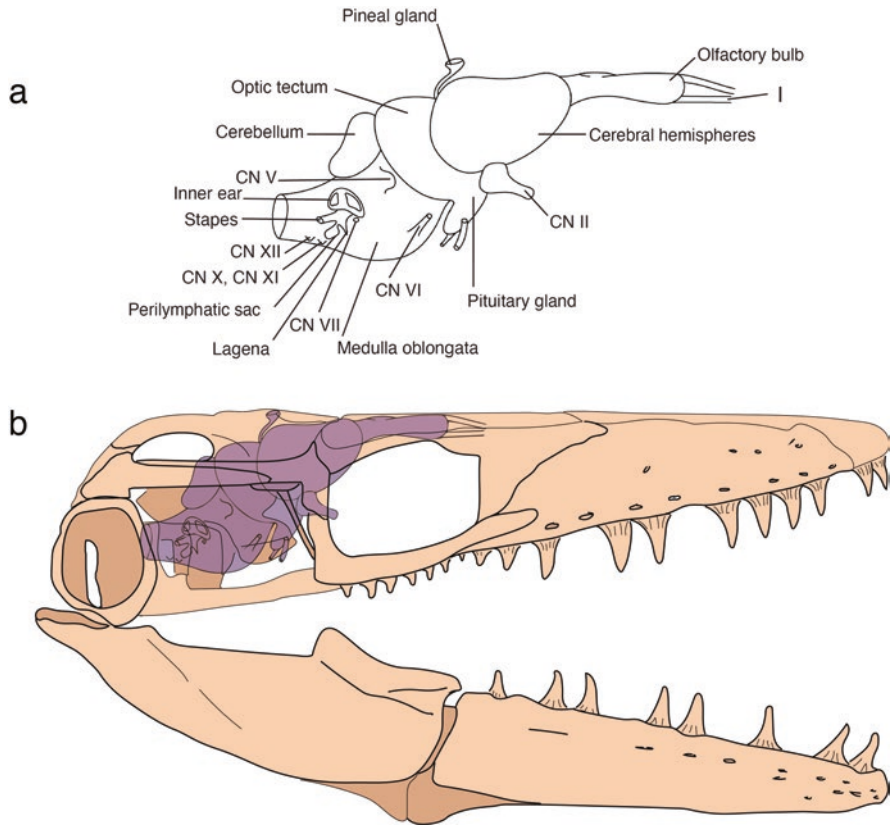


Fig. 5.15 Mosasaur brain. (a) Intertreted mosasaur brain anatomy based on endocasts; (b) *Platecarpus ictericus* showing the in situ brain. Brain and skull illustrations based on Russell (1967) and the estimated endocranial space modified from M. Everhart's Ocean of Kansas Paleontology website: <http://oceansofkansas.com/>

cerebellum. The optic lobes are ventrally displaced and can be observed at the level of the pituitary gland in lateral view. In *Tethysaurus*, the pituitary gland is well developed compared to *Platecarpus* (Camp 1942; Allemand 2017). A rounded protuberance on the dorsal surface of the endocast at the level of the parietal, corresponds to the cast of the pineal foramen. In *Tethysaurus* the pineal organ is relatively small based on the size of the parietal foramen, as in *Clidastes*, *Tylosaurus*, and *Mosasaurus* (Allemand 2017). However, Halisaurinae and Plioplatecarpinae species present a larger parietal foramen (Bardet et al. 2005; Konishi and Caldwell 2011; Páramo-Fonseca 2013; Konishi et al. 2015), suggesting the presence of a relatively larger pineal organ (Fig. 5.15). The position and size of the pineal foramen varies among Mosasauoidea. It is moderate in size and located at the midline of the parietal table in the yaguarasaurines (Páramo-Fonseca 2000; Polcyn and Bell Jr 2005), and large and bounded by the parietal in Halisaurinae and in *Plioplatecarpus*

houzeaui (Bardet et al. 2005; Páramo-Fonseca 2013; Konishi et al. 2015). Whereas in the tylosaurine *Tylosaurus proriger* the foramen can be fully located in the parietal or at the frontoparietal suture, being a variable character at intraspecific level (Jiménez-Huidobro and Caldwell 2016). The medulla oblongata is short and the dorsal surface is medially constricted indicating the development of the medullary eminence.

The cranial nerves and blood vessels were described by Russell (1967), Rieppel and Zaher (2000), Cuthbertson et al. (2015), and Allemand (2017). In the plioplatecarpine *Platecarpus* sp. and *Plioplatecarpus peckensis*, the basisphenoid bears a groove dorsal to the basiptyergoid process that corresponds to the vidian canal, which runs anteroposteriorly indicating the path of the internal carotid artery (Russell 1967; Cuthbertson et al. 2015). In *P. peckensis*, there is a pair of foramina and a single foramen in the floor of the dorsum sellae that bifurcates ventral within the vidian canal, more likely to transmit the cerebral branch of the carotid artery to the brain cavity into the ventral region of the orbit (Russell 1967; Cuthbertson et al. 2015; Allemand 2017). Posteriorly, a pair of foramina appear anterior to the foramen magnum, identified as the basilar artery, which would run along the basioccipital and basisphenoid (Russell 1967; Cuthbertson et al. 2015).

The passages for the optic nerve are large in diameter, long and anteriorly divergent. Endocranially, the foramina lateral to the dorsum sellae -as shown in *P. peckensis* and a reconstruction of *Clidastes* -, correspond to the abducens nerve that projects anteriorly and exits through foramina within the pituitary fossa (Russell 1967; Cuthbertson et al. 2015). There is a single foramen for the facial nerve, and two foramina for the vestibulocochlear nerve, as in *Tethysaurus nopcsai*. The opisthotic forms the posterior margin of the fenestra vestibuli, and ventral to it, a large foramen rotundum carries the perilymphatic sac (Bahl 1937; Russell 1967; Cuthbertson et al. 2015). The metotic foramen serves as a path for the vagus and accessory nerves (Allemand 2017), contrary to Cuthbertson et al. (2015) and Rieppel and Zaher (2000), who suggested that the foramen houses both glossopharyngeal and vagus nerves. According to Allemand (2017), the glossopharyngeal nerve is located posterior to the inner ear region of the endocast. Three posterior foramina have been identified for transmitting branches of the hypoglossal nerve.

Inner Ear of Extant and Extinct Lepidosaurians

The lepidosaurian inner ear consists of bony and membranous labyrinths differentiated in two main anatomically and functionally regions: the vestibular and lagenar systems. The vestibular system consists of three semicircular ducts -with the associate ampullae- that detect angular acceleration, and the vestibule (containing the sacule, utricle, and otolith organs) that detects linear accelerations (e.g. Retzius 1881). The lagena is in charge of sound perception, innervated by branches of the stato-acoustic nerve that project from the lagena to the auditory tectum. In general, reptiles hear in low frequencies being capable of detecting seismic vibrations (Liem et al. 2000). Vibrations of the footplate are transmitted to the sensory epithelium via

a fluid system consisting on the perilymphatic cistern juxtaposed to the oval window, the perilymphatic duct, the perilymphatic sac, and the perilymphatic diverticulum in contact with the medial surface of the basilar membrane (Peterson 1966). Osteological correlates comprise external features of the otic capsule (size of the fenestra vestibule, position and size of the periotic foramen, presence of crests that may indicate the extent of a lateral compensatory window), and the endosseous labyrinth formed by the lagena ventrally, and the vestibular apparatus dorsally (Evans 2016).

Variation of Inner Ear Morphology Among Lepidosauers The inner ear of *Sphenodon punctatus* was described and illustrated by Wyeth (1920). The three semicircular canals are slender and subtriangular, with an **asc** slightly larger than the **psc** and well differentiated anterior and posterior ampullae. The vestibule (sacculus) is not expanded. The vestibular apparatus in *S. punctatus* resembles that of other reptiles, although the lagena resembles that of turtles, with an oval basilar membrane, -a trait considered primitive (Schmidt 1964)-, with the auditory papilla located near its medial edge (having 225 hair cells in each inner ear). The fenestra pseudorotunda is absent, and the fluids inside the lagena mobilize using a reentrant fluid circuit, as in turtles, snakes, and amphisbaenians (Gans and Wever 1976). The aerial and vibratory sensitivity functions indicate a range of good sensitivity in the low frequencies for this group.

The general squamate inner ear is characterized by markedly low semicircular canals, short crus commune, somehow swollen ampullae, relatively large vestibule (sacculum), large oval window, and short lagena. The comparative gross anatomy of the lizard inner ear has been largely studied (Schmidt 1964 and references therein). The labyrinth is generally a conservative structure with the sacculum and the lagena showing the greatest variation among the studied families (e.g. Schmidt 1964; Boistel et al. 2011; Evans 2016; Palci et al. 2017). Compared to other squamates, snakes have shallower and less rounded semicircular canals (Boistel et al. 2011). The statistical analysis by Yi and Norell (2015) suggested that large and spherical vestibuli correspond to burrowing forms, including the extinct snake *Dinilysia*. However, a later analysis suggested that within squamates, in ecologically generalized (terrestrial) forms, the three semicircular canals are similar in size and the sacculus is small, in arboreal forms the anterior semicircular canal is larger, and aquatic forms tend to resemble generalist forms (Palci et al. 2017). Interestingly, although the small sacculus is present in generalized and aquatic forms, a large spherical sacculus is not unique to fossorial squamates, being present in some semi-aquatic forms as well. Additionally, some typical borrowers such as scolecophidian snakes, lack an enlarged sacculus (Palci et al. 2017). This implies a new interpretation of the life-style of *Dinilysia*, considered by some authors as a borrowing snake (e.g. Yi and Norell 2015). Another analysis, suggests that the size of the semicircular canals does not differ either among squamates with different life-styles (Boistel et al. 2011), indicating a difficulty in associating certain labyrinth traits with ecological behaviors.

Among extinct snakes, the inner morphology is known in *Dinilyisia* from a natural endocast (Triviño et al. 2018), and in *Yurlunggur* and *Wonambi* based on CT scans (Palci et al. 2017, 2018). The vestibular apparatus of *Dinilyisia* is characterized by a markedly enlarged spherical vestibule, surrounded by markedly thin and delicate semicircular canals. The inner ear of *Yurlunggur* is complete and exhibits an enlarged vestibule and relatively robust semicircular canals than those observed in *Dinilyisia*. The fenestra ovalis is circular and large while the lagena is short, a morphology that resembles that of both semiaquatic and semifossorial snakes (Palci et al. 2017, 2018). In turn, the inner ear of *Wonambi* is incomplete and paleoecological inferences are difficult to make. The preserved anatomy, however, differs from that of *Yurlunggur* having a relatively smaller vestibule and fenestra ovalis, which suggests a more generalistic ecology for this taxon (Palci et al. 2018). *Dinilyisia*, on the other hand, exhibits a vestibular morphology characterized by a notably enlarged spherical sacculus that is highly similar to that of some living burrowing squamates. Semi aquatic snakes (*Myron*) and some fossorial forms (*Xenopeltis*, *Cylindrophis*, *Teretrurus*) tend to have relatively larger sacculus. However, not all fossorial or semifossorial snakes have an expanded sacculus, and thus such morphology cannot be attributed to an exclusively burrowing ecology (Palci et al. 2017 contra Yi and Norell 2015). The large fenestra ovalis is present in the generalist snake *Naja siamensis*, but absent in scolecophidian snakes (burrowers).

As discussed by Evans (2016) there has been relatively little work on mosasauroid inner ear, and most of them correspond to conference abstracts (Caldwell et al. 2007; Polcyn 2008, 2010; Yi et al. 2012) rather than peer reviewed publications. Therefore, cranial elements will be used to discuss the possible paleoneurology of mosasauroids in a comparative approach. Russell (1967) described the inner ear of this group as similar to that of *Varanus*, although recent data based on CT scans showed that is not the case, as derived mosasauroids have slender and rounded semicircular canals compared to other squamates (Georgi 2008; Cuthbertson et al. 2015; Yi and Norell 2018). In *Platecarpus* and *Tylosaurus nepaeolicus*, the **asc** is oval, shorter than in *Varanus*; however, there is no statistical support for the reduced size of the otic region (Yi and Norell 2018). The same condition is found in *Tethysaurus nopcsai* (Allemand 2017) and *Plioplatecarpus peckensis* (Cuthbertson et al. 2015), where their **asc** is shorter than in *Varanus*. In *P. peckensis* the semicircular canals are strongly arched. The posterior ampulla in both *Tylosaurus* and *Tethysaurus* is almost leveled with the **lsc**, whereas in *Platecarpus*, unlikely, they are in different planes (Georgi 2008; Georgi and Sipla 2008; Allemand 2017). The ampulla of *Tethysaurus* is poorly expanded compared to other squamates. In *P. peckensis* the lagena appears to be relatively long (Cuthbertson et al. 2015), while is relatively shorter in *Tethysaurus* (Allemand 2017). Unfortunately, there is no available data on the inner ear of neither agalosaurids nor dolichosaurids.

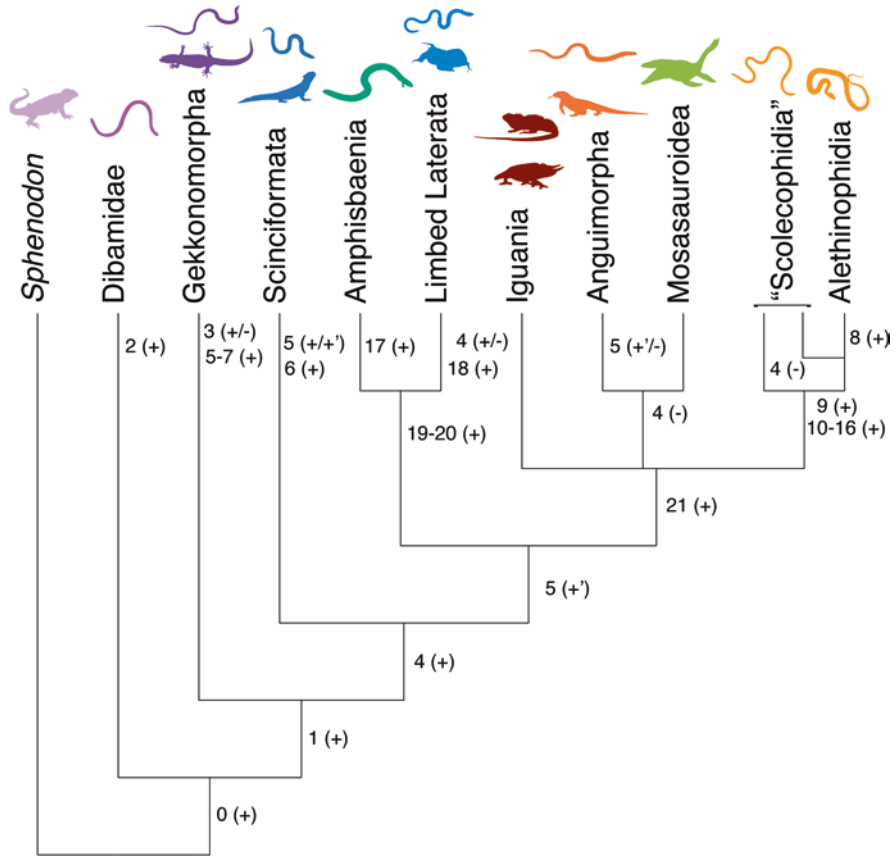


Fig. 5.16 Distribution of some braincase characters in a simplified lepidosaur phylogeny. Characters included are the less homoplastic. (0) Closed canal for the carotid artery and palatine nerve. (1) Divided metoptic fissure. (2) Lack of optic canal. (3) Foramen prootico. (4) Processus ascendens. (5) Orbitosphenoid: (+) cartilaginous, (+') ossified. (6) Crista prootica large. (7) Divided MARST. (8) Ophidiosphenoid. (9) Paired supraoccipitals. (10) Frontal and parietal constricts the parabasisphenoid, enclosing the braincase. (11) Supratemporal expanded on the lateral surface of the otoccipital. (12) Crista circumfenestralis. (13) Reduction of loss of the paroccipital process. (14) Loss of the synovial joint between the basiptyergoid process and the pterygoid. (15) Medial parietal pillars projected medially in the braincase. (16) Laterosphenoid. (17) Tabulosphenoid. (18) Orbitosphenoid bi or tri-radiated. (19) Relatively small basiptyergoid process. (20) parabasisphenoid rostrum with broad base. (21) Enlarged crista tuberalis, shifting the vagus foramen posteriorly. (+) indicates presence and (-) Absence of that character

5.6 Future Directions and Conclusions

Cranial endocasts provide an overview of the general morphology of the soft tissues and their relationship to the endocranial cavity. These anatomical data allow a better understanding on the possible ecological adaptations associated to determinate

neurological features, and provide insights on the senses, the behavior, and ultimately on the lifestyle of extinct taxa (Balanoff et al. 2016). In the particular case of the Lepidosauromorpha, the field of comparative neuroanatomy has benefited from the use of non-invasive techniques such as micro-CT scans, which are improving the study of braincase and endocranial cavities in fossil skulls (Fig. 5.16). There is also an expanding interest in digital data to visualize endocranial casts in both extinct and extant taxa (Balanoff et al. 2016). The available neuroanatomical information for extinct lepidosaurs is, however, quite poor. The braincase and neuroanatomical information reviewed here looks forward to providing a baseline tool for future paleoneurological studies. Up to day, few integrative studies have been made exploring multiple approaches to study brain evolution, the potential relationship between endocranial (brain) morphology and sensory-related ecology, locomotor specialization, etc. (e.g. Macri et al. 2019; Segall et al. 2021). There are yet important gaps regarding brain anatomy during the evolutionary history of lepidosauromorphs, and future investigations and research are needed to reach a better understanding and recognizing diverse endocranial arrangements, or in other words, which brain areas have evolved in each group, and what kind of specializations they reflect in terms of ecological niches, adaptations to different habitats, etc.

5.7 Conclusions

A low number of publications has been made on the paleoneurology of the clade Lepidosauromorpha. The dealing with brain endocasts of extant representatives of rhynchocephalians and squamates is poor, preventing further understanding of variability, insight on senses, behavior etc. As a result, the amount of paleoneurological data is yet limited to few non-closely related taxa, and there is a general lack of understanding of brain evolution and sensory perception (so far only hearing has been relatively more explored in this manner). Studies based on CT scans of the skull of extinct forms are still largely missing for Lepidosauromorpha as a whole, particularly the early forms. Non-invasive techniques, such as Micro-CT scan, are now widely used in the field of comparative neuroanatomy, allowing to visualize endocranial features that represent an amount of unexplored phylogenetic data (Balanoff et al. 2016; Allemand et al. 2017). As we have seen in this review, Micro-CT scans have been used recently to assess brain anatomy in living lepidosaurian taxa, and it is probably a matter of time for paleontologists to start using this technique to analyze well preserved braincases.

Acknowledgements The authors thank Dr. Evans for advice on identification of braincase structures; J. Gray for the DICECT scans, and M. Everhart from the Fort Hays Sternberg Museum for permissions to use a figure from the Oceans of Kansas Paleontology website. Funding: PICT-2020-SERIEA-01428 (to APC), Alexander von Humboldt Postdoctoral Fellowship (to PJH).

References

- Albino AM, Caldwell M (2003) Hábitos de vida de la serpiente cretácica *Dinilyisia patagonica* Woodward. *Ameghiniana* 40:407–414
- Albino A (2011) Evolution of Squamata reptiles in Patagonia based on the fossil record. *Biol J Linn Soc* 103:441–457
- Allemand R (2017) Endocranial microtomographic study of marine reptiles (Plesiosauria and Mosasauroida) from the Turonian (Late Cretaceous) of Morocco: palaeobiological and behavioral implications. Ph.D. Dissertation, Museum National d'Histoire Naturelle, Paris
- Allemand RR, Boistel G, Daghfous Z, Blanchet R, Cornette N, Bardet P, Vincent HA (2017) Comparative morphology of snake (Squamata) endocasts: evidence of phylogenetic and ecological signals. *J Anat* 231:849–868
- Anderson CL, Kabalka GW, Layne DG et al (2000) Non-invasive high field MRI brain imaging of the garter snake (*Tamnhophis sirtalis*). *Copeia* 1:265–269
- Apesteeguía S (2008) Esfenodontes (Reptilia, Lepidosauria) del Cretácico Superior de Patagonia: Anatomía y filogenia. Dissertation, Universidad Nacional de La Plata
- Apesteeguía S, Zaher H (2006) A Cretaceous terrestrial snake with robust hindlimbs and a sacrum. *Nature* 440:1037–1040
- Armstrong JA, Gamble HJ, Goldby F (1953) Observations on the olfactory apparatus and telencephalon of *Anolis*, a microsmatic lizard. *J Anat* 87:288–307
- Auen EL, Langebartel DA (1977) The cranial nerves of the colubrid snakes *Elaphe* and *Thamnophis*. *J Morphol* 154:205–222
- Bahl KN (1937) Skull of *Varanus* monitor. *Rec Ind Mus* 39:133–174
- Balanoff AM, Bever GS (2020) The role of endocasts in the study of brain evolution. In: Kaas J (ed) *Evolutionary neuroscience*. Elsevier, pp 29–49
- Balanoff AM, Bever GS (2017) The role of endocasts in the study of brain evolution. In: Kaas (ed) *Evolutionary Neuroscience*, Academic Press pp 29–49
- Balanoff AM, Bever GS, Colbert MW et al (2016) Best practices for digitally constructing endocranial casts: examples from birds and their dinosaurian relatives. *J Anat* 229:173e190
- Barbas-Henry HA (1988) The cranial nerves III–XII in the monitor lizard *Varanus exanthematicus*: a neuroanatomical tracing study. Free University Press, Amsterdam
- Bardet N, Suberbiola XP, Jalil NE (2003) A new mosasauroid (Squamata) from the Late Cretaceous (Turonian) of Morocco. *C R Palevol* 2:607–616
- Bardet N, Suberbiola XP, Iarochene M, Bouya B, Amaghaz M (2005) A new species of *Halisaurus* from the Late Cretaceous phosphates of Morocco, and the phylogenetical relationships of the Halisaurinae (Squamata: Mosasauridae). *Zool J Linn Soc* 143:447–472
- Bardet N, Falconnet J, Fischer V, Houssaye A, Jouve S, Pereda Suberbiola X, Pérez-García A, Rage JC, Vincent P (2014) Mesozoic marine reptile palaeobiogeography in response to drifting plates. *Gondwana Res* 26:869–887
- Bauer AM (1989) Extracranial endolymphatic sacs in *Eurydactyloides* (Reptilia: Gekkonidae), with comments on endolymphatic function in lizards in general. *J Herpetol* 23:172–175
- Bauer AM, Beach-Mehrotra M, Bermudez Y et al (2018) The tiny skull of the Peruvian gecko “*Pseudogonatodes barbouri*” (Gekkota: Sphaerodactylidae) obtained via a divide-and-conquer approach to morphological data acquisition. *S Am J Herpet* 13:102–116
- Bell GL Jr (1997) A phylogenetic revision of North American and adriatic Mosasauroida. In: Callaway JM, Nicholls EL (eds) *Ancient marine reptiles*. Academic Press, San Diego, pp 293–332
- Bell GL, Polcyn MJ (2005) *Dallasaurus turneri*, a new primitive mosasauroid from the Middle Turonian of Texas and comments on the phylogeny of Mosasauridae (Squamata). *Neth J Geosci* 84(3):177–194
- Bell CJ, Evans SE, Maisano JA (2003) The skull of the gymnophthalmid lizard *Neusticurus epleopus* (Reptilia: Squamata). *Zool J Linn Soc* 103:283–304

- Bellairs AA, Kamal AM (1981) The chondrocranium and the development of the skull in recent reptiles. In: Gans C (ed) *Biology of the reptilia*. Academic Press, New York
- Berman DS (1973) *Spathorhynchus fossorium*, a Middle Eocene amphisbaenian (Reptilia) from Wyoming. *Copeia* 1973:704–721
- Berman DS (1976) A new amphisbaenian (Reptilia: Amphisbaenia) from the Oligocene-Miocene John Day Formation, Oregon. *J Paleontol* 50:165–174
- Berman DS (1977) *Spathorhynchus natronicus*, a new species of rhineurid amphisbaenian (Reptilia) from the early Oligocene of Wyoming. *J Paleontol* 51:986–991
- Bever GS, Norell MA (2017) A new rhynchocephalian (Reptilia: Lepidosauria) from the Late Jurassic of Solnhofen (Germany) and the origin of the marine Pleurosauridae. *R Soc Open Sci* 4:170570
- Bever GS, Bell CJ, Maisano JA (2005) The ossified braincase and cephalic osteoderms of *Shinisaurus crocodilurus* (Squamata, Shinisauridae). *Palaeontol Electron* 8(1):1–36
- Boistel R, Herrel A, Lebrun R, Daghfous G et al (2011) Shake rattle and roll: The bony labyrinth and aerial descent in squamates. *Integr Comp Biol* 51:957–968
- Bolet A, Delfino M, Fortuny J, Almecija S, Robles JM, Alba DM (2014) An amphisbaenian skull from the European miocene and the evolution of Mediterranean worm lizards. *PLoS ONE* 9:e98082
- Bolet A, Stanley EL, Daza JD, Arias JS, Čerňanský A, Vidal-García M, Bevitt JJ, Peretti A, Evans SE (2021) Unusual morphology in the mid-Cretaceous lizard *Oculudentavis*. *Curr Biol* 31:3303–3314.e3303
- Borsuk-Białynicka M (1985) Carolinidae, a new family of xenosaurid-like lizards from the Upper Cretaceous of Mongolia. *Acta Palaeontol Pol* 30:151–176
- Borsuk-Białynicka M (1987) *Carusia*, a new name for the Later Cretaceous lizard Carolina. *Acta Palaeontol Pol* 32:153
- Borsuk-Białynicka M (1990) *Gobekko cretacicus* gen. et. sp. n., a new gekkonid lizard from the Cretaceous of the Gobi Desert. *Acta Palaeontol Pol* 35:67–76
- Brizuela S, Albino A (2017) Redescription of the extinct species *Callopiastes bicuspidatus* Chani, 1976 (Squamata, Teiidae). *J Herpetol* 51:343–354
- Broom R (1903) On the skull of a true Lizard (*Paliguana whitei*) from the Triassic beds of South Africa. *Rec AlbanyMus* 1:1–3
- Bruce LL (2006) Evolution of the nervous system in reptiles. In: Kaas JH (ed) *Evolution of nervous systems, vol II. The evolution of nervous systems in non-mammalian vertebrates*. Elsevier, pp 125–156
- Bruce L (2009) Evolution of the brain in reptiles. In: Binder, Hiokawa, Windhorst (eds), *Encyclopedia of Neuroscience*, Springer, Berlin pp 1295–1301
- Burbrink FT, Graziotin FG, Pyron RA et al (2020) Interrogating genomic-scale data for Squamata (Lizards, Snakes, and Amphisbaenians) shows no support for key traditional morphological relationships. *Syst Biol* 69:502–520
- Butler AB, Hodos W (2005) *Comparative vertebrate neuroanatomy: evolution and adaptation*, 2nd edn. Wiley, Hoboken
- Butler AB, Northcutt RG (1973) Architectonic studies of the diencephalon of *Iguana iguana* (Linnaeus). *J Comp Neurol* 149:439–462
- Caldwell MW (1999) Squamate phylogeny and the relationships of snakes and mosasauroids. *Zool J Linn Soc* 125(1):115–147
- Caldwell MW (2012) A challenge to categories: what, if anything, is a mosasaur? *Bull Soc Géol Fr* 183:7–34
- Caldwell MW, Konishi T, Dutchak A, Bell GB Jr, Lamb J (2007) Osteology of the middle ear in mosasaurs (Squamata): from impedance matching to underwater hearing. In: Everhart MJ (ed) *Second mosasaur meeting abstract booklet*. Fort Hays State University – Sternberg Museum of Natural History, Hays, p 10
- Caldwell MW, Nydam RL, Palci A, Apesteguía S (2015) The oldest known snakes from the Middle Jurassic-Lower Cretaceous provide insight on snake evolution. *Nat Commun* 6:5996

- Camaiti M, Evans AR, Hipsley CA, Chapple DG (2021) A farewell to arms and legs: a review of limb reduction in squamates. *Biol Rev Camb Philos Soc* 96:1035–1050
- Camp CL (1923) Classification of the lizards. *Am Mus Nat Hist Bull* 48:289–481
- Camp CL (1942) California mosasaurs. University of California Press, Berkeley
- Carroll RL, deBraga M (1992) *Aigialosaurs*: Mid-Cretaceous varanoid lizards. *J Vert Paleontol* 12(1):66–86
- Čerňanský A, Stanley EL, Daza JD et al (2022) A new Early Cretaceous lizard in Myanmar amber with exceptionally preserved integument. *Res Sq.* <https://doi.org/10.21203/rs.3.rs-952564/v1>
- Chambi-Trowell SAV, Whiteside DI, Benton MJ (2019) Diversity in rhynchocephalian *Clevosaurus* skulls based on CT reconstruction of two Late Triassic species from Britain. *Acta Paleontol Pol* 64
- Chou CY, Xing LD (2020) Vertebrate remains in amber around the world. *Acta Palaeontol Sin* 59:30–42
- Christensen K (1927) The morphology of the brain of *Sphenodon*. *Univ Iowa Stud Nat Hist* 12:1–29
- Conrad JL (2008) Phylogeny and systematics of Squamata (Reptilia) based on morphology. *Bull Am Mus Nat Hist* 310:1–182
- Conrad JL, Daza JD (2015) Naming and rediagnosing the Cretaceous Gekkonomorpha (Reptilia, Squamata) from Oosh (Ovorkhangai, Mongolia). *J Vert Paleontol* 35
- Conrad JL, Norell M (2006) High-resolution X-ray computed tomography of an Early Cretaceous gekkonomorpha (Squamata) from Öösh (Övorkhangai; Mongolia). *Hist Biol* 18:405–431
- Conrad JL, Norell M (2008) The braincase of two glyptosaurines (Anguillidae, Squamata) and anguillid phylogeny. *Am Mus Nov* 3613:1–24
- Conrad JL, Rieppel O, Grande L (2008) Re-assessment of varanid evolution based on new data from *Saniwa ensidens* Leidy, 1870 (Squamata, Reptilia). *Am Mus Nov* 3630:1–15
- Conrad JL, Rieppel O, Gauthier JA, Norell MA (2011) Osteology of *Gobiderma pulchrum* (Monstersauria, Lepidosauria, Reptilia) *Bull Am Mus. Nat Hist* 362:1–88
- Conrad JL, Balcarcel AM, Mehling CM (2012) Earliest Example of a Giant Monitor Lizard (*Varanus*, Varanidae, Squamata). *PLoS ONE* 7(8):e41767
- Cruzado-Caballero P, Castillo Ruiz C, Bolet A, Colmenero JR, De la Nuez J, Casillas R, Llacer S, Bernardini F, Fortuny J (2019) First nearly complete skull of *Gallotia auaritatae* (lower-middle Pleistocene, Squamata, Gallotiinae) and a morphological phylogenetic analysis of the genus *Gallotia*. *Sci Rep* 9:16629
- Cundall D, Irish F (2008) The snake skull. In: Gans C, Gaunt AS, Adler K (eds) *Biology of the reptilia*, Volume 20, Morphology H. Society for the Study of Amphibians and Reptiles, Ithaca, pp 349–692
- Cuny G, Jaeger JJ, Mahboubi M et al (1990) Les plus anciens serpentes (Reptilia, Squamata) connus. Mise au point sur l'âge géologique des Serpents de la partie moyenne du Crétacé. *C R Séances Acad Sci Paris Ser* 2(311):1267–1272
- Cuthbertson RS, Maddin HC, Holmes RB, Anderson JS (2015) The braincase and endosseous labyrinth of *Plioplatecarpus peckensis* (Mosasauridae, Plioplatecarpinae), with functional implications for locomotor behavior. *Anat Rec* 298:1597–1611
- deBraga M, Carroll RL (1993) The origin of mosasaurs as a model of macroevolutionary patterns and processes. *Evol Biol* 27:245–322
- Dakrory AI (2011a) Innervation of the Olfactory Apparatus of *Varanus Niloticus* (Squamata–Lacertilia-Varanidae). *J Am Sci* 7(9)
- Dakrory AI (2011b) Anatomical study on the cranial nerves of the spiny tail lizard *Uromastix aegypticus* (Squamata, Lacertilia, Agamidae) II-nervous facialis. *J Egypt Ge Soc Zool* 63B:99–129
- Daza JD, Bauer AM (2015) Cranial anatomy of the pygopodid lizard *Aprasia repens*, a gekkotan masquerading as a scolecophidian. In: Bininda-Emonds ORP, Powell GL, Jamniczky HA, Bauer AM, Theodor JM (eds) *All animals are interesting: a festschrift in honour of Anthony P. Russell*. BIS Verlag, Oldenburg, pp 303–350

- Daza JD, Abdala V, Thomas R, Bauer AM (2008) Skull anatomy of the miniaturized gecko *Sphaerodactylus roosevelti* (Squamata: Gekkota). *J Morphol* 239:1340–1364
- Daza JD, Bauer AM, Snively E (2013) *Gobekko cretacicus* (Reptilia: Squamata) and its bearing on the interpretation of gekkotan affinities. *Zool J Linn Soc* 167:430–448
- Daza JD, Mapps AA, Lewis PJ, Thies ML, Bauer AM (2015) Peramorphic traits in the tokay gecko skull. *J Morphol* 276:915–928
- Daza JD, Stanley EL, Wagner P, Bauer AM, Grimaldi DA (2016) Mid-Cretaceous amber fossils illuminate the past diversity of tropical lizards. *Sci Adv* 2
- Dendy A (1909) The intracranial vascular system of sphenodon. *Proc R Soc B* 81:403–427
- Dendy A (1910) On the structure, development and morphological interpretation of the pineal organs and adjacent parts of the brain in the tuatara (*Sphenodon punctatus*). *Philos Trans R Soc Lond B* 201:226e331
- Diaz RE, Trainor PA (2019) An integrative view of lepidosaur cranial anatomy, development, and diversification. In: Ziermann J, Diaz R Jr, Diogo R (eds) Heads, jaws, and muscles. Fascinating life sciences. Springer, Cham. https://doi.org/10.1007/978-3-319-93560-7_9
- Estes R (1983) *Handbuch der Paläherpetologie, Sauria terrestria, Amphisbaenia*. Gustav Fischer Verlag, Stuttgart
- Estes R, Frazzetta TH, Williams EE (1970) Studies on the fossil snake *Dinilysia patagonica* Woodward: part I. Cranial morphology. *Bull Mus Comp Zool* 140:25–74
- Estes R, de Queiroz K, Gauthier J (1988) Phylogenetic relationships within Squamata. In: Estes R, Pregill G (eds) Phylogenetic relationships of the lizard families. Essays commemorating Charles L. Camp. Stanford University Press, California, pp 119–281
- Evans SE (1980) The skull of a new eosuchian reptile from the Lower Jurassic of South Wales. *Zool J Linn Soc* 70:203–264
- Evans S (1984) The classification of the Lepidosauria. *Zool J Linn Soc* 82:87–100
- Evans SE (1987) The braincase of *Youngina capensis* (Reptilia: Diapsida; Permian). *N Jb Geol Paläont Mh* 4:293–203
- Evans SE (1991) A new lizard-like reptile (Diapsida: Lepidosauromorpha) from the Middle Jurassic of England. *Zool J Linn Soc* 103:391–412
- Evans SE (1998) Crown-group lizards (Reptilia, Squamata) from the Middle Jurassic of the British Isles. *Palaeontographica Ab* 250(4):123–154
- Evans SE (2008) The skull of lizards and tuatara. In: Gans C, Gaunt S, Adler K (eds) *Biology of the reptilia, Volume 20, Morphology*. Society for the Study of Amphibians and Reptiles, Ithaca, pp 1–347
- Evans SE (2016) The lepidosaurian ear: variations on a theme. In: Clack J, Fay R, Popper A (eds) *Evolution of the vertebrate ear*. Springer handbook of auditory research. Springer Nature, Cham, pp 245–284
- Evans SE (2022) The origin and early diversification of squamates. In: Gower, Zaher (eds), *The origins and early evolutionary history of snakes*, Cambridge University Press, pp 7–25
- Evans SE, Chure DC (1998) Paramacellodid lizard skulls from the Jurassic Morrison Formation at Dinosaur National Monument, Utah. *J Vert Paleontol* 18:99–114
- Evans SE, Jones MEH (2010) The origin, early history and diversification of lepidosauromorph reptiles. In: Bandyopadhyay S (ed) *New aspects of Mesozoic biodiversity, lecture notes in earth sciences*. Springer, Berlin, pp 27–44
- Ford DP, Evans SE, Choiniere JN, Fernandez V, Benson RBJ (2021) A reassessment of the enigmatic diapsid *Paliguana whitei* and the early history of Lepidosauromorpha. *Proc Biol Sci* 288:20211084
- Fraser NC (1982) A new rhynchocephalian from the British Upper Trias. *Palaeontology* 25:709–725
- Gamble T, Greenbaum E, Russell AP, Jackman TR, Bauer AM (2012) Repeated origin and loss of toepads in gekkotan lizards. *PLoS ONE* 7:e39429
- Gans C, Wever EG (1976) The ear and hearing in *Sphenodon punctatus*. *PNAS* 73 (11):4244–4246
- Gans C, Northcutt RG, Ulinski P (eds) (1979a) *Biology of the reptilia, Volume 9, Neurology A*. Academic Press, London

- Gans C, Northcutt RG, Ulinski P (eds) (1979b) *Biology of the reptilia*, Volume 10. Neurology B. Academic Press, London
- Gans C, Northcutt RG, Ulinski P (eds) (1992) *Biology of the reptilia*, Volume 17. Neurology C. Sensorimotor integration. Academic Press, London
- Gao K, Norell M (1998) Taxonomic revision of *Carusia* (Reptilia: Squamata) from the Late Cretaceous of the Gobi Desert and phylogenetic relationships of the anguimorph lizards. *Am Mus Nov* 3230:1–51
- Gao K, Norell MA (2000) Taxonomic composition and systematics of late cretaceous lizard assemblages from Ukhaa Tolgod and adjacent localities Mongolian Gobi Desert. *Bull Am Mus Nat Hist* 249:4–52
- García S (2021) Morfología neurocraneana del Teiidae (Squamata/Lacertilia) *Callopestes* cf. *rionegrensis* de la Formación Chichinales (Mioceno temprano), Provincia de Río Negro, Argentina. Undergraduate thesis, Universidad Nacional de Río Negro
- García S, Paulina-Carabajal A, Cruzado-Caballero P (2021) Reconstrucción del oído interno de la lagartija extinta *Callopestes* cf. *rionegrensis*. PE-APA 21(R2):R21. <https://doi.org/10.5710/PEAPA.08.06.2021.394>
- Garberoglio FF, Apesteuguía S, Simões T, Palci A, Gómez R, Nydam R, Larsson H, Lee M, Caldwell M (2019) New skulls and skeletons of the Cretaceous legged snake *Najash*, and the evolution of the modern snake body plan. *Sci Adv* 5:eaax5833
- Gardiner BG (1982) Tetrapod classification. *Zool J Linn Soc* 74:207–232
- Gardner NM, Holliday CM, O’Keefe FR (2010) The braincase of *Youngina capensis* (Reptilia, Dipsida): new insights from high-resolution CT scanning of the holotype. *Palaentol Electron* 13(19A):16
- Gauthier J, Estes R, Queiroz K (1988) A phylogenetic analysis of lepidosauromorpha. In: Estes, Despard, Gregory (eds), *Phylogenetic Relationships of the Lizard Families: Essays Commemorating Charles L. Camp*, Stanford University Press, pp 15–98
- Gauthier J, Kearney M, Maisano JA et al (2012) Assembling the squamate tree of life: Perspectives from the phenotype and the fossil record. *Bull Peabody Mus Nat Hist* 53:3–308
- Georgalis GL, Rabi M, Smith KT (2021) Taxonomic revision of the snakes of the genera *Palaeopython* and *Paleryx* (Serpentes, Constrictores) from the Paleogene of Europe. *Swiss J Palaentol* 140:18
- Georgi JA (2008) Semicircular canal morphology as evidence of locomotor environment in amniotes. PhD Thesis. New York: Stony Brook University
- Georgi JA, Sipla JS (2008) Comparative and functional anatomy of balance in aquatic reptiles and birds. In: Thewissen JGM, Nummela S (eds) *Sensory evolution on the threshold: adaptations in secondarily aquatic vertebrates*. University of California Press, Berkeley, pp 233–256
- Gilmore CW (1943) Fossil lizards of Mongolia. *Bull Amer Mus Nat Hist* 81:361–384
- Gisi J (1808) Das Gehirn von *Hatteria punctata*. *Zool Jhb Abt F Anat Ontog* 25:71–236
- Goldby F (1934) The cerebral hemispheres of *Lacerta viridis*. *J Anat* 68:157–215
- Goldby F, Gamble HJ (1957) The reptilian cerebral hemispheres. *Biol Rev* 32(4):383–420
- Gower DJ, Weber E (1998) The braincase of Euparkeria, and the evolutionary relationships of birds and crocodylians. *Biol Rev* 73(4):367–411
- Greenberg N, MacLean PD (1978) Behavior and neurology of lizards, an interdisciplinary colloquium. U.S. Department of health, education, and welfare publication No. (ADM) pp 77–491
- Greene HW (1997) *Snakes. The evolution of mystery in nature*. University of California Press, Berkeley
- Greer AE (1985) The relationships of the lizard genera *Anelytropsis* and *Dibamus*. *J Herpetol* 19:116–156
- Griffing AH, Sanger TJ, Daza JD et al (2019) Embryonic development of a parthenogenetic vertebrate, the mourning gecko (*Lepidodactylus lugubris*). *Dev Dyn* 248:1070–1090
- Griffiths E, Ford DE, Benson RB, Evans SE (2021) New information on the Jurassic lepidosauromorph *Marmorettaoxoniensis*. *Pap Palaentol* 7(4):2255–2278
- Grigoriev DV, Averianov AO, Arkhangel’sky MS et al (2009) A mosasaur from the Cenomanian of Russia. *Palaentol J* 43(3):311e317

- Guerra C, Montero R (2009) The skull of *Vanzosaura rubricauda* (Squamata: Gymnophthalmidae). *Acta Zool (Stockholm)* 90:359–371
- Güntürkün O, Stacho M, Strökens F (2017) The brains of reptiles and birds. In: Kaas JH (ed) *Evolution of nervous systems*, 2nd edn. Elsevier, New York, pp 171–221
- Güntürkün O, Stacho M, Strökens F (2020) The brains of reptiles and birds. In: Kaas JH (ed) *Evolutionary neuroscience*. Wiley, New York, pp 159–212
- Haas G (1964) Anatomical observations on the head of *Liotyphlops albirostris* (Typhlopidae, Ophidia). *Acta Zool* 45:1–62
- Haas G (1979) On a new snakelike reptile from the lower Cenomanian of 'Ein Yabrud, near Jerusalem. *Bull Mus Natl Hist Nat Paris* 4:51–64
- Haas G (1980a) Remarks on a new ophiomorph reptile from the Lower Cenomanian of Ein Jabrud, Israel. In: Jacobs LL (ed) *Aspects of vertebrate history, in Honor of E. H. Colbert*. Museum of Northern Arizona Press, Flagstaff, pp 177–192
- Haas G (1980b) *Pachyrhachis problematicus* Haas, snakelike Reptile from the lower Cenomanian: ventral view of the skull. *Bull Mus Natl Hist Nat Paris* 4:87–104
- Hay JM, Subramanian S, Millar CD et al (2008) Rapid molecular evolution in a living fossil. *Trends Genet* 24:106–109
- Hernández Morales C, Peloso PLV, Bolívar García W et al (2018) Skull morphology of the lizard *Ptychoglossus vallensis* (Squamata: Alopoglossidae) with comments on the variation within Gymnophthalmoidea. *Anat Rec* 302:1074–1092
- Herrera-Flores J, Elsler A, Stubs T et al (2021) Slow and fast evolutionary rates in the history of lepidosaurs. *Palaentology*. <https://doi.org/10.1111/pala.12579>
- Hoffstetter R, Rage J-C (1977) Le gisement de vertébrés miocènes de La Venta (Colombie) et sa faune de serpents. *Ann Paléontol* 63:161–190
- Holovacs NT, Daza JD, Guerra C et al (2019) You can't run, but you can hide: the skeleton of the sand-swimmer lizard *Calyptommatus leiolepis* (Squamata: Gymnophthalmidae). *Anat Rec* 303:1305–1326
- Hoops D, Desfilis E, Ullmann JFP et al (2018) A 3D MRI-based atlas of a lizard brain. *J Comp Neurol* 526:2511–2547
- Hoops D, Weng H, Shaid A et al (2021) A fully segmented 3D anatomical atlas of a lizard brain. *Brain Struct Funct* 226:1727–1741
- Hopson JA (1979) Paleoneurology. In: Gans C (ed) *Biology of the reptilia*, vol 9. Academic Press, New York, pp 39–146
- Houssaye A, Bardet N (2013) A baby mosasauroid (Reptilia, Squamata) from the Turonian of Morocco – *Tethysaurus* 'junior' discovered? *Cret Res* 46:208–215
- Hsiou AS (2007) A new Teiidae species (Squamata, Scincomorpha) from the Late Pleistocene of Rio Grande do Sul State, Brazil. *Rev Bras Paleontol* 10:181–194
- Hurlburt GR, Ridgely RC, Witmer LM (2013) Relative size of brain and cerebrum in tyrannosaurid dinosaurs: an analysis using brain-endocast quantitative relationships in extant alligators. In: Parrish, Molnar, Currie, Koppelhus (eds), *Tyrannosaurid paleobiology*, Indiana University Press, pp 135–154
- Islam A, Ashiq S (1972) The cranial nerves of *Uromastix hardwicki* Gray. *Biologia* 18:51–73
- Janensch W (1906) Über *Archaeophis proavus* Mass., eine Schlange aus dem Eocän des Monte Bolca. In: Neumayr M (ed) *Beiträge zur Paläontologie und Geologie Österreich-Ungarns und des Orients*, vol 19. Hansebooks, pp 1–33
- Jerison HJ (1973) *Evolution of the Brain and Intelligence*. New York, Academic Press
- Jiménez-Huidobro P (2016) Phylogenetic and palaeobiogeographical analysis of Tylosaurinae (Squamata: Mosasauroida). Dissertation, University of Alberta
- Jiménez-Huidobro P, Caldwell MW (2016) Reassessment and reassignment of the Early Maastrichtian mosasaur *Hainosaurus bernardi* Dollo, 1885, to *Tylosaurus* Marsh, 1872. *J Vert Paleontol* 36(3):e1096275–e1096212
- Jiménez-Huidobro P, Simões TR, Caldwell MW (2017) Mosasauroids from Gondwanan Continents. *J Herpetol* 51:355–364

- Jollie MT (1960) The head skeleton of the lizard. *Acta Zool* (Stockholm) 41:1–54
- Jones MEH (2008) Skull shape and feeding strategy in *Sphenodon* and other Rhynchocephalia (Diapsida: Lepidosauria). *J Morphol* 269:945–966
- Jones MEH, Curtis N, Fagan MJ et al (2011) Hard tissue anatomy of the cranial joints in *Sphenodon* (Rhynchocephalia): sutures, kinesis, and skull mechanics. *Paleontol Electron* 14(2):17A-1-17A-92
- Jones ME, Anderson CL, Hipsley CA et al (2013) Integration of molecules and new fossils supports a Triassic origin for Lepidosauria (lizards, snakes, and tuatara). *BMC Evol Biol* 13:208
- Kamal AM (1971) On the fissura metotica in Squamata. *Bull Zool Soc Egypt* 23:53–57
- Kearney M (2003) Systematics of the Amphisbaenia (Lepidosauria: Squamata) based on morphological evidence from recent and fossil forms. *Herpetol Monogr* 17(1):1–74
- Kearney M, Maisano JA, Rowe T (2005) Cranial anatomy of the extinct amphisbaenian *Rhineura hatcherii* (Squamata, Amphisbaenia) based on high-resolution X-ray computed tomography. *J Morphol* 264:1–33
- Kim R, Evans D (2014) Relationships among brain, endocranium, and body sizes in reptiles. Society of Vertebrate Paleontology 74th Annual Meeting, Berlin, Germany.
- Klembara J, Böhme M, Rummel M (2010) Revision of the anguine lizard *Pseudopus laurilardi* (Squamata, Anguillidae) from the Miocene of Europe, with comments on paleoecology. *J Paleontol* 84:159–196
- Kluge AG (1962) Comparative osteology of the eublepharid genus *Coleonyx* Gray. *J Morphol* 110:299–332
- Kluge AG (1967) Higher taxonomic categories of gekkonid lizards and their evolution. *Bull Am Mus Nat Hist* 135:1–60
- Kluge AG (1976) Phylogenetic relationships in the lizard family Pygopodidae: an evaluation of theory, methods and data. *Misc Publ Mus Zool Univ Mich* 152:1–72
- Konishi T, Caldwell MW (2011) Two new plioplatecarpine (Squamata, Mosasauridae) genera from the Upper Cretaceous of North America, and a global phylogenetic analysis of plioplatecarpines. *J Vert Paleontol* 31:754–783
- Konishi T, Caldwell MW, Nishimura T et al (2015) A new halisaurine mosasaur (Squamata: Halisaurinae) from Japan: the first record in the western Pacific realm and the first documented insights into binocular vision in mosasaurs. *J Syst Palaeontol*. <https://doi.org/10.1080/14772019.2015.1113447>
- Laver RJ, Morales CH, Heinicke MP et al (2020) The development of cephalic armor in the tokay gecko (Squamata: Gekkonidae: Gekko gecko). *J Morphol* 281:213–228
- Liem KF, Bemis WE, Walker WF, et al (2000) Functional anatomy of the vertebrates: an evolutionary perspective. 3rd ed. Thomson Learning, Belmont
- Longrich NR, Bhullar B-A S, Gauthier JA (2012) Mass extinction of lizards and snakes at the Cretaceous–Paleogene boundary. *Proc Natl Acad Sci* 109:21396–21396
- Macri S, Savriama Y, Khan I et al (2019) Comparative analysis of squamate brains unveils multi-level variation in cerebellar architecture associated with locomotor specialization. *Nat Comm* 10:5560. <https://doi.org/10.1038/s41467-019-13405-w>
- Maisano JA, Kearney M, Rowe T (2005) Cranial anatomy of the spade-headed amphisbaenian *Diplometopon zarudnyi* (Squamata, Amphisbaenia) based on high-resolution x-ray computed tomography. *J Morphol* 267(1):70–102
- Makádi L, Caldwell MW, Ősi A (2012) The first freshwater mosasauroid (Upper Cretaceous, Hungary) and a new clade of basal mosasauroids. *PLoS One* 7(12):e51781
- Martill DM, Tischlinger H, Longrich NR (2015) A four legged snake from the Early Cretaceous of Gondwana. *Nature* 349:416–419
- Martínez RN, Simões TR, Sobral G et al (2021) A Triassic stem lepidosaur illuminates the origin of lizard-like reptiles. *Nature* 597:235–238
- McDowell SB (2008) The skull of serpentes. In: Gans C, Gaunt AS, Adler K (eds) *Biology of the reptilia*, Volume 21, Morphology I. Society for the Study of Amphibians and Reptiles, Ithaca, pp 467–620

- McDowell SB, Bogert CM (1954) The systematic position of *Lanthanotus* and the affinities of the anguimorph lizards. *Bull Am Mus Nat Hist* 105:1–42
- Meloro C, Jones ME (2012) Tooth and cranial disparity in the fossil relatives of *Sphenodon* (Rhynchocephalia) dispute the persistent ‘living fossil’ label. *J Evol Biol* 25:2194–2209
- Montero R, Gans C (1999) The head skeleton of *Amphisbaena alba* Linnaeus. *Ann Carnegie Mus* 68:15–80
- Montero R, Gans C (2008) An atlas of amphisbaenian skull anatomy. In: Gans C, Gaunt AS, Adler K (eds) *Biology of the reptilia*, Vol 21, Morphology I (The Skull and appendicular locomotor apparatus of Lepidosauria). Society for the Study of Amphibians and Reptiles, Ithaca, pp 621–738
- Montero R, Gans C, Lions ML (1999) Embryonic development of the skeleton of *Amphisbaena darwini* heterozonata (Squamata: Amphisbaenidae) *J Morphol* 239:1–25
- Montero R, Abdala V, Moro S et al (2004) Atlas de *Tupinambis rufescens* (Squamata: Teiidae). Anatomía externa, osteología y bibliografía. *Cuad Herpetol* 18:17–32
- Montero R, Daza JD, Bauer AM et al (2017) How common are cranial sesamoids among squamates? *J Morphol* 278:1400–1411
- Motani R (2009) The evolution of marine reptiles. *Evol: Educ Outreach* 2:224–235
- Müller J, Hipsley CA, Head JJ et al (2011) Eocene lizard from Germany reveals amphisbaenian origins. *Nature* 473:364–367
- Müller J, Hipsley CA, Maisano JA (2016) Skull osteology of the Eocene amphisbaenian *Spathorhynchus fossorium* (Reptilia, Squamata) suggests convergent evolution and reversals of fossorial adaptations in worm lizards. *J Anat* 229:615–630
- Nieuwenhuys R (1998) Morphogenesis and general structure. In: Nieuwenhuys R, Ten Donkelaar HJ, Nicholson C (eds) *The central nervous system of vertebrates*. Springer, Berlin, pp 158–228
- Northcutt RG (1978) Forebrain and midbrain organization in lizards and its phylogenetic significance. In: Greenberg N, MacLean MPD (eds) *Behaviour and neurology of lizards*. National Institute of Mental Health, Rockville, pp 11–64
- Northcutt RG (2002) Understanding vertebrate brain evolution. *Integ Comp Biol* 42:743–756
- Northcutt RG (2013) Variation in reptilian brains and cognition. *Brain Behav Evol* 82:45–54
- O’Donoghue CH (1920) The blood vascular system of the Tuatara, *Sphenodon punctatus*. *Philos Trans R Soc London B* 2010:175–125
- Oelrich TM (1956) The anatomy of the head of *Ctenosaura pectinata* (Iguanidae). *Misc Publ Mus Zool Univ Mich* 94:1–122
- Olori JC (2010) Digital endocasts of the cranial cavity and osseous labyrinth of the burrowing snake *Uropeltis woodmansoni* (Alethinophidia: Uropeltidae). *Copeia* 2010:14–26
- Olori JC, Bell CJ (2012) Comparative skull morphology of uropeltid snakes (Alethinophidia: Uropeltidae) with special reference to disarticulated elements and variation. *PLoS ONE* 7
- Palci A, Caldwell MW, Papazzoni CA (2013) A new genus and subfamily of mosasaurs from the Upper Cretaceous of Northern Italy. *J Vert Paleontol* 33(3):599–612
- Palci A, Hutchinson MN, Caldwell MW et al (2017) The morphology of the inner ear of squamate reptiles and its bearing on the origin of snakes. *R Soc Open Sci* 4:170685
- Palci A, Hutchinson MN, Caldwell MW et al (2018) Paleocological inferences for the fossil Australian snakes *Yurlunggur* and *Wonambi* (Serpentes, Madtsoiidae). *R Soc Open Sci* 5(3):172012
- Paluh DJ, Bauer AM (2017) Comparative skull anatomy of terrestrial and crevice-dwelling *Trachylepis* skinks (Squamata: Scincidae) with a survey of resources in scincid cranial osteology. *PLoS ONE* 12:e0184414
- Pancioli E, Benson RBJ, Walsh SL et al (2020) Diverse vertebrate assemblage of the Kilmaluag Formation (Bathonian, Middle Jurassic) of Skye, Scotland. *Earth Environ Sci Trans R Soc Edinb* 111:135–156
- Páramo-Fonseca ME (2000) *Yaguarasaurus columbianus* (Reptilia, Mosasauridae), a primitive mosasaur from the Turonian (Upper Cretaceous) of Columbia. *Historical Biology* 14:121–131

- Páramo-Fonseca ME (2013) *Eonatator coellensis* nov. sp. (Squamata: Mosasauridae), a new species from the Upper Cretaceous of Colombia. *Revista Acad Colomb Ci Exact* 37:499–518
- Perez-Martinez C, Leal M (2021) Lizards as models to explore the ecological and neuroanatomical correlates of miniaturization. *Behaviour* 158:1121–1168
- Peterson EA (1966) Hearing in the lizard: some comments on the auditory capacities of a non-mammalian ear. *Herpetologica* 22:161–171
- Pianka ER, Vitt LJ (2003) *Lizards: windows to the evolution of diversity*. University of California Press, Berkeley
- Platel R (1975) Nouvelles données sur l'encéphalisation des reptiles squamates. *Z Zool Syst Evol* 13:161–184
- Platel R (1976) Comparative volumetric analysis of the main subdivisions of the brain in saurian reptiles. *J Hirnforsch* 17(6):513–537
- Platel R (1989) Anatomy of the brain of the New Zealand Gray *Sphenodon punctatus* (Sphenodontidae): a quantitative study of the principle subdivisions of the brain. *J Hirnforsch* 30:325–337
- Polcyn MJ (2008) Braincase evolution in plioplatecarpine mosasaurs. *J Vert Pal* 28(Suppl.3):128A
- Polcyn MJ (2010) Sensory adaptations in mosasaurs. *J Vert Paleontol* 30(Suppl 3):146A
- Polcyn MJ, Bell GL Jr (2005) *Russellosaurus coheni* n. gen., n. sp., a 92 million-year-old mosasaur from Texas (U.S.A.), and the definition of the parafamily Russellosaurina. *Neth J Geosci* 84:321–333
- Polcyn MJ, Jacobs LL et al (2014) Physical drivers of mosasaur evolution. *Palaeogeogr Palaeoclimatol Palaeoecol* 400:17–27
- Porter WR, Witmer LM (2015) Vascular patterns in Iguanas and other squamates: blood vessels and sites of thermal exchange. *PLoS One* 10:e0139215
- Pough FH, Andrews RM, Crump ML et al (2016) *Herpetology*, 4th ed, Sinauer Associates, Massachusetts
- Pratt CW (1948) The morphology of the ethmoidal region of *Sphenodon* and lizards. *Proc Zool Soc Lon* 118:171–201
- Pyron RA (2017) Novel approaches for phylogenetic inference from morphological data and total-evidence dating in squamate reptiles (lizards, snakes, and amphisbaenians). *Syst Biol* 66:38–56
- Quadros AB, Chafrat P, Zaher H (2018) A new teiid lizard of the genus *Callopiastes* Gravenhorst, 1838 (Squamata, Teiidae), from the Lower Miocene of Argentina. *J Vert Paleontol* 38:e1484754
- Rage J-C (1976) Les squamates du Miocène de Beni Mellal, Maroc. *Géol Méditerranéenne* 3:57–70
- Rage J-C, Escuillié F (2000) Un nouveau serpent bipède du Cénomane (Crétacé). Implications phylétiques. *C R Acad Sci Paris* 330:513–520
- Range JC, Bailon S (2005) Amphibians and squamate reptiles from the late early Miocene (MN 4) of Béon 1 (Montréal-du-Gers, southwestern France). *Geodiversitas* 27:413–441
- Reeder TW, Townsend TM, Mulcahy DG et al (2015) Integrated analyses resolve conflicts over squamate reptile phylogeny and reveal unexpected placements for fossil taxa. *PLoS ONE*:10
- Renesto S, Bernardi M (2014) Redescription and phylogenetic relationships of *Megachirella wachtleri* Renesto et Posenato, 2003 (Reptilia, Diapsida). *Paläontol Zeitsch* 88:197–210
- Retzius G (1881) *Das Gehörorgan der Wirbelthiere*, vol 1. Samson and Wallin, Stockholm
- Reynoso V-H (1998) *Huehucuetzpalli mixtecus* gen. et sp. nov.: a basal squamate (Reptilia) from the Early Cretaceous of Texepi de Rodríguez, Central Mexico. *Phil Trans R Soc Lon B* 353:477–500
- Rieppel O (1979a) The braincase of *Typhlops* and *Leptotyphlops* (Reptilia: Serpentes). *Zool J Linn Soc* 65:161–176
- Rieppel O (1979b) The evolution of the basicranium in the Henophidia (Reptilia: Serpentes). *Zool J Linn Soc* 66:411–431
- Rieppel O (1980) The phylogeny of anguimorph lizards. *Naturforschenden Gesellschaft, Basel*
- Rieppel O (1981) The skull and jaw adductor musculature in some burrowing scincomorph lizards of the genera *Acontias*, *Typhlosaurus* and *Feylinia*. *J Zool* 195:493–528

- Rieppel O (1984a) The cranial morphology of the fossorial lizard genus *Dibamus* with a consideration of its phylogenetic relationships. *J Zool* 204:289–327
- Rieppel O (1984b) The structure of the skull and jaw adductor musculature of the Gekkota, with comments on the phylogenetic relationships of the Xantusiidae (Reptilia: Lacertilia). *Zool J Linn Soc* 82:291–318
- Rieppel O (1993) Patterns of diversity in the reptilian skull. In: Hanken J, Hall BK (eds) *The skull*. The University of Chicago Press, Chicago, pp 344–390
- Rieppel O, Head JJ (2004) New specimens of the fossil snake genus *Eupodophis* Rage & Escuillié, from Cenomanian (Late Cretaceous) of Lebanon. *Mem Soc Sci Nat Mus Civ Stor Nat Milano* 32:1–26
- Rieppel O, Zaher H (2000) The braincase of mosasaurs and *Varanus*, and the relationships of snakes. *Zool J Linn Soc* 129:489–514
- Rieppel O, Kluge AG, Zaher H (2002) Testing the phylogenetic relationships of the Pleistocene snake *Wonambi naracoortensis* Smith. *J Vert Paleontol* 22:812–829
- Rieppel O, Kley NJ, Maisano JA (2009) Morphology of the skull of the white-nosed blindsnake, *Liotyphlops albirostris* (Scoleophidia: Anomalepididae). *J Morphol* 270:536–557
- Romer AS (1956) *Osteology of the Reptiles*. Chicago, University of Chicago Press
- Roscito JG, Rodrigues MT (2010) Comparative cranial osteology of fossorial lizards from the tribe Gymnophthalmini (Squamata, Gymnophthalmidae). *J Morphol* 271:1352–1365
- Ross CF, Sues H-D, Klerk WJ (1999) Lepidosaurian remains from the Lower Cretaceous Kirkwood Formation of South Africa. *J Vert Paleontol* 19:21–27
- Russell DA (1967) Systematics and morphology of American mosasaurs. *Bull Peabody Mus Nat Hist* 23:1–241
- Sánchez-Martínez PM, Daza JD, Hoyos JM (2021) Comparative anatomy of the middle ear in some lizard species with comments on the evolutionary changes within Squamata. *Peer J* 9
- Säve-Söderbergh G (1947) Notes on the brain-case in *Sphenodon* and certain Lacertilia. *Zool Bidr Uppsala* 25:489–516
- Scanferla A, Smith KT (2020a) Additional anatomical information on the Eocene minute boas *Messelophis variatus* and *Rieppelophis ermannorum* (Messel Formation, Germany). *Vertebr Zool* 70:615–620
- Scanferla A, Smith KT (2020b) Exquisitely preserved fossil snakes of Messel: insight into the evolution, biogeography, habitat preferences and sensory ecology of Early boas. *Diversity* 12:100. <https://doi.org/10.3390/d12030100>
- Scanferla A, Zaher H, Novas F, de Muizon C, Céspedes R (2013) A new snake skull from the Paleocene of Bolivia sheds light on the evolution of macrostomatans. *Plos One* 8:e57583
- Scanferla A, Smith KT, Schaal SFK (2016) Revision of the cranial anatomy and phylogenetic relationships of the Eocene minute boas *Messelophis variatus* and *Messelophis ermannorum* (Serpentes, Booidea). *Zool J Linn Soc* 176:182–206
- Scanlon JD (2003) The basicranial morphology of madtsoiid snakes (Squamata, Ophidia) and the earliest Alethinophidia (Serpentes). *J Vert Paleontol* 23:971–976
- Scanlon JD (2005) Cranial morphology of the Plio-Pleistocene giant madtsoiid snake *Wonambi naracoortensis*. *Acta Palaeontol Pol* 50:139–180
- Scanlon JD (2006) Skull of the large non-macrostomatian snake *Yurlunggur* from the Australian Oligo-Miocene. *Nature* 439:839–842
- Scanlon JD, Lee MSY (2000) The Pleistocene serpent *Wonambi* and the early evolution of snakes. *Nature* 403
- Schmidt RS (1964) Phylogenetic significance of lizard cochlea. *Copeia* 3:542–549
- Schoch RR, Sues H-D (2018) A new lepidosauromorph reptile from the Middle Triassic (Ladinian) of Germany and its phylogenetic relationships. *J Vertebr Paleontol* 38:e1444619
- Schwenk K (2000) Feeding in lepidosaurs. In: Schwenk (ed), *Feeding*. California, Academic Press, pp 175–291
- Segall M, Cornette R, Rasmussen AR et al (2021) Inside the head of snakes: influence of size, phylogeny, and sensory ecology on endocranium morphology. *Brain Struct Func* 226:2401–2415

- Shanklin WM (1930) The central nervous system of *Chameleo vulgaris*. Acta Zool (Stockholm) 11:425–490
- Shute CCD, Bellairs AA (1953) The cochlear apparatus of Geckonidae and Pygopodidae and its bearing on the affinities of these groups of lizards. Proc Zool Soc Lon 123:695–708
- Sienbenrock F (1893) Das Skelet von Uroplates fimbriatus Schneid. Ann K K Naturhist Hoormus ien 8:517–536
- Simões TR, Pyron RA (2021) The squamate tree of life. Bull Mus Comp Zool 163:1–95
- Simões TR, Caldwell MW, Talanda M et al (2018) The origin of squamates revealed by a Middle Triassic lizard from the Italian Alps. Nature 557:706–709
- Simões TR, Vernygora O, Caldwell MW et al (2020) Megaevolutionary dynamics and the timing of evolutionary innovation in reptiles. Nat Commun 11:3322. <https://doi.org/10.1038/s41467-020-17190-9>
- Smeets WJA, Hoogland PV, Lohman AH (1986) A forebrain atlas of the lizard *Gekko gekko*. J Comp Neurol 254:1–19
- Smith KT (2009) Eocene Lizards of the clade *Geiseltaliellus* from Messel and Geiseltal, Germany, and the early radiation of Iguanidae (Reptilia: Squamata). Bull Peabody Mus Nat Hist 50(2):219–306
- Smith KT, Bullar B-AS, Köhler et al (2018) The only known jawed vertebrate with four eyes and the bauplan of the pineal complex. Curr Biol 28(7):1101–1107.e2
- Smith KT, Habersetzer J (2021) The anatomy, phylogenetic relationships, and autecology of the carnivorous lizard “*Saniwa*” *feisti* Stritzke, 1983 from the Eocene of Messel, Germany. C R Palevol 20(23):441–506
- Smith KT, Scanferla A (2021) A nearly complete skeleton of the oldest definitive erycine boid (Messel, Germany). Geodiversitas 43:1–24
- Sobral G, Simões TR, Schoch RR (2020) A tiny new Middle Triassic stem-lepidosauromorph from Germany: implications for the early evolution of lepidosauromorphs and the Vellbert fauna. Sci Rep 10:2273
- Starck D (1979) Cranio-cerebral relations in recent reptiles. In: Gans AC, Northcutt RG, Ulinski P (eds) Biology of the reptilia, Vol 9, Neurology. Academic Press, London, pp 1–36
- Stepanova N, Bauer AM (2021) Phylogenetic history influences convergence for a specialized ecology: comparative skull morphology of African burrowing skinks (Squamata; Scincidae). BMC Ecol Evol 21:86
- Stocker MR, Kirk EC (2016) The first amphisbaenians from Texas, with notes on other squamates from the middle Eocene Purple Bench Locality. J Vert Paleontol 36(3):e1094081
- Strong CRC, Palci A, Caldwell MW (2020) Insights into skull evolution in fossorial snakes, as revealed by the cranial morphology of *Atractaspis irregularis* (Serpentes: Colubroidea). J Anat 238:146–172
- Sues H-D (2019) The rise of reptiles: 320 million years of evolution. Page 1 online resource. Johns Hopkins University Press, Baltimore
- Sues H-D, Reisz RT (1995) First record of the early Mesozoic sphenodontian *Clevosaurus* (Lepidosauria: Rhynchocephalia) from the Southern Hemisphere. J Paleontol 69:123–126
- Sulimski A (1975) Macrocephalosauridae and Polyglyphanodontidae (Sauria) from the Late Cretaceous of Mongolia. Acta Paleont Pol 33:25–102
- Szyndlar Z (1985) Ophidian fauna (Reptilia, Serpentes) from the uppermost Miocene of Algorta (Spain). Estudios geol 41:447–465
- Szyndlar Z (1988) Two new extinct species of the genera *Malpolon* and *Vipera* (Reptilia, Serpentes) from the Pliocene of Layna Spain. Acta Zool Cracov 31:687–706
- Szyndlar Z (1991) Ancestry of the Grass Snake (*Natrix natrix*): paleontological evidence. J Herpetol 25:412–418
- Szyndlar Z, Zarova GA (1990) Neogene Cobras of the genus *Naja* (Serpentes: Elapidae) of East Europe. Ann Naturhist Mus Wien 91:53–61
- Tatarinov LP (1988) The cranial structure of the lower Eocene sea snake “*Archaeophis*” *turkmenicus* from Turkmenia. Paleontol J 22:73–79

- Tchernov E, Rieppel O, Zaher H, Polcyn MJ, Jacobs LL (2000) A fossil snake with limbs. *Science* 287:2010–2012
- Triviño LN, Albino AM, Dozo MT et al (2018) First natural endocranial cast of a fossil snake (Cretaceous of Patagonia, Argentina). *Anat Rec* 301:9–20
- Uetz P, Freed P, JHTR Database (2022). <http://www.reptile-database.org>. Accessed 06 Sept 2022
- Underwood G (1957) On lizards of the family Pygopodidae. A contribution to the morphology and phylogeny of the Squamata. *J Morphol* 100:207–268
- Underwood G (1967) A contribution to the classification of snakes. British Museum of Natural History, London
- Versluys J (1898) Die mittlere und äussere Ohrsphäre der Lacertilia und Rhynchocephalia, Inaugural Dissertation Universität Giessen. Gustav Fischer, Jena.
- Vidal N, Hedges SB (2005) The phylogeny of squamate reptiles (lizards, snakes and amphisbaenians) inferred from nine nuclear protein-coding genes. *C R Biol* 328:1000–1008
- Villa AJ, Abella DM, Alba S et al (2018) Revision of *Varanus marathoniensis* (Squamata, Varanidae) based on historical and new material: morphology, systematics, and paleobiogeography of the European monitor lizards. *PLoS ONE* 13(12):e0207719
- Vitt LJ, Caldwell JP (2013) Herpetology: an introductory Biology of Amphibians and reptiles. 4th ed. Academic Press
- Watanabe A, Gignac PM, Balanoff AM, Green TL, Kley NJ, Norell MA (2019) Are endocasts good proxies for brain size and shape in archosaurs throughout ontogeny? *J Anat* 234(3):291–305
- Watkinson GB (1906) The cranial nerves of *Varanus bivittatus*. *Ge-genbauers Morph Jahrb* 35:450–472
- Weber EG (1978) The reptile ear: its structure and function. Princeton University Press, Princeton
- Werneburg I, Sánchez-Villagra MR (2015) Skeletal heterochrony is associated with the anatomical specialization of snakes among squamate reptiles. *Evolution* 69:254–263
- Whiteside DI (1986) The head skeleton of the Rhaetian sphenodontid *Diphydontosaurus avonensis* gen. et sp. nov., and the modernising of a living fossil. *Phil Trans R Soc B* 312(1156):379–430
- Wiens JJ, Kuczynski CA, Townsend TM et al (2010) Combining phylogenomics and fossils in higher-level squamate reptile phylogeny: molecular data change the placement of fossil taxa. *Syst Biol* 59:674–688
- Wiens JJ, Hutter CR, Mulcahy DG et al (2012) Resolving the phylogeny of lizards and snakes (Squamata) with extensive sampling of genes and species. *Biol Lett* 8(6):1043–1046
- Willard WA (1915) The cranial nerves of *Anolis carolinensis*. *Bull Mus Comp Zool Harv* 59:18–116
- Wilson JA, Mohabey DM, Peters SE, Head JJ (2010) Predation upon hatchling dinosaurs by a new snake from the Late Cretaceous of India. *PLoS Biol* 8:e1000322
- Witmer LM (1995) The extant phylogenetic bracket and the importance of reconstructing soft tissues in fossils. In: Thomason JJ (ed) *Functional morphology in vertebrate paleontology*. New York, Cambridge University Press, pp 19–33
- Witmer LM, Ridgely RC, Dufeau DL et al (2008) Using CT to peer into the past: 3D visualization of the brain and ear regions of birds, crocodiles, and nonavian dinosaurs. In: Endo H, Frey R (eds) *Anatomical imaging: towards a new morphology*. Springer, Tokyo, pp 67–88
- Wood PL, Guo X, Travers SL et al (2020a) Corrigendum to “Parachute geckos free fall into synonymy: Gekko phylogeny, and a new subgeneric classification, inferred from thousands of ultraconserved elements”. *Mol Phylogenet Evol* 146:106731
- Wood PL, Guo X, Travers SL et al (2020b) Parachute geckos free fall into synonymy: Gekko phylogeny, and a new subgeneric classification, inferred from thousands of ultraconserved elements. *Mol Phylogenet Evol* 146:107255
- Wu X, Brinkman D, Russell A et al (1993) Oldest known amphisbaenian from the Upper Cretaceous of Chinese Inner Mongolia. *Nature* 366:57–59
- Wyeth FJ (1924) The development of the auditory apparatus in *Sphenodon punctatus* with an account of the visceral pouches, aortic arches, and other accessory structures. *Phil Trans R Soc Lon (B)* 212:259–368
- Wyneken J (2007) Reptilian neurology: anatomy and function. *Vet Clin Exot Anim* 10:837–853

- Wyeth FJ (1920) On the development of the auditory apparatus in *Sphenodon punctatus*. *Proc Roy Soc Lon B* 91(639):224–228
- Xing L, O'Connor JK, Schmitz L et al (2020) Hummingbird-sized dinosaur from the Cretaceous period of Myanmar. *Nature* 579:245–249
- Yi H, Norell MA (2015) The burrowing origin of modern snakes. *Sci Adv* 1:e1500743
- Yi H, Norell MA (2018) The bony labyrinth of *Platecarpus* (Squamata: Mosasauria) and aquatic adaptations in squamate reptiles. *Palaeoworld*. <https://doi.org/10.1016/j.palwor.2018.12.001>
- Yi H, Norell M (2013) New Materials of *Estesia mongoliensis* (Squamata: Anguimorpha) and the Evolution of Venom Grooves in Lizards. *Am Mus Nov* 3767:1–31
- Yi H, Sampath D, Schoenfeld S et al (2012) Reconstruction of inner ear shape and size in mosasaurs (Reptilia: Squamata) reveals complex adaptation strategies in secondary aquatic reptiles. *J Vert Paleontol* 32:198A
- Young BA (1987) The cranial nerves of three species of sea snakes. *Can J Zool* 65(9). <https://doi.org/10.1139/z87-338>
- Zaher H, Scanferla CA (2012) The skull of the Upper Cretaceous snake *Dinilysia patagonica* Smith-Woodward, 1901, and its phylogenetic position revisited. *Zool J Linn Soc* 164:194–238
- Zaher H, Smith KT (2020) Pythons in the Eocene of Europe reveal a much older divergence of the group in sympatry with boas. *Biol Lett* 16:20200735
- Zaher H, Apestequí S, Scanferla CA (2009) The anatomy of the Upper Cretaceous snake *Najash rionegrina* Apestequí & Zaher, 2006, and the evolution of limblessness in snakes. *Zool J Linn Soc* 156:801–826
- Zaher H, Mohabey DM, Grazziotin FG et al (2022a) The skull of *Sanajeh indicus*, a Cretaceous snake with an upper temporal bar, and the origin of ophidian wide-gaped feeding. *Zool J Linn Soc*
- Zaher H, Augusta BG, Rabinovich R et al (2022b) A review of the skull anatomy and phylogenetic affinities of marine pachyophiid snakes. In: Gower DJ, Zaher H (eds) *The origin and early evolution of snakes*. Cambridge University Press, Cambridge
- Zheng Y, Wiens JJ (2016) Combining phylogenomic and supermatrix approaches, and a time-calibrated phylogeny for squamate reptiles (lizards and snakes) based on 52 genes and 4162 species. *Mol Phil Evol* 94:537–547

Chapter 6

Paleoneurology of the Early Diversification of Triassic Archosauriforms and Pseudosuchians



M. Belén von Baczko, Julia B. Desojo, M. Jimena Trotteyn,
and Michelle R. Stocker

Institutional Abbreviations

GR	Ruth Hall Museum of Paleontology at Ghost Ranch, New Mexico, USA
MCZ	Museum of Comparative Zoology, Harvard University, Boston, USA
NMT	National Museum of Tanzania, Dar es Salaam, Tanzania
PIN	Borissiak Paleontological Institute of the Russian Academy of Sciences, Moscow, Russia

M. B. von Baczko (✉)

Sección Paleontología de Vertebrados, Museo Argentino de Ciencias Naturales “Bernardino Rivadavia”, Ciudad Autónoma de Buenos Aires, Argentina

Consejo Nacional de Investigaciones Científicas y Técnicas (CONICET),
Ciudad Autónoma de Buenos Aires, Argentina
e-mail: belen_vb@macn.gov.ar

J. B. Desojo

Consejo Nacional de Investigaciones Científicas y Técnicas (CONICET),
Ciudad Autónoma de Buenos Aires, Argentina

División Paleontología Vertebrados, Facultad de Ciencias Naturales y Museo, Universidad Nacional de La Plata, La Plata, Argentina
e-mail: juliadeso@fcnym.unlp.edu.ar

M. J. Trotteyn

Consejo Nacional de Investigaciones Científicas y Técnicas (CONICET),
Ciudad Autónoma de Buenos Aires, Argentina

INGEO, Departamento de Biología, Departamento de Geología, Facultad de Ciencias Exactas, Físicas y Naturales, Universidad Nacional de San Juan, San Juan, Argentina
e-mail: jtrotteyn@unsj.edu.ar

M. R. Stocker

Department of Geosciences, Virginia Tech, Blacksburg, VA, USA
e-mail: stockerm@vt.edu

© Springer Nature Switzerland AG 2023

M. T. Dozo et al. (eds.), *Paleoneurology of Amniotes*,
https://doi.org/10.1007/978-3-031-13983-3_6

PULR	Paleontología, Universidad Nacional de La Rioja, La Rioja, Argentina
PVL	Instituto Miguel Lillo, Tucumán, Argentina
PVSJ	Sección de Paleontología de Vertebrados, Museo de Ciencias Naturales de la Universidad Nacional de San Juan, San Juan, Argentina
SAM-PK	Iziko South African Museum, Cape Town, South Africa
TTUP	Texas Tech University Museum, Lubbock, Texas, USA
UFRGS-PV	Departamento de Paleontologia e Estratigrafia, Instituto de Geociências, Universidade Federal do Rio Grande do Sul, Porto Alegre, Brazil
UMZC	Museum of Zoology, Cambridge University, Cambridge, UK
ZPAL	Institute of Paleobiology of the Polish Academy of Sciences, Warsaw, Poland

6.1 Systematic and Phylogenetic Context

Archosauriformes is a group of diapsids distributed around all Pangea that consist of very heterogeneous forms of reptiles including the clade Archosauria, the ruling reptiles, which are represented by the crocodylian (*Pseudosuchia*) and avian (*Avenmetatarsalia*) lineages. Non-archosaurian archosauriforms are recorded only in the Triassic Period, being the first continental forms recorded after the massive Permo-Triassic mass extinction (P-Tr, ~252 Ma) (Benton 1984, 1985). They include a vast range of animals with wide and flat skulls adapted to amphibious life habits as well as narrow and tall ones related to terrestrial habits. The small-bodied (1–2 m) proterochampsians present two general morphotypes, one with deeply ornamented flat skulls, markedly triangular in dorsal view (*Proterochampsia*, *Doswelliidae*) and resembling the shape of an extant crocodylian skull and the other with taller and narrow skulls (*Rhadinosuchinae*) ornamented by ridges. *Doswelliids* are found in Middle-Late Triassic continental deposits of the northern hemisphere (USA, Germany, China), whereas proterochampsids are restricted to South America (Argentina, Brazil) (Trotteyn and Ezcurra 2020; Wynd et al. 2019). Some smaller semiaquatic archosauriforms are grouped in *Proterosuchidae*, which are sprawling animals of medium body size (3.5–4 m) with no osteoderms and a bizarre cranial anatomy characterized by an anteroventrally expanded snout with numerous diverging premaxillary teeth in mature forms (Ezcurra and Butler 2015). *Proterosuchids* are found in Late Permian-Early Triassic outcrops of Russia, China, South Africa, India, and probably Brazil and Uruguay (De-Oliveira et al. 2022; Ezcurra et al. 2021; Ezcurra 2016). On the other hand, the more terrestrial forms include some large hypercarnivorous predators from the Early-Middle Triassic such as erythrosuchids, which reach up to 5 m long, have proportionally large skulls and robust skeletons but no osteoderms. They are recorded in Russia, China, South Africa, and probably South America (Gower 2003; Ezcurra 2016; Butler et al. 2019). Lastly, euparkeriids are relatively small-sized archosauriforms from the Early-Middle Triassic of South Africa, China, Russia, and Poland. They are generalized terrestrial

carnivorous forms with relatively deep and narrow skulls and paired paramedian osteoderms (Ewer 1965; Sookias et al. 2020).

The crown group Archosauria experienced a huge radiation during the Middle Triassic, which is represented by an enormous diversity of pseudosuchians and some of the first avemetatarsalians. Pseudosuchians dominated the continental environments during the Triassic and exhibited an impressive diversity of body forms, sizes, and life habits (Pradelli et al. 2022). During this time, they are usually divided into the following clades: Phytosauria, Aetosauria, Ornithosuchidae, Erpetosuchidae, Gracilisuchidae, Poposauroidae, and Loricata (Fig. 6.1). However, some of the relationships between these groups are still debated.

In some of the latest phylogenetic schemes (Nesbitt 2011 and subsequent modifications; Ezcurra et al. 2017), phytosaurs are recognized either as the basal-most group within Pseudosuchia or as the immediate sister group of Archosauria. They are recovered mainly from the Late Triassic deposits of most continents, except Australia, Antarctica, and South America, with a putative record from the Riograndia Assemblage Zone from Brazil (Kischlat and Lucas 2003; Schultz et al. 2020) and a Middle Triassic representative from China. Phytosaurs are sprawling quadrupedal animals with large bodies covered with multiple diamond-shaped osteoderms

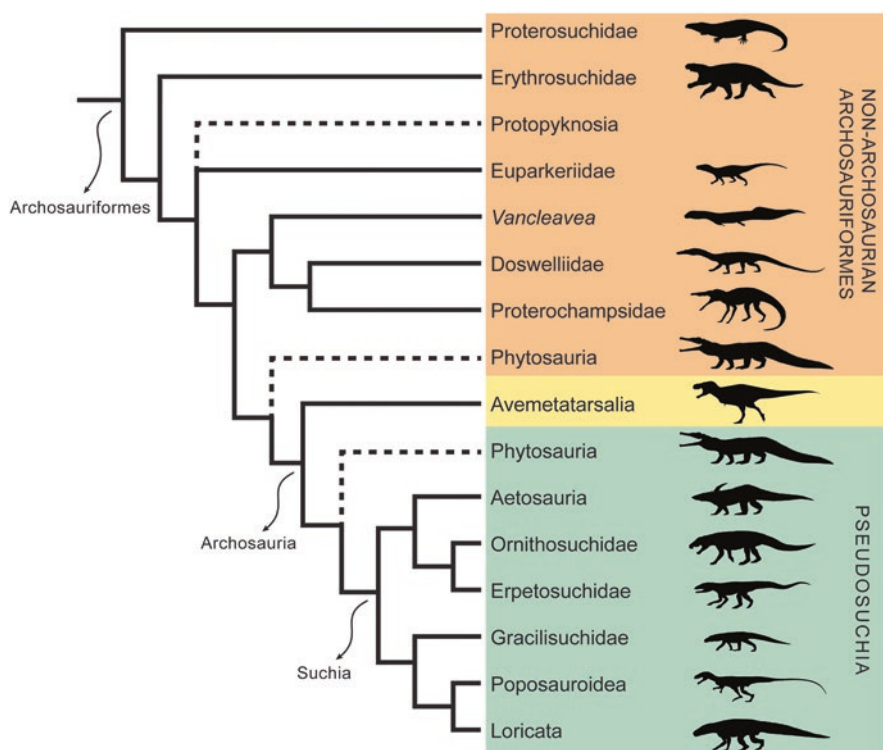


Fig. 6.1 Simplified cladogram showing the main groups of Triassic archosauriforms and pseudo-suchians. (Based on Nesbitt 2011; Stocker et al. 2016; and Ezcurra et al. 2017)

(arranged in two paramedian rows) and characteristic proportionally large and longirostrine skulls with non-terminal nares.

Ornithosuchids are recovered as either the basal-most group of Pseudosuchians (Nesbitt 2011; Marsh et al. 2020) or closely related to erpetosuchids and aetosaurs within Suchia (Ezcurra et al. 2017; Müller et al. 2020). They are registered in Late Triassic continental deposits of Scotland, Argentina, and Brazil. Ornithosuchids are quadrupedal to facultative bipedal reptiles with carnivorous or scavenger feeding habits and with bizarre cranial anatomy (anteroventrally expanded snout, large diastema between premaxilla and maxilla, short lower jaw) and a unique “crocodile-reverse” ankle joint.

Aetosaurs are a distinctive group recovered from Late Triassic outcrops of most continents, except Australia and Antarctica. Currently they are considered the sister group of erpetosuchids+ornithosuchids (Ezcurra et al. 2017) or grouped with *Revueltosaurus* and *Acaenosuchus* as sister of Erpetosuchidae (Marsh et al. 2020). Aetosaurs are quadrupedal, heavily armoured animals with small tapering skulls, edentulous anterior lower jaws, and extensively ornamented osteoderms forming the dorsal, lateral, ventral, and appendicular armor.

Erpetosuchids are a recently reevaluated group whose phylogenetic affinities are now better understood thanks to new abundant findings. They are registered from Middle-Late Triassic continental outcrops of Scotland, Germany, Tanzania, USA, Brazil, and Argentina (Ezcurra et al. 2017; Nesbitt et al. 2017). They are closely related to aetosaurs as well as ornithosuchids, depending on the phylogenetic analysis. Erpetosuchids are characterized by a heavily ornamented skull with the tooth row restricted to the anterior half of the maxilla, and thick ornamented paramedian and lateral dorsal rows of osteoderms as well as ventral and appendicular ones.

Gracilisuchids are small, gracile, terrestrial carnivorous pseudosuchians (~50 cm total length) found only in the Late Triassic continental beds of Argentina and the Middle-Late Triassic of China. Their phylogenetic affinities have been long debated but they are currently considered as the sister group of Paracrocodylomorpha (Butler et al. 2014; Lecuona et al. 2017).

Poposauroids are one of the most unique groups of pseudosuchians, being recorded in Middle-Late Triassic outcrops of Europe, Asia, North and South America, and Africa. They are nested within Paracrocodylomorpha, sister to Loricata, but their internal relationships are still debated because several of their representatives are very incomplete. Poposauroids are characterized by having four to five sacral vertebrae and lacking osteoderms. They include very diverse taxa with sizes ranging from 2–4 m, bipeds to quadrupeds, and strange adaptations like sail-backs or edentulous beaks (Nesbitt 2003, 2007; Butler et al. 2011; Schachner et al. 2020).

Non-crocodylomorph loricatans have been historically grouped as Rausuchidae and Prestosuchidae within “Thecodontia”, later on classified as the poorly defined “Rausuchia”, and their phylogenetic relationships have been strongly argued (Reig 1961; Parrish 1993; Gower 2000; Nesbitt et al. 2013a; Desojo et al. 2020). They are recorded from Middle-Late Triassic beds worldwide, except in Australia and Antarctica, and include the largest short-necked, quadrupedal, hypercarnivorous

predators within Pseudosuchia at the beginning of the Mesozoic, reaching sizes of 7–8 m long.

The skull has been extensively modified in each of the archosauriform groups previously mentioned allowing the filling of the continental niches available after the P-Tr mass extinction. Since the skull is the structure that contains and protects the encephalon and sensorial organs, the study of the endocranial spaces will reflect the morphology of the soft tissues contained within them. Therefore, the understanding of the braincase and the endocranial casts (endocast) of these animals will allow us to better comprehend their capabilities, their behavior, and the adaptations that they required when filling their ecological roles. Through the study of the endocranial anatomy of these reptiles we can take a look at how these structures evolved through time from the earliest archosauriforms that radiated in the Triassic to the modern crocodiles we see nowadays.

6.2 Historical Background

Some of the first studies showing the endocranial morphology of stem-archosaurs and pseudosuchians were published by the end of the nineteenth century and beginning of the twentieth century (Edinger 1975) mainly focused on the Late Triassic continental phytosaurs from the US. By that time, the endocranial cavities were studied either by the serial sectioning of a skull (which involved partial or complete destruction of the specimen), through natural endocasts exposed by the erosion of the cranial bones, or by developing artificial endocasts when filling these cavities with different materials and extracting them (e.g. plaster, gutta percha, latex). The physical artificial endocast of “*Belodon*” (= *Machaeropsopus buceros*) was described by Cope (1887, 1888) triggering the subsequent works on other species of phytosaurs from Germany and the US such as *Mesorhinus fraasi* (= *Mesorhinosuchus*) (Jaekel 1910), *Leptosuchus* (Case 1928, 1929; Gregory 1951), *Pseudopalatus* (= *Machaeropsopus*) *pristinus* (Mehl 1928; Camp 1930), *Brachysuchus megalodon* (Case 1929), and *Machaeropsopus* (= *Smilosuchus*) *gregorii* (Camp 1930; Goldby and Gamble 1957). Moreover, the first endocast of an aetosaur, *Desmotosuchus* “*haplocerus*” (= *D. spurensis*), was described by Case (1921) amongst these pioneering studies of early archosaurs (Fig. 6.2).

By mid-twentieth century, after the World War II, the revision of some South African non-avemetatarsalian archosauriforms included the descriptions of the cranial anatomy of *Erythrosuchus africanus*, “*Chasmatosaurus*” (= *Proterosuchus fergusi*), “*Vjushkovia*” *triplicostata* (= *Garjainia prima*), and *Euparkeria* (Brink 1955; Ewer 1965), as well as the Scottish aetosaur *Stagonolepis robertsoni* (Walker 1961). These studies had interesting details of their neuroanatomy, although no endocranial casts were included at that time. On the other hand, the exhaustive revision on Indian phytosaurs performed by Chatterjee (1978) not only included the detailed description of the braincase of *Parasuchus hislopi* but also provided the first artificial endocast for this species.

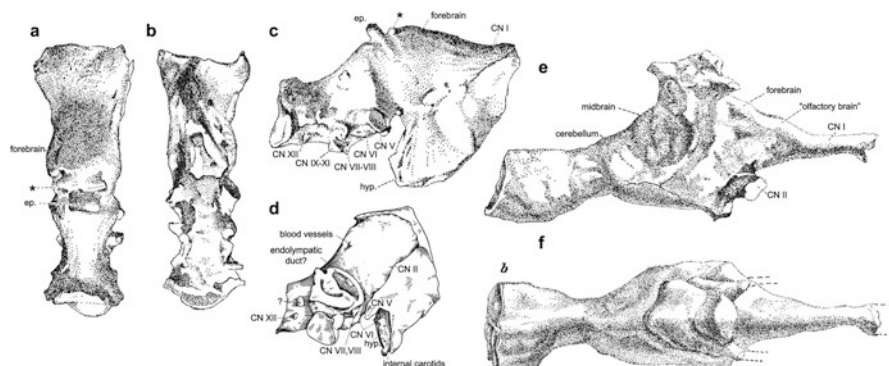


Fig. 6.2 First pseudosuchian endocasts published (modified from Edinger 1929). Endocast of the aetosaur *Desmatosuchus spurensis* in (a), dorsal, (b), ventral, and (c), lateral view. (d), Endocast of the phytosaur *Leptosuchus* in lateral view. Endocast of the phytosaur “*Belodon buceros*” (= *Machaeroprotopus*) in (e), lateral and (f), dorsal. Abbreviations: CN I–XII cranial nerves I–XII, ep. epiphysis, hyp. hypophysis, * “problematic protuberances”

The main integrative work in reptilian paleoneurology was carried out by Hopson (1979) as a contribution to the ninth volume of the book *Biology of the Reptilia* (Gans et al. 1979). In this chapter, Hopson considers several topics on the evolution, size, and problematics of the brain of fossil reptiles and addresses a comparative study of the brain in these groups. Within pseudosuchian archosaurs, he highlights the endocast descriptions of the aetosaur *Desmatosuchus* and several phytosaurs (e.g. *Machaeroprotopus*, “*Belodon*”, “*Leptosuchus*”) making some reinterpretations of their encephalon and cranial nerves and considering them as “unspecialized” forms similar to crocodylians and carnosaurian dinosaurs.

Groundbreaking works on cladistics helped establish the phylogenetic framework of stem and crown archosaurs (Gauthier and Padian 1985; Benton and Clark 1988; Sereno 1991; Sereno and Arcucci 1990), opening a clearer pathway for further studies on different macroevolutionary aspects of this lineage (Fig. 6.1). Paleoneurology was one of these aspects, and, in this new context, an important increase in the study of archosauriform neuroanatomy was boosted by Gower and colleagues. They provided numerous contributions, such as the detailed studies on the braincases of *Erythrosuchus africanus*, “*Vjushkovia*” “*triplicostata*”, *Xilousuchus sapingensis*, *Eupakeria broomi*, *Stagonolepis robertsoni*, *Batrachotomus kupferzellensis*, and *Arizonasaurus babbitti* (Gower and Sennikov 1996a, b; Gower 1997, 2002; Gower and Weber 1998; Gower and Walker 2002; Gower and Nesbitt 2006).

This was the stepping stone for paleoneurology of non-dinosaurian archosauriforms that had yet to be benefitted by the development of digital endocasts through the incorporation of modern techniques in this discipline (X-ray imaging, computed tomography, microCT, Neutron scanning). In addition, many researchers specialized in the field of paleoneurology, which further contributed to its development and expansion.

6.2.1 Problematics

The study of the brain of fossil archosauriforms carries the main problem seen in living reptiles concerning the correlation between the different regions of the brain and the endocranial cavity through different ontogenetic stages (Watanabe et al. 2019). In extant crocodylians, turtles, and squamates the brain does not fill the entire endocranial space, occupying only 50–70% of it, unlike in birds and mammals where the brain fills almost the entire endocranial cavity (95%) (Jerison 1973; Hopson 1979). For this reason, the structures identified on endocasts of fossil reptiles need to be addressed with care considering that the tissues surrounding the brain, such as the meninges and venous sinuses, can occupy an important portion of the endocranial spaces, and the brain-to-endocranial cavity correlation index must be taken into consideration (BEC index) (Jerison 1969; Hopson 1979; Balanoff et al. 2013; Evers et al. 2019).

The changes seen associated with the ontogeny of living reptiles also need to be considered when studying fossil endocasts because the morphology of the brain and the proportion it occupies within the endocranial cavity is drastically modified from embryos to adults (Jirak and Janacek 2017; Watanabe et al. 2019; Hu et al. 2020). In hatchling and juvenile crocodiles, the brain is relatively larger but anteroposteriorly shorter than in adults. The flexures between brain regions are more pronounced in embryos and juveniles than in adults, and for that reason the relative position of the cranial nerves is strongly modified during ontogeny (Evans et al. 2009; Jirak and Janacek 2017, Lessner and Holliday 2020). Therefore, if the ontogenetic stage of the specimens studied can affect the interpretations in living forms, in fossils it may be more difficult to determine the ontogenetic stage if we are dealing with fragmentary or incomplete specimens.

One of the main questions in paleontology concerns the paleobiology of extinct forms. In this regard, we intend to recognize if there is a correlation between the endocranial morphology and the paleoecological roles that are proposed for extinct animals based on other sources of information (osteology, histology, taphonomy, etc.). Traditionally, the ecological roles of extinct animals were inferred through the sedimentary environment in which they were found in combination with their general morphology and phylogenetic context (e.g. Bonaparte 1984). Paleoneurology allows us to test these hypotheses in order to better understand the paleobiology, paleoecology, and macroevolution of extinct animals.

The last decades have witnessed more detailed reanalysis of known specimens, as well as the discovery of more complete ones, providing crucial information about the neurocranial region, which was previously poorly understood (Gower and Sennikov 1996b; Gower and Nesbitt 2006; Gower and Walker 2002; Gower 2002; Trotteyn and Haro 2011, 2012; Mastrantonio et al. 2013; Sobral et al. 2016; Stocker et al. 2016; Nesbitt et al. 2017, 2020). However, this still is a low number of paleoneurological studies of Triassic archosauriforms compared to the diversity of known species, which might be a reflection of the low percentage of preserved braincases over the total amount of nominal species for these groups (Fig. 6.3a). Only 20% of

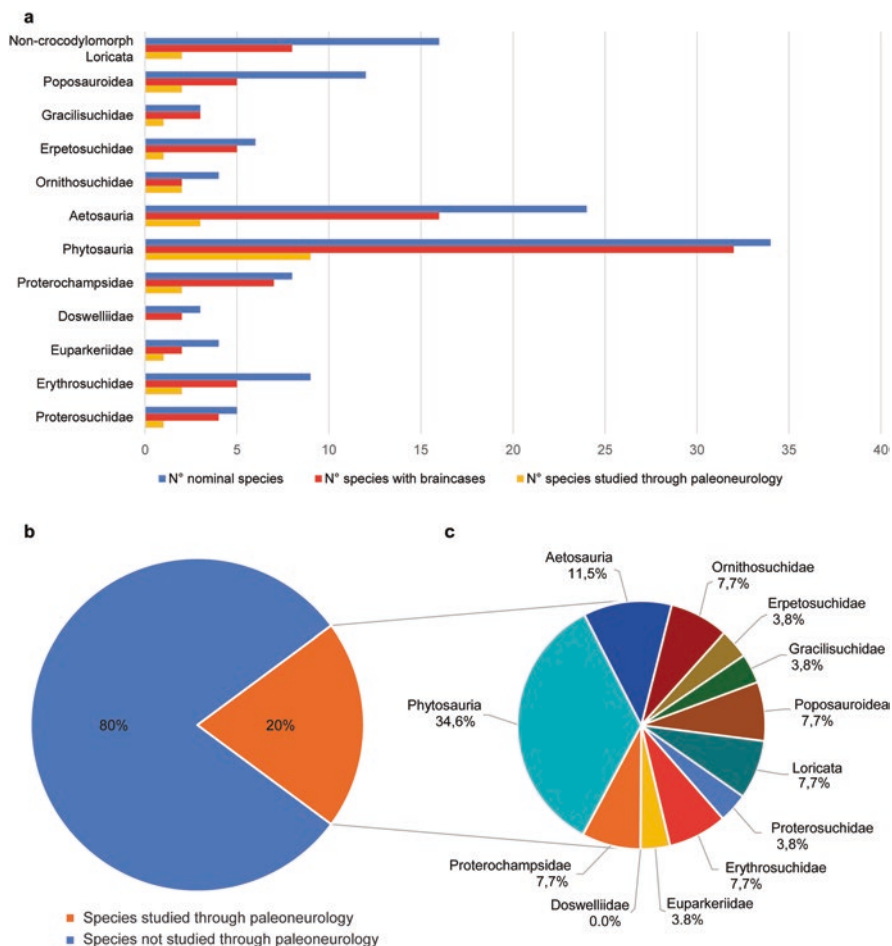


Fig. 6.3 (a), Histogram showing the number of nominal species of Triassic archosauriforms and pseudosuchians currently known (blue), the species with preserved neurocranial elements (red), and the number of species that have been studied from paleoneurological perspectives (yellow). (b), Pie chart showing the total percentage of Triassic archosauriform and pseudosuchian species with paleoneurological studies done and (c), detail indicating the representation of each group within those studies

the Triassic archosauriform and pseudosuchian species known to date have been studied through paleoneurological analysis, providing novel information about the soft tissues and sensorial organs of extinct species (Fig. 6.3b).

Fortunately, previously inaccessible aspects of the skull (e.g. unprepared specimens, tiny and/or articulated skulls, taphonomically distorted specimens) are now available thanks to the application of modern technologies such as computed tomographies (Fig. 6.4). This new information together with clearer taxonomic and phylogenetic schemes is contributing to expand the paleoneurological knowledge of

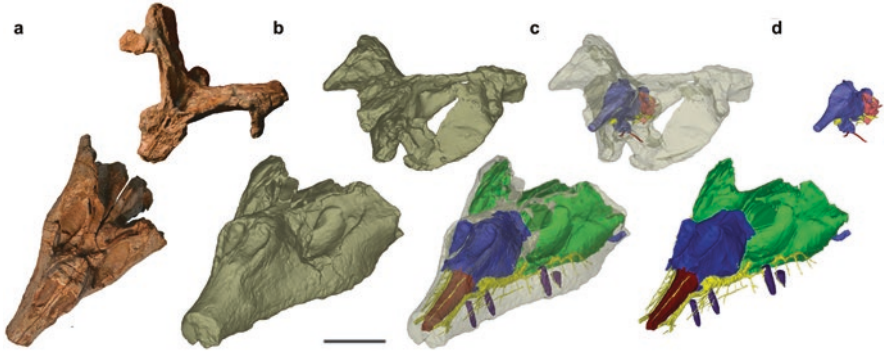


Fig. 6.4 Computed tomography applied to the fossil skull of the basal phytosaur *Wannia scurriensis* (TTUP-00539) and digital reconstructions of the skull and its soft tissues (modified from Lessner and Stocker 2017). (a), Dorsal view of the skull, (b), anterolateral view of CT scan of skull, (c), anterolateral view of transparent skull, and (d), anterolateral view of endocast (brain, inner ear, and sinuses). Snout section: Premaxillary cavity in red; airway in blue; antorbital sinus in green; neurovascular canal in yellow. Braincase section: Encephalon in blue, cranial nerves in yellow, labyrinth in pink, internal carotid arteries in red. Scale bar = 5 cm

archosauriforms and pseudosuchians and will hopefully allow us in the future to recognize macroevolutionary patterns in archosauriforms.

6.3 Overview of General and Comparative Anatomy

6.3.1 Non-archosaurian Archosauriforms

Proterosuchidae

The first study of the endocranial anatomy of *Proterosuchus fergusi*, recently published by Brown et al. (2020), was based on endocranial reconstructions and also discussed its life habits. That study presents the first assessment of the braincase and inner ear of *P. fergusi*. The endocranial cast of *Proterosuchus fergusi* is similar to that of extant crocodylians. The olfactory bulbs are slightly laterally expanded, and rostrally taper into two separate elements. The reconstructed forebrain is bulbous and horizontal, and the midbrain is anteroventrally directed. The hindbrain is medio-laterally narrow and expands ventrally more than the other parts of braincase. The floccular lobes are relatively small and do not expand through the anterior semicircular canal. The carotid canal is divided in two channels that extend away from each other laterally, and extends ventrally from the braincase. A small ventrally-oriented trochlear nerve canal (CN IV) and three branches of the trigeminal nerve canal (CN V) were reconstructed. The vestibular portion of the endosseous labyrinths of the inner ear has a pyramidal shape. The anterior semicircular canal and the posterior semicircular canal are relatively equal in proportions. The lagena is less ventrally

extended than in other archosauriform reconstructions (Witmer et al. 2008; Leahey et al. 2015; Lautenschlager and Butler 2016; Brusatte et al. 2016; Pierce et al. 2017), and the fenestra vestibuli extends posterolaterally away from the labyrinth.

Erythrosuchidae

Partial physical endocasts of *Erythrosuchus africanus* and *Garjainia prima* (= "*Vjushkovia triplicostata*") were developed and described by Gower and Sennikov (1996a). Both endocasts of *Erythrosuchus africanus* and *Garjainia prima* represent the middle and posterior region of the encephalon, part of the inner ear, and the exits for the cranial nerves V to XII. The position of CN II to IV were also recognized by Gower and Sennikov (1996a) based on additional disarticulated material and these were indicated in their brain reconstructions. These endocasts are described as being relatively low and broad and having subequal cerebral and pontine flexures of approximately 135°. A large floccular lobe is located anterior to the anterior semicircular canal of the labyrinth and is anteriorly surrounded by the middle cerebral vein, which runs vertically and curves posteroventrally to exit together with the trigeminal nerve (CN V). The abducens nerve (CN VI) exits anterolaterally, from a location ventromedial to the facial nerve (CN VII), which is located anterior to the inner ear, at the level of the fenestra ovalis. The metotic foramen is a single, wide, slit-like opening, just posterior to the fenestra ovalis, and CN XII exits through a single foramen as well, but slightly more ventrally located in *Garjainia prima* than in *Erythrosuchus africanus*. Concerning the inner ear, only part of the horizontal semicircular canal and common crus were identified by Gower and Sennikov (1996a). The anterior and posterior ampullae are undifferentiated in *Erythrosuchus africanus*, whereas these cannot be identified in *Garjainia prima*. However, the lagena (or pseudolagena) is identified in the latter as a ventrally directed projection that originates from the fenestra ovalis.

Few other erythrosuchid braincases are known that offer some information about the shape of their brain. The braincase of *Guchengosuchus shiguaiensis* has the impression of the dorsal surface of the brain, olfactory tracts and bulbs (Butler et al. 2019) and part of the lateral surface. A deep auricular recess/floccular fossa is apparently divided by an anterodorsally oriented ridge, differing from other erythrosuchids. The other endocranial features recognized in *Guchengosuchus shiguaiensis* (CN V, VII, IX-XI) do not differ from those seen in *Erythrosuchus africanus*. Gower and Sennikov (1996b) described the braincase of *Fugusuchus hejapanensis* indicating a morphology congruent with that of *Garjainia* (= "*Vjushkovia*"), but the better preservation of the ventral surface of the braincase of *Fugusuchus* allowed a clear identification of the foramina for the cerebral branch of the internal carotids. These are located on the ventral surface of the basisphenoid, between the posterior ends of the basiptyergoid processes.

Protopyknosia

Known only from partial cranial material, the protopyknosians *Triopticus primus* Stocker et al. 2016 and *Kranosaura kuttyi* Nesbitt et al. 2021 both preserve at least partial endocranial casts. These archosauriforms are characterized by their bizarre endocranial morphology, which includes a deep and wide pit (?= pineal foramen) extending from the posterodorsal surface of the skull through the skull roof to possibly contact and connect with the dorsal surface of the brain endocast. In *Triopticus*, the brain endocast, reconstructed neurovasculature, and endosseous labyrinths are well preserved overall due to hypermineralization of the braincase (Stocker et al. 2016). The overall structure of the brain endocast is relatively consistent with other non-archosaurian archosauriforms with some exceptions. The endocast is elongate with little midbrain flexure. Anteriorly, the forebrain preserves distinct cerebral hemispheres separated by a median interhemispheric sulcus. The olfactory tracts (CN I) are narrow with well-demarcated olfactory bulbs. In the midbrain, the optic lobes are not well-defined between the cerebrum and cerebellum, though the trunks of the optic tracts (CN II) are relatively large. There are prominent floccular lobes on the cerebellum that differ from the condition in any other non-archosaurian archosauriform and even from most early-diverging archosaurs. The labyrinths preserve unusually long canals for a non-archosaur archosauriform that are similar to those of some theropod dinosaurs (Bronzati et al. 2021), along with well-formed ampullae and elongate lagenae.

Euparkeriidae

The braincase of *Euparkeria* was described for the first time by Ewer (1965), based on the holotype (SAM-PK-5867) and two other specimens (SAM-PK-7696; UMZC T.692). Subsequently, Cruickshank (1970) redescribed the specimen SAM-PK-7696 after further acid preparation. On the basis of the same isolated specimen (SAM-PK-7696), Evans (1986) in her treatment compared the *Euparkeria* braincase with that of *Prolacerta broomi*. After a further mechanical preparation of the holotype and SAM-PK-7696, Welman (1995) figured both and compared the braincase of *Euparkeria* with that of birds, dinosaurs, and crocodiles. Gower and Weber (1998) redescribed exhaustively the specimen UMZC T.692 of *Euparkeria* and refuted the previous hypothesis (Welman 1995) that linked this taxon to birds to the exclusion of other archosaurs.

Building on the work of Gower and Weber (1998), Sobral et al. (2016) documented new information using CT information of UMZC T.692, SAM-PK-5867 (holotype), SAM-PK-6047A, and the isolated braincase SAM-PK-7696. The inner ear of *Euparkeria* shows relatively elongated semicircular canals, especially the anterior semicircular canal. The floccular fossa is much smaller in *Euparkeria* than in modern birds, but larger than in *Youngina* (Sobral et al. 2016). The metotic foramen and fenestra ovalis of *Euparkeria* are more enlarged than in *Captorhinus*

(Heaton 1979), *Youngina* (Evans 1987), or *Prolacerta* (Evans 1986), and there is further differentiation of a ventral region, which is a pressure-relief structure.

On the reevaluation of Euparkeriidae carried out by Sookias et al. (2014), *Dorosuchus neoetus* was described with details on the braincase, which was originally studied by Sennikov (1989). Sookias et al. (2014) focused on phylogeny, so their work had no paleoneurological inferences, but a description of the braincase was presented by the authors. The paratype of *Dorosuchus neoetus* (PIN 1579/62) is a mostly complete but damaged braincase including the basioccipital, supraoccipital, otooccipitals, prootics, parabasisphenoid, and stapes. The osteology of the basioccipital, opisthotic, and supraoccipital were described, but without paleoneurological features. The paleoneurological features include a matrix-infilled pit on the anterodorsal surface of the exoccipital, ventral to the base of the paroccipital process, which may be the foramen for the hypoglossal nerve (CN XII). The prootic forms the posterior part of a large oval foramen for the trigeminal nerve. A groove located anterodorsally to the *crista prootica* holds the exit of the facial nerve, with the hyomandibular branch, and the palatine branch. Although the exit for the abducens nerve (CN VI) was not described, the authors recognized that the surface expected to hold the external foramina for the abducens nerve is anteroventrally directed. The floccular recess is recognized on the internal surface of the prootic, which is a subcircular depressed area measuring one-third of the height of the lateral wall of the braincase. The foramen for the entrance of the cerebral branch of the internal carotid artery can be seen in posterior view on each side, posterior to the base of the basiptyergoid process. On the lateral surface of the parabasisphenoid is a large fossa; no foramina are present in this fossa. This shows that the cerebral branch of the internal carotid artery entered the braincase in a posteroventral position (not laterally, as in archosaurs). The mentioned fossa connects dorsally with the ventral end of the groove for the palatal branch of the facial nerve. The preserved stapes is a thin cylinder of bone that increases gradually towards its distal end, which has a shaft diameter of 20% of the dorsoventral width of the fenestra ovalis.

Vanclavea* and *Litorosuchus

The non-archosaurian archosauriforms, *Vanclavea campi* and *Litorosuchus somnii*, represent some of the best supported cases of a semi-aquatic lifestyle early in Archosauriformes. *Vanclavea* is known by several specimens across a range of nearly 20 million years of the Late Triassic, but the most complete endocranial material currently known was described by Nesbitt et al. (2009) for the specimen GR 138. Though well-preserved and nearly complete, GR 138 was preserved as a mediolaterally compressed and twisted skeleton, causing only parts of the braincase to be observed in lateral view. Attempts to μ CT scan the skull of GR 138 have resulted in unusable scan data because of hematite and barite within the bones, which are very reflective minerals that are detrimental to the contrast of the images obtained; thus, no endocast currently exists for *Vanclavea*. A similar flattened preservation affects the Middle Triassic sister taxon to *Vanclavea*, *Litorosuchus* (Li

et al. 2016). From the braincase elements themselves, the passage of cranial nerve V through the prootic appears to have been through a nearly closed notch in *Vanleavea* (identified as the ‘trigeminal foramen’ by Nesbitt et al. 2009), though compression has displaced some skull elements. It is unclear whether *Vanleavea* had one or two exits for CN XII, but there is at least one foramen visible on the lateral side of the exoccipital; CN XII exits through two foramina in *Litorosuchus*.

Doswelliidae

The braincase anatomy of *Doswellia* is known and was described in detail (Weems 1980; Dilkes and Sues 2009; Sues et al. 2013), but the endocast is not known yet. The known skull remains of this taxon consist of the postorbital portion, and it is crushed dorsoventrally. The skull of *Doswellia* is dorsoventrally flat, and it has no infratemporal fenestrae. A relevant character is the stapes preserved lying within an otic notch in the quadrates, which have a slender configuration, similar to sauropsids.

Proterochampsidae

There is little information on the braincase and endocranial morphology of this group. The braincases of *Pseudochampsia ischigualastensis* and *Proterochampsia barrionuevoi* from the Ischigualasto Formation were described in detail by Trotteyn and Haro (2011, 2012). Particularly, the skull of *Pseudochampsia ischigualastensis* (PVSJ 567), originally described as *Chanaresuchus ischigualastensis* (Trotteyn and Haro 2012; Trotteyn and Ezcurra 2014), is fairly complete but presents some degree of dorsoventral deformation and anterior displacement, exposing the posterior end of the endocranial cavity in dorsal view. This exposed region was occupied by the hindbrain. The anterior section, corresponding to the ventral part of the forebrain, was virtually reconstructed.

The inner ear and partial endocast of *Chanaresuchus bonapartei* (MCZ 4037) was briefly mentioned and illustrated by Stocker et al. (2016), showing a dorsoventrally flattened labyrinth with an anterior semicircular canal apparently larger than the posterior one, and a lagena that is almost equivalent in height to the labyrinth. The preserved portion of the endocast lacks a floccular fossa, but has a large exit for the metotic foramen, and a single internal passage for cranial nerve XII that bifurcates. Moreover, the endocasts of *Pseudochampsia ischigualastensis* and *Tropidosuchus romeri* from the Chañares Formation were described by Trotteyn and Paulina-Carabajal (2016).

The complete skull of *Tropidosuchus romeri* (PVL 4601) was scanned and studied; it presents some deformation, but it does not affect the braincase. The braincase is almost complete, missing the laterosphenoids, and the sutures between the braincase bones are difficult to observe. A partial cranial endocast was digitally rendered, and the forebrain was reconstructed based on the impressions left on the ventral surface of the frontals by the cerebral hemispheres, the olfactory tracts, and

olfactory bulbs. The general shape of the endocast is sub-horizontal and slightly sigmoidal in lateral view, as in extant crocodylians (e.g. Witmer et al. 2008; Bona and Paulina-Carabajal 2013). Among the endocasts known for proterochampsids, *Tropidosuchus romeri* is the one studied in more detail, with endocranial characters described, and presenting the most complete reconstruction.

The general morphology of the endocast of *P. ischigualastensis* and *T. romeri* suggest the presence of a large vascular sinuses, making the observation of any brain characters difficult. As in most archosaurs, a large dorsal longitudinal venous sinus covered the cerebellum, optic tectum, and brain stem, preventing observation of their morphology (Sedlmayr 2002; Witmer et al. 2008). However, the medullary section, hypophysis, cerebral hemispheres, and olfactory tracts and bulbs could be described. The Reptilian Encephalization Quotient (REQ) was calculated for *Tropidosuchus romeri* resulting in a range of 0.34–0.9, which is similar to the lower values of the living crocodylian *Alligator mississippiensis* (Hurlburt et al. 2013). The olfactory ratio of *Tropidosuchus romeri* is approximately 57.7%. When this ratio is plotted as a function of body mass (see Zelenitsky et al. 2009), it is similar to that of *Alligator*, which has an olfactory ratio significantly higher than those predicted for theropods of similar body mass (Zelenitsky et al. 2009). Additionally, when compared with other living crocodylians, non-avian dinosaurs (e.g. Zelenitsky et al. 2009; Lautenschlager et al. 2012; Paulina-Carabajal et al. 2016), and living and extinct birds (Zelenitsky et al. 2011; Tambussi et al. 2015), it appears that *Tropidosuchus romeri* had a great reliance on olfaction. The values of both olfactory ratio and REQ in *Tropidosuchus romeri* are similar to living crocodylians, supporting a predator status for this taxon.

6.3.2 Pseudosuchian Archosaurs

Phytosauria

Phytosaurs have a long history of endocranial research, beginning nearly 150 years ago with a plaster reconstruction of the endocast of *Machaeroprotopus buceros* (Cope 1888). These taxa share general external morphological similarities to extant crocodylians, which led to assumptions of ecological and biological similarity that were not well tested until more recent and thorough examinations of their endocasts. Much of the focus in those historical studies was on derived phytosaurs (Case 1928; Mehl 1928; Camp 1930; also Holloway et al. 2013). More recent work has added to the evolutionary context of phytosaur endocranial anatomy with examinations of the endocasts of the early-branching phytosaurs *Parasuchus hislopi* (Chatterjee 1978; Stocker et al. 2016), *Parasuchus angustifrons* and *Ebrachosuchus neukami* (Lautenschlager and Butler 2016), and *Wannia scurriensis* (Lessner and Stocker 2017). The incorporation of computed tomography and μ CT allowed additional insights not just into the structure and shape of the phytosaur brain, but also semicircular canals and the extensive paranasal sinuses (Holloway et al. 2013;

Lautenschlager and Butler 2016; Lessner and Stocker 2017). These digital endocasts are still rare for phytosaur specimens because of taphonomic distortion of many phytosaur skulls and an overall skull size that is often incompatible with the field of view in a μ CT scanner. However, multiple braincases of phytosaurs exist in collections and broader sampling of endocranial anatomy is still needed for this group.

The phytosaurian encephalon is anteroposteriorly elongate and mediolaterally narrow; the encephalon in more derived phytosaurian taxa tends to be more gracile and horizontally oriented than in early-branching phytosaurs (Lautenschlager and Butler 2016; Lessner and Stocker 2017). The elongate olfactory tract extends anteriorly from the main body of the encephalon, ending anteriorly in rounded olfactory bulbs when complete (Lautenschlager and Butler 2016). This olfactory tract is straighter in early-branching phytosaurs and appears dorsally curved in lateral view in more derived phytosaurs. Dorsally, a dural peak is present in the pineal region, which may be the result of a dural venous sinus, a paratympanic sinus, or an enlarged pineal body; no pineal foramen is present in any known phytosaur. The hypophysis in phytosaurs is generally large, but appears largest in the early branching taxa *Wannia*, *Parasuchus*, and *Ebrachosuchus* (Lessner and Stocker 2017); *Machaeroprotopus mccauleyi* appears to lack a hypophysis (Holloway et al. 2013). The internal carotid arteries extend posteroventrally from the ventralmost point of the hypophysis and exit the braincase ventrolaterally from the basisphenoid tubera. All phytosaurs appear to have both cephalic and pontine flexures, though the degree of flexure is smaller in more derived phytosaurs. Small floccular lobes are present. The optic tract (CN II) exits through a single foramen formed by the laterosphenoids. The trigeminal nerve (CN V) extends many small accessory nerve branches to the alveoli, facial region, and mandible, similar to the branching in extant crocodylians. These nerve endings are associated with small randomly distributed external pits concentrated at the anterior portions of the dentaries and premaxillae.

The endosseous labyrinths in phytosaurs (when reconstructed) tend to have longer anterior semicircular canals, with the three canals oriented at roughly right angles to one another (Holloway et al. 2013; Lautenschlager and Butler 2016; Stocker et al. 2016; Lessner and Stocker 2017). The lagenae are generally elongate, as in extant crocodylians (Lessner and Stocker 2017).

Aetosauria

The endocasts of only two aetosaurians are currently known based on natural and artificial moulds. The first aetosaurian endocast of one of the largest and most characteristic species of the group was published by Case (1921). This was an artificial physical endocast of the holotype of *Desmotosuchus spurensis* (*Desmotosuchus "haplocerus"* at that time) representing only the encephalon and surrounding soft tissues. On the other hand, the first natural endocast of an aetosaur was recently described for *Neoaetosauroides engaeus* (von Baczko et al. 2018) which includes the cast of the encephalon, surrounding soft tissues, and inner ear. This is

complemented by the digital endocast of the best-preserved skull (PVL 5698) and the natural endocast of the olfactory region of a third skull (PVL 4363).

Two different morphologies were recognized within aetosaurs. *Desmatosuchus spurensis* has short and wide olfactory tracts and rounded olfactory bulbs, whereas *Neoaetosauroides engaeus* has elongated and narrow tracts and elliptic olfactory bulbs. The inner ear of *Neoaetosauroides* also differs from that of *Desmatosuchus* as figured by Stocker et al. (2016) and von Baczko et al. (2021). The inner ear of the former has a dorsoventrally high endosseous labyrinth and a short lagena; furthermore, the anterior and posterior semicircular canals have similar curvatures, contrasting with those of *Desmatosuchus spurensis* that are different in size. Moreover, the endosseous labyrinth of the latter is wider than high, and the lagena is proportionally longer than in *Neoaetosauroides engaeus*. New digital endocasts of *Desmatosuchus spurensis* and *Desmatosuchus smalli* have been recently published by von Baczko et al. (2021), showing a more complete encephalon for *Desmatosuchus* than that previously published by Case (1921). A remarkable feature recognized in these new models is a dorsal midline structure between the cerebral hemispheres and optic lobes. The interpretation of this dorsal projection has been argued by previous authors (Case 1921; Edinger 1929; Hopson 1979) but von Baczko et al. (2021) suggest it corresponds to the dorsal dural venous sinus system because it has clear characteristics indicating a vascular origin (diploic veins). This interpretation would not be in conflict with the presence of an epiphysis (Case 1921; Edinger 1929) and the presence of both structures could be true.

The natural marks left by the encephalon on the ventral surface of the skull roof can also be seen in *Stagonolepis olenkae* (ZPAL AbIII/466/17). On this surface the area occupied by the cerebral hemispheres, olfactory bulbs and tracts can be recognized as well as some spaces occupied by the dorsal longitudinal venous sinus. The olfactory tract is wide, resembling that of *Desmatosuchus spurensis*. Several other braincases of aetosaurs have been published to date (e.g. *Stenomyti huangae*: Small and Martz 2013; *Longosuchus meadei*: Parrish 1994; *Paratypothorax coccinarum*: Schoch and Desojo 2016; *Scutarx deltatylus*: Parker 2016; *Aetosauroides scagliai*: Paes Neto et al. 2021) but their endocranial anatomy still awaits to be studied.

Ornithosuchidae

The cranial endocast of ornithosuchids is currently known for the digital reconstruction of *Riojasuchus tenuiseps* (von Baczko and Desojo 2016) (Los Colorados Formation, Argentina) and a partial natural endocast of *Venaticosuchus rusconii* (Ischigualasto Formation, Argentina). The general morphology of the encephalon of *Riojasuchus tenuiseps* (PVL 3827) is tall and sigmoid. The forebrain almost triples its width from the anterior edge to the widest region of the cerebral hemispheres, and these are slightly longer than wide. The angle between the anterior and mid-brain is approximately 130°. Few cranial nerves (CN) can be recognized on the endocast of *Riojasuchus tenuiseps*. The olfactory tracts (CN I) on the anterior end of the forebrain are short, the trigeminal nerve (CN V) exits through a single

foramen, which implies that the branches of this nerve diverge outside the braincase. The hypophysis can be identified projecting posteroventrally from the ventral region of the anterior brain.

Recently, a partial natural cranial endocast has been found in association with the skull of *Venaticosuchus rusconii* (PVL 2578) and represents part of the brain and the right inner ear (Fig. 6.5a–d). The partial endocast corresponds to the middle and posterior brain, from the level of the cephalic flexure up to the posterior end of the brain. The cephalic flexure cannot be measured because of the incompleteness of the endocast, but the pontine flexure is approximately 140°, as in *Riojasuchus tenuisiceps*. The anterior portion of the dorsal surface of the endocast has a transversal ridge that would correspond to the suture of the frontals and parietals. The dorsal surface of the posterior region of the endocast has two smooth longitudinal lines that probably correspond to the medial margins of the exoccipitals, which do not contact each other as in *Riojasuchus tenuisiceps* (von Baczko and Desojo 2016). The posterior end which corresponds to the foramen magnum is oval, being 1.75 times wider than tall, and resembling the condition of *Riojasuchus tenuisiceps* (von Baczko and Desojo 2016). A large subtriangular exit for the trigeminal nerve (CN V) can be recognized on the anteroventral margin of the middle brain, anterior to the labyrinth. A transversal ridge that corresponds to the ventral margin of the metotic foramen (CN IX–XI) is located posterior to the labyrinth. The midbrain is strongly constricted where the endosseous labyrinth is located, and no projection corresponding to the flocculus can be recognized anterior to this area as in *R. tenuisiceps*. The endosseous labyrinth is preserved within the partially eroded prootics and opisthotics that are attached to the cranial endocast. The anterior and posterior semicircular canals are exposed through the broken surface of the otic bones and form an angle of approximately 90° with each other.

Erpetosuchidae

The endocast of *Parringtonia gracilis* from the Middle Triassic of Tanzania was described in detail by Nesbitt et al. (2017) based on a growth series of three braincases, one of which (NMT RB426) was well-enough preserved to present a description of the encephalon, endosseous labyrinths, and cranial nerve trunks. This taxon was hypothesized to support a high degree of conservatism and homoplasy in braincase anatomy and brain architecture among pseudosuchians. The encephalon is anteroposteriorly elongate, with a cephalic flexure similar to that of phytosaurs, aetosaurs, and *Riojasuchus* (e.g. Case 1921, 1928; von Baczko and Desojo 2016; Nesbitt et al. 2017). The long olfactory tracts and rounded bulbs with a medial dividing sulcus were reconstructed based on their dorsal surface impressions into the ventral surface of the frontals; these tracts may have had their lengths elongated by displacement of the laterosphenoids. No hypophysis was reconstructed. A slight dural peak is present at the apex of the midbrain flexure. No flocculus is obvious in the hindbrain region. A small, laterally-opening foramen in the ventral ramus of the opisthotic was identified as the perilymphatic foramen. The internal carotids enter

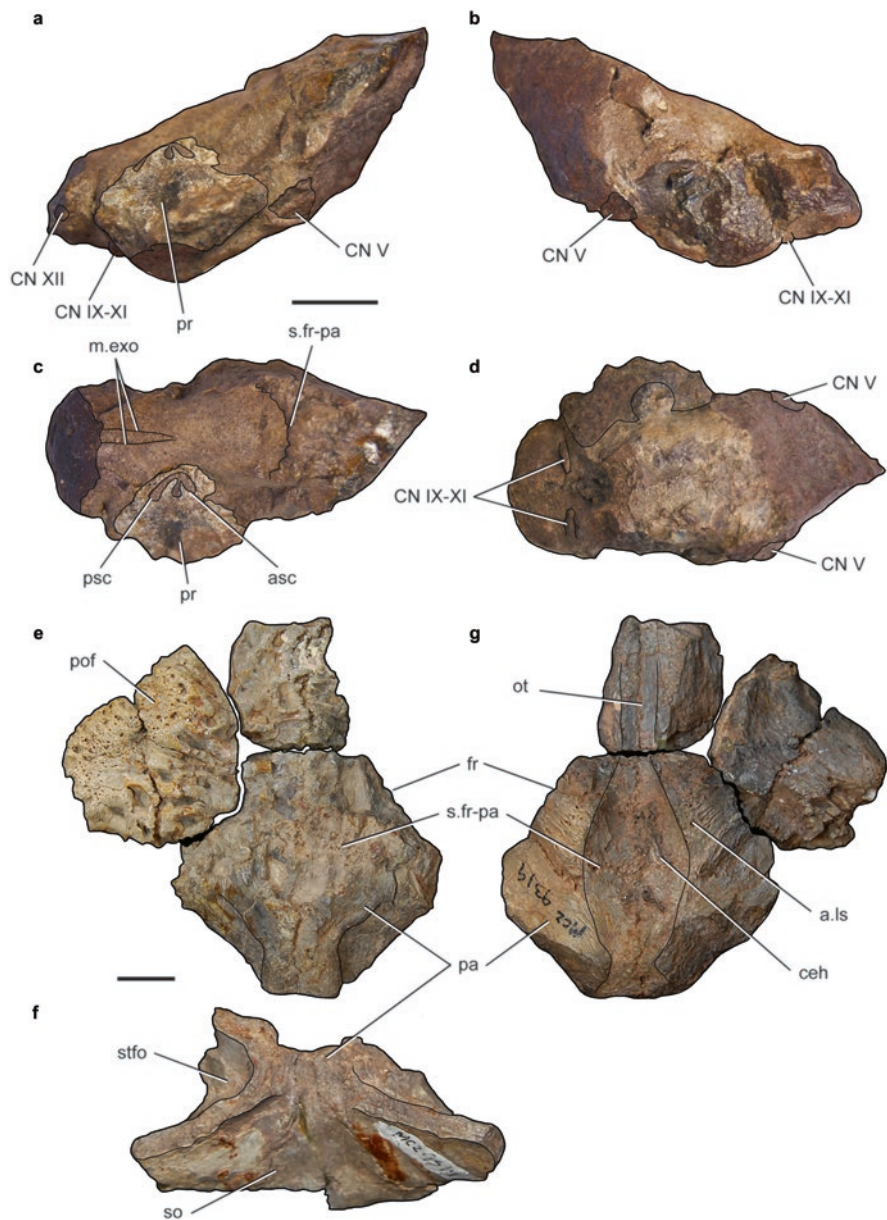


Fig. 6.5 Natural endocranial cast of the ornithosuchid *Venaticosuchus rusconii* (PVL 2578) in (a), right, (b), left, (c), dorsal, and (d), ventral views. Fragmentary skull roof of the erpetosuchid *Tarjadia ruthae* (MCZ 9319) in (e-f), dorsal and (g), ventral views. Abbreviations: *a.ls* articular surface for laterosphenoid, *asc* anterior semicircular canal, *ceh* cerebral hemispheres, *CN* cranial nerve foramina, *fr* frontal, *m.exo* medial margin of the exoccipitals, *ot* olfactory tract, *pa* parietal, *pof* postfrontal, *pr* prootic, *psc* posterior semicircular canal, *s.fr-pa* suture between frontal and parietal, *so* supraoccipital, *stfo* supratemporal fossa. Scale bars = 1 cm

the endocranial space ventrally unlike in other pseudosuchians. Cranial nerve V passes through an undivided trigeminal foramen formed by the prootic and laterosphenoid. Cranial Nerve VI exits through the parabasisphenoid. Two crests (Crest 1 and Crest 2 of Nesbitt et al. 2017) confine the hyomandibular path of CN VII, similar to the condition in *Revueltosaurus callenderi* (Parker et al. 2021) and aetosaurs (Gower and Walker 2002). The hypoglossal nerve (CN XII) exits through two foramina on each side. The endosseous labyrinths show that the semicircular canals were all roughly the same length, and the anterior and posterior canals were dorso-ventrally squat.

Archeopelta arborensis from the Middle-Late Triassic of Brazil was described by Desojo et al. (2011), who referred it together with *Tarjadia ruthae* to Doswelliidae. However, more recent studies recover both species within Erpetosuchidae (Ezcurra et al. 2017). The poorly preserved occipital region of the braincase of *Archeopelta* was described, including the identification of several cranial foramina (V-VII, IX-XII). A single exit was recognized for CN XII between the exoccipital and parabasisphenoid. Ezcurra et al. (2017) reinterpreted the putative foramina for CN VI as the exit for the cephalic branch of the internal carotid arteries located on the ventral surface of the parabasisphenoid at base of the basiptyergoid process. However, due to the poor preservation of the specimen no endocast was reconstructed.

The fragmentary holotype and MCZ referred specimen of *Tarjadia ruthae*, including a partial braincase, were described by Arcucci and Marsicano (1998), and some endocranial features such as the olfactory tracts and bulbs are mentioned. However, considering the new specimens currently available (Ezcurra et al. 2017) and after restudying by firsthand the referred specimen MCZ 9319 we reinterpret some of those features. For instance, the groove on the ventral surface of the frontal described as “olfactory channel” appears to correspond to the olfactory tract and the posterior depression at the suture of the frontal and parietal originally identified as “housing the olfactory bulbs” would correspond to the cerebral hemispheres (Fig. 6.5e–g). This interpretation is in accordance with the elongated cranial endocast described for *Parringtonia gracilis* (Nesbitt et al. 2017). The unpublished endocast of a new and more complete specimen of *Tarjadia ruthae* (CRILAR PV 478) is being studied by some of the authors (BvB, JBD, MJT) and also supports these new interpretations.

Gracilisuchidae

A partial artificial endocast from the holotype of *Gracilisuchus stipanicorum* PULR 08 was made, but few anatomical structures can be identified because it corresponds to the posterodorsal surface of the endocranial cavity. Unfortunately, a medical CT scan from the same type material did not allow the reconstruction of the encephalon because of its poor preservation and small size; only gross neurocranial features could be interpreted (e.g. skull roof, paroccipital processes, basiptyergoid processes, cultriform process).

On the other hand, a microtomography of the referred specimen MCZ 4117 was performed, but its detailed description is still pending. Stocker et al. (2016) figured the inner ear (semicircular canals and vestibule) and middle and posterior encephalon of this specimen; the anterior semicircular canal has a markedly larger curvature radius than the posterior one, and a moderately developed flocculus can be recognized. The exit for the transversooccipital veins can also be identified, but the lagena could not be reconstructed. Fabbri et al. (2017) only illustrated a preliminary digital reconstruction of the brain of the same specimen, but without the labyrinth. It is possible to recognize a low, elongated encephalon with low cephalic and pontine flexures, long and narrow olfactory tracts, and elliptic olfactory bulbs.

Poposauroidea

A physical artificial endocast of the encephalon of *Shuvosaurus inexpectatus* was carried out by Lehane (2005) as part of his unpublished Master's thesis and later figured by Holloway et al. (2013). Unfortunately, the endocast was only illustrated with hypothesized drawings, in which some regions of the encephalon are complete, but the actual braincases of *Shuvosaurus* did not preserve the corresponding part of the braincase.

The moulds left by the encephalon on the braincases of the holotype and referred specimen of *Shuvosaurus inexpectatus* (TTUP 9280 and 9282) exhibit well expanded cerebral hemispheres and marked floccular lobes. The ventral surface of the hypophyseal fossa is very shallow on the basisphenoid, so the extension of the hypophysis is not clear. A single large passage can be recognized for the trigeminal nerve (CN V); the metotic foramen (CN IX-XI) is large but cannot be separated from the opening for the fenestra ovalis because the region is slightly damaged (TTUP 9280). Considering the structure of the braincase of *Shuvosaurus inexpectatus*, the fenestra ovalis does not seem to be subdivided, and the element separating it from the metotic foramen probably corresponded to the ventral process of the opisthotic. Cranial nerve XII appears to have two internal foramina but a single external foramen on TTUP 9280 and 9282. The dorsal region of the midbrain that Lehane (2005) identified as a triangular-shaped cerebellum would more likely be occupied by the dorsal longitudinal venous sinus as well as the meninges which represent a large portion of the endocranial cavity in reptiles, unlike avian archosaurs.

The braincase and complete skull of *Effigia okeeffeae* was described and CT scanned by Nesbitt (2007), but no endocranial reconstruction was made – probably because the skull is partially crushed. Nevertheless, several structures corresponding to the encephalon were identified, such as the foramina for cranial nerves V, VII, and VIII on a disarticulated prootic. A putative small but deep hypophyseal fossa was identified on the dorsal surface of the basisphenoid, although it seems to be a continuation of the dorsal groove of the cultriform process. The exit for the cerebral branch of the internal carotids is on the lateral surface of the same element. Part of the floccular (= auricular) fossa can be recognized on the medial surface of the prootic.

Additionally, Gower and Nesbitt (2006) described a beautifully preserved braincase of *Arizonasaurus babbitti*, but no endocast was reconstructed. A remarkable feature present in this species is that the exits for the cerebral branches of the internal carotids are located on the ventral surface of the parabasisphenoid, resembling the condition of erpetosuchids and non-archosaurian archosauriforms and differing from most pseudosuchians, in which these exits are lateral.

Non-crocodylomorph Loricata

Little is known about the endocast morphology of non-crocodylomorph loricatans. Just the endocast of the prestosuchid *Prestosuchus chiniquensis* was published by Mastrantonio et al. (2019), and the posterior region of the endocast and partial inner ear of the rausuchid *Postosuchus kirkpatricki* was figured by Stocker et al. (2016).

The digital endocast of *Prestosuchus chiniquensis* (UFRGS-PV-0629-T) is high and sigmoid with strong flexures. It has large olfactory bulbs, although they are not as large as illustrated by Mastrantonio et al. (2019). In that reconstruction, the anterior half of the supposed olfactory bulbs actually corresponds to the nasal cavity proper, according to Fonseca et al. (2020). The olfactory tracts are narrow and longer than the cerebral hemispheres, being almost as long as the rest of the encephalon. Unfortunately, few cranial nerves were identified on the endocast of *Prestosuchus chiniquensis*. The olfactory tract, representing CN I, was mistakenly described as CN II by Mastrantonio et al. (2019). The trigeminal nerve (CN V) exhibits a single exit as in most pseudosuchians and non-archosaurian archosauriforms, and the hypoglossal nerve (CN XII) also appears to have a single internal and external passage in *Prestosuchus chiniquensis*. The general morphology of this endocast resembles that of theropod dinosaurs and contrasts with pseudosuchian living forms, the crocodylians. The inner ear of *Prestosuchus* has not been studied yet, but that of *Postosuchus* was illustrated by Stocker et al. (2016). The labyrinth of *Postosuchus kirkpatricki* is proportionally high and has asymmetrical anterior and posterior semicircular canals, with the anterior canal being almost twice the height of the posterior one. A moderately developed floccular lobe can be recognized through the anterior semicircular canal and appears to be smaller than that of *Triopticus* (Stocker et al. 2016). In his unpublished master's thesis, Weinbaum (2002) mentioned the development of an artificial endocast, but clarified that its description could not be included in said contribution. He only highlighted the similarity between the brain of *Postosuchus* and that of living crocodiles, and the presence of an enlarged hind-brain that probably explained its terrestrial habit and upright posture.

Few other well-preserved braincases of non-crocodylomorph loricatans were published describing their external morphology, namely *Batrachotomus kupferzellensis*, *Heptasuchus clarki*, *Postosuchus kirkpatricki*, and *Saurosuchus galilei* (Alcober 2000; Gower 2002; Weinbaum 2011; Nesbitt et al. 2020). However, the endocranial cavity of the last two are currently being studied by some of the authors (BvB, JBD) and will soon provide new information about the endocranial anatomy of this group.

6.4 Brain Evolution and Paleobiological Inferences

In general terms, the cranial endocasts of non-archosaurian archosauriforms (Fig. 6.6), derived phytosaurs, erpetosuchids, and crocodylomorphs are elongated, narrow, and share a more horizontal organization, with low cephalic and pontine flexures (e.g. *Triopticus primus*, *Tropidosuchus romeri*, *Erythrosuchus africanus*, *Garjainia prima* [=“*V. triplicostata*”], *Machaeropsopus pristinus*, *Parringtonia gracilis*, *Alligator mississippiensis*, *Caiman yacare*) (Gower and Sennikov 1996a; Lautenschlager and Butler 2016; Nesbitt et al. 2017; Lessner and Stocker 2017). Other pseudosuchians such as aetosaurs, ornithosuchids, gracilisuchids, basal loricatans, and poposauroids have slightly more pronounced flexures; however, they do not reach the marked flexures seen in the verticalized, robust endocasts of avemetatarsalian archosaurs (Lehane 2005; von Baczko and Desojo 2016; Stocker et al. 2016; Lessner and Stocker 2017; von Baczko et al. 2018; Mastrantonio et al. 2019).

The Reptile Encephalization Quotient (Hurlburt 1996) is a measurement that was not frequently considered among the literature of Triassic archosauriforms and pseudosuchians. A higher quotient is linked to a better capacity for processing and integrating neurosensorial information and responding to environmental stimuli. The REQ was only calculated for *Tropidosuchus romeri* considering ratios of 37% and 50% of the endocranial volume since the brain does not fill the entire cavity (Hopson 1979). The calculations resulted in a range of minimum and maximum REQs for the proterochampsid *Tropidosuchus romeri* of 0.34–0.9, which overlaps



Fig. 6.6 Comparison of the cranial endocasts of selected archosauriforms and pseudosuchians and their phylogenetic relationships (based on Stocker et al. 2016; Ezcurra et al. 2017; Wynd et al. 2019). Abbreviations: *Ar* Archosauria, *Arf* Archosauriformes, *Euc* Eucrocopoda, *Pr* Proterochampsia, *Ps* Pseudosuchia, *Su* Suchia. Encephalon in blue, cranial nerves in yellow, labyrinth in pink, cerebral branch of internal carotids in red

the lower range of REQs calculated for the living crocodile *Alligator mississippiensis*.

6.4.1 Sensory Evolution

The head posture in fossil reptiles has been inferred by orienting the lateral semicircular canal (LSC) of the endosseous labyrinth horizontal as in most living tetrapods (de Beer 1947), although some studies disagree with the use of the LSC as reference system. These studies documented a misalignment of the LSC and Earth horizontal and instead suggested aligning the ventral surface of the braincase to the horizontal plane (Hullar 2006; Taylor et al. 2009; Marugán-Lobón et al. 2013). Despite this debate, the horizontal LSC was still used to infer an anterodorsally inclined alert posture of the head for *Proterosuchus fergusi* (Brown et al. 2020) and for phytosaurs (Holloway et al. 2013; Lessner and Stocker 2017) as an adaptation to aquatic life habits. This would allow them to keep the nares and orbits over the waterline while the rest of the head and body remains hidden underwater. On the other hand, the head posture inferred for other terrestrial archosauriforms such as *Triopticus primus* and the aetosaurs *Neoaetosauroides engaeus*, *Desmatosuchus spurensis*, and *D. smalli* resulted in an anteroventral inclination of the head (Stocker et al. 2016; von Baczko et al. 2018, 2021) better adapted for terrestrial habits and potentially revealing behavioral aspects such as agonistic behavior.

Locomotor agility has been inferred through the development of the flocculus and the semicircular canals of the labyrinth, which are involved in coordinating the movements of the eyes and head to stabilize gaze and equilibrium (Voogd and Wylie 2004; Witmer et al. 2003, 2008; Georgi and Sipla 2008). The flocculus is very variable among archosauriforms and pseudosuchian archosaurs. A moderately developed flocculus is present in the archosauriforms *Triopticus* and *Euparkeria*, some phytosaurs, *Gracilisuchus*, *Shuvosaurus*, and basal loricatans (*Postosuchus*, *Batrachotomus*). But in other archosauriforms such as *Proterosuchus*, *Erythrosuchus*, *Tropidosuchus*, possibly *Chanaresuchus*, and aetosaurs (*Desmatosuchus*, *Neoaetosauroides*) the floccular fossa is very shallow and almost absent. A larger development of the flocculus might be expected in active predators because of the need to stabilize gaze after quick movements; however, this is not evidenced in the earliest forms such as *Proterosuchus* and *Erythrosuchus*.

The geometry of the semicircular canals has been proposed to be linked to certain locomotor habits. Particularly, in the case of non-avemetatarsalian archosauriforms, high labyrinths have been related to erect limb posture or/and bipedal gait, whereas low and wide labyrinths have been associated to aquatic habits (Witmer et al. 2003; Georgi and Sipla 2008; Hanson et al. 2021). Dorsoventrally low aspect ratios of the semicircular canals have been associated with aquatic habits as evidenced in phytosaurs, thalattosuchians, living crocodylians, and other reptiles like some aquatic turtles (Georgi and Sipla 2008; Schwab et al. 2020). However, other studies have recognized that, within Archosauromorpha and Pseudosuchia, there is

no significant correlation between the aquatic adaptation and low aspect ratios of semicircular canals or even the increase in diameter of the endosseous canals (Bronzati et al. 2021). Furthermore, early pseudosuchians show a remarkable disparity in the geometry of the labyrinth and for that reason the morphology seen in living crocodiles cannot be interpreted as the plesiomorphic reptilian condition.

The olfactory acuity of some archosauriforms has been inferred by calculating their olfactory ratio (OR) and comparing it to that of modern relatives or analogues (Zelenitsky et al. 2009). The olfactory ratio of *Proterosuchus fergusi* is similar to that of living crocodiles, which are considered to have a well-developed sense of smell, whereas that of *Tropidosuchus romeri* is slightly lower than *Alligator mississippiensis* (Brown et al. 2020; Trotteyn and Paulina-Carabajal 2016). Some works on pseudosuchian archosaurs mentioned the similarity in shape and relative size of their olfactory bulbs and those of living crocodiles, therefore assuming similar olfactory capacities; however, they did not quantitatively compare their ORs (Lautenschlager and Butler 2016; Lessner and Stocker 2017; von Baczko et al. 2018).

The estimation of visual acuity is a pending issue for Triassic archosauriforms and pseudosuchians because very few specimens have preserved sclerotic rings, which could provide information on optical function. Sclerotic rings are known in few pseudosuchians such as *Gracilisuchus stipanicorum* (Lecuona 2013; Lecuona et al. 2020) and *Quianosuchus admixtus* (Li et al. 2006), but no estimations of their visual acuity have been made. Despite the presence of some small bony elements in the orbit of aetosaurs, no sclerotic rings are present in these pseudosuchians as discussed by several authors (Walker 1961; Desojo and Báez 2007; Schoch 2007; Nesbitt et al. 2013b).

Sclerotic rings are registered in the non-archosaurian archosauriforms *Euparkeria capensis* and *Proterosuchus fergusi* (= *P. "vanhoepni"*), from which scotopic and mesopic vision have been tentatively proposed, respectively (Schmitz and Motani 2011). This implies that they were better adapted to dim light environments. However, because they were found in high latitudes near the polar circle, they probably experienced extended periods of daylight or darkness depending on the season. For that reason, it is uncertain if this inference can be properly supported.

Hearing sensitivity has been estimated considering the length of the lagena (=cochlear duct) in several archosauriforms and pseudosuchians (Sobral et al. 2016; Brown et al. 2020). These studies recognized that the plesiomorphic condition seen in the most basal archosauriforms, such as *Proterosuchus fergusi*, is the presence of a very short lagena, which in turn suggests an acoustic estimation near the lowest values known for modern crocodylians. Since sociality and vocality are strongly linked, the low auditory ranges of *P. fergusi*, and therefore low complexity in vocalization, might also be an indicative that it lived in small groups or even in solitary (Brown et al. 2020).

An increase in the length of the lagena can be recognized crownwards in other archosauriforms and in most archosaurs. A moderately elongate lagena can be identified in the archosauriforms *Euparkeria capensis*, *Triopticus primus*, and *Chañaresuchus bonapartei*, in phytosaurs (*Wannia*, *Ebrachosuchus*, *Parasuchus*), and in aetosaurs (*Neoaetosauroides*, *Desmotosuchus*), but not in the erpetosuchid

Parringtonia gracilis, whose lagena is remarkably shorter than that of extant crocodylians. In some particular cases, the lagena has a secondary tendency towards its reduction as is the case of some aquatic pseudosuchians like thalattosuchians crocodylomorphs and some living crocodiles (Schwab et al. 2020). The elongation of the lagena in these groups is related to an extension of their hearing range to high-frequencies and therefore a probable improved hearing ability and better pitch discrimination (Gleich and Manley 2000; Gleich et al. 2005).

6.5 Future Directions

As shown in the previous sections, paleoneurology of extinct Triassic archosauriforms and pseudosuchians is a flourishing area, though it still needs to be explored in more detail because at least the 80% of the known species of these groups have not been studied from a paleoneurological approach (Fig. 6.3b). Very few quantitative analyses have been made about the sensorial capacities of archosauriforms and pseudosuchians, which might be a consequence of the poor knowledge about these groups. Currently, a wide range of specimens with well-preserved braincases are available and new technologies applied to paleontology are allowing us the study of their internal structures, however their paleoneurological aspects remain unexplored (e.g. aetosaurs, loricatans, erpetosuchids) (Fig. 6.3a).

Their study will be essential in order to properly recognize the neuroanatomical diversity within groups as well as possible macroevolutionary trends concerning the brain and sensorial organs of these extinct reptiles. A further step in this area should be the quantification of the sensorial capacities, such as olfaction, vision, hearing, and encephalization, in order to draw paleobiological interpretations about extinct lifeforms and understand how they behaved and which role they occupied in the Triassic continental communities. The information obtained from these studies will be crucial to identify evolutionary patterns that occurred through the Triassic, when the rise of the major lineages of modern reptiles took place.

6.6 Concluding Remarks

This chapter presents an updated review of reptilian paleoneurology particularly focused on early extinct archosauriforms and pseudosuchians. We include the descriptions of known endocranial casts of the major clades as well as the paleobiological interpretations that can be inferred from them.

Moreover, we present the description of the first natural endocast of *Venaticosuchus rusconii*, an ornithosuchid from the Ischigualasto Formation (Carnian, Late Triassic) of Argentina. The paleoneurology of this group was previously known only from the digital endocast of *Riojasuchus tenuisiceps* (von Baczko and Desojo 2016), therefore this new information expands the knowledge for this group.

We provide a brief reinterpretation of the endocranial features of *Shuvosaurus inexpectatus*, a peculiar poposauroid from the Dockum Group (Norian, Late Triassic), USA, described by Lehane (2005) in his unpublished Master's thesis. Based on firsthand observation of the holotype and referred specimen, we recognize some differences from the original description that sheds light on the poorly understood neuroanatomy of poposauroids.

Modern studies are including certain paleoneurological features (e.g. shape of encephalon or labyrinth) in a wide range of analysis concerning morphological disparity of Archosauriformes (e.g. Fabbri et al. 2017; Brown et al. 2020; Bronzati et al. 2021; Hanson et al. 2021). However, many of the specimens included in those studies were not described in detail from a paleoneurological perspective and considered only partial information about the endocranial morphology. This supports the need for more detailed and complete descriptions of the endocranial anatomy of archosauriforms and pseudosuchians, which will allow us to explore more in depth their paleoneurology and sensorial biology, currently known from very scarce examples.

Acknowledgments We are thankful to the editors M.T. Dozo, A. Paulina-Carabajal, T.E. Macrini, and S. Walsh for inviting us to contribute to this special publication. We thank Lawrence Witmer, Ariana Paulina-Carabajal, David Gower, Martín Ezcurra, and Paula Bona for helpful comments on different aspects of this thematic volume. We thank A. Elbakyan, J. Bar, and Wikipaleo Group for allowing free literature sharing. Funded by Agencia Nacional de Investigaciones Científicas y Tecnológicas, PICT 2018-0717 (to JBD), PICT 2018-853 (to BvB), and the Department of Geosciences, VT (to MRS).

References

- Alcober O (2000) Redescription of the skull of *Saurosuchus galilei* (Archosauria: Rauisuchidae). *J Vertebr Paleontol* 20(2):302–316. [https://doi.org/10.1671/0272-4634\(2000\)020\[0302:ROTSOSJ2.0.CO;2](https://doi.org/10.1671/0272-4634(2000)020[0302:ROTSOSJ2.0.CO;2)
- Arcucci A, Marsicano CA (1998) A distinctive new archosaur from the Middle Triassic (Los Chañares Formation) of Argentina. *J Vertebr Paleontol* 18(1):228–232. <https://doi.org/10.1080/002724634.1998.10011046>
- Balanoff AM, Bever GS, Rowe TB et al (2013) Evolutionary origins of the avian brain. *Nature* 501(7465):93–96. <https://doi.org/10.1038/nature12424>
- Benton MJ (1984) The relationships and early evolution of the Diapsida. In: Ferguson MWJ (ed) *The structure, evolution, and development of reptiles*, vol 52. *Symposia of the Zoological Society of London*, London, pp 575–596
- Benton MJ (1985) Classification and phylogeny of the diapsid reptiles. *Zool J Linnean Soc* 84:97–164. <https://doi.org/10.1111/j.1096-3642.1985.tb01796.x>
- Benton MJ, Clark JM (1988) Archosaur phylogeny and the relationships of the Crocodylia. In: Benton MJ (ed) *The phylogeny and classification of the tetrapods*, vol 1. Clarendon Press, Oxford, pp 295–338
- Bona P, Paulina-Carabajal A (2013) *Caiman gasparinae sp. nov.*, a huge alligatorid (Caimaninae) from the late Miocene of Paraná, Argentina. *Alcheringa* 37(4):462–473. <https://doi.org/10.1080/003115518.2013.785335>
- Bonaparte JF (1984) Locomotion in rauisuchid thecodonts. *J Vertebr Paleontol* 3(4):210–218

- Brink AS (1955) Notes on some thecodonts. *Navors Nas Mus* 1(6):141–148
- Bronzati M, Benson RB, Evers SW et al (2021) Deep evolutionary diversification of semicircular canals in archosaurs. *Curr Biol* 31(12):2520–2529. <https://doi.org/10.1016/j.cub.2021.03.086>
- Brown EE, Butler RJ, Ezcurra MD et al (2020) Endocranial anatomy and life habits of the Early Triassic archosauriform *Proterosuchus fergusi*. *Palaeontology* 63(2):255–282. <https://doi.org/10.1111/pala.12454>
- Brusatte SL, Muir A, Young MT et al (2016) The braincase and neurosensory anatomy of an Early Jurassic marine crocodylomorph: implications for crocodylian sinus evolution and sensory transitions. *Anat Rec* 299(11):1511–1530. <https://doi.org/10.1002/ar.23462>
- Butler RJ, Brusatte SL, Reich M et al (2011) The sail-backed reptile *Ctenosauriscus* from the latest Early Triassic of Germany and the timing and biogeography of the early archosaur radiation. *PLoS One* 6(10):e25693. <https://doi.org/10.1371/journal.pone.0025693>
- Butler RJ, Sullivan C, Ezcurra MD et al (2014) New clade of enigmatic early archosaurs yields insights into early pseudosuchian phylogeny and the biogeography of the archosaur radiation. *BMC Evol Biol* 14(1):1–16. <https://doi.org/10.1186/1471-2148-14-128>
- Butler RJ, Ezcurra MD, Liu J et al (2019) The anatomy and phylogenetic position of the erythrosuchid archosauriform *Guchengosuchus shiguaiensis* from the earliest Middle Triassic of China. *Peer J* 7:e6435. <https://doi.org/10.7717/peerj.6435>
- Camp CL (1930) A study of the phytosaurs with description of new material from western North America, vol 10. University of California Press, Berkeley
- Case EC (1921) On an endocranial cast from a reptile, *Desmatosuchus spurensis*, from the Upper Triassic of western Texas. *J Comp Neurol* 33:132–147
- Case EC (1928) An endocranial cast of a phytosaur from the upper Triassic beds of western Texas. *J Comp Neurol* 45:161–168
- Case EC (1929) Description of the skull of a new form of Phytosaur. *Memoirs of the University of Michigan Museums-Museum of Paleontology-Volume II*
- Chatterjee S (1978) A primitive parasuchid (phytosaur) reptile from the Upper Triassic Maleri Formation of India. *Palaeontology* 21:83–127
- Cope ED (1887) A contribution to the history of the Vertebrata of the Trias of North America. *Proc Am Philos Soc* 24(126):209–228
- Cope ED (1888) The pineal eye in extinct vertebrates. *Am Nat* 22(262):914–917
- Cruikshank ARI (1970) Early thecodont braincases. In: *Proceedings of the international Gondwana symposium*, vol 2, pp 683–685
- de Beer GR (1947) Presidential address: how animals hold their heads. *Proc Linn Soc Lond* 159(2):125–139. <https://doi.org/10.1111/j.1095-8312.1947.tb00491.x>
- De-Oliveira TM, Kerber L, de França MAG, Pinheiro FL (2022) Archosauriform remains from the Lower Triassic Sanga do Cabral Formation of Brazil. *J Vertebr Paleontol* 41(6):e2068022. <https://doi.org/10.1080/02724634.2022.2068022>
- Desojo JB, Báez AM (2007) Cranial morphology of the Late Triassic South American archosaur *Neoaetosauroides engaeus*: evidence for aetosaurian diversity. *Palaeontology* 50(1):267–276. <https://doi.org/10.1111/j.1475-4983.2006.00608.x>
- Desojo JB, Ezcurra MD, Schultz CL (2011) An unusual new archosauriform from the Middle–Late Triassic of southern Brazil and the monophyly of *Doswelliidae*. *Zool J Linn Soc* 161(4):839–871. <https://doi.org/10.1111/j.1096-3642.2010.00655.x>
- Desojo JB, von Baczko MB, Rauhut OW (2020) Anatomy, taxonomy, and phylogenetic relationships of *Prestosuchus chiniquensis* (Archosauria: Pseudosuchia) from the original collection of von Huene, Middle-Late Triassic of southern Brazil. *Palaeontol Electron* 23:a04. <https://doi.org/10.26879/1026>
- Dilkes D, Sues HD (2009) Redescription and phylogenetic relationships of *Doswellia kaltensbachi* (Diapsida: Archosauriformes) from the Upper Triassic of Virginia. *J Vertebr Paleontol* 29(1):58–79. <https://doi.org/10.1080/02724634.2009.10010362>
- Edinger T (1929) Die Fossilen Gehirne. *Ergeb Anat und Entwicklungsgesch* 28:1–249
- Edinger T (1975) *Paleoneurology 1804–1966: an annotated bibliography*, vol 49. Springer, Berlin/Heidelberg

- Evans SE (1986) The braincase of *Prolacerta broomi* (Reptilia, Triassic). *Neues Jahrb Geol Palaontol Abh* 173(2):181–200
- Evans SE (1987) The braincase of *Youngina capensis* (Reptilia: Diapsida; Permian). *Neues Jahrb Geol Palaontol Monatsh* 4:193–203. <https://doi.org/10.1127/njgpm/1987/1987/193>
- Evans DC, Ridgely R, Witmer LM (2009) Endocranial anatomy of lambeosaurine hadrosaurids (Dinosauria: Ornithischia): a sensorineural perspective on cranial crest function. *Anat Rec* 292(9):1315–1337. <https://doi.org/10.1002/ar.20984>
- Evers SW, Neenan JM, Ferreira GS et al (2019) Neurovascular anatomy of the protostegid turtle *Rhinochelys pulchriiceps* and comparisons of membranous and endosseous labyrinth shape in an extant turtle. *Zool J Linnean Soc* 187(3):800–828. <https://doi.org/10.1093/zoolinnean/zlz063>
- Ewer RF (1965) The anatomy of the thecodont reptile *Euparkeria capensis* Broom. *Philos Trans R Soc B* 248(751):379–435. <https://doi.org/10.1098/rstb.1965.0003>
- Ezcurra MD (2016) The phylogenetic relationships of basal archosauromorphs, with an emphasis on the systematics of proterosuchian archosauriforms. *Peer J* 4:e1778. <https://doi.org/10.7717/peerj.1778>
- Ezcurra MD, Butler RJ (2015) Post-hatchling cranial ontogeny in the Early Triassic diapsid reptile *Proterosuchus fergusi*. *J Anat* 226(5):387–402. <https://doi.org/10.1111/joa.12300>
- Ezcurra MD, Fiorelli LE, Martinelli AG et al (2017) Deep faunistic turnovers preceded the rise of dinosaurs in southwestern Pangaea. *Nat Ecol Evol* 1(10):1477–1483. <https://doi.org/10.1038/s41559-017-0305-5>
- Ezcurra MD, Montefeltro FC, Pinheiro FL, Trotteyn MJ, Gentil AR, Lehmann OE & Pradelli LA (2021) The stemarchosaur evolutionary radiation in South America. *Journal of South American Earth Sciences* 105:102935. <https://doi.org/10.1016/j.jsames.2020.102935>
- Fabbri M, Koch NM, Pritchard AC et al (2017) The skull roof tracks the brain during the evolution and development of reptiles including birds. *Nat Ecol Evol* 1(10):1543–1550. <https://doi.org/10.1038/s41559-017-0288-2>
- Fonseca PHM, Martinelli AG, da Silva MT et al (2020) Morphology of the endocranial cavities of *Campinasuchus dinizi* (Crocodyliformes: Baurusuchidae) from the Upper Cretaceous of Brazil. *Geobios* 58:1–16. <https://doi.org/10.1016/j.geobios.2019.11.001>
- Gans C, Northcutt RG, Ulinski P (eds) (1979) *Biology of the reptilia, Neurology*, vol 9. Academic Press, London/New York/San Francisco
- Gauthier J, Padian K (1985) Phylogenetic, functional, and aerodynamic analyses of the origin of birds and their flight. In: Hecht MK, Ostrom JH, Viohl G, Wellnhofer P (eds) *The beginning of birds*. *Freunde des Jura Museums, Eichstatt*, pp 185–197
- Georgi JA, Sipla JS (2008) Comparative and functional anatomy of balance in aquatic reptiles and birds. In: Thewissen JGM, Nummela S (eds) *Sensory evolution on the threshold: adaptations in secondarily aquatic vertebrates*. University of California Press, Berkeley/Los Angeles, pp 233–256
- Gleich O, Manley GA (2000) The hearing organ of birds and crocodylia. In: *Comparative hearing: birds and reptiles*. Springer, New York, pp 70–138
- Gleich O, Dooling RJ, Manley GA (2005) Audiogram, body mass, and basilar papilla length; correlations in birds and predictions for extinct archosaurs. *Naturwissenschaften* 92(12):595–598. <https://doi.org/10.1007/s00114-005-0050-5>
- Goldby F, Gamble HJ (1957) The reptilian cerebral hemispheres. *Biol Rev* 32(4):383–420
- Gower DJ (1997) The braincase of the early archosaurian reptile *Erythrosuchus africanus*. *J Zool* 242(3):557–576. <https://doi.org/10.1111/j.1469-7998.1997.tb03855.x>
- Gower DJ (2000) Rausuchian archosaurs (Reptilia, Diapsida): an overview. *Neues Jahrb Geol Palaontol Abh* 218(3):447–488
- Gower DJ (2002) Braincase evolution in suchian archosaurs (Reptilia: Diapsida): evidence from the rausuchian *Batrachotomus kupferzellensis*. *Zool J Linnean Soc* 136(1):49–76. <https://doi.org/10.1046/j.1096-3642.2002.00025.x>
- Gower DJ (2003) Osteology of the early archosaurian reptile *Erythrosuchus africanus*, Broom. *Ann S Afr Mus* 110:1–88

- Gower DJ, Nesbitt SJ (2006) The braincase of *Arizonasaurus babbitti*—further evidence for the non-monophyly of ‘rauisuchian’ archosaurs. *J Vertebr Paleontol* 26(1):79–87. [https://doi.org/10.1671/0272-4634\(2006\)26\[79:TBOABE\]2.0.CO;2](https://doi.org/10.1671/0272-4634(2006)26[79:TBOABE]2.0.CO;2)
- Gower DJ, Sennikov AG (1996a) Endocranial casts of early archosaurian reptiles. *Paläontol Z* 70(3):579–589. <https://doi.org/10.1007/BF02988094>
- Gower DJ, Sennikov AG (1996b) Morphology and phylogenetic informativeness of early archosaur braincases. *Palaeontology* 39(4):883–906
- Gower DJ, Walker AD (2002) New data on the braincase of the aetosaurian archosaur (Reptilia: Diapsida) *Stagonolepis robertsoni* Agassiz. *Zool J Linnean Soc* 136(1):7–23. <https://doi.org/10.1046/j.1096-3642.2002.00023.x>
- Gower DJ, Weber E (1998) The braincase of *Euparkeria*, and the evolutionary relationships of birds and crocodylians. *Biol Rev* 73(4):367–411. <https://doi.org/10.1017/S0006323198005222>
- Gregory WK (1951) *Evolution emerging; a survey of changing patterns from primeval life to man*. Macmillan, New York. (No. 591.38 G74)
- Hanson M, Hoffman EA, Norell MA et al (2021) The early origin of a birdlike inner ear and the evolution of dinosaurian movement and vocalization. *Science* 372(6542):601–609. <https://doi.org/10.1126/science.abb4305>
- Heaton MJ (1979) Cranial anatomy of primitive captorhinid reptiles from the Late Pennsylvanian and Early Permian, Oklahoma and Texas, vol 127. University of Oklahoma
- Holloway WL, Claeson KM, O’keefe FR (2013) A virtual phytosaur endocranium and its implications for sensory system evolution in archosaurs. *J Vert Paleontol* 33(4):848–857. <https://doi.org/10.1080/02724634.2013.747532>
- Hopson JA (1979) Paleoneurology. In: Gans C, Northcutt R, Ulinski P (eds) *Biology of the Reptilia*, Vol, vol 9, pp 39–146
- Hu K, King JL, Romick CA et al (2020) Ontogenetic endocranial shape change in alligators and ostriches and implications for the development of the non-avian dinosaur endocranium. *Anat Rec* 304(8):1759–1775. <https://doi.org/10.1002/ar.24579>
- Hullar TE (2006) Semicircular canal geometry, afferent sensitivity, and animal behavior. *Anat Rec* 288(4):466–472. <https://doi.org/10.1002/ar.a.20304>
- Hurlburt GR, Ridgely RC, Witmer LM (2013) Relative size of brain and cerebrum in tyrannosaurid dinosaurs: an analysis using brain-endocranium quantitative relationships in extant alligators. In: Parrish JM, Molnar RE, Currie PJ, Koppelhus E (eds) *Tyrannosaurid Paleobiology*. Indiana University Press, Bloomington, pp 135–155
- Jaekel O (1910) Ueber einen neuen Belodonten aus dem Buntsandstein von Bernburg. *Sber Ges naturf Freunde*, Bed 5:197–229
- Jerison HJ (1969) Brain evolution and dinosaur brains. *Am Nat* 103(934):575–588. <https://doi.org/10.1086/282627>
- Jerison HJ (1973) *Evolution of the brain and intelligence*. Academic, New York
- Jirak D, Janacek J (2017) Volume of the crocodylian brain and endocranium during ontogeny. *PLoS One* 12(6):e0178491. <https://doi.org/10.1371/journal.pone.0178491>
- Kischlat EE, Lucas SG (2003) A phytosaur from the Upper Triassic of Brazil. *J Vertebr Paleontol* 23(2):464–467. [https://doi.org/10.1671/0272-4634\(2003\)023\[0464:APFTUT\]2.0.CO;2](https://doi.org/10.1671/0272-4634(2003)023[0464:APFTUT]2.0.CO;2)
- Lautenschlager S, Butler RJ (2016) Neural and endocranial anatomy of Triassic phytosaurian reptiles and convergence with fossil and modern crocodylians. *Peer J* 4:e2251. <https://doi.org/10.7717/peerj.2251>
- Lautenschlager S, Rayfield EJ, Altangerel P et al (2012) The endocranial anatomy of Therizinosauria and its implications for sensory and cognitive function. *PLoS One* 7(12):e52289. <https://doi.org/10.1371/journal.pone.0052289>
- Leahey LG, Molnar RE, Carpenter K et al (2015) Cranial osteology of the ankylosaurian dinosaur formerly known as *Minmi* sp. (Ornithischia: Thyreophora) from the Lower Cretaceous Allaru Mudstone of Richmond, Queensland, Australia. *Peer J* 3:e1475. <https://doi.org/10.7717/peerj.1475>
- Lecuona A (2013) Anatomía y relaciones filogenéticas de *Gracilisuchus stipanicicorum* y sus implicancias en el origen de Crocodylomorpha. Dissertation, Universidad de Buenos Aires

- Lecuona A, Desojo JB, Pol D (2017) New information on the postcranial skeleton of *Gracilisuchus stipanicorum* (Archosauria: Suchia) and reappraisal of its phylogenetic position. *Zool J Linnean Soc* 131(3):638–677. <https://doi.org/10.1093/zoolinnean/zlx011>
- Lecuona A, Desojo JB, Cerda IA (2020) New information on the anatomy and histology of *Gracilisuchus stipanicorum* (Archosauria: Pseudosuchia) from the Chañares Formation (early Carnian), Argentina. *C R Palevol* 19:40–62. <https://doi.org/10.5852/cr-palevol2020v19a3>
- Lehane J (2005) Anatomy and relationship of *Shuvosaurus*, a basal theropod from the Triassic of Texas. Dissertation, Texas Tech University
- Lessner EJ, Holliday CM (2020) A 3D ontogenetic atlas of *Alligator mississippiensis* cranial nerves and their significance for comparative neurology of reptiles. *Anat Rec (Special Issue)*:1–29. <https://doi.org/10.1002/ar.24550>
- Lessner EJ, Stocker MR (2017) Archosauriform endocranial morphology and osteological evidence for semiaquatic sensory adaptations in phytosaurs. *J Anat* 231(5):655–664. <https://doi.org/10.1111/joa.12668>
- Li C, Wu XC, Cheng YN, Sato T, Wang L (2006) An unusual archosaurian from the marine Triassic of China. *Naturwissenschaften* 93(4):200–206
- Li C, Wu XC, Zhao LJ et al (2016) A new armored archosauriform (Diapsida: Archosauromorpha) from the marine Middle Triassic of China, with implications for the diverse life styles of archosauriforms prior to the diversification of Archosauria. *Sci Nat* 103(11):1–23. <https://doi.org/10.1007/s00114-016-1418-4>
- Marsh AD, Smith ME, Parker WG et al (2020) Skeletal anatomy of *Acaenasuchus geoffreyi* Long and Murry, 1995 (Archosauria: Pseudosuchia) and its implications for the origin of the Aetosaurian Carapace. *J Vertebr Paleontol* 40(4):e1794885. <https://doi.org/10.1080/02724634.2020.1794885>
- Marugán-Lobón J, Chiappe LM, Farke AA (2013) The variability of inner ear orientation in saurischian dinosaurs: testing the use of semicircular canals as a reference system for comparative anatomy. *Peer J* 1:e124. <https://doi.org/10.7717/peerj.124>
- Mastrantonio BM, Schultz CL, Desojo JB et al (2013) The braincase of *Prestosuchus chiniquensis* (Archosauria: Suchia). *Geol Soc Spec Publ* 379(1):425–440. <https://doi.org/10.1144/SP379.10>
- Mastrantonio BM, von Baczko MB, Desojo JB et al (2019) The skull anatomy and cranial endocast of the pseudosuchid archosaur *Prestosuchus chiniquensis* from the Triassic of Brazil. *Acta Palaeontol Pol* 64(1):171–198. <https://doi.org/10.4202/app.00527.2018>
- Mehl MG (1928) *Pseudopalatus pristinus*: a new genus and species of Phytosaurs from Arizona. The University of Missouri Studies, Columbia, pp 3–25
- Müller RT, von Baczko MB, Desojo JB et al (2020) The first ornithosuchid from Brazil and its macroevolutionary and phylogenetic implications for late Triassic faunas in Gondwana. *Acta Palaeontol Pol* 65(1):1–10. <https://doi.org/10.4202/app.00652.2019>
- Nesbitt SJ (2003) *Arizonasaurus* and its implications for archosaur divergence. *Proc Royal Soc B* 270(supp2):S234–S237. <https://doi.org/10.1098/rsbl.2003.0066>
- Nesbitt S (2007) The anatomy of *Effigia okeeffeae* (Archosauria, Suchia), theropod-like convergence, and the distribution of related taxa. *Bull Am Mus Nat Hist* 302:1–84. [https://doi.org/10.1206/0003-0090\(2007\)302\[1:TAOEOA\]2.0.CO;2](https://doi.org/10.1206/0003-0090(2007)302[1:TAOEOA]2.0.CO;2)
- Nesbitt SJ (2011) The early evolution of archosaurs: relationships and the origin of major clades. *Bull Am Mus Nat Hist* 352:1–292
- Nesbitt SJ, Stocker MR, Small BJ, Downs A (2009) The osteology and relationships of *Vancleavea campi* (Reptilia: Archosauriformes). *Zool J Linnean Soc* 157(4):814–864. <https://doi.org/10.1111/j.1096-3642.2009.00530.x>
- Nesbitt SJ, Brusatte SL, Desojo JB, Liparini, A, De França MA, Weinbaum JC & Gower DJ (2013a) *Rauisuchia*. Geological Society, London, Special Publications 379(1):241–274.
- Nesbitt SJ, Turner AH, Weinbaum JC (2013b) A survey of skeletal elements in the orbit of Pseudosuchia and the origin of the crocodylian palpebral. *Earth Environ Sci Trans R Soc Edinb* 103(3–4):365–381. <https://doi.org/10.1017/S1755691013000224>
- Nesbitt SJ, Stocker MR, Parker WG et al (2017) The braincase and endocast of *Parringtonia gracilis*, a Middle Triassic suchian (Archosaur: Pseudosuchia). *J Vert Paleontol* 37(supp1):122–141. <https://doi.org/10.1080/02724634.2017.1393431>

- Nesbitt SJ, Zawiskie JM, Dawley RM (2020) The osteology and phylogenetic position of the loricatan (Archosauria: Pseudosuchia) *Heptasuchus clarki*, from the ?Mid-Upper Triassic, southeastern Big Horn Mountains, Central Wyoming (USA). Peer J 8:e10101. <https://doi.org/10.7717/peerj.10101>
- Nesbitt SJ, Stocker MR, Chatterjee S et al (2021) A remarkable group of thick-headed Triassic Period archosauromorphs with a wide, possibly Pangean distribution. J Anat 239:184–206. <https://doi.org/10.1111/joa.13414>
- Paes Neto VD, Desojo JB, Brust ACB et al (2021) The first braincase of the basal aetosaur *Aetosauroides scagliai* (Archosauria: Pseudosuchia) from the Upper Triassic of Brazil. J Vert Paleontol. <https://doi.org/10.1080/02724634.2021.1928681>
- Parker WG (2016) Osteology of the late Triassic aetosaur *Scutarx deltatylys* (Archosauria: Pseudosuchia). Peer J 4:e2411. <https://doi.org/10.7717/peerj.2411>
- Parker WG, Nesbitt S, Irmis R et al (2021) Osteology, histology, and relationships of *Revueltosaurus callenderi* (Archosauria: Suchia) from the Upper Triassic (Norian) Chinle Formation of Petrified Forest National Park, Arizona, USA. Anat Rec (Special Issue):1–62. <https://doi.org/10.1002/ar.24757>
- Parrish JM (1993) Phylogeny of the Crocodylotarsi, with reference to archosaurian and cruro-tarsan monophyly. J Vertebr Paleontol 13(3):287–308. <https://doi.org/10.1080/02724634.1993.10011511>
- Parrish JM (1994) Cranial osteology of *Longosuchus meadei* and the phylogeny and distribution of the Aetosauria. J Vertebr Paleontol 14(2):196–209. <https://doi.org/10.1080/02724634.1994.10011552>
- Paulina-Carabajal A, Lee YN, Jacobs LL (2016) Endocranial morphology of the primitive nodosaurid dinosaur *Pawpawsaurus campbelli* from the Early Cretaceous of North America. PLoS One 11(3):e0150845. <https://doi.org/10.1371/journal.pone.0150845>
- Pierce SE, Williams M, Benson RB (2017) Virtual reconstruction of the endocranial anatomy of the early Jurassic marine crocodylomorph *Pelagosaurus typus* (Thalattosuchia). Peer J 5:e3225. <https://doi.org/10.7717/peerj.3225>
- Pradelli LA, Leardi JM, Ezcurra MD (2022) Body size disparity of the Archosauromorph reptiles during the first 90 million years of their evolution. Ameghiniana 59(1):47–77. <https://doi.org/10.5710/AMGH.16.09.2021.3441>
- Reig OA (1961) Acerca de la posición sistemática de la familia Rausuchidae y del género *Saurosuchus* (Reptilia, Thecodontia). Rev Mus Munic Cienc Nat Tradic Mar del Plata 1:73–114
- Schachner ER, Irmis RB, Huttenlocker AK et al (2020) Osteology of the Late Triassic bipedal archosaur *Poposaurus gracilis* (Archosauria: Pseudosuchia) from Western North America. Anat Rec 303(4):874–917. <https://doi.org/10.1002/ar.24298>
- Schmitz L, Motani R (2011) Nocturnality in dinosaurs inferred from scleral ring and orbit morphology. Science 332(6030):705–708. <https://doi.org/10.1126/science.1200043>
- Schoch RR (2007) Osteology of the small archosaur *Aetosaurus* from the Upper Triassic of Germany. Neues Jahrb Geol Palaontol Abh 246(1):1–35. <https://doi.org/10.1127/0077-7749/2007/0246-0001>
- Schoch RR, Desojo JB (2016) Cranial anatomy of the aetosaur *Paratypothorax andressorum* Long & Ballew, 1985, from the Upper Triassic of Germany and its bearing on aetosaur phylogeny. Neues Jahrb Geol Palaontol Abh 279(1):73–95. <https://doi.org/10.1127/njgpa/2016/0542>
- Schultz CL, Martinelli AG, Soares MB et al (2020) Triassic faunal successions of the Paraná Basin, southern Brazil. J S Am Earth Sci 104:102846. <https://doi.org/10.1016/j.jsames.2020.102846>
- Schwab JA, Young MT, Neenan JM et al (2020) Inner ear sensory system changes as extinct crocodylomorphs transitioned from land to water. PNAS 117(19):10422–10428. <https://doi.org/10.1073/pnas.2002146117>
- Sedlmayr JC (2002) Anatomy, evolution, and functional significance of cephalic vasculature in Archosauria. Dissertation, Ohio University
- Sennikov AG (1989) A new euparkeriid (Thecodontia) from the Middle Triassic of the Southern Urals. Palaeontol J 22:66–73
- Sereno PC (1991) Basal archosaurs: phylogenetic relationships and functional implications. J Vertebr Paleontol 11(S4):1–53. <https://doi.org/10.1080/02724634.1991.10011426>

- Sereno PC, Arcucci AB (1990) The monophyly of crurotarsal archosaurs and the origin of bird and crocodile ankle joints. *Neues Jahrb Geol Palaontol Abh* 180(1):21–52
- Small BJ, Martz JW (2013) A new aetosaur from the Upper Triassic Chinle Formation of the Eagle Basin, Colorado, USA. *Geol Soc Spec Publ* 379(1):393–412. <https://doi.org/10.1144/SP379.18>
- Sobral G, Sookias RB, Bhullar BAS et al (2016) New information on the braincase and inner ear of *Euparkeria capensis* Broom: implications for diapsid and archosaur evolution. *R Soc Open Sci* 3(7):160072. <https://doi.org/10.1098/rsos.160072>
- Sookias RB, Sennikov AG, Gower DJ et al (2014) The monophyly of Euparkeriidae (Reptilia: Archosauriformes) and the origins of Archosauria: a revision of *Dorosuchus neoetus* from the Mid-Triassic of Russia. *Palaeontology* 57(6):1177–1202. <https://doi.org/10.1111/pala.12110>
- Sookias RB, Dilkes D, Sobral G et al (2020) The craniomandibular anatomy of the early archosauriform *Euparkeria capensis* and the dawn of the archosaur skull. *R Soc Open Sci* 7(7):200116. <https://doi.org/10.1098/rsos.200116>
- Stocker MR, Nesbitt SJ, Criswell KE et al (2016) A dome-headed stem archosaur exemplifies convergence among dinosaurs and their distant relatives. *Curr Biol* 26(19):2674–2680. <https://doi.org/10.1016/j.cub.2016.07.066>
- Sues HD, Desojo JB, Ezcurra MD (2013) Doswelliidae: a clade of unusual armoured archosauriforms from the Middle and Late Triassic. *Geol Soc Spec Publ* 379(1):49–58. <https://doi.org/10.1144/SP379.13>
- Tambussi CP, Degrange FJ, Ksepka DT (2015) Endocranial anatomy of Antarctic Eocene stem penguins: implications for sensory system evolution in Sphenisciformes (Aves). *J Vertebr Paleontol* 35(5):e981635. <https://doi.org/10.1080/02724634.2015.981635>
- Taylor MP, Wedel MJ, Naish D (2009) Head and neck posture in sauropod dinosaurs inferred from extant animals. *Acta Palaeontol Pol* 54(2):213–220. <https://doi.org/10.4202/app.2009.0007>
- Trotteyn MJ, Ezcurra MD (2014) Osteology of *Pseudochampsia ischigualastensis* gen. et comb. nov. (Archosauriformes: Proterochampsidae) from the early Late Triassic Ischigualasto Formation of northwestern Argentina. *PLoS One* 9(11):e111388. <https://doi.org/10.1371/journal.pone.0111388>
- Trotteyn MJ, Ezcurra MD (2020) Redescription of the holotype of *Chanaresuchus bonapartei* Romer, 1971 (Archosauriformes: Proterochampsidae) from the Upper Triassic rocks of the Chañares Formation of North-Western Argentina. *J Syst Palaeontol* 18(17):1415–1443. <https://doi.org/10.1080/14772019.2020.1768167>
- Trotteyn MJ, Haro JA (2011) The braincase of a specimen of *Proterochampsia* Reig (Archosauriformes: Proterochampsidae) from the Late Triassic of Argentina. *Paläontol Z* 85(1):1–17. <https://doi.org/10.1007/s12542-010-0068-7>
- Trotteyn MJ, Haro JA (2012) The braincase of *Chanaresuchus ischigualastensis* (Archosauriformes) from the Late Triassic of Argentina. *J Vert Paleontol* 32(4):867–882. <https://doi.org/10.1080/002724634.2012.670178>
- Trotteyn MJ, Paulina-Carabajal A (2016) Braincase and neuroanatomy of *Pseudochampsia ischigualastensis* and *Tropidosuchus romeri* (Archosauriformes, Proterochampsia). *Ameghiniana* 53(5):527–542. <https://doi.org/10.5710/AMGH.28.04.2016.2968>
- von Baczko MB, Desojo JB (2016) Cranial anatomy and palaeoneurology of the archosaur *Riojasuchus tenuisiceps* from the Los Colorados Formation, La Rioja, Argentina. *PLoS One* 11(2):e0148575. <https://doi.org/10.1371/journal.pone.0148575>
- von Baczko MB, Taborda JR, Desojo JB (2018) Paleoneuroanatomy of the aetosaur *Neoaeosauroides engaeus* (Archosauria: Pseudosuchia) and its paleobiological implications among archosauriforms. *Peer J* 6:e5456. <https://doi.org/10.7717/peerj.5456>
- von Baczko MB, Desojo JB, Gower DJ et al (2021) New digital braincase endocasts of two species of *Desmatosuchus* and neurocranial diversity within Aetosauria (Archosauria: Pseudosuchia). *Anat Rec (Special Issue)*:1–20. <https://doi.org/10.1002/ar.24798>
- Voogd J, Wylie DR (2004) Functional and anatomical organization of floccular zones: a preserved feature in vertebrates. *J Comp Neurol* 470(2):107–112. <https://doi.org/10.1002/cne.11022>
- Walker AD (1961) Triassic reptiles from the Elgin area: *Stagonolepis*, *Dasygnathus* and their allies. *Philos Trans R Soc B* 244(709):103–204. <https://doi.org/10.1098/rstb.1961.0007>

- Watanabe A, Gignac PM, Balanoff AM et al (2019) Are endocasts good proxies for brain size and shape in archosaurs throughout ontogeny? *J Anat* 234(3):291–305. <https://doi.org/10.1111/joa.12918>
- Weems RE (1980) An unusual newly discovered archosaur from the upper Triassic of Virginia, USA. *Trans Am Philos Soc* 70(7):1–53. <https://doi.org/10.2307/1006472>
- Weinbaum JC (2002) Osteology and relationships of *Postosuchus kirkpatricki* (Archosauria: Crurotarsi). Dissertation, Texas Tech University
- Weinbaum JC (2011) The skull of *Postosuchus kirkpatricki* (Archosauria: Paracrocodyliformes) from the upper Triassic of the United States. *PaleoBios* 30(1):18–44. <https://doi.org/10.5070/P9301021795>
- Welman J (1995) Euparkeria and the origin of birds. *S Afr J Sci* 91(10):533–537
- Witmer LM, Chatterjee S, Franzosa J et al (2003) Neuroanatomy of flying reptiles and implications for flight, posture and behaviour. *Nature* 425(6961):950–953. <https://doi.org/10.1038/nature02048>
- Witmer LM, Ridgely RC, Dufeau DL et al (2008) Using CT to peer into the past: 3D visualization of the brain and ear regions of birds, crocodiles, and nonavian dinosaurs. In: Endo H, Frey R (eds) *Anatomical imaging*. Springer, Tokyo, pp 67–87
- Wynd BM, Nesbitt SJ, Stocker MR et al (2019) A detailed description of *Rugarhynchos sixmilensis*, *gen. et comb. nov.* (Archosauriformes, Proterochampsia), and cranial convergence in snout elongation across stem and crown archosaurs. *J Vertebr Paleontol* 39(6):e1748042. <https://doi.org/10.1080/02724634.2019.1748042>
- Zelenitsky DK, Therrien F, Kobayashi Y (2009) Olfactory acuity in theropods: palaeobiological and evolutionary implications. *Proc Royal Soc B* 276(1657):667–673. <https://doi.org/10.1098/rspb.2008.1075>
- Zelenitsky DK, Therrien F, Ridgely RC et al (2011) Evolution of olfaction in non-avian theropod dinosaurs and birds. *Proc Royal Soc B* 278(1725):3625–3634. <https://doi.org/10.1098/rspb.2011.0238>

Chapter 7

An Overview on the Crocodylomorpha Cranial Neuroanatomy: Variability, Morphological Patterns and Paleobiological Implications



Francisco Barrios, Paula Bona, Ariana Paulina-Carabajal, Juan Martín Leardi, Casey M. Holliday, and Emily J. Lessner

F. Barrios (✉)

Departamento de Paleontología, Museo Provincial de Ciencias Naturales “Prof. Juan Olsacher”, Neuquén, Argentina

P. Bona

Facultad de Ciencias Naturales y Museo, División Paleontología de Vertebrados, Anexo Laboratorios, Buenos Aires, Argentina

CONICET, Consejo Nacional de Investigaciones Científicas y Técnicas, Buenos Aires, Argentina

e-mail: pbona@fcnym.unlp.edu.ar

A. Paulina-Carabajal

CONICET, Consejo Nacional de Investigaciones Científicas y Técnicas, Buenos Aires, Argentina

Instituto de Investigaciones en Biodiversidad y Medioambiente,

CONICET-Universidad Nacional del Comahue, San Carlos de Bariloche, Argentina

e-mail: a.paulinacarabajal@conicet.gov.ar

J. M. Leardi

CONICET, Consejo Nacional de Investigaciones Científicas y Técnicas, Buenos Aires, Argentina

Facultad de Ciencias Exactas y Naturales, Departamento de Ciencias Geológicas, Instituto de Estudios Andinos “Don Pablo Groeber” (IDEAN), Universidad de Buenos Aires, Buenos Aires, Argentina

Departamento de Biodiversidad y Biología Experimental, Facultad de Ciencias Exactas y Naturales, Universidad de Buenos Aires, Buenos Aires, Argentina

e-mail: idean@gl.fcen.uba.ar; jmleardi@gl.fcen.uba.ar

C. M. Holliday · E. J. Lessner

Department of Pathology and Anatomical Sciences, School of Medicine, University of Missouri, Columbia, MO, USA

e-mail: hollidayca@missouri.edu; ejlessner@mail.missouri.edu

Anatomical Abbreviations

ana	anterior ampulla
asc	anterior semicircular canal
bo	basioccipital
bs	basisphenoid
cb	cerebellum
cc	crus communis
cer	cerebral hemispheres
cf.	cerebellar flocculus
cCQ	cranioquadrate canal
cInt	integumentary canal
cMa	mandibular canal
CN I	olfactory nerve
CN II	optic nerve
CN III	oculomotor nerve
CN IV	trochlear nerve
CN IX	glossopharyngeal nerve
CN V	trigeminal nerve
CN V _{so}	supraorbital division of trigeminal nerve
CN V _{ty}	tympanic division of trigeminal nerve
CN V ₁	ophthalmic division of trigeminal nerve
CN V ₂	maxillary division of trigeminal nerve
CN V ₃	mandibular division of trigeminal nerve
CN VI	abducens nerve
CN VII	facial nerve
CN VII _{hy}	hyomandibular ramus of facial nerve
CN VII _{pal}	palatine ramus of facial nerve
CN VIII	vestibulocochlear nerve
CN VIII _{ch}	cochlear ramus of vestibulocochlear nerve
CN VIII _v	vestibular ramus of vestibulocochlear nerve
CN IX	glossopharyngeal nerve
CN X	vagus nerve
CN XI	accessory nerve
CN XII	hypoglossal nerve
CN XII ₁	anterior division of hypoglossal nerve
CN XII ₂	posterior division of hypoglossal nerve
edr	edentulous region
eo	exoccipital
faCA	foramen for carotid artery
fCNII	foramen for CN II
fCNIII	foramen for CN III
fCNIV	foramen for CN IV
fCNIX,X	foramen for CN IX and X

fCNIX,X,XI	foramen for CN IX, CN X and XI
fCNV	foramen for CN V
fCNV ₁	ophthalmic foramen
fCNV _{2,3}	maxillomandibular foramen
fCNVI	foramen for CN VI
fCNVII	foramen for CN VII
fCNVIII _{ch}	foramen for cochlear ramus of CN VIII
fCNVIII _v	foramen for vestibular ramus of CN VIII
fInt	integumentary foramina
fMag	foramen magnum
fMCV	foramen for middle cerebral vein
fMe	Meckelian fossa
foCNV	trigeminal fossa
fr	frontal
gCNV	trigeminal ganglion
gS	sympathetic ganglion
it	intertympanicum diverticulum
la	laterosphenoid
laa	lateral ampulla
lg	lagena
lsc	lateral semicircular canal
mo	medulla oblongata
ob	olfactory bulb
ol	optic lobe
orb	orbite
ot	olfactory tract
pa	parietal
pf	pituitary or hypophyseal fossa
pi	pituitary or hypophyseal gland
poa	posterior ampulla
pr	prootic
pt.	pterygoid
psc	posterior semicircular canal
so	supraoccipital
vd	vestibular depression
ve	vestibule
vs	venous sinus

Institutional Abbreviations

AMNH FARB American Museum of Natural History, Fossil Amphibians, Reptiles, and Birds Collection, New York, USA

BP	Evolutionary Studies Institute (formerly Bernard Price Institute for Palaeontological Research), University of the Witwatersrand, Johannesburg, South Africa
BRLSI	Bath Royal Literary and Scientific Institute, Bath, UK
CMC	Chinchilla Museum Collection, Queensland, Australia
CMNH	Cleveland Museum of Natural History, Cleveland, USA
CNRST-SUNY	Centre National de la Recherche Scientifique et Technologique, Mali-Stony Brook University, New York, USA
CPPLIP	Centro de Pesquisas Paleontológicas Llewellyn Ivor Price, Peirópolis, Brazil
DVZ M	Department of Vertebrate Zoology, Morphological Collection, Saint Petersburg State University, Saint Peterburg, Russia
FEF-PV	Fernandópolis Educational Foundation, São Paulo, Brazil
FMNH	Field Museum Natural History, Illionis, USA
FUP	University of Brasília, Campus Planaltina, Federal District, Brazil
IFSP-VTP	Federal Institute of Education, Science and Technology of São Paulo, Brazil
HUE	Museo de Paleontología de Castilla-La Mancha, Lo Hueco Collection, Cuenca, Spain
IVPP V	Institute of Vertebrate Paleontology and Paleoanthropology, Beijing, People's Republic of China
LACM	Natural History Museum of Los Angeles County, Los Angeles, USA
LPP	Institut de Paléoprimatologie, Paléontologie, Humaine Évolution et Paléoenvironnements, Université de Poitiers, Poitiers, France
LPRP	Laboratório de Paleontologia de Ribeirão Preto, Universidade de São Paulo, São Paulo, Brazil
MACN-He	Museo Argentino de Ciencias Naturales "Bernardino Rivadavia," Herpetology Collection, Buenos Aires, Argentina
MCD	Museu de la Conca Dellà, Lleida, Spain
MCZ	Museum of Comparative Zoology, Cambridge, USA
MDA	Museo del Desierto de Atacama, Antofagasta, Chile
MLP	Museo de La Plata, La Plata, Argentina
MNA	Museum of Northern Arizona, Arizona, USA
MNHN	Muséum National d'Histoire Naturelle, Paris, France
MNN	Musée National du Niger, Niamey, Republic of Niger
MOZ-PV	Museo Provincial de Ciencias Naturales "Prof. Dr. Juan A. Olsacher," Vertebrate Paleontology Collection, Zapala, Argentina
MPEF-PV	Museo Paleontológico Egidio Feruglio, Vertebrate Paleontology Collection, Chubut, Argentina
MUVC	University of Missouri Vertebrate Collection, Columbia, Missouri, USA

MZB	Museu Zoològic de Barcelona, Barcelona, Spain
NHMUK PV OR	Natural History Museum, London, UK
OUVV	Ohio University Vertebrate Collection, Ohio, USA
PVL	Instituto Miguel Lillo, Tucumán, Argentina
QMF	Queensland Museum, Brisbane, Australia
ROM	Royal Ontario Museum, Toronto, Canada
RRBP	Rukwa Rift Basin Project, Tanzanian Antiquities Unit, Dar es Salaam, Tanzania
SAM PK	Iziko South African Museum, Cape Town, South Africa
SMC	Sedgwick Museum, Cambridge, UK
SNSB-BSPG	Staatliche Naturwissenschaftliche Sammlungen Bayerns- Bayerische Staatssammlung für Paläontologie und Geologie, Munich, Germany
STUS	Sala de las Tortugas ‘Emiliano Jiménez’ de la Universidad de Salamanca, Salamanca, Spain
TMM	Texas Memorial Museum, Austin, Texas, USA
UA	Université d’Antananarivo, Antananarivo, Madagascar
UF	University of Florida, Florida Museum of Natural History, Florida, USA
UFRGS-PV-Z	Laboratório de Paleontologia de Vertebrados, Universidade Federal do Rio Grande do Sul, Zoological Collection, Porto Alegre, Brazil
UMZC	University Museum of Zoology, Cambridge, UK
UNM	University of New Mexico, New Mexico, USA
UOMNH	University of Oregon Museum of Natural and Cultural History, Eugene, USA
ZIN	Zoological Institute, Russian Academy of Sciences, Saint Peterburg, Russia
ZMMU MSU R	Zoological Museum of Moscow State University, Moscow, Russia

7.1 Phylogenetic Context and Introduction to Paleoneurology of Crocodylomorpha

Crocodylomorpha is an intriguing clade of archosauriforms recorded worldwide (except Antarctica) since the Late Triassic, which explored all environments, excluding the aerial. They survived the great Triassic-Jurassic and Cretaceous-Paleocene extinctions, diversifying during the Mesozoic and Cenozoic (e.g. Nesbitt 2011; Bronzati et al. 2015; Wilberg et al. 2019). Living crocodylomorphs (i.e. crown-group Crocodylia) are continental predators with amphibious habits; however, the group is ancestrally terrestrial and filled a wide variety of ecological niches in the past (e.g. Grigg and Kirshner 2015). Extinct crocodylomorphs include pelagic taxa (e.g. thalattosuchians as *Cricosaurus araucanensis*), small terrestrial

carnivores (e.g. protosuchids as *Protosuchus richardsoni*), herbivores (e.g. notosuchians as *Simosuchus clarki*) or omnivores (e.g. notosuchians as *Araripesuchus gomesii*, *Notosuchus terrestris*), and even large terrestrial predators (e.g. sebecosuchians as *Baurusuchus pachecoi*, *Sebecus icaeorhinus*), with a great diversity of body morphotypes (e.g. Ósi 2013; Godoy et al. 2019; Wilberg et al. 2019; Fig. 7.1). It is worth mentioning that the phylogenetic position of thalattosuchians is controversial (e.g. immediately outside Crocodyliformes, Wilberg 2015a, b; as sister taxon of Mesoeucrocodylia, Larsson and Sues 2007; or within Neosuchia, Pol and Gasparini 2009; Bronzati et al. 2012, 2015; Montefeltro et al. 2013; Pol et al. 2014; Turner 2015; Fig. 7.1), so their neuroanatomy was described in an independent section in this chapter. Within Thalattosuchia, *Pelagosaurus typus* is particularly interesting since its phylogenetic relationships are controversial, having teleosauroid (e.g. Wilberg 2015b) and metriorhynchid apomorphies (e.g. Buffetaut 1980; Young et al. 2013; Wilberg 2015a). Furthermore, in some analyzes, *Pelagosaurus* is hypothesized as a basal (e.g. Mueller-Töwe 2005) or *incertae sedis* (e.g. Pierce and Benton 2006) Thalattosuchia.

Paleoneurology is the study of the brain and associated organs of extinct vertebrates based on their cranial endocasts (e.g. Hopson 1979; Wharton 2002), being a powerful tool when interpreting the lifestyle of an organism (Hopson 1977; Hurlburt 1996; Wharton 2002; Franzosa 2004; Witmer et al. 2008). The first paleoneurological studies in Crocodylomorpha date back to the late 1800s and were based mainly on natural cranial endocast and/or sectioned braincases of thalattosuchian and eusuchian taxa, such as *Teleosaurus cadomensis* (formerly *T. eucephalus*; Eudes-Deslongchamps 1863; Seeley 1880; Koken 1887; Wilberg 2015a), *Pelagosaurus typus* (formerly *Teleosaurus temporalis*; Eudes-Deslongchamps 1863; Koken 1887), *Proexochokefalos heberti* (formerly *Steneosaurus heberti*; Morel de Glasville 1876), *Thoracosaurus isorhynchus* (formerly *Gavialis macrorhynchus*; Lemoine 1883–1884), *Pholidosaurus meyeri* (Koken 1887; Edinger 1938; Hopson 1979), and *Goniopholis* spp. (Koken 1887; Edinger 1938). Descriptions based on latex cranial endocasts were published for early crocodylomorphs (Walker 1990) and extinct mesoeucrocodylians such as *Charitomenosuchus leedsi* (formerly *Steneosaurus pictaviensis*, a thalattosuchian Teleosauroidea; Wharton 2000), *Sebecus icaeorhinus* and *Wargosuchus australis* (a sebecosuchian Notosuchia; Colbert 1946; Martinelli and Pais 2008) and *Caiman gasparinae* (a eusuchian Crocodylia; Bona and Paulina-Carabajal 2013). In the last 20 years, the advent of new non-invasive imaging technologies (as Axial Computed Tomography, Magnetic Resonance, X-ray Micro-CT, High-Resolution Computed Tomography, Synchrotron Computer Tomography), allowed more detailed neuroanatomical approaches and a resurgence of paleoneurology as a discipline (Walsh and Knoll 2011). Now there is important information available on extinct crocodylomorph neuroanatomy based on 3D digital cranial endocasts, as is the case of the non-crocodyliform crocodylomorph *Almadasuchus figarii* (Leardi et al. 2020), the notosuchians *Araripesuchus wegeneri*, *Anatosuchus minor* (Sereno and Larsson 2009), *Simosuchus clarki* (Kley et al. 2010), *Rukwasuchus yajabalijekundu* (Sertich and O'Connor 2014), *Baurusuchus* (Dumont Jr et al. 2020), and *Campinasuchus dinizi* (Fonseca et al. 2020), the thalattosuchians '*Metriorhynchus*' cf. '*M.* *westermanni*' (Fernández

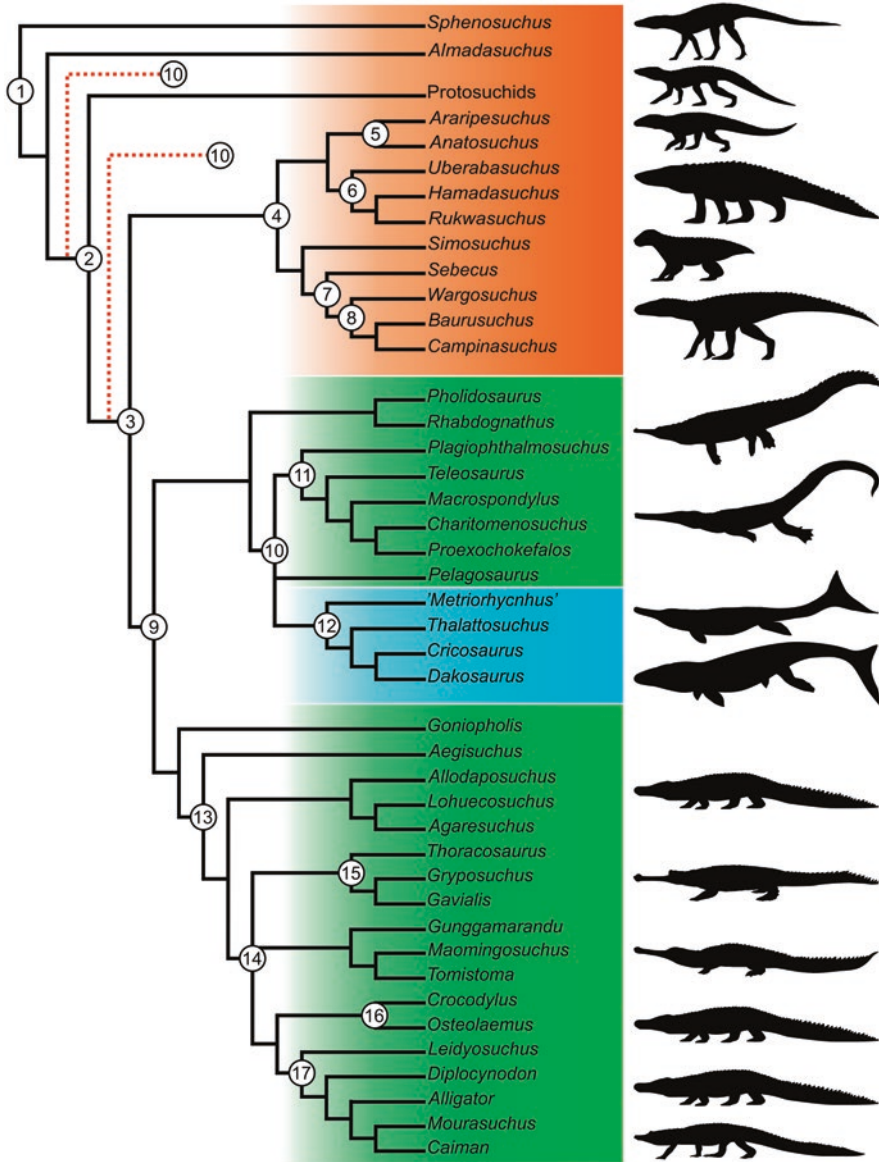


Fig. 7.1 Phylogenetic relationships of extant and fossil crocodylomorphs used in this study (based in Larsson and Sues 2007; Pol et al. 2013, 2014; Wilberg 2015a, b; Narváez et al. 2016; Young et al. 2016; Ristevski et al. 2021). Only showing taxa for which there are paleoneurological or neuroanatomical studies published. Numerical references: (1) Crocodylomorpha, (2) Crocodyliformes, (3) Mesoeucrocodylia, (4) Notosuchia, (5) Uruguayosuchidae, (6) Peirosauridae, (7) Sebecosuchia, (8) Baurusuchidae, (9) Neosuchia, (10) Thalattosuchia, (11) Teleosauroidea, (12) Metriorhynchoidea, (13) Eusuchia, (14) Crocodylia, (15) Gavialoidea, (16) Crocodyloidea, (17) Alligatoroidea. Dotted line indicates the alternate position of Thalattosuchia (sister clade of Crocodyliformes or sister clade of Mesoeucrocodylia). Color references: taxa with terrestrial (orange), semi-aquatic (green) or pelagic (light blue) habitats. Silhouettes based in the artworks of Ceri Thomas, Deverson da Silva, Dmitry Bogdanov, Felipe Alves Elias, Jeff Martz, Lucille Bettin-Nash and Nobu Tamura

et al. 2011), *Plagiophthalmosuchus* cf. *gracilirostris* (formerly *Steneosaurus* cf. *gracilirostris*; Brusatte et al. 2016), *Pelagosaurus typus* (Pierce et al. 2017), *Macrospondylus bollensis* (formerly *Steneosaurus bollensis*; Wilberg et al. 2021) and *Cricosaurus araucanensis* (Herrera et al. 2018), the neosuchians *Rhabdognathus aslerensis* (Erb and Turner 2021), *Allodaposuchus hulki* (Blanco et al. 2015), *Mourasuchus nativus* (Bona et al. 2013), *Gryposuchus neogaeus* (Bona et al. 2017), *Lohuecosuchus megadontos* (Serrano-Martínez et al. 2018), *Diplocynodon tormis* (Serrano-Martínez et al. 2019) and *Agaresuchus fontisensis* (Serrano-Martínez et al. 2020). For a summary of the different crocodylomorph taxa whose descriptions were published or mentioned in comparative paleoneurological studies, see Table 7.1.

Knowledge of the neuroanatomy (soft tissues) and their osteological correlates (cranial endocasts) of living crocodylians is crucial for accurate paleoneurological and paleobiological interpretations (Hopson 1979; Fig. 7.2). The endocranial cavity of living species has been described from cranial endocasts in *Gavialis gangeticus* (Owen 1850; Wharton 2000; Bona et al. 2017; Pierce et al. 2017), *Crocodylus acutus* (Owen 1850; Colbert 1946; Jirak and Janacek 2017), *Cr. johnstoni* (Witmer et al. 2008), *Cr. niloticus* (Eudes-Deslongchamps 1863; Koken 1887; Edinger 1938; Jirak and Janacek 2017; Beyrand et al. 2019), *Cr. moreletii* (Franzosa 2004), *Cr. siamensis* (Kawabe et al. 2009), *Alligator mississippiensis* (Lemoine 1883–1884; Koken 1887; Edinger 1938; Colbert 1946; Romer 1956; Witmer and Ridgely 2008; Sereno and Larsson 2009; George and Holliday 2013; Dufeu and Witmer 2015; Fabbri et al. 2017; Watanabe et al. 2019; Hu et al. 2020; Lessner and Holliday 2020), *Caiman crocodilus* (Hopson 1979; Brusatte et al. 2016; Jirak and Janacek 2017; Beyrand et al. 2019), *Ca. yacare* (Bona and Paulina-Carabajal 2013; Paulina-Carabajal et al. 2016), and *Paleosuchus trigonatus* (Balanoff and Bever 2017). Among living crocodylians, *Alligator mississippiensis* received the most attention as it has been frequently used as a comparative model for neuroanatomical studies of extinct archosaurs (e.g. Koken 1887; Edinger 1938; Witmer and Ridgely 2008; Holliday and Witmer 2009; Dufeu 2011; George and Holliday 2013; Hurlburt et al. 2013; Dufeu and Witmer 2015; Porter et al. 2016; Fabbri et al. 2017; Watanabe et al. 2019; Hu et al. 2020; Lessner and Holliday 2020).

In this contribution, we present an updated view of the cranial paleoneuroanatomy of Crocodylomorpha, describing the general morphology of the encephalon, cranial nerves, inner ear and principal cephalic blood vessels (e.g. cerebral carotid artery and venous sinuses-based on their osteological correlates) of the main groups within this clade: non-crocodyliform crocodylomorphs, thalattosuchians, notosuchian and neosuchian mesoeucrocodylians. Finally, we also discuss the paleobiological implications of the morphological patterns present in these groups. Definitions of major taxa of crocodylomorphs were considered as follows: Crocodylomorpha (“sphenodontians” and crocodyliforms; Clark 1986), Crocodyliformes (*Protosuchus richardsoni*, *Crocodylus niloticus*, and all descendants of their common ancestor; Sereno et al. 2001; following Clark 1986), Mesoeucrocodylia (all crocodyliforms more closely related to *Crocodylus niloticus* than to *Protosuchus richardsoni*; Sereno et al. 2001; following Whetstone and Whybrow 1983, Benton and Clark 1988), Notosuchia (all crocodyliforms more

Table 7.1 Background of publications on studies of Crocodylomorpha neuroanatomy, indicating habits and types of cranial endocast of taxa

Taxon	Specimens	Habitat	Provenance	Cranial endocast, brain or sectioned braincase	References
<i>Sphenosuchus acutus</i>	SAM PK 3014	Terrestrial	Early Jurassic of South Africa	Natural cranial endocast	Walker (1990)
<i>Almadasuchus figarii</i>	MPEF-V 3838	Terrestrial	Oxfordian of Argentina	Digital cranial endocast	Leardi et al. (2020)
<i>Eopneumatosuchus colberti</i>	MNA V2460	Terrestrial	Early Jurassic of United States	Digital cranial endocast	Dufeu (2011)
<i>Sebecus icaeorhinus</i>	AMNH 3160	Terrestrial	Eocene of Argentina	Latex cranial endocast	Colbert (1946), Hopson (1979)
<i>Aphaurosuchus escharafacies</i>	LPRP 0697	Terrestrial	Coniacian-Campanian of Brazil	Sectioned braincase	Darlim et al. (2021)
<i>Baurusuchus</i> sp.	IFSP-VTP/PALEO-0002, 0003; FEF-PV-R-1/9; FUP-Pv 000020, 000021	Terrestrial	Campanian-Maastrichtian of Brazil	Digital cranial endocast	Dumont et al. (2020)
<i>Campinasuchus dinizi</i>	CPPLIP 1360	Terrestrial	Turonian-Santonian of Brazil	Digital cranial endocast	Fonseca et al. (2020)
<i>Wargosuchus australis</i>	MOZ-PV 6134	Terrestrial	Santonian of Argentina	Latex cranial endocast	Martinelli and Pais (2008) and Fonseca et al. (2020)
<i>Araripesuchus wegneri</i>	MNN GAD18	Terrestrial	Aptian-Albian of Niger	Digital cranial endocast	Sereno and Larsson (2009)
<i>Anatosuchus minor</i>	MNN GAD19	Terrestrial	Aptian-Albian of Niger	Digital cranial endocast	Sereno and Larsson (2009)
<i>Simosuchus clarki</i>	UA 8679	Terrestrial	Maastrichtian of Madagascar	Digital cranial endocast	Kley et al. (2010)
<i>Hamadasuchus rebouli</i>	ROM 52560, 54511	Terrestrial	Aptian-Cenomanian of Morocco	Digital cranial endocast	Dufeu (2011) and George and Holliday (2013)
<i>Rukwasuchus yajabalijekundu</i>	RRBP 08630	Terrestrial	Aptian-Cenomanian of Tanzania	Digital cranial endocast	Sertich and O'Connor (2014)
<i>Uberabasuchus terrificus</i>	CPPLIP 1360	Terrestrial	Maastrichtian of Brazil	Digital cranial endocast	Fonseca et al. (2020)
<i>Pelagosaurus typus</i>	BRLSI M1413 NHMUK OR 32599	Semi-aquatic	Toarcian of England	Sectioned braincase Digital cranial endocast	Eudes-Deslongchamps (1863), Koken (1887), Dufeu (2011), Pierce et al. (2017) and Neenan et al. (2017)
<i>Proexochokefalos heberti</i>	MNHN.F unnumbered	Semi-aquatic	Callovian of France	Natural cranial endocast	Morel de Glasville (1876)
<i>Charitomenosuchus leedsi</i>	LPPM 35	Semi-aquatic	Callovian of France	Latex cranial endocast	Wharton (2000)

(continued)

Table 7.1 (continued)

Taxon	Specimens	Habitat	Provenance	Cranial endocast, brain or sectioned braincase	References
<i>Plagiophthalmosuchus</i> cf. <i>gracilirostris</i>	NHMUK PV OR 3395	Semi-aquatic	Toarcian of England	Digital cranial endocast	Brusatte et al. (2016)
<i>Macrospondylus bollensis</i>	SNSB-BSPG 1984 I258 MCZ VPRA-1063	Semi-aquatic	Toarcian of Germany	Digital cranial endocast	Herrera et al. (2018) and Wilberg et al. (2021)
<i>Teleosaurus cadomensis</i>	SMC J35177 MNHN AC 8746	Semi-aquatic	Bathonian of France	Sectioned braincase	Eudes-Deslongchamps (1863), Seeley (1880), Koken (1887), Jouve (2009), and Wilberg (2015a)
<i>Cricosaurus araucanensis</i>	MLP 72-IV-7-1 MOZ-PV 7201 MOZ-PV 7261	Pelagic	Tithonian of Argentina	Digital cranial endocast Natural cranial endocast	Herrera et al. (2013), Herrera et al. (2018) and Herrera (2015)
<i>Thalattosuchus superciliosus</i>	MNHN 1870-133	Pelagic	Callovian-Oxfordian of France	Sectioned braincase Natural cranial endocast	Wenz (1968)
' <i>Metriorhynchus</i> ' cf. ' <i>M.</i> <i>brachyrhynchus</i>	NHMUK PV OR 32617	Pelagic	Callovian-Oxfordian of France	Digital cranial endocast	Schwab et al. (2021)
' <i>Metriorhynchus</i> ' cf. ' <i>M.</i> <i>westermanni</i>	MDA 2	Pelagic	Oxfordian of Chile	Digital cranial endocast	Fernández et al. (2011) and Herrera et al. (2018)
<i>Dakosaurus</i> cf. <i>andiniensis</i>	MOZ-PV 089	Pelagic	Late Tithonian-early Berriasian of Argentina	Natural cranial endocast	Herrera (2015) and Herrera and Vennari (2014)
<i>Zoneait nargorum</i>	UOMNH F39539	Pelagic	Aalenian-Bajocian of United States	Natural cranial endocast	Wilberg (2015b)
<i>Pholidosaurus meyeri</i>	Unnumbered	Semi-aquatic	Berriasian of Germany	Natural cranial endocast	Koken (1887), Edinger (1938) and Hopson (1979)
<i>Pholidosaurus schauburgensis</i>	Unnumbered	Semi-aquatic	Berriasian of Germany	Natural cranial endocast	Koken (1887) and Edinger (1938)
cf. <i>Rhabdognathus</i>	CNRST-SUNY-190	Semi-aquatic	Maastrichtian-Paleocene of Mali	Digital cranial endocast	George and Holliday (2013)
<i>Rhabdognathus aslerensis</i>	AMNH FARB 33354	Semi-aquatic	Maastrichtian-Paleocene of Mali	Digital cranial endocast	Erb and Turner (2021)
<i>Goniopholis</i> sp.	Unnumbered	Semi-aquatic	Berriasian of England	Natural cranial endocast	Koken (1887) and Edinger (1938)
<i>Eutretauranosuchus delfsi</i>	CMNH 8028	Semi-aquatic	Kimmeridgian of United States	Digital cranial endocast	Smith (2008) and Dufeu (2011)

(continued)

Table 7.1 (continued)

Taxon	Specimens	Habitat	Provenance	Cranial endocast, brain or sectioned braincase	References
<i>Aegisuchus witmeri</i>	ROM 54530	Semi-aquatic	Cenomanian of Morocco	Digital cranial endocast	Holliday and Gardner (2012)
<i>Allodaposuchus hulki</i>	MCD 5139	Semi-aquatic	Maastrichtian of Spain	Digital cranial endocast	Blanco et al. (2015)
<i>Lohuecosuchus megadontos</i>	HUE-04498	Semi-aquatic	Campanian-Maastrichtian of Spain	Digital cranial endocast	Serrano-Martínez et al. (2018)
<i>Agaresuchus fontisensis</i>	HUE-02502	Semi-aquatic	Campanian-Maastrichtian of Spain	Digital cranial endocast	Serrano-Martínez et al. (2020)
<i>Thoracosaurus isorhynchus</i>	Unnumbered	Semi-aquatic	Maastrichtian of Spain	Natural cranial endocast	Lemoine (1883–1884)
<i>Gavialis gangeticus</i>	TMM M5490 AMNH R81802 MLP 602 UF 118998 UMZC R5792 ZIN 7249	Semi-aquatic	Recent of India	Sectioned braincase Latex cranial endocast Digital cranial endocast	Owen (1850), Koken (1887), Wharton (2000), Dufeu (2011), Gold et al. (2014), Pierce et al. (2017), Bona et al. (2017), Serrano-Martínez et al. (2018, 2019), and Kuzmin et al. (2021)
<i>Gryposuchus neogaeus</i>	MLP 68-IX-5-1	Semi-aquatic	Miocene of Argentina	Digital cranial endocast	Bona et al. (2017)
<i>Maomingosuchus petrolica</i>	IVPP V2303	Semi-aquatic	Eocene of China	Natural cranial endocast	Yeh (1958)
<i>Gunggamarandu maunala</i>	QMF14.547	Semi-aquatic	Pliocene-Pleistocene of Australia	Digital cranial endocast	Ristevski et al. (2021)
<i>Tomistoma schlegelii</i>	TMM M-6342 ZMMU MSU R-13859 ZMMU MSU R-9296	Semi-aquatic	Recent of Asian Southeastern	Sectioned braincase Digital cranial endocast	Serrano-Martínez et al. (2018, 2019) and Kuzmin et al. (2021)
<i>Paludirex vicenti</i>	CMC2019-010-5	Semi-aquatic	Pliocene-Pleistocene of Australia	Digital cranial endocast	Ristevski et al. (2020)
<i>Crocodylus niloticus</i>	Several specimens	Semi-aquatic	Recent of Africa	Sectioned braincase Digital cranial endocast	Eudes-Deslongchamps (1863), Koken (1887), Edinger (1938), George and Holliday (2013), Jirak and Janacek (2017), Beyrand et al. (2019) and Serrano-Martínez et al. (2018, 2019)
<i>Crocodylus acutus</i>	Several specimens	Semi-aquatic	Recent of America	Sectioned braincase Latex cranial endocast Digital cranial endocast	Owen (1850), Colbert (1946), Gold et al. (2014), Jirak and Janacek (2017), and Neenan et al. (2017)

(continued)

Table 7.1 (continued)

Taxon	Specimens	Habitat	Provenance	Cranial endocast, brain or sectioned braincase	References
<i>Crocodylus johnstoni</i>	OUV C 10425	Semi-aquatic	Recent of Australia	Digital cranial endocast	Witmer et al. (2008) and George and Holliday (2013)
<i>Crocodylus moreletii</i>	TMM M-4980	Semi-aquatic	Recent of Central America	Digital cranial endocast	Franzosa (2004)
<i>Crocodylus siamensis</i>	Unnumbered	Semi-aquatic	Recent of Asian Southeastern	Digital cranial endocast	Kawabe et al. (2009)
<i>Crocodylus porosus</i>	Unnumbered	Semi-aquatic	Recent of Australia	Sectioned braincase	Kundrát et al. (2018)
<i>Crocodylus novaeguineae</i>	DVZ M9/13	Semi-aquatic	Recent of New Guinea	Sectioned braincase	Kuzmin et al. (2021)
<i>Osteolaemus tetraspis</i>	MZB 2006-0039 DVZ M7/13	Semi-aquatic	Recent of Africa	Digital cranial endocast	Serrano-Martínez et al. (2018, 2019) and Kuzmin et al. (2021)
<i>Mecistops cataphractus</i>	DVZ M6/13	Semi-aquatic	Recent of Africa	Sectioned braincase	Kuzmin et al. (2021)
<i>Diplocynodon tormis</i>	STUS-344	Semi-aquatic	Eocene of Spain	Digital cranial endocast	Serrano-Martínez et al. (2019)
<i>Leidyosuchus?</i>	UNM B-401 A	Semi-aquatic	Paleocene of United States	Natural cranial endocast	Storrs et al. (1983)
<i>Leidyosuchus canadensis</i>	ROM 1903	Semi-aquatic	Campanian of Canada	Digital cranial endocast	George and Holliday (2013)
<i>Alligator mississippiensis</i>	Several specimens	Semi-aquatic	Recent of United States	BrainSectioned braincase Latex cranial endocast Digital cranial endocast	Rabl-Rückhard (1878), Lemoine (1883–1884), Koken (1887), Edinger (1938), Colbert (1946), Romer (1956), Chiasson (1962), Brochu (1999), Witmer and Ridgely (2008), Sereno and Larsson (2009), George and Holliday (2013), Hurlburt et al. (2013), Dufeu and Witmer (2015), Fabbri et al. (2017), Kundrát et al. (2018), Serrano-Martínez et al. (2018, 2019), Watanabe et al. (2019), Hu et al. (2020), Lessner and Holliday (2020), and Kuzmin et al. (2021)

(continued)

Table 7.1 (continued)

Taxon	Specimens	Habitat	Provenance	Cranial endocast, brain or sectioned braincase	References
<i>Alligator sinensis</i>	DVZ M 2/13, 3/13	Semi-aquatic	Recent of China	Sectioned braincase	Iordansky (1973) and Kuzmin et al. (2021)
<i>Paleosuchus palpebrosus</i>	FMNH 69869	Semi-aquatic	Recent of South America	Sectioned braincase Digital cranial endocast	Eudes-Deslongchamps (1863), Koken (1887) and Dufeu (2011)
<i>Paleosuchus trigonatus</i>	AMNH 137175	Semi-aquatic	Recent of South America	Digital cranial endocast	Balanoff and Bever (2017)
<i>Mourasuchus nativus</i>	MLP 73-IV-15-9	Semi-aquatic	Miocene of South America	Digital cranial endocast	Bona et al. (2013)
<i>Caiman crocodilus</i>	FMNH 73711	Semi-aquatic	Recent of America	Digital cranial endocast	Brusatte et al. (2016), Jirak and Janacek (2017), Beyrand et al. (2019), Serrano-Martínez et al. (2018, 2019), and Kuzmin et al. (2021)
<i>Caiman gasparinae</i>	MLP 73-IV-15-1	Semi-aquatic	Miocene of South America	Latex cranial endocast	Bona and Paulina-Carabajal (2013)
<i>Caiman yacare</i>	MLP 603 MACN-He 43694 ZMMU MSU R-6967	Semi-aquatic	Recent of South America	Sectioned braincase Latex cranial endocast Digital cranial endocast	Bona and Paulina-Carabajal (2013), von Baczko et al. (2018), and Kuzmin et al. (2021)
<i>Melanosuchus niger</i>	UFRGS-PV 003-Z	Semi-aquatic	Recent of South America	Digital cranial endocast	George and Holliday (2013) and Fonseca et al. (2020)

closely related to *Notosuchus terrestris* than to *Crocodylus niloticus*; Sereno et al. 2001; following Pol et al. 2014), and Neosuchia (all crocodyliforms more closely related to *Crocodylus niloticus* than to *Notosuchus terrestris*; Sereno et al. 2001; following Benton and Clark 1988).

7.2 Overview of General and Comparative Anatomy

7.2.1 Neuroanatomy of Extant Crocodylians

Brain

As in other amniotes, the brain of living crocodylians is anatomically (and functionally) initially divided into three principal parts: the prosencephalon or forebrain, the mesencephalon or midbrain and the rhombencephalon or hindbrain (e.g. Romer 1956; Vaage 1969; Hopson 1979; Vieira et al. 2010; Figs. 7.2 and 7.3). In advanced

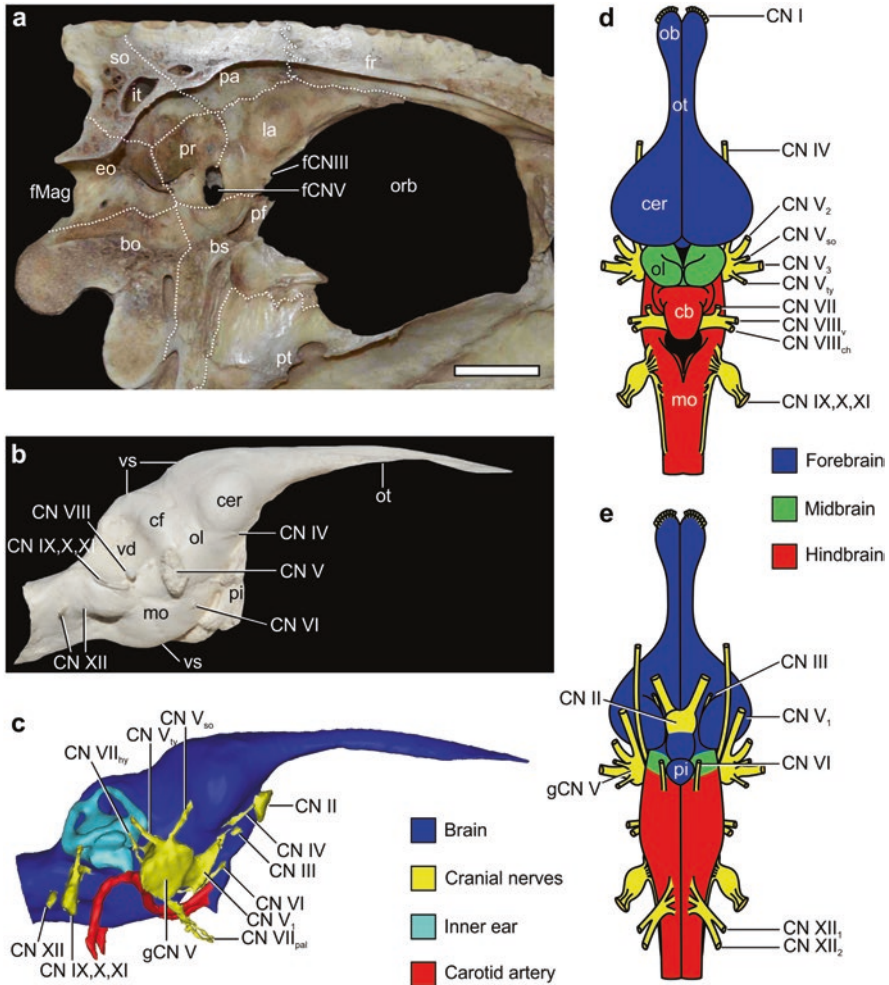


Fig. 7.2 Main sources of neuroanatomical information for paleoneurological studies, for example, *Caiman yacare* [a, b (MLP 603); c (MACN-He 43,694)] and *Alligator mississippiensis* (d, e). a, sectioned braincase; b, latex cranial endocast; c, digital cranial endocast. Brain in dorsal view (d) and ventral view (e); modified from Romer (1956). Scale bar in a = 1 cm

ontogenetic stages the prosencephalon becomes differentiated into a telencephalon or cerebral hemispheres (=cerebrum), and a less developed and posterior diencephalon (Fig. 7.2d). In living crocodylians as *Caiman crocodilus*, *Alligator mississippiensis* and *Crocodylus niloticus*, the brain and the cranial endocast become morphologically transformed during post-hatching ontogeny (e.g. Hopson 1979; Chentanez et al. 1983; George and Holliday 2013; Ngwenya et al. 2013; Jirak and Janacek 2017; Kundrát et al. 2018; Watanabe et al. 2019; Hu et al. 2020). As in other non-avian reptiles, the brain of adult crocodylians does not completely fill the

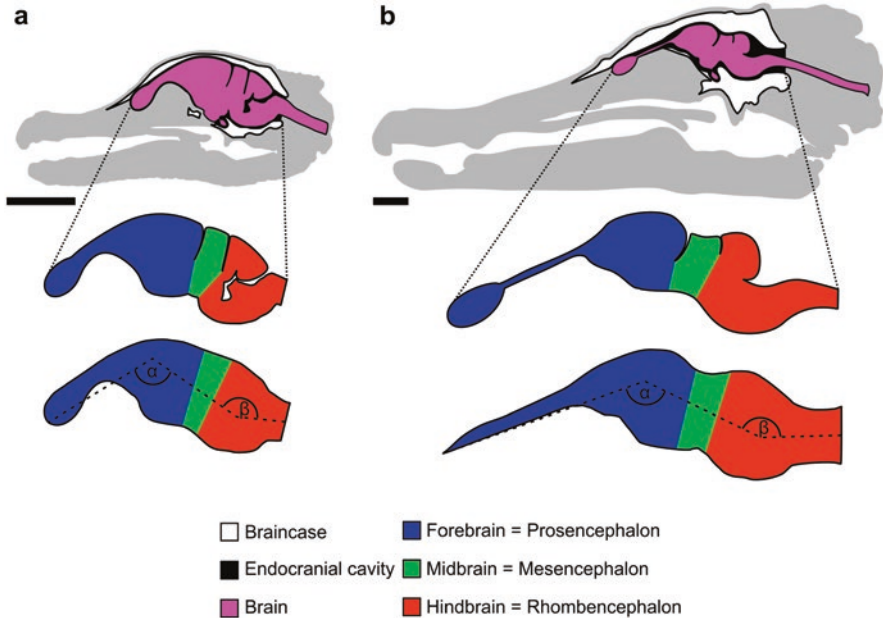


Fig. 7.3 Sagittal slices through the heads of *Alligator mississippiensis*, perinatal (a) and juvenile (b) individuals; modified from Watanabe et al. (2019, fig 1). Graphic interpretation, brain, and cranial endocast. Angle between forebrain and midbrain (α), angle between midbrain and hindbrain (β). Scale bar = 1 cm

endocranial cavity, contrary to what occurs in earliest post-hatching ontogenetic stages where the brain occupies nearly the 95% of the endocranial space (e.g. Hopson 1979; Hurlburt and Waldorf 2002; Jirak and Janacek 2017; Hu et al. 2020; Fig. 7.3). Jirak and Janacek (2017) reported that the brain changes its general shape through the ontogeny, going from an S-shaped configuration in early post-hatched juveniles to a more linearly organized brain in grown individuals (Table 7.2). This contrasts with the cranial endocast that elongates and expands interstitially throughout ontogeny. As a result, more mature (and larger) crocodylian specimens show higher values of cranial endocast volume/brain volume than that of immature (and smaller) specimens, where the brain occupies approximately 29% of cranial endocast volume in largest forms. These authors also find that during ontogeny, the highest proportion of brain tissue to cranial endocast volume is in the prosencephalon, followed by the rhombencephalon, as it was confirmed in later contributions by other authors (i.e. Watanabe et al. 2019; Hu et al. 2020). Thus, the larger the relative size of the crocodylian endocranial cavity, the less informative it is regarding the morphology and volume of the brain, especially for the rhombencephalon (Fig. 7.3). Despite this, the cranial endocast of adult crocodylians reflects the general shape and relative size of some parts of the brain (i.e., distinction and proportions between forebrain, midbrain and hindbrain, the angles between these regions, the lateral shape of the cerebral hemispheres, the olfactory bulbs and tracts, the pituitary gland,

and in some cases, it is also possible to recognize the optic lobes of the mesencephalic tectum and flocculi of the cerebellum). Therefore, qualitative and quantitative morphological features of these cranial endocast structures are often used in comparative paleoneurology (e.g. Rogers 1998; Larsson et al. 2000; Franzosa 2004; Witmer and Ridgely 2008; Witmer et al. 2008; George and Holliday 2013; Fig. 7.2b, c). Considering this, the neuroanatomy of the extinct forms described in this chapter is based on anatomical inferences of the cranial endocast made from the osseous correlates of soft organs and tissues. In this way, in the following sections, we

Table 7.2 Comparison of cranial endocast measurements of crocodylomorphs taxa

Taxa	Forebrain-midbrain angle	Midbrain-hindbrain angle	Source
<i>Almadasuchus figarii</i>	161°	170°	Leardi et al. (2020)
<i>Araripesuchus wegeneri</i>	157°	160°	Sereno and Larsson (2009)
<i>Anatosuchus minor</i>	157°	162°	Sereno and Larsson (2009)
<i>Rukwasuchus yajabaliyekundu</i>	149°	155°	Sertich and O'Connor (2014)
<i>Simosuchus clarki</i>	142°	165°	Kley et al. (2010)
<i>Baurusuchus</i> sp.	160°	163°	Dumont et al. (2020)
<i>Campinasuchus dinizi</i>	161°	163°	Fonseca et al. (2020)
<i>Sebecus icaeorhinus</i>	150°	160°	Colbert (1946)
<i>Steneosaurus bollensis</i>	175°	170°	Brusatte et al. (2016)
<i>Pelagosaurus typus</i>	160°	160°	Pierce et al. (2017)
<i>Cricosaurus araucanensis</i>	166°	162°	Herrera et al. (2018)
<i>Pholidosaurus meyeri</i>	143°	150°	Edinger (1938)
<i>Rhabdognathus aslerensis</i>	158°	152°	Erb and Turner (2021)
<i>Goniopholis</i> sp.	140°	161°	Edinger (1938)
<i>Agaresuchus fontisensis</i>	156°	151°	Serrano-Martínez et al. (2020)
<i>Thoracosaurus isorhynchus</i>	159°	165°	Lemoine (1883–1884)
<i>Gavialis gangeticus</i>	147°	158°	Pierce et al. (2017)
<i>Tomistoma schlegelii</i>	148°	147°	This study
<i>Crocodylus niloticus</i>	149°	159°	This study
<i>Osteolaemus tetraspis</i>	132°	149°	This study
<i>Leidyosuchus</i> sp.	153°	150°	Storrs et al. (1983)
<i>Diplocynodon tormis</i>	145°	142°	Serrano-Martínez et al. (2019)
<i>Alligator mississippiensis</i>	131°	146°	Witmer and Ridgely (2008)
<i>Caiman yacare</i>	126°	143°	This study

described the cast of the pituitary, olfactory tracts, cerebral hemispheres, etc. as the soft structures itself.

The principal anatomical features of the forebrain of living crocodylians are rather accurately represented in the cranial endocast (i.e. internal surfaces of parietal posterodorsally, frontal anterodorsally, laterosphenoids, laterally and basisphenoid, ventrally; Fig. 7.2a). The dural envelope surrounding the forebrain is relatively thin and the bony walls of the braincase lie close to the cerebral hemispheres, olfactory tracts and bulbs (Hopson 1979). The anterior forebrain of crocodylians is laterally expanded into a pair of cerebral hemispheres (Fig. 7.2d, e). As in other amniotes, both lateral hemispheres are medially separated by a deep cleft that is invaded by the dura and contains vascular structures like the longitudinal venous sinus and arteries, which run across the cleft it forward to the nasal cavity (the slight midline elevation reflected in several cranial endocasts at this level may correspond to these vascular elements; Hopson 1979, fig 2B, C). In living crocodylians, cerebral hemispheres are sub-spherical structures (but see comparisons below) enclosed by the medial surface of the laterosphenoid (Fig. 7.2a) that represent the transversely widest sector of the brain (Fig. 7.2d). As in other non-avian reptiles, excluding turtles, the olfactory neurons located at the anterior nuclei of the dorsal ventricular ridge of the telencephalic pallium project anteriorly from the cerebral hemispheres into a pair of olfactory tracts, each of them anteriorly expanded in an olfactory bulb (Billings et al. 2020; Fig. 7.2d). The olfactory tracts lie in the cavum suprasetale at the dorsal edge of the interorbital septum and are dorsally covered by the frontal (Starck 1979; Fig. 7.2a). As a consequence, the anteroposterior extension and shape of the tracts reflect the overall extension and morphology of the orbital region of the skull (which also grows allometrically during ontogeny). The relative size of the olfactory bulb is positively correlated with the magnitude of the olfactory system (Starck 1979) and its measurement is taken into account when estimating the olfactory acuity of an individual (Zelenitsky et al. 2009). The crocodylian diencephalon is macro-anatomically similar to other reptiles. The pineal complex (= parietal eye and more deeply situated pineal gland) present in several reptiles is absent as a discrete organ in crocodylians (e.g. Quay 1979; Starck 1979; Firth et al. 2010; Witmer 2018; Billings et al. 2020; however see Colbert 1946 and Hopson 1979 for a different point of view). As in other gnathostomes, the ventral aspect of the crocodylian diencephalon, the hypothalamus, is ventrally evaginated, forming the optic chiasm and tracts (from here on cranial nerves II or CN II) and the odd and posterior neurohypophysis, which projects ventrally by an infundibulum into the hypophyseal fossa (Fig. 7.2e). Together with the adenohypophysis (the anterior part of the gland that is formed from the embryonic stomodeum) the neurohypophysis forms the hypophysis (pituitary gland), which almost fills the hypophyseal fossa (Girons 1970). Part of the anterodistal portion of the hypophyseal fossa is also occupied by blood vessels (branches of the cerebral carotid arteries and cavernous sinus; Porter et al. 2016). This fossa is excavated in the basisphenoid (Fig. 7.2a) and its volume indicates the approximate maximum volume of the hypophysis during the animal's life.

The anatomical features and volume of the remaining parts of the brain of living crocodylians (i.e., mesencephalon and rhombencephalon) are lesser evidenced in the cranial endocast (e.g. Hopson 1979; Watanabe et al. 2019; Figs. 7.2b, c and 7.3). The dural covering of the mid- and hindbrain is generally much thicker. In addition, the interstitial space between the cranial endocast and the posterior portion of the midbrain and the entire hindbrain is occupied by vascular structures like the large longitudinal venous sinus and its principal branches, which obscures the underlying brain morphology (e.g. Hopson 1979; Porter et al. 2016). In crocodylians, as in other living reptiles, the mesencephalon consists of a roof containing the optic tectum and auditory torus semicircularis nuclei, and a floor that contains the rostral tegmentum (Senn 1979; Billings et al. 2020). The most conspicuous anatomical structures of the mesencephalon of almost all vertebrates are the optic lobes, which are a pair of dorsolateral projections of the optic tectum (Figs. 7.2d and 7.3). Although in living crocodiles, these are conspicuous sub-spherical structures located posterior to the cerebrum, they do not leave evidence of their size or shape on the cranial endocast (Fig. 7.2b, c). Nevertheless, the position of the optic tectum is indicated in the cranial endocast by the lateral constriction and drop in height of the cranial endocast caudal to the cerebral region (Hopson 1979; Hu et al. 2020; Figs. 7.2b, c and 7.3).

As in other vertebrates, the hindbrain comprises the cerebellum (=metencephalon) and the medulla oblongata (=myelencephalon) (Fig. 7.2d, e). The rhombencephalon is higher than wide, being laterally strangled by the development of the inner ear labyrinth. The medulla oblongata is more sharply confined and its posteriormost diameter is almost equal to the diameter of the occipital spinal cord (Figs. 7.2 and 7.3). Hopson (1979) describes that in caimans, the cerebellum is narrower but almost equal in height to the optic tectum. However, the cranial endocast posterior to the optic tectum provides more information about the morphology of the venous sinuses and its branches than it does about the cerebellum. The cerebellar flocculus is slightly laterally developed, leaving a smooth bony imprint or recess on the medial surface of the prootic, just anterior to the vestibular eminence, and posterodorsally to the foramen for CN V (e.g., *Alligator mississippiensis*, *Caiman yacare*, Fig 7.2a).

Inner Ear

As in other gnathostomes, the crocodylian inner ear consists of an internal membranous layer surrounded by bony labyrinths which are anatomically and functionally differentiated into two main distinct portions: one, the vestibular apparatus, formed by three semicircular canals (anterior, posterior and lateral; from here on ASC, PSC and LSC, respectively) ventrally connected by an utriculus which also communicates with a sacculus; and a posteroventrally projected and tubular lagena (Wever 1978; Manley 2016; Fig. 7.4). The vestibular apparatus and lagena are innervated by the vestibular and cochlear divisions of the vestibulocochlear nerve (CN VIII), respectively (Baird 1970; Wever 1978). Whereas the vestibular apparatus is linked

with equilibrium, spatial position and linear accelerations (utricle, saccule and ampullae at the base of each semicircular canal) and angular acceleration (semicircular canals), the lagena is responsible for sound perceptions (e.g. Liem et al. 2000; Georgi 2008). The general aspect of the endosseous labyrinth is similar within crocodylian species, with a triangular vestibular sector (with ASC and PSC forming angles near to 90° in dorsal view) and a relatively elongated lagena (Gleich and Manley 2000; Fig. 7.4). As in other archosaurs, the vertical semicircular canals (ASC and PSC) vary in height, ASC being the larger (e.g. Georgi 2008; Witmer et al. 2008).

Cranial Nerves of Crocodylomorphs

The cranial nerves of vertebrates (which in amniotes are the terminal nerve or CN 0 and the CNs I - XII) are quite conserved through evolution and often maintain consistent paths to their targets despite occasional, significant lineage-specific neurocranial element shifts (Hopson 1979). This conservation of the neurological system facilitates relatively accurate identifications of the foramina and pathways of the nerves and their branches when near the bony surfaces of the skull, including those of crocodylomorphs (Lessner and Holliday 2020; Kuzmin et al. 2021). Recently, the combination of contrast-enhanced CT imaging (Holliday et al. 2013; Gignac et al. 2016; Lessner and Holliday 2020; Lessner 2020) enabled morphologists to better trace the cranial nerves through the skull and its soft tissues of alligators and other crocodylians, offering a more clear resolution of pathways and anatomical relationships of structures. These data (Figs. 7.2 and 7.5) now serve as a rich template for

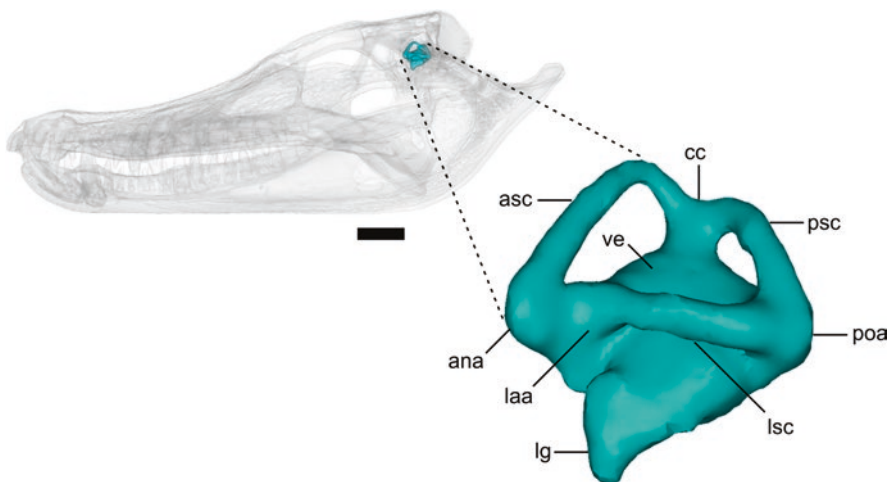


Fig. 7.4. Digital cranial endocast of the left inner ear of *Caiman yacare* (MACN-He 43694), showing the main components. The images are surface renderings of CT scan data. The skull is transparent revealing the location and size of the inner ear. Scale bar = 2 cm

reconstructing the paths of nerves in the skulls of extinct crocodylomorphs (Figs. 7.6, 7.7 and 7.8).

7.2.2 Comparative Anatomy of Crocodylomorph Brain and Inner Ear

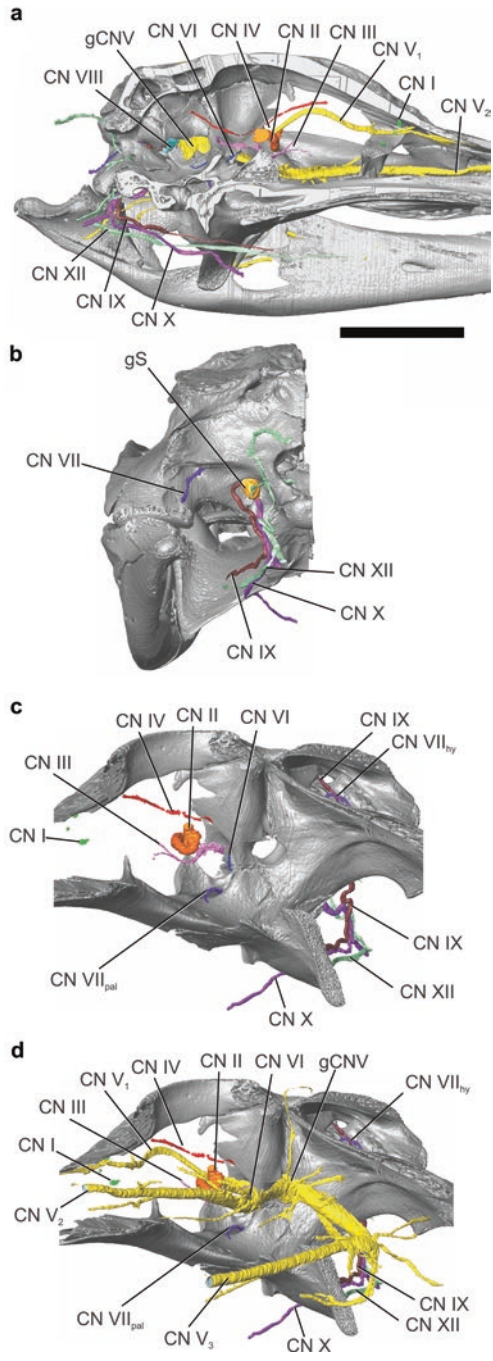
Non-crocodyliform Crocodylomorphs and Basal Crocodyliforms

Brain The knowledge of the brain of non-crocodyliform crocodylomorphs is limited to an almost complete cranial endocast of *Almadasuchus figarii* (MPEF-V 3838; Leardi et al. 2020) that partially preserves the olfactory bulbs, and a partial natural cranial endocast of *Sphenosuchus acutus* (SAM PK 3014; Walker 1990) that preserves the hindbrain. This limited number of specimens with known cranial endocasts contrasts with the absolute lack of published evidence in non-mesoeucrocodylian crocodyliforms. As a consequence, there is a gap in information and a lack of understanding of the major changes that might have happened in the brain during the initial diversification of crocodyliforms at the Late Triassic- Early Jurassic (Martínez et al. 2019; Leardi et al. 2020).

One taxon worthy of mention is *Eopneumatosuchus colberti* (Crompton and Smith 1980), whose cranial endocast has been reconstructed by Dufeu (2011, fig 1.5). This digital reconstruction is figured only in dorsolateral view and it is partially obscured by the dorsal pneumatic diverticula, which are present in most non-thalattosuchian crocodyliforms, allowing only clear observation of the olfactory bulbs (Dufeu and Witmer 2015; Leardi et al. 2020). *Eopneumatosuchus* has been classically considered a basal crocodyliform (Crompton and Smith 1980; Clark 1986; Benton and Clark 1988) and a formal redescription of this taxon has not been published to date. However, in recent phylogenetic analyses, it has been recovered, with low support values, within Mesoeucrocodylia, as the sister taxon of thalattosuchians (Ristevski et al. 2018; Johnson et al. 2020). Thus, comparisons among stem crocodyliforms including *Eopneumatosuchus* should be handled with caution.

The cranial endocast of *Almadasuchus* is tubular, as in other pseudosuchian archosaurs (Lautenschlager and Butler 2016; Pierce et al. 2017), and unlike the more sigmoidal cranial endocast of living crocodylians, non-avian dinosaurs and birds (e.g. Witmer et al. 2008; Bronzati et al. 2017; Fig. 7.9). This cylindrical shape of the cranial endocast is a result of low angles between the forebrain, midbrain and hindbrain, that in *Almadasuchus* present similar values as in thalattosuchians (161° and 170°, respectively; see Table 7.2). However, unlike thalattosuchians, where the dorsal border of the cranial endocast is basically straight (e.g. *Cricosaurus*, *Macrospondylus*, *Plagiophthalmosuchus*), in *Almadasuchus* it is slightly convex and resembles a series of waves. This is the result of dorsoventral inflexions located at the transition between the olfactory tract and the cerebral hemispheres, and at the level of the boundaries between midbrain and hindbrain (this last one probably

Fig. 7.5 Cranial anatomy and 3D models of cranial nerves of *Alligator mississippiensis* (MUVCL31) modified from Lessner and Holliday (2020). (a), left medial view; (b), caudal view; (c), left lateral view with deep structures; (d), left lateral view with more superficial structures. Scale bar = 2 cm



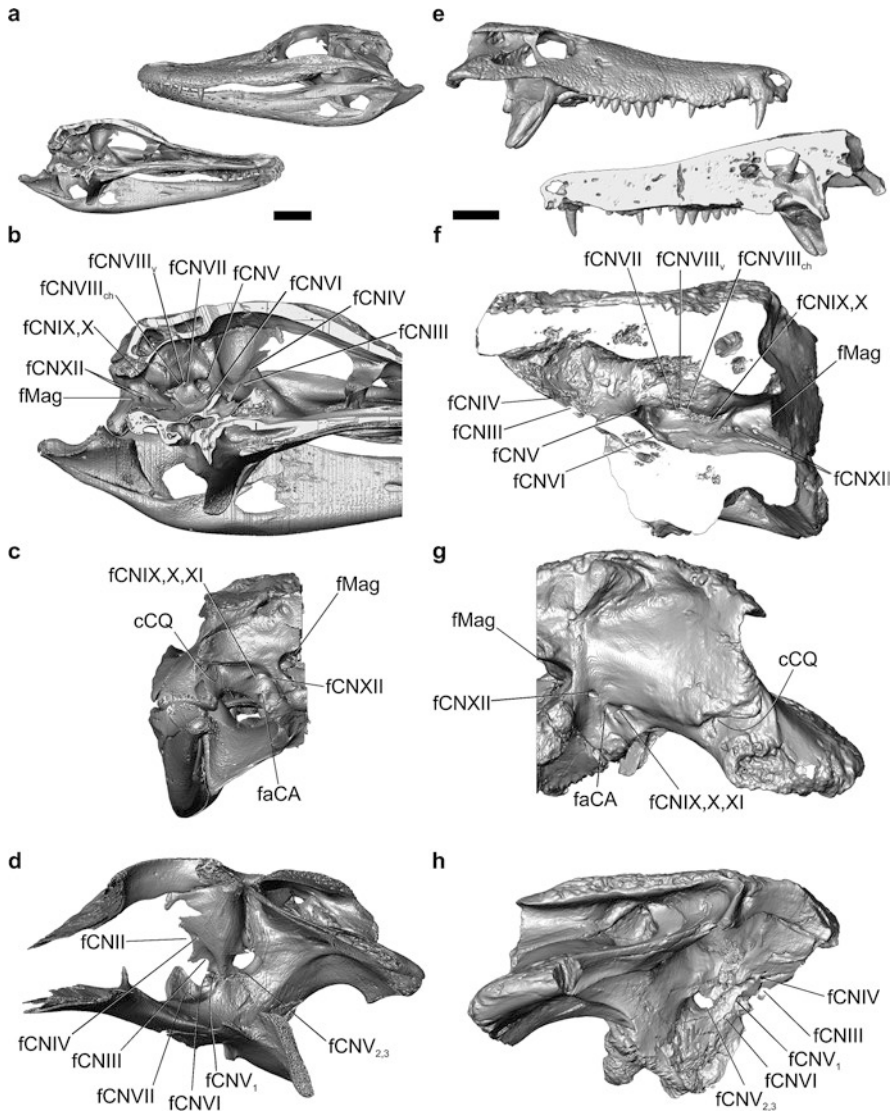


Fig. 7.6 Braincase anatomy and foramina of cranial nerves: *Alligator mississippiensis* (a; MUV AL623) in left medial (b), caudal (c) and left lateral (d) views; and *Hamadasuchus rebouli* (e; ROM 52620) in left medial (f), caudal (g) and left lateral (h) views. Scale bar = 2 cm (a) and 5 cm (e)

related to the shape and size of the dorsal longitudinal venous sinus), as in most crocodyliforms (Fig. 7.9). The dorsal shape of the cranial endocast of *Eopneumatosuchus* is unknown, but in *Sphenosuchus*, the preserved midbrain-hindbrain shows a more marked pontine flexure (angle between midbrain and hindbrain) and a more dorsally convex dorsal surface of the hindbrain (Walker 1990, fig

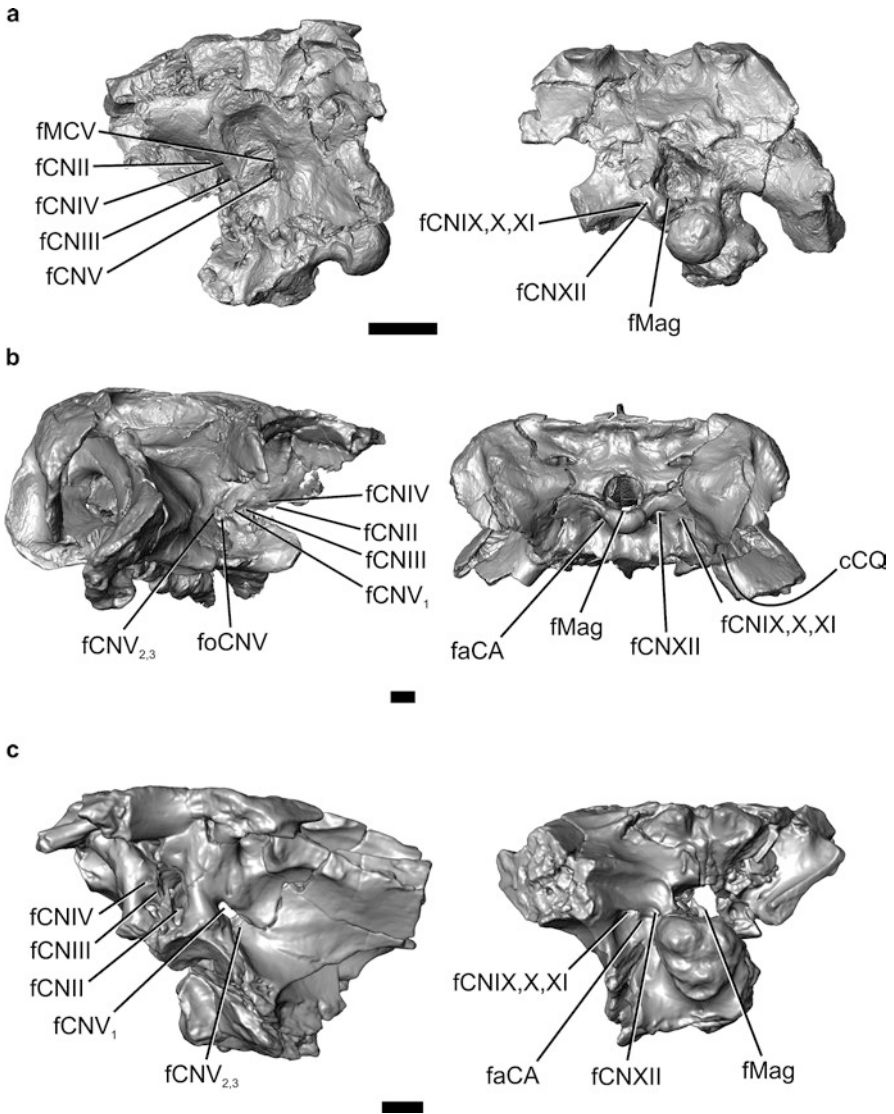
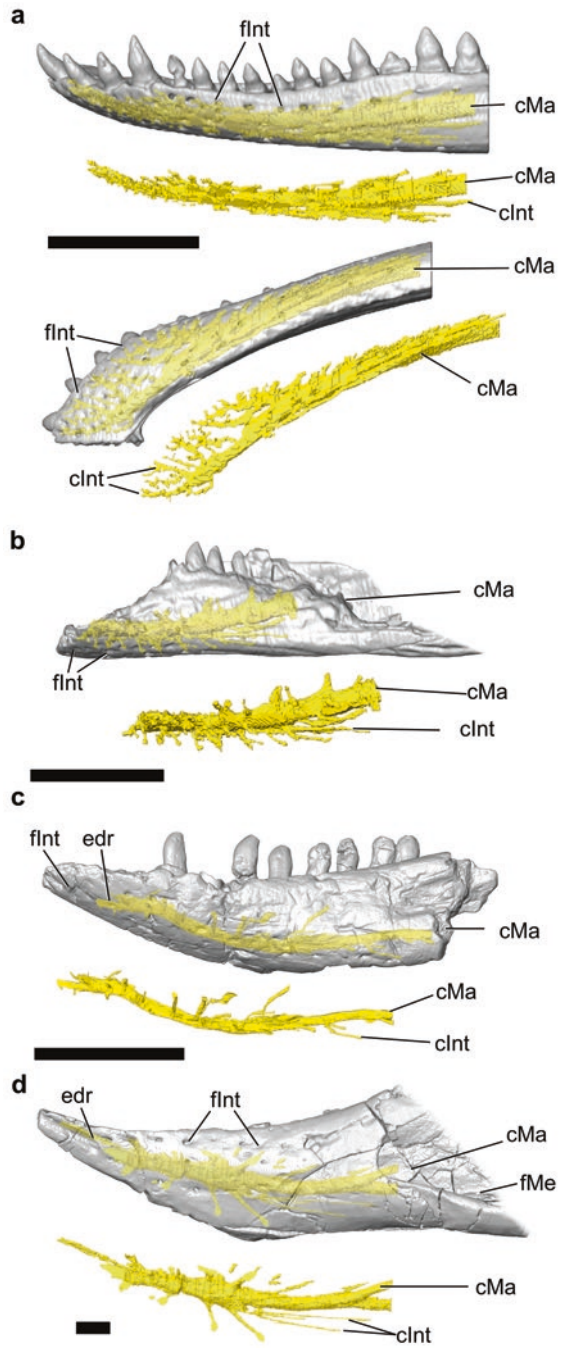


Fig. 7.7 Braincase anatomy and foramina of cranial nerves: *Longosuchus meadi* (a; TMM 31185-84B) in left lateral and caudal views; *Almadasuchus figarii* (b; MPEF-PV 3838) in right lateral and caudal views; and *Aegisuchus witmeri* (c; ROM 54530) in left lateral view and caudal views. Scale bar = 2 cm

46). In lateral view, this morphology of the cranial endocast contrasts with that of *Almadasuchus*; and is similar to several extinct and extant mesoeucrocodylians (e.g. *Araripesuchus*, *Simosuchus*, *Sebecus*, *Goniopholis*, *Leidyosuchus*, and living *Gavialis*, *Alligator*, *Crocodylus* and *Caiman*; Fig. 7.9).

Fig. 7.8 Mandibles and endocasts of mandibular canals of (a) *Alligator mississippiensis* (MUV AL31) in left lateral and ventral views; (b) *Araripesuchus gomesii* (AMNH 24450) in left lateral view; (c) *Macelognathus vagans* (LACM 5572/150148) in left lateral view; and (d) *Longosuchus meadi* (TMM 31185-84B) in left lateral view. Scale bar = 1 cm



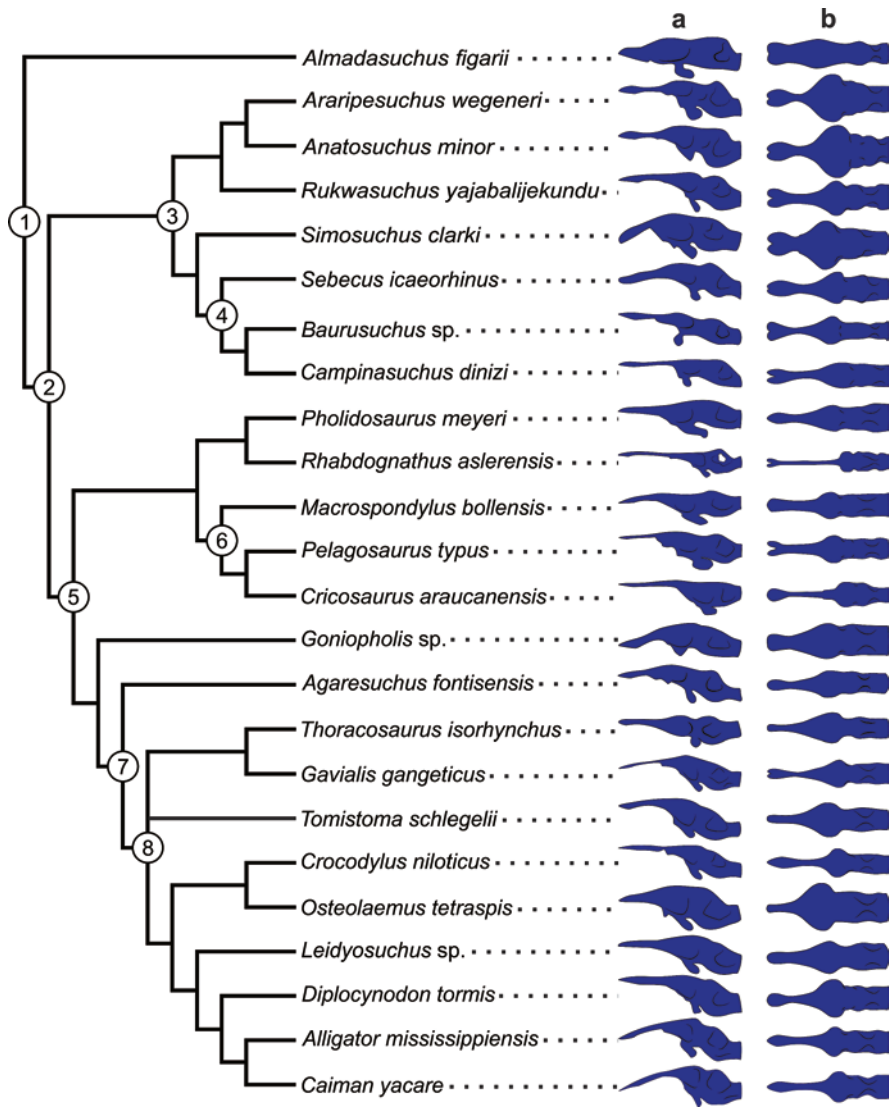


Fig. 7.9 Phylogenetic relationships of the crocodylomorph taxa with respective cranial endocast published, in lateral (a) and dorsal (b) views. Phylogenetic relationships are based in Pol et al. (2013, 2014) and Narváez et al. (2016). The cranial endocasts are scaled in their anteroposterior length. For *Araripesuchus wegeneri* and *Anatosuchus minor*, the olfactory tract and bulbs were reconstructed from unpublished data. Numerical references: (1) Crocodylomorpha, (2) Crocodyliformes, (3) Notosuchia, (4) Sebecosuchia, (5) Neosuchia, (6) Thalattosuchia, (7) Eusuchia and (8) Crocodylia

The forebrain of *Almadasuchus* is partially complete as the olfactory bulbs are not entirely preserved (Fig. 7.9). The olfactory bulbs are undivided medially (by bone) as in most crocodylomorphs except for *Eopneumatosuchus*, the

thalattosuchian *Pelagosaurus* (Pierce et al. 2017) and the notosuchians *Simosuchus* (Kley et al. 2010), *Rukwasuchus* (Sertich and O'Connor 2014) and *Baurusuchus* (Dumont Jr et al. 2020). Unlike most mesoeucrocodylians (e.g. *Simosuchus*, *Sebecus icaeorhinus*, *Cricosaurus araucanensis*, *Macrospodylus bollensis*, *Alligator mississippiensis*) and similar to other non-crocodylomorphs pseudosuchians (e.g. aetosaurs as *Desmotosuchus*, von Baczko et al. 2021), the olfactory tracts are markedly anteroposteriorly short and almost as mediolaterally wide as the olfactory bulbs, which are also slightly narrower than the cerebral hemispheres. The cerebral hemispheres of *Almadasuchus* are moderately laterally expanded, contrasting with mesoeucrocodylian crocodyliforms including thalattosuchians (e.g. *Pelagosaurus*, *Macrospodylus*, *Plagiophthalmosuchus*, *Araripesuchus*, *Simosuchus*, *Gavialis*, *Alligator*, *Crocodylus* and *Caiman*; Table 7.2). As in most crocodylomorphs, the interhemispheric fissure of *Almadasuchus* is obscured by the dorsal dural longitudinal venous sinus (e.g. Hopson 1979; Witmer et al. 2008; Kley et al. 2010). Ventral to the cerebral hemispheres, the cranial endocast of the hypophyseal fossa is anteroposteriorly longer than its mediolateral width. This anteroposterior enlargement of the pituitary cast probably reflects the anteroposterior enlargement of the gland, similar to that observed in thalattosuchians (e.g. *Pelagosaurus*, Pierce et al. 2017; *Macrospodylus bollensis*, *Cricosaurus araucanensis*, Herrera et al. 2018) and contrasts with the anteroposteriorly shorter pituitary casts of other crocodylomorphs (Fig. 7.9). As in other crocodylomorphs, the cerebral carotid arteries canals in *Almadasuchus* reach the hypophyseal fossa via the carotid pillars that enclose these arteries where they pierce the basisphenoid (Walker 1990). The cerebral carotid arteries branch from the internal carotid arteries immediately before they enter the braincase through the internal carotid foramen (Porter et al. 2016), which in *Almadasuchus* pierce each otoccipital near to the otoccipital-basioccipital suture at the neck of the occipital condyle. This most posterior placement of the carotid foramen is a derived condition within Crocodylomorpha, shared with hallopodids + crocodyliforms and absent in more basal forms of the clade and other pseudosuchians (i.e. Pol et al. 2013; Leardi et al. 2017, 2020).

In lateral view, the cranial endocast of *Almadasuchus* is expanded at the level of the cerebellum, being dorso-ventrally higher than the cerebral hemispheres due to the marked dorsal development of the longitudinal venous sinus, which also forms an abrupt step at the transition between the cerebellum and the medulla oblongata as in other crocodyliform cranial endocasts (Fig. 7.9). A well-developed cerebellar flocculus can be identified in the hindbrain of the *Almadasuchus*.

Inner Ear The inner ear anatomy of basal crocodylomorphs is better documented than that of the brain. Despite the bony labyrinth of *Almadasuchus* (Leardi et al. 2020), recent anatomical information of the inner ear shows a greater morphological diversity among non-crocodyliform crocodylomorphs and early crocodyliforms (e.g. *Junggarsuchus sloani*, *Protosuchus haughtoni*, and the conflictive *Eopneumatosuchus colberti*; Schwab et al. 2020). *Macelognathus vagans* (LACM 5572/150148) also preserves a partial left bony labyrinth (Leardi et al. 2017; but a description of the inner ear was not published nor figured). *Junggarsuchus* and

Almadasuchus are closely related to crocodyliforms (Leardi et al. 2017) and present marked morphological differences in their inner ears. This disparity prevents the interpretation of the primitive condition of the inner ear in basal Crocodyliformes. Major morphological differences among the inner ear of these species are in the vestibule and the lagena. *Junggarsuchus* (IVPP V 14010) has a relatively narrow vestibule, with a more marked constriction at the beginning of the lagena, similar to the condition seen in crocodyliforms (e.g. *Protosuchus haughtoni* BP/1/4770). On the other hand, *Almadasuchus* shows a more inflated (lateromedially expanded) vestibule with a robust crus commune. This condition resembles that of *Eopneumatosuchus* and some thalattosuchians (Schwab et al. 2020, fig 2). Another important difference between *Almadasuchus* and *Junggarsuchus* is the relative length of the lagena, which in the last species is dorsoventrally longer than the vestibular system. In contrast, in *Almadasuchus* the lagena seems to be shorter, a condition similar to *Eopneumatosuchus* and thalattosuchians (Fig. 7.10). However, in *Almadasuchus*, *Eopneumatosuchus* and *Junggarsuchus*, the lagena is straight in lateral view, contrasting strongly with the anteriorly concave lagenae of crocodyliforms, including thalattosuchians (Schwab et al. 2020, fig 2; Dumont Jr et al. 2020, fig 9). Besides the mentioned differences, *Junggarsuchus* and *Almadasuchus* show an inner ear similar to other non-crocodylomorph pseudosuchians (see Lautenschlager and Butler 2016), with a dorsoventrally low vestibular apparatus and an ASC that is dorsoventrally higher but anteroposteriorly longer than the PSC (Leardi et al. 2020; Schwab et al. 2020). The ASC and PSC are narrow, unlike the derived condition present in most metriorhynchids in which the diameter of the tube of those canals are relatively larger in cross section (Schwab et al. 2020). The lateral semicircular canal (LSC) is only known in *Junggarsuchus*.

Thalattosuchia (Teleosauroidea and Metriorhynchoidea)

Brain Because they have very subtle flexures, thalattosuchian cranial endocasts are in general almost tubular (Fig. 7.9 and Table 7.2). The cerebral hemispheres are bulbous structures that project laterally but not to the same extent observed in notosuchians and modern crocodylians. The optic lobes are visible as subtle swellings just posterior to the cerebral region, as in young specimens of *Caiman crocodilus* and *Alligator mississippiensis* (Hopson 1979; Dufeu and Witmer 2015; Jirak and Janacek 2017). The pituitary is relatively small, anteroposteriorly long and dorsoventrally low, except in *Pelagosaurus typus* (BRLSIM1413), *Plagiophthalmosuchus* cf. *gracilirostris* (NHMUK PV OR 33095) and *Macrospodylus bollensis* (MCZ VPRA-1063), which have an enlarged gland (Brusatte et al. 2016; Pierce et al. 2017; Wilberg et al. 2021). Whereas in ‘*Metriorhynchus*’ cf. ‘*M. brachyrhynchus*’ (NHMUK PV OR 32617) the pituitary is more bulbous and rounded compared to other thalattosuchians (Schwab et al. 2021). Paired channels extending anteriorly from the pituitary may have housed the orbital artery (Brusatte et al. 2016; Pierce et al. 2017; Herrera et al. 2018); a condition shared with the dyrosaurid *Rhabdognathus aslerensis* (AMNH FARB 33354; Erb and Turner 2021). Among

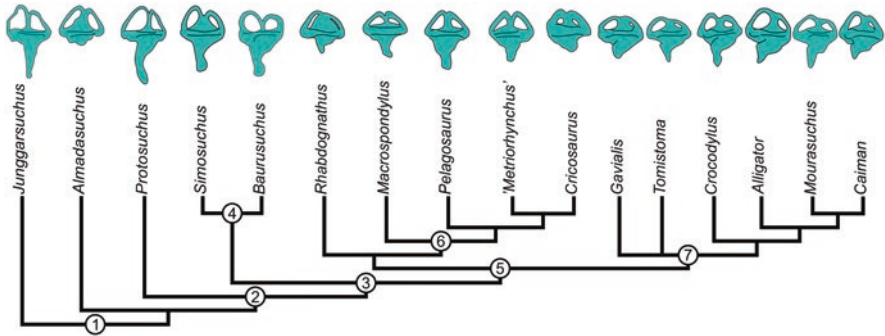


Fig. 7.10 Phylogenetic relationships of the crocodylomorph taxa with respective cranial endocast of inner ear published, in lateral view. Phylogenetic relationships are based in Pol et al. (2013, 2014). The inner ear are scaled in anteroposteriorly width and horizontally leveled with the LSC. For *Simosuchus clarki*, the lagena was reconstructed from *Baurusuchus* (*sensu* Dumont Jr et al. 2020). In all cases, the ASC is to the left. Numerical references: (1) Crocodylomorpha, (2) Crocodyliformes, (3) Mesoeucrocodylia, (4) Notosuchia, (5) Neosuchia, (6) Thalattosuchia, (7) Crocodylia

thalattosuchians, the anteroposterior length of the cranial endocast -excluding olfactory tracts and bulbs- is variable. In teleosauroids -as well as in *Pholidosaurus*, *Rhabdognathus* and most mesoeucrocodylians-, the cranial endocast is relatively more elongated anteroposteriorly than in metriorhynchoids (Fig. 7.9). The midbrain is particularly anteroposteriorly elongated in teleosauroids (as *Macrospondylus*, *Plagiophthalmosuchus*) and *Pelagosaurus*.

In the case of teleosauroid thalattosuchians, the best studied cranial endocast corresponds to that of *Macrospondylus bollensis*, from the Toarcian (SNSB-BSPG 1984 I258 by Herrera et al. 2018; MCZ VPRA-1063 by Wilberg et al. 2021), in which many regions of the brain were hypothesized, including the cerebral hemispheres, pituitary and most of the cranial nerves. Another studied species is *Plagiophthalmosuchus* cf. *gracilirostris* (NHMUK PV OR 3395), from the Early Jurassic (Brusatte et al. 2016). Only in *Macrospondylus bollensis* (MCZ VPRA-1063) the anterior region of the forebrain is known (olfactory apparatus), which accounts for about half of the total length of the cranial endocast (Wilberg et al. 2021). In all cases, the preserved portion of the cranial endocasts is long and narrow, similar in shape to other teleosauroids (e.g. a latex cranial endocast of *Charitomenosuchus leedsi*, LPP.M 35 by Wharton 2000, and those taxa with visible endocranial cavity in cross-section; Owen 1842; Seeley 1880; Wilberg 2015a), and metriorhynchoids (such as *Cricosaurus araucanensis*; Fernández et al. 2011; Herrera et al. 2013, 2018; Herrera and Vennari 2014).

Within Metriorhynchoidea, taxa with studied cranial endocasts -most of them missing the olfactory tracts and bulbs- include *Cricosaurus araucanensis* (MLP 72-IV-7-1; Herrera et al. 2013, 2018; Herrera 2015), *Dakosaurus* cf. *andiniensis* (MOZ-PV 089; Herrera 2015; Herrera and Vennari 2014), *Thalattosuchus superciliosus* (formerly *Metriorhynchus superciliosus*; MNHN 1870-133; Wenz 1968),

‘*Metriorhynchus*’ cf. *westermanni* (MDA 2; Fernández et al. 2011), ‘*Metriorhynchus*’ cf. ‘*M.* *brachyrhynchus*’ (NHMUK PV OR 32617; Schwab et al. 2021), and *Zoneait nargorum* (UOMNH F39539; Wilberg 2015b) (Table 7.1). ‘*Metriorhynchus*’ cf. ‘*M.* *brachyrhynchus*’ is unique in having a pronounced flexure at the forebrain/mid-brain region, a trait that seems to be present -but less pronounced- in *C. araucanensis* (Schwab et al. 2021; Table 7.2). In *C. araucanensis* (MLP 72-IV-7-1) the cranial endocast is complete (Herrera et al. 2018). It is anteroposteriorly elongated, narrow and almost straight in lateral view, with the dorsal border of the medulla oblongata level with the olfactory tract (Fig. 7.9). The olfactory tracts are long and form approximately half of the total length of the cranial endocast, –related to the relative length of the orbital region- as in other longirostrine crocodyliforms with enlarged orbits (e.g. dyrosaurids and gavialoids; Pierce et al. 2017; Bona et al. 2017; Erb and Turner 2021). The olfactory tracts widen anteriorly, forming relatively reduced olfactory bulbs when compared to the width of the cerebral hemispheres (Fig. 7.9).

The cephalic vasculature of thalattosuchians (e.g. orbital artery, carotid artery, caudal middle cerebral vein, cavernous sinus) is enlarged relative to most crocodylomorphs (e.g. Herrera et al. 2018; Schwab et al. 2021; Wilberg et al. 2021). Contrasting with teleosauroids, in which the particularly enlarged carotid canals are not included by bone as they pass through the pharyngotympanic sinus, in metriorhynchoids as *C. araucanensis* and ‘*M.*’ cf. ‘*M.*’ *brachyrhynchus* these canals are fully ossified and can be completely reconstructed (Herrera et al. 2018; Wilberg et al. 2021). The left and right carotid passages converge at the distal end of the pituitary, as in other mesoeucrocodylians. The cranial endocast of *Pelagosaurus typus* was fully described and presented features shared between teleosauroids and metriorhynchoids (Pierce et al. 2017).

Inner Ear The thalattosuchian inner ear morphology is reminiscent of other aquatic crocodyliforms (e.g. semi-aquatic neosuchians, including modern crocodiles), although living representatives have dorsoventrally taller semicircular canals (Georgi and Sipla 2008; Brusatte et al. 2016; Pierce et al. 2017; Herrera et al. 2018; Schwab et al. 2020; Fig. 7.10). However, important differences are observed in the thalattosuchian vestibular apparatus, which is relatively low and triangular, with semicircular canals and crus commune of similar diameter, and an anterior semicircular canal slightly larger than the posterior one. In teleosauroids and *Pelagosaurus* there are no great differences in the morphology of the labyrinth compared to living crocodylians. The pelagic metriorhynchoids in particular (more derived forms such as *Cricosaurus*) have developed a strongly dorsoventrally short labyrinth, with an anterior semicircular canal that is not particularly larger than the posterior one, and semicircular canals and crus commune, which are markedly more robust and thick in cross section than those of their semi-aquatic living relatives (Schwab et al. 2020, 2021).

Notosuchia (Uruguaysuchidae, Peirosauridae and Sebecosuchia)

Brain Cranial endocasts for Notosuchia are known for a handful of taxa (Fig. 7.9 and Table 7.1). Notosuchians that received the most attention so far are from Africa: the uruguaysuchids *Araripesuchus wegeneri* and *Anatosuchus minor* (MNN GAD19 and MNN GAD18, respectively; Sereno and Larsson 2009), the bizarre taxon *Simosuchus clarki* (UA 8679; Kley et al. 2010), and the peirosaurid *Rukwasuchus yajabaliyekundu* (RRBP 08630; Sertich and O'Connor 2014). Available descriptions of cranial endocasts of South American notosuchians are those of the sebecosuchian *Baurusuchus* sp. (IFSP-VTP/PALEO-0002, IFSP-VTP/PALEO-0003, FEF-PV-R-1/9, FUP-Pv 000020, FUP-Pv 000021; Dumont Jr et al. 2020), *Campinasuchus dinizi* (CPPLIP 1360; Fonseca et al. 2020), *Sebecus icaeorhinus* (AMNH 3160; Colbert 1946) and *Wargosuchus australis* (MOZ-PV 6134, a partial cranial endocast; Martinelli and Pais 2008) whereas cranial endocasts of the peirosaurids *Uberabasuchus terrificus* (CPPLIP 1360; Fonseca et al. 2020, fig 10C, D) and *Hamadasuchus rebouli* (ROM 52560; Dufeau 2011; George and Holliday 2013, fig 2A) were figured but not formally described.

The cranial endocast of Notosuchia presents the same general morphology of other extinct and living crocodylomorphs, except for the variation of the angles between the brain regions and other particularities mentioned below (Fig. 7.9). It is characterized by being anteroposteriorly elongated, with a sigmoidal shape (slightly sub-horizontal), and angles between fore- and midbrain, and mid and hindbrain of 142°–161° and 155°–165° respectively (see Table 7.2).

The olfactory bulbs are prominent, oval in outline and lateromedially expanded (Barrios 2015; Barrios et al. 2016; Fernández-Dumont et al. 2017a, b; Fonseca et al. 2020; Dumont Jr et al. 2020; Fig. 7.9). The length of the olfactory tracts varies among notosuchian species in terms of its anteroposterior extension and anteroventral inclination. They are shorter in *Simosuchus*, and longer in *Rukwasuchus*, *Baurusuchus*, *Campinasuchus* and *Sebecus*, which are also shorter-snouted and longer-snouted forms, respectively (Colbert 1946; Kley et al. 2010; Sertich and O'Connor 2014; Barrios 2015; Barrios et al. 2016; Dumont Jr et al. 2020; Fonseca et al. 2020; Fig. 7.9). In most known notosuchians, as in the peirosaurid *Rukwasuchus* and the baurusuchid *Campinasuchus*, the olfactory tracts are subhorizontally disposed (with the skull oriented according to the palate horizontally disposed), contrary to *Simosuchus* that presents anteroventrally inclined tracts (e.g. Barrios 2015). This latter condition is also present in some derived eusuchians such as *Alligator* and *Caiman* (Fig. 7.9).

In small-sized notosuchians, as *Araripesuchus*, *Anatosuchus* and *Simosuchus*, the cerebral hemispheres are relatively lateromedially expanded (Sereno and Larsson 2009; Kley et al. 2010), contrasting with the morphology present in large-sized notosuchians as *Rukwasuchus*, *Baurusuchus*, *Campinasuchus*, and *Sebecus*, which have lateromedially narrower cerebral hemispheres (Fig. 7.9 and Table 7.2). The cerebral hemispheres in *Araripesuchus*, *Anatosuchus* and *Simosuchus* are similarly lateromedially expanded than juvenile living crocodylians (e.g. Hopson 1979;

Jirak and Janacek 2017; Hu et al. 2020). In lateral view, the cerebral hemispheres are particularly dorsoventrally low in baurusuchids (such as *Baurusuchus*, *Campinasuchus*) and in *Araripesuchus* (Fig. 7.9). In *Araripesuchus* and *Simosuchus* the pituitary is relatively enlarged, contrasting with larger notosuchians (*Rukwasuchus*, *Sebecus*, *Baurusuchus* and *Campinasuchus*), in which this gland is smaller; however, the influence of the cavernous sinus on the pituitary cast in all these species is not ruled out.

The midbrain of notosuchians presents some degree of variation in terms of its anteroposterior length as well as in its lateromedial extent (Fig. 7.9). *Araripesuchus*, *Anatosuchus* and *Simosuchus* have a well lateromedially expanded but slightly anteroposteriorly elongated optic tectum. The lateromedially expanded optic tectum in these small-sized notosuchians is reminiscent of the condition observed in juvenile living crocodylians (e.g. Hopson 1979; Jirak and Janacek 2017; Hu et al. 2020; Barrios 2021). Larger sized notosuchians, as *Rukwasuchus*, *Baurusuchus* and *Sebecus*, have a lesser lateromedially expanded, but anteroposteriorly longer, midbrain (e.g. Barrios et al. 2017; Dumont Jr et al. 2020; Barrios 2021). The anteroposteriorly elongated midbrain of large notosuchians is similar to the stem crocodylomorph *Almadasuchus* (Leardi et al. 2020).

As in most eusuchians, the hindbrain varies among notosuchians in terms of its dorsoventral development (Fig. 7.9). In this region of the brain, the dorsal longitudinal venous sinus is largest in *Araripesuchus*, *Rukwasuchus*, *Sebecus* and *Campinasuchus* than in *Simosuchus* and *Baurusuchus* (Serenó and Larsson 2009; Kley et al. 2010; Sertich and O'Connor 2014; Barrios et al. 2016; Dumont Jr et al. 2020). The ventral longitudinal venous sinus is more developed in *Anatosuchus*, *Simosuchus*, *Rukwasuchus*, and *Sebecus*, contrary to the condition seen in *Baurusuchus* and *Campinasuchus* (e.g. Kley et al. 2010; Fonseca et al. 2020). The flocculus is more prominent in *Araripesuchus*, *Anatosuchus* and *Rukwasuchus* than in any other Crocodyliformes, similar to *Almadasuchus* (Sertich and O'Connor 2014; Barrios et al. 2016; Leardi et al. 2020). Unlike other crocodylomorphs, in notosuchians the depression for the otic capsule in the cranial endocast is more posteriorly placed, probably related to the anteroposterior elongation of the midbrain (Kley et al. 2010; Fonseca et al. 2020; Dumont Jr et al. 2020; Barrios 2021).

The carotid canal is difficult to identify and segment in most studied notosuchians. It is partially reconstructed in *Baurusuchus* (Dumont Jr et al. 2020, fig 5B, D) posterior to the pituitary gland. In the basicranium of notosuchians, the foramen for the internal carotid artery perforates the otoccipital in a dorsal position (lateral to the occipital condyle), very close to the metotic foramen (CNs IX, X, XI) or with the metotic foramen contents within a fossa (Barrios et al. 2018). This last condition contrasts with that observed in other mesoeucrocodylians (e.g. Crocodylia) in which the carotid foramen is more ventral with respect to the metotic foramen (e.g. Brochu 1999).

Inner Ear The inner ear is poorly known for most Notosuchia (e.g. Barrios 2021). The inner ear of *Baurusuchus* (FUP-Pv 000021) has been completely described by Dumont Jr et al. (2020), and a partial description of the preserved semicircular

canals is known for *Simosuchus* (Kley et al. 2010). In notosuchians, the vestibular apparatus formed by the semicircular canals is located more dorsal than in aquatic neosuchians (e.g. *Rhabdognathus*, *Gavialis*,) and thalattosuchians (e.g. *Pelagosaurus*, *Plagiophthalmosuchus*, *Macrospodylus*, ‘*Metriorhynchus*’, *Cricosaurus*), in which the semicircular canals have more elliptical contours (Fig. 7.10). In *Simosuchus* and *Baurusuchus*, the ASC is markedly more dorsal than the PSC, probably related to the relatively prominent cerebellar flocculus in these species (see below). In *Baurusuchus*, the lagena is dorsoventrally high (as in terrestrial non- mesoeucrocodylian crocodylomorphs such as *Junggarsuchus* and *Protosuchus*) and gently medially curved (as *Protosuchus* and living crocodylians), contrary to the dorsoventrally low lagena present in other crocodylomorphs (e.g. Schwab et al. 2020, fig 2; Fig. 7.10).

Early Eusuchians and Crocodylia

Brain The general morphology of the cranial endocast of early eusuchians and extinct Crocodylia is similar to that of living forms, in which the body size seems to constrain the general shape of the brain (e.g. Hu et al. 2020; Serrano-Martínez et al. 2020). Thus, the cranial endocast of larger non-crocodylian eusuchians as *Lohuecosuchus megadontos* (HUE-04498; Serrano-Martínez et al. 2018) presents a less sigmoidal shape than smallest forms as *Agaresuchus fontisensis* (HUE-02502; Serrano-Martínez et al. 2020; Fig. 7.9). This is also seen in the huge extinct caiman *Caiman gasparinae* (MLP 73-IV-15-1; Bona and Paulina-Carabajal 2013), which shows a more linear arrangement of the brain regions than in extant *Caiman yacare* and *Ca. latirostris*, similar to the largest *Crocodylus* species (e.g. *Cr. niloticus*; Fig. 7.9) and the extinct tomistomine *Gunggamarandu maunala* (QMF14.547; Ristevski et al. 2021). Among gavialoids, the cranial endocast of the large *Thoracosaurus isorhynchus* (Lemoine 1883–1884, pl. 4, fig 7; Table 7.1) is also more sub-horizontal than the smaller extant *Gavialis gangeticus* (e.g. Wharton 2000; Bona et al. 2017; Pierce et al. 2017). However, it should be mentioned that some large but probably young specimens of fossil caimanines such as *Mourasuchus nativus* (MLP 73-IV-15-9) present a cranial endocast that is more sigmoidal than expected (Bona et al. 2013, fig 5; see discussion below). It is interesting to note that cranial endocasts of small crocodylian species as *Paleosuchus trigonatus* (Balanoff and Bever 2017, fig 4A) and *Osteolaemus tetraspis* (Serrano-Martínez et al. 2019, fig 5) are sigmoidal and robust with relatively large hypophysis (Fig. 7.9), resembling the general shape of living juvenile crocodylians endocasts (e.g. Jirak and Janacek 2017; Watanabe et al. 2019; Hu et al. 2020; Table 7.2).

The olfactory tracts in crocodyliforms closely related to Eusuchia, as *Goniopholis*, are particularly transversely broad and relatively short (similar to *Almadasuchus*) when compared to eusuchians (Fig. 7.9). Within this clade, the olfactory tracts vary in shape, but they are always reconstructed as relatively narrow and elongated, especially in longirostrine forms (as *Gavialis gangeticus*; Bona et al. 2017; Pierce et al.

2017). Among living forms, which have more accurate cranial endocasts than extinct forms, the olfactory bulbs are transversally narrow in the more aquatic form *Gavialis gangeticus* compared to other crocodylians (Fig. 7.9).

As in living crocodiles, the maximum width of the endocranial cavity of early eusuchians and extinct Crocodylia is at the cerebral hemispheres (e.g. Hopson 1979; Table 7.2). *Goniopholis* (Edinger 1938, fig 2), non-crocodylian eusuchians, and probably crocodylians as crocodyloids, gavialoids and some basal alligatoroids as *Leidyosuchus* (UNM B-401 A; Storrs et al. 1983), present cerebral hemispheres with more elongated anterior surfaces in dorsal view (Fig. 7.9) contrasting with the apparently derived morphology shared by globidontian alligatoroids (e.g. *Diplocynodon tormis* STUS-344, *Alligator*, *Caiman*). Globidontians are represented by sub-spherical lateral cerebral hemispheres with symmetrical anterior and posterior surfaces (Bona and Paulina-Carabajal 2013; Serrano-Martínez et al. 2019). The large caiman *Caiman gasparinae* preserves vascular impressions on the ventral surface of the frontal, suggesting that the cerebral hemispheres filled most of the cavity (Evans 2005), a feature not evident in extant smaller *Caiman* species (*Ca. yacare* and *Ca. latirostris*).

In almost all fossil Eusuchia, the hindbrain portion is the most commonly preserved region of the cranial endocast (e.g. *Allodaposuchus hulki* MCD 5139, *Gryposuchus neogaeus* MLP 68-IX-5-1, *Mourasuchus nativus* MLP 73-IV-15-9, *Leidyosuchus* UNM B-401 A; Storrs et al. 1983; Bona et al. 2013, 2017; Blanco et al. 2015). In general, there is no evident impression of the cerebellar flocculus on the preserved section of the prootic.

Although the brain seems to be morphologically conservative in Eusuchia, there is some disparity in the cranial endocast shape, mainly due to the relative size of the pituitary and the development and arrangement of the principal blood vessels. Within Crocodylia, the pituitary fossa is apparently larger in smaller taxa as *Osteolaemus tetraspis* (Serrano-Martínez et al. 2019, fig 5; Fig. 7.9) and *Paleosuchus trigonatus* (Balanoff and Bever 2017, fig 4) as occurs in early ontogenetic stages of living forms (Hu et al. 2020). However, Bona et al. (2017) mentioned that in gavialoids (e.g. *Thoracosaurus isorhynchus*, *Gryposuchus neogaeus*, and *Gavialis gangeticus*), the pituitary fossa is relatively larger than in caimans.

The volume and extension of intracranial venous sinuses inferred from the cranial endocast shape are variable within Crocodylia. In some huge caimans (e.g. *Ca. gasparinae*; Bona and Paulina-Carabajal 2013, fig 5), there is no evidence of a large dorsal longitudinal sinus, as in *Cr. johnstoni* (Witmer et al. 2008) and *Gunggamarandu maunala* (Ristevski et al. 2021, fig 3). However, in other caimanines as *Mourasuchus nativus* (Bona et al. 2013, fig 5), the cranial endocast seems to be dominated by large dural and venous sinuses that obscure the main dorsal anatomical structures of the posterior forebrain, midbrain and hindbrain, as in many other eusuchians (e.g. *Agaresuchus*, *Alligator*, *Diplocynodon*, *Osteolaemus*, extant *Caiman*; Serrano-Martínez et al. 2019, 2020; Fig. 7.9) and other non-avian archosaurs (e.g. Witmer et al. 2008; Witmer and Ridgely 2008). This is also true for gavialoids, such as *Gryposuchus neogaeus* (Bona et al. 2017). Bona et al. (2017) described the ventral longitudinal venous sinus in gavialoids as *Gryposuchus neogaeus*, *Gavialis*

gangeticus and *Thoracosaurus isorhynchus*, concluding that it is also well developed and shows the same morphological pattern in the three species, being ovoidal-shaped in ventral view just posterior to the pituitary (Lemoine 1883–1884, pl. 4, fig 6; Bona et al. 2017, fig 6B, 7B). This feature of the posteroventral cranial endocast is also present in other eusuchians (e.g., *Agaresuchus*, *Diplocynodon*, *Osteolaemus*, *Caiman*, *Alligator*) and other non-eusuchian crocodylomorphs (Fig. 7.9).

As in other crocodylomorphs, in fossil eusuchians, the anterior limits of the optic lobes -at the cerebral hemisphere and optic tectum constriction-, is often obscured in the cranial endocast probably by the enlargement of the transverse venous sinus (Hopson 1979; Witmer et al. 2008; Porter et al. 2016). In almost all living crocodylians, except some species as *Cr. johnstoni* (Witmer et al. 2008), the optic lobes display no marked separation from the cerebral hemispheres as seen in other eusuchian cranial endocasts (Bona and Paulina-Carabajal 2013; Fig. 7.9). The intracranial branches of the internal carotid artery in Eusuchia (i.e. the cerebral carotid artery and its derivations; Porter et al. 2016) do not run endosseously throughout their entire trajectory. In Eusuchia, there is a variation in the trajectories of the basiesphenoidal carotid canals, just before entering the pituitary fossa (Bona et al. 2017). The widespread plesiomorphic condition within this group is the presence of anteriorly convergent carotid canals, contrary to the apomorphic condition seen in *Crocodylus* spp., in which both canals become parallel before entering at the hypophyseal fossa (e.g. *Cr. johnstoni*, *Cr. niloticus*; Witmer et al. 2008, fig 6.3; Barrios 2021, fig 2.15B).

Inner Ear Endosseous labyrinths in extinct Eusuchia are similar to living forms, with a triangular vestibular apparatus and relatively elongated lagena (Fig. 7.10). However, in gavialoids as *Gryposuchus neogaeus* and *Gavialis gangeticus*, the lagena is shorter, suggesting a reminiscent of the condition observed in marine crocodylomorphs (i.e. thalattosuchians) (e.g. Bona et al. 2017; Pierce et al. 2017; Schwab et al. 2020). The vertical semicircular canals are more dorsoventrally compressed in longirostrine forms as gavialoids, *Tomistoma schlegelii*, *Gungamarandu maunala* and *Mourasuchus nativus*, in which the ASC is also less differentiated in size than the PSC.

7.2.3 Cranial Nerves of Crocodylomorphs

Olfactory Nerve (CN I) The first cranial nerve emerges as a tuft of short nerves from the olfactory bulbs (Figs. 7.2 and 7.5). The nerves pierce the dura and membranous septum between the endocranial cavity and the ethmoidal region of the nasal cavity near the mid-sagittal plane (Lessner and Holliday 2020). Although the olfactory tracts and bulbs leave distinct and identifiable osteological correlates in the ventral surface of the frontals, nasals and ethmoids -if present-, the olfactory nerves do not. Living crocodylians have a keen olfactory sense (Weldon and Ferguson 1993), but their extinct relatives seem to have a variable sense of smell given the variety of sizes of olfactory bulbs found in the clade (Erb and Turner 2021

and references therein). Because this region of the skull rarely if ever ossifies in the lineage (as the cribriform plate does in mammals), little is known about the anatomy of the olfactory nerves proper. In this regard, recent data on the Paleocene dyrosaur *Rhabdognathus aslerensis* revealed a perforated bony laminae that envelopes the olfactory bulbs, suggesting an increased surface for olfaction (Erb and Turner 2021).

Optic (CN II), Oculomotor (CN III) and Trochlear (CN IV) Nerves The second, third, and fourth cranial nerves emerge from the brain and all pass through a variable number of ossified passages bounded by the orbitosphenoid -if present-, and laterosphenoid to innervate the retina (CN II), and the extraocular muscles (CNs III, IV) respectively (Lessner and Holliday 2020; Kuzmin et al. 2021; Figs. 7.2 and 7.5). Because this region of the skull is often unmineralized, unprepared or damaged due to its fragility, descriptions of these foramina are rarer than other nerves, although imaging methods help increasing the number of descriptions. The optic nerve emerges from the optic chiasm in the encephalic cavity and enters the orbit dorsal to the hypophyseal fossa in the basisphenoid, through a large single foramen along the medial edge of the laterosphenoid. In crocodylomorphs, this foramen is located along the ventral edge of the laterosphenoid near the contact with the basisphenoid (Fig. 7.2a). In the Early Triassic archosauriform *Proterosuchus* there is a gap for the oculomotor nerve between the medially positioned ‘slender’ process, likely the ossified pila metoptica or orbitosphenoid, and more lateral body of the laterosphenoid (Clark et al. 1993). The optic foramen is not typically preserved in crocodylomorphs, though aetosaurs appear to have partially mineralized orbitosphenoids (e.g. *Longosuchus*; Fig. 7.7a) and thus preserve a clear optic foramen. In crocodyliforms, the foramen for the oculomotor nerve pierces the wall of the ventral edge of the laterosphenoid just lateral to the optic nerve foramen, as in the thalattosuchian *Pelagosaurus* (NHMUK PV OR 32599) and the notosuchians *Araripesuchus* (AMNH 24450) and *Simosuchus* (UA 8679) (Holliday and Witmer 2009). The trochlear nerve foramen pierces the laterosphenoid dorsolateral to the oculomotor nerve and medial to the ophthalmic foramen or canal as a slit in *Sphenosuchus* (Walker 1990) or foramen in *Almadasuchus* (Leardi et al. 2020; Fig. 7.7b) and crocodyliforms (Fig. 7.6).

Trigeminal Nerve (CN V) The fifth cranial nerve is responsible for conveying somatosensory information from most of the head rostral to the jaw joints and the brain, as well as transmitting motor innervation to the adductor musculature (Soares 2002; Holliday and Witmer 2009; Leitch and Catania 2012; George and Holliday 2013). The large nerve emerges from the midbrain as a bundle of sensory roots to enter the trigeminal ganglion, which resides in the trigeminal fossa (Figs. 7.2 and 7.5). The trigeminal fossa is typically a relatively large spherical to cone-shaped space bounded by the laterosphenoid rostrally, the basisphenoid ventrally and the prootic caudally, and opens laterally, particularly in non-crocodyliform crocodylomorphs (as *Almadasuchus*; Leardi et al. 2020). As the quadrate and pterygoid become sutured to the braincase in the more derived lineages of sphenosuchians and crocodyliforms, these elements also share some of the lateral edges of the trigemi-

nal fossa as well as the foramina for the divisions (Holliday and Witmer 2009). Laterally the trigeminal ganglion divides into the three main branches of the trigeminal nerve: the ophthalmic, maxillary, and mandibular divisions. A similar pattern of separated exits for different ramii of the trigeminal nerve is also seen in braincase walls of other amniotes such as birds, turtles and mammals, which also have an increase in ossification in the lateral wall of the braincase.

Because the lateral wall of the crocodylomorph and crocodyliform braincase is the intersection between the orbit, adductor chamber, ear and throat, and is quite robustly ossified, the bony surfaces possess many osteological correlates of muscles, neurovasculature, and other soft tissues (e.g. Holliday and Witmer 2007, 2009). Proximally, several of the branches of the trigeminal divisions and related vasculature leave distinct foramina and grooves on the walls of the lateral braincase. This bony information enables relatively accurate inferences of the paths of the trigeminal nerve. In most crocodylomorphs, the trigeminal foramen is bilobate (e.g. Holliday and Witmer 2009; Bona and Desojo 2011; Barrios et al. 2018; Herrera et al. 2018), except in the thalattosuchian *Macrospodylus bollensis* (divided by prootic; Wilberg et al. 2021) and the eusuchian *Mourasuchus nativus* (divided by quadrate; Bona et al. 2013). The ophthalmic division passes rostrally from the trigeminal fossa and leaves a groove on the ventrolateral surface of the laterosphenoid in most crocodylomorphs before following the caudal surface of the orbital wall where its path diverges from the surface of the bone. The nerve continues rostrally to innervate the sclera of the eye, orbital walls, medial portions of the nasal cavity, integumentary surface of the premaxilla and nostrils, though not to the nasal muscles, which are innervated by sympathetic nerves (Lessner and Holliday 2020). Ventral to the ophthalmic groove on the laterosphenoid, there is often a set of small grooves for the neurovasculature of the cavum epitericum and the motor branch to the levator bulbi muscle in the floor of the orbit (Holliday and Witmer 2009) as well as the depressor auriculæ inferioris muscle of the external ear (Shute and Bellairs 1955). When present, as in some thalattosuchians (such as *Pelagosaurus*), notosuchians (such as *Simosuchus*, *Araripesuchus* and *Hamadasuchus*), and non-eusuchian crocodyliforms (such as *Sarcosuchus*, *Rhabdognathus*), the epipterygoid separates the adductor chamber from the cavum epitericum and thus also separates the maxillary and mandibular nerves from contacting the lateral wall of the braincase (Holliday and Witmer 2009; Fernández-Dumont et al. 2020). In more derived neosuchians, the epipterygoid appears to persist as an isolated element in contact with the body of the laterosphenoid, exposing the ophthalmic groove laterally, such as in *Hylaeochampsa* (NHMUK R177) and *Aegisuchus* (ROM 54530; Holliday and Gardner 2012; Fig. 7.7c). Within Eusuchia, a descending process of the laterosphenoid, the lateral bridge, extends ventrally to again cover the ophthalmic groove and cavum epitericum medially and is often laterally marked by a groove left by the maxillary nerve. Finally, in some specimens of crocodylians, further ossification of the laterosphenoid and quadrate can further enclose the maxillary and mandibular nerves, sealing off the maxillomandibular foramen and instead forming separate

foramina for each nerve (Holliday and Witmer 2009) as in the extinct caimanine *Mourasuchus* (Bona et al. 2013).

Upon diverging from the laterosphenoid, the maxillary division passes rostrally between the eyeball and pterygoideus dorsalis muscle in the orbit to enter the maxilla and innervates the lateral portions of the nasal cavity, maxillary teeth and skin of most of the rostrum (Lessner and Holliday 2020). The mandibular nerve passes ventrolaterally to enter the Meckelian fossa of the dentary and emits branches to the tongue, oral cavity, mandibular teeth, and integument (Fig. 7.8). All three divisions of the trigeminal nerve ultimately emerge from bones of the face to innervate the integument leaving an array of characteristic foramina that form the basis for the sensory array for the densely packed mechanoreceptors on the rostrum of crocodylians (Leitch and Catania 2012; George and Holliday 2013; Fig. 7.8).

Abducens Nerve (CN VI) In early crocodylomorphs and all crocodyliforms, the sixth cranial nerve emerges from the ventral surface of the medulla oblongata and characteristically transmits through a canal in the dorsal part of the basisphenoid across the dorsum sellae to emerge through small foramina in the exposed rostrodorsal surface of the basisphenoid lateral to the pituitary fossa (Kuzmin et al. 2021; Figs. 7.2, 7.5, 7.6 and 7.7). The abducens nerve innervates the lateral rectus muscle of the orbit, but also the pyramidalis muscle of the nictitating membrane (Lessner and Holliday 2020).

Facial Nerve (CN VII) The seventh cranial nerve emerges from the encephalic cavity through a foramen in the prootic (Kuzmin et al. 2021; Figs. 7.2 and 7.5). This exit is obscured in crocodyliforms as the quadrate has covered over the region (e.g. Crompton and Smith 1980; Clark 1986; Leardi et al. 2020). The nerve splits into two primary branches, the palatine ramus and hyomandibular ramus (Fig. 7.2). The palatine ramus passes rostrally along the lateral surface of the prootic and basisphenoid into the palatine-maxillary suture (Lessner and Holliday 2020), where it ramifies throughout the rostrum providing parasympathetic innervation of soft tissues. The hyomandibular ramus passes caudolaterally past the prootic-opisthotic suture to enter a canal along the margin of the suture of the quadrate and otoccipital. It then passes ventrally, innervating the depressor mandibulae muscle, the superior auricular muscles (Shute and Bellairs 1955) and ultimately the constrictor colli profundus muscle of the throat while also giving off the chorda tympani nerve to the tongue.

Vestibulocochlear Nerve (CN VIII) The eighth cranial nerve is quite short as it passes only from the medulla to the inner ear through the prootic, just caudal to the foramen for the facial nerve, extending vestibular divisions and a cochlear branch through individual, or shared foramina to the semicircular canals and lagena (Lessner and Holliday 2020; Kuzmin et al. 2021; Figs. 7.2 and 7.5). These structures are described elsewhere in the chapter.

Glossopharyngeal (CN IX), Vagus (CN X), and Accessory (CN XI) Nerves The ninth, tenth, and eleventh cranial nerves share a passage through the skull and thus

are discussed together (Kuzmin et al. 2021; Figs. 7.2 and 7.5). The glossopharyngeal nerve (CN IX) transmits sensory information from the tongue, pharynx, and middle ear, and motor information to the hyobranchial musculature. The vagus nerve (CN X) transmits sensory information from the larynx, motor information to muscles of the pharynx and larynx, and parasympathetic information to the thorax and abdomen (Lessner and Holliday 2020). The accessory nerve (CN XI) transmits motor information to shoulder musculature. CN XI originates in the cervical region, enters the skull through the foramen magnum, and joins the vagus nerve before exiting the skull with CNs IX and CN X (Benninger and McNeil 2010).

In extant crocodylians, CNs IX, X, and XI exit the skull through the metotic foramen (*sensu* Bellairs and Shute 1953; jugular foramen *sensu* de Beer 1937; vagus foramen *sensu* Iordansky 1973), which is present on the paroccipital process of the otoccipital (appearing at the junction of the ossification centres of the opisthotic and exoccipital in crocodylian embryos). Internally, the metotic foramen is an extension of the posterior opening of the subdivided metotic fissure, a relict of the homonymous embryonic metotic fissure (de Beer 1937; Fernández-Blanco 2018) which is a gap between the cartilaginous otic capsule and chondrocranium basicranium (Gower and Weber 1998; also named metotic foramen by Kuzmin et al. 2021). This anatomical arrangement is a consequence of the development and fusion of several structures in the posterolateral skull. In crocodylians, the metotic foramen results from the fusion of the metotic cartilage with the subcapsular process and the anterior and posterior juxtaotic lamina (membranous bone). The anterior juxtaotic lamina (outgrowth of the basal [=parachordal] plate) fuses with the posterior juxtaotic lamina (outgrowth of the occipital arch [=pila occipitalis]) to form the posteroventral wall of the metotic fissure (Klembara 2005). The internal boundaries of this canal form through ontogeny as the subcapsular process extends from the lateral surface of the occipital arch (exoccipital), just dorsal to the foramina for the branches of CN XII (Shiino 1914). The subcapsular process forms the floor of the anterior metotic fissure (=fenestra rotunda, fenestra pseudorotunda, foramen cochleare, apertura lateralis scalae tympani) and the roof of the posterior metotic fissure (de Beer 1937; Rieppel 1985; Gower and Weber 1998).

Leardi et al. (2017) noted two conditions within *Suchia* that ultimately must stem from various extents of this developmental process. The metotic foramen is present on the ventrolateral surface of the paroccipital process in *Almadasuchus*, thalattosuchians, and other crocodyliforms, whereas basal crocodylomorphs have no distinct foramen. In the basal taxa, the CNs IX, X, and XI exit through the metotic fissure, which extends (along the opisthotic-exoccipital junction) from the braincase internally to the ventrolateral region of the skull, externally (Walker 1990). Walker (1990) noted a partial ossification of the subcapsular process in *Sphenosuchus* and, therefore, incomplete division of the metotic fissure. In this case, CN X and CN XI, along with the posterior cerebral vein, pass through the more posterodorsal aspect of the metotic fissure and CN IX along with the perilymphatic duct pass through the anteroventral aspect (Walker 1990). The subcapsular process is more extensive in more-derived crocodylomorphs (Busbey and Gow 1984; see Leardi et al. 2017,

character 105 for a complete list), and therefore these taxa exhibit a unique metotic foramen for passage of CNs IX, X and XI. Thus, the extent of subcapsular and juxtaotic laminae ossification, the degree of closure of the metotic fissure, and the presence of a metotic foramen are useful characters in determining phylogenetic position in crocodylomorphs.

Hypoglossal Nerve (CN XII) The hypoglossal nerve (CN XII) carries motor information to the tongue musculature. The hypoglossal nerve exits the skull through one, two, or three foramina in the otoccipital near the foramen magnum. However, in most crocodylomorphs, there are two foramina for the divisions of the CN XII (e.g. Clark 1986). The foramina are located medial to the internal carotid foramen and posterior to the metotic fissure (Figs. 7.2 and 7.5). Foramina are not always symmetrical in number (e.g. *Sphenosuchus*; Walker 1990). In the case of multiple foramina, the anterior foramen tends to be smaller in diameter than the posterior foramina (e.g. *Sphenosuchus*, *Dibothrosuchus*; Walker 1990; Ruebenstahl 2019). Though CN XII foramen size has not been investigated across pseudosuchians, it may be indicative of innervation to the tongue and provide insight into the proposed reduction of tongue mobility through crocodyliforms (Li and Clarke 2015).

7.3 Paleobiological Implications of Crocodyliform Neuroanatomy

The knowledge of the entire anatomy and physiology of extinct forms is crucial to elaborate accurate hypotheses related to lifestyle. Together with postcranial anatomy, dentition, and osteohistology, neuroanatomical data is another source of evidence to infer paleobiology. There has been a recent proliferation of published data on neuroanatomy of Pseudosuchia, especially for crocodylomorphs (e.g. Brusatte et al. 2016; Pierce et al. 2017; Herrera et al. 2018; Leardi et al. 2020; Dumont Jr et al. 2020; Darlim et al. 2021; Erb and Turner 2021), and associations have been proposed between certain anatomical patterns (brain, cranial nerves and sense organs) and adaptations to terrestrial and aquatic habitats (e.g. Montefeltro et al. 2016; Neenan et al. 2017; Fonseca et al. 2020; Dumont Jr et al. 2020; Schwab et al. 2020; Barrios 2021; Bronzati et al. 2021). For example, prominent olfactory bulbs seem to relate to the terrestrial habitats inferred for notosuchians (as *Baurusuchus*, *Simosuchus*, *Rukwasuchus*), and therefore represent the ancestral condition present in basal crocodylomorphs (as *Almadasuchus*) and several non-crocodyliform pseudosuchians (e.g. *Parasuchus angustifrons*, *Ebranchosuchus neukami*, Laustenschlager and Butler 2016; *Prestosuchus chiniquensis*, Mastrantonio et al. 2019) (Fig. 7.9). Larger olfactory bulbs are also linked to greater olfactory acuity in terrestrial environments (e.g. Martinelli and Pais 2008; Zelenitsky et al. 2009; Fonseca et al. 2020). However, it should be taken into account that all these olfactory estimations should consider the correlation between the olfactory ratio and body size (see Zelenitsky et al. 2009; Dumont Jr et al. 2020). The elongation of the

olfactory tracts is linked with the anteroposterior extension of the orbital region of the skull (expressed by the length of the frontal) and not with the length of the snout (e.g. Starck 1979; Barrios 2021). However, the anteroposterior length of the rostrum, reflected by the elongation of nasals, maxilla and/or premaxilla (e.g. Wilberg 2015a), may influence somatosensation over olfactory acuity (e.g. Soares 2002).

When considering *Thalattosuchia* as crocodyliforms, we observed that within *Crocodylomorpha* the cast of the cerebral hemisphere expands laterally near the node *Crocodyliformes* (Fig. 7.9 and Table 7.2), contrasting with the narrower cerebrum observed in non-crocodyliform pseudosuchians (as *Almadasuchus*; see above). Relatively larger cerebral hemispheres indicate larger encephalization (*sensu* Jerison 1973), which is necessary for the processing of environmental information (e.g. foraging for food, escape from predators), and the development of more complex responses (Jerison 1977; Rogers 1999; Franzosa 2004; Witmer et al. 2008). It is worth mentioning that encephalization is negatively correlated with body size in living crocodylians, and it decreases with age (e.g. Jirak and Janacek 2017; Hu et al. 2020; Watanabe et al. 2019).

Prominent optic lobes endocasts in crocodylomorphs (such as notosuchians *Araripesuchus*, *Anatosuchus*, *Simosuchus*, and probably *Baurusuchus*) would correlate with greater visual capacity, which is also related to the greater relative size of the orbits observed in those groups (e.g. Schmitz and Motani 2011). In sauripsids, the development of the midbrain tectum is hypothesized to correspond to with a more adjusted perception of space (visual and auditory field and proprioception; Walls 1942; Ulinski et al. 1992) regarding a major animal activity. Even more, the major development of the optic tectum may indicate great dependence on the sense of vision to find food, detect danger, defend territory, and select a sexual partner (e.g. Shimizu et al. 2009). This higher dependence on the sense of sight would be also expressed as an increment in motor integrating centers at the cerebellum, and therefore a larger cerebellar flocculus, as visual stimuli need higher degrees of processing in the brain (e.g. Jerison 1973; Franzosa 2004; Witmer et al. 2008). A relatively larger cerebellar flocculus endocast, as is observed in the early crocodylomorphs (e.g. *Almadasuchus* and *Sphenosuchus*) and notosuchians (e.g. *Simosuchus* and *Rukwasuchus*), could be related to complex movements of the head in more active animals (e.g. Franzosa 2004; Witmer et al. 2008; Walsh et al. 2013; von Backzo et al. 2015; Trotteyn et al. 2015; Ferreira-Cardoso et al. 2017). Also, in *Simosuchus* and *Baurusuchus* the ASC is markedly higher than the PSC, a trait that seems to correlate with the prominent cerebellar flocculus and optic tectum endocasts in these species (see above), which in turn relates to the coordination of eye and head movements during gaze pursuit (e.g. Highstein 1998; Belton and McCrea 2000; Cox and Jeffery 2010).

As with all robust paleobiological inferences, size and pathways of the cranial nerves must rely on anatomical data from extant forms as well as data from the fossil record. To date, little attention has been paid to the size or number of the purely sensory nerves and their osteological correlates like the olfactory nerve (CN I) and optic nerve (CN II), which may offer details on olfaction or vision. This situation is more likely an artifact of preservation, as the bony passages of these nerves are in

general not preserved in the crocodylomorph fossil record. Similarly, it remains to be determined how biologically informative the size and reconstructed pathways of purely motor (e.g. CNs III, IV, VI, XII) or mixed (e.g. CNs VII, IX, X) cranial nerves are. On the other hand, the trigeminal nerve (CN V) has received significant attention, both because of the bony preservation of key parts -including the ganglion and facial branches-, as well as its clear correlation with somatosensation and the derived sense of face touch in living crocodylians (e.g. Soares 2002; Leitch and Catania 2012; Lessner and Holliday 2021). In extant species, as well as in closely related extinct neosuchians (see above), the number and density of trigeminal nerve-sourced rostral foramina are greater for these aquatic (continental or marine-pelagic) and semi-aquatic crocodyliforms. These foramina have been hypothesized to serve as proxies for facial somatosensation (Soares 2002), but their morphological patterns and distribution remain to be thoroughly tested. Regardless, George and Holliday (2013) found that the volume of the trigeminal fossa (a proxy for the size of the trigeminal ganglion) as well as the diameter of the maxillomandibular foramen (a proxy for nerve size), both relative to brain volume, showed an increase in size along the line to living crocodylians supporting a relationship between the sizes of nerve tissues, their osteological correlates and a derived sense of face touch. Moreover, putatively terrestrial crocodyliforms, such as protosuchids (e.g. *Protosuchus* MCZ 6727), as well as notosuchians (e.g. *Simosuchus*, Kley et al. 2010; *Notosuchus*, Barrios et al. 2018; *Hamadasuchus* ROM 52620; *Aphaurosuchus* LPRP 0697; Fig. 7.6e), possess very small trigeminal foramina -with relatively small trigeminal fossae-, further suggesting derived somatosensation evolved later in the clade than previously proposed by Soares (2002) or that the increase somatosensation evolved multiple times within crocodylomorphs, for example in *Thalattosuchia* and *Crocodylia* (George and Holliday 2013; Barrios 2021).

Recently, new CT scan-derived volumetric approaches have been employed to better characterize the morphology and distribution of trigeminal nerve-related structures (Lessner 2020), as well as those related to other cranial nerves (Lessner and Holliday 2020), revealing informative new approaches in crocodylomorph neurology (Figs. 7.5, 7.6, 7.7 and 7.8). For example, compared to the richly, dendritically branching array of nerves in *Alligator*, there are rather limited branches of the neurovascular canal in the dentary of the putatively terrestrial notosuchian *Araripesuchus gomesii* (AMNH 24450; Fig. 7.8b) and in the wide and anteriorly edentulous dentary of the non-crocodyliform crocodylomorph *Macelognathus* (LACM 4684/133772; Fig. 7.8c). Interestingly, the dentary of the aetosaur *Longosuchus* (TMM 31185-84B; Fig. 7.8d) shares a similar morphology with *Macelognathus* but possesses a lateral branch of the mandibular canal that radiates in a stellate pattern rather than the dense, dendritic array of canals found in crocodylians (Fig. 7.8a).

Regarding the sense of hearing, the dorsoventral extension of the lagena represents the areal surface of sensory epithelium (i.e. basilar papilla), and therefore serves as a proxy for hearing capability (Gleich and Manley 2000; Gleich et al. 2005; Walsh et al. 2009). The dorsoventral extension of the lagena of extinct and living crocodylomorphs is relatively variable (Schwab et al. 2020; Fig. 7.10). The

early crocodyliform *Protosuchus* (Schwab et al. 2020, fig 2) and the notosuchian *Baurusuchus* (Dumont Jr et al. 2020, fig 9), both putatively terrestrial, have considerably elongated lagenae -particularly the former- contrasting with the shorter lagenae found in aquatic forms, specifically in pelagic thalattosuchians (e.g. Neenan et al. 2017; Schwab et al. 2020). Furthermore, in *Protosuchus* and *Baurusuchus*, the lagena is bent anterior and medially as an incipient pseudo-cochlea (considering the mammalian cochlea; Manley 2000). This condition may indicate greater hearing acuity in these terrestrial forms. In thalattosuchians, the dorsoventral shortening of the vestibular apparatus, together with the more robust semicircular canals, have been related to aquatic environments and a higher buoyancy capacity based on the similar shape to living deep ocean animals where buoyancy is more important than in semi-aquatic forms (e.g. Georgi and Sipla 2008; Schwab et al. 2020). These authors proposed that there is a link between the shape of the semicircular canals and the initial phases of aquatic adaptation in crocodyliforms, and further modifications associated with a pelagic lifestyle. Although this hypothesis is consistent with what was observed for other terrestrial archosaurs (Fig. 7.10), Bronzati et al. (2021) found that this specific hypothesis was not supported, although as they did not test aquatic adaptation nor included pelagic taxa in the analyses, their work is not contrary to Schwab et al. (2020). More studies on the anatomy of the inner ear but also considering the general morphology of the skull in crocodylomorphs are necessary. For its part, Montefeltro et al. (2016) studied the anatomy of the outer ear (meatal chamber) in crocodyliforms and their implications in the auditory function, suggesting that airborne hearing played an important role in the origin of Crocodyliformes and evolution of its lineage.

7.4 Final Remarks

The neuroanatomy of Crocodylomorpha seems to have changed very little in the last 60 million years. However, and despite the few information on extinct forms, some transformations can be observed near relevant nodes of this clade (e.g. non-crocodyliform crocodylomorphs, thalattosuchians, eusuchian mesoeucrocodylians) some of them that could be related to general lifestyles (terrestrial vs aquatic), especially those referred to sense organs and linked brain parts. Within crocodylomorphs, the cranial endocast general shape seems to be dominated by body size and development in volume and position of the cephalic vasculature (e.g. venous sinuses, internal carotids and its main branches as the cerebral arteries; Hopson 1979; Witmer et al. 2008; Hu et al. 2020).

Unfortunately, the anatomical evidence for the brain of early crocodylomorphs, including basal crocodyliforms, is practically null and is biased to a few taxa such as *Almadasuchus*, which appears to have several apomorphic features in its cranial endocast (Leardi et al. 2020). Despite this, an endocast with lateromedially narrower cerebral hemispheres and a relatively large pituitary gland (hypophyseal fossa) could be the plesiomorphic condition for Crocodylomorpha (Fig. 7.9 and

Table 7.2). The slight lateral extension of the cerebral hemispheres probably changes near the node Crocodyliformes, to a notable more laterally expanded telencephalon, generally oval in outline, with the longest margin facing anteriorly (as occurring in early ontogenetic stages of living crocodylians; Watanabe et al. 2019). This condition of a cranial endocast with relatively laterally expanded cerebral hemispheres is mainly observed in the notosuchians *Simosuchus* and uruguayasuchids (e.g. *Araripesuchus*, *Anatosuchus*), and the dwarf crocodylian *Osteolaemus* (Fig. 7.9). Conversely, dyrosaurids (e.g., *Rhabdognathus*) and thalattosuchians (e.g. ‘*Metriorhynchus*’, *Cricosaurus*) have cranial endocast with a less lateral expansion of the cerebral hemispheres (Table 7.2), condition that could be interpreted as reversals, especially when thalattosuchians are considered within Crocodyliformes. In addition, some non-crocodylian eusuchians (e.g. *Goniopholis*) and crocodylians (e.g. *Leidyosuchus*, *Gavialis*, *Osteolaemus*) present more oval lateral hemispheres with more elongated anterior surfaces (as it is observed in dorsal view, Fig. 7.9), contrasting with the apparently derived morphology shared by globidontian alligatoroids (e.g. *Diplocynodon*, *Alligator*, *Caiman*) which present subspherical lateral hemispheres, with symmetrical anterior and posterior surfaces (e.g. Bona and Paulina-Carabajal 2013).

As observed in large crocodylomorphs, the cranial endocast is almost tubular. During the ontogeny of living crocodylians, the outline of the brain changes as size increases, from sigmoidal to more tubular (e.g. Jirak and Janacek 2017; Watanabe et al. 2019; Hu et al. 2020). As a result, more mature and larger animals have a more anteroposteriorly linearly disposed encephalon. This condition is observed in large fossil caimans (*Caiman gasparinae*) and thalattosuchians (e.g. *Cricosaurus*). However, in some huge extinct amphibious crocodylians such as the caimanine *Mourasuchus nativus*, the cranial endocast maintains a sigmoidal disposition in grown forms (Bona et al. 2013). This should be handled with care as this pedomorphic trait of the cranial endocast of *Mourasuchus* is one of the several peculiar craniomandibular features that this bizarre taxon has (e.g. Bona et al. 2013; Cidade et al. 2019) and markedly contrasts with the morphology seen in other closely related caimanines. Pedomorphic morphotypes of the cranial endocast can be also observed in adult “dwarf” forms of living crocodiles such as *Osteolaemus tetraspis* and *Paleosuchus trigonatus* (Balanoff and Bever 2017, fig 5; Serrano-Martínez et al. 2019, fig 5).

In addition to the angles between the forebrain, midbrain, and hindbrain, the dorsal and ventral outline of the brain in Crocodylomorpha varies from wavy to almost straight, according to the development of the venous sinuses that drain the cerebral cavity (e.g. Hopson 1979; Witmer et al. 2008; Porter et al. 2016; Fig. 7.9). Regarding the cranial vasculature, an important anatomical condition shared by most crocodylomorphs is that the internal carotids enter the skull more posteriorly than other pseudosuchians. The position of the internal carotid foramen for the passage of the cerebral carotid artery (*sensu* Porter et al. 2016) is placed on the occipital surface of the skull, and is a derived condition within Crocodylomorpha, shared with hallopodids + crocodyliforms and absent in more basal forms of the clade and other pseudosuchians (e.g. Benton and Clark 1988; Pol et al. 2013; Leardi et al.

2017, 2020). Although inside the braincase the arterial pattern of branching and pathways is similar among crocodylomorphs. In Eusuchia, a variation in the trajectories of the basiesphenoidal carotid canals, just before their opening in the pituitary fossa, is observed (e.g. Witmer et al. 2008; Bona et al. 2017). Finally, it should be mentioned that despite the practically absence of brain flexures (Table 7.2), thalattosuchian and dyrosaurid neuroanatomy include a well-developed cephalic vascular system with caudal middle cerebral vein and orbital artery, and an enlarged internal carotid artery in the former (e.g. Brusatte et al. 2016; Pierce et al. 2017; Herrera et al. 2018; Erb and Turner 2021; Wilberg et al. 2021). Also, the relatively large pituitary in thalattosuchians has been correlated with water regulation and with the hypertrophy of the cavernous sinus (Schwab et al. 2021; Wilberg et al. 2021).

The general morphology of early pseudosuchian inner ear is retained in most Crocodylomorpha; however, some differences were recognized. In non-crocodyliform crocodylomorphs (except *Almadasuchus*), early crocodyliforms, and notosuchians, the vestibular portion is relatively high with the ASC more dorsally projected than the PSC, contrasting with the morphology of most mesoeucrocodylians including thalattosuchians if they are considered within the clade (Fig. 7.10). Despite this, vertical semicircular canals (ASC and PSC) seem to be more unequally sized in more aquatic mesoeucrocodylians (i.e. thalattosuchians, gavialoids). As observed in non-crocodylomorph pseudosuchians (e.g. Stocker et al. 2016) and in non-crocodyliform crocodylomorphs, the condition of the inner ear of notosuchians coincides with that expected for terrestrial forms (Schwab et al. 2020). With respect to the ventral portion of the vestibule, the lagenae is relatively dorsoventrally elongated (except *Almadasuchus* and aquatic crocodylomorphs).

We conclude that there is a gap in information on neuroanatomy of the non-crocodyliform crocodylomorphs and early crocodyliforms (e.g. protosuchids), which is key to understanding the major changes that might have happened in the brain during the initial diversification of crocodyliforms at the Late Triassic–Early Jurassic, and understanding the basal condition for mesoeucrocodylians. Information on the neuroanatomy of various groups of Mesoeucrocodylia is poorly sampled or absent, in both notosuchians (e.g. sphagesaurids, peirosaurids, sebecosuchians) and neosuchians (e.g. pholidosaurids, dyrosaurids, atoposaurids, planocraniids), and necessary for a better understanding of the neurological novelties within Crocodyliformes and their implications in the evolutionary occupation of terrestrial and aquatic habitats. Morphogeometric studies are also needed to analyze shape variation in a more exhaustive way as well as quantitative studies on sensory capacities of extinct forms (i.e. olfactory, visual, hearing).

Acknowledgments We thank the Editors (María Teresa Dozo, Ariana Paulina-Carabajal, Thomas E. Macrini, and Stig Walsh) for the invitation to contribute to this important book, and for answering many questions that improved the final version of this manuscript. We also thank Diego Pol and Alan Turner for the availability of the unpublished CT data of *Araripesuchus gomesii* used in this manuscript for nerve reconstruction. Finally we also thank Yanina Herrera and Felipe Montefeltro for reviewing and improving this manuscript. This work was partly supported by grants from the Consejo Nacional de Investigaciones Científicas y Técnicas (F.B.), Agencia Nacional de Promoción

Científica y Tecnológica-FONCyT- PICT 2026-0159 (P.B.), PICT 2016-0267 (J.M.L.), PICT 2018-0605 (J.M.L.), and the University of Missouri Research Board, National Science Foundation (NSF IOS 1457319, NSF EAR 1631684) (C.M.H.). Ruth Elsey and the Rockefeller State Refuge for access to specimens.

References

- Baird II (1970) Chapter 3: The anatomy of the reptilian ear. In: Gans C, Parsons TS (eds) *Biology of the reptilia, Morphology B*, vol 2. Academic, pp 193–275
- Balanoff AM, Bever GS (2017) The role of endocasts in the study of brain evolution. In: Kaas J (ed) *Evolution of nervous systems*, vol 1, 2nd edn, pp 223–241. <https://doi.org/10.1016/B978-0-12-820584-6.00003-9>
- Barrios F (2015) Primera reconstrucción digital del endocráneo de un Crocodyliformes del Cretácico de Patagonia: análisis morfológico-comparativo. *Ameghiniana* 52(4):8
- Barrios F (2021) El neurocráneo de los Notosuquios (Crocodyliformes) del Cretácico Superior de la Cuenca Neuquina (Patagonia, Argentina): morfología endocraneana y sus inferencias paleoneurológicas. Dissertation, Universidad Nacional de La Plata
- Barrios F, Paulina-Carabajal A, Novas F et al (2016) Paleoneurology of *Yacarerani boliviensis* (Notosuchia) from the Cretaceous of Bolivia. *Ameghiniana* 53(6):7
- Barrios F, Paulina-Carabajal A, Bona P et al (2017) Moldes endocraneanos naturales de Crocodyliformes continentales de la Cuenca Neuquina. Abstract presented at the 1st Reunión de Paleovertebrados de la Cuenca Neuquina, Rincón de los Sauces, 2–3 November 2017
- Barrios F, Bona P, Paulina-Carabajal A et al (2018) Re-description of the cranio-mandibular anatomy of *Notosuchus terrestris* (Crocodyliformes, Mesoeucrocodylia) from the Upper Cretaceous of Patagonia. *Cret Res* 83:3–39. <https://doi.org/10.1016/j.cretres.2017.08.016>
- Bellairs AA, Shute CCD (1953) Observations on the narial musculature of Crocodylia and its innervation from the sympathetic system. *J Anat* 87(4):367–378
- Belton T, McCrear RA (2000) Role of the cerebellar flocculus region in the coordination of eye and head movements during gaze pursuit. *J Neurophysiol* 84(3):1614–1626. <https://doi.org/10.1152/jn.2000.84.3.1614>
- Benning B, McNeil J (2010) Transitional nerve: a new and original classification of a peripheral nerve supported by the nature of the accessory nerve (CN XI). *Neurol Res Int* 2010:476018. <https://doi.org/10.1155/2010/476018>
- Benton MJ, Clark JM (1988) Archosaur phylogeny and the relationships of the Crocodylia. In: Benton MJ (ed) *The phylogeny and classification of the tetrapods, Amphibians, reptiles, birds*, vol 1. Systematics Association, Clarendon Press, pp 295–338. Special Volume 35A
- Beyrand V, Voeten DFAE, Burès S et al (2019) Multiphase progenetic development shaped the brain of flying archosaurs. *Sci Rep* 9:10807. <https://doi.org/10.1038/s41598-019-46959-2>
- Billings BK, Behroozi M, Helluy X et al (2020) A three-dimensional digital atlas of the Nile crocodile (*Crocodylus niloticus*) forebrain. *Brain Struct Funct* 225:683–703. <https://doi.org/10.1007/s00429-020-02028-3>
- Blanco A, Fortuny J, Vicente A et al (2015) A new species of *Allodaposuchus* (Eusuchia, Crocodylia) from the Maastrichtian (Late Cretaceous) of Spain: phylogenetic and paleobiological implications. *Peer J* 3:e1171. <https://doi.org/10.7717/peerj.1171>
- Bona P, Desojo JB (2011) Osteology and cranial musculature of *Caiman latirostris* (Crocodylia: Alligatoridae). *J Morphol* 272(7):780–795. <https://doi.org/10.1002/jmor.10894>
- Bona P, Paulina-Carabajal A (2013) *Caiman gasparinae* sp. nov. a huge alligatorid (Caimaninae) from the late Miocene of Paraná, Argentina. *Alcheringa* 37:462–473. <https://doi.org/10.1080/003115518.2013.785335>

- Bona P, Degrange F, Fernández MS (2013) Skull anatomy of the bizarre crocodylian *Mourasuchus nativus* (Alligatoridae, Caimaninae). *Anat Rec* 296(2):227–239. <https://doi.org/10.1002/ar.22625>
- Bona P, Paulina-Carbajal A, Gasparini ZB (2017) Neuroanatomy of *Gryposuchus neogaeus* (Crocodylia, Gavialoidea): a first integral description of the braincase and endocranial morphological variation in extinct and extant gavialoids. *Earth Environ Sci Trans R Soc Edinb* 106(4):235–246. <https://doi.org/10.1017/S1755691016000189>
- Brochu CA (1999) Phylogenetics, taxonomy, and historical biogeography of Alligatoroidea. *J Vert Paleontol*, Memoir 6:9–100. <https://doi.org/10.2307/3889340>
- Bronzati M, Montefeltro FC, Langer MC (2012) A species-level supertree of Crocodyliformes. *Hist Biol* 24(6):598–606. <https://doi.org/10.1080/08912963.2012.662680>
- Bronzati M, Montefeltro FC, Langer MC (2015) Diversification events and the effects of mass extinctions on Crocodyliformes evolutionary history. *R Soc Open Sci* 2:140385. <https://doi.org/10.1098/rsos.140385>
- Bronzati M, Rauhut OWM, Bittencourt JS, Langer MC (2017) Endocast of the Late Triassic (Carnian) dinosaur *Saturnalia tupiniquim*: implications for the evolution of brain tissue in Sauropodomorpha. *Sci Rep* 7:11931. <https://doi.org/10.1038/s41598-017-11737-5>
- Bronzati M, Benson RBJ, Evers SW et al (2021) Deep evolutionary diversification of semicircular canals in archosaurs. *Curr Biol* 31(12):2520–2529. <https://doi.org/10.1016/j.cub.2021.03.086>
- Brusatte SL, Muir A, Young MT et al (2016) The braincase and neurosensory anatomy of an Early Jurassic marine crocodylomorph: implications for crocodylian sinus evolution and sensory transitions. *Anat Rec* 299(11):1511–1530. <https://doi.org/10.1002/ar.23462>
- Buffetaut E (1980) Teleosauridae et Metriohynchidae: l'évolution de eux familles de crocodyliens méso-suchiens marins du Mésozoïque. Paper presented at the 105th Congrès National des Sociétés Savantes, Caen, 8–9 April 1980
- Busbey AB III, Gow C (1984) A new protosuchian crocodile from the Upper Triassic Elliot Formation of South Africa. *Palaeontol Afr* 25:127–149
- Chentanez T, Huggins SE, Chentanez V (1983) Allometric relationships of the siamese crocodile, *Crocodylus siamensis*. *J Sci Soc Thail* 9:5–26. <https://doi.org/10.2306/scienceasia1513-1874.1983.09.005>
- Chiasson RB (1962) Laboratory anatomy of the alligator. WMC. Brown Company Publishers
- Cidade GM, Souza-Filho JP, Hsiou AS et al (2019) New specimens of *Mourasuchus* (Alligatoroidea, Caimaninae) from the Miocene of Brazil and Bolivia and their taxonomic and morphological implications. *Alcheringa* 43(2):261–278. <https://doi.org/10.1080/03115518.2019.1566495>
- Clark JM (1986) Phylogenetic relationships of the crocodylomorph archosaurs. Dissertation, University of Chicago
- Clark JM, Welman J, Gauthier JA et al (1993) The laterosphenoid bone of early archosauriforms. *J Vert Paleontol* 13(1):48–57
- Colbert EH (1946) *Sebecus*, representative of a peculiar suborder of fossil Crocodylia from Patagonia. *Bull Am Mus Nat Hist* 87(4):217–280
- Cox PG, Jeffery N (2010) Semicircular canals and agility: the influence of size and shape measures. *J Anat* 216(1):37–47. <https://doi.org/10.1111/j.1469-7580.2009.01172.x>
- Crompton AW, Smith KK (1980) A new genus and species of crocodylian from the Kayenta Formation (Late Triassic?) of Northern Arizona. In: Jacobs LL (ed) *Aspects of Vertebrate History: essays in honor of Edwin Harris Colbert*. Museum of Northern Arizona Press, Flagstaff, pp 193–217
- Darlim G, Montefeltro FC, Langer MC (2021) 3D skull modelling and description of a new baurusuchid (Crocodyliformes, Mesoeucrocodylia) from the Late Cretaceous (Bauru Basin) of Brazil. *J Anat* 239(3):622–662. <https://doi.org/10.1111/joa.13442>
- de Beer GS (1937) The development of the vertebrate skull. Clarendon Press, Oxford
- Dufeau DL (2011) The evolution of cranial pneumaticity in Archosauria: patterns of paratympanic sinus development. Dissertation, Ohio University

- Dufeu DL, Witmer LM (2015) Ontogeny of the middle-ear air-sinus system in *Alligator mississippiensis* (Archosauria: Crocodylia). PLoS One 10(9):e0137060. <https://doi.org/10.1371/journal.pone.0137060>
- Dumont MV Jr, Santucci RM, Andrade MB et al (2020) Paleoneurology of *Baurusuchus* (Crocodyliformes: Baurusuchidae), ontogenetic variation, brain size, and sensorial implications. Anat Rec. <https://doi.org/10.1002/ar.24567>
- Edinger T (1938) Über Steinkerne von Hirn-und Ohr-Höhlen der Mesosuchier *Goniopholis* und *Pholidosaurus* aus dem Bückeburger Wealden. Acta Zool 19(3):467–505. <https://doi.org/10.1111/j.1463-6395.1938.tb00693.x>
- Erb A, Turner AH (2021) Braincase anatomy of the Paleocene crocodyliform *Rhabdognathus* revealed through high resolution computed tomography. Peer J 9:e11253. <https://doi.org/10.7717/peerj.11253>
- Eudes-Deslongchamps JA (1863) Mémoires sur les Téléosauriens de l'Époque Jurassique du Département du Calvados. Premier Mémoire contenant l'exposé des caractères généraux des Téléosauriens comparés à ceux des crocodiliens et la description particulière des espèces du Lias Supérieur. Mém Soc Linn, Normandie XIII(3):1–138
- Evans DC (2005) New evidence on brain–endocranial cavity relationships in ornithischian dinosaurs. Acta Palaeontol Pol 50(3):617–622
- Fabbri M, Koch NM, Pritchard AC et al (2017) The skull roof tracks the brain during the evolution and development of reptiles including birds. Nat Ecol Evol 1:1543–1550. <https://doi.org/10.1038/s41559-017-0288-2>
- Fernández M, Paulina Carabajal A, Gasparini Z et al (2011) A metriorhynchid crocodyliform braincase from Northern Chile. J Vert Paleontol 32(2):369–377. <https://doi.org/10.1080/02724634.2011.550361>
- Fernández-Blanco MV (2018) Análisis morfológico del esqueleto de las especies argentinas del género *Caiman* (Alligatoridae: Caimaninae): Aportes al conocimiento de la historia evolutiva de los alligatíridos sudamericanos. Dissertation, Universidad Nacional de La Plata
- Fernández-Dumont ML, Bona P, Barrios F et al (2017a) Estudio preliminar del endocast de un ejemplar de *Araripesuchus* (Crocodyliformes, Uruguaysuchidae): aportes al conocimiento de la neuroanatomía de los notosúquios. PE-APA 18(2):R25
- Fernández-Dumont ML, Bona P, Barrios F et al (2017b) Anatomía endocraneana de *Araripesuchus* sp. (Crocodyliformes, Notosuchia) del Cretácico tardío de la Cuenca Neuquina. Abstract presented at the 1st Reunión de Paleovertebrados de la Cuenca Neuquina, Rincón de los Sauces, 2–3 November 2017
- Fernández-Dumont ML, Bona P, Pol D et al (2020) New anatomical information on *Araripesuchus buitreaensis* with implications for the systematics of Uruguaysuchidae (Crocodyliformes, Notosuchia). Cret Res 113:104494. <https://doi.org/10.1016/j.cretres.2020.104494>
- Ferreira-Cardoso S, Araújo R, Martins NE et al (2017) Floccular fossa size is not a reliable proxy of ecology and behaviour in vertebrates. Sci Rep 7:2005. <https://doi.org/10.1038/s41598-017-01981-0>
- Firth BT, Christian KA, Belan I et al (2010) Melatonin rhythms in the Australian freshwater crocodile (*Crocodylus johnstoni*): a reptile lacking a pineal complex? J Comp Physiol B 180(1):67–72. <https://doi.org/10.1007/s00360-009.0387-8>
- Fonseca PHM, Martinelli AG, Marinho TS et al (2020) Morphology of the endocranial cavities of *Campinasuchus dinizi* (Crocodyliformes: Baurusuchidae) from the Upper Cretaceous of Brazil. Geobios 58(1):1–16. <https://doi.org/10.1016/j.geobios.2019.11.001>
- Franzosa J (2004) Evolution of the brain in Theropoda (Dinosauria). Dissertation, University of Texas
- George ID, Holliday CM (2013) Trigeminal nerve morphology in *Alligator mississippiensis* and its significance for crocodyliform facial sensation and evolution. Anat Rec 296(4):670–680. <https://doi.org/10.1002/ar.22666>
- Georgi JA (2008) Semicircular canal morphology as evidence of locomotor environment in amniotes. Dissertation, Stony Brook University

- Georgi JA, Sipla JS (2008) Comparative and functional anatomy of balance in aquatic reptiles and birds. In: Thewissen JGM, Nummela S (eds) Sensory evolution on the threshold-adaptations in secondarily aquatic vertebrates. University of California Press, pp 233–256
- Gignac PM, Kley NJ, Clarke JA et al (2016) Diffusible iodine-based contrast-enhanced computed tomography (diceCT): an emerging tool for rapid, high-resolution, 3-D imaging of metazoan soft tissues. *J Anat* 228(6):889–909. <https://doi.org/10.1111/joa.12449>
- Girons HS (1970) Chapter 5: The pituitary gland. In: Gans C, Parsons TS (eds) *Biology of the reptilia, Morphology C*, vol 3. Academic, pp 135–199
- Gleich O, Manley GA (2000) The hearing organ of birds and crocodylian. In: Dooling RJ, Fay RR (eds) *Comparative hearing: birds and reptiles*. Springer, New York, pp 70–138
- Gleich O, Dooling RJ, Manley GA (2005) Audiogram, body mass, and basilar papilla length: correlations in bird and predictions for extinct archosaurs. *Naturwissenschaften* 92:595–598. <https://doi.org/10.1007/s00114-005-0050-5>
- Godoy PL, Benson RB, Bronzati M et al (2019) The multi-peak adaptive landscape of crocodylomorph body size evolution. *BMC Evol Biol* 19:167. <https://doi.org/10.1186/s12862-019-1466-4>
- Gold MEL, Brochu CA, Norell MA (2014) An expanded combined evidence approach to the *Gavialis* problem using geometric morphometric data from crocodylian braincase and Eustachian systems. *PLoS One* 9(9):e105793. <https://doi.org/10.1371/journal.pone.0105793>
- Gower DJ, Weber E (1998) The braincase of *Euparkeria*, and the evolutionary relationships of birds and crocodylians. *Biol Rev* 73(4):367–411. <https://doi.org/10.1017/S0006323198005222>
- Grigg G, Kirshner D (2015) *Biology and evolution of crocodylians*. Cornell University Press, Ithaca/London
- Herrera Y (2015) Metriorhynchidae (Crocodylomorpha: Thalattosuchia) from Upper Jurassic–Lower Cretaceous of Neuquén Basin (Argentina), with comments on the natural casts of the brain. In: Fernández M, Herrera Y (eds) *Reptiles Extintos – Volumen en Homenaje a Zulma Gasparini PE-APA* 15(1):159–171. <https://doi.org/10.5710/PEAPA.09.06.2015.104>
- Herrera Y, Vennari VV (2014) Cranial anatomy and neuroanatomical features of a new specimen of Geosaurini (Crocodylomorpha: Metriorhynchidae) from west-central Argentina. *Hist Biol* 27(1):33–41. <https://doi.org/10.1080/08912963.2013.861831>
- Herrera Y, Fernández MS, Gasparini Z (2013) The snout of *Cricosaurus araucanensis*: a case study in novel anatomy of the nasal region of metriorhynchids. *Lethaia* 46(3):331–340. <https://doi.org/10.1111/let.12011>
- Herrera Y, Leardi JM, Fernández MS (2018) Braincase and endocranial anatomy of two thalattosuchian crocodylomorphs and their relevance in understanding their adaptations to the marine environment. *Peer J* 6:65686. <https://doi.org/10.7717/peerj.5686>
- Highstein SM (1998) Role of the flocculus of the cerebellum in motor learning of the vestibulo-ocular reflex. *J Otolaryngol-Head N* 119(39):212–220. [https://doi.org/10.1016/S0194-5998\(98\)70056-7](https://doi.org/10.1016/S0194-5998(98)70056-7)
- Holliday CM, Gardner NM (2012) A new eusuchian crocodyliform with novel cranial integument and its significance for the origin and evolution of Crocodylia. *PLoS One* 7(1):e30471. <https://doi.org/10.1371/journal.pone.0030471>
- Holliday CM, Witmer LM (2007) Archosaur adductor chamber evolution: integration of musculoskeletal and topological criteria in jaw muscle homology. *J Morph* 268(6):457–484. <https://doi.org/10.1002/jmor.10524>
- Holliday CM, Witmer LM (2009) The epipterygoid of crocodyliforms and its significance for the evolution of the orbitotemporal region of eusuchians. *J Vert Paleontol* 29(3):715–733. <https://doi.org/10.1671/039.029.0330>
- Holliday CM, Tsai HP, Skiljan RJ et al (2013) A 3D interactive model and atlas of the jaw musculature of *Alligator mississippiensis*. *PLoS One* 8(6):e62806. <https://doi.org/10.1371/journal.pone.0062806>
- Hopson JA (1977) Relative brain size and behavior in archosaurian reptiles. *Annu Rev Ecol Evol Syst* 8:429–448. <https://doi.org/10.1146/annurev.es.08.110177.002241>

- Hopson JA (1979) Chapter 2: Paleoneurology. In: Gans C, Northcutt RG, Uliski P (eds) *Biology of the reptilia, Neurology A*, vol 9. Academic, pp 39–146
- Hu K, King JL, Romick CA et al (2020) Ontogenetic endocranial shape change in alligators and ostriches and implications for the development of the non-avian dinosaur endocranium. *Anat Rec* 304(8):1759–1775. <https://doi.org/10.1002/ar.24579>
- Hurlburt GR (1996) Relative brain size in recent and fossil amniotes: determination and interpretation. Dissertation, University of Toronto
- Hurlburt GR, Waldorf L (2002) Endocast volume and brain mass in a size series of alligators (*Alligator mississippiensis*). *J Vert Paleontol* 23(3, Suppl):69A
- Hurlburt GR, Ridgely RC, Witmer LM (2013) Relative size of brain and cerebrum in tyrannosaurid dinosaurs: an analysis using brain-endocast quantitative relationships in extant alligators. In: Parrish JM, Henderson M, Currie PJ, Koppelhus E (eds) *Origin, systematics, and paleobiology of the tyrannosauridae*. Northern Illinois University Press, pp 134–154
- Iordansky NN (1973) Chapter 3: The skull of the crocodylia. In: Gans C, Parsons TS (eds) *Biology of the reptilia, Morphology D*, vol 4. Academic, pp 201–262
- Jerison HJ (1973) Evolution of the brain and intelligence. Academic, New York
- Jerison HJ (1977) The theory of encephalization. *Ann NY Acad Sci* 299(1):146–160. <https://doi.org/10.1111/j.1749-6632.1977.tb41903.x>
- Jirak D, Janacek J (2017) Volume of the crocodylian brain and endocast during ontogeny. *PLoS One* 12(6):e0178491. <https://doi.org/10.1371/journal.pone.0178491>
- Johnson MM, Young MT, Brusatte SL (2020) The phylogenetics of Teleosauroida (Crocodylomorpha, Thalattosuchia) and implications for their ecology and evolution. *Peer J* 8:e9808. <https://doi.org/10.7717/peerj.9808>
- Kawabe S, Shimokawa T, Miki H et al (2009) A simple and accurate method for estimating the brain volume of birds: possible application in paleoneurology. *Brain Behav Evol* 74:295–301. <https://doi.org/10.1159/000270906>
- Klembara J (2005) Ontogeny of the partial secondary wall of the otoccipital region of the endocranium in prehatching *Alligator mississippiensis* (Archosauria, Crocodylia). *J Morphol* 266(3):319–330. <https://doi.org/10.1002/jmor.10380>
- Kley NJ, Sertich JJW, Turner AH et al (2010) Craniofacial morphology of *Simosuchus clarki* (Crocodyliformes: Notosuchia) from the Late Cretaceous of Madagascar. In: Krause DW, Kley NJ (eds) *Simosuchus clarki* (Crocodyliformes: Notosuchia) from the Late Cretaceous of Madagascar, vol 10. Memoir (Society of Vertebrate Paleontology), pp 13–98. <https://doi.org/10.1080/02724634.2010.532674>
- Koken E (1887) Die Dinosaurier, Crocodyliden und Sauropterygier des norddeutschen Wealden Palaeontologische Abhandlungen p 138
- Kundrát M, Xu X, Hančová M et al (2018) Evolutionary disparity in the endoneurocranial configuration between small and gigantic tyrannosauroids. *Hist Biol* 32(5):620–634. <https://doi.org/10.1080/08912963.2018.1518442>
- Kuzmin IT, Boitsova EA, Gombolevskiy VA et al (2021) Braincase anatomy of extant Crocodylia, with new insights into the development and evolution of the neurocranium in crocodylomorphs. *J Anat* 239(5):983–1038. <https://doi.org/10.1111/joa.13490>
- Larsson HCE, Sues HD (2007) Cranial osteology and phylogenetic relationships of *Hamadasuchus rebouli* (Crocodyliformes: Mesoeucrocodylia) from the Cretaceous of Morocco. *Zool J Linnean Soc* 149(4):533–567. <https://doi.org/10.1111/j.1096-3642.2007.00271.x>
- Larsson HCE, Sereno PC, Wilson JA (2000) Forebrain enlargement among nonavian theropod dinosaurs. *J Vert Paleontol* 20(3):615–618
- Lautenschlager S, Butler RJ (2016) Neural and endocranial anatomy of Triassic phytosaurian reptiles and convergence with fossil and modern crocodylians. *Peer J* 4:e2251. <https://doi.org/10.7717/peerj.2251>
- Leardi JM, Pol D, Clark JM (2017) Detailed anatomy of the braincase of *Macelognathus vagans* Marsh, 1884 (Archosauria, Crocodylomorpha) using high resolution tomography and new

- insights on basal crocodylomorph phylogeny. *Peer J* 5:e2801. <https://doi.org/10.7717/peerj.2801>
- Leardi JM, Pol D, Clark JM (2020) Braincase anatomy of *Almadasuchus figarii* (Archosauria, Crocodylomorpha) and a review of the cranial pneumaticity in the origins of Crocodylomorpha. *J Anat* 237(1):48–73. <https://doi.org/10.1111/joa.13171>
- Leitch DB, Catania KC (2012) Structure, innervation and response properties of integumentary sensory organs in crocodylians. *J Exp Biol* 215(23):4217–4230. <https://doi.org/10.1242/jeb.076836>
- Lemoine V (1883–1884) Note sur l'encephale du gavial du Mont-Aime, étudié sur trois moulages naturels. *Bull Soc Géol Fr* 12 (3): 158–162
- Lessner EJ (2020) Quantifying neurovascular canal branching patterns reveals a shared crocodylian arrangement. *J Morphol* 282(2):185–204. <https://doi.org/10.1002/jmor.21295>
- Lessner EJ, Holliday CM (2020) A 3D ontogenetic atlas of *Alligator mississippiensis* cranial nerves and their significance for comparative neurology of reptiles. *Anat Rec*. <https://doi.org/10.1002/ar.24550>
- Lessner EJ, Holliday CM (2021) Ecomorphology and morphological diversity of trigeminal nerve-mediated somatosensation in sauropsids. In: Abstracts of American Association for Anatomy Annual Meeting, Virtual, January 3–February 28, 2021
- Li Z, Clarke JA (2015) New insight into the anatomy of the hyolingual apparatus of *Alligator mississippiensis* and implications for reconstructing feeding in extinct archosaurs. *J Anat* 227(1):45–61. <https://doi.org/10.1111/joa.12320>
- Liem KF, Bemis WE, Walker WF et al (2000) Functional anatomy of the vertebrates: an evolutionary perspective, 3rd edn. *Harcourt College Publishers*
- Manley GA (2000) Cochlear mechanisms from a phylogenetic viewpoint. *Proc Natl Acad Sci* 97(22):11736–11743. <https://doi.org/10.1073/pnas.97.22.11736>
- Manley GA (2016) Comparative auditory neuroscience: understanding the evolution and function of ears. *J Assoc Res Otolaryngol* 18(1):1–24. <https://doi.org/10.1007/s10162-016-0579-3>
- Martinelli AG, Pais DF (2008) A new baurusuchid crocodyliform (Archosauria) from the Late Cretaceous of Patagonia (Argentina). *C R Palevol* 7(6):371–381. <https://doi.org/10.1016/j.crv.2008.05.002>
- Martínez RN, Alcober OA, Pol D (2019) A new protosuchid crocodyliform (Pseudosuchia, Crocodylomorpha) from the Norian Los Colorados Formation, Northwestern Argentina. *J Vert Paleontol* 38(4):1–12. <https://doi.org/10.1080/02724634.2018.1491047>
- Mastrantonio BM, von Baczko MB, Desojo JB et al (2019) The skull anatomy and cranial endocast of the pseudosuchid archosaur *Prestosuchus chiniquensis* from the Triassic of Brazil. *Acta Palaeontol Pol* 64(1):171–198. <https://doi.org/10.4202/app.00527.2018>
- Montefeltro FC, Larsson HCE, de França MAG et al (2013) A new neosuchian with Asian affinities from the Jurassic of northeastern Brazil. *Naturwissenschaften* 100(9):835–841. <https://doi.org/10.1007/s00114-013-1083-9>
- Montefeltro FC, Andrade DV, Larsson HCE (2016) The evolution of the meatal chamber in crocodyliforms. *J Anat* 228(5):838–863. <https://doi.org/10.1111/joa.12439>
- Morel de Glasville M (1876) Sur la cavité crânienne et la position du trou optique dans le *Steneosaurus heberti*. *Bull Soc Géol Fr* 3(4):342–348
- Mueller-Töwe IJ (2005) Phylogenetic relationships of the Thalattosuchia. *Zitteliana* A45:211–213
- Narváez I, Brochu CA, Escaso F et al (2016) New Spanish Late Cretaceous eusuchian reveals the synchronic and sympatric presence of two allodaposuchids. *Cret Res* 65(11):112–125. <https://doi.org/10.1016/j.cretres.2016.04.018>
- Neenan JM, Reich T, Evers SW et al (2017) Evolution of the sauropterygian labyrinth with increasingly pelagic lifestyles. *Curr Biol* 27(24):3852–3858-e31-7. <https://doi.org/10.1016/j.cub.2017.10.069>
- Nesbitt SJ (2011) The early evolution of archosaur: relationships and the origin of major clades. *Bull Am Mus Nat Hist* 352:1–292

- Ngwenya A, Patzke N, Spocter MA et al (2013) The continuously growing central nervous system of the Nile crocodile (*Crocodylus niloticus*). *Anat Rec* 296(10):1489–1500. <https://doi.org/10.1002/ar.22752>
- Ósi A (2013) The evolution of jaw mechanism and dental function in heterodont crocodyliforms. *Hist Biol* 26(3):279–414. <https://doi.org/10.1080/08912963.2013.777533>
- Owen R (1842) Report on British Fossil Reptiles, Part II. *Rep Br Ass Advmt Sci* 11:60–204
- Owen R (1850) On the communications between the cavity of the tympanum and the palate in the Crocodylia (gavials, alligators and crocodiles). *Philos Trans R Soc Lond* 140:521–527. <https://doi.org/10.1098/rstl.1850.0028>
- Paulina-Carabajal A, Lee YN, Jacobs LL, Iwaniuk A (2016) Endocranial morphology of the primitive nodosaurid dinosaur *Pawpawsaurus campbelli* from the Early Cretaceous of North America. *PLoS One* 11(3) e0150845. <https://doi.org/10.1371/journal.pone.0150845>
- Pierce SE, Benton MJ (2006) *Pelagosaurus typus* Bronn, 1841 (Mesoeucrocodylia: Thalattosuchia) from the Upper Lias (Toarcian, Lower Jurassic) of Somerset, England. *J Vert Paleontol* 26(3):621–635
- Pierce SE, Williams M, Benson RBJ (2017) Virtual reconstruction of the endocranial anatomy of the early Jurassic marine crocodylomorph *Pelagosaurus typus* (Thalattosuchia). *Peer J* 5:e3225. <https://doi.org/10.7717/peerj.3225>
- Pol D, Gasparini ZB (2009) Skull anatomy of *Dakosaurus andiniensis* (Thalattosuchia: Crocodylomorpha) and the phylogenetic position of Thalattosuchia. *J Syst Palaeontol* 7(2):163–197. <https://doi.org/10.1017/S1477201908002605>
- Pol D, Rauhut O, Lecuona A et al (2013) A new fossil from the Jurassic of Patagonia reveals the early basicranial evolution and the origins of Crocodyliformes. *Biol Rev* 88(4):862–872. <https://doi.org/10.1111/brv.12030>
- Pol D, Nascimento PM, Carvalho AB et al (2014) A new notosuchian from the late cretaceous of Brazil and the phylogeny of advanced notosuchians. *PLoS One* 9(4):e93105. <https://doi.org/10.1371/journal.pone.0093105>
- Porter WR, Sedlmayr JC, Witmer LM (2016) Vascular patterns in head of crocodylians: blood vessels and sites of thermal exchange. *J Anat* 229(6):800–824. <https://doi.org/10.1111/joa.12539>
- Quay WB (1979) Chapter 5: The parietal eye-pineal complex. In: Gans C, Northcutt RG, Ulinski P (eds) *Biology of the reptilia, Neurology A*, vol 9. Academic, pp 245–406
- Rabl-Rückhard H (1878) Das centralnervensystem des alligators. *Z Wiss Zool* 30:336–375
- Rieppel O (1985) The recessus scalae tympani and its bearing on the classification of reptiles. *J Herpetol* 19(3):373–384. <https://doi.org/10.2307/1564265>
- Ristevski J, Young MT, Andrade MB et al (2018) A new species of *Anteophthalmosuchus* (Crocodylomorpha, Goniopholidae) from the Lower Cretaceous of the Isle of Wight, United Kingdom, and a review of the genus. *Cret Res* 84:340–383. <https://doi.org/10.1016/j.cretres.2017.11.008>
- Ristevski J, Yates AM, Price GJ et al (2020) Australia’s prehistoric ‘swamp king’: revision of the Plio-Pleistocene crocodylian genus *Pallimnarchus* de Vis, 1886. *Peer J* 8:e10466. <https://doi.org/10.7717/peerj.10466>
- Ristevski J, Price GJ, Weisbecker V et al (2021) First record of a tomistomine crocodylian from Australia. *Sci Rep* 11:12158. <https://doi.org/10.1038/s41598-021-91717-y>
- Rogers SW (1998) Exploring dinosaur neuropaleobiology: computed tomography scanning and analysis of an *Allosaurus fragilis* endocast. *Neuron* 21:673–679. [https://doi.org/10.1016/S0896-6273\(00\)80585-1](https://doi.org/10.1016/S0896-6273(00)80585-1)
- Rogers SW (1999) *Allosaurus*, crocodiles, and birds: evolutionary clues from Spiral Computed Tomography of an endocast. *Anat Rec* 257(5):162–173. [https://doi.org/10.1002/\(SICI\)1097-0185\(1999105\)257:5<162::AID-AR5>3.0.CO;2-W](https://doi.org/10.1002/(SICI)1097-0185(1999105)257:5<162::AID-AR5>3.0.CO;2-W)
- Romer AS (1956) *Osteology of the reptiles*. University of Chicago Press
- Ruebenstahl AA (2019) *Junggarsuchus sloani*, An Early Late Jurassic Crocodylomorph with Crocodyliform Affinities. Dissertation, George Washington University

- Schmitz L, Motani R (2011) Nocturnality in dinosaurs inferred from scleral ring and orbit morphology. *Science* 332(6030):705–708. <https://doi.org/10.1126/science.1200043>
- Schwab JA, Young MT, Neenan JM et al (2020) Inner ear sensory system changes as extinct crocodylomorphs transitioned from land to water. *PNAS* 117(19):10422–10428. <https://doi.org/10.1073/pnas.2002146117>
- Schwab JA, Young MT, Herrera Y et al (2021) The braincase and inner ear of ‘*Metriorhynchus*’ cf. ‘*M. brachyrhynchus*’-implications for aquatic sensory adaptations in crocodylomorphs. *J Vert Paleontol* 41(1):e1912062. <https://doi.org/10.1080/02724634.2021.1912062>
- Seeley HG (1880) Note on the cranial characters of a large teleosaur from the Whitby Lias preserved in the Woodwardian Museum of the University of Cambridge, indicating a new species, *Teleosaurus eucephalus*. *Quart J Geol Soc* 36:627–637. <https://doi.org/10.1144/GSL.JGS.1880.036.01-04.46>
- Senn DG (1979) Chapter 4: Embryonic development of the central nervous system. In: Gans C, Northcutt RG, Ulinski P (eds) *Biology of the reptilia, Neurology A*, vol 9. Academic, pp 173–244
- Sereno PC, Larsson CE (2009) Cretaceous crocodyliforms from the Sahara. *Zookeys* 28:1–143. <https://doi.org/10.3897/zookeys.28.325>
- Sereno PC, Larsson HCE, Sidor CA, Gado B (2001) The giant crocodyliform *Sarcosuchus* from the Cretaceous of Africa. *Science* 294(5546):1516–1519. <https://doi.org/10.1126/science.1066521>
- Serrano-Martínez A, Knoll F, Narváez I et al (2018) Inner skull cavities of the basal eusuchian *Lohuecosuchus megadontos* (Upper Cretaceous, Spain) and neurosensory implications. *Cret Res* 93:66–77. <https://doi.org/10.1016/j.cretres.2018.08.016>
- Serrano-Martínez A, Knoll F, Narváez I et al (2019) Brain and pneumatic cavities of the braincase of the basal alligatoroid *Diplocynodon tormis* (Eocene, Spain). *J Vert Paleontol* 39(1):e1572612. <https://doi.org/10.1080/02724634.2019.1572612>
- Serrano-Martínez A, Knoll F, Narváez I et al (2020) Neuroanatomical and neurosensory analysis of the Late Cretaceous basal eusuchian *Agaresuchus fontisensis* (Cuenca, Spain). *Pap Palaeontol* 7(1):641–656. <https://doi.org/10.1002/spp2.1296>
- Sertich JJW, O’Connor PM (2014) A new crocodyliform from the middle Cretaceous Galula Formation, southwestern Tanzania. *J Vert Paleontol* 34(3):576–596. <https://doi.org/10.1080/02724634.2013.819808>
- Shiino K (1914) Studien zur Kenntniss des Wirbeltierkopfes. I. Das Chondrocranium in *Crocodylus* mit Berücksichtigung der Gehirnnerven und Kopfgefäße. *Anat Hefte* 50:254–381
- Shimizu T, Patton TB, Szafranski G et al (2009) Evolution of the visual system in reptiles and birds. In: Binder MD, Hirokawa N, Windhorst U (eds) *Encyclopedia of neuroscience*. Springer, Berlin, pp 1466–1472. https://doi.org/10.1007/978-3-540-29678-2_3179
- Shute CCD, Bellairs AD (1955) The external ear in Crocodilia. *Proc Zool Soc Lon* 124(4):741–749. <https://doi.org/10.1111/j.1469-7998.1955.tb07813.x>
- Smith D (2008) The cranial endocast of *Eutretauranosuchus delfsi* (Crocodyliformes, Goniopholidae) and its relationship to other cephalic spaces. *J Vert Paleontol* 28(3, Suppl):144A
- Soares D (2002) An ancient sensory organ in crocodylians. *Nature* 417:241–242. <https://doi.org/10.1038/417241a>
- Starck D (1979) Chapter 1: Cranio-cerebral relations in recent reptiles. In: Gans C, Northcutt RG, Ulinski P (eds) *Biology of the reptilia, Neurology A*, vol 9. Academic, pp 1–38
- Stocker MR, Nesbitt SJ, Criswell KE et al (2016) A dome-headed stem archosaur exemplifies convergence among dinosaurs and their distant relatives. *Curr Biol* 26(19):2674–2680. <https://doi.org/10.1016/j.cub.2016.07.066>
- Storrs GW, Lucas SG, Schoch RM (1983) Endocranial cast of an Early Paleocene crocodylian from the San Juan, New Mexico. *Copeia* 3:842–845. <https://doi.org/10.2307/1444362>
- Trotteyn MJ, Bona P, Barrios F et al (2015) Nuevas evidencias del desarrollo del flóculo en el cerebro de arcosauriformes: variabilidad, implicancias paleobiológicas. Abstract presented at the 5th Congreso Latinoamericano de Paleontología de Vertebrados, Colonia del Sacramento, 21–25 Setember 2015

- Turner AH (2015) A review of *Shamosuchus* and *Paralligator* (Crocodyliformes, Neosuchia) from the Cretaceous of Asia. PLoS One 10(2):e0118116. <https://doi.org/10.1371/journal.pone.0118116>
- Ulinski PS, Dacey DM, Sereno MI (1992) Chapter 4: Optic tectum. In: Gans C, Ulinski PS (eds) Biology of the reptilia, Neurology C, Sensorimotor integration, vol 17. University of Chicago Press, pp 242–366
- Vaage S (1969) The segmentation of the primitive neural tube in chick embryos (*Gallus domesticus*). A morphological, histochemical and autoradiographical investigation. *Ergeb Anat Entwicklungsgesch* 41(3):3–87
- Vieira C, Pombro A, Garcia-Lopez R et al (2010) Molecular mechanisms controlling brain development: an overview of neuroepithelial secondary organizers. *Int J Dev Biol* 54(1):7–20. <https://doi.org/10.1387/ijdb.092853cv>
- von Baczko B, Barrios F, Desojo JB et al (2015) New insights on the development of the flocculus on Pseudosuchia (Archosauria). *Ameghiniana* 52(4, Suppl):41–42
- von Baczko MB, Taborda JR, Desojo JB (2018) Paleoneuroanatomy of the aetosaur *Neoaetosauroides engaeus* (Archosauria: Pseudosuchia) and its paleobiological implications among archosauriforms. *Peer J* 6:e5456. <https://doi.org/10.7717/peerj.5456>
- von Baczko MB, Desojo JB, Gower DJ et al (2021) New digital braincase endocasts of two species of *Desmotosuchus* and neurocranial diversity within Aetosauria (Archosauria: Pseudosuchia). *Anat Rec*. <https://doi.org/10.1002/ar.24798>
- Walker AD (1990) A revision of *Sphenosuchus acutus* Haughton, a crocodylomorph reptile from the Elliot Formation (late Triassic or early Jurassic) South Africa. *Philos Trans R So Lon B* 330(1256):1–120. <https://doi.org/10.1098/rstb.1990.0185>
- Walls GL (1942) The vertebrate eye and its adaptive radiation. Hafner Publishing Company
- Walsh SA, Knoll MA (2011) Directions in palaeoneurology. *Spec Pap Palaeontol* 86:263–279
- Walsh SA, Barrett PM, Milner AC et al (2009) Inner ear anatomy is a proxy for deducing auditory capability and behavior in reptiles and birds. *Proc R Soc B* 276(1660):1355–1360. <https://doi.org/10.1098/rspb.2008.1390>
- Walsh SA, Iwaniuk AN, Knoll MA et al (2013) Avian cerebellar floccular fossa size is not a proxy for flying ability in birds. *PLoS One* 8(6):e67176. <https://doi.org/10.1371/journal.pone.0067176>
- Watanabe A, Gignac PM, Balanoff AM et al (2019) Are endocasts good proxies for brain size and shape in archosaurs throughout ontogeny? *J Anat* 234(3):291–305. <https://doi.org/10.1111/joa.12918>
- Weldon PJ, Ferguson MWJ (1993) Chemoreception in crocodylians: anatomy, natural history and empirical results. *Br Behav Evol* 41(3–5):239–245. <https://doi.org/10.1159/000113845>
- Wenz S (1968) Contribution à l'étude du genre *Metriorhynchus*: crâne et moulage endocranien de *Metriorhynchus superciliosus*. *Ann Paléontol* 54(2):149–183
- Wever EG (1978) The reptile ear. Its structure and function. Princeton University Press
- Wharton DS (2000) An enlarged endocranial venous system in *Steneosaurus pictaviensis* (Crocodylia: Thalattosuchia) from the Upper Jurassic of Les Lourdines, France. *C R Acad, Ser IIA, Earth Planet Sci* 331(3):221–226. [https://doi.org/10.1016/S1251-8050\(00\)01397-5](https://doi.org/10.1016/S1251-8050(00)01397-5)
- Wharton DS (2002) The evolution of the avian brain. Dissertation, University of Bristol
- Whetstone KN, Whybrow PJ (1983) A cursorial crocodylian from the Triassic of Lesotho (Basutoland) Southern Africa. *Occas Pap Mus Nat Hist Univ Kansas* 106:1–37
- Wilberg EW (2015a) What's in an Outgroup? The impact of Outgroup choice on the phylogenetic position of Thalattosuchia (Crocodylomorpha) and the origin of Crocodyliformes. *Syst Biol* 64(4):621–637. <https://doi.org/10.1093/sysbio/syv020>
- Wilberg EW (2015b) A new metriorhynchoid (Crocodylomorpha, Thalattosuchia) from the Middle Jurassic of Oregon and the evolutionary timing of marine adaptations in thalattosuchian crocodylomorphs. *J Vert Paleontol* 35(2):e902846. <https://doi.org/10.1080/02724634.2014.902846>
- Wilberg EW, Turner AH, Brochu CA (2019) Evolutionary structure and timing of major habitat shifts in Crocodylomorpha. *Sci Rep* 9:514. <https://doi.org/10.1038/s41598-018-36795-1>

- Wilberg EW, Beyl AR, Pierce SE et al (2021) Cranial and endocranial anatomy of a three-dimensionally preserved teleosauroid thalattosuchian skull. *Anat Rec.* <https://doi.org/10.1002/ar.24704>
- Witmer LM (2018) Paleoneurology: a sight for four eyes. *Curr Biol* 28(7):R311–R313. <https://doi.org/10.1016/j.cub.2018.02.071>
- Witmer LM, Ridgely RC (2008) The paranasal air sinuses of predatory and armored Dinosaurs (Archosauria: Theropoda and Ankylosauria) and their contribution to cephalic structure. *Anat Rec* 291(11):1362–1388. <https://doi.org/10.1002/ar.20794>
- Witmer LM, Ridgely RC, Dufeu DL et al (2008) Using CT to peer into the past: 3D visualization of the brain and ear regions of birds, crocodiles, and noavian dinosaurs. In: Endo H, Frey R (eds) *Anatomical imaging: towards a new morphology*. Springer, Tokyo, pp 67–88
- Yeh H (1958) A new crocodiles from Maoming Kwangtung. *Vert PalAs* 23(4):237–243
- Young MT, Andrade MB, Etches S et al (2013) A new metriorhynchid crocodylomorph from the Lower Kimmeridge Clay Formation (Late Jurassic) of England, with implications for the evolution of dermatocranium ornamentation in Geosaurini. *Zool J Linnean Soc* 169(4):820–848. <https://doi.org/10.1111/zoj.12082>
- Young MT, Hastings AK, Allain R, Smith TJ (2016) Revision of the enigmatic crocodyliform *Elosuchus felixi* de Lapparent de Broin, 2002 from the Lower–Upper Cretaceous boundary of Niger: potential evidence for an early origin of the clade Dyrosauridae. *Zool J Linn Soc.* <https://doi.org/10.1111/zoj.12452>
- Zelenitsky DK, Therrien F, Kobayashi Y (2009) Olfactory acuity in theropods: palaeontological and evolutionary implications. *Proc R Soc B* 276(1657):667–673. <https://doi.org/10.1098/rspb.2008.1075>

Chapter 8

Paleoneurology of Non-avian Dinosaurs: An Overview



Ariana Paulina-Carabajal, Mario Bronzati, and Penélope Cruzado-Caballero

8.1 Phylogenetic Context

Dinosaurs are reptile members of the clade Archosauria, which has living representatives in birds (descendants of theropod dinosaurs known as ‘avian dinosaurs’) and crocodylians. The clade Dinosauria Owen 1842, is a diverse group originated probably during the Early to Middle Triassic, around 243–231 million years ago, with the oldest dinosaur skeletons known from Carnian rocks of South America (e.g. Brusatte et al. 2010b; Benton 2004; Langer et al. 2010). Rapidly after their appearance, non-avian dinosaurs (hereafter ‘dinosaurs’) become the dominant vertebrates in all terrestrial ecosystems worldwide probably by the end of the Triassic to the Early Jurassic -about 210 million years (My) ago- when major clades were diversified (Brusatte 2012). The group (except for the avian theropods) became extinct at the end of the Cretaceous, approximately 65 My ago.

Dinosaurs were tiny to extremely large bodied bipedal and quadrupedal animals that occupied a wide range of continental niches, developing a wide spectrum of dietary, sensory and habitat adaptations. Traditionally, the clade Dinosauria was

A. Paulina-Carabajal (✉)
Instituto de Investigaciones en Biodiversidad y Medioambiente,
CONICET-Universidad Nacional del Comahue, San Carlos de Bariloche, Argentina
e-mail: a.paulinacarabajal@conicet.gov.ar

M. Bronzati
Department of Biology, Faculty of Philosophy, Sciences and Letters at Ribeirão Preto,
University of São Paulo, São Paulo, Brazil
e-mail: mariobronzati@usp.br

P. Cruzado-Caballero
Paleontology Area, Department of Animal Biology, Edaphology and Geology, University of
La Laguna, Santa Cruz de Tenerife, Spain
e-mail: pcruzado@ull.edu.es

broadly divided into Saurischia and Ornithischia on the basis of a single characteristic: the configuration of the hip (pelvis) structure (Seeley 1887). The dinosaur pelvis consists of three bones: ilium, ischium, and pubis. Saurischia were those dinosaurs with a more lizard-like hip, while Ornithischia had a more bird-like hip with the pubis pointing backwards and parallel to the ischium (living birds ironically descending from the lizard-like hip clade, Saurischia). The most recent phylogenetic definition (Langer et al. 2020) states that Dinosauria consists of the smallest clade containing *Iguanodon bernissartensis* Boulenger in Bedden 1881 (Ornithischia/Euornithopoda), *Megalosaurus bucklandii* Mantell 1827 (Theropoda/Megalosauroidae), and *Cetiosaurus oxoniensis* Philips 1871 (Sauropodomorpha) (Fig. 8.1). A recent phylogenetic analysis revived the term used by Huxley (1870) to refer to the ‘bird-footed’ dinosaurs: the clade Ornithoscelida. This hypothesis places theropods more closely related to the ornithischians than to Sauropodomorpha (see Baron et al. 2017), and has been questioned by many researchers (e.g. Langer et al. 2017). We follow here the traditional classification of Dinosauria.

8.1.1 Saurischia Seeley 1887

Saurischia comprises birds and all dinosaurs more closely related to them than to the ornithischians. The latest phylogenetic definition of Saurischia states that is the largest clade containing *Allosaurus fragilis* Marsh 1877 (Theropoda/Carnosauria) and *Camarasaurus supremus* Cope 1877 (Sauropodomorpha), but not *Stegosaurus stenops* Marsh 1887 (Ornithischia/Stegosauridae; Gauthier et al. 2020). In the most classic definitions, the clade includes sauropodomorphs and theropods (Eusaurischia), two main groups of dinosaurs that split early during the Mesozoic, probably during the Carnian (Late Triassic), about 230 My ago. Additional saurischians from South and North America such as herrerasaurids and *Tawa hallae*, have either being considered as theropods or as non-eusaurischians in different phylogenetic studies (e.g. see Ezcurra 2010; Langer 2014; and discussion therein). All of the oldest known dinosaurs are saurischians, and they were small sized, bipedal and probably carnivorous animals (Cabreira et al. 2016). Fossils of sauropodomorphs, theropods and ornithopods have been found in every continent, including Antarctica (e.g. Hammer and Hickerson 1994; Cerda et al. 2011).

Theropoda Marsh 1881

This clade includes dinosaurs closest to birds than to sauropodomorphs and ornithischians, characterized by pneumatized bones. The latest phylogenetic definition states that this group is largest clade containing *Allosaurus fragilis* Marsh 1877 (Theropoda) but neither *Plateosaurus engelhardti* Meyer 1837 (Sauropodomorpha) nor *Heterodontosaurus tucki* Crompton and Charig 1962 (Ornithischia). The oldest neotheropods are known from the early Norian (Late Triassic) of North America, whereas the rest of the Triassic species were found in South America, Europe and

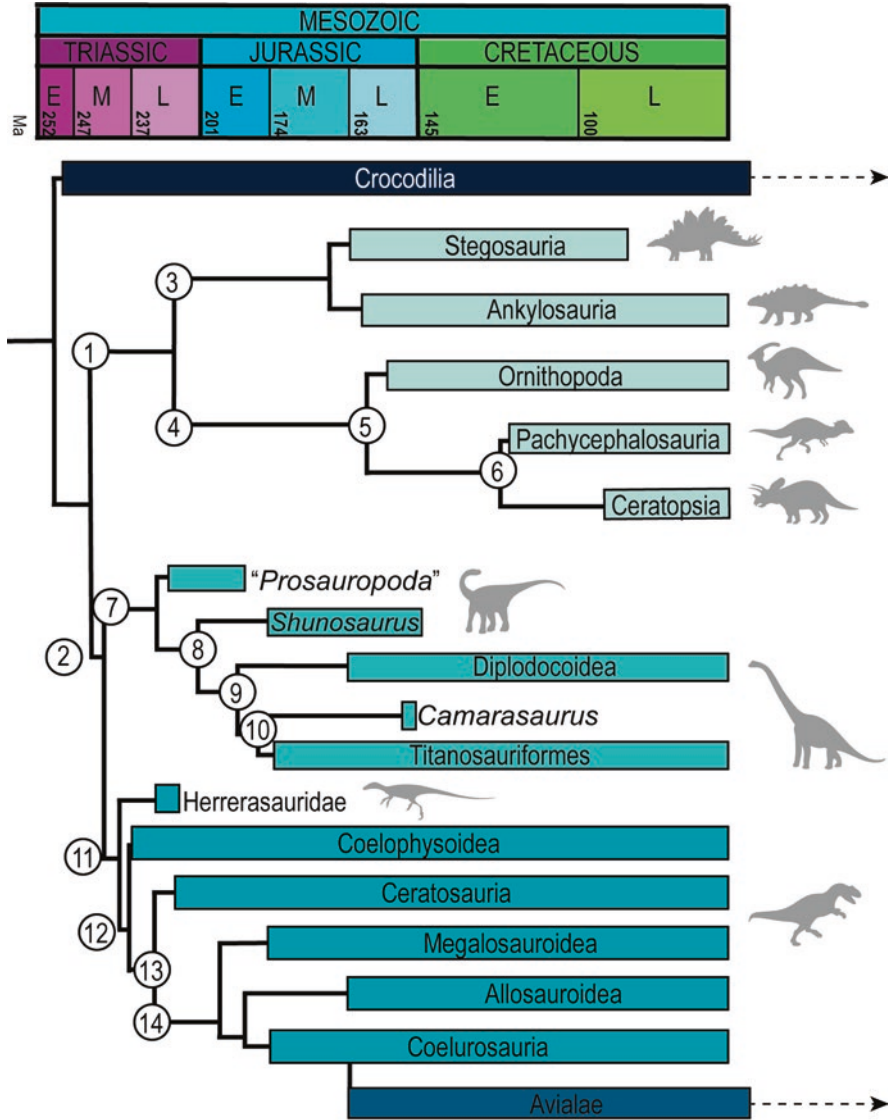


Fig. 8.1 Simplified calibrated cladogram of Dinosauria. The circles indicate the following nodes and clades: (1), Ornithischia; (2), Saurischia; (3), Tyrerophora; (4), Neornithischia; (5), Cerapoda; (6), Marginocephalia; (7), Sauropodomorpha (the term “Prosauropoda” is here used to refer to the paraphyletic assemblage of taxa known as prosauropods); (8), Eusauropoda; (9), Neosauropoda; (10), Macronaria; (11), Theropoda (note that the inclusion of Herrerasauridae within this clade have been largely discussed, being also proposed as a basal Saurischia); (12), Neotheropoda; (13), Averostra; (14), Tetanurae; (15), Maniraptora. (Based on Sampson 2011)

India (e.g. Nesbitt and Ezcurra 2015). Theropods radiate in two main lineages, Ceratosauria and Tetanurae, the last being the most diverse group of saurischians (e.g. Carrano et al. 2012; Ezcurra 2010). Primitively, theropods were bipedal non-specialized faunivorous dinosaurs. Later during the Mesozoic, they developed, however, different skull morphological features which can be related to dietary adaptations to insectivory (e.g. alvarezsauridae; Senter 2005; Holtz Jr 2018), piscivory (e.g. spinosaurids; Charig and Milner 1997; Sereno et al. 1998), and herbivory (e.g. therizinosaurs; Lautenschlager 2014). The largest members among theropods were found in Cretaceous formations, represented by spinosaurids, carcharodontosaurids and tyrannosaurids. These taxa could reach 14–9 m in length, and could weigh 10–20 tons, a marked phenotypic divergence from the 10–30 kg Triassic ancestors (e.g. Benson et al. 2014, 2018). Non-avian theropods (from now on ‘theropods’ in this chapter) disappear along with other dinosaurs during the Cretaceous-Paleogene extinction.

Sauropodomorpha von Huene 1932

Sauropodomorpha is defined as the largest clade containing *Saltasaurus loricatus* Bonaparte and Powell 1980 (Sauropodomorpha) but not *Allosaurus fragilis* Marsh 1877 (Theropoda), and *Iguanodon bernissartensis* Boulenger in Beneden 1881 (Ornithischia) (Fabbri et al. 2020). This group includes the largest animals to ever walk on Earth, the gigantic sauropods. They might represent the best example of a dinosaur that most people have in their mind: a quadrupedal animal with a long neck, long tail, and a relatively small skull (Rauhut et al. 2011). The biggest of these animals could reach 35–40 m in length and 60–95 tons in weight (e.g. Carballido et al. 2017; Benson et al. 2018). The fossil record indicates that sauropods were the most abundant large herbivorous animals during the Late Jurassic (around 150 My) until the Cretaceous/Paleogene extinction (Upchurch et al. 2004). During the last twenty-five years, an incredible diversity of sauropodomorphs were discovered from Late Triassic (c. 235–230 My) rocks from Brazil and Argentina. These represent not only the oldest sauropodomorphs, but actually the oldest dinosaurs to ever live. Unlike their gigantic relatives, the first sauropodomorphs were small animals, around c. 1.5 m in length and weighing less than 20 kg (Sereno 1999; Benson et al. 2017), and with either a faunivorous or omnivorous diet (Cabreira et al. 2016; Bronzati et al. 2017). Despite the extreme differences between sauropods and the first Triassic sauropodomorphs, the evolution of the conspicuous sauropod body plan can be traced in the fossil record. Anatomical modifications of the skeleton occurred in an apparently stepwise fashion, as evidenced by the Late Triassic and Early Jurassic fossil record of an assemblage of taxa classically known as ‘prosauropods’, which include all non-sauropodan sauropodomorphs with the exception of the oldest South American taxa (Bronzati 2017). There is not a consensual phylogenetic definition for Sauropoda Marsh 1878 (Peyre de Fabregues et al. 2015). One popular definition of Sauropoda considers the clade to comprise most inclusive group containing *Vulcanodon*, Eusauropoda and all their descendants (Salgado et al. 1997), whereas another definition regards the clade as including all sauropodomorphs more closely related to

Saltasaurus than to *Melanorosaurus* (Yates 2007). There are no paleoneurology studies on basal eusauropods yet. The main groups within Neosauropoda include Diplodocoidea (Rebbachisaurida, Dicraeosaurida and Diplodocidae) and Macronaria (*Camarasaurus* and Titanosauriformes).

8.1.2 *Ornithischia* Seeley 1888

The latest phylogenetic definition states that Ornithischia is the largest clade containing *Iguanodon bernissartensis* Boulenger in Beneden 1881 but not *Allosaurus fragilis* Marsh 1877a, and *Camarasaurus supremus* Cope 1877, this being a maximum-clade definition (Madzia et al. 2021). The ornithischian group includes a great variety of clades that have in common an ‘opisthopubic’ pelvis, the presence of a palpebral bone, reduction or full closure of the antorbital fenestra, a predentary—which is an unpaired scoop-shaped bone located in the front of the lower jaws—, lack of premaxillary teeth, and a jaw articulation lower than the level of the teeth (probably important for braincase form and crucial for the advanced masticatory adaptations in this group) (Butler et al. 2008; Fastovsky and Weishampel 2016; and references therein). This group has a global distribution and is divided in two sub-orders: Thyreophora with the infraorders Stegosauria and Ankylosauria, and Neornithischia that includes Cerapoda, with the clades Marginocephalia (subdivided into the infraorders Pachycephalosauria and Ceratopsia), and Ornithopoda (see Weishampel et al. 2004; Fig. 8.1). The evolutionary history told by the fossil record shows that during more than 130 My ornithischian dinosaurs developed great taxonomic diversity. The different groups exhibit morphological disparity particularly in their cranial characteristics, accompanying the development of a complex chewing apparatus that reached its maximum efficiency in the hadrosaurid clade (Fastovsky and Weishampel 2016; Madzia et al. 2021).

The moment when the ornithischian clade appeared is not clear, but seems to have happened during the late Triassic (e.g. Desojo et al. 2020; Müller and Garcia 2020) or the earliest Jurassic (Baron 2019), and they became extinct during the Cretaceous/Paleogene extinction along with most other groups of saurischian dinosaurs (Weishampel et al. 2004). Basal ornithischians have a poor fossil record, obscuring our knowledge about their origins and phylogenetic relationships with saurischian and silesaurid dinosaurs (see references in Dieudonné et al. 2020). During the last decade, new phylogenies have been proposed, but the interrelationships between the basal forms remain poorly resolved (Dieudonné et al. 2020; Madzia et al. 2021).

Thyreophora Nopcsa 1915

This clade is defined as the group containing *Ankylosaurus magniventris* Brown 1908 and *Stegosaurus stenops* Marsh 1887, but not *Iguanodon bernissartensis* Boulenger in Beneden 1881 and *Triceratops horridus* Marsh 1889 (see Madzia

et al. 2021). The clade radiated in two main lineages, Ankylosauria and Stegosauria, which were small to mid-body sized animals that may have reached a maximum length of about 10 m in some species, and become extinct at the end of the Cretaceous (Norman et al. 2004b; Weishampel et al. 2004). Stegosauria and ankylosauria were herbivorous dinosaurs with dorsal dermal armor. Their basal forms were bipedal but the derived Cretaceous forms were quadrupedal and exhibited a complex chewing mechanism (Breedon III et al. 2021). The most basal thyreophorans are from the Hettangian-Sinemurian (Early Jurassic) of North America, and have an extremely poor fossil record. Ankylosauria are known from the Middle Jurassic and are quadrupedal herbivorous dinosaurs with an armor of osteoderms and smaller ossicles covering the entire body from the head to the tail, with the presence in the most derived ankylosaurid family of a heavy club-tail (Vickaryous et al. 2004; Arbour and Currie 2016). In turn, stegosauria are quadrupedal animals with two rows of bony plates and spines extending from the neck to the end of the tail (Galton and Upchurch 2004; Arbour and Currie 2016).

Neornithischia Cooper 1985

Neornithischia is defined as the group containing *Iguanodon bernissartensis* Boulenger in Beneden 1881 and *Triceratops horridus* Marsh 1889, but not *Ankylosaurus magniventris* Brown 1908 and *Stegosaurus stenops* Marsh 1887 (Madzia et al. 2021). The fossil record of this clade extends from the Middle Jurassic to the end of the Cretaceous, with a worldwide distribution, and included Ceratopsia, Pachycephalosauria and Iguanodontia (Boyd 2015; Dieudonné et al. 2020).

Basal ornithischians were small to mid-sized bipedal animals, which lack the osteological ornamentation (e.g. *Triceratops* horns) typical of more derived groups (Norman et al. 2004a). Members of this group were bipedal and quadrupedal herbivorous dinosaurs that became very common during the Cretaceous, particularly in the Northern Hemisphere (Fastovsky and Weishampel 2016)

8.2 Historical Background

8.2.1 Brief Summary of the History of Dinosaur Paleoneurology

Brains vs. Spinal Cord

The focus of this review will be on the Central Nervous System (CNS) of dinosaurs, but particularly in the morphology and function of the brain, mainly because it is the most informative structure. In comparison, aspects on the anatomy of the spinal cord morphology have been poorly documented, with the earliest studies corresponding mostly to sauropod sacral casts made for *Apatosaurus* and *Camarasaurus*

by Marsh (1896), and *Barosaurus* and *Dicraeosaurus* by Janensch (1939), followed by fewer studies based on the ornithopod *Camptosaurus* (Marsh 1896) and the stegosaurs *Stegosaurus* (Marsh 1881) and *Kentrosaurus* (Janensch 1939). In both sauropods and ornithischians (but particularly in stegosaurs), the sacral casts exhibited expansions, which led to the old idea of the presence of a ‘sacral brain’ or a ‘second brain’ in these groups (e.g. Marsh 1881; Lull 1917). However, posterior calculations of the Spinal Quotient, which estimates the enlargement of the spinal cord at the inter-limb level, did not support at the end the presence of a ‘sacral brain’ in dinosaurs (Giffin 1990; see Buchholtz 2012 for a broader historical review of this topic). Most recent analyses focused on the expanded neural canals observed in caudal vertebrae of certain groups of sauropods. These dilatations are now interpreted as osteological correlates of expansions of the spinal cord, in this case, related with a high degree of innervation necessary for the large muscle groups of the pelvis and tail in these giant dinosaurs (Atterholt and Wedel 2019; Wedel et al. 2021).

Other tangentially related aspects to paleoneurology, such as the sensory biology in dinosaurs (e.g. vision, olfaction or hearing, among others) have been explored in other recent works (e.g. Rogers 2005; Ali et al. 2008; Zelenitsky et al. 2009, 2011; Schmitz and Motani 2011; Brusatte 2012; Choiniere et al. 2021; Paulina-Carabajal et al. [in press](#)) and will not be expanded here.

Early Studies and Current State of Knowledge of Dinosaur Paleoneurology

Dinosaur paleoneurology has a long history that goes back to more than 150 years ago. It was during the late 1800s when John W. Hulke made the first description of a dinosaur endocranial cavity, identifying impressions left by different regions of the brain on the internal surfaces of the braincase bones (Hulke 1871; Fig. 8.2a). This braincase belonged to *Iguanodon*, an ornithopod dinosaur, which was reanalyzed more than 20 years later by Andrews (1897), using this time a physical endocast. But this was not the first endocast ever created for a dinosaur. It was Othniel C. Marsh, the pioneer of dinosaur paleoneurology (see Edinger 1975 for a complete list of his work), who published the first dinosaur brain-cast in 1880 (Fig. 8.2b), comparing it with a living crocodile brain. Marsh described and illustrated the endocranial cavities and cranial endocasts of at least eight species of dinosaurs, including sauropods (e.g. *Camarasaurus*, *Diplodocus*), theropods (e.g. *Ceratosaurus*), thyreophorans (e.g. *Stegosaurus*), marginocephalians (e.g. *Triceratops*) and ornithopods (e.g. *Camptosaurus*, *Hadrosaurus*) from North America (Marsh 1880, 1881, 1884a, b, 1889, 1890, 1891, 1893, 1894, 1896; Table 8.1). Other early studies that followed Marsh’s work included aspects of the endocranial anatomy of the sauropods *Camarasaurus* (Fig. 8.2e), *Dicraeosaurus*, *Giraffatitan* (= *Brachiosaurus*) and *Tornieria* (= *Barosaurus*), the ornithischians *Edmontosaurus* and *Kentrosaurus*, and the theropods *Tyrannosaurus* (Fig. 8.2d) and “*Stenonychosaurus*” (= *Troodon*?), among others (e.g. Bürckhardt 1892; Osborn 1912; Brown 1914; Lambe 1920; Hennig 1925; Janensch 1935–1936; Lull and Wright 1942; Osborn and Mook 1921;

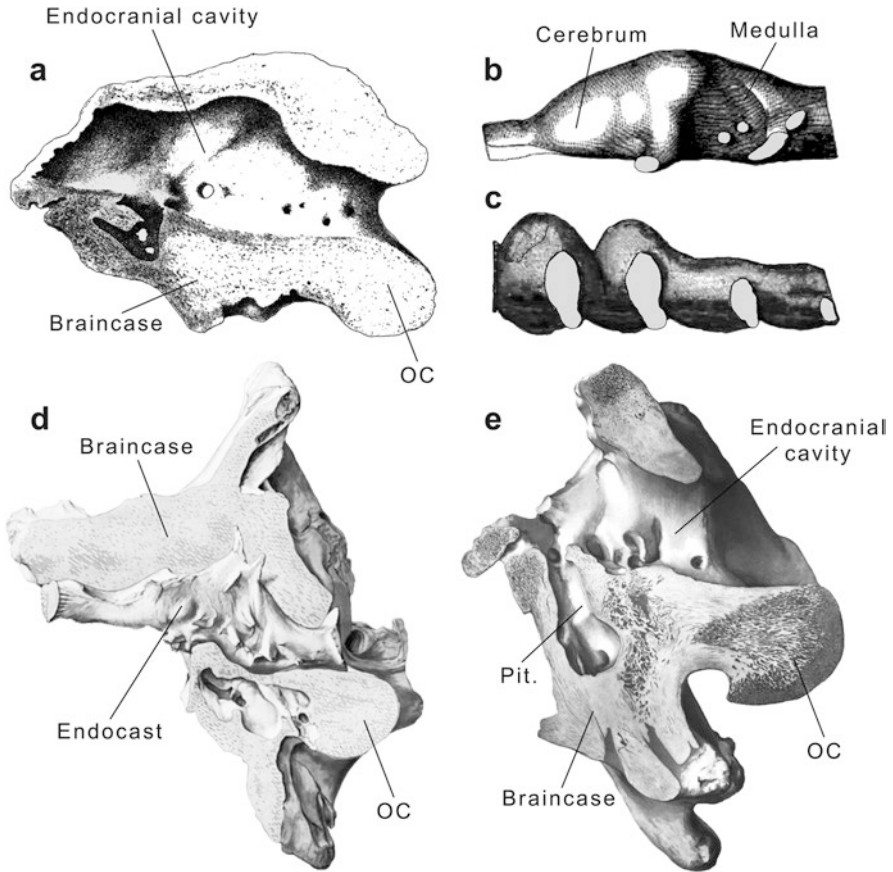


Fig. 8.2 Earliest described dinosaur endocranial cavities and endocasts in left lateral views. (a), *Iguanodon* endocranial cavity (from Hulke 1871); (b), oldest dinosaur endocast, *Stegosaurus* (from Marsh 1880); (c), sacral endocast of a sauropod (from Marsh 1896); (d), *Tyrannosaurus* sagittally sectioned braincase showing the cranial endocast inside (from Osborn 1912); (e), *Camarasaurus* sagittally sectioned braincase showing features of the endocranial cavity (from Osborn and Mook 1921). Not to scale

Ostrom 1961; Russell 1969; Table 8.1). The studies of cranial endocasts continued more or less sporadically during the first half of the twentieth century, but it was the outstanding work of Otilie ‘Tilly’ Edinger (known today as the ‘mother’ of paleoneurology), Harry J. Jerison (who developed the Encephalization Quotient as a method to assess relative brain size in vertebrates), and James A. Hopson (author of the chapter “Paleoneurology” for the book *The Reptilia*, Gans 1979) that created the bases of this science (see Jerison 1973; Hopson 1979; Buchholtz and Seyfarth 2001; and Buchholtz 2012 for a detailed historical review).

Up to today the endocranial anatomy –based mainly on three dimensional endocast descriptions– of nearly 150 taxa at genus or species level have been described

Table 8.1 List of dinosaur taxa with known endocranial anatomy

Taxon	Age	Proc	Cast	ie	Source
ORNITHISCHIA					
Ornithopoda					
<i>Amurosaurus riabinini</i>	K	As	A	–	Saveliev et al. (2012) and Lauters et al. (2013)
<i>Arenysaurus ardevoli</i>	K	Eu	D	✓	Cruzado Caballero et al. (2015)
<i>Bactrosaurus johnstoni</i>	K	As	A	–	Langston Jr (1960)
<i>Batyrosaurus rozhdestvenskyi</i>	K	As	A	✓	Godefroit et al. (2012)
<i>Camptosaurus</i> sp.	J	NA	A	–	Marsh (1896)
<i>Corythosaurus</i> sp.	K	NA	D	✓	Ostrom (1961), Evans (2006), Evans et al. (2009)
<i>Dryosaurus altus</i>	J	NA	A	✓	Galton (1989)
<i>Dysalotosaurus lettowvorbecki</i>	J	Af	AD	✓	Galton (1989), Lautenschlager and Hübner (2013*)
<i>Edmontosaurus annectens</i>	K	NA			Lull and Wright (1942) (=Anatosaurus)
<i>Edmontosaurus regalis</i> .	K	NA	A	✓	Lambe (1920), Ostrom (1961)
<i>Edmontosaurus</i> sp.	K	NA	A	–	Brown (1914) (=Trachodon, Anatosaurus in Ostrom (1961) and Lambe (1920)
<i>Gryposaurus notabilis</i>	K	NA	A	–	Ostrom (1961) (=Kritosaurus), Hopson (1979)
<i>Hadrosaurus agilis</i>	K	NA	A	–	Marsh (1893, 1896) (=Claosaurus)
<i>Hypacrosaurus altispinus</i>	K	NA	D	✓	Evans et al. (2009)
<i>Hypsilophodon foxii</i>	K	Eu	A	✓	Galton (1989)
<i>Iguanodon bernissartensis</i>	K	Eu+	D	–	Lauters et al. (2012)
<i>Iguanodon</i> sp.	K	Eu+	A	✓	Hulke (1871), Andrews (1897), Norman and Weishampel (1990), Norman et al. (2004a)
Iguanodontidae indet.	K	Eu+	N	–	Serrano-Brañas et al. (2006), Brasier et al. (2016)
<i>Kritosaurus notabilis</i>	K	NA	A	–	Hopson (1979)
<i>Lambeosaurus</i> sp.	K	NA	D	✓	Evans et al. (2009)
<i>Leaellysauro amica</i>	K	Au	N	–	Rich and Rich (1989), Galton (1989)
<i>Lophorhynchon atopus</i>	K	NA	A	✓	Langston Jr (1960)
<i>Mantellisaurus atherfieldensis</i>	K	Eu	D	–	Lauters et al. (2012)
<i>Parasaurolophus</i> sp.	K	NA	D	✓	Farke et al. (2013)
<i>Proa valdearinnoensis</i>	K	Eu	D	✓	Knoll et al. (2021)
<i>Secernosaurus koernerii</i>	K	SA	D	✓	Becerra et al. (2018)
<i>Sirindhorna khoratensis</i>	K	As	D	–	Shibata et al. (2016) (abstract)
<i>Tenontosaurus tilletti</i>	K	NA	AD	✓	Thomas (2015), Galton (1989)
<i>Thescelosaurus neglectus</i>	K	NA	A	✓	Galton (1989)

(continued)

Table 8.1 (continued)

Taxon	Age	Proc	Cast	ie	Source
<i>Tsintaosaurus spinorhinus</i>	K	As	A	–	Young (1958)
<i>Zephyrosaurus schaffi</i>	K	NA	A	✓	Galton (1989)
Ankylosauria					
<i>Bissektipelta archibaldi</i>	K	As	A	–	Alifanov and Saveliev (2019), Kuzmin et al. (2020)
<i>Cedarpelta bibleyhallorum</i>	K	NA	A	–	Carpenter et al. (2001)
<i>Euoplocephalus tutus</i>	K	NA	AD	✓	Coombs (1978), Hopson (1979), Miyashita et al. (2011)
<i>Hungarosaurus tormai</i>	K	Eu	A	–	Ösi et al. (2014)
<i>Kunbarrasaurus ieverisi nodosaurid indet</i>	K	Au	D	✓	Leahey et al. (2015)
<i>nodosaurid indet</i>	K	As	A	–	Hawakaya et al. (2005)
<i>Panoplosaurus minus</i>	K	NA	D	–	Witmer and Ridgely (2008a)
<i>Pawpawsaurus campbelli</i>	K	NA	D	✓	Paulina-Carabajal et al. (2016b)
<i>Polacanthus foxii</i>	K	Eu	A	–	Norman and Faiers (1996)
<i>Silvisaurus condrayi</i>	K	NA	N?	–	Eaton (1960)
<i>Struthiosaurus austriacus</i>	K	Eu	A	–	Pereda-Suberbiola and Galton (1994)
<i>Struthiosaurus transylvanicus</i>	K	Eu	A	–	Nopcsa (1929), Pereda-Suberbiola and Galton (1994)
<i>Talarurus plicatospineus</i>	K	As	D	–	Kurzanov and Tumanova (1978), Paulina-Carabajal et al. (2018b)
<i>Tarchia gigantea</i>	K	As	D	✓	Tumanova (1987), Paulina-Carabajal et al. (2018b)
Stegosauria					
<i>Kentrosaurus aethiopicus</i>	J	Af	A	✓	Hennig (1925), Galton (1988, 2001)
<i>Stegosaurus armatus</i>	J	NA	A	–	Gilmore (1914)
<i>Stegosaurus stenops</i>	J	NA	A	✓	Marsh (in Ostrom and McIntosh 1966), Galton (2001), Leahey et al. (2015)
<i>Stegosaurus unglulatus</i>	J	NA	A	–	Marsh (1880, 1890, 1881, 1891, 1896), Galton (2001)
Ceratopsia					
<i>Anchiceratops ornatus</i>	K	NA	N/A	✓	Brown (1914), Hopson (1979)
<i>Auroraceratops</i>	K	As	D	–	Zhang et al. (2019)
<i>Pachyrhinosaurus canadensis</i>	K	NA	A	–	Langston Jr (1975)
<i>Pachyrhinosaurus lakustai</i>	K	NA	D	✓	Witmer and Ridgely (2008b)
<i>Pachyrhinosaurus perotorum</i>	K	NA	D	✓	Tykoski and Fiorillo (2012)
<i>Protoceratops grangeri</i>	K	As	A	✓	Brown and Schlaikjer (1940), Hopson (1979)

(continued)

Table 8.1 (continued)

Taxon	Age	Proc	Cast	ie	Source
<i>Psittacosaurus amitabha</i>	K	As	D	✓	Napoli et al. (2019)
<i>Psittacosaurus lujiatunensis</i>	K	As	D	✓	Zhou et al. (2007), Bullar et al. (2019), King (2021)
<i>Triceratops horridus</i>	K	NA	A	–	Marsh (1889, 1890, 1891, 1896), Hay (1909), Forster (1996)
<i>Triceratops prorsus</i>	K	NA	A	–	Marsh (1896)
<i>Triceratops</i> sp.	K	NA	D	✓	Sakagami and Kawabe (2020)
Pachycephalosauria					
<i>Gravitholus albertae</i>	K	NA	A	–	Giffin (1989) (=Setegoceras?)
<i>Pachycephalosaurius wyomingensis</i>	K	NA	A	✓	Brown and Schlaikjer (1943) (=P. grangeri), Hopson (1979), Giffin (1989)
<i>Sphaerolitholus edmontonensis</i>	K	NA	D	✓	Bourke et al. (2014) (suppl info at WitmerLab site)
<i>Stegoceras validus</i>	K	NA	AD	✓	Lambe (1918), Maryanska and Osmólska (1974), Hopson (1979), Giffin (1989), Bourke et al. (2014)
<i>Stenolitholus kohleri</i>	K	NA	A	–	Giffin et al. (1987), Giffin (1989)
SAURISCHIA					
<i>Gnathovorax cabreira</i>	T	SA	D	✓	Pacheco et al. (2019)
Basal Sauropodomorpha					
<i>Buriolestes schultzi</i>	T	SA	D	✓	Müller et al. (2021)
<i>Macrocollum itaquii</i>	T	SA	D	✓	Müller et al. (2021)
<i>Massospondylus carinatus</i>	J	Af	D	✓	Sereno et al. (2007)
<i>Plateosaurus</i> sp.	T	Eu	AD	✓	Galton (1985), Bronzati et al. (2017*)
<i>Saturnalia tupiniquim</i>	T	SA	D	✓	Bronzati et al. (2017)
<i>Thecodontosaurus antiquus</i>	T	SA	D	✓	Ballell et al. (2021), King (2021)
Riojasaurid indet.	T	SA	D	✓	Paulina-Carabajal et al. (2019a) (abstract)
Eusauropoda					
<i>Amargasaurus cazau</i>	K	SA	D	✓	Paulina-Carabajal et al. (2014)
<i>Antarctosaurus wichmannianus</i>	K	SA	D	✓	von Huene and Matley (1933), Paulina-Carabajal (2012)
<i>Apatosaurus ajax</i>	J	NA	D	–	Balanoff et al. (2010)
“ <i>Barosaurus africanus</i> ”	J	Af	A	–	Janensch (1935–1936) (=Tornieria)
<i>Bonitan reigi</i>	K	SA	D	✓	Paulina-Carabajal (2012)
<i>Camarasaurus grandis</i>	J	NA	AD	✓	Marsh (1880), Osborn and Mook (1921), Zheng (1996), Chatterjee and Zheng (2005); Witmer et al. (2008*), Knoll et al. (2015a, b*)
<i>Cetiosaurus</i> cf.	J	Eu	AD	✓	von Huene (1906), Galton and Knoll (2006), Bronzati et al. (2017*)
<i>Diamantisaurus matildae</i>	K	Au	D	✓	Poropat et al. (2016)

(continued)

Table 8.1 (continued)

Taxon	Age	Proc	Cast	ie	Source
<i>Dicraeosaurus hansemanii</i>	J	Af	A	–	Janensch (1935–1936)
<i>Diplodocus longus</i>	J	NA	AD	✓	Marsh (1884a), (1896), Osborn (1912), Hopson (1979), Witmer et al. (2008)*
<i>Europasaurus hogeri</i>	J	Eu	–	–	Schmitt et al. (2015) (abstract)
<i>Galeamopus pabsti</i>	J	NA	D	✓	Franzosa (2004) (= <i>Diplodocus hayi</i>)
<i>Giraffatitan brancai</i>	J	Af	D	✓	Janensch (1935–1936), Clarke (2005), Knoll and Schwarz-Wings (2009) (= <i>Brachiosaurus</i>)
<i>Jainosaurus septentrionalis</i>	K	Eu	AD	✓	von Huene and Matley (1933), Wilson et al. (2009), Knoll et al. (2012*)
<i>Limaysaurus tessonei</i>	K	SA	D	✓	Paulina-Carabajal and Calvo (2021)
<i>Lohuecotitan pandaflandi</i>	K	Eu	D	✓	Knoll et al. (2013, 2019) (= <i>Ampelosaurus</i>)
<i>Malawisaurus dixeyi</i>	K	Af	D	✓	Andrzejewski et al. (2019)
<i>Narambuenatitan</i>	K	SA	D	✓	Paulina-Carabajal et al. (2020)
<i>Nigersaurus taqueti</i>	K	Af	D	✓	Sereno et al. (2007)
<i>Saltasaurus loricatus</i>	K	SA	A	–	Powell (2003), Paulina-Carabajal (2012)
<i>Sarmientosaurus musacchioi</i>	K	SA	D	✓	Martínez et al. (2016)
<i>Shunosaurus lii</i>	J	As	A		Zheng (1996), Chatterjee and Zheng (2002)
<i>Spinophorosaurus nigrensis</i>	J	Af	D	✓	Knoll et al. (2012)
<i>Suuwassee emilieae</i>	J	NA	–	–	Knoll et al. 2015a, b (abstract)
Dicraeosauridae indet.	K	SA	N	–	Paulina-Carabajal et al. (2018a)
Rebbachisauridae indet.	K	SA	A	✓	Paulina-Carabajal et al. (2016a)
Titanosauria indet.	K		D	✓	Sues et al. (2015)
Titanosauria indet.	K	SA	A	✓	Paulina-Carabajal et al. (2008)
Titanosauria indet.	K	Eu	D	✓	Knoll et al. (2015a, b)
Titanosauria indet.	K	SA	A	✓	Paulina-Carabajal (2012), Paulina-Carabajal and Salgado (2007)
Titanosauria indet.	K	Eu	D	✓	Knoll et al. (2019)
Theropoda					
<i>Acrocanthosaurus atokensis</i>	K	NA	D	✓	Franzosa (2004), Franzosa and Rowe (2005)
<i>Ajancingenia yanshini</i>	K	As	A	–	Osmólska (2004) (= <i>Ingenia</i>)
<i>Alioramus altai</i>	K	As	D	✓	Bever et al. (2013)
<i>Allosaurus fragilis</i>	J	NA	AD	✓	Hopson (1979) (natural), Rogers (1999) (digital)*, Franzosa (2004)
<i>Arcovenator escotae</i>	K	Eu	D	–	Beyrand et al. (2019)
<i>Aucasaurus garridoi</i>	K	SA	D	✓	Paulina-Carabajal and Succar (2015)
<i>Bambiraptor feinbergi</i>	K	NA	D	–	Burnham (2004)
<i>Bistahieversor sealeyi</i>	K	NA	D	✓	Mckeown et al. (2020)
<i>Byronosaurus jaffei</i>	K	As	D	–	Franzosa (2004)

(continued)

Table 8.1 (continued)

Taxon	Age	Proc	Cast	ie	Source
<i>Carcharodontosaurus</i>	K	NA	A	✓	Stromer (1931), Larsson (2001)
<i>Carnotaurus sastrei</i>	K	NA	D	✓	Cerroni and Paulina-Carabajal (2019)
<i>Ceratomykus oculus</i>	K	As	N	–	Alifanov and Barsbold (2009), Alifanov and Saveliev (2011)
<i>Ceratosaurus nasicronis</i>	J	NA	D	✓	Marsh (1884b), Franzosa (2004), Sanders and Smith (2005)
<i>Citipati osmolskai</i>	K	As	D	✓	Franzosa (2004), Balanoff et al. (2013, 2018)
<i>Conchoraptor gracilis</i>	K	As	D	–	Kundrát (2007), Balanoff et al. (2014)
<i>Daspletosaurus</i> sp.	K	NA	D	✓	Paulina-Carabajal et al. (2021)
<i>Daspletosaurus torosus</i>	K	NA	D	✓	Paulina-Carabajal et al. (2021)
<i>Deinonychus antirrhopus</i>	K	NA	D	✓	Witmer and Ridgely (2009)
<i>Dilong paradoxus</i>	K	As	D	✓	Kundrát et al. (2018)
<i>Dromiceiomimus breviterius</i>	K	NA	A	–	Russell (1972), Hopson (1979)
<i>Erlikosaurus andrewsi</i>	K	As	D	✓	Lautenschlager et al. (2012)
<i>Falcarius utahensis</i>	K	NA	D	✓	Lautenschlager et al. (2012)
<i>Fukuivenator paradoxus</i>	K	As	D	✓	Azuma et al. (2016) (only inner ear)
<i>Giganotosaurus carolinii</i>	K	SA	AD	✓	Paulina-Carabajal and Canale (2010); Paulina-Carabajal and Nieto (2019)
<i>Gorgosaurus libratus</i>	K	NA	D	✓	Witmer and Ridgely (2009)
<i>Halszkaraptor escuillei</i>	K	As	D	–	Beyrand et al. (2019)
<i>Incisivosaurus gauthieri</i>	K	As	D	✓	Balanoff et al. (2009)
<i>Indosaurus matleyi</i>	K	As	A	–	von Huene and Matley (1933)
<i>Iemirus medullaris</i>	K	As	EC	–	Kurzanov (1976)
<i>Irritator challengeri</i>	K	SA	D	✓	Schade et al. (2020)
<i>Khaan mckennai</i>	K	As	D	–	Balanoff et al. (2018)
<i>Llukalkan aliocranianus</i>	K	SA	D	✓	Gianechini et al. (2021)
<i>Majungasaurus crenatissimus</i>	K	Af	D	✓	Sampson and Witmer (2007)
<i>Megapnosaurus rhodesiensis</i>	J	Af	A	–	Raath (1977) (=Syntarsus)
<i>Megaraptor namunhuaiquii</i>	K	SA	D	✓	Paulina-Carabajal and Porfiri (2018) (abstract)
<i>Musraptor barrosaensis</i>	K	SA	D	✓	Paulina-Carabajal and Currie (2017)
<i>Nanotyrannus</i> sp.	K	SA	D	✓	Witmer and Ridgely (2010)
<i>Niebla antiqua</i>	K	SA	D	✓	Aranciaga Rolando et al. (2020)
<i>Nothronychus mckinleyi</i>	K	NA	D	✓	Lautenschlager et al. (2012), Smith et al. (2018)
<i>Ornithomimus edmontonicus</i>	K	NA	D	✓	Tahara and Larsson (2011) (only inner ear)
<i>Saurornitholestes lanstoni</i>	K	NA	A	–	Cast (TMP 85.07.4) at Royal Tyrrel Museum analyzed in Zelenitsky et al. (2009)
<i>Sinosaurus triassicus</i>	J	As	D	✓	Xing et al. (2014)

(continued)

Table 8.1 (continued)

Taxon	Age	Proc	Cast	ie	Source
<i>Sinraptor dongi</i>	J	As	D	✓	Paulina-Carabajal and Currie (2012)
<i>Struthiomimus altus</i>	K	NA	D	✓	Witmer and Ridgely (2009)
<i>Tarbosaurus bataar</i>	K	As	A	–	Maleev (1965), Saveliev and Alifanov (2007)
<i>Timurlengia euotica</i>	K	As	D	✓	Brusatte et al. (2016)
<i>Troodon formosus</i>	K	NA	A	–	Hopson (1979), Jerison (2004)
<i>Troodon inequalis</i>	K	NA	A	–	Russell (1969) (= <i>Stenonychosaurus</i> , <i>Latenivenatrix</i>)
<i>Tyrannosaurus rex</i>	K	NA	AD	✓	Osborn (1912); Brochu (2000*), Witmer et al. (2008*), Witmer and Ridgely (2009*)
<i>Velociraptor</i>	K	As	D	✓	King et al. (2020)
<i>Viavenator exxoni</i>	K	SA	D	✓	Paulina-Carabajal et al. (2018a, b)
<i>Yaverlandia bitholus</i>	K	Eu	A	–	Hopson (1979)
<i>Zanabazar junior</i>	K	As	D	–	Norell et al. (2009), Franzosa (2004) (= <i>Mongolodon</i>), Balanoff et al. (2018)
<i>Zupaysaurus rougieri</i>	T	SA	D	✓	Paulina-Carabajal et al. (2019b)
Abelisauridae indet.	K	SA	D	✓	Méndez et al. (2021) (MAU-Pv-LI-582)
Theropoda indet.	J	Eu	D	–	Knoll (1997), Knoll et al. (1999)
Troodontid indet.	K	As	D	–	Balanoff and Bever (2017) (IGM 100/1126)
Troodontid indet.	K	As	D	–	Franzosa (2004) (IGM 100/1005)

Modified and actualized from Burch et al. (in press)

Abbreviations: *A* artificial (any casting material), *Af* Africa, *As* Asia, *Au* Australia, *D* digital, *Eu* Europe, *ie* inner ear, *J* Jurassic, *K* Cretaceous, *N* natural, *NA* North America, *Proc* precedence, *SA* South America, *T* Triassic, *digital version of the same taxon/specimen

or illustrated (see Table 8.1). Notably, more than 60% of the publications made during the period 1871–2021 correspond to studies conducted only in the last 20 years, hand-in-hand with the use of non-invasive technologies such as X-ray Computed Tomography. Of this sample, the largest number of studied specimens and taxa correspond to saurischian dinosaurs (almost 60%), whereas among ornithischians the largest number of studied specimens correspond to ornithomimid dinosaurs (almost 20%) (Fig. 8.3a). The latter observation is likely related to the fact of hadrosaurids were extremely abundant in the Late Cretaceous, having a highly rich record of ontogenetic series, mummified remains, eggs and ichnites, and including complete braincases (see Lull and Wright 1942; Horner, Weishampel and Forster 2004).

Although the general characteristics of the brain morphology of representatives of all major clades of dinosaurs is known at least at a family level, the larger number of studies correspond to Cretaceous taxa (80%), whereas the early forms remain understudied (Fig. 8.3b). In this regard, the Jurassic taxa represent around 15% of the sample, including principally saurischian dinosaurs (such as the eusauropods *Apatosaurus*, *Barosaurus*, *Camarasaurus*, *Cetiosaurus*, *Dicraeosaurus*, *Giraffatitan*, *Shunosaurus*, *Spinophorosaurus*, and the theropods *Allosaurus*, *Ceratosaurus*, *Megapnosaurus*, *Sinosaurus*, and *Sinraptor*), whereas Ornithischia is represented by the ornithomimids *Dryosaurus* and *Dysalotosaurus* and the stegosaurs

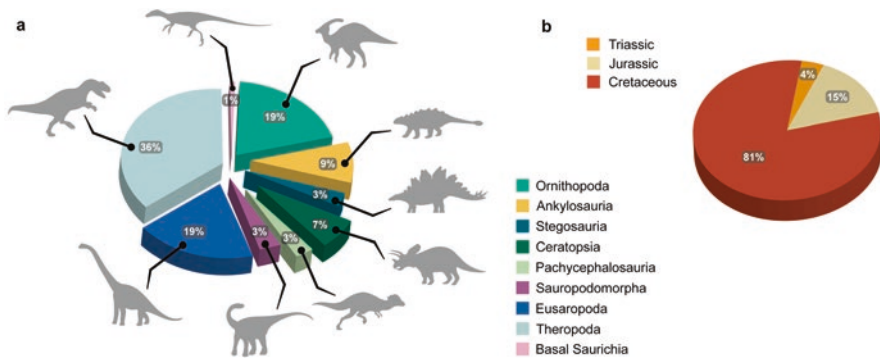


Fig. 8.3 Pie-charts showing the number of studied dinosaur endocasts by (a), taxonomic groups; and (b), by periods of time represented by the specimens of the sample

Kentrosaurus and *Stegosaurus* (Table 8.1). The Triassic studied taxa in turn represent less than 5% of the known dinosaur cranial endocasts (Table 8.1 and Fig. 8.3b). Except for the sauropodomorph *Plateosaurus*, for which details on the brain anatomy were already published in the 1980's (Galton 1985), data on all other Triassic species including the sauropodomorphs *Buriolestes*, *Thecodontosaurus*, *Saturnalia*, an indeterminate riojasaurid from Argentina, and the basal theropod *Zupaysaurus*, became available only recently, all of them studied using CT scans (Bronzati et al. 2017; Paulina-Carabajal et al. 2019a, b; Ballell et al. 2021; Müller et al. 2021; Table 8.1). The anatomical data from these early forms was really important from an evolutionary point of view, shedding some light on the primitive dinosaur neuro-anatomical morphology and the possible evolutionary trajectory along the history of the group.

8.2.2 Non-invasive Techniques and Paleoneurology

The use of non-invasive techniques certainly improved the field of dinosaur paleoneurology greatly, marking a landmark in the methodology for obtaining internal anatomical data (e.g. Witmer et al. 2008; Balanoff and Bever 2017; Balanoff et al. 2016b). In particular, X-ray computed tomography allows the observation of internal features with minimal manipulation of the sample, and the virtual extraction of structures through the rendering of digital three-dimensional models (Fig. 8.4). Also, this technique allows digital visualization of endocranial cavities, not only the brain cavity but also neurovascular passages, endosseous labyrinth and cranial pneumatic recesses, regardless of whether the braincase articulates with, or is covered by other skull bones, or if it is still encased by sediment. The digital technique has become such a useful tool that artificial physical endocast production has been minimized drastically nowadays, being replaced by 3D impressions of the available models for instance in online repositories.

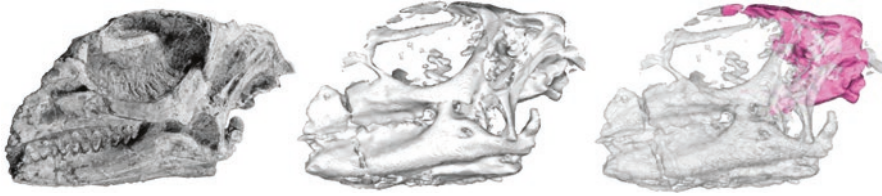


Fig. 8.4 Skull and braincase of *Gasparinisaura cincosaltensis*. In the 3D models the skull bones were rendered semitransparent to allow the observation of the braincase, which can virtually “extracted” for study (After Paulina-Carabajal et al. 2017 and Paulina-Carabajal, Dieudonné and Cruzado-Caballero in prep.; the photograph of the holotype specimen was courtesy of J. Meso). Not to scale

The first published dinosaur paleoneurology studies based on CT scans were made in the late 1990’s for *Allosaurus* and an indeterminate theropod from France, by Rogers (1998) and Knoll et al. (1999) respectively. The digital studies of *Tyrannosaurus* were published right after by Brochu (2000), followed in the next years by few dinosaur publications in which CT scan data was used to visualize both the braincase (and cranial nerve foramina) and the endocranial structures (e.g. Coria and Currie 2002; Ebner and Salgado 2003; Burnham 2004; Franzosa 2004). The boom of the studies based on CT scans (X-ray or neutron tomography) really started, however, after the first decade of the twenty-first century, and continues to expand (e.g. Witmer et al. 2008; Balanoff and Bever 2017; Balanoff et al. 2016b; Watanabe et al. 2019; Dumoncel et al. 2020; Table 8.1).

8.2.3 Problems for the Study of Dinosaur ‘Brains’

Vertebrate brains and cranial peripheral nerves pretty much never fossilize, except under exceptional circumstances, as for example the Cenozoic tadpole cranial soft tissues –eyes and peripheral nerves– preserved in slabs (e.g. Báez and Púgener 2003) and retinal traces in Devonian fishes (Davidson and Trewin 2005). And even then, those soft tissues might be difficult to identify without complementary microscopic or chemical analyses (e.g. Knoll and Kawabe 2020 and references therein). Among dinosaurs, possible part of brain-related tissue was identified in an iguanodontian natural endocast (Brasier et al. 2016), and cranial nerve fibers were identified inside a nerve passage on a *Triceratops* occipital condyle (Armitage 2021). However, in most cases, paleoneurological studies have been based on cranial endocasts because they are considered to be representations or approximations of the actual brain external morphology (e.g. Edinger 1929; Hopson 1979; Iwaniuk and Nelson 2002; Buchholtz 2012).

The problem of determining how much of the endocranial cavity is occupied by neural tissue is strongly influenced by the fact that certain regions of the reptilian brain fill the endocranial cavity more completely than others. In terms of regional

fit, olfactory bulbs, cerebrum and probably the pituitary are brain structures that fill better the endocranial space, whereas the optic tectum, cerebellum and medulla oblongata tend to leave poor osteological correlates across dinosaurs. In most non-avian dinosaurs there is a reduction in the correspondence between the brain and its endocast, except in smaller derived –and more encephalized– theropods and ornithopods (Witmer et al. 2008; Watanabe et al. 2019; Balanoff and Bever 2020). Thus, this ‘regional fit’ influences what we can tell about dinosaur paleoneurology by using Jerison’s Principle of Proper Mass (see below). For instance, the fidelity between the dorsal brain surface and endocranial surface of the skull roof is for example pretty good in smaller theropods, but quite poor in the larger ones (e.g. *Tyrannosaurus*). Also, there’s a fair amount of fidelity of the dorsal brain surface in some ornithopods to the extent that there is a degree of overlap between them and derived theropods (e.g. Rich and Rich 1989; Evans 2005; Knoll et al. 2021).

There are two main factors influencing the relative brain size and its relationship with the endocranial cavity: (1) a genuine selective increase in neural tissue mass (neural capacity) that has the brain competing with other cranial structures for space due to increases in processing capacity; and (2) the body size, which is another highly adaptive –and correlated– variable, where body size is outstripping brain size increase in larger taxa (the converse being body size reduction resulting in a ‘tight’ brain to brain cavity fit) (e.g. Smaers et al. 2012; Hurlburt et al. 2013; Walsh et al. 2009).

In other words, the accuracy of the cranial endocast as a source of neural information depends on the brain-endocranium relationship in each species, which in turn depends on different anatomical and evolutive factors (taxonomic group, ontogenetic stage and body size; Giffin 1989; Hurlburt et al. 2013). In this regard, the first paleobiological inferences based on cranial endocast anatomy were nearly speculations. But nowadays paleontologists look for, and use, testable evidence within a phylogenetic framework in order to make paleobiological inferences on dinosaur brain evolution and sensory biology (e.g. Hopson 1977; Witmer 1995; Witmer et al. 2008; Balanoff et al. 2014; Watanabe et al. 2019). These kind of studies rely, however, on indirect sources of data including the knowledge of extant reptile biology, and the osteological correlates –which are impressions left by a soft tissue on the surface of the bones–observed in both extinct and living representatives (Witmer 1995). Thus, the method known as Extant Phylogenetic Bracketing (Witmer 1995) allows paleontologists to infer presence/absence of soft tissue structures –in this case brain structures–using the mentioned osteological correlates.

In paleoneurology, important osteological correlates are the impressions of the different main regions and structures of the brain left on the surface of the endocranial cavity (Fig. 8.5a). The best way to visualize such morphology is through using 3D models (physical or digital) of the endocranial space, usually referred to as cranial endocasts. Dinosaur natural cranial endocasts are extremely rare in the fossil record (e.g. Hopson 1979; Rich and Rich 1989; Rogers 1998; Galton 2001; Serrano-Brañas et al. 2006; Jerison 2004; Brasier et al. 2016; Paulina-Carabajal et al. 2018a; Table 8.1), which is the reason early studies were based on the direct observation of the endocranial cavity. This was possible through natural fractures in the braincase,

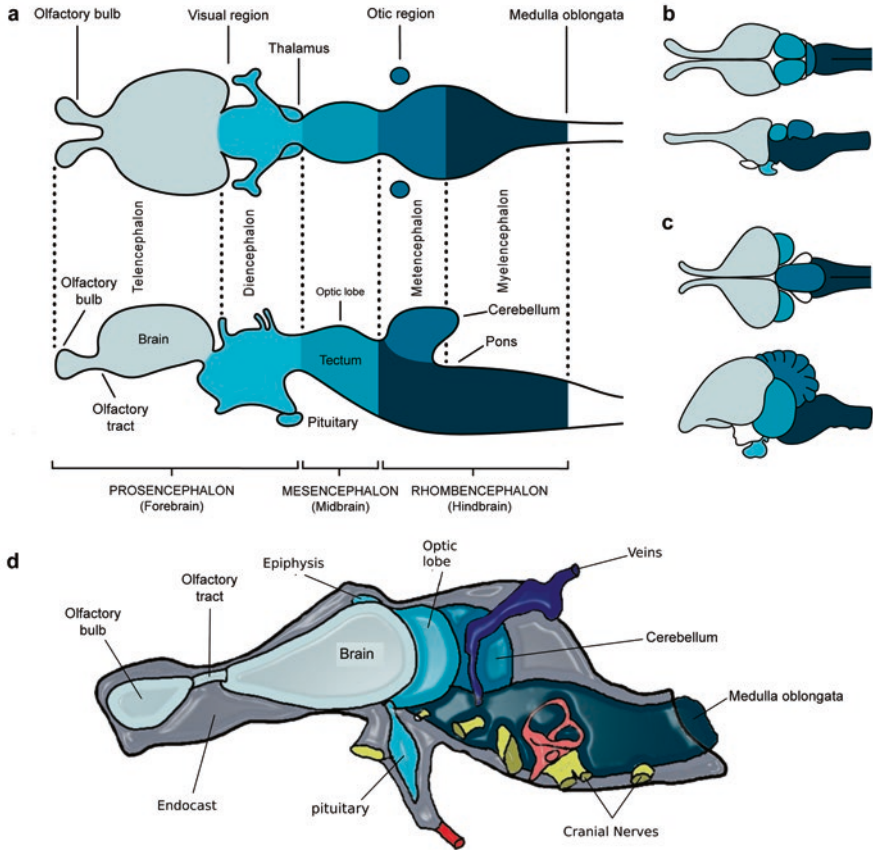


Fig. 8.5 Brain regions. (a), Scheme of embryonic differentiated regions of the vertebrate brain. (b), Relative development of brain regions in living crocodiles; and (c), birds. (d), Scheme of modeled brain parts within a theropod dinosaur endocast using the GABRA method (see Morhardt 2016; Morhardt et al. 2018) (a–c), based on Northcutt 2002; (d), line drawing based on Morhardt 2016, illustration published online (2017) at <https://www.earthtouchnews.com/discoveries/fossils/theres-a-lot-to-learn-about-dinosaur-brains/>

but also through sagittally sectioning complete skulls and braincases, a practice possible only if several specimens were available for study as is the case of *Diplodocus*, *Triceratops*, some hadrosaurids, and *Tyrannosaurus* (e.g. Osborn 1912; Lull 1933; Forster 1996; Brochu 2000). The sagittal section is quite informative because allows observation of all the three brain regions at the same time, and the study of such structures using photography or creation of wax models (Figs. 8.2d, e and 8.6a). Artificial cranial endocasts can be made using casting material –if sediment is not present in the endocranial cavity– or using CT scans, in which case the endocast model is digital. As mentioned, digital models are now the most common type of endocasts used by scientists (Table 8.1).

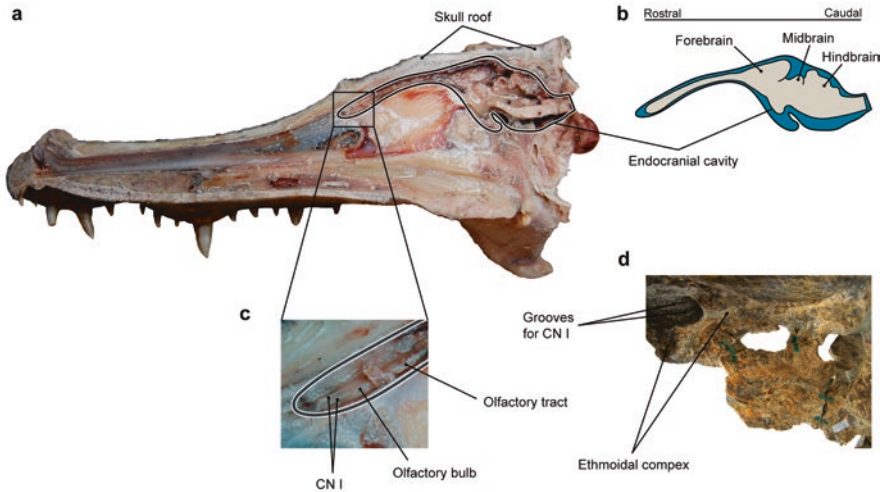


Fig. 8.6 Brain to endocranial cavity relationship. (a), Photograph of sagittally sectioned skull and brain of *Caiman* sp.; (b), line-drawing showing the brain-endocranium relationship in a living reptile, and (c), detail of olfactory nerves (CN I) running into the olfactory bulbs. (d), Detail of the ossified ethmoidal complex in the theropod *Abelisaurus*, showing horizontal grooves inside the olfactory bulb cavity left probably by olfactory nerves. (a, b), modified from Burch et al. *in press*; (d), from Paulina-Carabajal 2015. (Photo of *Caiman* courtesy of J. Desojo and P. Bona (Museo de La Plata))

8.2.4 Cranial Endocast Reliability

As mentioned above, cranial endocasts are the most important sources of data for the study of vertebrate brain evolution. However, endocasts can be good proxies for assessment of brain morphology in certain groups, such as mammals and birds, but not in most reptiles where the endocasts are not faithful copies of the unpreserved soft tissues (e.g. Iwaniuk and Nelson 2002; Balanoff et al. 2016a,b; Balanoff and Bever 2017; Morhardt et al. 2018; Watanabe et al. 2019; Dumoncel et al. 2020). This is the outcome of different factors, such as the development of large dorsal and ventral longitudinal venous sinuses or the presence of thick meninges, which separate the brain from the endocranial surface, obscuring the structures below (see Edinger 1951; Hopson 1979; Franzosa 2004; Evans 2005; Witmer et al. 2008; Porter et al. 2016; Balanoff and Bever 2017). Variation in endocast shape among the main clades of dinosaurs mostly results from the above-mentioned brain-endocranial relationship, plus the differential development of brain regions, a phenomenon that takes place particularly in the forebrain (see Larsson et al. 2000; Balanoff et al. 2010; Buchholtz 2012). The latter is also observed throughout the evolution of amniotes where there is a brain size increment that responds, mainly, to increases in forebrain size (Bruce 2006; Güntürkün et al. 2020). Finally, another source of dinosaur brain shape variation can result from flexion of the main axis (e.g. Balanoff

et al. 2014), although this is far less notable than that observed in the dinosaur descendants, the birds.

The recognition of brain structures is important also to the field of sense biology. Inferring of sensory adaptations is possible by means of Jerison's Principle of Proper Mass (PPM), which states that the size of a neural structure reflects its processing capacity and the relative importance of the specific processing tasks taking place within the structure (Jerison 1973). As such, the shape and size of certain brain structures (e.g. the optic or olfactory lobes), may be correlated with specific sensory capabilities (Jerison 1973; Wylie et al. 2015). For instance, an animal relying on vision would be expected to have larger optic lobes, whereas an animal relying more on olfaction would be expected to have larger olfactory lobes. Obtaining evidence on sensory biology in extant taxa helps to support hypotheses about the behavior in extinct animals (e.g. Zelenitsky et al. 2009; Brusatte 2012; Lautenschlager et al. 2012; Paulina-Carabajal et al. *in press*, and references therein). However, while the PPM approach to endocast analysis makes logical sense, it largely ignores the role of interconnections between brain regions, and its reliability has been questioned (see Striedter 2005 for discussion).

Paleoneurologists and vertebrate anatomists have made attempts to determine indicators of brain morphology, and how much of an endocast corresponds to neural anatomy (brain-endocast fidelity; Morhardt et al. 2012; Balanoff et al. 2013). In order to do this, it is evident that modern comparative methods (and knowledge of the conservative evolutionary pattern of the vertebrate brain) are essential to infer the general layout and function of the dinosaur brain (Jerison 1973; Hopson 1979, 1980; Butler and Hodos 2005; Balanoff and Bever 2017). Based on actualistic studies, nearly two dozen osteological correlates, which serve as informative anatomical landmarks and support a brain design typical of other vertebrates, can be identified in a dinosaur endocast (e.g. Hurlburt 1996; Witmer and Ridgely 2009; Balanoff et al. 2016b; Morhardt 2016; Morhardt et al. 2018; Watanabe et al. 2019). Thus, allowing an accurate interpretation of the location and relative size of the modeled brain regions (Morhardt et al. 2018; Fig. 8.5d).

8.2.5 *Brain to Endocranial Cavity Ratio*

As mentioned, one of the main problems with the study of cranial endocasts in extinct dinosaurs is that the brain does not completely fill the endocranial cavity (Fig. 8.6a, b). This particularity of the reptilian brain has been known since early anatomical studies, such as that of the lepidosaur *Sphenodon*, which exhibits a 50% filling of the endocranial cavity (e.g. Dendy 1910; Hopson 1979; Starck 1979). Based on that single study, there was for a long time a generalized assumption that in most adult dinosaurs the brains filled the same amount of endocranial space (e.g. Edinger 1951; Hopson 1979). More recent comparative neuroanatomy studies have shown that squamates (e.g. snakes, amphisbaenians and many lizards) actually have a wide range of brain-endocranial cavity proportions, some of which approach 90%

(e.g. Olori 2010; Hurlburt et al. 2013; Allemand et al. 2017; Macri et al. 2019). Among dinosaurs, derived theropods and some ornithopods have endocasts exhibiting features interpreted as indicators of a large percentage of cavity filling. These can be brain structures (such as a fissura interhemispherica separating cerebral hemispheres medially, optic lobes, or the cerebellum) or vascular structures (such as impressions of blood vessels on the bones enclosing the forebrain that indicates a thin dura mater) (Osmólska 2004; Evans 2005).

The variation of the ratio between the brain and the occupied space within the endocranial cavity in different dinosaurs has direct implications for the study of their endocasts. Balanoff et al. (2016a) referred to this differential relationship as the brain-to-endocranial cavity index (BEC index). *Sphenodon* therefore has a BEC index of 0.5. Higher BEC values indicate that the endocast reflects with more fidelity the brain morphology (size and shape), whereas low values are typical of more tubular endocasts that show less resemblance to the brain proper because there is a reduction of the correspondence between endocast and brain (Hopson 1979; Witmer et al. 2008; Balanoff et al. 2016a; Balanoff and Bever 2020).

8.2.6 Ontogeny

There are few studies regarding ontogenetic and developmental patterns in dinosaur brains, basically due limitations in the fossil record. In fact, when we talk about dinosaur paleoneurology, in most species the brains are known from a single studied specimen. Moreover, most studied braincases belong to adult or subadult individuals, and there is little information on juvenile dinosaurs except for a few exceptions (e.g. Lautenschlager and Hübner 2013; Bullar et al. 2019). This is, however, an interesting approach to the study of the relationship between the brain and the endocranial cavity: Do juvenile dinosaur brains fill the endocranial cavity better than the adult ones, or vice versa? Do they both, juvenile and adults, share the same brain architecture –and therefore– endocast morphology? So far, the brain-to-endocranial relationship has been studied in a few clades of dinosaurs with juvenile representatives, including ornithopods, ceratopsians and tyrannosaurids with interesting results (e.g. Evans et al. 2009; Bever et al. 2011; Lautenschlager and Hübner 2013; Romick 2013; Beyrand et al. 2019; Bullar et al. 2019). These studies showed a marked morphological variation between juvenile and adult cranial endocasts, plus a higher degree of endocranial occupation in juveniles of some groups (e.g. lambeosaurines, Evans et al. 2009). Differences in size and shape in ontogenetic stages indicate changes in the endocranial anatomy that were influenced by growth and other developmental factors, and in living crocodiles these changes are more marked during the embryonic period than after hatchling (e.g. Jirak and Janacek 2017). Such changes in the brain occurring during the ontogenic stages may have been related to changes in function (e.g. relative reliance on olfaction, respiration) although these aspects require further exploration (Ngwenya et al. 2013; Beyrand et al. 2019; Hu et al. 2021). On the other hand, the degree to which an endocast of a

particular taxon is brain-like may also influence assessments of the ontogenetic stage of the individual. For instance, the ‘brain-like’ endocast of *Nannotyrannus* may represent evidence for that taxon being a juvenile *Tyrannosaurus* (Witmer and Ridgely 2010; Hurlburt et al. 2013).

8.3 Overview of General and Comparative Brain Anatomy

8.3.1 *The Reptilian Central Nervous System*

The vertebrate brain is an organ formed of several functional regions whose patterns of location of processing centers, and sensory and motor signal transmissions are highly conservative, somehow facilitating their study and comparisons among non-related groups. In living reptiles, the brain is in general anatomically simple, with the three main embryonic subdivisions –the forebrain, midbrain and hindbrain– aligned in sequence, resulting in more or less ‘tubular’ brains (e.g. Romer 1956; Wyneken 2007; Fig. 8.5b).

The forebrain or prosencephalon is the most anterior part of the brain (Fig. 8.5a–c). This region subdivides into the telencephalon (comprising the olfactory apparatus, the cerebral hemispheres, and Cranial Nerve (CN) I), and the diencephalon (comprising pineal complex, pituitary gland, the optic chiasm, and CN II). Although foramina in the skull roof of some sauropodomorph dinosaurs had been referred to as ‘pineal’ structures, is now more widely accepted that those endocranial spaces (externally opened or not) included extensive dural sinuses or were casts of open skull sutures (see Harris 2006; Witmer et al. 2008; Balanoff et al. 2014). The loss of the pineal complex in dinosaurs has been related to endothermy (Benton 1979). The hypothalamus forms the optic chiasm and the neurohypophysis, housed –together with the adenohypophysis and blood vessels– within the pituitary fossa.

The midbrain or mesencephalon deals with visual processing and neuroendocrine regulation. This region of the brain comprises the optic lobes (generally well developed in reptiles), tegmentum (ventral part of the midbrain) and CNs III and IV. The paired optic lobes are expressed just posterior to the cerebrum, and are the most conspicuous structure in this region, whose size is related –among other variables– with visual stimuli (Wyneken 2007). In most reptile endocranial cavities the optic lobes are not large enough to leave visible osteological correlates.

The hindbrain or rhombencephalon is associated with the senses of hearing and balance. This region of the brain subdivides into the metencephalon (cerebellum), and the myelencephalon (medulla oblongata, CNs V–XII) (Fig. 8.5a). The cerebellum has a role in balance and equilibrium, integrating touch, proprioception, vision, hearing and motor input. The size of the cerebellar region varies among species, and particularly with locomotor behavior, tending to be smaller in cursorial species and larger in aquatic and arboreal species (Romer 1956; Nieuwenhuys et al. 1998; Wyneken 2007; Bruce 2009). However, the cerebellum is often not a recognizable structure in a dinosaur endocast, except for the paired cerebellar flocculi when they

are large enough to leave an osteological correlate on the anterior wall of the vestibular eminence. The medulla oblongata is easily discernible in the endocast because most of the posterior cranial nerves emerge from it, having in this sense an organization similar to that in birds and mammals.

8.3.2 *Characterization of Cranial Endocast Morphology in Dinosaurs*

Generalized Dinosaur Endocast

Forebrain The forebrain structures that can be observed in a dinosaur cranial endocast correspond to the olfactory bulbs, olfactory tracts, cerebral hemispheres, and pituitary gland. The anatomy, number, and spatial distribution of the cranial nerves in dinosaurs differ little from those of other reptiles (Franzosa 2004; Witmer et al. 2008).

The olfactory nerve (CN I) is often indicated in illustrations of braincases and/or endocasts, although in those cases the highlighted areas correspond more precisely to the olfactory tracts or the olfactory bulbs. Actual impressions of the olfactory nerves may be recognized on the internal walls of the ossified ethmoidal complex, which are the bones enclosing the cavity that houses the olfactory bulbs (see Ali et al. 2008: Fig 3; Fig. 8.6c). The median septum (mesethmoid?) which separates medially both olfactory bulbs may exhibit horizontal grooves that represent impressions left by the olfactory nerves, as observed in the ethmoidal complex of tyrannosaurids and abelisaurids, among others (e.g. Ali et al. 2008; Figs. 8.5d and 8.6b).

The optic tracts (CN II) are in general paired short passages, large in diameter, that may leave the endocranial cavity through a single or separate foramina (this depending on the degree of ossification of the orbitosphenoids). Casts of these large single or paired -but markedly short- passages can be found on the ventromedial surface of the endocast. The optic chiasm corresponds to the area where the axonic fibers of the right and left optic nerves partially intersect, continuing along the contralateral tract and in some cases leaving an osteological correlate. It is observed as a rounded median bulge bearing left and right CN II passages (and separating them from the surface of the endocast), on the ventral side of the forebrain in some titanosaur sauropods (Paulina-Carabajal 2012, 2015), ankylosaurs (Miyashita et al. 2011), some ceratopsians (e.g. Forster 1996), and lambeosaurines (Evans et al. 2009; Cruzado-Caballero et al. 2015).

The olfactory bulbs are oval structures that may be parallel or divergent from the midline. Most endocasts comprise more space within the endocranium for the olfactory structures (olfactory region of the nasal cavity) than that occupied by the bulbs themselves (e.g. see for instance the first and last reconstructions for *Tyrannosaurus*, Brochu 2000; Witmer and Ridgely 2009), which is the reason why a careful look for the true osteological correlates is needed. This is particularly necessary if

calculation of the Olfactory Ratio (Zelenitsky et al. 2009; see below) is intended. The conservative condition among archosaurs consists of relatively anteroposteriorly elongated olfactory tracts, a disposition that typically accompanies the interorbital septum in tropibasic skulls, and it clearly differentiated from the olfactory bulbs anteriorly and the cerebral hemispheres posteriorly by strong constrictions. This configuration is observed in non-maniraptoran theropods and basal sauropodomorphs (prosauropods), whereas most ornithischians (such as ornithomorphs, ceratopsians and pachycephalosaurs) still exhibit this condition but with relatively shorter and broader olfactory tracts. Markedly short olfactory tracts—often accompanied by relatively smaller olfactory bulbs—characterize the endocasts of derived sauropods, hadrosaurids, ankylosaurs and stegosaurs (Fig. 8.9). The Olfactory Ratio (OR, the ratio of the greatest diameter of the olfactory bulb to the greatest diameter of the cerebral hemisphere) is a value used to infer olfactory acuity (which is the capacity to distinguish between two odors) and behavioral traits through a quantitative approach and using the body size as a variable in the equation. Because of this, the OR is not an indicator of olfactory acuity by itself (Zelenitsky et al. 2009, 2011), although the measurement can be used as a comparative variable. Such analyzes have found a positive correlation between olfactory ratio and body size, indicating that the OR increases with body size. Among theropods there was no relative increase or decrease of olfactory acuity during the evolution of the clade, and olfactory bulbs larger than the predicted values were found only in tyrannosaurids and dromaeosaurids (Zelenitsky et al. 2009). Something similar is observed among sauropodomorphs, where ORs range from low to high (suggesting specialized olfactory capabilities), but being above the confidence interval of predicted values only in basal sauropodomorphs and *Camarasaurus* (Müller 2021). Beyond this, little information is available on the olfactory acuity for other groups of dinosaurs (Paulina-Carabajal et al. [in press](#)).

The widest section of the dinosaur endocast is at the cerebral hemispheres. These are paired laterodorsal expansions which appear separated dorsomedially by a sagittal groove (the fissura interhemispherica) only in derived maniraptorans (e.g. dromaeosaurids, troodontids, and birds). In the cranial endocasts of hadrosaurids, some sub-adult coelurosaurids (e.g. tyrannosaurids), and oviraptorosaurs, the cerebrum may bear impressions of small blood vessels (Fig. 8.7c, d). This vasculature (observed as impressions on the internal surfaces of the frontals and/or the laterosphenoids) indicates a thin dura mater, and thus, a close resemblance between the actual brain and its endocast (e.g. Brochu 2003; Osmólska 2004; Evans 2005). Such impressions, unfortunately, are better preserved and observable in physical artificial endocasts than in the virtual ones created using medical CT scans (e.g. Paulina-Carabajal et al. 2021) due to poor resolution in medical equipment. In the most other dinosaur groups, the surface morphology of the brain is often obscured by dorsal longitudinal venous sinuses, resulting in smooth endocasts (Witmer et al. 2008; Porter et al. 2016; Porter and Witmer 2020).

The cast of the pituitary fossa comprises the glandular (adenohypophysis) and the neural (neurohypophysis) parts of the pituitary, plus an important blood supply nourished principally by the cerebral branch of the internal carotid arteries. In most

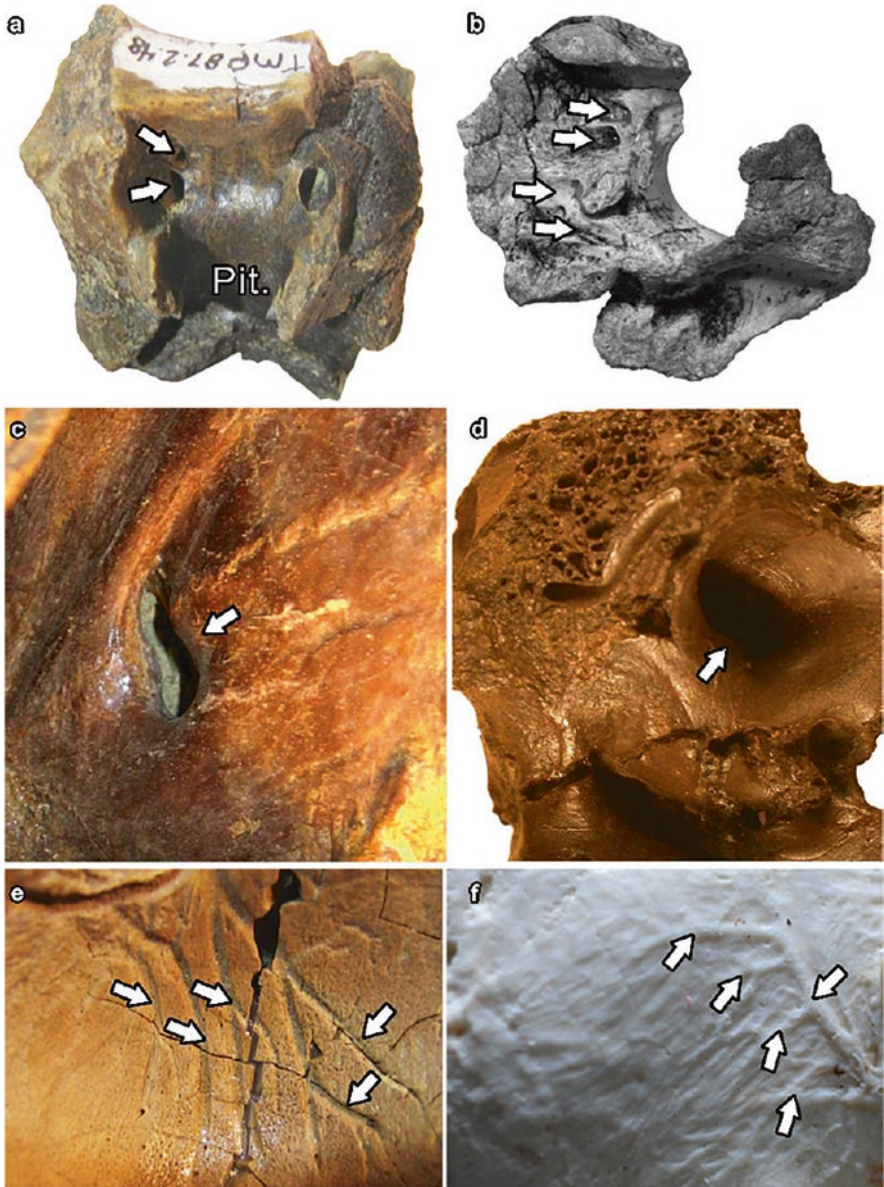


Fig. 8.7 Endocranial osteological correlates of brain structures and blood vessels. (a), ceratopsian basicranium in anterior view. The anterior wall of the pituitary fossa is missing exposing the dorsum sellae and the foramina for CN VI (above) and the internal carotid artery (below). (b), ethmoidal elements of the theropod *Sinraptor* in left lateral view showing grooves and passages within the cavity enclosing the olfactory bulbs, for CN I and probably other blood vessels. (c) and (d), floccular recesses in the endocranial cavity of the theropods *Daspletosaurus* (c) and *Troodon* (d). (e), impressions (grooves) of blood vessels in the ventral surface of an hadrosaurid frontal; (f), blood vessels on the lateroventral side of the cerebrum in a tyrannosaurid endocast (b, modified from Paulina-Carabajal and Currie 2012, c-f after Paulina-Carabajal 2015)

cases it is not possible to differentiate the two portions of the pituitary (except perhaps in some titanosaurs, Paulina-Carabajal 2012), and researchers refer to the entire cast as the ‘pituitary gland’. All dinosaur endocasts, from primitive to derived forms have a well-defined pituitary gland, in contrast to the smaller, less distinct bulges on the ventral surface of the endocasts of other reptiles, such as turtles and crocodiles. The pituitary is a ventral bulbous projection that connects dorsally to the main body of the cranial endocast through the infundibular stalk (Fig. 8.9b). Early theropods (i.e. *Zupaysaurus*, *Megapnosaurus*, and *Sinosaurus*) have a proportionally large and ventrally projected bulbous pituitary, a condition also present in the Triassic sauropodomorph *Plateosaurus* (but apparently not in *Buriolestes* which seems to have had a relatively smaller pituitary), and also in Jurassic basal ornithischians such as *Dysalotosaurus* and *Stegosaurus* (e.g. Galton 1985; Lautenschlager and Hübner 2013; Paulina-Carabajal et al. 2019a, b). This suggests that the presence of a relatively large and well-differentiated pituitary may represent a plesiomorphic trait among dinosaurs. By comparison, ceratosaurian and tetanuran theropods exhibit relatively smaller pituitaries, suggesting a reduction in the relative pituitary size occurred near or at the Averostra clade (following the definition of Ezcurra and Cuny 2007). In other words, the relatively small *Megapnosaurus* (ca. 2.5 m total length) has a pituitary that is proportionally larger than that of much larger theropods such as *Allosaurus* and *Acrocanthosaurus* (ca. 9–12 m total length) (Paulina-Carabajal et al. 2019b). Nonetheless, it is possible that a correlation is present between the absolute size of the pituitary and body size, as found in other amniotes (Edinger 1942). Sauropod cranial endocasts (and to a lesser extent those of ankylosaurs as well) exhibit hypertrophy of the pituitary gland, which in these endocasts is a posteroventrally oriented elongated finger-shaped projection. The reasons behind the striking enlargement of this structure have been debated for a long time (e.g. Edinger 1942; Balanoff et al. 2010; Miyashita et al. 2011; Paulina-Carabajal 2012; Paulina-Carabajal et al. 2018b). As mentioned above, possible explanations involve a simple positive allometric relationship of the pituitary gland with a large body size (e.g. Edinger 1942). However, various aspects of sauropod biology and selection pressure have been analyzed to understand the evolution of gigantism in sauropods, which resulted from a unique historical interaction of primitive and derived traits (see Sander et al. 2011; Sander 2013 and references therein). Other explanations for the enlargement of the pituitary lie in the continuous growth potential of these reptiles that was probably enhanced by this gland (e.g. Griebeler and Werner 2011), and also in the possible relationship with a reproductive strategy consisting of large egg production (hundreds per year) per individual (e.g. Sander et al. 2008; Werner and Griebeler 2013; García et al. 2015; and discussions and references therein).

Midbrain The midbrain is in general the least recognizable region in most dinosaur endocasts. Observed structures of the optic tectum correspond to the optic lobes, plus the oculomotor (CN III) and trochlear (CN IV) nerves. Cranial Nerves III and IV are usually very close to each other conservatively enclosed between the orbitosphenoid and laterosphenoid in the braincase either through separate foramina or a single foramen. Cranial Nerve III innervates four of the six extraocular

muscles of the eye and its passage is in general larger in size than CN IV, also because the exit foramen may house vascular elements as well. It locates in general ventrally to the CN IV, which is smaller in diameter and often dorsal to CN II.

The optic lobes are not observed in most dinosaur cranial endocasts. Among saurischians, these structures are recognizable in derived theropods such as maniraptorans. The evolutionary pattern in the avialan lineage (accompanied by a high degree of encephalization) shows a tendency towards an increase in the size of the optic lobes and a lateroventral migration. In *Saurornitholestes* the optic lobes are differentiated but still posterior to the cerebral hemispheres whereas in the dromaeosaurid *Bambiraptor* and the oviraptorosaur *Conchoraptor* the optic lobes have migrated lateroventrally, although they are yet observed in dorsal view (Burnham 2004; Balanoff et al. 2014) (Fig. 8.8b). Among ornithischians, optic lobes have only been described in the natural endocast of the Early Cretaceous basal ornithopod *Leaellynasaura*. In this Australian taxon, the relative increase in optic lobes has been interpreted as adapting to the decreased daylight at high latitudes (Rich and Rich 1989; Rich et al 2002). However, the brains of other closely related but lower

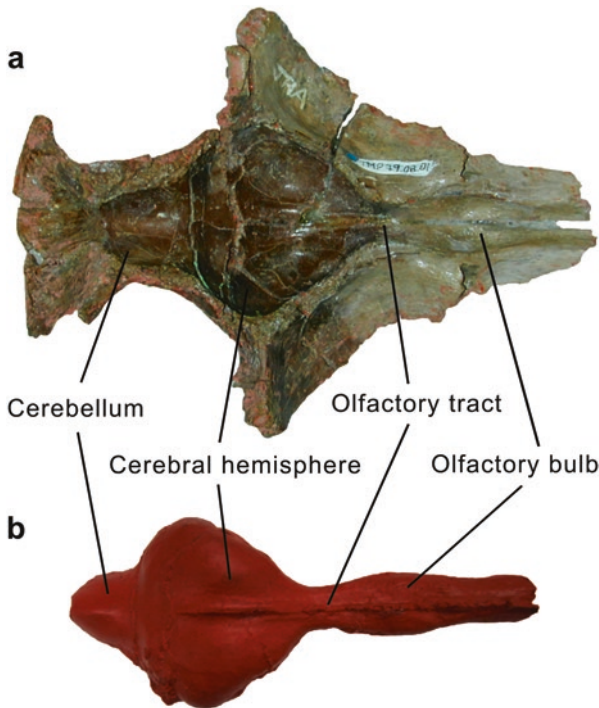


Fig. 8.8 Photographs of a derived troodontid theropod skull roof (TMP 79.8.1) and its endocast. (a), brain osteological correlates in the ventral surface of the skull roof; and (b), physical cranial endocast in dorsal view. (The specimen -hosted at the Royal Tyrrell Museum collections, in Canada- was described by Russell in 1969 as *Stenonychosaurus*; later the taxon was synonymized to *Troodon*, and more recently to *Latenivenatrix*)

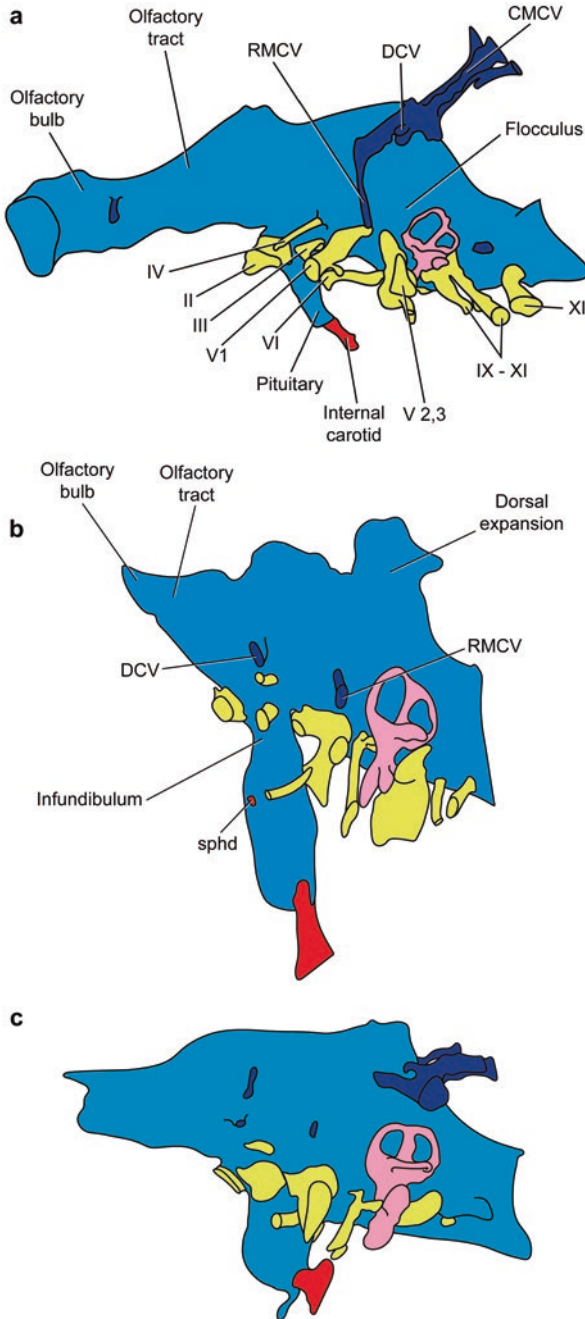


Fig. 8.9 Scheme of dinosaur comparative cranial endocast morphology. (a), Theropoda; (b), Sauropoda; and (c), Ornithischia. Line-drawings based on a, *Tyrannosaurus* (Witmer and Ridgely 2009), b, *Diplodocus* (Balanoff et al. 2010) and c, *Stegosaurus* (Leahey et al. 2015). Not to scale

latitude species need to be studied before the distribution of this feature can be better understood and its paleobiological implications tested.

Hindbrain Typical hindbrain structures recognized in dinosaur endocasts are the cerebellum, the medulla oblongata, and the trigeminal (CN V), abducens (CN VI), vestibulocochlear (CN VIII), glossopharyngeal (CN IX), vagus (CN X), accessory (CN XI) and hypoglossal (CN XII) cranial nerves (Franzosa 2004).

The cerebellum is not clearly distinguished in most dinosaur endocasts, except in derived theropods where it appears as a discrete dorsal prominence –which can be small or large– posteromedial to the cerebral hemispheres (e.g. oviraptorosaurs, dromaeosaurs). The paired cerebellar flocculi are posterolateral finger-like projections that, if large enough, leave an impression (called floccular recess) on the anterior wall of the vestibular eminence on both sides of the endocranial cavity. Smaller flocculi are barely detectable bulges on the endocasts, whereas well-defined flocculi can be finger-like or tongue-like structures projected well past the area of the anterior semicircular canal of the inner ear. Well-defined cerebellar flocculi are characteristic of basal saurischians and all theropod endocasts, with a tendency towards the enlargement in volume and diameter within the lineage of the maniraptorans (e.g. Lautenschlager et al. 2012; Bever et al. 2013; Balanoff et al. 2014; King et al. 2020; Paulina-Carabajal et al. 2021). Among sauropodomorphs, the cerebellar flocculi are typically present in all ‘prosauropods’ studied so far, whereas markedly reduced flocculi or floccular recesses (‘auricular recess’ in older works) have been described in *Giraffatitan*, *Dicraeosaurus* and rebbachisaurids (e.g. Janensch 1935–1936; Sereno et al. 2007; Knoll and Schwarz-Wings 2009; Paulina-Carabajal et al. 2014, 2016a). The cerebellar flocculi, together with the semicircular canals of the inner ear, have a major role in the control of visual gaze stabilization through compensatory head and neck movements via the Vestibulo-Ocular Reflex (Witmer et al. 2003; Walsh et al. 2013). Since the largest floccular processes are in flying reptiles (such as pterosaurs and birds) these structures were first correlated with the complex coordination of head-neck movements needed during the flight (e.g. Witmer et al. 2003). Thus, the presence of flocculus in theropods –and its apparent absence in most sauropods– was first related to bipedalism, the reason why bipedal ornithischians were expected to have an enlarged flocculus. However, this structure it is absent in most ornithischian clades and has been found only in a few taxa including the basal dryosaurid *Dysalotosaurus* (Galton 1989; Lautenschlager and Hübner 2013), and the quadrupedal ankylosaurs of the ankylosaurids family (Miyashita et al. 2011; Paulina-Carabajal et al. 2016b, 2018b), and stegosaurs (Galton 1988, 2001), making the paleobiological inferences of this structure, controversial at least. Recent works focused on bird brain evolution and the origins of flight assumed a positive relationship between floccular size and aerial maneuverability. However, the size of the floccular process has not been found to be a reliable indicator of locomotor behavior in vertebrates (Walsh et al. 2013; Ferreira-Cardozo et al. 2017). We are far from understanding the morphological variation, function, and distribution of this interesting brain feature among dinosaurs, particularly in the quadrupedal ones (see Sect. 8.3.2.3 for a possible explanation). Beyond this, there

is no doubt that the flocculus is at least a useful anatomical landmark for comparative neuroanatomy.

The medulla oblongata represents the posteroventral part of the endocast, from which the roots of the posterior cranial nerves emerge. The main transverse and longitudinal venous sinuses can be traced in this region of the endocast as well (e.g. Witmer et al. 2008; Witmer and Ridgely 2009; Porter et al. 2016). This section is one of the most conspicuous regions of the hindbrain. It is easily recognizable as it forms the floor of the endocast from the infundibulum anteriorly to the foramen magnum posteriorly, and because the roots of cranial nerves V–XII emerge from it, more or less aligned one behind the other. The ventral surface may be flat or convex, and smooth or presenting a median sulcus (in this case the osteological correlate is the medial eminence on the floor of the endocranial cavity or the basilar artery). On the lateral sides of the endocast, transverse venous sinuses can be identified (see below)

In most dinosaurs, the trigeminal nerve (CN V) emerges from the medulla oblongata and the ophthalmic (V_1), maxillary (V_2) and mandibular (V_3) branches leave the endocranial cavity together through an internal single foramen, anterior to the vestibular eminence. Externally in the braincase, the three branches may exit together (indicating that the Gasserian ganglion is extracranial) and in this case the cast of the passage must be indicated simply as ‘CN V’. In other cases, the ophthalmic branch separates from the maxillo-mandibular branches and as a result two passages (V_1 , V_{2-3}) will be observed in the endocast. There are few documented cases of three separated branches (and foramina), for instance as in therizinosaurs (e.g. Lautenschlager et al. 2012). The trigeminal is one of the few nerves that can be traced peripherally. The maxillary and mandibular branches leave osteological correlates (they are actually neurovascular canals) along the dorsal and ventral jaws respectively, as in living crocodylians (George and Holliday 2013). The degree of branching and size (diameter) of these nerves, together with the accompanying vasculature, have been related to a facial sensory system in certain carnivorous dinosaurs (Ibrahim et al. 2014; Barker et al. 2017; Carr et al. 2017; Kawabe and Hattori 2021).

The passages for the abducens nerve (CN VI) are the only ones emerging from the ventral surface of the medulla oblongata, a feature that makes them easily recognizable in any endocast. Right and left passages project anteroventrally passing lateral to the pituitary fossa or entering it, a character that is extremely variable among and within dinosaur groups.

The facial nerve (CN VII) is in general small in diameter and posterior to CN V. It is usually a short passage, except in the sauropod *Limaysaurus*, which has such an elongate passage that the external opening locates posteroventral in the braincase, behind the crista prootica. In most dinosaurs the palatine (VIIp) and hyomandibular (VIIh) branches of this nerve leave the endocranial cavity through a single passage and separate externally, leaving in some cases osteological correlates (grooves) on the prootic bone indicating the posterodorsal and ventral routes of each one respectively. The endocranial separation of these branches is rare, and has been described in only a few dinosaurs including the theropods *Acrocanthosaurus* (Franzosa and

Rowe 2005), *Alioramus* (Bever et al. 2013) and *Shaochilong* (Brusatte et al. 2010a), the sauropodomorph *Efraasia* (Bronzati and Rauhut 2017), and the sauropod *Cetiosaurus* (Galton and Knoll 2006). The size of this nerve –measured from the diameter of the cranial foramen– has been used as evidence against the presence of a proboscis in sauropods (Knoll et al. 2006), although the muscles forming the proboscis in elephants are not homologous to the muscles in the snouts of reptiles.

The vestibulocochlear nerve (CN VIII) is in general of small diameter, and as a result is rarely recreated in physical or virtual endocasts. The branches of this nerve leave the endocranial cavity and pass through the wall of the vestibular eminence to reach the vestibular region of the inner ear.

The glossopharyngeal (CN IX), vagus (CN X) and accessory (CN XI) cranial nerves may leave the endocranial cavity together with the internal jugular vein through a single foramen, called in this case the metotic foramen. Where this is the case, the cast of this passage is one of the largest in any endocast, similar in diameter to CN V. However, these nerves can also leave the endocranial cavity independently, in which case the nomenclature of the external foramina in the braincase changes and the interpretations of these separate foramina may be controversial (e.g. Sampson and Witmer 2007; see Gower and Weber 1998 for a discussion of these terms among reptiles).

Lastly, the hypoglossal nerve (CN XII) is the most posterior in the endocast, having a variate number of passages depending on the group. For example, in sauropods and ornithischians (particularly ankylosaurs and ceratopsians) there is a tendency towards the reduction of the number of external cranial foramina (1–2) for this nerve, but is highly variable among theropods, where one or two foramina are observed in general, but four foramina are observed in *Troodon* (e.g. Currie and Zhao 1993; Paulina-Carabajal 2015: fig. 7.3). There is also variability in the number of foramina for CN XII between the left and right sides of the same braincase in some coelurosaurs (P. J. Currie, Pers. Comm.), suggesting a degree of plasticity of this character, often used in phylogenies.

Blood Vessels Except for the cerebral branch of the internal carotid artery, which has a clearly visible passage on each side of the endocast, and few veins that leave osteological correlates in the braincase, the drainage of most of the blood of dorsal and ventral venous sinuses is through the foramen magnum and also through some of the larger cranial foramina, such as CNs III, V, and the metotic foramen (for CNs IX–XI and the internal jugular vein) (e.g. Witmer et al. 2008; Porter et al. 2016; Porter and Witmer 2020). In some cases, it is possible to identify separate passages for blood vessels in an endocast, and the most commonly found are the orbitocerebral vein, the rostral middle cerebral vein and the caudal middle cerebral vein, all which are part of the mid-cerebral vein system (Witmer and Ridgely 2009; Porter et al. 2016; Porter and Witmer 2020).

The cerebral branch of the carotid artery enters the basicranium through the vidian canal on its way to the pituitary fossa, with the largest carotid foramina observed in ornithischian dinosaurs (e.g. ceratopsians, stegosaurs and ankylosaurs). Left and right arteries may penetrate the posterior wall of the fossa separately (e.g.

prosauropods, sauropods, some theropods such as *Abelisaurus* and *Dromaeosaurus*, and most ornithischians including ankylosaurs, ceratopsians, and hadrosaurs, among others; Fig. 8.7a), or they may merge and enter the fossa via a single canal (e.g. theropods such as *Piatnitzkysaurus*, *Giganotosaurus*, tyrannosaurids and troodontids). This artery supplies endocranial tissues, and it is also an important blood supply to the nasal region, although recent studies suggest that in larger dinosaurs the cerebral internal carotid supplied mostly only the brain except perhaps in ankylosaurs (e.g. Porter and Witmer 2020; Porter et al. 2016). In their recent work, Porter and Witmer (2020) produced the most comprehensive comparative and quantitative analysis of the osteological correlates for blood supply in the craniofacial region of the skull of dinosaurs. Regarding the cerebral carotid artery, they found that the use of blood vessels in different sites of thermal exchange determines different thermoregulatory strategies, which in dinosaurs seem to be similar to those in living reptiles.

Inside the pituitary fossa small sphenopalatine arteries branch off the internal carotid artery (Sedlmayr 2002; Porter et al. 2016). When the anterior wall of the pituitary fossa is ossified these blood vessels exit anteriorly through foramina identified in theropods (e.g. *Majungasaurus*, Sampson and Witmer 2007), sauropods (e.g. *Bonatitan*, Paulina-Carabajal 2012), and many ceratopsians (e.g. *Pachyrhinosaurus*, Witmer and Ridgely 2008b and references therein).

The basilar artery is single median artery formed by merging of the paired branches of the caudal encephalic arteries, which extend caudomedially across the dorsum sellae, continuing through the foramen magnum as the ventral spinal artery (Rahmat and Gillard 2014; Porter et al. 2016). Some endocasts bear a rod-like elongate median protuberance on the ventral surface of the medulla oblongata, which seems to be a cast of this artery. In many dinosaur basicrania there is a median groove on the dorsal surface of the neck of the occipital condyle that has been identified also as an impression of the basilar artery (e.g. Rauhut 2003; Paulina-Carabajal 2015), although a similar groove is produced by the odontoid process in birds (*incisura mediana condyli*; Baumel and Witmer 1993). Another striking feature in some dinosaur basicrania is a median passage connecting the floor of the endocranial cavity (just behind the dorsum sellae) with the pituitary fossa. This passage has been identified in basal saurpodomorphs (*Plateosaurus*) and sauropods such as *Bonatitan*, *Limaysaurus*, *Giraffatitan*, *Malawisaurus*, *Narambuenatitan*, and *Spinophorosaurus* (Janensch 1935–1936; Galton 1985; García et al. 2008; Knoll and Schwarz-Wings 2009; Knoll et al. 2012; Paulina-Carabajal 2012; Sues et al. 2015; Andrzejewski et al. 2019; Paulina-Carabajal and Calvo 2021; Paulina-Carabajal et al. 2020 and references therein) as a possible basilar artery, which in this case would remain enclosed in bone. Other authors suggested a venous origin for this structure (Sues et al. 2015).

The orbitocerebral vein has a small diameter (Fig. 8.9b, c). It usually traverses the laterosphenoid-orbitosphenoid region, dorsally to CNs III and IV and near the contact with the frontal bone. In the absence of a foramen this vein probably leaves the endocranial cavity together with the passage for the trochlear nerve (CN IV) (e.g. Janensch 1935–1936; Knoll and Schwarz-Wings 2009). In some cases, there is

a larger opening in this region of the braincase, called epiotic fenestra (an unossified region of the braincase wall?) used probably for by CNs and blood vessels. This fenestra is present in the rebbachisaurid *Nigersaurus* and the dicraeosaurid *Dicraeosaurus* (Janensch 1935–1936; Sereno et al. 2007), although is not present in the south American representatives of those clades (Paulina-Carabajal et al. 2014, 2016a).

The dorsal longitudinal venous sinus (= superior sagittal venous sinus) and the occipital dural sinus are encephalic structures in the midline of the dorsal surface of the brain that drain blood from the endocranial cavity (e.g. Witmer et al. 2008; Porter et al. 2016). When these sinuses are large in volume, they produce dorsal protuberances within the endocranial cavity, which on the endocasts correspond to the dorsal expansions (= dural peaks) observed in many dinosaur endocasts. Enlarged sinuses, together with a thick dura mater, are factors that obscure the surface anatomy of the brain structures. Among sauropods the largest dural expansions are present in diplodocoid sauropods such as *Diplodocus* or dicraeosaurids, whereas markedly thinner sinuses characterize rebbachisaurids and most titanosaurids (e.g. Sereno et al. 2007; Paulina-Carabajal 2012; Knoll et al. 2012; Paulina-Carabajal and Calvo 2021). Theropods have in general well-developed dural expansions obscuring principally the mid- and hindbrain (e.g. *Zupaysaurus*, *Majungasaurus*, *Tyrannosaurus*), although derived maniraptorans exhibit reduction of both dorsal sinus and dura mater (e.g. Osmólska 2004). Among ornithischians the dorsal longitudinal sinus does not form markedly enlarged dural expansions. The venous sinuses are large enough to obscure the surface of the brain except in *Leaellynasaura* and hadrosaurs, which exhibit optic lobes or signals of thin dura mater (blood vessels over the cerebral hemispheres) respectively (Rich and Rich 1989; Evans 2005; Fig. 8.7e, f). The dorsal longitudinal sinus connects with a transverse sinus, connecting the middle cerebral vein system (rostral middle cerebral vein and dorsal middle cerebral veins may have exit foramina on the lateral wall of the braincase, whereas the caudal middle cerebral vein exits posteriorly through foramina on the occipital wall of the braincase).

The rostral middle cerebral vein is small in diameter and exits the endocranial cavity through a small foramen in the lateral wall of the braincase (the laterosphenoïd) near the contact with the skull roof. The dorsal head vein foramen is more dorsal and leads into the supratemporal fossa. In braincases lacking these two foramina the rostral middle cerebral vein and the dorsal vein extend ventrally and use the trigeminal foramen to leave the endocranial cavity (e.g. Rauhut 2003; Sampson and Witmer 2007; Witmer and Ridgely 2009). In this case, a transversal vertical sinus can leave an osteological correlate, which is observed on the lateral surface of the endocast as an elongated vertical bulge or ridge that ends at the base of CN V. This vertical ridge is more clearly observed in sauropods such as *Diplodocus*, *Limaysaurus*, *Sphinophorosaurus* and some titanosaurs (e.g. Witmer et al. 2008; Knoll et al. 2012; Martínez et al. 2016; Paulina-Carabajal and Calvo 2021). In theropods the vertical ridge is a more discrete bulge connecting the rostral middle cerebral vein with the root of the trigeminal nerve, often converging with the base of the cerebellar flocculus (e.g. *Allosaurus*, *Tyrannosaurus*). In this regard, the

8-shaped floccular recess in *Aucasaurus* and *Daspletosaurus* (Paulina-Carabajal 2015) suggests that while the ventral and larger recess hosted the neural tissue, the smaller dorsal section of the recess enclosed blood vessels supplying the flocculus of the cerebellum (Fig. 8.7c).

The caudal middle cerebral vein (= vena capitis dorsalis, dorsal head vein, in work prior to Sampson and Witmer 2007) is observed in the most posterodorsal region of the endocast (Sedlmayr 2002; Witmer et al. 2008). These paired passages drain blood from the posterior region of the dorsal longitudinal venous sinus, and the exit foramina for these veins are enclosed between the supraoccipital and the parietal, being easily recognizable at the occipital region of the skull.

The Cranial Endocast of Theropoda

The most complete Triassic theropod cranial endocast is that of the neotheropod *Zupaysaurus rougeri* from the Norian of South America (Fig. 8.10). A partial endocast has been described for the putative theropod *Gnathovorax* (Pacheco et al. 2019), an herrerasaurus, but the braincase and endocranial anatomy of other Triassic taxa is poorly known because of the lack of well-preserved material, or because the specimens remain incompletely studied (Paulina-Carabajal 2019a, b and references therein). *Zupaysaurus* has a relatively anteroposteriorly short but dorsoventrally tall endocast, as a result of marked angles between the forebrain, midbrain and hindbrain ('cerebral' and 'pontine' flexures in many works, although the terminology corresponds more correctly to embryonic stages of the brain), elongate olfactory tracts and bulbs and well-defined flocculi and pituitary. This general morphology is shared with another early dinosaurs, such as basal sauropodomorphs ('prosauropods' such as *Plateosaurus*), the early saurischian *Herrerasaurus* (Romick 2013: fig 7) and early Jurassic neotheropods. So far, the next oldest neotheropod with a described endocranial cavity is the Early Jurassic *Megapnosaurus* (= *Coelophysis*) *rhodesiensis* from Africa, followed by the basal tetanuran *Sinosaurus triassicus* from Asia, the allosauroids *Sinraptor dongi* and *Allosaurus fragilis* (from Asia and USA respectively), and the ceratosaur *Ceratosaurus nasicornis* from USA (Raath 1977; Rogers 1998; Sanders and Smith 2005; Paulina-Carabajal and Currie 2012; Xing et al. 2014). As mentioned, *Megapnosaurus* and *Sinosaurus* have endocasts with marked flexures, whereas basal allosauroids and ceratosauroids exhibit a more sub-horizontal endocast, meaning forebrain, midbrain and hindbrain have relatively less marked angles. The amount of available information on early forms is, however, poor and as a result, the early evolution of the endocranium of Neotheropoda is only beginning to be understood. On the other hand, the largest sample of studied theropod cranial endocasts correspond to Cretaceous taxa, representing all main groups of Theropoda (e.g. abelisaurids, allosauroids, coelurosaurians) (Table 8.1 and Fig. 8.3a).

Basal neotheropods and most non-coelurosaur theropods have in general terms anteroposteriorly long and narrow cranial endocasts (in dorsal view the lateral expansion of the cerebral hemisphere does not overpass the lateral semicircular

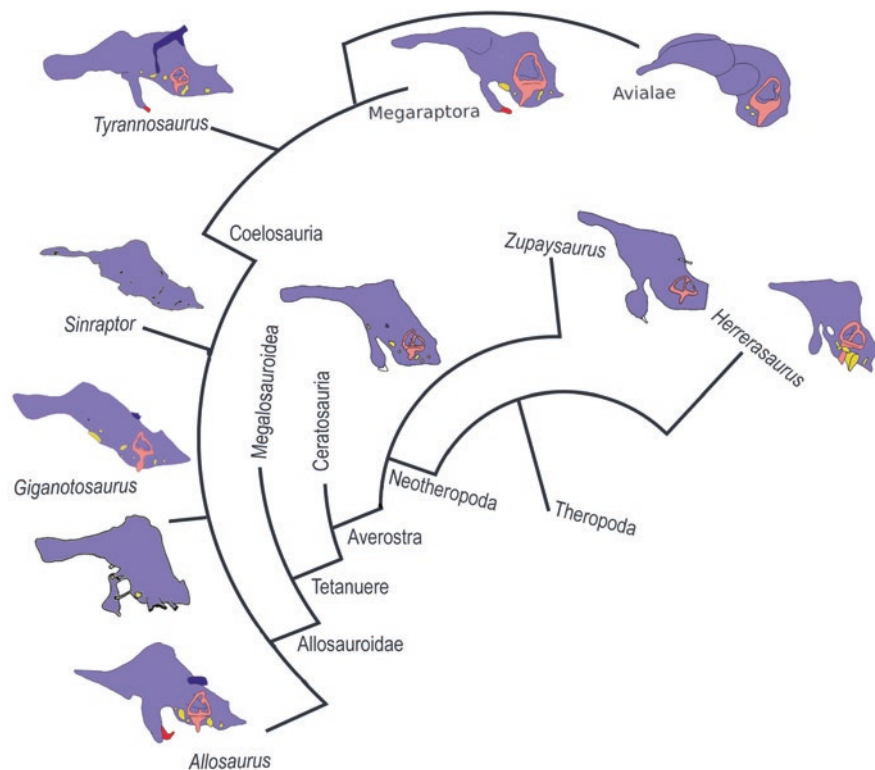


Fig. 8.10 Simplified cladogram of Theropoda showing the phylogenetic relationships of selected taxa and their endocasts. (line-drawings of endocasts based on: *Zupaysaurus* (Paulina-Carabajal et al. 2019b); *Majungasaurus* (Sampson and Witmer 2007), *Allosaurus*, *Tyrannosaurus*, *Deinonychus* and *Archaeopteryx* (Witmer and Ridgely 2009), *Acrocantnosaurus* (Franzosa and Rowe 2005), *Giganotosaurus* (Paulina-Carabajal and Canale 2010) and *Sinraptor* (Paulina-Carabajal and Currie 2012). Not to scale

canal of the inner), which is a conservative trait shared with other basal saurischians. The angles between forebrain, midbrain and hindbrain are in general wide, resulting in sigmoidal endocasts in lateral view, with the forebrain and hindbrain approximately horizontal and parallel to each other, and the midbrain obliquely angled between them as in *Zupaysaurus*, *Megapnosaurus*, ceratosaurs, *Sinraptor* and carcharodontosaurids (although the midbrain is more or less vertical in *Acrocantnosaurus*) (e.g. Larsson et al. 2000; Franzosa and Rowe 2005; Sanders and Smith 2005; Paulina-Carabajal et al. 2019b). In these endocasts, the venous sinuses largely obscure the details of the brain surface.

The olfactory apparatus, formed by olfactory bulbs and olfactory tracts, is elongated, with the most robust and transversely wide olfactory tracts observed in abelisaurids, carcharodontosaurids and tyrannosaurids (e.g. Brochu 2000; Larsson 2001; Sampson and Witmer 2007; Paulina-Carabajal and Canale 2010, Agnolfin

et al. 2022). The olfactory ratio (OR) however, is around 50% in most Ceratosauria and *Allosaurus*, around 56–58% in *Viavenator* and Carcharodontosauridae, and around 70% in Tyrannosauridae, while the value drops drastically in maniraptorans (28–35%) and Avialae (17%), which have relatively shorter olfactory tracts and smaller olfactory bulbs (Zelenitsky et al. 2009; Paulina-Carabajal and Filippi 2018). The ORs of theropods have been analyzed in order to infer the olfactory acuity, possible olfactory capacities and its implications for certain behaviors (Zelenitsky et al. 2009, 2011). The resulting phylogenetic trend in olfaction within Theropoda suggests that tyrannosaurids were the only group with a markedly specialized olfactory acuity. In this regard, along the evolutionary history of Theropoda there was a notable tendency towards the reduction of the olfactory bulb size and therefore, olfactory acuity (a trend not quite observed in sauropods and ornithischians).

The cerebral hemispheres are discernible as transversely expanded protuberances, which however, have no clear boundaries with other structures (such as optic lobes, cerebellum) in the endocasts of most theropods, except in derived maniraptorans (Fig. 8.8b). It was among the latter group (dromaeosaurids and troodontids) that a marked encephalization began, particularly due the enlargement of the cerebrum. This trend continued through the avialan lineage, through the derived oviraptorosaur brains (which shared endocranial traits with birds), to the highly encephalized brain (relative to body-size) and cerebrum (relative to total brain volume) observed in living birds (e.g. Larsson et al. 2000; Kundrát 2007; Balanoff et al. 2014). This long evolutionary history –leading to the high encephalization seen in living birds–indicates that most basal theropods had relative cerebral volumes and total brain volumes similar to those of living reptiles, whereas an increase of near 50% of total endocast volume occurred at Coelurosauria, produced in part by a disproportionate enlargement of the cerebrum (e.g. Larsson et al. 2000; Knoll and Kawabe 2020; and references therein).

The cerebellar flocculus is already present and relatively well-developed in the endocasts of Triassic basal saurischians such as *Herrerasaurus* (Romick 2013; Paulina-Carabajal pers. obs), *Gnathovorax* (Pacheco et al. 2019), and the neotheropod *Zupaysaurus* (Paulina-Carabajal et al. 2019b). Ceratosaur, tetanurans and basal Coelurosauria exhibit elongated flocculi (the structure varies from finger-shaped to blade-shaped morphologies) extended deep within the area of the anterior semicircular canal of the inner ear. In some theropods such as abelisaurids and the tyrannosaurid *Daspletosaurus*, the floccular recess is 8-shaped suggesting that the space was occupied not only by the neural tissue, but also by blood vessels (Paulina-Carabajal 2015; Paulina-Carabajal et al. 2021; Fig. 8.7c). On the other hand, derived–and smaller sized– maniraptoran theropods have relatively larger flocculi, which occupy a larger volume between the anterior and posterior semicircular canals (e.g. *Troodon*). The relative size of the flocculus correlates negatively with body size, meaning the structure is relatively larger in smaller theropods and most derived coelurosaurs. Walsh et al. (2013) suggested that the flocculus expression may be a result of expansion of the uvula nodulus (the structure involved with the nodding motion of walking birds) deep inside the cerebellum, in which case this –and not the flocculus– could have been the real link to bipedalism in early theropods. However,

a quantitative analysis of the floccular volume relative to brain size and body size has not been done yet for the complete clade Theropoda, nor for the complete Dinosauria.

More derived and smaller non-avian theropods such as maniraptorans (dromaeosaurids, troodontids, and particularly oviraptorosaurs) exhibit gradually more globose endocasts, with markedly shorter olfactory tracts, smaller olfactory bulbs, and markedly expanded cerebral hemispheres, which may be separated by a median groove as observed for example in *Bambiraptor feinbergi* and *Conchoraptor gracilis* (Burnham 2004; Kundrát 2007) (Figs. 8.7 and 8.10). A reduced olfactory apparatus, characterized by short olfactory bulbs and tracts is a shared feature of maniraptorans (in living birds an outgrowth of the cerebral hemispheres is covering the olfactory bulbs, which are then not visible in the endocasts). The extreme reduction, however, characterizes oviraptorosaurs and Aves, in which olfactory bulbs and tracts make up less than 0.5% of the total endocranial volume (Balanoff et al. 2014). Larger and visible optic lobes are located posteroventrally resembling the disposition observed in avian theropods and in pterosaurs, both groups with dominance of the sense of vision (e.g. Witmer et al. 2003; Stevens 2006; Kundrát 2007; Witmer and Ridgely 2009: fig.4; Buchholtz 2012; Balanoff et al. 2013, 2014, 2018). In these derived forms, the cerebellum is also observed but no cerebellar foliation has been reported, being probably obscured by dorsal venous sinuses (e.g. Kundrát 2007). The increase in encephalization index during non-avian theropod evolution has been largely explored by scientists, particularly for those interested in bird brain evolution. Now we know that the increased volume of the whole brain in early avian evolution largely relates to the enlargement of the midbrain and the cerebellum, two regions involved with visual perception and motor control abilities respectively: However, the largest brains observed in living birds today were molded by the strikingly increase of the telencephalon (e.g. Butler and Hodos 2005; Walsh et al. 2013; Wylie et al. 2015; Early et al. 2020).

The Endocast of Sauropodomorpha

After the first sauropod endocranial descriptions made by Marsh (e.g. 1980, 1984a), cranial endocasts of sauropod dinosaurs were described based on Late Jurassic specimens from the Morrison Formation in the USA (Osborn 1912) and the Tendaguru Beds in Tanzania (Janensch 1935–1936) (Table 8.1). Since then, a great quantity of studies on the neuroanatomy of sauropods has been published (e.g. Chatterjee and Zheng 2002; Sereno et al. 2007; Knoll and Schwarz-Wings 2009; Knoll et al. 2012, 2013, 2019; Balanoff et al. 2010; Paulina-Carabajal 2012; Paulina-Carabajal et al. 2008, 2014, 2016a, 2020; Table 8.1 and Fig. 8.11). Unlike the scenario in sauropods, endocasts of non-sauropodan sauropodomorphs are relatively scarce. In the last century, the only descriptive work of the endocast of a non-sauropodan taxa was that of *Plateosaurus* (Galton 1985). Yet, whereas the endocasts of other non-sauropodan sauropodomorphs have been used for comparative purposes in studies dealing with the evolution of neuroanatomy in dinosaurs during

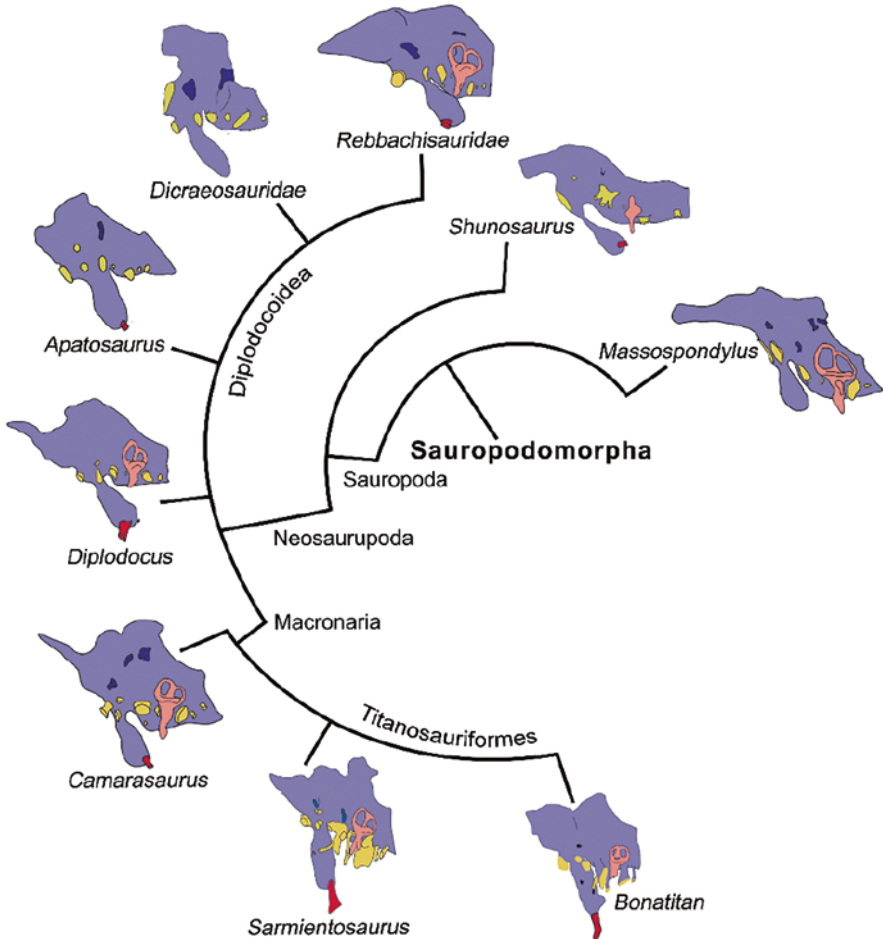


Fig. 8.11 Simplified cladogram of Sauropodomorpha showing the phylogenetic relationships of selected taxa and their endocasts (based on Balanoff et al. 2010). Endocasts were redrawn from: *Camarasaurus*, *Massospondylus*, *Nigersaurus* and *Diplodocus* (Sereno et al. 2007), *Shunosaurus* and (Chatterjee and Zheng 2002), *Dicraeosaurus* (based on photo kindly granted by F. Knoll), *Apatosaurus* (Balanoff et al. 2010), *Sarmientosaurus* (Martínez et al. 2016), and *Bonatitan* (Paulina-Carabajal 2012). Not to scale

the last two decades (e.g. Sereno et al. 2007; Knoll et al. 2012), it is only in the last five years that detailed descriptions of the brain and inner ear anatomy of non-sauropodan representatives became available (Bronzati et al. 2017; Chappelle and Choiniere 2018; Ballell et al. 2021; Müller et al. 2021; Table 8.1).

It would not be misleading to affirm that our knowledge of the neuroanatomy of sauropodomorph dinosaurs is still behind of that on their postcranial skeleton. However, the information provided by the studies on non-sauropodan taxa allows us to trace some major modifications on the neuroanatomy of sauropodomorphs.

Endocasts of the endocranial cavity are known for more than 25 specimens of sauropods (Table 8.1 and Fig. 8.9b). Thus, while we can certainly point out more than a handful of differences among them, some similarities are also present. Generally, it is difficult to discern the different regions of the brain in endocasts of sauropod dinosaurs (there are however some exceptions, as for example *Ampelosaurus* – see Knoll et al. 2013). This is an indication that the brain of sauropods did not fill the whole endocranial cavity, a feature that to a certain degree hampers the collection of accurate models of the brain of sauropods with all its subdivisions (Witmer et al. 2008).

As mentioned above, the flocculus of the cerebellum is present in the endocasts of sauropodomorphs usually known as ‘prosauropods’, but is absent in most sauropods. The osteological correlate of this cerebellar structure has been reported in all studied Triassic sauropodomorphs so far (e.g. Galton 1985; Bronzati et al. 2017, 2019; Ballell et al. 2021; Müller et al. 2021), whereas a comparatively reduced structure has been reported in the sauropods *Giraffatitan* (Janensch 1935–1936; Knoll and Schwarz-Wings 2009), the rebbachisaurids *Nigersaurus* and an indeterminate taxon from Argentina (Serenó et al. 2007; Paulina-Carabajal et al. 2016a), and the dicraeosaurid *Dicraeosaurus* (the ‘fossa subarcuata’ was mentioned by Janensch 1935–1936). Derived sauropods such as titanosaurids, are characterized by an absolute absence of a floccular recess in their braincases, and this suggests that the presence of large flocculi in sauropodomorphs is the retention of a primitive condition among saurischians. The evolution of the floccular lobe of the cerebellum in Sauropodomorpha has been recently analyzed in a series of papers (Bronzati et al. 2017; Ballell et al. 2021; Müller et al. 2021), but there remain important gaps in the fossil record, particularly for non-eusauropodan endocranial anatomy. The markedly reduced floccular lobe of sauropods was firstly associated with their quadrupedalism, which requires less balance coordination than in a bipedal type of locomotion (see Chatterjee and Zheng, 2002; Paulina-Carabajal 2012). However, facultative bipedal sauropodomorphs such as *Plateosaurus* also exhibit a reduced floccular lobe, and a different explanation for the reduction of this structure in Sauropodomorpha was recently presented in Bronzati et al. (2017). The floccular lobe is well-developed in taxa such as *Buriolestes*, *Saturnalia* and *Thecodontosaurus*. The diet of these three early sauropodomorphs has been inferred as faunivorous and/or omnivorous (see Cabreira et al. 2016; Ballell et al. 2021). Although the tooth morphology of *Plateosaurus* is also compatible with an omnivorous diet (Barrett and Upchurch 2007), some of its anatomical features, including a large body size, indicate that the diet of this animal was more plant based than that of the smaller omnivores such as *Saturnalia* and *Thecodontosaurus*. Thus, basal sauropodomorphs with larger floccular lobes correspond to those with a diet solely based and/or partially complemented by predation of other animals. In this context, Bronzati et al. (2017) argued that the reduction of the floccular lobe is congruent with a shift in the diet and feeding behavior of sauropodomorphs, given that an herbivorous diet does not require the same level of control and refinement of the movements of neck and head, nor the same degree of gaze stabilization as that of a predatory behavior. However, quantitative analyses of the floccular size in birds did not show a direct

relationship between a feeding behavior (in this case a predatory behavior) and larger floccular volumes, suggesting that this variable is not independent of other categories, such as could be the activity pattern (e.g. nocturnal vs diurnal) (see Walsh et al. 2013; Ferreira-Cardozo et al. 2017). Regarding dinosaurs, this hypothesis needs to be tested using a more comprehensive sample of sauropods and other dinosaurs with cerebellar flocculi, analyzing this feature throughout the evolutionary history of ornithischians and theropods as well.

In all sauropod endocasts known so far, the cerebellar region of the endocast does not exhibit any distinct protuberance, contrary to some derived theropods (e.g. Lautenschlager et al. 2012) and early sauropodomorphs (see below). One feature that is however, easily discernible in many sauropod endocasts is the presence of dural expansions (=dural peak) posterior to the cerebral region on the dorsal surface of the endocast (Witmer et al. 2008). These casts correspond to part of the intricate venous systems of the endocranial cavity of sauropods, which were connected to vascular systems of different regions of the skull (e.g. Witmer et al. 2008; Knoll et al. 2015a, b). Particularly large dorsal expansions, connecting to the dorsal surface of the skull roof through openings are present in dicraeosaurids, probably related to a thermoregulation function (Janensch 1935–1936; Paulina-Carabajal et al. 2014)

An enlarged ventrally-projected pituitary is a remarkable feature of the endocast of sauropods (Fig. 8.9b). The dorsoventral height of the gland is usually around half or the same as the height of the portion of the endocast dorsal to it. In some titanosaurs however, the height of the pituitary even surpasses that of the rest of the endocast (see Knoll et al. 2019 and references therein). Although the pituitary fossa was certainly filled with other soft tissues, the presence of a large pituitary gland in sauropods is expected as it has a relationship of positive allometry with body size (Edinger 1942). Excluding the pituitary, the rest of the brain endocast of sauropods usually exhibits a sigmoid shape in lateral view, a result of the presence of prominent flexures between forebrain, midbrain and hindbrain (called ‘cerebral and pontine’ flexures by other authors, although these are embryological terms) (Balanoff et al. 2010). Another characteristic that is also common to all sauropods, despite some variation, is the presence of a short olfactory tract and small olfactory bulbs.

There is a single passage for all branches of trigeminal nerve in most sauropods, but a separated V_1 (ophthalmic branch) is present in *Camarasaurus* (Zheng 1996; Paulina-Carabajal 2015). The most significant variation within Sauropoda might be that regarding the hypoglossal nerve (XII), with different specimens exhibiting either one or two foramina associated with the passage of this cranial nerve (see Balanoff et al. 2010). Within the more inclusive group Sauropodomorpha, another variation corresponds to the path for CNs IX–XI. Sauropods exhibit a single aperture on the lateral wall of the braincase between the fenestra ovalis anteriorly and the foramina for the hypoglossal nerve posteriorly, the metotic foramen, which likely corresponds to the path of CNs IX, X, and XI – this is different from the condition in most non-sauropod sauropodomorphs, which exhibit an additional foramen for CN X (see discussion below).

In relation to the neuroanatomy of sauropods, the endocast of the early sauropodomorph *Buriolestes schultzi* lies on the other side of the spectrum of morphological variation (Müller et al. 2021). So far, *Buriolestes* is the only non-sauropodan sauropodomorph for which the whole endocast including hind-, mid- and forebrain, as well as the inner ear, could be reconstructed. This taxon possesses a brain morphology that is mostly similar to the plesiomorphic condition of archosaurs. The endocast of *Buriolestes* do not exhibit flexures as marked as that of other sauropods. As a result, the endocast is less sigmoid in lateral view than in sauropods. Anteriorly, *Buriolestes* exhibits an elongated olfactory tract, with an anteroposterior length corresponding to around one third of the total length of its endocast. Another well-developed structure in the brain of *Buriolestes* is the floccular lobe of the cerebellum, which projects laterally within the space between the semicircular canals of the inner ear. On the other hand, the pituitary is reduced in size when compared to sauropods.

The Cranial Endocast of Ornithischia

The first described dinosaur endocranial cavity belonged to *Iguanodon* (Hulke 1871; Fig. 8.2a), but it appears the first endocast described came from a *Stegosaurus* (Marsh 1880; Fig. 8.2b). Unlike saurischians, more than a half of the known ornithischian brains were studied using physical endocasts. They are known for representatives of all main clades including Ornithopoda, Thyreophora (Ankylosauria and Stegosauria), and Marginocephalia (Ceratopsia and Pachycephalosauria), with stegosaurians and pachycephalosaurians remaining the less explored group in terms of number of studied taxa (Table 8.1 and Fig 8.12). Contrarily, the ornithopods are best known group due to their excellent fossil record, particularly of hadrosaurids (see Lull and Wright 1942; Horner et al. 2004 for reviews).

Most ornithischians have anteroposteriorly extended and transversely narrow endocasts, differing from that of many non-avian theropods in having relatively shorter olfactory apparatus, as observed in iguanodontians (*Dryosauridae*, *Iguanodon*), stegosaurs, and ceratopsians (although not particularly in basal representatives such as psittacosaur which have markedly elongated olfactory bulbs), and/or expanded cerebral hemispheres, as observed in hadrosaurids. On the other hand, ankylosaurs, and to some degree pachycephalosaurians, have short and transversely wide and bulbous endocasts that are more reminiscent of the morphology present in derived sauropods (Figs. 8.12 and 8.13d, g).

The pattern of angle flexures between forebrain, midbrain and hindbrain is equally angular in practically the entire clade except in iguanodontids and hadrosaurids (Giffin 1989). The variation in the pattern of angle flexion seems to depend on the absolute size of the skull and the relative size of the eye, and thus, the smallest taxa tend to have more sigmoidal endocasts (e.g. pachycephalosaurians, psittacosaurians, basal iguanodontians) than the largest forms, and the same variation is observed between juvenile and adult individuals of the same genus (e.g. Giffin

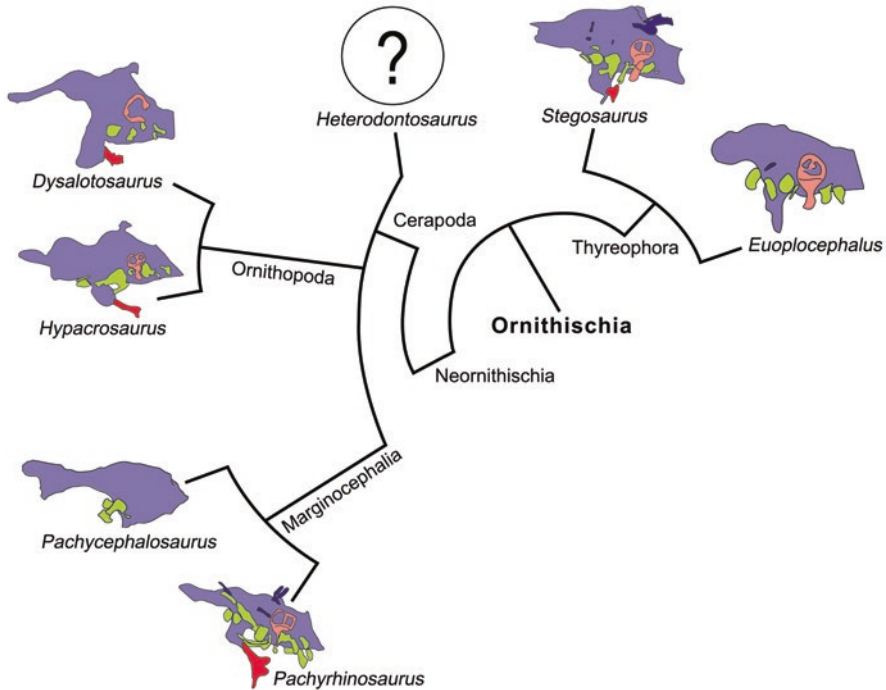


Fig. 8.12 Simplified cladogram of Ornithischia showing the phylogenetic relationships of selected taxa and their endocasts. Endocasts were redrawn from: *Pachyrhinosaurus* (Witmer and Ridgely 2008b), *Pachycephalosaurus* (Giffin 1989), *Hypacrosaurus* (Evans et al. 2009), *Dysalotosaurus* (Lautenschlager and Hübner 2013), *Stegosaurus* (Leahey et al. 2015), *Euoplocephalus* (Ösi et al. 2014). Not to scale

1989; Lautenschlager et al. 2012; Bullar et al. 2019), following a similar pattern as that observed in living birds (Walsh and Milner 2011).

There is a high variability on visible forebrain structures among ornithischian clades. The olfactory tracts are relatively anteroposteriorly elongated in basal and derived ceratopsians (Forster 1996; Zhou et al. 2007), but are shorter and the olfactory bulbs are just in front the cerebral hemispheres in hadrosaurids (Evans et al. 2009; Becerra et al. 2018), and ankylosaurs (e.g. Miyashita et al. 2011; Ösi et al. 2014; Paulina-Carabajal et al. 2016b, 2018b), with an intermediate situation observed in stegosaurs and pachycephalosaurs (Giffin 1989; Galton 2001; Bourke et al. 2014). The olfactory system in hadrosaurids constitutes between 3% and 7% of the endocranial volume, something similar to the sauropod *Nigersaurus* (Evans et al. 2009). This is, relatively smaller than in other dinosaurs including ceratopsians and theropods. However, more comprehensive analyses of olfactory bulb size ratio and olfactory acuity among ornithischians have not yet been done.

The cerebral hemispheres are well-defined in most clades, being separated from the olfactory tract by a conspicuous constriction. The cerebrum however, is not markedly laterally expanded in most groups, except in hadrosaurids where a dense

net of blood vessels suggests that this region of the endocast reflects the actual shape of the cerebral hemispheres (Osmólska 2004; Evans 2005; Witmer et al. 2008). In all ornithischians, the endocasts constrict markedly posterior to the cerebrum, maintaining a constant narrow width along the medulla. This post-cerebral region (hind-brain) is similar to most other dinosaurs in the lack of detailed morphology due the presence of a large longitudinal sinus, thus suggesting that it was not closely related to the endocranial wall (Evans 2005). The floccular lobes are so small and superficial in ornithischians that they are not distinguished in most endocasts: So far, this structure has been reported in primitive iguanodontians of the dryosaurid family (*Dryosaurus*: Galton 1989; Lautenschlager and Hübner 2013), small ornithopods of the thescelosaurid family (*Dysalotosaurus* and *Hypsilophodon*: Galton 1989), in ankylosaurids –but not in nodosaurids– (Miyashita et al. 2011; Paulina-Carabajal et al. 2016b, 2018b), and in stegosaurs (Galton 1988, 2001). Within the latter group the flocculus is however not reconstructed in the digital rendering of *Stegosaurus stenops* made by Leahey et al. (2015), whereas the floccular recess is absent in the endocranial cavity of the specimen YPM 1853 (*S. unguatus* at Yale Peabody Museum, APC pers. obs) suggesting some degree of intra and interspecific variation for the genus *Stegosaurus*.

Most of the data about ornithischian paleoneurology comes from derived Cretaceous forms, whereas Jurassic taxa are represented by a few basal ornithopods and stegosaurs (Table 8.1). Also, most of the data is from taxa from the Northern Hemisphere, whereas the endocranial anatomy of taxa from the Southern Hemisphere remains poorly explored, with only three studied species: *Secernosaurus australis* from South America (Becerra et al. 2018), the stegosaurid *Kentrosaurus aethiopicus* from Africa (Hennig 1925; Galton 1988, 2001), and the thyreophoran *Kunbarrasaurus ieverisi* from Australia (Leahey et al. 2015).

Ornithopoda Ornithopods are the better studied group with around 30 species with known neuroanatomy, although the Jurassic representatives remain yet poor compared to the Cretaceous forms (Table 8.1). According to Hopson (1979) the forebrain-midbrain flexion in iguanodontids and hadrosaurids is considerably reduced and the midbrain-hindbrain flexion is practically eliminated, resulting in a more or less straight endocranial cavity. Ornithopod endocasts characterize by transversely expanded cerebral hemispheres that are faithful copies of the soft tissues, as the blood vessels indicate (Evans 2005), whereas in the Early Cretaceous *Leallenyssaura* is possible to observe the optic lobes in dorsal view (Rich and Rich 1989). Particularly in lambeosaurines the cerebral hemispheres are strikingly large, globose and broad, surpassing the 40–50% of the total endocranial volume –without the olfactory system– (Evans et al. 2009; Cruzado-Caballero et al. 2015). The relative large brain size in some ornithopods (e.g *Proa*) represents a degree of encephalization compatible –or even larger– with theropods, suggesting a trend towards increased relative brain size during ornithopod evolution with (see Knoll et al. 2021 and references therein).

Thyreophora (Ankylosauria and Stegosauria) Ankylosaurs were among the least explored clades. Although nearly a dozen of species have been studied, all taxa

represent Cretaceous forms, and the current understanding of their evolution remain unclear (e.g. Nopcsa 1929; Pereda-Suberbiola and Galton 1994; Carpenter et al. 2001; Witmer and Ridgely 2008a; Ösi et al. 2014; Leahey et al. 2015; Paulina-Carabajal et al. 2016b, 2018b; Table 8.1). Most ankylosaurs share an anteroposteriorly short endocranium with globose forebrain and large pituitary and internal carotid arteries (Fig. 8.12). Relatively large olfactory bulbs have been also described for the ankylosaurs *Bissektipelta* (Kuzmin et al. 2020), *Euoplocephalus* (Miyashita et al. 2011) and *Tarchia* (Paulina-Carabajal et al. 2018b), suggesting a better sense of smell in ankylosaurids than in nodosaurids, although the nodosaurids *Hungarosaurus* and *Struthiosaurus* (Ösi et al. 2014) have relatively large olfactory bulbs as well. The Olfactory Ratios vary from 44% in nodosaurids to 52% in ankylosaurids (Paulina-Carabajal et al. 2016b). The flocculus of cerebellum is absent in all studied nodosaurids so far, but has been identified in some ankylosaurids, suggesting a differentiated brain pattern between these families (Paulina-Carabajal et al. 2018b).

Stegosaurian endocrania are among the first ones being studied, but only four or five Jurassic species have known neuroanatomy so far (e.g. Marsh 1880; Gilmore 1914; Galton 1988, 2001; Table 8.1). Stegosaurs have tubular, long and narrow endocrania with low flexures and large venous sinuses obscuring the shape of the brain. They exhibit low brain to body mass ratios, and the lowest calculated REQs among dinosaurs (e.g. Hopson 1979; Figs. 8.12 and 8.14).

Marginocephalia (Ceratopsia and Pachycephalosauria) The first ceratopsian endocranium was studied by Marsh (1889) and quite some time later the first pachycephalosaurian endocranium was made (Brown and Schlaikjer 1940), although a well-described and illustrated endocranium showing the shape of the cerebrum and olfactory bulbs was made by Lambe in 1918. The group remains poorly studied compared to other dinosaurs, and today cranial endocrania of less than ten species of ceratopsians (e.g. Marsh 1896; Langston Jr 1975; Forster 1996; Tykoski and Fiorillo 2012; Napoli et al. 2019; Zhang et al. 2019) and about five valid species of pachycephalosaurians (e.g. Maryanska and Osmólska 1974; Hopson 1979; Giffin et al. 1987; Giffin 1989) have been studied (Table 8.1).

Among ceratopsians the olfactory bulbs are relatively larger in basal (e.g. *Auroraceratops*, *Psittacosaurus*; Zhou et al. 2007; Napoli et al. 2019; Zhang et al. 2019) than in more derived forms (e.g. *Pachyrhinosaurus*; Witmer and Ridgely 2008b), although these lobes are relatively large compared to other dinosaurs, suggesting a well-developed sense of smell for the group in general. The cerebral hemispheres are poorly expanded and the dorsal venous sinus obscures other brain structures (e.g. Forster 1996). A well-differentiated pituitary connected with strikingly large passages for the cerebral internal carotid arteries characterize the ceratopsian endocranium (e.g. Zhou et al. 2007; Witmer and Ridgely 2008a, b; Zhang et al. 2019).

Pachycephalosaurs have simple and more or less tubular endocrania, although exhibit a more globose cerebrum and a marked sigmoidal shape than ceratopsians, probably responding to the differential position of the head in these bipedal

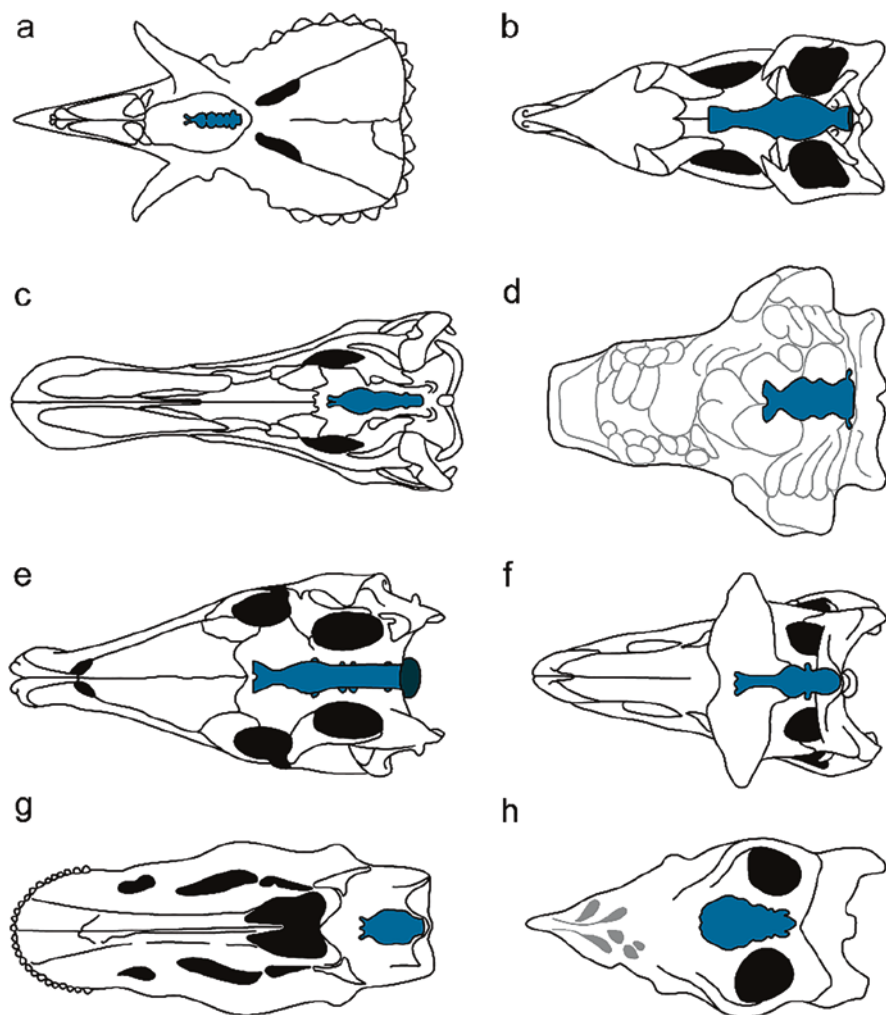


Fig. 8.13 Line drawings of the skull and brain (blue color) of main groups of dinosaurs in dorsal view. (a), Ceratopsia; (b), basal Sauropodomorpha; (c), hadrosauridae; (d), Ankylosauria; (e), Stegosauria; (f), non-maniraptoran Theropoda; (g), Sauropoda; (h), Oviraptorosauria. (a, c, e, g, redrawn from Marsh 1896; b, after Bronzati et al. 2019; d, after Paulina-Carabajal et al. 2016b; f, after Cerroni and Paulina-Carabajal 2019; h, after Balanoff and Norell 2012 and Kundrát 2007). Not to scale

dinosaurs, and to a reorganization of the skull bones to head butting behavior (e.g. Giffin 1989; Hopson 1979; Bourke et al. 2014). As in ceratopsians, the olfactory bulbs are relatively large, and the olfactory tracts are short but well defined, suggesting an acute sense of smell in this group (Giffin 1989). The cerebral hemispheres are laterally expanded (surpassing the olfactory bulbs width) and giving the endocast a convex shape dorsally (Fig. 8.12). One of the most complete endocasts is that of

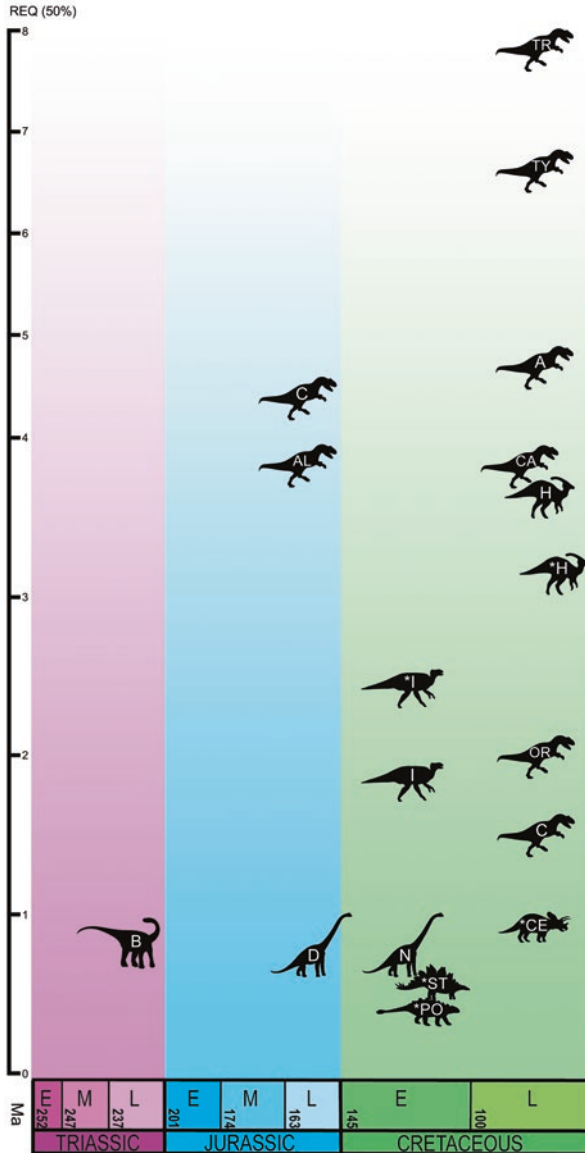


Fig. 8.14 Dinosaur (Reptile) Encephalization Quotient (REQ/EQ). Graphic showing the mean EQ and REQ (with asterisk) calculated for certain dinosaur taxa. Abbreviations: *A* allosauroidea, *C* Ceratosauria, *CA* Caenagnathoidea, *CE* ceratopsia, *D* *Diploducus*, *H* hadrosaurid, *I* iguanodontids, *N* *Nigersaurus*, *OR* ornithomimosauria, *PO* Polacanthus, *ST* Stegosauria, *TR* troodontidae, *TY*, tyrannosauroidae. (Sources of data: Hopson 1979; Franzosa 2004; Witmer et al. 2008; Zhou et al. 2007; Evans et al. 2009; Lauters et al. 2012; Hurlburt et al. 2013)

Pachycephalosaur (Brown and Schlaikjer 1943). It has the anterior margins of each cerebral hemisphere not rounded but pointed, a shape resulting from the presence of dorsal venous sinuses, as in the living *Alligator* (Witmer et al. 2008). The infundibulum is robust and the pituitary is relatively larger than that reconstructed for *Stegoceras* (Bourke et al. 2014).

8.4 Evolutionary Patterns in Dinosaur Neuroanatomy

8.4.1 Encephalization Quotient

Since the beginning of paleoneurological science, there have been attempts to correlate brain size with ‘intelligence’ or neuronal capacity, and now it is widely accepted that the analysis of brain size provides insights into different aspects of the nervous system (e.g. Jerison 1969, 1973; Hopson 1977, 1979, 1980; Larsson et al. 2000; Iwaniuk and Nelson 2002; Buchholtz 2012; Hurlburt et al. 2013; Morhardt 2016; Balanoff and Bever 2017; Dumoncel et al. 2020). However, cognitive characters of a given taxon may not be predicted from the brain size only, and there is also no easy or reliable way to measure brain size (or determine the development of certain regions of the brain) from an endocast. Also, brain size alone may not be sufficient data to predict cognitive capabilities in a given animal, although the analysis of this measure may help to understand the evolution of the central nervous system through comparative studies. Jerison (1973) developed an equation called Encephalization Quotient (EQ) to investigate the allometric relation between the brain and body size. This equation, which was modified by Hurlburt (1996) as the Reptile EQ to adjust the regression to the reptilian lineage, represents an individual’s actual brain size divided by the expected brain size for its particular body size, calculated in turn using an allometric relationship derived from a large extant sample (e.g. Jerison 1973; Evans et al. 2009). Hurlburt et al. (2013) made the first measurements of dinosaur relative brain size using REQ, and also estimated the dinosaur relative brain and cerebrum size by calculating the cerebrum: a cerebrocast ratio. The cerebrum fills the braincase more completely than other parts of the brain in living reptiles and many groups of dinosaurs, becoming the most recognizable feature in any endocast (Hopson 1977; Larsson et al. 2000). The REQ is then a useful tool to determine relative brain size and compare it with the same data for taxa of different body sizes. However, it should be used with caution because quantifying the ‘intelligence’ of a dinosaur is fraught with uncertainties, and many aspects should be considered: (1) there is no direct correlation between a larger brain and a greater intelligence, (2) dinosaur endocasts are poor models of the brain in general, and 3) corrections need to be done in order to estimate the most accurate brain size (e.g. Hurlburt et al. 2013), and also body size, since mass estimates in dinosaurs in general are questionable. Furthermore, different authors have obtained a wide range of brain volume and body size values even for a single taxon or specimen, and with body size estimates based on different formulas (see Christiansen and Fariña 2004;

Benson et al. 2014, 2018; Campione and Evans 2020). The influence of such measurement variations has not been comprehensively analyzed among dinosaurs yet. These uncertainties in the calculation of the base data (body size and brain volume) in extinct taxa do not prevent the REQ from being a useful comparative metric (Evans et al. 2009).

Among dinosaurs, some ornithischians have REQs in the same range as coelurosaur theropods (e.g. the iguanodont *Proa valdearinnensis*), whereas sauropods (but not sauropodomorphs) and marginocephalians exhibit the lowest values (Hopson 1977; Buchholtz 1997; Evans et al. 2009; Lautenschlager et al. 2012; Hurlburt et al. 2013; Knoll et al. 2021; Fig. 8.14). Within theropods, the analyses made using calculated REQs indicate that the brain becomes larger in derived groups, with dromaeosaurids and troodontids having the highest values. In the coelurosaurian lineage it has been suggested that most of the enlargement occurred within the forebrain, particularly in the relative cerebrum size (Larsson et al. 2000; Brusatte 2012). The mean values for most theropod taxa are, however, only slightly larger than in living crocodylians, except for certain small maniraptoriforms (*Bambiraptor*, *Ornithomimus*, *Troodon*) and particularly oviraptorosaurs which have an index that falls within the range of extant birds (and outside that of the non-avian dinosaurs) (Hurlburt et al. 2013; Balanoff et al. 2014). As mentioned above, high values within the range of living birds were found also in some ornithopods, and recent work on the paleoneurology of ornithischian dinosaurs showed a trend towards the increment of relative brain size during ornithopod evolution from the late Jurassic onwards (Knoll et al. 2021 and references therein). The high EQ/REQ values found in Cretaceous relatively large forms such as *Proa*, suggest that an increasing encephalization was fostered not only in theropods but also in parallel in the shorter-lived lineage of ornithopods (Knoll et al. 2021; Fig. 8.14).

Among non-sauropodan sauropodomorph taxa, an encephalization quotient can only be calculated for *Buriolestes schultzi*, and its REQ is higher than that of all sauropods for which this metric can be calculated, although is not higher than that in non-coelurosaur theropods (Müller et al. 2021). It is thus certainly tempting to consider the giant sauropods as slow-moving animals (although this was already suspected from their extremely large bodies), given that brain size has previously been proposed as a proxy for intelligence and agility (Jerison 1973). Therefore, there is nothing extraordinary in the fact that sauropods have relatively small brains, as the relation between brain and body sizes is of negative allometry (Hopson 1979). Furthermore, factors such as the number of cortical neurons and conduction velocity are better indicators of information-processing capacity, and hence better proxies for intelligence (Roth and Dicke 2005). However, it is interesting that even *Buriolestes* has a REQ value smaller than that of all other theropods for which the value is known (Müller et al. 2021). It is not possible to establish if the REQ of *Buriolestes* is the retention of an ancestral trait or if it corresponds to a derived feature of sauropodomorphs when compared to other dinosaurs. Apart from *Buriolestes*, so far REQ values could only be calculated for Jurassic and Cretaceous dinosaurs.

8.4.2 *Brain Architecture and Evolution*

Comparative neuroanatomists have long recognized the intimate connection between the development of the brain and evolution, and the degree of encephalization across vertebrates (e.g. Watanabe et al. 2021 and references therein). The plesiomorphic condition for reptiles is an elongate brain whose neuroanatomical regions are arranged almost linearly whereas birds exhibit a derived neuroanatomy with expanded cerebrum and cerebellum and displacement of the optic tectum ventrolaterally (Hopson 1979; Butler and Hodos 2005; Balanoff and Bever 2017). This plesiomorphic architecture of the reptile brain is conserved among dinosaurs, where a linear arrangement of the main brain regions is observed in all basal forms, including most ornithischians, sauropodomorphs and early theropods (Balanoff and Bever 2017; and references therein).

The derived transformation that resulted in the modern S-shaped brain in avian theropods does not appear in the dinosaurian fossil record until deep within the history of theropods, at the origins of the clade Maniraptora and prior to the origins of the avian crown clade (Balanoff and Bever 2017). Some closely-related non-avian theropods, such as oviraptorosaurs and troodontids, exhibit allometric trends in brain-to-body size similar to that in some living avian theropods (Balanoff et al. 2013; Watanabe et al. 2021). Recent work suggests that the evolution of each region of the brain occurs under a mosaic brain evolution mode (Balanoff et al. 2016b). During the transformation from the plesiomorphic linear brain into the derived sinusoidal brain, cerebral hyperinflation was the primary driver of encephalization and it was probably correlated with transformations of the maniraptoran cranial morphology such as expansion of the cranial vault, enlargement of the orbits, and shortening of the craniofacial region (Balanoff and Bever 2017 and references therein). Volumetric evidence indicating pulses of cerebral expansion occurring among non-avian maniraptoran dinosaurs suggests that an ancestrally more modular brain allowed for increasingly encephalized brains and globular cerebra to evolve prior to, and even after, the origin of Avialae (Balanoff et al. 2013; Ksepka et al. 2020; Watanabe et al. 2021).

Despite the fact that sauropods have no living representatives, a similar pattern is observed in the lineage with the basal sauropodomorph *Buriolestes schultzi* exhibiting a more anteroposteriorly elongated endocast whereas derived forms (e.g. titanosaurs) exhibit a more sigmoid shape in lateral view. *Buriolestes* is usually recovered as the sister group of all other sauropodomorphs in phylogenetic analyses of the group (see e.g. Müller et al. 2021). Thus, given its phylogenetic position and the presence of traits in its endocast that are mostly similar to those of other early dinosaurs, it is safe to consider the neuroanatomy of *Buriolestes* as very close to the ancestral morphology for Sauropodomorpha as a whole. As mentioned above, brain shape is highly correlated with the morphology of the skull roof in reptiles (Fabbri et al. 2017), and this also seems to hold true for sauropodomorph dinosaurs. One of the most distinctive features of sauropods is the presence of an anteroposteriorly short skull, with the length usually accounting for less than 50% of the length of the

femur. On the other hand, the oldest sauropodomorphs such as *Buriolestes* had proportionally longer skulls, with skull length accounting for more than 70% of the femoral length. The reduction of the skull in sauropods is mostly notable in the temporal region, where the braincase is located (Bronzati et al. 2018). Thus, the reduction of the anteroposterior length of the endocast in sauropods, with the accompanying reduction of the olfactory tract, and the appearance of more marked flexures, is more likely to be correlated with skull length reduction and verticalization of the occipital plate, rather than possessing any ecological significance.

8.5 Future Directions and Conclusions

Most research on dinosaur paleoneurology has focused on the neuroanatomy of the taxon under study only, and there are considerably fewer studies that go further towards a descriptive analysis in order to understand ontogenetic changes (e.g. Lautenschlager and Hübner 2013), evolutionary patterns (e.g. Witmer and Ridgely 2009; Balanoff et al. 2010; Lauters et al. 2012; Lautenschlager et al. 2012) or documenting neuroanatomical transformations of the modular brain in deep time (e.g. Balanoff and Bever 2017), in specific clades.

Most likely the fossil record will eventually provide information that will fill the gaps in our understanding of dinosaur endocranial anatomy and ontogeny. However, some authors have stated that the major constraints facing research in paleoneurology center on the accuracy and reliability of the correlation between the endocast morphology and the complexity and modularity of the actual brain (Balanoff and Bever 2017). Although the quantitative relationship between the osteological correlates (landmarks) and the neuroanatomy require verification in a broader sample of lineages, the approach appears useful in tracing the modular nature of the brain in deep time (Balanoff et al. 2013, 2015; Balanoff and Bever 2017). Futures studies that may improve our understanding of the pattern of neurosensory evolution in dinosaurs include the addition of unknown taxa (filling gaps in the phylogeny), more exhaustive integrative morphological analyses, seeking correlations between diversity radiations and evolutionary brain changes through the Mesozoic (do they occur in different lineages at the same time?), advances in the field of sensory biology and behavior, etc.

Finally, as pointed out by Balanoff and Bever (2017), the analysis of volume remains an important aspect of endocast vs brain comparative studies, however the complexity of the brain in terms of structure and function, will be always exceed the information we can obtain from the available structures in an endocast. No matter how far paleoneurology and sensory biology have progressed, we must keep in mind that it remains a challenge to obtain reliable information about behavior in modern relatives such as crocodylians and birds (e.g. Vergne et al. 2009).

Final Remarks Dinosaur paleoneurology is a growing discipline that seeks to understand the evolutionary pattern of the central nervous system in these extinct

animals, hand-in-hand with the field of comparative neurology of their living relatives. Today, the cranial endocast morphology of most dinosaur families is known, and hypotheses about the evolutionary pattern of their brains (particularly in the lineages leading into the flying dinosaurs) and senses (dealing especially with the senses commonly known as sight, smell, hearing and touch) have been proposed. Poorly explored aspects often hinge on lack of data in the fossil record, which particularly impedes our understanding of ontogenetic changes, inter- and intra-species morphological variation, and possible ecological adaptations and lifestyle. The arrival of non-invasive technologies, such as X-ray computed tomography or neutron micro-tomography, are increasing enormously the number of studied taxa, including those groups with smaller body sizes. In this sense, the improved knowledge of dinosaur brain anatomy and sensory systems is allowing, for the first time in many groups, more comprehensive analysis of the morphological data provided by the endocasts using quantitative methods. Thus, the trends and future directions in dinosaur paleoneurology will be oriented towards the analysis of macroevolutionary and morphofunctional patterns, but also to the field of sensory perception, seeking for adaptive signals and paleobiological implications on behavior and occupation of ecological niches, among others.

References

- Agnolín FL, Cerroni MA, Scanferla A et al (2022) First definitive abelisaurid theropod from the Late Cretaceous of Northwestern Argentina. *J Vertbr Paleontol* 41:e2002348
- Ali F, Zelenitsky D, Therrien F et al (2008) Homology of the “ethmoid complex” of tyrannosaurids and its implications for the reconstruction of the olfactory apparatus of non-avian theropods. *J Vertebr Paleontol* 28:123–133
- Alifanov VR, Barsbold R (2009) *Ceratomykus oculus* gen. et sp. nov., a new dinosaur (?Theropoda, Alvarezsauria) from the Late Cretaceous of Mongolia. *Paleontol J* 43:94–106
- Alifanov VR, Saveliev V (2011) Brain structure and neurobiology of alvarezsaurians (Dinosauria), exemplified by *Ceratomykus oculus* (Parvicursoridae) from the Late Cretaceous of Mongolia. *Paleontol J* 45:183–190
- Alifanov VR, Saveliev V (2019) The brain morphology and neurobiology in armored dinosaur *Bissekipelta archibaldi* (Ankylosauridae) from the Late Cretaceous of Uzbekistan. *Paleontol J* 53:315–321
- Allemand RR, Boistel G, Daghfous Z et al (2017) Comparative morphology of snake (Squamata) endocasts: evidence of phylogenetic and ecological signals. *J Anat* 231:849–868
- Andrews CW (1897) Note on a cast of the brain-cavity of *Iguanodon*. *Ann Mag Nat Hist (ser. 6)* 19:585–591
- Andrzejewski KA, Polcyn MJ, Winkler DA et al (2019) The braincase of *Malawisaurus dixeyi* (Sauropoda: Titanosauria): a 3D reconstruction of the brain endocast and inner ear. *PLoS One* 14:e0211423. <https://doi.org/10.1371/journal.pone.0211423>
- Aranciaga Rolando M, Cerroni MA, Garcia Marsà JA et al (2020) A new medium-sized abelisaurid (Theropoda, Dinosauria) from the late cretaceous (Maastrichtian) Allen Formation of Northern Patagonia, Argentina. *J S Am Earth Sci* 102915. <https://doi.org/10.1016/j.jsames.2020.102915>
- Arbour VM, Currie PJ (2016) Systematics, phylogeny and palaeobiogeography of the ankylosaurid dinosaurs. *J Syst Palaeontol* 14:385–444

- Armitage MH (2021) First report of peripheral nerves in bone from *Triceratops horridus* occipital condyle. *MTO* 29(2):20–25
- Atterholt J, Wedel MJ (2019) Neural canal ridges: A novel osteological correlate of post-cranial neurology in dinosaurs. *Peer J Preprints* 7:e27967v1. <https://doi.org/10.7287/peerj.preprints.27967v1>
- Azuma Y, Xu X, Shibata M et al (2016) A bizarre theropod from the Early Cretaceous of Japan highlighting mosaic evolution among coelurosaurians. *Sci Rep* 6:20478. <https://doi.org/10.1038/srep20478>
- Báez AM, Púgener A (2003) Ontogeny of a new Palaeogene pipid frog from southern South America and xenopodinomorph evolution. *Zool J Linn Soc* 139:439–476
- Balanoff AM, Bever GS (2017) The role of endocast in the study of brain evolution. In: Kaas JH (ed) *Evolution of nervous systems*, vol 1. Elsevier, Amsterdam, pp 223–241
- Balanoff AM, Bever GS (2020) The role of endocasts in the study of brain evolution. In: Kaas J (ed) *Evolutionary neuroscience*. Elsevier, pp 29–49
- Ballell A, King JL, Neenan JM et al (2021) The braincase, brain and palaeobiology of the basal sauropodomorph dinosaur *Thecodontosaurus antiquus*. *Zool J Linn Soc* 193:541–562
- Balanoff AM, Bever GS, Ikejiri T (2010) The braincase of *Apatosaurus* (Dinosauria, Sauropoda) based on Computed Tomography of a new specimen with comments on variations and evolution in sauropod neuroanatomy. *Am Nov* 3677:1–29
- Balanoff AM, Bever GS, Rowe TB et al (2013) Evolutionary origins of the avian brain. *Nature* 501(7465):93–96
- Balanoff AM, Bever GS, Norell MA (2014) Reconsidering the avian nature of the oviraptorosaur brain (Dinosauria: Theropoda). *PoS One* 9(12):e113559. <https://doi.org/10.1371/journal.pone.0113559>
- Balanoff AM, Norell M (2012) Osteology of *Khaan mckennai* (Oviraptorosauria: Theropoda). *Bull Am Mus Nat Hist* 372:1–77
- Balanoff AM, Smaers JB, Turner AH (2016a) Brain modularity across the theropod-bird transition: testing the influence of flight on neuroanatomical variation. *J Anat* 229(2):204–214
- Balanoff AM, Bever GS, Colbert MW et al (2016b) Best practices for digitally constructing endocranial casts: examples from birds and their dinosaurian relatives. *J Anat* 229:173–190
- Balanoff A, Norell MA, Hogan A et al (2018) The endocranial cavity of oviraptorosaur dinosaurs and the increasingly complex, deep history of the avian brain. *Brain Behav Evol* 91(3):125–135
- Ballell A, King JL, Neenan JM et al (2021) The braincase, brain and palaeobiology of the basal sauropodomorph dinosaur *Thecodontosaurus antiquus*. *Zool J Linn Soc* 193(2):541–562
- Baron MG (2019) *Pisanosaurus mertii* and the Triassic ornithischian crisis: could phylogeny offer a solution? *Hist Biol* 31:967–981
- Baron MG, Norman DB, Barrett PM (2017) A new hypothesis of dinosaur relationships and early dinosaur evolution. *Nature* 543:501–506
- Barker CT, Naish D, Newham E et al (2017) Complex neuroanatomy in the rostrum of the Isle of Wight theropod *Neovenator salerii*. *Sci Rep* 7:3749. <https://doi.org/10.1038/s41598-017-03671-3>
- Barrett PM, Upchurch P (2007) The evolution of feeding mechanisms in early sauropodomorph dinosaurs. In: PM Barrett, DJ Batten (eds), *Evolution and palaeobiology of early sauropodomorph dinosaurs*. *Special Pap Palaeontol* 77:91–112
- Baumel E, Witmer LM (1993) Osteology. In: Baumel E, King A, Breazile JE, Evans H, Vanden Bergue JC (eds) *Handbook of Avian anatomy: Nomina Anatomica Avium*. Cambridge University Press, pp 45–132
- Becerra MG, Paulina-Carabajal A, Cruzado-Caballero P et al (2018) First endocranial description of a South American hadrosaurid: The neuroanatomy of *Secernosaurus koernerii* from the Late Cretaceous of Argentina. *Acta Palaeontol Pol* 63(4):693–702
- Benson RBJ, Campione NE, Carrano MT et al (2014) Rates of dinosaur body mass evolution indicate 170 million years of sustained ecological innovation on the avian stem lineage. *PLoS Biol* 12(5):1001853. <https://doi.org/10.1371/journal.pbio.1001853>

- Benson RB, Hunt G, Carrano M et al (2017) Cope's rule and the adaptive landscape of dinosaur body size evolution. *Palaeontology* 61:13–48
- Benson RBJ, Hunt G, Carrano MT et al (2018) Cope's rule and the adaptive landscape of dinosaur body size evolution. *Palaeontology* 61(1):13–48
- Benton M (1979) Ectothermy and the success of dinosaurs. *Evol* 33(3):983–997
- Benton (2004) Origin and relationships of Dinosauria. In: D Weishampel (ed), *The Dinosauria*, University of California Press pp 6–19
- Bever GS, Brusatte SL, Balanoff AM et al (2011) Variation, variability, and the origin of the avian endocranium: insights from the anatomy of *Alioramus altai* (Theropoda: Tyrannosauroida). *PLoS One* 6:e23393. <https://doi.org/10.1371/journal.pone.0023393>
- Bever GS, Brusatte SL, Carr TD et al (2013) The braincase anatomy of the Late Cretaceous dinosaur *Alioramus* (Theropoda: Tyrannosauroida). *Bull Am Mus Nat Hist* 376:1–72
- Beyrand V, Voeten DFA, Bures S et al (2019) Multiphase progenetic development shaped the brain of flying archosaurs. *Sci Rep* 9:10807. <https://doi.org/10.1038/s41598-019-46959-2>
- Bourke JM, Porter WMR, Ridgely RC et al (2014) Breathing life into dinosaurs: tackling challenges of soft-tissue reconstruction and nasal airflow in extinct species. *Anat Rec* 297:2148–2186
- Boyd CA (2015) The systematic relationships and biogeographic history of ornithischian dinosaurs. *Peer J* 3:e1523. <https://doi.org/10.7717/peerj.1523>
- Brasier MD, Norman DB, Liu AG et al (2016) Remarkable preservation of brain tissues in an Early Cretaceous iguanodon dinosaur. *Geol Soc Spec Publ* 448:383–398
- Breeden BT III, Raven TJ, Butler RJ et al (2021) The anatomy and palaeobiology of the early armoured dinosaur *Scutellosaurus lawleri* (Ornithischia: Thyreophora) from the Kayenta Formation (Lower Jurassic) of Arizona. *R Soc Open Sci* 8(7):201676. <https://doi.org/10.1098/rsos.201676>
- Brochu CA (2000) A digitally-rendered endocast for *Tyrannosaurus rex*. *J Vertebr Paleontol* 20:1–6
- Brochu C (2003) Osteology of *Tyrannosaurus Rex*: insights from a nearly complete skeleton and high-resolution Computed Tomographic analysis of the skull. *J Vertebr Paleontol* 7:1–138
- Bronzati M (2017) Should the terms 'basal taxon' and 'transitional taxon' be extinguished from cladistic studies with extinct organisms? *Palaeontologia Electronica* 20.2.3E:1–12
- Bronzati M, Rauhut OWM (2017) Braincase redescription of *Efraasia minor* Huene, 1908 (Dinosauria: Sauropodomorpha) from the Late Triassic of Germany, with comments on the evolution of the sauropodomorph braincase. *Zool J Linn Soc* 182:173–224
- Bronzati M, Rauhut OWM, Bittencourt JS et al (2017) Endocast of the Late Triassic (Carnian) dinosaur *Saturnalia tupiniquim*: implications for the evolution of brain tissue in Sauropodomorpha. *Sci Rep* 7:11931. <https://doi.org/10.1038/s41598-017-11737-5>
- Bronzati M, Benson RB, Rauhut OWM (2018) Rapid transformation in the braincase of sauropod dinosaurs: integrated evolution of the braincase and neck in early sauropods? *Palaeontology* 61(2):289–302
- Bronzati M, Lagner M, Rauhut OWM (2019) Braincase anatomy of the early sauropodomorph *Saturnalia tupiniquim* (Late Triassic, Brazil). *J Vertebr Paleontol* e1559173
- Brown DB (1914) *Anchiceratops*, a new genus of horned dinosaurs from the Edmonton Cretaceous of Alberta; with discussion of the origin of the ceratopsian crest and the brain casts of *Anchiceratops* and *Trachodon*. *Bull Am Mus Nat Hist* 33:539–548
- Brown B, Schlaikjer EM (1940) The structure and relationships of *Protoceratops*. *Ann N Y Acad Sci* 40:133–266
- Brown B, Schlaikjer EM (1943) A study of the toodontid dinosaurs with the description of a new genus and four new species. *Bull Am Mus Nat Hist* 82(5):115–150
- Bruce LL (2006) Evolution of the nervous system in reptiles. In: Kaas JH (ed) *Evolution of nervous systems, The evolution of nervous systems in non-mammalian vertebrates*, vol II. Elsevier, Amsterdam, pp 125–156
- Bruce L (2009) Evolution of the brain in reptiles. In: Binder, Hiokawa, Windhorst (eds) *Encyclopedia of Neuroscience*, Springer, Berlin, pp 1295–1301
- Brusatte SL (2012) *Dinosaur paleobiology*. Wiley-Blackwell, Oxford

- Brusatte SL, Chure DJ, Benson RBJ et al (2010a) The osteology of *Shaochilong maortuensis*, a carcharodontosaurid (Dinosauria: Theropoda) from the Late Cretaceous of Asia. *Zootaxa* 2334:1–46
- Brusatte SL, Nesbitt SJ, Irmis RB et al (2010b) The origin and early radiation of dinosaurs. *Earth-Sci Rev* 101:68–100
- Brusatte SL, Averianov A, Sues H-D et al (2016) New tyrannosaur from the mid-Cretaceous of Uzbekistan clarifies evolution of giant body sizes and advanced senses in tyrant dinosaurs. *PNAS* 113:3447–3452
- Buchholtz E (1997) Paleoneurology. In: Currie PJ, Padian K (eds) *Encyclopedia of dinosaurs*. Academic Press, San Diego, pp 522–524
- Buchholtz E (2012) Dinosaur paleoneurology. In: Brett-Surman MK, Holtz TR Jr, Farlow JO (eds) *The complete dinosaur*. Indiana University Press, Bloomington, pp 191–208
- Buchholtz E, Seyfarth E-A (2001) The study of “Fossil Brains”: Tilly Edinger (1897–1967) and the beginnings of Paleoneurology. *BioScience* 51:674–682
- Bullar CM, Zhao Q, Benton MJ et al (2019) Ontogenetic braincase development in *Psittacosaurus lujiatunensis* (Dinosauria: Ceratopsia) using micro-computed tomography. *Peer J* 7:e7217. <https://doi.org/10.7717/peerj.7217>
- Burch SH, Paulina-Carabajal A, O’Connor P et al (in press). Dinosaur soft tissues. In: Weishampel D, Barret P, Carrano M, Mackovik P (eds), *The dinosauria*, 3rd edn. Cambridge University Press, Berkeley
- Bürckhardt R (1892) Das Gehirn von *Triceratops flabellatus* Marsh. *Neues Jahrb Min Geol Paläontol* 1892(Bd.2):71–72. [in German]
- Burnham DA (2004) New information on *Bambiraptor feinbergi* (Theropoda: Dromaeosauridae) from the Late Cretaceous of Montana. In: Currie PJ, Koppelhus E, Shugar MA, Wright J (eds) *The feathered dragons*. Indiana University Press, Bloomington, pp 67–111
- Butler AB, Hodos W (2005) *Comparative vertebrate neuroanatomy: evolution and adaptation*. Wiley-Liss, New York
- Butler RJ, Upchurch P, Norman DB (2008) The phylogeny of the ornithischian dinosaurs. *J Syst Palaeontol* 6:1–40
- Cabreira SF, Kellner AWA, Dias-da-Silva S et al (2016) A unique Late Triassic dinosauromorph assemblage reveals dinosaur ancestral anatomy and diet. *Curr Biol* 26:3090–3095
- Campione NE, Evans DC (2020) The accuracy and precision of body mass estimation in non-avian dinosaurs. *Biol Rev* 95:1759–1797
- Carballido JL, Pol D, Otero A et al (2017) A new giant titanosaur sheds light on body mass evolution among sauropod dinosaurs. *Proc R Soc B* 284:20171219
- Carpenter K, Kirkland JJ, Birge D et al (2001) Disarticulated skull of a new primitive ankylosaurid from the Lower Cretaceous of Utah. In: Carpenter K (ed) *The armored dinosaurs*. Indiana University Press, pp 211–238
- Carr TD, Varricchio DJ, Sedlmayr JC et al (2017) A new tyrannosaur with evidence for anagenesis and crocodile-like facial sensory system. *Sci Rep* 7:44942. <https://doi.org/10.1038/srep44942>
- Carrano MT, Benson RBJ, Sampson SD (2012) The phylogeny of Tetanurae (Dinosauria: Theropoda). *J Syst Palaeontol* 10(2):211–300
- Cerda I, Paulina-Carabajal A, Salgado L et al (2011) The first record of a sauropod dinosaur from Antarctica. *Naturwissenschaften* 99(1):83–87
- Cerroni MA, Paulina-Carabajal A (2019) Novel information on the endocranial morphology of the abelisaurid theropod *Carnotaurus sastrei*. *C R Palevol* 18(8):985–995
- Chapelle KEJ, Choiniere JN (2018) A revised cranial description of *Massospondylus carinatus* Owen (Dinosauria: Sauropodomorpha) based on computed tomographic scans and a review of cranial characters for basal Sauropodomorpha. *Peer J* 6:e4224. <https://doi.org/10.7717/peerj.4224>
- Charig AJ, Milner AC (1997) *Baryonyx walkeri*, a fish eating dinosaur from the Wealden of Surrey. *Bull Nat Hist Mus* 53:11–70
- Chatterjee S, Zheng Z (2002) Cranial anatomy of *Shunosaurus*, a basal sauropod dinosaur from the Middle Jurassic of China. *Zool J Linn Soc-Lond* 136:145–169

- Chatterjee S, Zheng Z (2005) Neuroanatomy and dentition of *Camarasaurus lentus*. In: Tidwell V, Carpenter K (eds) Thunder-lizards: the sauropodomorph dinosaurs. Indiana University Press, Bloomington, pp 199–211
- Choiniere JN, Neenan JM, Schmitz L et al (2021) Evolution of vision and hearing modalities in theropod dinosaurs. *Science* 232(6542):610–613
- Christiansen P, Fariña RA (2004) Mass Prediction in Theropod Dinosaurs. *Hist Biol* 16:85–92
- Clarke AH (2005) On the vestibular labyrinth of *Brachiosaurus brancai*. *J Vestib Res* 15:65–71
- Coombs WP (1978) An endocranial cast of *Euoplocephalus* (Reptilia, Ornithischia). *Palaeontogr Abt A* 161:176–182
- Coria RA, Currie PJ (2002) The braincase of *Giganotosaurus carolinii* (Dinosauria: Theropoda) from the Upper Cretaceous of Argentina. *J Vertebr Paleontol* 22:802–811
- Crompton AW, Charig AJ (1962) A new ornithischian from the Upper Triassic of South Africa. *Nature* 196:1074–1077
- Cruzado-Caballero P, Fortuny J, Lácer S et al (2015) Paleoneuroanatomy of the European lambeosaurine dinosaur *Arenysaurus ardevoli*. *Peer J* 3:e802. <https://doi.org/10.7717/peerj.802>
- Currie PJ, Zhao X-J (1993) A new troodontid (Dinosauria, Theropoda) braincase from the Dinosaur Park Formation (Campanian) of Alberta. *Can J Earth Sci* 30:2231–2247
- Davidson RG, Trewhin NH (2005) Unusual preservation of the internal organs of acanthodian and actinopterygian fish in the Middle Devonian of Scotland. *Scot J Geo* 41:129–134
- Dendy A (1910) On the structure, development, and morphological interpretation of the pineal organs and adjacent parts of the brain in the tuatara (*Sphenodon punctatus*). *Proc R Soc B* 82:629–637
- Desojo JB, Fiorelli LE, Ezcurra MD et al (2020) The Late Triassic Ischigualasto Formation at Cerro Las Lajas (La Rioja, Argentina): fossil tetrapods, high-resolution chronostratigraphy, and faunal correlations. *Sci Rep* 10:12782. <https://doi.org/10.1038/s41598-020-67854-1>
- Dieudonné PE, Cruzado-Caballero P, Godefroit P (2020) A new phylogeny of Cerapodan dinosaurs. *Hist Biol* 33(10):2335–2355
- Dumoncel J, Subsol G, Durrleman S et al (2020) Are endocasts reliable proxies for brains? A 3D quantitative comparison of the extant human brain and endocast. *J Anat* 238:480–488
- Early CM, Iwaniuk AN, Ridgely RC et al (2020) Endocast structures are reliable proxies for the sizes of corresponding regions of the brain in extant birds. *J Anat* 237:1162–1176
- Eaton TH (1960) A new armored dinosaur from the Cretaceous of Kansas, University of Kansas Paleontological Contributions 25. University of Kansas Press, Lawrence, pp 1–24
- Ebner R, Salgado L (2003) Computed tomographic scan of a dinosaur's skull: the optic canal. *Arch Ophthalmol* 121:294–295
- Edinger T (1929) Die fossilen Gehirne. *Ergebnisse der Anatomische Entwicklungsgeschichte*, 28:1–249
- Edinger T (1942) The pituitary body in giant animals fossil and living: a survey and a suggestion. *Q Rev Biol* 17:31–45
- Edinger T (1951) The brains of the Odontognathae. *Evolution* 5:6–24
- Edinger T (1975) Paleoneurology 1804–1966: an annotated bibliography. *Ad Anat Embryol Cell Biol* 49:1–6
- Evans DC (2005) New evidence on brain–endocranial cavity relationships in ornithischian dinosaurs. *Acta Palaeontol Pol* 50:617–622
- Evans DC (2006) Nasal cavity homologies and cranial crest function in lambeosaurine dinosaurs. *Paleobiology* 32:109–125
- Evans DC, Ridgely R, Witmer LM (2009) Endocranial anatomy of lambeosaurine hadrosaurids (Dinosauria: Ornithischia): a sensorineural perspective on cranial crest function. *Anat Rec* 292(9):1315–1337
- Ezcurra MD (2010) A new early dinosaur (Saurischia: Sauropodomorpha) from the Late Triassic of Argentina: a reassessment of dinosaur origin and phylogeny. *J Syst Palaeontol* 8:371–425
- Ezcurra MD, Cuny G (2007) The coelophysoid *Lophostropheus airelensis*, gen. nov.: A review of the systematics of “*Liliensternus*” *airelensis* from the Triassic–Jurassic outcrops of Normandy (France). *J Vertebr Paleontol* 27(1):73–86

- Fabbri M, Koch NM, Pritchard A et al (2017) The skull roof tracks the brain during the evolution and development of reptiles including birds. *Nat Ecol Evol* 1:1543–1550
- Fabbri M, Tschopp B, McPhee S et al (2020) Sauropodomorpha. In: de Queiroz K, Cantino PD, Gauthier JA (eds) *Phylogeny: a Companion to the PhyloCode*. CRC Press, Boca Raton, pp 1225–1234
- Farke AA, Chok DJ, Herrero A et al (2013) Ontogeny in the tube-crested dinosaur *Parasaurolophus* (Hadrosauridae) and heterochrony in hadrosaurids. *Peer J* 1:e182. <https://doi.org/10.7717/peerj.182>
- Fastovsky DE, Weishampel DB (2016) *Dinosaurs: a concise natural history*. Cambridge University Press, Cambridge
- Ferreira-Cardozo S, Araújo R, Martins NE et al (2017) Floccular fossa size not a reliable proxy of ecology and behavior in vertebrates. *Sci Rep* 7(1):1–11
- Forster CA (1996) New information on the skull of *Triceratops*. *J Vertebr Paleontol* 16:246–258
- Franzosa JW (2004) Evolution of the brain in Theropoda (Dinosauria). Dissertation, University of Texas
- Franzosa J, Rowe T (2005) Cranial endocast of the Cretaceous theropod dinosaur *Acrocanthosaurus atokensis*. *J Vertebr Paleontol* 25:859–864
- Galton PM (1985) Cranial anatomy of the prosauropod dinosaur *Plateosaurus* from the Knollenmergel (Middle Keuper, Upper Triassic) of Germany. *Geol Palaeontol* 19:119–159
- Galton PM (1988) Skull bones and endocranial casts of stegosaurian dinosaur *Kentrosaurus Hennig*, 1915 from Upper Jurassic of Tanzania, East Africa. *Geol Palaeontol* 22:123–143
- Galton PM (1989) Crania and endocranial casts from ornithopod dinosaurs of the families Dryosauridae and Hypsilophodontidae (Reptilia: Ornithischia). *Geol Palaeontol* 23:217–239
- Galton PM (2001) Endocranial casts of the plated dinosaur *Stegosaurus* (Upper Jurassic, western USA): a complete undistorted cast and the original specimens of Othniel Charles Marsh. In: Carpenter K (ed) *The armored dinosaurs*. Indiana University Press, Bloomington, pp 103–129
- Galton PM, Knoll F (2006) A saurischian dinosaur braincase from the Middle Jurassic (Bathonian) near Oxford, England: from the theropod *Megalosaurus* or the sauropod *Cetiosaurus*? *Geol Mag* 43:905–921. <https://doi.org/10.1017/S0016756806002561>
- Galton PM, Upchurch P (2004) Stegosauria. In: Weishampel DB, Dodson P, Olsólska H (eds) *The dinosauria*, 2nd edn. University of California Press, Berkeley, pp 343–362
- García R, Paulina-Carabajal A, Salgado L (2008) Un nuevo basicráneo de titanosaurio de la Formación Allen (Campaniano-Maastrichtiano), Provincia de Río Negro, Patagonia, Argentina. *Geobios* 41:625–633
- García RA, Salgado L, Fernández MS et al (2015) Paleobiology of titanosaur: reproduction, development, histology, pneumaticity, locomotion and neuroanatomy from the South American fossil record. *Ameghiniana* 52:29–68
- Gauthier JA, Langer MC, Novas FE et al (2020) Saurischia H. G. Seeley. In: de Queiroz K, Cantino PD, Gauthier JA (eds) *Phylogeny: a companion to the PhyloCode*. CRC Press, Boca Raton, pp 1219–1224
- George I, Holliday CM (2013) Trigeminal nerve morphology in *Alligator mississippiensis* and its significance for crocodyliform facial sensation and evolution. *Anat Rec* 296(4):670–680
- Gianechini FA, Méndez AH, Filippi LS et al (2021) A new furilesaurian abelisaurid from La Invernada (Upper Cretaceous, Santonian, Bajo de la Carpa Formation), northern Patagonia, Argentina. *J Vert Paleontol* 40(6):e1877151. <https://doi.org/10.1080/02724634.2020.1877151>
- Giffin EB (1989) Pachycephalosaur paleoneurology (Archosauria: Ornithischia). *J Vertebr Paleontol* 9(1):67–77
- Giffin EB (1990) Gross spinal anatomy and limb use in living and fossil reptiles. *Paleobiology* 16(4):448–458
- Giffin EB, Gabriel D, Johnson R (1987) A new pachycephalosaurid skull from the Cretaceous Hell Creek Formation of Montana. *J Vertebr Paleontol* 7:398–407
- Gilmore CW (1914) Osteology of the armored Dinosauria in the United States National Museum, with special reference to the genus *Stegosaurus*. *Bull US Natl Mus*, Smithsonian Institution, 89

- Godefroit P, Escuillié F, Bolotsky YL et al (2012) A new basal hadrosauroid dinosaur from the Upper Cretaceous of Kazakhstan. In: Godefroit P (ed) *Bernissart dinosaurs and early cretaceous terrestrial ecosystems*. Indiana University Press, Bloomington, pp 336–358
- Gower DJ, Weber E (1998) The braincase of *Euparkeria*, and the evolutionary relationships of birds and crocodylians. *Biol Rev* 73:367–411
- Griebeler EM, Werner J (2011) The life cycle of sauropod dinosaurs. In: Gans C, Glenn Northcutt R, Ulinski P (eds) *Biology of the reptilia*. Academic, London, pp 39–146
- Güntürkün O, Stacho M, Strökens F (2020) The brains of reptiles and birds. In: Kaas JH (ed) *Evolutionary neuroscience*. Elsevier, pp 159–212
- Hammer WR, Hickerson WJ (1994) A crested theropod dinosaur from Antarctica. *Science* 264(5160):828–830
- Harris JD (2006) Cranial osteology of *Suuwassea emiliae* (Sauropoda: Diplodocoidea: Flagellicaudata) from the Upper Jurassic Morrison Formation of Montana, USA. *J Vertebr Paleontol* 26:88–102
- Hawakaya H, Manabe M, Carpenter K (2005) Nodosaurid ankylosaur from the Cenomanian of Japan. *J Vert Paleontol* 25:240–245
- Hay OP (1909) On the skull and the brain of *Triceratops* with notes on the brain-cases of *Iguanodon* and *Megalosaurus*. *Proc U S Natl Mus* 36:95–108
- Hennig E (1925) *Kentrosaurus aethiopicus*, die Stegosaurier-Funde von Tendaguru, Deutsch-Ostafrika. *Palaeontogr Suppl.* 7:101–254
- Holtz T Jr (2018) Evolution: new branches on the alvarezsaur tree. *Curr Biol* 28(17):R941–R943
- Hopson JA (1977) Relative brain size and behavior in archosaurian reptiles. *Ann Rev Ecol Syst* 8:429–448
- Hopson JA (1979) Paleoneurology. In: Gans C, Northcutt RG, Ulinski P (eds) *Biology of the reptilia*. Academic, London, pp 39–146
- Hopson JA (1980) Relative brain size in dinosaurs. Implications for dinosaurian endothermy. In: Thomas RDK, Olson EC (eds) *A cold look at the warm-blooded dinosaurs*. Westview Press, Boulder, pp 287–310
- Horner JR, Weishampel DB, Forster CA (2004) Hadrosauridae. In: Weishampel DB, Dodson P, Osmólska H (eds) *The dinosauria*, 2nd edn. University of California Press, Berkeley, pp 438–463
- Hu K, King JL, Romick CA et al (2021) Ontogenetic endocranial shape change in alligators and ostriches and implications for the development of the non-avian dinosaur endocranium. *Anat Rec* 304:1759–1775
- Hulke JW (1871) Note on a large reptilian skull from Brooke, Isle of Wight, probably dinosaurian, and referable to the genus *Iguanodon*. *Quart J Geol Soc* 27:199–206
- Hurlburt GR (1996) Relative brain size in recent and fossil amniotes: determination and interpretation. Dissertation, University of Toronto
- Hurlburt GR, Ridgely RC, Witmer LM (2013) Relative size of brain and cerebrum in tyrannosaurid dinosaurs: an analysis using brain-endocast quantitative relationships in extant alligators. In: Parrish JM, Molnar E, Currie PJ et al (eds) *Tyrannosaurid paleobiology*. Indiana University Press, Bloomington, pp 134–154
- Huxley TH (1870) On the classification of the Dinosauria with observations on the Dinosauria of the Trias. *Quart J Geol Soc Lon* 26:32–51
- Ibrahim N, Sereno PC, Dal Sasso C et al (2014) Semiaquatic adaptations in a giant predatory dinosaur. *Science* 345(6204):1613–1616
- Iwaniuk AN, Nelson J (2002) Can endocranial volume be used as an estimate of brain size in birds? *Can J Zool* 80:16–23
- Janensch W (1935–1936) Die Schädel der Sauropoden *Brachiosaurus*, *Barosaurus* und *Dicraeosaurus* aus den Tendaguru-Schichten Deutsch-Ostafrikas. *Palaeontogr Suppl* 7:147–298
- Janensch W (1939) Der sakrale Neuralkanal einiger Sauropoden und anderer Dinosaurier. *Palaentol Z* 21:171–193
- Jerison HJ (1969) Brain evolution and dinosaur brains. *Am Nat* 103:575–588

- Jerison HJ (1973) Evolution of the brain and intelligence. Academic, New York
- Jerison HJ (2004) Dinosaur brains. In: Adelman G, Smith BH (eds) Encyclopedia of neuroscience, 3rd edn. Elsevier, Amsterdam
- Jirak D, Janacek J (2017) Volume of the crocodylian brain and endocast during ontogeny. PLoS One 12(6):e0178491. <https://doi.org/10.1371/journal.pone.0178491>
- Kawabe S, Hattori S (2021) Complex neurovascular system in the dentary of *Tyrannosaurus*. Hist Biol. <https://doi.org/10.1080/08912963.2021.1965137>
- King L (2021) Macroevolutionary and Ontogenetic Trends in the Anatomy and Morphology of the Non-Avian Dinosaur Endocranium. Dissertation, University of Bristol
- King L, Sipla JS, Georgi JA et al (2020) The endocranium and trophic ecology of *Velociraptor mongoliensis*. J Anat 237(5):861–869
- Knoll F (1997) La Boîte crânienne d'un Théropode (Saurischia) du Jurassique des Vaches Noires: Ostéologie et Paléoneurologie. Dissertation, Université des Sciences et Techniques du Languedoc
- Knoll F, Kawabe S (2020) Avian palaeoneurology: reflections on the eve of its 200th anniversary. J Anat 236(6):965–979
- Knoll F, Lautenschlager S, Valentin X et al (2019) First palaeoneurological study of a sauropod dinosaur from France and its phylogenetic significance. Peer J 7:e7991. <https://doi.org/10.7717/peerj.7991>
- Knoll F, Lautenschlager S, Kawabe S et al (2021) Palaeoneurology of the early cretaceous iguanodont *Proa valdearriñoensis* and its bearing on the parallel developments of cognitive abilities in theropod and ornithomimid dinosaurs. J Comp Neurol 529:3922–3945
- Knoll F, Schwarz-Wings D (2009) Paleoneuroanatomy of *Brachiosaurus*. Ann de Paléontol 95:165–175
- Knoll F, Buffetaut E, Bulow M (1999) A theropod braincase from the Jurassic of the Vaches Noires cliffs (Normandy, France): osteology and Paleoneurology. BSGF-Earth SCI B170:103–109
- Knoll F, Galton PM, Lopez-Antoñanzas R (2006) Paleoneurological evidence against a proboscis in the sauropod dinosaur *Diplodocus*. Geobios 39:215–221
- Knoll F, Witmer LM, Ortega F et al (2012) The braincase of the basal sauropod dinosaur *Spinophorosaurus* and 3D reconstructions of the cranial endocast and inner ear. PLoS One 7(1):e30060. <https://doi.org/10.1371/journal.pone.0030060>
- Knoll F, Ridgely RC, Ortega F et al (2013) Neurocranial osteology and neuroanatomy of a Late Cretaceous titanosaurian sauropod from Spain (*Ampelosaurus* sp.). PLoS One 8:e54991. <https://doi.org/10.1371/journal.pone.0054991>
- Knoll F, Ridgely RC, Witmer LM (2015a) Comparative paleoneurology of the basal dicraeosaurid sauropod *Suuwassea emilieae*. J Vertebr Paleontol (supp):156
- Knoll F, Witmer LM, Ridgely RC et al (2015b) A new titanosaurian braincase from the Cretaceous “Lo Hueco” locality in Spain sheds light on neuroanatomical evolution within Titanosauria. PLoS One 10:e0138233. <https://doi.org/10.1371/journal.pone.0138233>
- Ksepka DT, Balanoff AM, Smith A et al (2020) Tempo and pattern of avian brain size evolution. Current Biol 30:2026–2036.e3
- Kundrát M (2007) Avian-like attributes of a virtual brain model of the oviraptorid theropod *Conchoraptor gracilis*. Naturwissenschaften 94:499–504
- Kundrát M, Xu X, Hančová M et al (2018) Evolutionary disparity in the endoneurocranial configuration between small and gigantic tyrannosauroids. Hist Biol 32:620–634
- Kurzanov SM (1976) Braincase structure in the carnosaur *Itemirus* n. gen. and some aspects of the cranial anatomy of dinosaurs. Paleontol J 10:361–369
- Kurzanov SM, Tumanova TA (1978) Endo-cranium structure of some mongolian ankylosaurs. Paleontol J 3:90–96
- Kuzmin I, Petrov I, Averianov A et al (2020) The braincase of *Bissektipelta archibaldi*—new insights into endocranial osteology, vasculature, and paleoneurobiology of ankylosaurian dinosaurs. Biol Comm 65(2):85–156
- Lambe LM (1918) The Cretaceous genus *Stegoceras* typifying a new family referred provisionally to the Stegosauria. Trans Roy Soc Canada, Ser 3(12):23–36

- Lambe LM (1920) The hadrosaur *Edmontosaurus* from the Upper Cretaceous of Alberta, Canada Department of Mines. (Geological Survey of Canada) Memoir 120. T. Mulvey, Ottawa, pp 1–79
- Langer MC (2014) The origins of Dinosauria: much ado about nothing. *Palaeontology* 57:469–478
- Langer MC, Ezcurra MD, Bittencourt JS et al (2010) The origin and early evolution of dinosaurs. *Biol Rev* 85(1):5–110
- Langer MC, Ezcurra MD, Rauhut OWM et al (2017) Untangling the dinosaur family tree. *Nature* 551(7678):E1–E3. <https://doi.org/10.1038/nature24011>
- Langer MC, Novas FE, Bittencourt JS et al (2020) Dinosauria R. Owen. In: de Queirok K, Cantino PD, Gauthier JA (eds) *Phylonyms: a companion to the PhyloCode*. CRC Press, Boca Raton, pp 1209–1218
- Langston WL Jr (1960) The vertebrate fauna of the Selma Formation of Alabama. Part 6: the dinosaurs. *Fieldiana, Geol Mem* 3:313–363
- Langston WL Jr (1975) The ceratopsian dinosaurs and associated lower vertebrates from the St. Mary River Formation (Maestrichtian) at Scabby Butte, southern Alberta. *Can J Earth Sci* 12:1576–1608
- Larsson HCE (2001) Endocranial anatomy of *Carcharodontosaurus saharicus* (Theropoda: Allosauroidea) and its implications for theropod brain evolution. In: Tanke DH, Carpenter K (eds) *Mesozoic vertebrate life*. Indiana University Press, Bloomington, pp 19–33
- Larsson HCE, Sereno PC, Wilson JA (2000) Forebrain enlargement among nonavian dinosaurs. *J Vertebr Paleontol* 20:615–618
- Lautenschlager S (2014) Morphological and functional diversity in therizinosaur claws and the implications for theropod claw evolution. *Proc Biol Sci* 22(1785):281. <https://doi.org/10.1098/rspb.2014.0497>
- Lautenschlager S, Hübner T (2013) Ontogenetic trajectories in the ornithischian endocranium. *J Evol Biol* 26(9):2044–2050
- Lautenschlager S, Rayfield EJ, Altangerel P et al (2012) The endocranial anatomy of Therizinosauria and its implications for sensory and cognitive function. *PLoS One* 7:e52289. <https://doi.org/10.1371/journal.pone.0052289>
- Lauters P, Coudyzer W, Vercauteren M (2012) The brain of *Iguanodon* and *Mantellisaurus*: perspectives on ornithopod evolution. In: Godefroit P (ed) *Bernissart dinosaurs and early cretaceous terrestrial ecosystems*. Indiana University Press, Bloomington, pp 213–224
- Lauters P, Vercauteren M, Bolotsky YL et al (2013) Cranial endocast of the lambeosaurine hadrosaurid *Amurosaurus riabinini* from the Amur Region, Russia. *PLoS One* 8(11):e78899. <https://doi.org/10.1371/journal.pone.0078899>
- Leahey LG, Molnar RE, Carpenter K et al (2015) Cranial osteology of the ankylosaurian dinosaur formerly known as *Minmi* sp. (Ornithischia: Thyreophora) from the Lower Cretaceous Allaru Mudstone of Richmond, Queensland, Australia. *Peer J* 3:e1475. <https://doi.org/10.7717/peerj.1475>
- Lull RS (1917) On the functions of the “Sacral Brain” in dinosaurs. *Amer J of Sci* 4(44):471–477
- Lull RS (1933) A revision of the Ceratopsia or horned dinosaurs. *Mem Peabody Mus Nat Hist* 3:1–175
- Lull RS, Wright NE (1942) Hadrosaurian dinosaurs of North America. *Special Paper. Geol Soc Ame* 40:1–242
- Macri S, Savriama Y, Khan I, Di-Poï N (2019) Comparative analysis of squamate brains unveils multi-level variation in cerebellar architecture associated with locomotor specialization. *Nat Comm* 10:5560. <https://doi.org/10.1038/s41467-019-13405-w>
- Madzia D, Arbour VM, Boyd CA et al (2021) The phylogenetic nomenclature of ornithischian dinosaurs. *Peer J* 9:e12362. <https://doi.org/10.7717/peerj.12362>
- Maleev EA 1965. [On the brain of carnivorous dinosaurs.] *Paleontologeskii Zhurnal*, 2:141–143
- Marsh OC (1880) Principal characters of American Jurassic dinosaurs. Part III. *Am J Sci* 19:253–259
- Marsh OC (1881) Principal characters of American Jurassic dinosaurs. Part IV. *Am J Sci* 122:167–170

- Marsh OC (1884a) Principal characters of American Jurassic dinosaurs. Part VII. On the Diplodocidae, a new family of the Sauropoda. *Am J Sci* 27:161–168
- Marsh OC (1884b) Principal characters of American Jurassic dinosaurs. Part VIII. The order Theropoda. *Am J Sci* 27:329–340
- Marsh OC (1889) The skull of the gigantic Ceratopsidae. *Am J Sci* 228:501–506
- Marsh OC (1890) Additional characters of the Ceratopsidae, with notice of the new Cretaceous dinosaurs. *Am J Sci* 39:418–426
- Marsh OC (1891) The gigantic Ceratopsidae, or horned Dinosaurs, of North America. *Am J Sci* 41:168–178
- Marsh OC (1893) The skull and brain of *Claosaurus*. *Am J Sci* 3(265):83–86
- Marsh OC (1894) The typical Ornithopoda of the American Jurassic. *Am J Sci* 48:85–90
- Marsh OC (1896) The dinosaurs of North America. United States Geological Survey, sixteenth annual report, 1894–95:133–244
- Martínez RD, Lamanna MC, Novas FE et al (2016) A basal lithostrotian titanosaur (Dinosauria: Sauropoda) with a complete skull: implications for the evolution and paleobiology of Titanosauria. *PLoS One* 11(4):e0151661. <https://doi.org/10.1371/journal.pone.0151661>
- Maryanska T, Osmólska H (1974) Pachycephalosauria, a new suborder of ornithischian dinosaurs. *Paleontol Pol* 30:54–102
- Méndez A, Gianechini FA, Paulina-Carabajal A et al (2021) New furilesaurian remains from La Invernada (northern Patagonia, Argentina): A site of unusual abelisaurids abundance. *Cret Res* 129:104989. <https://doi.org/10.1016/j.cretres.2021.104989>
- Miyashita T, Arbour VM, Witmer LM et al (2011) The internal cranial morphology of an armoured dinosaur *Euoplocephalus* corroborated by X-ray computed tomographic reconstruction. *J Anat* 219(6):661–675
- Morhardt AC (2016) Gross anatomical brain region approximation (GABRA): assessing brain size, structure, and evolution in extinct archosaurs. Dissertation, Ohio University
- Morhardt AC, Ridgely RC, Witmer LM (2012) From endocast to brain: assessing brain size and structure in extinct archosaurs using gross anatomical brain region approximation (GABRA). *J Vertebr Paleontol* 32 (Suppl.), 145
- Morhardt AC, Ridgely RC, Witmer LM (2018) Gross anatomical brain region approximation (GABRA): a new landmark-based approach for estimating brain regions in dinosaurs and other archosaurs. *FASEB J* 31:251–252. https://doi.org/10.1096/fasebj.31.1_supplement.251.2
- Müller RT (2021) Olfactory acuity in early sauropodomorph dinosaurs. *Hist Biol* 34(2):346–351
- Müller RT, Garcia MS (2020) A paraphyletic ‘Silesauridae’ as an alternative hypothesis for the initial radiation of ornithischian dinosaurs. *Biol Lett* 16:20200417. <https://doi.org/10.1098/rsbl.2020.0417>
- Müller RT, Ferreira JD, Pretto FA et al (2021) The endocranial anatomy of *Buriolestes schultzi* (Dinosauria: Saurischia) and the early evolution of brain tissues in sauropodomorph dinosaurs. *J Anat* 238(4):809–827
- Napoli JG, Hunt T, Erickson GM (2019) *Psittacosaurus amitabha*, a new species of ceratopsian dinosaur from the Ondai Sayr locality, Central Mongolia. *Am Mus Novit* 2019(3932):1–36. <https://doi.org/10.1206/3932.1>
- Nesbitt SJ, Ezcurra MD (2015) The early fossil record of dinosaurs in North America: a new neotheropod from the base of the Dockum Group (Upper Triassic) of Texas. *Acta Palaeontol Pol* 60:513–526
- Ngwenya A, Patzke N, Spocter MA et al (2013) The continuously growing central nervous system of the Nile Crocodile (*Crocodylus niloticus*). *Anat Rec Adv Integr Anat Evol Biol* 296:1489–1500
- Nieuwenhuys R, Donkelaar HJ, Nicholson C (1998) The central nervous system of vertebrates. Springer Berlin, Heidelberg
- Nopcsa F (1929) Dinosaurierreste aus Siebenbürgen. *V. Geol Hung Palaeontol* 4:1–76
- Norell MA, Makovicky PJ, Bever GS et al (2009) A review of the mongolian Cretaceous dinosaur *Saurornithoides* (Troodontidae: Theropoda). *Am Mus Nov* 3654:1–63

- Norman DB, Faiers T (1996) On the first partial skull of an ankylosaurian dinosaur from the Lower Cretaceous of the Isle of Wight, Southern England. *Geol Mag* 133:299–310
- Norman DB, Weishampel DB (1990) Iguanodontidae and related ornithopods. In: Weishampel DB, Dodson P, Osmólska H (eds) *The dinosauria*. University of California Press, Berkeley, pp 510–533
- Norman DB, Sues H-D, Witmer LM et al (2004a) Basal ornithopoda. In: Weishampel DB, Dodson P, Osmólska H (eds) *The dinosauria*, 2nd edn. University of California Press, Berkeley, pp 393–412
- Norman DB, Witmer LM, Weishampel DB (2004b) Basal thyreophora. In: Weishampel DB, Dodson P, Osmólska H (eds) *The dinosauria*, 2nd edn. University of California Press, Berkeley, pp 335–342
- Northcutt RG (2002) Understanding vertebrate brain evolution. *Integr Comp Biol* 42:743–756
- Olori JC (2010) Digital endocasts of the cranial cavity and osseous labyrinth of the burrowing snake *Uropeltis woodmansoni* (Alethinophidia: Uropeltidae). *Copeia* 2010:14–26
- Osborn HF (1912) Crania of *Tyrannosaurus* and *Allosaurus*. *Mem Am Mus Nat Hist* 1:1–97
- Osborn HF, Mook CC (1921) *Camarasaurus*, *Amphicoelias*, and other sauropods of Cope, Memoirs of the AMNH, vol 3. American Museum of Natural History, New York, pp 247–287
- Osmólska H (2004) Brief report: evidence on relation of brain to endocranial cavity in oviraptorid dinosaurs. *Acta Palaeontol Pol* 49(2):321–324
- Ostrom JH (1961) Cranial morphology of the hadrosaurian dinosaurs of North America. *Bull Am Mus Nat Hist* 122:33–186
- Ostrom JH, McIntosh JS (1966) Marsh's dinosaurs. The collections from Como Buff. Yale University Press, New Heaven and London
- Ósi A, Pereda-Suberbiola X, Földes T (2014) Partial skull and endocranial cast of the ankylosaurian dinosaur *Hungarosaurus* from the Late Cretaceous of Hungary: implications for locomotion. *Palaeontol Electron* 17(1):1A. <https://doi.org/10.26879/405>
- Pacheco C, Müller RT, Langer M et al (2019) *Gnathovorax cabreirai*: a new early dinosaur and the origin and initial radiation of predatory dinosaurs. *Peer J* 7:e7963. <https://doi.org/10.7717/peerj.7963>
- Paulina-Carabajal A (2012) Neuroanatomy of titanosaurid dinosaurs from the Upper Cretaceous of Patagonia, with comments on endocranial variability within Sauropoda. *Anat Rec* 295:2141–2156
- Paulina-Carabajal A (2015) Guía para el estudio de la neuroanatomía de los dinosaurios Saurischia, con énfasis en Theropoda basales. *PE-APA* 15:108–142
- Paulina-Carabajal A, Currie JP (2017) The braincase of the theropod dinosaur *Murusraptor*: osteology, neuroanatomy and comments on the paleobiological implications of certain endocranial features. *Ameghiniana* 54:517–640
- Paulina-Carabajal A, Apaldetti C, Martínez R (2019a) Paleoneuroanatomy of a new riojasaurid (Dinosauria, Sauropodomorpha) from the Late Triassic of Argentina. Abstract presented at SVP annual Meeting, 9–12 October (Brisbane)
- Paulina-Carabajal A, Ezcurra M, Novas F (2019b) New information on the braincase and endocranial morphology of the Late Triassic neotheropod *Zupaysaurus rougieri* using CT scans. *J Vertebr Paleontol* 39(3):e1630421. <https://doi.org/10.1080/02724634.2019.1630421>
- Paulina-Carabajal A, Filippi L (2018) Neuroanatomy of the abelisaurid theropod *Viavenator*: the most complete reconstruction of cranial endocast and inner ear for a South American representative of the clade. *Cret Res* 83:84–94
- Paulina-Carabajal A, Calvo JO (2021) Re-description of the braincase of the rebbachisaurid sauropod *Limaysaurus tessonei* and novel endocranial information based on CT scans. *An Acad Bras Cienc* 93(2):e20200762. <https://doi.org/10.1590/0001-3765202102000762>
- Paulina-Carabajal A, Canale JI (2010) Cranial endocast of the carcharodontosaurid theropod *Giganotosaurus carolinii*. *Neues Jahrb fur Geol Palaontol Abh* 258:249–256
- Paulina-Carabajal A, Currie PJ (2012) New information on the braincase and endocast of *Sinraptor dongi* (Theropoda: Allosauroidea): Ethmoidal region, endocranial anatomy and pneumaticity. *Vert PalAs* 50:85–101

- Paulina-Carabajal A, Porfiri JD (2018) The neuroanatomy of *Megaraptor namunhuaiquii* (Theropoda: Megaraptoridae) from the Upper Cretaceous of Patagonia, a preliminary report. Abstract presented at Reunión de Comunicaciones de la Asociación Paleontológica Argentina (Madryn)
- Paulina-Carabajal A, Nieto MN (2019) Brief comment on the brain and inner ear of *Giganotosaurus carolinii* (Dinosauria: Theropoda) based on CT scans. *Ameghiniana* 57(1):58–62
- Paulina-Carabajal A, Salgado L (2007) El basicráneo de un titanosaurio (Dinosauria, Sauropoda) del Cretácico Superior del norte de Patagonia: descripción y aportes al conocimiento del oído interno de los dinosaurios. *Ameghiniana* 44:109–120
- Paulina-Carabajal A, Succar C (2015) Endocranial morphology and inner ear of the theropod *Aucasaurus garridoi*. *Acta Palaeontol Pol* 60(1):141–144
- Paulina-Carabajal A, Coria RA, Chiappe LM (2008) An incomplete Late Cretaceous braincase (Sauropoda: Titanosauria): new insights about the dinosaurian inner ear and endocranium. *Cret Res* 29:643–648
- Paulina-Carabajal A, Carballido J, Currie PJ (2014) Braincase, neuroanatomy and neck posture of *Amargasaurus cazaui* (Sauropoda: Dicraeosauridae) and its implications for understanding head posture in sauropods. *J Vert Paleontol* 34:870–882
- Paulina-Carabajal A, Canale JI, Haluza A (2016a) New rebbachisaurid cranial remains (Sauropoda, Diplodocoidea) from the Cretaceous of Patagonia, Argentina, and the first endocranial description for a South American representative of the clade. *J Vert Paleontol* 36:e1167067. <https://doi.org/10.1080/02724634.2016.1167067>
- Paulina-Carabajal A, Lee YN, Jacobs LL (2016b) Neuroanatomy of the primitive nodosaurid dinosaur *Pawpawsaurus campbelli* and paleobiological implications of some endocranial features. *Plos One* 11(3):e0150845. <https://doi.org/10.1371/journal.pone.0150845>
- Paulina-Carabajal A, Cruzado-Caballero P, Calvo J (2017) Novel information on the braincase morphology of *Gasparinisaura cincosaltensis* (Dinosauria, Ornithischia) based on CT scans. Abstract presented at 1st Reunión de Paleovertebrados de la Cuenca Neuquina, 2–3 November 2017 (Rincón de los Sauces)
- Paulina-Carabajal A, Coria RA, Currie PJ et al (2018a) A natural cranial endocast with possible dicraeosaurid (Sauropoda, Diplodocoidea) affinities from the Lower Cretaceous of Patagonia. *Cret Res* 84:437–441
- Paulina-Carabajal A, Lee YN, Kobayashi Y et al (2018b) Neuroanatomy of the ankylosaurid dinosaurs *Tarchia teresae* and *Talarurus plicatospineus* from the Upper Cretaceous of Mongolia, with comments on endocranial variability among ankylosaurs. *Palaeogeogr Palaeoclim Palaeoecol* 494:135–146
- Paulina-Carabajal A, Filippi L, Knoll F (2020) Neuroanatomy of the titanosaur sauropod *Narambuenatitan palomoi* from the Upper Cretaceous of Patagonia, Argentina. *PE-APA* 20(2):1–9. <https://doi.org/10.5710/PEAPA.21.05.2020.298>
- Paulina-Carabajal A, Currie PJ, Dungeon T et al (2021) Two braincases of *Daspletosaurus* (Theropoda: Tyrannosauridae): anatomy and comparison. *Can J Earth Sci.* <https://doi.org/10.1139/cjes-2020-0185>
- Paulina-Carabajal A, Bourke J, Morhardt A (in press) Senses. In: Zanno L, Arbour V, Holtz T (eds), *The complete dinosaur*, 3rd edn. Indiana University Press, Bloomington
- Pereda-Suberbiola J, Galton PM (1994) Revision of the cranial features of the dinosaur *Struthiosaurus austriacus* Bunzel (Ornithischia: Ankylosauria) from the Late Cretaceous of Europe. *Neues Jahrb Geol Paläontol Abhand* 191:173–200
- Peyre de Fabregues C, Allain R, Barriel V (2015) Root causes of phylogenetic incongruence observed within basal sauropodomorph interrelationships. *Zool J Linn Soc* 175:569–586
- Pol D, Otero A, Apaldetti C et al (2021) Triassic sauropodomorph dinosaurs from South America: the origin and diversification of dinosaur dominated herbivorous faunas. *J South Am Earth Sci* 107:103145. <https://doi.org/10.1016/j.jsames.2020.103145>
- Poropat SF, Mannion PD, Upchurch P et al (2016) New Australian sauropods shed light on Cretaceous dinosaur palaeobiogeography. *Sci Rep* 6:34467. <https://doi.org/10.1038/srep34467>

- Porter WR, Witmer LM (2020) Vascular patterns in the heads of dinosaurs: evidence for blood vessels, sites of thermal exchange, and their role in physiological thermoregulatory strategies. *Anat Record* 303:1075–1103
- Porter WR, Sedlmayr JC, Witmer LM (2016) Vascular patterns in the heads of crocodylians blood vessels and sites of thermal exchange. *J Anat* 229:800–824
- Powell JE (2003) Revision of South American titanosaurid dinosaurs: palaeobiological, palaeobiogeographical and phylogenetic aspects. *Rec Queen Vic Museum* 111:1–173
- Raath MA (1977) The anatomy of the Triassic theropod *Syntarsus rhodesiensis* (Saurischia: Podokesauridae) and a consideration of its biology. Dissertation, Rhodes University
- Rahmat S, Gilland E (2014) Comparative anatomy of the carotid-basilar arterial trunk and penetrating arteries in vertebrates. *Open Anat J* 6. <https://doi.org/10.2174/1877609401406010001>
- Rauhut OWM (2003) The interrelationships and evolution of basal theropod dinosaurs. *Spec Pap Palaeontol* 69:1–213
- Rauhut OWM, Fechner R, Remes K et al (2011) How to get big in the Mesozoic: the evolution of the sauropodomorph body plan. In: Klein N, Remes K, Gee CT, Sander PM (eds), *Biology of the Sauropod Dinosaurs: Understanding the life of giants*. Bloomington, Indiana University Press pp 119–149
- Rich T, Rich P (1989) Polar dinosaurs and biotas of the Early Cretaceous of southeastern Australia. *Nat Geograp Res* 5(1):15–53
- Rich TH, Vickers-Rich P, Gangloff RA (2002) Polar dinosaurs. *Science* 295:979–980
- Rogers SW (1998) Exploring dinosaur neuropaleobiology: computed tomography scanning and analysis of an *Allosaurus gracilis* endocast. *Neuron* 21:673–679
- Rogers SW (1999) *Allosaurus*, crocodiles, and birds: evolutionary clues from spiral computed tomography of an endocast. *Anat Rec* 257:162–173
- Rogers SW (2005) Reconstructing the behaviors of extinct species. *Am J Med Genet* 134A:349–358
- Romer AS (1956) *Osteology of the Reptiles*. California, University of Chicago Press
- Romick CA (2013) Ontogeny of the brain endocasts of ostriches (Aves: *Struthio camelus*) with implications for interpreting extinct dinosaur endocasts. Dissertation, Ohio University
- Roth G, Dicke U (2005) Evolution of the brain and intelligence. *Trends Cogn Sci* 9(5):250–257
- Russell DA (1969) A new specimen on *Stenonychosaurus* from the Oldman Formation (Cretaceous) of Alberta. *Can J Earth Sci* 6:595–612
- Russell DA (1972) Ostrich Dinosaurs from the Late Cretaceous of Western Canada. *Can J Earth Sci* 9:375–402
- Sakagami R, Kawabe S (2020) Endocranial anatomy of the ceratopsid dinosaur *Triceratops* and interpretations of sensory and motor function. *Peer J* 8:e9888. <https://doi.org/10.7717/peerj.9888>
- Salgado L, Coria RA, Calvo JO (1997) Evolution of titanosaurid sauropods. I: Phylogenetic analysis based on the postcranial evidence. *Ameghiniana* 34:2–32
- Sampson SD (2011) *Dinosaur odyssey: Fossil threads in the web of life*. University of California Press, Berkeley
- Sampson SD, Witmer LM (2007) Craniofacial anatomy of *Majungasaurus crenatissimus* (Theropoda: Abelisauridae) from the Late Cretaceous of Madagascar. *J Vertebr Paleontol* 8:32–102
- Sander PM (2013) An evolutionary cascade model for sauropod dinosaur gigantism – overview, update and tests. *PLoS One* 8(10):e78573. <https://doi.org/10.1371/journal.pone.0078573>
- Sander PM, Peitz C, Jackson FD et al (2008) Upper Cretaceous titanosaur nesting sites and their implications for sauropod dinosaur reproductive biology. *Palaeontographica A* 284:69–107
- Sander PM, Christian A, Clauss M et al (2011) Biology of the sauropod dinosaurs: the evolution of gigantism. *Biol Rev* 86:117–155
- Sanders RK, Smith DK (2005) The endocranium of the theropod dinosaur *Ceratosaurus* studied with computed tomography. *Acta Palaeontol Pol* 50:601–616
- Saveliev SV, Alifanov VR (2007) A new study of the brain of the predatory dinosaur *Tarbosaurus bataar* (Theropoda, Tyrannosauridae). *Paleontol J* 41:281–289

- Saveliev SV, Alifanov VR, Bolotsky YL (2012) Brain anatomy of *Amurosaurus riabinini* and some neurobiological peculiarities of duck-billed dinosaurs. *Paleontol J* 46:79–91
- Schade M, Rauhut OWM, Evers SW (2020) Neuroanatomy of the spinosaurid *Irritator challengeri* (Dinosauria: Theropoda) indicates potential adaptations for piscivory. *Sci Rep* 10:9259. <https://doi.org/10.1038/s41598-020-66261-w>
- Schmitt A, Knoll F, Tschopp E (2015) Paleoneurology of *Europasaurus holgeri*, an insular dwarf sauropod from northern Germany. *J Vertebr Paleontol* 35(suppl):209
- Schmitz L, Motani R (2011) Nocturnality in dinosaurs inferred from scleral ring and orbit morphology. *Science* 332:705–708
- Sedlmayr JC (2002) Anatomy, evolution, and functional significance of cephalic vasculature in Archosauria. Dissertation, Ohio University
- Sedlmayr JC (2022) Anatomy, Evolution, and Functional Significance of Cephalic Vasculature in Archosauria (Unpublished Ph.D.dissertation). Ohio University, 398
- Seeley HG (1887) On the classification of the fossil animals commonly named Dinosauria. *Proc R Soc Lon* 43:165–171
- Senter P (2005) Function in the stunted forelimbs of *Mononykus olecranus* (Theropoda), a dinosaurian anteater. *Paleobiol* 31:373–381
- Sereno PC (1999) The evolution of dinosaurs. *Science* 284:2137–2147
- Sereno PC, Beck AL, Dutheil D et al (1998) A long-snouted predatory dinosaur from Africa and the evolution of spinosaurids. *Science* 282(5392):1298–1302
- Sereno PC, Wilson JA, Witmer LM (2007) Structural extremes in a Cretaceous dinosaur. *PLoS One* 2:e1230. <https://doi.org/10.1371/journal.pone.0001230>
- Serrano-Brañas CI, Hernández-Rivera R, Torres-Rodríguez E et al (2006) A natural hadrosaurid endocast from the Cerro del Pueblo Formation (Upper Cretaceous) of Coahuila, Mexico. In: Lucas SG, Sullivan RM (eds) Late cretaceous vertebrates from the Western interior. *Bull N M Mus Nat Hist Sci* 35:317–321
- Shibata M, Kawabe S, Chokhaloemwong D et al (2016) Endocranial anatomy of *Sirindhorna khoratensis* (Ornithopoda, Hadrosauroida) and its implication. Abstract presented at the 76th SVP annual meeting, 26–29 October (Salt Lake City)
- Smaers JB, Dechmann DK, Goswami A et al (2012) Comparative analyses of evolutionary rates reveal different pathways to encephalization in bats, carnivorans and primates. *PNAS* 109(44):18006–18011
- Smith DK, Sanders RK, Wolfe DG (2018) A re-evaluation of the basicranial soft tissues and pneumaticity of the therizinosaurian *Nothronychus mckinleyi* (Theropoda; Maniraptora). *Plos One* 13(7):e0198155. <https://doi.org/10.1371/journal.pone.0198155>
- Starck D (1979) Cranio-cerebral relations in recent reptiles. In: Gans C, Northcutt RG, Ulinski P (eds) *Biology of the reptilia, Neurology A*, vol 9. Academic, London, pp 1–36
- Stevens KA (2006) Binocular vision in theropod dinosaurs. *J Vertebr Paleontol* 26:321–330
- Striedter G (2005) Principles of brain evolution. Sinauer Associates, Sunderland
- Stromer E (1931) Ergebnisse der Forschungsreisen Prof E. Stromers in den Wüsten Agyptens. II Wirbeltierreste der Baharije-stufe (unterstes Cenoman). 10. Ein Skelett-Rest von *Carcharodontosaurus* nov. gen. *Abh Bayer Akad Wissensch Math-Naturwiss Abt* 9:1–23
- Sues H-D, Averianov A, Ridgely RC et al (2015) Titanosauria (Dinosauria, Sauropoda) from the Upper Cretaceous (Turonian) Bissekty Formation of Uzbekistan. *J Vertebr Paleontol* 35:1–14
- Tahara R, Larsson HCH (2011) Cranial pneumatic anatomy of *Ornithomimus edmontonicus* (Ornithomimidae: Theropoda). *J Vertebr Paleontol* 31:127–143
- Thomas DA (2015) The cranial anatomy of *Tenontosaurus tilletti* Ostrom, 1970 (Dinosauria, Ornithopoda). *Palaeontol Electron* 18(2):37A. <https://doi.org/10.26879/450>
- Tumanova TA (1987) The armored dinosaurs of Mongolia, Transactions of the joint Soviet-Mongolian paleontological expedition, vol 32. Izdat. Nauka, Moskva, pp 1–76
- Tykoski RS, Fiorillo TR (2012) Beauty or brains? The braincase of *Pachyrhinosaurus perotorum* and its utility for species-level distinction in the centrosaurinae ceratopsid *Pachyrhinosaurus*. *Earth Environ Sci Trans R Soc Edin* 103:487–499

- Upchurch P, Barret PM, Dodson P (2004) Sauropoda. In: Weishampel DB, Dodson P, Osmólska H (eds) *The Dinosauria*, 2nd ed, University of California Press, Berkeley pp 259–322
- Vergne AL, Pritz MB, Mathevon N (2009) Acoustic communication in crocodylians: from behaviour to brain. *Biol Rev* 84:391–411
- von Huene F (1906) Ueber die Dinosaurier der aussereuropaischen Trisa. *Geol Palaeontol Abhandl* 8:97–156
- von Huene F, Matley CA (1933) The Cretaceous Saurischia and Ornithischia of the central provinces of India. *Mem Geol Surv India* 21:1–74
- Vickaryous MK, Maryanska T, Weishampel DB (2004) Ankylosauria. In: Weishampel DB, Dodson P, Osmólska H (eds) *The dinosauria*, 2nd edn. University of California Press, Berkeley, pp 362–392
- Walsh SA, Milner A (2011) Evolution of the avian brain and senses. In: Dyke G, Kaiser G (eds) *Living dinosaurs: the evolutionary history of modern birds*. Wiley, London, pp 282–305
- Walsh SA, Barrett PM, Milner AC et al (2009) Inner ear anatomy is a proxy for deducing auditory capability and behaviour in reptiles and birds. *Proc Royal Soc B* 276:1355–1360
- Walsh SA, Iwaniuk AN, Knoll MA et al (2013) Avian cerebellar floccular fossa size is not a proxy for flying ability in birds. *PLoS One* 8(6):e67176. <https://doi.org/10.1371/journal.pone.0067176>
- Watanabe A, Balanoff AM, Gignac PM et al (2021) Novel neuroanatomical integration and scaling define avian brain shape evolution and development. *eLife* 10:e68809
- Watanabe A, Gignac PM, Balanoff AM et al (2019) Are endocasts good proxies for brain size and shape in archosaurs throughout ontogeny? *J Anat* 234:291–305
- Wedel M, Atterholt J, Dooley AC Jr et al (2021) Expanded neural canals in the caudal vertebrae of a specimen of *Haplocanthosaurus*. *Academia Letters* 911:10.20935/AL911
- Weishampel DB, Dodson P, Osmólska K (2004) *The dinosauria*. University of California Press, Berkeley
- Werner J, Griebeler EM (2013) Reproduction in non-avian dinosaurs: linking information from the fossil record and from the allometries of extant close relatives. *PLoS ONE* 8(8):e72862. <https://doi.org/10.1371/journal.pone.0072862>
- Wilson J, D’Emic M, Rogers C et al (2009) Reassessment of sauropod dinosaur *Jainosaurus* (=“*Antarctosaurus*”) *septentrionalis* from the Upper Cretaceous of India. *Contrib Mus Paleontol Univ Mich* 32(2):17–40
- Witmer LM (1995) The extant phylogenetic bracket and the importance of reconstructing soft tissues in fossils. In: Thomason JJ (ed) *Functional morphology in vertebrate paleontology*. Cambridge University Press, New York, pp 19–33
- Witmer LM, Ridgely RC (2008a) The paranasal air sinuses of predatory and armored dinosaurs (Archosauria: Theropoda and Ankylosauria) and their contribution to cephalic structure. *Anat Rec* 291:1362–1388
- Witmer LM, Ridgely RC (2008b) Structure of the brain cavity and inner ear of the centrosaurine dinosaur *Pachyrhinosaurus* based on CT scanning and 3D visualization. In: Currie PJ, Langston W Jr, Tanke DH (eds) *A new horned dinosaur from an Upper Cretaceous bone bed in Alberta*. Canadian Science Publishing, Ottawa, pp 117–144
- Witmer LM, Ridgely RC (2009) New insights into the brain, braincase, and ear region of tyrannosaurs (Dinosauria, Theropoda), with implications for sensory organization and behavior. *Anat Rec* 292:1266–1296
- Witmer LM, Ridgely RC (2010) The Cleveland tyrannosaur skull (*Nanotyrannus* or *Tyrannosaurus*): new findings based on CT scanning, with special reference to the braincase. *Kirtlandia* 57:61–81
- Witmer LM, Chatterjee S, Franzosa J et al (2003) Neuroanatomy of flying reptiles and implications for flight, posture and behavior. *Nature* 425:950–953
- Witmer LM, Ridgely RC, Dufeu DL et al (2008) Using CT to peer into the past: 3D visualization of the brain and ear regions of birds, crocodiles, and nonavian dinosaurs. In: Endo H, Frey R (eds) *Anatomical imaging: towards a new morphology*. Springer, Tokyo, pp 67–88

- Wylie DRW, Gutiérrez-Ibáñez C, Iwaniuk A (2015) Integrating brain, behavior and phylogeny to understand the evolution of sensory systems in birds. *Front Neurosci* 9(31):281. <https://doi.org/10.3389/fnins.2015.00281>
- Wyneken J (2007) Reptilian neurology: anatomy and function. *Vet Clin Exot Anim* 10:837–853
- Xing L, Paulina-Carabajal A, Currie PJ et al (2014) Braincase anatomy of the basal theropod *Sinosaurus* from the Early Jurassic of China. *Acta Geol Sin* 88:1653–1664
- Yates AM (2007) The first complete skull of the Triassic dinosaur *Melanorosaurus* Haughton (Sauropodomorpha: Anchisauria). In Barret PM, Batten DJ (eds). *Evolution and palaeobiology of early sauropodomorph dinosaurs*. Special Pap Palaeontol 77:9–55
- Young C-C (1958) The dinosaurian remains of Laiyang, Shantung. *Palaeontol Sin, Ser C* 42(16):1–138
- Zelenitsky DK, Therrien F, Kobayashi Y (2009) Olfactory acuity in theropods: palaeobiological and evolutionary implications. *Proc R Soc B* 276:667–673
- Zelenitsky DK, Therrien F, Ridgely RC et al (2011) Evolution of olfaction in non-avian theropod dinosaurs and birds. *Proc R Soc B* 278:3625–3634
- Zhang Q-N, King L, Li D-Q et al (2019) Endocranial morphology of *Auroraceratops* sp. (Dinosauria: Ceratopsia) from the Early Cretaceous of Gansu Province, China. *Hist Biol* 32(10):1455–1366
- Zheng Z (1996). Cranial anatomy of *Shunosaurus* and *Camarasaurus* (Dinosauria: Sauropoda) and the phylogeny of the Sauropoda. Dissertation, Texas Tech University
- Zhou C-F, Gao K-Q, Fox RC et al (2007) Endocranial morphology of psittacosaur (Dinosauria: Ceratopsia) based on CT scans of new fossils from the Lower Cretaceous, China. *Palaeoworld* 16(4):285–293

Chapter 9

Anatomy and Evolution of Avian Brain and Senses: What Endocasts Can Tell Us



Federico J. Degrange, Julieta Carril, Ricardo S. De Mendoza, María M. Demmel Ferreira, and Claudia P. Tambussi

9.1 Systematic and Phylogenetic Context

Birds represent the most speciose and diverse group of terrestrial vertebrates. Nowadays, birds exhibit a great disparity regarding body shapes, body masses and behaviors, and they have conquered all present environments Brad Harris' character from the 2011 movie 'The Big Year' said "Who doesn't love birds? ... they're beautiful, and they fly, and they're capable of incredible things!". As highlighted by Harris' quote, birds' most noticeable feature is the ability to fly (or the ability to fly that their ancestors used to have). This fact was possible due to the evolution of feathers and other features related to sustained flight like the pneumatic bones, air sacs and even cranial kinesis (Zweers et al. 1997). The theropod-Bird transition was characterized by a reduction of body-size (Lee et al. 2014), which facilitated the evolution of other features such as the enhancement of flight and paedomorphic skulls, which in turn, enabled the development of large eyes and brain (Bhullar et al. 2012, 2016). Nevertheless, most of the features that characterize birds and their

F. J. Degrange (✉) · M. M. Demmel Ferreira · C. P. Tambussi
Centro de Investigaciones en Ciencias de la Tierra (CICTERRA), UNC, CONICET,
Córdoba, Argentina

Consejo Nacional de Investigaciones Científicas y Técnicas (CONICET),
Buenos Aires, Argentina
e-mail: fjdegrange@conicet.gov.ar; manuela.demmel@mi.unc.edu.ar;
tambussi.claudia@conicet.gov.ar

J. Carril · R. S. De Mendoza
Consejo Nacional de Investigaciones Científicas y Técnicas (CONICET),
Buenos Aires, Argentina

Laboratorio de Histología y Embriología Descriptiva, Experimental y Comparada
(LHYEDEC), Facultad de Ciencias Veterinarias, Universidad Nacional de La Plata,
La Plata, Argentina
e-mail: ricardo.demendoza@fcnym.unlp.edu.ar

ability to fly have been acquired in the non-avian theropods, implying that “there is no sharp line demarcating bird and non-bird, the distinction has become entirely arbitrary” (Witmer 2002: p 6).

It is worth mentioning here that the colloquial term “bird” refers to the clade Aves (in the sense of Chiappe 1997 *contra* Avialae in the sense of Gauthier 1986). Aves are maniraptoran theropod dinosaurs (or in a more encompassing sense, birds are dinosaurs), and together with Deinonychosauria, they constitute the group known as Paraves (Balanoff et al. 2013; Xu et al. 2011). Until recently, the first known bird was *Archaeopteryx* from the Upper Jurassic of Solnhofen, Germany, which was capable of performing active flight based on short-distance flapping (Voeten et al. 2018). However, its phylogenetic relation to birds has been challenged, alleging that *Archaeopteryx* is a non-avian dinosaur more closely related to Deinonychosauria, and flight may be a convergence between this last group and Aves (Xu et al. 2011). To add more controversy, more recently *Archaeopteryx* has been placed back into Aves (Lee and Worthy 2012; Field et al. 2018; Torres et al. 2021). By the Cretaceous, the most diverse and widespread birds were the Enantiornithes, a group with predominantly arboreal lifestyle (O’Connor et al. 2011). Other fossil birds registered in the Cretaceous period belonged to the Ornithuromorpha, a clade that included the iconic *Ichthyornis* (Field et al. 2018) and the aquatic *Hesperornis* (Bell and Chiappe 2016), among others. Modern birds, Neornithes (Aves in the sense of Gauthier 1986), appeared in the Upper Cretaceous (Clarke et al. 2005, 2006; Ksepka et al. 2017; Field et al. 2020). By the K-Pg extinction event most arboreal-dwelling birds became extinct. Only the ground-dwelling birds survived and diversified giving origin to the remaining groups of Neornithes, a radiation that occurred in the early Cenozoic (Field et al. 2018).

Neornithes are divided into two large groups based on the morphology of their palate: Paleognathae and Neognathae (Mindell and Brown 2005). Paleognathae includes the Tinamiformes (also known as inambues) and the ratites, a group of birds not capable of flying that includes kiwis, large and cursorial birds like rheas, cassowaries, emus, ostriches, and the gigantic extinct moas. Neognathae includes Galloanserae and Neoaves. Galloanserae includes landfowl and waterfowl, and Neoaves includes the remaining groups of birds whose phylogenetic relationships are still debated. Recent phylogenetic analyses based on molecular data (e.g. Prum et al. 2015) show that Neoaves comprises at least five large groups: (1) the Strisores, that includes the insectivorous nightjars, hyper-aerial birds such as swifts, and birds with extreme feeding adaptations to nectarivory such as hummingbirds; (2) Columbaves that includes arboreal birds such as turacos, large flying migrant birds such as bustards, and doves, (3) Gruiformes, that includes cranes, rails and trumpeters; (4) Aequirornithes, a group that includes birds mainly associated with aquatic environments, including extreme divers such as penguins, soaring sustained flyers such as petrels and albatrosses and the diverse Charadriiformes, among others; and (5) Inopinaves. This last group is the most diverse of all birds, including raptors, toucans, woodpeckers, seriemas, parrots, and the songbirds (i.e. Passeriformes) which is the largest order of birds, comprising ~60% of extant species (Barker 2014; Barker et al. 2004).

9.2 Historical Background

The evolutionary history of the avian brain is so far relatively poorly understood, despite the fact that the first mention of a fossil brain dates back almost two centuries. While some debate still remains over correlations between anatomy and function, brain morphology has been linked to a wide array of cognitive and behavioural capacities and sensory and motor abilities observed in Neornithes, such as tool use, sociability, complex vocalization, parental care and locomotion (Bennet and Harvey 1985; Ebinger 1995; Lefebvre et al. 2004).

As in other vertebrates, the avian brain shows a degree of modularity (Watanabe et al. 2021). Although there is no consensus about the degree of functional modularity in the brain, most researchers agree that some functional areas can be determined, some of which are purely dedicated to sensory processing, motor control and/or cognition (e.g. eminentia sagittalis to stereopsis or three-dimensional vision, Iwaniuk and Wylie 2006; Iwaniuk et al. 2008). As a consequence, we generally assume that the increase in a given region is correlated with an increase in the complexity of its functions. This is known as Jerison's Principle of Proper Mass (Jerison 1973), which states that the relative size of a brain structure correlates with an increase in either the number or the size of neurons present and, hence, with the relative importance of the information processed by that structure.

A very particular aspect of birds, shared only with mammals and the extinct pterosaurs, is that the brain nearly fills the brain or intracranial cavity (Iwaniuk and Nelson 2002; Witmer et al. 2003), resulting in a high brain-to-endocranial cavity correlation index (BEC index; Balanoff et al. 2016a). The two meninges are very thin, causing the brain's surface and its vascularization to be printed on the intracranial bone wall. From the natural (e.g., sediment) or artificial filling (with latex or by medical or design software) of the brain cavity, it is possible to obtain an endocranium cast: the endocast. Thus, the study of the endocast provides direct evidence of the surface morphology of the brain (Iwaniuk and Nelson 2002; Striedter 2005; Balanoff et al. 2016a; Watanabe et al. 2019). Early anatomical studies of the brain in fossil birds were based on rare natural endocasts, or on plaster casts of the endocranial cavity (Edinger 1928). However, the latter technique is partially or totally destructive. Modern studies are principally based on CT scan data that allow virtual reconstructions of the brain endocast and sensory organs accurately through 3D imaging techniques. Indeed, the study of 3D models generated from CT scans opened a range of research possibilities, and avian paleoneurology found through the incorporation of 3D modelling a new impulse from 2000 forward (Knoll and Kawabe 2020). This methodology presents obvious advantages: materials usually do not need treatment (beyond the possible removal of matrix and sediment in fossils) before entering the scanner, no deterioration occurs during the scan, and the results allow the reconstruction of high-quality 3D models from both paleontological and neontological specimens (Milner and Walsh 2009; Balanoff et al. 2016a; Tambussi et al. 2014, 2017). The datasets obtained by CT scans are in theory

permanent and easily portable, facilitating the comparison and study of the 3D models obtained, which are easily manipulated, sectioned and redescribed.

To combine neuroanatomical studies of extant and fossil animals occasionally seems challenging. Many studies of extant birds use histological techniques, and thus are not directly comparable with data from fossils. In contrast, most paleoneurological studies look to explain the main transformations of the brain in the different lineages of birds. These paleoneurological studies use the endocast as a proxy of the external brain morphology. At the present state, it is undeniable that the endocast is a faithful reflection of the morphology and volume of the brain in adult birds (Iwaniuk and Nelson 2002; Watanabe et al. 2019; Early et al. 2020a). Dissected fresh material has confirmed the similarity between the actual brain and the virtual endocast (Fig. 9.1; Ksepka et al. 2012; Tambussi et al. 2015; Carril et al. 2016; Degrange et al. 2018). However, extensive pneumatization and the dural venous system may interfere with this relationship (Balanoff and Bever 2017). For instance, the presence and number of cerebellar folia can be obscured by the presence of the occipital sinus in the endocast of some birds. Reconstruction techniques and best practices to reconstruct a bird endocast can be found in Balanoff et al. (2016a).

The present chapter deals with broad patterns of brain and sense organ morphology and evolution taking imaging technology as a starting point. Except when noted, endocasts are hereafter referred to as brain models or simply brains. It has to be pointed out that only recently, avian brain terminology has been updated (Reiner et al. 2004a, b). However, there is also still the need for an updated terminology for the endocast. For descriptions of endocasts, the osteological nomenclature proposed by Baumel and Witmer (1993) is used (see Table 9.1), and anatomical terminology for the central nervous system follows Breazile and Kuenzel (1993) and Jarvis et al. (2005).

9.3 The Bauplan of the Avian Brain

The brain of any vertebrate can be divided into the forebrain, midbrain and hindbrain. In birds (and also in mammals) the forebrain is notably enlarged (Reiner et al. 2005). The shape and volume of these regions vary greatly among the different lineages of modern birds or Neornithes.

The dorsal surface of the avian forebrain (also call prosencephalon) is smooth, without the grooves that characterize the brain of most mammals. It is constituted by the telencephalon and diencephalon. A pair of characteristic dorsal structures called eminentiae sagittales (or wulsts) mark the dorsal surface of the telencephalon. They are separated from one another by a *fissura interhemispherica*, and separated from the lateral surface of the rest of the telencephalon by a furrow called the *vallecula*. The eminentiae sagittales can vary in shape, size and position. They can be located rostrally in the telencephalon as in *Strigiformes* and *Caprimulgiformes* or caudally as in *Psittaciformes*, corresponding respectively to types A and B

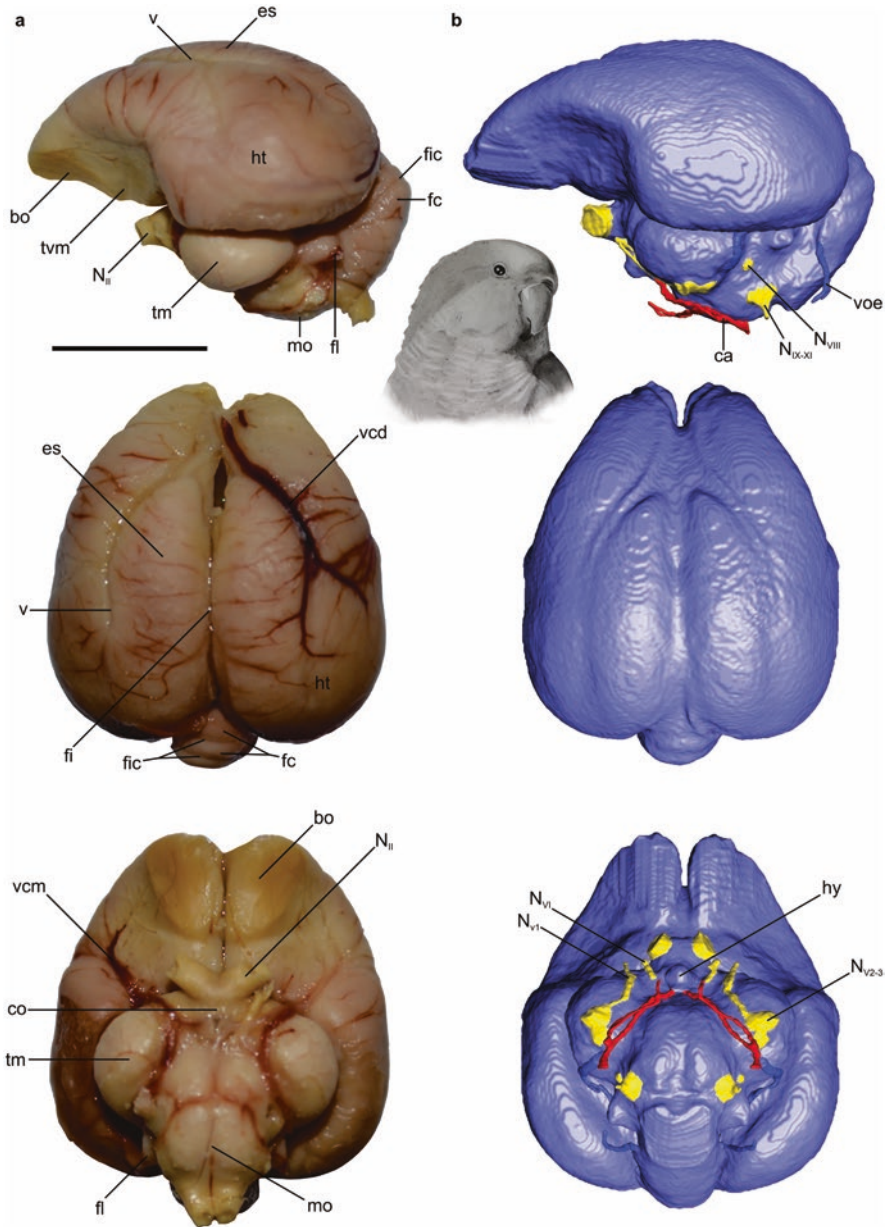


Fig. 9.1 Comparison of the (a) actual brain and (b) digital endocast of the monk parakeet *Myiopsitta monachus* (Psittaciformes) in lateral (top row), dorsal (middle row) and ventral (lower row) views. Scale = 1 cm. (Drawing by FJD)

according to the classification proposed by Stingelin (1957). In some other taxa, such as penguins, they occupy an intermediate position (Tambussi et al. 2015).

Table 9.1 Encephalic and sense organs terminology of Baumel et al. (1993), their most frequent vernacular names and abbreviations used in this work

Terminology	Vernacular Names	Abbreviations
Ampulla ossea anterior	Anterior ampulla	AA
Ampulla ossea lateralis	Lateral ampulla	La
Ampulla ossea posterior	Posterior ampulla	Pa
Anastomosis intercarotica	Intercarotid anastomosis	Ia
Arteria carotis cerebralis	Carotids	Ca
Auricula cerebelli	Flocculus	Fl
Auris interna	Inner ear	
Bulbus olfactorius	Olfactory bulbs	Bo
Canalis semicircularis anterior	Anterior/rostral semicircular canal	Asc
Canalis semicircularis lateralis	Horizontal/lateral semicircular canal	Hsc
Canalis semicircularis posterior	Caudal/posterior semicircular canal	Psc
Cavum cranii	Cranial cavity	
Cavum tympanicum	Middle ear region	
Cerebellum	Cerebellum	Ce
Chiasma opticum	Optic quiasm	Co
Cochlea	Cochlea	Dc
Crus communis	Crus communis	Cc
Diencephalon	Diencephalon	Di
Ductus semicircularis anterior	Anterior semicircular ductus	
Ductus semicircularis lateralis	Lateral semicircular ductus	
Ductus semicircularis posterior	Posterior semicircular ductus	
Endolympha	Endolymphatic fluid	
Epitellium corneae externum	Cornea	Co
Eminentia sagittalis	Sagittal eminentia or wulst	Es
Encephalon	Brain/endocast	
Fenestra cochlearis	Cochlear fenestra	Fco
Fenestra vestibularis	Vestibular fenestra	Fv
Fissura cerebelli	Cerebellar fissure	Fic
Fissura interhemisferica	Interhemispheric fissure	Fi
Flocculus (cerebellum)	Flocculus	Fl
Folia cerebelli	Cerebellar folia	Fc
Glandula pinealis	Pineal gland	
Hemispherium telencephali	Cerebral hemispheres	Ht
Humor aquosus	Aqueous humor	
Humor vitreum	Vitreous humor	V
Hypophysis	Hypophysis	Hy
Iris	Iris	i
Labyrinthus membranaceus	Membranous labyrinth	
Labyrinthus osseus	Bony labyrinth	
Labyrinthus vestibularis	Vestibular labyrinth	
Lentis	Lens	L

(continued)

Table 9.1 (continued)

Terminology	Vernacular Names	Abbreviations
Medulla oblongata	Medulla	Mo
Medulla spinalis	Spinal cord	
Mesencephalon	Mesencephalon/midbrain	Ms
Metencephalon	Metencephalon	Mt
Myelencephalon	Myelencephalon	My
Nervi craniales	Cranial nerves	N _{I-XII}
Oculi fovea	Fovea	Fo
Organum olfactorium	Olfactory organ	
Ossiculae sclerae	Scleral ossicles	Os
Pars cochlearis (inner ear)	Cochlea	
Pars vestibularis (inner ear)	Vestibulus	
Perylimpha	Perilymphatic fluid	
Prosencephalon	Forebrain	
Pupilla	Pupil	
Retina	Retina	Re
Pecten oculi	Pecten	Pe
Rhombencephalon	Hindbrain	
Sclera	Sclera	Sc
Sinus sagittalis dorsalis	Dorsal sagittal sinus	
Sinus transversus	Transversal sinus	
Systema nervosum Centrale	Central nervous system	
Tectum mesencephali	Optic lobe	Tm
Tectum opticum	Optic tectum	
Telencephalon	Telencephalum/cerebrum	Te
Tuber ventromediale	Ventromedial tuberosity	Tvm
Organum visum	Eye	
Vallecula telencephali	Valllecula	V
Vena cerebialis dorsorostralis	Dorsorostral cerebral vena	Vcd
Vena cerebialis media	Medial cerebral vena	Vcm
Vena occipitalis externa	Occipital vena externa	Voe

The forebrain is mostly involved in higher-level processing of sensory information, cognition, and memory. The eminentiae are related to visual and somatosensory inputs (Wild 2009). This is because the underlying soft-tissue structure, the hyperpallium, is part of the thalamofugal visual pathway linked to contour perception, distance discrimination, and spatial orientation among others (Güntürkün and Hahmann 1999; Shimizu and Bowers 1999). Early et al. (2020b) demonstrated that there is a very high correlation between the volume of the hyperpallium and the surface of the eminentia sagittalis expressed in the endocast. So, the size of the eminentia sagittalis can be used with confidence as an expression of the visual capabilities of a bird. Moreover, the eminentiae are very conspicuous in birds with strong visual specializations, such as owls and nightjars (Iwaniuk and Wylie 2006). In the

ventral and more rostral region of the telencephalon are the olfactory bulbs. They are paired structures (always small compared to reptiles) of variable size in the different birds. In seabirds and scavengers, for instance, they are larger compared to most other birds (Walsh and Milner 2011a). According to Cobb (1959), the bulbs can be discriminated in two types: the one-lobe type, in which the olfactory bulbs are a single mid-line structure (e.g. Suliformes); and the biantennary type, in which the bulbs are double (e.g. Procellariiformes). Rostrally to these bulbs extends the first pair of cranial nerves, the olfactory nerve (I).

The diencephalon is also part of the circuit of visual pathways; the tectofugal and thalamofugal pathways involved in visual input and processing. The pineal gland is very small, located on the dorso-caudal surface of the forebrain. The hypophysis (pituitary) has a variable shape and development, projecting ventrally between the caudal region of the optic chiasm and the rostral region of the hindbrain. The cranial nerves II (optic) leave the rostral portion of the diencephalon and branch before or after leaving the endocranial cavity. By crossing each other at the base of the brain, they form the optic chiasm projecting to various centers in the diencephalon and midbrain (Martin et al. 2007).

A paired tectum mesencephali (optic lobes) can be observed projecting laterally in the midbrain. However, due to the lateral expansion of the telencephalon, these lobes are occluded dorsally. The optic lobes receive visual information from the retina as part of the tectofugal visual pathway, considered the main visual pathway as it is involved in discrimination of brightness, colors and patterns. The optic lobe size is also influenced by the size of an underlying tissue, the nucleus lentiformis mesencephali, involved in the combination of fast and slow eye movement responses (optokinetic reflex). Eye and head movements help stabilize the image on the retina and, therefore, contribute to visual-spatial resolution (Schmid and Wildsoet 1998). The cranial nerve III (oculomotor) originates from this region of the brain, projecting rostrally towards the orbit, while cranial nerve IV (trochlear) originates from the ventro-lateral portion of the midbrain.

The hindbrain is constituted by the cerebellum and the medulla oblongata. In general terms, the hindbrain is in charge of motor control. Its autonomous centers also regulate heartbeat, respiration, and digestion and act as a bridge between the brain and the peripheral nervous system. The cerebellum is located caudally to the two telencephalic hemispheres (which hide part of the cerebellum) and dorsally to the medulla. Its most outstanding structures are the flocculi that project from their lateral walls through the arch of the anterior semicircular canal of the labyrinth of the inner ear. However, this extension is variable among Neornithes, being longest in seabirds and shortest in songbirds, parrots and woodpeckers. Cerebellar folia usually number eleven, and can be very well marked (e.g. Psittaciformes) or difficult to observe (e.g. Sphenisciformes) in the endocast. Iwaniuk et al. (2006a) stated that the differences in the degree of foliation (and folia size) among Neornithes are influenced by phylogeny. However, it is worth mentioning that the development of the occipital dural sinus may hide the cerebellar folia in the endocast.

According to Boire and Baron (1994) and Iwaniuk et al. (2006a, b), the size of the cerebellum may be related to flight abilities. However, an enlarged cerebellum

has been observed in aquatic birds and this has been related to tail and hindlimbs control. The flocculi play an important role in gaze stabilization through the vestibulo-ocular reflex (i.e. coordination of the eye movements with movements of the head, neck and body), and tend to be enlarged in taxa that rely on quick movements of the head (Witmer et al. 2003). Although estimating the size of the flocculi from the endocast can lead to errors due to the relationship between vascular and neuronal tissue (Walsh et al. 2013a), it is known that the size is related to the feeding strategy and nocturnality (see also Ferreira-Cardosa et al. 2017).

The medulla oblongata (or myelencephalon) is typically located ventrally to the cerebellum, and less frequently rostroventrally to it. It acts as a bridge between the rostral brain regions with the spinal cord and peripheral nerves. It contains nuclei related to heartbeat, digestion and respiration. Most nerves (V to XII) exit the brain from the medulla, either from the rostroventral portion (VI), lateral (V and VII), ventrocaudolateral (IX to XI) or ventral (XII).

9.4 Avian Brain Disparity

Bird brains exhibit a high variation in shape and size (Fig. 9.2). This variation is affected by multiple factors including the position of the brain within the skull (Dubbeldam 1989). Even the size of the eye has been correlated with brain morphology (Kawabe et al. 2013a). Also, the shape of the brain is, to some extent, a correlate of the relative size of specific regions such as those of the telencephalon, cerebellum, or midbrain optic lobes (Early et al. 2020b). In most birds, the main brain axis is at an angle with the axis of the spinal cord, so that in lateral view, a flexion is observed. Furthermore, the main axis of the brain and that of the beak can also be aligned (e.g. *Phalacrocorax* spp.) or in a strong angle (e.g. *Spheniscus* spp.) (Dubbeldam 1989; Marugán-Lobón and Buscalioni 2006; Walsh and Milner 2011a). In some birds, the telencephalon and the cerebellum are aligned (e.g., loons, cormorants). But in most birds, the cerebellum is located ventral to the telencephalon such that in dorsal view, the cerebellum is hidden totally or partially by the telencephalon. Most of this flexing occurs within the region of the mesencephalon (Pearson 1972), with a strong angle often developed between the long axis of the telencephalon and with the brain as a whole (Dubbeldam 1989). These types of brains are called orthocephalic and airecephalic respectively (Duijm 1951; Marugán-Lobón and Buscalioni 2006).

Iwaniuk and Hurd (2005) proposed the distinction of brain types of birds (i.e. cerebrotypes) based on the relative development of the regions as a whole, in an attempt to address two issues: first, that the development of a particular area may not be independent and may be correlated with other areas; and second, that the constitution of the brain is the product of the selective pressure of multiple factors in addition to the phylogenetic constraints. Using principal component and cluster analyses with 67 bird species, Iwaniuk and Hurd (2005) recognized five cerebrotypes associated with different environments. However, the cerebrotypes do not group species

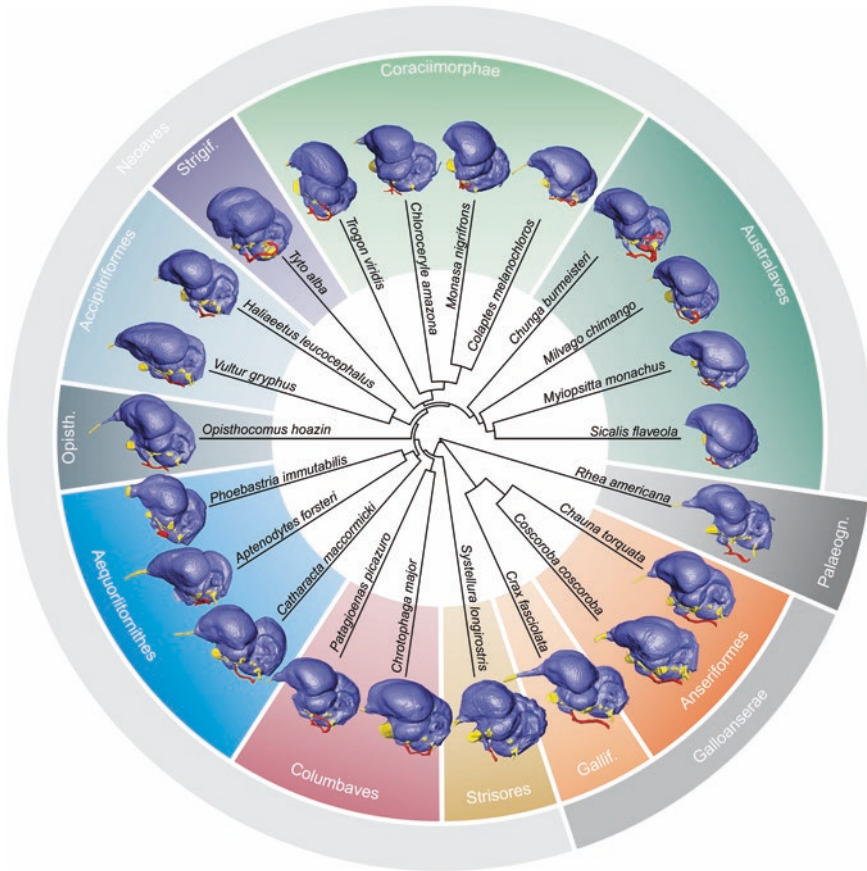


Fig. 9.2 Neornithes brain disparity (endocasts displayed in lateral view) mapped onto a simplified phylogeny taken from Prum et al. (2015). Not to scale

with similar development (e.g. precocial or altricial) nor with phylogenetically related species. As the same authors assume, in some cases the segregation is not conclusive, but it is a first step towards future multivariate analyzes with more species that could reveal more reliable relationships.

Bird brains are characterized by the increase of the size of the telencephalon, the cerebellum and the optic lobes, although features such as the degree of encephalization, the expansion of the telencephalon, the development of the eminentia sagittalis, or the total volume can be highly variable. The size or expansion relationships between the different regions of the brain as a whole is the result of an increment in neuronal packing which, in turn, is due to a greater preponderance in the functions performed by a certain regions (Striedter and Charvet 2008). In other words, the shape and size of the brain reflect some aspect of what a bird ‘does’ and therefore reflects its cognitive and sensory capacities, and possibly its ecology and behavior (Iwaniuk and Hurd 2005; Iwaniuk et al. 2004; Walsh and Milner 2011a).

Brain shape seems to be relatively consistent within clades (Fig. 9.2; Stingelin 1957) suggesting that the form of the brain may be phylogenetically constrained, although some variation may be observed (e.g., Pelecaniformes, see Kawabe et al. 2014; Psittaciformes, see Carril et al. 2016). However, little is known yet about how and how much the size and morphological variation observed in the birds' brain would be related to ethological, phylogenetic and/or life history aspects.

9.5 Cranial Nerves

Birds have twelve cranial nerves (Bubien-Waluszewska 1981), the four most rostral departing from the fore- and midbrain (the description of the nerves I to IV were made in Sect. 9.3), while the other eight leave the brain from the lateral and ventral surface of the hindbrain. The cranial nerve V (trigeminal) has two main branches: V_1 conducts sensory input on the eye, meanwhile the V_{2-3} branches (the most conspicuous) are subdivided into two main sub-branches, the maxillary and mandibular, which receive information from the beak and carry motor impulses to its muscles. Cranial nerve VI (abducens) leaves the medulla ventrally, in the most cranial part, carrying motor impulses to the muscles of the eye. Cranial nerve VII (facial) has motor and sensory functions such as taste. This nerve innervates facial musculature, but since in birds the facial musculature is practically absent, the development of cranial nerve VII is poor. Cranial nerve VIII (vestibulocochlearis) is exclusively involved in sensory functions such as audition, and equilibrium and acceleration, through the cochlear duct, ampullae and semicircular canals. Cranial nerve IX (glossopharyngeal) retransmits motor and sensory impulses such as taste. It generally shares an output with cranial nerves X (vagus) and XI (accessorius) on the lateral surface of the medulla. Cranial nerve X conducts sensory and motor impulses that regulate autonomic functions, mainly in the heart, digestive tract, and lungs. Cranial nerve XI carries motor impulses to the neck muscles. Finally, cranial nerve XII (hypoglossus) carries motor impulses to the tongue, trachea, syrinx (avian voice box), and some rostral cervical muscles.

9.6 Brain Vascularization

Paired carotid arteries run through the neck, extending laterally and dividing into two branches, the internal and external carotids, supplying arterial blood to the brain (Baumel 1993). The internal carotids run rostromedially through two bony carotid canals and transversely to the long axis of the skull, before contacting dorsally the distal portion of the hypophysis (Aslan et al. 2006; Porter and Witmer 2016). In most birds at this level, an intercarotid anastomosis is established through a transverse vessel that connects the right and left arteries. The anastomosis allows arterial blood to diffuse bilaterally to both hemispheres (Verduzco Mendoza et al. 2009).

Part of the literature affirms that it is functionally equivalent to the mammalian Circle of Willis (Baumel 1993) that helps blood flow from both the rostral and caudal regions of the brain.

Following Baumel and Gerchman (1968) and Pettit et al. (1981) four types of different shapes of the intercarotid anastomosis are recognized: the I-type has an elongated middle vessel formed by the merging of both internal carotids, the H-type has a long transverse anastomosis connecting the internal carotids, the X-type has a side-to-side anastomosis of the internal carotids, and the XH-type has a short transverse anastomosis of the internal carotids, being an intermediate state between the H- and X-types. The functional implications of these different types of anastomoses are still unknown, and at the moment it seems that there is no phylogenetic signal, especially at lower taxonomic levels, where it may be lost due to homoplasy. To give an example, the Magellanic penguin *Spheniscus magellanicus* has an anastomosis of type X or ‘side to side’ anastomosis, while the chinstrap penguin *Pygoscelis antarcticus* has type H (Tambussi et al. 2015). Also, phylogenetically distant taxa such as *Gallus* (Baumel 1981; Campos et al. 1995), the ostrich (Nazer and Campos 2011) or the Sparrowhawk (Ozudogru et al. 2016) have type H.

It is important to mention that in most birds, the bony carotid canals provide passage for the arteria carotis cerebialis and frequently also conduct the vena carotis cerebialis. Clearly, the cast of these conduits cannot discern between the arteria and the vena, so caution must be taken when describing the ‘carotids’ based on endocasts.

9.7 Brain Size

Brain size has become a measure for predicting cognitive, behavioral, sensory and motor abilities of vertebrates (Jerison 1973; Lefebvre et al. 2004; Lefebvre and Sol 2008; Corfield et al. 2008; Iwaniuk 2017). Although now controversial, the classical method used to estimate cognitive abilities is the encephalization coefficient (EQ) proposed by Jerison (1973). EQ is the ratio of the actual and expected brain size expressed by the volumetric measure (VEC, expressed in cm³) of an animal of a given body size (MC, expressed in grams). For birds the equation is as follows:

$$EQ = VEC / 0.137MC^{0.568}$$

Species with endocranial volumes larger than expected for their body mass will have EQ >1, while species with endocranial volumes smaller than expected for their body mass will have EQ values <1. Bird body masses can be obtained easily from collection data or bibliography (e.g., Dunning 2008) or by direct measurements. In the case of fossils, the mass can be estimated based on postcranial elements (see for example Campbell and Marcus 1992; Field et al. 2013) or from the virtual brain itself. Therefore, brain volume and body mass are highly variable depending on the applied method and, consequently, the analysis and comparison of the encephalization coefficients should be taken with caution.

Brain size varies mainly with body mass (Fig. 9.3), and this variation can be described through an allometric function (e.g. Ksepka et al. 2020). However, the way that the brain volume can be measured or estimated depends on the nature of the specimen. Iwaniuk and Nelson (2002) proposed the lead shot method in which the skull is filled with lead shot through the occipital foramen, then removed and weighed. Brain volume is calculated by dividing the total mass of lead shot by its density (11.4 g/ml), and the brain mass can be calculated by multiplying the volume obtained by the density of the brain, assumed to be the same as that of the nervous tissue (1.036 g/ml following Edinger 1995). Kawabe et al. (2009, 2013b) proposed a simple regression method in which the maximum brain width measured in the endocast is regressed against brain volume. Picasso et al. (2010) compared these three methods of volume estimation for different post-hatching stages of the greater rhea (*Rhea americana*). They concluded that indirect methods proved to be effective and constitute an alternative tool to direct measurements, which could be affected by post-mortem dehydration and rehydration of the nervous system in formalin or alcohol fixation solutions (Healy and Rowe 2007). The linear method of Kawabe et al. (2009), subsequently tested by Kawabe et al. (2013b) also proved to be a good estimator of brain volume. However, the values obtained by the lead shot method following the methodology of Iwaniuk and Nelson (2002) and by Iwaniuk et al. (2004, 2005) were lower than those obtained from 3D models, and in all cases very heterogeneous. Nowadays, the most common method used is the volume measurement from virtual endocasts (Balanoff et al. 2016a). It is well known that in adult birds, the brain occupies more than 90% of the cranial cavity; therefore, the volume

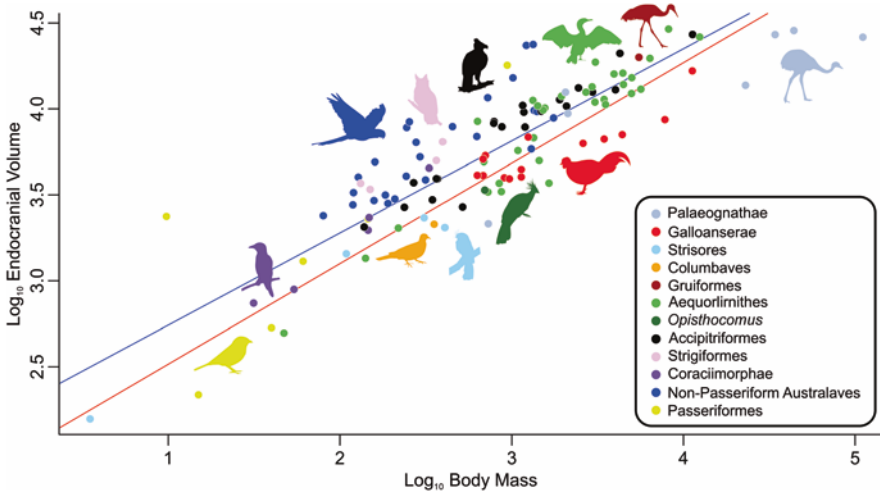


Fig. 9.3 Regression analyses between endocranial volume (mm^3) and body mass (g) in Neornithes. The red line represents the corrected phylogenetically regression line (pgls; $y = 0.5845x + 1.9306$, using Prum et al. 2015 phylogenetic proposal); meanwhile the blue line represents the regression without phylogenetic correction (OLS model; $y = 0.5x + 2.3103$). (Data taken from Walsh et al. 2013a)

of this cavity is a good estimate of the brain volume. However, in chicks (and in other adult archosaurs) the brain occupies only 60% of the endocranial cavity (Watanabe et al. 2019) so this approach is not applicable for these cases.

An increase in brain size is necessarily associated with an increase in the metabolic cost that is required for its maintenance and activity. In birds, there is an additional energy cost related to the parents' prolonged investment in taking care of the offspring, mainly in altricial species. It is generally accepted that precocial development is strongly associated with relatively small brains while the opposite occurs in birds with altricial development. Flight ability has also long been accepted as limiting brain size growth, while secondary loss flight removes this restriction. Some recent work points out the opposite and strictly flightless land birds have relatively smaller brains (Bennett and Harvey 1985; Iwaniuk and Nelson 2002). However, Iwaniuk et al. (2004) found that there is no correlation between the evolution of a relatively smaller brain and the secondary loss of flight. In other words, flightless birds generally do not have brain volumes noticeably different from those of flying species (Balanoff et al. 2016b). The current scenario is becoming increasingly complex and, apparently, more than one variable would be acting in this regard. For example, a study on brain size and climatic variables applied to parrots (Psittaciformes) states that relatively larger brains are favored in climatically variable environments (Sol et al. 2002, 2005). If this applies to all birds, species with brains of relatively larger sizes would be expected to tolerate better environments with a higher degree of environmental uncertainty (Marino 2005; Schuck-Paim et al. 2008). This complicates comparisons between different groups of birds as it is difficult to distinguish the effect of phylogenetic constraints from the effect of size, as well as from the environmental effect.

In a recent work based on endocast models, Carril et al. (2016) found (as expected) a positive correlation between body size and brain mass ($r^2 = 0.92$; $p < 0.05$) in Psittaciformes. EQ values obtained in 14 Neotropical parrot species suggested that these birds have higher brain volumes than expected for their body sizes, and reaffirms the idea that Psittaciformes have brains of greater relative sizes than other birds (Iwaniuk et al. 2005). As other authors argue, the relatively large brain sizes of Psittaciformes are potentially related to their advanced cognitive abilities (Carril et al. 2016), which include learning and vocal communication (Iwaniuk and Hurd 2005; Iwaniuk et al. 2005), a situation similar to that observed in crows (Passeriformes; Corvidae). However, it is important to point out here that brain volume alone can give a false or erroneous idea of cognition, since in Neornithes volume (and EQ) and neuronal packing/density are highly variable. Parrots and crows have high and similar EQs, but the neuronal density is superior (up to 30%) in the telencephalon of the crows (Olkowicz et al. 2016), which points to different cognitive capacities.

9.8 Senses

In this section, three of the main senses of birds are explored: vision, olfaction and hearing (Fig. 9.4). However, it is worth mention that birds have other senses that have been little investigated or are poorly understood.

Taste reception occurs in the beak and tongue, and is relayed to the brain through nerves VII and IX. It seems that this sense was not of prime importance during avian evolutionary history (Walsh and Milner 2011a) and, although some few cases, like the sandpipers and hummingbirds rely heavily on taste, this probably could be a trophic adaptation. In particular, sandpipers also rely on another sense poorly studied in birds: touch. Several corpuscles are located in small pits in the bill tip, allowing detection of prey buried in the sand using the trigeminal system (Gutiérrez-Ibáñez et al. 2009). A similar sense seems to be important in the nocturnal Kiwi (*Apteryx* spp.) that search for food on the floor during darkness. Early et al. (2018) state that

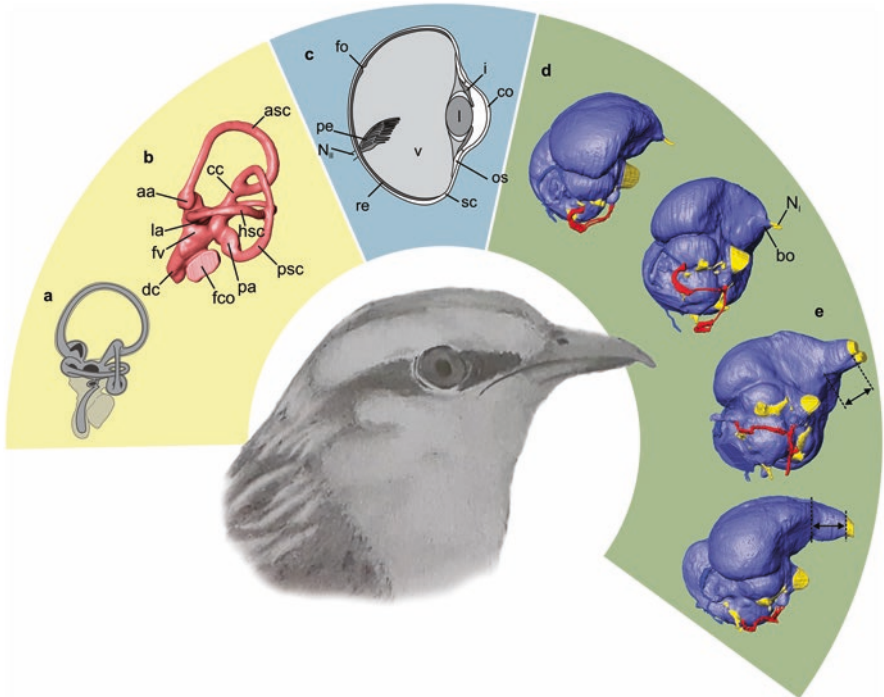


Fig. 9.4 Main avian senses. (a) schematic drawing of the inner ear showing differences between the membrane and osseous labyrinth, (b) 3D model of the inner ear of *Haliaeetus leucocephalus* (Accipitriformes), (c) Simplified structure of the avian eye (modified from Walsh and Milner 2011a), (d–e) olfactory bulb dimensions (after to Zelenitsky et al. 2009, 2011) indicated by the black arrow in the endocast of (d) *Milvago chimango* (Falconiformes) in right lateral and ventrolateral views, and (e) *Cathartes aura* (Cathartiformes) in ventrolateral and right lateral views. Not to scale. Drawing by FJD

most birds have pits and foramina in their beaks, so the generalizations about their functions are very speculative. Magnetoreception is another sense that has received attention only recently. It seems that the ophthalmic branch of the trigeminal nerve (V_1) and the mesencephalon are involved in feeling and processing of this input (Heyers et al. 2010; Wiltschko and Wiltschko 2019). Some birds, such as pigeons, have the ability to ‘see’ Earth’s magnetic field (Maeda et al. 2008; Wiltschko and Wiltschko 2019).

9.8.1 Inner Ear

The inner ear is a complex sensory organ, responsible for hearing and balance but also for space perception (Whitfield and Hammond 2007; Rabbitt et al. 2010). Here, its anatomy will be treated briefly and we will emphasize the functions associated with each structure.

The inner ear has ducts and cavities, known as the membranous labyrinth, through which endolymphatic fluid runs. It is enclosed within a bone cavity filled with perilymphatic fluid (Magariños et al. 2012) known as the bony labyrinth. Because this cavity is very thin, the bony labyrinth accompanies the shape of the membranous labyrinth (Fig. 9.4a). Thus, it is possible to build molds of the bony labyrinth to indirectly assess the anatomical characteristics of the membranous labyrinth (Fig. 9.4b; Witmer et al. 2008). From these data it is possible to explore its relationship with different capacities such as hearing, posture and locomotion (Walsh et al. 2009; Degrange et al. 2015), being of special relevance in the field of paleobiology.

The inner ear can be subdivided into two main parts (Walsh et al. 2009): the pars vestibularis and the pars cochlearis. The pars vestibularis is capable of perceiving linear and angular acceleration and changes in the position of the head. In combination with visual and somatosensory signals, it facilitates a wide range of automatic behaviors including stabilization of posture and coordination of body movement (de Beer 1947; Spoor et al. 2002; Sipla 2007; Cox and Jeffery 2010).

The pars vestibularis is formed by the three semicircular canals: the rostral and posterior canals inclined vertically, and the lateral canal inclined horizontally. The rostral canal is the longest of the three canals. Vertical canals control the adjustment of angular changes of the head within the longitudinal and medial axes of the skull (Cox and Jeffery 2010).

. It is assumed that the horizontal canal is associated with the sensitivity in the horizontal rotation of the head in such a way that, the longer it is, the greater the sensitivity. Moreover, the horizontal canal is usually aligned parallel or subparallel to the substrate plane during the alert position (Lebedkin 1924; de Beer 1947; Hullar 2006), giving information about the posture of the head (Duijm 1951). However, this assumption has been recently challenged, based on the premise that birds possess a range of horizontal canal orientations of $\sim 50^\circ$ in the alert posture (Marugán-Lobón et al. 2013). Although it has been shown that the orientation of the horizontal

canal is case-specific in mammals (Billet et al. 2012), this aspect needs further investigation among birds.

Both the position of the canals and their relative lengths provide information about the lifestyle of an animal, and they have been effectively applied in paleobiological studies (Hadžiselimović and Savković 1964; Milner and Walsh 2009; Walsh and Milner 2011b; Degrange et al. 2015; Tambussi et al. 2015). Shape and disposition of the canals have proven informative about flying capabilities. In general terms, the canals tend to be longer and thinner in good flyers than in other birds, and the most skilful flyers (e.g., *Falco*) tend also to have the rostral semicircular canals skewed medially. There are some exceptions and, therefore, inferences must be taken with caution.

In the pars cochlearis, the area most related to hearing, the cochlea, shows fairly uniform characteristics in all birds and, in general terms, the length increases relatively with decreasing body size (Schwartzkopff 1955). It is a ventrocranial elongated and medially curved finger-like tube that encloses the papilla basilaris (homologous to the mammalian organ of Corti). The papilla basilaris is made of ciliated sensory cells in a mosaic arrangement. The shape of these cells is an important factor in terms of hearing sensitivity, and they usually show a gradient in terms of width and length (Corfield et al. 2012). The function of the pars cochlearis is to convert the pressure levels of the middle ear into electrical impulses that are transmitted to the brain via the auditory nerve, in a process in which the perilymphatic fluid is also involved.

Because there is a correlation between the length of this papilla basilaris and the cochlea, it is possible to estimate hearing capacity by knowing the length of the cochlea (Gleich et al. 2005; Walsh et al. 2009). This finding is of singular importance for application to extinct or endangered species where access to the study of the papilla basilaris is difficult or impossible. This allowed subsequent authors to calculate hearing capabilities in fossil birds (e.g. Walsh et al. 2009; Walsh and Milner 2011b; Degrange et al. 2015; Tambussi et al. 2015) and relate these hearing capabilities to different behaviors. For example, estimation for hearing capacities in the extinct *Llallawavis scagliai* gave lower and upper ranges of 380.53 and 4229.63 respectively and a mean hearing sensitivity (~2300 Hz) below the average of living birds (Degrange et al. 2015).

Birds' best hearing frequency is between 1000 to 5000 Hz, but the greater sensitivity is between 2000 and 3000 (Schwartzkopff 1955; Dooling 2002). Some birds have larger ranges (owls) and others hear very low frequencies (emu, pigeons). The sound, produced by the syrinx is also used for echolocation in at least 16 living species (e.g., owls and oilbirds). To date, no apparent anatomical specializations in the auditory system or in higher processing centers of the encephalon have been found (Brinkløv et al. 2013).

9.8.2 Vision

Birds are well known to have large eyes and, indisputably, vision is their primary sense. Most of the things perceived during flight are visual or highly supplemented by vision. Thus, of all the senses, vision is the most important for a safe flight (Perrins 1990; Davies and Green 1994; Gill 2007; Martin and Osorio 2008). Obviously, visually related behaviours are not restricted to flight: perception of motion and orientation, but also to food detection and apprehension, prey capture and predator avoidance, group cohesion and mate selection are also related.

Two main functional divisions are recognized for the eye: its function as an image capture system and as a place where image processing begins. These statements lead to discussions about how variations in the form and structure of visual systems can be interpreted for some particular habits. This is a field of knowledge that is still full of gaps. It is not the objective of this section to focus on the anatomical and structural characteristics of the eye. We will make a brief summary of the main aspects and refer readers to the work of Hall and Ross (2007), Hall (2008) and Martin and Osorio (2008 and literature cited therein).

The lens and cornea are the main refractive structures of the eye of any vertebrate. In birds, there is an additional bone structure, the sclerotic ring (ossiculae sclerae), which houses a part of the eye that is not contained in the orbit (Fig. 9.4c; Hall 2008). The ossiculae sclerae is a series of bone segments that form a ring, variable in shape, size, number, curvature and overlap, and may or may not be fused (Lemmrich 1931; Curtis and Miller 1938; Bertelli et al. 2010). The number of ossicles is 12 to 16 in charadriiforms and gruiforms (Curtis and Miller 1938; Bertelli et al. 2010), between 12 and 14 in Phalacrocoracidae, and between 11 and 12 in Columbidae, Cuculidae, Trochilidae and some Psittacidae (Lemmrich 1931; Curtis and Miller 1938; Warheit et al. 1989).

The cavity with the lens is filled by the vitreous humor and opens to the most external cavity through the pupil. The pupil, which is under control of the iris, is always round in birds, except in the skimmers (Rynchopidae) which is like a slit reminiscent of that of some mammals and reptiles (Walls 1942; Zusi and Bridge 1981; Martin and Osorio 2008). The external cavity is filled with the aqueous humor. The pupil size and its control by the iris is the mechanism to adjust the levels of illumination of the retina, which size varies from more than a centimeter to the size of a pinhole (Martin and Osorio 2008). A notable property of the avian eye is that the accommodation is not only achieved by the lens but also by the cornea (Martin and Osorio 2008).

The retina is a layer of photosensitive tissue that covers the back of the eyeball, near the optic nerve. There is an intraocular, pigmented vascular structure called the pecten (pecten oculi) that nourishes the avascular retina (Kiama et al. 2001; Gültiken et al. 2012). The sector with the highest resolution of the retina is the fovea. Most birds have a single fovea, and only a few have two (e.g. hawks, seriemas, Wood 1917; Bringmann 2019). Modern birds have rods and five cone types (single and double cones) of photoreceptors while modern mammals have rods and two cone

types (Lamb et al. 2007; Baden and Osorio 2019; Seifert et al. 2020). The photoreceptors have different pigments allowing birds to capture different parts of the light spectrum. Single cones are related to chromatic reception and double cones with achromatic luminance reception. Rods have been shown to be inactive during the daylight, so the preponderance of some photoreceptors over others would give an idea of the preference of habits of the animal. Birds are probably tetrachromatic (Baden and Osorio 2019) and are sensitive to ultraviolet-A (UV, 350–400 nm spectrum), a condition that has evolved independently several times (Martin and Osorio 2008) and markedly separates them from mammals. This is possible because its ocular medium is transparent to UV and allows transmission of UV light to the retinal cones and the presence of a photoreceptor with maximum sensitivity for short wavelengths such as those seen in the UV spectrum (Toomey et al. 2016).

There is a wide variation of eye size, but they are indisputably large and can occupy up to 50% of the cranial volume (Seifert et al. 2020). As expected, the increase in eye size comes with a metabolic cost as the number of receptors and the eyeball mass (which is a large liquid-filled chamber) also increase (Martin and Osorio 2008). The size of the eye is positively correlated with the size of the eye-socket (Hall 2008; Schmitz 2009). An interesting observation is that there is a fixed relationship between brain and eye masses, and it is 0.68 (Brooke et al. 1999). Schmitz (2009) designed methods to estimate the dimensions of the soft tissues of the eyeball from the scleral ring and the dimensions of the orbit measured in the skull. These dimensions are highly correlated with visual capabilities (see above). It is widely accepted that the image resolution capacity is also related to the size of the eye. Bigger eyes and large pupils are optically better because they admit more light that stimulate the retina and increase spatial resolution (Land and Nilsson 2002; Lisney et al. 2020). The size of the eye and the cornea (which in turn limits the size of the pupil) is correlated with the activity of the bird. For example, the size ratio of the cornea and the eye is 0.7 or higher in nocturnal birds such as owls, kiwis and nightjars; it is less than 0.6 in diurnal raptors, passerines, gulls and parrots; and it is intermediate in crepuscular birds like some shorebirds, flamingos and ducks (Lisney et al. 2020 and literature cited therein).

A relationship between the size of the eye and the time of day in which the birds carry out their activity can be established, but not so clearly with the feeding strategy (Garamszegi et al. 2002). For example, passerines that begin to sing at the beginning of daylight have comparatively large eyes (Thomas et al. 2002) but, conversely, shorebirds with large eyes feed at night (Thomas et al. 2006). Both diurnal and nocturnal raptors have large eyes (Garamszegi et al. 2002). The diameter of the cornea is greater than the axial length of the eye in nocturnal birds, while in diurnal birds the relationship is the opposite. The first case would be related to the need to increase sensitivity to light, and the second would be correlated with greater visual acuity (Hall 2008).

Some examples about relationships between axial length of the eye and habits are: 39 mm in the ostriches, 29 mm in the tawny owls (*Strix aluco*) and 33 mm in the mountain eagle (*Aquila audax*). The latter has the highest known visual resolution (Reymond 1985): seven times higher than that estimated for the ostrich (Martin

and Osorio 2008). According to Boire et al. (2001), this condition would be associated with a high sensitivity to light of ostriches but to a high resolution in diurnal vision of eagles. Eye shape, corneal and pupil dimensions and habit relationships should be explored more thoroughly to be used as predictors.

The avian orbit orientation is directly related to the visual field that describes “the three-dimensional space about the head within which a bird can receive visual information at any one instant” (Martin 2007:548). The position of the eyes in the skull differs between the different species, and this probably has consequences for the visual information and the responses that are triggered by it. The visual field classification proposed by Martin (2007) includes three main types. Assuming that each type is determined primarily by feeding strategies, and secondarily by chick feeding requirements, the position of the beak is decisive. In type 1 (e.g. ostriches, penguins, albatross, some eagles) the beak is in the centre and there is a narrow binocular zone of maximum 20 or 30°, in type 2 (e.g. mallards) the beak is outside or at the margin of the visual field and the binocular zone is about 10° or less, and in type 3 (e.g. owls, band-winged nightjar) the binocular zone is huge (about 50°) and the tip of the beak below the lower periphery (Martin 2007; Salazar et al. 2019). Nevertheless, it is important to state here that birds with large movements of the eye are capable of modifying their visual field configuration, and that eye movements are highly variable among species.

Visual fields can be measured directly *in vivo* (Martin 2007) or indirectly from the volume of the eminentia sagittalis of the brain (Iwaniuk et al. 2008) or bony markers on the skull. Cerio and Witmer (2020) proposed a new methodology called virtual ophthalmoscopy methodology (VO) that allows comparison of schematic eyeballs and *in-silico* visual fields. It is a very promising field especially for its potential application in fossils. Visual abilities were estimated in the 3.3 million-year-old fossil of *Llallawavis scagliai*, known from a magnificent fossil specimen that preserved the entire sclerotic ring. *L. scagliai* would have had a binocular field of view between 18 and 38 degrees wide. Also, the tip of this phorusrhacid’s beak would have fallen directly into this binocular field, consistent with an animal that was using its beak to acquire food, a key perceptual challenge for birds (Cerio et al. 2018, 2019).

9.8.3 Olfaction

Olfaction is not of great importance in most birds (Walsh and Milner 2011a; Zelenitsky et al. 2011) since the olfactory bulbs are commonly very small compared to other vertebrates (Bang and Cobb 1968; Clark et al. 1993; Zelenitsky et al. 2011). However, in some species, the dependence on vision decreases in favor of smell (Potier et al. 2019; Hogan et al. 2020). Now, it is known that birds rely on this sense for behaviors like navigation and mating (Roper 1999; Nevitt 2000). Petrels and albatrosses (Procellariiformes), new world vultures (Cathartidae) and kiwis (Apterygidae) are birds with relatively good olfaction capacities. As more and more

is known about the anatomy of the brain in birds, the size and form of the olfactory bulbs is shown to be variable in the crown-group. It has been proposed that in tetrapods, the size of the olfactory bulbs (which connect to the olfactory nerve) and the olfactory capacity are correlated. Bang and Cobb (1968) designed a simple method to obtain an olfactory ratio that gives an idea of the olfaction capacity (Cobb 1959; Hieronymus 2008). This ratio expresses the relationship between the length of the olfactory bulb (Fig. 9.4d, e) with the maximum length of the telencephalic hemispheres expressed as a percentage. In the endocast, the length of the olfactory bulb can be measured as it is delimited by the most cranial constriction of the endocranium (rostral to the exit of the bulbs into the nasal cavity) and caudally by a ridge located between the fossa of the olfactory bulb and the most rostral brain cavity (Balanoff et al. 2013). Consequently, this method can be applied in fossils (Zelenitsky et al. 2009, 2011) or museum specimens without compromising their condition (Iwaniuk et al. 2020).

It is important to mention here that innervation and soft tissue of the conchae nasales play an important role in olfaction (Pearson 1972). Thus, the size of the olfactory lobes may not always provide reliable inferences about this sense and must be taken with caution. Another problem with the methodology proposed by Zelenitsky and collaborators (2009) is that the volume of the lobes is not taken exactly into account and some birds have short but voluminous lobes (e.g. some Procellariiformes). The ratio in these taxa may result smaller giving an erroneous inference about smelling capacity.

9.9 The Non-avian Theropod – Aves Brain and Senses Transition

One of the main features that have been stated to characterize the avian brain is its enlarged size compared to that of their theropod ancestors. In many vertebrates, such as fishes and amphibians, as well as in the early stages of brain development, the three forebrain, midbrain, and hindbrain (prosencephalon, mesencephalon and rhombencephalon respectively) areas are more or less equal in size. In birds and mammals, the forebrain becomes much larger than the other parts, and the midbrain becomes very small.

Early birds and theropods have similar brain size (Ksepka et al. 2020). *Archaeopteryx*'s brain is actually more similar to non-avian maniraptorans (Balanoff et al. 2013) and some avian-like structures such as the eminentia sagittalis identified in *Archaeopteryx* (Fig. 9.5a) have proven to be artifacts (Walsh et al. 2016; Beyrand et al. 2019). Bird brains are more 'packed' than those of their theropod ancestors (i.e. the shape is more sigmoidal), a condition accentuated in Neornithes. This packing means that the gap between the cerebellum and the telencephalon is smaller through the overlap of the cerebellum onto the cerebrum. Orbit size may have shaped the brain in extant birds (Kawabe et al. 2013a), with larger orbits

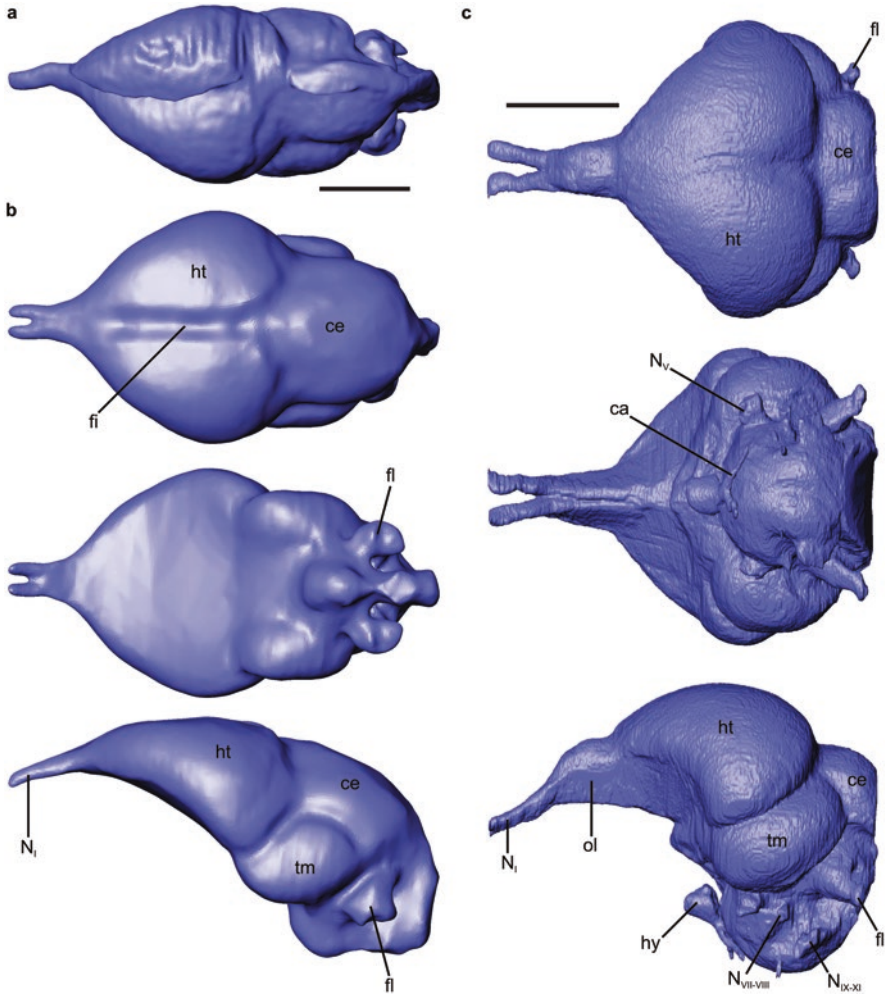


Fig. 9.5 Endocasts of Mesozoic birds. (a–b) *Archaeopteryx lithographica* NHMUK PAL PV OR 37001. (a) original in dorsal view, (b) restored in dorsal, ventral and lateral views. (c) *Cerebavis cenomanica* PIN 5028/2 in dorsal, ventral and lateral views. Scale = 5 mm

representing retention of a pedomorphic feature within Maniraptora (Bhullar et al. 2012). However, early stages of avian brain evolution remain unclear since there are no records of complete Cretaceous bird brains, mostly based on the fact that Cretaceous bird skulls are scarce or commonly found crushed or flattened. Little is known about brain morphology in basal Ornithurae, except for recent studies of the endocranial cavity of the Cretaceous *Ichthyornis* showing that the brain was quite similar to that observed in modern birds, even sharing the presence of eminentiae sagittales (Torres et al. 2021).

In Aves, the enlargement of the brain has been traditionally related to the ability to fly (e.g. Dominguez Alonso et al. 2004). However, modern studies reveal that the enlarged brain of birds does not relate with their flight capabilities but is an exaptation (Balanoff et al. 2013, 2016b, 2018; Balanoff and Bever 2017; Beyrand et al. 2019). While Ksepka et al. (2020) state that there are no substantial volume changes of the brain in the transition from non-avian Paraves to birds, and that this ‘larger brain’ could be the result of selection for smaller body sizes in neoavians after the K-Pg extinction; Torres et al. (2021) state the exact opposite, linking avian survivorship to the K-Pg extinction to sensory differences related to shifts in brain size and shape.

As previously stated, the modern bird brain is characterized by the enlargement of the regions related to visual inputs. Undoubtedly, the eminentiae sagittales represent key structures in the evolution of birds (Walsh and Milner 2011a, b). In the late Jurassic *Archaeopteryx* (Dominguez Alonso et al. 2004), in Enantiornithes (Kurochkin et al. 2006) and in some Late Cretaceous Ornithurinae (Walsh et al. 2016), the eminentiae sagittales are not evident. There is certain evidence that they were present in the Cretaceous Ornithurae *Ichthyornis* (Torres et al. 2021), the early Paleocene anseriforms (Tambussi et al. 2019; Degrange et al. 2018), in the lower Eocene *Halcorynis*, *Odontopteryx* and *Prophaeton* (Milner and Walsh 2009; Walsh and Milner 2011b), in some early Miocene-European Pliocene birds (Mlikovsky 1980, 1981, 1988) and in a late Miocene (9.0 to 6.8 Ma) accipitriform from Patagonia (Picasso et al. 2009).

During avian evolution, the optic lobes have undergone an enlargement and a ventrolateral displacement, probably as a result of the telencephalic expansion. Also, the cerebellum expands both laterally and rostrally, coming into contact with the telencephalon (Torres et al. 2021). A fourth structure that became enlarged in avian evolution, as in mammals, is the medulla oblongata (or ‘brainstem’). This increase may be related to the increasing number of tracts that connect the telencephalon with the cerebellum passing through the medulla.

Unfortunately, little is known about the evolution of the inner ear in birds. Inner ear morphology has been reconstructed in a few key fossil taxa including *Archaeopteryx*, *Enaliornis barretti* (figured but not described by Walsh et al. 2013b) and *Cerebavis cenomanica* (Walsh et al. 2016). Compared to theropods, the inner ear of birds is characterized by having a more developed cochlear duct, a shorter crus communis, and the posterior semicircular canal extends ventrally below the level of the lateral semicircular canal. In birds, a double perilymphatic communication develops (Gray 1908): the lateral canal communicates not only with the posterior canal but also with the rostral canal.

It seems that birds have similar hearing capabilities since the Cretaceous and even the Jurassic (Domínguez Alonso et al. 2004). According to Walsh et al. (2009), *Archaeopteryx* had a hearing range from 600 to 3400 Hz, which is quite similar to that of *Dromaius novaehollandiae* (Manley et al. 1997). The pars vestibularis of *Archaeopteryx* seems to be quite similar to that observed in modern birds (Domínguez Alonso et al. 2004), so its spatial perception and auditory abilities probably were similar to those observed in modern birds.

Enlargement of the eye may be also accompanied by a reduction of olfactory bulbs. The reduction of the olfactory system is observed in the lineage of Maniraptora. Olfactory bulb size in Mesozoic birds is smaller than those of non-avian theropods, while in *Cerebavis* (Fig. 9.5b) seems to be larger than in *Archaeopteryx*, although they seem small as in most birds when compared with the rest of the brain. *Archaeopteryx* possesses smaller olfactory bulbs than early maniraptorans but larger than most crown birds, reflecting its transitional development. This is consistent with the hypothesis that basal birds relied more upon the sense of smell (Zelenitsky et al. 2011). Olfactory bulb reduction appears to occur later in the evolution of more derived birds. On one hand, *Apteryx* retains large olfactory bulbs, however a reduction is observed in more derived groups (e.g., Struthioniformes) among palaeognaths. On the other hand, the most basal forms of Neognathae retain comparatively large bulbs (e.g. Degrange et al. 2018) when compared to more derived Neoaves such as Telluraves (e.g. Demmel Ferreira et al. 2021) and even, among Neoaves, it seems that basal taxa retain larger bulbs (e.g. Tambussi et al. 2015). This would demonstrate that the reduction of olfactory bulbs has occurred in a convergent way between Palaeognathae and Neognathae (Zelenitsky et al. 2011).

9.10 Concluding Remarks

While a part of the evolutionary history of the bird brain remains unresolved, bird diversification appears to have been marked by an increase in visual abilities and a decrease in sense of smell. Both capacities are reflected in the degree of development of the brain structures responsible for managing that particular sensory input. Similarly, more complex cognitive abilities would be accompanied by larger relative brain sizes in certain neornithine clades, such as parrots and songbirds. How can we not marvel at the intelligence exhibited by a crow carrying a walnut to a street so when a car crushes it, it becomes easier to access the nutritional content? How can we not be surprised when we see a grey parrot learning how to use a key to open a door?

Birds exhibit a wide range of niche occupation and dissimilar behaviors. This diversity seems to be reflected in the great disparity of brain structures. Although it is possible to identify widely varying degrees of encephalization, as well as modularity of functions, the functional interpretation of such differences is still speculative among birds. This places birds as an excellent subject for studying the correlation between brain, behavior and cognition.

The last few decades have brought important breakthroughs in the understanding of several features of the avian brain, while at the same time it has highlighted the increasing necessity for more descriptive and functional information. The picture of the evolution of avian brain and senses presented here shows that further investigation is needed, from improved availability of open-source visualization software, to increases in the number of brain and inner ear models in open databases, as well as a wider sample of living and extant species belonging to different families, orders

and lifestyle habits. Brain development in wild birds is also an unexplored field that would represent a great breakthrough. Complementing morphological studies of 3D virtual brain models with histology and establishing how the surface characteristics of the endocast correlate with different aspects of brain tissues would represent a great advance that will allow the study of micro- and macroevolutionary patterns in brain evolution.

Acknowledgements We thank the editors for the invitation to participate in the present book. This chapter is the result of an ongoing research activity that would not be possible without the interaction with several colleagues, doctors, technicians, collections managers and researchers. We especially thank M. Kaufman, M. Risso, N. Nissan, S. Salvarregui, N. Klinar, D. Cagnolo, and M. Risso (Investigaciones Médicas, Buenos Aires); G. Alcuaz and J. I. Cuesta (San Juan de Dios Hospital, La Plata); R. Simonetto, N. Perello, L. Lorenzi, L. Pereyra, and R. Quispe (Ipena, La Plata); M. E. Castrillón, N. Fábrega, Emanuel Restelli, and M. Murua (Hospital Nacional de Clínicas, Córdoba), and C. Capiel (Instituto Radiológico, Mar del Plata), and G.A. Tirao (FAMAF, UNC) for support with CT scanning and data management. S. Walsh provided the *Cerebavis* 3D model, and L. Witmer provided the *Archaeopteryx* 3D model. Thanks to the National Scientific and Technical.

Research Council (CONICET, Argentina) for constant support. This is a contribution to PUE 2016-CONICET-CICTERRA and funded by CONICET-PIP 2014 to CPT.

References

- Aslan K, Atalgin H, Kurtul I et al (2006) Patterns of the internal and cerebral carotid arteries in various avian species: a comparative study. *Rev Med Vet-Toulouse* 157:621–624
- Baden T, Osorio D (2019) The retinal basis of vertebrate color vision. *Annu Rev Vis Sci* 5:3.1–3.24
- Balanoff AM, Bever GS (2017) The role of endocasts in the study of brain evolution. In: Kaas J (ed) *Evolution of nervous systems*, 2nd edn. Elsevier, Oxford, pp 223–241
- Balanoff AM, Bever GS, Rowe TB et al (2013) Evolutionary origins of the avian brain. *Nature* 501:93–96
- Balanoff AM, Norell MA, Hogan AVC et al (2018) The endocranial cavity of Oviraptorosaur dinosaurs and the increasingly complex, deep history of the avian brain. *Brain Behav Evol* 91:125–135
- Balanoff AM, Bever GS, Colbert MW et al (2016a) Best practices for digitally constructing endocranial casts: examples from birds and their dinosaurian relatives. *J Anat* 229:173–190
- Balanoff AM, Smaers JB, Turner AH (2016b) Brain modularity across the theropod–bird transition: testing the influence of flight on neuroanatomical variation. *J Anat* 229:204–214
- Bang B, Cobb S (1968) The size of the olfactory bulb in 108 species of birds. *Auk* 85:55–61
- Barker FK (2014) Mitogenomic data resolve basal relationships among passeriform and passeridan birds. *Mol Phyl Evol* 79:313–324
- Barker FK, Cibois A, Schikler P et al (2004) Phylogeny and diversification of the largest avian radiation. *PNAS* 101:11040–11045
- Baumel JJ, Gerchman L (1968) The avian carotid anastomosis. *Am J Anat* 122:1–18
- Baumel JJ, Witmer L (1993) Osteologia. In: Baumel JJ, King AS, Breazile JE et al (eds) *Handbook of avian anatomy: nomina anatomica avium*, vol 23, 2nd edn. Nuttall Ornithological Club, Cambridge, pp 45–132
- Baumel JJ (1981) Coração e vasos sanguíneos das aves. In: Getty R (ed) *Sisson/Grossman's Anatomia dos Animais Domésticos*, 5th edn. Interamericana, Rio de Janeiro, pp p1842–p1869

- Baumel JJ (1993) Systema cardiovasculare. In: Baumel JJ, King AS, Breazile JE et al (eds) Handbook of avian anatomy: nomina anatomica avium, vol 23, 2nd edn. Nuttall Ornithological Club, Cambridge, pp 407–476
- Bell A, Chiappe LM (2016) A species-level phylogeny of the Cretaceous Hesperornithiformes (Aves: Ornithuromorpha): implications for body size evolution amongst the earliest diving birds. *J Syst Palaeontol* 14:239–251
- Bennett P, Harvey P (1985) Relative brain size and ecology in birds. *J Zool* 207:151–169
- Bertelli S, Lindow BEK, Dyke GJ et al (2010) A well-preserved ‘charadriiform-like’ fossil bird from the early Eocene Fur Formation of Denmark. *Palaeontol* 53:507–531
- Beyrand V, Voeten DFAE, Bureš S et al (2019) Multiphase progenetic development shaped the brain of flying archosaurs. *Sci Rep* 9:10807
- Bhullar B-AS, Marugán-Lobón J, Racimo F et al (2012) Birds have paedomorphic dinosaur skulls. *Nature* 487:223–226
- Bhullar B-AS, Hanson M, Fabbri M et al (2016) How to make a bird skull: major transitions in the evolution of the avian cranium, paedomorphosis, and the beak as a surrogate hand. *Integr Comp Biol* 56:389–403
- Billet G, Hautier L, Asher R et al (2012) High morphological variation of vestibular system accompanies slow and infrequent locomotion in three-toed sloths. *Proc R Soc B* 279:3932–3939
- Boire D, Baron G (1994) Allometric comparison of brain and main brain subdivisions in birds. *J Hirnforsch* 35:49–66
- Boire D, Dufour J-S, Théoret H et al (2001) Quantitative analysis of the retinal ganglion cell layer in the ostrich, *Struthio camelus*. *Brain Behav Evol* 58:343–355
- Breazile JE, Kuenzel WJ (1993) Systema nervosum centrale. In: Baumel JJ, King AS, Breazile JE et al (eds) Handbook of avian anatomy: nomina anatomica avium, vol 23, 2nd edn. Nuttall Ornithological Club, Cambridge, pp 493–554
- Bringmann A (2019) Structure and function of the bird fovea. *Anat Histol Embryol* 48:177–200
- Brinkløv S, Brock Fenton M, Ratcliffe JM (2013) Echolocation in oil birds and swiftlets. *Front Physiol* 4:1–12
- Brooke ML, Hanley S, Laughlin SB (1999) The scaling of eye size with body mass in birds. *Proc R Soc Lond B* 266:405–412
- Bubien-Waluszewska A (1981) The cranial nerves (pp 385–438). In: King AS, McLelland J (eds) Form and Function in Birds, vol 2. Academic Press, London
- Campbell K, Marcus L (1992) The relationship of hindlimb bone dimensions to body weight in birds. *Nat Hist Mus Los Angeles Sci Ser* 36:395–412
- Campos R, Ferreira N, Marrone ACH (1995) A systematic study of encephalic blood supply in *Gallus gallus*. I. Cerebral carotid arteries, collaterals and terminal branches, intercarotid anastomosis. *J Anat Embryo* 100:111–121
- Carril J, Tambussi CP, Degrange FJ et al (2016) Comparative brain morphology of Neotropical parrots (Aves, Psittaciformes) inferred from virtual 3D endocasts. *J Anat* 229:239–251
- Cerio DG, Witmer LM (2020) Modeling visual fields using virtual ophthalmoscopy: Incorporating geometrical optics, morphometrics, and 3D visualization to validate an interdisciplinary technique. *Vis Res* 167:70–86
- Cerio DG, Degrange FJ, Tambussi CP et al (2018). Modeling visual abilities in extinct species using Virtual Ophthalmoscopy, with a case study in predicting eye size, optical parameters, and visual fields in terror birds (Aves: Phorusrhacidae). Abstract presented at 78th Annual Meeting of The Society of Vertebrate Paleontology, New Mexico, 17–20 October 2018
- Cerio DG, Degrange FJ, Tambussi CP et al (2019) Optical properties, ecological differences, and Virtual Ophthalmoscopy: Morphometry of optical parameters in diapsids and a case study in restoring visual fields in terror birds (Aves: Phorusrhacidae). *J Morph* 280:S96
- Chiappe LM (1997) Aves. In: Currie PJ, Padian K (eds) The encyclopedia of dinosaurs. Academic Press, New York, pp 32–38
- Clark L, Avilova KV, Beans NJ (1993) Odor thresholds in passerines. *Comp Biochem Physiol A* 104:305–312

- Clarke JA, Tambussi CP, Noriega JI et al (2005) Definitive fossil evidence for the extant avian radiation in the Cretaceous. *Nature* 433:305–308
- Clarke JA, Tambussi CP, Noriega JI et al (2006) Corrigendum to Definitive fossil evidence for the extant avian radiation in the Cretaceous. *Nature* 444:780
- Cobb S (1959) A note on the size of the avian olfactory bulbs. *Epilep* 1:394–402
- Corfield JR, Wild M, Hauber ME et al (2008) Evolution of brain size in the Palaeognath lineage, with an emphasis on New Zealand Ratites. *Brain Behav Evol* 71:87–99
- Corfield JR, Kubke MF, Parsons S et al (2012) Inner-ear morphology of the New Zealand Kiwi (*Apteryx mantelli*) suggests high-frequency specialization. *J Assoc Res Oto* 135:629–639
- Cox PG, Jeffery N (2010) Semicircular canals and agility: the influence of size and shape measures. *J Anat* 216:37–47
- Curtis EL, Miller RC (1938) The sclerotic ring in North American birds. *Auk* 55:225–243
- Davies MNO, Green PR (1994) Multiple sources of depth information: an ecological approach. In: Davies MNO, Green PR (eds) *Perception and motor control in birds: an ecological approach*. Springer-Verlag, Berlin, pp 339–356
- de Beer G (1947) How animals hold their heads. *Proc Linn Soc Lond* 159:125–139
- Degrange FJ, Tambussi CP, Taglioreti M et al (2015) A new Mesembriornithinae (Aves, Phorusrhacidae) provides new insights into the phylogeny of phorusrhacids. *J Vert Pal* 35:e912656
- Degrange FJ, Tambussi CP, Witmer LM et al (2018) Endocranial anatomy of a Paleocene stem waterfowl (Aves, Anseriformes). *PE-APA* 19:R45
- Demmel Ferreira MM, Degrange FJ, Tirao GA et al (2021) Endocranial morphology of the Piciformes (Aves, Coraciimorphae): Functional and ecological implications. *J Anat* 239:167–183
- Domínguez Alonso P, Milner AC, Ketcham RA et al (2004) The avian nature of the brain and inner ear of *Archaeopteryx*. *Nature* 430:666–669
- Dooling R (2002) Avian hearing and the avoidance of wind turbines. *National Renewable Energy Laboratory*. <https://doi.org/10.2172/15000693>. Accessed 31 July 2020
- Dubbeldam JL (1989) Birds. In: Nieuwenhuys R, Ten Donkelaar HJ, Nicholson C (eds) *The central nervous system of vertebrates*, vol 3. Springer, Berlin, pp 1525–1636
- Duijm M (1951) On the head posture in birds and its relation features. *P K Ned Akad Wetensc* 54:202–271
- Dunning JB (2008) *CRC Handbook of Avian Body Masses*. CRC Press, Florida
- Early CM, James HF, Witmer LM (2018) The bill-tip organ: probing at tactile sensitivity in birds. *Int Comp Biol* 58:e55
- Early CM, Iwaniuk AN, Ridgely RC, Witmer LM (2020a) Endocast structures are reliable proxies for the sizes of corresponding regions of the brain in extant birds. *J Anat* 237:1162–1176
- Early C, Ridgely RC, Witmer LM (2020b) Beyond endocasts: using predicted brain-structure volumes of extinct birds to assess neuroanatomical and behavioral inferences. *Diversity* 12. <https://doi.org/10.3390/d12010034>
- Ebinger P (1995) Domestication and plasticity of brain organization in mallards (*Anas platyrhynchos*). *Brain Behav Evol* 45:286–300
- Edinger T (1928) Über einige fossile Gehirne. *Palaont Z* 9:379–402
- Ferreira-Cardoso S, Araújo R, Martins NE et al (2017) Floccular fossa size is not a reliable proxy of ecology and behaviour in vertebrates. *Sci Rep* 7. <https://doi.org/10.1038/s41598-017-01981-0>
- Field DJ, Lynner C, Brown C et al (2013) Skeletal correlates for body mass estimation in modern and fossil flying birds. *PLOS ONE* 8:e82000
- Field DJ, Hanson M, Burnham D et al (2018) Complete *Ichthyornis* skull illuminates mosaic assembly of the avian head. *Nature* 557:96–101
- Field DJ, Benito J, Chen A et al (2020) Late Cretaceous neornithine from Europe illuminates the origins of crown birds. *Nature* 579:397–401
- Garamszegi LZ, Møller AP, Erritzøe J (2002) Coevolving avian eye size and brain size in relation to prey capture and nocturnality. *Proc Roy Soc Lond B* 269:961–967

- Gauthier J (1986) Saurischian monophyly and the origin of birds. In: Padian K (ed) *The origin of birds and evolution of flight*. California Academy of Sciences, San Francisco, pp 1–55
- Gill FB (2007) *Ornithology*. Freeman, New York
- Gleich O, Dooling RJ, Manley G (2005) Audiogram, body mass, and basilar papilla length: correlations in birds and predictions for extinct archosaurs. *Naturwissenschaften* 92:595–598
- Gray AA (1908) *The labyrinth of animals, including mammals, birds, reptiles and amphibians*. Churchill, London
- Gültiken ME, Yıldız D, Onuk B et al (2012) The morphology of the pecten oculi in the common buzzard (*Buteo buteo*). *Vet Ophthalmol* 15:72–76
- Güntürkün O, Hahmann U (1999) Functional subdivisions of the ascending visual pathways in the pigeon. *Behav Brain Res* 98:193–201
- Gutiérrez-Ibáñez C, Iwaniuk AN, Wylie DR (2009) The independent evolution of the enlargement of the principal sensory nucleus of the trigeminal nerve in three different groups of birds. *Brain Behav Evol* 74:280–294
- Hadžiselimović H, Savković LJ (1964) Appearance of semicircular canals in birds in relation to mode of life. *Acta Anat* 57:306–315
- Hall MI (2008) The anatomical relationships between the avian eye, orbit and sclerotic ring: implications for inferring activity patterns in extinct birds. *J Anat* 212:781–794
- Hall MI, Ross CF (2007) Eye shape and activity pattern in birds. *J Zool* 271:437–444
- Healy S, Rowe C (2007) A critique of comparative studies of brain size. *Proc R Soc B* 274:453–464
- Heyers D, Zapka M, Hoffmeister M et al (2010) Magnetic field changes activate the trigeminal brainstem complex in a migratory bird. *PNAS* 107:9394–9399
- Hieronymus T (2008) Comparative anatomy and physiology of chemical senses in aquatic birds. In: Thewissen JGM, Nummela S (eds) *Sensory evolution on the threshold: adaptations in secondarily aquatic vertebrates*. University of California Press, Berkeley, pp 83–94
- Hogan AVC, Watanabe A, Balanoff AM et al (2020) Comparative growth in the olfactory system of the developing chick with considerations for evolutionary studies. *J Anat* 237:225–240
- Hullar TE (2006) Semicircular canal geometry, afferent sensitivity, and animal behavior. *Anat Rec A* 288:466–472
- Iwaniuk AN (2017) Functional correlates of brain and brain region sizes in nonmammalian vertebrates. In: Kaas J (ed) *Evolution of nervous systems*, 2nd edn. Elsevier, Oxford, pp 335–348
- Iwaniuk AN, Nelson J (2002) Can endocranial volume be used as an estimate of brain size in birds? *Can J Zool* 80:16–23
- Iwaniuk AN, Hurd L (2005) The evolution of cerebrotypes in birds. *Brain Behav Evol* 65:215–230
- Iwaniuk AN, Wylie D (2006) The evolution of stereopsis and the Wulst in caprimulgiform birds: a comparative analysis. *J Comp Physiol A* 192:1313–1326
- Iwaniuk AN, Nelson JE, James H et al (2004) A comparative test of the correlated evolution of flightlessness and relative brain size in birds. *J Zool* 263:317–327
- Iwaniuk AN, Dean KM, Nelson JE (2005) Interspecific allometry of the brain and brain regions in parrots (Psittaciformes): comparisons with other birds and primates. *Brain Behav Evol* 65:40–59
- Iwaniuk AN, Hurd PL, Wylie DR (2006a) Comparative morphology of the avian cerebellum: I. Degree of foliation. *Brain Behav Evol* 68:45–62
- Iwaniuk AN, Hurd PL, Wylie DR (2006b) The comparative morphology of the cerebellum in caprimulgiform birds: evolutionary and functional implications. *Brain Behav Evol* 67:53–68
- Iwaniuk AN, Heesy CP, Hall MI et al (2008) Relative wulst volume is correlated with orbit orientation and binocular visual field in birds. *J Comp Physiol A Neuroethol Sens Neural Behav Physiol* 194:267–282
- Iwaniuk AN, Keirnan AR, Janetzki H et al (2020) The endocast of the night parrot (*Pezoporus occidentalis*) reveals insights into its sensory ecology and the evolution of nocturnality in birds. *Sci Rep* 10:9258
- Jarvis ED, Güntürkün O, Bruce L et al (2005) Avian brains and a new understanding of vertebrate brain evolution. *Nat Rev Neurosci* 6:151–159

- Jerison H (1973) *Evolution of the Brain and Intelligence*. Academic Press, New York
- Kawabe S, Shimokawa T, Miki H et al (2009) A simple and accurate method for estimating the brain volume of birds: possible application in paleontology. *Brain Behav Evol* 74:295–301
- Kawabe S, Shimokawa T, Miki H et al (2013a) Variation in avian brain shape: relationship with size and orbital shape. *J Anat* 223:495–508
- Kawabe S, Shimokawa T, Miki H et al (2013b) Relationship between brain volume and brain width in mammals and birds. *Paleontol Res* 17:282–293
- Kawabe S, Ando T, Endo H (2014) Enigmatic affinity in the brain morphology between plotopterids and penguins, with a comprehensive comparison among water birds. *Zool J Linn Soc* 170:467–493
- Kiama SG, Maina JN, Bhattacharjee J et al (2001) Functional morphology of the pecten oculi in the nocturnal spotted eagle owl (*Bubo bubo africanus*), and the diurnal black kite (*Milvus migrans*) and domestic fowl (*Gallus gallus* var. *domesticus*): a comparative study. *J Zool* 254:521–528
- Knoll F, Kawabe S (2020) Avian palaeoneurology: Reflections on the eve of its 200th anniversary. *J Anat* 236:965–979
- Ksepka DT, Balanoff AM, Walsh SA et al (2012) Evolution of the brain and sensory organs in Sphenisciformes: new data from the stem penguin *Paraptendytes antarcticus*. *Zool J Linn Soc* 166:202–219
- Ksepka DT, Stidham TA, Williamson TE (2017) Early Paleocene landbird supports rapid phylogenetic and morphological diversification of crown birds after the K-Pg mass extinction. *PNAS* 114:8047–8052
- Ksepka DT, Balanoff AM, Smith NA et al (2020) Tempo and Pattern of Avian Brain Size Evolution. *Curr Biol* 30:1–11
- Kurochkin EN, Saveliev SV, Postnov AA et al (2006) On the brain of a primitive bird from the Upper Cretaceous of European Russia. *Paleontol J* 40:655–666
- Lamb TD, Collin SP, Pugh EN Jr (2007) Evolution of the vertebrate eye: Opsins, photoreceptors, retina and eye cup. *Nat Rev Neurosci* 8:960–975
- Land MF, Nilsson DE (2002) *Animal eyes*. Oxford University Press, Oxford
- Lebedkin S (1924) Über die lage des canalis semicircularis bei Säugern. *Anat Anzeiger* 58:449–460
- Lee MSY, Worthy TH (2012) Likelihood reinstates *Archaeopteryx* as a primitive bird. *Biol Lett* 8:299–303
- Lee MSY, Cau A, Naish D et al (2014) Sustained miniaturization and anatomical innovation in the dinosaurian ancestors of birds. *Science* 435:562–566
- Lefebvre L, Reader SM, Sol D (2004) Brains, innovations and evolution in birds and primates. *Brain Behav Evol* 63:233–246
- Lefebvre L, Sol D (2008) Brains, lifestyles and cognition: are there general trends? *Brain Behav Evol* 72:135–144
- Lemmrich W (1931) Der Skleralring der vögel. *Jen Z Natur* 65:513–586
- Lisney TJ, Potier S, Isard P et al (2020) Retinal topography in two species of flamingo (Phoenicopteriformes: Phoenicopteridae). *J Comp Neurol* 528:2848–2863
- Maeda K, Henbest KB, Cintolesi F et al (2008) Chemical compass model of avian magnetoreception. *Nature* 453:387–390
- Magariños M, Contreras J, Aburto MR et al (2012) Early development of the vertebrate inner ear. *Anat Rec* 295:1775–1790
- Manley GA, Köppl C, Yates GK (1997) Activity of primary auditory neurones in the cochlear ganglion of the Emu *Dromaius novaehollandiae*: spontaneous discharge, frequency tuning, and phase locking. *J Acoust Soc Am* 101:1560–1573
- Marino L (2005) Big brains do matter in new environments. *PNAS* 102:5306–5307
- Martin GR (2007) Visual fields and their functions in birds. *J Ornithol* 148:547–562
- Martin GR, Osorio D (2008) Vision in birds. In: Basbaum AI, Kaneko A, Shepherd GM et al (eds) *The senses: a comprehensive reference*. Academic Press, Amsterdam, pp 25–52
- Martin GR, Wilson K-J, Wild JM et al (2007) Kiwi forego vision in the guidance of their nocturnal activities. *PLOS ONE* 2:e198

- Marugán-Lobón J, Buscaglioni A (2006) Avian skull morphological evolution: exploring exo- and endo-cranial covariation with two block partial least squares. *Zool* 109:217–230
- Marugán-Lobón J, Chiappe LM, Farke AA (2013) The variability of inner ear orientation in sau- rischian dinosaurs: testing the use of semicircular canals as a reference system for comparative anatomy. *PeerJ* 1:e124
- Milner AC, Walsh SA (2009) Avian brain evolution: new data from Palaeogene birds (Lower Eocene) from England. *Zool J Linn Soc* 155:198–219
- Mindell DP, Brown JW (2005) Neornithes. *Modern birds*. <http://tolweb.org/Neornithes/15834/2005.12.14>
- Mlíkovský J (1980) Zwei Vogelgehirne aus dem Miozän Böhmens. *Casopis Min Geol* 25:409–413
- Mlíkovský J (1981) Ein fossile Vogelgehirn aus dem Oberpliozän Ungarns. *Frag Min Palaeontol* 10:71–74
- Mlíkovský J (1988) Notes on the brains of the middle Miocene birds (Aves) of Hahnenberg (F.R.G.). *Casopis Min Geol* 33:53–61
- Nazer MB, Campos R (2011) Systematization of the brain base arteries in ostrich (*Struthio camelus*). *J Morph Sci* 28:268–274
- Nevitt GA (2000) Olfactory foraging by Antarctic procellariiform seabirds: life at high Reynolds numbers. *Biol Bull* 198:245–253
- O'Connor JK, Chiappe LM, Gao C et al (2011) Anatomy of the Early Cretaceous enantiornithine bird *Rapaxavis pani*. *Acta Palaeontol Pol* 56:463–475
- Olkowicz S, Kocourek M, Lučan RK et al (2016) Birds have primate-like numbers of neurons in the forebrain. *PNAS* 113:7255–7260
- Ozudogru Z, Balkaya H, Ozdemir D (2016) The morphology of the brain base arteries in the Sparrowhawk (*Accipiter nisus*). *Isr J Vet Med* 71:43–47
- Pearson R (1972) *The Avian Brain*. Academic Press, London
- Perrins CM (1990) *The illustrated encyclopedia of birds*. Prentice Hall Editions, New York
- Pettit TN, Causey-Whittow G, Grant SG (1981) Rete mirabile ophthalmicum in Hawaiian sea- birds. *Auk* 98:844–846
- Picasso MJB, Tambussi C, Dozo MT (2009) Neurocranial and brain anatomy of a Late Miocene eagle (Aves, Accipitridae) from Patagonia. *J Vert Pal* 29:831–836
- Picasso M, Tambussi CP, Degrange FJ (2010) Virtual reconstructions of the endocranial cavity of *Rhea americana* (Aves, Palaeognathae): postnatal anatomical changes. *Brain Behav Evol* 76:176–184
- Porter WM, Witmer LM (2016) Avian cephalic vascular anatomy, sites of thermal exchange, and the rete ophthalmicum. *Anat Rec* 299:1461–1486
- Potier S, Duriez O, Célérier A et al (2019) Sight or smell: which senses do scavenging raptors use to find food? *Anim Cogn* 22:49–59
- Prum RO, Berv JS, Dornburg A et al (2015) A comprehensive phylogeny of birds (Aves) using targeted next-generation DNA sequencing. *Nature* 526:569–573
- Rabbitt RD, Boyle R, Highstein SM (2010) Mechanical amplification by hair cells in the semicir- cular canals. *PNAS* 107:3864–3869
- Reiner A, Perkel DJ, Bruce LL et al (2004a) The avian brain nomenclature forum: terminology for a new century in comparative neuroanatomy. *J Comp Neurol* 473:E1–E6
- Reiner A, Perkel DJ, Bruce LL et al (2004b) Revised nomenclature for avian telencephalon and some related brainstem nuclei. *J Comp Neurol* 473:377–414
- Reiner A, Yamamoto K, Karten HJ (2005) Organization and evolution of the avian forebrain. *Anat Rec A* 287:1080–1102
- Reymond L (1985) Spatial visual acuity of the eagle *Aquila audax*: A behavioural, optical and anatomical investigation. *Vis Res* 25:1477–1491
- Roper TJ (1999) Olfaction in birds. *Adv Stud Behav* 28:247–332
- Salazar JE, Severin D, Vega-Zuniga T et al (2019) Anatomical specializations related to forag- ing in the visual system of a nocturnal insectivorous bird, the Band-Winged Nightjar (Aves: Caprimulgiformes). *Brain Behav Evol* 94:27–36

- Schmid KL, Wildsoet CF (1998) Assessment of visual acuity and contrast sensitivity in the chick using an optokinetic nystagmus paradigm. *Vis Res* 38:2629–2634
- Schmitz L (2009) Quantitative estimates of visual performance features in fossil birds. *J Morphol* 270:759–773
- Schuck-Paim C, Alonso W, Ottoni E (2008) Cognition in an ever changing world: climatic variability is associated with brain size in Neotropical parrots. *Brain Behav Evol* 71:200–215
- Schwartzkopff J (1955) On the hearing of birds. *Auk* 72:340–347
- Seifert M, Baden T, Osorio D (2020) The retinal basis of vision in chicken. *Semin Cell Dev* 106:106–115
- Shimizu T, Bowers AN (1999) Visual circuits of the avian telencephalon: evolutionary implications. *Behav Brain Res* 98:183–191
- Sipla JS (2007) The semicircular canals of birds and nonavian dinosaurs. Dissertation, Stony Brook University
- Sol D, Timmermans S, Lefebvre L (2002) Behavioural flexibility and invasion success in birds. *Anim Behav* 63:495–502
- Sol D, Dunca RP, Blackburn TM et al (2005) Big brains, enhanced cognition, and response of birds to novel environments. *PNAS* 102:5460–5465
- Spoor F, Bajpai S, Hussain ST et al (2002) Vestibular evidence for the evolution of aquatic behaviour in early cetaceans. *Nature* 417:163–166
- Stingelin W (1957) Vergleichende morphologische Untersuchungen am Vorderhirn der Vögel auf cytologischer und cytoarchitektonischer Grundlage. Verlag Helbing and Lichtenhahn, Basel
- Striedter GF, Charvet CJ (2008) Developmental origins of species differences in telencephalon and tectum size: morphometric comparisons between a parakeet (*Melopsittacus undulatus*) and a quail (*Colinus virginianus*). *J Comp Neurol* 507:1663–1675
- Striedter G (2005) Principles of brain evolution. Sinauer Associates, Sunderland
- Tambussi CP, Degrange FJ, Tirao G (2014) Neo y paleo ornitología virtual. *El Hornero* 29:51–60
- Tambussi CP, Degrange FJ, Ksepka DT (2015) Endocranial anatomy of Antarctic Eocene stem penguins: implications for sensory system evolution in Sphenisciformes (Aves). *J Vert Paleont* 35:e981635
- Tambussi CP, Degrange FJ, Carril J et al (2017) Anatomía virtual del cerebro y órganos de los sentidos en Aves: aplicaciones en paleobiología. In: Vassallo A, Manzano A, Abdala V (eds) *Morfología de Vertebrados: Conceptos, métodos y grupos de investigación en Argentina*. EUEM, Mar del Plata, pp 197–228
- Tambussi CP, Degrange FJ, De Mendoza R et al (2019) A stem anseriform from the early Paleocene of Antarctica provides new key evidence in the early evolution of waterfowl. *Zool J Linn Soc* 186:673–700
- Thomas RJ, Székely T, Cuthill IC et al (2002) Eye size in birds and the timing of song at dawn. *Proc Roy Soc Lond B* 269:831–837
- Thomas RJ, Székely T, Powell RF et al (2006) Eye size, foraging methods and the timing of foraging in shorebirds. *Funct Ecol* 20:157–165
- Toomey MB, Lind O, Frederiksen R et al (2016) Complementary shifts in photoreceptor spectral tuning unlock the full adaptive potential of ultraviolet vision in birds. *eLife* 5:e15675
- Torres CR, Norell MA, Clarke JA (2021) Bird neurocranial and body mass evolution across the end-Cretaceous mass extinction: The avian brain shape left other dinosaurs behind. *Sci Adv* 7:eabg7099
- Verduzco Mendoza A, Arch TE, Contreras Figueroa ME et al (2009) Descripción anatómica de la vasculatura arterial carotídea-cerebral en el gallo doméstico *Gallus gallus* Linnaeus (Aves: Galliformes: Phasianidae). *Act Zool Mex* 25:465–477
- Voeten FAE, Cubo J, de Margerie et al (2018) Wing bone geometry reveals active flight in *Archaeopteryx*. *Nature commun* 9:923
- Walls GL (1942) The vertebrate eye and its adaptive radiation. The Cranbrook Institute of Science, Michigan

- Walsh SA, Milner A (2011a) Evolution of the avian brain and senses. In: Dyke G, Kaiser G (eds) *Living dinosaurs: the evolutionary history of modern birds*. John Wiley and Sons, United Kingdom, pp 282–305
- Walsh SA, Milner A (2011b) *Halcyornis toliapicus* (Aves: Lower Eocene, England) indicates advanced neuromorphology in Mesozoic Neornithes. *J Syst Palaeontol* 9:173–181
- Walsh SA, Barrett PM, Milner AC et al (2009) Inner ear anatomy is a proxy for deducing auditory capability and behavior in reptiles and birds. *Proc Roy Soc B* 276:1355–1360
- Walsh SA, Iwaniuk AN, Knoll MA et al (2013a) Avian cerebellar floccular fossa size is not a proxy for flying ability in birds. *PLOS ONE* 8:e67176
- Walsh SA, Luo Z, Barret PM (2013b) Modern imaging techniques as a window to prehistoric auditory worlds. In: Köppl C, Manley GA, Popper AN et al (eds) *Insights from Comparative Hearing Research*. Springer, New York, pp 227–261
- Walsh SA, Milner AC, Bourdon E (2016) A reappraisal of *Cerebavis cenomanica* (Aves, Ornithurae), from Melovodka, Russia. *J Anat* 229:215–227
- Warheit KI, Good KI, De Queiroz K (1989) Variation in numbers of scleral ossicles and their phylogenetic transformations within the Pelecaniformes. *Auk* 106:383–388
- Watanabe A, Gignac PM, Balanoff AM et al (2019) Are endocasts good proxies for brain size and shape in archosaurs throughout ontogeny? *J Anat* 234:291–305
- Watanabe A, Balanoff AM, Gignac PM et al (2021) Novel neuroanatomical integration and scaling define avian brain shape evolution and development. *eLife* 10:e68809
- Whitfield TT, Hammond KL (2007) Axial patterning in the developing vertebrate inner ear. *Int J Develop Biol* 51:507–520
- Wild JM (2009) Evolution of the wulst. In: Binder MD, Hirokawa N, Windhorst U (eds) *Encyclopedia of Neuroscience*. Springer, Berlin/Heidelberg. https://doi.org/10.1007/978-3-540-29678-2_3181
- Wiltshcko R, Wiltshcko W (2019) Magnetoreception in birds. *J R Soc Interface* 16:20190295
- Witmer LM (2002) The debate on avian ancestry: phylogeny, function, and fossils. In: Chiappe LM, Witmer LM (eds) *Mesozoic birds: above the head of dinosaurs*. University of California Press, Los Angeles, pp 3–30
- Witmer LM, Franzosa CJ, Rowe T (2003) Neuroanatomy of flying reptiles and implications for flight, posture and behaviour. *Nature* 425:950–953
- Witmer LM, Ridgely RC, Dufeu DL et al (2008) Using CT to peer into the past: 3D visualization of the brain and ear regions of birds, crocodiles, and non avian dinosaurs. In: Endo H, Frey R (eds) *Anatomical imaging: towards a new morphology*. Springer-Verlag, Tokyo, pp 67–88
- Wood CA (1917) *The fundus oculi of birds*. The Lakeside Press, Chicago
- Xu X, You H, Du K et al (2011) An *Archaeopteryx*-like theropod from China and the origin of Avialae. *Nature* 475:465–470
- Zelenitsky DK, Therrien F, Kobayashi Y (2009) Olfactory acuity in theropods: palaeobiological and evolutionary implications. *Proc R Soc Lond B* 276:667–673
- Zelenitsky DK, Therrien F, Ridgely RC et al (2011) Evolution of olfaction in non-avian theropod dinosaurs and birds. *Proc Biol Sci* 278:3625–3634
- Zusi RL, Bridge D (1981) On the slit pupil of the Black Skimmer (*Rynchops niger*). *J Field Ornithol* 52:338–340
- Zweers AG, Vanden Berge JC, Berkhoudt H (1997) Evolutionary patterns of avian trophic diversification. *Zool* 100:25–57

Chapter 10

Evolution of the Mammalian Neurosensory System: Fossil Evidence and Major Events



Timothy B. Rowe

Anatomical Abbreviations Used in the Figures

<i>Ali</i>	Alisphenoid
<i>Alv</i>	Alveoli for the dentition
<i>Ang</i>	Angular
<i>Art</i>	Articular
<i>Bs</i>	Basisphenoid
<i>c</i>	Lower canine
<i>C</i>	Upper canine
<i>Cb</i>	Cerebellum
<i>choa</i>	Choana
<i>cr</i>	cheek tooth crown
<i>cve</i>	Cavum epipterygium
<i>D cond</i>	Condylar process of dentary
<i>D cor</i>	Coronoid process of dentary
<i>D ctx</i>	Dorsal cortex (endocast)
<i>Den</i>	Dentary
<i>D ang</i>	Angular process of dentary
<i>D ram</i>	Dentary ramus
<i>Ec</i>	Ectopterygoid
<i>Eoc</i>	Exoccipital
<i>Et 1-5</i>	Ethmoid turbinals 1-5
<i>F ann</i>	Annular fissure
<i>F mag</i>	Foramen magnum
<i>Fr</i>	Frontal
<i>Fv</i>	Fenestra vestibuli

T. B. Rowe (✉)

Jackson School of Geological Sciences, University of Texas at Austin, Austin, TX, USA

e-mail: rowe@mail.utexas.edu

© Springer Nature Switzerland AG 2023

M. T. Dozo et al. (eds.), *Paleoneurology of Amniotes*,

https://doi.org/10.1007/978-3-031-13983-3_10

<i>Hyp</i>	Hypophysis (endocast)
<i>i</i>	1-4 Lower incisors
<i>I 1-3</i>	Upper incisors
<i>iam</i>	Internal auditory meatus (endocast)
<i>II</i>	Cranial nerve II (endocast)
<i>Ju</i>	Jugal
<i>Lac</i>	Lacrimal
<i>m 1-3</i>	Lower molars
<i>M 1-3</i>	Upper molars
<i>Max</i>	Maxilla
<i>Mt</i>	Maxilloturbinal
<i>Nas</i>	Nasal
<i>Ncx</i>	Neocortex
<i>Nt</i>	Nasoturbinal
<i>Ob</i>	Olfactory bulb
<i>Ocx</i>	Olfactory (piriform) cortex
<i>Opl</i>	Optic lobes (endocast)
<i>p 1-5</i>	Lower premolars
<i>P 1-2</i>	Upper premolars
<i>Pa</i>	Parietal
<i>Pal</i>	Palatine
<i>Pet</i>	Petrosal
<i>Pin</i>	Pineal body (endocast)
<i>Pfl</i>	Paraflocculus (endocast)
<i>Pmx</i>	Premaxilla
<i>Prom</i>	Promontorium of petrosal
<i>Pt</i>	Pterygoid
<i>Qu</i>	Quadrate
<i>Re lam</i>	Reflected lamina of angular (=ectotympanic)
<i>Rf</i>	Rhinal fissure
<i>rt</i>	tooth root
<i>Smx</i>	Septomaxilla
<i>Soc</i>	Supraoccipital
<i>Spc</i>	Spinal cord (endocast)
<i>Sq</i>	Squamosal
<i>sss</i>	Superior sagittal sinus (endocast)
<i>Sv</i>	Sinus venosus
<i>V</i>	Cranial nerve V (endocast)
<i>Vo</i>	Vomer

10.1 Phylogenetic Context

One of the central features in pan-mammalian evolution is enlargement of the brain relative to body size (encephalization) and emergence of the unique mammalian neocortex (Rowe 1996a; Rowe et al. 2011). This chapter focuses on what can be inferred about pan-mammalian neurosensory evolution, beginning with divergence of the mammalian total clade from the ancestral amniote, and culminating in the origin of crown clade *Mammalia* (Fig. 10.1). It attempts to summarize contemporary answers to basic questions articulated by Northcutt (2001): what happened, when did it happen, how did it happen, and why did it happen?

The following discussion employs conventions recommended by *PhyloCode* (Cantino and de Queiroz 2020), as illustrated in practice in its companion volume *Phylonoms* (de Queiroz et al. 2020) to designate particular subsets in a hierarchy of clades that includes *Mammalia* and its closest extinct relatives (Fig. 10.2). The Phylogenetic System is rankless and all taxonomic names, including known paraphyla, are italicized. The name *Mammalia* is used in reference to the ‘crown clade’ (Rowe 1988, 2020a, b; de Queiroz and Gauthier 1990, 1992, 1994; de Queiroz 1994). Fossil taxa more closely related to *Mammalia* than to other living taxa, that

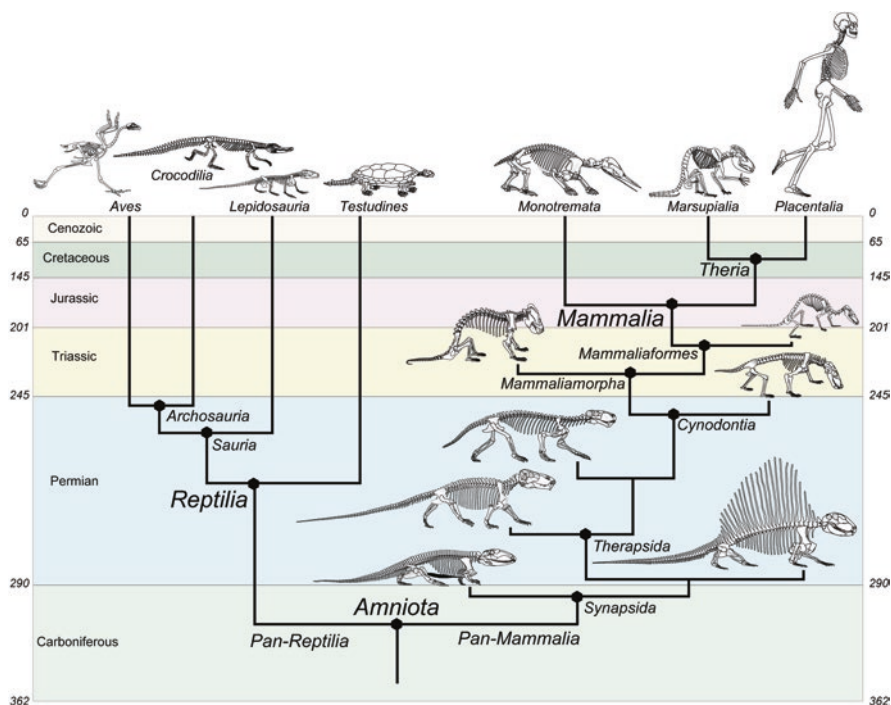


Fig. 10.1 Phylogeny of the major clades of *Pan-Mammalia* discussed here distributed across the geological time scale. (Modified after Rowe 2020a)

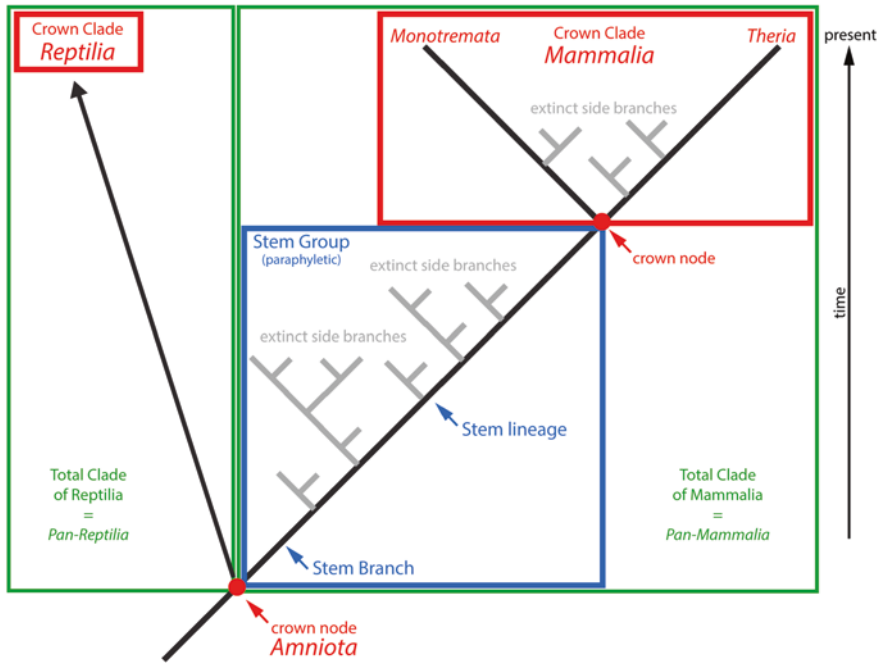


Fig. 10.2 Categories of clades and groups employed under the Phylogenetic System of taxonomic nomenclature. (Modified from de Queiroz 2007)

lie outside its crown clade, are considered to be members of the mammalian ‘stem’ or the paraphyletic extinct mammalian ‘stem-group’ while also belonging to the monophyletic ‘total clade’ of *Mammalia*. The ‘pan-clade’ naming convention attaches the prefix *Pan-* (for all) to the crown clade name to reflect its total clade (Rowe 2004; de Queiroz 2007). *Pan-Mammalia* (Rowe 2020c) is the total clade of *Mammalia* (Rowe 2020a), and the name *Pan-Reptilia* designates the total clade of *Reptilia*. Together *Pan-Reptilia* and *Pan-Mammalia* and their last common ancestor comprise the crown clade *Amniota*. A characterization of the ancestral amniote is where our discussion begins.

The discussion below is based on a series of phylogenetic and developmental analyses, using increasingly sophisticated taxon/character matrices and imaging instruments that are detailed elsewhere (Gauthier et al. 1988a, b, 1989; Donoghue et al. 1989; Rowe 1988, 1993; Rowe et al. 1995, 2005; Rubidge and Sidor 2001; Kielan-Jaworowska et al. 2004; Meng et al. 2006; Ji et al. 2006; Rowe et al. 2011; Kirk et al. 2014; Rowe and Shepherd 2016; Rowe 2020a).

10.2 Historical Background

Evidence from the fossil record has enjoyed a remarkable resurgence from digital endocasts thanks to computed tomography (e.g. Rowe et al. 1995; Macrini 2006; Balanoff et al. 2016; Balanoff and Bever 2020) and similar non-destructive digital imaging technologies, as well as a flurry of new discoveries of fossils lying along the mammalian stem and in basal positions within the crown clade. Data from the fossil record is augmented and extended far beyond what endocasts alone provide by comparative studies on genome, ontogeny, and mature organization of neurosensory systems of living amniotes, using what Witmer (1995) termed the ‘extant phylogenetic bracket’ – a realm that is enjoying its own renaissance.

A basic tenet of vertebrate paleoneurology is that in order to function properly the central nervous system and many peripheral sensory organs require rigid armatures that are provided mostly by the skeleton and associated connective tissues (Rowe and Shepherd 2016; Rowe 2020a). For example, early development of the brain is driven by a combination of tissue growth and a growing volume of cerebrospinal fluid in the ventricular cavities. In effect the ventricles become an expanding hydrostatic reservoir that places considerable loads on the connective tissues surrounding the brain and sensory organs in early ontogeny. Proper intraventricular pressure is required to drive normal brain expansion and normal skull formation. Epigenetic plasticity of the skull during ontogeny is highly responsive to the mechanical force regime imposed by the developing brain (reviewed in Rowe 1996b; Weisbecker et al. 2021). Similar epigenetic responses occur as the developing olfactory epithelium induces ossification of the bony turbinals (or turbinates) of the ethmoid bone (Rowe et al. 2005; Rowe and Shepherd 2016), and in other systems discussed below.

An integrative approach is used here to infer ancestral states of the neurosensory system in *Amniota* based on its two living clades, *Mammalia* and *Reptilia*, and their fossil records. This ancestral character state reconstruction helps to identify the evolution of novel morphological characters and character states preceding the origin of *Mammalia*. Patterns of successive correlated transformations identify potential driving factors behind the evolution of mammalian neurosensory systems that extend into genetic and epigenetic controls of development. We will see support for the idea that elaboration of peripheral sensory arrays, including olfactory receptors, teeth, and hair, influenced central organization with a cascade of new inputs. Through epigenetic population matching (Katz and Lasek 1978; Krubitzer and Kaas 2005; Streidter 2005) or some other mechanism, peripheral innovations were important drivers in central reorganization and successive increases in encephalization (Rowe and Shepherd 2016; Shepherd and Rowe 2017; Rowe 2020a).

A corollary is that peripheral sensory structures are not independent; they are parts of larger, integrated neurosensory systems. Generations of paleontologists have speculated on whether certain extinct stem-mammals had evolved whiskers, turbinals, endothermy, etc. (Broom 1932; Brink 1957; Crompton et al. 1978). These studies launched the exciting field of ‘paleobiology’ but hypotheses about soft

structures, physiology, and behavior in extinct taxa are often difficult to test. However, in cases where the neurosensory system is implicated or directly involved, tying hypothesized peripheral sensory structures into the larger systems of which they are a part can serve as a test. For example, as detailed below, expression of the huge olfactory receptor (OR) gene family in mammals induces growth of the expansive olfactory receptor epithelium, which in turn induces ossification of its scaffold of turbinals. The expanded number of olfactory neuron axons induces expansion of the olfactory bulb, whose axons in turn induce expansion of the olfactory (piriform) cortex. Hence, hypotheses that an unpreserved system of cartilaginous turbinals was present in early stem-mammal (e.g. Hillenius 1992, 1994) implicitly predict corresponding expansion of olfactory bulb and olfactory cortex that leave corresponding impressions in bones surrounding the endocranial cavity. The hypothesis of cartilaginous nasal turbinals in stem-mammals can be corroborated or falsified by evidence from the braincase and endocasts of the other components of the system.

Additional insights can be gained from Günter Wagner's (2014) conceptualization of two basic types of morphological innovation or novelty in animal evolution. Type I novelties involve the origin of a novel '*character identity*', and as examples Wagner cites the vertebrate head and the insect wing. The emergence of Type I innovations is not predicted by conventional Darwinian natural selection, and instead Wagner recognizes a special role for cascading effects of gene duplication and new gene regulatory networks. Pan-mammalian history reveals effects by the brain on skull morphogenesis from inferred gene duplications, particularly in the olfactory receptor sub-genome (Niimura 2012), and in genes regulating the radial units of cortical organization (Rakic 1988, 2000, 2007, 2009).

Type II innovations involve the origin of novel '*character-states*' and as examples Wagner cites emergence of the tetrapod limb from paired fins, and the emergence of feathers from epidermal scales. In an added level of complexity, Wagner also identifies novel '*variational modality*' in systems of repeated structures. We will see evidence of Type II innovations and transformations of *variational modality* in regionalization of the tetrapod vertebral column, differentiation and accelerated evolution in the occlusal dentition and inferred elaboration of olfactory receptors in cynodonts, each with its own special relationship to the neurosensory system.

Finally, the contours of pan-mammal history raise the provocative question of whether the mammalian neocortex, and possibly the masticatory apparatus, qualify as Type I innovations. The heuristic value of asking this question lies in the intricate dissection necessary for such a determination, and may be more informative than arriving at a final answer by advancing our understanding of the remarkable balance between individuation of novel character identities, new character states, and transformed variational modalities, with their functional integration into individual organisms and clades (Fig. 10.3).

Jerison's (1973) innovative 'encephalization quotients' (EQs) are commonly used to quantify the relationships between brain (or endocast) size and body size, but caveats should be acknowledged. Different authors have used different landmarks in fossils to delimit the floor and sides of the anterior half of the endocranial cavity where a bony enclosure is lacking, leading to different endocast

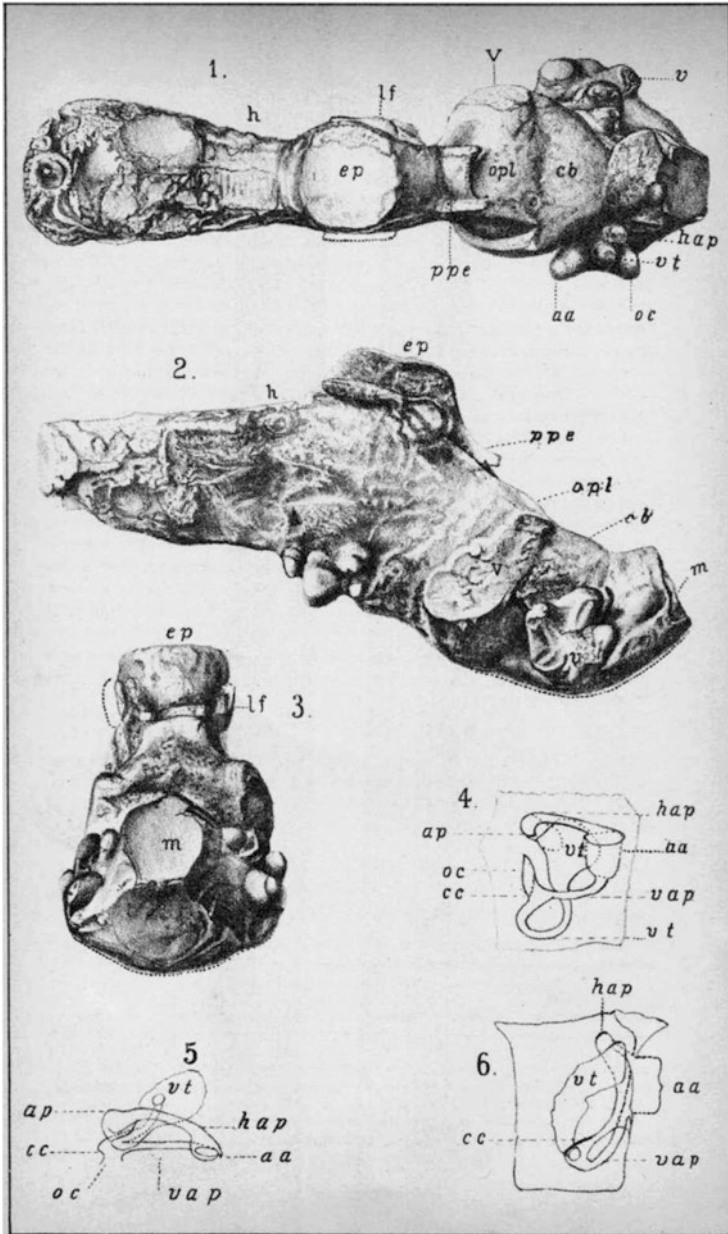


Fig. 10.4 Endocast of the stem amniote *Diadectes* (see Fig. 10.3) (From Cope 1886). Edinger (1975: 34) notes that this reconstruction “is not the endocast of one cranium, but a composite; that is, Cope’s introductory sentences stating that observations were made on a part of one skull, and a few other characters derived from two other skulls, apply also to the “brain” specimen.” (1) Dorsal view of endocast. (2) Left lateral view of endocast. (3) Posterior view of endocast. (4) Ventral view of semicircular canals. (5) Anterior view of semicircular canals. (6) Ventral view of semicircular canals. Abbreviations (from Cope)

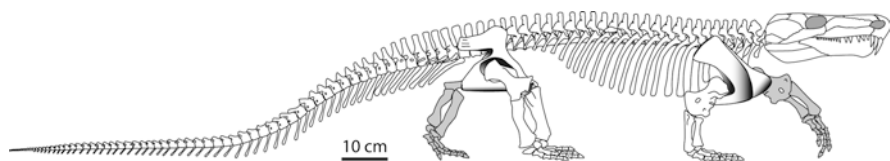


Fig. 10.5 *Limnoscelus paludis* – a stem-amniote that is very close to crown *Amniota* (see Fig. 10.3). (From Rowe 2020a)

10.3 The Ancestral Amniote

Pan-Reptilia (including birds) and *Pan-Mammalia* diverged from the ancestral amniote (Figs. 10.1 and 10.2) during the early Carboniferous, between 340 and 322 million years ago (Didier and Laurin 2020). The latest census of *Amniota* includes 6399 extant mammal species (Burgin et al. 2018), and more than 20,000 extant reptile species, a number that could rise by 5000–10,000 more, depending on ongoing reassessments of avian subspecies (Barrowclough et al. 2016). The ancestral amniote was a small predatory quadruped, about a half-meter in length, nearly half of which was the tail. The Carboniferous *Limnoscelus paludis* (Fig. 10.5) is either a basal amniote or a close relative on the amniote stem (Gauthier et al. 1988a), and provides an informative comparison for understanding subsequent amniote history. Early amniote fossils are generally found in deposits formed by what were then circumequatorial forests along rivers and deltas. The early terrestrial ecosystem would seem bizarre from today's vantage point, consisting mostly of predatory tetrapods who preyed on each other, and on non-vertebrates that were intermediates to the base of the food pyramid (Olson 1966).

10.3.1 The Amniote Skeleton

Whereas aquatic vertebrates are in effect neutrally buoyant, those who successfully moved onto land faced the effects of gravity and this underlies many skeletal innovations in basal amniotes. Because kinetic energy scales to the fifth power of linear dimension (McMahon and Bonner 1983), gravitational challenges increase



Fig. 10.4 (continued) Figures 1, 2 and 3 cast of cranial cavity, natural size. As the basicranial axis is lost, the inferior outline posteriorly is provisional only. Figure 1, from above. Figure 2, from the left side. Figure 3, from behind

The letters signify as follows: *m.* medulla, *cb.* cerebellum, *opl.* optic lobe, *ep.* epiphysis, *ppe.* posterior process of epiphysis, *If.* lateral foramen, *h.* region of cerebral hemispheres, *v.* cast of vestibule, *hap.* do. of orifice of horizontal anteroposterior semicircular canal, *vt.* do. of vertical transverse canal, *oc.* do. of os commune of vertical anteroposterior and vertical transverse canals, *aa.* do. of anterior ampulla, *V.* cast of foramen of fifth pair of nerves

Figures 4, 5 and 6 diagrams of the semicircular canals, natural size. Figure 4, interior view. Figure 5, anterior view. Figure 6, inferior view

exponentially with increase in body size. This probably explains why the first amniotes were small, and how similar strategies in strengthening the skeleton enabled different amniote clades to independently evolve large body sizes (Romer 1956, 1966). Amniotes initiated a trend towards simplification of the skeleton by consolidating primitively compound structures into single stronger elements (Sidor 2001). This occurred through ontogenetic re-patterning of regions of the skeleton in which primitively separate ossification centers failed to differentiate and a single element grew in their place, or where separate bones differentiated earlier in ontogeny and quickly fused.

Amniotes abandoned a larval stage and functional gills, and ventilation was achieved through two different systems. The first probably began in stem tetrapods, who co-opted the former pharyngeal skeleton into a branchial pump as lungs became the main site of metabolic gas exchange. The former gill arches were modified through reductions in their numbers, and in the number of elements per arch (Goodrich 1930). Some of these bones would later be co-opted to augment mobility of a fleshy tongue and unique swallowing behaviors (Crompton and Parker 1978; Crompton et al. 2018), and in both stem-mammals and stem-reptiles some were independently co-opted into an impedance matching middle ear (Gauthier et al. 1988a; Clack 2012; Kitazawa et al. 2015). The second system involved a musculo-skeletal system in the trunk in which hinged ribs and intercostal muscles acted to move the ribs away from the body center, expanding the cavity surrounding the lungs for aspirational breathing (Janis and Keller 2001; Brainerd 2015). This second system probably originated in support of the branchial pump, which gradually gave way to rib-driven aspirational breathing. This system arose in stem-amniotes and had probably become the dominant of the two systems in early amniotes and stem-mammals (Janis and Keller 2001; Brainerd and Owerkowicz 2006).

Like their aquatic ancestors, the first amniotes were macro-predators, but life on land entailed profound change in how they fed (Lemberg et al. 2021). The ancestral mode of gape-and-suck feeding worked in a water column, but terrestrial feeding entailed precise movements of the jaws, head, and neck, as the amniote mouth became a finely tuned prehensile device for biting and seizing prey items (Romer 1956, 1966). Swallowing also posed a new problem. Amniotes initially solved it with a fleshy tongue and by using inertial swallowing, i.e., by lunging the head and mouth forward against the inertia of a subdued, stationary prey item (Heiss et al. 2018). This implies new levels of coordination between vision and actions of the jaws, head and neck. Many such innovations imply neurosensory elaboration that can only be inferred, but nevertheless paint a more vivid picture of evolving neuro-sensory capacity.

Along with rib-driven aspirational breathing, the amniote craniovertebral joint reflects continuation of a new variational modality begun in early tetrapods involving increased regionalization of the axial skeleton. The amniote skull articulated with two specialized vertebrae – the ‘atlas-axis complex’ - that enhanced stable mobility of the head on a longer neck. A primitive neck enabling the head to be raised can be traced into early stem-tetrapods (Gauthier et al. 1988b, 1989). Early amniotes further modified this joint to facilitate prey capture and inertial

swallowing. It also raised the head somewhat, broadening sensory horizons and directional sensory perception. A design requirement of the craniovertebral joint is to ensure the spinal cord is not stretched or kinked by extended head movements (Jenkins Jr. 1969, 1971; Kemp 2005). At many points in pan-mammalian history, subtle skeletal modifications balanced seemingly conflicting demands of increased head and neck mobility against increases in diameter of the spinal cord that accompanied encephalization and peripheral sensory elaboration (Rowe et al. 2011; Rowe 2020a).

The limbs in early amniotes and stem-mammals were a bit longer than in the first tetrapods, but they were still very short and widely sprawled to the sides of the body. Fossil trackways are wide, showing a short stride, and they must have been quite slow (Romer and Price 1940). The pectoral girdle and forelimbs were heavily built and pulled the body forward by rotating a propeller-shaped humerus at the shoulder. The hindlimb was comparatively short and weakly developed, but strong femoral retractor muscles originating from the base of the tail provided thrust. Alternating lateral undulation of the axial skeleton augmented by the pull-push forces of the limbs also contributed thrust (Romer 1956; Kemp 2005; Hopson 2015). However, asymmetrical axial undulation precluded symmetrical, bilateral expansion of the ribs and must have limited aspirational breathing, and considerably limited metabolic scope during locomotion (Carrier 1987). Some consider the earliest stem-mammals to have been sit-and-wait ambush predators (Hopson 2015).

Compared to their descendants, early amniotes were limited in speed, agility, and gait. They could walk and probably still swim, but it is doubtful they could run, and any locomotion at speed was metabolically limited to short bursts (Carrier 1987). From such an ancestor, running, galloping, jumping, hopping, climbing, gliding, diving, and flying would eventually emerge in pan-mammals, but not without profound skeletal modifications and corresponding neurosensory elaboration (Rowe 2020a). The importance of feeding and locomotion in pan-mammal evolution has long been emphasized by paleontologists (e.g. Goodrich 1930; Romer 1966; Gauthier et al. 1988a). Paleoneurology can now begin to identify correlative neurosensory transformations in response to questions about what, when, how, and why the mammalian neurosensory system evolved (Northcutt 2001).

10.3.2 *Peripheral Sensory System*

Many characteristics of the amniote neurosensory system can be explained by a commitment to terrestrial life that altered acuity and balance between individual sensory modalities. For example the lateral line system was present in vertebrates ancestrally to detect electrical impulses transmitted through water, as well as water temperature, chemistry, and turbulence (Rowe 2004). But these signals are not perceptible in air, and in amniotes this entire system was quickly lost; early stem-amniote fossils are recognizable by the absence of lateral line canals on their skulls (Gauthier et al. 1988b, 1989). In contrast, the amniote visual system underwent a

vast adaptive radiation in response to a greater diversity of reflective objects on land than in water (Walls 1942). So too, the amniote olfactory system adapted to a more diverse and rapidly changing chemical environment encountered in terrestrial ecosystems (Rowe et al. 2011) and olfactory receptor genes became the fastest evolving gene family in tetrapods (Yohe et al. 2020) and especially pan-mammals.

Olfactory system

Amniotes inherited a dual olfactory system consisting of the main olfactory system and the vomeronasal system (accessory olfactory system) (Farbman 1992), that are encoded by separate gene subfamilies (Niimura and Nei 2005, 2006; Niimura 2009). The amniote olfactory system was profoundly transformed as the medium of ventilation and metabolic gas exchange moved from water to air, and it diversified further among the different amniote clades. The following discussion is exclusive to mammals, where genetic and ontogenetic paths are best-known. The vomeronasal system is absent in aquatic mammals, some bats, and platyrrhine and anthropoid primates (Bertmar 1981; Bhatnagar and Meisami 1998), but the dual system is present in monotremes, marsupials, as was the case in mammals ancestrally and across the mammalian stem-group.

Differentiation of the main olfactory and vomeronasal systems is induced as a single pair of ectodermal olfactory placodes at the rostral extremity of the neural plate invaginates to contact the rostral end of the developing forebrain (Farbman 1988, 1990; Schlosser 2010, 2017). This contact initiates differentiation and growth of separate main olfactory and vomeronasal epithelia, which together carpet the inner walls of the placode. Once induced, the main olfactory and vomeronasal systems follow separate ontogenetic trajectories, but their divergent synaptic pathways eventually converge in the accessory olfactory bulb (Farbman 1992).

Shortly thereafter, olfactory neurons (OSNs) differentiate in the olfactory epithelium, whose axons induce differentiation of glomeruli in the presumptive olfactory bulb (Figs. 10.6 and 10.7); once contact is made, the expression of a particular olfactory gene is induced, and the expression of other OR genes is suppressed (Chen and Shepherd 2005; Shepherd et al. 2021). Axonal projections from the olfactory bulb in turn induce differentiation of the olfactory cortex (Schlosser 2010; Shepherd et al. 2021). Lying between the olfactory bulb and olfactory cortex is the accessory olfactory bulb; it is probably induced by main olfactory bulb projections and/or vomeronasal receptor axons, but direct evidence is lacking. The rostral position of the olfactory placodes may explain why olfaction is the only peripheral sensory system that projects directly to the telencephalon, whereas the other cranial sensory placodes are positioned lateral or caudal to the presumptive diencephalon and follow different pathways to the telencephalon via the thalamus (Schlosser 2010, 2017; Shepherd et al. 2021).

In aquatic non-tetrapod vertebrates, both the main olfactory receptors, vomeronasal receptors, and the associated terminal nerve (cranial nerve 0) are sensitive to odorant molecules suspended in the water column. In early stem-tetrapods, what

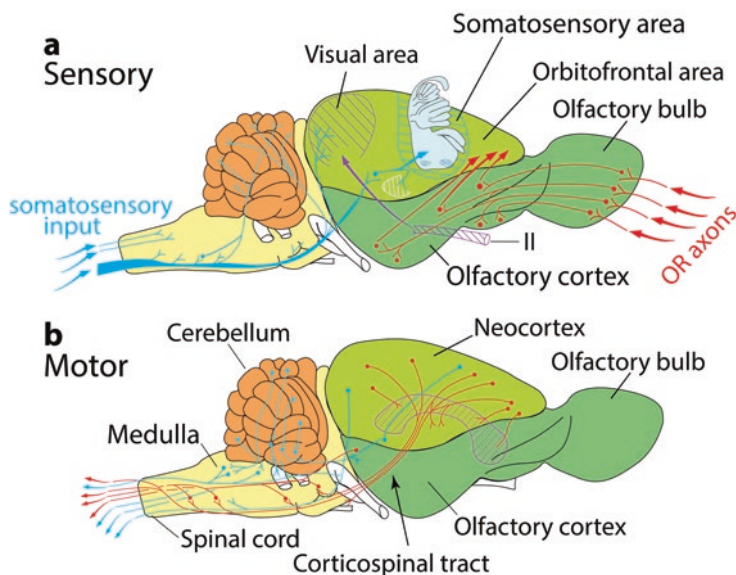


Fig. 10.6 Circuitry schematic of brain of modern opossum (*Didelphis*) brain showing (a) sensory inputs and (b) motor outputs. (Modified after Rowe et al. 2011). See anatomical abbreviations

formerly were diffusely distributed vomeronasal receptors became organized into an encapsulated vomeronasal organ on the floor of the nasal capsule (Rowe 2004; Rowe et al. 2005). Its receptors are activated primarily by pheromones and other large molecules that are not carried far by air (Baxi et al. 2006; Streidter and Northcutt 2020). Its axons and those from the terminal nerve make their first synapse in the accessory olfactory bulb, where they induce formation of glomeruli that are independent from those of the main olfactory system (Demski 1993; Demski and Schwanzel-Fukuda 1987). Whereas both olfactory systems are important in stem-mammal evolution, unequivocal evidence of transformations in the vomeronasal organ have yet to be recognized in stem-mammal fossils, and our focus now turns to the main olfactory system, which mediates conscious odor perception (Shepherd et al. 2021).

Genes that once coded receptors activated by waterborne molecules were either lost or transformed into new gene families that encode odorant receptors activated by volatile airborne odorants. A great breakthrough in understanding olfactory organization was made by Buck and Axel (1991) in identifying the genes that encode olfactory receptors (ORs), and the finding that each gene codes a receptor that is narrowly tuned to a single odorant molecule, or a narrow family of molecules. Then came the discovery that most vertebrates, including reptiles, have ~100 OR genes, but that the ancestral mammal was inferred to have had ~1200 OR genes based on comparisons among living species (Niimura and Nei 2005, 2006; Niimura 2012; Niimura et al. 2014; Zhou et al. 2021). The discovery that several derived turtle clades have expanded OR genomes (Wang et al. 2013) does not affect the estimated number for amniotes ancestrally, and underscores that the OR genome is the most

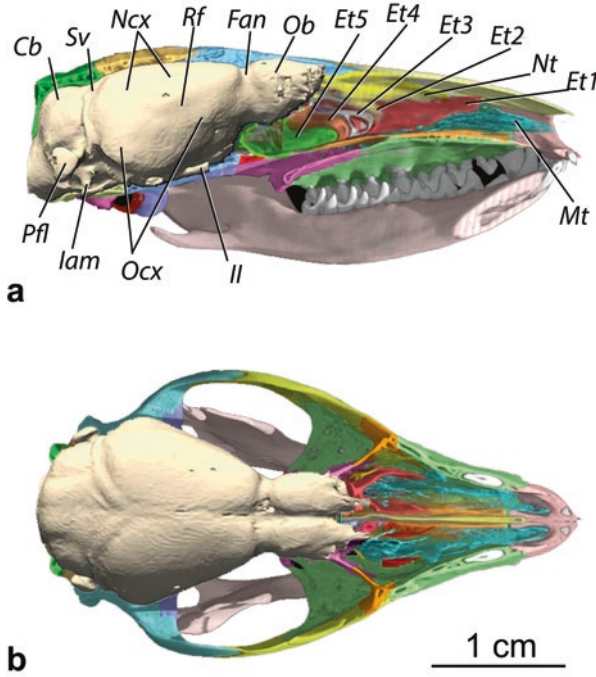


Fig. 10.7 Skull of mature *Monodelphis domestica*, reconstructed in 3D from computed tomography, in cut-away sagittal (**a**) and horizontal (**b**) views. The endocranial cavity was rendered solid beige to show the endocast of the brain in relation to the various bones of the skull, which were individually segmented and colored using VGStudio Max 2.0 software. (Modified after Rowe et al. 2011). See anatomical abbreviations

rapidly evolving subfamily in the tetrapod genome (Yohe et al. 2020). During the evolution of stem-mammals, therefore, a series of OR gene duplications must have increased their numbers by an order of magnitude beyond the numbers inferred present in the ancestral amniote. This was probably a result of multiple tandem gene duplications that led the OR genome to become the largest and most rapidly evolving subfamily in the mammalian genome; this must have occurred by or before the origin of *Mammalia* (Young et al. 2010; Yohe et al. 2020).

With the origin of *Amniota*, airflow through the nasal chamber became tied to two distinct functions. Each function is supported by a primary ‘choncha’ or epithelial fold, supported by a low ridge of cartilage protruding into the lumen from the lateral wall of the nasal capsule (Parsons 1967; Gauthier et al. 1988a). The anterior choncha supports mucociliary respiratory epithelium, while the posterior choncha supports olfactory epithelium. In *Mammalia*, (Fig. 10.7) both conchae evolved hypertrophied epithelia supported by elaborate skeletons of paper-thin filigreed scrolls, arbors, and plates of bone known as turbinals (or turbinates), as olfactory and respiratory functions elaborated (Taylor 1977; Rowe et al. 2005; Crompton et al. 2017a).

Visual System

There are far more reflective surfaces on land, less light scatter or absorption in air, and more light energy in air than in water (Walls 1942). The ancestral amniote entered a world of new visual information and is inferred to have been diurnal with a retina rich in cones compared to rods (Walls 1942). It may have traded light sensitivity for a marked increase in visual acuity and sharp resolving power because predaceous vertebrates generally require sharp vision to pursue and capture prey, and animals that feed on small objects like insects must be able to resolve them, which is best achieved in a cone-rich eye (Walls 1942). Most genomic accounts suggest the ancestral amniote had tetrachromatic vision (e.g. Streidter and Northcutt 2020). However, the recent discovery that the Tuatara (*Sphenodon*) has all five of the visual opsin genes found in vertebrates ancestrally (Gemmell et al. 2020), is consistent with the view that the ancestral amniote may have had pentachromatic color vision based on visual pigments of the RhA/Rh1, RhB/Rh2, SWS1, SWS2, and LWS opsin gene families (Collin 2010). Diurnal vision probably led the other senses in the ancestral amniote and in early stem-mammals. However, the RhB/Rh2 opsin genes are absent in *Mammalia* and must have been lost in its stem group. Further reductions in opsin genes occurred in different clades within *Mammalia*, and dichromatic crepuscular to nocturnal behaviors in monotremes (Davies et al. 2007; Ashwell 2013) and therians (Ashwell 2010) probably evolved independently (Walls 1942; Collin 2010; Gemmell et al. 2020).

Auditory System

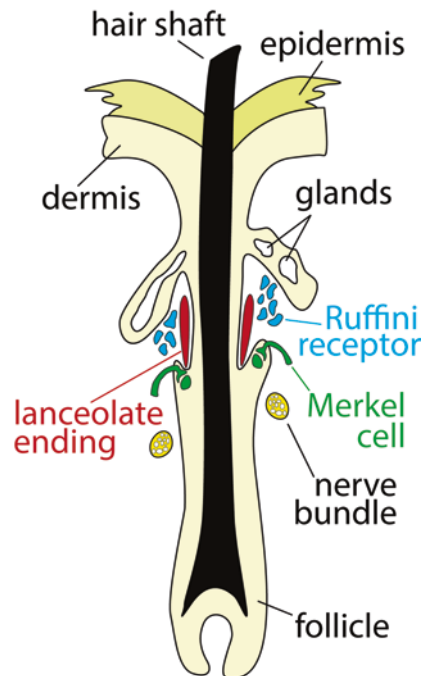
The sensitivity and resolving power of hearing in the ancestral amniote and early pan-mammals must have diminished in the transition to airborne acoustic information. Still, the ancestral amniote and its living descendants conserved basic functions of hearing involving frequency discrimination, signal to noise ratio enhancement, and sound localization. They also conserved the plesiomorphic transmission pathway involving transduction of acoustic information by sensory hair cells of the inner ear, which in amniotes involved a basilar papilla and membrane (Streidter and Northcutt 2020), and from there via the auditory nerve to brainstem auditory neurons (Carr and Soares 2002, 2009; Carr and Christiansen-Dalsgaard 2016). The fossil record indicates that an impedance matching middle ear evolved independently in amphibians, stem-reptiles, and stem-mammals (Gauthier et al. 1988a, b, 1989). In each clade, the middle ear has its own distinct anatomical organization and neural mechanisms for sound localization (Carr and Soares 2009). However, in each case, the middle ear develops from elements of the first and/or second branchial arches. Each clade also introduced a tympanic membrane connected via a lever system of bone and/or cartilage that matched airborne sound impedance to the fluid-filled inner ear (Grothe et al. 2005, 2010). Terrestrial hearing was probably limited at first to low frequency vibrations from the ground via the jaws and branchial arches as early amniotes rested their heads on the ground. This

may explain the independent derivation of impedance matching middle ears from components of the branchial arches.

Peripheral Somatosensory System

Bony scales were lost from the skin in stem amniotes, and in their place are tiny epidermal condensations – body placodes – induced by neural crest cells that would eventually evolve into mammalian hair and reptilian scales and feathers. Amniote body placodes share common spatial expression of placode molecular markers such as *Shh*, *Ctmb1*, and *Edar*, as well as conserved localized signaling in the dermis underlying the placode by *Bmp4*, corroborating shared common ancestry (Di-Pöi and Milinkovitch 2016). The appearance of placode-induced epidermal structures began an amazing diversification of integumentary specializations to prevent water loss, protect the skin from solar radiation, enhance sensory perception over the body surface and in the space around it, insulate the body, assist locomotion, provide camouflage, and attract mates. At some late point in stem-mammal history, hair follicles would evolve from body placodes and deliver a deluge of new peripheral information to the brain (Fig. 10.8). Exceptional preservation of a Jurassic stem-mammal indicates that fur evolved before the origin of crown *Mammalia* (below).

Fig. 10.8 Diagram of a hair follicle and its innervation (Modified after Rowe et al. 2011)



The Ancestral Amniote Brain

So little of the endocranial cavity is enclosed by bone that much speculation attends any attempt to reconstruct a basal amniote endocranium. Most relevant fossils are badly crushed or incomplete and their state of preservation often defeats CT scanning. As a result, few attempts have been made to reconstruct individual endocrania in a basal or stem-amniote (Fig. 10.4; Cope 1886; Case 1907; Romer and Edinger 1942). Nevertheless, general conclusions can be assembled from fossils and from comparative development of extant amniotes. Anteriorly, the orbitosphenoid formed a thin, Y-shaped ossification that cupped the forebrain from beneath. When preserved, the orbitosphenoid indicates a long narrow forebrain positioned close to the skull roof (Crompton et al. 2017b). The olfactory bulbs were probably closely appressed against the anterior telencephalon, as in extant lissamphibians and turtles (Gauthier et al. 1988a), and in all the later stem-mammal fossils from which endocrania can be extracted (e.g. Macrini 2006; Kemp 2009; Benoit et al. 2016, 2017). Whereas an interhemispheric sulcus divides the cerebral hemispheres in all extant vertebrates, there is no evidence of an interhemispheric ridge along the inferior side of the parietal. This suggests the brain was not strongly inflated in early development and did not exert the profound effect on cranial morphogenesis it would eventually have in some of the later stem-mammals (below). The floor and rear parts of the braincase were ossified and surrounded a cerebellum that was twice as wide as the forebrain. A large pineal stalk was present, and the midbrain was exposed dorsally between the telencephalon and cerebellum (Fig. 10.4).

Telencephalon Comparative and developmental anatomy in extant amniotes indicate the telencephalon in the ancestral amniote consisted of four basic divisions that surrounded the ventricle. The olfactory (piriform) cortex was positioned laterally, the hippocampus formed the medial wall, the telencephalic roof or dorsal pallium formed the dorsal cortex, and the basal ganglia differentiated in the telencephalic floor. The three cortical areas – dorsal cortex, olfactory cortex and hippocampus – in non-mammalian amniotes (except archosaurs; Briscoe and Ragsdale 2018) have a three-layer construction, consisting of a middle layer of pyramidal neuron bodies and interneurons with an underlying layer of axons and an overlying layer of dendrites of the pyramidal cells and interneurons (Shepherd and Rowe 2017).

The principal cells in the amniote forebrain are pyramidal cells (Shepherd 2011). This cell type is present in amphibians but lacks basal dendrites, whereas in amniotes the basal dendrites are not only present but have become extensively branched and interconnected in a vast synaptic web (Streidter 2005; Shepherd 2011). Pyramidal cells are present in the forebrains of all reptiles except crocodylians and birds, where they were secondarily transformed or lost (Streidter 2005). The amniote cortex surrounded a ventricular zone throughout its extent, and a subventricular zone in its lateral regions from which neurogenesis occurred in an inside-out pattern (Marín and Rubenstein 2001). Neurogenesis proceeded throughout much of ontogeny, and established the basic neurogenerative pattern that gave a degree of radial

and columnar organization to the forebrain that was carried to the extreme in *Mammalia* (Rakic 1988, 2000, 2007, 2009).

In its basic circuitry, the olfactory cortex has a similar neural organization in turtles and lizards (Ulinski 1983; Haberly 1985; Bruce 2007, 2009; Bruce and Braford Jr 2009) and in monotremes (Ashwell 2013), marsupials and placentals (Ashwell 2010; Shepherd 2011), supporting the inference that this organization was present in amniotes ancestrally. Olfactory receptors deliver signals to the olfactory bulb where they form an ‘odor image’. The unique degree of elaboration in mammals involves a chain of more than 20 separate microcircuits (Shepherd et al. 2021). The ‘odor image’ is passed to the olfactory cortex which transforms it into a higher level representation known as an ‘odor object’ with content addressable memory. The ‘odor object’ is passed to the dorsal cortex (or to neocortex in *Mammalia*) for further associative processing (Shepherd 1991; Wilson and Stevenson 2006). Anatomical and physiological studies in the hippocampus have shown that across amniotes the neurons and circuits are similar to those in the olfactory cortex, with similar long association fibers and interconnections for excitation and inhibition (Connors and Kriegstein 1986; Haberly 2001). In these regards, the intrinsic organization of olfactory cortex and hippocampus are similar to higher association cortical areas, for example the face area of inferotemporal cortex (Haberly 1985; Shepherd and Rowe 2017). There is a close similarity between the intrinsic organization of the hippocampus and the olfactory cortex in terms of layering of inputs on the apical dendrites and long association fibers (Neville and Haberly 2004). Since inputs to the hippocampus consist exclusively of central sites in the limbic regions, it is clear that the three-layered hippocampus was devoted to higher order processing such as learning and memory from the very start of amniote evolution (Rowe and Shepherd 2016; Shepherd and Rowe 2017). In this view, the three-layer dorsal cortex of the ancestral amniote, from which six-layer mammalian neocortex evolved, was not a ‘simple’ cortex for low-level processing, but rather had an organization that subserved high-level association functions analogous to those in olfactory cortex and hippocampus (Rowe and Shepherd 2016; Shepherd and Rowe 2017; Shepherd et al. 2021).

Thalamus The thalamus switches circuits passing in both directions from the dorsal cortex to the rest of the body. Compared to other tetrapods, amniotes have an expanded and highly differentiated thalamus (Butler 1994; Butler and Hodos 2005; Nieuwenhuys et al. 1998; Streidter and Northcutt 2020). It took on a new level of complex organization in amniotes, one that was further elaborated during stem-mammalian history in association with the emergence of neocortex. Amniotes have an elaborated dorsal thalamus that is larger and contains many more individual cell masses or nuclei than anamniotes (Butler 1994; Butler and Hodos 2005; Nieuwenhuys et al. 1998). Highly characteristic of amniotes is differentiation of discrete specialized nuclei that function as a complex of way-stations for visual, auditory, and somatosensory inputs interposed between the environmental sensory world and dorsal cortex (Butler 1994; Butler and Hodos 2005).

Hypothalamus The amniote hypothalamus differs from anamniotes in receiving input from those regions with responsibility to memory and the resonance of experience (Butler 1994; Butler and Hodos 2005). Many functions of the hypothalamus are tied to light, to the daily cycle of light from dawn to dusk; the influence of light on the hypothalamus extends to seasonal variability, to the shorter winter days and longer summer days. This is consistent with evidence that the ancestral amniote was diurnal with tetrachromatic or pentachromatic color vision (above). The hypothalamus also regulates water balance by directing kidney function – a crucial process in terrestrial vertebrates. The hypothalamus also controls the production of hormones involved in reproductive physiology, involving the movement of ova in the oviduct, contractions of muscles of the reproductive organs, and many behaviors involved in courtship. Finally, the suprachiasmatic nucleus of the hypothalamus is an autonomous circadian pacemaker. Thus, circadian cycles and seasonality were influential in early amniote and stem-mammal behaviors (Butler and Hodos 2005).

Spinal Cord The spinal cord is segmented at multiple levels of organization. Each segment forms dorsal (afferent) and ventral (efferent) spinal nerves that correspond in the neck and trunk to the numbers of vertebral segments. The amniote spinal cord is thicker than anamniotes and extends through the entire length of the dorsal vertebral column, and in *Mammalia* for a variable distance into the tail. It has more different types of cells than anamniotes, and many of these secondary neurons send axons across the midline to the contralateral side for left-right coordination of movement (Butler 1994; Nieuwenhuys et al. 1998). A distinct lateral column of motor neurons provides innervation to the limbs; and there are now expanded cervical enlargements (segments 7 – 10) and lumbosacral enlargements (segments 19 – 22) that represent the initial integrating centers of the brachial and sacral plexi, which innervate muscle complexes during locomotion and control reflexive action in the limbs. Their size is correlated with the lengths of the corresponding extremities (Nieuwenhuys et al. 1998). Another innovation was the aggregation of spinal neurons into discrete ‘motor pools’ that innervate single muscles, probably allowing them to be controlled independently (Streidter and Northcutt 2020). Additionally, the autonomic neuronal groups (i.e. ‘fright and flight reflexes’) of the brainstem and spinal cord were highly developed, indicating that the spinal cord was performing more internal decision-making processes that are independent of the brain (Streidter 2005).

In summary, compared to the first stem-tetrapods the ancestral amniote neurosensory system enjoyed an increase in numbers of genes, more neuronal types, and more complex pyramidal cells with greater interconnectivity, faster rates of neuron proliferation that produced a larger forebrain, and elaboration in complexity and computing power on the new world of terrestrial information amniotes had entered. It controlled more highly coordinated body movements using a more complex muscular system. While abandoning the lateral line system, it began a trend to integrate peripheral information from more acute visual and airborne olfactory systems. This underscores that three-layer dorsal cortex of amniotes ancestrally operated at the

level of higher order associations underlying analysis, discrimination, learning, and memory (Rowe and Shepherd 2016; Shepherd and Rowe 2017), and a remarkable capacity for detailed analysis of their environment (Nieuwenhuys et al. 1998). Basal amniotes were probably more introspective and reflective of experience, using a more highly developed sense of memory as a guide to action (Butler 1994; Butler and Hodos 2005).

Such was the general organization of the skeleton and neurosensory system in the ancestral amniote. From such an ancestor, we now turn to the fossil record of stem-mammals and the major events in neurosensory evolution culminating with the origin of *Mammalia*.

10.4 Early Pan-Mammalian History

Pan-Mammalia diverged onto its own evolutionary trajectory in the Early Carboniferous, 340 – 322 million years ago (Didier and Laurin 2020). In most (pre-Phylocode) literature *Pan-Mammalia* (Rowe 2020c) is referred to by the name ‘*Synapsida*’ which is used as a synonym for both the paraphyletic stem-group of mammals (e.g. Romer 1956, 1966), and for the total clade of *Mammalia* (e.g. Gauthier et al. 1988a; Laurin and Reisz 2020). I use the name for an apomorphy-based clade stemming from the first pan-mammal possessing the synapsid arch (Fig. 10.3, node 1) (Rowe 2020c). The early fossil record of stem-mammals is confined to what were then circumequatorial belts of Pangaea in the Carboniferous and Early Permian. They include several extinct side-branches, including *Varanopidae*, *Caseasauria*, *Ophiacodontidae*, *Edaphosauridae*, *Haptodontidae*, and *Sphenacodontidae* (Fig. 10.3, nodes 1–3; Fig. 10.9) that were long clustered in the paraphylum ‘*Pelycosuaria*’ (e.g. Romer and Price, 1940; Olson 1959). Beginning in the late nineteenth century, ‘pelycosaurs’ were recognized as representing the most primitive ‘grade’ of evolution involved in the distant ancestry of *Mammalia* (Rowe 2020a, b), and became known in the vernacular as “mammal-like reptiles”. It was their retention of numerous plesiomorphic amniote characters that persuaded virtually all paleontologists to classify them in what was then conceptualized as ‘paraphylum *Reptilia*’ which was considered ancestral to all the living amniote clades.

The endocranial skeleton in early stem-mammals differs little from stem-amniotes and offers few details on brain size and shape. The endocranial cavity is open anteriorly, the forebrain enclosed laterally and ventrally by the (rarely-preserved) orbitosphenoid bone, and only posterior to the hypophysis is the endocranial cavity fully enclosed by bone. The forebrain was a featureless narrow cylinder, and there is no evidence of the interhemispheric sulcus (although it must have been present in life). Comparisons to the lepidosaur *Sphenodon* are closer than to any living mammal, and indeed these early endocasts only obscured the true relationships of early stem-mammals (e.g. Baur and Case 1899).

Subtle skeleton changes in early stem-mammals with implied neurosensory effects are detailed elsewhere (Rowe and Shepherd 2016; Rowe 2020a). Suffice it

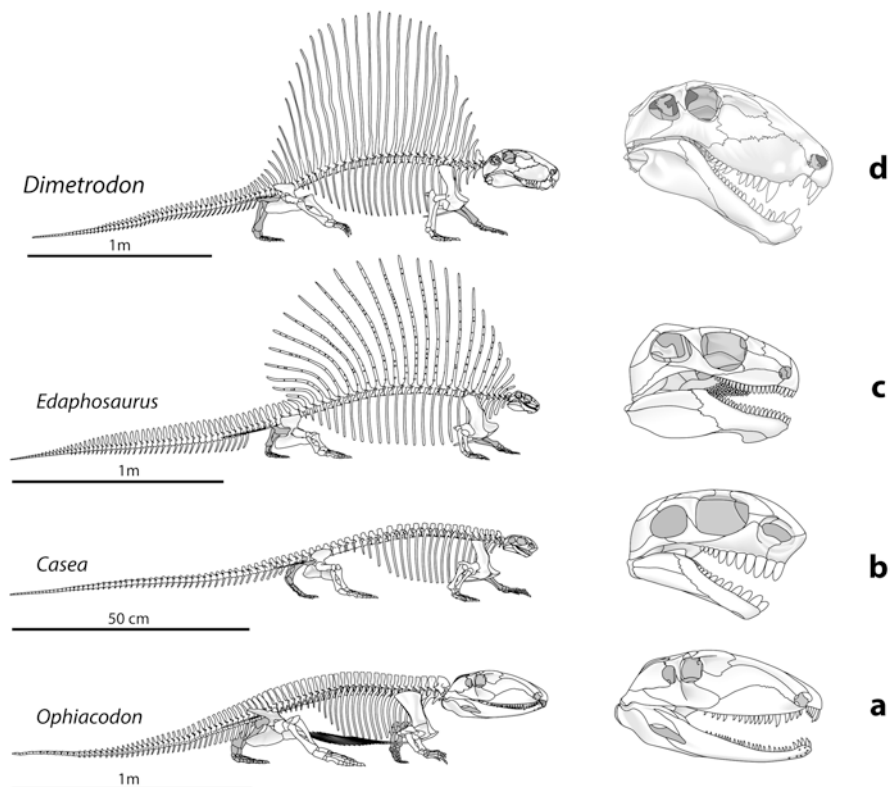


Fig. 10.9 Skulls and skeletons of ‘pelycosaur-grade’ Early Permian stem-mammals: (a) *Ophiacodon*, (b) *Casea*, (c) *Edaphosaurus*, and (d) *Dimetrodon*. Drawn to same lengths. (Modified after Rowe 2020a)

here to highlight the main diagnostic feature of *Pan-Mammalia* currently known, viz. the single temporal fenestra, bounded below by the homolog of the mammalian zygomatic arch (Gauthier et al. 1988a; Laurin and Reisz 2020; Rowe 2020c). The single fenestra and underlying arch comprise the ‘synapsid condition’ (Fig. 10.9), which allowed mandibular adductor musculature room to flex and expand outwards as the jaws snapped together without compressing the brain and blood vessels that lie deep to the adductor muscles. This exemplifies the epigenetic balancing act by the developing skull in supporting both the brain and masticatory system.

The ancestral amniote had small external nostrils that were directed laterally, and the internal nostrils (choanae) formed small openings near the front of the palate (Fig. 10.10). The space between nostril and choana allowed only a small nasal capsule and olfactory epithelium. However, in early stem-mammals the choana were considerably elongated, indicating a larger nasal capsule and expanded olfactory epithelium, beginning a trend in which enhanced olfaction would eventually become a major driver of pan-mammalian evolution (below).

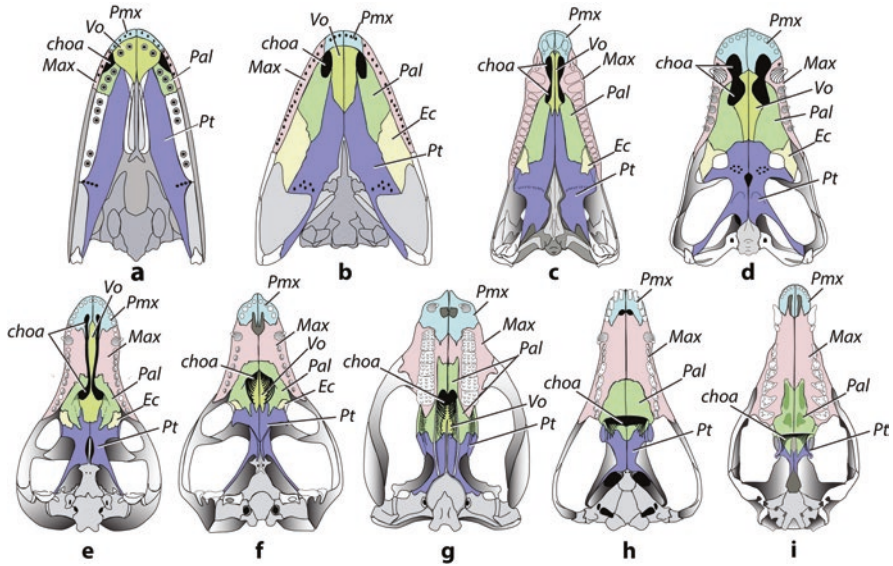


Fig. 10.10 Stages in the evolution of mammalian secondary palate and the ortho-retronasal olfaction duality. (a) *Eusthenopteron*, a stem-tetrapod; (b) *Seymouria*, a stem amniote; (c) *Dimetrodon*, a basal synapsid; (d) *Syodon*, a more advanced non-cynodontian synapsid; (e) *Procynosuchus*, the basal-most cynodont with an incipient secondary palate; (f) *Thrinaxodon*, an early cynodont with a complete secondary palate; (g) *Kayentatherium*, a basal mammaliaform with a complex dentition; (h) *Morganucodon*, a basal mammaliaform, with secondary palate extending to back of tooth row; (i) *Didelphis*, with secondary palate extending behind tooth row. (From Rowe and Shepherd 2016). See anatomical abbreviations

At maturity, most of the early stem-mammals had longer faces than other early amniotes, with more than half of the skull lying in front of the orbits, and a jaw articulation displaced to a level behind the occiput that further widened jaw gape. The mouth was lined with a long row of sharp, recurved teeth that were replaced continuously throughout life. Most early stem-mammals had a faster and more powerful bite than other early amniotes. Locomotor evolution involved increased power and speed, with the two sacral ribs attaching to the ilium at a level above the acetabulum, lowering the hip joint beneath the vertebral column and conveying slightly greater stride and lunge capability (Romer and Price 1940; Romer 1956). Some of these taxa, sphenacodontines in particular (Fig. 10.9, top), were the apex predators of the Late Carboniferous and Early Permian (Romer and Price 1940; Romer 1956; Kemp 2005). Indirectly, this implies a greater measure of neural velocity in perception and response to their environmental interactions.

From the start, stem-mammal orbits were large and opened laterally or dorsolaterally, and they held relatively large, mobile eyeballs. The bones enclosing the orbit would undergo multiple evolutionary transformations that redirected the orbits frontally, expanding their fields of stereoscopic vision, and probably altering the range of eyeball movements (Walls 1942; Romer 1956; Kemp 2005; Rowe 2020a).

An auditory innovation arising in *Sphenacodontia* (Fig. 10.3, node 3) is a notch in the angular bone at the back of the jaw that freed a thin ‘reflected lamina’ that enclosed a narrow air space against the jaw. The ‘reflected lamina’ is the distant transformational homolog of the mammalian ectotympanic, which supports the tympanic membrane. Whether the notch above the reflected lamina held a functional tympanum at this stage is unknown; the delicate reflected lamina itself may have functioned as a crude tympanum. Its significance in audition is clear only in retrospect and its overall mature size and form were unlike any auditory element in living mammals. It probably responded only to loud, low frequency sound, and the sacculus of the inner ear occupied only a shallow depression in the floor of the otic capsule (Olson 1944; Romer and Price 1940; Romer 1956).

Diurnal vision, followed distantly by olfaction, were the leading sensory modalities for much of early stem-mammalian history. Successive subtle changes in the craniovertebral joint and neck raised the head above the body (Jenkins Jr. 1969), and early pan-mammals surveyed broader information horizons than other early amniotes.

10.4.1 Node 4: *Therapsida*

Therapsida (Rowe 2020d) (Fig. 10.3, node 4) is the clade stemming from the last common ancestor *Mammalia* shares with the mid-Permian *Biarmosuchia*, and all its descendants. In its traditional conceptualization as an extinct paraphylum or ‘grade of evolution’, *Therapsida* included only the extinct side branches *Biarmosuchia*, *Deinocephalia*, *Gorgonopsia*, *Dicynodontia*, *Terocephalia*, and a paraphyletic *Cynodontia* that excluded *Mammalia* (Fig. 10.11). Kemp (2006) summarized the features separating early *Therapsida* from more basal stem-mammals: “It has always been recognized that therapsids are in a general way more ‘advanced’, or ‘progressive’ in their biology than their pelycosaurian forebears”. Whether viewed as a grade or a clade, therapsids “... had evolved a higher rate of food assimilation and of ventilatory capacity, a more agile, faster, more energetic mode of locomotion, more elaborate and therefore more sensitive olfaction and hearing, and an increased growth rate” (Kemp 2006:1237).

The face in basal therapsids presents an increasingly anterior or frontal axis of attention and activity, and bilateral directional coordination of visual and olfactory fields. The nostrils were redirected anterolaterally, enhancing stereoscopic directional perception of olfactory cues that are important in many mammals (Louis et al. 2008; Catania 2013; Catania and Catania 2015). The choanae are further elongated (Fig. 10.10d) over the condition of the basal-most stem-mammals (Sidor 2003), indicating further expansion of the nasal capsule and olfactory epithelium. The trenchant upper canine is longer than in ‘pelycosaurian grade’ stem-mammals and separates specialized enlarged incisors from unicuspid, recurved postcanine teeth. Early therapsids were increasingly specialized in apprehending and dismembering prey with a bite from their canines and incisors (Gauthier et al. 1988a; Kemp 2005,

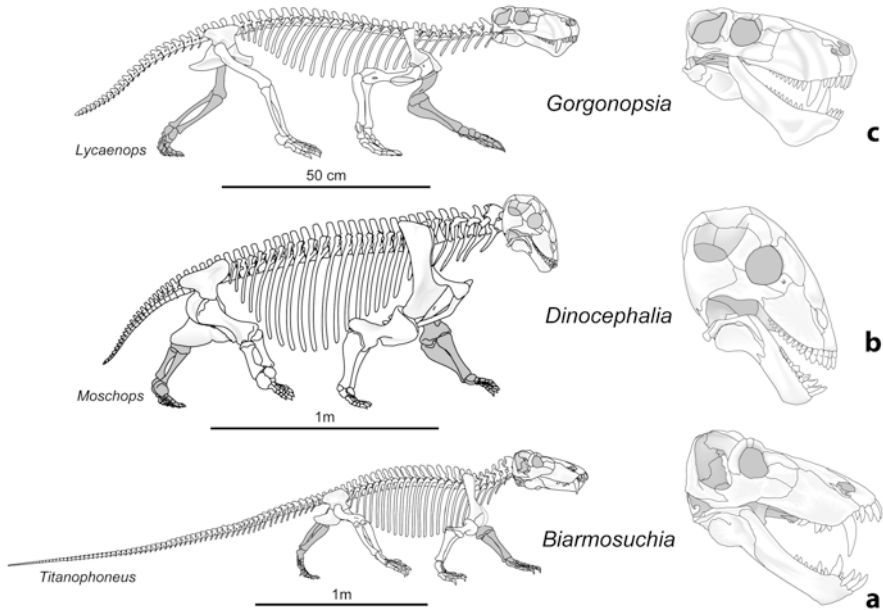


Fig. 10.11 Skulls and skeletons of Late Permian basal therapsids. (a) *Titanophoneus*, (b) *Moschops*, and (c) *Lycaenops*, drawn to the same lengths. (Modified after Rowe 2020a)

2006). The orbits are more frontal in orientation, with an increased field of binocular stereoscopic vision focused in front of the nose and mouth, a characteristic of terrestrial mammalian predators (Walls 1942).

An important new character state in basal therapsids involved their mode of tooth implantation. In the ‘pelycosaur-grade’ stem-mammals, the teeth had shallow implantation and were ankylosed to the jaws. In early therapsids the roots were elongated and held in deep alveoli by the periodontal ligament or ‘gomphosis’ (Osborn 1984; Gaengler and Metzler 1992; Rowe 1993, 2020a; Kemp 2005; LeBlanc et al. 2018). The roots and innervated periodontal ligament signal a new role for neural crest cells in the head that would eventually have a profound impact on mammalian neurosensory systems at multiple levels of organization (Hall 2009). Initially, the dental gomphosis provided a cushion to resist the compressive and shear forces associated with biting (LeBlanc et al. 2018). It would eventually become highly innervated and a key innovation in the evolution of an occlusal dentition and food mastication (see *Cynodontia*, below).

In the mandible, the reflected lamina of the angular is deeply incised along its dorsal margin, and probably now functioned as a tympanum. However, it remained attached to the mandible along with several other bones in the sound transduction pathway, and any transmitted vibrations had to cross the craniomandibular joint to reach the inner ear. Bones of the middle ear chain had a new measure of individual movement but the sacculus remained little more than a shallow depression (Olson 1944).

An important visual characteristic of living mammals that must have evolved along the mammalian stem involves their manner of eye movement. While the origin of this behavior cannot be pin-pointed, it is expeditious to mention it here. Gordon Walls describes it as follows: “in the matter of eye movements, mammals are at once set off from all other vertebrates by the fact that whenever voluntary movements are possible at all, the two eyes are never independent but are always conjugated. This universal conjugation is associated with the fact that mammals (whales, rabbits, and some others excepted) examine things only binocularly – even the bats, small rodents, insectivores, and other nose- or ear-minded nocturnal forms whose eyes never move even reflexively. Where the eyes are placed laterally as in the rabbits, there usually is no area centralis, let alone a fovea, and there are no spontaneous movements at all. But even the rabbits have the gyroscopic reflex eye movement, including the optomotor reaction. These compensatory movements in mammals are always most extensive in the plane of greatest biological usefulness, which usually means horizontal. The voluntary eye movements of mammals are really best correlated with visual acuity, which, it so happens, does go pretty well with intelligence in this group of vertebrates” (Walls 1942: 310–311).

The early therapsid neck became longer and more flexible, increasing mobility of the head and expanding horizons of the special senses. Basal therapsids had six cervical vertebrae, but soon settled on the seven cervicals almost invariably present in mammals. The mammalian vestibular system helps direct muscles of the neck that are responsible for reflexive compensatory movements of the head and eyes that keep a stereo visual image stable and in focus as the head is otherwise jostled in walking and running (Walls 1942). Maintenance of these reflexes may explain the invariance in number of cervical vertebrae in mammals. We can only speculate that this vestibular feedback traces to early therapsids.

A surprising claim reported that the basal therapsid *Kawingasaurus fossilis* has an endocast with an EQ that overlaps with the lower range of crown *Mammalia* and preserves evidence of a ‘neocortex-like structure’ (Laaß and Kaestner 2017). *Kawingasaurus* is a member of the extinct Permo-Triassic stem-mammal side branch *Dicynodontia*, and is interested within its highly specialized fossorial clade *Cistecephalidae* (Cluver 1978). The labeled CT imagery that accompanied this report reveals a fundamental misinterpretation of the bones of the braincase. For example, the structure identified as the ethmoid (Laaß and Kaestner 2017, figs. 2a,b,c,e) is actually the orbitosphenoid, and demonstrates unequivocally a narrow cylindrical forebrain just as in other dicynodonts (e.g. Cluver 1971) and basal therapsids (Rowe et al. 1995; Benoit et al. 2016; Crompton et al. 2018).

In basal *Therapsida* the vertebral column became more robust and regionalized, and the limbs were longer with the elbows turned back and the knees turned forward. This marks a significant shift from the sprawling sigmoid vertebral propulsion of basal stem-mammals, toward more strident parasagittal gait with limbs playing a more forceful role in locomotion, enhanced aspirational breathing, and enhanced metabolic scope. This implies greater activity levels and more sustained high levels of neurosensory activity. Whether the earliest stem-mammals could run is doubtful, but basal therapsids almost certainly could, implying neurosensory

elaboration that sets them apart. Unexpected shape variation was recently documented in endocasts of some early extinct therapsid side branches (Benoit et al. 2016); however, none has obvious bearing on neurosensory events on the direct path to the origin of *Mammalia*.

10.4.2 Node 9: *Cynodontia*

Cynodontia (Rowe 2020e) (Fig. 10.3, node 9) arose in the Late Permian ~230 million years ago, and today it includes the 6399 species of extant mammals (Burgin et al. 2018), plus many extinct Mesozoic and Cenozoic side branches. Many unique features of the mammalian skeleton and neurosensory system trace to the first cynodonts, as well as the first of several successive reductions in body size that effected shifts in ecology and life history strategy with profound neurosensory consequences.

Early cynodonts (Fig. 10.12) manifest the first episode in pan-mammalian history in which the braincase became more fully ossified than in earlier stem-mammals. EQs are slightly higher in basal cynodonts (Benoit et al. 2016), and innovations in brain evolution can be qualitatively appreciated in modifications of the osteocranium in its epigenetic responsiveness to brain development (Rowe 1996a, b; Fabbri et al. 2017). The posterolateral braincase walls became more fully ossified by ventral sheets from the frontal and parietal, and an anterior lamina from the prootic. Most important was the ‘newly formed’ alisphenoid bone. Long thought to be an expanded epipterygoid, it arose as a compound element joining the embryonic ala temporalis (footplate) of the epipterygoid with a new, membranous ossification induced within the spheno-obturator membrane (Presley 1981; Gauthier et al. 1988a). The alisphenoid is thus a compound element. Its ‘new’ portion is induced by expansion of the caudolateral pole of the olfactory cortex in most living mammals (Rowe 1996a, b; Rowe and Shepherd 2016). Given the ontogenetic interdependencies of the different components of the olfactory system (above) this event may reflect the onset of expression of a larger set of OR genes.

In cynodonts a secondary palate appeared, separating the nasopharyngeal passageway from the oral cavity, and displacing the choana to the back of the mouth (Fig. 10.10e). It forms as shelves of the maxillae and palatines grow toward the midline and fuse together to provide a bony floor beneath the nasal capsule and nasopharyngeal passageway, and a bony roof over the oral cavity. An occlusal dentition arose at the same time (Crompton 1963, 1972, 1989; Kemp 2005; Rowe and Shepherd 2016). The new ability to masticate food items yielded faster, enriched caloric return, enabling higher activity levels. Mastication occurs at the posterior (distal) part of the tooth row, where the mandibular adductor musculature was reorganized to exert its greatest force. We may infer that the tongue also took on a new role using the secondary palate as a substrate against which to move food within the oral cavity toward the teeth for mastication (Crompton and Parker 1978). Oral breakdown of food prior to swallowing also enabled more thorough inspection and

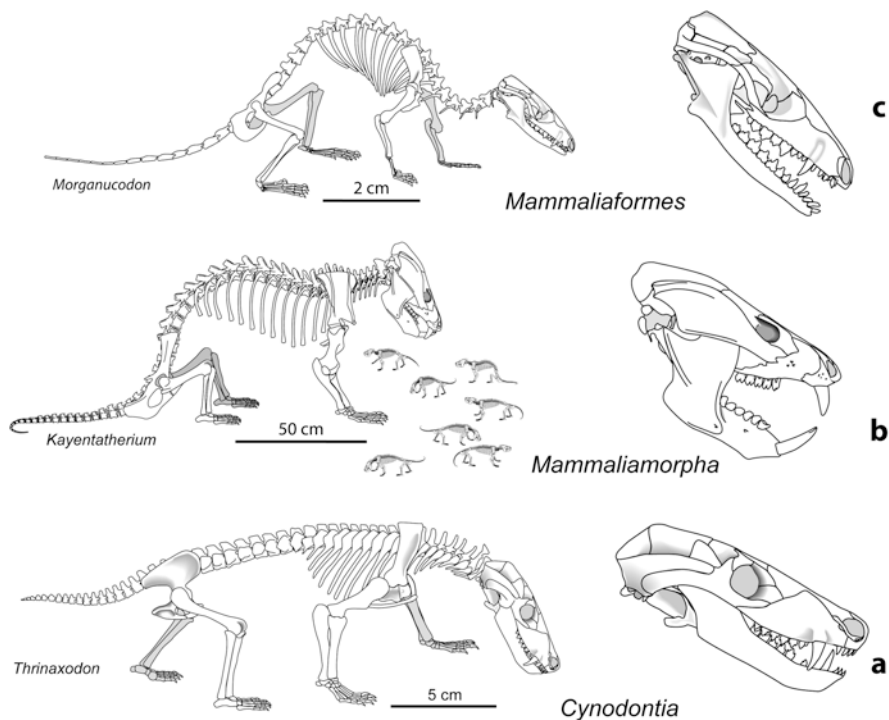


Fig. 10.12 Skulls and skeletons of Triassic basal cynodonts. (Bottom) *Thrinaxodon*; (Middle) *Kayentatherium* and its clutch of perinates; (Top) *Morganucodon*. Note the differentiation of thoracic and lumbar vertebrae, indicating presence of the diaphragm. (a, c modified after Rowe 2020a)

analysis of food items, and the ability to extract and process new kinds of information from food.

Early cynodont postcanine teeth had ‘triconodont’ crowns in which there are generally three principal cusps aligned longitudinally, with the middle cusp the tallest, and with a row of smaller cuspules on a narrow shelf at the base of the inner surface (Crompton 1963; Rowe 2020e; Rowe et al. 1995). Along the rear of the postcanine tooth row, the outer (buccal) surfaces of lower teeth occluded against the inner (lingual) surfaces of the upper teeth and produced irregular wear facets that are evidence of crown-to-crown occlusion (Fig. 10.13). A small degree of jaw rotation and a mobile symphysis facilitated occlusion, which was irregular at first, but eventually became intricately patterned. The rate of tooth replacement in early cynodonts was greatly reduced (Hopson 1971; Osborn and Crompton 1978). This initiated a new ‘variational modality’ involving unprecedented diversification of postcanine crown structure, function, and development that eventually enabled cynodonts to pierce, slice, dice, shred, and grind their food in ever more complex and efficient ways (Rowe and Shepherd 2016; Rowe 2020a). Up to this point, stem-mammal teeth were not subject to much variation, but in cynodonts almost every species has cheek teeth with its own diagnostic crown structure.

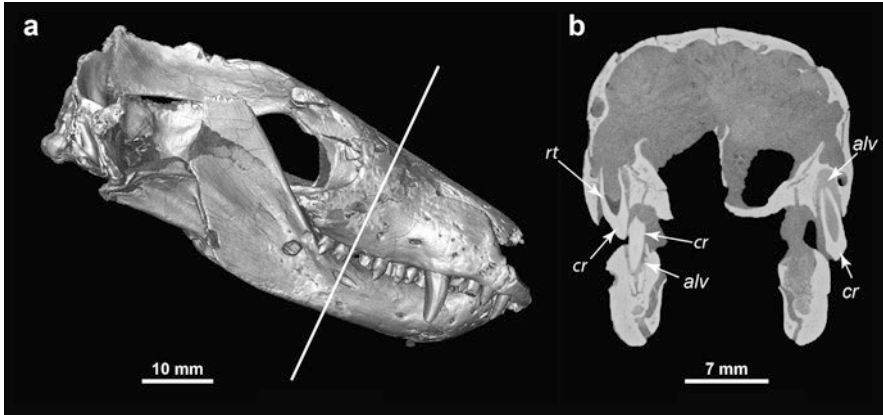


Fig. 10.13 CT cross-section through the snout of the early Triassic cynodont *Thrinaxodon*, showing the deep implantation of postcanine teeth (*Therapsida*) as well as the occlusal relationship between upper and lower teeth (*Cynodontia*) on the right. (a) lateral view of skull (reconstructed from CT slices using VGStudio Max) showing slice plane (b), a coronal slice through the snout. See anatomical abbreviations

The cynodont dentition eventually assembled into a new peripheral sensory array of considerable anatomical and neural complexity (Fig. 10.14), thanks in large part the ‘gomphosis’ mode of tooth implantation inherited from more basal therapsids, and to greatly reduced rates of postcanine replacement (Hopson 1971; Osborn and Crompton 1978). Ontogenetic malleability of the periodontal ligament enabled tooth crowns to establish precise occlusal relationships during eruption (Ten-Cate 1969, 1997). The cynodont periodontal ligament eventually became richly innervated, affording a considerable degree of learning and memory about food items during mastication. Recordings from single nerve fibers demonstrated that human periodontal receptors adapt slowly to maintained tooth loads (Trulsson 2006; Trulsson et al. 2010). Most receptors are broadly tuned to the direction of force application, and about half respond to forces applied to adjacent teeth. Information about the magnitude of tooth loads is made available in the mean firing rate response of periodontal receptors, and they precisely record intensity and spatiotemporal aspects of forces applied to a tooth. These mechanoreceptors are particularly important when biting and chewing because they efficiently encode tooth loading during intraoral food manipulation and are involved in jaw motor control and memory (Trulsson 2006; Trulsson et al. 2010).

In *Mammalia*, signals from periodontal mechanoreceptors project to separate oral fields of the primary somatosensory cortex (Remple et al. 2003; Kaas et al. 2006; Iyengar et al. 2007; Trulsson et al. 2010; Hlusko et al. 2011). Periodontal receptors encode information about the teeth stimulated and provide a detailed organizational map that adds representation of the dentition to the classic neocortical sensory animunculus (Kubo et al. 2008). There is also strong evidence for bilateral representation of the teeth into the primary sensory cortex coming directly from the

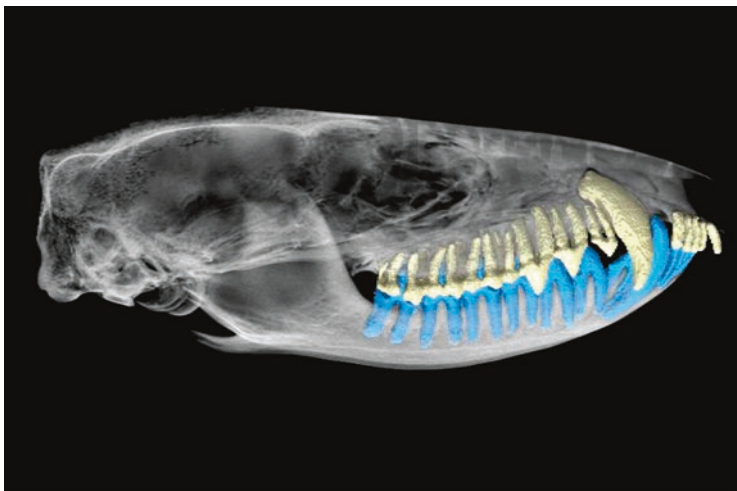


Fig. 10.14 Mature skull of *Monodelphis* reconstructed from CT data, with the bones of the skull rendered translucent, and the dentition opaque, to show the relationship of the dental array to the skull

thalamus or via transcallosal projections (Kaas et al. 2006; Iyengar et al. 2007; Habre-Hallage et al. 2014). Projections from the somatosensory oral cavity integrate cutaneous stimuli and movements of the tongue and jaws that are important for mastication and for the ability to recognize and discriminate the form of objects by using intraoral or perioral sensors. In the tongue, 80% or more of neurons are tactile, and 2–10% are taste receptors (Iyengar et al. 2007). The connections between the somatosensory representation of the teeth and tongue and adjoining motor and premotor representations of the oral cavity and jaw may help to coordinate motor control in chewing and swallowing (Iyengar et al. 2007), which becomes increasingly complex in the latest stem-mammals and *Mammalia* (Crompton 1989; Crompton et al. 2018).

Mastication plus a secondary palate liberated an entirely new class of odors and scents from food as it was chewed and broken down, and with this new behavior a new duality was introduced into the main olfactory system, known as ‘orthoretranasal olfaction’ (Fig. 10.15) (Rowe and Shepherd 2016; Rowe 2020a). The primitive behavior of inhaling external environmental odorant molecules through the naris into the mouth, known as ‘orthonasal’ olfaction, was inherited from early stem-tetrapods. They were the first vertebrates in which the nasal capsule had both an external opening, the naris (nostril), and the internal naris or choana which opened through its floor into the roof of the mouth (Jarvik 1942). The counterpart to orthonasal smell is ‘retranasal’ smell, in which air exhaled from the lungs carries an entirely new information domain of odor molecules liberated through the breakdown of food by chewing, saliva, and actions of the tongue. These molecules pass forward from the caudal part of the oropharynx and via the choana they cross the main olfactory epithelium before being expelled through the nares. Orthonasal

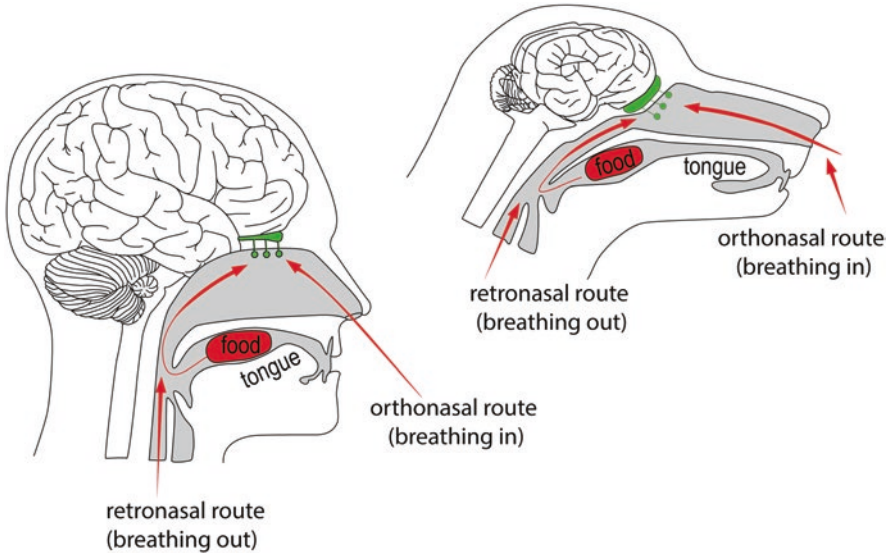


Fig. 10.15 Diagrammatic representation of orthonasal and retronasal olfactory modes in a dog and human. (Modified from Rowe and Shepherd 2016)

smell, retronasal smell, taste, and somatosensory signals from the lips, gums, cheeks, tongue and teeth passed along different pathways, but all eventually evolved convergence onto individual neurons in the neocortical area known as the orbito-frontal cortex that integrate the complex multisensory amalgam called ‘*flavor*’ (Shepherd 2004, 2006, 2012; De Araujo et al. 2003; Small et al. 2007; Rolls and Grabenhorst 2008; Rowe and Shepherd 2016; Rowe 2020a). The beginnings of this elaborate network trace to the first cynodonts, and its fullest measure of integration occurred as the orbitofrontal region of the neocortex emerged in *Mammalia* (below).

Also apomorphic of *Cynodontia* is the ‘double occipital condyle’ formed by the right and left exoccipitals positioned at the ventrolateral edges of the foramen magnum. This double articulation expanded the range of stable excursion of the head without impairing passage of an enlarged spinal cord through the foramen magnum (Jenkins Jr. 1969, 1971). The ventrolateral position of the condyles and orientation of the semicircular canals (Berlin et al. 2013; Ekdale 2016) also suggest that the head was habitually held at a tilt with the nose toward the ground.

Separate thoracic and lumbar regions were differentiated such that ribs that encircle the thorax persist anteriorly, while the posterior three to five ribs form attenuated processes that fuse to their respective neural arches (i.e. lumbar ribs). Differentiation of separate thoracic and lumbar regions (Fig. 10.12) marks more symmetrical axial movement during locomotion, and the development of a muscular diaphragm, separating the thoracic and abdominal cavities, and a far more complete decoupling of aspirational breathing from locomotion. The vacuum-chamber or bellows-like tidal diaphragmatic ventilation of *Mammalia* allows ventilation while moving or at rest, and a sustained supply of oxygen to the brain for greater

activity levels (Jenkins Jr. 1971; Gauthier et al. 1988a; Hirasawa and Kuratani 2013; Brainerd 2015). We may speculate that it brought the onset of new olfactory-mediated behaviors such as territorial scent-marking, the rapid sniffing behavior that drives scent tracking (Rowe and Shepherd 2016) and, more speculatively, reproductive behaviors related to parental care of the young.

10.4.3 Node 11 (*Unnamed*)

Node 11 is the unnamed clade stemming from the last common ancestor that *Mammalia* shares with *Diademodon* (Fig. 10.3, node 11). It is diagnosed by further elaboration of the molariform (postcanine) tooth roots, in which each cheek tooth crown has an ‘incipiently divided’ root. That is, there were two separate root canals, each conveying its own dental nerve to the pulp cavity, but a web of bone still connected the roots. This ‘incipient’ division of the roots occurred in Early and Middle Triassic cynodonts, and suggests they were mining more information in the differential loading of individual tooth crowns in mastication of different food types.

10.4.4 Node 12: *Probainognathia*

Probainognathia designates the clade stemming from the last common ancestor shared by the mid-Triassic *Probainognathus* and *Mammalia* (Fig. 10.3, node 12). EQ values in basal probainognathians are about the same as in more basal cynodonts (Quiroga 1979, 1980, 1984, Macrini 2006; Rowe et al. 2011; Benoit et al. 2016). However, EQ values fail to reveal what may be deeper insights into brain evolution based on other features of the endocasts (Wallace 2018).

In early probainognathians (Fig. 10.16) the endocast is more ‘brain-like’ than before, in that it is robustly ‘inflated’ against the braincase walls and embossed into them more vivid details of its external shape. Basal probainognathian endocasts convey the general impression of a much more strongly inflated brain very tightly packaged within a container whose proportions are constrained by competing functions of the skull such as supporting the masticatory system, in the type of relationship demonstrated by Weisbecker et al. (2021) in living and fossil marsupials. We may speculate that this is a time in stem-mammal evolution when the increased numbers and tighter packing of telencephalic neurons progressed, foreshadowing the cellular architecture that became characteristic of mammalian neocortex (Rubenstein and Rakic 1999; Rakic 2000, 2007, 2009; Molnár and Butler 2002; Shepherd and Rowe 2017).

The olfactory bulbs are larger and more distinctly separated by an encircling annular fissure from the rostral end of the cerebral hemispheres. The caudolateral poles of the olfactory (piriform) cortex diverge laterally to a greater degree than in basal cynodonts, and are now approximately as wide as the cerebellum. The

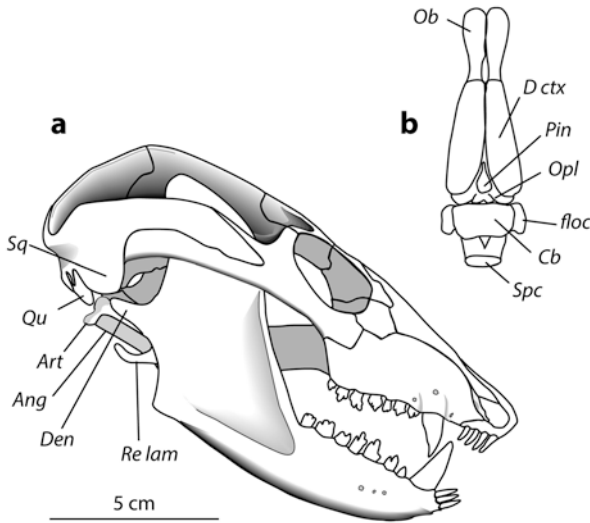


Fig. 10.16 Reconstructed skull of the Triassic cynodont *Probainognathus* (a) in lateral view, and (b) reconstructed dorsal view of its endocranium. Note that the dentary and squamosal are in very close approximation. (a: Modified after Romer 1970; b: Modified after Quiroga 1980). See anatomical abbreviations

forebrain was still long and narrow, but for the first time the interhemispheric sulcus is clearly visible on the endocranium, and the cerebral hemispheres are convex and high-domed. Basal probainognathians retain the plesiomorphic absence of an osseous enclosure around the lateral and ventral surfaces of the olfactory bulb and the cerebrum behind the orbitosphenoid (Crompton et al. 2017b), and there remains a measure of subjectivity in reconstructing the complete endocranium (Kemp 2009). To be clear, early probainognathians retained primitive endocrania when compared to even the least-encephalized mammal. But from enlarged olfactory bulbs and olfactory cortex, and doming of the dorsal cortex, it seems likely that another increase in expression of duplicated olfactory receptor genes had begun, that olfaction was exerting a far more dominant influence than ever before, and perhaps a new threshold in organization not revealed by the uncertainties in EQ estimates had been crossed. In any event, probainognathian cynodonts with approximately this general state of cerebral organization underwent a significant diversification during the Triassic.

The bones of the jaw lying behind the tooth-bearing dentary are considerably reduced, marking the onset of their negative allometric growth with respect to the skull and mandible (Rowe 1996a, b), and their increasing individuation as components of the auditory chain of the middle ear in a trend toward higher-frequency sound sensitivity.

10.4.5 Node 14: *Mammalia* *morph*

Mammalia (Rowe 1988, 2020f) is the clade stemming from the most recent common ancestor *Mammalia* shares with the extinct side branch *Tritylodontidae* (Fig. 10.3, Node 14, Fig 10.10g) (Kemp 1983; Rowe 1988). *Mammalia* arose ~230 million years ago, diversified into a number of extinct side branches across Pangea in the Late Triassic thru Middle Jurassic. There are several extinct Triassic to Early Jurassic side branches that may lie just within or just outside of *Mammalia*, but all share endocasts comparable in most respects to more basal probainognathians (Quiroga 1979, 1980, 1984; Benoit et al. 2016; Rodrigues et al. 2013, 2014, 2019; Wallace 2018; Hoffmann et al. 2019; Pavanatto et al. 2019). These include several taxa referred to as ‘brasilodonts’ (Bonaparte et al. 2005, 2013), a group of uncertain monophyly, *Trithelodontidae* (Martinelli and Rougier 2007; Sidor and Hancox 2006), and *Pseudotherium argentinus* (Wallace et al. 2019).

Further reduction in body size may have arisen in basal mammaliaforms (the last common ancestor of *Mammalia* unequivocally very small; Rowe 1988, 1993, 2020a; Rowe and Shepherd 2016). The most basal tritylodontid is probably *Oligokyphus* (Clark and Hopson 1985), and its shrew-sized body is about the same size as *Morganucodon* and other early mammaliaforms (Fig. 10.17). Miniaturization was attained in part by accelerated maturation of the skeleton at smaller and smaller sizes (Koyabu et al. 2014; Hoffman and Rowe 2018). Numerous descendant clades secondarily attained large body sizes, but most mammaliaforms remained tiny from the Late Triassic until after the origin of crown *Mammalia*. Miniaturized mammaliaforms encountered greater spatial and environmental heterogeneity than their larger ancestors. Entry into new microhabitats promoted dietary diversification, where new food items such as seeds, grains, fungi, small fruiting bodies, and small invertebrates were available for the first time, altering activity patterns and life history strategies (Harvey et al. 1980; Eisenberg 1990; Mace et al. 1981; Hayden et al. 2010). The mammaliaform postcanine teeth now have two or more fully divided roots, each with its own dental canal and nerve, and molariform crowns occluded in complex patterns. Molariform teeth were not replaced, and their permanence potentially enabled the subtle textural information from different kinds of

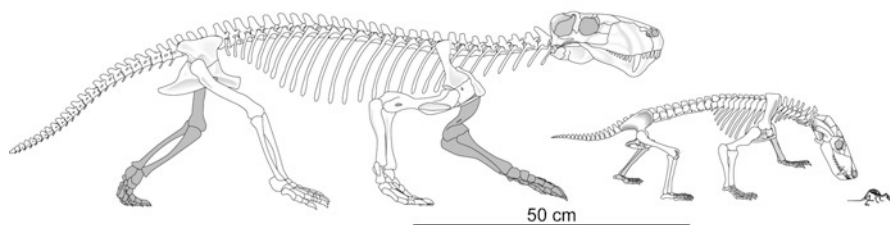


Fig. 10.17 Skeletons drawn to scale of *Lycaenops* (a Late Permian basal therapsid), *Thrinaxodon* (an Early Triassic basal cynodont), and *Morganucodon* (a late Triassic basal mammaliaform) showing the reduction in body sizes towards miniaturization. (From: Rowe and Shepherd 2016)

food to be learned and remembered to an increasing degree. Miniaturization involved greater excursion of the limbs and increased agility moving over complex three-dimensional habitats, implying muscle spindles and joint proprioceptors that were recording more information produced by the greater ranges of movement than before. Agile scampering and climbing were now added to the locomotion repertoire of the mammalian stem group (Kemp 1983, 1988, 2005; Rowe and Shepherd 2016; Rowe 2020a).

Early mammalian morph endocasts are generally similar to basal probainognathians. However, the pineal stalk was covered by rapid ontogenetic expansion of the cerebral hemispheres over the midbrain to contact the cerebellum, and the pineal foramen closed. Forebrain expansion may be reflected in ossification of the orbital wall by joined sheets of the frontal and palatine bones (Rowe 1988). The cerebellum has a distinguishable vermis and left and right cerebellar hemispheres bulge on either side (Wallace 2018), but this is probably more a consequence of packaging (Weisbecker et al. 2021) than functional differentiation. In basal mammalian morphs, the internal auditory meatus is walled medially with separate foramina for the vestibular and cochlear nerves (Kemp 1983; Rowe 1988), and the cochlea underwent a first pulse in elongation, in some cases also curving over an arc of about 70° and suggesting greater sensitivity to a wider range of high frequencies (Luo et al. 2001, 2004; Kielan-Jaworowska et al. 2004; Rodrigues et al. 2013, 2019; Wallace et al. 2019). The angular is now nearly circular, and almost certainly held a tympanic membrane although it was still anchored to the mandible.

A μ CT study of the stem-mammalian morph *Brasilitherium* (Rodrigues et al. 2014) reported small ossifications in the nasal capsule that were interpreted as primordia of the nasoturbinal and the first ethmoturbinal, which support olfactory epithelium (Rowe et al. 2005). The posterior nasal septum is partly ossified and contributes to an ossified mesethmoid, which also supports olfactory epithelium in mammals. In addition, the nasal cavity expanded posteriorly forming a distinctive ethmoidal recess separated ventrally from the nasopharyngeal duct by an ossified lamina terminalis. Similar structures were reported in the nasal chamber of the closely related mammalian morph *Pseudotherium* (Wallace et al. 2019), and possibly in tritylodonts (Kielan-Jaworowska et al. 2004). A primitive, relatively simple skeleton of ossified turbinals in fossils near the mammalian crown should not be surprising. However, in these two cases, the ossifications are very small and are not co-ossified to the wall of the nasal chamber, and other discernible features of the olfactory system leave uncertainty about their identity. Wallace (2018) pointed out that the reconstructed olfactory bulb in *Brasilitherium* seems excessively large and there is no corresponding expansion of the olfactory cortex. In her study of *Pseudotherium*, Wallace reconstructed a more conservative flat floor beneath the preserved impressions of the olfactory bulb, reducing endocranial volume by 15%, which placed it within the range of other basal mammalian morphs. Applying a similar correction to *Brasilitherium* reduces its endocranial volume into the same cluster. In either case, we may be seeing another incremental increase in expression of OR genes.

Paleontologists have long speculated about whether there may have been an extensive network of cartilaginous turbinals in non-mammalian therapsids (e.g. Brink 1957; Hillenius 1992, 1994; Crompton et al. 2017b). As noted, olfactory gene expression initiates cascading ontogenetic interdependencies of olfactory epithelium surface area, ethmoid turbinal surface area, total area of foramina in the cribriform plate, olfactory bulb size, and olfactory cortex size. The individual components of the olfactory system offer general proxies for the system as a whole (Bird et al. 2018; Garrett and Steiper 2014; Hayden et al. 2010; Pihlström et al. 2005; Rowe et al. 2005; Rowe and Shepherd 2016; Schlosser 2010). However, it is important to recognize that turbinals do not exist as separate parts independent of the rest of the olfactory system. The recent data from endocasts suggests that the degree of olfactory development in basal cynodonts and early mammaliomorphs was still insufficient to induce an extensive scaffold of rigid support that approaches the degree in *Mammalia*, and the olfactory bulb and olfactory cortex remained relatively small. Moreover, at no time in mammalian ontogeny is there a free-standing extensive network of cartilaginous turbinals in any known mammal (Rowe et al. 2005). Nothing within the ‘extant phylogenetic bracket’ offers support for the hypothesis of an expansive network of cartilaginous turbinals in any stem-mammal. Nevertheless, as imaging technologies improve and larger samples of fossils are scanned, more compelling evidence may yet materialize to document intermediate states in the evolution of an ossified scaffold in late stem-mammals.

In another study based on μ CT, Benoit et al. (2016) reported in tritylodontids that the maxillary canal carried the “true” infraorbital nerve and that it supplied vibrissae and a mobile rhinarium. These claims are doubtful because evidence of the other parts of the system to which they communicate is absent. Whiskers and the rhinarium are both parts of the cutaneous field of the trigeminus that develops in mammals in close association with the differentiation of complex facial muscles and a system of intricate circuitry with corresponding representations in the somatosensory area of neocortex, and outputs to the motor cortex (Huber 1930; Grant et al. 2013). Moreover, whiskers are not universally present in therian mammals (Catania and Catania 2015), and ancestral state reconstruction suggests that they evolved independently as many as seven times among therians (Muchlinski et al. 2020) and were never present in monotremes (Huber 1930). Whiskers and the rhinarium are inevitably linked to large numbers of efferent nerve axons, a much thicker infraorbital nerve and an considerably enlarged infraorbital foramen (Muchlinski 2008; Muchlinski et al. 2020). No such enlargement occurs in the “infraorbital canal” illustrated by Benoit et al. (2016). Presence of a mobile rhinarium can probably be dismissed in all stem-mammals because they retain the ossified internasal (prenasal) process of the premaxilla (Rowe 1988, 1993). This process was lost in mammals ancestrally, and a rhinarium seems to have appeared for the first time in therian or stem-therian mammals, along with fully differentiated facial muscles (Huber 1930) associated with a wide repertoire of learned orofacial motor skills (below). Developmental evidence suggests that monotreme facial musculature was apomorphically derived from the ancestral amniote sphincter coli and platysma muscles, and that a limited degree of facial muscle differentiation probably reflects the

ancestral state for mammals (Huber 1930; Lightoller 1942). In light of the discovery that a pelt of modern aspect was present in basal mammaliaforms (below), it is conceivable (if speculative) that a primitive cover of innervated hair was present in basal mammaliomorphs. However, the sophisticated cortical barrels that map sensations from whiskers, and other neocortical areas that map sensory stimuli from whiskers, rhinarium, and their associated facial musculature requires cortical computing power for which there is no evidence at this point in stem-mammal evolution.

10.4.6 Node 15: *Mammaliaformes*

Mammaliaformes is the clade stemming from the last common ancestor that *Mammalia* shares with *Morganucodonta* (Rowe 1988, 2020g) (Fig. 10.3, Node 15). It arose by ~210 million years ago, diversified into a number of extinct side branches across Pangea in the Late Triassic thru Middle Jurassic, and *Mammalia* arose within it by ~170 million years ago. The most striking feature of early mammaliaforms is that their brains had almost doubled in relative size compared to basal mammaliomorphs, and the endocast is strongly ‘inflated’ and now looks very much like a mammalian brain (Figs. 10.18 and 10.19). Using the Eisenberg (1981) equation, the EQ of non-mammaliaform cynodonts was found to range from ~0.16 to 0.23, whereas the EQ of *Morganucodon* is ~0.32, reflecting an increase of 30–50% over basal cynodonts (Rowe et al. 2011). The olfactory bulb and olfactory cortex are by far the regions of greatest expansion. A deep annular fissure encircles the olfactory tract, marking a distinctive external division of the brain between the inflated olfactory bulbs and the cortex. The cerebellum is also enlarged, implying expansion of the basal nuclei, thalamus, and medulla.

The dentition evolved a more complex occlusal pattern. The diphyodont pattern of tooth postcanine tooth replacement characteristic of mammals seems unequivocally established at this point in stem-mammal phylogeny, if not arising earlier in basal mammaliomorphs (Cifelli et al. 1996; Luo et al. 2004). The evolution of non-replacing molars marks a landmark in dental function, learning, and memory. Trulsson et al. (2010) compared the responses to tooth stimulation with those produced by identical vibrotactile stimulation of fingers. The results suggest that the periodontal ligament mechanoreceptors in living mammals play a significant role in specifying forces used to hold and manipulate food between teeth, and in these respects the masticatory system appears analogous to fine finger-control mechanisms used during precision manipulation of small objects. Their fMRI studies revealed activations in posterior insular cortex, leading them to speculate that the dentition, via the periodontal ligament mechanoreceptors, are involved in an important aspect of the feeling of body ownership (Trulsson 2006; Trulsson et al. 2010).

A pelt of modern aspect, with guard hairs and velus underfur, was discovered in the exceptionally preserved *Castorocauda lutrasimilis* (Ji et al. 2006), a late-surviving non-mammalian member of *Mammaliaformes* from the Middle Jurassic (~165 million years old) of China. Hair follicles have been called ‘dynamic

another pulse in encephalization that raised its EQ to ~ 0.5 , a level within the range of crown mammals (Rowe et al. 2011). This reflects a further increase in relative size of olfactory bulbs and olfactory cortex. Its cerebellum also expanded to such a degree that the occipital plate bulges backwards, where it enclosed a relatively large foramen magnum and thick spinal cord, and possible evidence that the corticospinal tract had emerged.

10.4.8 Node 17: *Mammalia*

Far more justifiable inferences can be made regarding the ancestral species of *Mammalia* because we have two major living sister lineages to compare, and thus their most recent common ancestor lies within the ‘extant phylogenetic bracket’ (Rowe 1988, 2020b; Witmer 1995). The fossil record indicates that *Monotremata* (Rowe et al. 2020) and *Theria* had diverged by or before the Middle Jurassic, ~ 170 million years ago (Rowe 1988, 2020a). Perhaps the most remarkable feature in all of pan-mammalian history is the emergence of six-layer neocortex from the three-layer dorsal cortex of amniotes ancestrally, and with it arose the uniquely diverse cognitive and behavioral abilities of mammals (Harris and Shepherd 2015; Rowe and Shepherd 2016; Shepherd and Rowe 2017; Rowe 2020a).

The rhinal fissure is an anatomical boundary between dorsal neocortex and lateral olfactory cortex that is clear in histological samples, and when visible in endocasts it demarcates the two regions. However, in small mammals the meninges are sufficiently thick that they often prevent the inner wall of the parietal from forming a ridge that enters the fissure; the rhinal fissure can be present in life, but not represented in an endocast. In other words, there is no unambiguous anatomical marker for neocortex in endocasts from stem-mammals and many crown mammals. However, histological studies of brains in monotremes (Ashwell 2013) and therians (Ashwell 2010) indicate neocortex is present in both, and its inferred presence in mammals ancestrally is unequivocal.

As noted, the three layer dorsal cortex of basal amniotes functions as an associative network of higher level functions and, over the course of stem-mammal evolution, six-layer neocortex emerged as a further elaboration of this network that enhanced computationally more demanding functions involving multidimensional perceptions, memory, planning, and execution (Shepherd and Rowe 2017). The extinct taxa *Morganucodon* and *Hadrocodium* closely approached and then overlapped the lower range of EQ in *Mammalia* (Fig. 10.20); if neocortex emerged prior to the origin of crown *Mammalia*, it was more likely present in basal *Mammaliaformes* than in more distant stem-mammals.

The computational power of neocortex derives in part from its subdivisions within and across layers into functionally distinct and specialized regions known as ‘fields’ or ‘areas’, and independent elaboration in numbers of neocortical areas is characteristic of different mammalian clades in association with independent evolutionary increases in encephalization (Kaas 2009, 2020). The outputs from cortical

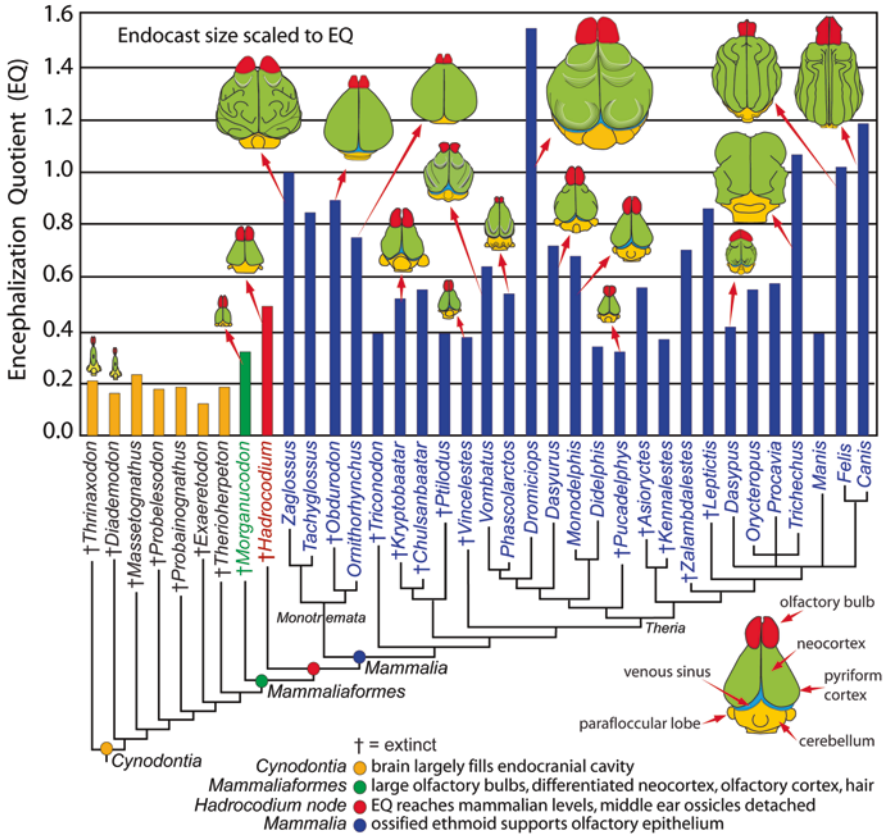


Fig. 10.20 Patterns of brain evolution in phylogeny of basal Triassic cynodonts and selected crown Mammalia. Encephalization Quotient (EQ) is shown as a histogram, and selected endocasts are scaled to EQ. (From Rowe et al. 2011)

areas provide input to other cortical areas where computational functions are reiterated. The increased numbers of cortical areas increase the numbers of computations that are possible, resulting in more sophisticated computations overall (Kaas 2009, 2020; Krubitzer and Hunt 2009). Reconstructing the number and types of areas present in the ancestral mammal is problematic in that most studies have focused on a few model species, and appropriate comparisons between monotremes and therians are limited. That said, estimates are that the ancestral mammal probably had ~20 neocortical areas, including a primary (S1) and secondary (S2) somatosensory areas, and possibly three or four others; primary (V1) and secondary (V2) visual areas, and perhaps one or two others; a primary auditory area (A1), and possibly a second area; a primary motor area (M1); and other areas of limbic, orbitofrontal, and endorhinal cortex (Kaas 2009, 2020; Krubitzer and Hunt 2009; Molnár et al. 2014). The general trend is for larger brains to have more cortical areas, and as many as 200 areas have been tentatively identified in humans (Kaas 2013).

At the cellular level, the pyramidal neuron populations are greatly expanded compared to other tetrapods, and their cell bodies are densely packed in the six-layered neocortex (e.g. Kaas 2009; Molnár et al. 2009). Moreover, during the course of pan-mammalian evolution the basic pyramidal cell present in the ancestral amniote diversified into four main types that lie at different layers in the six-layered neocortex (Shepherd and Rowe 2017). Migration of neuron precursors along radial glial columns generate its columnar organization and increased neocortical thickness (Rakic 1988, 2000, 2007, 2009). Neocortical organization is broadly similar between cortical areas and between species, leading to the idea of a ‘canonical microcircuit’ that employs a similar computational strategy to process multiple types of information (Shepherd 2011; Harris and Shepherd 2015). As the OR genome increased by more than an order of magnitude over the ancestral amniote, and the repertoire of perceptible odorants increased exponentially, the number of microcircuits in the olfactory bulb and olfactory cortex increased correspondingly (Shepherd et al. 2021). The expanded numbers of nuclei in the dorsal thalamus of amniotes (Butler and Hodos 2005; Nieuwenhuys et al. 1998) was carried to extreme degrees in mammals in association with the proliferation of specialized neocortical areas.

In the three-layer dorsal cortex of basal amniotes, peripheral afferent projections to the dorsal and olfactory cortex coursed over the outer layer, while efferents projected from the inner layer to other parts of the brain and body. In mammalian neocortex, peripheral afferents may reach multiple layers of neocortex, efferents may be intratelencephalic projections, corticothalamic projections, or corticospinal projections, effecting a fundamental reorganization of connectivity to, from, and within the primitive three-layer dorsal dorsal cortex (Shepherd 2011; Shepherd and Rowe 2017). In all amniotes, projections from the dorsal cortex innervate the basal ganglia and brainstem, but in mammals (possibly originating in basal *Mammaliaformes*), neocortical projections can pass directly into the spinal cord as well, forming the unique corticospinal (pyramidal) tract. The uniqueness of neocortex involves not only the elaboration of inherited associative networks, but also new connections through the corticospinal tract that give higher neocortical functions direct access to virtually the entire neuraxis (Shepherd and Rowe 2017).

Ossified Ethmoid Complex

Ossification of an elaborate skeleton of ethmoid turbinals occurred by or before the origin of *Mammalia*. Its beginnings probably extend to early mammaliomorphs or even more basal cynodonts, but so far the evidence in fossils remains open to interpretation (above). The turbinal skeleton in *Mammalia* afforded a 10-fold or greater increase in the surface area of olfactory epithelium that could be deployed inside the nasal cavity (Rowe et al. 2005). The ethmoid turbinals coalesce around the olfactory nerve fascicles to form the bony cribriform plate, a compound structure that separates the olfactory recess from the cavum cranii. The turbinals grow rostrally from the cribriform plate as the olfactory epithelium matures, and their mature geometry

is highly variable among mammals (Rowe et al. 2005; Macrini 2012, 2014). Also ossifying in the nose is the maxillary turbinal (Fig. 10.7), which increases the epithelial surface area by nearly an order of magnitude that is involved in regulating respiratory moisture and heat exchange, (Taylor 1977; Van Valkenburgh et al. 2004; Rowe et al. 2005; Green et al. 2012).

The Mammalian Middle Ear

An extraordinary morphogenic consequence of the expanded olfactory cortex in *Mammalia* is that the auditory chain was disrupted during ontogeny, and those ossicles directly involved in the auditory chain were detached from their ancestral and embryonic position on the mandible, relocated a short distance behind the mandible, and suspended exclusively from beneath the braincase during early ontogeny as the brain grows in circumference (Rowe 1996a, b). The result is that the middle ear was more sensitive and receptive to an extended range of high frequency sound. This left the dentary as the sole element of the mandible in mature *Mammalia*. Other mechanisms have been hypothesized, and whether detachment is a unique autapomorphy of *Mammalia*, or *Mammalia* plus *Hadrocodium*, or if it represents wide spread convergent evolution among stem-mammals is controversial (Rowe 1988, 1996a, b; Wang et al. 2001; Bever et al. 2005; Luo 2007; Ji et al. 2006; Meng et al. 2006).

Suspension of the middle ear from beneath the cranium offered the mammalian middle ear enhanced sensitivity, and possibly also an extended range of high frequency sound perception. In *Mammalia*, the cochlea added a bony lamina which supports the basilar membrane and two distinct types of hair cells. Inner hair cells located along the central axis of the cochlea carried efferent signals to cochlear nuclei, as before. But outer hair cells receive efferents from the brain that are thought to amplify sound induced vibrations of the basilar membrane, and in the rodent in which it was first reported, at least, this make the inner hair cells more responsive to sound by a factor of ~100 times (Ren et al. 2011; Streidter and Northcutt 2020). It is doubtful that this degree of amplification was present in the ancestral mammal, since its cochlea was still short, and it surely became a more potent factor in therian mammals that have a long coiled cochlea.

Orofacial Motor Skills

Cynodont mastication eventually became linked to a complex of novel orofacial muscles and behaviors involving diverse orofacial motor skills including learned orofacial movements in suckling, chewing, and swallowing (Crompton et al. 2018). Such behaviors were long attributed to brain stem circuits, but it is now apparent from anatomical, electrophysiological imaging, and behavioral studies of the facial sensorimotor cortex in mammals that the face primary motor cortex and the face primary somatosensory cortex make important contributions to the control of these

learned movements (Avivi-Arber et al. 2011). Hence, the new function of mastication would eventually be reflected in a large neocortical presence, but these were much later developments that arose within *Mammalia* and carried to their extreme in therians (Rowe 2020a).

Spinal Cord

A double-occipital condyle arose in basal *Cynodontia*, and in *Mammalia* the condyles expanded to surround the entire ventral half of the foramen magnum. Correspondingly, the mammalian atlas, or first vertebra, is highly distinctive in forming a bony ring through ontogenetic fusion of the three separate ossification centers (centrum, right & left neural arches) that had remained separate throughout life in all stem-mammals. The limbs and girdles develop secondary ossification centers, the most obvious of which are the cartilaginous epiphyses of the long bones. Sesamoid bones form in tendons of the flexor muscles of the hands and feet, and in the hindlimb a single large sesamoid forms the patella (Rowe 1988, 1993). These modifications correlate with increased thickness and regionalization of the spinal cord, owing in part to the advent of the corticospinal tract, and to increased agility to which the sesamoid bones may contribute.

Nocturnality

A popular interpretation is that early mammals and mammaliaforms were nocturnal (e.g. Kermack and Kermack 1984). There is no evidence in extant mammals of RhB/Rh2 opsin genes, which must have been lost somewhere along the mammalian stem. Further reductions in opsin genes occurred in different clades within crown *Mammalia*, where the SWS1 opsin gene became dysfunctional in monotremates, while the SWS2 opsin gene was lost in therians (Collin 2010, Jacobs 2009, 2013; Wakefield et al. 2008). Thus, as Walls (1942) surmised, the ancestral mammal may have been diurnal with trichromatic vision, and that dichromatic crepuscular to nocturnal behaviors in monotremes and therians evolved independently (with a gene duplication restoring trichromatic vision to some primates). The sclerotic ossicles were also lost in *Mammalia* (or perhaps *Mammaliaformes*) ancestrally, allowing the eyeball to become nearly spherical (Walls 1942).

10.5 Discussion

The poorly ossified braincase in basal ‘pelycosaur-grade’ stem-mammals offers little direct evidence of neurosensory organization beyond what can be inferred about the ancestral amniote brain. Diversification in feeding and minor advances in locomotion were the major trends in evolution. Inferred neurosensory elaboration

in a few of these taxa, particularly the sphenacodontines, included slightly greater frontality of the orbits, consistent with their inferred role as apex predators. Most show elongation of the choana, suggesting increased size of the olfactory capsule and its olfactory epithelium. In Wagner's (2014) terms these all qualify as novel character states (Type II innovations).

With the origin of *Therapsida*, the novel tooth implantation via long roots held in deep alveoli by an innervated periodontal ligament would eventually become a key innovation in evolution of the cynodont masticatory system. Formation of tooth roots and the periodontal ligament marked a new role for neural crest cells in pan-mammalian evolution that eventually had far-reaching neurosensory and morphogenic consequences for stem-mammals.

Increased individuation of regions in the vertebral column occurred in the atlas-axis complex, establishment of seven cervical vertebrae in the neck, and in a shift toward parasagittal movement of the dorsal vertebrae and ribs that may have begun the process of decoupling aspirational breathing from locomotion. Inferences of increased aerobic ventilation and metabolic scope, more agile locomotion, and presumed higher levels of activity are consistent with these anatomical transformations, and with expanded geographic distribution of early therapsids.

Most of the innovations seen in basal therapsids can be categorized as new variational modalities in systems of repeated parts. At this point in stem-mammal history, they probably fit best into Wagner's category of Type II innovations. In retrospect, however, they foreshadow the later individuation of Type I novelties as the dentition took on a new character identity as an integrated sensory array involved in the novel function of mastication.

Digital endocasts of early therapsids (Benoit et al. 2017) provide the earliest models for comparison to later stem-mammals, but at present there is little direct evidence of how they differed from the most basal (pelycosaur grade) stem-mammals. Compared with their living descendants, early therapsids possessed low-resolution olfaction, weak hearing, coarse tactile sensitivity, poorly refined motor coordination, and sensory-motor integration that commanded little cerebral territory. Vision may have been their leading sensory modality.

The origin of *Cynodontia* signals onset of integration in previously distinct anatomical systems and sensory inputs that were recruited into the masticatory system. The new functions of occlusion and mastication involved further specialization of established incisor, canine, and postcanine regions, and in the complexity and diversity of functions that different parts of the dentition could now perform. A new variational modality ensued in which virtually every species evolved a unique crown structure, whereas rates of tooth replacement slowed (Rowe and Shepherd 2016; Rowe 2020a, e). This was correlated with the appearance of the secondary palate and separation of oral and nasopharyngeal passageways, and initiation of the compound sense of 'ortho-retronasal olfaction', which combines with sensory information from the tongue, lips, and cheeks that converges on single neurons in the orbitofrontal region of neocortex. Ossification of the alisphenoid was initiated by expansion of the caudolateral pole of the olfactory cortex, implying elaboration of the olfactory system that was probably induced, ultimately, by expression of a larger

number of olfactory receptor genes. The ontogenetic interdependencies that connect the various parts of the olfactory system were probably inherited from the ancestral amniote, but in cynodonts olfaction became sufficiently elaborated to induce visible changes in cranial morphogenesis.

Further individuation of regions of the axial skeleton occurred and, if not from the start, they later gained a surprising degree of integration with the olfactory and masticatory system. The double occipital condyle gave the skull a new kind of articulation to the atlas-axis complex and neck, providing a greater degree of stable dorsoventral and lateral movement by the head and neck and probably refined directional scent detection. At the same time, differentiation of distinct thoracic and lumbar regions indicate the onset of diaphragmatic ventilation, and more complete decoupling of aspirational breathing and sniffing from locomotion.

Basal cynodonts had begun to forge new functional linkages between biting, chewing, swallowing, sniffing and breathing, orthonasal and retronasal olfaction, taste, flavor and, more speculatively, territorial scent marking, scent-tracking, and odorant-moderated reproductive behaviors. The cynodont dentition eventually became individuated into a unique functional unit and sensory array that would eventually project to a large neocortical territory worthy of consideration as a Type 1 novelty. Diversification of the masticatory system became a major feature of cynodont evolution, including major clades within *Mammalia*. The neural implications are largely unexplored, but it is already clear that the cynodont masticatory system produced a rising tide of new kinds of peripheral information to the brain that imply linkages in the dorsal cortex for the first time of multiple previously independent sensory systems.

With the origin of *Mammaliaformes* (or possibly earlier, in basal *Mammaliomorpha*) miniaturization of adult body size occurred. For most of its Late Triassic, Jurassic and Cretaceous history, pan-mammals were mostly shrew-sized animals; a few reached the size of domestic cats, but it was not until the Cenozoic that huge body sizes evolved in crown *Mammalia*. Miniaturization corresponded with increased precision movements and agility of the skeleton, as well as the volume and kinds of internal information passing between the brain and the musculoskeletal system. Indirect evidence of further encephalization is reflected in ossification of the orbital walls. Ossification of rear parts of the nasal capsule and possible ossified primordia of the ethmoid skeleton suggest expression of another increase in OR genes. The brain in basal *Mammaliaformes* more than doubled in relative size. Most of this volume increase occurred in the olfactory bulb and olfactory cortex, and in all likelihood their projection to an emerging orbitofrontal region in the dorsal cortex. This probably reflects the largest increase in numbers of expressed olfactory receptor genes yet to occur in stem-mammal history. A pelt of modern aspect was also present. Induced by many thousands of body placodes, the 'dynamic miniorgans' (Schneider et al. 2009) that body hair represents must have provided a flood of new peripheral information to dorsal cortex; in *Mammalia* it has a large presence in somatosensory areas of neocortex. Moreover, from this point onwards the brain as a whole entered a new variational modality in which independent evolutionary increases in encephalization characterize many clades within

Mammalia (Fig. 10.20). Instances of secondary reduction in encephalization are rare (Macrini et al. 2006; Kruska 2007; Castiglione et al. 2021).

The discovery of fur in a Jurassic mammaliaform has additional implications for understanding mammalian neurosensory evolution. During ontogeny in mammals, hair performs first as a tactile organ and only later does it insulate as underfur thickens and matures (Zelená 1994; Schneider et al. 2009). Body temperature in newborn mammals is initially regulated by their mothers. This sequence implies that parental care and endothermy may have been present in *Mammaliaformes* ancestrally. Endothermy may have been an evolutionary consequence of mammaliaform encephalization because a large brain operates properly only within narrow thermal tolerances, and it is metabolically the most expensive organ to maintain. However, metabolism is under hormonal control that does not command large cerebral regions; thus endothermy did not itself drive encephalization (Rowe et al. 2011).

Reproductive strategies may also have been reorganized in basal *Mammaliaformes*. Fossil evidence was recently discovered of a large clutch of perinates in the Early Jurassic tritylodontid *Kayentatherium wellsi* (Fig. 10.12b) with a presumed maternal skeleton (Hoffman and Rowe 2018). The single clutch comprises at least 38 individuals, well outside the range of litter sizes documented in extant mammals. This confirms that production of high numbers of offspring represents the ancestral condition for amniotes and also constrains the timing of a reduction in clutch size along the mammalian stem to a late point in stem-mammalian history. Tritylodontids diverged from the mammalian stem just before the pulse of brain expansion that occurred with the origin of *Mammaliaformes* (Rowe et al. 2011). The association of a high number of offspring and largely isometric cranial growth in *Kayentatherium* is consistent with a scenario in which increased encephalization, and attendant shifts in metabolism and cranial allometry, drove later changes to reproductive strategy and smaller clutch sizes (Hoffman and Rowe 2018). This was in place in *Mammalia* ancestrally, but may trace to the origin of *Mammaliaformes*.

With the origin of *Mammalia*, we enter the phylogenetic bracket of extant monotremes and therians, which allows a much larger number of justifiable inferences regarding novelties arising in (or before) the last common ancestor of the crown clade. Neocortex, including the corticospinal tract, was undoubtedly present in the ancestral mammal, and the profound integration of the ancestrally distinct structures and systems that neocortex now integrates diagnoses it as a Type I novelty. As we have seen, many of the individual components of the larger system integrated by neocortex can be traced into the mammalian stem-group, to their roots as more-or-less discrete anatomical and functional elements, with plesiomorphic variational modalities. With such a rich fossil record of intermediate forms all along the mammalian stem, it is doubtful that a precise point of emergence of neocortex as a Type I novelty is susceptible to strict definition, and exactly where along the mammalian stem one draws this somewhat arbitrary boundary depends on one's research interests and goals (Wagner 2014).

The emergence of neocortex, lying as it does at the integral core of mammalian brain organization, was a central theme in stem-mammal evolution and the origin of *Mammalia*.

Olfaction, and its integration with other sensory modalities in the orbitofrontal region of neocortex, was a central driver in neocortical evolution (Shepherd and Rowe 2017). Olfactory genes form the largest and most rapidly evolving subfamily in the vertebrate (Niimura 2009, 2012), tetrapod (Yohe et al. 2020), and mammalian (Young et al. 2010) genomes. This reflects the selective importance of responding to ever-changing chemical environments that mammals exploited to a degree exceeding other vertebrates. Gene duplication is the primary mechanism of OR gene increases throughout vertebrate history (Bargmann 2006; Niimura 2012; Wagner 2014). In the transition from water onto land, the pace of olfactory receptor gene evolution accelerated into what has been called ‘evolutionary overdrive’ (Yohe et al. 2020), as tetrapods adapted to the more diverse and rapidly changing chemical environment encountered in terrestrial ecosystems. *Mammalia* carried this trend to its greatest extreme, as measured by the relative size of the mammalian olfactory genome, the complexity of microcircuitry in the mammalian olfactory pathway (Shepherd et al. 2021), and at gross anatomical levels in the size and complexity of epithelial and skeletal structures induced in an ontogenetic cascade that follows olfactory gene expression. The rapid rate of OR pseudogenation observed in many mammalian clades (Young et al. 2010; Niimura 2012) is further evidence of rapid OR evolution, and further emphasizes the rapidity of change in chemical environments successfully occupied by early mammals. As Aboitiz and Montiel (2015) comment: “our hypothesis has common ground with those proposed by Lynch (1986), Rowe et al. (2011) and Rowe and Shepherd (2016) that olfactory systems were key in early mammalian evolution. Here we add to these hypotheses the role of the emergent isocortex [neocortex] as a multimodal interface in the olfactory-hippocampal axis for behavioral navigation”.

The evolving ontogeny of mammalian neocortex proceeded as a surging flood of new peripheral information ascended to the brain (Rowe and Shepherd 2016; Rowe 2020a). Whether through connectional invasions and epigenetic population matching (Katz and Lasek 1978; Krubitzer and Kaas 2005; Streidter 2005), or some other developmental mechanism, hypertrophy of peripheral sensory arrays involving olfaction, dentition, musculoskeletal system, and elaborate integument produced cascading influences on central organization that are so distinctive of mammalian neocortex today. Early mammaliaformes and many early members of crown *Mammalia* immersed themselves in a wealth of new information in microhabitats dominated to an unprecedented degree by scents, odors, and smells. Their unsurpassed abilities to perceive and process olfactory information and to diversify and exploit the fast-changing chemical environments they faced throughout much of their history is one of the keys to understanding the major features of pan-mammal evolution.

References

- Aboitiz F, Montiel JF (2015) Olfaction, navigation, and the origin of isocortex. *Front Neurosci* 9(402):1–12
- Ashwell K (ed) (2010) *The neurobiology of Australian marsupials*. Cambridge University Press, Cambridge, UK
- Ashwell K (ed) (2013) *Neurobiology of monotremes: brain evolution in our distant mammalian cousins*. CSIRO Publishing, Collingwood
- Avivi-Arber L, Martin R, Lee JC et al (2011) Face sensorimotor cortex and its neuroplasticity related to orofacial sensorimotor functions. *Arch Oral Biol* 56(12):1440–1465
- Balanoff AM, Bever GS (2020) The role of endocasts in the study of brain evolution. In: Kaas J (ed) *Evolutionary neuroscience*, 2nd edn. Academic, New York, pp 223–241
- Balanoff AM, Bever GS, Colbert MW et al (2016) Best practices for digitally constructing endocranial casts: examples from birds and their dinosaurian relatives. *J Anat* 229(2):173–190
- Bargmann CI (2006) Comparative chemosensation from receptors to ecology. *Nature* 444:295–301
- Barrowclough GF, Cracraft J, Klicka J et al (2016) How many kinds of birds are there and why does it matter? *PLoS One* 11(11):e0166307
- Baur G, Case EC (1899) The history of the pelycosauria with a description of the genus *Dimetrodon*. *Trans Am Phil Soc* 20:5–62
- Baxi KN, Dorries KM, Eisthen HL (2006) Is the vomeronasal system really specialized for detecting pheromones? *Trends Neurosci* 29(1):1–7
- Benoit J, Manger PR, Rubidge BS (2016) Palaeoneurological clues to the evolution of defining mammalian soft tissue traits. *Sci Rep* 6(1):1–10. <https://doi.org/10.1038/srep25604>
- Benoit J, Fernandez V, Manger PR et al (2017) Endocranial casts of pre-mammalian therapsids reveal an unexpected neurological diversity at the deep evolutionary root of mammals. *Brain Behav Evol* 90(4):311–333
- Berlin JC, Kirk EC, Rowe TB (2013) Functional implications of ubiquitous semicircular non-orthogonality in mammals. *PLoS One* 8(11):e79585. <https://doi.org/10.1371/journal.pone.0079585>
- Bertmar G (1981) Evolution of vomeronasal organs in vertebrates. *Evolution* 35:359–366
- Bever GS, Rowe TB, Ekdale EG et al (2005) Comment on “Independent origins of middle ear bones in monotremes and therians”. *Science* 309:1492a
- Bhatnagar KP, Meisami E (1998) Vomeronasal organ in bats and primates: extremes of structural variability and its phylogenetic implications. *Microscopy ResTech* 43(6):465–475
- Bird DJ, Murphy WJ, Fox-Rosales L et al (2018) Olfaction written in bone: cribriform plate size parallels olfactory receptor gene repertoires in Mammalia. *Proc R Soc B* 285:20180100. <https://doi.org/10.1098/rspb.2018.0100>
- Bonaparte JF, Martinelli AG, Schultz CL et al (2005) New information on *Brasilodon* and *Brasilitherium* (Cynodontia, Probainognathia) from the late Triassic of southern Brazil. *Rev Bras Paleontolog* 8(1):25–46
- Bonaparte JF, Soares MB, Martinelli AG (2013) Discoveries in the Late Triassic of Brazil improves knowledge on the origin of mammals. *Hist Nat* 3rd Ser 2:5–30
- Brainerd EL (2015) Major transformations in vertebrate breathing mechanisms. In: Dial KP, Shubin N, Brainerd EL (eds) *Great transformations in vertebrate evolution*. University of Chicago Press, Chicago, pp 47–61
- Brainerd EL, Owerkowicz T (2006) Functional morphology and evolution of aspirational breathing in tetrapods. *Resp Physiol Neeurobi* 154:73–88
- Brink AS (1957) Speculations on some advanced mammalian characteristics in the higher mammal-like reptiles. *Palaeontol Africana* 4:77–96
- Briscoe SD, Ragsdale CW (2018) Molecular anatomy of the alligator dorsal telencephalon. *J Comp Neurol* 526(10):1613–1646
- Broom R (1932) *The mammal-like reptiles of South Africa and the origin of mammals*. HF & G Witherby, London

- Bruce LL (2007) Evolution of the nervous system in reptiles. In: Bullock TH, Rubenstein LR, Kaas JH (eds) *Evolution of nervous systems: a comprehensive reference, The evolution of nervous systems in non-mammalian vertebrates, vol II*. Elsevier/Academic, Oxford, pp 125–156
- Bruce LL (2009) Evolution of the nervous system in reptiles. In: Kaas JH (ed) *Evolutionary neuroscience*, 1st edn. Academic, New York, pp 233–265
- Bruce LL, Braford MR Jr (2009) Evolution of the limbic system. In: Squire LR (ed) *New encyclopedia of neuroscience*. Elsevier Academic, Oxford, pp 43–55
- Buck L, Axel R (1991) A novel multigene family may encode odorant receptors: a molecular basis for odor recognition. *Cell* 65:175–187
- Burgin CJ, Colella JP, Kahn PL et al (2018) How many species of mammals are there? *J Mammal* 99(1):1–14
- Butler AB (1994) The evolution of the dorsal pallium in the telencephalon of amniotes: cladistic analysis and a new hypothesis. *Brain Res Rev* 19(1):66–101
- Butler AB, Hodos W (2005) *Comparative vertebrate neuroanatomy: evolution and adaptation*, 2nd edn. Wiley, New York
- Cantino PD, De Queiroz K (eds) (2020) *PhyloCode: a phylogenetic code of biological nomenclature*. CRC Press, Boca Raton
- Carr EC, Christiansen-Dalsgaard J (2016) Evolutionary trends in directional hearing. *Curr Opin Neurobiol* 40:111–117
- Carr CE, Soares D (2002) Evolutionary convergence and shared computational principles in the auditory system. *Brain Behav Evol* 59:294–311
- Carr CE, Soares D (2009) Shared and convergent features of the auditory system of vertebrates. In: Kaas JH (ed) *Evolutionary neuroscience*, 1st edn. Academic, New York, pp 479–493
- Carrier DR (1987) The evolution of locomotor stamina in tetrapods: circumventing mechanical constraint. *Paleobiology* 13:326–341
- Case EC (1907) *Revision of the pelycosauria of North America, vol 55*. Carnegie Inst Washington Publ, Washington, pp 1–176
- Castiglione S, Serio C, Piccolo M et al (2021) The influence of domestication, insularity and sociality on the tempo and mode of brain size evolution in mammals. *Biol J Linn Soc* 132(1):221–231
- Catania KC (2013) Stereo and serial sniffing guide navigation to an odour source in a mammal. *Nat Commun* 4:1441–1449
- Catania KC, Catania EH (2015) Comparative studies of somatosensory systems and active sensing. In: Krieger P, Groth A (eds) *Sensorimotor integration in the whisker system*. Springer, New York, pp 7–30
- Chen WR, Shepherd G (2005) The olfactory glomerulus: a cortical module with specific functions. *J Neurocytol* 34:353–360
- Cifelli RL, Rowe TB, Luckett WP et al (1996) Fossil evidence for the origin of the marsupial pattern of tooth replacement. *Nature* 379:715–718
- Clack JA (2012) *Gaining ground*. Indiana University Press, Bloomington
- Clark JM, Hopson JA (1985) Distinctive mammal-like reptile from Mexico and its bearings on the phylogeny of Tritylodontidae. *Nature* 315:398–400
- Cluver MA (1971) The cranial morphology of the Genus *Lystrosaurus*. *Ann S Afr Mus* 56:155–273
- Cluver MA (1978) The skeleton of the mammal-like reptile *Cistecephalus* with evidence for a fossorial mode of life. *Ann S Afr Mus* 76:213–246
- Collin SP (2010) Evolution and ecology of retinal photoreception in early vertebrates. *Brain Behav Evol* 75:174–185
- Connors BW, Kriegstein AR (1986) Cellular physiology of the turtle visual cortex: distinctive properties of pyramidal and stellate neurons. *J Neurosci* 6:164–177
- Cope ED (1886) On the structure of the brain and auditory apparatus of a theromorphous reptile of the Permian Epoch. *Proc Am Phil Soc* 23:234–238
- Crompton AW (1963) Tooth replacement in the cynodont *Thrinaxodon Liorhinus*. *Ann S Afr Mus* 46:479–521

- Crompton AW (1972) Postcanine occlusion in cynodonts and tritylodontids. *Bull Br Mus Nat Hist Geol* 21:27–71
- Crompton AW (1989) The evolution of mammalian mastication. In: Wake DB, Roth G (eds) *Complex organismal functions: integration and evolution in vertebrates*. Wiley, New York, pp 23–40
- Crompton AW, Parker P (1978) Evolution of the mammalian masticatory apparatus. *Am Sci* 66(2):92–201
- Crompton AW, Taylor CR, Jagger JA (1978) Evolution of homeothermy in mammals. *Nature* 272:333
- Crompton AW, Owerkowicz T, Bhullar BAS et al (2017a) Structure of the nasal region of non-mammalian cynodonts and mammaliaforms: speculations on the evolution of mammalian endothermy. *J Vert Paleontol* 37(1):e1269116
- Crompton AW, Musinsky C, Rougier GW et al (2017b) Origin of the lateral wall of the mammalian skull: fossils, monotremes and therians revisited. *J Mammal Evol* 25(3):301–313. <https://doi.org/10.1007/s10914-017-9388-7>
- Crompton AW, Musinsky C, Bonaparte J et al (2018) Evolution of the mammalian fauces region and the origin of suckling. <https://nrs.harvard.edu/URN-3:HUL.INSTREPOS:37364482>
- Davies WL, Carvalho LS, Cowing JA et al (2007) Visual pigments of the platypus: a novel route to mammalian colour vision. *Curr Biol* 17(5):R161–R163
- De Araujo IE, Rolls ET, Kringelbach ML et al (2003) Taste olfactory convergence, and the representation of the pleasantness of flavour, in the human brain. *Eur J Neurosci* 18:2059–2068
- de Queiroz K (1994) Replacement of an essentialistic perspective on taxonomic definitions as exemplified by the definition of “Mammalia”. *Syst Biol* 43(4):497–510
- de Queiroz K (2007) Toward an integrated system of clade names. *Syst Biol* 56:956–974
- de Queiroz K, Gauthier JA (1990) Phylogeny as a central principle in taxonomy: phylogenetic definitions of taxon names. *Syst Biol* 39(4):307–322
- de Queiroz K, Gauthier JA (1992) Phylogenetic taxonomy. *Annu Rev Ecol Evol Syst* 23(1):449–480
- de Queiroz K, Gauthier JA (1994) Toward a phylogenetic system of biological nomenclature. *Trends Ecol Evol* 9(1):27–31
- de Queiroz K, Cantino PD, Gauthier JA (eds) (2020) *Phylonyms: a companion to the PhyloCode*. CRC Press, Boca Raton
- Demski LS (1993) Terminal nerve complex. *Cells Tissues Organs* 148(2-3):81–95
- Demski LS, Schwanzel-Fukuda M (eds) (1987) The terminal nerve (*Nervus Terminalis*) structure, function and evolution. *Ann NY Acad Sci* 519:1–49
- Didier G, Laurin M (2020) Exact distribution of divergence times from fossil ages and tree topologies. *Syst Biol* 69(6):1068–1087
- Di-Pöi N, Milinkovitch MC (2016) The anatomical placode in reptile scale morphogenesis indicates shared ancestry among skin appendages in amniotes. *Sci Adv* 2016:e1600708
- Donoghue MJ, Doyle J, Gauthier JA et al (1989) Importance of fossils in phylogeny reconstruction. *Annu Rev Ecol Evol Syst* 20:431–460
- Edinger T (1975) *Paleoneurology 1804–1966: an annotated bibliography*. *Adv Anat Embryol Cell Biol* 49:3–258
- Eisenberg JF (1981) *The mammalian radiations: an analysis of trends in evolution, adaptation, and behaviour*. University of Chicago Press, Chicago
- Eisenberg JF (1990) The behavioral/ecological significance of body size in the Mammalia. In: Damuth J, MacFadden B (eds) *Body size in mammalian paleobiology: estimation and biological implications*. Cambridge University Press, Cambridge, UK, pp 25–37
- Ekdale EG (2016) Form and function of the mammalian inner ear. *J Anat* 228(2):324–337
- Fabbri MN, Mongiardino M, Pritchard AC et al (2017) The skull roof tracks the brain during evolution and development of reptiles including birds. *Nat Ecol Evol* 1(10):1543–1550. <https://doi.org/10.1038/s41559-017-0288-2>

- Farbman AI (1988) Cellular interactions in the development of the vertebrate olfactory system. In: Margolis FL, Getchell TV (eds) *Molecular neurobiology of the olfactory system*. Plenum Press, New York, pp 319–332
- Farbman AI (1990) Olfactory neurogenesis: genetic or environmental controls? *Trends Neurosci* 13:362–365
- Farbman AI (1992) *Cell biology of olfaction*. Cambridge University Press, CITY
- Gaengler P, Metzler E (1992) The periodontal differentiation in the phylogeny of teeth – an overview. *J Periodontal Res* 27:214–225. <https://doi.org/10.1111/j.1600-0765.1992.tb01671.x>
- Garrett EC, Steiper ME (2014) Strong links between genomic and anatomical diversity in both mammalian olfactory chemosensory systems. *Proc B Roy Soc Lond* 281:2013–2828
- Gauthier JA, Kluge AG, Rowe TB (1988a) Amniote phylogeny and the importance of fossils. *Cladistics* 4:105–209
- Gauthier JA, Kluge AG, Rowe TB (1988b) The early evolution of the Amniota. In: Benton M (ed) *The phylogeny and Classification of the Tetrapods, Vol. 1: Amphibians, Reptiles and Birds, Syst Assoc Spec Vol Ser special vol No. 35a*. Clarendon Press, Oxford, pp 103–155
- Gauthier JA, Cannatella D, de Queiroz K et al (1989) Tetrapod phylogeny. In: Fernholm B, Bremer H, Jornvall H (eds) *The hierarchy of life, Nobel sympos 70*. Excerpta Medica, Amsterdam, pp 337–353
- Gemmell NJ, Rutherford K, Prost S et al (2020) The tuatara genome reveals ancient features of amniote evolution. *Nature* 584:403–409
- Goodrich ES (1930) *Studies on the structure and function of vertebrates*. Constable & Co, London
- Grant R, Haidarliu S, Kennerley NJ et al (2013) The evolution of active vibrissal sensing in mammals: evidence from vibrissal musculature and function in the marsupial opossum *Monodelphis domestica*. *J Exp Biol* 216(18):3483–3494
- Graybeal A, Rosowski JJ, Ketten DR et al (1989) Inner ear structure in Morganucodon, an early Jurassic mammal. *Zool J Linn Soc* 96(2):107–117
- Green PA, Van Valkenburgh B, Pang B et al (2012) Respiratory and olfactory turbinal size in canid and arctoid carnivorans. *J Anat* 221(6):609–621
- Grothe B, Carr CE, Cassidy JH et al (2005) The evolution of central pathways and their neural processing patterns. In: Manley GA, Popper AN, Fay AN (eds) *Evolution of the vertebrate auditory system*. Springer, New York, pp 289–359
- Grothe B, Pecka M, McAlpine D (2010) Mechanisms of sound localization in mammals. *Physiol Rev* 90(3):983–1012
- Haberly LB (1985) Neuronal circuitry in olfactory cortex: anatomy and functional implications. *Chem Senses* 10:219–238
- Haberly LB (2001) Parallel-distributed processing in olfactory cortex: new insights from morphological and physiological analysis of neuronal circuitry. *Chem Senses* 26:551–576
- Habre-Hallage P, Dricot L, Hermoye L et al (2014) Cortical activation resulting from the stimulation of periodontal mechanoreceptors measured by functional magnetic resonance imaging (fMRI). *Clin Oral Investig* 18(8):1949–1961
- Hall BK (2009) *The neural crest and neural crest cells in vertebrate development and evolution*. Springer, New York
- Harris KD, Shepherd GM (2015) The neocortical circuit: themes and variations. *Nat Neurosci* 18(2):170–181
- Harvey PH, Clutton-Brock TH, Mace GM (1980) Brain size and ecology in small mammals and primates. *PNAS* 77:4387–4389
- Hayden S, Bekaert M, Crider TA et al (2010) Ecological adaptation determines functional mammalian olfactory subgenomes. *Genome Res* 20:1–9
- Heiss E, Aerts P, Van Wassenbergh S (2018) Aquatic–terrestrial transitions of feeding systems in vertebrates: a mechanical perspective. *J Exp Biol* 221(8):221, jeb154427. <https://doi.org/10.1242/jeb.154427>

- Herculano-Houzel S, Manger PR, Kaas JH (2014) Brain scaling in mammalian evolution as a consequence of concerted and mosaic changes in numbers of neurons and average neuronal cell size. *Front Neuroanat* 8:1–28
- Hillenius WJ (1992) The evolution of nasal turbinates and mammalian endothermy. *Paleobiology* 18:17–29
- Hillenius WJ (1994) Turbinates in therapsids: evidence for late Permian origins of mammalian endothermy. *Evolution* 48:207–229. <https://doi.org/10.1111/j.1558-5646.1994.tb01308.x>
- Hirasawa T, Kuratani S (2013) A new scenario of the evolutionary derivation of the mammalian diaphragm from shoulder muscles. *J Anat* 222(5):504–517
- Hlusko LJ, Sage RD, Mahaney MC (2011) Modularity in the mammalian dentition: mice and monkeys share a common dental genetic architecture. *J Exp Zool B Mol Dev Evol* 316(1):21–49
- Hoffman EA, Rowe TB (2018) Jurassic stem-mammal perinates and the origin of mammalian reproduction and growth. *Nature* 561(7721):104–108
- Hoffmann CA, Rodrigues PG, Soares MB et al (2019) Brain endocast of two non-mammaliaform cynodonts from southern Brazil: an ontogenetic and evolutionary approach. *Hist Biol* 2019:1–12
- Hopson JA (1971) Postcanine replacement in the gomphodont cynodont *Diademodon*. In: Kermack DM, Kermack KA (eds) *Early Mammals*. *Zool J Linn Soc* 50(suppl 1):1–21
- Hopson JA (2015) Fossils, trackways, and transitions in locomotion: a case study of *Dimetrodon*. In: Dial KP, Shubin N, Brainerd EL (eds) *Great transformations in vertebrate evolution*. University of Chicago Press, Chicago, pp 125–141
- Huber E (1930) Evolution of facial musculature and cutaneous field of Trigemini. Part I. *Quart Rev Biol* 5(2):133–188
- Hurlburt GR, Ridgely RC, Witmer LM (2013) Relative size of brain and cerebrum in tyrannosaurid dinosaurs: an analysis using brainendocast quantitative relationships in extant alligators. In: Parrish JM, Molnar RE, Currie PJ, Koppelhus EB (eds) *Tyrannosaurid paleobiology*. Indiana University Press, Bloomington, pp 135–155
- Iyengar S, Qi HX, Jain N et al (2007) Cortical and thalamic connections of the representations of the teeth and tongue in somatosensory cortex of new world monkeys. *J Compar Neurol* 501(1):95–120
- Jacobs GH (2009) Evolution of colour vision in mammals. *Phil Trans B Royal Soc Lond* 364(1531):2957–2967
- Jacobs GH (2013) Losses of functional opsin genes, short-wavelength cone photopigments, and color vision – a significant trend in the evolution of mammalian vision. *Visual Neurosci* 30(1-2):39–53
- Janis CM, Keller JC (2001) Modes of ventilation in early tetrapods: costal aspiration as a key feature of amniotes. *Acta Palaeontol Pol* 46(2):137–170
- Jarvik E (1942) On the structure of the snout of crossopterygians and lower gnathostomes in general. *Zool Bidr Upps* 21:235–675
- Jenkins FA Jr (1969) The evolution and development of the dens of the mammalian axis. *Anat Rec* 164:173–184
- Jenkins FA Jr (1971) The postcranial skeleton of African cynodonts: problems in the early evolution of the mammalian postcranial skeleton. *Bull Peabody Mus Nat Hist* 36:1–216
- Jerison H (1973) *Evolution of the brain and intelligence*. Academic, New York
- Ji Q, Luo Z-X, Yuan C et al (2006) A swimming mammaliaform from the Middle Jurassic and ecomorphological diversification of early mammals. *Science* 311:1123–1127
- Kaas JH (2009) The evolution of the dorsal thalamus in mammals. In: Kaas JH (ed) *Evolutionary neuroscience*, 1st edn. Elsevier, Oxford, pp 569–586
- Kaas JH (2013) The evolution of brains from early mammals to humans. *Wiley Interdiscip Rev Cogn Sci* 4(1):33–45
- Kaas JH (2020) The organization of neocortex in early mammals. In: Kaas JH (ed) *Evolutionary neuroscience*, 2nd edn. Elsevier, Oxford, pp 333–348
- Kaas JH, Qi HX, Iyengar S (2006) Cortical network for representing the teeth and tongue in primates. *Anat Rec* 288(2):182–190

- Katz MJ, Lasek RJ (1978) Evolution of the nervous system: role of ontogenetic mechanisms in the evolution of matching populations. *PNAS* 75(3):1349–1352
- Kemp TS (1983) The relationships of mammals. *Zool J Linn Soc* 77:353–384
- Kemp TS (1988) A note on the Mesozoic mammals, and the origin of therians. In: Benton MJ (ed) *The phylogeny and classification of the tetrapods, volume 2: mammals*, Syst Assoc Spec Vol Ser special vol No. 35b. Clarendon Press, Oxford, pp 23–29
- Kemp TS (2005) *The origin and evolution of mammals*. Oxford University Press, Oxford
- Kemp TS (2006) The origin and early radiation of the therapsid mammal like reptiles: a palaeobiological hypothesis. *J Evol Biol* 19(4):1231–1247
- Kemp TS (2009) The endocranial cavity of a nonmammalian cynodonts *Chiniquodon theotenicus* and its implications for the origin of the mammalian brain. *J Vert Paleontol* 29(4):1188–1198
- Kermack DM, Kermack KE (1984) *The evolution of mammalian characters*. Springer, New York
- Kielan-Jaworowska Z, Cifelli RL, Luo Z-X (2004) *Mammals from the age of dinosaurs*. Columbia University Press, New York
- Kirk EC, Daghighi P, Macrini T et al (2014) Cranial anatomy of the Duchesnean primate *Rooneyia viejaensis*: New insights from high resolution computed tomography. *J Hum Evol* 74:82–95
- Kitazawa T, Takechi M, Hirasawa T et al (2015) Developmental genetic bases behind the independent origin of the tympanic membrane in mammals and diapsids. *Nat Commun* 6(1):1–7
- Koyabu D, Werneburg I, Morimoto N et al (2014) Mammalian skull heterochrony reveals modular evolution and a link between cranial development and brain size. *Nat Commun* 5(1):1–9
- Krubitzer L, Hunt DL (2009) Captured in the new of space and time: understanding cortical field evolution. In: Kaas JH (ed) *Evolutionary neuroscience*, 1st edn. Elsevier, Oxford, pp 545–568
- Krubitzer L, Kaas J (2005) The evolution of the neocortex in mammals: how is phenotypic diversity generated? *Curr Opin Neurobiol* 15(4):444–453
- Kruska DCT (2007) The effects of domestication on brain size. In: Bullock TH, Rubenstein LR, Kaas JH (eds) *Evolution of nervous systems: a comprehensive reference, volume II, the evolution of nervous systems in non-mammalian vertebrates*. Elsevier Academic, Oxford, pp 143–153
- Kubo K, Shibukawa Y, Shintani M et al (2008) Cortical representation area of human dental pulp. *J Dental Res* 87(4):358–362
- Laaß M, Kaestner A (2017) Evidence for convergent evolution of a structure comparable to the mammalian neocortex in a Late Permian therapsid. *J Morph* 278:1033–1057
- Laurin M, Reisz RR (2020) Synapsida. In: de Queiroz K, Cantino PD, Gauthier JA (eds) *Phylonyms: a companion to the PhyloCode*. CRC Press, Boca Raton, pp 811–814
- LeBlanc AR, Brink KS, Whitney MR et al (2018) Dental ontogeny in extinct synapsids reveals a complex evolutionary history of the mammalian tooth attachment system. *Proc Royal Soc B* 285(1890):20181792. <https://doi.org/10.1098/rspb.2018.1792>
- Lemberg JB, Daeschler EB, Shubin NH (2021) The feeding system of *Tiktaalik roseae*: an intermediate between suction feeding and biting. *PNAS* 118(7):1–10. e2016421118
- Lightoller GS (1942) Matrices of the facialis musculature: homologization of the musculature in monotremes with that of marsupials and placentals. *J Anat* 76(3):258–269
- Louis M, Huber T, Benton R et al (2008) Bilateral olfactory sensory input enhances chemotaxis behavior. *Nat Neurosci* 11(2):187–199
- Luo Z-X (2007) Transformation and diversification in early mammal evolution. *Nature* 450:1011–1019
- Luo Z-X, Crompton AW, Sun A-L (2001) A new mammal from the Early Jurassic and evolution of mammalian characteristics. *Science* 292:1535–1540
- Luo Z-X, Kielan-Jaworowska Z, Cifelli RL (2004) Evolution of dental replacement in mammals. *Bull Carnegie Mus Nat Hist* 36:159–175
- Luo Z-X, Ruf I, Martin T (2012) The petrosal and inner ear of the Late Jurassic cladotherian mammal *Dryolestes leiirensis* and implications for ear evolution in therian mammals. *Zool J Linn Soc* 166(2):433–463

- Luo Z-X, Gatesy SM, Jenkins FA Jr et al (2015) Mandibular and dental characteristics of Late Triassic mammaliaform *Haramiyavia* and their ramifications for basal mammal evolution. PNAS 112(51):E7101–E7109. <https://doi.org/10.1073/pnas.1519387112>
- Lynch G (1986) Synapses, circuits, and the beginnings of memory. MIT Press, Cambridge, MA
- Mace GM, Harvey PH, Clutton-Brock TH (1981) Brain size and ecology in small mammals. J Zool 193:333–354
- Macrini TE (2006). The evolution of endocranial space in mammals and non-mammalian cynodonts. Dissertation, University of Texas
- Macrini TE (2012) Comparative morphology of the internal nasal skeleton of adult marsupials based on x-ray computed tomography. Bull Am Mus Nat Hist 2012:1–91
- Macrini TE (2014) Development of the ethmoid in *Caluromys philander* (Didelphidae, Marsupialia) with a discussion on the homology of the turbinal elements in marsupials. Anat Rec 297(11):2007–2017
- Macrini TE, Rowe TB, Archer M (2006) Description of a cranial endocast from a fossil platypus, *Obdurodon dicksoni* (Monotremata, Ornithorhynchidae), and the relevance of endocranial characters to monotreme monophyly. J Morph 267:1000–1015
- Manger PR (2006) An examination of cetacean brain structure with a novel hypothesis correlating thermogenesis to the evolution of a big brain. Biol Rev 81(2):293–338
- Marín O, Rubenstein JL (2001) A long, remarkable journey: tangential migration in the telencephalon. Nat Rev Neurosci 2(11):780–790
- Martinelli AG, Rougier GW (2007) On *Chalimnia musteloides* (Eucynodontia: Tritheledontidae) from the Late Triassic of Argentina, and a Phylogeny of Ictidosauria. J Vert Paleontol 27:442–460
- McMahon TA, Bonner JT (1983) On size and life. Scientific American Library, New York
- Meng J, Hu Y, Wang Y et al (2006) A Mesozoic gliding mammal from northeastern China. Nature 444:889–893
- Molnár Z, Butler AB (2002) Neuronal changes during forebrain evolution in amniotes: an evolutionary developmental perspective. Progr Brain Res 136:21–38
- Molnár Z, Tavare A, Cheung AFP (2009) The origin of Neocortex: lessons from comparative embryology. In: Kaas JH (ed) Evolutionary neuroscience, 1st edn. Elsevier, Oxford, pp 509–522
- Molnár Z, Kaas JH, de Carlos JA et al (2014) Evolution and development of the mammalian cerebral cortex. Brain Behav Evol 83:126–139
- Muchlinski MN (2008) The relationship between the infraorbital foramen, infraorbital nerve, and maxillary mechanoreception: implications for interpreting the paleoecology of fossil mammals based on infraorbital foramen size. Anat Rec 291(10):1221–1226
- Muchlinski MN, Wible JR, Corfe I et al (2020) Good vibrations: The evolution of whisking in small mammals. Anat Rec 303(1):89–99
- Neville KR, Haberly LB (2004) Olfactory cortex. In: Shepherd GM (ed) The synaptic organization of the brain. Oxford University Press, New York, pp 415–454
- Nieuwenhuys RHJ, ten Donkelaar HJ, Nicholson C (1998) The central nervous system of vertebrates. Springer, Berlin/Heidelberg
- Niimura Y (2009) On the origin and evolution of vertebrate olfactory receptor genes: comparative genome analysis among 23 chordate species. Genome Biol Evol 1:34–44
- Niimura Y (2012) Olfactory receptor multigene family in vertebrates: from the viewpoint of evolutionary genomics. Curr Genom 13:103–114
- Niimura Y, Nei M (2005) Evolutionary dynamics of olfactory receptor genes in fishes and tetrapods. Proc Natl Acad Sci 102(17):6039–6044
- Niimura Y, Nei M (2006) Evolutionary dynamics of olfactory and other chemosensory receptor genes in vertebrates. J Hum Genet 51(6):505–517
- Niimura Y, Matsui A, Touhara K (2014) Extreme expansion of the olfactory receptor gene repertoire in African elephants and evolutionary dynamics of orthologous gene groups in 13 placental mammals. Genome Res 24(9):1485–1496
- Northcutt RG (2001) Changing views of brain evolution. Brain Res Bull 55(6):663–674

- Olson EC (1944) Origin of mammals based upon cranial morphology of the therapsid suborders. *Geol Soc Amer Spec Pap* 55:1–130
- Olson EC (1959) The evolution of mammalian characters. *Evolution* 13:344–353
- Olson EC (1966) Community evolution and the origin of mammals. *Ecology* 47(2):291–302
- Osborn JW (1984) From reptile to mammal: evolutionary considerations of the dentition with emphasis on tooth attachment. *Symp Zool Soc Lond* 52:549–574
- Osborn JW, Crompton AW (1978) The evolution of mammalian from reptilian dentitions. *Breviora* 399:1–18
- Parsons TS (1967) Evolution of the nasal structure in the lower tetrapods. *Amer Zool* 7:397–413
- Pavanatto AE, Kerber L, Dias da Silva S (2019) Virtual reconstruction of cranial endocasts of traversodontid cynodonts (Eucynodontia: Gomphodontia) from the upper Triassic of Southern Brazil. *J Morph* 280(9):1267–1281
- Pihlström H, Fortelius M, Hemilä S et al (2005) Scaling of mammalian ethmoid bones can predict olfactory organ size and performance. *Proc B Royal Soc* 272:957–962
- Presley R (1981) Alisphenoid equivalents in placentals, marsupials, monotremes and fossils. *Nature* 294:668–670
- Quiroga JC (1979) The brain of two mammal-like reptiles (Cynodontia – Therapsida). *J Hirnforsch* 20:341–350
- Quiroga JC (1980) The brain of the mammal-like reptile *Probainognathus jenseni* (Therapsida, Cynodontia), a correlative paleo-neurological approach to the neocortex at the reptile-mammal transition. *J Hirnforsch* 21:299–336
- Quiroga JC (1984) The endocranial cast of the advanced mammal-like reptile Therioherpeton *cargnini* (Cynodontia – Therapsida) from the middle Triassic of Brazil. *J Hirnforsch* 25:285–290
- Rakic P (1988) Specification of cerebral cortical areas. *Science* 241:170–176
- Rakic P (2000) Radial unit hypothesis of neocortical expansion. In: Bock G, Cardew G (eds) *Evolutionary developmental biology of the cerebral cortex*. Novartis found sympos chichester. Wiley, New York, pp 30–52
- Rakic P (2007) The radial edifice of cortical architecture: from neuronal silhouettes to genetic engineering. *Brain Res Rev* 55(2):204–219
- Rakic P (2009) Evolution of the neocortex: a perspective from developmental biology. *Nature Rev Neurosci* 10:724–735
- Remple MS, Henry EC, Catania KC (2003) Organization of somatosensory cortex in the laboratory rat (*Rattus norvegicus*): evidence for two lateral areas joined at the representation of the teeth. *J Comp Neurol* 467(1):105–118
- Ren T, He W, Gillespie PG (2011) Measurement of cochlear power gain in the sensitive gerbil ear. *Nat Comm* 2(1):1–7
- Rodrigues PG, Ruf I, Schultz CL (2013) Digital reconstruction of the otic region and inner ear of the non-mammalian cynodont *Brasilitherium riograndensis* (Late Triassic, Brazil) and its relevance to the evolution of the mammalian ear. *J Mammal Evol* 20(4):291–307
- Rodrigues PG, Ruf I, Schultz CL (2014) Study of a digital cranial endocast of the non-mammaliaform cynodont *Brasilitherium riograndensis* (Late Triassic, Brazil) and its relevance to the evolution of the mammalian brain. *Paläontol Z* 88:329–352
- Rodrigues PG, Martinelli AG, Schultz CL et al (2019) Digital cranial endocast of *Riograndia guaibensis* (Late Triassic, Brazil) sheds light on the evolution of the brain in non-mammalian cynodonts. *Hist Biol* 31(9):1195–1212
- Rolls ET, Grabenhorst F (2008) The orbitofrontal cortex and beyond: from affect to decision-making. *Prog Neurobiol* 86:216–244
- Romer AS (1956) *Osteology of the reptilia*. University of Chicago Press, Chicago
- Romer AS (1966) *Vertebrate paleontology*. University of Chicago Press, Chicago
- Romer AS (1970) The Chanares (Argentina) Triassic reptile fauna: 6. A chiniquodontid cynodont with an incipient squamosal-dentary jaw articulation. *Breviora* 344:1–18
- Romer AS, Edinger T (1942) Endocranial casts and brains of living and fossil Amphibia. *J Comp Neurol* 77(2):355–389

- Romer AS, Price LW (1940) Review of the pelycosauria. *Geol Soc Amer Spec Pap* 28:1–534
- Rowe TB (1988) Definition, diagnosis and origin of Mammalia. *J Vertebr Paleontol* 8(3):241–264
- Rowe TB (1993) Phylogenetic systematics and the early history of mammals. In: Szalay FS, Novacek MJ, McKenna MC (eds) *Mammalian phylogeny*. Springer, New York, pp 129–145
- Rowe TB (1996a) Coevolution of the mammalian middle ear and neocortex. *Science* 273:651–654
- Rowe TB (1996b) Brain heterochrony and evolution of the mammalian middle ear. In: Ghiselin MG, Pinna, G (eds) *New perspectives on the history of life*. Calif Acad Sci Memoir 20:71–96
- Rowe TB (2004) Chordate phylogeny and development. In: Cracraft J, Donoghue MJ (eds) *Assembling the tree of life*. Oxford University Press, Oxford/New York, pp 384–409
- Rowe TB (2020a) The emergence of mammals. In: Kaas JA (ed) *Evolutionary neurosciences*, 2nd edn. Elsevier, New York, pp 263–319
- Rowe TB (2020b) Mammalia. In: de Queiroz K, Cantino PD, Gauthier JA (eds) *Phylonyms: a companion to the PhyloCode*. CRC Press, Boca Raton, pp 841–847
- Rowe TB (2020c) Pan-Mammalia. In: de Queiroz K, Cantino PD, Gauthier JA (eds) *Phylonyms: a companion to the PhyloCode*. CRC Press, Boca Raton, pp 783–791
- Rowe TB (2020d) Therapsida. In: de Queiroz K, Cantino PD, Gauthier JA (eds) *Phylonyms: a companion to the PhyloCode*. CRC Press, Boca Raton, pp 797–808
- Rowe TB (2020e) Cynodontia. In: de Queiroz K, Cantino PD, Gauthier JA (eds) *Phylonyms: a companion to the PhyloCode*. CRC Press, Boca Raton, pp 813–823
- Rowe TB (2020f) Mammaliaomorpha. In: de Queiroz K, Cantino PD, Gauthier JA (eds) *Phylonyms: a companion to the PhyloCode*. CRC Press, Boca Raton, pp 825–831
- Rowe TB (2020g) Mammaliaformes. In: de Queiroz K, Cantino PD, Gauthier JA (eds) *Phylonyms: a companion to the PhyloCode*. CRC Press, Boca Raton, pp 833–839
- Rowe TB, Shepherd GM (2016) The role of ortho-retronasal olfaction in mammalian cortical evolution. *J Comp Neurol* 524:471–495. <https://doi.org/10.1002/cne.23802>
- Rowe TB, Carlson W, Bortorff W (1995) *Thrinaxodon*: digital atlas of the skull. CD-ROM, 2nd edn. University of Texas Press, Austin
- Rowe TB, Eiting TP, Macrini TE et al (2005) Organization of the olfactory and respiratory skeleton in the nose of the gray short-tailed Opossum *Monodelphis domestica*. *J Mammal Evol* 12:303–336
- Rowe TB, Rich TH, Vickers-Rich P et al (2008) The oldest *Platypus*, and its bearing on divergence timing of the *Platypus* and *Echidna* Clades. *PNAS* 105:1238–1242
- Rowe TB, Macrini TE, Luo Z-X (2011) Fossil evidence on origin of the mammalian brain. *Science* 332:955–957. <https://doi.org/10.1126/science.1203117>
- Rowe TB, Wallace RVS, Bhullar BAS (2020) Monotremata. In: de Queiroz K, Cantino PD, Gauthier JA (eds) *Phylonyms: a companion to the PhyloCode*. CRC Press, Boca Raton, pp 833–839
- Rubenstein JL, Rakic P (1999) Genetic control of cortical development. *Cereb Cortex* 9(6):521–523
- Rubidge BS, Sidor CA (2001) Evolutionary patterns among Permo-Triassic therapsids. *Ann Rev Ecol Syst* 32:449–480
- Schlosser G (2010) Making senses: development of vertebrate cranial placodes. *Int Rev Cell Mol Biol* 283:129–234
- Schlosser T (2017) Evolution of neural crest and cranial placodes. In: Kaas JA (ed) *Evolution of nervous systems*, vol 1. Elsevier, New York, pp 25–36
- Schneider MR, Schmidt-Ullrich R, Paus R (2009) The hair follicle as a dynamic miniorgan. *Curr Biol* 19(3):R132–R142
- Sengel P (1976) *Morphogenesis of skin*. Cambridge University Press, Cambridge
- Shepherd GM (1991) Computational structure of the olfactory system. In: Eichenbaum HM, Davis J (eds) *Olfaction: a model for computational neuroscience*. MIT Press, Cambridge, MA, pp 3–42
- Shepherd GM (2004) The human sense of smell: are we better than we think? *PLoS Biol* 2:e146
- Shepherd GM (2006) Smell images and the flavour system in the human brain. *Nature* 444:316–321
- Shepherd GM (2011) The microcircuit concept applied to cortical evolution: from three-layer to six-layer cortex. *Front Neuroanat* 5(30):1–15

- Shepherd GM (2012) *Neurogastronomy: how the brain creates flavor and why it matters*. Columbia University Press, New York
- Shepherd GM, Rowe TB (2017) Neocortical lamination: insights from neuron types and evolutionary precursors. *Front Neuroanat* 11:100. <https://doi.org/10.3389/fnana.2017.00100>
- Shepherd GM, Rowe TB, Greer CA (2021) An evolutionary microcircuit approach to the neural basis of high dimensional sensory processing in olfaction and vision. *Front Cell Neurosci* 15(658480):1–23
- Sidor CA (2001) Simplification as a trend in synapsid cranial evolution. *Evolution* 55:1419–1442
- Sidor CA (2003) The naris and palate of *Lycaenodon longiceps* (*Therapsida: Biarmosuchia*), with comments on their early evolution in the Therapsida. *J Paleontol* 77:977–984
- Sidor CA, Hancox PJ (2006) *Elliotherium kersteni*, a new tritheledontid from the Lower Elliot Formation (Upper Triassic) of South Africa. *J Vert Paleontol* 80:333–342
- Small DM, Bender G, Veldhuizen MG et al (2007) The role of the human orbitofrontal cortex in taste and flavor processing. *Ann NY Acad Sci* 1121:136–151
- Streidter GF (2005) *Principles of brain evolution*. Sinauer, Sunderland
- Streidter GF, Northcutt G (2020) *Brains through time – a natural history of vertebrates*. Oxford University Press, Oxford
- Taylor CR (1977) Exercise and environmental heat loads: different mechanisms for solving different problems? *Internat Rev Physiol* 15:119–145
- Ten-Cate AR (1969) The mechanism of tooth eruption. In: Melcher AH, Bowen WH (eds) *Biology of the Periodontium*. Academic, New York, pp 91–103
- Ten-Cate AR (1997) The development of the periodontium—a largely ectomesenchymally derived unit. *Periodontology* 2000 13(1):9–19
- Trulsson M (2006) Sensory motor function of human periodontal mechanoreceptors. *J Oral Rehabil* 33(4):262–273
- Trulsson M, Francis ST, Bowtell R et al (2010) Brain activations in response to vibrotactile tooth stimulation: a psychophysical and fMRI study. *J Neurophysiol* 104(4):2257–2265
- Ulinski PS (1983) *Dorsal ventricular ridge: a treatise on forebrain organization in reptiles and birds*. Wiley, New York
- Van Valkenburgh B, Theodor J, Friscia A et al (2004) Respiratory turbinates of canids and felids: A quantitative comparison. *J Zool* 264:1–13
- Wagner G (2014) *Homology, genes, and evolutionary innovation*. Princeton University Press, Princeton
- Wakefield MJ, Anderson M, Chang E et al (2008) Cone visual pigments of monotremes: filling the phylogenetic gap. *Visual Neurosci* 25(3):257–264
- Wallace RVS (2018) *A new close mammal relative and the origin and evolution of the mammalian central nervous system*. Dissertation, University of Texas at Austin
- Wallace RVS, Martínez R, Rowe T (2019) First record of a basal mammalian morph from the early Late Triassic Ischigualasto Formation of Argentina. *PLoS ONE* 14(8):e0218791. <https://doi.org/10.1371/journal.pone.0218791>
- Walls GL (1942) *The vertebrate eye and its adaptive radiation*. Hafner Publishing Company, New York
- Wang Y, Hu Y, Meng J et al (2001) An ossified Meckel's cartilage in two Cretaceous mammals and origin of the mammalian middle ear. *Science* 294:357–361
- Wang Z, Pascual-Anaya J, Zadissa A et al (2013) The draft genomes of soft-shell turtle and green sea turtle yield insights into the development and evolution of the turtle-specific body plan. *Nat Genet* 45(6):701–706
- Weisbecker V, Rowe TB, Wroe S et al (2021) Global elongation and high shape flexibility as an evolutionary hypothesis of accommodating mammalian brains into skulls. *Evolution* 75(3):625–640
- Wilson DA, Stevenson RJ (2006) *Learning to smell - olfactory perception from neurobiology to behavior*. Johns Hopkins University Press, Baltimore

- Witmer L (1995) The extant phylogenetic bracket and the importance of reconstructing soft tissues in fossils. In: Thomason J (ed) *Functional morphology in vertebrate paleontology*. Cambridge University Press, Cambridge, pp 19–33
- Yohe LR, Fabbri M, Hanson M et al (2020) Olfactory receptor gene evolution is unusually rapid across Tetrapoda and outpaces chemosensory phenotypic change. *Curr Zool* 66(5):505–514
- Young JM, Massa HF, Hsu L, Trask BJ (2010) Extreme variability among mammalian V1R gene families. *Genome Res* 20(1):10–18
- Zelená J (1994) *Nerves and mechanoreceptors: the role of innervation in the development and maintenance of mammalian mechanoreceptors*. Springer, Dordrecht
- Zhou Y, Shearwin-Whyatt L, Li J et al (2021) Platypus and echidna genomes reveal mammalian biology and evolution. *Nature* 2021(1). <https://doi.org/10.1038/s41586-020-03039-0>

Chapter 11

Evolution of the Brain and Sensory Structures in Metatherians



Thomas E. Macrini, Michael Leary, and Vera Weisbecker

11.1 Marsupial Origins, Diversity, and Phylogenetic Relationships

11.1.1 Marsupial Biogeography

The marsupials are a clade of mammals comprising around 375 (Voss and Jansa 2021) mostly South American and Australian living species and their most recent ancestor. “Marsupialia” is a “crown clade”, a term applied to a group of living species and their last common ancestor. Marsupialia is embedded in the larger “stem clade” of Metatherians, which includes mammals that are more closely related to living marsupials than to other species but do not share the common ancestor with extant species (Williamson et al. 2014). We note this here because “Marsupialia” and “Metatheria” are sometimes erroneously used interchangeably (see Weisbecker and Beck 2015).

Although marsupials are a Southern Hemisphere radiation, probably originating in South America (e.g. Eldridge et al. 2019), their metatherian origins are probably in Laurasia (the northern-hemisphere supercontinent including North America, Europe, and Asia). The location of the earliest metatherians within Laurasia is unknown because of a large gap in the fossil record (Bi et al. 2018; Eldridge et al. 2019), but is generally estimated to have occurred between 125 and 160 million years ago (Eldridge et al. 2019).

T. E. Macrini (✉) · M. Leary
Department of Biological Sciences, St. Mary’s University, San Antonio, TX, USA
e-mail: tmacrini@stmarytx.edu

V. Weisbecker (✉)
College of Science and Engineering, Flinders University, Bedford Park, SA, Australia
e-mail: vera.weisbecker@flinders.edu.au

Laurasian metatherians of the Late Cretaceous spread across North America, Europe, Asia and even Africa before going extinct in the Miocene. While they appear to have been very diverse and morphologically disparate locally (Williamson et al. 2014; Maga and Beck 2017), their early diversity is difficult to assess because of a poor fossil record (Bennett et al. 2018). Metatherians, including the ancestor of marsupials, are thought to have entered South America around the K-PG boundary and probably evolved exclusively in Gondwana (the southern-hemisphere supercontinent including South America, Antarctica, and Australia; reviewed in (Voss and Jansa 2021)). Sadly, we only have a few tantalising cues as to how marsupials radiated across Gondwana, owing to difficulties of obtaining fossils from Antarctica (Gelfo et al. 2019). However, by the late Cretaceous, Gondwana had all but broken apart and South America was probably fully isolated from the remainder of Antarctica (Reguero and Goin 2021). This deep separation is also reflected in the split of living marsupials into two major groups, the American Ameridelphia and the mostly Australian Australidelphia. There is a single Australidelphian in South America, the Monito del Monte (*Dromiciops gliroides*); the ongoing debate as to how this can be explained (Nilsson et al. 2010; Eldridge et al. 2019) serves to remind us of how little we know of the radiation events of marsupials in Gondwana.

South American and Australian marsupials separately re-entered the northern hemisphere in two relatively recent events. Marsupials migrated to North America roughly 2.8 million years ago as part of the Great American Biotic Interchange, a biogeographically momentous meeting of the northern and southern American subcontinents. Most of these species stayed in the very south of the North American subcontinent, although the Virginia opossum has famously become widely distributed in North America even in very recent times (Voss and Jansa 2021). The Asian distribution of marsupials is restricted to New Guinea east of Wallace's line. The relationship between Australian and New Guinean marsupial faunas is complicated and marred by a lack of understanding on past connectivity. However, it was probably marked by multiple migration events of diverse antiquity since the Miocene (Mitchell et al. 2014).

11.1.2 Marsupial Diversity

Living marsupials are far less taxonomically diverse than placentals, with the most recent tally standing at 375 species (Voss and Jansa 2021) compared to over 5000 extant species of placentals (Wilson and Reeder 2005). Marsupial species are distributed in seven orders of very variable size and ecology (see Fig. 11.1).

The two main radiations of Australidelphia and Ameridelphia differ drastically in their diversity. Ameridelphians include seven species of Paucituberculata, or shrew opossums. These are unusual in having procumbent lower incisors like the unrelated diprotodontian marsupials, giving rise to much debate as to how diprotodonty relates to marsupial phylogenetic relationships (summarized in Weisbecker and Beck 2015). The other living ameridelphian order is the diverse Didelphimorphia,

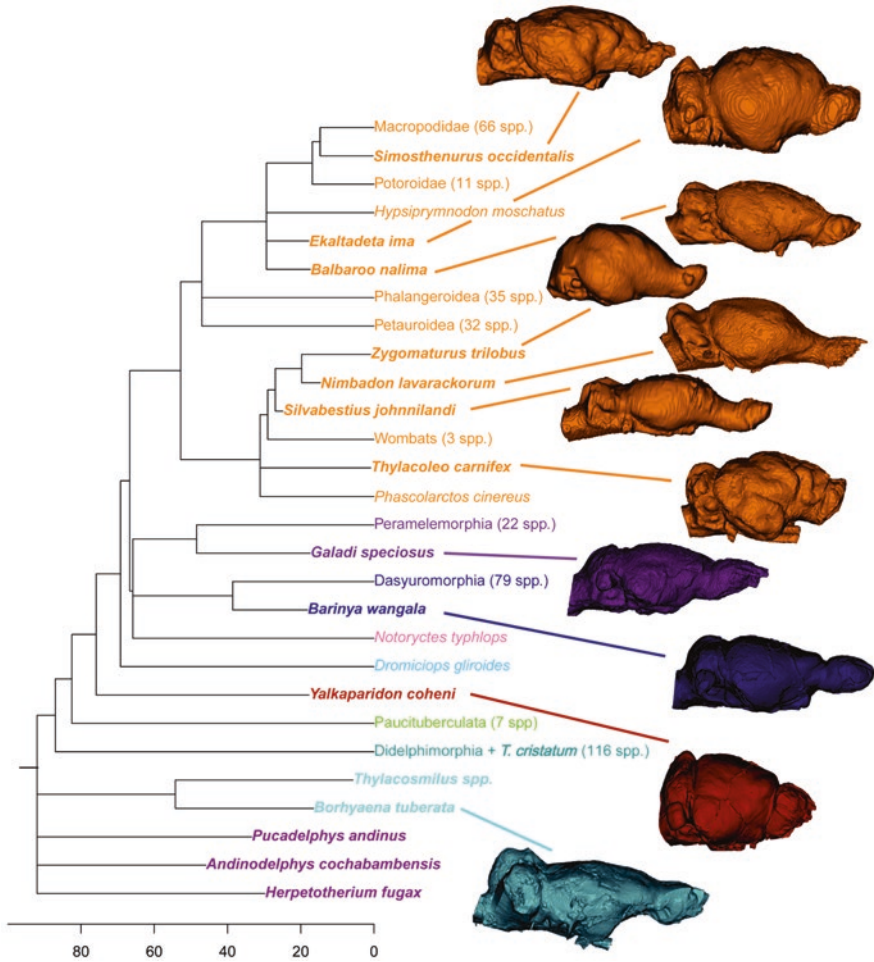


Fig. 11.1 Phylogeny of living marsupial orders of major diprotodontian clades, including species numbers of extant species from Voss and Jansa (2021). Species in bold are extinct. The time scale for most species is derived from the phylogeny used in Weisbecker et al. (2021), with addition of timing for the Metatherians *incertae sedis* and *Thylacosmilus* species from Eldridge et al. (2019)

or opossums, which occupy a variety of ecological niches particularly in Southern and Central America (Voss and Jansa 2021). Didelphimorphians also include the only semi-aquatic marsupial, the Yapok or water opossum. Australidelphians include the South American *Dromiciops gliroides* (see above) but all other Australidelphians are Australian. They include the carnivorous/insectivorous Dasyuromorphia, which contain many small insectivores but also large iconic species such as the Tasmanian devil and tiger; the omnivorous Peramelemorphia, or bilbies and bandicoots; the Notoryctemorphia, with two highly derived, eyeless

species of burrowing marsupial mole; and the large and diverse order of Diprotodontia, encompassing kangaroos, wombats, koalas, and possums.

While today's marsupials are ecologically quite diverse, the fossil record holds several extinct morphologically and ecologically unusual forms. These include the enigmatic, carnivorous marsupial sabretooth tiger *Thylacosmilus ferox* from the South American Pliocene; the probably hopping (Abello and Candela 2020) argyrolagids that survived in South America until the Pliocene; and the large-bodied Australian vombatiform megafaunal radiation, which include wombat relatives such as the ferocious *Thylacoleo carnifex* (or “marsupial lion”), and the biggest-ever marsupial, the roughly 3-ton (Wroe et al. 2004) *Diprotodon optatum*.

11.1.3 Are Marsupials Representative of a Small-Brained, Primitive Mammalian Ancestor?

The relevance of marsupials in research on mammalian brain evolution has long been diminished by the prejudice that marsupials represent a less advanced stage of mammalian evolution compared to placentals. This prejudice goes back to Charles Darwin and even before (reviewed in Weisbecker 2015). Ironically, the chief reason for the assumption of marsupial “primitiveness” turned out to be a developmental trajectory that in fact seems to be highly derived (Weisbecker 2011). Marsupial mammals are born after very short gestation times, and at minute sizes (between a rice grain and a jelly bean). The tiny marsupial neonates all need to actively move towards the pouch and attach to the teat unaided (Gemmell et al. 2002). This is reflected in well-developed neonatal forelimb (Weisbecker et al. 2008) and jaw (Sánchez-Villagra et al. 2008) bones, whereas hind limbs (Weisbecker et al. 2008) and the brain (Smith 2006) develop more slowly and mostly postnatally. It is currently debated whether this developmental peculiarity reduces the ability of the marsupial limb and skull to evolve into the same level of morphological disparity (Bennett and Goswami 2013; Sánchez-Villagra 2013; Garland et al. 2017; Martín-Serra and Benson 2020; Fabre et al. 2021; Pevsner et al. 2022).

Since the dawn of western research into marsupial biology, the development of marsupials was singled out as the reason for supposed anatomical and cognitive inferiority (Owen and Carlisle 1834). This was later compounded by Portman's widely-cited work on bird brain size (Portman 1947), which associated a bird's evolutionary “niveau” (“level”) with the maturity of hatchlings. This interpretation influenced Fabiola Müller's (Müller 1969) conclusion that the immature neonates of the marsupials would also result in a lower evolutionary stage of their brains. Müller's argumentation was a major factor in the persistent stereotype (e.g. by Lillegraven et al. 1987) that the marsupial brain was unable to reach the same level of brain size relative to body mass (“encephalization”) compared to placental mammals. It probably also did not help that most mid-late twentieth century studies on marsupial brain anatomy were on *Didelphis virginiana*, the Virginia opossum (see

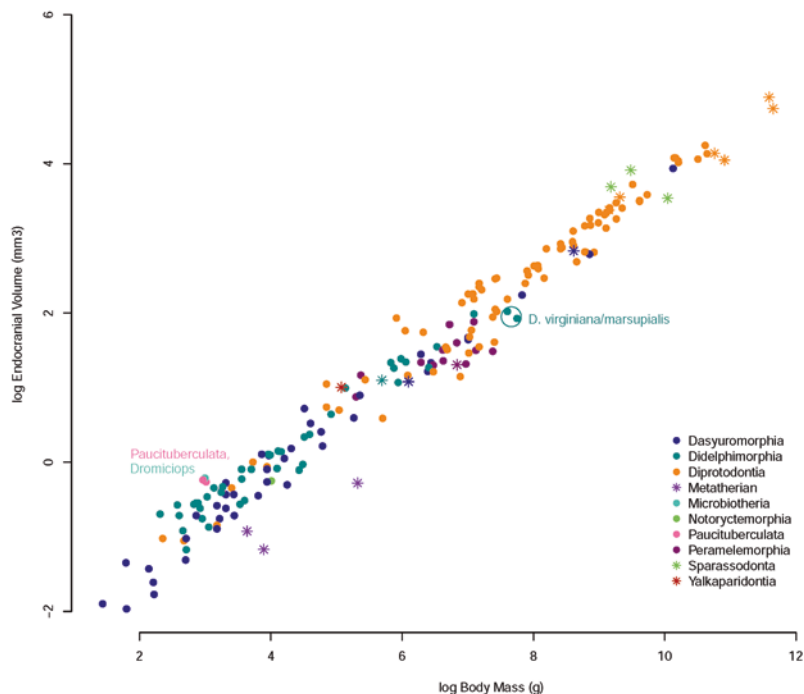


Fig. 11.2 Log endocranial volume vs log body mass in 194 species of marsupials, including 18 extinct species (the coloration corresponds with the phylogeny in Fig. 11.1). “Metatherian” designates three metatherians “*incertae sedis*” (Eldridge et al. 2019). Endocranial volume and body mass data for the fossil specimens are presented in Table 11.1

Johnson 2012 for a comprehensive bibliography on the marsupial central nervous system). As the only marsupial in the USA, the Virginia opossum was probably the most available marsupial until its gradual replacement by the more easily bred relative, the gray short-tailed opossum (*Monodelphis domestica*; Saunders et al. 1989; Macrini 2004). *D. virginiana* is among the smaller-brained marsupials for their body mass (Fig. 11.2; Pirlot 1981; Nelson and Stephan 1982), which would have further served to prejudice “western” science against marsupial mammals as a whole.

The idea that marsupials reflect ancestral mammalian brain organization survives in the more recent literature (but see Dos Santos et al. 2017). However, the adult marsupial brain appears fundamentally similar to placentals (for a summary of anatomical differences see Sect. 11.4.4), for example in the contexts of relative brain size (Weisbecker and Goswami 2010; Smaers et al. 2021), histological structure and development (Ashwell 2010c, 2015; Johnson 2012; Ashwell and Shulruf 2016; Suárez et al. 2018; Jyothilakshmi et al. 2020), and cellular scaling (Dos Santos et al. 2017).

Table 11.1 Endocranial volume (ECV) and body mass data for fossil crown marsupials and stem marsupials based on data from the literature

Species	Clade	ECV	Body Mass	ECV reference	Body mass reference
<i>Balbaroo nalima</i>	Diprotodontia	9400	29.257	Weisbecker et al. (2021)	Travouillon et al. (2009)
<i>Barinya wangala</i>	Dasyuromorphia	445	2.941	Weisbecker et al. (2021)	Travouillon et al. (2009)
<i>Borhyaena tuberosa</i>	Sparassodonta	23,000	34.324	Weisbecker et al. (2021)	Argot (2003)
<i>Ekaltadeta ima</i>	Diprotodontia	11,100	34.845	Weisbecker et al. (2021)	Travouillon et al. (2009)
<i>Galadi speciosus</i>	Peramelemorphia	929	3.687	Weisbecker et al. (2021)	Travouillon et al. (2009)
<i>Nimbacinus dicksoni</i>	Dasyuromorphia	5500	17.022	Weisbecker et al. (2021)	Travouillon et al. (2009)
<i>Nimbadon lavarackorum</i>	Diprotodontia	54,800	57.245	Weisbecker et al. (2021)	Black et al. (2012)
<i>Silvabestius johnlandi</i>	Diprotodontia	46,960	62.733	Weisbecker et al. (2021)	Travouillon et al. (2009)
<i>Simosthenurus occidentalis</i>	Diprotodontia	115,000	114.331	Weisbecker et al. (2021)	Turney et al. (2008)
<i>Thylacoleo carnifex</i>	Diprotodontia	108,000	133.105	Weisbecker et al. (2021)	Wroe et al. (1999)
<i>Yalkaparidon coheni</i>	Yalkaparidontia	160	2.729	Weisbecker et al. (2021)	Travouillon et al. (2009)
<i>Zygomaturus trilobus</i>	Diprotodontia	589,000	376.859	Weisbecker et al. (2021)	Sharp (2016)
<i>Herpotherium fugax</i>	Metatherian	38 ^b	0.397	Horovitz et al. (2008)	Unpublished ^a
<i>Pucadelphys andinus</i>	Metatherian	49 ^b	0.311	Macrini et al. (2007a)	Macrini et al. (2007a)
<i>Andinodelphys cochabambensis</i>	Metatherian	205 ^b	0.758	de Muizon and Ladevèze (2020)	de Muizon and Ladevèze (2020)
<i>Thylacosmilus atrox</i>	Sparassodonta	9702	40	Quiroga and Dozo (1988)	Quiroga and Dozo (1988)
<i>Thylacosmilus atrox</i>	Sparassodonta	13,117	50	Quiroga and Dozo (1988)	Quiroga and Dozo (1988)
<i>Thylatheridium cristatum</i>	Didelphimorphia	297	3	Dozo (1989)	Dozo (1989)

ECV data are presented in cm³ and body mass data in g. ^aBody mass of *Herpotherium fugax* was estimated using the skull length of MB.Ma.50671 of 29.44 mm (Horovitz et al. 2008) and Myers' (2001) equation. ^bNote that the ECVs of the three metatherians are potentially underestimates, and should not be used without this caveat in quantitative analysis

Acknowledging this fundamental comparability of marsupial and placental brains is important because it emphasizes the role of marsupial brain evolution as a

useful contrast to the more widely studied placental mammals. Marsupials are also a particularly tractable group because they are a phylogenetically very well-resolved, ecologically diverse radiation of mammals on which most standard hypotheses of sensorimotor or cognitive association of neuroanatomy can be tested (Weisbecker 2015).

11.2 Historical Background

11.2.1 *The Record of Endocranial Morphology and any Other Paleoneurological Approaches in the Group Under Study*

The paleoneurological record for Metatheria is rather sparse considering the longevity and fossil record of the group. However, natural and artificial endocasts from some South American species have been described. For example, two endocasts of *Thylacosmilus atrox* (Sparassodonta) from skulls from the Pliocene of Argentina were described by Quiroga and Dozo (1988). Dozo (1994) expanded the description of the endocasts of *Thylacosmilus atrox* and provided a description of the cranial endocast of *Borhyaena tuberata* (Sparassodonta) from the Miocene of Argentina.

The relatively recent use of high-resolution X-ray computed tomography (CT) has allowed for the study of the cranial cavities of additional stem marsupials (non-marsupial metatherians), and therefore, has advanced studies of the paleoneurology of Metatheria. *Pucadelphys andinus*, a Paleocene stem marsupial from Bolivia, is well represented by multiple skulls and postcranial elements (de Muizon 1992, 1998; Marshall and de Muizon 1995; Marshall and Sigogneau-Russell 1995). A digital cranial endocast was extracted from a CT scan of one of the skulls of *Pucadelphys* and described in comparison to extant marsupial cranial endocasts (Macrini et al. 2007a). A digital brain endocast was recently described for another early Paleocene stem marsupial from Bolivia, *Andinodelphys cochabambensis* (de Muizon and Ladevèze 2020).

Digital cranial endocasts were generated from CT images of a skull of *Herpetotherium fugax* from the White River Formation (Early Oligocene) of Wyoming (Sánchez-Villagra et al. 2007; Horovitz et al. 2008). The exact phylogenetic position of *Herpetotherium* is unclear with some analyses finding this taxon to be a stem marsupial just outside of the crown group (e.g. Sánchez-Villagra et al. 2007; Horovitz et al. 2009; Ladevèze et al. 2020), whereas others place it within crown Marsupialia (Wilson et al. 2016).

Relatively few descriptions of cranial endocasts of fossil crown marsupials were published prior to the 1970s (see Edinger 1975 for a list), to the point that Jerison (1973) largely skips over the group in his book. However, some fossils such as *Thylacoleo carnifex*, the marsupial lion, received attention in the literature with a description of an artificial cranial endocast (Woods 1956 and citations within).

More recently, Haight and Murray (1981) examined a latex cranial endocast of the Early Miocene marsupial *Wynyardia bassiana* from Tasmania and compared it to the external brain anatomy of extant marsupials. Cranial endocasts from two Miocene didelphids from Argentina (*Thylatheridium cristatum* and *Thylophorops chapalmalensis*) were described by Dozo (1989). Two natural limestone cranial endocasts of macropodoids from the early Eocene Riversleigh locality in northwestern Queensland were described by Kear (2003). One specimen was attributed to the kangaroo *Balbaroo*, and the other was found in isolation and cannot be confidently identified (Kear 2003).

Many studies of cranial endocasts of crown marsupials have relied heavily on extant taxa (e.g. Macrini et al. 2007a, b, c; Ashwell 2008; Weisbecker et al. 2021). Recently a study including two of us (V.W. and T.M.) Weisbecker et al. (2021) analyzed brain shape evolution in 57 species of marsupials including 45 extant species and 12 fossils.

Aside from endocasts, a wealth of potential information particularly on the locomotion and phylogenetic relationships (e.g. Schmelzle et al. 2007; Macrini et al. 2013) of metatherians can be gained from several reconstructions of the inner ear. Although no complete description of the inner ear of *Pucadelphys* has been published, reference is made to this region of the skull in the literature (de Muizon et al. 2018; de Muizon and Ladevèze 2020; Ladeveze et al. 2020). However, the digital inner ear endocasts were recently described for the sparassodont *Allqokirus australis* (de Muizon et al. 2018) and *Andinodelphys cochabambensis* (de Muizon and Ladevèze 2020), both from the Paleocene of Tiupampa, Bolivia. The digital inner ear endocasts were also described from CT images of a skull of *Herpetotherium fugax* (Sánchez-Villagra et al. 2007; Horovitz et al. 2008), and the inner ears of the European herpetotheriids (*Peratherium* and *Amphiperatherium*) were also recently described (Selva and Ladevèze 2017; Ladevèze et al. 2020). The inner ear of *Necrolestes patagonensis*, a possible metatherian from the Miocene of Argentina was described by Ladevèze et al. (2008); however, a more recent study suggests that *Necrolestes* belongs to a non-therian mammalian lineage, rather than a metatherian (Rougier et al. 2012). Digital endocasts of the inner ears of the sparassodonts *Thylacosmilus atrox*, *Borhyaena tuberata*, and *Sipalocyon gracilis* were recently reconstructed from CT imagery (Forasiepi et al. 2019).

Relatively few inner ear studies of fossil crown marsupials have been published, but see the description of the inner ear and petrosal morphology of *Mimoperadectes houdei* from early Eocene aged rocks of the Clark Fork Basin of Wyoming (Horovitz et al. 2009). *M. houdei* is considered a crown marsupial based on multiple phylogenetic analyses (Horovitz et al. 2009; Wilson et al. 2016). Similarly, Meng and Fox (1995) described the internal anatomy of isolated petrosal bones from the Bug Creek Anthills locality of Montana (Late Cretaceous) and reconstruct the inner ear anatomy based on radiography and scanning electron microscopy. A comparative study of marsupial bony labyrinths included the inner ear endocasts of *Diprotodon*, *Thylacoleo*, and a number of extant diprotodontians (Alloing-Séguier et al. 2013). Another study included a digital endocast of the inner ear of *Palaeotheres lemoinei*, a paucituberculatan marsupial from the Early Miocene of Patagonia (Forasiepi

et al. 2014). Studies of the inner ears of extant species are more common (Sánchez-Villagra and Schmelzle 2007; Schmelzle et al. 2007; Ekdale 2010; Berlin et al. 2013; Ashwell and Shulruf 2014). These reveal some evidence that inner ear morphology is associated with the locomotor mode of marsupials, but due to space constraints of this chapter, we will not go into much detail about the anatomy, evolution, and functionality of the inner ears of marsupials.

11.2.2 Problematics

While diverse separate aspects of marsupial brain anatomy have been studied in the past (see summary in Ashwell 2008), there has not been a comprehensive study of the comparative anatomy of the brain or central nervous system of marsupials. This would be an important contribution for coding morphological variation of the nervous system of marsupials into phylogenetic analyses of the group, as well as understanding the ecological and sensory motor correlates of anatomical variation.

Another glaring gap in our knowledge of the paleoneurology of marsupials is due to the lack of a temporally continuous record from fossil marsupials of Australia, with famous and rich faunas such as the Riversleigh locality yielding fossils from discrete but widely spaced time periods (but see Kear 2003). Digital cranial endocasts were recently extracted from CT data from some additional marsupial fossils (Weisbecker et al. 2021), but anatomical descriptions have not been published for these taxa. There is future work to be done in this area.

This review provides a summary and synthesis of previously published paleoneurological studies of marsupials and their closest extinct relatives (non-marsupial metatherians). We contribute a comprehensive dataset of endocranial volume and body masses for fossil and extant marsupials and non-marsupial metatherians.

11.3 Overview of General and Comparative Anatomy

11.3.1 Endocast Morphology

Unlike most other amniotes except birds, the mammalian brain resides in a fully ossified brain cavity so that the endocast is often easily reconstructed from CT-scanned fossils. This makes it easy to distinguish the overall shape of the brain, and identify broad divisions of the main brain regions - olfactory bulb, cerebrum, cerebellum, and brain stem as well as homologous sulci on the cerebrum (e.g. Macrini et al. 2007a, b, c; Weisbecker et al. 2021). However, the endocast of mammals is characterized not just by the brain; nerves, meninges, ganglia, veins and their sinuses, and arteries are also variably imprinted into the bones of the cranial vault. Compared to the brain of birds, which is tightly packed into the skull, the

outline of the mammalian brain is therefore not always easily apparent. For studies of phylogeny, this can be an asset because the course and topology of blood vessels and sinuses and nerves can provide important phylogenetic information. However, the fact that endocasts do not purely reflect the shape of the brain poses difficulties for the functional interpretation of endocast shape.

Although no comprehensive comparative studies of marsupial cranial endocasts or gross brain anatomy have been published, as previously mentioned, there are several studies dealing with specific marsupial groups and stem marsupials. Below we provide an anatomical description of the cranial endocast of a didelphid marsupial (*Caluromys philander*), which shows the relevant endocast traits very clearly, and make comparisons with endocasts from other marsupial groups based on published descriptions.

The skull of an adult *Caluromys philander*, the bare-tailed woolly opossum, (AMNH 95526) was CT scanned at the University of Texas High-Resolution X-Ray Computed Tomography Facility in Austin, TX. Details about the CT scanning of this specimen are provided by Macrini (2014). Digital segmentation and volume measurement of the cranial endocast were done using Amira (ver. 6; Thermo Fisher Scientific 2017) by M. L. following protocols described by Macrini (2009). Anatomical labels on Fig. 11.3 identify the names of brain and other soft tissue structures represented by the corresponding space on the endocast. This labelling convention is used to conserve space, but with the understanding that the actual soft tissue structures are not represented on an endocast.

In general, the cranial endocast of *Caluromys philander* (Fig. 11.3) more closely resembles the shape and form of an adult *Monodelphis domestica*, the gray short-tailed opossum, than that of *Didelphis virginiana*, the Virginia opossum (Macrini et al. 2007c). However, the cranial flexure reflected in the endocast of *C. philander* is more similar to that of *D. virginiana* (Macrini et al. 2007c). The endocranial volume (EV) for AMNH 95526 is 3.267 ml, a value that is intermediate between the EVs for adult *M. domestica* and *D. virginiana* (Macrini et al. 2007a, c). Compared to the endocasts from fossil taxa examined here (Figs. 11.4, 11.5, and 11.6), the endocast of *Caluromys* superficially resembles those of *Barinya wangala* and *Galadi speciosus*.

Forebrain In dorsal view, the endocast of *Caluromys philander* is pear-shaped with the cerebral hemisphere casts expanding more laterally than the cerebellar space, including the parafloccular lobes (Fig. 11.3). This form is similar to what is seen in the adult endocasts of *Monodelphis domestica* but unlike that of endocast of *Didelphis virginiana*, in which the parafloccular lobes extend well lateral of the cerebral hemispheres (Macrini et al. 2007c). A well-defined circular fissure separates the large olfactory bulbs from the rest of the brain similar to what is seen on endocasts of other didelphids, as well as all of the fossil taxa shown in Fig. 11.4, and other mammals. The median sulcus is clearly represented on the dorsal surface of the endocast of *C. philander*, as is the case for *M. domestica* (Macrini et al. 2007c), and it separates the lissencephalic cerebral hemisphere casts (Fig. 11.3). Casts of the transverse sinuses and prootic veins extend around the posterior border of the cer-

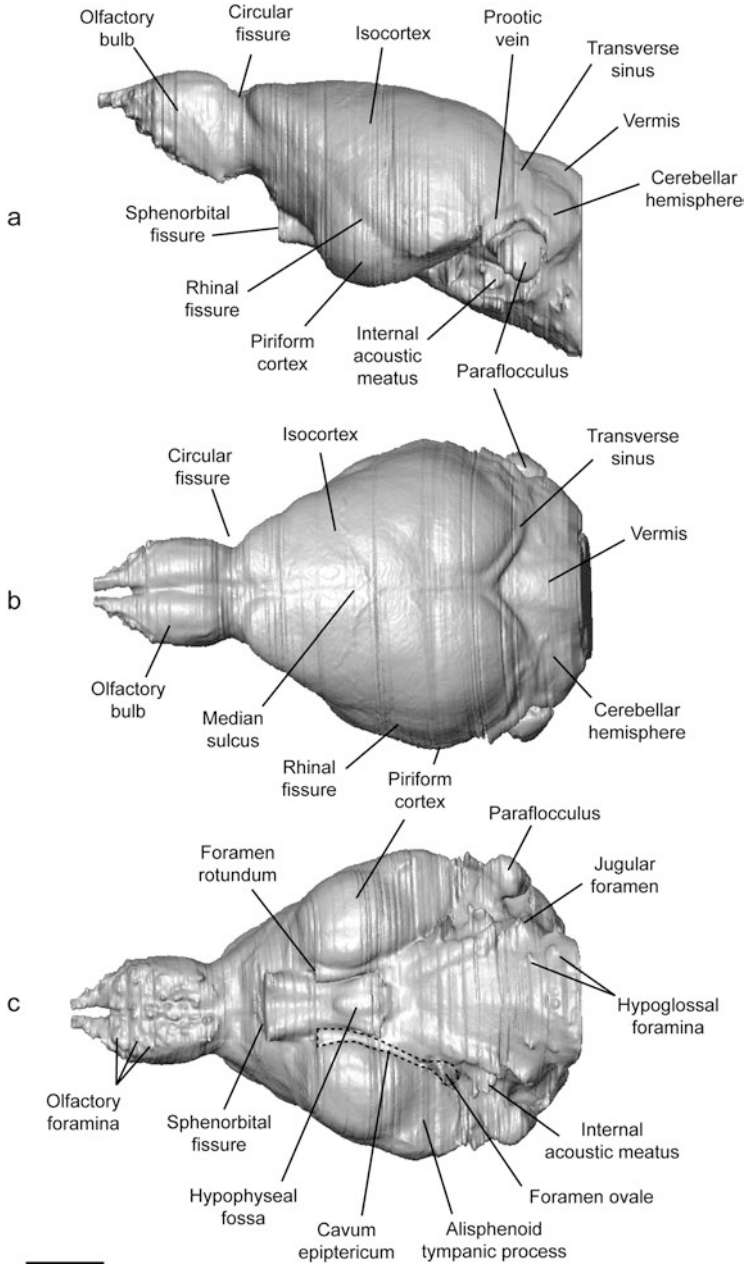


Fig. 11.3 Digital cranial endocast of *Caluromys philander*, the bare-tailed woolly opossum, (AMNH 95526) shown in (a), left lateral, (b), dorsal, and (c), ventral views. Scale bar equals 5 mm. See Macrini (2014) for details about the CT scanning of this specimen. Digital segmentation of the cranial endocast was done using Amira following protocols described by Macrini (2009)

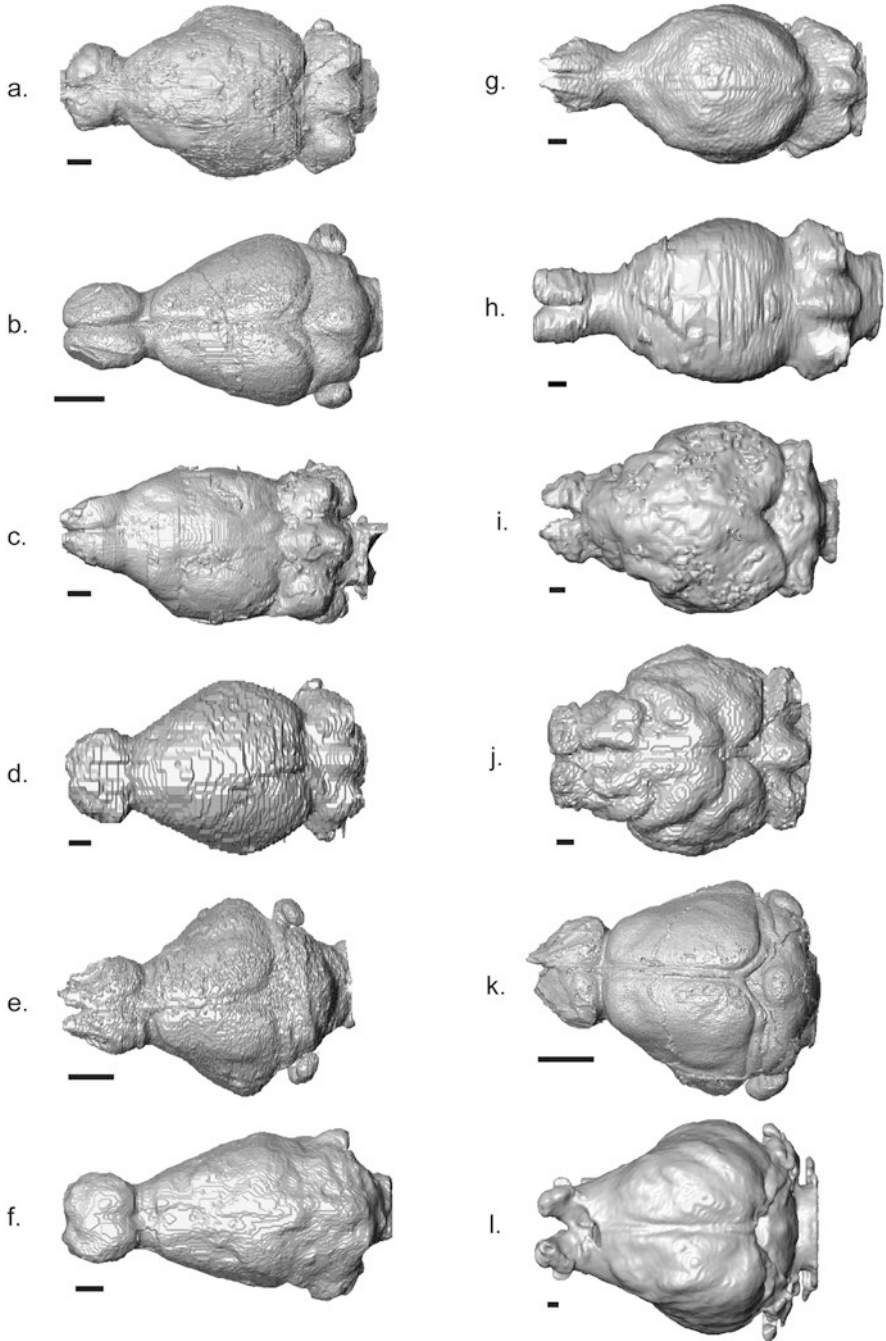


Fig. 11.4 Dorsal views of cranial endocasts from select fossil marsupials. Endocast data were previously published by Weisbecker et al. (2021). All scale bars equal 5 mm. (a). *Balbaroo nalima*

ebellar hemispheres of *C. philander* similar to what is seen in endocasts of *M. domestica* and *D. virginiana* (Macrini et al. 2007c). The rhinal fissure is seen in lateral view on the endocasts of *C. philander* (Fig. 11.3) and *D. virginiana*, but not in the smaller-brained didelphid *M. domestica* (Macrini et al. 2007c). The piriform cortex of the cerebrum is seen bulging in lateral view of the endocast of *C. philander* (Fig. 11.3), but similar to the rhinal fissure, the piriform lobe cannot be seen in lateral view in *M. domestica* (Macrini et al. 2007c).

On the ventral surface of the forebrain region of the endocast of *Caluromys philander* there is a groove between the right and left casts of the sphenorbital fissure canals (Fig. 11.3). *Monodelphis domestica* also shows this groove on its endocast but not as well defined as in *C. philander* (Fig. 11.3) or *Didelphis virginiana* (Macrini et al. 2007c). The hypophyseal fossa is not as well defined as in *M. domestica* or *D. virginiana* (Macrini et al. 2007c). The piriform lobes of the cerebrum bulge ventrally on the endocast of *C. philander* unlike what is seen in the other two didelphids (Macrini et al. 2007c). Finally, within the piriform cortex an indentation caused by the alisphenoid tympanic process is present on the endocasts of *C. philander* and *M. domestica*, but not in *D. virginiana* (Macrini et al. 2007c).

Midbrain/Hindbrain As in other didelphids and mammals, the cerebral hemispheres are expanded posteriorly to cover the dorsal surface of the midbrain (Fig. 11.3). The cerebral expansion combined with the prominent transverse sinuses completely obscures the tectum (e.g. superior and inferior colliculi) of the midbrain from being represented on the endocast of *Caluromys philander* (Fig. 11.3). Likewise, the tegmentum of the midbrain is not visible on the ventral surface of the endocast of *C. philander* as is the case in other marsupial and mammal endocasts.

The cerebellum is well represented on the endocast of *Caluromys philander* posterior to the cerebral hemispheres. Casts of the vermis, cerebellar hemispheres, and the paraflocculi of the cerebellum are well differentiated in dorsal and lateral views of the endocast (Fig. 11.3). The shape of the parafloccular casts of *C. philander* is more similar to that of *Monodelphis domestica*, but significantly different from the paraflocculi of *Didelphis virginiana* (Macrini et al. 2007c). The lobus anterior of the cerebellum is not visible on the dorsal surface of the endocast of *C. philander*, similar to the condition in *M. domestica* and in contrast to *D. virginiana*, in which this structure is visible on the endocast (Macrini et al. 2007c). The posteroventral surface of the endocast of *C. philander* preserves the hindbrain but there is no visible differentiation into brain structures such as the pons or medulla oblongata (Fig. 11.3). However, casts of various openings in the skull for transmission of cranial nerves are represented on the ventral hindbrain endocast. The internal acoustic meatus

←

Fig. 11.4 (continued) (QMF31408), (b). *Barinya wangala* (QMF36295), (c). *Borhyaena tuberosa* (YPMPU15120), (d). *Ekaltadeta ima* (QMF12436), (e). *Galadi speciosus* (QMF23393), (f). *Nimbacinus dicksoni* (QMF36357), (g). *Nimbadon lavarackorum* (QMF42677), (h). *Silvabestius johnnilandi* (QMF30504), (i). *Simosthenurus occidentalis* (SAMP1668), (j). *Thylacoleo carnifex* (SAM280507), (k). *Yalkaparidon coheni* (QMF13008), (l). *Zygomaturus trilobus* (QVM1992_GFV73)

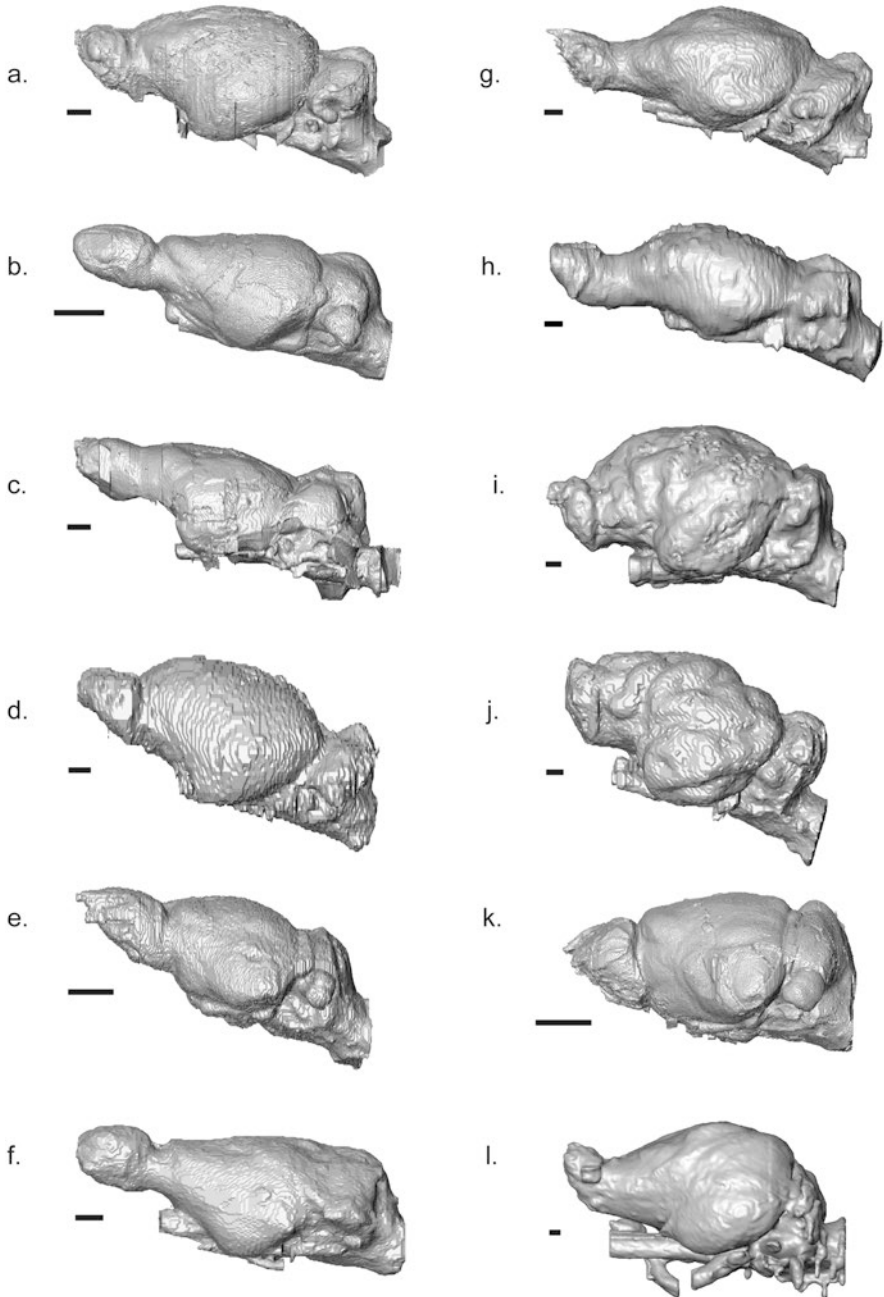


Fig. 11.5 Left lateral views of cranial endocasts from select fossil marsupials. Endocast data were previously published by Weisbecker et al. (2021). All scale bars equal 5 mm. (a), *Balbaroo nalima* (QMF31408), (b), *Barinya wangala* (QMF36295), (c), *Borhyaena tuberata* (YPMPU15120), (d), *Ekaltadeta ima* (QMF12436), (e), *Galadi speciosus* (QMF23393), (f), *Nimbacinus dicksoni* (QMF36357), (g), *Nimbadon lavarackorum* (QMF42677), (h), *Silvestrius johnnlandi* (QMF30504), (i), *Simosthenurus occidentalis* (SAMP1668), (j), *Thylacoleo carnifex* (SAM280507), (k), *Yalkaparidon coheni* (QMF13008), (l), *Zygomaturus trilobus* (QVM1992_GFV73)

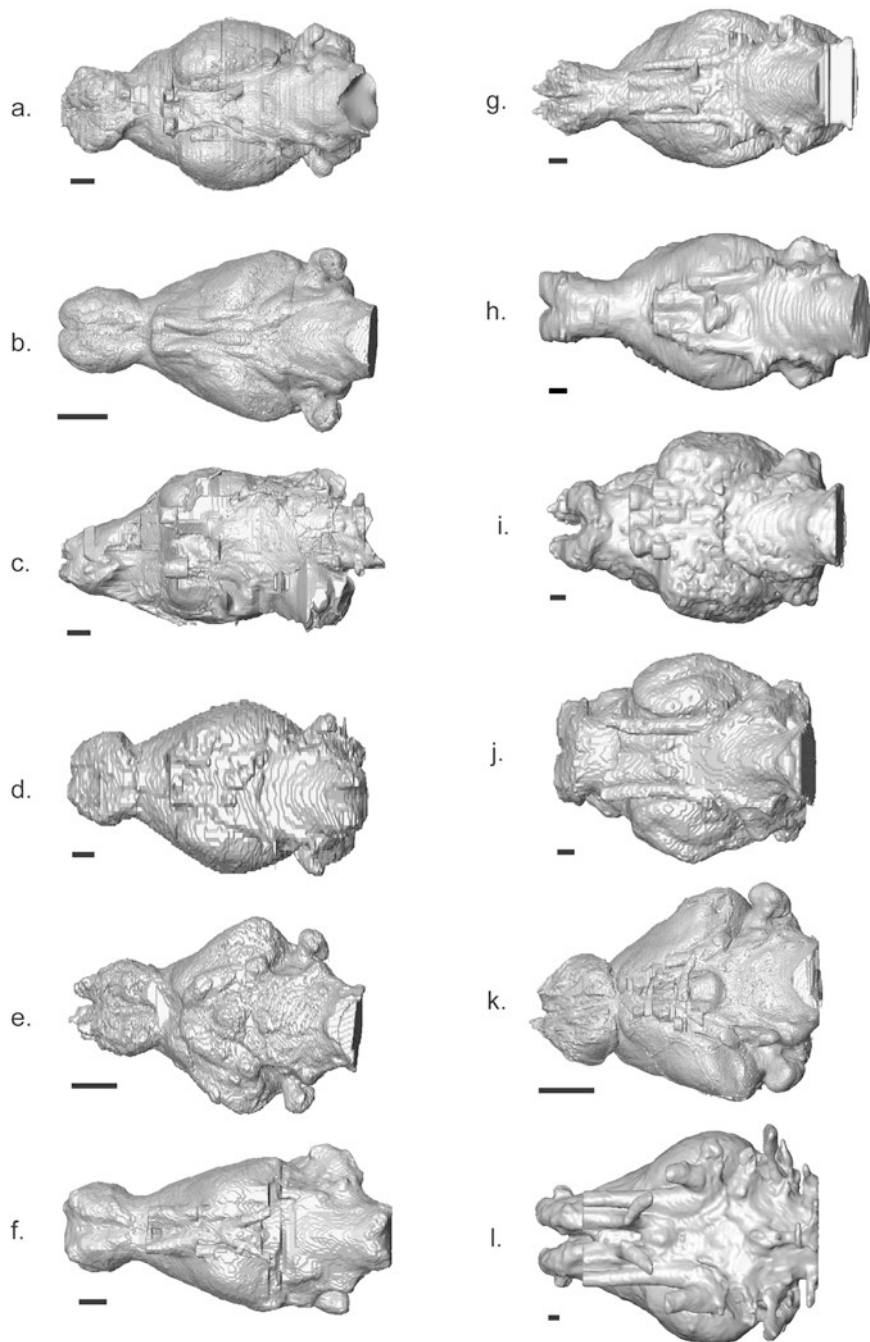


Fig. 11.6 Ventral views of cranial endocasts from select fossil marsupials. Endocast data were previously published by Weisbecker et al. (2021). All scale bars equal 5 mm. (a), *Balbaroo nalima*

allows passage of cranial nerves VII and VIII, the jugular foramen provides passage of cranial nerves IX, X, and XI, and the hypoglossal foramina (two per side) provide passage for cranial nerve XII (Fig. 11.3). All of these openings are also seen on the ventral hindbrain surface of endocasts of *M. domestica* and *D. virginiana* (Macrini et al. 2007c).

Comparative Anatomy Descriptions of the cranial endocasts of the stem marsupials *Pucadelphys andinus* (Macrini et al. 2007a), *Andinodelphys cochabambensis* (de Muizon and Ladevèze 2020), and *Herpetotheium fugax* (Horovitz et al. 2008) suggest that the ancestral metatherian had a very “didelphid-like” brain with lissencephalic cerebral hemispheres, a small isocortex, large olfactory bulbs, large paraflocculi of the cerebellum, and large cerebellar hemispheres (Figs. 11.3, 11.4, 11.5, and 11.6). The transverse sinuses are well-represented on the dorsal surface of the cranial endocasts of these taxa and contribute to covering the dorsal surface of the midbrain along with the dura mater. Similarly, *Barinya wangala*, *Galadi speciosus*, and *Yalkaparidon coheni* show the transverse sinuses on their endocasts (Fig. 11.4). Cranial endocasts of didelphids also typically do not preserve the rhinal fissure marking the ventral border of the isocortex, although this seems to be brain size-dependent (Dozo 1989; Macrini et al. 2007a, c; Fig. 11.3). The cranial endocasts of some non-diprotodontians such as *Dasyurus hallucatus*, the Northern quoll, have lissencephalic endocasts with large olfactory bulbs similar to didelphids but show more expansion of the isocortex of the cerebral hemispheres (Macrini 2006). The koala, *Phascolarctos cinereus*, has relatively small cerebral hemispheres, a smooth brain and corresponding lissencephalic endocast (Haight and Nelson 1987; Macrini 2006), and the cranial cavity includes expansive cisterns and dural sinuses (de Miguel and Henneberg 1998; Taylor et al. 2006).

Other Australian marsupials such as macropodids, *Sarcophilus harrisii*, the Tasmanian Devil, and *Thylacoleo carnifex*, the marsupial lion, however, show extensive gyrification of the cerebral hemispheres on their endocasts (Woods 1956; Haight and Murray 1981; Kear 2003; Macrini 2006; Figs. 11.4 and 11.5). Similarly, the South American *Dromiciops gliroides*, the monito del monte, shows substantial gyrification and encephalization of the brain and corresponding endocast (Macrini 2006; Macrini et al. 2007a; Rowe et al. 2011) as do the endocasts of the extinct sparassodonts *Thylacosmilus atrox* and *Borhyaena tuberata* (Quiroga and Dozo 1988; Dozo 1994). Gyrification of the brain has occurred independently in multiple lineages of marsupials and stem marsupials, likely as a function of brain size and packaging within the cranial cavity (Macrini et al. 2007a; Mota and Herculano-Houzel 2015; Weisbecker et al. 2021).

←
Fig. 11.6 (continued) (QMF31408), (b). *Barinya wangala* (QMF36295), (c). *Borhyaena tuberata* (YPM15120), (d). *Ekaltadeta ima* (QMF12436), (e). *Galadi speciosus* (QMF23393), (f). *Nimbacinus dicksoni* (QMF36357), (g). *Nimbadon lavarackorum* (QMF42677), (h). *Silvabestius johnnilandi* (QMF30504), (i). *Simosthenurus occidentalis* (SAMP1668), (j). *Thylacoleo carnifex* (SAM280507), (k). *Yalkaparidon coheni* (QMF13008), (l). *Zygomaturus trilobus* (QVM1992_GFV73)

11.3.2 Spaces Associated with Cranial Blood Supply

Similar to other mammals, marsupial cranial endocasts show a number of vascular structures that occupy the cranial cavity such as dural sinuses (e.g. superior sagittal sinus, transverse sinus, sigmoid sinus, prootic sinus) and cisterns, which are expanded subarachnoid spaces filled with cerebrospinal fluid (Butler and Hodos 1996; Macrini et al. 2007a, c). The superior sagittal, transverse, sigmoid, and prootic sinuses are visible on cranial endocasts of extant didelphids (Macrini et al. 2007c). Similarly, the superior sagittal and transverse sinuses are visible on the cranial endocasts of the fossil didelphids *Thylatheridium cristatum* and *Thylophorops chapalmalensis* (Dozo 1989). Dural sinuses are also visible on endocasts of *Wynyardia bassiana* (Haight and Murray 1981) and on fossil macropodoids (Kear 2003). The transverse and prootic sinuses are visible on the endocast of the metatherian *Herpetotherium fugax* (Horovitz et al. 2008) and the transverse sinus is visible on the endocast of *Andinodelphys cochabambensis* (de Muizon and Ladevèze 2020).

The cranial cavity of *Phascolarctos cinereus*, the koala, houses particularly large cisterns around the medulla oblongata (Taylor et al. 2006). The koala is notorious among marsupials for having a brain that poorly fills the cranial cavity (Haight and Nelson 1987). Although the koala is not as poorly encephalized as originally reported by Haight and Nelson (1987), the brain does not completely fill the cranial cavity during life even when the voluminous brain ventricles and cisterns are filled with cerebrospinal fluid (de Miguel and Henneberg 1998; Taylor et al. 2006).

11.4 Brain Evolution and Paleobiological Inferences Based on Endocast Morphology

11.4.1 Morphological Brain Diversity

Endocasts and Phylogenetic Traits

Cranial endocasts provide the best direct evidence for studying the form and external morphology of the brains of extinct taxa. Previous studies of various groups of mammals have suggested that there is phylogenetic signal in anatomical differences in cranial endocasts (e.g. Macrini et al. 2007b; Perini et al. 2022; Weisbecker et al. 2021).

The brain of the ancestral marsupial was reconstructed by Horovitz et al. (2008) based on an analysis of the endocasts of *Herpetotherium* cf. *fugax*, *Pucadelphys andinus*, and a handful of extant taxa (also see Macrini et al. 2007a). The hypothetical ancestor of crown Marsupialia possessed relatively large olfactory bulbs that are posteriorly separated from the rest of the brain by a deep circular fissure, lissencephalic cerebral hemispheres that combined are wider than long, no rhinal fissure on the endocast, the vermis of the cerebellum being longer than wide, and relatively

large, broad, and rounded paraflagella. All of these character states are plesiomorphic for Theria (Macrini et al. 2007b).

The digital cranial endocast of *Andinodelphys cochabambensis* was described by de Muizon and Ladevèze (2020) and compared to those of *Pucadelphys* and endocasts of some extant marsupials (Macrini et al. 2007a). The endocast of *Andinodelphys* shows a number of similarities to those of *Pucadelphys* and extant didelphids such as *Didelphis virginiana* and *Monodelphis domestica*. However, the phylogenetic analysis by de Muizon and Ladevèze (2020) did not include data directly related to cranial endocasts, highlighting the need for a more comprehensive comparative analysis of metatherian endocasts with the goal of coding variation into phylogenetic characters.

A comparison of the gross anatomy of extant marsupial brains with the cranial endocast of *Wynyardia bassiana* placed species into three types (Haight and Murray 1981). One group including the Australian marsupials *Isoodon obesulus* (brown bandicoot), *Antechinus swainsonii* (dusky antechinus), *Dasyurus viverrinus* (tiger cat), and *Sarcophilus harrisii* (Tasmanian Devil), shows brain morphology that most closely resembles that of non-diprotodontian and stem marsupials. This isocortex hemispheres of the cerebrum are trapezoid-shaped when viewed above, the brain is straight with little or no dorsoventral flexion, and the olfactory bulbs are large compared to those of diprotodonts (Haight and Murray 1981). A second grouping includes diprotodont marsupials including *Petaurus breviceps* (sugar glider), *Trichosurus vulpecula* (brush-tailed possum), *Phalanger maculatus* (spotted cuscus), *Vombatus ursinus* (common wombat), *Thylacoleo carnifex* (marsupial lion), and *Wynyardia bassiana*, but excluding macropodids. The isocortex hemispheres of the cerebrum of this group is more ovoid in shape when viewed dorsally because of lateral expansion of the parietofrontal region of the brain, the brain is slightly flexed dorsoventrally when viewed laterally, and the olfactory bulbs and the rest of the “rhinencephalon” are relatively small (Haight and Murray 1981). *Wynyardia bassiana* shows similarities with the external morphology of the extant phalangerid, *Trichosurus vulpecula*. The third group of marsupials, the macropodids, includes *Potorous tridactylus* (rat kangaroo), *Thylagale billardierii* (Tasmanian pademelon), and *Macropus giganteus* (grey kangaroo). The macropodid brains possess a sulcus β , which separates the parietofrontal lobe from the temporal lobe of the cerebrum, the isocortical hemispheres of macropodoids are generally triangular in dorsal outline, and the brains show significant anteroposterior flexion in lateral view due to depression of rostral parts of the skull relative to the braincase (Haight and Murray 1981; Kear 2003). A fourth type of external brain anatomy was identified by Ashwell (2010a) for notoryctids, the extant marsupial moles, which have brains with exaggerated olfactory bulbs, no dorsoventral flexion of the forebrain, and a cerebellum that is not well differentiated. A more recent analysis suggests that there is moderate phylogenetic signal in brain shape of marsupials (Weisbecker et al. 2021).

Functional and/or Behavioral Interpretations of Endocast Morphology

The chief interest of endocasts in palaeoneurology lies in the fact that they reflect the morphology of the brain, and are often the only soft-tissue inference that can be made from a fossil. It is therefore an intuitive expectation that adaptations relating to brain function might also be inferred from endocast morphology. Much of this work has been done in the context of Euarchontoglires and particularly primates (e.g. Silcox et al. this book, Chap. 12). However, aside from the studies of endocast sizes outlined below, relatively few studies have assessed how the mammalian brain evolves across longer time spans, diverse ecologies, and large body mass ranges. In such a broad context, little is known about how the brain and surrounding soft tissues interact with the hard tissue of the cranial vault to give rise to endocast shape (Weisbecker et al. 2021). Investigations in this field are complex because the brain and its surroundings do not adapt like the more tractable musculo-skeletal system of mammals, whose biomechanical function is relatively clear. Instead, a truly bewildering diversity of factors that can, and probably do, impact endocast shape without any relevance to interpretations of brain function at all. At the level of neuronal wiring, the mammalian brain is likely subject to internal tensions that give it a basic shape (Koser et al. 2016). However, brains are probably very flexible in their shape development: during the growth of an individual, the brain appears to mold itself to the endocranial space it “finds” (Toro 2012; Budday et al. 2015). Brain shape is also not always static during an individual’s lifetime: different parts of the brain appear to grow and shrink seasonally in shrews and mustelids (Dechmann et al. 2017). In addition, the requirement for mammalian skulls to be highly adapted to food acquisition and housing of the sensory organs means that either the skull or the brain must accommodate the other. Lastly, accommodation of the brain into the skull posits a special challenge for mammals because it is so large relative to body size. The dorsal cranial vault may have adapted to evolutionary brain enlargement through a heterochronic delay of ossification (Koyabu et al. 2014). However, even within mammals, there are substantial differences in how much the brain contributes to skull evolution because the brain of nearly all mammals scales negatively with body mass (Jerison 1973; Smaers et al. 2021). This means that smaller mammals have a substantially greater contribution of the brain to their skull space (e.g. larger endocranial cavity relative to skull size) than larger species even when they have the same relative brain size (or an encephalization of 1), leading to the expectation that brain shape could be allometric.

All of the factors noted above – developmental and evolutionary flexibility of brain tissue, functional adaptation of the skull, and size-related issues of brain accommodation – could plausibly impact the evolution of endocranial shape without revealing anything about sensorimotor or cognitive abilities of the brain itself. Separating these factors from “true” functional signal of the brain represents a major challenge, which is only just starting to be approached thanks to the increasing speed of digital data acquisition (Bruner 2018).

The diversity of ecology, wide range of body masses, and good phylogenetic resolution make the marsupial clade an excellent group to test how endocast

morphology may aid interpretation of sensorimotor or cognitive abilities of fossil mammals (Pirlot 1981; Macrini et al. 2007c; Todorov et al. 2021; Weisbecker et al. 2021). This was recently assessed in a study including two of us (V.W. and T.M.; Weisbecker et al. 2021), focusing on 3D geometric morphometrics of endocast shape and its association with virtual dissections of the endocasts into its main four components (olfactory bulb, cerebrum, cerebellum, and brain stem). The results showed substantial phylogenetic signal that was congruent with the phylogenetic divisions of external brain morphology identified by others (see above; Haight and Murray 1981). However, contrary to expectations of allometry and locomotor signal, endocast shape could not be associated with absolute or relative endocranial volume or ecology. Even the specialized locomotor types of the gliding possums or hopping kangaroos were not associated with endocast shape, even though this was expected based on their cranial re-arrangement and sensorimotor adaptations (Russo and Kirk 2013; Bertrand et al. 2019). Furthermore, the information contained in endocast 3D shape does not capture the proportions of the externally discernable divisions of the brain (olfactory bulb, cerebrum, cerebellum, and brain stem), and also gives no structural information on neocortical grey or white matter volume.

Unexpectedly, the brain shapes of marsupials primarily fall out along a strikingly clear pattern of variation where brain shapes ranged from elongate and nearly tubular to compressed and angled (Compare shapes in Figs. 11.3, 11.4, 11.5, and 11.6). This range of shape also encompassed extinct species, with particularly varied endocast shapes among the vombatiforms. Intriguingly, this variation is very similar to the pattern of “spatial packing”, postulated as a way of accommodating the increasingly large brains of primates into the skull (Ross and Henneberg 1995; Lieberman et al. 2008; Bastir et al. 2011). The hypothesis of “spatial packing” suggests that larger brains can fit into a limited space in the cranial cavity by evolving flexure at the base and a round overall shape. The data for marsupial brains raise the exciting possibility that “spatial packing” patterns in the primate skull reflect a more global tendency of the brain to vary along the axis of global elongation found in marsupials.

We still have a long way to go in explaining why the marsupial brain displays this pattern of elongation because there seems so little functional significance to the distribution of this shape variation. It might be either resulting from a constraint on brain shape, or simply encompass all shapes that are required to fit the brain into a diversity of cranial contexts. However, the latter seems more likely because we also found substantial variation in endocast shapes among individuals of the same species, and some very unusual forms superimposed over the main variation (Figs. 11.3, 11.4, 11.5, and 11.6 for some examples). This suggests that flexibility of shape (as discussed above) is an important property of the marsupial brain, which would also explain why neural adaptation is unlikely to be strongly expressed on the endocast.

11.4.2 *Brain-Size Evolution and Encephalization Quotient*

Encephalization quotients (EQs) or comparisons of brain size relative to body size in closely related taxa (Jerison 1973) have been widely used to assess brain size evolution in vertebrates. However, EQs have also been frequently criticized (e.g. Deacon 1990; Striedter 2005) because of the variable ways they are calculated (e.g. Jerison 1973, Eisenberg 1981), because of questions around their biological significance, and because different mammalian clades clearly show substantial differences in slope and intercept, making a one-fits-all calculation of EQs fairly meaningless (Smaers et al. 2021). In this chapter we compiled endocranial volume and estimated body mass data on fossil marsupials and non-marsupial metatherians based on previously published studies (Table 11.1). Figure 11.2 shows a log-log plot of these data (see interpretation below), but readers are, of course, able to freely analyze these data in different ways (e.g. EQ analyses) if they so choose.

Marsupial Brain Size and Behavioral Correlates

In terms of brain size, the relatively uniform reproduction of marsupials and their mostly postnatal brain development may be an important advantage in refining the many different hypotheses of how brain sizes can be used to interpret behavioral, ecological, or reproductive traits. Reproductive and developmental traits, particularly the maturity of neonates, are noted for their associations with brain size in placentals (Bennett and Harvey 1985; Martin 1996; Barton and Capellini 2011). However, many of these are also strongly associated with particular behaviors thought to select for larger brain sizes, such that there is a risk of confounding selection *versus* constraint of a behavioral trait (Weisbecker and Goswami 2011; Todorov et al. 2021). Marsupials all have extremely altricial (immature) offspring, and their maternal investment into the brain is nearly entirely through lactation. This should reduce the number of confounding correlations between behavior, reproduction, and brain size (Weisbecker and Goswami 2011; Todorov et al. 2021). Indeed, testing a number of behavioral and reproductive hypotheses of brain size evolution revealed no evidence that relative brain size was a useful indicator of particular behaviors, ecological traits, or metabolic activity (measured as basal or field metabolic rate; Todorov et al. 2021). However, relative brain size tended to be smaller in marsupials with smaller litters (Weisbecker and Goswami 2010; Todorov et al. 2021).

The lack of association between metabolic rate and marsupial brain size is counter to the long-standing suggestion that brain tissue should require elevated metabolic rates because it is metabolically expensive (Armstrong 1983; for a synopsis, see Isler and van Schaik 2009). It is possible that placental mammals have this association because their long gestation and placentation allows the offspring to benefit from higher maternal metabolic rates (Capellini et al. 2010), which is not possible during the short marsupial placentation (Weisbecker and Goswami 2010,

2011). Regardless, inferring metabolic capacity of extinct mammals based on relative brain sizes is probably not appropriate, at least for studies involving therians.

Despite the lack of a clear association of brain size with metabolic rates at the level of living mammals, it seems very likely that the large increase of brain sizes that occurred between early synapsid amniotes and mammals is related to increases in metabolic rates (among other factors; see Rowe et al. 2011, Rowe this book, Chap. 10). The premise of the association between BMR and brain size – that brains are a particularly energy-hungry tissue – is definitely correct (Magistretti et al. 2015). In addition, the largest relative brain sizes appear in birds and mammals, whose metabolic rates have soared relative to other amniotes (White et al. 2006). The transition of mammals and birds from their reptile-like amniote ancestors involved metabolic changes at far greater scales than what is observed within both mammals and birds. The appearance of substantially increased brain sizes is therefore likely to be tied to increases in metabolic rate of a magnitude that is not observable among living species.

It is somewhat frustrating that there are no dependable behavioral predictors of mammalian brain size that could be used to interpret fossil behavior. However, endocranial volumes may relate to reproductive and/or life history constraints. Litter size in particular is regularly associated with brain size (summarized in Todorov et al. 2021), as is longevity in at least some mammals (Pontzer et al. 2014; DeCasien et al. 2018). Cautious interpretation of relative endocranial volumes in this context might add to interpretation of basic life history variables, particularly in combination with evidence from parts of the body.

With regards to the diversity of endocranial volume across Marsupialia, a compilation of available endocast data (Todorov et al. 2021) for living species and as per Table 11.1 for extinct species, reveals that overall, fossil marsupials and the metatherians do not deviate substantially from the overall distribution of brain *versus* body mass relationships among marsupials (Fig. 11.2). It is moreover notable that *D. virginiana* and *D. marsupialis* are both quite small-brained for their size compared to similarly sized marsupials. This is important because Didelphidae have been considered an early-diverging group of marsupials in a variety of contexts, with the presumption that they show plesiomorphic traits (Dooley et al. 2013; Bhullar et al. 2019). In the older literature, this included suggestions that their brain size is small because they represent a small-brained “ancestral” state (Pirlot 1981; Nelson and Stephan 1982). However, the genus *Didelphis* is not relatively smaller-brained than many diprotodontians and particularly the peramelemorphians, which both belong to much later-diverging and anatomically derived clades (see Fig. 11.1). By contrast, representatives of some of the oldest divergences – the Australidelphian *Dromiciops* and the Paucituberculata (shrew opossums) – both have notably larger relative brain sizes than diverse similarly sized marsupials (Fig. 11.2). An association between antiquity of divergence of the clade and small brain size can, therefore, not be made for living marsupials.

In contrast to the relatively even distribution of ECV/body mass scaling in living species, the three very old (Paleocene and Oligocene) metatherians *incertae sedis* stand out as being clearly much smaller-brained relative to their estimated body

mass (Fig. 11.2). This is an intriguing result because it would support Jerison's suggestion that "generally, the early mammals were less encephalized than their descendants" (Jerison 1979), which has been mirrored in the literature (Rowe 1996; Kielan-Jaworowska et al. 2004; Rowe et al. 2011). However, all three specimens of these early metatherians are severely crushed, so that their ECVs may well be substantial under-estimates; in addition, the relatively fragmentary nature of the fossils makes it difficult to establish a reliable measure of body mass. These data, while compiled here (Table 11.1), should be re-visited before they can be included in quantitative comparative analyses.

11.4.3 *Sensory Evolution: Vision, Somatosensory System, Auditory System, Vestibular Sense, Olfaction*

Because many marsupial and stem marsupial endocasts are lissencephalic (e.g. Macrini et al. 2007a, b, c; Horovitz et al. 2008; Weisbecker et al. 2021), there are no reliable landmarks on endocasts to properly delimit sensory regions of the brain with the exception of the olfactory bulbs. Therefore, much of the discussion below is based on what is known about the brains of extant marsupials, particularly didelphids (e.g. Brunjes et al. 1992; Aitkin et al. 1997; Huffman et al. 1999; Catania et al. 2000; Frost et al. 2000; Kahn et al. 2000), and Australian marsupials (Ashwell 2010b). Because the inner ears of extant and fossil metatherians have been studied in a number of taxa (e.g. Meng and Fox 1995; Sánchez-Villagra and Schmelzle 2007; Schmelzle et al. 2007; Ladevèze et al. 2008; Ekdale 2010; Berlin et al. 2013; Ashwell and Shulruf 2014), more can be discussed about the evolution of vestibular sense and hearing.

The visual systems of marsupials vary from those of placental mammals in a few ways. The retinæ of marsupials possess oil droplets and double celled-cones similar to extant reptiles but unlike those of placental mammals (Beazley et al. 2010). These features are advantageous for diurnal vision. Some Australian marsupials possess trichromatic color vision, which is only found in Primates among placental mammals (Beazley et al. 2010). Also, ultraviolet-sensitive (UVS) shortwave sensitive pigments are found in a number of marsupial species such as *Tarsipes rostratus*, the honey possum; *Sminthopsis crassicaudata*, the fat-tailed dunnart; *Monodelphis domestica*, the gray short-tailed opossum; and *Didelphis aurita*, the big-eared opossum, whereas only a subset of rodents contain UVS pigments among placental mammals (Beazley et al. 2010).

Generally speaking, the somatosensory system of marsupials resembles that of placental mammals, particularly the trigeminal pathway to the vibrissae, the most widely studied facet of this system (Marotte et al. 2010). Much of the work on the somatosensory portions of the trigeminal pathway are based on studies of *Macropus eugenii*, the tammar wallaby (Marotte et al. 2010).

The auditory system of marsupials was reviewed by Aitkin and Shepherd (2010). The auditory neurobiology of didelphids (*Monodelphis domestica* and *Didelphis virginiana*) has been studied in the greatest detail (Aitkin and Shepherd 2010). The auditory pathways have only been studied in a few species such as *Trichosurus vulpecula*, the brush-tailed possum, and *Dasyurus hallucatus*, the northern quoll (Aitkin and Shepherd 2010). Based on these few studies, the auditory systems of marsupials show many similarities with those of placental mammals.

The inner ear (cochlea, utriculus, sacculus, semicircular ducts) and the corresponding bony labyrinth of the petrosal bone has been studied in a larger number of species of marsupials. The cochlea in marsupials shows coiling similar to placental mammals, with the degree of coiling being variable between species (Gray 1908). In general, the anatomy of the cochlea of marsupials is similar to that of placental mammals (Aitkin and Shepherd 2010).

A study of ontogenetic variation of the bony labyrinth in *Monodelphis domestica*, the gray short-tailed opossum, examined individuals as young as 27 days postnatal (when the inner ear chambers have ossified) up to sexually mature adults (Ekdale 2010). Many of the inner ear measurements examined by Ekdale (2010) did not show a correlation with age, and in general, adult dimensions of inner ear structures such as the arcs of the semicircular canal and degree of coiling of the cochlea are achieved before the inner ear is functional.

As in all vertebrates, the ampullae of the semicircular canals are involved in detection of angular acceleration of the head. Historically, the canonical model of the semicircular canals suggested that ipsilateral canals of the inner ear are orthogonal with respect to one another, corresponding left and right canal pairs show angle symmetry, and contralateral synergistic canals are coplanar (i.e. they occupy parallel planes; Berlin et al. 2013). In a study including the inner ears of a number of extant mammals including several marsupial species, Berlin et al. (2013) found that the canonical model was invalid for nearly all species examined.

The olfactory system in mammals includes the olfactory epithelium, found on the ossified turbinates of the ethmoid bone and other surfaces of the nasal cavity; the olfactory nerve fibers, which pass through the cribriform plate to synapse with the mitral neurons in the main olfactory bulb (MOB); and the olfactory tract (mitral neuron axons), which extends from the MOB to the piriform cortex and other regions of the telencephalon (Butler and Hodos 1996; Ashwell 2010a). The accessory component of the olfactory system includes the vomeronasal organ of the nasal cavity, which projects to the accessory olfactory bulb of the brain via the terminal nerve. The main olfactory system is involved with detection and processing of airborne odorant molecules, whereas the accessory olfactory system processes pheromones.

Aspects of the olfactory system of the brain have only been studied in a handful of marsupial species (Ashwell 2010a). However, the olfactory bulb is highly variable in volume across species (Weisbecker et al. 2021), thus making it a likely candidate for ecological associations that are less easy to be made using whole brain volumes. Similarly, the olfactory components of the nasal cavity, especially the nasal skeleton, have been studied in multiple species of marsupials (e.g. Paulli

1900; Toeplitz 1920; Denison and Terry 1921; Osgood 1921; Wood Jones 1949; Kratzing 1978, 1982, 1984; Sánchez-Villagra 2001; Rowe et al. 2005; Macrini 2012, 2014). However, for the most part the components of the olfactory system in the nasal cavity (turbinals and olfactory epithelium) have not been studied integrated with the components of the brain (olfactory bulbs, olfactory track, olfactory pathways in the brain). Regardless, olfactory bulb volume is highly variable among marsupials; it explains most of the main variation in a principal components analysis of marsupial brain partition volumes (Weisbecker et al. 2021). It therefore seems important to study the association of olfactory bulb volume with ecological traits in extant marsupials and extrapolate the insights to extinct species.

11.4.4 Brain Anatomy in Marsupials Versus Placentals

As mentioned previously, the central nervous system of marsupials shows some limited anatomical differences with the CNS of placental and monotreme mammals (Ashwell 2010b). Most of these features are internally located within the brain or cranial cavity and unfortunately do not touch the external anatomy of the brain; therefore, these features are not represented on cranial endocasts. Therefore, these features cannot be assessed on fossil taxa, but nonetheless these characters are discussed below based on extant marsupials. In particular, marsupials lack the corpus callosum, a derived forebrain commissure between the cerebral hemispheres that is found in placental mammals (Ashwell 2010b), although marsupials do share a basic interhemispheric connectome with placentals (Suárez et al. 2018). Diprotodonts have a derived fiber bundle (fasciculus aberrans) that extends from the internal capsule of each inferior cerebral hemisphere to the anterior commissure (Ashwell 2010b). The fibers of the dorsal lateral olfactory tract in most marsupials and monotremes pass under the accessory olfactory formation unlike many placental mammals in which these fibers pass through the accessory olfactory formation (Ashwell 2010b).

Despite the overall anatomical similarity between marsupials and placentals, marsupials display a heterochronic delay of brain development relative to placentals (Smith 2006) and limited data suggest that it is possible that their neurogenetic development is more variable than that of placentals (Darlington et al. 1999). Lastly, in terms of blood supply, marsupials differ in the arterial blood supply to the brain (Johnson 2012; Ashwell and Shulruf 2016), such that the arterioles of the central nervous system of marsupials terminate in individual capillary loops that do not form free capillary anastomoses with venules as in other mammals (Johnson et al. 1982a, b). This is considered a derived condition for marsupials.

In monotremes and marsupials, cranial nerve VII (facial nerve) exits the brainstem dorsal to the sensory nuclei of cranial nerve V (trigeminal nerve). In contrast, the facial nerve passes either through the trigeminal nuclei or completely ventral to them in placentals (Ashwell 2010b). Finally, the accessory nucleus (IOV) of the inferior olivary nuclear complex of the medulla oblongata lies ventral and lateral in

monotremes and marsupials but the IOV is found medially in many placental mammals (Ashwell 2010b).

11.5 Future Directions: Outstanding Questions and Perspectives

Marsupials are an excellent radiation for testing hypotheses of mammalian brain evolution, which necessitates a good understanding of the brain morphology in extinct species. However, marsupial fossils are understudied in nearly every modality of data. Whereas we now have a good selection of data points for fossil species across the marsupial tree of life (Fig. 11.1; phylogeny), better and more reliable sampling particularly from lower parts of the tree is necessary for improving the robustness of models of brain size evolution within the clade. It is clear from this compilation that there is a need for a comprehensive comparative study of brain and cranial endocast morphology in marsupials and their closest extinct relatives. Similarly, there is a need for a similar study for the inner ear and bony labyrinth of metatherians, including both crown and stem marsupials. Such studies would allow for proper integration of neurological character data into phylogenetic analyses of metatherians.

Analyses of brain shape reveal that the marsupial brain displays a pattern of elongation in some taxa whereas others have compressed and rounded brains, but that the main variation within this pattern is not associated with either volume or surface areas of parts of the brain (Weisbecker et al. 2021). Whereas this is an intriguing, and possibly generalizable, pattern, there seems to be little functional significance to its distribution among species. The drivers of marsupial and mammalian brain shape are therefore still to be determined. It will also be important to understand if studies on endocast surface areas can improve our understanding of how the shape of the brain and its volumes and surfaces interact, because these variables seem to contain very different types of information (Weisbecker et al. 2021).

The complexity of the olfactory system of mammals sets us apart from other vertebrates (Kielan-Jaworowska et al. 2004; Rowe et al. 2005) and is perhaps a contributing factor to increased encephalization in this clade (Rowe et al. 2011). However, the olfactory system of marsupials, and mammals in general, has not been studied as a whole such that the components of the olfactory system in the nasal cavity (turbinals and olfactory epithelium) have not been examined in integration with the components of the brain (olfactory bulbs, olfactory track, olfactory pathways in the brain). Therefore, work needs to be done in examining relationships between olfactory bulb size and olfactory epithelial size (or its proxy on bony turbinals) and measuring olfactory receptor neuron numbers and density in extant species. Having an understanding of these parameters and their relationships to bony

correlates (e.g. turbinals and ethmoidal cavity in the braincase) in extant species will allow for extrapolation to the fossil record.

11.6 Concluding Remarks

Prior to the 1970s, relatively few descriptions of cranial endocasts of fossil crown marsupials and stem marsupials were published (see Jerison 1973; Edinger 1975). However, with the increased discovery of new fossil marsupial taxa from the Eocene Riversleigh locality in northwestern Queensland, including natural cranial endocasts (e.g. Kear 2003), our knowledge of the paleoneurology of the group has increased. Similarly, subsequent descriptions of natural cranial endocasts of metatherians from South America (e.g. Quiroga and Dozo 1988; Dozo 1989, 1994) have added to the knowledge of the paleoneurology of marsupials and their closest extinct relatives.

Additionally, the increased use of high-resolution X-ray computed tomography to image rare and unique fossil skulls of crown and stem marsupials (e.g. Macrini et al. 2007a, Horovitz et al. 2008; de Muizon and Ladevèze 2020) has provided a better picture of the evolution of brain in basal marsupials. In particular, descriptions of the digital cranial endocasts of the stem marsupials *Pucadelphys andinus* (Macrini et al. 2007a), *Andinodelphys cochabambensis* (de Muizon and Ladevèze 2020), and *Herpetotheium fugax* (Horovitz et al. 2008) suggest that the ancestral metatherian had a brain that closely resembled the brains of didelphids (e.g. *Caluromys philander*, Fig. 11.3).

Access to CT scans of marsupial skulls has also allowed for extraction of digital cranial endocasts from a range of crown marsupial taxa, both extant and fossil. These digital endocasts have made it possible to study the evolution of endocast (and the corresponding brain) shape variation in marsupials (Weisbecker et al. 2021) and has provided a rich dataset of endocranial volumes to study the evolution of brain size in fossil marsupials and their closest relatives (Table 11.1). A comparison between brain size and body size in fossil and extant metatherians shows a tightly constrained allometric relationship between the two variables (Fig. 11.2). Only three metatherians outside of crown Marsupialia fall substantially below other taxa. Within the crown, variation in relative brain size is not correlated with the timing of divergence of clades of marsupials, such that some of the earliest diverging clades such as Microbiotheriidae and Paucituberculata have larger relative brain sizes than similarly sized marsupials, whereas some didelphids do not show smaller relative brain size compared to later-diverging and anatomically derived Australasian clades (Fig. 11.2). It is also possible to deduce from the available datasets and anatomical descriptions that there is a significant range of variation in not only brain shape, but the degree of gyrification in various marsupial groups reflecting brain size differences and spatial packing within limited space in the braincase.

Despite these advances in the study of paleoneurology of marsupials, above we identified some areas for future work. In particular, a comprehensive comparison for

cranial endocast morphology in marsupials and stem marsupials is needed to allow for integration of neurological character into phylogenetic analyses to uncover phylogenetic signal within this anatomical system.

Acknowledgments VW was supported by an Australian Research Council Future Fellowship FT180100634; thanks to Meg Martin for assistance with figures. TEM was supported by the Biaggini Research Fund in the Department of Biological Sciences at St. Mary's University. ML was supported by a scholarship from the San Antonio Livestock Show and Exhibition. We thank A. Balcarcel and M. Sánchez-Villagra for helpful reviews of this chapter.

References

- Abello MA, Candela AM (2020) Paleobiology of *Argyrolagus* (Marsupialia, Argyrolagidae): an astonishing case of bipedalism among South American mammals. *J Mamm Evol* 27:419–444
- Aitkin LM, Shepherd RK (2010) Auditory system. In: Ashwell KWS (ed) *The neurobiology of Australian marsupials: brain evolution in the other mammalian radiation*. Cambridge University Press, New York, pp 184–191
- Aitkin L, Cochran S, Frost S et al (1997) Features of the auditory development of the short-tailed Brazilian opossum, *Monodelphis domestica*: evoked responses, neonatal vocalizations and synapses in the inferior colliculus. *Hear Res* 113:69–75
- Alloing-Séguier L, Sánchez-Villagra MR, Lee MSY et al (2013) The bony labyrinth in diprotodontian marsupial mammals: diversity in extant and extinct forms and relationships with size and phylogeny. *J Mamm Evol* 20:191–198
- Argot C (2003) Functional adaptations of the postcranial skeleton of two Miocene borhyaenoids (Mammalia, Metatheria), *Borhyaena* and *Prothylacinus*, from South America. *Palaeontology* 46:1213–1267
- Armstrong E (1983) Relative brain size and metabolism in mammals. *Science* 220:1302–1304
- Ashwell KWS (2008) Encephalization of Australian and New Guinean marsupials. *Brain Behav Evol* 71:181–199
- Ashwell KWS (2010a) Olfactory system. In: Ashwell KWS (ed) *The neurobiology of Australian marsupials: brain evolution in the other mammalian radiation*. Cambridge University Press, New York, pp 192–201
- Ashwell KWS (2010b) Overview of marsupial brain organisation and evolution. In: Ashwell KWS (ed) *The neurobiology of Australian marsupials: brain evolution in the other mammalian radiation*. Cambridge University Press, New York, pp 18–39
- Ashwell KWS (2010c) *The neurobiology of Australian marsupials: brain evolution in the other mammalian radiation*. Cambridge University Press, New York
- Ashwell KWS (2015) Quantitative analysis of somatosensory cortex development in eutherians, with a comparison with metatherians and monotremes. *Somatosens Mot Res* 32:137–152
- Ashwell KWS, Shulruf B (2014) Vestibular development in marsupials and monotremes. *J Anat* 224:447–458
- Ashwell KWS, Shulruf B (2016) Quantitative comparison of cerebral artery development in metatherians and monotremes with non-human eutherians. *J Anat* 228:384–395
- Barton RA, Capellini I (2011) Maternal investment, life histories, and the costs of brain growth in mammals. *Proc Natl Acad Sci U S A* 108:6169–6174
- Bastir M, Rosas A, Gunz P et al (2011) Evolution of the base of the brain in highly encephalized human species. *Nat Commun* 2:588
- Beazley LD, Arrese C, Hunt DM (2010) Visual system. In: Ashwell KWS (ed) *The neurobiology of Australian marsupials: brain evolution in the other mammalian radiation*. Cambridge University Press, New York, pp 155–166

- Bennett CV, Goswami A (2013) Statistical support for the hypothesis of developmental constraint in marsupial skull evolution. *BMC Biol* 11:1–14
- Bennett PM, Harvey PH (1985) Brain size, development and metabolism in birds and mammals. *J Zool B* 207:491–509
- Bennett CV, Upchurch P, Goin FJ et al (2018) Deep time diversity of metatherian mammals: implications for evolutionary history and fossil-record quality. *Paleobiology* 44:171–198
- Berlin JC, Kirk EC, Rowe TB (2013) Functional implications of ubiquitous semicircular canal non-orthogonality in mammals. *PLoS One* 8(11):e79585
- Bertrand O, San Martín-Flores G, Silcox M (2019) Endocranial shape variation in the squirrel-related clade and their fossil relatives using 3D geometric morphometrics: Contributions of locomotion and phylogeny to brain shape. *J Zool* 308:197–211
- Bhullar BAS, Manafzadeh AR, Miyamae JA et al (2019) Rolling of the jaw is essential for mammalian chewing and tribosphenic molar function. *Nature* 566:528–532
- Bi S, Zheng X, Wang X et al (2018) An early cretaceous eutherian and the placental–marsupial dichotomy. *Nature* 558:390–395
- Black KH, Camens AB, Archer M et al (2012) Herds overhead: *Nimbadon lavarackorum* (Diprotodontidae), heavyweight marsupial herbivores in the Miocene forests of Australia. *PLoS One* 7:e48213
- Bruner E (2018) The brain, the braincase, and the morphospace. In: Bruner E, Ogiwara N, Tanabe HC (eds) *Digital endocasts: from skulls to brains*. Springer, Tokyo, pp 93–114
- Brunjes PC, Jazaeri, Sutherland MJ (1992) Olfactory bulb organization and development in *Monodelphis domestica* (grey short-tailed opossum). *J Comp Neurol* 320:544–554
- Budday S, Steinmann P, Goriely A et al (2015) Size and curvature regulate pattern selection in the mammalian brain. *Extreme Mech Lett* 4:193–198
- Butler AB, Hodos W (1996) *Comparative vertebrate neuroanatomy: evolution and adaptation*. Wiley-Liss, New York
- Capellini I, Venditti C, Barton RA (2010) Placentation and maternal investment in mammals. *Am Nat* 177:86–98
- Catania KC, Jain N, Franca JG et al (2000) The organization of somatosensory cortex in the short-tailed opossum (*Monodelphis domestica*). *Somatosens Mot Res* 17:39–51
- Darlington R, Dunlop S, Finlay B (1999) Neural development in metatherian and eutherian mammals: variation and constraint. *J Comp Neurol* 411:359–368
- de Miguel C, Henneberg M (1998) Encephalization of the koala, *Phascolarctos cinereus*. *Aust Mammal* 20:315–320
- de Muizon C (1992) La fauna de mamíferos de Tiupampa (Paleoceno inferior, Formación Santa Lucía) Bolivia. *Rev Téc Yacim Pet Fisc Bol* 12:575–624
- de Muizon C (1998) *Mayulestes ferox*, a borhyaenoid (Metatheria, Mammalia) from the early Paleocene of Bolivia. Phylogenetic and palaeobiologic implications. *Géodiversitas* 20:19–142
- de Muizon C, Ladevèze S (2020) Cranial anatomy of *Andinodelphys cochabambensis*, a stem metatherian from the early Palaeocene of Bolivia. *Géodiversitas* 42:597–739
- de Muizon C, Ladevèze S, Selva C et al (2018) *Allqokirus australis* (Sparassodonta, Metatheria) from the early Palaeocene of Tiupampa (Bolivia) and the rise of the metatherian carnivorous radiation in South America. *Géodiversitas* 40:363–459
- Deacon TW (1990) Rethinking mammalian brain evolution. *Am Zool* 30:629–705
- DeCasien AR, Thompson NA, Williams SA et al (2018) Encephalization and longevity evolved in a correlated fashion in Euarchontoglires but not in other mammals. *Evolution* 72:2617–2631
- Dechmann DKN, LaPoint S, Dullin C et al (2017) Profound seasonal shrinking and regrowth of the ossified braincase in phylogenetically distant mammals with similar life histories. *Sci Rep* 7:42443
- Deason W, Terry RJ (1921) The chondrocranium of *Caluromys*. *Wash Univ Stud* 8:161–181
- Dooley JC, Franca JG, Seelke AM et al (2013) A connection to the past: *Monodelphis domestica* provides insight into the organization and connectivity of the brains of early mammals. *J Comp Neurol* 521:3877–3897

- Dos Santos SE, Porfirio J, da Cunha FB et al (2017) Cellular scaling rules for the brains of marsupials: not as “primitive” as expected. *Brain Behav Evol* 89:48–63
- Dozo MT (1989) Estudios paleoneurologicos en Didelphidae extinguidos (Mammalia, Marsupialia) de la Formacion Chapadmalal (Plioceno tardío), Provincia de Buenos Aires, Argentina. *Ameghiniana* 26:43–54
- Dozo MT (1994) Estudios paleoneurologicos en marsupiales “carnívoros” extinguidos de America del Sur: neuromorfología y encefalización. *Mastozool Neotrop* 1:5–16
- Edinger T (1975) Paleoneurology 1804-1966. An annotated bibliography. *Ergeb Anat Entwicklungsgesch* 49:1–258
- Eisenberg JF (1981) The mammalian radiations. University of Chicago Press, Chicago
- Ekdale EG (2010) Ontogenetic variation in the bony labyrinth of *Monodelphis domestica* (Mammalia: Marsupialia) following ossification of the inner ear cavities. *Anat Rec* 293:1896–1912
- Eldridge MD, Beck RM, Croft DA et al (2019) An emerging consensus in the evolution, phylogeny, and systematics of marsupials and their fossil relatives (Metatheria). *J Mammal* 100:802–837
- Fabre A-C, Dowling C, Portela Miguez R et al (2021) Functional constraints during development limit jaw shape evolution in marsupials. *Proc R Soc Lond (Biol)* 288:20210319
- Forasiepi AM, Sánchez-Villagra MR, Schmelzle T et al (2014) An exceptionally well-preserved skeleton of *Palaeotheres* from the early Miocene of Patagonia, Argentina: new insights into the anatomy of extinct paucituberculatan marsupials. *Swiss J Palaeontol* 133:1–21
- Forasiepi AM, MacPhee RDE, del Pino SH (2019) Caudal cranium of *Thylacosmilus atrox* (Mammalia, Metatheria, Sparassodonta), a South American predaceous sabertooth. *Bull Am Mus Nat Hist* 433:1–66
- Frost SB, Milliken GW, Plautz EJ et al (2000) Somatosensory and motor representations in cerebral cortex of a primitive mammal (*Monodelphis domestica*): a window into the early evolution of sensorimotor cortex. *J Comp Neurol* 421:29–51
- Garland K, Marcy A, Sherratt E et al (2017) Out on a limb: bandicoot limb co-variation suggests complex impacts of development and adaptation on marsupial forelimb evolution. *Evol Dev* 19:69–84
- Gelfo JN, Goin F, Bauzá N et al (2019) The fossil record of Antarctic land mammals: commented review and hypotheses for future research. *Adv Polar Sci* 30:274–292
- Gemmell RT, Veitch C, Nelson J (2002) Birth in marsupials. *Comp Biochem Physiol B Biochem Mol Biol* 131:621–630
- Gray H (1908) The labyrinth of animals: including mammals, birds, reptiles and amphibians, vol 2. J & A Churchill, London
- Haight JR, Murray PF (1981) The cranial endocast of the early Miocene marsupial, *Wynyardia bassiana*: an assessment of taxonomic relationships based upon comparisons of recent forms. *Brain Behav Evol* 19:17–36
- Haight JR, Nelson JE (1987) A brain that doesn't fit its skull: a comparative study of the brain and endocranium of the koala, *Phascolarctos cinereus* (Marsupialia: Phascolarctidae). In: Archer M (ed) Possums and opossums: studies in evolution, vol 1. Surrey Beatty and Sons Pty Limited, New South Wales, pp 331–352
- Horovitz I, Ladevèze S, Argot C et al (2008) The anatomy of *Herpotherium* cf. *fugax* Cope, 1873, a metatherian from the Oligocene of North America. *Palaeontogr Abt A* 284:109–141
- Horovitz I, Martin T, Bloch J et al (2009) Cranial anatomy of the earliest marsupials and the origin of opossums. *PLoS One* 4(12):e8278
- Huffman KJ, Nelson J, Clarey J et al (1999) Organization of somatosensory cortex in three species of marsupials, *Dasyurus hallucatus*, *Dactylopsila trivirgata*, and *Monodelphis domestica*: neural correlates of morphological specializations. *J Comp Neurol* 403:5–32
- Isler K, van Schaik CP (2009) The expensive brain: a framework for explaining evolutionary changes in brain size. *J Hum Evol* 57:392–400
- Jerison HJ (1973) Evolution of brain and intelligence. Academic, London

- Jerison HJ (1979) The evolution of diversity in brain size. In: Development and evolution of brain size: behavioral implications. Academic, New York, pp 29–57
- Johnson JI (2012) Central nervous system of marsupials. The biology of marsupials: 157
- Johnson JI, Switzer RC, Kirsch JAW (1982a) Phylogeny through brain traits: Fifteen characters which adumbrate mammalian genealogy. Brain Behav Evol 20:72–83
- Johnson JI, Switzer RC, Kirsch JAW (1982b) Phylogeny through brain traits: The distribution of categorizing characters in contemporary mammals. Brain Behav Evol 20:97–117
- Jyothilakshmi TK, Gurovich Y, Ashwell KWS (2020) Numerical analysis of the cerebral cortex in diprotodontids (Marsupialia; Australidelphia) and comparison with eutherian brains. Zoology 143:125845
- Kahn DM, Huffman KJ, Krubitzer L (2000) Organization and connections of V1 in *Monodelphis domestica*. J Comp Neurol 428:337–354
- Kear BP (2003) Macropodoid endocranial casts from the early Miocene of Riversleigh, northwestern Queensland. Alcheringa 27:295–302
- Kielan-Jaworowska Z, Cifelli RL, Luo Z-X (2004) Mammals from the Age of Dinosaurs: origin, evolution, and structure. Columbia University Press, New York
- Koser DE, Thompson AJ, Foster SK et al (2016) Mechanosensing is critical for axon growth in the developing brain. Nat Neurosci 19:1592–1598
- Koyabu D, Werneburg I, Morimoto N et al (2014) Mammalian skull heterochrony reveals modular evolution and a link between cranial development and brain size. Nat Commun 5:3625
- Kratzing JE (1978) The olfactory apparatus of the bandicoot (*Isoodon macrourus*): fine structure and presence of a septal olfactory organ. J Anat 123:601–613
- Kratzing JE (1982) The anatomy of the rostral nasal cavity and vomeronasal organ in *Tarsipes rostratus* (Marsupialia: Tarsipedidae). Aust Mammal 5:211–219
- Kratzing JE (1984) The anatomy and histology of the nasal cavity of the koala (*Phascolarctos cinereus*). J Anat 138:55–65
- Ladevèze S, Asher RJ, Sánchez-Villagra MR (2008) Petrosal anatomy in the fossil mammal *Necrolestes*: evidence for metatherian affinities and comparisons with the extant marsupial mole. J Anat 213:686–697
- Ladevèze S, Selva C, de Muizon C (2020) What are "opossum-like" fossils? The phylogeny of herpetotheriid and peradectid metatherians, based on new features from the petrosal anatomy. J Syst Palaeontol 18:1463–1479
- Lieberman DE, Hallgrímsson B, Liu W et al (2008) Spatial packing, cranial base angulation, and craniofacial shape variation in the mammalian skull: testing a new model using mice. J Anat 212:720–735
- Lillegraven JA, Thompson SD, McNab BK et al (1987) The origin of eutherian mammals. Biol J Linn Soc 32:281–336
- Macrini TE (2004) *Monodelphis domestica*. Mamm Species 760:1–8
- Macrini TE (2006) The evolution of endocranial space in mammals and non-mammalian cynodonts. Dissertation, University of Texas at Austin
- Macrini TE (2009) Description of a digital cranial endocast of *Bathygenys reevesi* (Merycoidodontidae; Oreodontoidea) and implications for apomorphy-based diagnosis of isolated, natural endocasts. J Vertebr Paleontol 29:1199–1211
- Macrini TE (2012) Comparative morphology of the internal nasal skeleton of adult marsupials based on X-ray computed tomography. Bull Am Mus Nat Hist 365:1–91
- Macrini TE (2014) Development of the ethmoid in *Caluromys philander* (Didelphidae, Marsupialia) with a discussion on the homology of the turbinal elements in marsupials. Anat Rec 297:2007–2017
- Macrini TE, de Muizon C, Cifelli RL et al (2007a) Digital cranial endocast of *Pucadelphys andinus*, a Paleocene metatherian. J Vertebr Paleontol 27:99–107
- Macrini TE, Rougier GW, Rowe T (2007b) Description of a cranial endocast from the fossil mammal *Vincelestes neuquenianus* (Theriiiformes) and its relevance to the evolution of endocranial characters in therians. Anat Rec 290:875–892

- Macrini TE, Rowe T, VandeBerg JL (2007c) Cranial endocasts from a growth series of *Monodelphis domestica* (Didelphidae, Marsupialia): a study of individual and ontogenetic variation. *J Morphol* 268:844–865
- Macrini TE, Flynn JJ, Ni X et al (2013) Comparative study of notoungulate (Placentalia, Mammalia) bony labyrinths and new phylogenetically informative inner ear characters. *J Anat* 223:442–461
- Maga AM, Beck RM (2017) Skeleton of an unusual, cat-sized marsupial relative (Metatheria: Marsupialiformes) from the middle Eocene (Lutetian: 44–43 million years ago) of Turkey. *PLoS One* 12:e0181712
- Magistretti PJ, Pierre J, Allaman I (2015) A cellular perspective on brain energy metabolism and functional imaging. *Neuron* 86:883–901
- Marotte LR, Leamey CA, Waite PME (2010) Somatosensory system. In: Ashwell KWS (ed) *The Neurobiology of Australian Marsupials: Brain Evolution in the Other Mammalian Radiation*. Cambridge University Press, New York, pp 167–183
- Marshall LG, de Muizon C (1995) Part II. The skull. In: Muizon C de (ed) *Pucadelphys andinus* (Marsupialia, Mammalia) from the Early Paleocene of Bolivia. *Mém Mus Natl Hist Nat* 165:21–90
- Marshall LG, Sigogneau-Russell D (1995) Part III. Postcranial skeleton. In: Muizon C de (ed) *Pucadelphys andinus* (Marsupialia, Mammalia) from the Early Paleocene of Bolivia. *Mém Mus Natl Hist Nat* 165:91–164
- Martin RD (1996) Scaling of the mammalian brain: The maternal energy hypothesis. *News Physiol Sci* 11:149–156
- Martín-Serra A, Benson RBJ (2020) Developmental constraints do not influence long-term phenotypic evolution of marsupial forelimbs as revealed by interspecific disparity and integration patterns. *Am Nat* 195:547–560
- Meng J, Fox RC (1995) Osseous inner ear structures and hearing in early marsupials and placentals. *Zool J Linnean Soc* 115:47–71
- Mitchell KJ, Pratt RC, Watson LN et al (2014) Molecular phylogeny, biogeography, and habitat preference evolution of marsupials. *Mol Biol Evol* 31:2322–2330
- Mota B, Herculano-Houzel S (2015) Cortical folding scales universally with surface area and thickness, not number of neurons. *Science* 349:74–77
- Müller F (1969) Zur frühen Evolution der Säuger-Ontogenesetypen: Versuch einer Rekonstruktion auf Grund der Ontogenese-Verhältnisse bei den Marsupialia. S. Karger
- Myers TJ (2001) Marsupial body mass prediction. *Aust J Zool* 49:99–118
- Nelson J, Stephan H (1982) Encephalization in Australian marsupials. *Carnivorous marsupials*. Royal Zoological Society of New South Wales, Sydney, pp 699–706
- Nilsson MA, Churakov G, Sommer M et al (2010) Tracking marsupial evolution using archaic genomic retroposon insertions. *PLoS Biol* 8:e1000436
- Osgood (1921) A monographic study of the American marsupial, *Caenolestes*. *Field Mus Nat Hist, Zool* 14:1–162
- Owen R, Carlisle A (1834) XVII. On the generation of the marsupial animals, with a description of the impregnated uterus of the kangaroo. *Philos Trans R Soc* 124:333–364
- Paulli S (1900) Über die Pneumaticität des Schädels bei den Säugetieren. Eine morphologische Studie. I. Über den Bau des Siebbeins. Über die Morphologie des Siebbeins und die Pneumaticität bei den Monotremen und den Marsupialiern. *Gegenbaurs Morphol Jahrb* 28:147–178
- Perini FA, Macrini TE, Flynn JJ et al (2022) Comparative endocranial anatomy, encephalization, and phylogeny of Notoungulata (Placentalia, Mammalia). *J Mamm Evol* 29:369–394
- Pevsner SK, Grossnickle DM, Luo Z-X (2022) The functional diversity of marsupial limbs is influenced by both ecology and developmental constraint. *Biol J Linn Soc* 135:569–585
- Pirlot P (1981) A quantitative approach to the marsupial brain in an eco-ethological perspective. *Rev Can Biol* 40:229–250

- Pontzer H, Raichlen DA, Gordon AD et al (2014) Primate energy expenditure and life history. *Proc Natl Acad Sci U S A* 111:1433–1437
- Portman A (1947) Études sur la cérébralisation chez les oiseaux. *Alauda* 15:27
- Quiroga JC, Dozo MT (1988) The brain of *Thylacosmilus atrox*. Extinct south American saber-tooth carnivore marsupial. *J Hirnforsch* 29:573–586
- Reguero MA, Goin FJ (2021) Paleogeography and biogeography of the Gondwanan final breakup and its terrestrial vertebrates: New insights from southern South America and the “double Noah's Ark” Antarctic Peninsula. *J S Am Earth Sci* 108:103358
- Ross C, Henneberg M (1995) Basicranial flexion, relative brain size, and facial kyphosis in *Homo sapiens* and some fossil hominids. *Am J Phys Anthropol* 98:575–593
- Rougier GW, Wible JR, Beck RMD et al (2012) The Miocene mammal *Necrolestes* demonstrates the survival of a Mesozoic nontherian lineage into the late Cenozoic of south American. *Proc Natl Acad Sci U S A* 109:20053–20058
- Rowe T (1996) Coevolution of the mammalian middle ear and neocortex. *Science* 273:651–654
- Rowe TB, Eiting TP, Macrini TE et al (2005) Organization of the olfactory and respiratory skeleton in the nose of the gray short-tailed opossum *Monodelphis domestica*. *J Mamm Evol* 12:303–336
- Rowe TB, Macrini TE, Luo Z-X (2011) Fossil evidence on origin of the mammalian brain. *Science* 332:955–957
- Russo GA, Kirk EC (2013) Foramen magnum position in bipedal mammals. *J Hum Evol* 65:656–670
- Sánchez-Villagra MR (2001) Ontogenetic and phylogenetic transformations of the vomeronasal complex and the nasal floor elements in marsupial mammals. *Zool J Linnean Soc* 131:459–479
- Sánchez-Villagra MR (2013) Why are there fewer marsupials than placentals? On the relevance of geography and physiology to evolutionary patterns of mammalian diversity and disparity. *J Mamm Evol* 20:279–290
- Sánchez-Villagra MR, Schmelzle T (2007) Anatomy and development of the bony inner ear in the woolly opossum, *Caluromys philander* (Didelphimorphia, Marsupialia). *Mastozool Neotrop* 14:53–60
- Sánchez-Villagra MR, Ladevèze S, Horovitz I et al (2007) Exceptionally preserved North American Paleogene metatherians: Adaptations and discovery of a major gap in the opossum fossil record. *Biol Lett* 3:318–322
- Sánchez-Villagra MR, Goswami A, Weisbecker V et al (2008) Conserved relative timing of cranial ossification patterns in early mammalian evolution. *Evol Dev* 10:519–530
- Saunders N, Adam E, Reader M et al (1989) *Monodelphis domestica* (grey short-tailed opossum): An accessible model for studies of early neocortical development. *Anat Embryol* 180:227–236
- Schmelzle T, Sánchez-Villagra MR, Maier W (2007) Vestibular labyrinth diversity in diprotodontian marsupial mammals. *Mammal Study* 32:83–97
- Selva C, Ladevèze S (2017) Computed microtomography investigation of the skull of Cuvier's famous 'opossum' (Marsupialiformes, Herpetotheriidae) from the Eocene of Montmartre. *Zool J Linnean Soc* 180:672–693
- Sharp AC (2016) A quantitative comparative analysis of the size of the frontoparietal sinuses and brain in vomatiform marsupials. *Mem Mus Vic* 74:331–342
- Smaers JB, Rothman RS, Hudson DR et al (2021) The evolution of mammalian brain size. *Sci Adv* 7(eabe2101)
- Smith KK (2006) Craniofacial development in marsupial mammals: developmental origins of evolutionary change. *Dev Dyn* 235:1181–1193
- Striedter GF (2005) Principles of brain evolution. Sinauer Associates, Sunderland, Massachusetts
- Suárez R, Paolino A, Fenlon LR et al (2018) A pan-mammalian map of interhemispheric brain connections predates the evolution of the corpus callosum. *Proc Natl Acad Sci U S A* 115:9622
- Taylor J, Rühli FJ, Brown E et al (2006) MR imaging of brain morphology, vascularisation and encephalization in the koala. *Aust Mammal* 28:243–247

- Todorov OS, Blomberg SP, Goswami A et al (2021) Testing hypotheses of marsupial brain size variation using phylogenetic multiple imputations and a Bayesian comparative framework. *Proc R Soc Lond (Biol)* 288:20210394
- Toeplitz C (1920) Bau und Entwicklung des Knorpelschädels von *Didelphys marsupialis*. *Zoologica* 70:1–84
- Toro R (2012) On the possible shapes of the brain. *Evol Biol* 39:600–612
- Travouillon KJ, Legendre S, Archer M et al (2009) Palaeoecological analyses of Riverleigh's oligo-Miocene sites: implications for the oligo-Miocene climate change in Australia. *Palaeogeogr Palaeoclimatol Palaeoecol* 276:24–37
- Turney CSM, Flannery TF, Roberts RG et al (2008) Late-surviving megafauna in Tasmania, Australia, implicate human involvement in their extinction. *Proc Natl Acad Sci U S A* 105:12150–12153
- Voss RS, Jansa SA (2021) Opossums: an adaptive radiation of new world marsupials. Johns Hopkins University Press
- Weisbecker V (2011) Monotreme ossification sequences and the riddle of mammalian skeletal development. *Evolution* 65:1323–1335
- Weisbecker V (2015) Are monotremes primitive and marsupials inferior? In: Marsupials and monotremes: nature's enigmatic mammals. Nova Science Publishers, Inc, pp 397–411
- Weisbecker V, Beck RM (2015) Marsupial and monotreme evolution and biogeography. In: Klieve A, Hogan L, Johnston S, Murray P (eds) Marsupials and monotremes: nature's enigmatic mammals. Nova Science Publishers, New York, pp 1–25
- Weisbecker V, Goswami A (2010) Brain size, life history, and metabolism at the marsupial/placental dichotomy. *Proc Natl Acad Sci U S A* 107:16216–16221
- Weisbecker V, Goswami A (2011) Neonatal maturity as the key to understanding brain size evolution in homeothermic vertebrates. *BioEssays* 33:155–158
- Weisbecker V, Goswami A, Wroe S et al (2008) Ossification heterochrony in the therian postcranial skeleton and the marsupial–placental dichotomy. *Evolution* 62:2027–2041
- Weisbecker V, Rowe T, Wroe S et al (2021) Global elongation and high shape flexibility as an evolutionary hypothesis of accommodating mammalian brains into skulls. *Evolution* 75:625–640
- White CR, Phillips NF, Seymour RS (2006) The scaling and temperature dependence of vertebrate metabolism. *Biol Lett* 2:125–127
- Williamson TE, Brusatte SL, Wilson GP (2014) The origin and early evolution of metatherian mammals: the cretaceous record. *ZooKeys* 1
- Wilson DE, Reeder DM, eds (2005) Mammal species of the world. Johns Hopkins University Press, Baltimore, 2 volumes, 142 p
- Wilson GP, Ekdale EG, Hoganson et al (2016) A large carnivorous mammal from the late cretaceous and the north American origin of marsupials. *Nat Commun* 7:13734
- Wood Jones F (1949) The study of a generalized marsupial (*Dasyercus cristicauda* Krefft). *Trans Zool Soc Lond* 26:409–503
- Woods (1956) The skull of *Thylacoleo carnifex*. *Mem Queensl Mus* 13:125–140
- Wroe S, Myers TJ, Wells RT et al (1999) Estimating the weight of the Pleistocene marsupial lion, *Thylacoleo carnifex* (Thylacoleonidae: Marsupialia): implications for the ecomorphology of a marsupial super-predator and hypotheses of impoverishment of marsupial carnivore faunas. *Aust J Zool* 47:489–498
- Wroe S, Crowther M, Dortch J et al (2004) The size of the largest marsupial and why it matters. *Proc R Soc Lond (Biol)* 271:S34–S36

Chapter 12

Early Evolution of the Brain in Primates and Their Close Kin



Mary T. Silcox, Ornella C. Bertrand, Arianna R. Harrington,
Madlen M. Lang, Gabriela A. San Martín-Flores, and Sergi López-Torres

12.1 Systematic and Phylogenetic Context

This chapter focuses on the early phases of brain evolution in the order Primates, with only a brief discussion (Sect. 12.6) of evolutionary events occurring higher in the primate tree. Therefore, this section is largely focused on the taxa (and taxonomic framework) most relevant to that perspective.

Supplementary Information The online version contains supplementary material available at https://doi.org/10.1007/978-3-031-13983-3_12.

M. T. Silcox (✉) · M. M. Lang · G. A. San Martín-Flores
Department of Anthropology, University of Toronto Scarborough, Toronto, ON, Canada
e-mail: mary.silcox@utoronto.ca; madlen.lang@mail.utoronto.ca;
gabriela.sanmartinflores@mail.utoronto.ca

O. C. Bertrand
School of Geosciences, Grant Institute, University of Edinburgh, Edinburgh, Scotland
e-mail: ornella.bertrand@ed.ac.uk

A. R. Harrington
Department of Biology, Dixie State University, St. George, UT, USA

Southern Utah University, Cedar City, USA
e-mail: Arianna.Harrington@dixie.edu; ariannaharrington@suu.edu

S. López-Torres
Institute of Evolutionary Biology, Biological and Chemical Research Centre, Faculty of
Biology, University of Warsaw, Warsaw, Poland
e-mail: s.lopez-torres@uw.edu.pl

12.1.1 *The Phylogenetic Position of Primates Within Mammalia*

Identifying the mammalian orders most closely related to Primates is central to providing a context for studying primate brain evolution, particularly when considering the earliest phases of this process. Historically there were two main hypotheses about the closest relatives to Primates. First, an ancestry among “insectivores” (i.e. shrews, moles, hedgehogs, desmans, solenodons, and historically golden moles and tenrecs [now considered afrotheres]) has long been posited for the order (e.g. Simpson 1945; McKenna 1966; Szalay 1975). In particular, the general dental similarities with erinaceomorphs (i.e. hedgehogs) suggested to some workers that primates may have arisen from among this group or shared a common ancestor with it (see discussion in MacPhee et al. 1988). With respect to the evolution of the brain, this suggested link formed part of the basis for comparisons between living “insectivores” and Primates in the classic compilation of volumetric data by Stephan and colleagues (Stephan et al. 1970, 1981). These authors also posited that extant insectivores formed a good general model for the primitive form of the brain, and in particular identified a subset of taxa (shrews and hedgehogs) as showing what they inferred to be relatively primitive cerebral patterns. This dataset formed the basis for a series of publications focusing on the evolution of different regions of the brain (Stephan 1972), such as the neocortex (e.g. Frahm et al. 1982), in a framework that was explicitly rooted in “insectivores” as models for what was primitive for Primates. These works played a central role in framing ideas about early transitions in the size and form of the brain around the origin of the order (see for example Martin 1990).

Second, the alternative perspective, dating back to Gregory (1910), was that Primates were most closely related to treeshrews (Scandentia), elephant shrews (Macroscelididae), colugos (Dermoptera) and bats (Chiroptera), with these various orders being grouped with Primates in Archonta. Unpopular for several decades after its proposal, this idea was re-vivified starting in the 1970s, based on a version of Archonta that excluded elephant shrews (e.g. McKenna 1975; Szalay 1977). Although treeshrews (often as putative primitive primates) were included in early discussions of the evolution of the brain in Primates (e.g. Elliot Smith 1902; Le Gros Clark 1945; Stephan et al. 1970, 1981; Martin 1973), a perspective that considered Archonta as the critical comparative context *rather than* “Insectivora” was absent.

Molecular analyses of mammalian inter-ordinal relationships have led to a broad-based consensus about which taxa should be considered Primates’ closest kin (Fig. 12.1). There is strong support for a modified version of Archonta (i.e. Euarchonta Waddell et al. 1999) that includes Primates, Scandentia, and Dermoptera, but not Chiroptera. Within Euarchonta there is some lingering debate about which order(s) is the sister taxon of Primates, with there being analyses supporting all possible resolutions (i.e. Dermoptera, e.g. Janečka et al. 2007; Scandentia, e.g., Liu et al. 2009; or Sundatheria [Dermoptera + Scandentia], e.g. O’Leary et al. 2013).

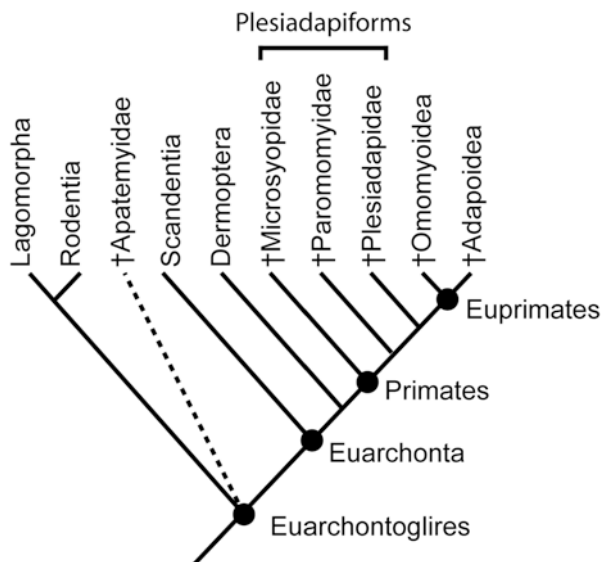


Fig. 12.1 Hypothesis of relationships for members of Euarchontoglires discussed in this chapter, based largely on Silcox et al. (2010b). Dermoptera has been positioned as the sister taxon to Primates based on Mason et al. (2016)

Recent genomic analyses seem to support a resolution to this debate, with Dermoptera being Primates' sister group (Mason et al. 2016; Zhang et al. 2019). The closest relatives of Euarchonta are not “insectivores” but rather rodents, rabbits and pikas (i.e. Glires [Rodentia + Lagomorpha]), a relationship recognized by the supraordinal name Euarchontoglires (Murphy et al. 2001). “Insectivora” as historically conceptualized is no longer considered to be a valid grouping; instead, supposed “insectivores” are thought to be spread between two broadly divergent supraordinal groups, the endemic African Afrotheria (Stanhope et al. 1998) and the more northerly evolving Laurasiatheria (Murphy et al. 2001). Hedgehogs in particular are included in Eulipotyphla, which is part of Laurasiatheria, and as such are more closely related to bats, carnivores, and ungulates than they are to Primates (Murphy et al. 2001).

Although this phylogenetic framework is broadly agreed upon, lingering effects of the history of considering “insectivores” as relevant to establishing what is primitive for Primates remain, with analyses as recent as 2016 (e.g. Ni et al. 2016) still including hedgehogs as outgroups to Euarchonta, rather than members of Glires (see also Beaudet and Gilissen 2018). This is also true for considerations of brain evolution (e.g. Gingerich and Gunnell 2005), so that even in our own work (Silcox et al. 2009b, 2010a), “insectivores” were used as proxies for what is primitive in Primates, in the absence of better available options.

With respect to the paleoneurological record, part of the challenge with studying the early evolution of the brain in Primates is that there are no fossil crania of

Scandentia or Dermoptera that are complete enough to produce an endocast for the purposes of comparison. As noted above, data from living treeshrews have been incorporated, to some degree, into discussions of primate brain evolution, and there exist very detailed histological descriptions of the modern treeshrew brain in a small selection of species (e.g. *Tupaia glis*, Tigges and Shantha 1969; *Tupaia belangeri*, Zhou and Ni 2016), as well as a database of endocasts for a greater diversity of extant forms (San Martín-Flores et al. 2018). However, based on comparisons to early primates, modern treeshrews make a poor proxy for a primitive stage of primate brain evolution, likely as a result of parallel increases in some areas of the brain (e.g., the neocortex; San Martín-Flores et al. 2018). Dermopterans, who have encephalization quotients (EQ) that are low relative to those of living Primates (Gingerich and Gunnell 2005), nonetheless have gyrencephalic brains that are very different from what would be expected for a primitive primate (San Martín-Flores et al. 2019).

From a paleoneurological perspective, this makes the endocasts of fossil Glires very relevant to studying primitive states in Primates, as the only extant group of non-primate euarchontoglires for which well-preserved fossil crania are known. Meng et al. (2003) published natural endocasts of the primitive member of Glires *Rhombomylus turpanensis*, although unfortunately they did not provide any quantitative data. There is a growing record of endocasts for fossil rodents (e.g. Dechaseaux 1958; Dozo 1997a, b; Dozo et al. 2004; Bertrand and Silcox 2016; Bertrand et al. 2016, 2017, 2018, 2019a; Ferreira et al. 2020), including some fairly primitive taxa (i.e. ischyromyids; see Bertrand and Silcox, Chap. 16, this book). Less well known is the form of the brain in extinct members of Lagomorpha, with Cope (1884) providing a few details about a natural endocast of *Paleolagus*, but otherwise only a few natural endocasts for relatively recent specimens being available (Edinger 1929; Sych 1967; Czyżewska 1985). More recently, virtual endocasts for extant lagomorphs and one virtual endocast for a more basal member of that order (*Megalagus turgidus*; López-Torres et al. 2020) have been described. Although still limited, the record that is available for Rodentia and Lagomorpha does help to frame primitive states for Primates, as discussed below.

Also, potentially relevant to assessing the primitive form of the brain in Primates are extinct groups that have been inferred to be members of Euarchontoglires (e.g. Apatemyidae [Silcox et al. 2010b], Anagalidae [Meng 2004], Mixodectidae [Szalay and Lucas 1996; Sargis et al. 2018]). Of these, the Apatemyidae is notable because virtual endocasts have been published for two species (see discussion below; von Koenigswald et al. 2009; Silcox et al. 2011). Apatemyids were arboreal animals (von Koenigswald 1990; von Koenigswald et al. 2005) sharing some features in the postcranium with euarchontans (Bloch et al. 2004), and with similarities to plesiadapiforms in the presence of enlarged, procumbent upper and lower incisors (e.g. see Silcox et al. 2010b: fig 2). An analysis based on craniodental traits grouped them within Euarchontoglires, with weak support tying them to *Rhombomylus* (Silcox et al. 2010b). As such, they have been suggested to be relevant to the larger context of euarchontoglian brain evolution (Silcox et al. 2011).

12.1.2 *Taxonomy and Phylogeny of Primates*

For extant primates, there is a broad-based consensus on the major framework for relationships within the order (e.g. Springer et al. 2012; Fleagle 2013). The first major division into suborders is between Strepsirrhini (lorises, lemurs and galagos) and Haplorhini (tarsiers, monkeys, apes and humans). Within Haplorhini, tarsiers are considered the most basally divergent group; their behavioral and morphological similarities with some strepsirrhines (e.g., nocturnal activity period; vertical clinging and leaping locomotion; faunivorous diet etc.) had traditionally caused them to be allied with strepsirrhines in Prosimii (engendering the term “prosimian”, which is still in broad usage), but those similarities are now thought to be primitive or convergent. The group that includes all non-tarsiiform haplorhines is variously referred to as Anthroidea or Simiiformes. It is divided into Platyrrhini (Panamerican monkeys) and Catarrhini (apes and humans [Hominoidea] and Afroeurasian monkeys [Cercopithecoidea]).

Although this phylogenetic and taxonomic framework is nearly universally accepted for living primates, fitting fossil taxa into the picture is not always straightforward, particularly for primitive species. The oldest potential primates are part of a radiation of over 140 species in 11 families that are generally referred to as plesiadapiforms (Silcox et al. 2017a). The first plesiadapiforms appear not long after the non-avian dinosaurs went extinct, in the early Paleocene (Fox and Scott 2011; Wilson Mantilla et al. 2021), whereas the latest occurring plesiadapiforms are late Eocene in age (Kihm and Tornow 2014). In the intervening >27 million years, members of the group evolved an impressive diversity of adaptations, although all known species have enlarged upper and lower central incisors and all species known from postcranial material were non-leaping arborealists. The primate status of plesiadapiforms continues to be a matter of debate. Whereas they share similarities to living primates in aspects of the dentition (e.g., low-crowned, bunodont molars with broad talonid basins) and in adaptations of the postcranium for arboreality, plesiadapiforms lack some traits that have traditionally been considered important to identifying primates, such as the postorbital bar. In recent years, the continuation of the debate stems in part from the challenge of choosing between the results of cladistic analyses based on larger matrices that were not designed with plesiadapiform character states in mind (e.g. Ni et al. 2016), and smaller matrices that were more explicitly tailored to the problem of sorting out events near the base of the primate tree (e.g. Bloch et al. 2007; Silcox 2008; Silcox et al. 2010b; Chester et al. 2017, 2019; see discussion in Silcox et al. 2017a). In the current paper we consider plesiadapiforms to be stem primates—so members of the order, but without a particular tie to any modern groups (Fig. 12.1). It is worth noting, however, that even analyses that come to a divergent conclusion about their primate status still finds that they are members of Euarchonta (e.g. Ni et al. 2016). As such, they are relevant to assessing primitive states for Primates whether or not they are classified as such. Within this framework it is useful to make a distinction between Plesiadapiformes, as a likely

paraphyletic array of stem primate families, and Euprimates Hoffstetter, 1977, as (probable) crown primates (Fig. 12.1).

The other two groups that are particularly critical for studying early brain evolution in Primates are Adapoidea and Omomyoidea, extinct euprimate superfamilies that both appear in the earliest Eocene (approx. 56 mya; Ni et al. 2004; Smith et al. 2006; Beard 2008; Rose et al. 2011, 2012). Most workers would agree that omomyoids are probably related to tarsiiiforms, or at least are haplorhines (e.g. Ni et al. 2016), but relationships of adapoids are more controversial, with various authors putting them on different sides of the haplorhine/strepsirrhine split (e.g. Gingerich et al. 2010; Williams et al. 2010). The consensus leans towards considering them strepsirrhines, in part because that is where they fall out in all large scale cladistic analyses (e.g. Ni et al. 2016; Seiffert et al. 2018). However, it is worth noting that they lack traits such as the toothcomb that are often thought to be distinctive of strepsirrhines (e.g. Fleagle 2013), implying that they are at best stem strepsirrhines. With respect to the paleoneurological record, adapoids and omomyoids are critically important, because there are no endocasts of early crown strepsirrhines (the oldest being the natural endocast of the Miocene lorisiiform *Komba*; Le Gros Clark and Thomas 1952; Simpson 1967), or other early, non-anthropoid haplorhines, but there is a burgeoning record of endocasts for adapoids and omomyoids.

12.2 Historical Background

12.2.1 *The Record of Endocranial Morphology and Any Other Paleoneurological Approaches in the Group Under Study*

There is a long history of study for endocasts of fossil primates, likely motivated by an interest in situating the exceptionally large brains of humans in a broader evolutionary context. The discussion below is divided into “Pre-CT” and “Post-CT” because the widespread availability of high-resolution X-ray computed tomography has re-framed the type of data that can be extracted from fossil primate crania.

Pre-CT

Discussion of the paleoneurology of early primates extends back to at least 1884, when Cope (1884, 1885) provided some brief commentary on the apparent form of the brain from the cranium of “*Anaptomorphus*” (now considered *Tetonius*) *homunculus*. Critical references in the early study of primate endocasts include Neumayer (1906), Gregory (1920), Le Gros Clark (1945), Hürzeler (1948), Piveteau (1958), Hofer (1962), Gazin (1965), Hofer and Wilson (1967), Radinsky (1967, 1970, 1974, 1975, 1977, 1982), Szalay (1969), Jerison (1973, 1979), Gingerich (1976), Gingerich

and Martin (1981), Gurche (1982), Martin (1990), and Gingerich and Gunnell (2005). Gurche (1982) published a useful summary of the state of knowledge known at the time for endocranial data of early primates, which includes consideration of most of the data available pre-CT. Although he deemed the sample available at that point to be “disappointingly small” (p. 227), he nonetheless provided a compilation of volume estimates for six species: the adapoids *Smilodectes gracilis*, *Adapis parisiensis*, and *Notharctus tenebrosus*; the omomyoids *Necrolemur antiquus* and *Tetonius homunculus*; and the taxonomically controversial *Rooneyia viejaensis* (often considered an omomyoid, but see Rosenberger et al. 2008). Prior to 1982, there were also published estimates of endocranial volume for the plesiadapiform *Plesiadapis tricuspidens* (Gingerich 1976; Radinsky 1977) that Gurche did not include, presumably because they were based on “the external appearance of crushed skulls” (p. 235). Of the specimens available in 1982, the most complete are attributed to the adapoids *Smilodectes gracilis*, known from a fairly complete natural endocast (USNM 23276; but missing the olfactory bulbs) published with excellent illustrations by Gazin (1965); and *Adapis parisiensis*, known from two endocasts, and for which direct estimates of volume could be calculated using both glass beads and mustard seed (Le Gros Clark 1945; Martin 1973, 1980; Gingerich and Martin 1981). While not discussed in any detail by Gurche (1982), there was also a partial latex endocast published for the microsyoipid plesiadapiform *Megadelphus lundeliusi* (AMNH 55284) by Szalay (1969; see also Radinsky 1977), although he did not provide any associated quantitative data. All the other endocranial data had to be gleaned from partial natural endocasts still partly or largely entombed in the crania or estimated from external cranial dimensions.

The interpretation of the data from this array of specimens was the focus of a historic debate in the literature between Leonard Radinsky and Harry Jerison (Radinsky 1970, 1977, 1982; Jerison 1973, 1979). Key areas of disagreement included (1) varying estimates of the endocranial capacity for the euprimate specimens; (2) differing interpretations about what the available data for *Plesiadapis* could tell us about the very earliest phases of primate brain evolution (i.e., with respect to the size of the brain and the degree to which it could be considered “spheroidal” like a primate’s); (3) differences of opinion over how to assess *relative* brain size (i.e. based on varying body mass estimators, and the use of different proxies for body mass such as foramen magnum dimensions); and (4) divergent views about the appropriate comparative context (i.e., modern primates vs. contemporary fossil taxa). Ultimately, the central difference of opinion between these authors was whether or not the evidence was adequate to assert that “encephalization was probably a characteristic adaptation in the order Primates from the earliest times,” (Jerison 1979: 615), with Radinsky (1977, 1982) disagreeing with this perspective. Gurche’s (1982) reassessment of the relevant data (including his own set of volume estimates) concluded, that, apart from *Rooneyia*, the Eocene euprimates had small brains relative to those of modern prosimians, with the adapoids in particular being notably less encephalized.

From Gurche’s (1982) summary to the beginning of the CT era, additional data for only three early Tertiary fossil primate species were added to the picture: the

adapoids *Leptadapis magnus* and *Pronycticebus gaudryi* (Martin 1990; note that the endocast referred to as “*Adapis magnus*” by Piveteau, 1958, actually pertains to *A. parisiensis* [Gingerich and Martin 1981]), and the plesiadapiform *Plesiadapis cookei* (Gingerich and Gunnell 2005). The latter was extremely revelatory with respect to the earlier arguments about the size and form of the brain in *Plesiadapis*. Gingerich and Gunnell (2005) made an estimate of cranial capacity using a full-scale model based on a partial natural endocast, and on dimensions drawn from a fairly completely preserved skull roof. Although the dorsoventral depth had to be approximated from “comparison with a range of endocasts of similar living mammals” (p. 188), this calculation is nonetheless much better constrained than earlier attempts to estimate the form and volume of the brain in the closely related species *P. tricuspidens* (Gingerich 1976; Radinsky 1977; Jerison 1979). The endocranial volume measured was much, much smaller than estimated for the similarly sized *P. tricuspidens* (i.e. 5 cc for *P. cookei* compared to estimates of 18.6 cc [Gingerich 1976]; 12–17 cc [Radinsky 1977]; and 16.6 cc [Martin 1990] for *P. tricuspidens*), and the shape of the endocast was far from spheroidal (Gingerich and Gunnell 2005: fig. 3). An excellent estimate of body mass can also be made for this specimen (UM 87990) because it is associated with much of a skeleton (Gingerich and Gunnell 2005; Boyer and Gingerich 2019). The ultimate message from these analyses is that *P. cookei* had a brain that was relatively very small compared to living primates and living dermopterans, and actually within the range of variation for Paleocene archaic ungulates. These data provided a first suggestion that Jerison’s generalization about encephalization being an ancient trait for Primates may not hold for “the first evolutionary radiation of primates” (Radinsky 1982: p. 34).

Post-CT

The small size and fragility of the cranium in most primitive primates limited the data available from traditional approaches. The increasing availability of high-resolution X-ray CT data has begun to revolutionize our understanding of their endocranial anatomy, particularly with respect to gathering accurate quantitative data. Virtual endocasts have been published for plesiadapiforms from three families: Plesiadapidae, Paromomyidae, and Microsypidae (Fig. 12.2; Silcox et al. 2009b, 2010a; Orliac et al. 2014; White et al. 2016). With respect to adapoids and omomyoids, virtual endocasts have been published for many of the same species whose significance was debated by Radinsky, Jerison, and Gurche, including *Smilodectes gracilis*, *Adapis parisiensis*, *Notharctus tenebrosus*, *Rooneyia viejaensis*, and *Necrolemur antiquus* (Fig. 12.3; Kirk et al. 2014; Harrington et al. 2016, 2020); notably Harrington et al. (2016) were able to provide endocasts for multiple specimens of *N. tenebrosus* (N = 3) and *S. gracilis* (N = 4), including a subadult specimen of *S. gracilis* (UM 32773 [=MPM 2612]), allowing for some first glimpses into intraspecific variation and ontogenetic change. Ramdarshan and Orliac (2016) provided a substantively complete endocast for the omomyoid *Microchoerus erinaceus*, a close relative of *N. antiquus*.

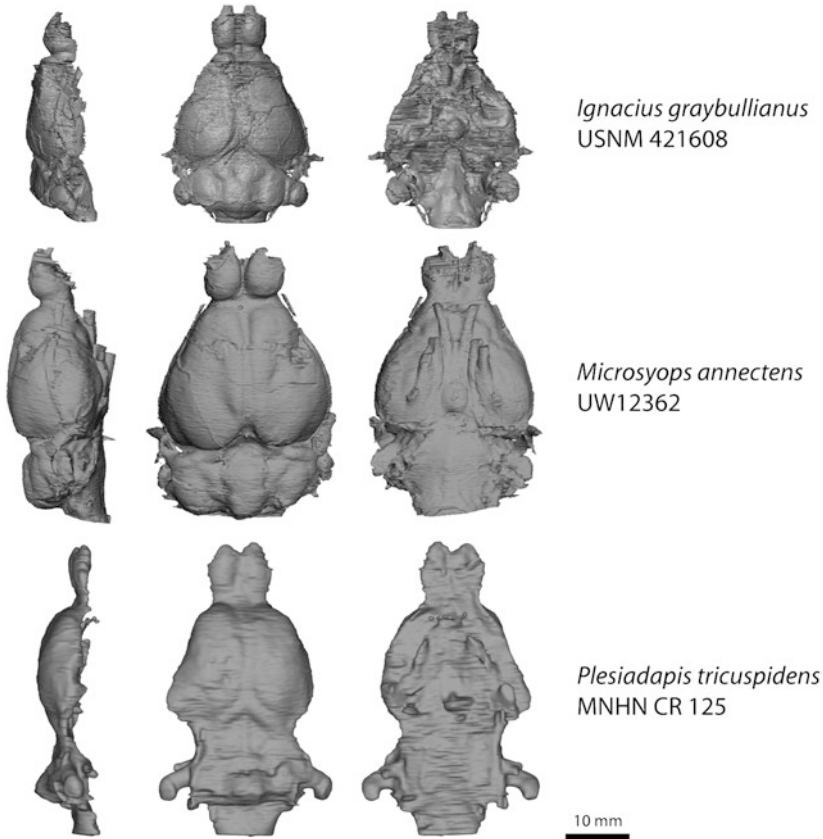


Fig. 12.2 Virtual endocasts of fossil stem primates from the families Paromomyidae (*Ignacius graybullianus*, USNM 421608), Microsyopidae (*Microsyops annectens*, UW 12362), and Plesiadapidae (*Plesiadapis tricuspidens*, MNHN CR 125) in lateral, dorsal, and ventral views. Endocasts originally published in Silcox et al. (2009b, 2010a) and Orliac et al. (2014)

For the taxa now known from virtual endocasts, it is possible to assess the previously made estimates of volume (see Gurche 1982: table 2; Martin 1990: table 8.12), with the assumption being that the virtual estimate is likely to be more accurate than estimates based on external dimensions or water displacement of “restored” endocasts (Gurche 1982: p. 228; Table 12.1). For *Adapis parisiensis*, the volume estimate made by Martin (1973) using mustard seed is a very close match to the volume calculated for the virtual endocast (8.8 cc; Harrington et al. 2016) for the same specimen, higher than Gurche’s (1982) estimate (8.31 cc), and lower than estimates calculated by Jerison and Radinsky using double integration methods (9.00 cc, 9.40 cc). Harrington et al. (2016) did not create virtual endocasts for the same specimens previously assessed for *S. gracilis* and *N. tenebrosus*, but in general their range of estimates is lower than those produced by other methods (i.e. range of 7.44–8.63 cc for *S. gracilis* vs. 9.12–9.95 cc [Gurche 1982]; range of 7.38–8.06 cc

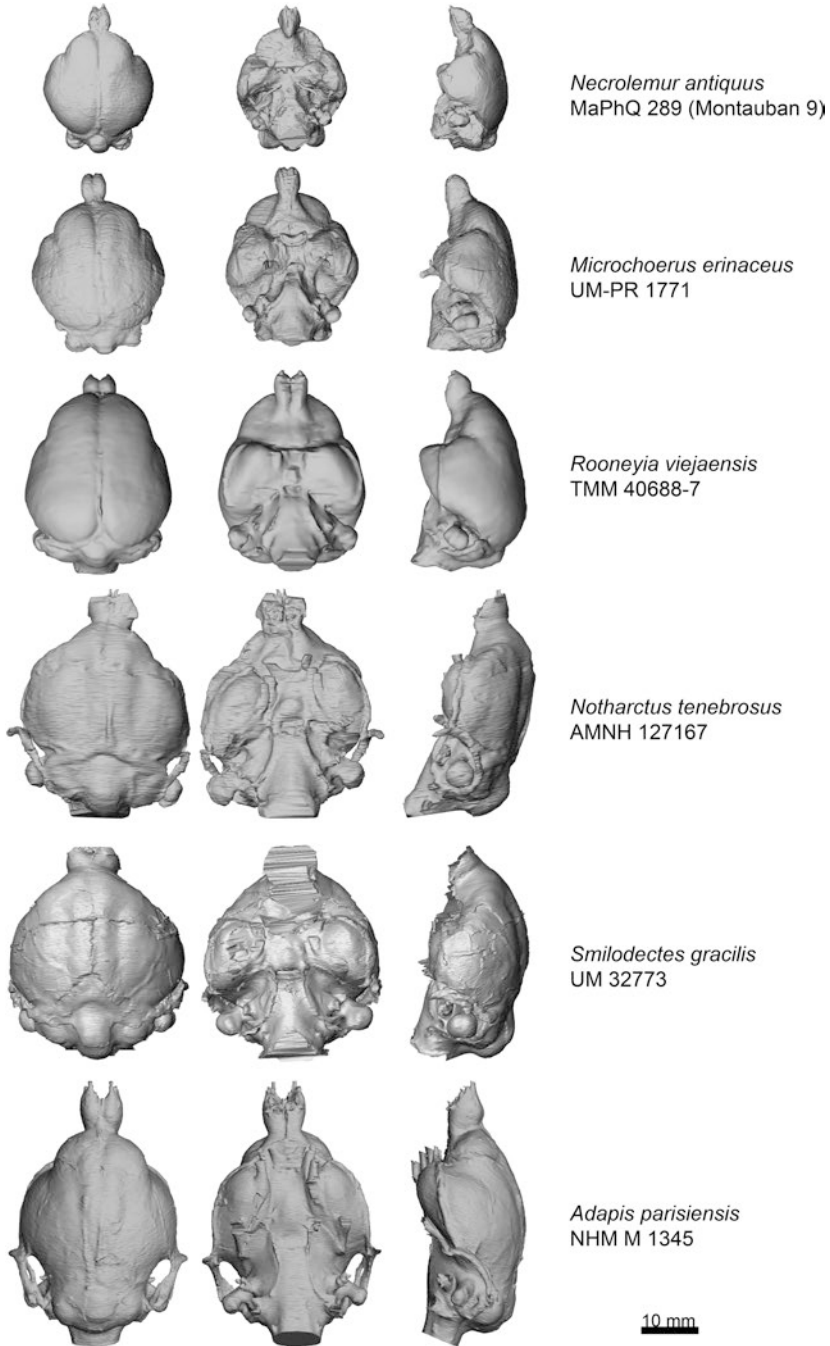


Fig. 12.3 Virtual endocasts of fossil euprimates from the superfamilies Omomyoidea (*Necrolemur antiquus*, MaPhQ 289 [Montauban 9]; *Microchoerus erinaceus*, UM-PR 1771) and Adapoidea (*Notharctus tenebrosus*, AMNH 127167; *Smilodectes gracilis*, UM 32773; *Adapis parisiensis*, NHM M 1345). *Rooneyia viejaensis* (TMM 40688-7) is of somewhat ambiguous systematic affiliation, but is often included in the Omomyoidea. Endocasts in dorsal, ventral, and lateral views. Endocasts originally published in Kirk et al. (2014), Harrington et al. (2016, 2020), and Ramdarshan and Orliac (2016)

Table 12.1 Compilation of data on early Tertiary primate endocasts

Taxon	<i>Necrolemur antiquus</i>	<i>Microchoerues erinaceus</i>	<i>Rooneyia viajaensis</i>	<i>Notharctus tenebrosus</i>	<i>Smilodectes gracilis</i>	<i>Adapis parisiensis</i>	<i>Microsypops annectens</i>	<i>Ignacius graybullianus</i>	<i>Plesiadapis cooket*</i>	<i>Plesiadapis tricuspidens</i>
Specimen	MaPhQ 289	UM-PRR1771	TMM 406887	MEAN	MEAN	NHM MI345	UW 12362	USNM 421608	UM 87990	MNHN CR 125
Total endocast volume	2355	4260	7230	7623.3	8353.3	8810	5900	2140	5000	5210
Total endocast length	25.4	31.4	35	40.6	40.3	45.7	41.25	30.79	42	43.5
Maximum endocast width	19.4	23.1	25.6	26.8	28.6	36.6	24	19.44	22	18.2
Maximum endocast height (=depth)	13.3	14.4	17.5	17	17.8	19	16.1	12.15	~12-13	22
Olfactory bulb length	4.6	4.5	4.1	4.8	5.8	9.1	8	6.28	10	9.7
Olfactory bulb width	4	4.5	5.9	8.5	8.7	7.5	5	3.935	5	-
Volume of olfactory bulbs	45.6	41	94	149	140.1	212	0.3	0.12	-	0.136
% of endocast composed of olfactory bulbs	1.94	0.96	1.3	1.95	1.68	2.41	5.1	5.53	7.8*	4.9

(continued)

Table 12.1 (continued)

Taxon	<i>Necrolemur antiquus</i>	<i>Microchoerus erinaceus</i>	<i>Rooneyia vijaensis</i>	<i>Notharctus tenebrosus</i>	<i>Smilodectes gracilis</i>	<i>Adapis parisiensis</i>	<i>Microslops amnectens</i>	<i>Ignacius graybullianus</i>	<i>Plesiadapis cookei*</i>	<i>Plesiadapis tricuspidens</i>
Total surface area of endocast	1266	1866.7	2409.3	2963.3	3300	3170	2956.19	1306.62	–	2960
Surface area of the neocortex	–	771.8	1054.6	905.3	1036.7	986	632.56	439.91	–	590
Neocortical ratio (calculated excluding olfactory bulbs)	–	0.43	0.46	0.32	0.34	0.33	0.243	0.218	–	0.22

Taken from Gingerich and Gunnell (2005), Silcox et al. (2009b, 2010a), Orliac et al. (2014), Long et al. (2015), Ramdarshan and Orliac (2016), Harrington et al. (2016, 2020). For *Plesiadapis cookei* values given are from Gingerich and Gunnell (2005) except for those listed with an asterisk which come from Orliac et al. (2014). Data for *Rooneyia vijaensis* as reported by Harrington et al. (2020), measured from the endocast described by Kirk et al. (2014). Values are given in mm, mm² or mm³

for *N. tenebrosus* vs. 10.43 cc [Gurche 1982]). Previous estimates for the only known cranium of *R. viejaensis* were close to the volume calculated from the virtual endocast, with Gurche (1982) actually being the closest (7.234 cc [Kirk et al. 2014] compared to 7.5 cc [Radinsky 1977]; 7.0 cc [Jerison 1979]; 7.38 cc [Gurche 1982]). Gurche (1982) also provided the endocranial volume estimate (2.65 cc) for *N. antiquus* that is closest to the value calculated from the digital endocast of the Montauban 9 cranium (MaPhQ 289; 2.36 cc [Harrington et al. 2020]), and markedly lower than estimates made by Radinsky (1977; 4.35 cc) and Jerison (1973, 1979, 4.20 cc,) although as Harrington et al. (2020) note, those estimates depended on composite illustrations that were based in part on other specimens (see Harrington et al. 2020: fig. 1). Bearing out the prediction made by Gingerich and Gunnell (2005), the estimate of cranial capacity for *P. tricuspidens* based on the virtual endocast (5.21 cc; corrected for deformation [Orliac et al. 2014]) is much lower than previous estimates for that taxon (18.6 cc [Gingerich 1976]; 12–17 cc [Radinsky 1977]; 16.6 cc [Martin 1990]), resulting in EQ estimates that overlap with that calculated for *P. cookei*.

The virtual endocasts currently available therefore address the first two issues that drove the Jerison-Radinsky debate. First, virtual endocasts provide direct measures of volume, so they do not depend on differing methods for estimation. Incomplete or damaged specimens do still require some additional interpretation—for example, the volume for the “undeformed” endocast of *P. tricuspidens* calculated by Orliac et al. (2014) is still likely a bit low, because they used the endocast of *Ignacius graybullianus* published by Silcox et al. (2009b) as their model, which comes from a skull that is also slightly pancaked. Nonetheless, these estimates come with fewer assumptions than (for example) those based on the double integration method, which models the brain as a cylinder (Jerison 1973). Second, we now have better data not only for *Plesiadapis*, but for several taxa (*Ignacius graybullianus*, *Microsyops annectens*) from the primate stem, all of which make clear that early primate brains retained a lot of primitive features (see discussion below).

12.2.2 Problematics

The other two issues in the Jerison-Radinsky debate remain sources of differing opinions. The best way to make comparisons of *relative* brain size continues to be an issue, although Martin (1990) provided a compelling argument that foramen magnum area is a poor proxy to use for body mass because of its lack of independence from brain size. The approach most recent authors have taken (e.g. Silcox et al. 2009b, 2010a; Orliac et al. 2014; Ramdarshan and Orliac 2016) has been to calculate multiple body mass estimates using equations based on different sample populations and measurements, and correspondingly provide a range of EQ estimates. Kirk et al. (2014) did not go even that far, giving no estimate of EQ for *Rooneyia* (but see Harrington et al. 2016 and Table 12.S1). Differences of opinion about how to best control for body mass led to a critique (Gilbert and Jungers 2017)

of one of the conclusions of the Harrington et al. (2016) analysis, specifically that changes in the organization of the brain in early euprimates preceded significant brain size increase. Gilbert and Jungers (2017) raised many valid concerns over the use of the encephalization quotient to consider relative brain size in that context. However, their approach of making narrow allometric comparisons (i.e. between taxa of like inferred body mass) was flawed in largely relying on body mass estimates for diverse taxa based on cranial length, which is problematic since plesiadapiform crania are less flexed, and have longer snouts, than euprimate crania (Bloch and Silcox 2006: fig. 28; Silcox et al. 2009a). As such, their inferences are confounded by the different scaling relationships of plesiadapiform and euprimate crania. This problem makes it difficult to assess whether their conclusion that relative brain size was notably smaller in plesiadapiforms than in early euprimates is a true signal, or a by-product of that difference (see further discussion in Sect. 12.4.2). Simply put, there is no ideal way to account for body mass in discussions of relative brain size, which means that debates about these questions are likely to continue.

The final issue in the Jerison-Radinsky debate was the appropriate comparative context in which to view the endocranial data for euprimates. In making comparisons, it is important to be clear on which question one is asking. Although differing body mass estimates make the situation somewhat murky (i.e. see discussions in Kirk et al. 2014; Ramdarshan and Orliac 2016), it does seem as though early Tertiary euprimates likely had somewhat smaller brains than living euprimates (Gurche 1982; Silcox et al. 2009b, 2010a; Harrington et al. 2016, 2020; Gilbert and Jungers 2017), with *Rooneyia* potentially being an exception to this generalization (Kirk et al. 2014: fig. 5; note that *Necrolemur* also appears to be an exception in that figure, but the endocranial volume estimate used was probably too high [Harrington et al. 2020]). Jerison (1973) suggested that there is a temporal effect on brain size, a hypothesis supported for Primates in a recent analysis by Bertrand et al. (2019a: fig. 17c) who found a significant (but rather weak) relationship between EQ estimates and geological time ($p < 0.05$; $r^2 = 0.507$; Bertrand et al. 2019a: table S11). However, this perspective does not provide an answer to two questions that are critical to establishing whether or not “encephalization was... a characteristic adaptation in the order Primates from the earliest times” (Jerison 1979, p. 615).

First, it does not answer the question of whether primates were encephalized relative to other mammals from the early Tertiary. Radinsky (1982) made comparisons between ranges of EQ values he had calculated (Radinsky 1978) for archaic carnivores and ungulates and concluded that contemporaneous primates were not exceptional; as noted above, Gingerich and Gunnell (2005) reached the same conclusion for *Plesiadapis cookei*. However, subsequent analyses using a slightly expanded archaic sample (e.g., Silcox et al. 2009b, 2010a; Bertrand et al. 2019a) reached a divergent conclusion, with primates generally (including plesiadapiforms) having relative brain sizes that are typically a bit higher than found in other “archaic” groups. There are many ways those analyses could be improved. In particular, they are still heavily dependent on Radinsky’s (1978) endocranial volume estimates, which were calculated using double integration. As the database of virtual endocasts expands, it would be preferable to use a sample of endocranial volume estimates

that are not so model dependent. Second, it would be beneficial to incorporate a phylogenetic factor (alongside a temporal one) into the analysis, rather than treating all non-primates as an undifferentiated mass (see discussion in Sect. 12.4.4).

The approach of formulating comparisons to other “archaic” mammals still does not answer the question of whether or not the earliest primates had larger (or differently organized) brains compared to their ancestors. The Radinsky (1978) sample that is central to such analyses is made up of carnivores and ungulates, which are only distantly related to Primates. As such, this sample does not provide the appropriate context to consider this question. With the expanded sample of closer primate relatives (i.e. rodents, lagomorphs, and apatemyids) available, it is starting to be possible to address this question (see Sect. 12.4.2).

12.3 Overview of General and Comparative Anatomy

12.3.1 Characterization of Cranial Endocast Morphology

Plesiadapiformes

There are reasonably complete endocasts published for four species of plesiadapiforms, in three families: Paromomyidae (*Ignacius graybullianus*: USNM 421608, Silcox et al. 2009b; UF 26000, Boyer et al. 2011; Long et al. 2015); Microsypidae (*Microsyps annectens*: UW 12362, UW 14559, Silcox et al. 2010a); and Plesiadapidae (*Plesiadapis cookei*: UM87990, Gingerich and Gunnell 2005; Orliac et al. 2014; *Plesiadapis tricuspiciens*: MNHN CR 125, Orliac et al. 2014; Kristjanson et al. 2016) (Fig. 12.2). Endocasts for two other species have been mentioned in abstracts, but have not yet been published in detail (*Niptomomys* cf. *N. doreenae*: USNM 530198, White et al. 2016; *Carpolestes simpsoni*: USNM 482354; Silcox et al. 2017b); discussion of these specimens here is limited to what was included in the abstracts. As noted above, Szalay (1969) published a partial latex endocast for the microsypid *Megadelphus lundeliusi* (AMNH 55284; see also Radinsky 1977). He did not provide any quantitative data. One of us (MTS) located the remnants of the endocast in the AMNH collection, but unfortunately it is degraded beyond usefulness. Szalay (1969), Silcox et al. (2010a), and Chester et al. (2019) also provided some endocranial details from partial cranial specimens of *Microsyps annectens* (AMNH 12595), *Microsyps* sp. cf. *M. elegans* (UM 99843) and *Torrejonia wilsoni* (NMMNH P-54500) respectively.

All the plesiadapiform endocasts that have been published show some basic points of similarity (Fig. 12.2). All have pedunculated olfactory bulbs separated from the rostral end of the cerebrum by a well demarcated circular fissure (Fig. 12.4a, b) implying that there was no overlap of the cerebrum onto the olfactory bulbs. The volume of the olfactory bulbs relative to the endocast as a whole is around 5% (Table 12.1) for *P. tricuspiciens*, *M. annectens*, and *I. graybullianus*. Orliac et al. (2014) produced a partial virtual endocast of *P. cookei*, which yielded a somewhat

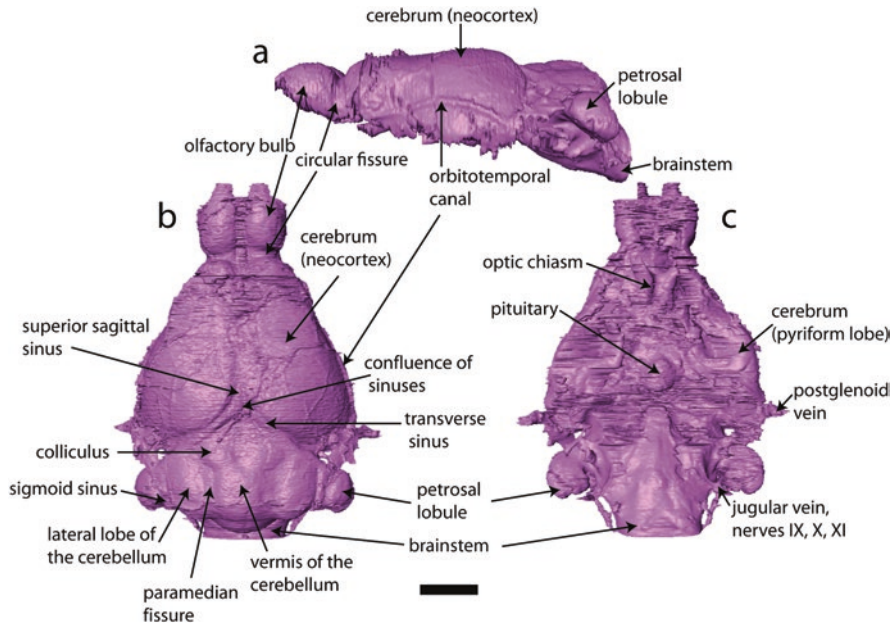


Fig. 12.4 Virtual endocast of *Ignacius graybullianus* (USNM 421608) in (a) left lateral, (b) dorsal and (c) ventral views, labelled with key structures discussed in the text. Endocast originally published in Silcox et al. (2009b). Scale = 5 mm

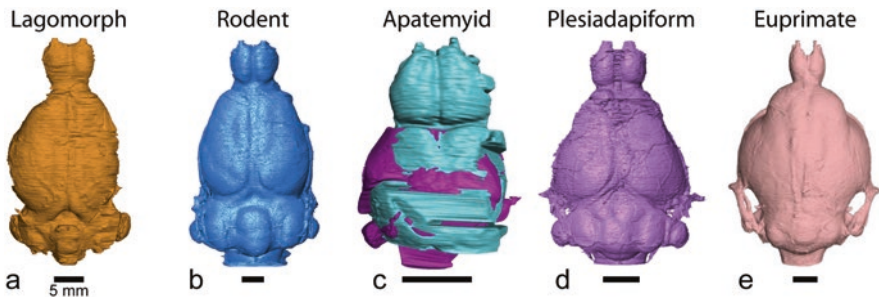


Fig. 12.5 Endocasts for early primates and members of closely related groups in dorsal view. (a) lagomorph *Megalagus turgidus* (FMNH UC 1642); (b) rodent *Paramys delicatus* (AMNH 12506); (c) apatemyid *Labidolemur kayi* (composite endocast based on USNM 530208 [purple] and USNM 530221 [teal]); (d) plesiadapiform *Ignacius graybullianus* (USNM 421608); (e) euprimate *Adapis parisiensis* (NHM M 1345). Endocasts originally published in Silcox et al. (2009b, 2011), Harrington et al. (2016), Bertrand et al. (2016), and López-Torres et al. (2020)

higher (7.8%) estimate of relative olfactory bulb size. However, this value is likely inflated as much of the ventral aspect of the endocast caudal to the olfactory bulbs is missing (see Orliac et al. 2014: fig. S2). In contrast, White et al. (2016) found that the olfactory bulbs in *Niptomomys* cf. *N. doreenae* were relatively somewhat larger

(8.61%); in this case the estimate (made from the more complete side of the endocast) likely represents a real difference from the other plesiadapiforms. Whether this large size is interpreted as primitive or derived depends on the taxa used for comparison. Early rodents (i.e. *Paramys copei*, 6.05%; *Paramys delicatus*, 4.75%; Bertrand et al. 2016; Fig. 12.5b) and an early lagomorph (*Megalagus turgidus* 3.96%; López-Torres et al. 2020; Fig. 12.5a) have olfactory bulbs that are smaller than reconstructed for *Niptomomys* cf. *N. doreenae*, which suggests that *Niptomomys* may have been specialized rather than exhibiting the primitive condition. However, the large olfactory bulbs of the basal apatemyid *Labidolemur kayi* (~12–15%; Silcox et al. 2011; Fig. 12.5c) send a contrary message.

In terms of the cerebrum, all plesiadapiforms are similar in having a narrow rostral end (suggesting small frontal lobes) and a caudal extent that does not fully cover the midbrain (Figs. 12.2 and 12.4a, b). There is some variation in the degree of exposure of the colliculi: in *I. graybullianus* (Fig. 12.4b; Silcox et al. 2009b), *Plesiadapis cookei* (Gingerich and Gunnell 2005), *P. tricuspidens* (Orliac et al. 2014), and *Carpolestes simpsoni* (Silcox et al. 2017b) a pair of colliculi (presumably the caudal or inferior colliculi) are exposed. The inner surface of the cranium of the palaeoarchonid plesiadapiform (*Torrejonia wilsoni*; Chester et al. 2019: fig. 3) also shows indentations for exposed colliculi. Within Microsyopidae there is some variability. A pair of colliculi are exposed in *Niptomomys* cf. *N. doreenae* (White et al. 2016), *Microsyops* sp. cf. *M. elegans* (Silcox et al. 2010a), and one specimen of *Microsyops annectens* (UW 14559; Silcox et al. 2010a). However, in the other known specimen of *M. annectens* (UW 12362) and in *Megadelphus lundeliusi* (see Szalay 1969: pl. 41) the colliculi are not exposed; although there is a small patch of midbrain visible, and it appears as though the transverse sinus is roofing the midbrain rather than the cerebrum (Szalay 1969; Silcox et al. 2010a). This contrast may relate to some small expansion of the cerebrum within the Microsyopidae, perhaps associated with more visual processing (Silcox et al. 2010a), because the taxa in which the colliculi are not consistently exposed are later occurring. Edinger (1964) made the point that exposure of the midbrain on the endocast is not necessarily primitive—it could also result from expansion of the colliculi for functional reasons. Interestingly, newborn *Tupaia* actually exhibit exposed rostral (superior) colliculi (Tigges and Shantha 1969), which is likely a reflection of the fact that the relevant part of the brain is very expanded in treeshrews (Kaas 2002). With respect to plesiadapiforms, however, midbrain exposure seems likely to be primitive, based on comparison to a range of relevant outgroups. The colliculi are exposed in the apatemyid *L. kayi* (Silcox et al. 2011; Fig. 12.5c), and there is very broad midbrain exposure in *Rhombomylus turpanensis* (Meng et al. 2003: fig. 51). Among early rodents, all the ischyromyids show some degree of midbrain exposure, with a couple of species showing clearly exposed colliculi (Bertrand et al. 2019a: table S14). The endocast of *Megalagus turgidus* does not exhibit exposed colliculi but does have a small patch of exposed midbrain (López-Torres et al. 2020; Fig. 12.5a). In sum, then, it appears likely that the exposure of the midbrain is primitive for plesiadapiforms, and likely characterized the common ancestor of Euarchontoglires.

No plesiadapiforms known from adequate material possess a Sylvian sulcus, or a well-defined temporal pole, which means that the ventral aspect of the cerebrum is nearly in line with, or ventral to, the brain stem (Fig. 12.4a). The same is also true in *L. kayi*, *R. turpanensis*, *M. turgidus*, and in early rodents (Meng et al. 2003; Silcox et al. 2011; Bertrand et al. 2016, 2019a; López-Torres et al. 2020). Interestingly tupaiid treeshrews actually have fairly well-defined temporal poles (e.g. see Le Gros Clark 1924: fig. 1), and some modern sciurids also develop a similar morphology, with at least one species (*Rhinosciurus laticaudatus*) even exhibiting a Sylvian sulcus (Bertrand et al. 2017: fig. 5). The fact that the temporal lobe is relatively small in the most basal living treeshrew, *Ptilocercus lowii* (e.g. see Le Gros Clark 1926: fig. 17), and in the fossil sciurid *Cedromus wilsoni* (Bertrand et al. 2017) suggests that the primitive state for Euarchontoglires is likely to be a poorly defined temporal pole, and suggest that the superficial similarity between euprimate (see below) and treeshrew endocasts in this feature arose independently.

The larger plesiadapiforms (*M. cf. elegans*, *M. lundeliusi*, *M. annectens*, *P. tricuspiciens*, *P. cookei*) all possess a lateral (=coronolateral, longitudinal, marginal) sulcus that runs approximately parallel to the superior sagittal sinus (Silcox et al. 2010a; Orliac et al. 2014; Fig. 12.2). The absence of this sulcus in the smaller plesiadapiforms (e.g., *Ignacius graybullianus*; Silcox et al. 2009b, 2010a; Fig. 12.4) likely relates to the fact that their endocranial volumes are less than 5 cc, the cut-off point below which brains typically fail to exhibit neocortical sulci (Macrini et al. 2007). There is some variability in the presence of the lateral sulcus in other fossil euarchontoglires (Silcox et al. 2011; Bertrand et al. 2016, 2019a; López-Torres et al. 2020), but this likely reflects variation in size rather than being informative about primitive states. Similarly, modern dermopterans have a lateral sulcus (Gingerich and Gunnell 2005: fig. 5) but modern treeshrews do not (Le Gros Clark 1924, 1926), which is probably a matter of their differing cranial capacities.

The location of the rhinal sulcus (=fissure; ventral edge of the neocortex) has been interpreted as corresponding to the orbitotemporal canal (=sinus canal) in plesiadapiforms that preserve the relevant region (Silcox et al. 2009b, 2010a; Orliac et al. 2014); these features are associated in modern lemuriforms (Martin 1990) and at least some rodents (Bertrand and Silcox 2016; Bertrand et al. 2016, 2017, 2018, 2019a). The orbitotemporal canal is located approximately two-thirds of the way down the lateral side of the cerebrum in *M. annectens*; the position was likely similar in *I. graybullianus* (Fig. 12.4a; see also Long et al. 2015: fig. 3F) and possibly *P. tricuspiciens*, although compression in the latter makes its position difficult to discern. As noted by Silcox et al. (2010a) and Orliac et al. (2014), the indentation identified as the rhinal fissure on the reconstructed endocast of *P. cookei* by Gingerich and Gunnell (2005) is likely to be too far ventral. Instead, *P. cookei* may have been like *M. annectens*, and possibly *M. lundeliusi*, in having an additional faint neocortical sulcus (?suprasylvian; Silcox et al. 2010a). The significance of the position of the rhinal sulcus is discussed further below (Sect. 12.4.4).

The morphology of the cerebellum in *I. graybullianus* and *M. annectens* is similar. In both cases there is a well demarcated vermis separated from the lateral lobes by paramedian fissures (Silcox et al. 2009b, 2010a; Figs. 12.2 and 12.4b). There is

no clear evidence of a fissura prima. The petrosal lobules (often referred to as the paraflocculi) are well-rounded and connect to the rest of the cerebellum with a short stem. In both cases the cerebellum accounts for between a quarter and a third of the total length of the endocast. It is difficult to form more refined quantitative comparisons about the cerebellum, since it is challenging to separate it from other parts of the brain in endocasts. However, based on the relative length of the cerebellum, it could be interpreted as making up a smaller proportion of the brain in *Plesiadapis* than in other plesiadapiforms, because it only accounts for about 17% of the total length of the endocast in *P. tricuspis* (Orliac et al. 2014). Damage to the relevant specimen makes the precise position of the front of the cerebellum a matter of interpretation, so it would be beneficial to be able to assess this in another specimen (unfortunately the full length of the endocast is not preserved for *P. cookei*). The petrosal lobules are also quite distinctive in shape in *P. tricuspis* compared to *I. graybullianus* and *M. annectens*, being more elongate and cylindrical, and less globular (Fig. 12.2), a contrast Orliac et al. (2014: p. 3) argue is real based on the “perfect preservation of both petrosals” in *P. tricuspis*.

Adapoids and Omomyoids

This discussion will focus on species for which three-dimensional endocasts are available (i.e., the adapoids *Smilodectes gracilis*, *Adapis parisiensis*, and *Notharctus tenebrosus*; the omomyoids *Microchoerus erinaceus* and *Necrolemur antiquus*; and *Rooneyia viejaensis*; Gazin 1965; Gingerich and Martin 1981; Kirk et al. 2014; Harrington et al. 2016, 2020; Ramdarshan and Orliac 2016) (Fig. 12.3) with additional details from specimens known only from natural endocasts that are partially visible through breaks in the cranium (see Gurche 1982: fig. 6) as warranted. As noted above there are endocranial volume estimates that have been calculated for the adapoids *Pronycticebus gaudryi* and *Leptadapis magnus* (Martin 1990), but these species are not yet known from published endocasts.

The adapoids and omomyoids known from endocasts are similar to plesiadapiforms in having pedunculated olfactory bulbs separated from the cerebrum by a distinct (if narrow) circular fissure (Figs. 12.3 and 12.5). The volume of the olfactory bulbs relative to the overall endocranial volume is typically lower in euprimates than in plesiadapiforms. For specimens with volumes directly measured from CT data the range of variation is 0.94% (*Rooneyia viejaensis*; Kirk et al. 2014) – 2.40% (*Adapis parisiensis*; Harrington et al. 2016). Estimates for taxa not yet known from virtual endocasts extend this range (i.e., 3.4% for *Tetonius homunculus*; Gurche 1982; Ramdarshan and Orliac 2016). These values generally lie within the range of variation observed for living strepsirrhines (0.39%–3.38%; Stephan et al. 1981; Kirk et al. 2014), but above the value for *Tarsius* sp. (0.53%; Stephan et al. 1981; Kirk et al. 2014). Although the contrast between plesiadapiforms and euprimates could be interpreted as evidence for reduced importance in the sense of smell through evolutionary time, it is worth noting that the distinction mostly disappears when the size of the olfactory bulbs is assessed against body mass rather than

endocranial volume (i.e., see Harrington et al. 2016: fig. 12). Therefore, the difference in *relative* size may relate more to increases in other parts of the brain than to decreases in the size of the olfactory apparatus, a point Martin (1990) also made with respect to the relative size of the olfactory bulbs in living strepsirrhines compared to non-primates (see Martin 1990: fig. 8.16; see also Heritage 2014).

The presence of a clear circular fissure on the endocast is a contrast with the situation in living euprimates, in which the cerebrum typically overlaps at least somewhat onto the olfactory bulbs. Alongside the relatively narrow rostral end of the cerebrum evident in adapoids and omomyoids (Fig. 12.3), this lack of overlap could signal a lesser development of the frontal lobes in primitive euprimates relative to extant species (Radinsky 1970; Jerison 1973; Kirk et al. 2014), although actually quantifying the relative size of this part of the brain is not possible (Jerison 2007). In contrast to plesiadapiforms, however, the cerebrum has a well-defined temporal pole in all euprimates known from endocasts. Associated with this, most fossil euprimate taxa have a fairly well distinguished Sylvian sulcus, which is a trait that has long been considered a distinctive feature of the primate brain (Elliot Smith 1902; although as noted above, this feature does occasionally develop in other groups; Bertrand et al. 2017). The sole exception to this generality among fossil euprimates is *Smilodectes gracilis*, which is variable in the presence of the Sylvian sulcus (Gazin 1965; Harrington et al. 2016; it is also only weakly expressed in a specimen of *N. tenebrosus*, AMNH 127167). The importance of this variable presence is somewhat ambiguous because it could reflect obscuring by dural vessels or thick meningeal tissues rather than a real absence from the brain (see discussion in Harrington et al. 2016). In any case, the expansion of the cerebrum (so that in lateral view the temporal pole extends ventrally beyond the level of the ventral border of the brain stem; Fig. 12.3) is a distinct difference from plesiadapiforms (Figs. 12.2 and 12.4a), suggestive of expansions to the temporal lobe.

In all the fossil euprimates known from endocasts that preserve the relevant area, the orbitotemporal canal (and therefore presumably the rhinal fissure) is located near the ventral extent of the temporal lobe (Fig. 12.3), in a position that is farther ventral than observed in the plesiadapiforms that preserve this feature, and similar to some small-bodied modern strepsirrhines (e.g., *Microcebus*; Kirk et al. 2014: fig. 4). As discussed below, this contrast is likely associated with a relative expansion of the neocortex at the euprimate node. Expansion of the cerebrum distally is also likely associated with increased neocorticalization, so that there is no exposure of the midbrain on the surface of the endocast (Fig. 12.3), unlike in plesiadapiforms (Fig. 12.2). This contrast suggests, therefore, some expansion of the occipital lobe with the evolution of Euprimates.

As in the plesiadapiforms, the larger taxa (*Adapis parisiensis*, *Smilodectes gracilis*, *Notharctus tenebrosus*; Gazin 1965; Gingerich and Martin 1981; Gurche 1982; Harrington et al. 2016) among the adapoids and omomyoids have a well-defined lateral sulcus running approximately parallel to the superior sagittal sinus, but this feature is missing from the smaller forms (*Rooneyia viejaensis*, *Tetonius homunculus*, *Necrolemur antiquus* Radinsky 1970; Kirk et al. 2014; Ramdarshan and Orliac 2016; Harrington et al. 2020; Fig. 12.3). A lateral sulcus has been identified in

Microchoerus erinaceus (Ramdarshan and Orliac 2016; Fig. 12.3), which is somewhat surprising because that species' endocranial volume is 4.26 cc, and so below the 5 cc boundary that is typically associated with lissencephaly (Macrini et al. 2007). Endocasts of *S. gracilis* and *N. tenebrosus* are variable in the expression of a faint dorsolateral sulcus in the region between the lateral sulcus and the orbitotemporal canal (e.g., see Harrington et al. 2016: fig. 5F), which has been referred to as a possible suprasylvian sulcus (Gurche 1982; Harrington et al. 2016); the position is similar to the faint ?suprasylvian sulcus evident in the plesiadapiform *M. annectens* (and also possibly *M. lundeliusi* and *P. cookei*; Silcox et al. 2010a). The expression of this feature varies not only among specimens, but even within particular specimens (e.g., it is better defined on the left size of AMNH 127167 [*N. tenebrosus*] than it is on the right; see Harrington et al. 2016: fig. 5). A shallow sulcus near the anteroventral border of the temporal lobe was identified in *Microchoerus erinaceus* (i.e., "temporal sulcus" of Ramdarshan and Orliac 2016: fig. 3C). Interestingly, a faint sulcus in a very similar position was identified in two specimens (Montauban 9 [MaPhQ 289] and BMM 4490) of *N. antiquus* by Gurche (1982; fig. 6f, g); he likened it to the postsylvian sulcus of *Tarsius*, which would be interesting in light of the historical tie suggested between those taxa (Rosenberger 1985). However, this feature is not evident on the virtual endocast of Montauban 9 (Harrington et al. 2020).

In general, it would be fair to say that early euprimate brains are characterized by the usual presence of the Sylvian sulcus, with evidence of independent development of additional subtle sulci, starting with the longitudinal sulcus, as brains start to increase in size. The pair of sulci on the relatively small brain of *M. erinaceus* stands out as notable, although it is unclear if this pattern represents a part of any kind of larger evolutionary picture.

All early euprimates known from endocasts (Fig. 12.3) share a basically similar morphology of the cerebellum with the plesiadapiforms *Ignacius graybullianus* and *Microsyops annectens* (Figs. 12.2 and 12.4). There is a clear division, by way of paramedian fissures, between the vermis and the lateral lobes, and the petrosal lobe is globular and attached to the rest of the cerebellum by a short stem. It is difficult to formulate any quantitative comparisons about the cerebellum from the endocranial evidence, because in early euprimates there are varying degrees of coverage of this part of the brain by the cerebrum (not covered in *S. gracilis*, *N. tenebrosus*, *A. parisiensis*; partly covered in *N. antiquus*, *T. homunculus*, *N. antiquus*, *M. erinaceus*, *R. viejaensis*; Harrington et al. 2016, 2020; Fig. 12.3). The relative length of the cerebellum on the ventral surface of the endocast likely has more to do with the degree of flexion of the cranium than with the actual size of the cerebellum. So, for example, the cerebellum appears very short in dorsal view in *R. viejaensis* (Kirk et al. 2014: fig. 3A) and much longer in *A. parisiensis* (Harrington et al. 2016: fig. 9B), but this is likely because the cranium of *R. viejaensis* is much more strongly flexed (with a cranial base angle of 176° compared to 187° in *A. parisiensis*; Harrington et al. 2020: table 1). Gurche (1982) provided an equation for calculating relative cerebellar size, but because it is based on brain mass, it is not possible to use it to consider cerebellar size as independent from overall brain size. For this reason,

unfortunately data from the endocasts of early primates cannot currently contribute to debates about the relative importance of the cerebellum in primate evolutionary history (e.g. Barton 2012).

12.3.2 *Spaces Associated with Cranial Blood Supply*

Endocasts of early primates possess casts of several spaces associated with arterial blood supply and venous drainage of the brain and cranium. Generally, the brains of fossil and extant haplorhine primates (including omomyoids), fossil anthropoids, most adapoids, and some plesiadapiforms (e.g., *Microsyops annectens*) are thought to be supplied by the vertebral artery and the promontorial branch of the internal carotid artery, whereas extant strepsirrhines, subfossil lemurs, some adapoids (e.g., *Adapis parisiensis*) and some plesiadapiforms (e.g., *Ignacius graybullianus*) are believed to have had non-patent (i.e., non-functional and/or absent) promontorial arteries (Bugge 1974, Conroy and Wible 1978; MacPhee and Cartmill 1986, Boyer et al. 2016). Among extant strepsirrhines with non-patent promontorial arteries, several groups (e.g., cheirogaleids and lorisiforms) supplement their encephalic blood supply via branches of the ascending pharyngeal artery, which stems from the external carotid arteries (Cartmill 1975; MacPhee and Cartmill 1986). There is some ambiguity in the pattern of evolution of internal carotid arterial reduction in strepsirrhine evolution, driven in part by variation among adapoids (e.g., the promontorial artery was involuted in *Adapis parisiensis* but not in its close relative *Leptadapis*), which indicates that there must have been some measure of homoplasy in this trait (Boyer et al. 2016).

The impressions of grooves, which presumably marked the paths of the promontorial arteries, are observed caudal or lateral to the cast of the hypophyseal fossa on the ventral surface of the endocasts of several species. These species include the plesiadapiform *Microsyops annectens* (Silcox et al. 2010a), the omomyoid *Necrolemur antiquus* (Harrington et al. 2020) and the adapoids *Notharctus tenebrosus* (Harrington et al. 2016) and *Smilodectes gracilis* (Gazin 1965; Harrington et al. 2016). These species are consistent with those identified by Boyer et al. (2016) to have likely had patent promontorial arteries (i.e., that supplied the brain), on the basis of the area of the ossified promontorial canal relative to brain size.

Inferring arterial blood supply to the brain from endocasts is limited in species which do not have patent promontorial arteries. The vertebral arteries enter the endocranial space through the foramen magnum and do not leave a cast of their course on endocasts. In addition, branches of the ascending pharyngeal arteries supplying the brain enter the endocranium via a foramen lacerum medium (Cartmill 1975; Conroy and Packer 1981; MacPhee and Cartmill 1986), which may also pass other structures and thus may not be correlated to the presence of the artery.

Far more numerous than the traces of arterial features on the endocast are the impressions of venous features. Chief among these are venous sinus spaces enclosed by folds in the dura mater. In mammals, the superior sagittal sinus, which forms at

the apex of the falx cerebri, drains into the transverse sinus (Fig. 12.4b; sometimes referred to as the lateral sinus, e.g., Gazin 1965 and Gingerich and Martin 1981) in the edge of tentorium cerebelli before continuing to the sigmoid sinus. In turn, the sigmoid sinus (Fig. 12.4b), as well as the inferior petrosal sinus on the ventral surface of the brain, empties into the internal jugular vein in the jugular foramen, which is one major path for blood exiting the endocranial cavity (Butler 1967; Wible 1990). Primitively for eutherian mammals, the transverse sinus is also continuous with a sinus variably called the petrosquamous or capsuloparietal emissary vein, which drains into the postglenoid vein exiting the endocranial cavity via the postglenoid foramen (Wible 1990; Wible and Zeller 1994). In treeshrews, the capsuloparietal emissary vein is also continuous anteriorly with the cranio-orbital sinus, which travels along the cranio-orbital canal to the orbits (Wible 2011; Wible and Zeller 1994). Hence, the capsuloemissary vein, cranio-orbital sinus, and postglenoid vein share a confluence in treeshrews. With a few exceptions, endocasts of plesiadapiforms and early euprimates preserve features which suggest they shared the above-described general primitive pattern of endocranial venous drainage (Fig. 12.4).

The impression of the superior sagittal sinus is prominent on the dorsal surface of many early fossil primate endocasts, particularly on the surface of the caudal half of the cerebrum (Fig. 12.4b). Macrini et al. (2007) suggested that the absence of a cast of the superior sagittal sinus may indicate a relatively deep position of this sinus within the meninges in life. This could suggest that in certain endocasts where the superior sagittal sinus is more prominent caudally (e.g., as seen in adapoids; Harrington et al. 2016; Fig. 12.3), that the sinus was deeper within the meninges surrounding the rostral half of the brain, and/or perhaps became more salient as it collected blood from more contributing veins caudally.

The cast of the confluence of the superior sagittal sinus and transverse sinuses are also well-preserved on the dorsal surface of early primate endocasts (Fig. 12.4b). The sigmoid sinus typically courses caudal to the petrosal lobules (Fig. 12.4b) but were either absent or not well-preserved on the endocasts of *P. tricuspidens*, *M. erinaceus*, and *N. antiquus* (Orliac et al. 2014; Ramdarshan and Orliac 2016; Harrington et al. 2020). On the ventral surface, bilateral casts of the inferior petrosal sinus have been identified on endocasts of early primates with the exception of *P. tricuspidens* and *I. graybullianus* (Orliac et al. 2014; Silcox et al. 2009b).

The portion of the petrosquamous sinus/capsuloparietal emissary vein connecting the transverse sinus to the postglenoid foramen (Fig. 12.4c) is evidently completely enclosed by bone in many plesiadapiforms, adapoids, and omomyoids, although this condition was not observed on the virtual endocast of *P. tricuspidens* or *N. antiquus* (Harrington et al. 2016, 2020; Orliac et al. 2014; Ramdarshan and Orliac 2016; Silcox et al. 2009b, 2010a). A distinct cast of the canal for the postglenoid vein and the orbitotemporal canal are also visible on virtual endocasts of early primates, except in that of *N. antiquus* (MaPhQ 289), for which it could not be discerned from a CT scan whether a definitive orbitotemporal canal was present (Harrington et al. 2020). It does not seem likely that this canal was entirely absent in *Necrolemur*, as *M. erinaceus*, which does possess a bilateral cast of the

orbitotemporal canals on its endocast, and has been hypothesized to be a direct descendent of *N. antiquus* (Minwer-Barakat et al. 2017). Thus, it is unlikely that this primitive endocranial feature was lost in *Necrolemur*, then regained in *Microchoerus*; the more likely alternative is that its absence on the endocast is a product of preservation.

12.4 Brain Evolution and Paleobiological Inferences Based on Endocast Morphology

12.4.1 Morphological Brain Diversity

As detailed above, we now have some understanding of the form of the brain both in stem primates, and in early euprimates, and can reach some tentative conclusions about directions in evolutionary change occurring near the base of the primate tree. Plesiadapiforms can be inferred to have had quite primitive looking brains, sharing fundamental similarities with endocasts that have been reconstructed for early fossil rodents (i.e., ischyromyids; Bertrand and Silcox 2016; Bertrand et al. 2016, 2019a) and for a stem lagomorph (López-Torres et al. 2020). In particular, like the endocasts in those taxa, they have fairly large, pedunculated olfactory bulbs, have a cerebrum that does not overlap onto the circular fissure or entirely cover the midbrain, and lack a Sylvian fissure and a clearly demarcated temporal pole (Fig. 12.5). As in early rodents and *Megalagus*, larger plesiadapiforms develop a lateral sulcus, with their brains otherwise being basically lissencephalic (with the exception of the very shallow ?suprasylvian sulcus of *M. annectens* and possibly *M. lundeliusi* and *P. cookei*). As noted above, there is some ambiguity in the direction of evolutionary change in the relative size of the olfactory bulbs based on the conflicting signal from rodents and lagomorphs on one hand, and the apatemyid *Labidolemur kayi* on the other. So perhaps the basal primate node was associated with some decrease in the relative size of these bulbs (but perhaps not; see also Heritage 2014). In all, there are few clear indications of special similarities in the brain between plesiadapiforms and euprimates. One possible exception to this was highlighted by Orliac et al. (2014: p. 1), who suggested that, in spite of being at the low end of the known variation in plesiadapiforms for both EQ and relative neocortical size, *P. tricuspidentis* was similar to euprimates in having a "...domed neocortex and downwardly shifted olfactory-bulb axis", differing in this way from *Ignacius graybullianus* and *Microsyops annectens*. Phylogenetic analyses (e.g. Bloch et al. 2007; Silcox et al. 2010b; Chester et al. 2019) suggest that plesiadapids are more closely related to euprimates than paromomyids and microsypids are. This shift could represent some re-organization of the brain in stem primates, prior to any kind of significant expansion in the relative size of the brain overall, or of the neocortex specifically. However, that conclusion is based on a very heavily pancaked specimen, so this

inference merits testing in other plesiadapoid specimens (i.e., including carpolestids or saxonellids).

What is more certain is that there was a quite significant re-organization of the brain associated with the euprimate node, with all euprimates showing evidence of expansion in the temporal and occipital lobes (associated with the development of a Sylvian sulcus and strong temporal pole, and coverage of the midbrain) compared to plesiadapiforms. The more ventral position of the rhinal fissure suggests expansion of the neocortex (see Sect. 12.4.4). The relative size of the olfactory bulbs is lower, but this may represent stasis, where in other regions were expanding, rather than an actual decrease in their absolute size. In all, early euprimates have brains that are similar in morphology in many ways to extant small strepsirrhines, differing predominantly in an inferred lesser development of the frontal lobes. Whether this reorganization was associated with a significant increase in overall size is a matter of some debate (Harrington et al. 2016; Gilbert and Jungers 2017; see discussion above and in Sect. 12.4.2), but as noted above, if an increase did occur, it did not lead to relative brain sizes that were comparable to living primates in most cases.

12.4.2 Brain-Size Evolution and Encephalization Quotient

As detailed above, the availability of quantitative data on encephalization for both plesiadapiforms and early euprimates has increased significantly in the last 15 years (Gingerich and Gunnell 2005; Silcox et al. 2009b, 2010a; Kirk et al. 2014; Orliac et al. 2014; Harrington et al. 2016, 2020; Ramdarshan and Orliac 2016; Table 12.1). This information allows us to explore quantitatively the question of when increases in encephalization occurred in early primate evolution, placing this question within the updated evolutionary framework of Euarchontoglires. Quantitative encephalization data for fossil primates is also extensive for higher nodes of the tree, including anthropoids (Martin 1993; Begun and Kordos 2004; Bush et al. 2004a,b; Holloway et al. 2004; Guy et al. 2005; Nargolwalla et al. 2005; Falk 2007; Harvati and Frost 2007; Simons et al. 2007; Weston and Lister 2009; White et al. 2009; Kay et al. 2012; Gonzales et al. 2015; Ni et al. 2019) and crown strepsirrhines (Ryan et al. 2008). Therefore, the encephalization data collected from fossil primates, combined with the brain and body mass data that exist for a great diversity of living primates (Table 12.S1), allows us to comprehensively probe this question through the means of ancestral state reconstruction analyses. Taxa for which endocranial volume estimates were made from external measurements of the cranium were generally excluded from this analysis.

To accurately reconstruct deep nodes in the primate tree, such as those of the ancestral euprimate or the ancestral primate, it is necessary to include the same type of quantitative information for other euarchontoglires. Previous attempts at reconstructing the ancestral euprimate relative brain size (Montgomery et al. 2010; Steiper and Seiffert 2012) used a sample exclusively made up of primates without putting them in an euarchontoglian context. Boddy et al. (2012) reconstructed the

ancestral euprimate EQ using a mammalian tree that included Scandentia, Rodentia and Lagomorpha (but not Dermoptera), but that did not include fossils. Fortunately, recent work in the last decade has provided relevant data for dermopterans (San Martin-Flores et al. 2019), scandentians (San Martin-Flores et al. 2018), fossil rodents (Bertrand and Silcox 2016; Bertrand et al. 2016, 2017, 2018, 2019a; Ferreira et al. 2020), fossil lagomorphs (López-Torres et al. 2020), and apatemyids (Silcox et al. 2011), allowing for an examination of change in brain size on the primate (and euarchontogliran) tree that at least partially overcomes the limitations of previous studies.

The taxa for which there are estimates of endocranial volume and body mass available (Table 12.S1) were assembled into a supertree based on Kobayashi (1995), Takai et al. (2008), Silcox et al. (2010b), Roberts et al. (2011), Springer et al. (2012), Gudde et al. (2013), Baab et al. (2014), Martins Jr. et al. (2015), Strait et al. (2015), Ni et al. (2016, 2019), Byrne et al. (2018), Mongle et al. (2019), and Bertrand et al. (2021). This tree was used as the basis for an analysis of ancestral states for EQ in Mesquite 3.2 (Maddison and Maddison 2017) under parsimony (i.e., using the Analysis:Tree Trace All Characters Parsimony Ancestral States option). We performed the analysis using estimates of EQ based on both Jerison's (1973) and Eisenberg's (1981) equations, and for topologies that support both Sundatheria (i.e., treeshrews and colugos as sister taxa) and Primatomorpha (i.e., primates and colugos as sister taxa). Figures 12.6 and 12.S1 were made with the software FigTree and depict the results of the analysis using Jerison's (1973) equation and the topology that supports Primatomorpha, while Table 12.2 includes reconstructed values for key nodes from all 4 analyses. Our results suggest that there is a marked increase in EQ from the ancestral primate to the ancestral euprimate nodes (Table 12.2, Fig. 12.6). Using Jerison's (1973) EQ, the ancestral primate would have had an EQ of 0.41 and the ancestral euprimate an EQ of 0.68; using Eisenberg's (1981) EQ, they would have had EQs of 0.57 and 0.92, respectively. These results are obtained using a phylogeny of Euarchontoglires that supports Primatomorpha (i.e., a monophyletic clade that includes Primates and Dermoptera; Janečka et al. 2007). There is a negligible change in these numbers if we use instead a phylogeny that supports Sundatheria; the ancestral primate node decreases its reconstructed EQs by only 0.01 (Table 12.2). Given these results, the ancestral primate is inferred to have been similarly encephalized to plesiadapiforms, dermopterans, ischyromyid rodents, and apatemyids, but also to adapoids. The ancestral euprimate would have had a higher EQ, more similar to those of omomyoids. There are additional increases associated with the lineages leading to Strepsirrhini and Haplorhini, and further increases within those clades, highlighting the rampant parallelism that was clearly a characteristic of the evolution of brain size in Primates (Table 12.2; see discussion below).

Although one interpretation of this pattern could be that the strepsirrhine-like brain organization that is observed in early euprimates (Kirk et al. 2014; Harrington et al. 2016, 2020; Ramdarshan and Orliac 2016) was associated with a notable increase in encephalization, the fact that all the adapoids in our sample (Table 12.S1) have EQs that are notably below the value inferred for the ancestral euprimate complicates this interpretation. As it stands, in our analysis a reversal to a lower EQ

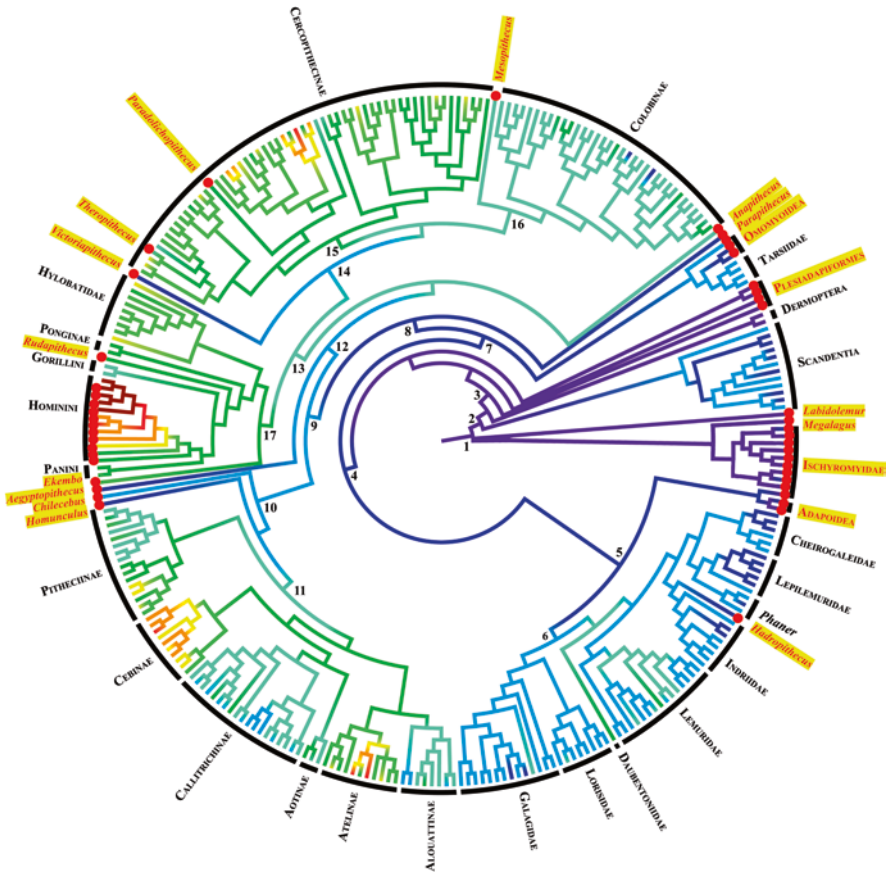


Fig. 12.6 Visualization of the ancestral state reconstruction analysis on a supertree representing a hypothesis of relationships among Euarchontoglires (see Sect. 12.4.2). Colors represent values of Jerison's (1973) encephalization quotient (EQ), with colder colours showing lower EQ values and warmer colours showing higher EQ values: 0.1–0.5, purple; 0.5–0.9, dark blue; 0.9–1.3, medium blue; 1.3–1.7, light blue; 1.7–2.1, dark green; 2.1–2.5, light green; 2.5–2.9, yellow; 2.9–3.5, orange; 3.5–3.9, light red; over 3.9, dark red. Fossils marked with a red dot. The analysis was performed in Mesquite 3.2 (Maddison and Maddison 2017) using parsimony. Combined cladogram from Kobayashi (1995), Takai et al. (2008), Silcox et al. (2010b), Roberts et al. (2011), Springer et al. (2012), Guddé et al. (2013), Baab et al. (2014), Martins Jr. et al. (2015), Strait et al. (2015), Ni et al. (2016, 2019), Byrne et al. (2018), Mongle et al. (2019), and Bertrand et al. (2021). The current tree supports Primatomorpha. For a more detailed tree, see Fig. 12.S1. Node names and associated ancestral state reconstruction values are given in Table 12.2

is reconstructed as having occurred in adapoids. This is one possibility, but it is also worth considering whether or not this pattern is a product of the ancestral state reconstruction methodology, and of this particular topology. Specifically, the location of the middle Eocene *Rooneyia* (with an EQ in the range of living strepsirrhines) at the base of the tarsiiform clade in this topology is driving up the

Table 12.2 Encephalization quotients for critical nodes reconstructed based on the analysis detailed in Sect. 12.4.2 and figured in Figs. 12.6 and 12.S1

Node number		Tree supporting Primatomorpha		Tree supporting Sundatheria	
		Jerison's (1973) EQ	Eisenberg's (1981) EQ	Jerison's (1973) EQ	Eisenberg's (1981) EQ
1	Ancestral euarchontoglires	0.39	0.58	0.34	0.50
2	Ancestral euarchontan	0.56	0.87	0.44	0.65
3	Ancestral primate	0.41	0.57	0.40	0.56
4	Ancestral euprimate	0.68	0.92	0.68	0.92
5	Ancestral strepsirrhine	0.77	1.02	0.77	1.02
6	Ancestral crown strepsirrhine	1.10	1.47	1.10	1.47
7	Ancestral haplorhine	0.80	1.10	0.80	1.10
8	Ancestral anthropoid	0.80	1.05	0.80	1.05
9	Ancestral crown anthropoid	0.90	1.15	0.90	1.15
10	Ancestral platyrrhine	0.99	1.3	0.99	1.3
11	Ancestral crown platyrrhine	1.54	1.97	1.54	1.97
12	Ancestral catarrhine	0.92	1.10	0.92	1.10
13	Ancestral crown catarrhine	1.53	1.73	1.53	1.73
14	Ancestral cercopithecoïd	1.29	1.49	1.29	1.48
15	Ancestral cercopithece	1.77	2.08	1.77	2.08
16	Ancestral colobine	1.48	1.71	1.48	1.71
17	Ancestral hominoid	1.97	2.20	1.97	2.20

See Table 12.S1 for data upon which this analysis was based

reconstructed primitive euprimate value. It is questionable whether the endocast of *Rooneyia viejaensis* is a good representative of what is primitive for that clade, in light of its specialized morphology and the late age of this species (Rosenberger et al. 2008; Kirk et al. 2014). These ambiguities mean that the differing interpretations of Harrington et al. (2016) and Gilbert and Jungers (2017) about whether shape changes preceded size increases in the earliest phases of euprimate evolution remain in contention. Endocranial data for more basal members of the tarsiiiform clade (i.e., older and/or more primitive omomyoids) would likely help to resolve this issue.

The reconstructed EQ value for the ancestral euarchontan is actually higher than that of the ancestral primate, but lower than that of the ancestral euprimate (Table 12.2). Whereas it is possible that the primate lineage suffered a decrease in

EQ at its basalmost node, it is important to acknowledge that the most closely related taxa (Dermoptera and Scandentia) are solely composed of extant species, since no fossil colugo or treeshrew crania have been recovered. The offset between the estimates for the ancestral euarchontan and the ancestral euarchontogloran (Table 12.2) may also reflect this issue, since all of the included members of Glires are fossil taxa. Extant treeshrews are particularly encephalized and they certainly have an important impact on the reconstruction of the basal euarchontan node. However, it can be concluded that there is no clear evidence for an increase in relative brain size at the basal primate node; as such, our analysis supports Radinsky's perspective that the most ancient primates were not necessarily encephalized over their mammalian contemporaries in the historical debate (see Sect. 12.2).

Extant strepsirrhines show the lowest EQ values among modern primates. Here we have considered adapoids as stem strepsirrhines; as noted above they have very low EQs (particularly *Notharctus* and *Adapis*, Harrington et al. 2016). This probably explains the low EQ inferred for the ancestral strepsirrhine. Among living strepsirrhines, there are a few reversals in EQ that stand out. Lepilemurids seem to have particularly low EQs compared to other lemuriforms. Lepilemurids are highly folivorous but have also been observed to practice caecotrophy (i.e., the reingestion of soft faeces or caecotrophs, Hladik 1978), which serves to improve the absorption of vitamins and microbial proteins (Hirakawa 2001). It is possible that the suboptimal absorption of nutrients from plant material in lepilemurids serves as a limiting factor in brain development. Another reversal among lemuriforms pertains to *Cheirogaleus*. This might be explained by strong seasonal variation in body mass in dwarf lemurs. *Cheirogaleus* is unusual among primates in storing large amounts of fat subcutaneously during the rainy season to prepare for a long period of torpor during the winter months, which makes their body mass increase up to 50% (Lemelin and Schmitt 2004). However, the sources we used for *Cheirogaleus*' body mass (Stephan et al. 1981; Boddy et al. 2012) do not report what time of the year they were taken, so it is hard to tell if this is the true reason behind the low EQ in this genus. The high degree of variation in body mass throughout the year will nonetheless impact the calculation of the EQ in that genus, with *Cheirogaleus* having its highest EQ after finishing torpor and its lowest before starting it, which is a good example of why EQ is a problematic tool to measure intelligence.

There is a consistent association in our analysis between lower EQ values and folivory (see also DeCasien et al. 2017). A prime example is the clear dichotomy in EQ trends between the cercopithecine and the colobine radiations (Table 12.2). There are a couple of explanations, not necessarily mutually exclusive, for this pattern. The Expensive-Tissue Hypothesis (Aiello and Wheeler 1995) suggests that the metabolic requirements of relatively large brains are offset by a corresponding reduction of the gut. Colobines, which are largely folivorous cercopithecoids, have stomachs that differ from any other primate and resemble those of ungulates, with a pseudoruminant anterior fermentation area in a large multichambered stomach (Fleagle 2013). Another possible explanation is that folivores depend on food that is more easily accessible and more predictable in time and space than that of frugivores. Consequently, folivores may not experience the types of cognitive demands for

efficient exploitation of their food supply encountered by primates in other dietary categories (Clutton-Brock and Harvey 1980). This pattern is also observed in other areas of the primate tree: gorillas compared to other great apes, alouattines compared to atelines, *Avahi* compared to other indriids, and lepilemurids compared to other lemuriforms.

Finally, there are a few lineages that show evidence of increased EQ that are worth mentioning. The hominin lineage, of course, stands out for clustering the highest EQs in the tree. Other groups with high EQ compared to their close relatives are cebines and aye-eyes. Cebinae groups together some of the most encephalized platyrrhines, which may have some relationship to the use of tools by cebines for a variety of purposes. For example, they are known to use stones to crack nuts, sticks to strike a conspecific or push objects, or leaves to be used as a cup, making them more proficient in tool use than most other non-ape anthropoids (Visalberghi 1990; Phillips 1998). The aye-aye (*Daubentonia madagascariensis*) is one of the most encephalized strepsirrhines. Aye-eyes evolved a context-specific form of manual extractive foraging involving a long, thin third digit for extracting grubs from within tree bark. This type of convergent evolution with other primates who practice omnivorous extractive foraging (i.e., cebines, chimpanzees and humans) may potentially be related to the observed parallel increase in encephalization in these lineages (Gibson 1986; Kaufman et al. 2006; Parker 2015). However, aye-eyes do not achieve the same level of sensorimotor cognition and comprehension of tool use as their anthropoid relatives do (Sterling and Povinelli 1999).

12.4.3 Sensory Evolution: Vestibular Sense, Vision, Hearing, Olfaction, Taste, etc.

As the brain is where sensory input is processed into actionable information, the evolution of the primate brain from a sensory perspective has become the subject of extensive research. Exploration into the connection between sensory adaptation and brain evolution operates on Jerison's (1973) Principle of Proper Mass, which ties the size of a brain structure to the information processing requirements of its function. This principle therefore suggests that an adaptation requiring an increase in the information sent to certain neural tissues will result in an increase in the size of those tissues. This principle serves as the foundation for interpreting size changes in the brain overall, and in specific neuroanatomical structures. Whereas much research into the sensory specialization of the primate brain has focused on smaller, more functionally specific brain regions (e.g. the striate cortex and the parvocellular and magnocellular layers of the lateral geniculate nucleus; Barton 1998), comparable analyses are largely not possible in endocast analyses as endocasts cannot provide information about internal structures. Consequently, only structures which can be measured accurately on the surface of the endocast are discussed here. Traditionally, these brain regions have included the neocortex, responsible for processing visual,

auditory, somatosensory, motor, sensorimotor, and prefrontal sensory information (Kaas 2012); and the olfactory bulbs, responsible for processing olfactory information (Heritage 2014).

As one of the defining features of primate sensory adaptation (Silcox et al. 2007), specializations of the visual system have been thoroughly examined in the primate brain. Often, visual specializations are cited as a driving force behind primate encephalization and the expansion of the neocortex (Barton 1996, 1998; Kirk 2006) as a large portion of the neocortex is devoted to processing visual information, most notably in diurnal anthropoids (Felleman and Van Essen 1991; van Essen et al. 1992). To this end, several analyses have focused on the scaling relationship between visually demanding ecological behaviors and the size of the neocortex within extant haplorhines and strepsirrhines (Barton 1996, 1998). Overall, these analyses indicate that haplorhines have significantly larger neocortices relative to the size of the rest of the brain, compared to strepsirrhines, and neocortex size is correlated with ecological behaviors including social group size, diet, and activity pattern (Barton 1996; DeCasien et al. 2017; DeCasien and Higham 2019). Among extant primates, diurnal frugivorous anthropoids living in large groups exhibit the highest degree of cortical expansion (Barton 1996; DeCasien and Higham 2019). It has been suggested that this scaling relationship is the product of the increased visual demands of primate communication and/or visually oriented foraging behaviors (Barton 1996, 1998, 2000).

However, the neocortex is also responsible for functions outside of vision (Joffe and Dunbar 1997). Analyses into more functionally specific visual structures, including the striate cortex and the lateral geniculate nucleus, identify similar scaling relationships associated with activity pattern, diet, and social group size (Barton 1998; DeCasien and Higham 2019). But, only a small portion of the variation in total neocortex size can be attributed to expansion of these visual structures (lateral geniculate nucleus: $r^2 = \sim 0.18$; $p = 0.014$ and striate cortex: $r^2 = \sim 0.14$; $p = 0.03$, Barton 1998). Given the diversity of sensory functions the neocortex performs, it is somewhat problematic to use neocortical expansion as an indicator for specialization in a single sensory modality. Nevertheless, researchers have examined the size and shape of the neocortex in connection with other ecological factors to help explain variation between closely related fossils. For example, caudal expansion of the neocortex, where the striate visual cortex is located, in later occurring microsyopids compared to other stem primates may indicate greater visual specialization among these taxa (Silcox et al. 2010a). Similarly, the lack of midbrain exposure in early fossil euprimates may be related to expansion of the neocortex related to improvements to visual processing (Harrington et al. 2016).

Brain size has also been examined in relation to the total amount of visual input. Kirk (2006) examined the relationship between total endocranial volume and optic foramen area, as the latter is strongly correlated with the size of the optic nerve and the number of ganglion cells in the retina (Kay and Kirk 2000; Kirk and Kay 2004). Body mass-controlled analysis of the relationship between these two variables in a large sample of extant primates indicated that visual input is significantly correlated with brain size, as relative orbital foramen area accounts for 43% ($p < 0.0001$) of the

variation found in relative endocranial volume (Kirk 2006). Furthermore, anthropoids were found to have relatively larger optic foramina, indicative of increased visual input, and correspondingly larger brains compared to strepsirrhines regardless of ecology. The same analysis was performed on six fossil euprimates: three late Eocene adapoids *Adapis parisiensis*, *Leptadapis* sp., *Pronycticebus gaudryi*; a late Eocene omomyoid, *Necrolemur antiquus*; the early Oligocene stem anthropoid, *Parapithecus* (= *Simonsius*) *grangeri*; and *Rooneyia viejaensis* (see discussions above about its taxonomic position). The three adapoids, *A. parisiensis*, *Leptadapis* sp., and *P. gaudryi*, fell outside of the extant primate distribution, having relatively small orbital foramen areas associated with relatively small endocranial volumes (Kirk 2006). The haplorhines, *N. antiquus* and *P. grangeri*, along with *R. viejaensis*, plot within the distribution of extant primates (Kirk 2006). These results were interpreted to reflect a grade-shift in brain size between haplorhines and strepsirrhines that was linked to the amount of visual input to the brain. This point may relate to the ambiguities discussed above about when EQ increased on primate evolution (see Sect. 12.4.2)—specifically the increase inferred as pertaining to the primitive euprimate may be a primarily haplorhine event. These results are also consistent with other research which indicates that haplorhines, specifically anthropoids, are visually specialized as they possess greater degrees of orbital convergence (Ross 1995), greater visual acuity (Kirk and Kay 2004), and in some cases, trichromatic vision (Regan et al. 2001). However, it is worth noting that this conclusion depends in part on an estimate of endocranial capacity in *N. antiquus* that has since been reassessed (Harrington et al. 2020).

Extant primates have long been considered to have a poor sense of smell (microsmatic), an idea that can be traced back to Elliot-Smith (1927) who suggested that olfaction would have been less important to primates than to other mammals because of their arboreal niche. Whether or not extant primates are microsmatic has been and continues to be discussed from genetic, behavioral, and anatomical perspectives (Smith et al. 2007). Concerning neuroanatomy, numerous studies have identified a clear grade-shift in the size of the olfactory bulbs relative to brain size between haplorhines and strepsirrhines, with haplorhines having significantly smaller olfactory bulbs (Stephan et al. 1981; Baron et al. 1983; Barton et al. 1995; Barton 2006; Heritage 2014; DeCasien and Higham 2019). A recent study modelling olfactory bulb evolution using extinct and extant taxa found evidence that the size of the olfactory bulbs (relative to the rest of the brain and absolute size) decreased in haplorhines and increased within the strepsirrhines (Heritage 2014).

The distinct difference in relative size of the olfactory bulbs between haplorhines and strepsirrhines is hypothesized to reflect differences in sensory specialization related to ecology in the two clades (Barton 2006; Heritage 2014). Ecological analyses suggest that the size of the olfactory bulbs (relative to the medulla, Barton 2006; and to the rest of the brain, Barton et al. 1995; DeCasien and Higham 2019) are significantly influenced by diet and activity pattern. Additionally, a negative correlation exists between visual and olfactory structures such that taxa with large olfactory structures tend to have smaller visual structures and vice versa depending on ecological condition. Specifically, nocturnal frugivores have larger olfactory

structures and smaller visual structures while diurnal frugivores have larger visual structures and smaller olfactory structures (Barton et al. 1995; DeCasien and Higham 2019). Activity pattern may have played a major role in the variation of olfactory and visual structures between the two suborders as extant haplorhines are almost exclusively diurnal, and likely ancestrally diurnal (Kay et al. 1997; Ross and Kirk 2007) compared to the more variable activity patterns observed in extant strepsirrhines (Ankel-Simons and Rasmussen 2008).

Endocranial analysis of Paleocene and Eocene stem primates *Plesiadapis cookei* (Gingerich and Gunnell 2005), *Plesiadapis tricuspidens* (Orliac et al. 2014), *Ignacius graybullianus* (Silcox et al. 2009b), and *Microsyops annectens* (Silcox et al. 2010a) indicate that the size of the olfactory bulbs relative to endocranial volume are larger than in extinct and extant euprimates, but smaller than early eutherians (Kielan-Jaworowska 1984; Kielan-Jaworowska and Trofimov 1986) and apatemyids (Silcox et al. 2010b), and similar in size to fossil rodents and lagomorphs (Bertrand et al. 2016, 2017, 2018, 2019a; Bertrand and Silcox 2016; López-Torres et al. 2020; see Sect. 12.3.1). As noted above, of the plesiadapiforms only one taxon diverges from this pattern. The Early Eocene *Niptomomys* cf. *N. dorenae* (White et al. 2016), possesses larger olfactory bulbs (relative to endocranial volume) than other plesiadapiforms and stem rodents, and smaller olfactory bulbs than early apatemyids, suggesting it was more specialized for olfaction than other plesiadapiforms and stem rodents, but not compared to apatemyids (Silcox et al. 2011; Fig. 12.5c). Analyses of *I. graybullianus* and *M. annectens* found that the size of the olfactory bulbs relative to body mass, as opposed to endocranial volume, fell within the range of extant strepsirrhines (Silcox et al. 2010a). This result suggests that the size of the olfactory bulbs may have been relatively stable from the primate stem through the early evolution of euprimates and ultimately in the common ancestor of strepsirrhines, although they accounted for a smaller percentage of the brain (Harrington et al. 2016). However, it is unclear whether stem primates showed reduction in the relative size of the olfactory bulbs relative to the ancestral condition given the conflicting signals about the primitive states from apatemyids and members of Glires. As the expansion seen in the rest of the euprimate brain is often attributed to visual specialization (Barton 1998; DeCasien and Higham 2019), the proportionally large olfactory bulbs in stem primates (i.e., plesiadapiforms) suggest they relied more on olfactory signals than their extant relatives (Silcox et al. 2009b, 2010a; Orliac et al. 2014).

Among early euprimates (i.e., adapoids and omomyoids), the smallest olfactory bulbs relative to endocranial volume are found in the omomyoid *Microchoerus erinaceus* (Ramdarshan and Orliac 2016; Table 12.1), which could suggest that the grade shift in the relative size of the olfactory bulbs observed in extant strepsirrhines and haplorhines may have occurred early in the diversification of the two clades. However, the olfactory bulbs of *M. erinaceus*' close relative, *Necrolemur antiquus*, are more similar in relative size to adapoids (Harrington et al. 2020; Table 12.1), making it less clear that the shift has an ancient origin. The onset of the apparent grade shift in relative olfactory bulb size that differentiates extant strepsirrhines and haplorhines is not clearly evident even in stem anthropoids. The olfactory bulbs of

the stem anthropoid, *P. grangeri*, are large relative to both brain volume and body mass, within the range of extant strepsirrhines (Bush et al. 2004b). Similarly, early catarrhines (*Victoriapithecus* and *Aegyptopithecus*) possess relatively large olfactory bulbs, also within the range of extant strepsirrhines (Gonzales et al. 2015). In contrast, the earliest stem platyrrhine known from an endocast, *Chilecebus carrascoensis*, has small olfactory bulbs, smaller than the average for extant haplorhines (Ni et al. 2019). This suggests that the extreme reduction in the size of the olfactory bulbs in extant catarrhines and platyrrhines occurred independently (Heritage 2014; Gonzales et al. 2015; Ni et al. 2019) and not at the base of Anthropoidea, which is a powerful example of the importance of the fossil record to establishing the evolutionary context of evolutionary changes.

It is also unclear when or how the trade-off between visual and olfactory structures, observed particularly among anthropoids, occurred. For example, the stem anthropoid *P. grangeri* had large olfactory bulbs for a euprimate (Bush et al. 2004b) and large optic foramen areas and endocranial volume (Kirk 2006), which suggests it both retained the apparatus for strong olfactory abilities while also possessing adaptations for higher acuity vision. Phylogenetically controlled regressions of total visual input to the brain (measured using optic foramen area and orbit size) and olfactory bulb size relative to body mass in a sample of extant and fossil euprimates, including *P. grangeri*, *Aegyptopithecus*, and *C. carrascoensis*, failed to identify a significant correlation between the two, indicating that changes in olfactory and visual structures occurred independent of one another (Ni et al. 2019). Again, the inclusion of fossils re-frames conventional stories of evolutionary change within Primates.

Endocranial reconstructions of the inner ear, and particularly the semicircular canals, have also been used to investigate the connection between ecology and sensory capability in early Tertiary primates (Silcox et al. 2009a; Ryan et al. 2012; Bernardi and Couette 2017). The three arcs (anterior, lateral, and posterior) of the semicircular canals help detect the angle and velocity of an animal's head movements. This information, alongside visual, proprioceptive, and otolithic information, is used to control body movements and stabilize gaze, functions suggested to be especially important for fast moving and arboreal animals (Spoor and Zonneveld 1998). The potential relationship between locomotor behavior and the semicircular canals was examined in a large sample of primates and mammals by Spoor et al. (2007). Multiple regression of average canal radius against body mass and locomotor agility indicated that fast, more agile species tend to have larger semicircular canals relative to body mass. Within primates, taxa with the smallest semicircular canals included slow quadrupedal arborealists (i.e., lorises) and large bodied great apes whereas taxa with the largest semicircular canals included specialized leapers (i.e., tarsiers and galagos) and acrobatic brachiators (i.e., gibbon).

Analysis of stem primates of the families Micromomyidae, Paromomyidae, Plesiadapidae, Carpolestidae, and Microsypidae; adapoids of the families Adapidae and Notharctidae; and omomyoids of the families Omomyidae and Microchoeridae, found that the agility estimates from the semicircular canals were largely consistent with the reconstructions of locomotor behavior derived from postcrania (Silcox

et al. 2009a; Bernardi and Couette 2017). Stem primates, adapids, and the primitive notharctid *Cantius nuniensis* had smaller semicircular canal radii relative to body mass, and therefore, were relatively slow-moving animals, a conclusion that is supported by postcranial material (when available) which suggests they were not specialized leapers. Omomyids and most notharctids, whose postcrania indicate occasional leaping, had relatively larger semicircular canals, similar to extant galagids, which engage in some leaping but are mostly arboreal quadrupeds. These analyses were unable to identify fine scale distinctions between locomotor behaviors within the stem primates (Silcox et al. 2009a), which reflects the ability of this method to only speak to relatively coarse differences in locomotor type. Ryan et al. (2012) assessed semicircular canal size and agility in anthropoids, reconstructing early anthropoids and catarrhines as being relatively slow moving, whereas early platyrrhines were more agile compared to earlier forms.

It is worth acknowledging that these analyses rest on a scale of agility scores that was generated entirely subjectively (Spoor et al. 2007). A much more rigorous, quantitative approach was taken by Malinzak et al. (2012), who took actual 3D vector measurements from a sample of primates while they were locomoting. These authors found that rotational head speed was more strongly correlated with the angles of the three semicircular canals (and how closely they approach orthogonality) than with their size. Unfortunately attempts to apply these methods to predictions of locomotion for fossil euarchontoglires have failed to produce results that are consistent with what is known from postcranial data (Bernardi and Couette 2017; Bhagat et al. 2020), perhaps because the sample of modern animals was fairly narrow in scope (11 species, all strepsirrhines). Certainly, more data of this type would enhance our ability to probe the limits of semicircular canal data for inferring aspects of behavior in fossil taxa.

In recent years, several analyses have attempted to expand the scope of the data that can be used to examine fossil endocasts, and help understand the sensory significance of endocranial variation, by using geometric morphometrics and landmark based analyses (e.g., Pereira-Pedro and Bruner 2018). Notably, some of these studies have used sulci to delimit functionally specific brain regions in phylogenetically constrained groups (Kobayashi et al. 2018; Pereira-Pedro et al. 2019, 2020). Whereas this new method will be useful for analysis of recent fossil primates, its application to phylogenetically diverse groups with significant variation in sulcal anatomy, groups which contain fossils whose sulcal configuration is not well known, or lissencephalic species, has not been investigated in any fully published work (but see Makedonska et al. 2008; Allen 2014; Lang et al. 2019). Regardless, as this method continues to develop, there may be more information which can be gained from currently under-investigated aspects of sensory neuroanatomy in fossil primates, specifically related to taste, touch, and hearing. As new specimens emerge, and these new methods are developed, we will be able to expand and refine our understanding of primate sensory neuroanatomy.

12.4.4 *Evolution, Form and Function of Derived Brain Structures*

In addition to providing new perspectives on old questions, 3D data make it possible to ask a new range of questions based on the ability to more accurately quantify volumes for individual parts of the endocast, such as the olfactory bulbs (see Sect. 12.4.3) or petrosal lobules (Lang et al. 2018, 2022), as well as providing measures of surface areas. With respect to the latter, Jerison (2012) developed a method for measuring the relative size of the neocortical surface using laser scans of physical endocasts. He found a relationship between the degree of neocorticalization and time, with fossil euprimates standing out as always having larger relative neocortices than their contemporaries (Jerison 2012: fig. 6). Long et al. (2015) further elaborated on this method using X-ray CT data, and added values calculated from endocasts of plesiadapiforms (see also Orliac et al. 2014; Harrington et al. 2016; Ramdarshan and Orliac 2016). Although they found that Jerison's conclusion was supported for euprimates, plesiadapiforms were inferred to be more like contemporary fossil non-primates in their degree of neocorticalization.

There was an issue with the dataset used by Long et al. (2015), however—it lacked any other euarchontoglires. As such, it does not directly answer the question of whether or not there were shifts in relative neocortical surface area at the primate (vs. euprimate) node. Unfortunately, the endocast of *Labidolemur kayi* is not well enough preserved to indicate the location of the rhinal fissure. However, data on neocorticalization are available for the stem lagomorph *Megalagus turgidus* (López-Torres et al. 2020) and for various early rodents (i.e., ischyromyids; Bertrand and Silcox 2016; Bertrand et al. 2016, 2019a; Bertrand and Silcox this book). If the comparison is limited to the oldest and some of the most basal rodents for which there are quantitative data (i.e., members of the genus *Paramys*) and to *Megalagus* (as the only stem lagomorph for which there are data), then it does appear that early primates may have been slightly neocorticalized relative to primitive members of Glires (i.e., see Bertrand et al. 2016: fig. 6). However, if the comparative frame is expanded to include a broader range of ischyromyids, then the contrast is less clear, with their range of variation in the neocortical ratio overlapping the range known for plesiadapiforms (Bertrand et al. 2019a; see also López-Torres et al. 2020: fig. 4b). It would be helpful if quantitative data were available for a basal taxon that was not already a rodent or a lagomorph. Unfortunately, the known natural endocasts of *Rhombomylus turpanensis* (as the best-known candidate for this position) do not preserve the rhinal fissure (Meng et al. 2003; contrary to the impression provided by Orliac et al. 2014: fig 4). There are several nicely preserved crania of *R. turpanensis* (i.e., see Meng et al. 2003: fig. 26) so perhaps this issue might be solved by the CT-scanning and digital extraction of an endocast from one or more of them.

12.5 Future Directions: Outstanding Questions and Perspectives

There are three main directions that the study of early primate brain evolution using endocasts are likely to take in the coming years. The **first** relates to the comparative context for studying changes near the base of the primate tree. A lot of progress has been made in expanding the dataset relevant to assessing plesiomorphic states in Primates and Euprimates. This includes the first virtual endocasts for plesiadapiforms (Silcox et al. 2009b, 2010a; Orliac et al. 2014), which allow for high quality quantitative data to be captured and compared to the data from fossil and living euprimates. Also, very important has been the expansion of our knowledge of fossil members of primates' close relatives (Silcox et al. 2011; Bertrand and Silcox 2016; Bertrand et al. 2016, 2019a, b; López-Torres et al. 2020). However, there remain critical holes in this sample. There are endocasts of plesiadapiforms that have not yet been published in full (*Niptomomys* cf. *N. doreenae* [White et al. 2016]; *Carpolestes simpsoni* [Silcox et al. 2017b]; *Ignacius graybullianus* [Boyer et al. 2011; Long et al. 2015]; *Plesiadapis tricuspidens* [Kristjanson et al. 2016]). But even when these specimens are published, it will still be the case that all plesiadapiform endocasts are known from relatively derived members of their respective families, and from branches several nodes from the base of the primate tree. It would be a tremendous boon to add a more basal plesiadapiform (e.g. a pugatoriid or palaechthonid) to the sample, beyond the very limited information that can be gleaned from *Torrejonia wilsoni* (Chester et al. 2019: fig. 3). Additional data for early Euprimates would also be beneficial. Extracting virtual endocasts from specimens that have already been studied in the context of early primate brain evolution (e.g., *Leptadapis magnus*, *Pronycticebus gaudryi*, *Tetoniuss homunculus*) would be an obvious first step. There is also an abstract published that mentions endocranial data for several additional specimens of European adapoids (Makedonska et al. 2008), but that study has never been published in full. However, even with these additions we would still be lacking endocranial data for the most basal adapoids and omomyoids (i.e., *Teilhardina*, *Cantius*, *Donrussellia*), which would be beneficial to characterizing the primitive states for these groups. As noted above, data for early omomyoids would be particularly valuable for assessing the timing of changes in relative brain size near the base of the primate tree. There are some cranial specimens known for some of these genera, which may be able to provide at least select endocranial details (e.g. Rose et al. 1999; Ni et al. 2004).

Beyond primates, it would be beneficial to have additional data for early members of Euarchontoglires. As discussed above, *Rhombomylus turpanensis* is one obvious candidate for this, and additional data for apatemyids would also be of interest (e.g., quantitative data for the endocast of the derived apatemyid *Carcinella sigei*; von Koenigswald et al. 2009). But probably even more exciting would be data for other fossil groups of Euarchontoglires, which could add additional perspectives on primitive states for that group (e.g., mixodectids, anagalids). Finally, having data for more than a single stem lagomorph would be crucial, particularly since

Megalagus turgidus is early Oligocene in age (López-Torres et al. 2020), and so notably more recent than the primate taxa under discussion here. Obviously, the situation is much better for early rodents (Bertrand and Silcox 2016; Bertrand et al. 2016, 2019a), with both a larger number of endocasts, and a greater temporal depth, extending back to the early Eocene. However, the oldest endocast for which good quantitative data are available is from Wa7 (Wasatchan North American Land Mammal Age 7, ~52.4–50.1 mya; Bertrand et al. 2016; note that there is an endocast for a specimen from Wa6 [*Notoparamys costilloi*] but it is too compressed to provide good quality quantitative data; Bertrand et al. 2019a), which is several million years after Rodentia entered North America at the start of the Clarkforkian (Rose 1981, 2006; Korth 1994) and so certainly well separated in time from the origin of the order. In sum, further understanding the primitive context of primate evolution requires not only a better sample for early primates, but also for relevant out-group taxa.

Second, future work will likely enhance our knowledge of intraspecific variation in fossil primate taxa. The best samples currently known are for adapoids, although the maximum sample size for any one taxon is only $N = 5$ for *Smilodectes gracilis* (Gazin 1965; Harrington et al. 2016), of which one (UM 32773) is subadult. Nonetheless, it would be of value to study this sample through the lens of intraspecific shape variation. Apart from the North American notharctid adapoids, the best candidates for understanding variation in closely related taxa are probably the large bodied European adapoids, known from numerous three-dimensionally preserved crania (e.g., Godinot and Couette 2008; Makedonska et al. 2008). A complication to such studies is the confounding effect of body mass, in light of the divergent estimates from different equations (e.g., see Harrington et al. 2016). The ideal situation is for the cranial specimen from which the endocast is extracted to be associated with postcranial material, allowing for a completely independent body mass estimate, but there are only a very few instances in which this is the case (e.g., *Plesiadapis cookei* [Gingerich and Gunnell 2005; Boyer and Gingerich 2019]; one specimen of *Smilodectes gracilis* [USNM V 17994; Harrington et al. 2016]).

Third, and finally, much of the discussion about endocranial variation in early Primates has focused on size, so an area of future growth is to expand our understanding of variation in shape. There have been some analyses mentioned in abstracts or unpublished theses that have looked at shape variation using geometric morphometric methods (e.g., Makedonska et al. 2008; Allen 2014; Lang et al. 2019), but these studies have not yet been published in full. A critical element in the interpretation of such analyses is the degree to which differences in shape can be interpreted with respect to function. Although there is obviously a very large literature on functional aspects of the brain in Primates, integrating the details of this literature with the data that can be observed or measured from an endocast is an ongoing challenge. For example, studies of function in the cerebral cortex that require the brain to be flattened for examination can be difficult to translate into the three-dimensional surface of an endocast. Application of new 3D imaging techniques such as DICE-CT may help in successfully integrating functional data with

the type of shape data available for endocasts, permitting more direct inferences to be made about differences among endocasts from fossil taxa.

12.6 Concluding Remarks/Final Considerations

The last 15 years have seen a renaissance in the study of endocranial morphology in early primates, largely spurred by the growing availability of high-resolution X-ray CT scanners. The endocasts that have emerged for early primates have confirmed some historical perspectives, answered some questions, but also spurred some new research directions. In spite of their areas of disagreement, Jerison and Radinsky did agree on some major elements of the interpretation of the pre-CT record of early euprimate endocasts, including the evidence for likely expansion of the temporal and occipital lobes and development of the Sylvian sulcus, and the presence of a less developed frontal lobe than in living primates. As discussed in Sect. 12.2.1, some of the elements that fueled their debates have effectively been answered by the data made available by CT. It is no longer necessary to rely on methods that make major assumptions about the shape of the brain to derive an estimate of volume. And we now have some good quality quantitative data for the first radiation of fossil primates, which show that the distinctively primate-like traits of euprimates actually do not characterize the first members of the order. However, as discussed in Sects. 12.2.2 and 12.4.2, the appropriate context for looking at relative brain size continues to be problematic, and more data are needed to help interpret the patterns seen in the endocasts we do have.

Although this chapter has by necessity focused mainly on the record of early primates and euprimates, there is also a burgeoning record of virtual endocasts for later non-hominid primates (e.g., Bush et al. 2004a,b; Simons et al. 2007; Ryan et al. 2008; Kay et al. 2012; Allen 2014; Gonzales et al. 2015; Beaudet et al. 2016; Ni et al. 2019). A few generalities about the broader picture of primate brain evolution are emerging from these studies, which have relevance to the interpretation of the earlier fossils. As discussed above, there is growing evidence for rampant parallelism in brain size evolution among lineages of fossil primates (Sect. 12.4.2, Table 12.2 and Fig. 12.6; see also Allen 2014; Gonzales et al. 2015; Ni et al. 2019). It is worth noting these parallel expansions make analyses of primate brain size evolution that do not integrate fossils quite problematic. Such analyses generally assume the process of brain size change will follow the most parsimonious or likely path over the entirety of the 65+ million years of primate evolution. The fossil record suggests that it does not.

There is also evidence from a few points in the primate tree that changes in form precede changes in size (Allen 2014; Gonzales et al. 2015; Ni et al. 2019). So, for example, the endocast of the stem cercopithecoid *Victoriapithecus* had already evolved the pattern of gyrification characteristic of cercopithecoids, but at a small endocranial volume (Gonzales et al. 2015). This finding parallels the conclusion of Harrington et al. (2016) that the major structural changes associated with the

euprimate node preceded significant relative change in brain size, although as noted above this conclusion was critiqued by Gilbert and Jungers (2017). In our opinion, we cannot reach an unambiguous answer on this point with the currently available fossil record (see discussion in Sect. 12.4.2).

Interpreting these patterns in an adaptive context poses a final challenge to our understanding of brain evolution. There are various factors that have been identified as critical to the process of brain evolution in the order including the evolution of visual processing (Barton 1998; Kirk 2006), the importance of social behavior (Dunbar 1998; Dunbar and Schultz 2007), the necessity of processing complex information from the arboreal environment (Falk 2007), and the impact of variation in diet (Harvey et al. 1980; DeCasien et al. 2017). The paleoneurological data have provided some possible insights into these competing influences on primate encephalization. In particular, the fact that plesiadapiforms, who were arboreal, exhibit plesiomorphic endocranial features suggests that moving into the trees did not have a marked impact on the form or size of the brain (Silcox et al. 2009b, 2010a). In contrast, improvements associated with visual processing were likely critical to at least some major transformations in the primate brain (Kirk 2006; Silcox et al. 2009b, 2010a). Studying the impact of other factors, such as diet, in a context that includes data from fossil primates has the potential to enrich our understanding of the reasons behind change over the course of primate brain evolution.

Acknowledgments Thanks to M. Orliac for providing the stl file for *Plesiadapis tricuspidens* used to generate the relevant part of Fig. 12.2, and to E.C. Kirk for providing images of *Rooneyia*. We are also thankful to T.E. Macrini and two anonymous reviewers for comments that substantially improved this paper. Support from an NSERC Discovery Grant to MTS; Marie Skłodowska-Curie Actions: Individual Fellowship (H2020-MSCA-IF-2018-2020; No. 792611) to OCB; and a Kalbfleisch Postdoctoral Research Fellowship to SLT.

References

- Aiello LC, Wheeler P (1995) The expensive-tissue hypothesis. *Curr Anthropol* 36:199–221
- Allen KL (2014) Endocranial volume and shape variation in early anthropoid evolution. Duke University, Doctoral dissertation
- Ankel-Simons F, Rasmussen DT (2008) Diurnality, nocturnality, and the evolution of primate visual systems. *Am J Phys Anth* 137(S47):100–117
- Baab KL, Perry JM, Rohlf FJ et al (2014) Phylogenetic, ecological, and allometric correlates of cranial shape in Malagasy Lemuriformes. *Evolution* 68:1450–1468
- Baron G, Frahm HD, Bhatnagar KP et al (1983) Comparison of brain structure volumes in Insectivora and Primates. III. Main olfactory bulb (MOB). *J Hirnforschung* 24:551
- Barton RA (1996) Neocortex size and behavioural ecology in primates. *Proc Roy Soc B-Biol Sci* 263:173–177
- Barton RA (1998) Visual specialization and brain evolution in primates. *Proc Roy Soc B-Biol Sci* 265:1933–1937
- Barton RA (2000) Primate brain evolution: cognitive demands of foraging or of social life. In: Boinski S, Garber PA (eds) *On the move: how and why animals travel in groups*. University of Chicago Press, Chicago, pp 204–237

- Barton RA (2006) Olfactory evolution and behavioral ecology in primates. *Am J Primatol* 68:545–558
- Barton RA (2012) Embodied cognitive evolution and the cerebellum. *Phil Trans R Soc B* 367:2097–2107
- Barton RA, Purvis A, Harvey PH (1995) Evolutionary radiation of visual and olfactory brain systems in primates, bats and insectivores. *Phil Trans R Soc B* 348:381–392
- Beard KC (2008) The oldest North American primate and mammalian biogeography during the Paleocene-Eocene Thermal Maximum. *Proc Natl Acad Sci USA* 105:3815–3818
- Beaudet A, Gilissen E (2018) Fossil primate endocasts: perspectives from advanced imaging techniques. In: Bruner E, Ogihara N, Tanabe H (eds) *Digital endocasts*. Springer, Tokyo, pp 47–58
- Beaudet A, Domuncel J, de Beer F et al (2016) Morphoarchitectural variation in South African fossil cercopithecoid endocasts. *J Hum Evol* 101:65–78
- Begun DR, Kordos L (2004) Cranial evidence of the evolution of intelligence in fossil apes. In: Russon AE, Begun DR (eds) *The evolution of thought: evolutionary origins of great ape intelligence*. Cambridge University Press, Cambridge, pp 260–279
- Bernardi M, Couette S (2017) Eocene paleoecology of *Adapis parisiensis* (primate, Adapidae): from inner ear to lifestyle. *Anat Rec* 300:1576–1588
- Bertrand OC, Silcox MT (2016) First virtual endocasts of a fossil rodent: *Ischyromys typus* (Ischyromyidae, Oligocene) and brain evolution in rodents. *J Vert Paleontol* 36:e1095762
- Bertrand OC, Amador-Mughal F, Silcox MT (2016) Virtual endocasts of Eocene *Paramys* (Paramyinae): oldest endocranial record for Rodentia and early brain evolution in Euarchontoglires. *Proc Roy Soc B-Biol Sci* 283:20152316
- Bertrand OC, Amador-Mughal F, Silcox MT (2017) Virtual endocast of the early Oligocene *Cedromus wilsoni* (Cedromurinae) and brain evolution in squirrels. *J Anat* 230:128–151
- Bertrand OC, Amador-Mughal F, Lang MM et al (2018) Virtual endocasts of fossil Sciuroidea: brain size reduction in the evolution of fossoriality. *Palaeontology* 61:919–948
- Bertrand OC, Amador-Mughal F, Lang MM et al (2019a) New virtual endocasts of Eocene Ischyromyidae and their relevance in evaluating neurological changes occurring through time in Rodentia. *J Mamm Evol* 26:345–371
- Bertrand OC, San Martin-Flores G, Silcox MT (2019b) Endocranial shape variation in the squirrel-related clade and their fossil relatives using 3D geometric morphometrics: contributions of locomotion and phylogeny to brain shape. *J Zool* 308:197–211
- Bertrand OC, Püschel HP, Schwab JA, Silcox MT, Brusatte SL (2021) The impact of locomotion on the brain evolution of squirrels and close relatives. *Comm Biol* 4:460
- Bhagat R, Bertrand OC, Silcox MT (2020) Evolution of arboreality and fossoriality in squirrels and aplodontid rodents: Insights from the semicircular canals of fossil rodents. *J Anat* 238:96–112
- Bloch JJ, Silcox MT (2006) Cranial anatomy of the Paleocene plesiadapiform *Carpolestes simpsoni* (Mammalia, Primates) using ultra high-resolution X-ray computed tomography, and the relationships of plesiadapiforms to Euprimates. *J Hum Evol* 50:1–35
- Bloch JJ, Boyer DM, Silcox MT et al (2004) New skeletons of Paleocene-Eocene *Labidolemur kayi* (Mammalia, Apatemyidae): ecomorphology and relationship of apatemyids to Primates and other mammals. *J Vert Paleontol* 24(Suppl. 3):40A
- Bloch JJ, Silcox MT, Boyer DM et al (2007) New Paleocene skeletons and the relationship of “plesiadapiforms” to crown-clade primates. *Proc Natl Acad Sci USA* 104:1159–1164
- Boddy AM, McGowen MR, Sherwood CC et al (2012) Comparative analysis of encephalization in mammals reveals relaxed constraints on anthropoid primate and cetacean brain scaling. *J Evol Biol* 25:981–994
- Boyer DM, Gingerich PD (2019) Skeleton of Late Paleocene *Plesiadapis cookei* (Mammalia, Euarchonta): life history, locomotion, and phylogenetic relationships. *Univ Mich Pap Paleontol* 38:1–269
- Boyer DM, Silcox MT, Bloch JJ et al (2011) New skull and associated postcrania of *Ignacius graybullianus* (Mammalia, ?Primates) from the Eocene of Wyoming. *J Vertebr Paleontol* 76A

- Boyer DM, Kirk EC, Silcox MT et al (2016) Internal carotid arterial canal size and scaling in Euarchonta: Re-assessing implications for arterial patency and phylogenetic relationships in early fossil primates. *J Hum Evol* 97:123–144
- Bronson RT (1981) Brain weight-body weight relationships in 12 species of nonhuman primates. *Am J Phys Anthropol* 56:77–81
- Bugge J (1974) The cephalic arterial system in insectivores, primates, rodents and lagomorphs, with special reference to the systematic classification. *Acta Anat* 87(Suppl 62):1–160
- Burger JR, George MA Jr, Leadbetter C et al (2019) The allometry of brain size in mammals. *J Mammal* 100:276–283
- Bush EC, Simons EL, Dubowitz DJ et al (2004a) Endocranial volume and optic foramen size in *Parapithecus grangeri*. In: Ross CF, Kay RF (eds) *Anthropoid origins: new visions*. Kluwer, Boston, pp 603–614
- Bush EC, Simons EL, Allman JM (2004b) High-resolution computed tomography study of the cranium of a fossil anthropoid primate, *Parapithecus grangeri*: new insights into the evolutionary history of primate sensory systems. *Anat Rec* 281:1083–1087
- Butler H (1967) The development of mammalian dural venous sinuses with special reference to the post-glenoid vein. *J Anat* 102(Pt 1):33–56
- Byrne H, Lynch-Alfaro JW, Sampaio I et al (2018) Titi monkey biogeography: parallel Pleistocene spread by *Plecturocebus* and *Cheracebus* into a post-Pebas western Amazon. *Zool Scr* 47:499–517
- Cartmill M (1975) Strepsirhine basicranial structures and the affinities of the Cheirogaleidae. In: Lockett WP, Szalay FA (eds) *Phylogeny of the Primates: a multidisciplinary approach*. Plenum, New York, pp 313–354
- Chester SG, Williamson TE, Bloch JI et al (2017) Oldest skeleton of a plesiadapiform provides additional evidence for an exclusively arboreal radiation of stem primates in the Palaeocene. *Roy Soc Open Sci* 4:170329
- Chester SG, Williamson TE, Silcox MT et al (2019) Skeletal morphology of the early Paleocene plesiadapiform *Torrejonia wilsoni* (Euarchonta, Palaechthonidae). *J Hum Evol* 128:76–92
- Clutton-Brock TH, Harvey PH (1980) Primates, brains and ecology. *J Zool* 190:309–323
- Conroy G, Packer D (1981) The anatomy and phylogenetic significance of the carotid arteries and nerves in strepsirhine primates. *Folia Primatol* 35:237–247
- Conroy GC, Wible JR (1978) Middle ear morphology of *Lemur variegatus*. *Folia Primatol* 29:81–85
- Cope ED (1884) The Vertebrata of the Tertiary formations of the West. Report of the United States Geological Survey of the Territories vol. 3
- Cope (ed) (1885) The Lemuroidea and the Insectivora of the Eocene period of North America. *Am Nat* 19:457–471
- Crile G, Quiring DP (1940) A record of the body weight and certain organ and gland weights of 3690 animals. *Ohio J Sci* 40:219–259
- Czyżewska T (1985) Natural endocranial casts of *Hypolagus brachygnathus* Kormos, 1934 (Leporidae, Lagomorpha) from Węże I near Działoszyn. *Acta Zool Crac* 29:1–12
- DeCasien AR, Higham JP (2019) Primate mosaic brain evolution reflects selection on sensory and cognitive specialization. *Nat Ecol Evol* 3:1483–1493
- DeCasien AR, Williams SA, Higham JP (2017) Primate brain size is predicted by diet but not sociality. *Nat Ecol Evol* 1:0112
- Dechaseaux C (1958) Encéphales de Simplicidentés fossiles. In: Piveteau J (ed) *Traité de paléontologie: L'origine des mammifères et les aspects fondamentaux de leur évolution*. 2. v. Masson, Paris, pp 819–821
- Dozo MT (1997a) Paleoneurología de *Dolicavia minuscula* (Rodentia, Caviidae) y *Paedotherium insigne* (Notoungulata, Hegetotheriidae) del Plioceno de Buenos Aires, Argentina. *Ameghiniana* 34:427–435
- Dozo MT (1997b) Primer estudio paleoneurológico de un roedor caviomorfo (Cephalomyidae) y sus posibles implicancias filogenéticas. *Mastozoología Neotropical* 4:89–96

- Dozo MT, Vucetich MG, Candela AM (2004) Skull anatomy and neuromorphology of *Hypsosteirromys*, a Colhuehuapian erethizontid rodent from Argentina. *J Vert Paleontol* 24:228–234
- Dumont ER, Ryan TM, Godfrey LR (2011) The *Hadropithecus* conundrum reconsidered, with implications for interpreting diet in fossil hominins. *Proc Roy Soc B-Biol Sci* 278:3654–3661
- Dunbar RIM (1998) The social brain hypothesis. *Evol Anthropol* 6:178–190
- Dunbar RIM, Schultz S (2007) Understanding primate brain evolution. *Phil Trans R Soc B* 362:649–658
- Edinger T (1929) Die fossilen Gehirne. *Zeitschrift für die gesamte Anatomie* 28:1–221
- Edinger T (1964) Midbrain exposure and overlap in mammals. *Am Zool* 4:5–19
- Eisenberg JF (1981) The mammalian radiations: an analysis of trends in evolution, adaptation, and behavior. University of Chicago Press, Chicago
- Elliot Smith G (1902) On the morphology of the brain in Mammalia, with special reference to that of lemurs, recent and extinct. *Trans Linn Soc Lond (Zool.)* 8:319–432
- Elliot-Smith G (1927) The evolution of man. Oxford University Press, London
- Falk D (2007) Evolution of the primate brain. In: Henke W, Tattersall I (eds) *Handbook of Paleoanthropology*, vol 2. Springer, Heidelberg, pp 1133–1162
- Felleman DJ, Van Essen DC (1991) Distributed hierarchical processing in the primate cerebral cortex. *Cerebral Cortex* 1:1–47
- Ferreira JD, Negri FR, Sánchez-Villagra MR et al (2020) Small within the largest: brain size and anatomy of the extinct *Neoeopiblema acreensis*, a giant rodent from the Neotropics. *Biol Lett* 16(2):20190914
- Fleagle JG (2013) Primate adaptation and evolution, 3rd edn. Academic Press, New York
- Fox RC, Scott CS (2011) A new, early Puercan (earliest Paleocene) species of *Purgatorius* (Plesiadapiformes, Primates) from Saskatchewan, Canada. *J Paleontol* 85:537–548
- Frahm HD, Stephan H, Stephan M (1982) Comparison of brain structure volumes in Insectivora and Primates. I. Neocortex. *J Hirnforschung* 23:375–389
- Gazin CL (1965) An endocranial cast of the Bridger Middle Eocene primate *Smilodectes gracilis*. *Smithsonian Misc Coll* 149:1–14
- Gibson KR (1986) Cognition, brain size and the extraction of embedded food sources. In: Else JG, Lee P (eds) *Primate ontogeny, cognition and social behaviour*. Cambridge University Press, Cambridge, pp 93–104
- Gilbert CC, Jungers WL (2017) Comment on relative brain size in early primates and the use of encephalization quotients in primate evolution. *J Hum Evol* 109:79–87
- Gingerich PD (1976) Cranial anatomy and evolution of early Tertiary Plesiadapidae (Mammalia, Primates). *Univ Michigan Pap Paleontol* 15:1–141
- Gingerich PD, Gunnell GF (2005) Brain of *Plesiadapis cookei* (Mammalia, Proprimates): surface morphology and encephalization compared to those of Primates and Dermoptera. *Contrib Univ Mich Herb* 31:185–195
- Gingerich PD, Martin RD (1981) Cranial morphology and adaptations in Eocene Adapidae. II. The Cambridge skull of *Adapis parisiensis*. *Am J Phys Anthropol* 56:235–257
- Gingerich PD, Franzen JL, Habersetzer J et al (2010) *Darwinius masillae* is a Haplorhine—Reply to Williams et al., 2010. *J Hum Evol* 59:574–579
- Glendenning KK, Masterton RB (1998) Comparative morphometry of mammalian central auditory systems: variation in nuclei and form of the ascending system. *Brain Behav Evol* 51:59–89
- Godinot M, Couette S (2008) Morphological diversity in the skulls of large adapines (Primates, Adapiformes) and its systematic implications. In: Sargis EJ, Dagosto M (eds) *Mammalian Evolutionary Morphology*. Springer, Dordrecht, pp 285–313
- Gonzales LA, Benefit BR, McCrossin ML et al (2015) Cerebral complexity preceded enlarged brain size and reduced olfactory bulbs in Old World monkeys. *Nat Comm* 6:1–9
- Gregory WK (1910) The orders of mammals. *Bull Am Mus Nat Hist* 27:1–524
- Gregory WK (1920) On the structure and relationships of *Notharctus*, an American Eocene primate. *Mem Bull Am Mus Nat Hist* 3:49–243

- Gudde RM, Joy JB, Mooers AO (2013) Imperilled phylogenetic endemism of Malagasy lemuriformes. *Divers Distrib* 19:664–675
- Gunz P, Kozakowski S, Neubauer S et al (2020) Skull reconstruction of the late Miocene ape *Rudapithecus hungaricus* from Rudabánya, Hungary. *J Hum Evol* 138:102687
- Gurche JA (1982) Early Primate Brain Evolution. In: Armstrong E, Falk D (eds) *Primate brain evolution: methods and concepts*. Springer US, Boston, pp 227–246
- Guy F, Lieberman DE, Pilbeam D et al (2005) Morphological affinities of the *Sahelanthropus tchadensis* (Late Miocene hominid from Chad) cranium. *Proc Natl Acad Sci USA* 102:18836–18841
- Harrington AR, Silcox MT, Yapuncich GS et al (2016) First virtual endocasts of adapiform primates. *J Hum Evol* 99:52–78
- Harrington AR, Yapuncich GS, Boyer DM (2020) The digital endocast of *Necrolemur antiquus*. *Palaeovertebrata* 43(2):e1. <https://doi.org/10.18563/pv.43.2.e1>
- Harvati K, Frost S (2007) Dental eruption sequences in fossil colobines and the evolution of primate life histories. *Int J Primatol* 28:705–728
- Harvey PH, Clutton-Brock TH, Mace GM (1980) Brain size and ecology in small mammals and primates. *Proc Natl Acad Sci USA* 77:4387–4389
- Heritage S (2014) Modeling olfactory bulb evolution through primate phylogeny. *PLoS One* 9(11):e113904
- Hirakawa H (2001) Coprophagy in leporids and other mammalian herbivores. *Mammal Rev* 31:61–80
- Hladik CM (1978) Adaptive strategies of primates in relation to leaf eating. In: Montgomery GG (ed) *The ecology of arboreal folivores*. Smithsonian Institution Press, Washington, pp 373–395
- Hofer HO (1962) Über die interpretation der ältesten fossilen primatengehirne. *Bibliogr Primatol* 1:1–31
- Hofer HO, Wilson JA (1967) An endocranial cast of an early Oligocene primate. *Folia Primatol* 5:148–152
- Hoffstetter R (1977) Phylogénie des primates. *Bull Mém Soc Anthropol Paris* 4:327–346
- Holloway RL, Broadfield DC, Yuan MS (2004) *The human fossil record: brain endocasts*. Wiley, Hoboken
- Hrdlička AL (1925) Weight of the brain and of the internal organs in American monkeys. With data on brain weight in other apes. *Am J Phys Anthropol* 8:201–211
- Hürzeler J (1948) Zur Stammesgeschichte der Necrolemuriden. *Schweiz palaont Abh* 66:3–46
- Isler K, van Schaik CP (2012) Allomaternal care, life history and brain size evolution in mammals. *J Hum Evol* 63:52–63
- Isler K, Kirk EC, Miller JM et al (2008) Endocranial volumes of primate species: scaling analyses using a comprehensive and reliable data set. *J Hum Evol* 55:967–978
- Janečka JE, Miller W, Pringle TH et al (2007) Molecular and genomic data identify the closest living relative of primates. *Science* 318:792–794
- Jerison HJ (1973) *Evolution of the Brain and Intelligence*. Academic Press, New York
- Jerison HJ (1979) Brain, body and encephalization in early primates. *J Hum Evol* 8:615–635
- Jerison HJ (2007) Evolution of the frontal lobes. In: Cummings JL, Miller BL (eds) *The human frontal lobes: functions and disorders*, 2nd edn. Guilford Press, New York, pp 107–120
- Jerison HJ (2012) Digitized fossil brains: neocorticalization. *Biolinguistics* 6:383–392
- Joffe TH, Dunbar RIM (1997) Visual and socio-cognitive information processing in primate brain evolution. *Proc Roy Soc B-Biol Sci* 264:1303–1307
- Kaas JH (2002) Convergences in the modular and areal organization of the forebrain of mammals: implications for the reconstruction of forebrain evolution. *Brain Behav Evol* 59:262–272
- Kaas JH (2012) The evolution of neocortex in primates. *Prog Brain Res* 195:91–102
- Kaufman JA, Ahrens E, Laidlaw D et al (2006) Anatomical analysis of an aye-aye brain (*Daubentonia madagascariensis*, Primates: Prosimii) combining histology, structural magnetic resonance imaging and diffusion tensor imaging. *Anat Rec* 287:1026–1037

- Kay RF, Kirk EC (2000) Osteological evidence for the evolution of activity pattern and visual acuity in primates. *Am J Phys Anthropol* 113:235–262
- Kay RF, Ross C, Williams BA (1997) Anthropoid origins. *Science* 275:797–804
- Kay RF, Perry JMG, Malinzak M et al (2012) Paleobiology of Santacrucian primates. In: Vizcaino SF, Kay RF, Bargo MS (eds) *Early Miocene Paleobiology in Patagonia: high-latitude paleocommunities of the Santa Cruz Formation*. Cambridge University Press, Cambridge, pp 306–330
- Kielan-Jaworowska Z (1984) Evolution of the therian mammals in the Late Cretaceous of Asia. Part VI. Endocranial casts of eutherian mammals. *Acta Palaeontol Pol* 46:157–171
- Kielan-Jaworowska Z, Trofimov BA (1986) Endocranial cast of the Cretaceous eutherian mammal *Barumlestes*. *Acta Palaeontol Pol* 31:137–144
- Kihm AJ, Tornow MA (2014) First occurrence of plesiadapiform primates from the Chadronian (latest Eocene). *Paludicola* 9:176–182
- Kirk EC (2006) Visual influences on primate encephalization. *J Hum Evol* 51:76–90
- Kirk EC, Kay RF (2004) The evolution of high visual acuity in the Anthropoidea. In: Ross CF, Kay RF (eds) *Anthropoid origins: new visions*. Kluwer, Boston, pp 539–602
- Kirk EC, Daghighi P, Macrini TE et al (2014) Cranial anatomy of the Duchesnean primate *Rooneyia viejaensis*: new insights from high resolution computed tomography. *J Hum Evol* 74:82–95
- Kobayashi S (1995) A phylogenetic study of titi monkeys, genus *Callicebus*, based on cranial measurements: I. Phyletic groups of *Callicebus*. *Primates* 36:101–120
- Kobayashi Y, Matsui T, Ogihara N (2018) Inferring cortical subdivisions based on skull morphology. In: Bruner E, Ogihara N, Tanabe H (eds) *Digital endocasts*. Springer, Tokyo, pp 33–46
- Korth WW (1994) *The Tertiary record of rodents in North America*. Plenum, New York
- Kristjanson H, Silcox MT, Perry J (2016) A new partial cranium of *Plesiadapis tricuspidens* and insights into plesiadapiform cranial anatomy. *J Vertebr Paleontol*:169–170
- Lang MM, Bertrand OC, San Martin-Flores G, Law CJ, Abdul-Sater J, Spakowski S, Silcox MT (2022) Scaling patterns of cerebellar petrosal lobules in Euarchontoglires: Impacts of ecology and phylogeny. *Anat Rec* 1–32
- Lang MM, Bertrand OC, Silcox MT (2018) Scaling pattern of primate paraflocculi does not correlate with ecological factors (activity pattern and diet/foraging strategy). *Am J Phys Anthropol* 165(S66):152–153
- Lang MM, San Martin-Flores GA, Bertrand OC et al (2019) Endocranial shape variation within Euarchontoglires using 3D Geometric Morphometrics. *J Vert Paleontol Prog Abstr* 2019:137
- Le Gros Clark WE (1924) On the brain of the tree-shrew (*Tupaia minor*). *Proc Zool Soc Lond* 1924:559–567
- Le Gros Clark WE (1926) On the anatomy of the pen-tailed tree-shrew (*Ptilocercus lowii*). *Proc Zool Soc Lond* 96:1179–1309
- Le Gros Clark WE (1945) Note on the palaeontology of the lemuroid brain. *J Anat* 79:123–126
- Le Gros Clark WE, Thomas DP (1952) *The Miocene lemuroids of East Africa, Fossil Mammals of Africa, No. 5*. British Museum (Natural History), London
- Lemelin P, Schmitt D (2004) Seasonal variation in body mass and locomotor kinetics of the fat-tailed dwarf lemur (*Cheirogaleus medius*). *J Morphol* 260:65–71
- Liu L, Yu L, Pearl DK et al (2009) Estimating species phylogenies using coalescence times among species. *Syst Biol* 58:468–477
- Long A, Bloch JI, Silcox MT (2015) Quantification of neocortical ratios in stem primates. *Am J Phys Anthropol* 157:363–373
- López-Torres S, Bertrand OC, Lang MM et al (2020) Cranial endocast of the stem lagomorph *Megalagus* and brain structure of basal Euarchontoglires. *Proc Roy Soc B-Biol Sci* 287:20200665
- MacPhee RD, Cartmill M (1986) Basicranial structures and primate systematics. In: Swisher DR, Erwin J (eds) *Comparative primate biology: systematics, evolution, and anatomy*. Alan R. Liss, New York, pp 219–275
- MacPhee RDE, Novacek MJ, Storch G (1988) Basicranial morphology of early Tertiary erinaceomorphs and the origin of Primates. *Am Mus Novit* 2921:1–42

- Macrini TE, Rougier GW, Rowe T (2007) Description of a cranial endocast from the fossil mammal *Vincelestes neuquenianus* (Theriiiformes) and its relevance to the evolution of endocranial characters in therians. *Anat Rec* 290:875–892. <https://doi.org/10.1002/ar.20551>
- Maddison WP, Maddison DR (2017) Mesquite: a modular system for evolutionary analysis. Version 3.2. <http://www.mesquiteproject.org>
- Makedonska JA, Lebrun R, Tafforeau P et al (2008) Comparative analysis of the endocasts of fossil and modern strepsirrhines using microtomography and 3D geometric morphometrics. *Am J Phys Anthropol* S46:147
- Malinzak MD, Kay RF, Hullar TE (2012) Locomotor head movements and semicircular canal morphology in primates. *Proc Natl Acad Sci* 109:17914–17919
- Marino L (1998) A comparison of encephalization between odontocete cetaceans and anthropoid primates. *Brain Behav Evol* 51:230–238
- Martin RD (1973) Comparative anatomy and primate systematics. *Symp Zool Soc Lond* 33:301–337
- Martin RD (1980) Adaptation and body size in primates. *Z Morphol Anthropol* 71:115–124
- Martin RD (1990) Primate origins and evolution: a phylogenetic reconstruction. Chapman Hall, London
- Martin RD (1993) Allometric aspects of skull morphology in *Theropithecus*. In: Jablonski NG (ed) *Theropithecus: the rise and fall of a primate genus*. Cambridge University Press, Cambridge, pp 273–298
- Martins AMG Jr, Amorim N, Carneiro JC et al (2015) Alu elements and the phylogeny of capuchin (*Cebus* and *Sapajus*) monkeys. *Am J Primatol* 77:368–375
- Mason VC, Li G, Minx P et al (2016) Genomic analysis reveals hidden biodiversity within colugos, the sister group to primates. *Sci Adv* 2(8):e1600633
- McKenna MC (1966) Paleontology and the origin of primates. *Folia Primatol* 4:1–25
- McKenna MC (1975) Toward a phylogenetic classification of the Mammalia. In: Luckett WP, Szalay FA (eds) *Phylogeny of the Primates: a multidisciplinary approach*. Plenum, New York, pp 21–46
- Meng J (2004) Phylogeny and divergence of basal Glires. *Bull Am Mus Nat Hist* 285:93–109
- Meng J, Hu Y, Li C (2003) The osteology of *Rhombomylus* (Mammalia, Glires): implications for phylogeny and evolution of Glires. *Bull Am Mus Nat Hist* 275:1–247
- Minwer-Barakat R, Marigó J, Femenias-Gual J et al (2017) *Microchoerus hookeri* nov. sp., a new late Eocene European microchoerine (Omomyidae, Primates): new insights on the evolution of the genus *Microchoerus*. *J Hum Evol* 102:42–66
- Mongle CS, Strait DS, Grine FR (2019) Expanded character sampling underscores phylogenetic stability of *Ardipithecus ramidus* as a basal hominin. *J Hum Evol* 131:28–39
- Montgomery SH, Capellini I, Barton RA et al (2010) Reconstructing the ups and downs of primate brain evolution: implications for adaptive hypotheses and *Homo floresiensis*. *BMC Biology* 8:9
- Murphy WJ, Eizirik E, O'Brien SJ et al (2001) Resolution of the early placental mammal radiation using Bayesian phylogenetics. *Science* 294:2348–2351
- Nargolwalla MC, Begun DR, Dean MC et al (2005) Dental development and life history in *Anapithecus heryaki*. *J Hum Evol* 49:99–121
- Neumayer L (1906) Über das Gehirn von *Adapis parisiensis* Cuv. *Neues Jahrb Min Geol Palaont* 2:100–104
- Ni X, Wang Y, Hu Y et al (2004) A euprimate skull from the early Eocene of China. *Nature* 427:65–68
- Ni X, Li Q, Li L et al (2016) Oligocene primates from China reveal divergence between African and Asian primate evolution. *Science* 352:673–677
- Ni X, Flynn JJ, Wyss AR et al (2019) Cranial endocast of a stem platyrrhine primate and ancestral brain conditions in anthropoids. *Sci Adv* 5(8):eaav7913
- Nowak RM (1991) Walker's mammals of the world. John Hopkins Press, Baltimore
- O'Leary MA, Bloch JI, Flynn JJ et al (2013) The placental mammal ancestor and the post-K-Pg radiation of placentals. *Science* 339:662–667

- Orliac MJ, Ladevèze S, Gingerich PD et al (2014) Endocranial morphology of Palaeocene *Plesiadapis tricuspidens* and evolution of the early primate brain. *Proc Roy Soc B-Biol Sci* 281:20132792
- Parker ST (2015) Re-evaluating the extractive foraging hypothesis. *New Ideas Psychol* 37:1–12
- Pereira-Pedro AS, Bruner E (2018) Landmarking endocasts. In: Bruner E, Ogiyama N, Tanabe H (eds) *Digital endocasts*. Springer, Tokyo, pp 127–142
- Pereira-Pedro AS, Beaudet A, Bruner E (2019) Parietal lobe variation in cercopithecoid endocasts. *Am J Primatol* 81(7):e23025
- Pereira-Pedro AS, Bruner E, Gunz P et al (2020) A morphometric comparison of the parietal lobe in modern humans and Neanderthals. *J Hum Evol* 142:102770
- Phillips KA (1998) Tool use in wild capuchin monkeys (*Cebus albifrons trinitatis*). *Am J Primatol* 46:259–261
- Piveteau J (1958) Recherches sur l'encéphale des primates. I.-L'encéphale d'un prosimien Lémuriforme: l'*Adapis*. *Ann Paléontol* 44:253–255
- Radinsky LB (1967) The oldest primate endocast. *Am J Phys Anthropol* 27:385–388
- Radinsky LB (1970) The fossil evidence of prosimian brain evolution. In: Novack CR, Montagna W (eds) *The primate brain: advances in primatology*, vol 1. Appleton Century Crofts, New York, pp 209–224
- Radinsky LB (1974) Prosimian brain morphology: functional and phylogenetic implications. In: Martin RD, Doyle GA, Walker AC (eds) *Research seminar on prosimian biology 1972*: London University. University of Pittsburg Press, Pittsburg, pp 781–798
- Radinsky LB (1975) Primate brain evolution. *Am Scient* 63:656–663
- Radinsky LB (1977) Early primate brains: facts and fiction. *J Hum Evol* 6:79–86
- Radinsky LB (1978) Evolution of brain size in carnivores and ungulates. *Amer Nat* 112:815–831
- Radinsky LB (1982) Some cautionary notes on making inferences about relative brain size. In: Armstrong E, Falk D (eds) *Primate brain evolution: methods and concepts*. Plenum, New York, pp 29–37
- Ramdarshan A, Orliac MJ (2016) Endocranial morphology of *Microchoerus erinaceus* (Euprimates, Tarsiiformes) and early evolution of the Euprimates brain. *Am J Phys Anthropol* 159:5–16
- Regan BC, Julliot C, Simmen B et al (2001) Fruits, foliage and the evolution of primate colour vision. *Phil Trans R Soc B* 356:229–283
- Rilling JK, Insel TR (1999) Differential expansion of neural projection systems in primate brain evolution. *NeuroReport* 10:1453–1459
- Roberts TE, Lanier HC, Sargis EJ et al (2011) Molecular phylogeny of treeshrews (Mammalia: Scandentia) and the timescale of diversification in Southeast Asia. *Mol Phylogenet Evol* 60:358–372
- Rose KD (1981) The Clarkforkian land-mammal age and mammalian faunal composition across the Paleocene-Eocene boundary. *Univ Mich Pap Paleontol* 26:1–197
- Rose KD (2006) *The Beginning of the Age of Mammals*. Johns Hopkins University Press, Baltimore
- Rose KD, MacPhee RD, Alexander JP (1999) Skull of early Eocene *Cantius abditus* (Primates: Adapiformes) and its phylogenetic implications, with a reevaluation of "*Hesperolemur*" *actius*. *Am J Phys Anthropol* 109:523–539
- Rose KD, Chester SGB, Dunn RH et al (2011) New fossils of the oldest North American euprimate *Teilhardina brandti* (Omomyidae) from the Paleocene-Eocene Thermal Maximum. *Am J Phys Anthropol* 146:281–305
- Rose KD, Chew AE, Dunn RH et al (2012) Earliest Eocene mammalian fauna from the Paleocene-Eocene Thermal Maximum at Sand Creek Divide, southern Bighorn Basin, Wyoming. *Univ Mich Pap Paleontol* 36:1–122
- Rosenberger AL (1985) In favor of the *Necrolemur*-tarsier hypothesis. *Folia Primatol* 45:179–194

- Rosenberger AL, Hogg R, Wong SM (2008) *Rooneyia*, postorbital closure, and the beginnings of the age of Anthropoidea In: Sargis EJ, Dagosto M (eds) *Mammalian Evolutionary Morphology*. Springer, Dordrecht, pp 325–346
- Ross CF (1995) Allometric and functional influences on primate orbit orientation and the origins of the Anthropoidea. *J Hum Evol* 29:201–227
- Ross CF, Kirk EC (2007) Evolution of eye size and shape in primates. *J Hum Evol* 52:294–313
- Rowe N, Goodall J, Mittermeier R (1996) *The pictorial guide to the living primates*. Pogonias Press, New York
- Ryan TM, Burney DA, Godfrey LR et al (2008) A reconstruction of the Vienna skull of *Hadropithecus stenognathus*. *Proc Natl Acad Sci USA* 105:10699–10702
- Ryan TM, Silcox MT, Walker A et al (2012) Evolution of locomotion in Anthropoidea: the semi-circular canal evidence. *Proc Roy Soc B-Biol Sci* 279:3467–3475
- San Martin-Flores GA, Nagendren L, Silcox MT (2018) Geometric Morphometrics on treeshrew cranial endocasts: a comparative analysis of scandentian and plesiadapiform brain shapes. *J Vert Paleontol Prog Abstr* 2018:209
- San Martin-Flores GA, Nagendren L, Lang MM et al (2019) Cranial endocasts of colugos, and their relevance to understanding the early phases of the evolution of the brain in Euarchonta and Primates. *J Vert Paleontol Prog Abstr* 2019:186
- Sargis EJ (2002) A multivariate analysis of the postcranium of treeshrews (Scandentia: Tupaiidae) and its taxonomic implications. *Mammalia* 66:579–598
- Sargis EJ, Chester SGB, Bloch JI et al (2018) Functional morphology of a remarkably complete skeleton of *Mixodectes pungens*: evidence for arboreality in an enigmatic eutherian from the Early Paleocene. *J Vert Paleontol Prog Abstr* 2018:210
- Seiffert ER, Boyer DM, Fleagle JG et al (2018) New adapiform primate fossils from the late Eocene of Egypt. *Hist Biol* 30:204–226
- Sherwood CC, Subiaul F, Zawidzki TW (2008) A natural history of the human mind: tracing evolutionary changes in brain and cognition. *J Anat* 212:426–454
- Silcox MT (2008) The biogeographic origins of Primates and Euprimates: east, west, north, or south of Eden? In: Sargis EJ, Dagosto M (eds) *Mammalian Evolutionary Morphology*. Springer, Dordrecht, pp 199–231
- Silcox MT, Sargis EJ, Bloch JI et al (2007) Primate origins and supraordinal relationships: morphological evidence. In: Henke W, Tattersall I (eds) *Handbook of Paleoanthropology*, vol 2. Springer, Heidelberg, pp 831–859
- Silcox MT, Bloch JI, Boyer DM et al (2009a) Semicircular canal system in early primates. *J Hum Evol* 56:315–327
- Silcox MT, Dalmyn CK, Bloch JI (2009b) Virtual endocast of *Ignacius graybullianus* (Paromomyidae, Primates) and brain evolution in early primates. *Proc Natl Acad Sci USA* 106:10987–10992
- Silcox MT, Benham AE, Bloch JI (2010a) Endocasts of *Microsyops* (Microsyopidae, Primates) and the evolution of the brain in primitive primates. *J Hum Evol* 58:505–521
- Silcox MT, Bloch JI, Boyer DM et al (2010b) Cranial anatomy of Paleocene and Eocene *Labidolemur kayi* (Mammalia: Apatotheria) and the relationships of the Apatemyidae to other mammals. *Zool J Linn Soc* 160:773–825
- Silcox MT, Dalmyn CK, Hrenchuk A et al (2011) Endocranial morphology of *Labidolemur kayi* (Apatemyidae, Apatotheria) and its relevance to the study of brain evolution in Euarchontoglires. *J Vert Paleontol* 31:1314–1325
- Silcox MT, Bloch JI, Boyer DM et al (2017a) The evolutionary radiation of plesiadapiforms. *Evol Anthropol* 26:74–94
- Silcox MT, Rusen R, Bloch JI (2017b) Endocranial anatomy of Late Paleocene (Clarkforkian NALMA) *Carpolestes simpsoni* (Plesiadapoidea, Primates) from the Bighorn Basin, Wyoming. *Am J Phys Anthropol* 162(S64):359
- Silva M, Downing JA (1995) *Handbook of mammalian body masses*. CRC Press, Boca Raton

- Simons EL, Seiffert ER, Ryan TM et al (2007) A remarkable female cranium of the early Oligocene anthropoid *Aegyptopithecus zeuxis* (Catarrhini, Propliopithecidae). *Proc Natl Acad Sci USA* 104:8731–8736
- Simpson GG (1945) The principles of classification and a classification of mammals. *Bull Am Mus Nat Hist* 85:1–350
- Simpson GG (1967) The Tertiary loriform primates of Africa. *Bull Comp Zool* 136:39–61
- Smith T, Rose KD, Gingerich PD (2006) Rapid Asia–Europe–North America geographic dispersal of earliest Eocene primate *Teilhardina* during the Paleocene–Eocene thermal maximum. *Proc Natl Acad Sci USA* 103:11223–11227
- Smith TD, Rossie JB, Bhatnagar KP (2007) Evolution of the nose and nasal skeleton in primates. *Evol Anth* 16:132–146
- Spitzka EA (1903) Brain-weights of animals with special reference to the weight of the brain in the Macaque monkey. *J Comp Neurol* 13:9–17
- Spoor F, Zonneveld F (1998) Comparative review of the human bony labyrinth. *Am J Phys Anthropol* 107(S27):211–251
- Spoor F, Garland T, Krovitz G et al (2007) The primate semicircular canal system and locomotion. *Proc Natl Acad Sci USA* 104:10808–10812
- Springer MS, Meredith RW, Gatesy J et al (2012) Marcoevolutionary dynamics and historical biogeography of primate diversification inferred from a species supermatrix. *PLoS ONE* 7:e49521
- Stanhope MJ, Waddell VG, Madsen O et al (1998) Molecular evidence for multiple origins of Insectivora and for a new order of endemic African insectivore mammals. *Proc Natl Acad Sci USA* 95:9967–9972
- Steiper ME, Seiffert ER (2012) Evidence for a convergent slowdown in primate molecular rates and its implications for the timing of early primate evolution. *Proc Natl Acad Sci USA* 109:6006–6011
- Stephan H (1972) Evolution of primate brains: a comparative anatomical investigation. In: Tuttle R (ed) *The functional and evolutionary biology of Primates*. Aldine-Atherton, New York, pp 155–174
- Stephan H, Bauchot R, Andy OJ (1970) Data on size of the brain and of various brain parts in insectivores and primates. In: Noback CR, Montagna W (eds) *The primate brain*. Appleton-Century-Crofts, New York, pp 289–297
- Stephan H, Frahm H, Baron G (1981) New and revised data on volumes of brain structures in insectivores and primates. *Folia Primatol* 35:1–29
- Sterling EJ, Povinelli DJ (1999) Tool use, aye-ayes, and sensorimotor intelligence. *Folia Primatol* 70:8–16
- Strait D, Grine FE, Fleagle JG (2015) Analyzing hominin phylogeny: cladistic approach. In: Henke W, Tattersall I (eds) *Handbook of paleoanthropology*, 2nd edn. Springer Reference, New York, pp 1989–2014
- Sych L (1967) Fossil endocranial cast of *Hypolagus brachygnathus* Kormos (Leporidae, Mammalia). *Acta Zool Crac* 12:27–30
- Szalay FS (1969) Mixodectidae, Microsyopidae, and the insectivore-primate transition. *Bull Am Mus Nat Hist* 140:195–330
- Szalay FS (1975) Phylogeny of primate higher taxa: the basicranial evidence. In: Lockett WP, Szalay FA (eds) *Phylogeny of the Primates: a multidisciplinary approach*. Plenum, New York, pp 91–125
- Szalay FS (1977) Phylogenetic relationships and a classification of the eutherian Mammalia. In: Hecht MK, Goody PC, Hecht BM (eds) *Major patterns in vertebrate evolution*. Plenum Press, New York, pp 315–374
- Szalay FS, Lucas SG (1996) The postcranial morphology of Paleocene *Chriacus* and *Mixodectes* and the phylogenetic relationships of archontan mammals. *New Mexico Mus Nat Hist Sci Bull* 7:1–47

- Takai M, Maschenko EN, Nishimura TD et al (2008) Phylogenetic relationships and biogeographic history of *Paradolichopithecus sushkini* Trofimov 1977, a large-bodied cercopithecine monkey from the Pliocene of Eurasia. *Quatern Int* 179:108–119
- Tigges J, Shantha TR (1969) A stereotaxic brain atlas of the tree shrew (*Tupaia glis*). Williams and Wilkins, Baltimore
- Van Essen DC, Anderson CH, Felleman DJ (1992) Information processing in the primate visual system: an integrated systems perspective. *Science* 255:419–423
- van Woerden JT, Willems EP, van Schaik CP et al (2012) Large brains buffer energetic effects of seasonal habitats in catarrhine primates. *Evolution* 66:191–199
- Visalberghi E (1990) Tool use in *Cebus*. *Folia Primatol* 54:146–154
- von Bonin G (1937) Brain-weight and body-weight of mammals. *J Gen Psychol* 16:379–389
- von Koenigswald W (1990) Die Paläobiologie der Apatemyiden (Insectivora s.l.) und die Ausdeutung der Skelettfunde von *Heterohyus nanus* aus dem Mittelozän von Messel bei Darmstadt. *Paleontographica A* 210:41–77
- von Koenigswald W, Rose KD, Grande L et al (2005) First apatemyid skeleton from the Lower Eocene Fossil Butte Member, Wyoming (USA), compared to the European apatemyid from Messel, Germany. *Paleontographica A* 272:149–169
- von Koenigswald W, Ruf I, Gingerich PD (2009) Cranial morphology of a new apatemyid, *Carcinella sigei* n. gen. n. sp. (Mammalia, Apatotheria) from the late Eocene of southern France. *Paleontographica A* 288:53–91
- Waddell PJ, Okada N, Hasegawa M (1999) Towards resolving the interordinal relationships of placental mammals. *Syst Biol* 48:1–5
- Warnke P (1908) Mitteilungen neuer Gehirn-und Körpergewichtsbestimmungen bei Säugern, nebst Zusammenstellung der gesamten bisher beobachteten absoluten und relativen Gehirngewichte bei den verschiedenen Spezies. *J Psychol Neurol* 13:355–403
- Weston EM, Lister AM (2009) Insular dwarfism in hippos and a model for brain size reduction in *Homo floresiensis*. *Nature* 459:85–88
- White TD, Asfaw B, Beyene Y et al (2009) *Ardipithecus ramidus* and the paleobiology of early hominids. *Science* 326:64–86
- White C, Bloch JI, Silcox MT (2016) Virtual endocast of late Paleocene *Niptomomys* (Microsypidae, Primates) and early primate brain evolution. *J Vertebr Paleontol*:248
- Wible JR (1990) Petrosals of Late Cretaceous marsupials from North America, and a cladistic analysis of the petrosal in therian mammals. *J Vert Paleontol* 10:183–205
- Wible JR (2011) On the treeshrew skull (Mammalia, Placentalia, Scandentia). *Ann Carnegie Mus* 79:149–231
- Wible JR, Zeller U (1994) Cranial circulation of the pen-tailed tree shrew *Ptilocercus lowii* and relationships of Scandentia. *J Mamm Evol* 2:209–230
- Williams BA, Kay RF, Kirk EC et al (2010) *Darwinius masillae* is a strepsirrhine—a reply to Franzen et al. (2009). *J Hum Evol* 59:567–573
- Wilson Mantilla GP, Chester SG, Clemens WA et al (2021) Earliest Palaeocene purgatoriids and the initial radiation of stem primates. *R Soc Open Sci* 8:210050
- Zhang ML, Li ML, Ayoola AO et al (2019) Conserved sequences identify the closest living relatives of primates. *Zool Res* 40:532–540
- Zhou JN, Ni RJ (2016) The tree shrew (*Tupaia belangeri chinensis*) brain in stereotaxic coordinates. Springer, Singapore

Chapter 13

Paleoneurology of Artiodactyla, an Overview of the Evolution of the Artiodactyl Brain



Maeva J. Orliac, Jacob Manguoust, Ana Balcarcel, and Emmanuel Gilissen

13.1 Systematic and Phylogenetic Context

The name “artiodactyl” (Owen 1848) comes from the ancient Greek *ἄρτιος*, pair, and *δάκτυλος*, finger, and unites ungulate mammals that have an even number of digits and paraxonian limbs (i.e. the axis of the limb is between digits III and IV; Thewissen and Hussain 1990; Lockett and Hong 1998). They are generally characterized by a “double pulley” astragalus with a distal trochlea and a large articular surface for the cuboid (Schaeffer 1947; Thewissen and Hussain 1990; Martinez and Sudre 1995; Rose 1996; Lockett and Hong 1998; Thewissen and Madar 1999; Geisler 2001; Gingerich et al. 2001; Thewissen et al. 2001; Geisler et al. 2007), and a trilobed lower deciduous fourth premolar (e.g. Lockett and Hong 1998; Geisler et al. 2007).

Behind the name “artiodactyl” lies one of the greatest mammalian evolutionary successes. Indeed, artiodactyls occupy today the second rank in terms of family diversity after rodents, and rank third in terms of generic and specific diversity (Burgin et al. 2018), overtaken there by chiropterans.

Supplementary Information The online version contains supplementary material available at https://doi.org/10.1007/978-3-031-13983-3_13.

M. J. Orliac (✉) · J. Manguoust
Institut Des Sciences de L'Évolution de Montpellier, Université de Montpellier,
Montpellier, France
e-mail: maeva.orliac@umontpellier.fr; jacob.manguoust@umontpellier.fr

A. Balcarcel
Palaeontological Institute and Museum, Zurich, Switzerland

E. Gilissen
Department of African Zoology, Royal Museum for Central Africa, Tervuren, Belgium
e-mail: emmanuel.gilissen@africamuseum.be

Artiodactyla today encompass five major crown groups: the tylopods (Tylopoda Illiger 1811), the suoids (Suoidea Gray 1821 sensu Gentry and Hooker 1988), the ruminants (Ruminantia Scopoli 1777), the hippopotamoids (Hippopotamoidea Gray 1821 sensu Gentry and Hooker 1988), and the cetaceans (Cetacea Brisson 1762).

Artiodactyls appeared quite abruptly in the fossil record ca. 55.8 Ma ago in the Holarctic, followed by an intense adaptive radiation in the early-middle Eocene (50–45 Ma; Theodor et al. 2007; Rose et al. 2012; Boivin et al. 2018). Past generic diversity is at least seven times larger than today's, with more than 40 extinct families and nearly 950 fossil genera recognized (Janis et al. 1998; Uhen 1998; Williams 1998; Uhen 2007; Prothero and Foss 2007; Gingerich 2010; Marx et al. 2016).

Despite a major breakthrough in Artiodactyla phylogenetic relationships made through molecular analyses, that is, the identification of the close affinities between hippopotamids and cetaceans (e.g. Miyamoto and Goodmann 1986; Irwin et al. 1991; Montgelard et al. 1997; Hassanin et al. 2012), basal relationships of the group remain largely unresolved and the origin of modern clades is still problematic when morphological characters are considered (e.g. O'Leary and Gatesy 2008; Geisler and Theodor 2009). According to most recent phylogenetic analyses, Tylopoda would be the first modern artiodactyl group to differentiate, followed by Suoidea; Ruminantia shares a close relationship with the Cetancodonta clade gathering hippos and cetaceans (Arnason et al. 2000, 2002; Hassanin et al. 2012; Gatesy et al. 2013). Total-evidence analyses, combining morphological and molecular characters, have been performed in the 2000s in order to enhance resolution of the early radiation and clarify the relationship of extinct artiodactyl groups relative to modern ones, although with unsuccessful results (e.g. Geisler and Uhen 2005; O'Leary and Gatesy 2008; Geisler and Theodor 2009; Spaulding et al. 2009). Since 2009, no new comprehensive contribution to artiodactyl phylogeny based on morphological characters including all four modern families and fossils has been published, and major questions remain about the placement of extinct taxa in the artiodactyl phylogenetic tree. The huge diversity of artiodactyls is perceptible in their brain pattern. Modern representatives show a wide array of brain morphologies (Fig. 13.1), including some of the biggest and most convoluted mammalian brains (Welker 1990) in those of delphinid cetaceans (e.g. *Tursiops truncatus*), where brain size expressed as a function of the body mass ('encephalization quotient = EQ', Jerison 1970) ranks second after that of humans (Marino 1998, 2002).

13.2 Historical Background

It is worth noting that the first definition of the endocranial cast was provided by Cuvier (1822) after an observation based on a natural endocast of an artiodactyl, *Anoplotherium commune*, from Montmatre gypsum. He wrote: "... it was moulded in the cavity of the skull; and as this cavity itself in the living animal was moulded on the brain, the clay necessarily represents the true shape of the latter..." Like many other mammalian groups, the first descriptions of artiodactyl endocranial

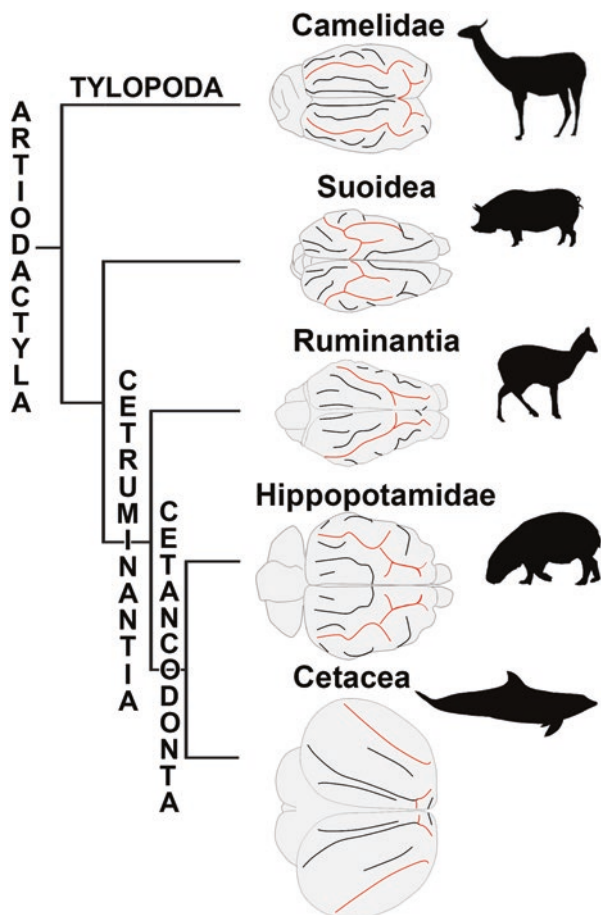


Fig. 13.1 Phylogenetic relationships and general neocortical pattern of modern artiodactyl groups. Suprasylvia and connected sulci (coronal and ansate sulci) are highlighted in red. Not to scale

casts mainly date from the second half of the nineteenth century and are based on natural endocasts. Among them are included those of European cainotheriids (Gratiolet 1859) and ruminants (Gaudry 1873), North American oreodontids (Leidy 1869; Bruce 1883), and North African archaeocete whales (Gervais 1871). Descriptions of these endocranial features are directly related to the discovery and scientific exploitation of major fossil outcrops that yielded abundant and well-preserved remains in a taphonomic context that allowed for natural preservation of casts of the endocranial cavity. Thus, the historical knowledge of endocranial anatomy is much contrasted depending on the taxonomic group and the geological period considered.

The brain of modern artiodactyls is remarkable by the expansion and by the folding of the neopallium. Modern artiodactyl groups are all highly gyrencephalic

(Kazu et al. 2014) and differ in their neocortical pattern (Fig. 13.1), and most of the early works on fossil artiodactyl endocranial casts pay special attention to the foldings of the neopallium and their identification. Detailed identification of the different sulci of the neopallium of artiodactyls was established during the end of the nineteenth century (Krueg 1878) and the first half of the twentieth century based on the study of embryologic/ontogenetic series by Anthony and Grzybowski (1931, 1934, 1936) for suids (*Sus scrofa*) and domestic bovids (sheep *Ovis aries*, and cow *Bos taurus*), and by Friant (1937, 1940) for hippopotamids. The study of artiodactyl endocranial casts during the nineteenth and twentieth centuries can be divided into two approaches: qualitative studies focusing on anatomy from the second half of nineteenth century until the 1970s (see for instance the chapter of Dechaseaux 1961 in the “*Traité de Paléontologie*” tome 6 of Piveteau for a remarkable summary of the knowledge of artiodactyl endocranial casts in the 1960s), and quantitative focusing on the increase of brain size through time that mainly developed in the 1980s (e.g., Jerison 1970, 1973; Radinsky 1987). Most of these observations were performed in a systematic framework separating artiodactyls in two categories on the basis of tooth morphology: Bunodontia (pigs, hippos and extinct relatives) and Selenodontia (ruminants – including camelids – and extinct relatives). The lack of a clear phylogenetic context (or basically the lack of phylogenetic concepts for earliest works) has limited the scope of the thorough, highly detailed, first observations performed on artiodactyl endocranial casts (see next Sect. 13.2.1).

Endocranial studies did not progress much until the democratization of CT-scan investigations due to the small number of natural endocranial casts available (and the limitation of their taxonomic attribution if not associated with dental remains) and to the often destructive nature of preparation of plaster/silicone endocranial casts. Yet descriptions of fossil artiodactyl endocranial casts based on virtual intracranial investigations and 3D reconstructions of the internal mould of the cranial cavity remain scarce and are only available for early representatives of the group (Oreodontoidea, Macrini 2009; *Diacodexis*, Orliac and Gilissen 2012), for early Hippopotamoidea (Thiery and Ducrocq 2015), for Cetacea and their closest relative (Raoellidae, Orliac and Thewissen 2021; Remingtonocetidae, Bajpai et al. 2011; crown Cetacea, Marino et al. 2003; Racicot and Rowe 2014; Boessenecker et al. 2017), and for crown Ruminantia (Cervidae, Fontoura et al. 2020).

13.2.1 Documentation of Artiodactyl Endocranial Casts in the Fossil Record

Endocranial Morphology of Extinct Artiodactyla Clades

The Endocranial Morphology of *Diacodexis*, Earliest Artiodactyla The oldest known artiodactyl endocranial casts described in the literature belong to the genus *Diacodexis* and originate from the Early Eocene of North America (*Diacodexis ilicis*, earliest Wasatchian, ca. 55 Ma; Orliac and Gilissen 2012, 3D reconstruction of the virtual endocranial cast) and

from the early Middle Eocene of Pakistan (*Diacodexis pakistanensis*, ca. 48 Ma; Sigogneau-Russell and Russell 1983, partial composite reconstruction based on nine skull fragments). The presence of a simple neopalleal pattern in *Diacodexis*, shared by other early artiodactyls, allowed for proposing a reconstruction of the ancestral neopalleal pattern for Artiodactyla.

Endemic European Artiodactyls (EEA) Several extinct artiodactyl genera and families (including Cebochoeridae, Mixtotheridae, Robiacinidae, Cainotheriidae, Choeropotamidae, Anoplotheriidae, Xiphodontidae, and Amphimerycidae) are geographically restricted to Europe. They derive from several endemic radiations that took place during the late early and middle Eocene when Europe was geographically isolated from other land masses in a general context of high sea level (Prothero 1994). Phylogenetic relationships among the basal families of artiodactyls remain unclear and greatly differ between analyses (e.g. Geisler et al. 2007; Luccisano et al. 2020; Weppe et al. 2020a, b). Endocasts of European endemic artiodactyls were among the first mammalian endocasts to be studied (Cuvier 1822; Gratiolet 1859). Most of them have been described based on exceptionally well-preserved fossil material from the early Miocene lacustrine deposits of Saint-Gérand-le-Puy (Allier department, France), and from Paleogene karstic infillings from the Quercy Phosphorite Formation (Southwestern France). Among the first taxa described were the cainotheriids, considered then to be early ruminant representatives (Gratiolet 1859; Milne-Edwards 1864; Gervais 1973; Hürzeler 1936). The endocast of *Cainotherium* was extensively studied by Anthony and Friant (1938) who concluded that it represented the primitive pattern of the ruminant brain. Dechaseaux (1961, 1968, 1969a, b, 1970, 1973) described then in great detail the endocranial casts of a variety of European endemic artiodactyls (*Tapirulus*, *Mouillacitherium*, *Cebochoerus*, *Dichobune*, *Dacrytherium*, *Cainotherium*, *Oxacron*, *Diplobune*, *Amphimeryx*, *Pseudamphimeryx*, *Mixtotherium*), and the general trends in neocortical fissuration patterns in Artiodactyla. These works from the second half of the twentieth century benefitted from the identification of cortical patterns established by Anthony and Grzybowski (1931, 1934, 1936) and from the sharp reflections on external brain features by the works of Friant (1937, 1939, 1940), together with a more integrative evolutionary context (e.g. Dobzhansky 1937; Mayr 1942; Huxley 1942; Simpson 1944; Stebbins Jr 1950).

Oreodontoidea Among the earliest works on artiodactyl endocranial casts are the studies on oreodontoids from North America. Oreodontoidea include two families, Agriocheridae and Merycoidodontidae, they include a wide variety of subfamilies documented from the middle Eocene to the middle Miocene. The phylogenetic relationships of, and within, Oreodontoidea are still unclear (Ludtke 2007; Stevens and Steven 2007). Natural endocasts of multiple oreodontoid taxa are particularly well described in the literature of the second half of the nineteenth century and the first half of the twentieth (Gratiolet 1859; Leidy 1869; Bruce 1883; Scott 1899; Moodie 1916, 1922; Black 1920; Thorpe 1931, 1937; Friant 1939, 1948). Most of these natural endocasts came from the Oligocene

White River fauna of the Western U.S. (Scott and Jepsen 1940), and the Eocene of West Texas (Wilson 1971). Among the taxa described or mentioned are the agriocherid *Protoreodon* (Macrini 2009) and the merycoidodontids *Merycoidodon* (Gratiolet 1859; Bruce 1883; Black 1920; Friant 1948; Leidy 1869), *Eporeodon* (Marsh 1886; Thorpe 1931), *Merycochoerus* (Moodie 1915, 1922), *Promerycochoerus* (Thorpe 1931), and *Leptauchenia* (originally described as *Cyclopidius* Cope 1878; Prothero and Sanchez 2008). Among these descriptive works, the incredible preservation of a specimen and the thorough description of the smallest details of its brain allowed Black (1920: Fig. 23–24) to propose a restoration of the “*Oreodon*” brain (in fact rather derived *Merycoidodon* species) with unrivalled precision. Black noticed the strikingly complex cerebellum contrasting with the small and relatively simply arranged neopallium and questioned, as early as the beginning of the twentieth century, the possible independent evolution of these parts of the brain. Black (1920) and Moodie (1916, 1922) noticed the association of ruminant and “suilline” characters in merycoidodontid brains and qualified them as “pig-like ruminants.” Oreodontid brain features were then discussed in a wider comparative frame by Friant (1939) and Dechaseaux (1961, 1969a). More recently, the endocranial cast of *Bathysgenys reevesi* was described by Macrini (2009) based on μ CT-scan data, together with a general discussion about morphological diversity within Merycoidodontidae.

Endocasts of Modern Artiodactyl Groups

Tylopoda The evolution of brain morphology in Tylopoda is documented mainly by camelids from the Eocene to the Miocene; whose origin is the Holarctic zone of North America. In geochronological order, the camelid brain is represented by endocasts of *Protylopus* (Eocene), *Eotylopus* (Eocene), *Poebrotherium* (early and late Oligocene), and lastly, *Protolabis* (late Miocene) and *Procamelus* (late Miocene). As the earliest known member of Camelidae, the brain of *Protylopus* (ca. 40 Ma) is considered the precursor to the modern camelid brain. The Oligocene camelid brain is known from two specimens: *Poebrotherium wilsoni* of the early Oligocene, and the relatively larger *Poebrotherium labiatum* in the late Oligocene (Bruce 1883; Cope 1886; Jerison 1971). Edinger (1966) briefly described the basic pattern of evolution from these earlier forms to the late Miocene, the latter stage represented by two endocasts of *Procamelus*. The smaller of the two, first recognized as *Procamelus occidentalis* (see Cope 1877a, b), was later re-assigned to the genus *Protolabis* (Jerison 1971). The larger endocast, which remains as *Procamelus*, was referred to as a late Pliocene form by many researchers (Edinger 1966; Jerison 1971; Repérant 1971a, b; Kruska 1982). Recent investigations have clarified, as previously considered by Jerison (1971), that this is actually a Miocene *Procamelus* (ca. 12–10 Ma) (Balcarcel et al. unpublished data). The major trends in neocortical evolution, spanning the Eocene to late Miocene, were described by Repérant (1970, 1971a). Recently, newly described endocasts including that of *Camelops hesternus* (artificial), a giant camelid, and one of what is likely a “*Palaeolama*” (natural),

highlight the degree of brain complexity reached during the Pleistocene (Balcarcel et al. unpublished data).

Suoidea The external features of the brain of *Sus scrofa*, the domestic pig, are well known and described in detail (e.g., Saikali et al. 2010), including its developmental aspects (Krueg 1878; Anthony and Grzybowski 1931). This is not the case for other modern suid genera, which have only been partly documented (Anthony and Grzybowski 1931). The external morphology of the brain of modern Tayassuidae is also described in very few works (Krueg 1878; Allanson 1971; Saraiva 2017). To our knowledge, there is no documentation of a fossil suoid endocast in the literature.

Ruminantia The general morphology of the brain of ruminant artiodactyls and the evolution of brain features has been described and discussed by Friant (1939), and subsequently augmented by Dechaseaux (1961). These works largely build on the studies of embryologic/ontogenetic series in domestic bovids (sheep *Ovis aries*, and cow *Bos taurus*) by Anthony and Grzybowski (1934, 1936). Several endocranial casts (natural or plaster) of fossil ruminants from the Quaternary and the Neogene are described and figured in the literature, and the morphological features are generally described in great detail. Among the first descriptions are those of *Gazella deperdita* (Bovidae), described Gaudry (1873) from the late Miocene deposits of Mont Luberon (France), and *Samotherium* (Giraffidae), described by Black (1915) from the late Miocene of the Samos Island. The endocranial morphology of extinct Bovidae was further documented by natural and silicone endocasts of the Plio-Pleistocene insular bovid *Myotragus* (Dechaseaux 1961: Fig. 16, 1962; Köhler and Moyà-Solà 2004; Palombo et al. 2008) and of the Pliocene ovine *Megalovis* (Dechaseaux 1961). The endocast of the cervoid Palaeomerycidae *Aletomeryx* was described from the late Miocene of Nebraska (Lull 1920; Friant 1939; Dechaseaux 1961) and the endocranial morphology of the fossil stem Cervidae *Dicrocerus* and *Megaceros* is known from the middle Miocene and the Pliocene of France (Dechaseaux 1961). More recently the small *Candiacervus* from the Plio-Pleistocene of the Mediterranean islands (Angelelli 1980; Palombo et al. 2008), and the late Pleistocene *Antifer ensenadensis* from southern Brazil (Fontoura et al. 2020) further documented the brain morphology of extinct cervids. The earliest ruminant endocranial casts described in the literature are, to our knowledge, that of *Dremotherium* (unknown family) and *Amphitragulus?* (unknown family) from the late Oligocene-early Miocene deposits of Saint-Gérard-le-Puy (Sigogneau 1968; Dechaseaux 1961, 1969a, b).

Hippopotamoidea A first illustration and very brief mention of a fossil hippopotamid endocast (artificial) was made by Friant (1940: Fig. 4). To our knowledge, studies of fossil Hippopotamidae endocasts in the literature are limited to *Hippopotamus protamphibius* from the Pleistocene of Ethiopia (uncertain locality from Omo valley), *H. madagascariensis* and *H. lemerlei* from the?late Pleistocene to Holocene of Madagascar, and *H. minor* from the Pleistocene of Cyprus (Anthony 1948). The latter notice the thickness of the dura mater preventing access to most of the cerebellar structures, and the presence of a large “K lobe”, characteristic of the brain of

Hippopotaminae (see Sect. 13.3.1.3). This work on natural and artificial plaster endocasts was then integrated by Dechaseaux (1961) in her discussions of adaptation to amphibiosis in hippopotamuses. The fossil record of Hippopotamidae only goes back to the Oligocene (ca. 30 Ma, Lihoreau et al. 2015) whereas hippopotamoids (i.e. “Anthracotheriidae”) appear in the fossil record in Asia during the middle Eocene (Lihoreau and Ducrocq 2007). The endocranial morphology of Hippopotamoidea is still poorly documented. Only two “anthracotheriid” taxa are described in the literature, a representative of the Microbunodontinae *Microbunodon minimum* and of a more derived Botriodontinae *Merycopotamus medioximus* (Thiery and Ducrocq 2015). Description of the endocast of *M. minimum* (late Oligocene from La Milloque, France) relies on a virtual reconstruction of the endocranial cavity of a well-preserved specimen, allowing a precise description of the external brain features of this small-sized animal. The external features of the brain of *M. medioximus* are only partly documented from a partial natural cranial endocast from Potwar Plateau, Pakistan, dated from the late Miocene (Lihoreau et al. 2004). Given the scarcity of available data, the evolutionary history of brain features of hippopotamoids remains widely undocumented.

Cetacea The first descriptions of cetacean endocasts are, to our knowledge, by Gervais who described plaster endocasts of extant Mysticeti (Gervais 1871), a partial braincase referred to the Eocene basilosaurid *Zeuglodon cetoides* (Watchita river, Louisiana, U.S.), and one of the Miocene delphinid *Glyphidelphis sulcatus* (Hérault, France, now referred to as *Schizodelphis sulcatus*) (Gervais 1874). Natural endocranial casts of basilosaurids, fully aquatic archaeocetes sister taxa to Neoceti, have been described based on *Dorudon* by Smith (1903), Andrews (1906), and Stromer (1903), and Dart (1923) who provided an extensive description of Zeuglodontidae endocasts. These works on basilosaurids were integrated with those of Edinger (1955) and Dechaseaux (1961). Following the concerns of Marples (1949) about the interpretation of fossil cetacean endocasts, Breathnach (1955) revised the brain/endocast shape correspondence for a sample of modern cetaceans and concluded that regarding the cerebellar region of odontocetes and the brain of mysticetes in general, the endocranial cast is “little less than a poor and misleading caricature” (Breathnach 1955: 541). The earliest evolutionary history of the cetacean brain is only partly documented back to the early middle Eocene by early diverging, non-fully aquatic archaeocetes, pakicetid (Nummela et al. 2006; Kishida et al. 2015), protocetids (*Indocetus* sp., cf. *I. ramani*, Bajpai et al. 1996), and remingtonocetids (Bajpai et al. 2011; Kishida et al. 2015). The endocranial morphology of *Indohyus* belonging to the Raoellidae, the sister taxon to Cetacea, recently provided some additional insights into the onset of cetacean brain characteristics (Orliac and Thewissen 2021). The endocranial morphology of Neoceti, the clade gathering modern cetaceans, is still partially documented relative to their diversity. Odontocetes are the best documented and include records of Xenorophidae (*Albertocetus* from early Oligocene, South Carolina, Boessenecker et al. 2017, and *Xenorophus* from late Oligocene North Carolina, Marino et al. 2003), Eurhinodelphinidae (*Xiphiacetus* sp. described as *Eurhinodelphis morrissi* by Marino et al. 2003, Middle Miocene of Maryland), Eoplatanistidae (Pilleri

and Gihl 1982, from Italy, originally referred to *Schizodelphis*, transferred to *Eoplatanista* by Muizon 1988), Delphinidae (Globicephalinae Boessenecker et al. 2015), Phocoenidae (Racicot and Rowe 2014), and several records of indeterminate odontocetes. These include “*Squalodon*” from the Oligocene of New Zealand (Marples 1949; specimen C.34.7; see Fordyce 1978 for systematic reassessment), “*Prosqualodon davidi*” by Dart (1923) from the Miocene of Tasmania, and a specimen from the middle Miocene of Poland (Stefaniak 1993, originally referred to as Delphinidae indet.). Bisconti et al. (2020) recently restudied the natural endocast of an early Miocene Odontocete from Piedmont, Italy, previously studied by Dal Piaz (1905), Parona (1923) and Pilleri and Gihl (1982). Natural endocasts of extinct mysticetes are very scantily documented in the fossil record, which is, to our knowledge, limited to the cetotherids *Cetotherium* (Strobel 1881:pl1, Fig. 2) and *Imerocetus* (Mchedlidze 1988), to *Pinocetus polonicus* (middle Miocene of Poland; Czyżewska 1988, originally placed in the Cetotheriidae but recently found outside this clade by Marx et al. 2019), to the Llanocetidae *Llanocetus denticrenatus* (Mitchell 1989) from the latest Eocene of Seymour Island (see Fordyce and Marx 2018 for familial referral), and to *Willungacetus* from the early Oligocene of South Australia (Pledge 2005, placed in Mysticeti indet. by Fitzgerald 2010). Few endocasts of extant cetaceans are also available in the literature, via physical endocasts (e.g. *Balaenoptera rostrata*, *Balaena mysticetes*, *Megaptera novaeangliae* by Gervais 1871; sperm-whale *Physeter microcephalus* by Flower 1867; foetal fin-whale, common porpoise *Phocaena phocaena* by Breathnach 1955; *Balaenoptera musculus* by Dechaseaux 1961), or digital reconstructions (e.g. Phocoenidae by Racicot and Colbert 2013; narwhal *Monodon monoceros* and beluga *Delphinapterus leucas* by Racicot et al. 2018).

13.2.2 Problematics

As exposed above, endocasts of artiodactyls have been actively described and studied from the second half of the nineteenth century to the 1970s. These works widely take place outside the frame of phylogenetic concerns, or in a paradigm mainly splitting Artiodactyla in two/three groups based on their dental morphology (bunodont/selenodont/bunoselenodont), and, naturally, separating cetaceans from artiodactyls. The phylogenetic context has drastically evolved since the end of the twentieth and the beginning of the twenty-first centuries, and the relationships between modern artiodactyl groups are now pretty consensual. Integrating Cetacea within a broader definition for Artiodactyla is now necessary, as is the clarification of the evolutionary history of brain structures within this new phylogenetic context. In the meantime, phylogenetic relationships at the order scale including fossil taxa remains highly debated and no consensus has yet been reached today. Major artiodactyl groups can be differentiated by their endocast morphology (Dechaseaux 1969a, b; Macrini 2009), and inclusion of endocranial characters will certainly bring a source of relevant characters to define clades and clarify basal relationships within Artiodactyla. Gathering an increasing corpus of data for artiodactyl

endocasts is now crucial to address these evolutionary issues. Indeed, documentation of endocranial morphology of the various artiodactyl groups remains scant compared to their amazing diversity. Most data regarding endocranial morphology of artiodactyls derives from natural and artificial endocasts and the number of available virtual models remains limited so that quantitative parameters such as relative volume of the different components (e.g. olfactory bulb, cerebrum, and cerebellum) or relative neocortical surface cannot currently be discussed at the order scale, hampering a quantitative assessment of brain evolution in the group.

Among major questions that are currently investigated is to what extent ecological specialisation has shaped the neocortical pattern and different components of the artiodactyl brain. The general overview of published endocasts suggests a complicated pattern of evolutionary history of the different structures with decoupling of evolutionary stages between cerebrum and cerebellum; each clade shows a mosaic pattern of derived and plesiomorphic features that has to be put in perspective with both the history and the ecology of taxa. Artiodactyla therefore appears to be a perfect group for a case study of brain evolution and its associated drivers because of their broad temporal and spatial repartition, and their incredible diversity within mammals, including a wide array of body masses and ecological specialisations (e.g. terrestrial and aquatic).

Domestication is also a crucial aspect of the evolution of the artiodactyl brain. Artiodactyls comprise an impressive proportion of today's domestic livestock, including suids, camelids, and a wide variety of ruminants (cervids, bovids). Each group represents a model for exploring morphological changes to the brain in correlation with the domestic niche: selection for tameness, environmental and dietary alterations, and life cycle changes (Zeder 2012). Brain size differences have already been noted between many wild and domestic mammals, particularly in artiodactyls (Kruska 1988), but neuroanatomical differences are less known. This is currently an area of great scientific interest, as behavioral and cognitive abilities are increasingly being inferred from brain morphology (e.g. Balcarcel et al. 2021; Hecht et al. 2019).

In this chapter, we provide a first step to discussing brain morphology and evolutionary history at the Artiodactyla scale, including Cetacea, based on a first compilation of available data and including recent, yet still very scant, 3D models deriving from μ CT-scan acquisitions.

13.3 Overview of General and Comparative Anatomy

13.3.1 *Characterization of Cranial Endocast Morphology*

Overview of Modern Artiodactyl Brain Morphology, Primary Identification of Structures

Modern Artiodactyla are characterized by an important extension of their neopallium that covers most of the cerebral surface and extends posteriorly over the midbrain, partially hiding the cerebellum. If terrestrial groups mostly differ by the sulcal

pattern of their neopallium, Cetacea stand as an exception with a highly morphologically divergent brain, with, among others, drastic reduction or lack of olfactory bulbs, very strong telencephalic flexure, and special cortical characteristics (i.e. simple cortical organization, Glezer et al. 1988; Morgane et al. 1988; Glezer et al. 1988, 1993; Raghanti et al. 2019). Due to these unique features, Cetacea have always been studied outside the Artiodactyla framework. The literature relating to the study of gyrencephaly abounds with diverse and often contradictory nomenclatures. We principally use here the revised nomenclature of Repérant (1971b), mainly built on the work of Smith (1902) and Anthony and Grzybowski (1930) and based on various homology criteria (topographical, morphological, anatomical, histological, ontological, phylogenetic). We add here some other support to homology based on the morphological intermediate criteria as defined by Repérant (1971b). The main neocortical sulci of Artiodactyla observed on endocasts (i.e. exposed on the external aspect of the brain) are, from the rhinal fissure on the ventral margin of the neopallium (delimiting the paleopallium from the neopallium, Smith 1902) to the interhemispheric fissure (at the sagittal plane): the ectosylvia, the suprasylvia, the coronal and the lateral (Figs. 13.1 and 13.2). The cruciate and the splenial sulci, originating from the internal aspect of the neopallium at the interhemispheric fissure, are also exposed on the dorsal surface of the hemispheres in some taxa (see Sect. 13.3.1.3). There are also typical secondary grooves: the diagonal sulcus (“*sillon γ* ” of Anthony and Grzybowski 1931, 1934, 1936; Friant 1939; Anthony 1961; Dechaseaux 1961), the arcuate sulcus (“*sillon α* ” of Friant 1952 – observed in Camelidae), and the oblique sulcus (“*sillon β* ” of Anthony and Grzybowski 1936; Friant 1939; Sigogneau 1959; Anthony 1961; Dechaseaux 1961, 1969a, b, 1973). In all modern artiodactyls, the pseudosylvia, observed in gyrencephalic mammal groups such as carnivorans (Smith 1902) is very small or lacking (Repérant 1971b). If the homology of the various artiodactyl sulci has been discussed based on the primitive carnivoran pattern (as exemplified by the dog; e.g. Krueg 1878; Smith 1902), it has never been discussed at the Artiodactyla scale based on a global comparison of extant and extinct taxa.

A hallmark of the complexity of the brain of artiodactyls is the operculization, often incomplete, of the central area (the region delimited by the rhinals, the suprasylvia and the presylvia sulci) of the neopallium. It consists of an invagination of a more or less large surface of neopallium, localized between the rhinal and the ectosylvia and recognized as the gyrus arcuatus I (yellow area on Fig. 13.3) based on topographical similarities with the carnivoran neocortical pattern (see Repérant 1971b for considerations on homologies). The sylvian complex resulting from this operculization has various orientation depending of artiodactyl clades (Fig. 13.3).

Modern representatives show different patterns, recognizable from each other, and with different degrees of operculization (Fig. 13.3). It is, for example, almost complete to complete in suoids (Anthony and Grzybowski 1931), while the gyrus arcuatus I remains variously exposed in hippopotamids (Friant 1939, 1940), camelids (Repérant 1971b), cetaceans (Hof and Van der Gucht 2007; Knopf et al. 2016), and ruminants (Anthony and Grzybowski 1934, 1936; Friant 1939). Operculization is related to the expansion of the surface of the neopallium, the part of the brain dedicated to higher cognitive functions. As such, this phenomenon has been central to the study of artiodactyl endocasts and to the evolutionary history of their brains.

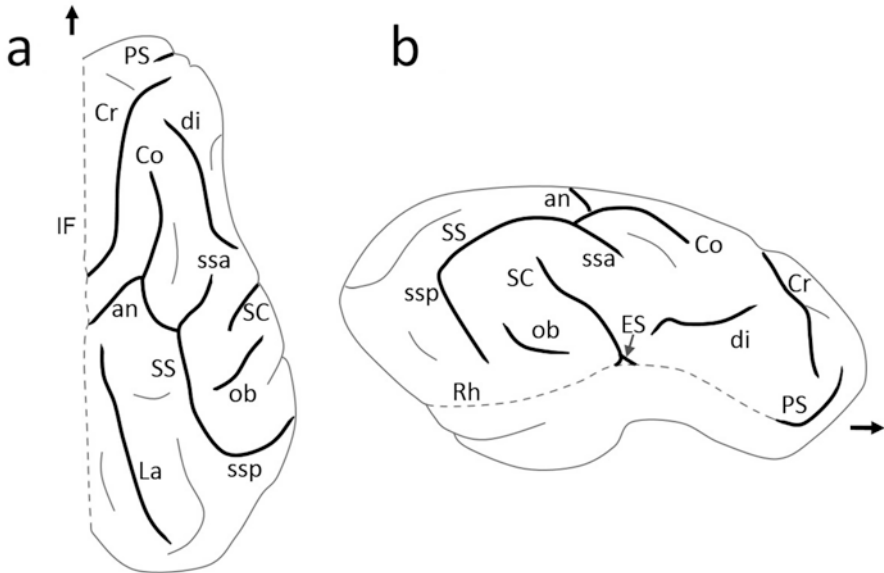


Fig. 13.2 Dorsal (a) and lateral (b) views of the right cerebral hemisphere of the domestic pig (*Sus scrofa*) illustrating the sulcal nomenclature used in this chapter. Arrow points anteriorwards. Abbreviations: *an* ansate sulcus, *Co* coronal sulcus, *Cr* cruciate sulcus, *di* diagonal sulcus, *ES* ectosylvia, *IF* interhemispheric fissure, *La* lateral sulcus, *Ob* oblique sulcus, *PS* presylvia, *Rh* rhinal fissure, *SC* sylvian complex, *SS* suprasylvia, *SSa* suprasylvia anterior, *SSp* suprasylvia posterior. The interhemispheric and the rhinal fissures are in dotted lines

The endocranial cast only gives access to the external structures of the brain, providing no clues as to the internal folds of the neopallium. This partial access to the morphology of the brain sometimes makes it difficult to identify first steps of operculization based on extinct taxa.

Most works on the brain cavity of artiodactyls have focused mainly on the morphology of the neopallium, while studies on the cerebellum are scarce. Modern artiodactyls exhibit a complicated cerebellum with highly convoluted and folded vermis and hemispheres (e.g. Suidae, domestic pig *Sus scrofa*, Saikali et al. 2010; Hippopotamidae, common hippopotamus *Hippopotamus amphibius*, Garrod 1880; Camelidae, Repérant 1971b), but most of these delicate foldings are generally not visible on endocasts. Given the particular attention devoted to the study of the artiodactyl neopallium in the literature and the paucity of data available concerning the cerebellum, this chapter focuses essentially on the former.

Endocranial Morphology of Extinct Artiodactyla Clades

Earliest Artiodactyls/Primitive Pattern The endocranial morphology of earliest artiodactyls is documented by the early and early middle Eocene *Diacodexis* (Sigogneau-Russell and Russell 1983; Orliac and Gilissen 2012), *Homacodon* (Fig. 13.4a–c; Orliac 2022) and *Helohyus* (Fig. 13.4d–f; Orliac 2022).

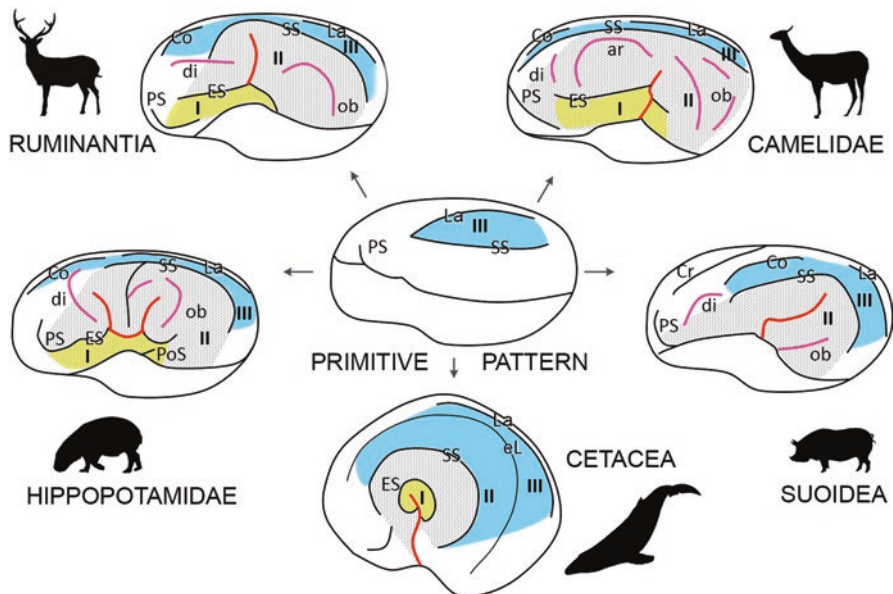


Fig. 13.3 Lateral left view of the cerebral hemisphere of crown Artiodactyla, compared to the primitive pattern (highlighted in central position), showing the operculization of the central territory of the neopallium (yellow, gyrus I). Abbreviations: *ar* arched sulcus, *Co* coronal, *Cr* Cruciate, *di* diagonal, *eL* ectolateral, *L* lateral, *ob* oblique, *PS* presylvia, *SS* suprasylvia; I-III refers to the neopallial gyri. The sylvian complex, sulci resulting from the operculization, is highlighted in red, diagonal and oblique sulci are highlighted in pink, arcuate is highlighted in orange; yellow, gyrus I; blue, gyrus III; gray sanded area and gray corresponds to the central area

Olfactory Bulbs These are only documented from the specimen of *Diacodexis ilicis* (Orliac and Gilissen 2012) and from fragmentary specimens of *Diacodexis pakistanensis* (Sigogneau-Russell and Russell 1983). This genus exhibits very large olfactory bulbs (13% of the total endocranium volume), so far the largest observed in Artiodactyla (Table 13.1).

Cerebral Hemispheres In *Diacodexis*, *Homacodon* and *Helohyus*, the extension of the neopallium on the surface of the cerebral hemispheres is reduced (43–44% of the surface of the cerebral hemisphere) and the paleopallium is visible in dorsal view. The ventral extension is weak and the caudal part of the cerebrum does not abut the cerebellum, letting a wide portion of the midbrain dorsally exposed (Fig. 13.4a–f). Their groove pattern is very simple with two deep sulci, the suprasylvia and the lateral sulcus (closer to the interhemispheric fissure), converging in their anterior-most part and delimiting an almond-shaped gyrus III. A small groove interpreted as the presylvia is also observed merging to the anterior segment of the rhinal fissure in the anterior most portion of the neopallium. The pyriform lobes are large. *Diacodexis* and *Homacodon* also show large olfactory tubercles. The lateral aspect of *Helohyus* endocranium cannot be described due to deformations (Fig. 13.4f).

It is worth to note that in earliest artiodactyls the orbitotemporal canal lies ventral to the rhinal fissure and is not a hallmark of the paleopallium/neopallium limit like it is the case in Primates (Microsyopidae, Silcox et al. 2010; although in some cases it is suggested dorsally, Proprimates, Gingerich and Gunnell 2005) and rodents (Ischyromyidae, Bertrand and Silcox 2016).

Midbrain Exposure The midbrain is widely exposed in *Diacodexis*, *Homacodon* and *Helohyus*. Midbrain exposure is observed in few other early artiodactyls (Figs. 13.4 and 13.5), but it is clearly wider in early and middle Eocene taxa (see also *Indohyus*).

Cerebellum Fine morphological details of the cerebellum are not visible on the endocasts, but all three taxa show a rather wide vermis compared to paramedian lobes. On *Diacodexis* (Orliac and Gilissen 2012) and *Helohyus* (Fig. 13.4d–f), the fissure prima can be identified on the dorsal aspect of the vermis, its position makes the paleocerebellum (lobus rostralis) widely exposed on the anterior part of the vermis. The lobus caudalis bears few fissures, and the fissure secunda is identifiable as a deep groove on the vermis endocast.

Endemic European Artiodactyls (EEA) Endocranial casts of EEA are documented from the late Eocene until the late Oligocene, most of them known from Quercy localities or from Saint-Gérard-le-Puy and described by Dechaseaux (1961, 1969a, b, 1973). They show a wide array of morphologies reflecting the radiation of the group in the “Island Europe” context.

Olfactory Bulbs *Cebochoerus*, *Dichobune*, *Mouillacitherium* as well as *Anoplotherium* present a rather similar relative size of the olfactory bulb with values comprised between 5.7 and 7.5% (Table 13.1). These values are smaller than what is observed in *Diacodexis* (13.8%). Among EEA, the cainotherid *Caenomeryx* exhibits the smallest olfactory bulbs, representing less than 4% of the total volume of the endocast (Table 13.1). In all these taxa, olfactory bulbs are joined on most of their length and separated from the anterior margin of the neopallium by a short circular fissure.

Cerebral Hemispheres The EEA show a great disparity of neocortical folding pattern, with a very simple pattern (two sulci delimiting the almond shapes gyri) observed in *Cebochoeridae* (Dechaseaux 1969a: Fig. 13) and in *Mouillacitherium* (Figs. 13.4g–i; Orliac 2022), and more complicated ones found in other groups documented. The dichobunoid *Dichobune* shows a slightly more complex pattern, with a long presylvia widely visible on the dorsal aspect and three accessory sulci notching the gyrus III (entolaterals, Figs. 13.4j–l; Orliac 2022). Cainotheriidae also present additional sulci, with a long coronal sulcus linked to both the lateral sulcus and the suprasylvia, and a diagonal sulcus, sometimes branched. The cainotheriids taxa analyzed *Caenomeryx filholi* (Fig. 13.4m–o; Orliac 2022), and *Cainotherium* (Anthony and Friant 1938; Friant 1939; Dechaseaux 1969a: Fig. 12) shows a small

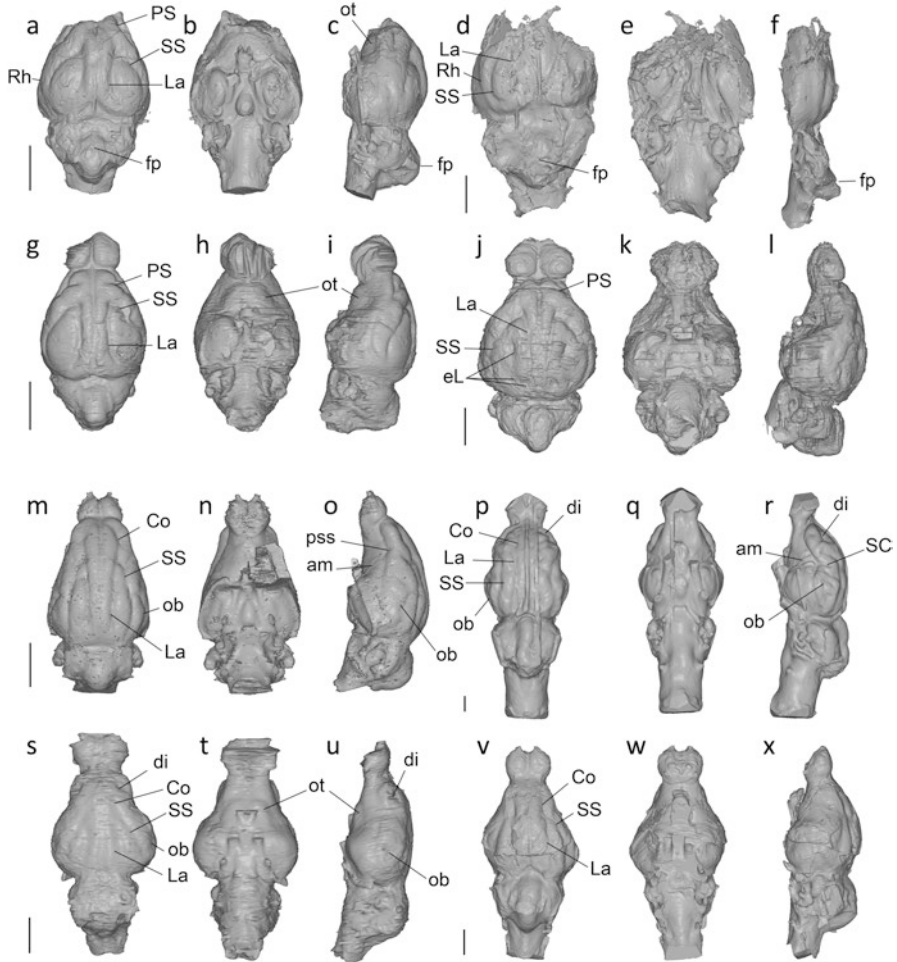


Fig. 13.4 Endocast morphology of extinct artiodactyl clades. a-c, *Homacodon vagans* (AMNH 12695); d-f, *?Helohyus* (AMNH 13079); g-i, *Mouillacitherium elegans* (UM ACQ 6625); j-l, *Dichobune leporina* (MNHN.F.QU16586); m-o, *Caenomeryx filholi* (UM PDS 2570); p-r, *Anoplotherium* sp. (3D surface of plaster cast illustrated by Dechaseaux 1969a, b: Fig. 6); s-t, *Leptauchenia* sp. (AMNH 45508); v-x, *Agriochoerus* sp. (AMNH 95330). 3D models are available in Orliac (2022). Illustrations in dorsal (a, d, g, j, m, p, s, v), ventral (b, e, h, k, n, q, t, w), and lateral (c, f, i, l, o, r, u, x) views. Scale bars = 1 cm

sulcus linking the rhinal fissure, here interpreted as a pseudosylvia, and most probably had partial operculization of the central area, highlighted by the pathway of the middle meningeal artery, partly hidden by the gyrus II (Dechaseaux 1961, 1969a; Fig. 13.4o). Anoplotherioidea exhibit another type of folding pattern. The dacrytherid *Dacrytherium* (Dechaseau 1969a: Fig. 2) is very close to the cainotherioid plan, with elongated lateral sulcus, suprasylvia and coronal sulcus, and also a small oblique sulcus. Anoplotheriidae exhibit more elongated, parallel sulci, and a coro-

Table 13.1 Measurements of the area and volume of the artiodactyls (Endemic European artiodactyls -EEA-, and crown artiodactyls) discussed in the text

	Specimen	Cerebrum surface (mm ²)	Neopallium surface (mm ²)	% neocortical surface	Endocranial volume (cm ³)	Olfactory bulbs volume (cm ³)	% olfactory bulbs volume
<i>Diacodexis ilicis</i>	AMNH 16141	944.02	404.34	42.8	4.70	0.65	13.8
<i>Homacodon vagans</i>	AMNH 12695	1384.93	613.82	44.3	#	#	#
<i>Monillactherium elegans</i> ^{EEA}	UM ACQ 6625	1313.55	567.14	43.2	8.77	0.51	5.8
<i>Dichobune leporina</i> ^{EEA}	MNHN QUI16586	2503.02	1107.44	44.2	7.41	0.57	7.7
<i>Cebochoerus</i> sp. ^{EEA}	MNHN QUI17151	#	#	#	17.20	1.20	7.0
<i>Caenomeryx filholi</i> ^{EEA}	UM PDS 2570	4033.04	2674.96	66.3	8.19	0.30	3.6
<i>Anoplotherium</i> sp. ^{EEA}	MNHN. No number	7173.92	4419.56	61.6	416.09	31.18	7.5
<i>Bathygenys reevesi</i>	TMM 40209-198	#	#	#	14.37	0.46	3.2
<i>Agriochoerus</i> sp.	AMNH 95330	2967.02	1606.20	54.1	33.00	1.64	5.0
<i>Leptauchenia</i> sp.	AMNH 45508	1748.33	909.04	52.0	13.73	0.75	5.5
<i>Palaeochoerus</i> sp.	MHNT_2014_0_3075	4450.78	2462.48	55.3	#	#	#
<i>Tayassu pecari</i>	UM V 79	7744.90	5748.38	74.2	94.86	3.08	3.3
<i>Sus scrofa</i>	TMM M 454	8568.78	6535.22	76.3	130.59	4.88	3.7
<i>Microbunodon minimum</i>	UP LM1967MA300	151057.00	95121.60	63.0	#	#	#
<i>Hippopotamus madagascariensis</i>	MNHT-pal-2012-0-218-1	19054.84	13445.16	70.6	486.90	14.01	2.9
<i>Hippopotamus amphibius</i>	AF RG 78	#	#	#	782.21	24.03	3.1
<i>Choeropsis liberitensis</i>	**	13400.30	9389.46	70.1	359.32	7.73	2.2
<i>Leptomeryx</i> sp.	AMNH 53596	2208.72	1249.59	56.6	17.25	0.89	5.15
<i>Moschiola memmina</i>	UM V 68	2037.02	1252.84	61.5	14.06	0.54	3.86
<i>Moschus chrysogaster</i>	UM N 401	4829.50	3244.68	67.2	51.03	1.58	3.1
<i>Tragelaphus scriptus</i>	AF RG35620	11648.02	9125.36	78.3	169.79	4.28	2.52

The cerebrum surface was measured using the tag tool of MorphoDig (Lebrun 2018) ^{##} volumes for *Choeropsis liberienis* correspond to the mean value of four specimens (AF RG 77-51-M1 . 31723. 35715. 35716); missing data are indicated by a #. Institution abbreviations: *AMNH* American Museum of Natural History, *MNHN* Muséum National d'Histoire Naturelle, Paris, *MHNT* Muséum d'Histoire Naturelle de Toulouse, *AF* Africa Museum, Tervuren, *UM* Université de Montpellier, *UP* Université de Poitiers, *TMM* Texas Memorial Museum

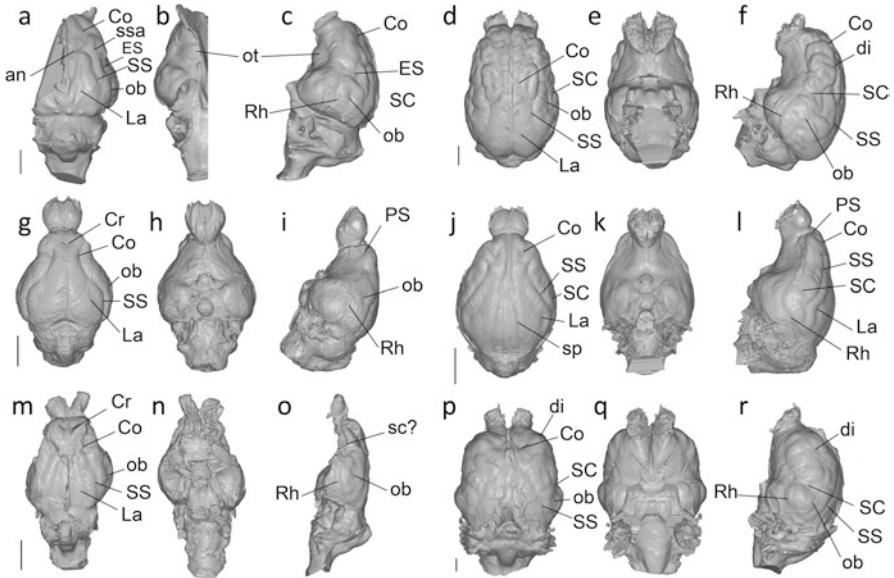


Fig. 13.5 Endocast morphology of crown artiodactyl clades: a-f (top line), Suoidea; g-l (middle line), Ruminantia; m-r (bottom line), Hippopotamoidea with a-c, *Palaeochoerus* sp. (MHNT_2014_0_3075); d-f, *Tajassu pecari* (UM V79); g-i, *Leptomeryx* sp. (AMNH 53596); j-l, *Moschiola memmina* (UM V68); m-o, *Microbunodon minimum* (UP LM1967MA300); p-r, *Choeropsis liberiensis* (MRAC RG 35715). Illustrations in dorsal (a, d, g, j, m, p), ventral (b, e, h, k, n, q), and lateral (c, f, i, l, o, r) views. Scale bars = 1 cm

nal sulcus preferentially linked to the lateral sulcus. *Anoplotherium* presents a complex folding pattern of the neopallium with additional ramifications (Fig. 13.4p, r); an additional sulcus located anterior to the coronal sulcus (“sulcus γ ” of Dechaseaux 1969a) would correspond to a diagonal sulcus according to the nomenclature of Repérant (1971b). *Anoplotherium* shows a clear operculization of the central area, with a deep sylvian complex. The oblique sulcus is sinuous and ramified. The extension of the neopallium on the surface of the cerebral hemispheres of *Dichobune* and *Mouillacitherium* is similar to *Diacodexis* and *Homacodon* (ca. 43%, see Table 13.1), but the paleopallium is not visible in dorsal view for the former (Fig. 13.4g, j). The relative sizes of the neopallium of the Oligocene taxa *Caenomeryx* and *Anoplotherium* is larger than that of other EEA and exceeds 60% (see Table 13.1).

Midbrain Exposure Midbrain exposure varies greatly depending on taxa. Although the exposure is smaller than in early Eocene taxa, the midbrain is exposed in *Cebochoerus* and colliculi are even visible (Dechaseaux 1969a: Fig. 13). Despite a relatively simple folding pattern and general weak extension of the neopallium, the midbrain exposure is small in *Dichobune* (Fig. 13.4g) and *Mouillacitherium* (Fig. 13.4j), *Tapirulus* (Dechaseaux 1969a, b: Fig. 12) and *Mixtotherium* (Dechaseaux 1973: Fig. 3), smaller than in *Diacodexis*, *Homacodon* and *Helohyus*.

The midbrain is not exposed in Cainotheriidae (*Caenomeryx*; Fig. 13.4m) and Anoplotheriidae (*Anoplotherium*; Fig. 13.4p).

Cerebellum Just like in other groups, the cerebellum of EEA has received little attention in the literature. They differ by the folding pattern, size and shape of their vermis (Fig. 13.4). Compared to the size of the cerebrum, the cerebellum is relatively large in Anoplotherioidea where the anterior extension of the vermis reaches that of the cerebellar hemispheres (Dechaseaux 1969a, b: Figs. 2,6,10; Fig. 13.4p). It is relatively smaller in other EEA taxa such as cainotheriids, *Mouillacitherium* or *Dichobune*. In these taxa, the cerebellar hemispheres extend anteriorly to the anterior margin of the vermis, like in early Eocene taxa (Fig. 13.4g, j, m).

Oreodontoidea Endocranial casts of oreodontoids are best illustrated in the literature by the late Eocene oreodontine *Bathygenys reevesi* (Macrini 2009), and by natural endocasts of the early Oligocene merycoidodontine *Merycoidodon culbertsoni* (Leidy 1869:pl. 14, Fig. 11; Black 1920: Fig. 18: specimen IV; Moodie 1922: Fig. 22) and middle Eocene *Merycoidodon gracilis* (Dechaseaux 1961: Fig. 10). We complete here the picture with 3D models of the leptachenine merycoidodontid *Leptauchenia* sp. from Washington County, South Dakota (AMNH-FAM 45508; Fig. 13.4s–u) and of the agriochoerid *Agriochoerus* sp. from Sage Creeck, Chadron Mont. (AMNH- FAM-95330, Late Eocene; Fig. 13.4v–x) (see Orliac and Gilissen 2012: Fig. 3).

Olfactory Bulbs Olfactory bulbs are proportionally smaller than in early artiodactyls described above (values comprised 3.2–5.5%, Table 13.1), but larger than in crown Artiodactyla. Unfortunately, most of the oreodontoid specimens are natural endocasts and the volume of the olfactory bulbs is not provided in their original description.

Cerebral Hemispheres Oreodontoids described in the literature present different degrees of neopallium sulcal complexity, from few sulci arranged in a rectilinear disposition, without ramifications, to complex, ramified, sulci and an operculization of the central area. The simplest pattern illustrated is described in *Bathygenys* which only presents a suprasylvia prolonged by a coronal sulcus, and a lateral sulcus delimiting a gyrus III (Macrini 2009: Fig. 3). A more complex pattern is observed in *Merycoidodon culbertsoni* and *Miniochoerus gracilis* from the middle Oligocene. An ectolateral sulcus divides the gyrus III in *Mi. gracilis* (Dechaseaux 1961: Fig. 10). *Me. culbertsoni* (Black 1920: Fig. 18) presents several ramifications branching on the suprasylvia, including a small sulcus x, originating from the suprasylvia and joining the interhemispheric cleft, and an oblique sulcus located on the lateral margin, posterior to the sylvian complex. We agree with the conclusions of Friant (1939, 1948) and Dechaseaux (1961) that the gyrus I is operculized in those species. Yet, there is no indication of operculization of the central area in *Bathygenys* (see Macrini 2009). A noticeable variability of the neocortical pattern has been described in the literature in *Merycoidon* and *Bathygenys* (Macrini 2009). The vir-

tual endocranial cast of *Leptauchenia* reveals a rather simple cortical pattern with two main sulci, a long oblique suprasylvia/coronal and a small lateral sulcus delimiting a closed gyrus III, and two accessory sulci, an oblic and a diagonal (Fig. 13.4s–u). There is no indication of operculization. The endocranial morphology of Agriocheridae is here documented by *Agriocherus* (Fig. 13.4v–x). It shows a simple sulcal pattern with only a suprasylvia, a coronal sulcus and a lateral sulcus delimiting a closed gyrus III, without accessory sulcus. It is worth noting that in this taxon, the coronal sulcus is in line with the lateral sulcus and not with the suprasylvia. The extension of the neopallium on the surface of the cerebral hemispheres in *Leptauchenia* and *Agriocherus* is more important than in *Diacodexis* and *Homacodon* and exceeds 50% (Table 13.1). The pyriform lobes and the olfactory tubercles are proportionally smaller in oreodontids than in *Diacodexis* (Orliac and Gilissen 2012: Figs. 1c and 2d) and *Homocadon* (Fig. 13.4a).

Midbrain Exposure The posterior development of the neopallium and the transverse sinus cover the midbrain in oreodontoid endocasts.

Cerebellum All oreodontoid taxa show a wide vermis compared to the cerebellar hemispheres. Black (1920: Figs. 9 and 10) illustrated an incredibly well preserved cerebellum of an oreodont from middle Oligocene of the White River group, South Dakota. The different lobules and crura can be identified in great detail. The fissura prima lies rather anteriorly, especially compared to *Bathygenys*, and the exposition of the lobus rostralis on the anterior part of the vermis is reduced compared to *Diacodexis* and *Helohyus*. Details of the vermis structures cannot be observed on the endocasts of *Leptauchenia* and *Agriocherus* (see Fig. 13.4).

The endocranial casts of oreodontoids show a diversity of shape and folding pattern. Our sample is restricted to the Late Eocene/Early Oligocene and it would be very interesting to document endocranial casts of all Merycoidodontidae subfamilies and more recent taxa.

Endocranial Morphology of Crown Artiodactyla Clades

Tylopoda Endocranial casts of the Camelidae are known from the late Eocene to the late Pleistocene. At least one endocast is known from each epoch in this timespan, allowing the observation of a tremendous brain size increase in this lineage (Edinger 1966; Jerison 1971, 2007). Basic qualitative descriptions for this group were made by Edinger (1966).

Olfactory Bulbs Descriptions of relative sizes of different brain regions, particularly of the anterior region and olfactory bulbs, are largely lacking for this group. These structures are missing from the known *Protylopus* endocast. However, if its brain proportions parallel those of Oligocene camelids, olfactory bulbs would have been about 8 mm in length (Edinger 1966).

Cerebral Hemispheres Detailed descriptions of gyrification patterns across multiple fossil taxa and modern camelids were made by Repérant (1970, 1971a, b). The late Eocene *Protylopus* brain is more complex than that of earliest artiodactyls and bears three longitudinal sulci: a corono-suprasylvian sulcus prolonged medially by a short ansate sulcus, a lateral sulcus and an entolateral sulcus (Repérant 1971a). By the Oligocene, in *Poebrotherium*, the suprasylvian sulcus moved toward the midline and developed a descending branch at its anterior end. Lateral and entolateral sulci get close to the sagittal plane as new sulci, ectolateral and the sylvian complex, began to form and move dorsally from the lateral edges of the brain. At this time, the presylvian sulcus is faintly visible in the anterior brain, and the appearance of sulcus “*oblique 1*” begins to define the oblique posterior brain. Operculization is observed in *Poebrotherium* where a long ectosylvia and a short sylvian complex occur (Repérant 1971a: Fig. 2). More sulci developed by the early Pliocene in *Procamelus*, when we observe the greatest expansion of the forebrain. The suprasylvian becomes more complex as its anterior portion couples with the ansate and coronal sulci, forming a branching pattern. All longitudinal sulci continue to move closer to the sagittal plane, as outer sulci develop further, and the rhinal fissure has moved further down the lateral edges of the brain (Repérant 1971a). Operculization is more extended. The main distinction in camelid brain evolution is the pattern of gradual introversion of posterior longitudinal sulci into the sagittal plane, and simultaneous eversion of sulci from the frontal region (Repérant 1971a).

Cerebellum Enlargement of the cerebral hemispheres was paralleled by enlargement of the cerebellum, whereas the vermis becomes less dominant (Edinger 1966). Fine details of cerebellar surface anatomy are scarce in this clade.

Suoidea As mentioned above there is, to our knowledge, no endocast of fossil suoid described in the literature. We document here the endocranial cast of *Palaeochoerus* sp. from an unknown locality in Quercy, France (ancient collections from the Museum d’Histoire Naturelle of Toulouse; MHNT PAL2014.0.3075.1; Fig. 13.5a–c). Given the biochronological repartition of this taxon in Quercy, it is most likely of late Oligocene age. Phylogenetic analyses (Orliac et al. 2010; Orliac 2012) support a basal position of Palaeochoeridae, before the split between Suidae and Tayassuidae.

Olfactory Bulbs The palaeochoerid specimen consists of a partial braincase and unfortunately does not preserve the olfactory bulbs. The small portion preserved indicated that they were of decent size, separated from the cerebral hemispheres by a short circular fissure.

Cerebral Hemispheres The neopallium sulcal complexity of *Palaeochoerus* sp. already strongly recalls that of modern suoids (Fig. 13.5a–c). The lateral sulcus is rather short and close to the interhemispheric fissure, the suprasylvia is prolonged anteriorly by an anterior branch and medially by an ansate sulcus that joins a long coronal sulcus. The later extends anteriorly and bifurcates in its anterior-most por-

tion. On the lateral aspect of the neopallium, there is a clear sylvian complex that forms an open area, letting part of the gyrus I be exposed. There is a short deep oblique sulcus. Contrary to the domestic pig, *Sus scrofa*, there is no trace of a cruciate sulcus (we follow here the identification of Anthony and Grzybowski 1931, and Barone and Bortolami 2004, that the anterior most sulcus in *Sus scrofa* is the anterior prolongation of the splenial; for alternative interpretation see Krueg 1878). The neopalleal pattern of *Palaeochoerus* is closer to that of Tayassuidae that do not seem to present a dorsal exposure of the anterior portion of the splenial sulcus (Saraiva 2017: Figs. 2, 5). The neopallium is widely expanded on the cerebral hemisphere and covers 55% of it, a slightly inferior value compared to *Tayassu* (Table 13.1).

There are wide, salient, olfactory tubercles on the *Palaeochoerus* endocast (Fig. 13.5b–c), just like in modern representatives of the group (Saraiva 2017: Fig. 4; Barone and Bortolami 2004:pl.158).

Midbrain Exposure and Cerebellum In *Palaeochoerus*, the midbrain is not exposed dorsally and the posterior expansion of the neopallium covers the anteriormost part of the vermis and the paramedian lobes. It is also the case in modern Tayassuidae (*Tayassu pecari*, Saraiva 2017: Fig. 7) and Suidae (*Sus scrofa domesticus*, Saikali et al. 2010). The vermis of *Palaeochoerus* is wide relative to the paramedian lobes, and its subdivisions are impossible to identify; the shape of the paramedian lobes is masked by the sinuses surrounding the petrosal region. In modern suoids, the vermis appears smaller than the paramedian lobes (Barone and Bortolami 2004:pl.113; Saraiva 2017).

Knowledge of the endocranial morphology of Suoidea remains highly limited, even for modern taxa. The general morphology of the brain of *Palaeochoerus* indicates an advanced stage of neopalleal expansion (Fig. 13.5a, c), as soon as the lower Oligocene, even if it is less convoluted than that of modern suoids. Its pattern is closer to Tayassuidae than to Suidae.

Ruminantia Compared to their great specific diversity, documentation of ruminant endocasts remains limited, especially for Paleogene times. We briefly describe and illustrate here the endocast of *Leptomeryx* sp. (AMNH 53596; Fig. 13.5g–i) from the Early Oligocene of South Dakota (Brule Formation, Orellan stage). In addition, we report the endocast of the Early Pleistocene cervid *Antifer ensenadensis* (Fontoura et al. 2020).

Olfactory Bulbs The endocast of *Leptomeryx*, earliest Ruminantia from our sample (early Oligocene) presents large olfactory bulbs (Fig. 13.5g–i) compared to modern representatives of the group (Table 13.1). The olfactory bulb chamber, or ethmoidal fossa, is globular and the two bulbs are closely apposed on their whole length. The endocasts of *Dremotherium* (Sigogneau 1968: Fig. 16–18) and of *Amphitragulus*? (Sigogneau 1968: Fig. 28–29) from the late Oligocene–early Miocene of Saint-Gérand-le-Puy show less globular, divergent olfactory bulb chambers. Unfortunately, 3D models of these specimens are not available yet, and the olfactory bulb chamber volume cannot be measured. Regarding olfactory bulb chamber morphology,

Leptomeryx is closer to modern tragulids (e.g. *Moschiola memmina* Fig. 13.5j–l), than to extant or extinct bovids or cervids (for illustrations of the latter see Palombo et al. 2008: Figs. 7–9, 11). The endocast of the cervoid Palaeomerycidae *Aletomeryx* from the late Miocene of Nebraska (Lull 1920) does not preserve the olfactory bulbs portion. As for *Dremotherium* and *Amphitragulus*?, the endocast of the late Miocene giraffid *Samotherium* (Black 1915) also presents set apart, rather slender olfactory bulb chambers. The olfactory lobes of *Antifer ensenadensis* are strongly separated, similar to those of the current cervid species with which they are compared (*Mazama*, *Blastocerus*, *Ozoterus*; Fontoura et al. 2020).

Cerebral Hemispheres Modern Ruminantia show a wide panel of neopalleal pattern from rather simple patterns like in Tragulidae (e.g. *Moschiola memmina* Fig. 13.5j–l; *Hyaemoschus aquaticus* Friant 1939: Fig. 21), to complex, highly convoluted neopallium (e.g. Giraffidae, Bovidae, Cervidae, Friant 1940; Palombo et al. 2008; Graić et al. 2017). The gyrification pattern has been demonstrated to be relevant at a systematic level, between families (Palombo et al. 2008) and within (Oboussier 1979). Regarding the main neopalleal sulci, the early Oligocene *Leptomeryx* shows the simplest pattern with a small, faint, lateral sulcus, and a long suprasylvia prolonged by an anteriorly extended coronal sulcus. A short cruciate and a short oblique sulci are also present, as well as a short presylvia (Fig. 13.5g–i). On the lateral aspect, the rhinal fissure lies fairly high and shows a marked inflexion between the pre- and postsylvia; however, no pseudosylvia, the hallmark of an incipient operculization, is visible. The simple pattern observed in *Leptomeryx* is close to that of modern tragulids (*Moschiola memmina*, Fig. 13.5j–l) that also show a very faint lateral sulcus and a long suprasylvia anteriorly prolonged by the coronal sulcus. However, tragulids show a long dorsal exposure of the splenial sulcus and a clear operculization of the central area with a marked sylvian complex. The neopalleal pattern of the late Oligocene/early Miocene *Amphitragulus*? (Sigogneau 1968: Fig. 28–29) is slightly more complex than that of *Leptomeryx* and shows a long anterior suprasylvia and a diagonal sulcus; pathway of the middle cerebral artery indicates that some part of the ventral margin of the neopallium is operculized. The pattern of *Dremotherium* (Sigogneau 1968: Fig. 16–18), of similar age, is even more complex, with more ramifications and elongation of the diagonal and oblique sulci. Operculization is also more important and the sylvian complex is visible as a deep depression on the surface of the endocast. A complex pattern is also observed in the late Miocene palaeomerycidae *Aletomeryx* (Lull 1920: Fig. 6) where the ansate also seems to be present. Highly complex, branched, neopalleal pattern are observed in late Miocene and plio-pleistocene Bovidae, Giraffidae and Cervidae.

The neopallium of *Leptomeryx* covers ca. 56% of the cerebral hemisphere; this value is slightly inferior to that of the modern tragulid *Moschiola* (Table 13.1). The olfactory tubercles are not salient on ruminant endocasts.

Midbrain Exposure and Cerebellum The midbrain is not exposed in ruminant endocasts documented so far. In *Leptomeryx* the posterior extension of the neopallium abuts the cerebellum and most probably covers part of the paramedian lobes.

The vermis is slender and posterior divisions are visible on the endocast (Fig. 13.5g-i). The vermis is also slender in *Amphitragulus?* (Sigogneau 1968: Fig. 28) and *Dremotherium* (Sigogneau 1968: Fig. 16). In bovids and cervids, the paramedian lobes seem to be smaller in dorsal view, the vermis looking relatively wider in these taxa.

Hippopotamoidea As mentioned above the number of endocasts of fossil hippopotamoids described in the literature remains very limited. Recent data about two phylogenetically distant taxa, the Microbunodontinae *Microbunodon minimum* and the Bothriodontinae *Merycopotamus medioximus* shed some light on important steps in their brain evolution (Thiery and Ducrocq 2015). Again, most of the discussions is focused on the evolution of the neopallium. Regarding modern hippopotamines, some morphological specificities of their endocast are related to modifications of their skull for semiaquatic habits. Indeed, focus has been made on the angle between the two optic nerves (Fig. 13.5q), considered as an indicator of laterally projected, dorsally protruding eyes related to amphibiosis (Anthony 1948; Dechaseaux 1961). Documentation of hippopotamoid endocasts remains very fragmentary and nothing is known prior to the late Oligocene.

Olfactory Bulbs Hippopotaminae present among the smallest relative size of the olfactory bulb chamber of our artiodactyl sample (2–3%; Table 13.1). Compared to other Artiodactyla, olfactory bulbs of modern hippopotamines are separated along their entire length (e.g. pygmy hippopotamus, *Choeropsis liberiensis*, Fig. 13.5p–r). Despite deformations of the fossil specimens, the olfactory bulbs of *Microbunodon* are obviously proportionally larger than that of modern and subfossil hippopotamines (Fig. 13.5m–o).

Cerebral Hemispheres The neopallium of modern hippopotamines is extended on a very large portion of the cerebral hemisphere (Table 13.1). It shows a complex folding pattern (Garrod 1880; Anthony 1948; Pilleri 1962; Butti et al. 2014), with a partial operculization of the gyrus I. Identification of the cortical foldings in *Choeropsis liberiensis* differs slightly depending on the authors (see Friant 1940; Pilleri 1962; Butti et al. 2014). Friant (1940) describes a rather linear organisation of the sulci, and characterizes modern hippos by the presence of a “K lobe” corresponding to a special folding induced by a bifid sylvian complex (Friant 1940: Fig. 2). Instead, Butti et al. (2014) highlight a pattern similar to cetaceans, with a concentric organization of the three main gyri of the lateral aspect (suprasylvian gyrus, ectosylvian gyrus, and perisylvian gyrus) around an almost vertical Sylvian fissure (Butti et al. 2014: 675). Organization of the foldings relative of the Sylvian fissure in *Choeropsis* rather seems to be close to that of *H. amphibius* and we follow here the interpretation of Friant (1940) that main foldings have a mostly longitudinal organization. Our observations indicate that the recording of neopalleal structure on endocasts is quite blunt in *C. liberiensis* (Fig. 13.5p) and *H. madagascariensis* due to meninges thickness and sulci only leaving faint depressions (see Friant 1940: p14, Figs. 4–5). The rhinal fissure is only distinct in its posterior part and the

cleft visible anterior to the rhinal angle corresponds to the pseudosylvia (Fig. 13.5r). Neopalleal structures are almost completely obscured in *H. amphibius*. A complex neopalleal pattern is retrieved on the natural endocast of the “advanced bothriodontine” *Merycopotamus medioximus* with the potential presence of a “K lobe” (Thiery and Ducrocq 2015). The partial preservation of the specimen, however, does not allow for precise description. The microbunodontine *Microbunodon minimum*, phylogenetically more distant from modern hippopotamines than is *Merycopotamus*, shows a much simpler pattern with only two main elongated parallel sulci: a long lateral sulcus and a long corono-sylvia (Thiery and Ducrocq 2015: Fig. 2; Fig. 13.5m–o). Anterior to the coronal sulcus, joining the interhemispheric fissure is a small cruciate sulcus, and, on the lateral aspect, the neopallium shows a shallow oblique sulcus. The specimen is damaged at the level of the rhinal angle making the presence of a Sylvian complex uncertain, the presence of a K lobe seems most unlikely. There is no apparent olfactory tubercles on hippopotamoid endocasts (Fig. 13.5n–o; q–r), even though modern hippopotamines do present large tubercles on the ventral aspect of actual brains (Pilleri 1962: Figs. 2, 4).

Midbrain Exposure and Cerebellum The packing of the posterior part of the cranium in modern hippos drastically impacts the braincase; besides, the presence of wide sinuses dorsal to the cerebellum completely hides the dorsal aspect of the latter. In modern hippopotamuses, the anterior part of the cerebellum is covered dorsally by the posterior extension of the cerebrum (e.g. Garrod 1880: Fig. 2; Butti et al. 2014: Fig. 1). The late Oligocene *Microbunodon minimum* shows no midbrain exposure (Fig. 13.5m). Its vermis is salient and protrudes dorsally above the level of the cerebrum (Fig. 13.5o). The cerebellum is not preserved in *Merycopotamus* and cannot be described.

Cetacea Endocranial morphology of cetaceans is only partly documented back to late Eocene. However, correspondence between the brain size and shape and the endocranial cast is not complete due to the presence of extensive adnexa.

Olfactory Bulbs The brain of modern cetaceans is characterized by a great reduction of the olfactory apparatus (e.g. Edinger 1955; Pihlström 2008; Godfrey et al. 2013; Berta et al. 2014; Kishida et al. 2015), and modifications of the olfactory tract occur in the earliest phase of cetaceans’ history (e.g. Orliac and Thewissen 2021). An elongation of the olfactory tract has been described in archaeocetes (Pakicetidae, Kishida et al. 2015; Remingtonocetidae, Bajpai et al. 2011; Basilosauridae, Edinger 1955; Uhen 2004; Godfrey et al. 2013) and in raellids (Orliac and Thewissen 2021). Regarding Neoceti, early mysticetes present massive, elongated, olfactory peduncles (*Llanocetus*, Mitchell 1989); these peduncles and associated ethmoidal chambers are still present, though relatively small in modern representatives of the group (e.g. *Balaena mysticetus*, Duffield et al. 1992; *Balaenoptera acutorostrata*, Godfrey et al. 2013; *Megaptera novaeangliae*, Hof and Van der Gucht 2007). In early foetal stages of odontocetes, the olfactory bulbs, nerve, and tracts are present, but these structures then degenerate and are completely absent from mature onto-

cete brains (Ridgway 1988; e.g. *Platanista*, Kamiya and Pirlot 1980). The olfactory apparatus is present in archaic odontocetes and has been described in Oligocene taxa (*Simocetus*, Fordyce 2002; USNM 299482, Fig. 5E, platanistoid odontocete, Hoch 2000, Figs. 6–7), in the early Miocene prosqualodontid *Prosqualodon davidi* (Flynn 1948), and in the Miocene *Squalodon* sp. (Dart 1923).

Cerebral Hemispheres Increased neocortical size and complexity is one of the hallmarks of the modern cetacean brain (Marino et al. 2000, 2004, 2007), however, the presence of endocranial vascular networks and other adnexa makes it impossible to access the neopallial pattern of most fossil cetaceans, as evidenced by basilosaurids in which the pattern could not be described (Pilleri 1991). In protocetids and remingtonocetids, the extension of the retia is limited; three faint oblique sulci have been mentioned on a natural endocranial cast of the protocetid *Indocetus* (Bajpai et al. 1996) and a faint one, close to the cerebral midline, is visible on the 3D reconstruction of the endocast of *Remingtonocetus harudiensis* (Bajpai et al. 2011: Fig. 7). The raoellid *Indohyus*, sister taxon to the Cetacea clade, shows a very simple neocortical pattern, limited to two major sulci (suprasylvia and lateral sulcus) plus a small coronal sulcus (Orliac and Thewissen 2021). This pattern is similar to the primitive neocortical pattern retrieved in Eocene terrestrial artiodactyls (see Orliac and Gilissen 2012). Endocasts of extant and extinct Neoceti mainly give access to the overall shape of the cerebral hemispheres and to the cranial vasculature. Some major neocortical sulci might be observed too, such as the Sylvian fissure, and sulci in the anterior portion (Pilleri 1991; Racicot and Colbert 2013; Bisconti et al. 2020), however, the groove pattern cannot be described nor compared with accuracy. The brain-stem flexure is highly pronounced in the modern representatives of Cetacea (Kruger 1966), and they show a concentric organization of the three main gyri of the lateral side of the cortex (suprasylvian gyrus, ectosylvian gyrus, and perisylvian gyrus) around an almost vertical Sylvian fissure. As far as we know, this organization, potentially linked to the highly derived conformation of the cranium of crown cetaceans, is not documented in the earliest archaeocetes (e.g. Dart 1923; Bajpai et al. 1996; Bajpai et al. 2011).

Midbrain Exposure and Cerebellum In modern cetaceans, the caudal extension of the neopallium covers a large part of the cerebellum, both in mysticetes (e.g. *Balaena*, Raghanti et al. 2019: Fig. 1B) and in odontocetes (e.g. *Stenella*, Kamiya and Pirlot 1974:pl.1; *Platanista*, Kamiya and Pirlot 1980: Fig. 10D). Regarding extinct taxa, the midbrain area is impossible to visualize on endocasts of Neoceti and basilosaurids because of the presence of endocranial vascular networks and other adnexa. In archaeocetes, *Indocetus* (Bajpai et al. 1996: Fig. 1C) and *Remingtonocetus* (Bajpai et al. 2011: Fig. 7) have a posteriorly expended neopallium that most probably covers the midbrain and abuts the cerebellum. Compared to archaeocetes, *Indohyus indirae* has a much limited extension of the neopallium and a wide midbrain exposure (Orliac and Thewissen 2021: Fig. 2), greater than in middle and late Eocene endemic European artiodactyls (e.g. *Dichobune*, *Cebochoerus*, Dechaseaux 1961, 1969a; Orliac and Gilissen 2012; Fig. 13.4j–k), and Eocene

North American taxa (e.g. *Agriochoerus*, *Bathxygenys*, Whitmore 1953; Macrini 2009; Orliac and Gilissen 2012; and *Leptauchenia* Fig. 13.4s–u). The brain of modern Cetacea shows a small and narrow vermis compared to the two voluminous, highly convoluted, cerebellar hemispheres (e.g. Ries and Langworthy 1937; Pilleri 1966a, b; Hanson et al. 2013; Bisconti et al. 2020). Regarding archaeocete endocasts, most of the surface of the cerebellum of basilosaurids is covered with a large rete mirabile (e.g. Breathnach 1955; Pilleri 1991; Geisler and Luo 1998; Uhen 2004), making it impossible to accurately observe the relative size of the vermis. The endocasts of *Indocetus* (Bajpai et al. 1996) and *Remingtonocetus* (Bajpai et al. 2011) show no major shift in the proportions of the different elements of the cerebellum compared to other artiodactyl groups, with a wide vermis relative to the plausible representation of the cerebellar hemispheres. *Indohyus* has a relatively large vermis compared to its cerebellar hemispheres (Orliac and Thewissen 2021: Fig. 2), as in earliest artiodactyls, *Diacodexis* (Orliac and Gilissen 2012) or *Dichobune* (Fig. 13.4j).

13.3.2 Space Associated with Cranial Blood Vessels

Mentions of cranial blood vessels in fossil artiodactyls are mostly based on descriptions of the external aspect of the basicranium or on petrosal morphology (e.g. Coombs and Coombs 1982; O’Leary 2010). Works describing endocasts of terrestrial artiodactyls based on intracranial investigations and μ CT-scan data (Merycoidontidae, Macrini 2009; early artiodactyls, Orliac and Gilissen 2012; Hippopotamoidea, Thiery and Ducrocq 2015) do not include detailed descriptions of cranial blood supply beyond mention of the orbito-temporal canal. Studies on endocasts of crown cetacean and their relatives do focus more on circulatory casts and sinuses (e.g. Racicot and Rowe 2014; Bajpai et al. 2011; Orliac and Thewissen 2021), mainly in relation with the presence and extension of the retia mirabilia (“wonderful net”, Slijper 1936; Ridgway et al. 2016).

Modern artiodactyls indeed present a selective brain cooling system (Baker and Hayward 1967) enabling them to lower their brain temperature below their body temperature. This system is mediated by the carotid rete, a subdural arterial meshwork that anatomically and functionally replaces the internal carotid artery (O’Brien 2018). It lies on the basisphenoid roof, slightly posterior to the hypophyseal fossa (O’Brien 2015: Fig. 1; O’Brien and Bourke 2015). The arterial meshwork of the carotid rete is housed within the venous cavernous sinus, a large pool of venous blood that drains from the sphenoparietal and frontal regions of the cerebrum and from the nasal area of the face (O’Brien 2017) and that receives blood that has been evaporatively cooled by the nasal turbinates. This contact between cooled venous blood and the high surface area of the arterial rete enables rapid heat exchange and cooling of the arterial blood destined for the brain. Nearly all modern artiodactyls possess a carotid rete and perform selective brain cooling. However, major arteries supplying the rete are derived from different embryonic aortic arches in the different

artiodactyl families (for review see O'Brien 2018). The results of O'Brien (2020) based on ancestral character reconstructions support that this pattern of variation results from independent evolutionary processes and suggest that different modern artiodactyls groups developed a carotid rete convergently. Unfortunately, presence of a carotid rete cannot be determined using endocasts for most artiodactyls, and the presence of a carotid rete is mostly correlated with the absence of major correlates for the internal carotid artery (O'Brien and Bourke 2015). Bony correlates therefore mostly imply the petrosal morphology or the region close to the petrosal and are best seen on bony material than on endocasts.

The intracranial retia of modern cetaceans greatly differ from that of other artiodactyl groups by their size and position: (i) the rostral arterial rete is more extensive (e.g. McFarland 1979; Vogl and Fisher 1981), (ii) there is a caudal endocranial arterial and venous rete mirabile (in mysticetes only; Breathnach 1955; Pilleri 1991; Melnikov 1997), and (iii) there are various retia in the basicranium and thus a high vascularization of the pneumatic sinuses around the petrosal and the ectotympanic bulla (Fraser and Purves 1960). The presence of these retia widely masks the external morphology of the brain, and therefore greatly impacts the shape of the endocasts of modern cetaceans and in basilosaurids (i.e. Pelagiceti; see Sect. 13.3.1.3). The presence and extension of retia is variable in non-basilosaurid archaeocetes: the protocetid *Indocetus* sp. presents a venous rete, dorsal to the cerebellum, and a caudal rete, medial and dorsomedial to the petrosal (Bajpai et al. 1996:fig. 1A), whereas in the remingtonocetids *Dalanistes ahmedi* (Gingerich et al. 1995) and *Remingtonocetus harudiensis* (Bajpai et al. 2011), a rete also probably fills the region dorsomedial to the petrosals, but there is little evidence of the presence of caudal or rostral rete. The raoellid *Indohyus indirae* has no extensive rostral or lateral retia mirabilia, but an intraosseous space dorsal to the cerebellum might have housed a network of diploic veins and arteries (Orliac and Thewissen 2021: Figs. 3–4) that might represent the first steps of an incipient caudal venous rete mirabile.

13.4 Brain Evolution and Paleobiological Inferences Based on Endocast Morphology

Artiodactyls follow the same broad lines of evolution of the brain as other gyrencephalic mammals, with general increase of the relative size of the brain, and of the size and complexity of the neopallium, from the early Eocene to modern times. Yet, despite a decent number of endocasts description in the literature, the picture of brain evolution at the Artiodactyla scale remains limited and major gaps remain to be filled regarding the earliest history of modern groups such as Suoidea, Hippotamoidea and Cetacea. Besides, quantitative data remain very scanty and the trends described in the following paragraphs are built on a very limited sample and only provide a very first step to understand brain evolution at the Artiodactyla scale.

13.4.1 *Morphological Brain Diversity: General Picture of Brain Evolution in Artiodactyla*

Olfactory Bulbs

Still very few data are available regarding the relative size of the olfactory bulbs in Artiodactyla, or in mammal in general. The data collected for terrestrial artiodactyls (Table 13.1) based on 3D models suggest a general trend toward a reduction of relative olfactory bulb size through time at the Artiodactyla scale (Fig. 13.6a). Morphologically speaking, the earliest artiodactyls show bulbous olfactory chambers, joined on most of their length (Figs. 13.4 and 13.7). The shape of the olfactory chamber is quadrangular in modern taxa and they are separated on most of their length in most extant representatives of modern groups (Figs. 13.5 and 13.7). In the latter, the olfactory chambers appear anteroposteriorly compressed and a large portion of their surface corresponds to the cribriform plate and bears imprints of the foramina for olfactory nerves.

Cetacea show progressive lengthening of the olfactory tract and concurrent reduction of the relative size of the olfactory bulb chamber. Indeed, the nose of cetaceans underwent great modifications as a result of their adaptation to obligate aquatic lifestyle. The raoellid *Indohyus* shows an elongated olfactory tract, with narrow olfactory bulbs and peduncles (Orliac and Thewissen 2021). An elongation of the olfactory tract has also been described in archaeocetes, Pakicetidae (Kishida et al. 2015), Remingtonocetidae (Bajpai et al. 2011), and Basilosauridae (Edinger 1955). This narrowing and lengthening of the olfactory tract might be directly related to modifications of the intertemporal region in early cetaceans and relatives and has been proposed as a synapomorphy of the clade (Orliac and Thewissen 2021: Fig. 5). These authors also suggest that the modification of the postorbital morphology and the concurrent elongation of the olfactory tract would primarily originate from modifications of the masticatory apparatus, related to specialized diet. Neoceti exhibit a reduction of the major olfactory structures (ethmoturbinates, cribriform plate and maxilloturbinates) including olfactory bulbs, with further reductions and subsequent losses within Odontoceti (Berta et al. 2014).

Neopallium Size and Complexity

The representation of a global picture of artiodactyl brain evolution in a rough phylogenetic and temporal context shows that the size of the neopallium relative to other components of the brain shows an increase with time in Artiodactyla in general and within all artiodactyl clades (Table 13.1 and Fig. 13.7). The expansion of the neopallium surface can notably be appreciated through (i) its posterior extend, (ii) its lateral extent and the location of the rhinal fissure on the lateral aspect of the endocast, (iii) the operculization of the central area and the invagination of the external part with increasing neopalleal surface.

Earliest artiodactyls from the early Eocene show the smallest neopallium surface relative to the surface of the cerebral hemisphere (Table 13.1 and Fig. 13.6b), and a concurrent wide midbrain exposure (Fig. 13.7). *Indohyus indirae* from the middle Eocene also shows a widely exposed midbrain and concurrent small neocortex expansion (Orliac and Thewissen 2021), and some middle Eocene European endemic taxa also show small midbrain exposure (Figs. 13.6b and 13.7). All artiodactyls from the Oligocene and on, have extended neopallium and no midbrain exposure. The area of the neopallium relative to the total surface of the cerebral hemisphere shows a trend to increase with time (Table 13.1 and Fig. 13.6b), with the lowest values retrieved in Early Eocene and middle/Late Eocene taxa, and highest values observed for modern taxa. Yet, relatively high values are also found in endemic European Paleogene taxa (Fig. 13.6b) such as the large bodied *Anoplotherium* (Anoplotheriidae; body mass estimate = 150 kg, Hooker 2007) and the small *Caenomeryx* (Cainotheriidae, body mass estimate = 1.5 kg) highlighting that the picture will get more complicated as the data available increase and that independent tempos are to be expected in the various artiodactyl clades. Besides, as soon as operculization occurs, the external surface of the neopallium is necessarily an underestimation of the total neopallial surface, which tempers the relevance of direct comparisons of values.

Earliest artiodactyls exhibit a very simple sulcal pattern of the neopallium with only two sulci, the suprasylvia and the lateral sulcus, converging in their anterior-most part and delimiting an almond-shape gyrus III + presylvia. This simplest pattern, found in early Eocene diacodexeids, homacodontids, and helohyids, is also observed in some middle/late Eocene endemic European taxa (“Dichobunoidea” with *Mouillacitherium* Fig. 13.4g, Amphimerycidae with *Pseudamphimeryx*, *Amphimeryx*, Dechaseaux 1969a: Fig. 17). A slightly more complicated pattern with the addition of a coronal sulcus occurs in middle/late Eocene taxa such as early oreodontoids, some endemic European taxa (*Tapirus*, Orliac and Gilissen 2012; *Cebochoerus*, Dechaseaux 1969a, b: Fig. 13), and the raellid *Indohyus*. Small additional sulci such as ectolaterals (*Dichobune* Fig. 13.4j), diagonal sulcus and/or oblique sulcus (*Leptauchenia* Fig. 13.4j; *Dacrytherium* Dechaseaux 1969a: Fig. 2) also occur in middle/late Eocene taxa. Anoplotheriidae, which include the largest of endemic European taxa, *Anoplotherium*, present, as soon as the late Eocene, a rather complex and extended neopallium with: (i) a longitudinal organization of the coronal sulcus and suprasylvia and additional sulci, (ii) the presence of a sylvian complex, hallmark of an operculization. A growing cortical complexity and diversity is observed in the different artiodactyl clades in the Oligocene, with branched patterns resulting from ramification of the main sulci and from the extension of the anterior part of the suprasylvia (suoids, oreodontids, ruminants, camelids), of the ansate sulcus (suoids, oreodontids, camelids), and of the oblique sulcus (cainotheriids, suoids, oreodontids, ruminants, camelids). Dorsal exposure of the cruciate and splenial sulci is variously present in ruminants, suids and hippopotamoids. Camelids, on the contrary, experience gradual introversion of posterior longitudinal sulci into the sagittal plane, and simultaneous eversion of sulci from the frontal region (Repérant 1971a). The presence of a small neopallium and very simple neopallial

pattern in raellids, sister taxon to Cetacea and therefore lying very high in the Artiodactyla tree, implies that a simple pattern was most probably present at the base of all modern groups and that neopallium complexity arose independently in the different crown clades of artiodactyls. This is consistent with the differences in neopalleal patterns observed today. The overview of neopalleal pattern in Artiodactyla through time highlights their diversity and the relevance of a neocortical pattern blueprint for phylogenetic and taxonomic purpose. The same is true for neopalleal extension and concurrent operculization of part of the central territory. Based on the available sample, operculization seems to be present in all artiodactyl taxa from the Oligocene onward. But the extension of the neopallium in the various artiodactyl clades did not imply the same areas, and operculization occurred independently in all crown clades and in major extinct clades. This is highlighted by the variety of operculization patterns observed, with the Sylvian complex following the rhinal margin plan only (Cainotheriidae), forming an open triangle on the rhinal (Anoplotheriidae), not connecting the rhinal (Hippopotaminae), or with the anterior ectosylvia pointing anteriorly (e.g. ruminants), or posteriorly (e.g. suines).

13.4.2 Brain-Size Evolution and Encephalization Quotient

Encephalization corresponds to the increase in brain size beyond that expected from the allometric brain-body relation (see Jerison 1970, 1973 and 1982 for historical reviews). It is often determined by calculating the residual value for a given species relative to the allometric regression line (Jerison 1985). Specifically, the encephalization quotient (EQ, Jerison 1970) has been defined as the ratio of the observed brain mass over the expected brain mass for a given body mass. The EQ is therefore rather straightforward to interpret; if a species/specimen has a greater brain mass than expected, the ratio is above 1, and if not, the ratio is under 1.

Before going further, a point must be raised. In a large brain a high quotient of encephalization might correspond to the addition of many grams of brain tissue (and a correspondingly large number of brain cells), whereas in a small brain the same quotient of encephalization would correspond to the addition of a comparatively small amount of brain tissue. When comparing species, brain size is often considered as proportional to neural information processing capacity, and the evolution of encephalization as the evolution of an increase in information processing capacity. It would therefore appear that large brains require more tissue than small brains to achieve the same increase in information processing capability. This paradox, raised by H. B. Barlow in Jerison (1985) has not yet been answered satisfactorily and must be kept in mind when interpreting trends in brain size evolution.

The main challenge in calculating the EQ is to estimate the expected brain mass, which is commonly calculated by an allometric formula with defined parameters. The general allometry formula $Y = aX^b$ can be used to calculate an expected brain mass (Y) for a given body mass (X). As a power function, this relationship can be illustrated by plotting the logarithm of the measurement against the logarithm of the

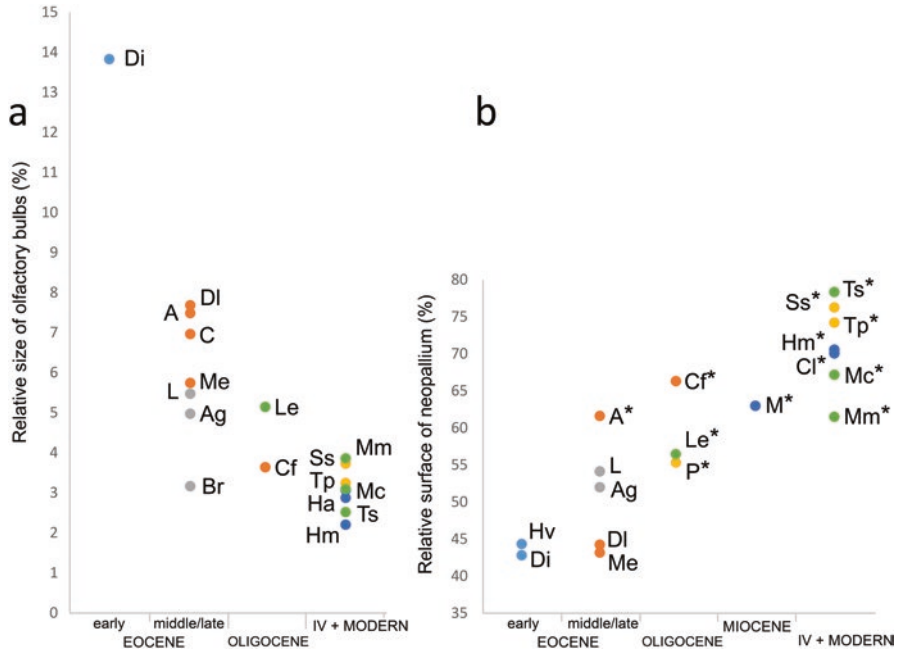


Fig. 13.6 Proportions of olfactory bulbs volume (a) and neopallium area (b) through time, generated on the basis of the data in Table 13.1. Colors: light blue, *Diacodexis*; orange, European Endemic artiodactyls; gray, Oreodontoidea; green, Ruminantia; dark blue, Hippopotamidae; yellow, Suoidea. Asterisks (*) indicate operculized taxa. Time periods abbreviations: *EE* early Eocene, *M/LE* middle /late Eocene, *O* Oligocene, *MI* Miocene, *IV + M* quaternary plus modern. Taxa abbreviations: A *Anoplotherium* sp., Ag *Agriochoerus* sp., Br *Bathygenys reevesi*, C *Cebochoerus* sp., Cf *Caenomeryx filholi*, Cl *Choeropsis liberiensis*, Di *Diacodexis ilitic*, DI *Dichobune leporina*, Ha *Hippopotamus amphibius*, Hm *Hippopotamus madagascariensis*, Hv *Homacodon vagans*, L *Leptauchenia* sp., Le *Leptomeryx* sp., Me *Mouillacatherium elegans*, Mc *Moschus chrysogaster*, M *Microbunodon minimum*, Mm *Moschiola memmina*, P *Palaeochoerus* sp., Ss *Sus scrofa*, Tp *Tayassu pecari*, Ts *Tragelaphus scriptus*

size, thus transforming the previous equation into a linear relationship: $\log(Y) = b \log(X) + \log(a)$.

Authors have used various values for the parameters a and b, and at various scales: some at the class level (e.g. Mammalia, Jerison 1970; Eisenberg and Wilson 1978), others at the order scale (e.g. rodents, Pilleri et al. 1984; primates, Martin 1990). The parameters used are assumed to represent the group of interest (i.e. that they do not vary much within this group); the relevance of parameters a and b therefore depends of the group of interest, and may not be relevant/suitable to another group or scale.

More precise and complex methods often deal with phylogenetic comparative methods (PCM; Cornwell and Nakagawa 2017) but these require a well-supported phylogenetic context. The phylogenetic relationships within Artiodactyla are still debated and if the relationships between crown groups are rather consensual on

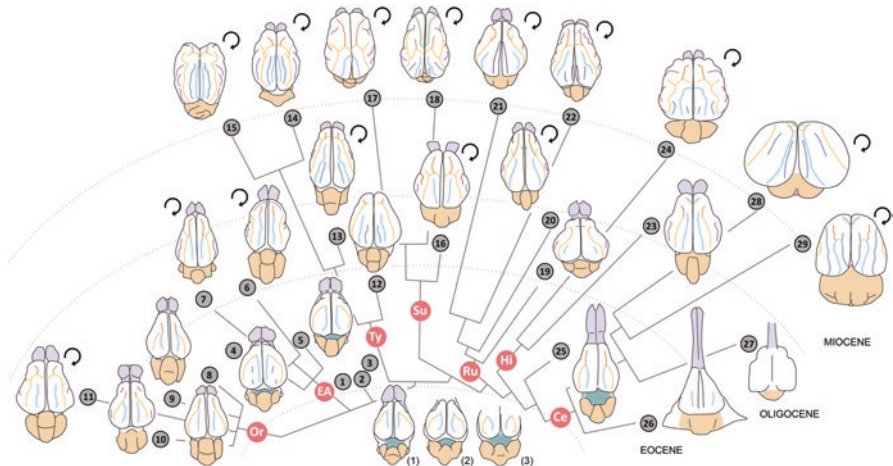


Fig. 13.7 Morphology, phylogenetic relationships and temporal distribution of artiodactyl endocasts and brains. Endocasts and brains are figured in dorsal view, anterior tip (olfactory bulbs) pointing upwards. Taxa: 1, *Diacodexis ilicis* (AMNH 16141); 2, *Homacodon vagans* (AMNH 12695); 3, ?*Helohyus* (AMNH 13079); 4, *Dichobune leporina* (MNHN QU16586); 5, *Mouillacitherium elegans* (UM ACQ 6625); 6, *Anoplotherium* sp. (3D surface of plaster cast illustrated by Dechaseaux 1969a, b: Fig. 6); 7, *Caenomeryx filholi* (UM PDS 2570); 8, *Bathygenys* sp. (after Macrini 2009: Fig. 1); 9, *Agriochoerus* sp. (AMNH 95330); 10, *Leptauchenia* sp. (AMNH 45508); 11, *Merycoidodon culbertsoni* (after Black 1920: Fig. 18); 12, *Protylopus* (after Edinger 1966: Fig. 1 and Repérant 1971a: Fig. 1); 13, *Poebrotherium* (after Repérant 1971a: Fig. 1); 14, *Procamelus* (after Edinger 1966: Fig. 3 and Repérant 1971a: Fig. 1); 15, *Lama glama* (after Repérant 1971b: pl. VIII); 16, *Palaeochoerus* sp. (MHNT_2014_0_3075); 17, *Tajassu pecari* (UM V79); 18, *Sus scrofa* (after Anthony and Grzybowski 1931); 19, *Leptomeryx* sp. (AMNH 53596); 20, *Dremotherium feignouxii* (after Sigogneau 1968); 21, *Moschiola memmina* (UM V68); 22, *Moschus chrysogaster* (UM N401); 23, *Microbunodon minimum* (UP LM1967MA300); 24, *Choeropsis liberiensis* (after Pilleri 1962: Fig. 1); 25, *Indohyus indirae* (NM RR 207); 26, *Remingtonocetus harudiensis* (after Bajpai et al. 2011: Fig. 6); 27, *Xenorophus* sp. (after Marino et al. 2003: Fig. 6C); 28, *Tursiops truncatus* (after Morgane et al. 1990: Fig. 2); 29, *Balaena mysticetus* (after Duffield et al. 1992: Fig. 7B, and Raghanti et al. 2019: Fig. 1C). Color code: light orange, cerebellum; turquoise, midbrain exposure; violet, olfactory bulbs and peduncles; neopal-leal sulci: blue, lateral; orange, coronal; yellow, suprasylvia (+ anterior suprasylvia and ansate for some taxa); green, cruciate; purple, splenial; pink, oblique and diagonal. Turning arrows indicate operculization. Abbreviations: *Ce* Cetacea, *EA* endemic artiodactyls, *Hi* Hippopotamoidea, *Or* Oreodontoidea, *Ru* Ruminantia, *Su* Suoidea, *Ty* Tylopoda. Phylogenetic relationships are based on Hassanin et al. (2012) for crown groups branching, fossil taxa relationships rely on Thewissen et al. (2007) for Cetacea, Geisler et al. (2007) for Tylopoda, Métais and Vislobokava (2007) for Ruminantia, Orliac (2012) for Suoidea, Oreodontoidea and endemic European taxa are here considered as monophyletic groups, relationships within endemic European taxa rely on Weppe et al. (2020a). Not to scale

molecular grounds (Hassanin et al. 2012), the position of extinct taxa is still highly disputed (e.g. Geisler and Theodor 2009). This lack of a clear/robust phylogenetic framework deprives us of the use of phylogenetic comparative methods on residuals at the artiodactylan scale. We therefore use here the EQ to provide (limited) state-of-the-art of the data.

Brain Size in Artiodactyla

To accurately describe the evolution of brain size through time within Artiodactyla, we define and use an empirical EQ formula based on a sample of 113 extant artiodactyl species. Figure 13.8a shows a plot of log (brain mass) against log (body mass) with the regression line based on extant species only. The equation for the regression is $0.6008x - 1.1278$. The expected brain mass equation is thus $0.3237(\text{body mass})^{0.6008}$ and the corresponding EQ formula for Artiodactyla (EQartio) is as follows: observed brain mass / $0.3237(\text{body mass})^{0.6008}$. The previous scaling exponents of Jerison (1970) and of Eisenberg and Wilson (1978) for Mammalia are, respectively, 0.667 and 0.74, which are slightly higher than the scaling exponent of 0.6008 proposed here for artiodactyls. With a lower slope value, a negative allometry between brain and body mass in artiodactyls is thus clear in our study compared to previous works at the Mammalia scale. A striking fact about artiodactylans relative brain size (Fig. 13.8a) is the duality between Cetacea and non-cetacean artiodactyls. Indeed, convex hulls for both groups of extant species do not overlap, and both extant and fossil cetaceans are generally above the regression line of Artiodactyla, while non-cetaceans are below this line. We therefore calculated two separate EQ formulas, one for non-cetacean artiodactyls with $\text{EQ}_{\text{noncet}} = \text{observed brain mass} / 0.3405(\text{body mass})^{0.5603}$, and one for cetacean artiodactyls with $\text{EQ}_{\text{cet}} = \text{observed brain mass} / 16.0007(\text{body mass})^{0.3490}$. Linear models of log(brain mass) relative to log(body mass) for extant species of non-Cetacea and Cetacea reveal a correlation between log(brain mass) and log(body mass) ($p < 2.2 \times 10^{-16}$) and a difference between both groups ($p < 2.2 \times 10^{-16}$ in both tests). Additionally, there is a difference between the slopes of each group over time ($p = 6.053 \times 10^{-7}$ in a t-test of slope comparisons), highlighting a difference in allometry equations between each group (Fig. 13.8a). In a comparable analysis (but using phylogenetic generalized least squares - GLS - regressions), Smaers et al. (2021) also found a lower encephalization slope for cetaceans and a higher encephalization intercept for cetaceans (both odontocetes and delphinids compared to ferungulates). Brain/body mass allometry is more negative in Cetacea (scaling exponent of 0.3490) than in other artiodactyls (scaling exponent of 0.5603, closer to that of the whole order, 0.6008). This does not imply a lower encephalization (their EQ is greater than other artiodactyls, as is their EQ variation; Fig. 13.8b), but may rather results from a massive increase in body mass for this clade (see Montgomery et al. 2013; Fig. 13.8a) and/or may simply reflect the greater homogeneity of Cetacea when compared to other artiodactyls.

Encephalization differences between cetaceans and non-cetacean artiodactyls is even clearer in a temporal framework (Fig. 13.8b). In both groups, there is a significant linear increase in EQ through time until the present ($p = 9.401 \times 10^{-4}$ and $R^2 = 0.13$ in cetaceans, $p < 2.2 \times 10^{-16}$ and $R^2 = 0.58$ in non-cetacean artiodactyls). Cetaceans EQ appears to increase particularly between late Eocene and Oligocene, while the EQ increase in non-cetacean artiodactyls seems to only start in the Oligocene. Moreover, residuals of both regressions are not homoscedastic ($p = 0.00305$ in cetaceans and $p = 0.01022$ in non-cetacean artiodactyls for

Breusch-Pagan tests) and their variance increases through time ($p = 2.669 \times 10^{-3}$ in cetaceans and $p = 9.956 \times 10^{-3}$ in non-cetacean artiodactyls for linear models). This highlights two differing and diachronic patterns of EQ increase for cetacean and non-cetacean artiodactyls during the Cenozoic.

Brain Size in Non-cetacean Artiodactyls

Figure 13.8c illustrates the evolution of EQ in non-cetacean artiodactyls over time, based on the non-cetacean artiodactyl equation. There is a significant difference between EQ values of Paleogene (Eocene-Oligocene), and Neogene (Miocene-Pliocene) and Quaternary non-cetacean artiodactyls ($p < 2.2 \times 10^{-16}$ in a t-test). There are no significant differences between Paleogene modalities in EQ ($p = 0.7104$ in an ANOVA, $p = 0.4122$ in a Kruskal-Wallis test, $p = 0.4212$ in a linear model), translating a stasis in EQ values during Paleogene times, while there is an increase in EQ values from the Oligocene onward supported by differences between each time section ($p = 1.546 \times 10^{-12}$ in an ANOVA, $p = 1.384 \times 10^{-8}$ in a Kruskal-Wallis test, 1.538×10^{-13} in a linear model). There also seems to be an increase in EQ variation during the Neogene and Quaternary, but this is not confirmed by linear models based on squared residuals of each linear model against time ($p = 0.1775$ in ANOVA and $p = 0.5652$ in Kruskal-Wallis test for Paleogene, $p = 0.1258$ and $p = 0.0461$ since Oligocene). The Oligocene Epoch corresponds to the massive appearance of artiodactyl crown groups in the fossil record (except for Cetacea) that progressively replaced stem artiodactyl lineages. Considering EQ variation over time within crown groups, Ruminantia is the only crown group that indubitably shows an increase in EQ ($p = 2.4 \times 10^{-4}$ in an ANOVA, $p = 0.0053$ in a Kruskal-Wallis test, $p = 4 \times 10^{-5}$ in a linear model). EQ increase for Suoidea and Tylopoda, as illustrated in Fig. 13.8c by the median line, is statistically not as well supported as in Ruminantia. Tylopoda shows significant increase according to ANOVA and linear models ($p = 0.0032$ and $p = 2.7 \times 10^{-4}$), while Suoidea do not ($p = 0.0918$). By contrast, Kruskal-Wallis test results are in conflict: Suoidea are significant ($p = 0.0455$), and Tylopoda are not ($p = 0.0687$). Hippopotamoidea EQ seems to remain constant over time ($p = 0.1896$ in ANOVA and linear model, $p = 0.1213$ in a Kruskal-Wallis test). However, EQ increase over time in non-cetacean artiodactyl crown groups (Fig. 13.8c) is based on unbalanced fossil records and has to be interpreted with caution. Further documentation of extinct taxa may change the picture.

Brain Size in Cetacea

Studies relative to brain size evolution in cetaceans describe two major encephalization pulses related to two major events: the onset of odontocetes near the Eocene-Oligocene boundary, and within odontocetes, the differentiation of Delphinoidea (15 Ma; e.g., Marino et al. 2004). Regarding the trends accompanying the early

steps of their evolutionary history, which comprises the transition to a fully aquatic environment, Marino et al. (2004) concluded that there was no significant increase in brain size during archaeocete evolution, ruling out the hypothesis of a correlation between relative brain size increase and aquatic habitats. These conclusions were challenged by Gingerich (2015), based on revised and more robust body mass estimates for archaeocetes but with a smaller sample, who concluded that the relative size of the brain in archaeocetes had doubled between the middle and late Eocene.

Figure 13.8d illustrates EQ variation over time for Archaeoceti, Mysticeti, non-delphinoid Odontoceti, and Delphinoidea, using the EQcet equation. It shows the general EQ increase during the Cenozoic for Cetacea ($p = 3.604 \times 10^{-4}$ in an ANOVA, $p = 3.489 \times 10^{-6}$ and $R^2 = 0.24$ in a linear model) and crown cetaceans (Neoceti; $p = 1.503 \times 10^{-3}$ in an ANOVA, $p = 4.983 \times 10^{-4}$ and $R^2 = 0.15$ in a linear model). In the literature, scaling patterns for these groups are based on other (less specific) formulas or other statistical treatment (e.g. Marino et al. 2004; Montgomery et al. 2013; Gingerich 2015; Serio et al. 2019; McCurry et al. 2021; Smaers et al. 2021). Some results are nonetheless congruent in an increase of cetacean relative brain size (see Serio et al. 2019 and McCurry et al. 2021). It also shows an EQ increase over time in Archaeoceti ($p = 0.01939$ in an ANOVA, $p = 7.693 \times 10^{-3}$ and $R^2 = 0.91$ in a linear model), as supported by Gingerich (2015), but contra Marino et al. (2004), and indicates a very early pulse of encephalization during cetacean evolutionary history. Regression parameters of archaeocetes and neocetes are not significantly different (t-test; $p = 0.2603$ for slope, $p = 0.6329$ for intercept), indicating no special pulse at the onset of Neoceti. Similarly, the encephalization pulse corresponding to the differentiation of odontocetes near the Eocene-Oligocene boundary is not supported here because the t-tests of the archaeocetes vs. odontocete and neocetes vs. odontocete regression parameters as a whole are not significant ($p = 0.1190$ and $p = 0.3859$, and $p = 0.7173$ and $p = 0.5672$ for slope and intercept of each comparison). An EQ increase over time is nevertheless observed in odontocetes as a whole ($p = 4.127 \times 10^{-4}$ in an ANOVA, $p = 1.417 \times 10^{-4}$ and $R^2 = 0.19$ in a linear model).

The differentiation of Delphinoidea (at ca. 15 Ma) is assumed to coincide with an encephalization pulse at the onset of this superfamily (Marino et al. 2004). In our analyses, Delphinoids and non-delphinoid odontocetes are normally distributed groups regarding their EQ ($p = 0.1561$ and $p = 0.075$ in Shapiro-Wilk tests respectively), which has not increased over time ($p = 0.05785$ and $p = 0.3098$ in linear models respectively). The EQ however differ in their means ($p = 1.334 \times 10^{-6}$ in a bilateral t-test, mean EQs are 1.23 and 0.71 respectively) and variance ($p = 9.775 \times 10^{-5}$ in a bilateral F-test, EQ variances are 0.23 and 0.05 respectively). Even though EQ did not increase over time in each odontocete subgroup, delphinoids have a general higher EQ together with a larger EQ range (as seen in Fig. 13.8d). The hypothesis of the initial encephalization pulse at the onset of delphinoids is thus supported, and the increase of EQ over time described at the Odontoceti scale (since Oligocene) might reflect that EQ pulse (since the Miocene). The more thorough analyses of Serio et al. (2019) found the high relative brain mass of odontocetes to be plesiomorphic, meeting partially our results: they found a high

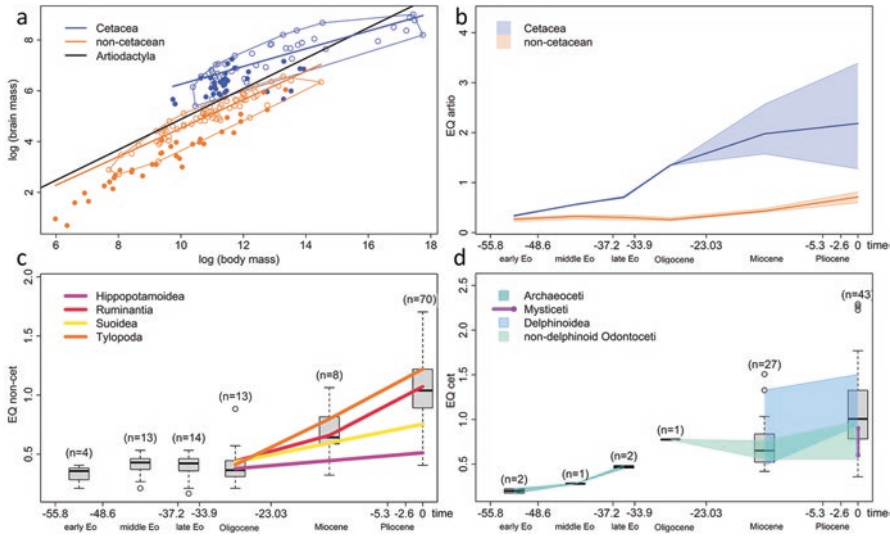


Fig. 13.8 Encephalization within Artiodactyla. **(a)** log brain mass vs log body mass plot in Artiodactyla; empty circles indicate extant taxa, full circles indicate fossil taxa; lines indicate regression lines of extant groups; convex hulls group extant taxa. **(b)** evolution of encephalization through time in Artiodactyla using the EQ ratio; bold central line is the median, thin lateral lines are the quartiles. **(c)** evolution of encephalization through time in non-cetacean artiodactyls using the corresponding EQ formula; colored lines are the median in each non-cetacean crown group; values above the boxes indicate the total number of taxa for the corresponding time section. **(d)** evolution of encephalization through time in cetacean artiodactyls using the corresponding EQ formula; interquartile range is represented by a semi-transparent range in non-mysticete cetaceans and by a segment in mysticetes (due to the absence of fossil values in this group); values above the boxes indicate the total number of taxa for the corresponding time section. Brain and body data for extant non-cetaceans artiodactyls are from Perez-Barberia et al. (2007), Schultz and Dunbar (2010), and Weston and Lister (2009), for fossil non-cetaceans artiodactyls from Jerison (1973), Orliac and Gilissen (2012), Lyras (2018), Thiery and Ducrocq (2015), Radinsky (1978), Berthet (2003), Macrini (2009), Janis (1982), Schultz (2009), and Köhler and Moyà-Solà (2004); data for cetacean mainly come from Marino et al. (2004), and Gingerich (2015). Detailed information about EQ dataset are provided in Supplementary Information

relative brain mass at the onset of odontocetes (as found here), but without increase since (as also found by McCurry et al. 2021). Smaers et al. (2021), using phylogenetic GLS regressions, also found that encephalization increases in mean at the onsets of odontocetes (both body and brain size decreasing, the former faster than the latter), but tightens in variance (variance of brain size diminishing faster than do that of body size). They also found, concurrently to our results, another encephalization increase at the onset of delphinids, both in mean (with decreasing body size and increasing brain size) and in variance (variance of brain size increasing faster than do that of body size). Finally, within Neoceti, EQ values of extant mysticetes do not differ from those of Oligocene odontocetes ($p = 0.8594$ in a t-test and $p = 0.8438$ in a Mann-Whitney test). Of the two clades, the odontocetes are particularly diverse and more frequently documented in the fossil record than mysticetes.

Assuming that Oligocene odontocetes are the closest estimates for ancestral EQ values in Neoceti would imply that EQ did not change during mysticete evolution. As a corollary, non-delphinoid odontocetes and extant mysticetes do not differ in EQ. Based on an EQ formula built solely on cetacean artiodactyls, there would only be two EQ increases/pulses in Cetacean history: a first one during archaeocete evolutionary history (in agreement with Gingerich 2015) and a second one at the onset of delphinoids (in agreement with Marino et al. 2004).

13.5 Future Directions: Outstanding Questions and Perspectives

A long tradition of paleoneurological studies in artiodactyls, based both on rich fossil documentation and solid neontological foundations, provides a substantial body of data to discuss the evolutionary history of brain structures in artiodactyls. μ CT-scan imagery techniques now allow for a detailed investigation of all endocranial structures as well as for quantitative studies of the evolution of the brain components. Yet, the number of these studies remains small and entire sections of Artiodactyla brain history remain undocumented, particularly concerning modern crown groups, especially Hippopotamoidea and Suoidea. Increasing the documentation of extinct and present-day species endocasts, both for qualitative and quantitative perspectives, is now crucial to complete the picture of artiodactyl brain evolutionary history and fully exploit this promising source of data for phylogenetic and palaeoecological reconstructions.

The nomenclature used to describe the artiodactyl neopallium is largely based on the resemblance between the sulcal pattern of present-day artiodactyls and that of the dog, but it is clear that the first artiodactyls have a very different pattern and that the recognition of the different cortical areas is only partially applicable. This is all the more difficult for large clades without extant representatives because (i) following the placement of the sulci during ontogeny is impossible or highly improbable (mainly used to formulate homologies between crown groups), and (ii) some patterns have no equivalent in modern artiodactyls, which themselves most probably have convergent complex patterns. Increasing the documentation of endocasts morphology of extinct representatives of crown artiodactyl clades is necessary to refine homology hypotheses. Finally, the study of the brain of artiodactyls has so far been largely synonymous with the study of their neopallium, but the cerebellum also shows great variation in form and structure and its study will allow for comparing cerebrum and cerebellum evolutionary trajectories.

Regarding quantitative prospects, quantitative works focused on the size of the brain as a whole, notably through EQ calculation, to discuss cognitive abilities (Jerison 1973), or habitat predation intensity (Jerison 1973), or to question the impact of socialization (Schultz and Dunbar 2010; Pérez-Barbería et al. 2007), domestication (e.g. Ballarin et al. 2016; Minervini et al. 2016), or differential

locomotor faculties (Pilleri et al. 1984) on brain size would be needed. Consideration of other quantitative data such as olfactory bulb size, cerebellum size, or neopallial surface will allow for addressing questions relating to species abilities that could be put into perspective with their ecology. Again, the constitution of a large database on modern taxa endocranial casts is necessary to be able to exploit further the data collected on fossils.

13.6 Concluding Remarks

We provide here a very first glance into artiodactyl brain evolutionary history, including Cetacea. The diversity highlighted in this first overview of the external morphology of the brain at the scale of Artiodactyla underlines the potentiality of a “neopallial blueprint” and its relevance at the systematic and phylogenetic level. The inclusion of endocast characters to taxon-character matrices will certainly bring a promising new phylogenetic signal. Yet, our understanding of the setting up of neopallium folding in the different artiodactyl groups is still very partial and at this point, the poor resolution of the phylogenetic relationships at the base of the artiodactyl tree, and small number of endocast of extinct representatives of moderns clades limit our understanding of brain evolution at the order scale. A better resolution of the phylogenetic relationships of Artiodactyla and a substantial increase of quantitative and qualitative data for extinct members of crown clades are now needed in order to take advantage of the increasing quality of data extracted from endocasts and to further exploit endocasts for paleobiological inferences.

Acknowledgments We thank R. Lebrun for the access to scanning facilities (MRI platform member of the national infrastructure France-BioImaging supported by the French National Research Agency [ANR-10-INBS-04, «Investments for the future»], the LabEx CEMEB [ANR-10-LABX-0004] and NUMEV [ANR-10-LABX-0020]). We thank J. Meng and M. O’Leary for their help in accessing to the AMNH collections. We are grateful to G. Thiery and S. Ducrocq (PALEVOPRIM) for granting access to the μ CT scan data of the *Microbunodon minimum* cranium from La Milloque, and to O. Lambert for his help with literature related to cetacean endocasts. This work was, in part, financially supported by the ANR program DEADENDER (ANR-18-CE02-0003-01) headed by M. J. Orliac.

References

- Allanson M (1971) Observations on the pituitary gland of some members of the suborder Suiformes (Mammalia: Artiodactyla). *J Zool* 164:451–461
- Andrew CW (1906) A descriptive catalogue of the Tertiary Vertebrata of Fayum, Egypt. British Museum of Natural History, London
- Angelelli F (1980) Endocranial morphology of the dwarf deer of Crete. *Quaderni dell’Accademia Nazionale dei Lincei* 249:101–109
- Anthony J (1948) Étude de moulages endocranien d’hippopotames disparus. *Mus Nation Hist Nat Paris (NS)* 26:31–56

- Anthony J (1961) Encéphale. Morphologie encéphalique et moulages endocraniens. In: Piveteau J (ed) *Traité de Paleontologie*, VI. Masson, Paris, pp 436–453
- Anthony R, Friant M (1938) Recherches sur le télencéphale des ruminants primitifs. *Le Cainotherium*, Arch Mus Na His Nat, 6e série 15:5–21
- Anthony R, Grzybowski J (1930) Le Neopallium des Équidés: Étude du Développement de ses Plissements. *J Anat* 64:147–169
- Anthony R, Grzybowski J (1931) Le neopallium des suidés: étude de son développement et interprétation de ses plissements. *Arch Zool Exp Gén* 74:1–24
- Anthony R, Grzybowski J (1934) Le Neopallium du Bœuf. Étude de son Développement et Interprétation de ses Plissements. *J Anat* 68:558–570
- Anthony R, Grzybowski J (1936) Le néopallium du mouton—Étude de son développement et interprétation de ses plissements. *J Anat* 71:41–53
- Arnason U, Gullberg A, Gretarsdottir S, Ursing B, Janke A (2000) The mitochondrial genome of the sperm whale and a new molecular reference for estimating eutherian divergence dates. *J Mol Evol* 50:569–578
- Arnason U, Adegoke JA, Bodin K et al (2002) Mammalian mitogenomic relationships and the root of the eutherian tree. *Proc Natl Acad Sci* 99:8151–8156
- Bajpai S, Thewissen JGM, Sahni A (1996) *Indocetus* (Cetacea, Mammalia) endocasts from Kachchh (India). *J Vertebr Paleontol* 6:582–584
- Bajpai S, Thewissen JGM, Conley RW (2011) Cranial anatomy of middle Eocene Remingtonocetus (Cetacea, Mammalia) from Kutch, India. *J Paleontol* 85:703–718
- Baker MA, Hayward JN (1967) Carotid rete and brain temperature of cat. *Nature* 216:139–141
- Balcarcel AM, Veitschegger K, Clauss M et al (2021) Intensive human contact correlates with smaller brains: differential brain size reduction in cattle types. *Proc Roy Soc B* 288:20210813
- Ballarin C, Povinelli M, Granato A et al (2016) The brain of the domestic *Bos taurus*: weight, encephalization and cerebellar quotients, and comparison with other domestic and wild Cetartiodactyla. *PLoS One* 11(4):e0154580
- Barone R, Bortolami R (2004) *Neurologie I: Système nerveux central*. Vigot, Paris
- Berta A, Ekdale EG, Cranford TW (2014) Review of the cetacean nose: form, function, and evolution. *Anat Rec* 297:2205–2215
- Berthet D (2003) Le genre *Cainotherium* (Mammalia, Artiodactyla): étude morphométrique, révision systématique, implications évolutives et paléogéographiques, extinction. *Travaux et Documents des Laboratoires de Géologie de Lyon* 159:3–205
- Bertrand OC, Silcox MT (2016) First virtual endocasts of a fossil rodent: *Ischyromys typus* (Ischyromyidae, Oligocene) and brain evolution in rodents. *J Vert Paleontol* 36(3):e1095762
- Bisconti M, Damarco P, Tartarelli G et al (2020) A natural endocast of an early Miocene odontocete and its implications in cetacean brain evolution. *J Comp Neurol* 529:1198–1227
- Black D (1915) A study of the endocranial casts of *Ocapia*, *Giraffa* and *Samotherium*, with special reference to the convolution pattern in the family Giraffidae. *J Comp Neurol* 25:329–360
- Black D (1920) Studies on endocranial anatomy. II. On the endocranial anatomy of *Oreodon* (Merycoidodon). *J Comp Neurol* 32:271–327
- Boessenecker RW, Perry FA, Geisler JH (2015) Globicephaline whales from the mio-pliocene purisima formation of Central California, USA. *Act Palaeontol Pol* 60:113–122
- Boessenecker RW, Ahmed E, Geisler JH (2017) New records of the dolphin *Albertocetus meffordorum* (Odontoceti: Xenorophidae) from the lower Oligocene of South Carolina: encephalization, sensory anatomy, postcranial morphology, and ontogeny of early odontocetes. *PLoS One* 12(11):e0186476
- Boivin M, Orliac MJ, Antunes MT et al (2018) New material of *Diacodexis* (Mammalia, Artiodactyla) from the early Eocene of Southern Europe. *Geobios* 51:285–306
- Breathnach AS (1955) Observations on endocranial casts of recent and fossil cetaceans. *J Anat* 89:532–546
- Bruce AT (1883) Observations upon the brain casts of tertiary mammals. *Contrib E. M. Mus Geol Archaeol Princeton College* 3:36–45

- Burgin CJ, Colella JP, Kahn PL et al (2018) How many species of mammals are there? *J Mammal* 99:1–14
- Butti C, Fordyce ER, Raghanti AM et al (2014) The cerebral cortex of the pygmy hippopotamus, *Hexaprotodon liberiensis* (Cetartiodactyla, Hippopotamidae): MRI, cytoarchitecture, and neuronal morphology. *Anat Rec* 297:670–700
- Coombs MC, Coombs WP (1982) Anatomy of the ear region of four Eocene artiodactyls, *Gobiohyus*, *?Helohyus*, *Diacodexis* and *Homacodon*. *J Vertebr Paleontol* 2:219–236
- Cope ED (1886) The phylogeny of the Camelidae. *Amer Nat* 20(7):611–624
- Cope ED (1877a) Chapter XII. Fossil of the Loup Fork Epoch. In: Cope ED (ed) Report upon the extinct Vertebrata obtained in New Mexico by parties of the expedition of 1874, pp 1–370
- Cope ED (1877b) On the brain of *Procamelus occidentalis*. *Proc Am Philos Soc* 17:49–52
- Cornwell W, Nakagawa S (2017) Phylogenetic comparative methods. *Curr Biol* 27:R333–R336. <https://doi.org/10.1016/j.cub.2017.03.049>
- Cuvier G (1822) Recherches sur les ossemens fossiles: où l'on rétablit les caractères de plusieurs animaux dont les révolutions du globe ont détruit les espèces. Dufour G et d'Ocagne E, Paris
- Czyżewska T (1988) Natural endocranial casts of the whales *Pinocetus polonicus* Czyżewska and Ryziewicz, 1976, from the Pińczów Limestones (Middle Miocene; southern slopes of the Holy Cross Mountains, Central Poland). *Acta Geol Pol* 38:45–50
- Dal Piaz G (1905) Sugli avanzi di *Cyrtodelphis sulcatus* dell'arenaria di Belluno. *Palaeontographia Ital* 11:253–278
- Dart RA (1923) The brain of the Zeuglodontidae (Cetacea). *Proc Zool Soc London* 42:615–654
- Dechaseaux C (1961) Encéphales d'artiodactyles fossiles. In: Piveteau J (ed) *Traité de Paléontologie*. VI. Masson, Paris, pp 1085–1104
- Dechaseaux C (1962) Cerveaux d'animaux disparus: essai de paléoneurologie, vol 24. Masson, Paris
- Dechaseaux C (1968) Les débuts de l'histoire de la fissuration du néopallium chez les carnivores fissipèdes et chez les artiodactyles. *C R Acad Sci* 266:2320–2323
- Dechaseaux C (1969a) Moulages endocrâniens d'artiodactyles primitifs. Essai sur l'histoire du néopallium. *Ann Paléontol* 60:195–248
- Dechaseaux C (1969b) Les grandes lignes de l'histoire de la fissuration du néopallium des artiodactyles. *C R Acad Sci D* 268:653–655
- Dechaseaux C (1970) Récents résultats en paléoneurologie. *Bulletin trimestriel de l'Académie et de la Société Lorraine des Sciences. Section 17 Paléontologie* 1:223–233
- Dechaseaux C (1973) Essais de paléoneurologie. *Ann Paléontol* 59:115–132
- Dobzhansky T (1937) Genetic nature of species differences. *Am Nat* 71:404–420
- Duffield DW, Haldiman JT, Henk WG (1992) Surface morphology of the forebrain of the bowhead whale, *Balaena mysticetus*. *Mar Mamm Sci* 8:354–378
- Edinger T (1955) Hearing and smell in cetacean history. *Eur Neurol* 129:37–58
- Edinger T (1966) Brains from 40 million years of camelid history. In: Hassler R, Stephan H (eds) *Evolution of the forebrain*. Springer, Boston, MA, pp 153–161
- Eisenberg JF, Wilson DE (1978) Relative brain size and feeding strategies in the Chiroptera. *Evolution* 32:740. <https://doi.org/10.2307/2407489>
- Fitzgerald EM (2010) The morphology and systematics of *Mammalodon colliveri* (Cetacea: Mysticeti), a toothed mysticete from the Oligocene of Australia. *Zool J Linnean Soc* 158:367–476
- Flower WH (1867) On the osteology of the cachalot or sperm-whale (*Physeter macrocephalus*). *Trans Zool Soc London* 6:309–372
- Flynn TT (1948) Description of *Prosqualodon davidi* Flynn, a fossil cetacean from Tasmania. *Trans Zool Soc London* 26:153–197
- Fontoura E, Ferreira JD, Bubadué J et al (2020) Virtual brain endocast of Antifer (Mammalia: Cervidae), an extinct large cervid from South America. *J Morphol* 281:1223–1240
- Fordyce RE (1978) The morphology and systematics of New Zealand fossil Cetacea. PhD Thesis, University of Canterbury

- Fordyce RE (2002) *Simocetus rayi* (Odontoceti: Simocetidae) (new species, new genus, new family), a bizarre new archaic Oligocene dolphin from the eastern North Pacific. In: Emry RJ (ed) Cenozoic mammals of land and sea: tributes to the career of Clayton E. Ray, Smithsonian Contrib Paleobiol. Smithsonian Institution Press, Washington, DC, pp 185–222
- Fordyce RE, Marx FG (2018) Gigantism precedes filter feeding in baleen whale evolution. *Cur Biol* 28:1670–1676.e2
- Fraser FC, Purves PE (1960) Anatomy and function of the cetacean ear. *Proc Roy Soc* 152:62–77
- Friant M (1937) Interprétation du cerveau de l'hippopotame par l'étude d'un stade embryonnaire. *C R Acad Sci* 205:1257–1259
- Friant M (1939) Morphologie, développement et évolution du Cerveau des Ongulés artiodactyles sélénodontes: exposé des recherches originales du Laboratoire d'Anatomie comparée. *Mém Mus Natl Hist Nat* 10:117–188
- Friant M (1940) Le Téléncéphale des Hippopotamidae. *Arch Mus Natl Hist Nat* 6e série 16:35–54
- Friant M (1948) Interprétation du cerveau de l'*Oreodon*. *C R Acad Sci* 227:780–781
- Friant M (1952) Les caractéristiques fondamentales du cerveau des Giraffidae. *C R Acad Sci* 235:978–979
- Garrod AH (1880) On the brain and other parts of the Hippopotamus (*H. amphibius*). *Trans Zool Soc London* 11:11–17
- Gatesy J, Geisler JH, Chang J et al (2013) A phylogenetic blueprint for a modern whale. *Mol Phyl Evol* 66(2):479–506
- Gaudry A (1873) Vertébrés fossiles du Mont Luberon. In: Gaudry A, Fischer P, Tournouër R (eds) Animaux fossiles du Mont Léberon (Vaucluse). F. Savy, Paris, pp 5–112
- Geisler JH (2001) New morphological evidence for the phylogeny of Artiodactyla, Cetacea, and Mesonychidae. *Am Mus Novit* 3344:1–53
- Geisler JH, Luo Z (1998) Relationships of Cetacea to terrestrial ungulates and the evolution of cranial vasculature in Cete. In: Thewissen JGM (ed) The emergence of whales. Plenum Press, New York, pp 163–212
- Geisler JH, Theodor JM (2009) *Hippopotamus* and whale phylogeny. *Nature* 458:E1
- Geisler JH, Uhen MD (2005) Phylogenetic relationships of extinct cetartiodactyls: results of simultaneous analyses of molecular, morphological, and stratigraphic data. *J Mamm Evol* 12:145–160
- Geisler JH, Theodor JM, Uhen MD et al (2007) Phylogenetic relationships of cetaceans to terrestrial artiodactyls. In: Prothero DR, Foss S (eds) The evolution of Artiodactyla. John Hopkins University Press, Baltimore, pp 19–31
- Gentry A, Hooker JJ (1988) The phylogeny of the Artiodactyla. In: Benton MJ (ed) The phylogeny and classification of the tetrapods, vol 2: mammals. Clarendon Press, Oxford, pp 72–235
- Gervais P (1871) Remarques sur l'anatomie des cétacés de la division des balénidés. *Nouv Arch Mus Hist Nat* 7:65–141
- Gervais P (1874) Remarques sur les formes cérébrales propres aux thalassothériens. *J Zool* 3:571–583
- Gervais P (1973) Mémoire sur les formes cérébrales propres à différents groupes de Mammifères. *J Zool* 3:425–469
- Gingerich PD, Gunnell GF (2005) Brain of *Plesiadapis cookei* (Mammalia, Proprimates): surface morphology and encephalization compared to those of Primates and Dermoptera. *Contrib Mus Paleontol, University of Michigan* 31(8):185–195
- Gingerich PD (2010) Cetacea. In: Werdelin L (ed) Cenozoic mammals of Africa. University of California Press, Oakland, pp 873–900
- Gingerich PD (2015) New partial skeleton and relative brain size in the Late Eocene Archaeocete *Zygorhiza kochii* (Mammalia, Cetacea) from the Pachuta Marl of Alabama, with a note on contemporaneous *Pontogeneus brachyspondylus*. *Contrib Mus Paleontol Univ Michigan* 32:161–188

- Gingerich PD, Arif M, Clyde W (1995) New archaeocetes (Mammalia, Cetacea) from the middle Eocene Domanda Formation of the Sulaiman Range, Punjab (Pakistan). *Smithsonian Contrib Mus Paleontol* 2:291–239
- Gingerich PD, Ul-Haq M, Zalmout IS et al (2001) Origin of whales from early artiodactyls: hands and feet of Eocene Protocetidae from Pakistan. *Science* 293:2239–2242
- Glezer II, Jacobs MS, Morgane PJ (1988) Implications of the “initial brain” concept for brain evolution in Cetacea. *Behav Brain Sci* 11:75–89
- Glezer II, Hof PR, Leranth C et al (1993) Calcium-binding protein-containing neuronal populations in mammalian visual cortex: a comparative study in whales, insectivores, bats, rodents, and primates. *Cereb Cortex* 3:249–272
- Godfrey SJ, Geisler J, Fitzgerald EM (2013) On the olfactory anatomy in an archaic whale (Protocetidae, Cetacea) and the minke whale *Balaenoptera acutorostrata* (Balaenopteridae, Cetacea). *Anat Rec* 296:257–272
- Graïc JM, Peruffo A, Ballarin C et al (2017) The brain of the giraffe (*Giraffa camelopardalis*): surface configuration, encephalization quotient, and analysis of the existing literature. *Anat Rec* 300:1502–1511
- Gratiolet P (1859) Sur l'encéphale de *Oreodon gracilis*. *Proc Verb Soc Phil*:52–53
- Hanson A, Grisham W, Sheh C et al (2013) Quantitative examination of the bottlenose dolphin cerebellum. *Anat Rec* 296:1215–1228
- Hassanin A, Delsuc F, Ropiquet A et al (2012) Pattern and timing of diversification of Cetartiodactyla (Mammalia, Laurasiatheria), as revealed by a comprehensive analysis of mitochondrial genomes. *C R Biol* 335:32–50
- Hecht EE, Smaers JB, Dunn WD, Kent M, Preuss TM, Gutman DA (2019) Significant neuroanatomical variation among domestic dog breeds. *J Neurosci* 39(39):7748–7758
- Hoch E (2000) Olfaction in whales: evidence from a young odontocete of the Late Oligocene North Sea. *Hist Biol* 14:67–89
- Hof PR, Van der Gucht E (2007) Structure of the cerebral cortex of the humpback whale, *Megaptera novaeangliae* (Cetacea, Mysticeti, Balaenopteridae). *Anat Rec* 290:1–31
- Hooker JJ (2007) Bipedal browsing adaptations of the unusual Late Eocene–earliest Oligocene tylopod *Anoplotherium* (Artiodactyla, Mammalia). *Zool J Linnean Soc* 151:609–659
- Hürzeler J (1936) Osteologie und odontologie der Caenotheriden. *Abh Schweiz Palaeontol Gesel* 58–59:1–111
- Huxley J (1942) *Evolution. The modern synthesis*. George Allen and Unwin Ltd, London
- Irwin DM, Kocher TD, Wilson AC (1991) Evolution of the cytochrome b gene of mammals. *J Mol Evol* 32:128–144
- Janis C (1982) Evolution of horns in ungulates: ecology and paleoecology. *Biol Rev* 57:261–318. <https://doi.org/10.1111/j.1469-185x.1982.tb00370.x>
- Janis CM, Scott KM, Jacobs LL (1998) *Evolution of Tertiary mammals of North America: volume 1, Terrestrial carnivores, ungulates, and ungulate like mammals*. Cambridge University Press, Cambridge
- Jerison HJ (1970) Brain evolution: new light on old principles. *Science* 170:1224–1225
- Jerison HJ (1971) Quantitative analysis of the evolution of the camelid brain. *Am Nat* 105:227–239
- Jerison HJ (1973) *Evolution of brain and intelligence*. Academic, New York
- Jerison HJ (1982) The evolution of biological intelligence. In: Sternberg RJ (ed) *Handbook of human intelligence*. Cambridge University Press, New York/London, pp 723–791
- Jerison HJ (1985) Animal intelligence and encephalization. *Phil Trans R Soc Lond B* 308:21–35
- Jerison HJ (2007) Chapter 20. How can fossils tell us about the evolution of the neocortex? In: Kaas J (ed) *Evolutionary neuroscience*. Academic Press, Elsevier, pp 497–508
- Kamiya T, Pirlot P (1974) Brain morphogenesis in *Stenella coeruleoalba*. *Sci Rep Whales Res Inst* 26:245–253
- Kamiya T, Pirlot P (1980) Brain organization in *Platanista gangetica*. *Sci Rep Whales Res Inst Tokyo* 32:105–126

- Kazu RS, Maldonado J, Mota B et al (2014) Cellular scaling rules for the brain of Artiodactyla include a highly folded cortex with few neurons. *Front Neuroanat* 8:1–19
- Kishida T, Thewissen JGM, Hayakawa T et al (2015) Aquatic adaptation and the evolution of smell and taste in whales. *Zool Lett* 1:1–10
- Knopf JP, Hof PR, Oelschläger HH (2016) The neocortex of Indian River dolphins (genus *Platanista*): comparative, qualitative and quantitative analysis. *Brain Behav Evol* 88:93–110
- Köhler M, Moyà-Solà S (2004) Reduction of brain and sense organs in the fossil insular bovid *Myotragus*. *Brain Behav Evol* 63:125–140
- Krueg J (1878) Über die Furchung der Grosshirnrinde der Ungulaten. *Z Wiss Zool* 31:297–345
- Kruger L (1966) Specialized features of the cetacean brain. In: Norris K (ed) *Whales, dolphins, and porpoises*. University of California Press, Berkeley, pp 232–254
- Kruska D (1982) Hirngroßenänderungen bei Tylopoden während der Stammesgeschichte und in der Domestikation. *Verh Dtsch Zool Ges* 1982:173–183
- Kruska D (1988) Effects of domestication on brain structure and behavior in mammals. *Hum Evol* 3:473–485
- Lebrun R (2018) MorphoDig, an open-source 3D freeware dedicated to biology. 5th International Palaeontological Congress (IPC5) – the fossil week, p 399
- Leidy J (1869) The extinct mammalian fauna of Dakota and Nebraska, including an account of some allied forms from other localities, together with a synopsis of the mammalian remains of North America. *J Acad Nat Sci Philadelphia* 2(7):1–472
- Lihoreau F, Ducrocq S (2007) Family Anthracotheriidae. In: Prothero DR, Foss SE (eds) *The evolution of artiodactyls*. John Hopkins University Press, Baltimore, pp 89–105
- Lihoreau F, Barry J, Blondel C et al (2004) A new species of Anthracotheriidae, *Merycopotamus medioximus* nov. sp. from the Late Miocene of the Potwar Plateau, Pakistan. *C R Palevol* 3:653–662
- Lihoreau F, Boisserie JR, Manthi FK et al (2015) Hippos stem from the longest sequence of terrestrial cetartiodactyl evolution in Africa. *Nat Commun* 6:1–8
- Luccisano V, Sudre J, Lihoreau F (2020) Revision of the Eocene artiodactyls (Mammalia, Placentalia) from Aumelas and Saint-Martin-de-Londres (Montpellier limestones, Hérault, France) questions the early European artiodactyl radiation. *J Syst Palaeontol* 18:1631–1656
- Luckett WP, Hong N (1998) Phylogenetic relationships between the orders Artiodactyla and Cetacea: a combined assessment of morphological and molecular evidence. *J Mamm Evol* 5:127–182
- Ludtke JA (2007) Family Agriocheridae. In: Prothero DR, Foss SE (eds) *The evolution of artiodactyls*. John Hopkins University Press, Baltimore, pp 151–156
- Lull RS (1920) New tertiary artiodactyls. *Am J Sci* 4:83–130
- Lyras GA (2018) Brain changes during phyletic dwarfing in elephants and hippos. *Brain Behav Evol* 92:167–181. <https://doi.org/10.1159/000497268>
- Macrini TE (2009) Description of a digital cranial endocast of *Bathygenys reevesi* (Merycoidodontidae; Oreodontoidea) and implications for apomorphy-based diagnosis of isolated, natural endocasts. *J Vert Paleontol* 29:1199–1211
- Marino L (1998) A comparison of encephalization between odontocete cetaceans and anthropoid primates. *Brain Behav Evol* 51:230–238
- Marino L (2002) Convergence of complex cognitive abilities in cetaceans and primates. *Brain Behav Evol* 59:21–32
- Marino L, Uhen MD, Frohlich B et al (2000) Endocranial volume of mid-late Eocene archaeocetes (Order: Cetacea) revealed by computed tomography: implications for cetacean brain evolution. *J Mamm Evol* 7:81–94
- Marino L, Uhen MD, Pyenson ND et al (2003) Reconstructing cetacean brain evolution using computed tomography. *Anat Rec* 272:107–117
- Marino L, McShea DW, Uhen MD (2004) Origin and evolution of large brains in toothed whales. *Anat Rec A* 281:1247–1255

- Marino L, Connor RC, Fordyce RE et al (2007) Cetaceans have complex brains for complex cognition. *PLoS Biol* 5(5):e139
- Marples BJ (1949) Two endocranial casts of cetaceans from the Oligocene of New Zealand. *Am J Sci* 247:462–471
- Marsh OC (1886) *Dinocerata: a monograph of an extinct order of gigantic mammals* (Vol. 10). Govt. print. Off., 243 p
- Martin RD (ed) (1990) *Primate origins and evolution: a phylogenetic reconstruction*. Chapman and Hall, London
- Martinez JN, Sudre J (1995) The astragalus of Paleogene artiodactyls: comparative morphology, variability and prediction of body mass. *Lethaia* 28:197–209
- Marx FG, Lambert O, Uhen MD (2016) Cetacean Paleobiology. In: Schoch RR (ed) *Amphibian evolution, the life of early land vertebrates*. Wiley, Chichester, pp 276–345
- Marx FG, Post K, Bosselaers M et al (2019) A large Late Miocene cetotheriid (Cetacea, Mysticeti) from the Netherlands clarifies the status of *Tranatocetidae*. *Peer J* 7:e6426
- Mayer E (1942) *Systematics and the origin of species, from the viewpoint of a zoologist*. Columbia University Press, New York
- McCurry MR, Marx FG, Evans AR et al (2021) Brain size evolution in whales and dolphins: new data from fossil mysticetes. *Biol J Linn Soc*:1–9. <https://doi.org/10.1093/biolinnean/blab054>
- McFarland WL (1979) Blood supply to the brain of the dolphin *Tursiops truncatus*, with comparative observations on special aspects of the cerebrovascular supply of other vertebrates. *Neurosci Behav Rev* 3:1–93
- Mchedlidze GA (1988) *Fossil cetacea of the caucasus*. Smithsonian Institution Libraries and National Science Foundation, Washington, DC
- Melnikov VV (1997) The arterial system of the sperm whale (*Physeter macrocephalus*). *J Morphol* 234:37–50
- Métais G, Vislobokava I (2007) Basal ruminants. In: Prothero DR, Foss SE (eds) *The evolution of artiodactyls*. John Hopkins University Press, Baltimore, pp 189–212
- Milne-Edwards A (1864) *Recherches anatomiques, zoologiques et paléontologiques sur la famille des chevrotains*. *Ann Sci Nat* 2:49–167
- Minervini S, Accogli G, Pirone A et al (2016) Brain mass and encephalization quotients in the domestic industrial pig (*Sus scrofa*). *PLoS One* 11(6):e0157378
- Mitchell ED (1989) A new cetacean from the late Eocene La Meseta formation Seymour Island, Antarctic peninsula. *Can J Fish Aqua Sci* 46:2219–2235
- Miyamoto M, Goodmann M (1986) Biomolecular systematics of eutherian mammals: phylogenetic patterns and classifications. *Syst Zool* 35:230–240
- Montgelard C, Catzeflis FM, Douzery E (1997) Phylogenetic relationships of artiodactyls and cetaceans as deduced from the comparison of cytochrome b and 12S rRNA mitochondrial sequences. *Mol Biol Evol* 14:550–559
- Montgomery SH, Geisler JH, McGowen MR et al (2013) The evolutionary history of cetacean brain and body size. *Evolution (NY)* 67:3339–3353. <https://doi.org/10.1111/evo.12197>
- Moodie RL (1915) A new fish brain from the Coal Measures of Kansas, with a review of other fossil brains. *J Comp Neurol* 25:135–131
- Moodie RL (1916) On the sinus paranasales of two early Tertiary mammals. *J Morphol* 28:135–144
- Moodie RL (1922) On the endocranial anatomy of some Oligocene and Pleistocene mammals. *J Comp Neurol* 34:343–379
- Morgane PJ, Glezer II, Jacobs MS (1988) Visual cortex of the dolphin: an image analysis study. *J Comp Neurol* 273:3–25
- Morgane PJ, Glezer II, Jacobs MS (1990) Comparative and Evolutionary Anatomy of the Visual Cortex of the Dolphin. In: Jones EG, Peters A (eds) *Cerebral Cortex*. Springer, Boston, MA, pp 215–262
- Muizon C (1988) Le polyphylétisme des Acrodelphidae, odontocètes longirostres du Miocène européen. *Bull Mus Natl Hist Nat* 10:31–88

- Nummela AS, Hussain ST, Thewissen JGM (2006) Cranial anatomy of Pakicetidae (Cetacea, Mammalia). *J Vertebr Paleontol* 26:746–759
- O'Brien HD (2015) Cranial arterial pattern of the Sri Lankan spotted chevrotain, *Moschiola memmina*, and comparative basicranial osteology of the Tragulidae. *Peer J* 3:e1451
- O'Brien HD (2018) Augmenting trait-dependent diversification estimations with fossil evidence: a case study using osmoregulatory neurovasculature. *Brain Behav Evol* 91:148–157
- O'Brien HD, Bourke J (2015) Physical and computational fluid dynamics models for the hemodynamics of the artiodactyl carotid rete. *J Theor Biol* 386:122–131
- Oboussier H (1979) Evolution of the brain and phylogenetic development of African Bovidae. *Afric Zool* 14:119–124
- O'Brien HD (2017) Cranial arterial patterns of the alpaca (Camelidae: *Vicugna pacos*). *R Soc Open Sci* 4:160967
- O'Brien HD (2020) From anomalous arteries to selective brain cooling: parallel evolution of the artiodactyl carotid rete. *Anat Rec* 303:308–317
- O'Leary MA (2010) An anatomical and phylogenetic study of the osteology of the petrosal of extant and extinct artiodactylans (Mammalia) and relatives. *Bull Am Mus Nat Hist* 335:1–206
- O'Leary MA, Gatesy J (2008) Impact of increased character sampling on the phylogeny of Cetartiodactyla (Mammalia): combined analysis including fossils. *Cladistics* 24:397–442
- Orliac MJ (2012) Osteology of the petrosal bone of Suoidea (Artiodactyla, Mammalia). *J Syst Palaeontol* 37:765–779
- Orliac MJ (2022) 3D models associated to Paleoneurology of Artiodactyla, a general picture of artiodactyl brain evolution. *MorphoMuseuM*. 180. <https://doi.org/10.18563/journal.m3.180>
- Orliac MJ, Gilissen E (2012) Virtual endocranial cast of earliest Eocene Diacodexis (Artiodactyla, Mammalia) and morphological diversity of early artiodactyl brains. *Proc R Soc B* 279:3670–3677
- Orliac MJ, Thewissen JGM (2021) The endocranial cast of *Indohyus* (Artiodactyla, Raoellidae): the origin of the cetacean brain. *J Mamm Evol* 28:831–843
- Orliac MJ, Antoine PO, Ducrocq S (2010) Phylogenetic relationships of the Suidae (Mammalia, Cetartiodactyla): new insights on the relationships within Suoidea. *Zool Script* 39:315–330
- Owen R (1848) Description of teeth and portions of jaw of two extinct anthracotheriid quadrupeds (*Hyopotamus vectianus* and *Hyop. bovinus*) discovered by the Marchioness of Hastings in the Eocene deposits of the N.W. coast of the Isle of Wight: with an at. Q. *J Geol Soc Lond* 4:103–141
- Palombo MR, Kohler M, Sola SM et al (2008) Brain versus body mass in endemic ruminant artiodactyls: a case studied of *Myotragus balearicus* and smallest *Candiacervus* species from Mediterranean Islands. *Quat Int* 182:160–183
- Parona CF (1923) Fossili rari. *Natura* 14:127–129
- Pérez-Barbería FJ, Shultz S, Dunbar RIM (2007) Evidence for coevolution of sociality and relative brain size in three orders of mammals. *Evolution* 61(12):2811–2821. <https://doi.org/10.1111/j.1558-5646.2007.00229.x>
- Pihlström H (2008) Comparative anatomy and physiology of chemical senses in aquatic mammals. In: Thewissen JGM, Nummela S (eds) *Sensory evolution on the threshold*. University of California Press, Berkeley, pp 95–110
- Pilleri G (1962) Zur Anatomie des Gehirnes von *Choeropsis liberiensis* Morton (Mammalia, Artiodactyla). *Act Zool* 43:229–245
- Pilleri G (1966a) Morphology of the brain of the Sei whale, *Balaenoptera borealis* lesson (Cetacea, Mysticeti, Balaenopteridae). *J Hirnforsch* 8:221–267
- Pilleri G (1966b) Über die Anatomie des Gehirns des Ganges Delphins, *Platanista gangetica*. *Rev Suisse Zool* 73:113–118
- Pilleri G (1991) Betrachtungen über das Gehirn der Archaeoceti (Mammalia, Cetacea) aus dem Fayum Ägyptens. *Investigations on Cetacea* 23:193–211
- Pilleri D, Gahr M (1982) Das Zentralnervensystem der Zahn und Bartenwale. *Rev Suisse Zool* 76:995–1037

- Pilleri G, Gihl M, Kraus C (1984) Cephalization in rodents with particular reference to the Canadian beaver (*Castor canadensis*). In: Pilleri G (ed) Investigations on beavers. Brain Anatomy Institute, Bern, pp 11–102
- Pledge NS (2005) A new species of early Oligocene cetacean from Port Willunga, South Australia. *Mem Queensl Mus* 51:123–133
- Prothero DR (1994) The late Eocene-Oligocene extinctions. *Annu Rev Earth Planet Sci* 22:145–165
- Prothero DR, Foss SE (2007) The evolution of artiodactyls. The Johns Hopkins University Press, Baltimore
- Prothero DR, Sanchez F (2008) Systematics of the leptauchenine oreodonts (Mammalia: Artiodactyla) from the Oligocene and earliest Miocene of North America. In: Lucas SG, Morgan GS, Spielmann JA, Prothero DR (eds) Neogene Mammals. New Mexico Museum of Natural History and Science, Albuquerque, pp 335–356
- Racicot RA, Colbert MW (2013) Morphology and variation in porpoise (Cetacea: Phocoenidae) cranial endocasts. *Anat Rec* 296:979–992
- Racicot RA, Rowe T (2014) Endocranial anatomy of a new fossil porpoise (Odontoceti, Phocoenidae) from the Pliocene San Diego Formation of California. *J Paleontol* 88:652–663
- Racicot RA, Darroch SA, Kohno N (2018) Neuroanatomy and inner ear labyrinths of the narwhal, *Monodon monoceros*, and beluga, *Delphinapterus leucas* (Cetacea: Monodontidae). *J Anat* 233:421–439
- Radinsky L (1978) Evolution of brain size in carnivores and ungulates. *Am Nat* 112:815–831. <https://doi.org/10.1086/283325>
- Radinsky LB (1987) The evolution of vertebrate design. University of Chicago Press, Chicago
- Raghanti MA, Wicinski B, Meierovich R et al (2019) A comparison of the cortical structure of the bowhead whale (*Balaena mysticetus*), a basal mysticete, with other cetaceans. *Anat Rec* 302:745–760
- Repérant J (1970) Moulages endocrâniens de tyloposes fossiles. *Ann Paléontol* 56:111–145
- Repérant J (1971a) Les grandes lignes de l'histoire de la gyrencéphalisation chez les Caméliés. *Mammalia* 35:658–665
- Repérant J (1971b) Morphologie comparée de l'encéphale et du moulage endocrânien chez les Tyloposes actuels (Mammifères, Artiodactyles). *Bull Mus Natl Hist Nat* 4:185–321
- Ridgway SH (1988) The cetacean central nervous system. In: Adelman G (ed) Comparative neuroscience and neurobiology. Readings from the encyclopedia of neuroscience. Birkhäuser, Boston, pp 20–25
- Ridgway SH, Carlin KP, Van Alstyne KR et al (2016) Comparison of dolphins' body and brain measurements with four other groups of cetaceans reveals great diversity. *Brain Behav Evol* 88:235–257
- Ries FA, Langworthy OR (1937) A study of the surface structure of the brain of the whale (*Balaenoptera physalus* and *Physeter catodon*). *J Comp Neurol* 68:1–47
- Rose KD (1996) On the origin of the order Artiodactyla. *Proc Natl Acad Sci* 93:1705–1709
- Rose KD, Chew AE, Dunn RH et al (2012) Earliest Eocene mammalian fauna from the Paleocene-Eocene thermal maximum at Sand Creek Divide, southern Bighorn Basin, Wyoming. *Pap Paleontol* 36:1–122
- Saikali S, Meurice P, Sauleau P et al (2010) A three-dimensional digital segmented and deformable brain atlas of the domestic pig. *J Neurosci Met* 192:102–109
- Saraiva J (2017) Macroscópia do encéfalo de catetos (*Pecari tajacu*, Linnaeus, 1758). PhD Thesis, Universidade Federal Rural do Semi-Árido (UFERSA)
- Schaeffer B (1947) Note on the origin and function of the artiodactyl tarsus. *Am Mus Novit* 1356:1–24
- Schultz WA (2009) Body size evolution in *Leptomeryx* and Rhinocerotinae (*Subhyracodon* and *Trigonias*) across the Eocene-Oligocene (Chadronian-Orellan) boundary. MSc Thesis, University of Colorado
- Schultz S, Dunbar R (2010) Encephalization is not a universal macroevolutionary phenomenon in mammals but is associated with sociality. *Proc Natl Acad Sci* 107:21582–21586

- Scott WB (1899) The Mammalia of the Uinta Formation. Part I. The geological and faunal relations of the Uinta Formation. Part II. The Creodonts, Rodentia, and Artiodactyla. *Trans Amer Philos Soc* 16:462–504. (462–470, 479–504)
- Scott WB, Jepsen GL (1940) The mammalian fauna of the White River Oligocene. Part IV. Artiodactyla. *Trans Am Phil Soc* 28:363–746
- Serio C, Castiglione S, Tesone G et al (2019) Macroevolution of toothed whales exceptional relative brain size. *Evol Biol* 46:332–342. <https://doi.org/10.1007/s11692-019-09485-7>
- Sigogneau D (1959) Contribution à l'étude du télencéphale des «elaphoïdes» (Elaphoidea Frechkop 1948). *Mammalia* 23:477–541
- Sigogneau D (1968) Le genre *Dremotherium* (Cervoidea): anatomie du crâne, denture et moulage endocranien. *Ann Paléontol* 54:39–100
- Sigogneau-Russell D, Russell DE (1983) A new dichobunoid artiodactyl (Mammalia) from the Eocene of North-West Pakistan—III reconstitution du moulage endocrânien. *Proc K Ned Akad B Phys* 3:319–330
- Silcox MT, Benham AE, Bloch JI (2010) Endocasts of *Microsypops* (Microsypopidae, Primates) and the evolution of the brain in primitive primates. *J Hum Evol* 58:505–521
- Simpson GG (1944) *Tempo and mode in evolution*. Columbia University Press, New York
- Slijper EJ (1936) Die Cetaceen. Vergleichend-anatomisch und systematisch. *Capita Zool* 6–7:1–590
- Smaers JB, Rothman RS, Hudson DR et al (2021) The evolution of mammalian brain size. *Sci Adv* 7:eabe2101. <https://doi.org/10.1126/sciadv.abe2101>
- Smith GE (1902) On the homologies of the cerebral sulci. *J Anat Physiol* 36:309–319
- Smith GE (1903) The brain of the Archaeoceti. *Proc R Soc London* 71:322–331
- Spaulding M, O'Leary MA, Gatesy J (2009) Relationships of Cetacea (Artiodactyla) among mammals: increased taxon sampling alters interpretations of key fossils and character evolution. *PLoS One* 4(9):1–14
- Stebbins CL Jr (1950) *Variation and evolution in plants*. Columbia University Press, New York
- Stefaniak K (1993) Natural endocranial cast of a delphinid (Cetacea, Delphinidae) from the Pińczów limestones (middle Miocene; Holy Cross Mountains, Central Poland). *Act Geol Pol* 43:115–120
- Stevens MS, Steven JB (2007) The family Mericoiodontidae in: Prothero DR, Foss SE (eds) *the evolution of artiodactyls*. The Johns Hopkins University Press, Baltimore, pp 158–168
- Strobel P (1881) Iconografia comparata delle ossa fossili del gabinetto di storia naturale dell'Università di Parma Fascicolo I Balenopteridae (Cetoterio e Megattera?). Battei, Parma
- Stromer E (1903) *Zeuglodon*-reste aus dem Oberen Mitteleocan des Fajum. *Beit Palaontol Geol Osterreich-Ungarns und des Orients* 15:65–100
- Theodor JM, Erfurt J, Métais G (2007) The earliest artiodactyls: Diacodexidae, Dichobunidae, Homacodontidae, Leptochoeridae, and Raoellidae. In: Prothero DR, Foss SE (eds) *The evolution of artiodactyls*. The Johns Hopkins University Press, Baltimore, pp 32–58
- Thewissen JGM, Hussain ST (1990) Postcranial osteology of the most primitive artiodactyl: *Diacodexis pakistanensis* (Dichobunidae). *Anat Histol Embryol* 19:37–48
- Thewissen JG, Madar SI (1999) Ankle morphology of the earliest cetaceans and its implications for the phylogenetic relations among ungulates. *Syst Biol*:4821–4830
- Thewissen JG, Williams EM, Roe LJ et al (2001) Skeletons of terrestrial cetaceans and the relationship of whales to artiodactyls. *Nature* 413:277
- Thewissen JGM, Cooper LN, Clementz MT et al (2007) Whales originated from aquatic artiodactyls in the Eocene epoch of India. *Nature* 450:1190–1194
- Thiery G, Ducrocq S (2015) Endocasts and brain evolution in Anthracotheriidae (Artiodactyla, Hippopotamoidea). *J Anat* 227:277–285
- Thorpe MR (1931) Natural brain casts of merycoidodonts. *Am J Sci* 21:13–203
- Thorpe MR (1937) The Merycoidodontidae: an extinct group of ruminant mammals. *Mem Peabody Mus Nat Hist* 3:1–428

- Uhen MD (1998) Middle to late Eocene Basilosaurines and Dorudontines. In: Thewissen JGM (ed) The emergence of whales: evolutionary patterns in the origin of Cetacea. Plenum Press, New York, pp 29–61
- Uhen MD (2004) Form, function, and anatomy of *Dorudon atrox* (Mammalia, Cetacea): an archaeocete from the middle to late Eocene of Egypt. *Pap Paleontol* 34:1–222
- Uhen MD (2007) Evolution of marine mammals: back to the sea after 300 million years. *Anat Rec* 290:514–522
- Vogl AW, Fisher HD (1981) Arterial circulation of the spinal cord and brain in the Monodontidae (order cetacea). *J Morphol* 170:171–180
- Welker W (1990) Why does cerebral cortex fissure and fold? In: Jones EG, Peters A (eds) Cerebral cortex, Comparative structure and evolution of cerebral cortex, Part II, vol 8B. Springer, Boston, pp 3–136
- Weppe R, Blondel C, Vianey-Liaud M et al (2020a) Cainotheriidae (Mammalia, Artiodactyla) from Dams (Quercy, SW France): phylogenetic relationships and evolution around the Eocene–Oligocene transition (MP19–MP21). *J Syst Palaeontol* 18:541–572
- Weppe R, Blondel C, Vianey-Liaud M et al (2020b) A new Cainotherioidea (Mammalia, Artiodactyla) from Palembert (Quercy, SW France): phylogenetic relationships and evolutionary history of the dental pattern of Cainotheriidae. *Palaeontol Electron* 23(3):a54
- Weston EM, Lister AM (2009) Insular dwarfism in hippos and a model for brain size reduction in *Homo floresiensis*. *Nature* 459:85–88. <https://doi.org/10.1038/nature07922>
- Whitmore F (1953) Cranial morphology of some Oligocene Artiodactyla. *US Geol Surv Prof Pap* 243:117–159
- Williams EM (1998) Synopsis of the earliest cetaceans pakicetidae, ambulocetidae, remingtonocetidae, and protocetidae. In: Thewissen JGM (ed) The emergence of whales. Plenum Press, New York/London, pp 1–28
- Wilson JA (1971) Early tertiary vertebrate faunas, vieja group, trans-pecos, texas: Agriocoeuridae and Merycoidodontidae. *Bull Texas Mem Mus* 18:1–83
- Zeder MA (2012) The domestication of animals. *J Anthropol Res* 68:161–190

Chapter 14

Evolution of the Brain and Sensory Structures in Sirenia



Thomas E. Macrini and Johanset Orihuela

14.1 Sirenian Biogeography, Fossil Record, and Phylogenetic Context

Sirenians or sea cows are large-bodied, aquatic mammals with paddle-like pectoral flippers, no hindlimbs, and a horizontal tail fluke (Berta et al. 2006). Sirenia comprises three extant species of manatees (Trichechidae) and one species of dugong (Dugongidae; Berta et al. 2006). Today, *Dugong dugong* is distributed in the Indian and Pacific Oceans and bordering landmasses (Husar 1978a), and the species of *Trichechus* manatees are found in the New World Atlantic Ocean, the Amazon Basin, and along the Atlantic coast of West Africa as well as some west African rivers (Husar 1977, 1978b, c). *Hydrodamalis gigas*, Steller's sea cow, is a recently extinct species of large dugong that lived in the northern Pacific (Berta et al. 2006).

Although there are only a handful of extant species within Sirenia, the fossil record for the group is diverse with dozens of species of dugongs and manatees extending back to the early Eocene (~50 million years ago; e.g. Simpson 1932; Savage 1976; Domning 1982, 1988, 1989a, b, 1990, 1997, 2005; Domning et al. 1982; Savage et al. 1994; Domning and Aguilera 2008, Vélez-Juarbe and Domning 2014a, b, 2015). Fossil sirenians are distributed globally, including deposits from the North Atlantic and Pacific, Caribbean, Indian Ocean, Mediterranean, western Europe, U.S., and South America (Berta et al. 2006). Basal sirenians such as *Pezosiren portelli* from the middle Eocene of Jamaica and *Sobrarbesiren cardieli*

T. E. Macrini (✉)
Department of Biological Sciences, St. Mary's University, San Antonio, TX, USA
e-mail: tmacrini@stmarytx.edu

J. Orihuela
Department of Earth and Environment (Geosciences), Florida International University,
Miami, FL, USA

from the Eocene of Spain clearly possessed well-developed limbs, indicating the ability to freely walk on land (Domning 2001; Díaz-Berenguer et al. 2020).

Pezosiren portelli, *Prorastomus sirenoides*, and other transitional fossil sirenians (Savage et al. 1994; Domning 2001) support the alignment of the group with elephants and desmostylids in the group Tethytheria (e.g. Domning et al. 1986). However, subsequent studies suggested that desmostylids might not belong to Afrotheria, and therefore, might not be closely aligned with Sirenia (e.g. Cooper et al. 2014). More recently, Tethytheria and additional placental groups were recovered within the clade Afrotheria (Springer et al. 1997, 2015; Murphy et al. 2001a, b, 2021), a group that includes Afrosoricida (e.g. tenrecs, golden moles), Macroscelidea (elephant shrews), Tubulidentata (aardvarks), Proboscidea (elephants), Sirenia, and Hyracoidea (hyraxes). Within Afrotheria, Sirenia forms the clade Paenungulata with Hyracoidea and Proboscidea.

Sirenian monophyly is well supported by morphological synapomorphies (Domning 1994), including the following: (1) external nares retracted and enlarged, reaching to or beyond the level of the anterior margin of the orbit; (2) premaxilla contacts the frontal; (3) sagittal crest absent; (4) five premolars, or secondarily reduced from the condition by loss of anterior premolars; (5) mastoid inflated and exposed through occipital fenestra; (6) ectotympanic inflated and drop-like; (7) pachyostosis and osteosclerosis present in the skeleton. Traditionally, phylogenetic analyses of Sirenia found that Trichechidae, including the extant *Trichechus* and closely related fossil taxa, is monophyletic, whereas Dugongidae is paraphyletic (Domning 1994). A recent phylogenetic analysis by Vélez-Juarbe and Wood (2019) included new phylogenetic definitions of sirenian clades. Sirenia was defined as the crown group comprising Trichechidae and a monophyletic Dugongidae (e.g. Fig. 14.1; Vélez-Juarbe and Wood 2019). Some fossil sirenians such as *Prorastomus*, *Pezosiren*, and the paraphyletic *Eotheriodes* fell on the stem to Sirenia within the more inclusive Pan-Sirenia group (Fig. 14.1), and we refer to these taxa as “stem sirenians.” We follow the phylogenetic definitions of Vélez-Juarbe and Wood (2019) in this chapter.

14.2 Historical Background

14.2.1 *The Record of Endocranial Morphology and Any Other Paleoneurological Approaches to Sirenia*

The first known published description of the brain of a sirenian came from Steller (1751) who described a freshly killed manatee from Bering Island, presumably *Hydrodamalis gigas*. Since then, multiple other descriptions of the brains of extant sirenians and the cranial endocasts of fossil taxa were published (see Edinger 1975 for a list of publications prior to 1966). The number of paleoneurological studies of

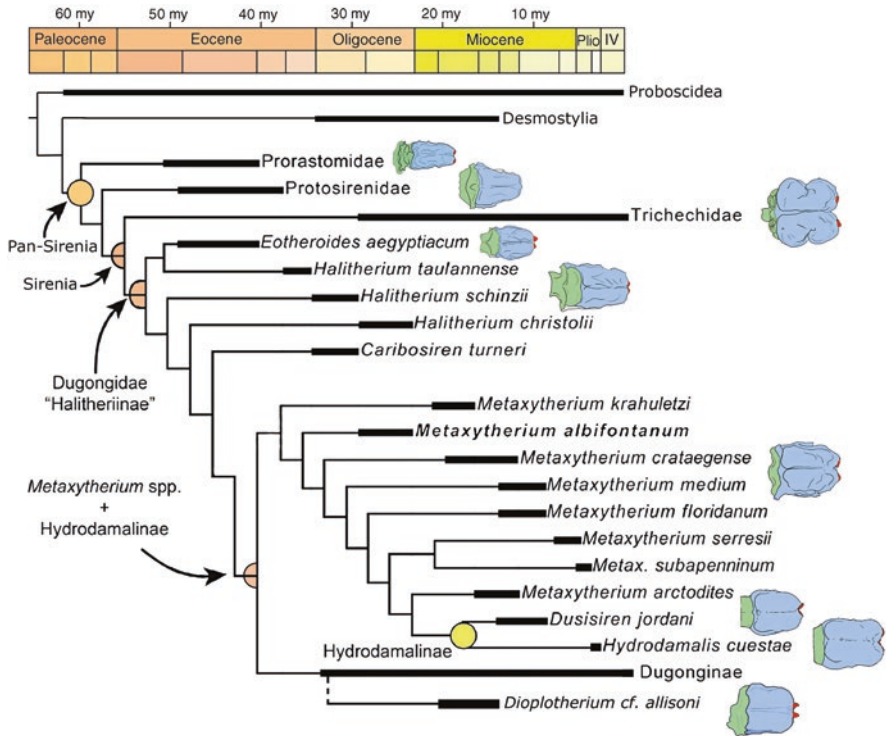


Fig. 14.1 Sirenian phylogeny and dorsal views of endocasts. Phylogenetic relationships based on Vélez-Juarbe and Wood (2019). The geological time scale is redrawn from Cohen et al. (2013) and modified from Vélez-Juarbe and Domning (2014a). See Fig. 14.2 caption for sources of endocasts

sirenians is small relative to the length of the evolutionary history of the group, going back to the Eocene.

Some of the most important paleoneurological studies include a description of the endocast of *Eotheroides* (= *Eosiren* and *Eotherium*) by Andrews (1906; Fig. 14.2). Subsequently, Edinger (1933) described new material from endocasts of pan-sirenians from Egypt and central Europe. In a later publication, Edinger (1939) added to the description of the cranial endocast of *Protosiren fraasi* based on additional fossil material (Fig. 14.2). More recently, a natural cranial endocast of *Metaxytherium* sp. from the Lower Miocene of Spain was described by Pilleri (1990; Fig. 14.2). Also, cranial endocasts of different species of *Hydrodamalis* were described and compared by Furusawa (2004). A natural endocast of *Rytidodus heali*, a dugongine from the Miocene of Libya, was described by Domning and Sorbi (2011; Fig. 14.2).

Additional recent studies of cranial endocasts of sirenians have relied on X-ray computed tomography (CT) imaging of skulls to extract digital endocasts. Computed tomography imagery of the holotype skull of *Protosiren fraasi* provided more details about the endocranial cavity of this taxon (Gingerich et al. 1994). The digital

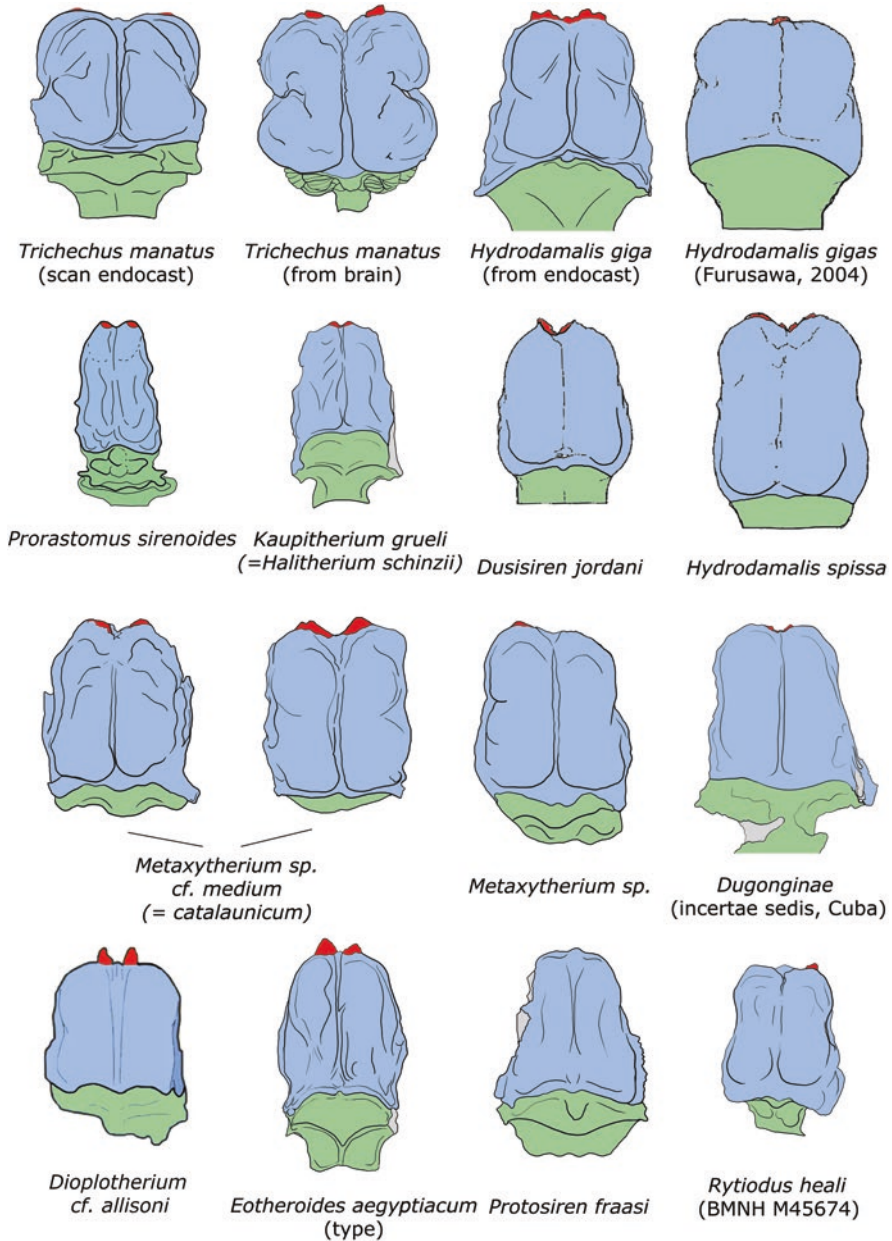


Fig. 14.2 Dorsal views of cranial endocasts of sirenians. *Trichechus manatus* (scan endocast) is an artificial, digital endocast drawn from specimen in <https://brains.anatomy.msu.edu/museum/Manatee/index.html>. Second *Trichechus manatus* endocast is redrawn from Edinger (1933). *Hydrodamalis giga* (endocast) is redrawn from Edinger (1933) and Furusawa (2004). *Prorastomus sirenioides* is redrawn from Benoit et al. (2013b), *Kaupitherium grueli* is redrawn from Furusawa (2004) and Edinger (1933) (= as *Halitherium schinzi*). *Hydrodamalis spissa* and *Dusisiren jordani*

cranial endocast of *Prorastomus sirenooides*, the basalmost stem sirenian (Fig. 14.1) from the Eocene of Jamaica, was reconstructed by Benoit et al. (2013b). The first cranial endocasts of early Miocene dugongs from the West Indies were described by Orihuela et al. (2019; Fig. 14.2). Descriptions in that paper were based on both digital and natural cranial endocasts. The cranial endocast of *Diplotherium* cf. *allisoni* from the middle Miocene of South America was recently described by Kerber and Moraes-Santos (2021; Fig. 14.2).

The bony labyrinth endocasts of fossil sirenians have been studied in only a couple of taxa. Digital endocasts of the bony labyrinth were extracted from CT imagery of the skull of *Prorastomus* and an isolated sirenian petrosal bone from the Eocene of Tunisia (Benoit et al. 2013a). Comparative data are available from the extant *Trichechus* and *Dugong* (Benoit et al. 2013a; Ekdale 2013).

14.2.2 Problematics

As mentioned above the paleoneurological record for Sirenia is sparse despite the group's long evolutionary history. More complete skulls of various fossil taxa are needed to get a better picture of the paleoneurology of the group. For what is known, there is a need for the incorporation of comparative data on the paleoneurology of Sirenia into phylogenetic characters. Previous work by Furusawa (2004) and Orihuela et al. (2019) provide a stepping stone. Furusawa (2004) examined phylogenetic characters of endocasts within Hydrodamalinae, whereas Orihuela et al. (2019) analyzed 17 endocast characters among 15 fossil and extant sirenian taxa.

14.3 Overview of General and Comparative Anatomy

14.3.1 Cranial Endocast Morphology

Cranial endocasts, or endocranial casts, are three-dimensional representations of the space inside the cranial cavity or braincase of vertebrates. The cranial endocasts of mammals tend to mostly fill the endocranial cavity (e.g. Jerison 1973; Macrini et al. 2007b) and so provide a fair representation of the external anatomy, shape, and volume of the corresponding brain. However, other soft tissue structures such as the meninges, blood vessels, dural sinuses, cisterns, and cranial nerves fill portions of



Fig. 14.2 (continued) are redrawn from Furusawa (2004). *Metaxytherium* sp. cf. *medium* and *Metaxytherium* sp. endocasts are redrawn from Pilleri (1989, 1990). Dugonginae (incertae sedis, Cuba) is redrawn from Orihuela et al. (2019). *Eotheroides aegyptiacum* is redrawn from Owen (1875) and Edinger (1933). *Protosiren fraasi* is redrawn from Gingerich et al. (1994). *Rytiodus heali* is redrawn from Domning and Sorbi (2011). *Diplotherium* cf. *allisoni* from Kerber and Moraes-Santos (2021). Olfactory bulbs are colored in red, the cerebrum is blue, and the cerebellum is green. Not to scale

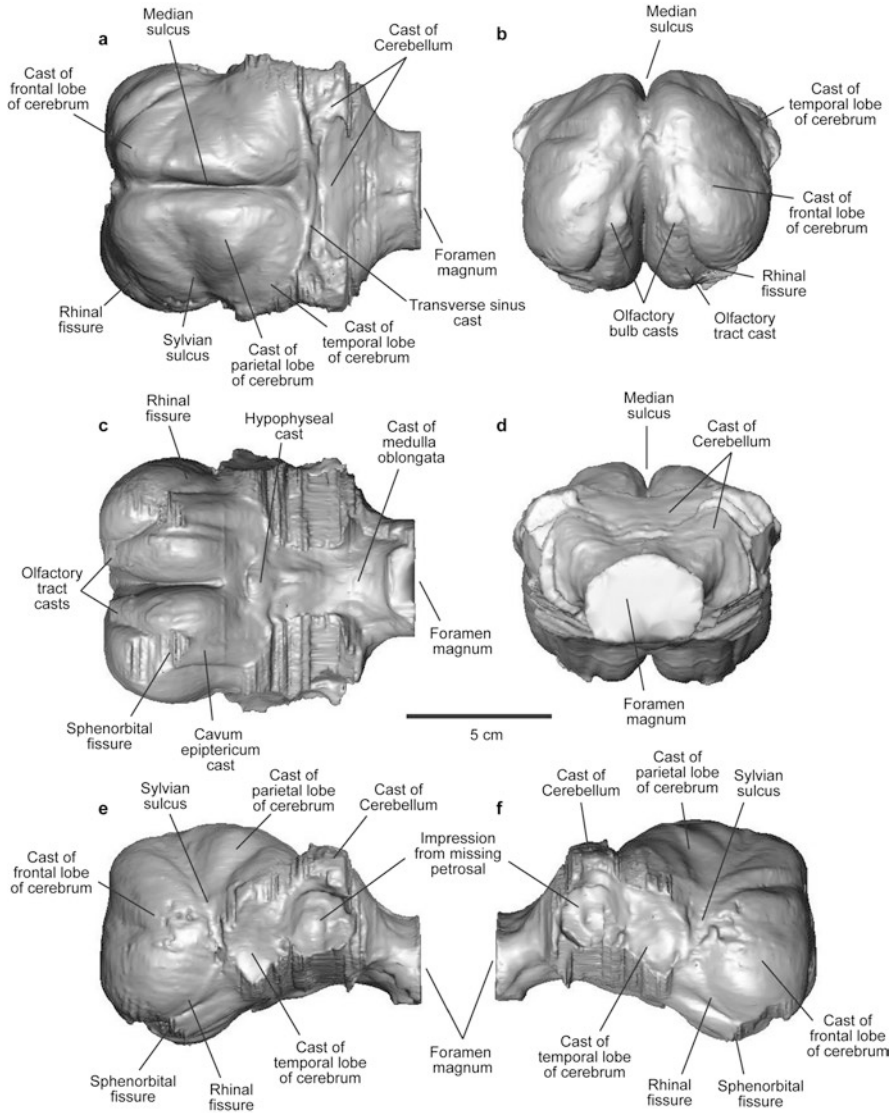


Fig. 14.3 Dorsal (a), anterior (b), ventral (c), posterior (d), left lateral (e), and right lateral views (f) of a digital cranial endocast extracted from a skull of *Trichechus senegalensis* (AMNH 53939). This figure is modified from Fig. 9 of Orihuela et al. (2019). See Macrini (2006) for details about CT scanning and how the endocast was extracted

the cranial cavity (Butler and Hodos 1996) and can obscure portions of the brain, such that they are not represented on the corresponding cranial endocast (Macrini et al. 2007a, b).

Below we describe a cranial endocast of *Trichechus senegalensis*, the African manatee (Fig. 14.3), and make comparisons with the brain of other extant sirenians. We chose to include this description for an extant taxon because there is no complete published description of the cranial endocast of *Trichechus*, but there are notably multiple descriptions of the gross anatomy of the brain of manatees (e.g. Reep and O'Shea 1990) and dugongs (e.g. Pirlot and Kamiya 1985). Given that paleoneurology is grounded in what is known from extant taxa for which we can compare brains directly with endocasts of the same species, the anatomical description that follows below is relevant and warranted in this chapter on the paleoneurology of Sirenia.

This particular description is based on the skull of an adult, female *T. senegalensis* (AMNH 53939) that was imaged at the University of Texas High-Resolution X-ray Computed Tomography Facility in Austin, TX. Details about the CT scanning and extraction of the digital endocast of this specimen are provided by Macrini (2006). This same endocast was figured in Orihuela et al. (2019).

Forebrain The dominant feature of the forebrain region of the endocast of *T. senegalensis* is the large and lissencephalic (smooth) cerebral hemisphere, which is consistent with the condition of the brains of manatees (Reep and O'Shea 1990) and dugongs (Pirlot and Kamiya 1985). The most pronounced sulci of the brain, such as the rhinal fissure, median sulcus, and Sylvian fissure, are represented on the cranial endocast (Fig. 14.3). The rhinal fissure, as in other mammals (Jerison 1991), marks the ventral boundary of the isocortex (or neocortex), the median sulcus divides the right and left cerebral hemispheres, and the Sylvian fissure separates the frontal and temporal lobes of the cerebrum. The parietal lobes of the cerebrum are also clearly separated from the rest of the cerebrum by the Sylvian sulcus (Fig. 14.3). In dorsal view, each cerebral hemisphere has the shape of a cashew nut, with an indentation on the lateral face representing the position of the Sylvian sulcus (Fig. 14.3a), which is a deep lateral fissure on the brain of *Trichechus manatus* (Reep and O'Shea 1990). The structure of the Sylvian fissure on the endocast of *T. senegalensis* is similar to what is seen on the brain of *Dugong dugong* (Pirlot and Kamiya 1985). The cerebral hemispheres on the endocast are roughly as long (rostrocaudal direction) as wide (Fig. 14.3a).

In anterior and ventral views, the much reduced olfactory bulb casts are visible (Figs. 14.1c and 14.3b). The corresponding cribriform plate of the skull is reduced or non-existent as are the bony turbinates of the nasal cavity. The olfactory bulbs are widely separated due to the robust crista galli of the skull as is the case in some fossil taxa (e.g. Gingerich et al. 1994). Casts of the olfactory tracts are visible on the ventral side of the endocast as is the case with the actual brain of *T. manatus* (Reep and O'Shea 1990). Similarly, the reduced olfactory bulbs and olfactory tracts are visible on the brain of *Dugong dugong* (Pirlot and Kamiya 1985).

The hypophyseal fossa is prominent in the middle of the ventral side of the endocast, although it is rather shallow. The right and left cava epiptERICA are widely separated at the level of the sphenorbital fissure. These openings transmit cranial nerves II, III, IV, V₁, and VI as is the case for many other mammals. Casts of many other

openings for cranial nerves such as the foramen ovale for cranial nerve V₃ are not visible on this endocast. There is no clear indication of a separate optic foramen for cranial nerve II on the endocast.

Midbrain and Hindbrain The dorsal midbrain (tectum) is not visible on the cranial endocast due to the posterior expansion of the cerebral hemispheres. The cast of the transverse sinus also overlies the position of the superior and inferior colliculi and obscures those structures from view on the endocast.

Although the cast of the cerebellum is visible in dorsal view on the endocast of *Trichechus* (Fig. 14.3a), details of this region of the brain (see Pirlot and Kamiya 1985, and Reep and O'Shea 1990), such as the cerebellar hemispheres, paraflocculi, and vermis are not clearly distinguishable on the endocast. The petrosal bones are missing from this skull, preventing the paraflocculi and internal acoustic meati from being represented on this endocast (Figs. 14.1e, f). The medulla oblongata is visible on the ventral side of the endocast but the pons is not (Fig. 14.3c).

Comparative Anatomy In general, sirenian endocasts have lissencephalic cerebral hemispheres, a reduced olfactory system (e.g., reduced or absent olfactory nerve and bulbs), reduced optic nerves, presence of a large trigeminal nerve and associated components, and thick meninges of the central nervous system (Benoit et al. 2013b; Kerber and Moraes-Santos 2021). Below we provided some details about a few fossil taxa that were previously described. Comparisons are made with the digital endocast of *Trichechus senegalensis* (Fig. 14.3) that was described above.

A natural cranial endocast of *Metaxytherium* sp. from the Lower Miocene of Cerro Gordo, Almeria, Spain (Fig. 14.2; Pilleri 1990), shows a more rectangular-shaped forebrain, with a less dorsally bulging cerebrum and a more flattened cerebellar region similar to other dugongid endocasts (e.g. Orihuela et al. 2019). The endocast of *Metaxytherium* has lissencephalic cerebral hemispheres, relatively large olfactory bulbs (much larger than those of *T. senegalensis*, Fig. 14.3), a large hypophyseal fossa, and large trigeminal nerve tracks (Pilleri 1990). *Hydrodamalis gigas* and *H. spissa* both have spherical olfactory bulbs and relatively large olfactory nerves compared to other sirenians (Fig. 14.2; Furusawa 2004). The olfactory bulbs of *Dioplotherium allisoni*, a dugongine from the middle Miocene of Brazil, are small but are elongated and clearly defined on the endocast (Kerber and Moraes-Santos 2021). In contrast, the olfactory bulbs of the Miocene dugongine *Rytiodus heali* are large and oval (Domning and Sorbi 2011), and similarly the olfactory bulbs of *Prorastomus* are large (Fig. 14.4; Benoit et al. 2013b).

The skull of the holotype of *Protosiren fraasi* from the Mokattam Limestone (Middle Eocene) of Cairo, Egypt (Fig. 14.2), was imaged using computed tomography (CT) and observations of the endocranial cavity were made by Gingerich et al. (1994) and compared to the descriptions of natural endocasts of the same species by Edinger (1933, 1939) and a natural endocast of *Eotheroides aegyptiacum* described by Owen (1875; Fig. 14.2). Gingerich et al. (1994) confirmed that *P. fraasi* and *E. aegyptiacum* are separate species, and the endocasts of the two species overlap in multiple measurements, with that of *P. fraasi* being 23% larger. The olfactory bulbs

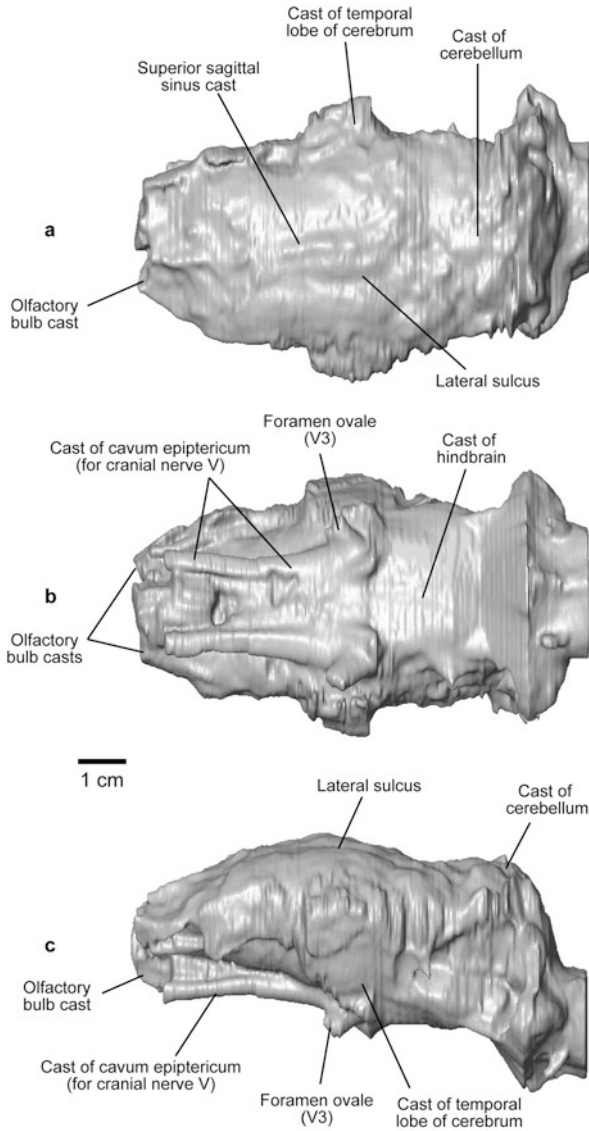


Fig. 14.4 Dorsal (a), ventral (b), and lateral (c) views of the cranial endocast of *Prorastomus sirenoides* (BMNH 44897) that was extracted from CT imagery by Benoit et al. (2013b)

of *P. fraasi* are small and widely separated by the crista galli (Edinger 1933; Gingerich et al. 1994), as is the case in other fossil sirenians (e.g. Orihuela et al. 2019; Kerber and Moraes-Santos 2021) and extant manatees (Fig. 14.3).

Computed tomography images of the skull of *Protosiren fraasi* show a narrow (2 mm diameter) optic canal, providing evidence for a separate optic foramen in at

least some sirenians (e.g. Owen 1875; Gingerich et al. 1994; Furusawa 2004). Due to its small size (e.g. *P. fraasi*; Edinger 1939), and in some cases close proximity to the casts of the trigeminal nerve paths (e.g. *Halitherium schinzii* and *Dusisiren jordani*; Furusawa 2004), the optic nerve is difficult to trace on sirenian endocasts. The optic nerve and optic foramen are not visible on endocasts of extant *T. senegalensis* (Fig. 14.3c), and some fossil taxa (e.g. Fig. 14.2; Benoit et al. 2013b; Orihuela et al. 2019). *Hydrodamalis gigas* and *H. spissa* both have optic nerves that are located dorsal to the trigeminal nerve (Furusawa 2004). The optic nerves of *Dioplotherium allisoni* are long and thin (Kerber and Moraes-Santos 2021).

The CT study of the skull of *P. fraasi* also confirmed that an osseous tentorium separating the cerebrum and cerebellum, and a median sagittal bony flax cerebri dividing the right and left cerebral hemispheres are well developed (Gingerich et al. 1994). A median sagittal bony flax cerebri is also present in *E. aegyptiacum* (Owen 1875; Gingerich et al. 1994).

Casts of the trigeminal nerve tracts and cavum epiptericum are large in all known sirenian endocasts (e.g. Owen 1875; Edinger 1933, 1939; Gingerich et al. 1994; Furusawa 2004; Benoit et al. 2013b; Orihuela et al. 2019; Kerber and Moraes-Santos 2021). The corresponding sphenorbital fissure and mandibular canals of the skulls in fossil and extant sirenians tend to be wide for the passage of branches of the trigeminal nerve.

14.3.2 Spaces Associated with Cranial Blood Supply

Casts of the transverse sinus are visible on the endocasts of fossil dugong from the Miocene of Cuba (Orihuela et al. 2019) and in *Trichechus senegalensis* (Fig. 14.3). Computed tomography images of the skull of *Protosiren fraasi* indicate the presence of a superior sagittal sinus (or “longitudinal dorsal sagittal venous sinus”) located near the roof of the skull, anteriorly. The sinus becomes buried in the dura mater posteriorly, and therefore, disappears from dorsal view on the endocast (Gingerich et al. 1994).

In at least some fossil sirenians, the brain stem (e.g. pons and medulla oblongata) is not represented on the ventral surface of the endocast (e.g. Edinger 1939; Orihuela et al. 2019). This suggests that thick meninges and/or large cisterns, (i.e. expansive subarachnoid spaces that are filled with cerebrospinal fluid in life), prevented them from being represented on the endocast. Orihuela et al. (2019) examined character #8 of Macrini et al. (2007a) pertaining to whether a cast of the superior sagittal sinus or the median sulcus was not visible on endocasts (0), visible but very shallow (1), or visible and deep (2). This was listed as character #10 in the Orihuela et al. (2019) matrix. *Hydrodamalis cuetae*, *H. spissa*, *Protosiren fraasi*, *Rytiodus heali*, and *Prorastamus sirenoides* showed character state 1, whereas all other taxa in the matrix were scored as character state 2 (Orihuela et al. 2019). No taxa in this matrix were scored with character state 0, but this character state has been observed in other mammals (Macrini et al. 2007a).

14.4 Brain Evolution and Paleobiological Inferences Based on Endocast Morphology

14.4.1 Morphological Brain Diversity

As noted previously by several authors, cranial endocasts provide the only direct evidence of brain morphology and evolution in extinct taxa. Earlier comparative and phylogenetic studies of different groups of mammals have incorporated endocranial characters in their matrices (e.g. Macrini et al. 2007a; Perini et al. 2022), but only two studies dealt exclusively with sirenians (Furusawa 2004; Orihuela et al. 2019). Furusawa (2004) included four endocast characters in a matrix containing 31 total morphological characters scored for eight total taxa including members of Hydrodamalinae and one outgroup taxon. Subsequently, Orihuela et al. (2019) examined 17 endocast characters on 15 taxa including both fossil and extant sirenians. The taxa examined included MNHNCu. P71.005310-11, an early Miocene dugongid from western Cuba; *Metaxytherium* sp. C. Gordo; *Metaxytherium* sp.; *Dugong dugon*; *Kaupitherium* sp.; *Dusisiren jordani*; *Hydrodamalis cuestae*; *H. spissa*; *H. gigas*; *Trichechus manatus*; *T. senegalensis*; *Protosiren fraasi*; *Rytiodus heali*; *Eotheroides aegyptiacum*; and *Prorastomus sirenoides*. Below we review some of the phylogenetic characters from these two studies that show some signal within the context of sirenian evolution, but we recognize that there is further work to be done in this area. We discuss these characters within the context of shape change in the cranial endocasts of sirenians.

Stem sirenians (e.g. *Prorastomus* and *Protosiren*) have cylindrically-shaped endocasts (when viewed dorsally) that show some posterior expansion near the boundary between the cerebrum and cerebellum (Figs. 14.1, 14.2 and 14.4). Crown sirenians show expansion of the cerebrum, particularly the frontal and transverse lobes. Orihuela et al. (2019) examined whether swelling of the frontal lobe of the cerebrum is absent (0), or present anterior to the Sylvian fissure (1). This swelling was not visible on the endocasts of *Prorastomus*, *Metaxytherium* sp., or the hydrodamalines examined by Furusawa (2004), which includes *Dusisiren jordani*, *Hydrodamalis cuestae*, *H. spissa*, and *H. giga*. All the taxa examined by Orihuela et al. (2019) were scored as character state 1. This character state distribution suggests that the swelling of the frontal lobe of the cerebrum anterior to the Sylvian fissure was derived in stem sirenians (exclusive of *Prorastomus*), and was secondarily lost in the clade containing *Metaxytherium* and Hydrodamalinae (Fig. 14.1). Trichechids show expanded parietal lobes of the cerebrum that are separated by the Sylvian sulcus (Fig. 14.3).

The olfactory bulbs of the stem sirenia *Prorastomus* are reportedly large (Fig. 14.4; Benoit et al. 2013b), whereas those of *Protosiren* are described as small (Edinger 1933; Gingerich et al. 1994). Crown sirenians generally have small olfactory bulbs with exceptions being *Metaxytherium* (Pilleri 1990) and the dugongine *Rytiodus heali* (Domning and Sorbi 2011). It is evident that there is a need to

quantify the size of the olfactory bulbs of stem and crown sirenians to better understand the evolution of the olfactory bulb size in this clade.

Orihuela et al. (2019) examined character #21 of Furusawa (2004) about the shape of the olfactory bulbs (character #1 in the Orihuela et al. matrix) but using a larger taxonomic sample. In addition to *Hydrodamalis spissa* and *H. gigas* showing character state 1 (circular or spherical shaped olfactory bulbs) as documented by Furusawa (2004), *Trichechus senegalensis*, and potentially *Protosiren fraasi* and *Rytiodus heali* also have this character state. All of the other taxa examined by Orihuela et al. (2019) were scored as character state 0: olfactory bulbs are elongated and compressed laterally with an elliptical outline.

Orihuela et al. (2019) also examined the position of the inferior sulcus on endocasts, a structure that is inferred to result from a robust crista galli of the ethmoid (Edinger 1939; Gingerich et al. 1994). Character #8 of Orihuela et al. (2019) examined the extent of the inferior sulcus as being either (0) anterior to the trigeminal nerve cast, or (1) reaching its vertices. This character was scored as (0) for *Metaxytherium*, *Rytiodus*, and MNHNCu. P71.005310–11, an early Miocene dugongid from western Cuba that was described by Orihuela et al. (2019). *Prosiren* and *Prorastomus* were scored as unknown for this character and all other taxa examined by Orihuela et al. (2019) were scored as having character state 1.

Perhaps the one of the most diagnostic of characters pertains to the depth of the transverse sulcus, which separates the cerebellum from the cerebrum (character #14 of Orihuela et al. 2019). In the stem sirenians *Protosiren* and *Prorastomus*, the transverse sulcus is shallow, whereas in the stem sirenian *Eotheroides*, and all crown sirenians, this sulcus is deep (Fig. 14.2).

14.4.2 Brain-Size Evolution and Encephalization Quotient

The evolution of brain size in sirenians has historically been examined using encephalization quotients (EQs), as has been done in other vertebrate groups (Jerison 1973). We summarize some of the most significant analyses of EQ in Sirenia below, while also recognizing the drawbacks and criticisms of this methodology (e.g. Deacon 1990; Striedter 2005, and see discussions in the Metatheria chapter of this book).

Estimating body size in fossil taxa has always been contentious as estimates using different skeletal parameters can vary greatly (Damuth and MacFadden 1990). In general, body mass estimates from postcranial elements tend to be the most realistic (Damuth and MacFadden 1990). However, the weight-bearing limb elements that are typically used to estimate body mass in terrestrial vertebrates are absent in obligatory aquatic mammals, and so the axial skeleton must be used for body mass estimation in these taxa (Sarko et al. 2010). Because many fossil taxa lack complete vertebral columns, measures of the skull are typically used to estimate body mass. Particularly for sirenians, the condylobasal length of the skull is usually considered

a more accurate predictor of body size in extant Florida manatees and dugongs compared to occipital condyle width and foramen magnum width (Sarko et al. 2010).

Endocranial volume (EV) can be accurately measured from CT images of skulls. However, sirenians and tethytherians, in general, have particularly thick meninges covering the brain (Benoit et al. 2013b), suggesting that the EV in these taxa is an overestimate of their brain size. Benoit (2015) provided a method to correct this issue and to provide more realistic estimates of brain size in fossil tethytherians.

The most comprehensive analysis of encephalization quotients for sirenians was published by Kerber and Moraes-Santos (2021). Endocranial volumes of sirenians were obtained from the literature and brain sizes were calculated following Benoit (2015), and body masses were estimated for fossil taxa following Sarko et al. (2010). Kerber and Moraes-Santos (2021) applied ancestral character state reconstruction for EQ using a phylogeny for sirenian relationships and found an EQ value of 0.27 ancestrally for Pan-Sirenia, 0.29 for crown Sirenia, 0.32 for Dugongidae and a slight increase to 0.36 for Dugonginae. The ancestral reconstruction for Trichechidae was the highest with an EQ of 0.42.

O'Shea and Reep (1990) recognized that sirenians have particularly low EQs compared to other marine mammals such as cetaceans or pinnipeds, despite showing life-history, ecological, and behavioral traits that are more consistent with large-brained species. It was suggested that the low-quality food diet and low metabolic rates of sirenians may account for their relatively small brain size, and that natural selection favored an increase in body size without a comparative increase in brain size (O'Shea and Reep 1990).

Compared to other members of Afrotheria, sirenians show a decrease in EQ, as is the case in some other afrotherian groups such as Tubulidentata, Bibymalagasia, and Tenrecoidea (Benoit et al. 2013b). The reduction of EQ in these different afrotherian clades seems to have occurred independently.

In this chapter, we include data on the endocranial volume and estimated body mass in fossil and extant sirenians (Table 14.1) that were previously compiled by Kerber and Moraes-Santos (2021). Figure 14.5 shows a log-log plot of the endocranial volume and body mass data in Table 14.1. The data plot tightly without any significant outliers, though *Prorastomus sirenooides* does plot slightly below the others, suggesting that it had a relatively small brain for its body size compared to other sirenians. *Hydrodamalis gigas* has the largest estimated body mass and endocranial volume of the taxa sampled, however, it does not deviate from the other taxa plotted here.

In general, these results suggest that brain and body mass evolved nearly isometrically in sirenians and thus, that there was little or no selection towards higher EQ (or higher body mass) in sirenians. This is quite unlike other marine mammals (i.e. pinnipeds and cetaceans), which belong to the “over 700-gram quartet” described by Manger et al. (2013). This is, in fact, unlike the trend observed in most mammalian lineages, including those of the closest relatives of sirenians—the proboscideans and embrithopods (Manger et al. 2013).

Table 14.1 Endocranial volume (ECV), brain mass, and body mass data for extinct and extant sirenians

Taxa	ECV (cm ³)	Brain mass (g)	Body Mass (g)	EQ Jerison (1973)	EQ Manger (2006)
<i>Dioplotherium cf. allisoni</i>	413.4	377.13	802,000	0.36	0.34
<i>Dugong dugon</i>	422	385	251,000	0.81	0.82
<i>Trichechus manatus</i>	396	361.13	756,000	0.37	0.35
<i>Trichechus inunguis</i>	277.5	252.13	363,000	0.41	0.41
<i>Trichechus senegalensis</i>	409	373.09	460,000	0.52	0.51
<i>Trichechus senegalensis</i>	374	341.36	460,000	0.48	0.47
<i>Hydrodamalis gigas</i>	1225	1123.53	6,738,250	0.26	0.21
<i>Hydrodamalis gigas</i>	1150	1054.55	6,738,250	0.25	0.20
<i>Hydrodamalis gigas</i>	1110	1017.77	6,738,250	0.24	0.19
<i>Hydrodamalis gigas</i>	1650	1514.38	6,738,250	0.35	0.29
<i>Metaxytherium sp.</i>	500	476.78	1,303,400	0.33	0.30
<i>Protosiren fraasi</i>	185	167.08	542,000	0.21	0.20
<i>Prorastomus sirenoides</i>	86.9	76.87	98,156	0.30	0.32
Dungongidae indet. Cuba	551.7	486.80	?	?	?

“EQ Jerison (1973)” was calculated using the equation of Jerison (1973), and “EQ Manger (2006)” was calculated using the equation of Manger (2006). Note: brain mass, rather than ECV, was used to calculate EQ’s. Data and EQ values are from Table 2 of Kerber and Moraes-Santos (2021), except for “Dungongidae indet. Cuba,” which is from Orihuela et al. (2019); brain mass for this specimen was estimated following Kerber and Moraes-Santos (2021)

14.4.3 Sensory Evolution: Vision, Vestibular Sense, Hearing, Mechanoreception, Olfaction

Vision Extant manatees have small eyes and a correspondingly thin optic nerve (Moore et al. 2021). The cranial endocast of *Dioplotherium cf. allisoni* (Kerber and Moraes-Santos 2021) shows a narrow optic canal. However, the cranial endocasts of Miocene dugongs from Cuba (Orihuela et al. 2019) do not clearly show the optic canals and so the optic nerve size cannot be estimated.

Vestibular Sense The inner ears of sirenians show that manatees and dugongs have semicircular canals with small arcs of curvature (Spoor 2018; Moore et al. 2021). This is consistent with the fact that sirenians typically do not make quick head movements and that they have a reduced range of motion due to fused and reduced number of cervical vertebrae (Spoor 2018; Moore et al. 2021). Noticeably, the semicircular canal radii of *Prorastomus* and a fossil sirenian from the Eocene of Tunisia (based on an isolated petrosal) also show small arcs of curvature even

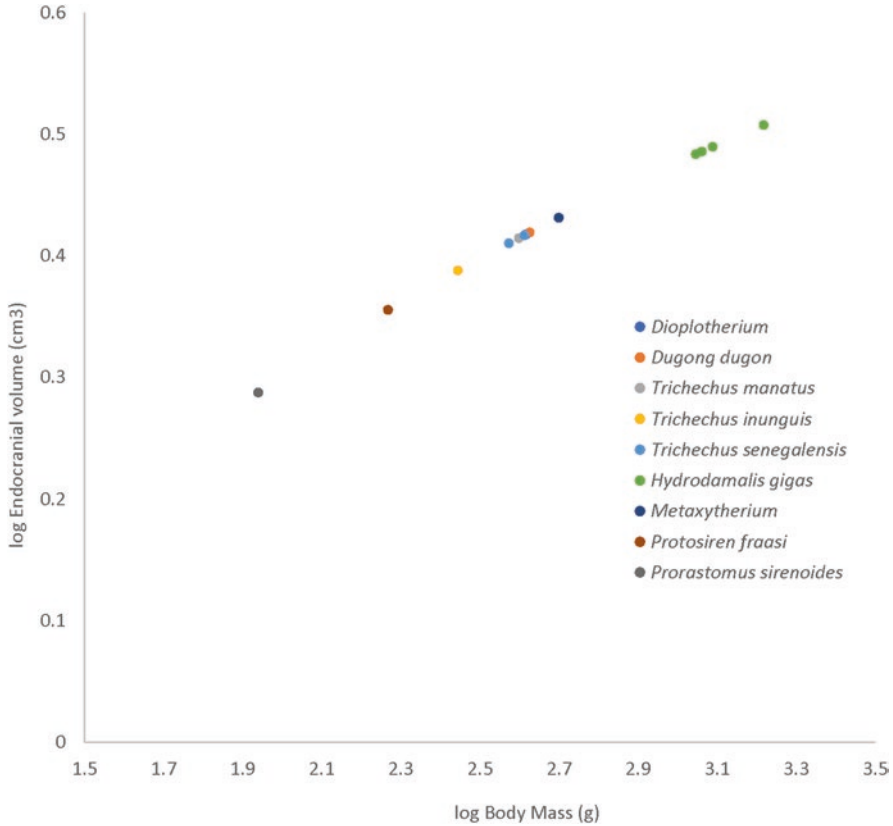


Fig. 14.5 Log endocranial volume vs log body mass in 10 species of sirenians, including six extinct species. Endocranial volume and body mass data for specimens used for this plot are presented in Table 14.1

though these basal taxa were likely not fully aquatic (Savage et al. 1994; Benoit et al. 2013a).

Hearing Sirenians have no pinnae, a small external auditory meatus, and a relatively large middle ear cavity and tympanic membrane (Moore et al. 2021). Their middle ear ossicles are reportedly the densest of any mammal, being even denser than the petrosal bone (Moore et al. 2021). The vocalizations of Florida manatees were recorded between 0.5 and 25 kHz, and manatees reportedly have good hearing at 5–20 kHz, although their hearing range is wider (Moore et al. 2021).

The cochlea of *Trichechus* completes just over 1.1 turns (407°; Ekdale 2013), whereas that of *Dugong* shows nearly 1.5 turns (514°; Benoit et al. 2013a). Among fossil sirenians, the bony labyrinth endocast of *Prorastomus* has just over 1.5 cochlear turns (550°) and an isolated fossil sirenian petrosal from the Eocene of

Tunisia shows 2.5 cochlear turns (900°; Benoit et al. 2013a). This might suggest that the more terrestrial basal sirenians had a wider range of hearing than extant taxa.

Mechanoreception Sirenians have vibrissae covering their face and postcranial regions, with the densest concentration being the facial vibrissae (Moore et al. 2021). Facial vibrissae consist of bristles, hair, and bristle-like hair, with the bristles being the stiffest and thickest and the hair being similar to the postcranial vibrissae (Moore et al. 2021). The facial vibrissae are innervated by the trigeminal sensory system, which is large in sirenians as reflected by the large sphenorbital fissure and rostral trigeminal canal (Kerber and Moraes-Santos 2021). Postcranial vibrissae in sirenians serve a mechanoreceptor function and are, in fact, the only type of hair found on sirenians body (Moore et al. 2021).

Olfaction Although extant sirenians (e.g., *Trichechus*) lack bony turbinals, a cribriform plate, and have reduced olfactory bulbs, some fossil taxa show differences in these structures. As mentioned above, *Prorastomus* has large olfactory bulbs according to Benoit et al. (2013b). The holotype of *Protosiren fraasi* preserves turbinals and a cribriform plate (Gingerich et al. 1994). A natural endocast of *Eotheroides aegyptiacum* (originally figured by Owen 1875) shows preservation of fairly large olfactory bulbs (Gingerich et al. 1994). Similarly, Miocene dugongs from Cuba (Orihuela et al. 2019) and *Dioplotherium* cf. *allisoni* (Kerber and Moraes-Santos 2021) show very reduced olfactory bulbs on their cranial endocasts.

14.4.4 Evolution and Form of Sirenian Brain Compared to Close Mammalian Relatives

An analysis of cranial endocasts in fossil and extant taxa, and extant brain morphology was used to reconstruct the endocranial morphology of the most recent common ancestor of Afrotheria (Benoit et al. 2013b). The ancestral condition of the afrotherian brain was reconstructed as having a straight (or linear) arrangement of the brain parts, absence of midbrain exposure on the dorsal surface, presence of three sulci on the neopallium (praesylyvia, suprasylvia, and sulcus lateralis), absence of the intercalary (splenial) sulcus, a ventral expansion of the neopallium such that it covers 50% of the lateral face of the brain, and absence of parafloccular lobes of the cerebellum (Benoit et al. 2013b).

The ancestral brain condition for Tethytheria, a group that includes Proboscidea and Sirenia, included the presence of very thick meninges and significant anteroposterior flexion resulting in the non-linear organization of the components of the brain (Benoit et al. 2013b). The thickness of meninges in members of Tethytheria obscures the sulcal pattern on the surface of the brain, making the cranial endocasts lissencephalic (Benoit et al. 2013b). The brains of extant elephants are highly gyrencephalic despite the smoothness of their endocasts, however, the brains of sirenians, despite showing some shallow sulci, are largely considered to be lissencephalic (Benoit

et al. 2013b). The endocast of the stem sirenian *Prorastomus* also differs from the tethytherian condition as it shows little endocranial flexion with the brain components being linearly arranged, and it shows a lateral sulcus on the cerebral hemispheres.

So, in general, the lissencephalic condition, linear arrangement of brain components, and low relative brain size of sirenians seem to be the result of a reversal rather than a retention of the ancestral conditions for Afrotheria.

14.5 Future Directions: Outstanding Questions and Perspectives

As is the case with many mammalian groups, there is a need to incorporate comparative data on sirenian endocasts into phylogenetic analyses. Furusawa (2004) and Orihuela et al. (2019) provide the only published analyses that directly include endocast characters of sirenians. However, the study by Furusawa (2004) examined only Hydrodamalinae. The analysis by Orihuela et al. (2019) included a broader taxonomic sampling, however, subsequent studies have described new sirenian endocast material that needs to be accounted for, too (e.g. Kerber and Moraes-Santos 2021). Additionally, many of the characters used by Orihuela et al. (2019) show phylogenetic variations at broad taxonomic levels but little variation among sirenians and appear to have little phylogenetic utility. There is certainly work to be done to develop an endocast character matrix that is more specific for capturing taxonomic variation for sirenians.

Also, bony labyrinth endocasts have been described for only a couple of fossil sirenians (Benoit et al. 2013a). There is work to be done to extract digital endocasts from complete petrosals of fossil sirenian and pan-sirenian taxa to better understand the functionality of the inner ear for hearing and balance in fossil taxa.

Furthermore, despite the extensive fossil record for Sirenia and Pan-Sirenia, relatively few taxa have complete skulls or preserved endocast material that can be studied. Considering the vast majority of sirenian diversity is represented by extinct species, sampling bias certainly affects our understanding of the paleoneurology of the group. Hopefully, future fossil discoveries will increase this dataset and provide a more complete picture of the sirenian paleoneurology.

Additionally, relatively little work has been done on the paleoneurology of Desmostylia, the purported sister taxon of Sirenia. Such data would be helpful for polarizing characters related to the paleoneurology of Sirenia.

Finally, there has yet to be a rigorous, quantitative study on shape change in the cranial endocasts of sirenians, similar to what has been done in marsupials (see Weisbecker et al. 2021; Chap. 11, this volume). Certainly there is not as much brain shape diversity in sirenians as in marsupials, but nonetheless such a study would be informative for gaining a more complete picture of the evolution of the brain in Sirenia.

14.6 Concluding Remarks

Despite the limitations of the fossil record mentioned above, computed tomography has allowed for expanded sampling of the paleoneurology of sirenians and pan-sirenians over the last three decades. Recent comparative studies of sirenian cranial endocasts have provided a better understanding of the evolution of the brain and brain size in this group (e.g. Orihuela et al. 2019; Kerber and Moraes-Santos 2021). In contrast to other afrotherians, sirenians have lissencephalic brains whose components are linearly arranged and small relative brain sizes. Sirenian brains are characterized by lissencephalic cerebral hemispheres, a reduced olfactory system, the reduction of the optic nerves, presence of an enlarged trigeminal nerve and associated components, and thickened meninges (Benoit et al. 2013b; Kerber and Moraes-Santos 2021).

Accessible data are still scarce though, and efforts will have to be made to code the paleoneurological differences between sirenian taxa. Similarly, there is work to be done on the comparative anatomy of the inner ear of sirenians as few anatomical studies of this system have been published for fossil sirenians.

Acknowledgments TEM was supported by the Biaggini Research Fund in the Department of Biological Sciences at St. Mary's University. JO was supported by Lazaro Viñola and Jorge Velez-Juarbe. We thank Julien Benoit for a helpful review of this chapter and for access to the digital cranial endocast of *Prorastomus*.

References

- Andrews CW (1906) A descriptive catalogue of the Tertiary Vertebrata of the Fayum, Egypt. British Museum (Natural History), London
- Benoit J (2015) A new method of estimating brain mass through cranial capacity in extinct proboscideans to account for the non-neural tissues surrounding their brain. *J Vertebr Paleontol* 35:e991021
- Benoit J, Adnet S, El Mabrouk E et al (2013a) Cranial remain from Tunisia provides new clues for the origin and evolution of Sirenia (Mammalia, Afrotheria) in Africa. *PLoS One* 8(1):e54307
- Benoit J, Crumpton N, Méridgeaud S et al (2013b) A memory already like an elephant's? The advanced brain morphology of the last common ancestor of Afrotheria (Mammalia). *Brain Behav Evol* 81:154–169
- Berta A, Sumich JL, Kovacs KM (2006) Chapter 5. Sirenia and other marine mammals: evolution and systematics. In: *Marine mammals: evolutionary biology*, 2nd edn. Elsevier, Burlington, MA, pp 89–110
- Butler AB, Hodson W (1996) *Comparative vertebrate neuroanatomy: evolution and adaptation*. Wiley-Liss, New York
- Cohen KM, Finney SC, Gibbard PL et al (2013) The ICS international chronostratigraphic chart. *Episodes* 36:199–204
- Cooper LN, Seiffert ER, Clementz M et al (2014) Anthracobunids from the Middle Eocene of India and Pakistan are stem perissodactyls. *PLoS One* 9(10):e109232
- Damuth JD, MacFadden BJ (1990) *Body size in mammalian paleobiology: estimation and biological implications*. Cambridge University Press, New York

- Deacon TW (1990) Rethinking mammalian brain evolution. *Am Zool* 30:629–705
- Díaz-Berenguer E, Houssaye A, Badiola A et al (2020) The hind limbs of *Sobrarbesiren cardieli* (Eocene, Northeastern Spain) and new insights into the locomotion capabilities of the quadrupedal sirenians. *J Mammal Evol* 27:649–675
- Domning DP (1982) Evolution of manatees: a speculative history. *J Paleontol* 56:599–619
- Domning DP (1988) Fossil Sirenia of the West Atlantic and Caribbean region. I. *Metaxytherium floridanum* Hay, 1922. *J Vertebr Paleontol* 8:395–426
- Domning DP (1989a) Fossil Sirenia of the West Atlantic and Caribbean region. II. *Dioplotherium manigaulti* Cope, 1883. *J Vertebr Paleontol* 9:415–428
- Domning DP (1989b) Fossil Sirenia of the West Atlantic and Caribbean region. III. *Xenosiren yucateca*, gen. et sp. nov. *J Vertebr Paleontol* 9:429–437
- Domning DP (1990) Fossil Sirenia of the West Atlantic and Caribbean region. IV. *Corystosiren varguezi*, gen. et sp. nov. *J Vertebr Paleontol* 10:361–371
- Domning DP (1994) A phylogenetic analysis of the Sirenia. *Proc San Diego Soc Nat Hist* 29:177–189
- Domning DP (1997) Fossil Sirenia of the West Atlantic and Caribbean region. VI. *Crenatosiren olseni* (Reinhart, 1976). *J Vertebr Paleontol* 17:397–412
- Domning DP (2001) The earliest known fully quadrupedal sirenian. *Nature* 413:625–627
- Domning DP (2005) Fossil Sirenia of the West Atlantic and Caribbean region. VII. Pleistocene *Trichechus manatus* Linnaeus, 1758. *J Vertebr Paleontol* 25:685–701
- Domning DP, Aguilera OA (2008) Fossil Sirenia of the West Atlantic and Caribbean region. VIII. *Nanosiren garciae*, gen. et sp. nov. and *Nanosiren sanchezi*, sp. nov. *J Vertebr Paleontol* 28:479–500
- Domning DP, Sorbi S (2011) *Rytiodus heali*, sp. nov., a new sirenian (Mammalia, Dugonginae) from the Miocene of Libya. *J Vertebr Paleontol* 31:1338–1355
- Domning DP, Morgan GS, Ray CE (1982) North American Eocene sea cows. *Smithson Contrib Paleobiol* 52:1–69
- Domning DP, Ray CE, McKenna MC (1986) Two new Oligocene desmostylians and a discussion of Tethytherian systematics. *Smithson Contrib Paleobiol* 59:1–56
- Edinger T (1933) Ergebnisse der Forschungsreisen Prof. E. Stromer's in den Wüsten Ägyptens. V. Tertiäre Wirbeltiere 5. Über Gehirne tertiärer Sirenia Ägyptens und Mitteleuropas sowie der rezenten Seekühe. *Abh Bayer Akad Wiss, Math naturw Abt* 20:5–36
- Edinger T (1939) Two notes on the central nervous system of fossil Sirenia. *Bull Fac Sci Fouad I Univ* 19:43–58
- Edinger T (1975) Paleoneurology 1804–1966: an annotated bibliography. *Ergeb Anat Entwicklungsgesch* 49:1–258
- Ekdale EG (2013) Comparative anatomy of the bony labyrinth (inner ear) of placental mammals. *PLoS One* 8(6):e66624
- Furusawa H (2004) A phylogeny of the North Pacific Sirenia (Dugongidae: Hydrodamalinae) based on a comparative study of endocranial casts. *Paleontol Res* 8:91–98
- Gingerich PD, Domning DP, Blane CE et al (1994) Cranial morphology of *Protosiren fraasi* (Mammalia, Sirenia) from the middle Eocene of Egypt: a new study using computed tomography. *Contrib Mus Paleontol Univ Michigan* 29:41–67
- Husar SL (1977) *Trichechus inunguis*. *Mamm Species* 72:1–4
- Husar SL (1978a) *Dugong dugong*. *Mamm Species* 88:1–7
- Husar SL (1978b) *Trichechus manatus*. *Mamm Species* 93:1–5
- Husar SL (1978c) *Trichechus senegalensis*. *Mamm Species* 89:1–3
- Jerison HJ (1973) Evolution of the brain and intelligence. Academic, New York
- Jerison HJ (1991) Fossil brains and the evolution of the neocortex. In: Finlay BL, Innocenti G, Scheich H (eds) The neocortex: ontogeny and phylogeny, NATO ASI Series A, Life sciences, vol 200. Plenum Press, New York, pp 5–19
- Kerber L, Moraes-Santos H (2021) Endocranial morphology of a Middle Miocene South American dugongid and the neurosensorial evolution of sirenians. *J Mammal Evol* 28:661–678

- Macrini TE (2006) The evolution of endocranial space in mammals and non-mammalian cynodonts. Ph.D. dissertation, University of Texas at Austin
- Macrini TE, Rougier GW, Rowe T (2007a) Description of a cranial endocast from the fossil mammal *Vincelestes neuquenianus* (Theriiiformes) and its relevance to the evolution of endocranial characters in therians. *Anat Rec* 290:875–892
- Macrini TE, Rowe T, VandeBerg JL (2007b) Cranial endocasts from a growth series of *Monodelphis domestica* (Didelphidae, Marsupialia): a study of individual and ontogenetic variation. *J Morph* 268:844–865
- Manger PR (2006) An examination of cetacean brain structure with a novel hypothesis correlating thermogenesis to the evolution of a big brain. *Biol Rev* 81:293–338
- Manger PR, Spocter MA, Patzke N (2013) The evolutions of large brain size in mammals: the ‘over 700-gram club quartet’. *Brain Behav Evol* 82:68–78
- Moore AM, Hartstone-Rose A, Gonzalez-Socoloske D (2021) Review of sensory modalities of sirenians and the other extant Paenungulata clade. *Anat Rec*:1–21
- Murphy WJ, Eizirik E, Johnson WE et al (2001a) Molecular phylogenetics and the origins of placental mammals. *Nature* 409:614–618
- Murphy WJ, Eizirik E, O’Brien SJ et al (2001b) Resolution of the early placental mammal radiation using Bayesian phylogenetics. *Science* 294:2348–2351
- Murphy WJ, Foley NM, Bredemeyer KR et al (2021) Phylogenomics and the genetic architecture of the placental mammal radiation. *Annu Rev Anim Biosci* 9:29–53
- O’Shea TJ, Reep RL (1990) Encephalization quotients and life-history traits in the Sirenia. *J Mamm* 71:534–543
- Orihuela J, Viñola LW, Macrini TE (2019) First cranial endocasts of early Miocene sirenians (Dugongidae) from the West Indies. *J Vertebr Paleontol* 39(2):e1584565
- Owen R (1875) On fossil evidence of sirenian mammal (*Eotheres aegypti*) from the nummulitic Eocene of the Mokaham Cliffs near Cairo. *Quat Journ Geol Soc* 31:100–105
- Perini FA, Macrini TE, Flynn JJ et al (2022) Comparative endocranial anatomy, encephalization, and phylogeny of Notoungulata (Placentalia, Mammalia). *J Mamm Evol* 29:369–394
- Pilleri G (1989) Endocranial cast of *Metaxytherium* (Mammalia: Sirenia) from the Miocene of Cerro Gordo, Almería, Spain. In: Pilleri G (ed) Contributions to the paleontology of some Tethyan Cetacea and Sirenia (Mammalia). Brain Anatomy Institute, Ostermundigen, pp 103–109
- Pilleri G (1990) Endocranial cast of *Metaxytherium* (Mammalia: Sirenia) from the Miocene of Cerro Gordo, Almería, Spain. *Treb Mus Geol Barcelona* 1:35–42
- Pirlot G, Kamiya T (1985) Qualitative and quantitative brain morphology in the sirenian *Dugong dugong* Erxl. *Z zool Syst Evolut-forsch* 23:147–155
- Reep RL, O’Shea TJ (1990) Regional brain morphometry and lissencephaly in Sirenia. *Brain Behav Evol* 35:185–194
- Sarko DK, Domning DP, Marino L et al (2010) Estimating body size of fossil sirenians. *Mar Mamm Sci* 26:937–959
- Savage RJG (1976) Review of early Sirenia. *Syst Zool* 25:344–351
- Savage RJG, Domning DP, Thewissen JGM (1994) Fossil Sirenia of the West Atlantic and Caribbean region. V. The most primitive known sirenian, *Prorastomus sirenoides* Owen, 1855. *J Vertebr Paleontol* 14:427–449
- Simpson GG (1932) Fossil Sirenia of Florida and the evolution of the Sirenia. *Bull Am Mus Nat Hist* 59:419–503
- Spoor F (2018) Balance. In: Würsig B, Thewissen JGM, Kovacs KM (eds) Encyclopedia of marine mammals, 3rd edn. Academic, New York, pp 59–60
- Springer MS, Cleven GC, Madsen O et al (1997) Endemic African mammals shake the phylogenetic tree. *Nature* 388:61–64
- Springer MS, Signore AV, Pajjmans JLA et al (2015) Interordinal gene capture, the phylogenetic position of Steller’s Sea cow based on molecular and morphological data, and the macroevolutionary history of Sirenia. *Mol Phylogenet Evol* 91:178–193

- Steller GW (1751) De Bestiis Marinis (The beasts of the sea). *Novi Commentarii Academiae Scientiarum Imperialis Petropolitanae*, Tom. II, (Petropoli [St. Petersburg]: Typia Academiae Scientiarum), pp. 289–398 (translated by Miller W, Miller JE)
- Striedter GF (2005) Principles of brain evolution. Sinauer Associates, Sunderland
- Vélez-Juarbe J, Domning DP (2014a) Fossil Sirenia of the West Atlantic and Caribbean region. IX. *Metaxytherium albifontanum*, sp. nov. *J Vertebr Paleontol* 34:444–464
- Vélez-Juarbe J, Domning DP (2014b) Fossil Sirenia of the West Atlantic and Caribbean region. X. *Priscosiren atlantica*, gen. et sp. nov. *J Vertebr Paleontol* 34:951–964
- Vélez-Juarbe J, Domning DP (2015) Fossil Sirenia of the West Atlantic and Caribbean region. XI. *Callistosiren boriquirensis*, gen. et sp. nov. *J Vertebr Paleontol* 35(1):e885034
- Vélez-Juarbe J, Wood AR (2019) An early Miocene dugonginae (Sirenia: Dugongidae) from Panama. *J Vertebr Paleontol* 38(5):e1511799
- Weisbecker V, Rowe T, Wroe S et al (2021) Global elongation and high shape flexibility as an evolutionary hypothesis of accommodating mammalian brains into skulls. *Evolution* 75:625–640

Chapter 15

Paleoneurology of the Proboscidea (Mammalia, Afrotheria): Insights from Their Brain Endocast and Labyrinth



Julien Benoit, George A. Lyras, Arnaud Schmitt, Mpilo Nxumalo,
Rodolphe Tabuce, Teodor Obada, Vladislav Mararsecul, and Paul Manger

Institutional Abbreviations

AMNH	American Museum of Natural History, New York, USA
AMPG	Museum of Palaeontology and Geology, National and Kapodistrian University of Athens, Athens, Greece
LACM	Natural History Museum of Los Angeles County

Supplementary Information The online version contains supplementary material available at [\[https://doi.org/10.1007/978-3-031-13983-3_15\]](https://doi.org/10.1007/978-3-031-13983-3_15).

J. Benoit (✉) · M. Nxumalo
Evolutionary Studies Institute (ESI), University of the Witwatersrand,
Johannesburg, South Africa
e-mail: julien.benoit@wits.ac.za

G. A. Lyras
Department of Geology and Geoenvironment, National and Kapodistrian University of
Athens, Athens, Greece
e-mail: glyras@geol.uoa.gr

A. Schmitt
Centre de Recherche en Paléontologie, Museum National d'Histoire Naturelle, Paris, France

R. Tabuce
Institut des Sciences de l'Évolution (UM, CNRS, IRD, EPHE), Université Montpellier,
Montpellier, France
e-mail: Rodolphe.Tabuce@umontpellier.fr

T. Obada · V. Mararsecul
Institute of Zoology, National Museum of Ethnography and Natural History of Moldova,
Chişinău, Moldova

P. Manger
School of Anatomical Sciences, Faculty of Health Sciences, University of the Witwatersrand,
Johannesburg, South Africa
e-mail: paul.manger@wits.ac.za

MCFFM	Academy of Sciences of Moldova, Institute of Zoology
MNHN	Muséum national d'Histoire Naturelle, Paris, France
NHM-UK	Natural History Museum, London, UK
MGG	Museo Geologico e Paleontologico G.G. Gemmellaro, Palermo, Italy
NMNH	National Museum of Natural History of Sofia
SMNS	Stuttgart Museum für Naturkunde
UM	Université de Montpellier, France

15.1 Historical Review and Current Data on the Variations of the Endocranial Cast Across Proboscidean Phylogeny

15.1.1 Introduction

Extant elephants are known for displaying a wide array of complex behaviors, equalling, if not surpassing, that of many primates, including such features as a detailed long-term memory storage and retrieval, behavioral adaptability, self-awareness, mourning of the dead, sophisticated problem-solving abilities, and the ability to modify their environment and to manufacture tools with their trunk (see Cozzi et al. 2001; Shoshani et al. 2006; Hart et al. 2008 for reviews). In addition, they are the shortest sleepers of all mammals studied to date (Gravett et al. 2017). As such, studying the brain of elephants to understand how it produces the array of complex behavioral repertoires observed has a long-standing fascination.

In the past two decades, many detailed studies have been conducted on various aspects of the neuroanatomy of extant elephants (e.g. Cozzi et al. 2001; Kupsky et al. 2001; Shoshani et al. 2006; Hart et al. 2008; Manger et al. 2009, 2010, 2012; Hakeem et al. 2009; Pettigrew et al. 2010; Bianchi et al. 2011; Jacobs et al. 2011; Ngwenya et al. 2011; Maseko et al. 2012, 2013a, b; Herculano-Houzel et al. 2014; Stoeger and Manger 2014; Patzke et al. 2014; Kharlamova et al. 2015, 2016; Limacher-Burrell et al. 2018). Unfortunately, the paucity of extant proboscidean species, the three species belonging to the sole extant family Elephantidae, limits comparative neuroanatomical analyses related to variations in behavioral repertoires (Byrne and Bates 2007). The paleoneurology of extinct species, although limited to the study of the shape and size of the endocranial casts, in part compensates for this lack of extant diversity, as almost 200 extinct species of proboscideans are known across the Cenozoic fossil record (Shoshani and Tassy 2005; Sanders et al. 2010; Shauer 2010). Earlier studies describing endocranial casts of proboscideans have been based on the rather rare natural casts of the braincase (e.g. Simionescu and Morosan 1937; Bever et al. 2008), on artificial casts of the braincase made with the least fragile fossil skulls (e.g. Andrews 1906; Dechaseaux 1958; Jerison 1973), or on sections of fossil skulls (e.g. Warren 1855; Boule and Thevenin 1920) (Fig. 15.1). Unfortunately, the former two types of material are quite uncommon because the extensive sinuses that comprise the majority of the volume of the proboscidean skull make it almost impossible for the *tabula interna* to withstand the natural or artificial processes that generate an endocranial cast. Sectioning fossil

skulls, being destructive, has never been routinely performed. Recently, micro-computed tomography X-ray (CT-scan) has become common in paleontology laboratories, and palaeoneurological studies can now be conducted more easily and without risk of damage to the fossils (Benoit et al. 2013b). Nevertheless, the cost of a CT scan and the large size and weight of most fossil proboscidean skulls remain two major obstacles to the study of proboscidean palaeoneurology.

Here we aim to provide a comprehensive review of published data on the endocranial anatomy of extinct proboscideans, summarizing the research undertaken over the past two hundred years aimed at increasing our knowledge of proboscidean brain evolution, bringing the number of species for which data are available from three (Shoshani et al. 2006) to twenty species (Table 15.1; the classification and phylogeny of fossil species follows Sanders et al. (2010), Shauer (2010), and Fisher (2018)). This chapter highlights some major aspects of the paleoneurological history of the proboscidean endocranial cast, i.e. endocranial capacity, endocranial morphology, and cortical gyrification.

Akin to humans, elephants are large-brained terrestrial mammals that originated in Africa and dispersed out of the African continent to populate most major landmasses, making them one of the best analogs to humans for tracing the evolution of brain size and behavioral complexity (Roca and O'Brien 2005; Goodman et al. 2009; Jebb and Hiller 2018). For example, paedomorphic scaling of brain size occurring during the evolution of insular dwarfing in elephants has stimulated the debate on whether *Homo floresiensis* should be considered a dwarf human species or a pathological case (Weber et al. 2005; Weston and Lister 2009). In addition, proboscidean brain size increased under an herbivorous diet, which also offers a unique opportunity to test whether an enlarged brain requires high-quality food to evolve (Finlay et al. 2001). Understanding how the elephantine brain evolved during the Cenozoic, therefore, has implications beyond proboscidean palaeoneurology alone as it may directly echo our own origin and evolution.

15.2 Evolution of Endocranial Capacity

15.2.1 *The Tools to Study the Evolution of Brain Size in Extinct Proboscideans*

To estimate the mass or volume of the brain in a fossil proboscidean is a difficult task, primarily because the endocranial volume comprises the volume of the brain and that of meninges that encapsulate it (Manger et al. 2009). Discrepancies surround the estimation of brain volume based on differing concepts of the meningeal thickness in proboscideans. For example, Osborn (1931, 1936, 1942) estimated that the meninges could represent as much as 20% of the endocranial capacity in recent species. This is consistent with the observations made by Kharlamova et al. (2016,

Table 15.1 Data on proboscideans cranial capacity, encephalization quotients (EQ) and primary bibliographic references

Taxon	Epoch	Endocranial capacity (cm ³)	Brain mass (g)	Body mass (g)	Jerison's EQ	Manger's EQ	Primary bibliographic references
Elephantoida	Modern	5211 (average)	4789	3030982 (average)	1.91	1.69	Benoit et al. (2019), Benoit (2015), Benoit et al. (2013a) and Shoshani et al. (2006)
	Modern	4927 (average)	4528	3850370 (average)	1.54	1.34	Benoit et al. (2019), Benoit (2015), Benoit et al. (2013a) and Shoshani et al. (2006)
	Plio- Quaternary	6807 ^a	6257	3649880	2.20	1.93	Benoit (2015) and Osborn (1931, 1942)
	Plio- Quaternary	9000 ^b	8274	11000000	1.39	1.14	Lyras (2018), Benoit et al. (2019), Benoit (2015), Weston and Lister (2009), Palombo and Giovinazzo (2005), Accordi and Palombo (1971) and Maccagno (1962)
	Plio- Quaternary	1800 ^c	1652	189000	4.87	4.42	Lyras (2018), Benoit et al. (2019), Weston and Lister (2009), Palombo and Giovinazzo (2005) and Accordi and Palombo (1971)
	Plio- Quaternary	4260 ^d	3951	1380000	2.63	2.45	Lyras (2018)
	Plio- Quaternary	4300 ^d	3951	1380000	2.66	2.48	Lyras (2018)
	Plio- Quaternary	3000 ^d	2756	727000	2.84	2.76	Lyras (2018)
	Plio- Quaternary	6232 ^e	5728	9800000	1.04	0.86	Benoit et al. (2019), Benoit (2015) and Bever et al. (2008)
	Plio- Quaternary						

	Plio- Quaternary	<i>Mammuthus primigenius</i> (juvenile, Yuka)	5025 ^f	4618	460000	6.46	6.45	Kharlamova et al. (2015, 2016)
	Plio- Quaternary	<i>Mammuthus primigenius</i> (juvenile, Khroma)	2300 ^g	2112	–	–	–	Fisher et al. (2014)
	Plio- Quaternary	<i>Mammuthus primigenius</i>	4687 ^h	4307	600000	1.09	0.92	Benoit et al. (2019), Benoit (2015), Kubacka (1944) and Simionescu and Morosan (1937)
	Plio- Quaternary	<i>Mammuthus meridionalis</i>	5828 ⁱ	5357	1100000	0.90	0.74	Benoit et al. (2019), Benoit (2015), Benoit et al. (2013a) and Dechaseaux (1958)
	Miocene	<i>Stegodon insignis</i>	3838 ^j	3527	200000	1.85	1.69	Benoit et al. (2019) and Gervais (1872)
Mammutida	Plio- Quaternary	<i>Mammut americanum</i>	3862 ^k	3549	6384056	0.86	0.73	Benoit et al. (2019), Benoit (2015), Benoit et al. (2013a) and Andrews (1906)
	Plio- Quaternary	<i>Mammut americanum</i>	4600 ^l	4227	800000	0.88	0.74	Benoit et al. (2019), Benoit (2015), Shoshani et al. (2006) and Jerison (1973)
	Plio- Quaternary	<i>Zygodon borsoni</i>	5133 ^m	4718	1600000	0.62	0.50	Benoit et al. (2019)
	Oligocene	<i>Palaeomastodon beadhelli</i>	771 ⁿ	706	250000	0.32	0.29	Benoit et al. (2019), Andrews, in Larger (1917)
	Oligocene	<i>Moeritherium lyonsi</i>	240 ^o	218	810000	0.21	0.20	Benoit et al. (2019), Benoit (2015), Jerison (1973), Andrews (1906)
Sirenia	Eocene	<i>Prorastomus sirenoideus</i>	87 ^o	90	98156	0.35	0.39	Benoit et al. (2013a)

(continued)

Table 15.1 (continued)

Taxon	Epoch	Endocranial capacity (cm ³)	Brain mass (g)	Body mass (g)	Jerison's EQ	Manger's EQ	Primary bibliographic references
Hyracoidea	Eocene	5 °	5	2932	0.21	0.29	Benoit et al. (2013a)

^aCranial capacity after Osborn (1931, 1942, water displacement?)

^bCranial capacity after Maccagno (1962, water displacement)

^cCranial capacity after Palombo and Giovino (2005, water displacement?)

^dCranial capacity after Lyras (2018, silica balls) (see Fig. 15.3)

^eCranial capacity after Bever et al. (2008, water displacement)

^fCranial capacity after Kharlamova et al. (2016, CT scan)

^gCranial capacity after Fisher et al. (2014, CT scan)

^hCranial capacity after Benoit (2015), calculated using double graphic integration including olfactory bulbs on the figures by Simionescu and Morosan (1937) (see Fig. 15.1)

ⁱCranial capacity after Benoit et al. (2013b), calculated using double graphic integration including olfactory bulbs on the figures by Dechaseaux (1958)

^jCranial capacity after Benoit et al. (2019), photogrammetry on an artificial endocast made by Gervais (1872) (see Fig. 15.1)

^kCranial capacity after Benoit et al. (2013b), calculated using double graphic integration including olfactory bulbs on the figures by Andrews (1906)

^lCranial capacity after Jerison (1973, water displacement)

^mCranial capacity after Benoit et al. (2019), photogrammetry on an artificial endocast made by the authors) (see Fig. 15.1)

ⁿCranial capacity after Benoit et al. (2019), calculated using double graphic integration on a drawing of the endocast

^oCranial capacity after Benoit et al. (2013b, CT scan)

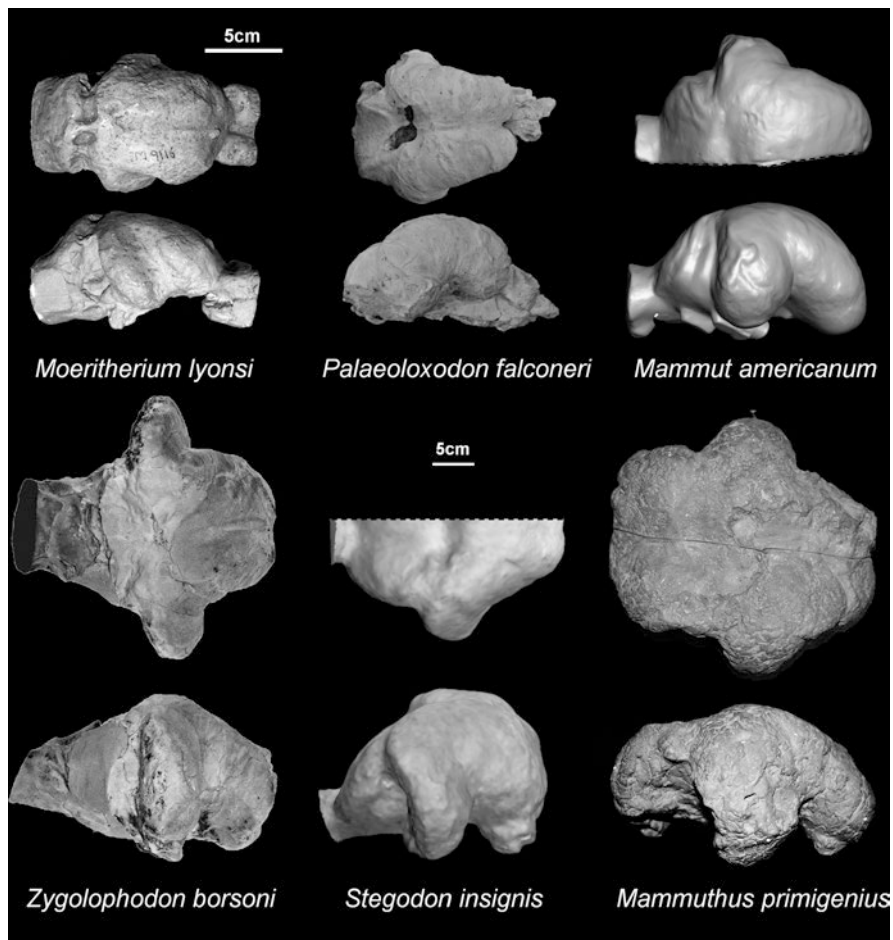


Fig. 15.1 Endocranial casts of *Moeritherium lyonsi* (NHM-UK M9116), *Palaeoloxodon falconeri* (MGG RSAL 47), *Mammuth americanum* (LACM-M40977), *Zygolophodon (Mammuth) borsoni* (MCFM-CLB-1), *Stegodon insignis* (MNHN-A952) and *Mammuthus primigenius* (No number, from Naslavcea, Moldova, see Simionescu and Morosan 1937) in dorsal and lateral views. Scale bar is the same size for all proboscideans except *Moeritherium lyonsi*. The endocranial casts of *Mammuth americanum* and *Palaeoloxodon falconeri* are mirrored for comparison

2021) in the juvenile mammoth Yuka, in which the *dura mater* occupied 18.56% of the endocranial volume. In contrast, the *dura mater* was proposed to constitute only 11% of the total mass of the tissue filling the endocranial space in extant elephants according to Shoshani et al. (2006). Benoit (2015) and Kharlamova et al. (2016) independently proposed a systematic method to estimate meningeal thickness in extinct proboscidean species. It is based on a regression using data on brain and endocranial volume primarily from Rohrs and Ebinger (2001). The equation proposed by Benoit (2015) is the most commonly used (Lyras 2018; Benoit et al. 2019), as it includes more data. The derived regression is:

$$\text{Brain volume} = 0.8877 \times \text{endocast volume} - 2.9408$$

The resulting estimates of meningeal volume indicate that the meninges occupy, on average, 14% of the endocranial space in proboscideans (Benoit 2015). Historically, the specific gravity of endocranial tissues in proboscideans was considered to be the same as that of water (e.g. Jerison 1973; but see Lyras 2018). Accordingly, these authors consider that brain mass is essentially equal to the calculated brain volume. More recently, brain tissue has been considered to be denser than water, with a specific gravity of 1.036 (Stephan et al. 1970; Palombo and Giovinazzo 2005; Benoit 2015; Benoit et al. 2019; Kharlamova et al. 2016), which is the approach taken herein (Table 15.1). In this case, brain mass equals 1.036 times brain volume; however, this assumption has been criticized by Lyras (2018) who argues that the specific gravity of the brain has been found to range from 1.027 to 1.100 g.cm³.

The resulting brain mass can be compared using the encephalization quotient (EQ) (Jerison 1973), a ratio between the observed brain mass (or volume) of an animal and the expected brain mass (or volume) of an animal of the same body mass (these expected values are calculated using a regression of known brain mass to body mass data across mammalian species). Mammals with a brain larger than expected have an EQ above 1, whereas mammals with a brain smaller than expected have a value below 1. Many methods of calculating EQs exist, but those of Jerison (1973) and Manger (2006) have been the most commonly used to compare encephalization across proboscideans (Jerison 1973; Palombo and Giovinazzo 2005; Shoshani et al. 2006; Benoit et al. 2013b, 2019; Benoit 2015; Lyras 2018). They are expressed as follow:

$$\text{Jerison's EQ} = (\text{Brain mass}) / (0.12 * \text{Body mass}^{2/3})$$

$$\text{Manger's EQ} = (\text{Brain mass}) / (0.0535 * \text{Body mass}^{0.7294})$$

Manger's EQ is similar to, but preferred over Eisenberg's EQ (Eisenberg 1981) as it includes more species to calculate the regression, and excludes outliers such as primates and cetaceans (Manger 2006).

15.2.2 *Patterns of Encephalization Evolution in Proboscideans*

The brains of extant elephants are the largest in absolute size amongst terrestrial animals (Shoshani et al. 2006; Manger et al. 2013; Herculano-Houzel et al. 2014). On average, the EQs of extant elephants range between 1 and 2, with an average of 1.88 for Jerison's EQ (Shoshani et al. 2006) and 1.51 for Manger's EQ (Benoit et al. 2019). Though not markedly different from that of an animal of similar body mass (Manger et al. 2013), modern proboscideans usually have a larger brain than predicted (Jerison 1973; Shoshani et al. 2006; Benoit et al. 2013b, 2019; Benoit 2015).

This implies that both absolute and relative brain size increased sometime during the phylogenetic history of elephants, and thus effort has been made to understand the causal factors and evolutionary timing of the enlarged brain in proboscideans (Jerison 1973; Shoshani et al. 2006; Benoit et al. 2013b, 2019; Benoit 2015; Jebb and Hiller 2018).

The geologically earliest endocranial cast of a proboscidean belongs to the ‘plesielephantiform’ *Moeritherium lyonsi* and dates from the late Eocene (~40–35 Ma) of the Fayum (Egypt; Andrews 1906; Jerison 1973; Fig. 15.1). Its endocast volume was estimated as 240 cm³ by Jerison (1973) using the water displacement method for determining endocast volume on the cast of the braincase made by Andrews (1906). Jerison’s and Manger’s EQs of *Moeritherium* provide an estimate of 0.2 (Table 15.1), an EQ that is an order of magnitude smaller than the EQ of extant elephants. Similar low EQ values have also been reported in the hyracoid *Seggeurius* and the sirenian *Prorastomus* (Table 15.1), two early Eocene Paenungulata, and the closest relatives of proboscideans (Benoit et al. 2013b, 2016). As a consequence, Jerison (1973), Benoit et al. (2013b), Manger et al. (2013), and Benoit (2015) hypothesized that a small relative and absolute brain size is the primitive condition for Proboscidea. This has since been supported by Benoit et al. (2019), who used ancestral character state reconstruction based on maximum likelihood to reconstruct that the last common ancestor of Proboscidea most likely had a Manger’s EQ of 0.24 (Fig. 15.2). The relatively small size of the brain cavity compared to the skull in *Phosphatherium* and *Numidotherium*, two basal ‘plesielephantiforms’ from the Early Eocene of North Africa (–56 to –48 Ma) depicted by Gheerbrant et al. (2005) and Benoit et al. (2013b: appendix B), also support this conclusion (Fig. 15.2a). Unfortunately, the endocast of *Moeritherium* remains the only complete one currently known for a ‘plesielephantiform’.

All other fossil proboscidean endocasts described, and for which endocranial capacity has been estimated, belong to the Elephantiformes (Table 15.1). The basal-most elephantiform, and only non-elephantimorph elephantiform taxon for which the endocranial capacity has been estimated is *Palaeomastodon beadnelli*, from the Oligocene of Egypt (Benoit et al. 2019). As early as 1917, Larger (1917: p.397) reported a personal communication from Andrews who hypothesized that *Palaeomastodon* and *Moeritherium* would have shared a similar brain size, roughly equivalent to that of a tapir (about 200 g according to Pérez-Barbería and Gordon 2005). Given that *Palaeomastodon* is the basal-most Elephantiformes (Gheerbrant and Tassy 2009; Fisher 2018), and that the Elephantimorpha have long been known for having high EQ values (Jerison 1973), this would imply that the endocranial volume likely did not increase prior to the origin of the Elephantimorpha (or, less parsimoniously, convergently in the Mammutida and Elephantoida). The endocranial capacity of *Palaeomastodon* was measured for the first time by Benoit et al. (2019) using double graphic integration on a drawing of the reconstructed endocast, a method for which the accuracy has been validated by Radinsky (1977, p.48). The *Palaeomastodon* brain has a volume of approximately 771 cm³, which is almost four times as large as that of *Moeritherium*, but since the estimated body mass of

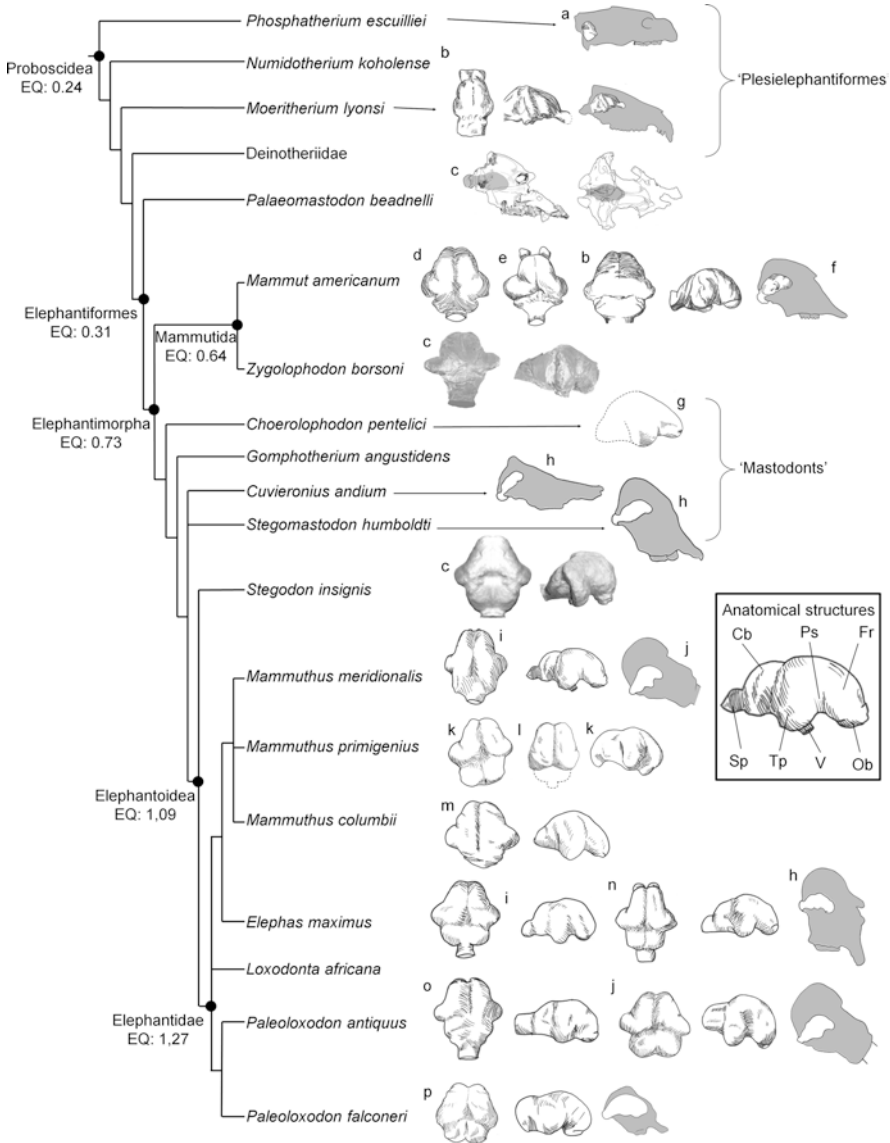


Fig. 15.2 The evolution of endocast shape in dorsal and lateral views in proboscideans. Redraw after: (a) Gheerbrant et al. 2005, (b) Andrews 1921 (c) Benoit et al. 2019, (d) Marsh 1873, (e) Jerison 1973, (f) Warren 1855, (g) Schlesinger 1922, (h) Boule and Thevenin 1920, (i) Dechaseaux 1958, (j) Palombo and Giovinazzo 2005, (k) Simionescu and Morosan 1937, (l) Kubacska 1944, (m) Bever et al. 2008, (n) Elliot Smith 1902, (o) Osborn 1931, (p) Accordi and Palombo 1971. Abbreviations: *Cb*, cerebellum; *EQ*, reconstructed ancestral Manger’s encephalization quotient after Benoit et al. 2019; *Fr* frontal lobe, *Ob* olfactory bulb, *Ps* pseudosylvia, *Sp* spinal cord, *Tp* temporal lobe, *V* trigeminal nerve. Drawings not to scale

Palaeomastodon is three times larger than *Moeritherium*, the resulting EQs are quite similar (about 0.3, Table 15.1). Accordingly, the ancestral Manger's EQ for the Elephantiformes clade is 0.31 (Benoit et al. 2019), which is similar to that seen in basal proboscideans and other Eocene paenungulates (Table 15.1). Encephalization was thus relatively stable, and brain mass seems to have co-varied tightly with body mass, in Palaeogene proboscideans, as hypothesized by Manger et al. (2013), although the endocast of some noticeably large-bodied non-elephantiform taxa such as the deinotheriids and *Barytherium* still need to be studied in detail to confirm this trend (Benoit et al. 2019). In this respect, the exposed braincase of a specimen of *Deinotherium bosazii* from the National Museums of Kenya (KNM-ER 1087) measuring about 14 cm across, and that shows no sign of expanded temporal lobes would support this prediction (J.B. Pers. Obs.).

The Elephantimorpha most likely originated during the late Oligocene (~28–24 Ma) according to both molecular dating techniques (Rohland et al. 2007; Palkopoulou et al. 2018) and the fossil record (Gheerbrant and Tassy 2009; Sanders et al. 2010; Shauer 2010); however, no data on endocranial volume is known for elephantimorphs prior to the late Miocene (Benoit 2015; Benoit et al. 2019). Benoit (2015) was the first to hypothesize that the EQ increased beyond the value of 1 in the Elephantimorpha, although crucial supportive data for elephantiforms was missing. Building upon Benoit's (2015) work, Benoit et al. (2019) showed that the relative brain size (calculated using Manger's EQ) doubled in the last common ancestor of Elephantimorpha compared to the primitive paenungulate-like condition, reaching a value of 0.73 (Fig. 15.2).

This value is close to that reconstructed for the last common ancestor of the Mammutida by Benoit et al. (2019), which is 0.64 (Fig. 15.2). The Mammutida include the largest species in the dataset, *Zygodon borsoni*, from the Pliocene of Moldova, for which body mass is estimated to 16 tons (Larramendi 2015). The endocranial size of *Zygodon* was acquired through digitization of an artificial endocast using photogrammetry (Benoit et al. 2019). It is noteworthy that despite its large body mass, both Jerison's and Manger's EQs of *Zygodon* (0.62 and 0.50 respectively) are only about 30% lower than the EQs of the two Pleistocene *Mammuth americanum*, which have body masses about half of that of *Zygodon* (Table 15.1). This illustrates that the evolution of encephalization in proboscideans is strongly tied to phylogeny, even compared to the effect of body mass (Benoit et al. 2019).

The other major clade of the Elephantimorpha is the Elephantoida (Fig. 15.2). Benoit et al. (2019) additionally found that another steep increase in relative brain size occurred in the more derived Elephantoida, for which the Manger's EQ of the last common ancestor was reconstructed as equalling 1.09 (Fig. 15.2). Jerison's and Manger's EQs appear to stabilize at this phylogenetic level, as the EQ values of the basal-most elephantoid, the late Miocene *Stegodon insignis* (1.85 and 1.69 respectively) are comparable to those in later, more derived, Elephantidae (on average 1.75 and 1.58 respectively) (Benoit et al. 2019).

15.2.3 The Effect of Insular Dwarfism on Brain Size

A pervasive pattern exhibited across island mammals worldwide is the general trend for gigantism in smaller-bodied species and dwarfism in larger-bodied species, a trend coined ‘the Island Rule’ by Van Valen (1973) and subsequent authors. A major factor in evolution under insular conditions is the ecological release from mammalian competitors and predators resulting in dwarfism in insular representatives of large-bodied taxa (Lomolino et al. 2012, 2013). Elephants provide some of the most spectacular cases of body size decrease under insular conditions. For example, the Middle Pleistocene elephant *Palaeoloxodon falconeri* from Spinagallo Cave (Sicily) evolved a body mass reduction to just 2% of the size (body mass) of its mainland ancestor *P. antiquus* (Lomolino et al. 2012, 2013). More than 20 extinct species of dwarf proboscideans are known from 17 islands worldwide (Herridge and Lister 2012; van der Geer et al. 2016). Nevertheless, available data for their brain is limited to just three *Palaeoloxodon* species: *P. aff. mnaidriensis* (late Middle Pleistocene of Sicily), *P. tiliensis* (Late Pleistocene of Tilos) and *P. falconeri* (early Middle Pleistocene of Sicily) (Accordi and Palombo 1971; Benoit 2015; Larramendi 2015; Larramendi and Palombo 2015; Lyras 2018; Benoit et al. 2019) (Fig. 15.3). Of

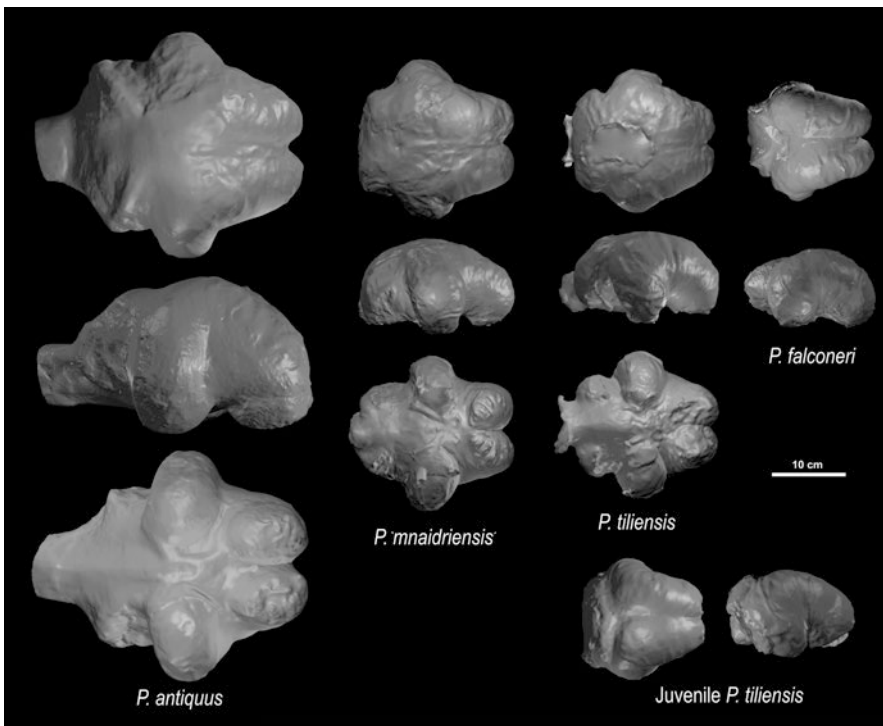


Fig. 15.3 Endocranial casts of *Palaeoloxodon antiquus* (AMNH 22634), *Palaeoloxodon* aff. *mnaidriensis* (MGG skull), *Palaeoloxodon tiliensis* (adult, AMPG T189/96; juvenile, AMPG T189/96), and *Palaeoloxodon falconeri* (MGG RSAL 47). Scale bar = 10 cm

these, a detailed description of the endocranial morphology has been published only for *P. falconeri* (Accordi and Palombo 1971).

A major challenge in estimating the relative brain size of insular proboscideans is to accurately predict their body size relative to that of their direct mainland ancestor. This applies especially to *P. falconeri*, the smallest of all insular elephants, given the magnitude of its dwarfing. As a result, the EQ estimates of *P. falconeri* range from 3.75 (Lyras 2018), 3.94 (Larramendi and Palombo 2015), 4.30 (Palombo and Giovinazzo 2005), 5.22 (Benoit et al. 2019), up to even 7.08 (Benoit 2015). This wide range is due to differences that exist in the literature between individual estimates of the body masses of dwarf elephants in general. The body mass of insular *Palaeoloxodon* species has been estimated using skeletal scaling relationships (Roth 1990; Palombo and Giovinazzo 2005; Lomolino et al. 2012, 2013; van der Geer et al. 2014, 2016) or volumetric reconstructions (Larramendi and Palombo 2015; Romano et al. 2019). Prediction regressions are hampered by two main issues: (1) many dwarf elephants, such as those of Sicily and Tilos, were considerably smaller than the smallest mature individuals of the extant species; and (2) the small-sized living relatives of elephants have significantly different body proportions compared to the island forms. Roth (1990) developed prediction equations after examining the relationship between lengths of long limb bones and body masses in 33 mammalian species ranging from mice to African elephants. Thus, in the absence of small-sized living relatives with similar physical proportions, she used a reference dataset of «all» mammals. Using the length of long limb bones Roth (1990) estimated the body mass of *P. falconeri* to 60–90 kg. Christiansen (2004) and Palombo and Giovinazzo (2005) restricted their datasets to elephants only. Palombo and Giovinazzo (2005) used regressions that predict body mass from pad circumferences and shoulder height. Their calculations for *P. falconeri* range between 51.1 kg and 141.1 kg. Christiansen (2004) on the other hand developed prediction equations using the skeletal measurements from seven Asian elephant individuals of known body mass and thus restricted his dataset to elephants only. His equations were used by Lomolino et al. (2013), who estimated the body mass of *P. falconeri* to be 189 kg, of *P. tiliensis* to be 727 kg, and that of *P. aff. mnaidriensis* to be 1380 kg. Instead of using individual bones, Larramendi and Palombo (2015) and Romano et al. (2019) used composite skeletal mounts and applied volumetric approaches. Their estimates for the body mass of *P. falconeri* range from 150 to 304.5 kg.

Using the mass estimations of Lomolino et al. (2013) the Manger EQ rises from 1.14 in *P. antiquus* to 2.45–2.48 in *P. aff. mnaidriensis*, 2.76 in *P. tiliensis*, and 4.42 in *P. falconeri* (Table 15.1). Although the brain of insular dwarfs is larger than predicted for a mammal of their size, their brain is smaller than what is predicted by the allometric trend of continental Elephantidae (Lyras 2018). Furthermore, their brains are smaller than what the static and late ontogenetic allometries of modern elephants predict (Fig. 15.4). This is particularly evident for the smallest Sicilian dwarf, *P. falconeri*.

Different values of EQ arise when alternative body mass estimations are taken into consideration, but in all cases, there is a progressive increase of EQ with

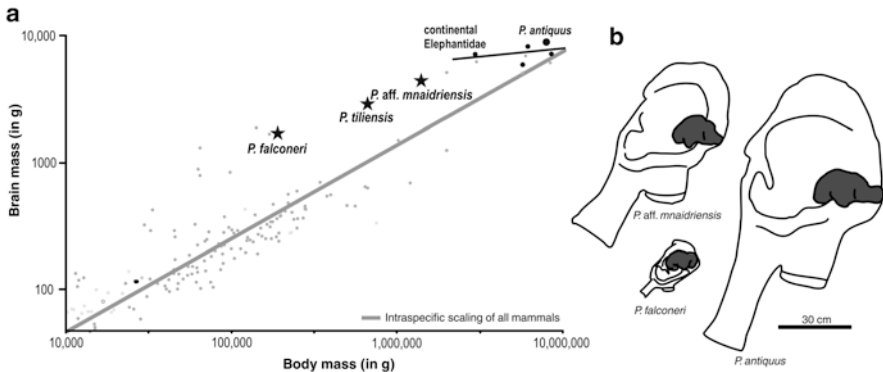


Fig. 15.4 Allometric relationships of the brain and body weight in the genus *Palaeoloxodon* (from Lyras 2018). (a) Plot of brain weight versus body weight and regressions of intra-specific scaling in continental Elephantidae (blue line) and “all” mammals excluding Cetacea and Primates (from Manger 2006) (gray line). (b) comparison of the skull and endocranial cast of *Palaeoloxodon antiquus*, *Palaeoloxodon aff. mnaidriensis*, and *Palaeoloxodon falconeri* to scale (Scale bar = 30 cm)

reduced body mass (Fig. 15.4). It appears that the larger the difference in body mass between the insular and its mainland ancestral species, the more their EQ differs.

The brains of the dwarf elephants of Sicily and Tilos are not simply scaled-down models of their mainland relative, *P. antiquus*. Their cerebellum is relatively smaller; there is a relative reduction of the temporal lobes; the frontal lobe is more massive; the olfactory bulbs are placed more caudally (Fig. 15.3). These changes seem to be gradual and are most pronounced in *P. falconeri*, the smallest species. Some of these changes might be related to ‘packaging’ problems. In insular dwarfs, the brain is contained in a much smaller space than in the continental forms. The relatively massive frontal lobe of *P. falconeri* could thus be just the result of tighter packing. A similar phenomenon has been observed in some small-sized dog breeds, which also have massive and downward rotated frontal lobes (Seiferle 1966; Radinsky 1973). The position of the olfactory bulbs is related to changes in the position of the respiratory axis. In *P. falconeri*, the skull’s center of gravity is shifted anteriorly (van der Geer et al. 2018). This has an impact on the orientation of the respiratory axis, which is more horizontal in *P. falconeri* than in *P. antiquus* (Palombo and Giovinazzo 2005). The reduction of the temporal lobes could be the result of a spatial constraint in the postnatal development of the lobe. The relative size of the temporal lobe of modern elephants increases during ontogenetic development (Shoshani et al. 2006). The temporal lobes of *P. falconeri* resemble those of juvenile *P. tiliensis*. Although the two species are not phylogenetically related, this resemblance is in line with previous suggestions that the relatively large brain of *P. falconeri* (for an average mammal of that size) is the result of heterochrony (Palombo and Giovinazzo 2005). An alternative explanation is that the small temporal lobes of *P. falconeri* are the result of allometric scaling. The morphology of the skull in insular elephants is, to

a significant extent, a function of size (van der Geer et al. 2018). Therefore, the morphology of the brain in dwarf elephants could be the result of their smaller size.

15.2.4 Why Did Elephantimorpha Evolve an Enlarged Brain?

Many hypotheses have been proposed in the literature to account for the origin and evolution of the absolutely and relatively larger brains in elephants, and these can be divided into four categories.

The first category is composed of hypotheses that aimed to find a correlation between brain size and a given life-history trait. Many life-history traits correlate with brain size in mammals, such as longevity, sexual maturation, body mass, or metabolic rate (Jerison 1973; Martin 1981; Hofman 1993; González-Lagos et al. 2010; Weisbecker and Goswami 2011; DeCasien et al. 2018). According to Manger et al. (2013), brain size in proboscideans scales almost normally with their body mass (except for *P. falconeri*), which implies that a large brain would have co-evolved with large body size since the Paleogene in proboscideans. This is only partly supported by the study of Benoit et al. (2019), who found a significant correlation between brain and body mass variations in proboscideans, but also found that brain size increased faster than body size in the last common ancestors of Elephantimorpha and Elephantoidea, resulting in two pulses of increase in both absolute and relative brain size. Pérez-Barbería and Gordon (2005) also pointed out a positive correlation between large brain mass and gestation length in paenungulates, artiodactyls, and perissodactyls, an interesting point given that elephants have the longest gestation period of all mammals (two years) (Shoshani and Tassy 1996), but yet impossible to address due to deficiencies in the fossil record.

The second category of hypotheses proposed to explain brain enlargement in proboscideans are those related to the ‘social brain’ hypothesis. Pérez-Barbería and Gordon (2005), and Shultz and Dunbar (2006) suggested that life in herds and group size are highly correlated with brain enlargement in paenungulates, artiodactyls, and perissodactyls. In support of this hypothesis, they argue that gregariousness would represent a gain of fitness primarily because it provides defence against predators. The corollary is an increase in social complexity that positively selects for larger brains in order to manage social interactions that require rapid and elaborate responses (Pérez-Barbería and Gordon 2005; Shultz and Dunbar 2006). Indeed, elephants share tight social bonds (Hart et al. 2008) and gregariousness is documented in the fossil record of Elephantimorpha (presumably in *Stegotetrabelodon*) as early as the Late Miocene, by footprints indicating that a family of 13 individuals (which is about the average for extant elephants) lived as a herd (Bibi et al. 2012). Elephants are known for possessing long-term social memory that involves: (i) chemical memory (e.g. recognition of other individuals using chemosensory characteristics of their urine), which is proposed to correlate to the enlargement of the hippocampus (Hakeem et al. 2005; Hart et al. 2008; Shultz and Dunbar 2006; but see Kupsky et al. 2001; Patzke et al. 2014 who demonstrated that the hippocampus

of elephants is not enlarged beyond what one would expect for a 5-kg mammalian brain); and (ii) acoustic memory (it has been reported that elephants can discriminate the calls of more than hundred individuals [Hart et al. 2008]), which could also be linked to the seemingly large, but unverified, size of their temporal lobe (Shoshani et al. 2006).

The third category of hypotheses are the adaptationist hypotheses. They are based on the fact that brain tissue is metabolically expensive, and natural selection usually does not maintain such costly tissue without any adaptive functions (Shultz and Dunbar 2006). Accordingly, Jerison (1973: p. 8–9) has formulated his principle of proper mass: “the mass of neural tissue controlling a particular function is appropriate to the amount of information processing involved in performing the function. This implies that in comparisons among species the importance of a function in the life of each species will be reflected by the absolute amount of neural tissue for that function in each species.” This principle has been applied to elephants by Shoshani et al. (2006) who associated their brain size with proposed extensive memory capacities and intelligence, such as the capacity to use tools, the ability to ‘think’ and consciousness. The fitness benefit of long-term memory has been emphasized by many authors as it is thought to help matriarchs to recall the location of water holes during dry seasons (Hart et al. 2008; Benoit et al. 2019). Lister (2013) also proposed that behavioral accommodation has preceded morphological adaptation to a grazing diet (i.e. increase in teeth hypsodonty and lamellar number) in proboscideans during the late Miocene (~7 Ma). It seems, however, unlikely that this triggered an increase in brain size since: (i) no pulse of absolute or relative brain enlargement is documented in late Miocene proboscideans (Benoit et al. 2019); and (ii) because Pérez-Barbería and Gordon (2005) found no indisputable correlation between diet and brain size in paenungulates, artiodactyls, and perissodactyls.

Finally, it has been hypothesized that absolute and relative brain enlargement in proboscideans may reflect an increase in intelligence and/or behavioral flexibility to cope with some major environmental, climatic and biogeographic changes that occurred in Africa between the end of the Oligocene and the beginning of the Miocene (Benoit 2015; Benoit et al. 2019). Benoit et al. (2019) noted two pulses of relative increase in brain size that roughly coincide with increased aridity, rapid temperature changes, and megafauna dispersal events in and out of Africa. According to Kappelman et al. (2003), competition with the continuous influx of artiodactyls and perissodactyls from Asia since the Late Eocene perhaps contributed to the fragmentation of proboscidean populations and increased the selective pressure on proboscideans, which then underwent a period of rapid adaptive radiation. Whether the arrival of these newcomers influenced the evolution of the cognitive capacities of endemic fauna still remains to be tested quantitatively as this hypothesis relies heavily on the apparent coincidence of variations in relative brain size and environmental changes pointed out by Benoit et al. (2019).

15.3 Evolution of Brain Morphology

15.3.1 *Neuroanatomy of Modern Elephants*

The extant elephants possess the largest terrestrial brains coupled with the largest terrestrial bodies. Despite these large brains, until recently very little was known about the structure, and through inference, functional capacities of the elephant brain. A 2001 review of the neuroanatomical data available for the elephant brain (Cozzi et al. 2001) demonstrated that only 52 scientific papers had been published that were specifically dedicated to structural aspects of the elephant brain, and that 20 of these were written in the nineteenth century. It was concluded by Cozzi et al. (2001, p.255) that the lack of interest in the elephant brain is: "...probably due to the feeling that no 'front line' discovery can be derived from these studies...", and a lack of interest in support for such studies from funding agencies. Since the publication of this review, a number of detailed studies of the elephant brain have been published (e.g. Kupsy et al. 2001; Shoshani et al. 2006; Manger et al. 2009, 2010, 2012; Hakeem et al. 2009; Pettigrew et al. 2010; Ngwenya et al. 2011; Maseko et al. 2011, 2012, 2013a,b; Herculano-Houzel et al. 2014; Stoeger and Manger 2014; Patzke et al. 2014; Limacher-Burrell et al. 2018), the majority on the brain of the African elephant (Manger et al. 2009), with these studies providing a great deal more information regarding the structure and potential functional capacities of the elephant central nervous system. Rather than provide an exhaustive review of this work, here we examine five central themes of elephant neuroanatomy, and their associated proposed behavioral parallels, that are of most interest in terms of understanding the extant elephants, and contextualizing studies of the evolution of the proboscidean brain. The five aspects of interest to be discussed here include: (1) the cerebral cortex, due to the reported behavioral complexity and flexibility of extant elephants (Hart et al. 2008); (2) the hippocampal formation, due to the near-mythical status assigned to the memory of elephants (Patzke et al. 2014); (3) the olfactory system, due to the large olfactory sensory range of the elephants (Ngwenya et al. 2011; Niimura et al. 2014); (4) the cerebellum, due to its potential association with control of the trunk (Maseko et al. 2012, 2013a); and (5) the production and reception of infrasound, due to the central involvement of the somatosensory, auditory and motor systems in this aspect of elephant communication (Maseko et al. 2013b; Stoeger and Manger 2014). Many of these features potentially brought about changes in the shape and size of the proboscidean brain throughout their evolutionary history, and therefore are important to our interpretation of fossil proboscidean endocasts and what the variations observed may indicate regarding the evolution of brain and behavior.

The cerebral cortex is an important structure because this is where the most complex processing of neural information occurs. Although debunked, for many years it was believed that brains with cerebral cortices that were more highly fissured and folded (gyrencephalic) reflected greater cognitive capacities of the species in which these features were present. The cerebral cortex of the extant elephant appears, at a superficial glance to be highly gyrencephalic, but when measured systematically and compared to other mammals, while clearly having many gyri and sulci, the

elephant brain is no more gyrencephalic than one would expect for a mammal brain weighing 5 kg (Manger et al. 2012). A similar conclusion can be reached regarding the cerebral cortex of the extinct woolly mammoth (Kharlamova et al. 2015, 2016). The cerebral cortex of the African elephant has a mass that approaches 3 kg (including both grey and white matter, 1.4 kg of grey matter alone), and contains approximately 5.59×10^9 neurons, approximately 1/3 of the neurons found in the human cerebral cortex, and less than the approximately 9×10^9 cortical neurons observed in the cerebral cortex of great apes (Herculano-Houzel et al. 2014). Thus, despite having a cerebral cortical mass far greater than apes, including humans, the number of neurons is far lower. However, there is evidence of regional variation in cortical structure and neuronal density (Herculano-Houzel et al. 2014), and evidence for the presence of very large, complexly organized neurons that rival the most complex neurons observed in the cerebral cortex of humans (Jacobs et al. 2011, 2016a). Thus, there are mixed lines of evidence regarding the level of complexity of information processing in the elephant cerebral cortex, some that hint at high levels of complexity, and some that hint at lower levels of complexity. It is only with further study that greater certainty regarding the level of complexity of the cerebral cortex of the elephant can be attained and how this may relate to their observable behaviors. In addition, it must be noted that the surface of the cerebral cortex is covered by thick meninges, in places being up to 15 mm thick (Shoshani et al. 2006; Manger et al. 2009), which effectively obscures the impression of the pattern of gyri sulci on the inner surface of the cortical mantle, making it very difficult to infer structural or regional variation of the cerebral cortex over proboscidean evolutionary history through the examination of fossil endocasts. It is only through the examination of large-scale structural units of the cortex, such as cortical lobes, that any hints regarding the evolutionary history of the elephant cerebral cortex can be gleaned. In this sense, the temporal (see below), occipital and frontal lobes are the most salient features of the elephant cerebral hemisphere for palaeoneurological analysis.

The apparently extraordinary capacities of the elephant memory system are a feature of their behavior that has been dramatically exaggerated by the field of evolutionary psychology, leading to misrepresentations of the size and complexity of the hippocampal formation (the central structure that functions to form and recall memories) in the extant elephants (Hakeem et al. 2005). Indeed, when placed in an appropriate context, the elephant hippocampal formation, having a volume of 10.84 cm^3 , is very close to the size that one would expect for a mammal with an approximately 5-kg brain (Patzke et al. 2014, 2015). The general structure of the hippocampal formation of the elephant is quite similar to that observed in other mammals, with one exception – the molecular layer of the dentate gyrus appears to have double the number of sublamina observed in other mammalian species (Patzke et al. 2014), although the effect this may have on the formation and recall of memories is unclear. At present it is best to be pragmatic about elephant memory capacities, assuming that the quality, quantity, and clarity of memories stored within the elephant brain parallel the needs of a long-lived terrestrial mammal. In this sense, “enlargement” of the hippocampal formation, putatively leading to an enlargement of the temporal lobe in which it is found, is an unlikely scenario leading to

variations in the shape and size of the fossil proboscidean endocast and can be excluded from palaeoneurological analyses as a factor in the evolution of the shape of the brain in fossil proboscideans.

The olfactory bulbs of the extant elephant are large in size, with a combined mass of almost 42 g, and 908.37 million neurons (Herculano-Houzel et al. 2014). Within the olfactory bulbs of the elephant, the typically mammalian layered organization is observed, although the glomerular layer expresses a honey-combed appearance compared to the mono-layered appearance observed in other mammals (Ngwenya et al. 2011). This large size and complexity of the glomerular layer are clearly associated with the presence of up to 2000 active olfactory receptor genes in the elephants (Niimura et al. 2014). These observations indicate that the sense of smell is a crucial aspect of the life history of the elephant. While there is a distinct and functional vomeronasal organ in the elephant (Johnson and Rasmussen 2002), interestingly, the accessory olfactory bulb, part of the pathway that processes information acquired through the vomeronasal organ for the odorous detection of pheromones, is absent in the elephant olfactory bulb (Ngwenya et al. 2011), as are the more central nuclei of the brain that are known to process accessory olfactory odorant information (Limacher-Burrell et al. 2018). This would indicate that pheromones are not detected as odorants by the elephants, but rather as tactile sensations (presumably *via* the trigeminal nerve), which may be of great importance in understanding the effects of pheromones on elephant behavior (Limacher-Burrell et al. 2018). Despite these microstructural intricacies, it is clear that the large size and anteroventral location of the elephant olfactory bulbs create important skeletal markers in the study of fossil endocasts and the evolution of behavioral repertoires associated with olfaction in the proboscideans.

The cerebellum of the elephant, with a volume of approximately 925 ml, is relatively the largest cerebellum of all mammals studied to date (Maseko et al. 2012). The African elephant cerebellum is composed of 250.71×10^9 neurons (Herculano-Houzel et al. 2014), and these neurons are far more complex, in terms of dendritic length and branching complexity, than observed in other mammalian species (Maseko et al. 2013a). As the cerebellum functions to control the force, extent, and duration of muscular contractions, this large volume and enormous population of complex neurons appear to be related to the control of the intricate musculature of the trunk and perhaps the production of the varied elephantine vocalizations. In this sense, understanding when in proboscidean evolutionary history the cerebellum obtained its large proportions is likely to provide circumstantial evidence regarding the evolution of the trunk and vocal communication systems in this lineage.

The last aspect of the extant elephant brain, and possibly that most amenable to elucidation through the examination of the fossil endocasts, involves the production and reception of infrasonic and other vocalizations. Indeed, for both the production and reception of vocalizations by the elephants there are numerous specific neural specializations (Maseko et al. 2013a; Stoeger and Manger 2014), but the majority of these specializations are unlikely to be reflected in fossil endocasts. It is well-known that across mammals the temporal lobe is involved in the processing of the auditory sense, and it is reasonable to assume that the temporal lobe of the elephant plays a

similar role. It is also known that the temporal lobe of the elephant appears to be expanded, thus creating a very specific signature that can be readily observed in the fossil endocasts. It would be reasonable to assume, given the specializations of the auditory system, especially in the dorsal thalamus where a unique nucleus ideally situated to process infrasonic sound is found within the medial geniculate body (Maseko et al. 2013b), that the expansion of the temporal lobe of the elephant was driven by the need for greater cortical processing of auditory information (Shoshani et al. 2006). This expanded temporal lobe may be responsible for the extraction of the semantic content of elephant vocalizations and the integration of seismic and air-borne infrasonic vocalizations for the localization of the source of infrasound (Maseko et al. 2013a; Stoeger and Manger 2014). Given this potentially vital role of the cerebral cortex forming the temporal lobe, the expansion of the temporal lobe in the evolutionary history of the proboscideans is likely to be an important marker of the timing when the auditory sense became very prominent, likely reflecting the evolution of the production, reception, and use of infrasonic vocalizations.

This survey of the extant elephant brain, while mostly derived from studies of the African elephant brain, has indicated that the evolution of morphological and behaviorally important aspects of the elephant brain that may be elucidated through the study of fossils include: (1) The lobes of the cerebral hemisphere, most specifically the temporal lobe, but also the frontal and occipital lobes; (2) the olfactory bulbs; (3) and the cerebellum. This survey also indicates that inferences regarding the patterns of sulci and gyri of the cerebral cortex and the relationship between the expansion of the temporal lobe and the hippocampal formation are not likely to contribute to changes in the shape of the endocast during proboscidean evolution. Using this more focused approach we re-evaluate the evolution of the proboscidean endocast.

15.3.2 *Morphology of the Endocranial Cast in Stem Proboscideans*

The endocast of modern elephants reflects their highly derived neuroanatomy. It is characterized by: (i) its rostrally prominent and flexed frontal lobe; (ii) its laterally and ventrally protruding temporal lobe; (iii) the unclearly defined occipital lobe; and (iv) its large cerebellum (Fig. 15.2i). In stem proboscideans, the endocast was very different. In *Moeritherium*, the endocranial cast has been investigated by numerous authors (primarily Andrews (1906) and Jerison (1973), but see Edinger (1975) for a complete list of workers). Unlike in modern elephants, the brain is rather linearly arranged as the olfactory bulbs are completely exposed dorsally (Fig. 15.1). A linearly arranged endocast is a primitive feature for proboscideans as it is also found in basal paenungulates such as early sirenians and hyracoids (Benoit et al. 2013b). The dorsal surface of the hemispheres is however slightly more rounded and protruding dorsally in *Moeritherium* than in other Paleogene paenungulates (Benoit et al. 2013b) (Fig. 15.1), which foreshadows the flexed condition of the hemisphere in more derived species. The cerebellum is dorsally exposed in *Moeritherium* and contributes to about one-third of the dorsal and lateral surface of

the endocast, which suggests that it was already enlarged as in modern proboscideans (Fig. 15.1). There are no visible dorsal delineating features of the occipital lobe in *Moeritherium*, though this cortical region might be obscured by the presence of the superior sagittal sinus (Fig. 15.1). The neopallium is smooth as in all Tethytheria (Benoit et al. 2013b). The temporal lobes appear large, but do not protrude laterally and ventrally to the extent that they do in the Elephantimorpha (Fig. 15.1). Friant (1951, 1954) noted that the lengthened and rather primitive aspect of the endocast of *Moeritherium* appears reminiscent to that of the brain of a twelve-month-old fetus of *Loxodonta africana*.

Comparative anatomy, isotopic analyses, ancestral molecular sequence reconstruction, and other data of various types have given substantial support to the hypothesis that *Moeritherium* was a semi-aquatic mammal (e.g. Osborn 1936; Clementz et al. 2008; Liu et al. 2008; Mirceta et al. 2013). Noticeably, adaptation to a semi-aquatic life history is known to dramatically affect brain function and morphology as it increases corticalization and decreases the size of olfactory bulbs (primarily because the sense of smell is less efficient underwater) (Bauchot and Stephan 1968; Pirlot and Kamiya 1985). This brings into question whether the endocranial morphology of *Moeritherium* is truly representative of the typical stem proboscidean condition, or if it autapomorphically reflects its adaptation to a semiaquatic lifestyle. In this respect, Matsumoto and Andrews (1923) noted that the endocast of *Moeritherium* looks like that of a terrestrial mammal as its volume is comparatively small (as stated above, its EQs reflect the primitive condition for Paenungulata, Table 15.1) and its olfactory bulbs are large and pedunculated. These features are in sharp contrast with what would be expected from a brain affected by adaptation to a semi-aquatic environment, which indicates that the endocast of *Moeritherium* is a reliable estimate of the primitive condition in Proboscidea. To test this assertion, more work will have to be done on other “plesiephantiform” taxa. Unfortunately, as stated above, *Moeritherium* is the only specimen sufficiently documented to date. In *Phosphatherium*, one of the basal-most proboscideans, the exposed braincase has not been studied in detail. The brain cavity is described as globular and two times smaller than the rostrum of the skull (~50 mm in length) (Gheerbrant et al. 2005). The cerebral cavity in *Numidotherium*, as illustrated by Benoit et al. (2013c), is too badly crushed to give any reliable indication of endocast morphology.

15.3.3 Morphology of the Endocranial Cast in Elephantiformes

Evolution of the Temporal Lobe

Descriptions of the evolution of the temporal lobe in fossil proboscideans are scarce. In Elephantimorpha, a deep pseudosylvian sulcus marks the anterior limit of the temporal lobe, which protrudes laterally and appears almost vertical in lateral view (Fig. 15.1d–p) (Elliot Smith 1902). This gives the temporal lobe of Elephantimorpha

a hypertrophied appearance in dorsal view (Fig. 15.1d–p), even compared to that of Primates (Shoshani et al. 2006).

The temporal lobe in the basal elephantiform *Palaeomastodon beadnelli* (as reconstructed in Benoit et al. [2019], based on the exposed braincase of specimen NHM-UK PV M 8464), does not protrude laterally to the same extent as in more derived Elephantimorpha. This condition is similar to that observed in *Moeritherium* (and seemingly *Deinotherium* and *Phosphatherium*), and the temporal lobe is similarly ill-defined in other basal paenungulates such as sirenians, embrithopods, and hyracoids (Andrews 1906; Edinger 1960; Benoit et al. 2013b). These observations indicate that an unspecialized temporal lobe is most likely the plesiomorphic condition for proboscideans (Benoit et al. 2013b).

The temporal lobe is especially prominent in the largest taxa for which complete endocasts are known, *Zygodolophodon borsoni* (16-ton body mass) and *Mammuthus meridionalis* (11-ton body mass) (Fig. 15.1; Benoit et al. 2019). In contrast, the endocast of the dwarf *P. falconeri* appears globular with rather blunt, weakly demarcated temporal lobes (Accordi and Palombo 1971; Palombo and Giovinazzo 2005). These observations indicate that the dimensions of the temporal lobe may vary in concert with body and/or brain size rather than to a particular function, which would be consistent with the appearance of an enlarged temporal lobe in Elephantimorpha. In *Choerolophodon* and *Gomphotherium*, the shape of the temporal lobe and the whole cerebral hemisphere seems to slightly differ from that in other Elephantimorpha according to Gervais (1872) and Schlesinger (1922), but these authors have also emphasized the poor state of preservation of their specimens.

The temporal lobe is involved in the processing of auditory stimuli, which is noteworthy given that the auditory capabilities of proboscideans and their acoustic environment have dramatically changed in elephantimorphs (Shoshani 1998; Shoshani et al. 2006; Benoit et al. 2013b; but see Sect. 15.3.1). In elephants, social communications are transmitted by infrasonic vocalizations (15–25 Hz) and foot-stomping to produce seismic waves (10–40 Hz) (Langbauer 2000; O’Connell-Rodwell 2007). The necessity to maintain communication and recognition within and between herds may have placed a major selective pressure leading to temporal lobe enlargement in elephantimorphs (Benoit 2015; Benoit et al. 2019). Bolstering this possibility is the fossil evidence that suggests that the morphological adaptations to produce infrasonic vocalization (inferred from muscle scars on fossil hyoid bones of mammoths, mammutids, and gomphotheres) and to perceive infrasonic calls (wide interaural distance, enlarged middle ear ossicles, absence of a secondary bony lamina on the bony labyrinth) were both present in the last common ancestor of the Elephantimorpha (Meng et al. 1997; Shoshani 1998; Shoshani et al. 2001; Shoshani and Tassy 2005; Benoit et al. 2013b; see Sect. 15.2.3).

Frontal Lobes and Olfactory Bulbs

According to Edinger (1960), proboscideans retain the ‘ancestral sausage shape’ of the frontal lobe encountered in their close relatives the extinct tethytheres *Arsinoitherium*, desmostylians, extant and extinct sirenians (Andrews 1906; Edinger

1975) and Mesozoic mammals (Edinger 1964; Kielan-Jaworowska 1986). Nevertheless, the frontal lobe of elephants does not appear so primitive according to Maccagno (1962), Shoshani et al. (2006), and Bever et al. (2008) who argue that the evolution of the proboscidean frontal lobe is characterized by a progressive ventral bending of its anterior-most part that ultimately results in the covering of the olfactory bulbs in dorsal view (Fig. 15.2). A similar pattern of ventral bending and flexion of the frontal lobe is observed during ontogeny in extant elephants (Friant 1957; van der Merwe et al. 1995). On the one hand, a ventral flexion of the frontal lobe leading to the covering of the olfactory bulbs in dorsal view is present in most Elephantidae (Fig. 15.2), the most extreme example being observed in the dwarf elephant of Sicily, in which the olfactory bulbs are oriented ventrally (Accordi and Palombo 1971) (Fig. 15.3). *Stegodon insignis* (Stegodontiidae, the sister group to the Elephantidae) from the Miocene of the Himalayas displays a morphology similar to that of extant elephantids, with short and large olfactory bulbs completely covered by the flexed frontal lobe (Fig. 15.1). Some noticeable exceptions among elephantids are worth mentioning. The specimen of *Paleoloxodon antiquus* depicted by Osborn (1931, 1942) displays a small dorsal exposure of olfactory bulbs anteriorly, whereas in specimen MPUR sn1 from Pian dell'Olmo the olfactory bulbs are not exposed at all in dorsal view (Maccagno 1962; Accordi and Palombo 1971; Palombo and Giovino 2005). The endocast of an Asian elephant depicted by Elliot Smith (1902: figs. 175, 177), also appears to have the olfactory bulbs exposed dorsally, whereas that shown by Dechaseaux (1958: fig. 4) does not (Fig. 15.2n). Finally, the olfactory bulbs are partially visible in the dorsal view of the endocast of *Mammuthus meridionalis* (Dechaseaux 1958), but not in *M. columbii* (Bever et al. 2008) and *M. primigenius* (Simionescu and Morosan 1937) (Fig. 15.2i, k, m).

On the other hand, the olfactory bulbs are indisputably exposed in the dorsal view of the *Moeritherium* endocast (Jerison 1973; Shoshani et al. 2006; Bever et al. 2008) (Fig. 15.1). These observations would concur with Maccagno (1962), Shoshani et al. (2006) and Bever et al. (2008), that the frontal lobe increasingly flexes from basal to derived proboscideans, but the condition and polarity of this character in basal elephantiforms are far from clear. In *Palaeomastodon*, the olfactory bulbs were not clearly reconstructed (Benoit et al. 2019, SI 1) (Fig. 15.2c). Among the Mammutida, the anterior tips of the olfactory bulbs are partially visible in dorsal view in *Zygodon borsoni* (Benoit et al. 2019, SI 1), but there is much debate about their appearance in *Mammuth americanum*. According to Jerison (1973), Shoshani et al. (2006) and Bever et al. (2008) the olfactory bulbs should be readily apparent in the dorsal view of the endocast in *M. americanum*, but Warren (1855: plate 17), Marsh (1873: fig. 74), Andrews (1906: fig. 42), and Edinger (1960: fig. 2d), depicted specimens in which the olfactory bulbs are not visible in dorsal view (Fig. 15.2d, e, b). Our own observations of specimen PV OR 40977 indicate that its olfactory bulbs are only partially visible when examining the specimen from the dorsal aspect. The extent to which the olfactory bulbs lie below the frontal lobe is also unclear among "mastodonts". According to Gervais (1872), the endocast of a juvenile *Gomphotherium angustidens* from Sansan (France) has large and anteriorly protruding olfactory bulbs. Two other gomphotheres, *Cuvieronius* and

Stegomastodon, also possess a rather non-flexed brain cavity at the level of the frontal lobe (Boule and Thevenin 1920) (Fig. 15.2h). In contrast, the olfactory bulbs in *Choerolophodon pentelici* are oriented ventrally (Fig. 15.2g), though the frontal lobe does not appear significantly flexed (Schlesinger 1922).

It is important to note that the uncertainty surrounding the polarity of this character in basal elephantiformes and the discrepancies between previous observations might be due to differences in the orientation of the braincase/endocast. A braincase/endocast tilted upward anteriorly is more likely to expose the olfactory bulbs, as in the *Cuvieronius* and *Stegomastodon* specimens described in Boule and Thevenin (1920) (Fig. 15.2h). As a consequence, the state of exposure of the olfactory bulbs in dorsal views of the endocasts may have been affected by the orientation of the specimens depicted by the original authors (a parameter that cannot be controlled) instead of the actual state of this character. Even though this does not invalidate that a ventral flexion of the frontal lobe occurred during proboscidean evolution, further observations are necessary to better understand when and how this phenomenon occurred.

The Cerebellum and Evolution of the Trunk

The cerebellum is readily visible in dorsal views of the endocranial cast in all extant and extinct proboscideans, but the occipital lobe is ill-defined (Fig. 15.1). This greatly differs from the condition seen in humans, in which the occipital lobe is well developed and overlies the cerebellum in dorsal view (Jerison 1973; Holloway 2013; Beaudet et al. 2019). In this regard, Shoshani et al. (2006) indicated that as the occipital lobe is the center of vision, vision is not an elaborated sense in elephants (but see Pettigrew et al. 2010; Maseko et al. 2013a, b). The cerebellum of extant elephants is proportionately and absolutely the largest of all mammals examined to date (Maseko et al. 2012). The large size of the cerebellum likely plays an important role in the coordination of pharyngeal muscles for vocalizations and complex motions of the proboscis (Shoshani et al. 2006; Maseko et al. 2012). The proboscis alone represents 150,000 muscle bundles capable of lifting 350 kg, whereas its finger-like tips can achieve extremely delicate actions such as shelling peanuts or making tools (Shoshani 1998). As a consequence, it has been proposed that cerebellum size would have co-evolved with the development of the proboscis (Maseko et al. 2012).

Although a rich fossil record chronicles the evolutionary history of Proboscidea, the evolution of their most defining feature, the trunk (or proboscis) is not well documented as soft tissues do not readily preserve (Shoshani 1998). Historically, authors made use of osteological correlates to estimate the presence and dimensions of the proboscis such as the size of the infraorbital foramen (for the infraorbital ramus of the maxillary branch of the trigeminal nerve), retraction of the osseous naris, and length of the mandibular symphysis and other osteological proxies (Osborn 1936, 1942; Wall 1980; Witmer et al. 1999; Knoll et al. 2006; Muchlinski

2008, 2010; Crumpton and Thompson 2013; Nabavizadeh 2015; Nabavizadeh and Reidenberg 2019).

The trigeminal nerve is one of the largest nerves in proboscideans as it is responsible for mostly providing tactile sensation to the face, narial area, trunk, and dentition of the upper (V1, V2) and lower jaws (V3), as well as carrying out some motor functions to the lower jaw (Boas 1908; Shoshani 1982; Rodella et al. 2012; Higashiyama and Kuratani 2014; Nabavizadeh and Reidenberg 2019). The infraorbital ramus of the maxillary branch (V2) of the trigeminal nerve innervates the follicles of the sensory hairs and skin of the elephant trunk (Osborn 1936, 1942; Wall 1980; Witmer et al. 1999; Knoll et al. 2006; Muchlinski 2008, 2010; Crumpton and Thompson 2013; Nabavizadeh 2015; Nabavizadeh and Reidenberg 2019). It passes through a bony tunnel through the maxilla called the infraorbital canal, which opens caudally within the orbit (maxillary foramen) and rostrally on the lateral aspect of the maxilla (infraorbital foramen) (Muchlinski 2008; Crumpton and Thompson 2013; Benoit et al. 2019). The dimensions of the infraorbital foramen are directly correlated to the number of nerve fibers passing through the infraorbital canal in mammals (Muchlinski 2008, 2010). As the proboscis developed during proboscidean evolution, it is thus inferred that the size of the infraorbital foramen on fossilized skulls would reflect the increasing innervation of the “growing” trunk (Andrews 1904; Osborn 1936, 1942). To the best of our knowledge, no quantitative approach to tracing the evolution of the dimensions of the proboscidean infraorbital foramen has been undertaken, and only qualitative accounts are available.

It is noteworthy that even the basal-most “Plesielephantiformes”, such as *Eritherium*, *Phosphatherium*, and *Numidotherium* (Mahboubi et al. 1984; Gheerbrant et al. 2005; Gheerbrant 2009; Gheerbrant et al. 2012), already present with a relatively large infraorbital foramen, surrounded by a deep infraorbital fossa (or canine fossa) for the attachment of a presumably well-developed *levator alae nasi* muscle (Boas 1908; Shoshani 1982). This strongly suggests that a mobile and prehensile upper lip was already present in the basal-most proboscideans and is likely a plesiomorphic feature of the Tethytheria (Gheerbrant et al. 2005) (Fig. 15.5). Deinotheriidae and Elephantiformes, including the basal elephantiform *Palaeomastodon*, possess a very large infraorbital foramen, comparable to that of modern elephants (Andrews 1904; Osborn 1936, 1942; Sanders et al. 2010), although some variations exist and remain to be fully explored, like in *Gomphotherium angustidens*, which exhibits a condition where the infraorbital canal is divided into a small dorsal foramen and a relatively larger ventral one (Tassy 2013). In general, the infraorbital canal is long and runs horizontally in basal “plesielephantiforms”, but becomes relatively short and more obliquely oriented in deinotherids and elephantiforms as the rostrum shortens and the external nares are retracted (Andrews 1904; Osborn 1936, 1942; Sanders et al. 2010) (Fig. 15.5).

The proboscis, molars, and tusks weigh altogether hundreds of kilograms (Shoshani and Eisenberg 1982; Larramendi 2015) contributing 5–10% of the total body mass in modern elephants. The proboscideans skull, therefore developed a highly pneumatized skull and deep insertions for the nuchal ligaments to

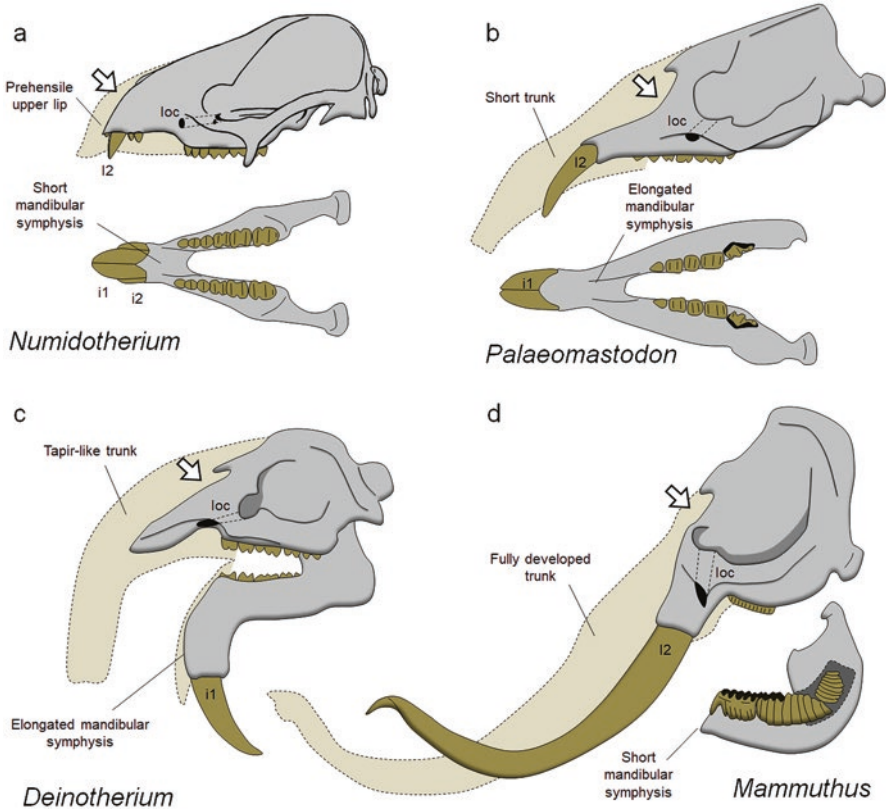


Fig. 15.5 Reconstruction of the proboscis in (a) *Numidotherium koholense*, (b) *Palaeomastodon beadnelli*, (c) *Deinotherium giganteum*, and (d) *Mammuthus primigenius* (after Osborn 1936, 1942; Scheele 1955; Markov and Spassov 2001). Abbreviations: *i1* first lower incisor, *i2* second lower incisor, *I2* second upper incisor, *loc* infraorbital canal. The white arrow indicates the nasal opening

compensate for the cranial extra weight (Andrews 1904; Osborn 1936, 1942; van der Merwe et al. 1995; Shoshani and Tassy 1996; Sanders et al. 2010). *Eritherium*, *Phosphatherium*, and *Moeritherium* show little signs of cranial pneumatization, whereas *Numidotherium* and *Barytherium* do (Mahboubi et al. 1984; Delmer 2005; Gheerbrant et al. 2005; Gheerbrant 2009; Gheerbrant and Tassy 2009; Gheerbrant et al. 2012; Benoit et al. 2013c), which makes it difficult to point out the exact origin of a pneumatized skull among “plesiephantiforms”. It is nevertheless likely that *Moeritherium* secondarily lost its cranial pneumaticity as an adaptation to a semi-aquatic lifestyle (Matsumoto and Andrews 1923; Tassy 1981). The deinotherids, *Palaeomastodon*, and more derived elephantiformes all share the presence of cranial pneumaticity and deep nuchal fossae for ligamentous attachment (Andrews 1904; Osborn 1936, 1942; Shoshani and Tassy 1996; Sanders et al. 2010).

Due to the evolution of the proboscis, the proboscidean skull changed in overall gross morphology to accommodate attachments of the heavy labial and nasal

musculature needed to operate the massive trunk, i.e. the nares became increasingly large and retracted, the snout shortened and the premaxilla became wider (Andrews 1904; Osborn 1936, 1942; Shoshani 1998; Gheerbrant and Tassy 2009). The earliest proboscidean to display an enlarged narial opening is *Numidotherium koholense*, whereas the first hints of narial retraction appear with *Barytherium* and *Moeritherium* (Andrews 1906; Mahboubi et al. 1984; Delmer 2005; Sanders et al. 2010). These anatomical changes are consistent with a gradual increase in size of the pre-existing mobile upper lip. Among early proboscideans, the deinotheriid *Deinotherium* achieved some of the widest premaxilla and largest nasal opening (Andrews 1921; Harris 1973; Sanders et al. 2010), although as it retains a relatively long and flexible neck and limbs, and shallow facial muscle attachments, it is traditionally reconstructed with a wide but short tapir-like trunk (Markov and Spassov 2001; Larramendi 2015).

Andrews (1904) and subsequent authors (e.g., Nabavizadeh 2015; Nabavizadeh and Reidenberg 2019) hypothesized that the onset of a very long mandibular symphysis in basal elephantiforms (i.e. *Palaeomastodon*, Mammutida, Gomphotheriinae, Choerolophodontinae, Amebelodontinae and other “gomphotheres”) and deinotheriids accompanied the evolution of the proboscis. The proboscis would occlude with the symphysis to enhance trophic activities and food processing, and as such the growth of the trunk would parallel the lengthening of the symphysis throughout phylogeny (Nabavizadeh 2015). This initial lengthening is coupled with the formation of tusk-like upper and shovel-shaped lower incisors (Andrews 1904; Noubhani et al. 2008; Nabavizadeh 2015). The maximum length of the mandibular symphysis is reached in Choerolophodontinae, and Amebelodontinae indicating that a trunk comparable to that in modern elephants was present as early as the middle Miocene, and is followed by the convergent, secondary reduction of the symphysis in the late Miocene and Pliocene in the Mammutida and Stegodontidae (modern elephant ancestors) while the proboscis remained stable (Andrews 1904; Osborn 1936, 1942; Van der Made 2010; Tassy 2013; Nabavizadeh 2015) (Fig. 15.5). The convergent loss of lower tusks may be correlated to the decrease of global temperature and humidity in the upper Miocene and Pliocene as the presence of four tusks would enhance heat loss (Mothé et al. 2016).

Based on the retraction of the narial opening, length of the mandibular symphysis, enlargement of the infraorbital foramen, and other cranial adaptations, it is most likely that basal “plesielementiforms” had a prehensile upper lip (Fig. 15.5). The facial and narial musculature eventually evolved into a large and mobile proboscis in the last common ancestor of the Deinotheriidae and Elephantiformes in the late Eocene (Andrews 1904; Osborn 1936, 1942; Nabavizadeh 2015).

The presence of a prehensile upper lip would account for the relatively large cerebellum of *Moeritherium* which makes up about one-third of the total length of the endocast in dorsal view (Fig. 15.1). The endocasts of all known Elephantiformes display an enlarged cerebellum comparable to that in modern elephants (Benoit 2015; Benoit et al. 2019) (Fig. 15.2). In the rare occasion when it is preserved and depicted, the cast of the trigeminal nerve is correspondingly large on the endocranial cast of elephantiforms (Andrews 1906; Dechaseaux 1958; Palombo and

Giovinazzo 2005; Shoshani et al. 2006). Though the cerebellar morphology of deinotherids is unknown, the size of the *foramen rotundum* indicates that the trigeminal nerve was relatively large (Andrews 1921; Harris 1973).

Cortical Sulcation and Gyrfication

One of the most striking features of the elephantine brain surface anatomy is the extent to which the cerebral cortex is fissured and folded, termed gyrencephaly (Cozzi et al. 2001; Shoshani et al. 2006). It has been shown that, broadly across mammalian species, the larger the brain (in absolute size), the more gyrencephalic the cerebral cortex (Manger et al. 2012). It should be noted that the extent of gyrencephaly of the elephant brain is what would be considered typical for a mammal with a brain mass of 5 kg (Manger et al. 2012). Nevertheless, the endocranial cast of proboscideans, including fossils, is surprisingly lissencephalic (smooth; Figs. 15.1, 15.2 and 15.3; Andrews 1906; Simionescu and Morosan 1937; Dechaseaux 1958; Palombo and Giovinazzo 2005; Benoit et al. 2013b). This is likely due to the thickness of the meninges (which comprise meningeal vessels, the pia mater, the arachnoid, and the dura mater) that encapsulate the brain and obfuscate the cortical gyral and sulcal patterns (Osborn 1931; Dechaseaux 1962; Manger et al. 2009). The functional significance of this thick layer of meninges and meningeal vessels in elephants include mechanical protection, blood supply and drainage, thermoregulation (through a possible rete mirabile formed by meningeal arteries), a housing of stem cells in case of injury, and as a ‘vascular hydraulic skeleton’ through blood pressure (Shoshani et al. 2006; Bruner et al. 2011; Decimo et al. 2012). The thickness of meninges in extant elephants ranges between five and fifteen millimeters, depending on the location sampled (Shoshani et al. 2006; Manger et al. 2009), and this thickness obscures the cortical sulci on the endocranial cast (Figs. 15.1, 15.2 and 15.3). Meningeal thickness co-varies with brain size (Edinger 1948; Benoit 2015; Kharlamova et al. 2016) and as such, a smooth endocast is often found in mammals with large absolute brain size, such as humans, cetaceans, proboscideans, ground sloths, *Arsinoitherium*, *Elasmotherium*, and *Paraceratherium* (Andrews 1906; Granger et al. 1936; Dechaseaux 1958; Milne-Edwards 1868; Gervais 1872; Jerison 1973). It may be hypothesized that the smaller brained proboscideans (e.g. *Phosphatherium* and *Eritherium*) (Gheerbrant et al. 2005; Gheerbrant 2009) may have had a visibly gyrencephalic endocast, although a visibly lissencephalic condition appears to be the most likely primitive condition (Benoit et al. 2013b). The endocast of *Moeritherium lyonsi* is lissencephalic (Jerison 1973). The Sirenia, which are the closest living relatives of elephants (Poulakakis and Stamatakis 2010; Kuntner et al. 2011) have, since the early Eocene, been observed to have visibly lissencephalic endocasts (Ronald et al. 1978; O’Shea and Reep 1990; Furusawa 2004; Benoit et al. 2013b; Orihuela et al. 2019). The brains and endocasts of the extant Sirenia are also lissencephalic for the most part (O’Shea and Reep 1990). A visibly lissencephalic endocast is also found in *Arsinoitherium* and *Desmostylus* (Andrews 1906; Edinger 1963, 1975), two extinct representatives of the orders

Embrithopoda and Desmostylia respectively, which also belong to the Tethytheria along with the sirenians and the proboscideans (Novacek and Wyss 1987; Seiffert 2007a; Asher 2007). As such, addressing the precise evolution of the gyral and sulcal pattern in extinct proboscideans is not tenable, except in the case of the well-preserved frozen brain tissue in *Mammuthus primigenius* (Kharlamova et al. 2016).

For more than 150 years, biologists and palaeobiologists have investigated the cranial cavity of frozen woolly mammoths from Siberia in order to study the soft brain tissue of this extinct species. As early as 1846 and 1904, Gleboff (1846) and Salensky (1904) respectively investigated the fleshy brain of *Mammuthus primigenius*, but they did not find anything more than a heavily decayed substance in place of the brain. Nonetheless, they could distinguish a distinct dura mater. Gleboff even depicted some identifiable neural cells that remained intact (Gleboff 1846: 111–119, plate VII). About one hundred years later, Kreps et al. (1979, 1981) recorded the presence of a large variety of lipids in the brain of various specimens of *Mammuthus primigenius* and again later, Vereschagin (1981, 1999) and Maschenko et al. (2013) provided the first descriptions of partly preserved neural tissues from a variety of frozen calves. Fisher et al. (2014) briefly described the first endocast of a well-preserved *Mammuthus primigenius* neonate, although endocasts of adult specimens had been known for a long time already (Simionescu and Morosan 1937; Kubacska 1944). Lastly, a very well-preserved brain of a juvenile *M. primigenius* has been thoroughly described (Kharlamova et al. 2015, 2016). The analysis of this approximately ten-year-old specimen, nicknamed Yuka, shows that the overall external morphology of the brain, including the sulcal pattern, is quite comparable to that of extant elephants. As in extant elephants, the whole brain surface is densely sulcated, the temporal lobe is disproportionately large and laterally expanded, the cerebellum is large, with a narrow vermis, and is widely exposed dorsally. This represents the first time that the anatomy of the *true* brain of an extinct species is described (Kharlamova et al. 2015, 2016).

15.4 Evolution of the Bony Labyrinth, Hearing, and Balance

15.4.1 Historical Review

The first detailed study of the ear region and bony labyrinth of an elephant dates back to 300 years ago (Blair 1710a, b, 1717). A hundred years later, the labyrinth of an elephant was described again by Fick (1844) and Hyrtl (1845). These early studies were completed by Watson (1874), Buck (1888, 1890), Richards (1890), and Eales (1926) who described several aspects of soft tissue anatomy, osteology, and ontogeny of the ear region and petrosal of the African and Asian elephants.

The study by Claudius (1865) of the bony labyrinth of *Deinotherium giganteum* was the first known attempt to describe the bony labyrinth of an extinct member of the Proboscidea (Fig. 15.6c). Apart from this, the bony labyrinth of extinct proboscideans has only been investigated in recent years. A natural endocast of the cochlear

canal of *Moeritherium* from the Eocene of Libya was briefly described by Tassy (1981) (Fig. 15.6b). A more complete study of a natural cast of the cochlear canal of *Numidotherium* from El Kohol (Algeria) (Fig. 15.6a) suggested that they were not adapted to low-frequency hearing (Court 1992), which was later confirmed by the CT-assisted study and digital reconstruction of a more complete bony labyrinth of *N. koholense* (Benoit et al. 2013c). The petrosal of *Moeritherium* was described in detail for the first time by Court (1994) as displaying an undivided perilymphatic foramen which demonstrated that this genus was more derived than *Numidotherium*. In 2013, Tassy provided the first detailed description of the petrosal of *Gomphotherium*

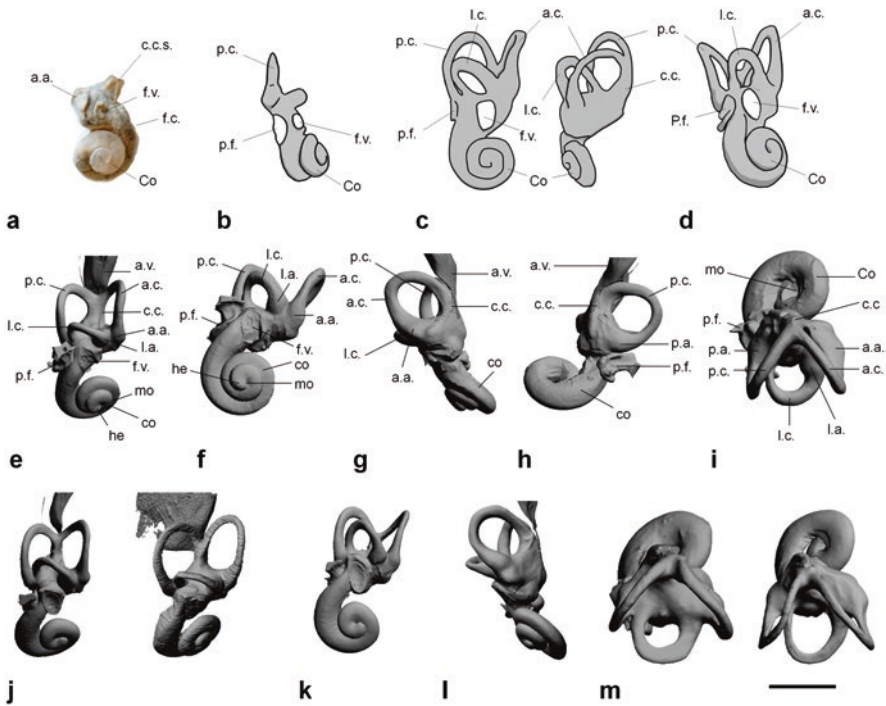


Fig. 15.6 The bony labyrinth of the Proboscidea. (a) natural cast of the cochlear canal of *Numidotherium* studied by Court (1992), (b) natural cast of the partial bony labyrinth of *Moeritherium* redrawn after Tassy (1981), (c) the bony labyrinth of *Deinotherium* in lateral and anterior views redrawn after Claudius (1865), (d) the bony labyrinth of an indeterminate elephant-timorph redrawn after Ekdale (2011), (e–i) the bony labyrinth of *Elephas maximus* MNHN.ZM.AC.1904-273 in lateral (e), ventral (f), anterior (g), posterior (h), and dorsal (i) views, (j) lateral view of the bony labyrinths of MNHN.ZM.AC.2008-71 and CEB130168, (k) ventral view of the bony labyrinth of MNHN.ZM.AC.2008-71, (l) anterior view of the bony labyrinth of MNHN.ZM.AC.2008-81, (m) dorsal view of the bony labyrinths MNHN.ZM.AC.1956-194 and MNHN.ZM.AC.1957-465, illustrating the variability of the bony labyrinth in modern elephants. Abbreviations: a.a. anterior ampulla, a.c. anterior semicircular canal, a.v. aquaeductus vestibuli, c.c. crus commune, co cochlear canal, f.v. fenestra vestibuli, he helicotrema, l.a. lateral ampulla, l.c. lateral semicircular canal, mo modiolus (apical lacuna), p.a. posterior ampulla, p.c. posterior semicircular canal, p.f. perilymphatic foramen. Scale bar = 1 cm

angustidens. The development and increasing use of CT-scanning techniques paved the way for further study of extinct proboscideans, starting with the dwarf elephant *Palaeoloxodon tiliensis* (Provatidis et al. 2011), although these authors did not focus their study on the ear region. The first thorough CT study and 3D reconstruction of the bony labyrinth of an extinct proboscidean were performed by Ekdale (2011) on an isolated petrosal (presumably *Mammuthus* or *Mammut*) from Texas (Fig. 15.6d). The bony labyrinths of *Numidotherium* and *Arsinoitherium* studied by Benoit et al. (2013c) later evidenced the convergent evolution of low-frequency hearing in elephantiforms and embrithopods. Further studies of the basal “plesiephantiforms” *Eritherium* and *Phosphatherium* later refined the understanding of early proboscidean labyrinthine evolution (Schmitt and Gheerbrant 2016).

As is evident from this historical review, only a handful of proboscidean bony labyrinths has been described and published. The main objective of this work is thus to provide the first comprehensive description of morphological variations and evolution of the bony labyrinth in modern elephants, including *Elephas maximus*, *Loxodonta cyclotis*, and *L. africana* and 14 genera of extinct proboscideans (*Eritherium azzouorum*, *Phosphatherium escuilliei*, *Numidotherium koholense*, *Moeritherium lyonsi*, *M. cf. lyonsi*, *M. trigodon*, *Prodeinotherium bavaricum*, *Deinotherium giganteum*, *Mammut americanum*, *Gomphotherium angustidens*, *Cuvieronius* sp., *Stegomastodon* sp., *Platybelodon grangeri*, *Anancus arvernensis*, *Stegodon orientalis*, and *Palaeoloxodon antiquus*) using published data, CT scanning, manual segmentation, 3D reconstructions, and measurements (see details in the Online Supplementary Material). This increases the number of proboscidean taxa for which the bony labyrinth is documented from six (including Ekdale’s (2011) unidentified elephantimorph and Claudius’ (1865) *Deinotherium*) to seventeen. The petrosal and bony labyrinth of *Palaeoloxodon tiliensis* were described too recently to be considered here, but their morphology is almost identical to that of modern elephants (Liakopoulou et al. 2021).

15.4.2 Bony Labyrinth Anatomy of Extant Elephants

The petrosal and bony labyrinth of modern elephants show no clear distinctive features between genera or species (Tables 15.2 and 15.3). In general, the semicircular canals of extant elephants appear stocky and thick compared to other mammals (Fig. 15.6e–i). They are flattened in cross-section, a feature previously observed in *Arsinoitherium* (Benoit et al. 2013c). In general, the semicircular canals appear flatter in *Loxodonta*. The average semicircular canals thickness ratio tends to be higher in *Elephas* than in *Loxodonta*, but this character strongly varies intraspecifically (see Table 15.2). The angles between semicircular canals show great variability but usually, the most acute angle is between the anterior and lateral semicircular canals, whereas the most obtuse angle is between the posterior and lateral canals (Table 15.2). The ampullae of the canals are poorly defined, as the distinction

Table 15.2 Measurements of the semicircular canals of extant elephants

	Crus commune length (mm)	Crus commune section radius (mm)	Crus commune thickness ratio	ASC length (mm)	PSC length (mm)	LSC length (mm)	SCC average thickness ratio	Angle ASC-PSC (°)	Angle ASC-LSC (°)	Angle LSC-PSC (°)	ASC radius of curvature	PSC radius of curvature	LSC radius of curvature
<i>Elephas</i> 1904-273	7.11	1.51	21.19	22.45	22.44	20.33	4.64	72.6	75.7	88.8	5.25	5.20	3.16
<i>Elephas</i> 1941-209	5.58	1.20	21.53	22.79	22.49	23.06	4.13	76.5	74.2	83.2	5.19	5.23	3.52
<i>Elephas</i> 2008-81	6.53	1.48	22.62	26.66	24.56	26.07	3.52	76.6	75.0	85.8	5.97	5.60	4.06
<i>Elephas</i> CEB150009	3.07	1.51	49.20	23.47	21.01	24.10	4.86	78.9	67.9	85.7	5.04	4.65	3.65
<i>Loxodonta</i> 1932-523	5.47	1.38	25.26	24.99	23.65	21.26	3.02	70.9	72.4	85.8	5.66	5.37	3.21
<i>Loxodonta</i> 2008-71 (average)	5.63	1.13	20.09	22.49	22.31	22.54	3.90	75.9	59.8	83.5	5.18	5.14	3.56
<i>L. africana</i> 1861-53	5.50	1.82	27.27	27.42	24.36	21.04	3.57	81.1	73.8	82.2	5.86	5.25	3.54
<i>L. africana</i> CEB130168	4.05	1.51	37.23	27.44	25.40	24.07	3.28	84.8	72.7	78.0	5.80	5.55	3.72
<i>L. cyclotis</i> 1950-728	5.89	1.64	27.87	23.85	21.40	21.06	3.69	83.3	72.3	88.5	5.41	4.91	3.35
<i>L. cyclotis</i> 1956-194	5.37	1.57	29.20	31.98	29.92	23.44	2.74	76.7	72.9	93.8	6.87	6.25	4.09
<i>L. cyclotis</i> 1957-465	4.84	1.94	40.15	23.99	21.88	20.50	4.01	74.7	80.0	85.0	5.48	4.98	3.15
<i>L. cyclotis</i> 1961-69	4.46	1.40	31.33	22.30	20.61	21.16	4.77	80.9	68.1	80.6	5.06	4.78	3.37

Abbreviations: ASC anterior semicircular canal, LSC lateral semicircular canal, PSC posterior semicircular canal, SCC semicircular canals

Table 15.3 Measurements of the cochlear canal of extant elephants

Specimens	Number of turns	Coiling (°)	Length (mm)	Aspect ratio	Radii ratio (Manoussaki et al. 2008)
<i>Elephas</i> 1904-273	2.375	855	74.13	0.38	7.16
<i>Elephas</i> 1941-209	2.375	855	80.46	0.38	6.18
<i>Elephas</i> 2008-81	2.375	855	80.28	0.43	6.88
<i>Elephas</i> CEB 150009	2.25	810	73.11	0.36	5.95
<i>Loxodonta</i> sp 1932-523	2.25	810	77.13	0.41	6.82
<i>Loxodonta</i> sp 2008-71 (average)	1.81	653	67.92	0.32	6.90
Left ear	2.00	720	73.61	0.34	6.33
Right ear	1.625	585	62.18	0.30	7.47
<i>Loxodonta africana</i> 1861-53	2.375	855	71.54	0.45	7.38
<i>Loxodonta africana</i> CEB130168	2	720	70.84	0.37	6.50
<i>Loxodonta cyclotis</i> 1950-728	2.25	810	69.16	0.40	8.47
<i>Loxodonta cyclotis</i> 1956-194	2.625	945	74.16	0.40	8.85
<i>Loxodonta cyclotis</i> 1957-465	2.625	945	79.03	0.44	5.35
<i>Loxodonta cyclotis</i> 1961-69	2.625	945	81.55	0.44	8.23

between a canal and the swelling of the corresponding ampulla is poorly marked, unlike in most mammals (Fig. 15.6e–i). In both genera, the anterior semicircular canal is oval in anterior view (Fig. 15.6g) and the posterior one is circular in posterior view (Fig. 15.6h). Compared to other mammals, the lateral canal appears shorter and smaller than the two vertical canals (Fig. 15.6i). Unlike the vertical canals, the shape of the lateral semicircular canal in dorsal view varies greatly, from oval to almost circular between specimens of the same species. The lateral canal is also the one that shows the most variation in deviation from planarity (Fig. 15.6j), whereas the anterior and posterior canals do not undulate. The average values of the radii of curvature are similar between *Elephas* and *Loxodonta* (respectively 5.4 mm and 5.7 mm for the anterior canal, 5.2 mm and 5.3 mm for the posterior canal and 3.6 mm and 3.5 mm for the lateral canal on average). In general, the radii in *Elephas* are less variable than in *Loxodonta* (Table 15.2). In both genera, the anterior canal is consistently larger than the posterior one in terms of radii of curvature and length (Table 15.2). The dorsal apex of the anterior canal projects higher than that of the posterior canal (Fig. 15.6e, j). The point of entry of the lateral canal into the vestibule is located low and close to the posterior ampulla, but there is usually no secondary common crus (Fig. 15.6e, j), except a short one in two specimens of *Elephas* (MNHN.AC.ZM.1904-273 and 2008-81) and one of *Loxodonta* (MNHN.AC.ZM.2008-71). The crus commune is usually stocky in elephants but may appear slightly more elongated and slender in some specimens of *Loxodonta*. Many

specimens exhibit bumps and ridges on their crus commune (Fig. 15.6g, h, l) that seem to occur randomly. They may represent ossification scars or grooves that contained blood vessels in life (although this last hypothesis seems unlikely as specimen CEB150009 shows no blood vessels preserved in this area). Similar ridges are also present in some extinct proboscideans and *Arsinoitherium* (Benoit et al. 2013c).

The stapedia ratio varies greatly in elephants from a rather rounded *fenestra vestibuli* (1.53) to a rather oval one (1.83). This is consistent with the extreme values that Ekdale (2011) found in a large sample of Pleistocene elephantimorphs (1.4 to 2.1). On the cochlear canal, the secondary bony lamina (*lamina secundaria*) is absent in both genera (Fig. 15.6g, h). This is interpreted as an adaptation to low-frequency hearing since the absence of a secondary bony lamina widens the basilar membrane, making it less stiff and therefore more sensitive to low frequencies (Court 1992; Ketten 1992; Meng et al. 1997). Elephants are known to have the lowest low-frequency hearing limit of all extant terrestrial mammals (17Hz at 60dB in *Elephas*, Manoussaki et al. 2008), which aligns well with the infrasound they can produce by both vocalization (20Hz) and foot-drumming (10 to 40Hz) (Payne et al. 1986; Poole et al. 1988, 2005; O'Connell-Rodwell et al. 2001, 2007; Günther et al. 2004; O'Connell-Rodwell 2007; Nair et al. 2009; Stoeger et al. 2011; Stoeger and Manger 2014). The radii ratio of the cochlear canal (the quotient between the radius of the basal turn over that of the apical turn) is between 5.35 and 8.85, which is consistent with low-frequency hearing (Manoussaki et al. 2008). The average relative volume of the cochlear canal is the same between *Elephas* and *Loxodonta* (respectively 47.7% and 47.0%). Viewed in profile, the cochlear canal appears planispiral (Fig 15.6g) and both genera share the same mean aspect ratios (0.39). The aspect ratio of the cochlear canal varies within species but remains between 0.30 and 0.45 (Table 15.3).

The number of turns of the cochlea is not a constant feature in extant elephants as it varies from less than two to almost three full turns (Table 15.3 and Fig. 15.6f, j, k); it varies less in *Elephas* than in *Loxodonta* (Table 15.3). Noticeably, specimen MNHN.ZM.AC.2008-71 displays the smallest number of turns in the right ear (1.625 turns, 585°), but two turns (720°) in the left ear (Table 15.3). In contrast, the relative volume of the cochlear canal seems to be quite conservative in extant elephants as it varies mostly around 50% of the total volume of the bony labyrinth (except in specimens MNHN.ZM.AC.1956-194 and MNHN.ZM.AC.1957-465, in which it is 39.5% and 43.4% respectively, Table 15.3).

15.4.3 Evolution of the Ear Region and Bony Labyrinth in Proboscidea

To reconstruct the evolutionary history of the bony labyrinth in Proboscidea, we mapped ear region characters on a phylogenetic tree of proboscideans (Fig. 15.7). The consensus tree used to map the characters is a synthesis of Tassy (1994), Shoshani and Tassy (1996), Shoshani (1998), and Fisher (2018). The character

matrix, originally designed for phylogenetic analysis at the scale of the superorder Afrotheria (Schmitt 2016), includes 12 petrosal characters and 20 bony labyrinth characters (Online Supplementary Material).

Basal Proboscideans

The ear region morphotype of extant elephants was not acquired at the evolutionary root of the Proboscidea clade, but gradually during the evolutionary history of the Proboscidea (Fig. 15.7). Compared to modern proboscideans, *Eritherium* and *Phosphatherium* display a primitively slender and unspecialized vestibular morphology common to basal Paenungulata (Gheerbrant et al. 2014; Benoit et al. 2013a, 2016; Schmitt and Gheerbrant 2016), i.e. the outline of their semicircular canals form a circle, their cross-section is round, the lateral semicircular canal is long, the anterior semicircular canal does not project dorsally, the ampullae are well defined, the *crus commune* is slender (Table 15.4), and a secondary common crus (*crus commune secundaria*) is present (Figs. 15.8, 15.9, 15.10, 15.11 and 15.12). The secondary common crus is short in *Eritherium*, but is longer in *Phosphatherium*, *Numidotherium*, and is likely present and short in *Moeritherium* (Figs. 15.8, 15.9, 15.10, 15.11 and 15.12). The presence of a secondary common crus is generally considered plesiomorphic for Eutheria (Ekdale 2013) and Afrotheria (Benoit et al. 2013a, 2015). However, a secondary common crus is absent and the lateral canal enters the posterior ampulla in the oldest and basal-most paenungulate *Ocepeia daouiensis* (Gheerbrant et al. 2014) and the basal hyracoid *Seggeurius* (Benoit et al. 2016) (a condition also found in *Mammut*, *Palaeoloxodon*, *Platybelodon* and some specimens of *Loxodonta* among more derived proboscideans, Figs. 15.8, 15.9, 15.10, 15.11 and 15.12), which makes the polarity of this character uncertain for paenungulates. Since a secondary common crus is consistently present in the basal-most proboscideans as well as in basal sirenians (Benoit et al. 2013a), it appears reasonable to consider its presence plesiomorphic for Proboscidea.

Eritherium exhibits the most slender semicircular canals (thickness ratio of 1.08, Table 15.5), whereas the canals in *Phosphatherium* and *Numidotherium* are slightly thicker (thickness ratio of 2.24 and 2.16 respectively), but still relatively more slender than in *Prodeinotherium* (thickness ratio of 2.82) and the Elephantimorpha (thickness ratio around or 3.00 and up to 4.86). It appears that the semicircular canals of proboscideans were primitively thin and became progressively thicker during their evolutionary history. This is supported by comparisons with *Ocepeia* (Gheerbrant et al. 2014), the early sirenians *Prorastomus* and that from Chambi (Benoit et al. 2013a), the basal hyracoid *Seggeurius* (Benoit et al. 2016) and the basal embrithopod *Stylolophus* (Gheerbrant et al. 2021), which all exhibit slender semicircular canals. Additionally, *Eritherium*, *Phosphatherium*, and *Numidotherium* display well-defined and bulbous ampullae, which contrasts with the poorly defined ampullae of more derived proboscideans (Figs. 15.8, 15.9, 15.10, 15.11 and 15.12). The condition in *Moeritherium* is unclear from the CT scan (Figs. 15.8, 15.9, 15.10, 15.11 and 15.12d), but judging from Tassy's (1981) figure, the ampullae appear

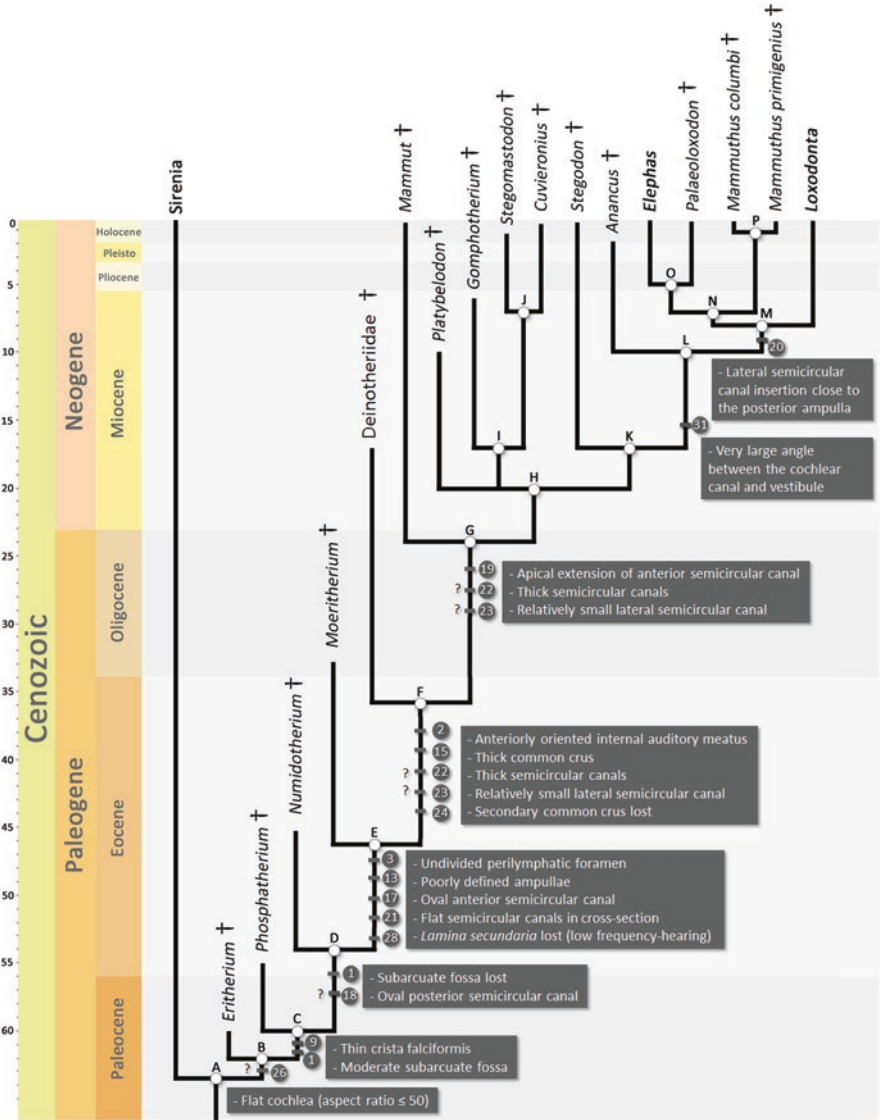


Fig. 15.7 Summary of the principal evolutionary changes of the ear region of the Proboscidea. Only taxa studied in this work are represented. Clades: (A) Tethytheria, (B) Proboscidea, (C, D, E, F) Unnamed clades, (G) Elephantimorpha, (H) Elephantida, (I, J, K, L) Unnamed clades (M) Elephantidae, (N) Elephantini, (O) Unnamed clade, (P) *Mammuthus* genus. Phylogeny and time range after Tassy (1994), Shoshani and Tassy (1996), Shoshani (1998), Shauer (2010), and Fisher (2018)

poorly defined, as in more derived proboscideans (Fig. 15.7). In basal paenungulates such as *Ocepeia* (Gheerbrant et al. 2014), *Seggeurius* (Benoit et al. 2016), *Prorastomus* and the sirenian from Chambi (Benoit et al. 2013a), and *Arsinoitherium*

(Benoit et al. 2013c), the ampullae are well defined too, which indicates that the condition in *Eritherium*, *Phosphatherium*, and *Numidotherium* is plesiomorphic.

The *fenestra cochleae* and cochlear aqueduct are separated in *Eritherium*, as in *Phosphatherium*, and *Numidotherium* (Figs. 15.8 and 15.10). On the cochlear canal, there is a well-defined secondary bony lamina that expands on the $\frac{3}{4}$ turn of the cochlear canal in *Eritherium* and the $\frac{1}{2}$ turn in *Phosphatherium* (Figs. 15.10 and 15.11a, b). The cochlear canal makes two full turns in *Eritherium* (Table 15.4; not preserved in *Phosphatherium*). The basal turn of the cochlear canal is especially thick in *Phosphatherium* (Fig. 15.10b), resulting in a high cochlear volume (69% of the bony labyrinth volume). This is similar to *Ocepeia*, in which the cochlear canal represents about two-thirds of the total volume of the bony labyrinth (Table 15.4). In contrast, *Eritherium* and every other proboscidean have a vestibular canal contributing about 50% of the labyrinthine volume or less (Table 15.4), which suggests that the condition in *Phosphatherium* might be autapomorphic. An apical lacuna for the modiolus is present in most “plesielephantiformes”, except *Deinotherium* (Claudius 1865) and one specimen of *Numidotherium* (Court 1992) (Fig. 15.9). This character may be considered plesiomorphic for proboscideans given its presence in *Ocepeia* (Gheerbrant et al. 2014); however, it is very variable in modern elephants, which prevents any definitive conclusion.

The cochlear aspect ratio is remarkably low in *Eritherium* (0.35, Table 15.4), which indicates a rather flat cochlea. A cochlear canal with a high aspect ratio (>0.6 , character 26) seems to be plesiomorphic for Paenungulata. The “condylarthran” *Ocepeia*, and the basal sirenian from Chambi both have a rather high aspect ratio (0.72 and 0.67 respectively) (Benoit et al. 2013a; Gheerbrant et al. 2014). In contrast, the aspect ratio is consistently low (always inferior to 0.6) in all studied proboscideans preserving a complete cochlear canal (Table 15.4). A rather flat cochlear canal may thus constitute a synapomorphy of the Proboscidea; however, it should be noted that the basal hyracoid *Seggeurius* (Benoit et al. 2016) and the basal sirenian *Prorastomus* (Benoit et al. 2013a) both have low cochlear aspect ratios (0.48 and 0.34 respectively). This casts some doubts about the polarity of this character and, in addition to the plesiomorphic aspect of the bony labyrinth of *Eritherium*, suggests that the origin of proboscideans may not have been accompanied by any unambiguous inner ear synapomorphies (Fig. 15.7).

While *Eritherium* exhibits a generalized morphology similar to more basal Paenungulata, *Phosphatherium* already displays a few proboscidean features: in the unnamed node C (Fig. 15.7) the *crista falciformis* becomes thinner and deeply embedded in the external auditory meatus (character 9) as in *Numidotherium* and more derived taxa (node D) (Court 1994; Benoit et al. 2013c), and the subarcuate fossa (character 1) becomes less deep before becoming shallow or absent at node E (Fig. 15.7). This last character change may seem surprising, as a shallow subarcuate fossa has long been recognized as a derived feature shared by Paenungulata (Novacek and Wyss 1986). Nevertheless, recent findings of a deep subarcuate fossa in *Eritherium* and the basal paenungulate *Ocepeia* (Gheerbrant et al. 2014; Schmitt and Gheerbrant 2016), and that of a moderately deep one in the hyracoid *Seggeurius*, the basal sirenian from Chambi and *Phosphatherium* (Gheerbrant et al. 2005; Benoit

Table 15.4 Measurements of the bony labyrinth of fossil proboscideans and outgroups

	Volume			Cochlea					Cris commune				Angles		
	Bony labyrinth volume (mm ³)	Cochlea volume (mm ³)	Relative volume of the cochlea (%)	Stapedial ratio	Number of turns of cochlea	Aspect ratio of the cochlea	Length of the cochlea (mm)	Radii ratio (after Manoussaki et al., 2008)	Cris commune length (mm)	Cris commune average section radius (mm)	Cris commune average thickness ratio	Angle between the ASC and the PSC (°)	Angle between the ASC and the LSC (°)	Angle between the LSC and the PSC (°)	Vestibulo-cochlear angle (°)
<i>Oreopelia daouienensis</i> MNHN-PM45	17.5	11.7	66	2.05	2.13	0.72	19.2	3.47	1.75	0.30	17.4	91.6	80.1	87.8	102
<i>Sylolophus</i> MNHN-PM53	?	?	?	?	?	?	?	?	3.92	0.53	13.7	86.0	83.4	98.6	?
<i>Ananias arvernensis</i> NMNHS.FM2991A	934.6	468.3	50	1.7	2.5	0.43	72.3	7.03	5.11	1.06	20.8	90.5	58.2	77.6	150
<i>Ananias arvernensis</i> NMNHS.FM2991B	?	?	?	?	?	?	?	?	6.70	1.34	20.1	81.0	58.9	78.0	?
<i>Ananias arvernensis</i> NMNHS.FM2991C	957.5e	442.2e	46e	1.6	2.5	0.41	?	7.36	3.28	1.32	40.4	79.8	63.8	81.3	166
<i>Ananias arvernensis</i> NMNHS.FM2991D	1151e	539.3e	47e	1.7	2.5	0.37	78e	7.24	4.58	1.64	35.8	92.4	70.4	81.2	154
<i>Ananias arvernensis</i> NMNHS.FM2991E	1440.5	701.8	49	1.6	2.5	0.37	80.1	7.22	6.39	1.38	21.7	87.5	70.4	87.9	145
<i>Ananias arvernensis</i> NMNHS.FM2991F	1215e	502.1e	41e	1.8	2.5	0.47	78e	9	7.23	1.33	18.4	88.6	68.9	80.5	150
<i>Ananias arvernensis</i> NMNHS.FM2991G	933.9e	394.1e	42e	1.6	>2.5	0.45	73e	?	6.04	1.23	20.3	78.5	64.6	79.7	147
<i>Cuvieronius</i> sp FM103247	?	?	?	?	?	?	?	?	9.52	1.65	17.4	82.1	77.4	85.5	?
<i>Erethium azouzeorum</i> MNHN-PM88	11.22	5.91	53	1.57	2	0.35	16.8	3.10	2.33	0.27	11.46	93.8	83.5	91.4	117
<i>Gomphotherium angustidens</i> CBar coll. V2	988.3	497.0	50	1.5	2.63	0.47	90.1	6.65	8.73	1.24	14.2	79.2	67.8	85.3	132

<i>Gomphotherium angustidens</i> SEP38	814.4	400.2	49	1.5	2.38	0.47	69.3	5.72	6.82	1.27	18.7	85.7	72.8	91.1	120
<i>Mammuth americanum</i> AMNH-FM14293A	936.3	343.1	37e	?	2.38	0.44	68.0	?	7.74	1.18	15.2	86.5	68.8	81.4	153
<i>Mammuth americanum</i> AMNH-FM14293B	?	?	?	?	?	?	?	?	7.21	1.55	21.6	80.5	65.1	80.9	?
<i>Mammuthus columbi</i> FM1-44658	?	?	?	?	?	?	?	?	5.23	1.41	27	76.6	73.3	87.2	?
<i>Mammuthus primigenius</i> MNHN.F.1904-12	1131	480.1	42	?	2.25	0.46	67.6	8.02	5.57	1.42	25.5	68.6	71.4	88.0	148
<i>Moeritherium</i> 68436	?	?	?	?	1.5e	?	?	?	?	?	?	?	?	?	?
<i>Numidotherium kohlense</i> UM-UOK5	84.4	35.1	42	?	1.5	0.48	27.1	2.88	4.50	0.67	14.9	78.0	75.5	96.1	128
<i>Palaeoloxodon antiquus</i> M82706	?	?	?	?	?	?	?	?	6.35	1.41	22.2	77.1	76.2	92.6	?
<i>Phosphatherium escuilliei</i> MNHN.F.FM17	32.54	22.38	69	1.62	>1	>0.41	?	?	2.56	0.32	12.45	85.6	77.1	89.7	102
<i>Platybelodon grangeri</i> 26S64 (824+)	854.5	373.8	44	?	2	0.41	56.8	?	4.20	1.17	27.9	73.9	67.4	98.8	132
<i>Prodeinotherium bavaricum</i> 2013.01108E	674.4	322.1	48e	?	2.25	0.29	?	6.75	5.91	1.26	21.4	77.2	67.6	90.7	132
<i>Stegodon orientalis</i> FM18632	1117.5	507.8	45	?	2	0.50	68.7	6.74	5.34	1.37	25.7	108	74.9	94.0	122
<i>Stegomastodon</i> sp FM21807	?	530	?	?	2	0.45	65.8	7.04	6.67	1.29	19.4	96.6	?	?	139

Abbreviations: ASC anterior semicircular canal, LSC lateral semicircular canal, PSC posterior semicircular canal

et al. 2013c, 2016) now makes the presence of a rather deep subarcuate fossa the plesiomorphic condition at the root of the Proboscidea clade without ambiguity.

In *Numidotherium* and more derived species (Clade D), the subarcuate fossa is lost (character 1) and the posterior semicircular canal defines a more oval space (character 18, although this character is quite variable). The petrosal of *Numidotherium* is unique as its *pars cochlearis* is excavated by a transpromontory sulcus (Court and Jaeger 1991; Benoit et al. 2013c) for the internal carotid artery (van der Klaauw 1931; Wible 1986). A transpromontorial (or lateral) course of the internal carotid artery is considered primitive for Placentalia (Wible 1986), whereas the derived condition (a medial or perbullar course) is documented or reconstructed based on the absence of a transpromontory sulcus in every other extant and extinct proboscidean, sirenian and hyracoid currently known, including *Eritherium* and *Phosphatherium* (Blair 1717; van der Klaauw 1931; Wible 1986; Fischer 1990, 1992; Court 1990, 1994; Court and Jaeger 1991; Gheerbrant et al. 2005; Ekdale 2011; Benoit et al. 2013a, 2015, 2016; Tassy 2013). *Ocepeia* and *Numidotherium* are the only known paenungulates in which a transpromontory sulcus is present (Court and Jaeger 1991; Benoit et al. 2013c; Gheerbrant et al. 2014), suggesting that this feature is not homologous in the two taxa and better interpreted as a homoplasy.

In *Moeritherium* and more derived proboscideans (node E) the anterior semicircular canal becomes more oval (Fig. 15.10d) (character 17). As stated above, the semicircular canals (particularly the anterior one) were all rounded in *Eritherium* and *Phosphatherium* (Fig. 15.10a–c), as well as in *Ocepeia* (Gheerbrant et al. 2014), the fossil hyracoid *Seggeurius* (Benoit et al. 2016), embrithopods (*Arsinoitherium* and *Stylolophus*; Benoit et al. 2013c; Gheerbrant et al. 2021), and *Prorastomus* and the sirenian from Chambi (Benoit et al. 2013a). *Moeritherium*, the Deinotheriidae, and more derived proboscideans also differ from more basal “plesielephantiforms” by the flattening of the semicircular canals in cross-section (character 21), the poorly defined ampullae (character 13), the loss of the *lamina secundaria* (character 28), and the fusion of the *aquaeductus cochleae* and the *fenestra cochleae* to form the perilymphatic canal (character 3). The paedomorphic retention of a single perilymphatic foramen during ontogeny instead of separated *fenestra cochleae* and *aquaeductus cochleae* is a derived feature encountered in extant elephants and sirenians (Fischer 1990). Such a single perilymphatic foramen is present in *Moeritherium*

←
Fig. 15.8 (continued) mirrored), (j) *Gomphotherium angustidens* (MNHN.F.SEP38), (k) *Cuvieronius* sp. (FM103247, mirrored), (l) *Stegomastodon* sp. (FM21807, mirrored), (m) *Platybelodon grangeri* (MNHN 26564-824+), (n) *Anancus arvernensis* (NMNHS.FM2991A), (o) *Anancus arvernensis* (NMNHS.FM2991B), (p) *Anancus arvernensis* (NMNHS.FM2991C, mirrored), (q) *Anancus arvernensis* (NMNHS.FM2991D, mirrored), (r) *Anancus arvernensis* (NMNHS.FM2991E, mirrored), (s) *Anancus arvernensis* (NMNHS.FM2991F, mirrored), (t) *Anancus arvernensis* (NMNHS.FM2991G), (u) *Stegodon orientalis* (FM18632), (v) *Mammuthus primigenius* (MNHN.F.1904-12), (w) *Mammuthus columbi* (FM144658), (x) *Mammuthus columbi* (FM144658, mirrored), (y) *Palaeoloxodon antiquus* (M82706, mirrored). Scale bar = 1 cm. Abbreviations: *a.a.* anterior ampulla, *a.c.* anterior semicircular canal, *a.v.* aquaeductus vestibuli, *aq aquaeductus cochleae*, *c.c.* crus commune, *c.c.r.* crus commune ridge, *c.c.s.* crus commune secundaria, *co* cochlear canal, *f.c.* fenestra cochleae, *f.v.* fenestra vestibuli, *l.a.* lateral ampulla, *l.c.* lateral semicircular canal, *p.a.* posterior ampulla, *p.c.* posterior semicircular canal, *p.f.* perilymphatic foramen

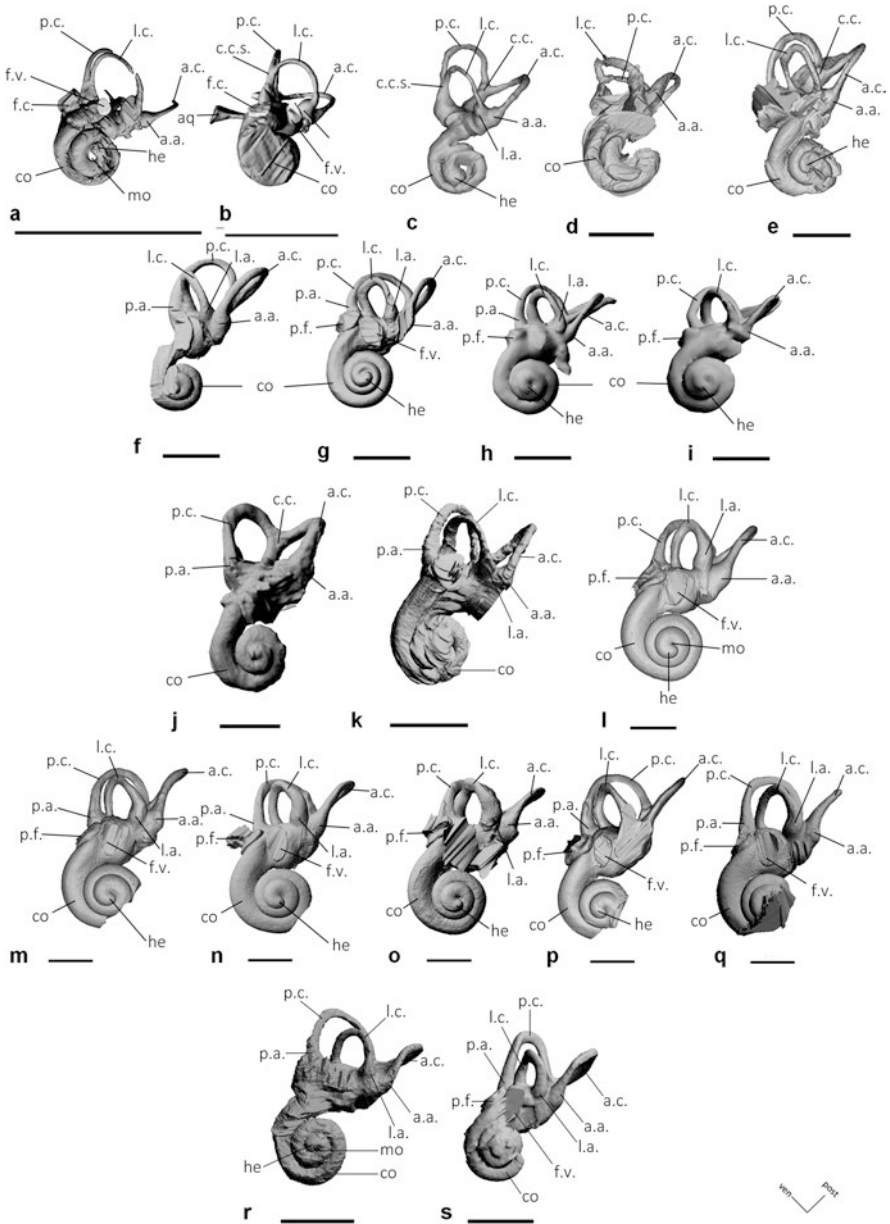


Fig. 15.9 3D reconstructions of the bony labyrinths of fossil proboscideans in ventral view. (a) *Eriitherium azzouzor* (MNHN-PM88), (b) *Phosphatherium esculliei* (MNHN.F PM17), (c) *Numidotherium koholense* (UM-UOK5, mirrored), (d) *Moeritherium* sp. (68436, mirrored), (e) *Prodeinotherium bavaricum* (MNHN 2013.01108E), (f) *Mammuth americanum* (AMNH-FM14293A, mirrored), (g) *Gomphotherium angustidens* (MNHN CBar coll. V2, mirrored), (h) *Gomphotherium angustidens* (MNHN.F.SEP38, mirrored), (i) *Gomphotherium angustidens* (MNHN.F.SEP38), (j) *Stegomastodon* sp. (FM21807, mirrored), (k) *Platybelodon grangeri*

(Court 1994), *Prodeinotherium*, and all elephantimorphs studied here (Figs. 15.8, 15.9, 15.10, 15.11 and 15.12), as well as in the embrithopod *Arsinoitherium* and was previously considered a synapomorphy of the clade Tethytheria (Fischer 1990; Court and Jaeger 1991). In contrast, the basal “plesiephantiforms” *Eritherium*, *Phosphatherium*, and *Numidotherium*, the basal sirenians *Prorastomus* and the unidentified specimen from Chambi all display a cochlear fenestra separated from the aqueduct (Court and Jaeger 1991; Benoit et al. 2013a, c; Schmitt and Gheerbrant 2016). As the separated condition is plesiomorphic for placental mammals (Court and Jaeger 1991; Ekdale 2011), the single perilymphatic foramen condition most likely evolved in a convergent manner in derived Proboscidea, Embrithopoda and Sirenia (Court 1990; Court and Jaeger 1991; Benoit et al. 2013a, c). Court and Jaeger (1991) hypothesized that it could be the result of independent adaptations to low-frequency hearing in Proboscidea and Sirenia (see below).

The Evolution of Low-Frequency Hearing

Both elephants (Manoussaki et al. 2008) and sirenians (Ketten et al. 1992; Gaspard et al. 2012) exhibit adaptations allowing low-frequency hearing; however, low-frequency hearing might not be primitive for paenungulates as *Ocepeia*, hyracoids, *Prorastomus*, the basal embrithopod *Stylolophus*, and basal proboscideans all possess a secondary bony lamina (or *lamina secundaria*) that narrows and stiffens the basilar membrane at the base of the cochlear canal, making it more sensitive to high frequencies (West 1985; Court 1992; Ketten 1992; Meng et al. 1997; Benoit et al. 2013a, 2016; Gheerbrant et al. 2014; Schmitt and Gheerbrant 2016; Ekdale 2016). *Numidotherium* differs from other “plesiephantiforms” by its lower number of cochlear turns. Most proboscideans display a cochlear canal making a least two full turns (Table 15.4) but those of the two specimens of *Numidotherium* examined here only complete 1.5 and 1.62 turns. The cochlear canal of the specimen described by Court (1992) also completes 1.5 turns (Fig. 15.6a). Thus, although this feature appears extremely variable in modern elephants, it seems stable in *Numidotherium*. As the basilar membrane becomes wider in the apical turns of the cochlea, it becomes more sensitive to low-frequency sounds (West 1985; Ketten et al. 1992). The low number of turns of the cochlear canal in *Numidotherium* might then reflect poorly developed low-frequency hearing. This is supported by the presence of a

←
Fig. 15.9 (continued) (MNHN 26564-824+), (l) *Anancus arvernensis* (NMNHS.FM2991A), (m) *Anancus arvernensis* (NMNHS.FM2991C, mirrored), (n) *Anancus arvernensis* (NMNHS.FM2991D, mirrored), (o) *Anancus arvernensis* (NMNHS.FM2991E, mirrored), (p) *Anancus arvernensis* (NMNHS.FM2991F, mirrored), (q) *Anancus arvernensis* (NMNHS.FM2991G), (r) *Stegodon orientalis* (FM18632), (s) *Mammuthus primigenius* (MNHN.F.1904-12). Scale bar = 1 cm. Abbreviations: *a.a* anterior ampulla, *a.c.* anterior semicircular canal, *a.v.* aquaeductus vestibuli, *aq* aquaeductus cochleae, *c.c.* *crus commune*, *c.c.r.* *crus commune* ridge, *c.c.s.* *crus commune secundaria*, *co* cochlear canal, *f.c.* fenestra cochleae, *f.v.* fenestra vestibuli, *l.a.* lateral ampulla, *l.c.* lateral semicircular canal, *p.a.* posterior ampulla, *p.c.* posterior semicircular canal, *p.f.* perilymphatic foramen

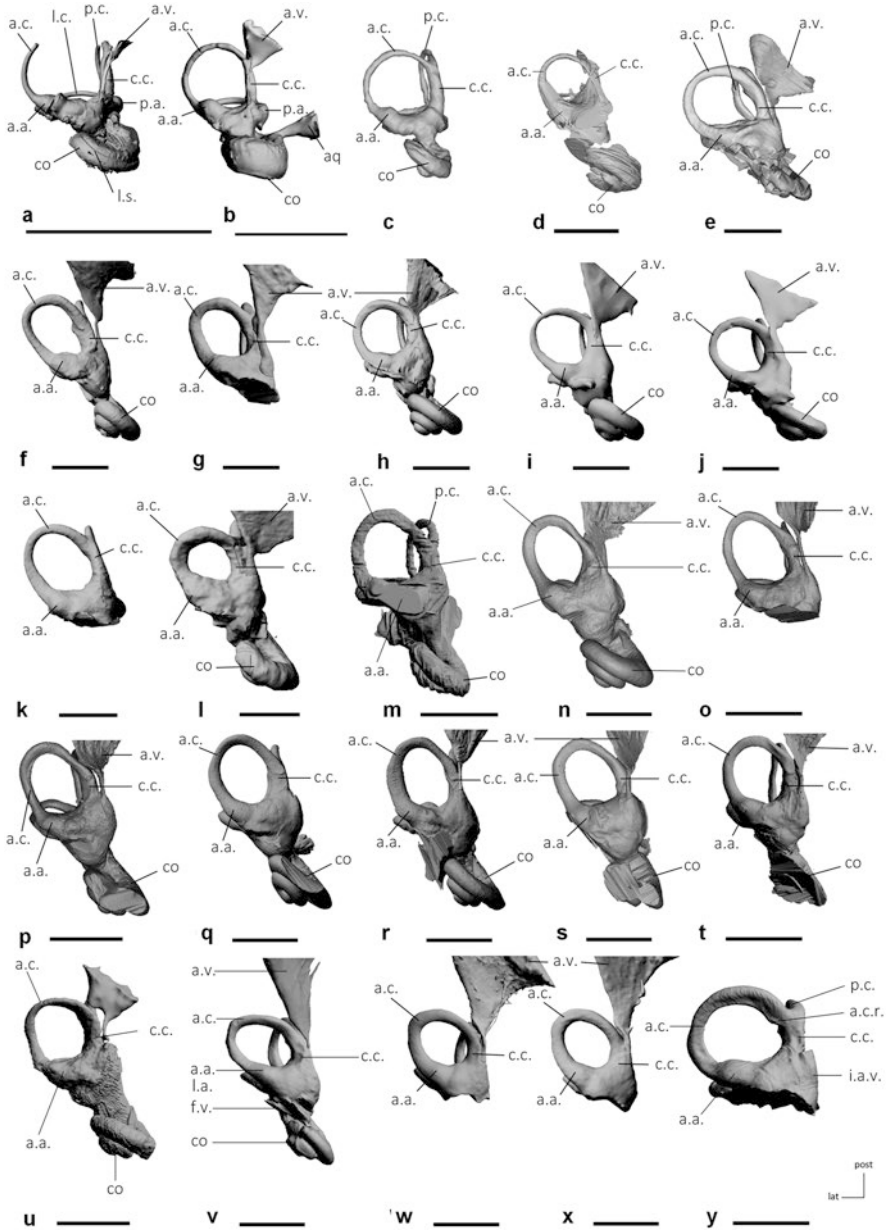


Fig. 15.10 3D reconstructions of the bony labyrinths of fossil proboscideans in anterior view. (a) *Eritherium azouzorum* (MNHN-PM88), (b) *Phosphatherium escuilliei* (MNHN.F PM17), (c) *Numidotherium koholense* (UM-UOK5, mirrored), (d) *Moeritherium* sp. (68436, mirrored), (e) *Prodeinotherium bavaricum* (MNHN 2013.01108E), (f) *Mammut americanum* (AMNH-FM14293A, mirrored), (g) *Mammut americanum* (AMNH-FM14293B), (h) *Gomphotherium angustidens* (MNHN CBar coll. V2, mirrored), (i) *Gomphotherium angustidens* (MNHN.F.SEP38, mirrored), (j) *Gomphotherium angustidens* (MNHN.F.SEP38), (k) *Cuvieronius* sp. (FM103247,

secondary bony lamina in *Numidotherium* (Court 1992). The secondary bony lamina is present in the cochlear canal of most mammals (Ekdale 2013, 2016), but it is absent in all the proboscideans studied herein except *Eritherium*, *Phosphatherium*, and *Numidotherium* (Figs. 15.10, 15.11). In *Phosphatherium*, it is extremely shallow and in *Numidotherium* it has only been observed in the specimen described by Court (1992); its absence in the specimens studied here may be explained by the resolution of the CT scan, preservation, or a genuine intraspecific variability. Its absence in proboscideans more derived than *Numidotherium* (Node E), modern sirenians (Ketten et al. 1992; Benoit et al. 2013a; Ekdale 2013) and *Arsinoitherium* is interpreted as a secondary loss due to adaptation to low-frequency hearing (Benoit et al. 2013c). This is supported by our measurements of the radii ratio in proboscideans, which indicates that even though *Moeritherium* had lost the secondary bony lamina, its radii ratio remains quite low, which is indicative of poorly developed, or non-specialized, low-frequency hearing according to Manoussaki et al. (2008). A relatively small radii ratio is likely plesiomorphic for the Proboscidea as it is also present in *Ocepeia* (Table 15.4) and most hyracoids (Benoit et al. 2016). A radii ratio within the range of variation observed in modern elephants is only seen in deinotheriids and elephantimorphs (Table 15.4), suggesting a lag between the loss of the secondary bony lamina and the change in cochlear geometry, and possibly a gradual adaptation to more specialized low-frequency hearing across the Eocene and Oligocene. A more recent evolution of the capacity for low-frequency hearing in proboscideans is consistent with the works by Shoshani (1998) and Meng et al. (1997) who studied the middle ear, hyoid apparatus and interaural distance in *Mammuth*, *Gomphotherium*, *Stegodon*, *Palaeloxodon*, and *Mammuthus*, and concluded that the ability to hear and produce infrasonic calls likely evolved in the last common ancestor of Elephantimorpha.

Deinotheriidae and Elephantimorpha

The bony labyrinth and ear region become essentially elephant-like in the last common ancestor of the Deinotheriidae and Elephantimorpha (Node F, Fig. 15.7), concurrent with the presence of most of the defining features of modern elephants. This



Fig. 15.10 (continued) mirrored), (l) *Stegomastodon* sp. (FM21807, mirrored), (m) *Platybelodon grangeri* (MNHN 26564-824+), (n) *Anancus arvernensis* (NMNHS.FM2991A), (o) *Anancus arvernensis* (NMNHS.FM2991B), (p) *Anancus arvernensis* (NMNHS.FM2991C, mirrored), (q) *Anancus arvernensis* (NMNHS.FM2991D, mirrored), (r) *Anancus arvernensis* (NMNHS.FM2991E, mirrored), (s) *Anancus arvernensis* (NMNHS.FM2991F, mirrored), (t) *Anancus arvernensis* (NMNHS.FM2991G), (u) *Stegodon orientalis* (FM18632), (v) *Mammuthus primigenius* (MNHN.F.1904-12), (w) *Mammuthus columbi* (FM144658), (x) *Mammuthus columbi* (FM144658, mirrored), (y) *Palaeloxodon antiquus* (M82706, mirrored). Scale bar = 1 cm. Abbreviations: *a.a.* anterior ampulla, *a.c.* anterior semicircular canal, *a.c.r.* anterior semicircular canal ridge, *a.v.* aquaeductus vestibuli, *aq* aquaeductus cochleae, *c.c.* *crus commune*, *c.c.s.* *crus commune secundaria*, *co* cochlear cana, *f.c.* fenestra cochleae, *i.a.v.* insertion of the aquaeductus vestibuli, *l.a.* lateral ampulla, *l.c.* lateral semicircular canal, *l.s.* lamina secundaria, *p.a.* posterior ampulla, *p.c.* posterior semicircular canal, *p.f.* perilymphatic foramen

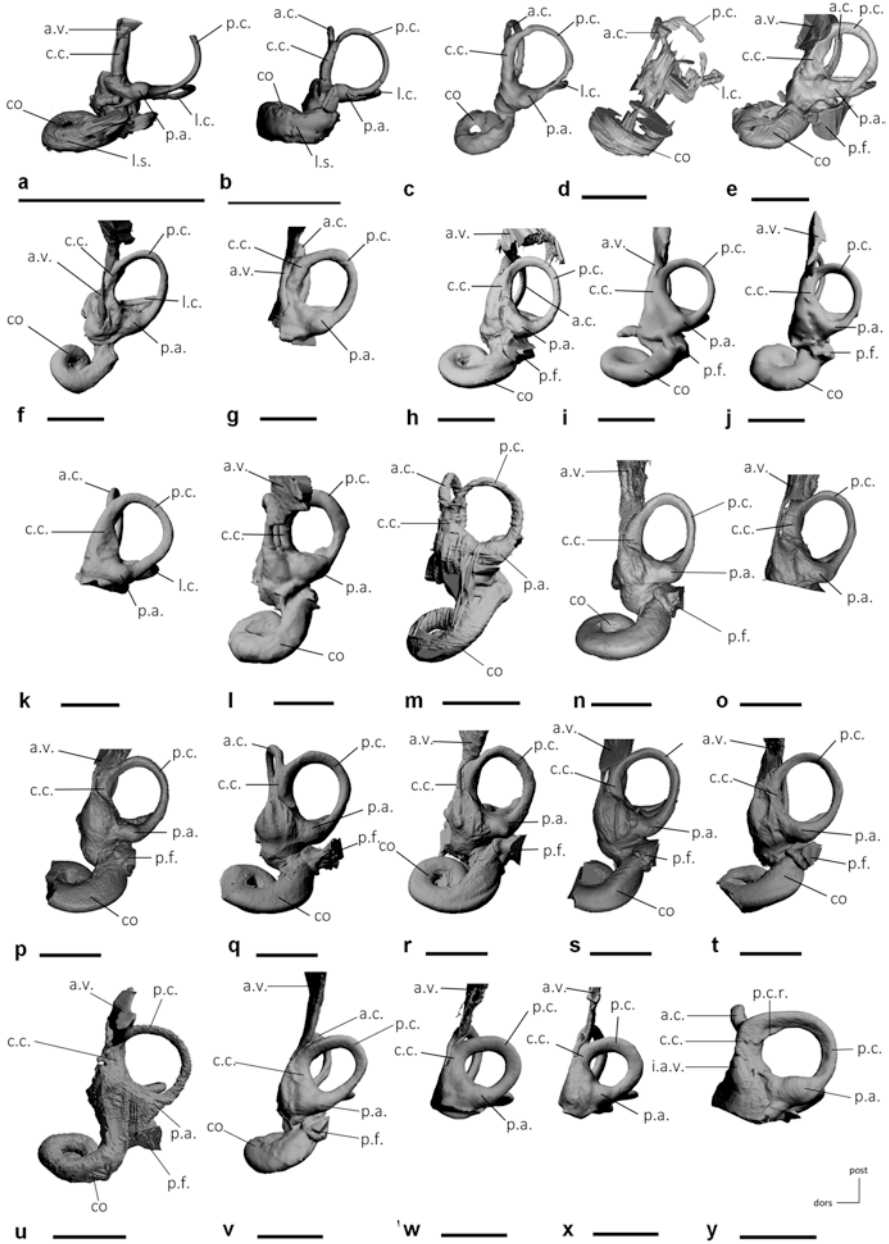


Fig. 15.11 3D reconstructions of the bony labyrinths of fossil proboscideans in posterior view. (a) *Eritherium azzouzorum* (MNHN-PM88), (b) *Phosphatherium esculliei* (MNHN.F PM17), (c) *Numidotherium koholense* (UM-UOK5, mirrored), (d) *Moeritherium* sp. (68436, mirrored), (e) *Prodeinotherium bavaricum* (MNHN 2013.01108E), (f) *Mammuth americanum* (AMNH-FM14293A, mirrored), (g) *Mammuth americanum* (AMNH-FM14293B), (h) *Gomphotherium angustidens* (MNHN CBar coll. V2, mirrored), (i) *Gomphotherium angustidens* (MNHN.F.SEP38,

is reflected distinctly in the vestibular morphology, as the studied proboscideans belonging to this clade have lost the secondary common crus (character 24) and exhibit a short and stocky common crus (character 15). A short lateral semicircular canal (character 23) and thickened semicircular canals (character 22) may also have evolved in this clade or the next one (node G) as these characters appear to be present in the *Deinotherium giganteum* specimen figured by Claudius (1865) (Fig. 15.6d) but not in *Prodeinotherium* (Figs. 15.8, 15.9, 15.10, 15.11 and 15.12e). The more elephant-like aspect of the vestibular morphology of Claudius's *Deinotherium* compared to *Prodeinotherium* (if not due to an artistic license or misidentification) may be due to the difference in body mass between these two taxa (up to ten tons according to Larramendi (2015)). The presence of thickened semicircular canals, a stocky common crus, and a shortened lateral semicircular canal is commonly encountered in many large tetrapods such as *Arsinoitherium* (Benoit et al. 2013c), *Hippopotamus* (Hyrtil 1845), the giant subfossil lemur *Megaladapis* (Walker et al. 2008), the giant wombat *Diprotodon* (Alloing-Séguier et al. 2013), and many sauropod dinosaurs (Witmer et al. 2008; Knoll et al. 2012). The exact allometric relationship and possible functional significance of the more robust aspect of the vestibule in these taxa have not yet been investigated. If not synapomorphic, characters 22 and 23 may thus be the result of a convergent evolution toward a more robust morphology of the vestibular apparatus due to an increase in body mass.

Clade F is also marked by a change in the position of the internal auditory meatus, which becomes more anteriorly oriented, whereas it was dorsally positioned in basal proboscideans (character 2). This reorientation affects the bony labyrinth as it results in a more obtuse angle between the basal turn of the cochlear canal and the vestibule in *Prodeinotherium* and more derived species (Table 15.4). As such, the basal turn of the cochlear canal is aligned with the ampullary limb of the anterior semicircular canal in anterior view, whereas it is not in more basal proboscideans (Fig. 15.10). The vestibulocochlear angle increases even further in node L (character 31), which includes *Anancus* and the Elephantidae (Table 15.4).

The Deinotheriidae nevertheless retain some noticeable plesiomorphies, such as the absence of a dorsal extension of the anterior canal (character 19). The apices of

←
Fig. 15.11 (continued) mirrored), (j) *Gomphotherium angustidens* (MNHN.F.SEP38), (k) *Cuvieronius* sp. (FM103247, mirrored), (l) *Stegomastodon* sp. (FM21807, mirrored), (m) *Platybelodon grangeri* (MNHN 26564-824+), (n) *Anancus arvernensis* (NMNHS.FM2991A), (o) *Anancus arvernensis* (NMNHS.FM2991B), (p) *Anancus arvernensis* (NMNHS.FM2991C, mirrored), (q) *Anancus arvernensis* (NMNHS.FM2991D, mirrored), (r) *Anancus arvernensis* (NMNHS.FM2991E, mirrored), (s) *Anancus arvernensis* (NMNHS.FM2991F, mirrored), (t) *Anancus arvernensis* (NMNHS.FM2991G), (u) *Stegodon orientalis* (FM18632), (v) *Mammuthus primigenius* (MNHN.F.1904-12), (w) *Mammuthus columbi* (FM144658), (x) *Mammuthus columbi* (FM144658, mirrored), (y) *Palaeoloxodon antiquus* (M82706, mirrored). Scale bar = 1 cm. Abbreviations: *a.a.* anterior ampulla, *a.c.* anterior semicircular canal, *a.v.* aquaeductus vestibuli, *aq aquaeductus cochleae*, *c.c.* crus commune, *co* cochlear canal, *f.c.* fenestra cochleae, *i.a.v.* insertion of the *aquaeductus vestibuli*, *l.a.* lateral ampulla, *l.c.* lateral semicircular canal, *l.s.* lamina secundaria, *p.a.* posterior ampulla, *p.c.* posterior semicircular canal, *p.c.r.* posterior semicircular canal ridge, *p.f.* perilymphatic foramen

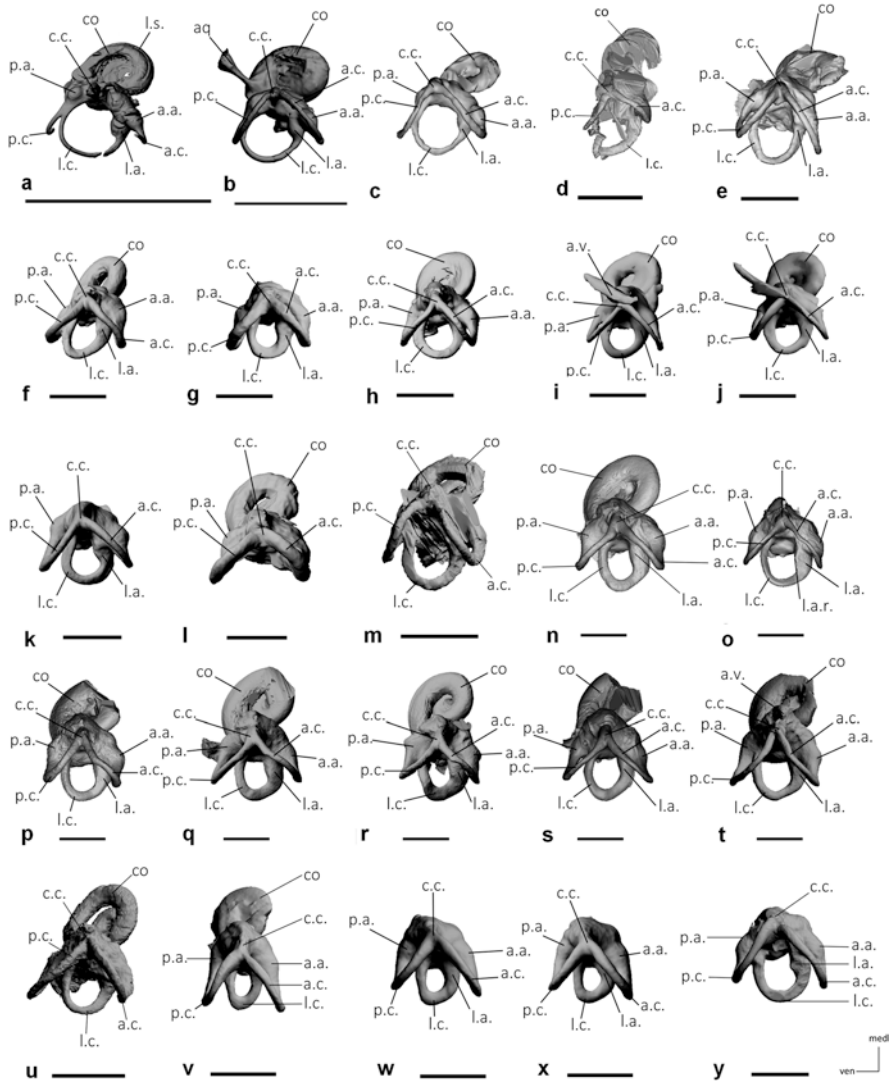


Fig. 15.12 3D reconstructions of the bony labyrinths of fossil proboscideans in dorsal view. (a) *Eriotherium azzouzorom* (MNHN -PM88), (b) *Phosphatherium esculliei* (MNHN.F PM17), (c) *Numidothierium koholense* (UM-UOK5, mirrored), (d) *Moeritherium* sp. (68436, mirrored), (e) *Prodeinotherium bavaricum* (MNHN 2013.01108E), (f) *Mammuth americanum* (AMNH-FM14293A, mirrored), (g) *Mammuth americanum* (AMNH-FM14293B), (h) *Gomphotherium angustidens* (MNHN CBar coll. V2, mirrored), (i) *Gomphotherium angustidens* (MNHN.F.SEP38, mirrored), (j) *Gomphotherium angustidens* (MNHN.F.SEP38), (k) *Cuvieronius* sp. (FM103247, mirrored), (l) *Stegomastodon* sp. (FM21807, mirrored), (m) *Platybelodon grangeri* (MNHN 26564-824+), (n) *Anancus arvernensis* (NMNHS.FM2991A), (o) *Anancus arvernensis* (NMNHS.FM2991B), (p) *Anancus arvernensis* (NMNHS.FM2991C, mirrored), (q) *Anancus arvernensis* (NMNHS.FM2991D, mirrored), (r) *Anancus arvernensis* (NMNHS.FM2991E, mirrored), (s) *Anancus arvernensis* (NMNHS.FM2991F, mirrored), (t) *Anancus arvernensis* (NMNHS.FM2991G, mirrored).

these two vertical semicircular canals reach the same height in *Phosphatherium*, *Numidotherium*, *Moeritherium*, and *Prodeinotherium* (the condition could not be evaluated from Claudius's figures of *Deinotherium*) (Fig. 15.1c). In contrast, the anterior canal apex always extends higher than the posterior one in more derived proboscidean taxa, except for *Stegomastodon* (Fig. 15.8). The relative dorsal extension is variable, from slightly higher (as in *Anancus*, Fig. 15.10n–q) to much higher (as in e.g. *Mammuthus columbi*, Fig. 15.8w, x).

The bony labyrinth morphology remains quite conservative among the Elephantimorpha (node G) as the differences observed between taxa do not depart significantly from the intraspecific variability observed in modern species (Tables 15.2, 15.3, 15.4 and 15.5). *Gomphotherium* stands out in this respect, as its *crus commune* is extremely large at its base and progressively tapers dorsally, forming a conical shape in lateral view (Fig. 15.8h, i, j). In *Prodeinotherium*, *Anancus*, *Cuvieronius*, *Gomphotherium*, *Mammuthus*, and *Stegodon* the lateral canal is completely separated from the posterior canal and ampulla (character 20) and enters the vestibule in a higher position than in the Elephantidae *Loxodonta*, *Elephas*, *Mammuthus* and *Palaeoloxodon* (Figs. 15.8, 15.9, 15.10, 15.11 and 15.12), in which the point of insertion of the lateral canal into the vestibule migrates back toward the posterior ampulla (node M). This character may constitute a synapomorphy of the Elephantidae (Fig. 15.7).

15.5 Final Considerations

The ear region is a key anatomical complex useful for anatomical, evolutionary, and functional studies. Its peculiar but poorly known morphology in proboscideans deserves further investigation. The petrosal of extant elephants is solidly fused to the skull and therefore difficult to access. While this region has already been described in the past, many previous studies failed to provide most of the anatomical details taken into account in recent studies of the petrosal and bony labyrinth of extant and extinct mammals. This study is the first comprehensive attempt to document the morphological diversity of the ear region and bony labyrinth of extant and extinct proboscideans using CT scanning. We found no feature that could discriminate between the bony labyrinths of the three extant elephant species. The bony labyrinth is described in sixteen extinct genera, covering most major proboscidean groups. We show that the modern morphotype evolved gradually in

←
Fig. 15.12 (continued) FM2991G), (u) *Stegodon orientalis* (FM18632), (v) *Mammuthus primigenius* (MNHN.F.1904-12), (w) *Mammuthus columbi* (FM144658), (x) *Mammuthus columbi* (FM144658, mirrored), (y) *Palaeoloxodon antiquus* (M82706, mirrored). Scale bar = 1 cm. Abbreviations: a.a. anterior ampulla, a.c. anterior semicircular canal, a.v. aquaeductus vestibuli, aq aquaeductus cochleae, c.c. crus commune, co cochlear canal, f.c. fenestra cochleae, l.a. lateral ampulla, l.c. lateral semicircular canal, l.s. lamina secundaria, p.a. posterior ampulla, p.c. posterior semicircular canal

Table 15.5 Measurements of the semicircular canals of fossil proboscideans and outgroups

	Radius of curvature			Lateral canal ratio (%)			Central streamline length (mm)			Average section radius (mm)			Average thickness ratio					
	ASC	PSC	LSC	ASC	PSC	LSC	ASC	PSC	LSC	ASC	PSC	LSC	ASC	PSC	LSC	ASC	PSC	LSC
<i>Ocepeia daouienensis</i> MNHN-PM145	1.64	1.55	1.24	78.5	6.87	7.49	6.79	0.15	0.16	0.14	2.22	2.18	2.04	2.15				
<i>Stylolophus</i> MNHN-PM53	3.26	3.13	2.3e	71.7	12.6	13.4	11e	0.22	0.21	0.12	1.72	1.57	1.1e	1.46				
<i>Anancus arvernensis</i> NMNHS.FM2991A	5.02	4.79	3.19	65	22.7	20.9	20.3	0.70	0.70	0.74	3.09	3.37	3.63	3.36				
<i>Anancus arvernensis</i> NMNHS.FM2991B	5.91	5.63	4.06	70.4	25.4	23.9	24.4	0.58	0.64	0.66	2.29	2.66	2.72	2.56				
<i>Anancus arvernensis</i> NMNHS.FM2991C	5.15	4.89	3.39	67.6	23.8	21.5	21.7	0.76	0.74	0.78	3.18	3.43	3.58	3.40				
<i>Anancus arvernensis</i> NMNHS.FM2991D	5.24	5.39	3.39	64.5	23.5	24.1	21.7	0.79	0.82	0.84	3.36	3.40	3.86	3.54				
<i>Anancus arvernensis</i> NMNHS.FM2991E	5.52	5.37	3.54	65.1	24.3	23.0	21.8	0.91	0.92	1.06	3.75	3.99	4.87	4.20				
<i>Anancus arvernensis</i> NMNHS.FM2991F	5.68	5.67	3.92	69.1	24.6	25	23.6	0.83	0.78	0.83	3.39	3.10	3.50	3.33				
<i>Anancus arvernensis</i> NMNHS.FM2991G	5.33	5.67	3.58	66.8	23.2	25.8	22.2	0.79	0.70	0.79	3.39	2.70	3.56	3.21				
<i>Cuvieronius</i> sp FM103247	6.18	6.06	3.57	58.5	25.0	25.4	21.4	0.85	0.86	0.89	3.41	3.37	4.18	3.65				
<i>Erethrum azoucorum</i> MNHN-PM188	1.74	1.83	1.78	77.5	6.99	10.8	7.31	0.07	0.05	0.13	0.94	0.49	1.79	1.08				
<i>Gomphotherium angustidens</i> CBar coll. V2	5.26	5.56	3.71	66	20.4	23.2	22.2	0.77	0.76	0.78	3.78	3.26	3.50	3.51				
<i>Gomphotherium angustidens</i> SEP38	5.45	5.11	3.36	63.7	22.8	21.6	19.1	0.64	0.71	0.78	2.82	3.29	4.09	3.40				

<i>Mammuth americanum</i> AMNH-FM14293A	6.33	6.09	3.82	61.8	28.8	25.5	24.1	0.95	0.95	0.92	3.30	3.70	3.82	3.61
<i>Mammuth americanum</i> AMNH-FM14293B	5.43	5.68	2.96	52.7	23.6	23.8	18.4	1.04	1.01	0.87	4.30	4.33	4.74	4.47
<i>Mammuthus columbi</i> FMI44658	5.71	4.84	3.08	60.1	25.9	21.2	21.3	1.2	1.10	0.99	4.24	5.65	4.65	4.85
<i>Mammuthus primigenius</i> MNHN.F.1904-12	5.80	5.53	2.92	51.6	26.8	25.3	19.7	0.88	1.01	0.93	3.28	3.99	4.69	3.99
<i>Numidotherium koholense</i> UM-UOK5	3.52	3.28	2.56	73.3	13.9	14.7	13.9	0.34	0.30	0.28	2.47	2.03	1.99	2.16
<i>Palaeoloxodon antiquus</i> M82706	5.87	5.14	3.93	72.4	26.2	22.2	24.1	0.92	0.93	0.91	3.51	4.18	3.78	3.82
<i>Phosphatherium escuilliei</i> MNHN.F.PM17	1.91	1.88	1.9	78.5	7.77	8.77	7.95	0.19	0.17	0.18	2.41	1.99	2.31	2.24
<i>Platybelodon grangeri</i> 26564	5.16	4.89	3.54	69.7	22.0	22.0	22	0.81	0.65	0.68	3.69	2.93	3.11	3.25
<i>Prodeinotherium bavaricum</i> 2013.01108E	5.60	5.01	3.98	75	24.7	22.5	22.7	0.69	0.69	0.59	2.79	3.06	2.62	2.82
<i>Stegodon orientalis</i> FMI8632	5.36	7.48	3.27	51	23.7	23.4	15.2	0.83	0.82	0.77	3.51	3.51	5.10	4.04
<i>Stegomastodon sp</i> FM21807	4.91	5.30	?	?	19.4	22.5	?	1.32	1.18	?	6.8	5.24	?	6.02

Abbreviations: ASC anterior semicircular canal, LSC lateral semicircular canal, PSC posterior semicircular canal. Average thickness ratio is calculated = average section radius/central streamline length*100

“plesiephantiforms” to become essentially elephant-like during the Oligocene, in the clade that includes deinotheriids and elephantiforms.

Although more data on the bony labyrinth of *Palaeomastodon* and the endocranial cast of deinotheriids would be necessary to confirm this trend, it is noteworthy that both the bony labyrinth and braincase morphology underwent an evolutionary limp toward an essentially elephant-like condition simultaneously around the late Eocene - Early Oligocene. This suggests that the brain and inner ear coevolved in the common ancestors of elephantiforms and deinotheriids (Fig. 15.13). Examples of brain-ear region coevolution are not uncommon in mammals (e.g. Rowe 1996; Sánchez-Villagra 2002). It has been proposed that complex social interactions may result in brain size increase in paenungulates, artiodactyls, and perissodactyls (Pérez-Barbería and Gordon 2005; Shultz and Dunbar 2006). Such social bonds are supported by long-term memory of chemical scents and sounds of relatives in elephants (Payne et al. 1986; Poole et al. 1988, 2005; O’Connell-Rodwell et al. 2001, 2007; Günther et al. 2004; O’Connell-Rodwell 2007; Hart et al. 2008). As the overall African climate became dryer in the Oligocene, droughts became more frequent and pockets of more humid environments (e.g., in Egypt and equatorial Africa) became more isolated (Boureau et al. 1983; Zachos et al. 2001; Kappelman et al. 2003; Bobe 2006; Seiffert 2007b; Feakins and Demenocal 2010; Mudelsee et al. 2014; Jacobs et al. 2016b; de Vries et al. 2021). We here speculate that the necessity to locate and remember the location of widely spaced sources of water and maintain social communication despite this distance using infrasonic vocalizations and foot drumming might have fuelled the coevolution of brain and inner ear morphology (Poole et al. 1988, 2005; Langbauer 2000; O’Connell-Rodwell et al. 2001, 2007; Günther et al. 2004; O’Connell-Rodwell 2007; Hart et al. 2008). Low-frequency sounds propagate long distances as seismic waves (O’Connell-Rodwell 2007), and modern elephants use these seismic waves as alarms, to locate mates and to maintain intra- and intergroup cohesion (Poole et al. 1988; Langbauer 2000; Günther et al. 2004; O’Connell-Rodwell et al. 2007). Elephants may even be able to locate places where rain falls and underground water reservoirs using infrasounds (Arnason et al. 2002; Garstang et al. 2014). A tight correlation between the onset of low-frequency hearing and the increase in drought frequency is supported by studies of the hyoid apparatus (Shoshani 1998; Shoshani et al. 2001; Meng et al. 1997), which show that the ability to store water in a pharyngeal pouch and that of producing infrasonic calls are correlated and were already present in the last common ancestor of the Elephantimorpha. The possible evolutionary origin of the trunk in elephantiforms, an organ essential to infrasound vocalizations and filling up the pharyngeal pouch (Shoshani 1998; Shoshani et al. 2001; Meng et al. 1997), concurrently involved an increase in the size of the cerebellum to coordinate its movements (Maseko et al. 2012). The presence of a trunk also aided drinking and smelling at ground level as proboscideans evolved a larger body size, taller shoulder height and a shorter neck in the Oligocene (Larramendi 2015). As explained earlier in this chapter, a larger body mass is correlated to changes in the encephalization quotient (Manger et al. 2013) and the morphology of the bony labyrinth (thickening of the semicircular canals and common crus, reduced lateral canal). Low-frequency sound

production and hearing are also more likely to evolve in larger species (e.g. rhinos and hippos) as large absolute body size increases the size of vocal organs and interaural distance (von Muggenthaler and Reinhart 2003; Barklow 2004a, b; Policht et al. 2008; Benoit et al. 2013c; Mourlam and Orliac 2017; Shoshani et al. 2001). It is noteworthy that low-frequency hearing may also be an adaptation to underwater hearing (Barklow 2004a, b; Mourlam and Orliac 2017), while the earliest proboscidean for which the loss of the *lamina secundaria* is documented coincidentally is *Moeritherium*, a species that has long been reconstructed as semiaquatic (Osborn 1936; Clementz et al. 2008; Liu et al. 2008). Finally, herbivores living in open habitats have more chance to be grazers, and thus to display higher body mass, as a large body consumes less energy per unit of mass than a small one, and can accommodate a larger gut that improves digestion of coarse, comparatively nutrient deficient, grass (Peters 1983; Christiansen 2004; Franzen, 2010; Sander et al. 2011). Incidentally, living in an open habitat also increases the probability to live in large social and hierarchized groups, which in turn correlates with an increase in encephalization (Pérez-Barbería and Gordon 2005). As such, it is possible that a dryer climate in Africa during the Oligocene had long-term cascading and self-reinforcing effects on body mass, encephalization, and bony-labyrinth morphology (Fig. 15.13). This hypothesis will have to be tested when more data become available, particularly from key late Eocene and Oligocene taxa such as early Elephantiformes, Deinotheriidae and other “Plesielephantiformes” for which reasonably small, yet highly relevant material could be CT scanned, such as specimen AMNH 13468 of the basal elephantiform *Phiomia serridens* and specimen Dt1008-1 of the “plesielephantiform” *Barytherium grave* (Andrews 1906; Sanders et al. 2010; Jaeger et al. 2012).

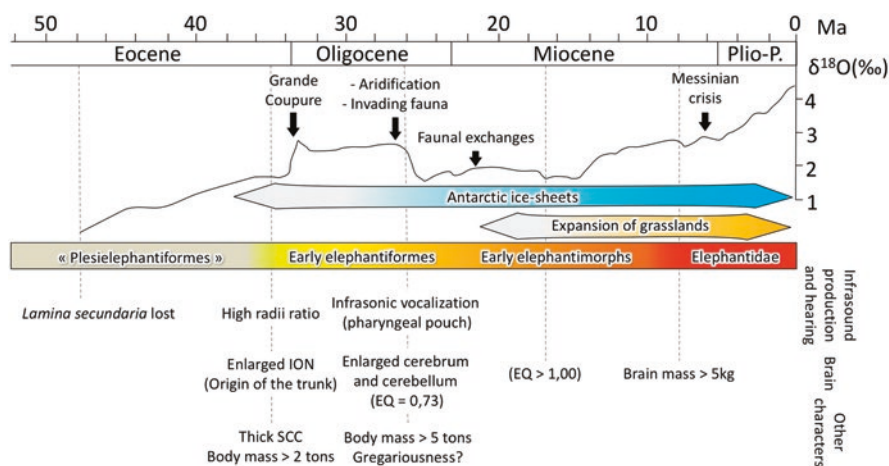


Fig. 15.13 Palaeoenvironmental context of proboscidean brain, inner ear and other related characters co-evolution. δ¹⁸O curve and climatic events after Zachos et al. (2001). Abbreviations: EQ: encephalization quotient, ION infraorbital nerve, SCC semicircular canals

Acknowledgments The authors would like to thank the financial support of La Fondation des Treilles, créée par Anne Gruner Schlumberger, a notamment pour vocation d’ouvrir et de nourrir le dialogue entre les sciences et les arts afin de faire progresser la création et la recherche contemporaines. Elle accueille également des chercheurs et des écrivains dans le domaine des Treilles (Var, France). www.les-treilles.com. T.O. thanks Dr. Ștefan Vasile, University of Bucharest for access to the mammoth endocast from Naslavcea. A.S. thanks Emmanuel Gheerbrant and Pascal Tassy (MNHN, Paris, France) for supervising him during his PhD, and Erik Seiffert (Keck School of Medicine of USC, Los Angeles), Marcelo Sánchez (Paläontologisches Institut und Museum, Zürich), Pierre-Olivier Antoine (Université de Montpellier 2), and Guillaume Billet (MNHN, Paris) for taking part of his defense jury and improvement of his work. A.S. and J.B. thank Christine Argot, Joséphine Lesur, Aurélie Verguin, Marc Herbin, Eric Pellé and Jacques Cuisin (MNHN, Paris), Pip Brewer, Dan Sykes, and Farah Ahmed (Natural History Museum, London), Reinhard Ziegler (State Museum of Natural History, Stuttgart), Judith Galkin, Henry Tobin, Alana Gishlick, Ruth O’Leary, Morgan Hill and Meng Jin (AMNH) for providing access to the specimens studied here. A.S. also thanks the Department of Human Evolution of the Max Planck for Evolutionary Anthropology (Leipzig, Germany) for welcoming him twice and allowing him to scan some specimens described in this study - in particular, Fred Spoor for providing some dataset and Romain David for his support. G.L. thanks Carolina di Patti (MGG), Pip Brewer (NHM-UK), Judith Galkin and Meng Jin (AMNH) for providing access to specimens studied here and Bartholomeus van der Geer for digitizing the endocasts. The authors finally thank Thomas E. Macrini and another anonymous reviewer for their comments on the manuscript.

References

- Accordi FS, Palombo MR (1971) Morfologia endocranica degli elefanti nani pleistocenici di Spinagallo (Siracusa) e comparazione con l’endocranio di *Elephas antiquus*. Rendiconti della Accademia Nazionale Lincei, serie VIII 51:111–124
- Alloing-Séguier L, Sánchez-Villagra MR, Lee MSY et al (2013) The bony labyrinth in Diprotodontian marsupial mammals: diversity in extant and extinct forms and relationships with size and phylogeny. *J Mammal Evol* 20:191–198. <https://doi.org/10.1007/s10914-013-9228-3>
- Andrews CW (1904) On the evolution of the Proboscidea. *Philos Trans R Soc Lond B Biol Sci* 196:99–118. <https://doi.org/10.1098/rstb.1904.0004>
- Andrews CW (1906) A descriptive catalogue of the Tertiary Vertebrata of the Fayum, Egypt. Order of the Trustees of the British museum, London
- Andrews CW (1921) Note on the skull of *Dinotherium giganteum* in the British Museum. *Proc Zool Soc London* 91:525–534. <https://doi.org/10.1111/j.1096-3642.1921.tb03278.x>
- Arnason BT, Hart LA, O’Connell-Rodwell CE (2002) The properties of geophysical fields and their effects on elephants and other animals. *J Comp Psychol* 116:123–132. <https://doi.org/10.1037/0735-7036.116.2.123>
- Asher RJ (2007) A web-database of mammalian morphology and a reanalysis of placental phylogeny. *BMC Evol Biol* 7:108. <https://doi.org/10.1186/1471-2148-7-108>
- Barklow WE (2004a) Amphibious communication with sound in hippos, *Hippopotamus amphibius*. *Anim Behav* 68:1125–1132. <https://doi.org/10.1016/j.anbehav.2003.10.034>
- Barklow WE (2004b) Low-frequency sounds and amphibious communication in *Hippopotamus amphibius*. *J Acoust Soc Am* 115:2555–2555. <https://doi.org/10.1121/1.4783854>
- Bauchot R, Stephan H (1968) Etude des modifications encéphaliques observées chez les insectivores adaptés à la recherche de nourriture en milieu aquatique. *Mammalia* 32:228–275. <https://doi.org/10.1515/mamm.1968.32.2.228>
- Beaudet A, Clarke RJ, de Jager EJ et al (2019) The endocast of StW 573 (“Little Foot”) and hominin brain evolution. *J Hum Evol* 126:112–123. <https://doi.org/10.1016/j.jhevol.2018.11.009>

- Benoit J (2015) A new method of estimating brain mass through cranial capacity in extinct proboscideans to account for the non-neural tissues surrounding their brain. *J Vertebr Paleontol* 35:e991021. <https://doi.org/10.1080/02724634.2014.991021>
- Benoit J, Adnet S, El Mabrouk E et al (2013a) Cranial remain from Tunisia provides new clues for the origin and evolution of Sirenia (Mammalia, Afrotheria) in Africa. *PLoS One* 8:e54307. <https://doi.org/10.1371/journal.pone.0054307>
- Benoit J, Crumpton N, Méridgeaud S et al (2013b) A memory already like an elephant's? The advanced brain morphology of the last common ancestor of Afrotheria (Mammalia). *Brain Behav Evol* 81:154–169. <https://doi.org/10.1159/000348481>
- Benoit J, Merigeaud S, Tabuce R (2013c) Homoplasy in the ear region of Tethytheria and the systematic position of Embrithopoda (Mammalia, Afrotheria). *Geobios* 46:357–370. <https://doi.org/10.1016/j.geobios.2013.07.002>
- Benoit J, Lehmann T, Vatter M et al (2015) Comparative anatomy and three-dimensional geometric-morphometric study of the bony labyrinth of *Bibymalagasia* (Mammalia, Afrotheria). *J Vertebr Paleontol* 35:e930043. <https://doi.org/10.1080/02724634.2014.930043>
- Benoit J, Crochet J-Y, Mahboubi M et al (2016) New material of *Seggeurius amourensis* (Paenungulata, Hyracoidea), including a partial skull with intact basicranium. *J Vertebr Paleontol* 36:e1034358. <https://doi.org/10.1080/02724634.2015.1034358>
- Benoit J, Legendre LJ, Tabuce R et al (2019) Brain evolution in Proboscidea (Mammalia, Afrotheria) across the Cenozoic. *Sci Rep* 9:1–8. <https://doi.org/10.1038/s41598-019-45888-4>
- Bever G, Macrini T, Jass C (2008) A natural endocranial cast of a fossil proboscidean with comments on elephant endocranial evolution and the scientific value of “no data” specimens. *Unlocking the unknown: Papers honouring Dr Richard Zakrewski, Fort Hays Studies, Special Issue No 1, Fork Hays State University, Hays, Kansas*, pp 11–22
- Bianchi S, Bauernfeind AL, Gupta K et al (2011) Neocortical neuron morphology in Afrotheria: comparing the rock hyrax with the African elephant. *Ann N Y Acad Sci* 1225:37–46. <https://doi.org/10.1111/j.1749-6632.2011.05991.x>
- Bibi F, Kraatz B, Craig N et al (2012) Early evidence for complex social structure in Proboscidea from a late Miocene trackway site in the United Arab Emirates. *Biol Lett* 8:670–673. <https://doi.org/10.1098/rsbl.2011.1185>
- Blair P (1710a) A continuation of the osteographia elephantina: or, a description of the bones of an elephant, which died near Dundee, April the 27th, 1706. *Philos Trans R Soc Lond* 27:117–168. <https://doi.org/10.1098/rstl.1710.0009>
- Blair P (1710b) Osteographia Elephantina: a full and exact description of all the bones of an elephant, which died near Dundee, April the 27th, 1706. with their several dimensions. Communicated in a letter to Dr. Hans Sloane, R, S, Secr. By Mr Patrick Blair, Surgeon. *Philos Trans R Soc Lond* 27:53–116. <https://doi.org/10.1098/rstl.1710.0008>
- Blair P (1717) A description of the organ of hearing in the elephant, with the figures and situation of the ossicles, labyrinth and cochlea, in the ear of that large animal. *Philos Trans R Soc Lond* 30:885–899
- Boas JEV (1908) The elephant's head: studies in the comparative anatomy of the organs of the head of the Indian Elephant and other mammals. Fischer in Komm, Copenhagen
- Bobé R (2006) The evolution of arid ecosystems in eastern Africa. *J Arid Environ* 66:564–584. <https://doi.org/10.1016/j.jaridenv.2006.01.010>
- Boule M, Thevenin A (1920) Mammifères fossiles de Tarija. Imprimerie Nationale, Paris
- Boureau E, Cheboldaëff-Salard M, Koeniguer J-C et al (1983) Evolution des flores et de la végétation Tertiaires en Afrique, au nord de l'Equateur. *Bothalia* 14:355–367. <https://doi.org/10.4102/abc.v14i3/4.1180>
- Bruner E, Mantini S, Musso F et al (2011) The evolution of the meningeal vascular system in the human genus: from brain shape to thermoregulation. *Am J Hum Biol* 23:35–43. <https://doi.org/10.1002/ajhb.21123>
- Buck AH (1888) A contribution to the anatomy of the elephant's ear. *Trans Am Otol Soc*:240–253

- Buck AH (1890) A revised description of the anatomy of the elephant's ear. *Trans Am Otol Soc*:3–15
- Byrne RW, Bates LA (2007) Sociality, evolution and cognition. *Curr Biol* 17:R714–R723. <https://doi.org/10.1016/j.cub.2007.05.069>
- Christiansen P (2004) Body size in proboscideans, with notes on elephant metabolism. *Zool J Linn Soc* 140:523–549. <https://doi.org/10.1111/j.1096-3642.2004.00113.x>
- Claudius M (1865) Das Gehörlabyrinth von *Dinotherium giganteum* nebst Bemerkungen über den Werth der Labyrinthformen für die Systematik der Säugethiere. *Palaeontographica* (1846–1933):65–74
- Clementz MT, Holroyd PA, Koch PL (2008) Identifying aquatic habits of herbivorous mammals through stable isotope analysis. *Palaios* 23:574–585. <https://doi.org/10.2110/palo.2007.p07-054r>
- Court N (1990) Periotic anatomy of *Arsinoitherium* (Mammalia, Embrithopoda) and its phylogenetic implications. *J Vertebr Paleontol* 10:170–182. <https://doi.org/10.1080/02724634.1990.10011806>
- Court N (1992) Cochlea anatomy of *Numidotherium koholense*: auditory acuity in the oldest known proboscidean. *Lethaia* 25:211–215. <https://doi.org/10.1111/j.1502-3931.1992.tb01385.x>
- Court N (1994) The periotic of *Moeritherium* (Mammalia, Proboscidea): homology or homoplasy in the ear region of Tethytheria McKenna, 1975? *Zool J Linn Soc Lond* 112:13–28. <https://doi.org/10.1111/j.1096-3642.1994.tb00310.x>
- Court N, Jaeger J-J (1991) Anatomy of the periotic bone in the Eocene proboscidean *Numidotherium koholense*: an example of parallel evolution in the inner ear of tethytheres. *C R Acad Sci* 312:559–565
- Cozzi B, Spagnoli S, Bruno L (2001) An overview of the central nervous system of the elephant through a critical appraisal of the literature published in the XIX and XX centuries. *Brain Res Bull* 54:219–227. [https://doi.org/10.1016/S0361-9230\(00\)00456-1](https://doi.org/10.1016/S0361-9230(00)00456-1)
- Crumpton N, Thompson RS (2013) The holes of moles: osteological correlates of the trigeminal nerve in Talpidae. *J Mammal Evol* 20:213–225. <https://doi.org/10.1007/s10914-012-9213-2>
- de Vries D, Heritage S, Borths MR et al (2021) Widespread loss of mammalian lineage and dietary diversity in the early Oligocene of Afro-Arabia. *Commun Biol* 4:1172. <https://doi.org/10.1038/s42003-021-02707-9>
- DeCasien AR, Thompson NA, Williams SA et al (2018) Encephalization and longevity evolved in a correlated fashion in Euarchotheriids but not in other mammals. *Evolution* 72:2617–2631. <https://doi.org/10.1111/evo.13633>
- Dechaseaux C (1958) L'encéphale d'*Elephas meridionalis*. *Ann Paléontol* 64:269–278
- Dechaseaux C (1962) Cerveaux d'animaux disparus: essai de paléoneurologie. Masson
- Decimo I, Fumagalli G, Berton V et al (2012) Meninges: from protective membrane to stem cell niche. *Am J Stem Cells* 1:92–105
- Delmer C (2005) Les premières phases de différenciation des Proboscidiens (Tethyria, Mammalia): le rôle du Barytherium grave de Lybie. These de doctorat, Paris, Muséum national d'histoire naturelle
- Eales NB (1926) XI.—The Anatomy of the head of a foetal African elephant, *Elephas africanus* (*Loxodonta africana*). *Earth Environ Sci Trans R Soc Edinb* 54:491–551. <https://doi.org/10.1017/S0080456800016082>
- Edinger T (1948) Evolution of the horse brain. *Geol Soc Am Mem* 25:1–177
- Edinger T (1960) Anthropocentric misconceptions in paleoneurology. *Proc Rudolf Virchow Med Soc City N Y* 19:56–107. <https://doi.org/10.1159/000405771>
- Edinger T (1963) Neues aus der Paläoneurologie. *Paläont Z* 37:49–55. <https://doi.org/10.1007/BF02989599>
- Edinger T (1964) Midbrain exposure and overlap in mammals. *Am Zool* 4:5–19
- Edinger T (1975) Paleoneurology 1804–1966: an annotated bibliography. *Adv Anat Embryol Cell Biol* 49:3–258

- Eisenberg JF (1981) The mammalian radiations: an analysis of trends in evolution, adaptation, and behaviour. University of Chicago Press, Chicago
- Ekdale EG (2011) Morphological variation in the ear region of pleistocene elephantimorpha (Mammalia, Proboscidea) from central Texas. *J Morphol* 272:452–464. <https://doi.org/10.1002/jmor.10924>
- Ekdale EG (2013) Comparative anatomy of the bony labyrinth (inner ear) of placental mammals. *PLoS One* 8:e66624. <https://doi.org/10.1371/journal.pone.0066624>
- Ekdale EG (2016) Form and function of the mammalian inner ear. *J Anat* 228:324–337. <https://doi.org/10.1111/joa.12308>
- Elliot Smith G (1902) The brains of the mammalia. In: Owen R (ed) Descriptive and illustrated catalogue of the physiological series of comparative anatomy contained in the Museum of the Royal College of Surgeons of England. Taylor and Francis, London, pp 138–481
- Feakins SJ, Demenocal PB (2010) Global and African regional climate during the Cenozoic. In: Werdelin L (ed) Cenozoic mammals of Africa. University of California Press, Berkeley, pp 45–56
- Fick L (1844) Über das Labyrinth des Elefanten. *Archiv für Anatomie, Physiologie und wissenschaftliche Medizin*:431–432
- Finlay BL, Darlington RB, Nicastro N (2001) Developmental structure in brain evolution. *Behav Brain Sci* 24:263–278
- Fischer MS (1990) Un trait unique de l'oreille des éléphants et des siréniens (Mammalia): un paradoxe phylogénétique. *C R Acad Sci, Sér 3, Sci vie* 311:157–162
- Fischer MS (1992) Hyracoidea. *Handbuch der Zoologie: Mammalia* 8:1–169
- Fisher DC (2018) Paleobiology of Pleistocene proboscideans. *Annu Rev Earth Planet Sci* 46:229–260. <https://doi.org/10.1146/annurev-earth-060115-012437>
- Fisher DC, Shirley EA, Whalen CD et al (2014) X-ray computed tomography of two mammoth calf mummies. *J Paleontol* 88:664–675. <https://doi.org/10.1666/13-092>
- Franzen J (2010) The rise of horses: 55 million years of evolution. The Johns Hopkins University Press, Baltimore
- Friant M (1951) Sur la forme du cerveau, au cours de l'Ontogénie, chez les éléphants (Elephantidae). *C R Acad Sci - Sér 3, Sci vie* 232:2137–2138
- Friant M (1954) Sur la forme du cerveau de l'éléphant (*Loxodonta africana* Blum.), au cours de la vie prénatale. *C R Acad Sci - Sér 3, Sci vie* 238:1534–1535
- Friant M (1957) Morphologie et développement du cerveau des mammifères euthériens. III. Série des ongulés. *Ann Soc R Zool Belg* 88:321–367
- Furusawa H (2004) A phylogeny of the North Pacific Sirenia (Dugongidae: Hydrodamalinae) based on a comparative study of endocranial casts. *Paleontol Res* 8:91–98. <https://doi.org/10.2517/prpsj.8.91>
- Garstang M, Davis RE, Leggett K et al (2014) Response of African elephants (*Loxodonta africana*) to seasonal changes in rainfall. *PLoS One* 9:e108736. <https://doi.org/10.1371/journal.pone.0108736>
- Gaspard JC, Bauer GB, Reep RL et al (2012) Audiogram and auditory critical ratios of two Florida manatees (*Trichechus manatus latirostris*). *J Exp Biol* 215:1442–1447. <https://doi.org/10.1242/jeb.065649>
- Gervais P (1872) Mémoire sur les formes cérébrales propres à différents groupes de mammifères. *Journal de Zoologie, Paris* 1:425–469
- Gheerbrant E (2009) Paleocene emergence of elephant relatives and the rapid radiation of African ungulates. *Proc Natl Acad Sci USA* 106:10717–10721. <https://doi.org/10.1073/pnas.0900251106>
- Gheerbrant E, Tassy P (2009) L'origine et l'évolution des éléphants. *C R Palevol* 8:281–294. <https://doi.org/10.1016/j.crpv.2008.08.003>
- Gheerbrant E, Sudre J, Tassy P et al (2005) Nouvelles données sur *Phosphatherium escul-liei* (Mammalia, Proboscidea) de l'Eocène inférieur du Maroc, apports à la phylogénie des Proboscidea et des ongulés lophodontes. *Geodiversitas* 27:239–333

- Gheerbrant E, Bouya B, Amaghazaz M (2012) Dental and cranial anatomy of *Eritherium azzouzum* from the Paleocene of Morocco, earliest known proboscidean mammal. *Palaeontogr Abt A* 297:151–183. <https://doi.org/10.1127/pala/297/2012/151>
- Gheerbrant E, Amaghazaz M, Bouya B et al (2014) *Ocepeia* (Middle Paleocene of Morocco): the oldest skull of an Afrotherian mammal. *PLoS One* 9:e89739. <https://doi.org/10.1371/journal.pone.0089739>
- Gheerbrant E, Khaloune F, Schmitt A et al (2021) Earliest embrithopod mammals (Afrotheria, Tethytheria) from the Early Eocene of Morocco: anatomy, systematics and phylogenetic significance. *J Mamm Evol* 28:245–283. <https://doi.org/10.1007/s10914-020-09509-6>
- Gleboff J (1846) Recherches microscopiques sur les parties molles du mammouth (*Elephas primigenius* Blumenbach, *Mammonteus* Fischer). *Bulletin de la Société impériale des naturalistes de Moscou* 19:108–134
- González-Lagos C, Sol D, Reader SM (2010) Large-brained mammals live longer. *J Evol Biol* 23:1064–1074. <https://doi.org/10.1111/j.1420-9101.2010.01976.x>
- Goodman M, Sterner KN, Islam M et al (2009) Phylogenomic analyses reveal convergent patterns of adaptive evolution in elephant and human ancestries. *Proc Natl Acad Sci USA* 106:20824–20829. <https://doi.org/10.1073/pnas.0911239106>
- Granger W, Gregory WK, William K et al (1936) Further notes on the gigantic extinct rhinoceros, *Baluchitherium*, from the Oligocene of Mongolia. *Bull Am Mus Nat Hist* 72:1–73
- Gravett N, Bhagwandin A, Sutcliffe R et al (2017) Inactivity/sleep in two wild free-roaming African elephant matriarchs – does large body size make elephants the shortest mammalian sleepers? *PLOS ONE* 12:e0171903. <https://doi.org/10.1371/journal.pone.0171903>
- Günther RH, O'Connell-Rodwell CE, Klemperer SL (2004) Seismic waves from elephant vocalizations: a possible communication mode? *Geophys Res Lett* 31:L11602. <https://doi.org/10.1029/2004GL019671>
- Hakeem AY, Hof PR, Sherwood CC et al (2005) Brain of the African elephant (*Loxodonta africana*): neuroanatomy from magnetic resonance images. *Anat Rec* 287A:1117–1127. <https://doi.org/10.1002/ar.a.20255>
- Hakeem AY, Sherwood CC, Bonar CJ et al (2009) Von Economo Neurons in the Elephant Brain. *Anat Rec* 292:242–248. <https://doi.org/10.1002/ar.20829>
- Harris JM (1973) *Prodeinotherium* from Gebel Zelten, Libya. *Bull Br Mus Nat Hist* 23:283–348
- Hart BL, Hart LA, Pinter-Wollman N (2008) Large brains and cognition: where do elephants fit in? *Neurosci Biobehav Rev* 32:86–98. <https://doi.org/10.1016/j.neubiorev.2007.05.012>
- Herculano-Houzel S, Avelino-de-Souza K, Neves K et al (2014) The elephant brain in numbers. *Front Neuroanat* 8:46. <https://doi.org/10.3389/fnana.2014.00046>
- Herridge VL, Lister AM (2012) Extreme insular dwarfism evolved in a mammoth. *Proc Biol Sci* 279:3193–3200. <https://doi.org/10.1098/rspb.2012.0671>
- Higashiyama H, Kuratani S (2014) On the maxillary nerve: the maxillary nerve in vertebrates. *J Morphol* 275:17–38. <https://doi.org/10.1002/jmor.20193>
- Hofman MA (1993) Encephalization and the evolution of longevity in mammals. *J Evol Biol* 6:209–227. <https://doi.org/10.1046/j.1420-9101.1993.6020209.x>
- Holloway RL (2013) The evolution of the hominid brain. In: Henke W, Tattersall I (eds) *Handbook of paleoanthropology*. Springer, Berlin/Heidelberg, pp 1–23
- Hyrtil J (1845) Vergleichend-anatomische untersuchungen über das innere gehörorgan des menschen und der säugethiere. F. Ehrlich
- Jacobs B, Lubs J, Hannan M et al (2011) Neuronal morphology in the African elephant (*Loxodonta africana*) neocortex. *Brain Struct Funct* 215:273–298. <https://doi.org/10.1007/s00429-010-0288-3>
- Jacobs B, Lee L, Schall M et al (2016a) Neocortical neuronal morphology in the newborn giraffe (*Giraffa camelopardalis tippelskirchi*) and African elephant (*Loxodonta africana*). *J Comp Neurol* 524:257–287. <https://doi.org/10.1002/cne.23841>

- Jacobs LL, Polcyn MJ, Mateus O et al (2016b) Post-Gondwana Africa and the vertebrate history of the Angolan Atlantic coast. *Mem Mus Vic* 74:343–362. <https://doi.org/10.24199/jmmv.2016.74.24>
- Jaeger J-J, Salem MJ, Bilal AA et al (2012) Dūr at Ṭalaḥ vertebrate locality revisited: new data on its stratigraphy, age, sedimentology and mammalian fossils. In: Salem MJ, Elbakai MT, Abutarruma Y (eds) *Earth science*. Society of Libya, Tripoli, pp 241–258
- Jebb D, Hiller M (2018) Recurrent loss of HMGS2 shows that ketogenesis is not essential for the evolution of large mammalian brains. *eLife* 7:e38906. <https://doi.org/10.7554/eLife.38906>
- Jerison H (1973) *Evolution of the brain and intelligence*. Elsevier Science, Saint Louis
- Johnson EW, Rasmussen L (2002) Morphological characteristics of the vomeronasal organ of the newborn Asian elephant (*Elephas maximus*). *Anat Rec* 267:252–259. <https://doi.org/10.1002/ar.10112>
- Kappelman J, Rasmussen DT, Sanders WJ et al (2003) Oligocene mammals from Ethiopia and faunal exchange between Afro-Arabia and Eurasia. *Nature* 426:549–552. <https://doi.org/10.1038/nature02102>
- Ketten DR (1992) The marine mammal ear: specializations for aquatic audition and echolocation. In: Webster DB, Popper AN, Fay RR (eds) *The evolutionary biology of hearing*. Springer, New York, pp 717–750
- Ketten DR, Odell DK, Domning DP (1992) Structure, function, and adaptation of the manatee ear. In: Thomas JA, Kastelein RA, Supin AY (eds) *Marine mammal sensory systems*. Springer, Boston, pp 77–95
- Kharlamova AS, Saveliev SV, Protopopov AV et al (2015) The mummified brain of a pleistocene woolly mammoth (*Mammuthus primigenius*) compared with the brain of the extant African elephant (*Loxodonta africana*). *J Comp Neurol* 523:2326–2343. <https://doi.org/10.1002/cne.23817>
- Kharlamova A, Saveliev S, Kurtova A et al (2016) Preserved brain of the woolly mammoth (*Mammuthus primigenius* (Blumenbach 1799)) from the Yakutian permafrost. *Quat Internat* 406:86–93. <https://doi.org/10.1016/j.quaint.2014.09.073>
- Kharlamova AS, Pavlov IS, Saveliev SV (2021) Unique 39 thousand cal. BP brain of the “Yuka” mammoth mummified fossils: A history and methods of the examination: paleoneurological perspectives. *Paleontol J* 55:1260–1269. <https://doi.org/10.1134/S0031030121110034>
- Kielan-Jaworowska Z (1986) Brain evolution in Mesozoic mammals. In: Flanagan KM, Lillegraven JA (eds) *Vertebrates, phylogeny, and philosophy*. University of Wyoming, Laramie, pp 21–34
- Knoll F, Galton PM, López-Antoñanzas R (2006) Paleoneurological evidence against a proboscis in the sauropod dinosaur *Diplodocus*. *Geobios* 39:215–221. <https://doi.org/10.1016/j.geobios.2004.11.005>
- Knoll F, Witmer LM, Ortega F et al (2012) The braincase of the basal sauropod dinosaur *Spinophorosaurus* and 3D reconstructions of the cranial endocast and inner ear. *PLoS One* 7:e30060. <https://doi.org/10.1371/journal.pone.0030060>
- Kreps EM, Chirkovskaia EV, Pomazanskaia LF et al (1979) Brain lipids of a mammoth, *Elephas primigenius*, which died more than 40,000 years ago. *Zh Evol Biokhim Fiziol* 15:227–238
- Kreps EM, Avrova NF, Chebotarëva MA et al (1981) Brain lipids in fossilized mammoths, *Mammuthus primigenius*. *Comp Biochem Physiol B Comp Biochem* 68:135–140. [https://doi.org/10.1016/0305-0491\(81\)90192-9](https://doi.org/10.1016/0305-0491(81)90192-9)
- Kubacska AT (1944) Der natürliche Schädelhöhlenausschnitt eines Mammut aus tatra. In: *Annales Historico-Naturales Musei Nationalis Hungarici*, pp 3–40
- Kuntner M, May-Collado LJ, Agnarsson I (2011) Phylogeny and conservation priorities of afrotherian mammals (Afrotheria, Mammalia). *Zool Scr* 40:1–15. <https://doi.org/10.1111/j.1463-6409.2010.00452.x>
- Kupsky WJ, Marchant GH, Cook K et al (2001) Morphologic analysis of the hippocampal formation in *Elephas maximus* and *Loxodonta africana* with comparison to that of human. In: *Proceedings of the first international congress of La Terra degli Elefanti, the world of elephants*. Consiglio Nazionale delle Ricerche, Rome, pp 643–647

- Langbauer WR (2000) Elephant communication. *Zoo Biol* 19:425–445. [https://doi.org/10.1002/1098-2361\(2000\)19:5<425::AID-ZOO11>3.0.CO;2-A](https://doi.org/10.1002/1098-2361(2000)19:5<425::AID-ZOO11>3.0.CO;2-A)
- Larger R (1917) Théorie de la contre-évolution, ou Dégénérescence par l'hérédité pathologique. Félix Alcan, Paris
- Larramendi A (2015) Shoulder height, body mass, and shape of proboscideans. *Acta Palaeontol Pol* 61:537–574. <https://doi.org/10.4202/app.00136.2014>
- Larramendi A, Palombo MR (2015) Body size, biology and encephalization quotient of *Palaeoloxodon* ex gr. *P. falconeri* from Spinagallo Cave (Hyblean plateau, Sicily). *Hystrix* 26:102–109. <https://doi.org/10.4404/hystrix-26.2-11478>
- Liakopoulou DE, Theodorou GE, van Heteren AH (2021) The inner morphology of the petrosal bone of the endemic elephant of Tilos Island, Greece. *Palaeontol Elec* 24(a23):10.26879/1034
- Limacher-Burrell A, Bhagwandin A, Maseko BC et al (2018) Nuclear organization of the African elephant (*Loxodonta africana*) amygdaloid complex: an unusual mammalian amygdala. *Brain Struct Funct* 223:1191–1216. <https://doi.org/10.1007/s00429-017-1555-3>
- Lister AM (2013) The role of behaviour in adaptive morphological evolution of African proboscideans. *Nature* 500:331–334. <https://doi.org/10.1038/nature12275>
- Liu AGSC, Seiffert ER, Simons EL (2008) Stable isotope evidence for an amphibious phase in early proboscidean evolution. *Proc Natl Acad Sci USA* 105:5786–5791. <https://doi.org/10.1073/pnas.0800884105>
- Lomolino MV, Sax DF, Palombo MR et al (2012) Of mice and mammoths: evaluations of causal explanations for body size evolution in insular mammals. *J Biogeogr* 39:842–854. <https://doi.org/10.1111/j.1365-2699.2011.02656.x>
- Lomolino MV, van der Geer AA, Lyras GA et al (2013) Of mice and mammoths: generality and antiquity of the island rule. *J Biogeogr* 40:1427–1439
- Lyras GA (2018) Brain changes during phyletic dwarfing in elephants and hippos. *Brain Behav Evol* 92:167–181. <https://doi.org/10.1159/000497268>
- Maccagno AM (1962) Gli elefanti di Riano (Roma). *Geologica Romana* 1:33–131
- Mahboubi M, Ameur R, Crockett JY et al (1984) Earliest known proboscidean from early Eocene of north-west Africa. *Nature* 308:543–544. <https://doi.org/10.1038/308543a0>
- Manger PR (2006) An examination of cetacean brain structure with a novel hypothesis correlating thermogenesis to the evolution of a big brain. *Biol Rev* 81:293. <https://doi.org/10.1017/S1464793106007019>
- Manger PR, Pillay P, Maseko BC et al (2009) Acquisition of brains from the African elephant (*Loxodonta africana*): perfusion-fixation and dissection. *J Neurosci Methods* 179:16–21. <https://doi.org/10.1016/j.jneumeth.2009.01.001>
- Manger PR, Hemingway J, Haagensen M et al (2010) Cross-sectional area of the elephant corpus callosum: comparison to other eutherian mammals. *Neuroscience* 167:815–824. <https://doi.org/10.1016/j.neuroscience.2010.02.066>
- Manger PR, Prowse M, Haagensen M et al (2012) Quantitative analysis of neocortical gyrencephaly in African elephants (*Loxodonta africana*) and six species of cetaceans: comparison with other mammals. *J Comp Neurol* 520:2430–2439. <https://doi.org/10.1002/cne.23046>
- Manger PR, Spocter MA, Patzke N (2013) The evolutions of large brain size in mammals: the 'Over-700-Gram Club Quartet'. *Brain Behav Evol* 82:68–78. <https://doi.org/10.1159/000352056>
- Manoussaki D, Chadwick RS, Ketten DR et al (2008) The influence of cochlear shape on low-frequency hearing. *Proc Natl Acad Sci USA*:6162–6166. <https://doi.org/10.1073/pnas.0710037105>
- Markov G, Spassov N (2001) A reconstruction of the facial morphology and feeding behaviour of the deinotheres. In: Proceedings of the 1st international congress. Roma, pp 652–655
- Marsh OC (1873) On the gigantic fossil mammals of the order Dinocerata. *Am J of Sci* s3-5:117–122. <https://doi.org/10.2475/ajs.s3-5.26.117>
- Martin RD (1981) Relative brain size and basal metabolic rate in terrestrial vertebrates. *Nature* 293:57–60. <https://doi.org/10.1038/293057a0>

- Maschenko EN, Boeskorov GG, Baranov VA (2013) Morphology of a mammoth calf (*Mammuthus primigenius*) from Ol'chan (Oimiakon, Yakutia). *Paleontol J* 47:425–438. <https://doi.org/10.1134/S0031030113040096>
- Maseko BC, Spocter MA, Haagensen M et al (2011) Volumetric analysis of the African elephant ventricular system. *Anat Rec* 294:1412–1417. <https://doi.org/10.1002/ar.21431>
- Maseko BC, Spocter MA, Haagensen M et al (2012) Elephants have relatively the largest cerebellum size of mammals. *Anat Rec* 295:661–672. <https://doi.org/10.1002/ar.22425>
- Maseko BC, Jacobs B, Spocter MA et al (2013a) Qualitative and quantitative aspects of the micro-anatomy of the African elephant cerebellar cortex. *Brain Behav Evol* 81:40–55. <https://doi.org/10.1159/000345565>
- Maseko BC, Patzke N, Fuxe K et al (2013b) Architectural organization of the African Elephant diencephalon and brainstem. *Brain Behav Evol* 82:83–128. <https://doi.org/10.1159/000352004>
- Matsumoto H, Andrews CW (1923) A contribution to the knowledge of *Moeritherium*. *Bull Am Mus Nat Hist* 48(article 4):97–140
- Meng J, Shoshani J, Ketten D (1997) Evolutionary evidence for infrasonic sound and hearing in proboscideans. *J Vertebr Paleontol* 17:64–65A. <https://doi.org/10.1080/02724634.1997.10011028>
- Milne-Edwards H (1868) Observations sur le stéréocère de Gall. *Annales des Sciences Naturelles*, Paris 10:203–221
- Mirceta S, Signore AV, Burns JM et al (2013) Evolution of mammalian diving capacity traced by myoglobin net surface charge. *Science* 340(6138):1234192. <https://doi.org/10.1126/science.1234192>
- Mothé D, Ferretti MP, Avilla LS (2016) The dance of tusks: rediscovery of lower incisors in the Pan-American proboscidean *Cuvieronius hyodon* revises incisor evolution in Elephantimorpha. *PLoS One* 11:e0147009. <https://doi.org/10.1371/journal.pone.0147009>
- Mourlam MJ, Orliac MJ (2017) Infrasonic and ultrasonic hearing evolved after the emergence of modern whales. *Curr Biol* 27:1776–1781.e9. <https://doi.org/10.1016/j.cub.2017.04.061>
- Muchlinski MN (2008) The relationship between the infraorbital foramen, infraorbital nerve, and maxillary mechanoreception: implications for interpreting the paleoecology of fossil mammals based on infraorbital foramen size. *Anat Rec* 291:1221–1226. <https://doi.org/10.1002/ar.20742>
- Muchlinski MN (2010) Ecological correlates of infraorbital foramen area in primates. *Am J Phys Anthropol* 141:131–141. <https://doi.org/10.1002/ajpa.21137>
- Mudelsee M, Bickert T, Lear CH et al (2014) Cenozoic climate changes: a review based on time series analysis of marine benthic $\delta^{18}\text{O}$ records. *Rev Geophys* 52:333–374. <https://doi.org/10.1002/2013RG000440>
- Nabavizadeh A (2015) Proboscidean jaw mechanics and the evolution of the proboscis and feeding apparatus in extant elephants. *FASEB J* 29:867.10. https://doi.org/10.1096/fasebj.29.1_supplement.867.10
- Nabavizadeh A, Reidenberg JS (2019) Anatomy of the proboscidean nerve in the proboscis of the African elephant (*Loxodonta africana*). *FASEB J* 33:lb148. https://doi.org/10.1096/fasebj.2019.33.1_supplement.lb148
- Nair S, Balakrishnan R, Seelamantula CS et al (2009) Vocalizations of wild Asian elephants (*Elephas maximus*): structural classification and social context. *J Acoust Soc Am* 126:2768–2778. <https://doi.org/10.1121/1.3224717>
- Ngwenya A, Patzke N, Ihunwo AO et al (2011) Organisation and chemical neuroanatomy of the African elephant (*Loxodonta africana*) olfactory bulb. *Brain Struct Funct* 216:403–416. <https://doi.org/10.1007/s00429-011-0316-y>
- Niimura Y, Matsui A, Touhara K (2014) Extreme expansion of the olfactory receptor gene repertoire in African elephants and evolutionary dynamics of orthologous gene groups in 13 placental mammals. *Genome Res* 24:1485–1496. <https://doi.org/10.1101/gr.169532.113>
- Noubhani A, Hautier L, Jaeger J-J et al (2008) Variabilité dentaire et crânienne de *Numidotherium koholense* (Mammalia, Proboscidea) de l'Éocène d'El Kohol, Algérie. *Geobios* 41:515–531. <https://doi.org/10.1016/j.geobios.2007.09.002>

- Novacek MJ, Wyss AR (1986) Higher-level relationships of the recent Eutherian orders: morphological evidence. *Cladistics* 2:257–287. <https://doi.org/10.1111/j.1096-0031.1986.tb00463.x>
- Novacek MJ, Wyss AR (1987) Selected features of the desmostylian skeleton and their phylogenetic implications. *Desmostylian skeleton*. *Am Mus Novit* 2870:7–8
- O’Connell-Rodwell CE (2007) Keeping an “ear” to the ground: seismic communication in elephants. *Physiology* 22:287–294. <https://doi.org/10.1152/physiol.00008.2007>
- O’Connell-Rodwell CE, Hart LA, Arnason BT (2001) Exploring the potential use of seismic waves as a communication channel by elephants and other large mammals. *Integr Comp Biol* 41:1157–1170. <https://doi.org/10.1093/icb/41.5.1157>
- O’Connell-Rodwell CE, Wood JD, Kinzley C et al (2007) Wild African elephants (*Loxodonta africana*) discriminate between familiar and unfamiliar conspecific seismic alarm calls. *J Acoust Soc Am* 122:823–830. <https://doi.org/10.1121/1.2747161>
- O’Shea TJ, Reep RL (1990) Encephalization quotients and life-history traits in the sirenia. *J Mammal* 71:534–543. <https://doi.org/10.2307/1381792>
- Orihuela J, López LWV, Macrini TE (2019) First cranial endocasts of early Miocene sirenians (Dugongidae) from the West Indies. *J Vertebr Paleontol* 39:e1584565. <https://doi.org/10.1080/002724634.2019.1584565>
- Osborn HF (1931) *Palaeoloxodon antiquus italicus* sp. nov., final stage in the ‘*Elephas antiquus*’ phylum. *Am Mus Nov* 460:1–24
- Osborn HF (1936) Proboscidea: a monograph of the discovery, evolution, migration and extinction of the mastodonts and elephants of the world, vol 1. Published on the J. Pierpont Morgan Fund by the trustees of the American Museum of Natural History: American Museum Press, New York
- Osborn HF (1942) Proboscidea: a monograph of the discovery, evolution, migration and extinction of the mastodonts and elephants of the world, vol 2. Published on the J. Pierpont Morgan Fund by the trustees of the American Museum of Natural History: American Museum Press, New York
- Palkopoulou E, Lipson M, Mallick S et al (2018) A comprehensive genomic history of extinct and living elephants. *Proc Natl Acad Sci USA* 115:E2566–E2574. <https://doi.org/10.1073/pnas.1720554115>
- Palombo MR, Giovinazzo C (2005) *Elephas falconeri* from Spinagallo Cave (south-eastern Sicily, Hyblean Plateau, Siracusa): a preliminary report on brain to body weight comparison. In: Proceedings of the International Symposium “Insular Vertebrate Evolution: the Palaeontological Approach”: September, 16–19 Mallorca. Societat d’Història Natural de les Balears, pp 255–264
- Patzke N, Olalaye O, Haagenen M et al (2014) Organization and chemical neuroanatomy of the African elephant (*Loxodonta africana*) hippocampus. *Brain Struct Funct* 219:1587–1601. <https://doi.org/10.1007/s00429-013-0587-6>
- Patzke N, Spocter MA, Karlsson KÆ et al (2015) In contrast to many other mammals, cetaceans have relatively small hippocampi that appear to lack adult neurogenesis. *Brain Struct Funct* 220:361–383. <https://doi.org/10.1007/s00429-013-0660-1>
- Payne KB, Langbauer WR, Thomas EM (1986) Infrasonic calls of the Asian elephant (*Elephas maximus*). *Behav Ecol Sociobiol* 18:297–301. <https://doi.org/10.1007/BF00300007>
- Pérez-Barbería FJ, Gordon IJ (2005) Gregariousness increases brain size in ungulates. *Oecologia* 145:41–52. <https://doi.org/10.1007/s00442-005-0067-7>
- Peters RH (1983) The ecological implications of body size. Cambridge University Press, Cambridge
- Pettigrew JD, Bhagwandin A, Haagenen M et al (2010) Visual acuity and heterogeneities of retinal ganglion cell densities and the tapetum lucidum of the African elephant (*Loxodonta africana*). *Brain Behav Evol* 75:251–261. <https://doi.org/10.1159/000314898>
- Pirlot P, Kamiya T (1985) Qualitative and quantitative brain morphology in the sirenian *Dugong dugong*. *J Zool Syst Evol Res* 23:147–155. <https://doi.org/10.1111/j.1439-0469.1985.tb00577.x>

- Policht R, Tomášová K, Holečková D et al (2008) The vocal repertoire in Northern White Rhinoceros *Cerathotherium simum cottoni* as recorded in the last surviving herd. *Bioacoustics* 18:69–96. <https://doi.org/10.1080/09524622.2008.9753591>
- Poole JH, Payne K, Langbauer WR et al (1988) The social contexts of some very low frequency calls of African elephants. *Behav Ecol Sociobiol* 22:385–392. <https://doi.org/10.1007/BF00294975>
- Poole JH, Tyack PL, Stoeger-Horwath AS et al (2005) Elephants are capable of vocal learning. *Nature* 434:455–456. <https://doi.org/10.1038/434455a>
- Poulakakis N, Stamatakis A (2010) Recapitulating the evolution of Afrotheria: 57 genes and rare genomic changes (RGCs) consolidate their history. *System Biodivers* 8:395–408. <https://doi.org/10.1080/14772000.2010.484436>
- Provatidis CG, Theodorou EG, Theodorou GE (2011) Computed tomography and CAD/CAE methods for the study of the osseous inner ear bone of Greek quaternary endemic mammals. *Mediterr Archaeol Archaeom* 11:121–127
- Radinsky L (1973) Evolution of the canid brain. *Brain Behav Evol* 7:169–185. <https://doi.org/10.1159/000124409>
- Radinsky L (1977) Early primate brains: facts and fiction. *J Hum Evol* 6:79–86. [https://doi.org/10.1016/S0047-2484\(77\)80043-2](https://doi.org/10.1016/S0047-2484(77)80043-2)
- Richards H (1890) A further report on the anatomy of the elephant's ear. *Trans Am Otol Soc* 4:587–604. <https://doi.org/10.5962/bhl.title.101959>
- Roca AL, O'Brien SJ (2005) Genomic inferences from Afrotheria and the evolution of elephants. *Curr Opin Genet Dev* 15:652–659. <https://doi.org/10.1016/j.gde.2005.09.014>
- Rodella LF, Buffoli B, Labanca M et al (2012) A review of the mandibular and maxillary nerve supplies and their clinical relevance. *Arch Oral Biol* 57:323–334. <https://doi.org/10.1016/j.archoralbio.2011.09.007>
- Rohland N, Malaspinas A-S, Pollack JL et al (2007) Proboscidean mitogenomics: chronology and mode of elephant evolution using mastodon as outgroup. *PLoS Biol* 5:e207. <https://doi.org/10.1371/journal.pbio.0050207>
- Rohrs N, Ebinger P (2001) How is cranial capacity related to brain volume in mammals? *Mamm Biol* 66:102–110
- Romano M, Manucci F, Palombo MR (2019) The smallest of the largest: new volumetric body mass estimate and in-vivo restoration of the dwarf elephant *Palaeoloxodon ex gr. P. falconeri* from Spinagallo Cave (Sicily). *Hist Biol* 33:340–353. <https://doi.org/10.1080/08912963.2019.1617289>
- Ronald K, Selley LJ, Amoroso EC (1978) Biological synopsis of the manatee. International Development Research Centre, Ottawa
- Roth VL (1990) Insular dwarf elephants: a case study in body mass estimation and ecological inference. In: Damuth J, MacFadden BJ (eds) *Body size in mammalian paleobiology: estimation and biological implications*. Cambridge University Press, New York, pp 151–179
- Rowe T (1996) Coevolution of the mammalian middle ear and neocortex. *Science* 273:651–654. <https://doi.org/10.1126/science.273.5275.651>
- Salensky W (1904) Über die Hauptresultate der Erforschung des im Jahre 1901 am Ufer der Beresowka entdeckten männlichen Mammutkadavers. *Compte-rendu des séances du sixième Congrès international de zoologie* 6:67–86
- Sánchez-Villagra MR (2002) The cerebellar paraflocculus and the subarcuate fossa in *Monodelphis domestica* and other marsupial mammals – ontogeny and phylogeny of a brain-skull interaction. *Acta Theriol* 47:1–14. <https://doi.org/10.1007/BF03193561>
- Sander PM, Christian A, Clauss M et al (2011) Biology of the sauropod dinosaurs: the evolution of gigantism. *Biol Rev* 86:117–155. <https://doi.org/10.1111/j.1469-185X.2010.00137.x>
- Sanders W, Gheerbrant E, Harris J et al (2010) Proboscidea. In: Werdelin L, Sanders WJ (eds) *Cenozoic mammals of Africa*. University of California Press, Berkeley
- Scheele WE (1955) *The first mammals*. World Pub. Co., New York
- Schlesinger G (1922) Die Mastodonten der Budapester Sammlungen. *Geol Hung* 2:1–284

- Schmitt A (2016) La région de l'oreille osseuse chez les Proboscidea (Afrotheria, Mammalia): anatomie, fonction, évolution. Thèse de doctorat, Paris, Muséum national d'histoire naturelle
- Schmitt A, Gheerbrant E (2016) The ear region of earliest known elephant relatives: new light on the ancestral morphotype of proboscideans and afrotherians. *J Anat* 228:137–152. <https://doi.org/10.1111/joa.12396>
- Seiferle E (1966) On the topography of the brain on long and short skulls in dog breeds. *Acta Anat* 63:346–362
- Seiffert ER (2007a) A new estimate of afrotherian phylogeny based on simultaneous analysis of genomic, morphological, and fossil evidence. *BMC Evol Biol* 7:224. <https://doi.org/10.1186/1471-2148-7-224>
- Seiffert ER (2007b) Evolution and Extinction of Afro-Arabian Primates Near the Eocene-Oligocene Boundary. *Folia Primatol* 78:314–327. <https://doi.org/10.1159/000105147>
- Shauer K (2010) Commentary and sources for the evolutionary diagram of the Proboscidea in Africa and Eurasia. In: Meller H (ed) *Elefantenreich – Eine Fossilwelt in Europa*. Landesamt für Denkmalpflege und Archäologie Sachsen-Anhalt & Landesmuseum Vorgeschichte, pp 631–650
- Shoshani J (1982) On the dissection of a female Asian elephant (*Elephas maximus maximus* Linnaeus, 1758) and data from other elephants. *Elephant* 2:3–93. <https://doi.org/10.22237/elephant/1521731887>
- Shoshani J (1998) Understanding proboscidean evolution: a formidable task. *Trends Ecol Evol* 13:480–487. [https://doi.org/10.1016/S0169-5347\(98\)01491-8](https://doi.org/10.1016/S0169-5347(98)01491-8)
- Shoshani J, Eisenberg JF (1982) *Elephas maximus*. *Mamm Species* 182:1–8. <https://doi.org/10.2307/3504045>
- Shoshani J, Tassy P (1996) *The Proboscidea: evolution and palaeoecology of elephants and their relatives*. Oxford University Press
- Shoshani J, Tassy P (2005) Advances in proboscidean taxonomy & classification, anatomy & physiology, and ecology & behavior. *Quat Int* 126–128:5–20. <https://doi.org/10.1016/j.quaint.2004.04.011>
- Shoshani J, Marchant GH, Cavarretta G (2001) Hyoid apparatus: a little known complex of bones and its “contribution” to proboscidean evolution. In: *La terra degli elefanti: atti del 1. Congresso internazionale; Roma, 16–20 ottobre 2001; Proceedings of the 1st international congress. Consiglio nazionale delle ricerche, Roma*
- Shoshani J, Kupsky WJ, Marchant GH (2006) Elephant brain. *Brain Res Bull* 70:124–157. <https://doi.org/10.1016/j.brainresbull.2006.03.016>
- Shultz S, Dunbar RIM (2006) Both social and ecological factors predict ungulate brain size. *Proc Biol Sci* 273:207–215. <https://doi.org/10.1098/rspb.2005.3283>
- Simionescu I, Morosan N (1937) Sur le moulage endocrânien d'*Elephas primigenius* de Roumanie. *Bulletin de la section scientifique de l'Académie de Roumanie* 19:1–7
- Stephan H, Bauchot R, Andy OJ (1970) Data on size of the brain and of various brain parts in insectivores and primates. In: Noback CR, Montagna W (eds) *The primate brain*. Appleton-Century-Crofts, New York, pp 289–297
- Stoeger AS, Manger P (2014) Vocal learning in elephants: neural bases and adaptive context. *Curr Opin Neurobiol* 28:101–107. <https://doi.org/10.1016/j.conb.2014.07.001>
- Stoeger AS, Charlton BD, Kratochvil H et al (2011) Vocal cues indicate level of arousal in infant African elephant roars. *J Acoust Soc Am* 130:1700–1710. <https://doi.org/10.1121/1.3605538>
- Tassy P (1981) Le crâne de *Moeritherium* (Proboscidea, Mammalia) de l'Eocène de Dor El Talha (Libye) et le problème de la classification phylogénétique du genre dans les Tethytheria McKenna, 1975. *Bull Mus Natl Hist Nat*, 4 sér, sect C 3:87–147
- Tassy P (1994) Gaps, parsimony, and early Miocene elephantoids (Mammalia), with a re-evaluation of *Gomphotherium annectens* (Matsumoto, 1925). *Zool J Linn Soc* 112:101–117. <https://doi.org/10.1111/j.1096-3642.1994.tb00313.x>

- Tassy P (2013) L'anatomie cranio-mandibulaire de *Gomphotherium angustidens* (Cuvier, 1817) (Proboscidea, Mammalia): données issues du gisement d'En Pélouan (Miocène moyen du Gers, France). *Geodiversitas* 35:377–445. <https://doi.org/10.5252/g2013n2a6>
- van der Geer AA, Lyras GA, van den Hoek Ostende LW et al (2014) A dwarf elephant and a rock mouse on Naxos (Cyclades, Greece) with a revision of the palaeozoogeography of the Cycladic Islands (Greece) during the Pleistocene. *Palaeogeogr Palaeoclimatol Palaeoecol* 404:133–144
- van der Geer AAE, van den Bergh GD, Lyras GA et al (2016) The effect of area and isolation on insular dwarf proboscideans. *J Biogeogr* 43:1656–1666. <https://doi.org/10.1111/jbi.12743>
- van der Geer AA, Lyras GA, Mitteroecker P et al (2018) From Jumbo to Dumbo: cranial shape changes in elephants and hippos during phyletic dwarfing. *Evol Biol* 45:303–317
- van der Klaauw CJ (1931) The auditory bulla in some fossil mammals: with a general introduction to this region of the skull. On the auditory bulla in some fossil mammals. *Bull Am Mus Nat Hist* 62:1–352
- Van der Made J (2010) The evolution of elephants and their relatives in the context of a changing climate and geography. In: Meller H (ed) *Elefantenreich – Eine Fossilwelt in Europa*. Landesamt für Denkmalpflege und Archäologie Sachsen-Anhalt & Landesmuseum Vorgeschichte, pp 341–360
- van der Merwe NJ, Bezuidenhout AJ, Seegers CD (1995) The skull and mandible of the African elephant (*Loxodonta africana*). *Onderstepoort J Vet Res* 62:245–260
- Van Valen L (1973) Body size and numbers of plants and animals. *Evolution*:27–35
- Vereschagin NK (1981) Morfometricheskoe opisanie mamontenka. In: Vereschagin NK, Mikhelson VM (eds) *Magadanskii Mamontenok*. Nauka, Leningrad, pp 52–80
- Vereschagin NK (1999) Yamal'skiy Mamontenok: Morfometricheskoye Opisanie Skeleta. *Trudy Zool Inst RAS* 275:32e38. (in Russian). *Proceedings of the Zoological Institute RAS* 275:32–38
- von Muggenthaler E, Reinhart P (2003) Songlike vocalizations from a Sumatran rhinoceros calf (*Dicerorhinus sumatrensis*). *J Acoust Soc Am* 113:2277–2277. <https://doi.org/10.1121/1.4780553>
- Walker A, Ryan TM, Silcox MT et al (2008) The semicircular canal system and locomotion: the case of extinct lemuroids and lorisoids. *Evol Anthropol* 17:135–145. <https://doi.org/10.1002/evan.20165>
- Wall WP (1980) Cranial evidence for a proboscis in *Cadurcodon* and a review of snout structure in the Family Amarynodontidae (Perissodactyla, Rhinoceroidea). *J Paleontol* 54:968–977
- Warren JC (1855) *The Mastodon giganteus* of North America. Wilson, Boston
- Watson M (1874) Contributions to the anatomy of the Indian elephant: Part IV. Muscles and blood-vessels of the face and head. *J Anat Physiol* 9:118–133
- Weber J, Czarnetzki A, Pusch CM (2005) Comment on “The Brain of LB1, *Homo floresiensis*”. *Science* 310:236b. <https://doi.org/10.1126/science.1114789>
- Weisbecker V, Goswami A (2011) Neonatal maturity as the key to understanding brain size evolution in homeothermic vertebrates. *BioEssays* 33:155–158. <https://doi.org/10.1002/bies.201000128>
- West CD (1985) The relationship of the spiral turns of the cochlea and the length of the basilar membrane to the range of audible frequencies in ground dwelling mammals. *J Acoust Soc Am* 77:1091–1101. <https://doi.org/10.1121/1.392227>
- Weston EM, Lister AM (2009) Insular dwarfism in hippos and a model for brain size reduction in *Homo floresiensis*. *Nature* 459:85–88. <https://doi.org/10.1038/nature07922>
- Wible JR (1986) Transformations in the extracranial course of the internal carotid artery in mammalian phylogeny. *J Vertebr Paleontol* 6:313–325. <https://doi.org/10.1080/02724634.1986.10011628>
- Witmer LM, Sampson SD, Solounias N (1999) The proboscis of tapirs (Mammalia: Perissodactyla): a case study in novel narial anatomy. *J Zool* 249:249–267. <https://doi.org/10.1111/j.1469-7998.1999.tb00763.x>

- Witmer LM, Ridgely RC, Dufeu DL et al (2008) Using CT to peer into the past: 3D visualization of the brain and ear regions of birds, crocodiles, and nonavian dinosaurs. In: Endo H, Frey R (eds) *Anatomical imaging*. Springer, Tokyo, pp 67–87
- Zachos J, Pagani M, Sloan L et al (2001) Trends, rhythms, and aberrations in global climate 65 Ma to present. *Science* 292:686–693. <https://doi.org/10.1126/science.1059412>

Chapter 16

Brain Evolution in Fossil Rodents: A Starting Point



Ornella C. Bertrand and Mary T. Silcox

16.1 Systematic and Phylogenetic Context

The clade Glires is composed of Rodentia and Lagomorpha (rabbits) and has been recovered in molecular (e.g. Murphy et al. 2001a; Huchon et al. 2002; Poux et al. 2006) and morphological (e.g. Chuan-Kuei et al. 1987; Meng et al. 2003; Marivaux et al. 2004; Meng 2004) analyses. In a broader context, Glires and Euarchonta (Primates, Scandentia, Dermoptera) are sister-clades belonging to Euarchontoglires (Murphy et al. 2001b).

Today, rodents encompass more than 2500 species, representing 40% of mammalian diversity (Burgin et al. 2018). The monophyly of rodents is well-supported and has only rarely been contested (e.g., Graur et al. 1991). In contrast, the internal relationships of rodents have been disputed throughout the last century since Tullberg's first classification in 1899 (Tullberg 1899). Rodents used to be divided into two groups, Sciurognathi and Hystricognathi, based on the angular process position compared to the incisor plane. This hypothesis remained popular among rodentologists for decades (e.g. Lavocat 1973; Luckett and Hartenberger 1985; McKenna and Bell 1997; Nowak 1999; Wilson and Reeder 2005) because it helped to reconcile molecular and morphological results, at least for extant hystricognath rodents, for which it is well-supported by both types of data (e.g. Bugge 1985; Marivaux et al. 2004; Huchon et al. 2000). Another hypothesis surfaced, based on distinct muscle attachment configurations of the masticatory apparatus, leading to the recognition of three groups: Sciuromorpha, Hystricomorpha and Myomorpha (e.g. Simpson 1945). The issue with this classification was that some groups could

O. C. Bertrand (✉)

School of Geosciences, Grant Institute, University of Edinburgh, Edinburgh, Scotland, UK
e-mail: ornella.bertrand@ed.ac.uk

M. T. Silcox

Department of Anthropology, University of Toronto Scarborough, Toronto, ON, Canada
e-mail: mary.silcox@utoronto.ca

not be included in any of the three categories, including Aplodontidae (i.e. mountain beavers), which display a fourth state known as Protrugomorphy that was considered the plesiomorphic condition for rodents (Wood 1955).

Based on molecular data, Rodentia is now divided into three distinct groups: the Squirrel-related clade (squirrels, mountain beavers, dormice), Ctenohystrica (African porcupines, gundis, chinchillas, pacas) and the mouse-related clade which includes Myodonta (rats and mice), Castorimorpha (beavers, kangaroo rats) and Anomaluromorpha (scaly-tailed squirrels, springhares; Huchon et al. 1999; Douzery et al. 2003; Blanga-Kanfi et al. 2009; Meredith et al. 2011; Fabre et al. 2015). There are still major aspects of rodent phylogeny that are under intense debate. First, the relationships within the mouse-related clade are still not resolved, so the relationships among its three members remain unclear (Blanga-Kanfi et al. 2009; Fabre et al. 2013; Fabre et al. 2015). Second, and most important in the context of this chapter, any of the three major rodent clades could potentially be considered the most basal. The Squirrel-related clade has been recovered the most often as the sister taxon to Ctenohystrica plus the mouse-related clade (e.g. Huchon et al. 2000; Douzery et al. 2003; Blanga-Kanfi et al. 2009) but the two other combinations have been found as well (e.g. Montgelard et al. 2008; Meredith et al. 2011).

With respect to the origins of the group from fossil taxa, based solely on morphological data Lockett and Hartenberger (1985) viewed modern rodents emerging from two groups, one from Asian ctenodactyloids and one from North American and Eurasian ischyromyoids. Wible et al. (2005) recovered Ctenohystrica (Huchon et al. 2000) as sister-clade to a North American and Eurasian clade (Ischyromyidae, Sciuravidae, and Theridomyidae).

In this chapter, we will focus specifically on the Squirrel-related clade and its closest fossil relatives, Ischyromyidae; and on South American caviomorph rodents, because virtual endocasts for extant and extinct species have been studied for these groups. The Squirrel-related clade is composed of Gliridae and Sciuroidea (including Sciuridae and Aplodontidae as sister-clades). This grouping was found using molecular (Blanga-Kanfi et al. 2009; Churakov et al. 2010; Fabre et al. 2012) and morphological data (Meng 1990; Korth and Emry 1991; Korth 1994). Aplodontidae is represented by a single species today, the mountain beaver *Aplodontia rufa*. However, this family was very diverse in the past and was distributed across the Holarctic region, with cranio-dental material of fossil aplodontids being recovered in North America, Europe and Asia (e.g. Rensberger 1981, 1983; Hopkins 2008; Vianey-Liaud et al. 2013). In total, the known fossil record for this family encompasses 27 genera and more than 100 species (Hopkins 2008). Sciuridae is the second most diverse family of extant rodents today with 58 genera in 285 species (Burgin et al. 2018). Members of this family are native to all continents except Australia and Antarctica (Mercer and Roth 2003). The fossil record of Sciuridae extends to the late Eocene and fossils have mainly been recovered in North America and Europe (Emry and Thorington 1982; Thorington et al. 2012). Gliridae (dormice) includes nine extant genera and 26 species (Holden 2005). The glirid fossil record is almost entirely from Europe and the oldest occurrence for the group is dated from the early Eocene (Rose 2006).

Ischyromyidae includes the oldest rodents recovered to date (Late Paleocene) and extends to the Late Oligocene; Ctenodactyloidea is also known from very early specimens, coming from the early Eocene of Asia (Wible et al. 2005; Dawson 2015). Ischyromyidae is considered to be either at the base of Rodentia (Matthew 1910; Wilson 1949; Wood 1962) or the ancestor to Sciuridae and Castoridae (Hartenberger 1980; Dawson et al. 1984; Korth 1984, 1994; Flynn et al. 1986). Fossil ischyromyids have been recovered from North America (late Paleocene to early Oligocene), Europe (early to late Eocene), and East Asia (early Oligocene; Anderson 2008) and classified into four different subfamilies: Paramyinae, Ischyromyinae, Reithroparamyinae, and Ailuravinae (Korth 1994). In phylogenetic analyses Ischyromyidae was found to be polyphyletic (Meng 1990; Marivaux et al. 2004), but these studies used only a handful of species; no study to date has incorporated taxa belonging to all four subfamilies in the same analysis. Potential synapomorphies for Ischyromyidae include (1) large portion of the mastoid separates the bulla from the back of the skull, and (2) the stapedia muscle only located inside the bulla and does not extend outside of it (Lavocat and Parent 1985). One aspect common to different studies is that Paramyinae (and more specifically the genus *Paramys*) has repeatedly been found near the base of Rodentia (Meng 1990; Meng et al. 2003; Wible 2005; O’Leary et al. 2013). A debate persists regarding the relationships among the four subfamilies. Paramyinae and Reithroparamyinae might be more closely related to one another than either is to Ischyromyinae (Wood 1962; Asher et al. 2019); however, another phylogenetic analysis found no evidence of a strong relationship between Paramyinae and Reithroparamyinae (Meng 1990). Meng’s (1990) phylogenetic analysis, using the anatomy of the ear region, suggested that Reithroparamyinae was the closest fossil relative to the Squirrel-related clade. Previous studies have considered Ischyromyinae to be the most derived subfamily based on craniodental features (Korth 1994), and that the ischyromyine *Ischyromys* was sister-clade to Sciuroidea, with Gliridae as outgroup (Asher et al. 2019). Under that hypothesis of relationships, Ischyromyinae would be part of the Squirrel-related clade and Ischyromyidae would be polyphyletic (Fig. 16.1a, b). Ailuravinae represents a distinct subfamily found mainly in Europe (Michaux 1968; Wood 1976; Dawson 2003) and its relationship to the other ischyromyids is unclear.

Caviomorpha is one of the most successful groups of rodents today and is composed of four superfamilies, 11 families and more than 244 extant species (Fig. 16.1c; Huchon and Douzery 2001; Upham and Patterson 2015). Caviidae and Chinchillidae include the largest rodents that ever lived, including the largest living rodent, the capybara, and the extinct Pliocene *Josephoartigasia monesi*, which is the largest rodent known (Ferreira et al. 2020; Rinderknecht and Blanco 2008). Their closest relatives are Hystricidae and Phiomorpha from Africa and Asia (Upham and Patterson 2015). At a higher taxonomic level, Ctenohystrica includes these groups and Ctenodactylomorpha (Ctenodactylidae + Diatomyidae; Fabre et al. 2012; Upham and Patterson 2015; Patterson and Upham 2014). Caviomorpha are endemic to South America, but their ancestors immigrated from Africa probably during the Eocene (Antoine et al. 2012; Vucetich et al. 2015) via one or more crossings of the South Atlantic, which would have been ~1000–1500 km wide (Houle 1999). Fossil

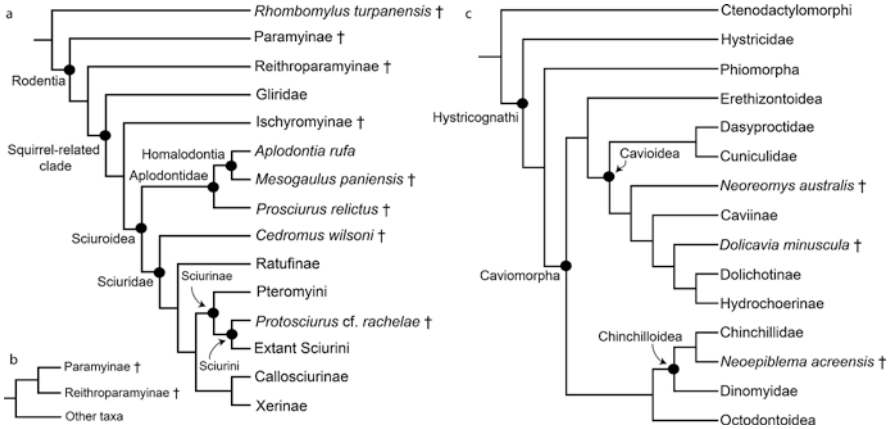


Fig. 16.1 Cladograms representing the relationships of the taxa discussed in the text. (Hopkins 2008; Korth and Emry 1991; Mercer and Roth 2003). For Ischyromyidae: (a), Topology based on Meng (1990) and Asher et al. (2019) and (b), alternative topology based on Asher et al. (2019). The symbol † indicates extinct taxa. (c), Cladogram for Ctenohystrica including Caviomorpha following different studies (Fabre et al. 2012; Patterson and Upham 2014; Upham and Patterson 2015; Kerber et al. 2017; Pérez et al. 2017; Rasia and Candela 2019)

caviomorphs have been recovered from Argentina, Peru, Chile, Bolivia, and Brazil (Bertrand et al. 2012).

In this chapter we limit our discussion of extant species to those that have been studied from endocasts, since they are known from data that is directly comparable to that which can be collected from fossils. Additionally, we note that a full consideration of the brain in living rodents is beyond the scope of this chapter, especially considering the amount of work that has been done on mouse and rat brains and other rodent animal models.

16.2 Historical Background

16.2.1 *The Record of Endocranial Morphology and Any Other Paleoneurological Approaches in the Group Under Study*

Before the widespread use of X-ray Computed Tomographic (CT) data, only a limited number of partial natural endocasts had been published (see Table 16.1). No quantitative data were produced for any of the published natural endocasts of rodents except encephalization quotient values for *Dolicavia minuscula* (Dozo 1997a). Outside rodents, the publication of natural endocasts for the primitive gliroid mammal *Rhombomylus turpanensis* (Meng et al. 2003) provides a starting point for thinking about the early stages of rodent brain evolution. The authors described *R. turpanensis* as having a small and unconvoluted cerebrum and

Table 16.1 Natural endocasts of fossil rodents

Family/Suborder	Specimen	Catalogue #	Epoch	Locality	Reference
Ischyromyidae	<i>Reithroparamys sciurooides</i>	YPM VPPU 011555	Eocene	North America	Scott and Osborn (1887) and Wood (1962)
Ischyromyidae	<i>Pseudotomus hians</i>	AMNH 5025	Eocene	North America	Scott and Osborn (1887, 1890) and Wood (1962)
Ischyromyidae	<i>Ischyromys</i> sp.	–	Oligocene	North America	Scott et al. (1937)
Cylindrodontidae	<i>Pseudocylindrodon texanus</i>	TMM 40840-1	Eocene	North America	Wood (1974)
Pseudosciuridae	<i>Adelomys vaillanti</i>	–	Eocene	Europe	Dechaseaux (1958)
Theridomyindae	<i>Trechomys bonduelli</i>	–	Eocene	Europe	Dechaseaux (1958)
Castoridae	<i>Trogotherium boisvillei</i>	–	Pliocene	Europe	Dechaseaux (1958)
Phiomorpha	<i>Paraphiomys</i>	–	Miocene	Africa	Lavocat (1973)
Caviomorpha	<i>Hypsosteiromys</i> sp.	MPEF-PV 6029	Miocene	South America	Dozo et al. (2004)
Caviomorpha	<i>Cephalomyidae</i> indet.	MACN CH 909	Miocene	South America	Dozo (1997b)
Caviomorpha	<i>Dolicavia minuscula</i>	MMP 386-S	Miocene	South America	Dozo (1997a)
Caviomorpha	<i>Metacaremys primitiva</i> comb. nov.	PVSJ-LT104	Miocene	South America	Piñero et al. (2021)

cerebellum, broadly exposed midbrain, and large olfactory bulbs compared to rodents (Fig. 16.2e). However, no measurements were recorded from the endocast for *R. turpanensis*.

In recent years, virtual endocasts of fossil ischyromiid and sciuroid rodents were produced (Fig. 16.2a–d, f–g). More specifically, data were generated for 11 species of ischyromiid rodents including several Eocene genera (*Paramys*, *Pseudotomus*, *Notoparamys*, *Rapamys*, *Reithroparamys*) and species of the Oligocene genus *Ischyromys typus* (Table 16.2; Bertrand and Silcox 2016; Bertrand et al. 2016a, 2019). For Sciuridae, virtual endocasts of extant squirrels, the Oligocene squirrels *Cedromus wilsoni* and *Protosciurus* cf. *rachelae* were reconstructed (Bertrand et al. 2017, 2018) and for Aplodontidae, endocasts of the extant *Aplodontia rufa*, the Oligocene *Prosciurus relictus* and *Mesogaulus paniensis* were produced (Bertrand et al. 2018). Finally, a recent study described virtual endocasts of nine extant and two extinct South American caviomorphs: *Neoepiblema acreensis* and *Neoreomys australis* belonging to the two clades Chinchilloidea and Cavoidea, respectively (Ferreira et al. 2020). Some quantitative data were provided for all the recently published virtual endocasts including endocranial, olfactory bulb and petrosal

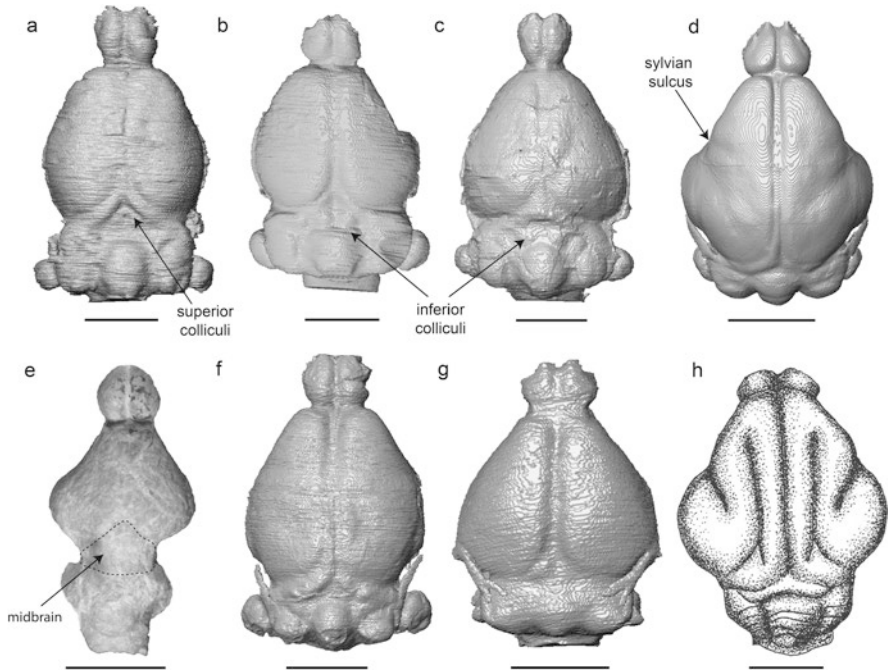


Fig. 16.2 Variation in midbrain exposure in specimens described in the text. Virtual endocasts of (a), *Rapamys atramontis* (AMNH128704) (Bertrand et al. 2019), (b), *Reithroparamys delicatissimus* (AMNH 12561) (Bertrand et al. 2021), (c), *Ischyromys typus* (AMNH: FAM 144836) (Bertrand and Silcox 2016), (d), *Rhinosciurus laticaudatus* (USNM 488511) (Bertrand et al. 2017); (e), Natural endocast of *Rhombomylus turpanensis* (IVPP V5286) (Modified from Meng et al. 2003); Virtual endocasts of (f), *Protosciurus cf. rachelae* (YPM 14737) (Bertrand et al. 2018), (g), *Mesogaulus paniensis* (AMNH F:AM 65511) (Bertrand et al. 2018); (h), Drawing of the natural endocast of *Dolicavia minuscula* (MMP 386-S). (Modified from Dozo 1997a). Scale equals 10 mm

lobule volumes. However, data for the neocortex have only been generated for Sciuroidea and Ischyromyidae.

16.2.2 Problematics

Before the CT scan era, descriptions and comparisons of rodent endocasts were extremely limited and no attempts at quantifying the size of the brain of fossil rodents was made until the very end of the twentieth century (Dozo 1997a). Unfortunately, attempts to acquire quantitative data for natural endocasts has been hampered by challenges in locating and identifying material described in historical references. One natural endocast of the Oligocene *Ischyromys* described and illustrated by Scott et al. (1937) was of interest, for example, because it shows exposed caudal colliculi. One of the authors (OCB) tried to find this natural endocast, but

Table 16.2 Virtual endocasts of fossil rodents

Family/Suborder	Specimen	Catalogue #	Epoch	Locality	Reference
Ischyromyidae	<i>Paramys copei</i>	AMNH 4756	Eocene	North America	Bertrand et al. (2016a)
Ischyromyidae	<i>Paramys delicatus</i>	AMNH 12506	Eocene	North America	Bertrand et al. (2016a)
Ischyromyidae	<i>Pseudotomus horribilis</i>	USNM 17159	Eocene	North America	Bertrand et al. (2019)
Ischyromyidae	<i>Pseudotomus oweni</i>	USNM 17161	Eocene	North America	Bertrand et al. (2019)
Ischyromyidae	<i>Pseudotomus petersoni</i>	AMNH 2018	Eocene	North America	Bertrand et al. (2019)
Ischyromyidae	<i>Pseudotomus hians</i>	AMNH 5025	Eocene	North America	Bertrand et al. (2019)
Ischyromyidae	<i>Reithroparamys delicatissimus</i>	AMNH 12561	Eocene	North America	Bertrand et al. (2019)
Ischyromyidae	<i>Rapamys atramontis</i>	AMNH 128706; AMNH 128704	Eocene	North America	Bertrand et al. (2019)
Ischyromyidae	<i>Ischyromys typus</i>	ROMV 1007; AMNH 12252; AMNH F:AM 144638	Oligocene	North America	Bertrand and Silcox (2016)
Sciuridae	<i>Cedromus wilsoni</i>	USNM 256584	Oligocene	North America	Bertrand et al. (2017)
Sciuridae	<i>Protosciurus rachelae</i>	YPM 14736; YPM 14737	Oligocene	North America	Bertrand et al. (2018)
Aplodontiidae	<i>Prosciurus relictus</i>	USNM 437793	Oligocene	North America	Bertrand et al. (2018)
Aplodontiidae	<i>Mesogaulus paniensis</i>	AMNH F:AM 65511	Miocene	North America	Bertrand et al. (2018)
Caviomorpha	<i>Neoeptlema acreensis</i>	UFAC 4515; UFAC 3576	Miocene	South America	Ferreira et al. (2020)
Caviomorpha	<i>Neoreomys australis</i>	PIMUZ A/V 5265	Miocene	South America	Ferreira et al. (2020)

was unable to locate it, in part because no catalogue number was given. A partial natural endocast of *Reithroparamys sciuroides* (YPM VPPU 011555 = *Leptotomus sciuroides*) was mentioned by Scott and Osborn (1887) and Scott and Osborn (1890). The authors described the olfactory bulbs but interestingly, when YPM VPPU 011555 was borrowed for CT scanning by OCB, the olfactory bulbs were not attached to the rest of the endocast, and in fact, were still enclosed inside the cranium. It is unclear if another specimen belonging to the same species was available to the original authors.

Despite the increased number of virtual endocasts generated for rodents, the current sample is limited to three groups: Ischyromyidae, the Squirrel-related clade and Caviomorpha. It is challenging to relate sciuroid/ischyromyid data to the caviomorph data. Also challenging is the lack of endocranial data for the earliest rodents, which is currently limited to Ischyromyidae. Crania pertaining to the Eocene ctenodactyloid rodents *Exmus mini* (Wible et al. 2005), and *Cocomys lingchaensis* (Li et al. 1989) are known and the analysis of their endocranial structures could be extremely useful for establishing what features are primitive for rodents. Additionally, as mentioned above, there is the lack of quantitative data for the gliroid *R. turpanensis* (Meng et al. 2003), the only extinct taxon closely related to rodents (besides other fossil Euarchontoglires such as lagomorphs and primates [see Silcox et al. this volume]) with endocranial material known. Another gliroid, *Matutinia nitidulus* (Ting et al. 2002), is known from cranial remains, but has yet to be CT scanned.

Beyond gathering additional endocranial data, a better resolved phylogenetic context is crucial to make hypotheses about brain evolution. As previously mentioned, the phylogenetic relationships among Ischyromyidae and with other orders is still under debate and a robust phylogeny is currently lacking for the group. Also, among the main modern divisions of Rodentia it remains unclear which is the most basal for the order. Although the Squirrel-related clade has been recovered most often in this position, there is still some measure of support for the two other hypotheses. Mapping the evolution of the brain, or any other biological aspects of rodent evolution, will remain challenging until we better understand the deep nodes of the rodent phylogeny.

16.3 Overview of General and Comparative Anatomy

16.3.1 Characterization of Cranial Endocast Morphology

Ischyromyidae

For ischyromyid rodents, endocasts have been generated for three subfamilies: Paramyinae (*Notoparamys costilloi*, *Pseudotomus* [*Ps. horribilis*, *Ps. hians*, *Ps. oweni*, and *Ps. petersoni*], and *Paramys* [*Pa. delicatus* and *Pa. copei*; Bertrand et al. 2016a, 2019]); Reithroparamyinae (*Rapamys atramontis* [two specimens] and

Reithroparamys [*Re. delicatissimus* and *R. sciuroides*; Bertrand et al. 2019]); and Ischyromyinae (*Ischyromys typus* [Bertrand and Silcox 2016; see Table 16.2]).

Ischyromyid endocasts are similar in terms of overall organization and all display pedunculated olfactory bulbs, which are separated from the cerebrum by a marked circular fissure, suggesting that there was no overlap between these two endocranial regions (e.g. Bertrand et al. 2019). The position of the olfactory bulbs within the cranium varies among ischyromyid rodents. The olfactory bulbs are located above the M2 in Paramyinae (*Paramys*, *Pseudotomus* and *Notoparamys*; Fig. 16.3g), whereas in Reithroparamyinae (*Reithroparamys* and *Rapamys*) and the ischyromyine *I. typus*, they are located above the M1 (Bertrand and Silcox 2016; Bertrand et al. 2016a, 2019). The olfactory bulb volume ratio ranges from 3.2% in *I. typus* to 6.1% in *Pa. copei*. Generally, members of Paramyinae have relatively larger olfactory bulbs (4.1–6.1%, values for *Paramys* and *Pseudotomus*) compared to members of Reithroparamyinae (3.2–3.8%, *Rapamys* and *Reithroparamys*) and Ischyromyinae (3.2–3.7%, *I. typus*).

In terms of the cerebrum, the rostral region does not overlap with the circular fissure, which suggests that the frontal lobes were not very well developed. The caudal region of the cerebrum also shows limited expansion, and never overlaps onto the cerebellum. As a result, the midbrain is always visible in the dorsal view of fossil ischyromyid rodents, as in *Pa. delicatus* (Fig. 16.3a). Variation exists in the degree of midbrain coverage; for example, the inferior colliculi are visible in Reithroparamyinae (*Ra. atramontis*, *Re. delicatissimus* and *Re. sciuroides*; Fig. 16.2a, b) and in the ischyromyine *I. typus* (Bertrand and Silcox 2016; Bertrand et al. 2019; Fig. 16.2c), whereas in Paramyinae (*Paramys*, *Pseudotomus*, and

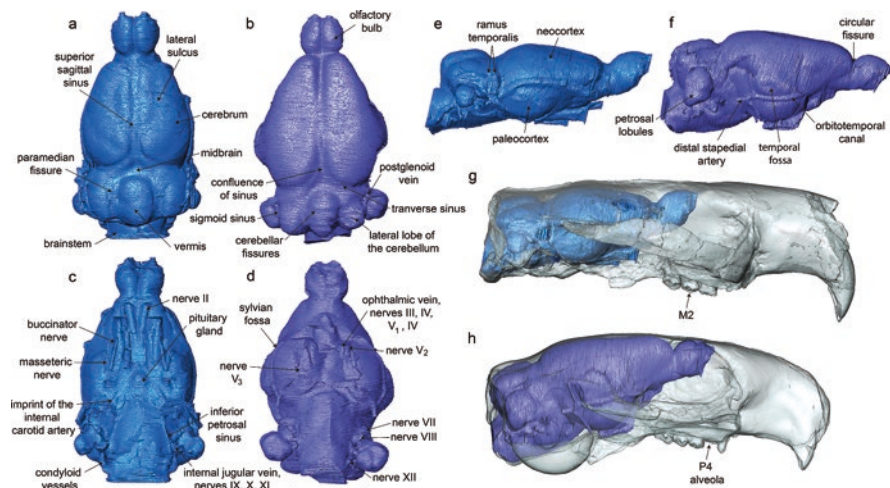


Fig. 16.3 General endocranial anatomy for the rodent described in the text; (a, c, e, g), *Paramys delicatus* (AMNH 12506) (Bertrand et al. 2016a); (b, d, f, h), *Cedromus wilsoni* (USNM 256584) (Bertrand et al. 2017). (a) and (b), dorsal; (c) and (d), ventral; (e) and (f), lateral views; (g) and (h), lateral views of the endocasts inside translucent crania. Scales equal 10 mm

Notoparamys), the midbrain is partially exposed with no visible colliculi (Bertrand et al. 2016a, 2019; Fig. 16.3a). Although limited preservation can sometimes prevent the identification of the colliculi (e.g., as may possibly be the case for *Rhombomylus*, with its broad expanse of exposed midbrain), in the case of Paramyinae, the close approximation of the transverse sinuses and rostral extent of the cerebellum in those specimens in which the colliculi are not observed means that there would not have been adequate space on the surface of the brain for such exposure.

Regarding the presence of sulci on the surface of the cerebrum (Fig. 16.3a), the majority of Ischyromyidae sampled display lateral sulci and only *N. costilloi* and Reithroparamyinae (*Re. delicatissimus*, *R. sciuroides* and *Ra. atramontis*) are completely lissencephalic (Bertrand et al. 2019). The development of neocortical sulci appears to be related to the size of the brain, with brains below 5 cc typically being lissencephalic in mammals (Macrini et al. 2007). For rodents, both gyrencephalic and lissencephalic brains are found in an interval of brain masses between 3 and 30 cc (Pilleri et al. 1984). All sampled ischyromyids have an endocranial volume between 5 and 12 cc. The lissencephalic *Rapamys atramontis* (6–7 cc) has an approximately equivalent endocranial volume compared to *I. typus* (5–7 cc), which displays lateral sulci, showing that there is some variation independent of simple size in which taxa exhibit neocortical sulci. In euarchontoglires, the presence of the orbitotemporal canal has been used as a landmark to identify the location of the rhinal fissure, which separates the neocortex from the paleocortex (Martin 1990; Bertrand et al. 2019). The orbitotemporal canal is visible in all Ischyromyidae sampled, although it is very narrow in *I. typus* compared to other taxa such as in *Pa. delicatus* (Fig. 16.3e). The position of the orbitotemporal canal varies among Ischyromyidae but it is approximately two-thirds of the way down the lateral side of the cerebrum except in *Pseudotomus* for which it appears to be more dorsally positioned (Bertrand et al. 2019). The orbitotemporal canal is always dorsal to the temporal fossa when the latter is visible in lateral view (see *Ps. horribilis*, *Ps. hians* and *I. typus*, AMNH F: AM 144638; Bertrand et al. 2019). The relative neocortical surface area varies among Ischyromyidae. Paramyinae (18–22%), and *Re. delicatissimus* (17.3%) include some of the lowest neocortical surface area ratios, whereas *I. typus* (20–23%) and *Ra. atramontis* (23%) are in the upper range of variation for Ischyromyidae (Bertrand et al. 2021).

The morphology of the cerebellum is overall similar among Ischyromyidae, with the presence in dorsal view of a centrally positioned vermis separated from the lateral cerebellar lobes by the paramedian fissures. The petrosal lobules (=paraflocculi) are globular in shape and attached to the rest of the cerebellum by a short stem. The cerebellum represents about one-fifth to one-quarter of the total length of the endocast in ischyromyid rodents. Quantifying the volume of the entire cerebellum is challenging as the boundaries of this part of the brain are not easily identifiable on endocasts (Bertrand and Silcox 2016). However, relative size of the petrosal lobules has been quantified; they represent 0.6% in the paramyine *Ps. petersoni*, which has the lowest petrosal lobule volume ratio, whereas the reithroparamyine *Ra. atramontis* (AMNH 128704) and *Re. delicatissimus* display the highest ratios

(2.1% and 2.3% respectively; Bertrand et al. 2016a, 2019, 2021). Finally, the fossa for the pituitary gland is visible on the surface of all endocasts of Ischyromyidae except in *Ra. atramontis* for which the fossa is not visible despite high quality preservation (Bertrand et al. 2016a, 2019).

Sciuroidea

Virtual endocasts of several fossil members of Sciuroidea have been published including three squirrel specimens: the cedromurine *C. wilsoni*, the sciurine *Prot. cf. rachelae* (two specimens), and three apodontid species: the prosciurines *Pros. relictus* and *Pros. aff. saskatchewaensis* and the mesogauline *M. paniensis* (Bertrand et al. 2018; Table 16.2). Additionally, virtual endocasts of extant Sciuroidea have been published (Bertrand et al. 2017, 2018, 2021).

There is more variation among the members of this group compared to Ischyromyidae. However, they all display pedunculated olfactory bulbs, which are separated from the cerebrum by the circular fissure. In extant and fossil squirrels, and in the apodontid *Prosciurus*, the circular fissure is narrower compared to the apodontids *M. paniensis* and *A. rufa* (Bertrand et al. 2017, 2018). The position of the olfactory bulbs is similar in all fossil Sciuroidea, in which they are located above the P4 (Fig. 16.3h). In extant squirrels, they are positioned either above the P4, P4-P3 or the diastema, differing from the conditions found in Ischyromyidae (above M1-M2) and in *A. rufa* (above M1). In terms of size, the olfactory bulb volume ratio represents 3.0% in the squirrel *C. wilsoni* and 3.7% to 4.8% in the squirrel *Prot. cf. rachelae*, whereas it corresponds to 3.6% and 3.3% in the apodontids *Pros. relictus* and *M. paniensis* respectively (Bertrand et al. 2018). The olfactory bulb volume ratios of extant Sciuroidea overlap with extinct relatives, ranging from 1.64% to 4.73%.

The rostral region of the cerebrum covers at least a portion of the circular fissure in lateral view in extant and extinct squirrels *C. wilsoni* (Fig. 16.3f), *Prot. cf. rachelae*, and in the apodontid *Pros. relictus*. The opposite pattern is visible in *A. rufa* and *M. paniensis* in which the circular fissure is quite broad (Fig. 16.2g), suggesting that the frontal lobes are not very well developed in these taxa. The caudal region of the cerebrum varies among fossil Sciuroidea, with more expansion visible in *Prot. cf. rachelae*, *C. wilsoni* and *Pros. aff. saskatchewaensis* compared to Ischyromyidae as the midbrain is more visible in the latter taxa (Figs. 16.2f and 16.3b). In extant Sciuroidea and in *Mesogaulus paniensis*, the midbrain is not visible, suggesting expansion of the cerebrum (Bertrand et al. 2017, 2018; Fig. 16.2d, g).

In contrast to Ischyromyidae, fossil Sciuroidea, *A. rufa*, and the majority of extant squirrels lack sulci on the surface of the cerebrum, which may relate to their low endocranial volume, being between 0.9 and 9.7 cc (Bertrand et al. 2017, 2018). However, some extant squirrels display neocortical sulci despite their low endocranial volume, such as *Rhinosciurus laticaudatus* (4.4 cc) and *Callosciurus* sp. (7.0cc). The flying squirrels *Aeromys tephromelas* and *Petaurista petaurista* with high endocranial volumes (11.5 and 12.3 cc respectively) exhibit lateral sulci, while the

Callosciurinae *R. laticaudatus* displays a sylvian sulcus (Fig. 16.2d). A sylvian fossa is present in *C. wilsoni* and in the majority of extant squirrels (Bertrand et al. 2017; Fig. 16.3d), but is absent in other fossil Sciuroidea and in *A. rufa* (Bertrand et al. 2018). The orbitotemporal canal is clearly visible and broad in most extant squirrels, the fossil squirrels *C. wilsoni* and *Prot. cf. rachelae*, and in the aplodontid *Pros. relictus*, whereas its presence is hardly distinguishable in some extant flying squirrels, *M. paniensis* and *A. rufa* (Bertrand et al. 2018; Bertrand et al. 2017; Fig. 16.3f). The position of the orbitotemporal canal is approximately three-quarters of the way down the lateral side of the cerebrum in all fossil Sciuroidea except in *M. paniensis* and *A. rufa* in which it appears more dorsally located (Bertrand et al. 2018). In extant squirrels, the position of the orbitotemporal canal is variable, sometimes being similar to *C. wilsoni*, but it can also be as far as ventral as the ventral extent of the lateral side of the cerebrum (i.e. *Ratufa affinis* and *Protoxerus stangeri*; Bertrand et al. 2017). The orbitotemporal canal is ventral to the temporal fossa in all extant and fossil Sciuroidea (Fig. 16.3f) except in *M. paniensis*, which shows the opposite pattern and is therefore similar to the ischyromyid condition. The temporal fossa is absent in the extant *A. rufa* (Bertrand et al. 2018). The neocortical surface area ratio is between 30 and 32% in the fossil squirrels *C. wilsoni* and *Prot. cf. rachelae*, which is higher than in the aplodontids *Pros. relictus* (29.7%), *M. paniensis* (26.8%) and *A. rufa* (27.1%; Bertrand et al. 2018, 2021). In extant squirrels, the neocortical surface area ratio is higher, being from 33% to 38% (Bertrand et al. 2021).

The morphology of the cerebellum is overall similar to that seen in Ischyromyidae. However, some variation can be noted, such as the vermis being better demarcated in *C. wilsoni*, *Prot. cf. rachelae*, *Pros. relictus*, and extant squirrels compared to *M. paniensis* and *A. rufa*, in which the paramedian fissures are not clearly visible. The petrosal lobules show the same configuration as in Ischyromyidae; however, they are relatively larger in *C. wilsoni*, *Prot. cf. rachelae* and *Pros. relictus*. Relative to the overall endocranial volume the petrosal lobules represent 3.2% in *C. wilsoni*, 3.0–3.3% in *Prot. cf. rachelae* and 3.4% in *Pros. relictus*. In contrast, *M. paniensis* has relatively smaller petrosal lobules compared to other fossil Sciuroidea (1.3%). Extant squirrels have a lower petrosal lobule ratio ranging from 0.9% to 2.3%, while *A. rufa* has an even lower ratio of 0.8%. The cerebellum represents about one-fifth of the total length of the endocast in fossil Sciuroidea and *A. rufa*, and one-fifth to one-seventh in extant squirrels, which is less than in Ischyromyidae. Cerebellar fissures are visible in both fossil squirrels *C. wilsoni* and *Prot. cf. rachelae*, and many extant squirrels (e.g. Callosciurinae and Ratufinae), but are absent in fossil Aplodontidae (Bertrand et al. 2017, 2018; Fig. 16.3b). Finally, the fossa for the pituitary gland is clearly visible on the endocranial surface of the fossil *M. paniensis* and in a few extant squirrels (*Ratufa affinis*, *Sciurus carolinensis*) but less well demarcated in *A. rufa*. Despite relatively good preservation, this area is not visible in other sciuroids (Bertrand et al. 2017, 2018).

Caviomorpha

Limited endocranial material has been published on caviomorph rodents. Two virtual endocasts of fossil caviomorphs have recently been analyzed: the chinchilloid *Neoe. acrensis* and the cavioid *Neor. australis* (Ferreira et al. 2020). A few other natural endocasts have also been described: the erethizontoid *Hypsosteiromys* sp., the chinchilloid Cephalomyidae indet., the cavioid *Dolicavia minuscula*, and *Metacaremys primitiva* comb. nov. (Fig. 16.3h; Dozo 1997a, b; Dozo et al. 2004; Piñero et al. 2021). Additionally, 14 virtual endocasts of extant caviomorph rodents have been published (Ferreira et al. 2020; Piñero et al. 2021 but see also, Ferreira et al. 2022).

Most extant caviomorph specimens, the chinchilloid *Neoe. acrensis*, and the cavioid *Neor. australis* display pedunculated olfactory bulbs, which are separated from the cerebrum by the circular fissure. In the cavioid *D. minuscula*, the chinchilloid Cephalomyidae indet., the erethizontoid *Hypsosteiromys* sp. and in the extant *Coendou spinosus*, the olfactory bulbs appear to be directly connected to the cerebrum and there is no clearly demarcated olfactory tract. The olfactory bulb volume for *Neor. australis* represents 3.3% of the total endocranial volume and ratios for extant taxa range from 1.5% to 3.6% (based on the volumes provided in Ferreira et al. (2020)). The olfactory bulbs are not preserved in *Metacaremys primitiva* comb. nov. and quantitative data on the olfactory bulbs were not obtained for extant Octodontidae, *Abrocoma*, and Echimyidae (Piñero et al. 2021).

The rostral region of the cerebrum covers the circular fissure in the cavioid *D. minuscula* (Fig. 16.2h) and to a lesser degree in the chinchilloid *Neoe. acrensis* and the cavioid *Neor. australis* (Ferreira et al. 2020). In contrast, the circular fissure is uncovered in extant caviomorphs. The caudal region of the cerebrum appears to be expanded, as the midbrain is covered in all extinct and extant caviomorph endocasts under study, except perhaps in the chinchilloid Cephalomyidae indet. in which the midbrain might be exposed (ambiguous [likely as a result of preservation] based on the drawing from Dozo 1997b) and *Metacaremys primitiva* comb. nov. in which the midbrain presence cannot be assessed because of limited preservation of the area (Piñero et al. 2021).

Sulci are present on the cerebral surface of caviomorph endocasts. Lateral and suprasylvian sulci are visible on the endocast of the chinchilloid *Neoe. acrensis* and the cavioid *D. minuscula* and in the extant *Lagostomus maximus*, *Dinomys branickii*, and *Hydrochoerus hydrochaeris* (Dozo 1997a; Ferreira et al. 2020). Lateral sulci are visible in *Octomys mimax*, *Abrocoma cinerea*, *Euryzygomatomys spinosus*, and *Kannabateomys amblyonyx* (see Fig. 2 in Piñero et al. 2021). Additionally, a pseudosylvian sulcus is visible in *D. minuscula* (Dozo 1997a). Despite its high endocranial volume (12.6 cc), the cavioid *Neor. australis* is lissencephalic, similar to its close relative the smaller extant *Cavia porcellus* (4.5 cc). Interestingly, the endocast of *D. minuscula* displays more sulci than *Neoe. acrensis* in spite of the former being much smaller (5.7 cc vs. 47.2 cc). The erethizontoid *Coendou spinosus* appears to display some sulci but they cannot be easily identified. Other extant caviomorphs, *Dasyprocta* sp., *Lagostomus maximus*, *Chinchilla*

lanigera, *Dinomys branickii*, *Myocastor coypus*, *H. hydrochaeris* and *Phyllomys dasythrix*, all display a lateral sulcus and have endocranial volumes ranging from 2.6 and 94.8 cc. This suggests that the presence of sulci might not be correlated to endocranial volume in caviomorphs. The orbitotemporal canal is not visible on any of the extinct and extant caviomorph endocasts and no quantification of the neocortex has been attempted for these specimens.

The vermis is separated from the lateral lobes of the cerebellum by the paramedian fissure visible on the endocast of extant caviomorphs, the cavioid *Neor. australis* and *D. minuscula*, the octodontoid *Metacaremys primitiva* comb. nov. and in the chinchilloid Cephalomyidae indet. The cavioid *Cavia porcellus* is the exception as it does not display a clear paramedian fissure on its endocast (Ferreira et al. 2020). The cerebellum is not well enough preserved in *Neoe. acrensis* nor in *Hypsosteiromys* sp. to make any comparisons (Dozo et al. 2004). The petrosal lobules are present in all extant caviomorphs (except *Coendou spinosus*) and the cavioid *Neor. australis* but their size was not estimated (Ferreira et al. 2020; Piñero et al. 2021). These structures are not visible on the natural endocast of *Metacaremys primitiva* comb. nov. because of limited preservation (Piñero et al. 2021). Petrosal lobule volumes were measured for six caviomorphs including one fossil, the octodontoid *Prospaniomys priscus* (Arnaudo et al. 2020). The cerebellum represents about one-quarter to one-third of the total length of the endocast in *Neor. australis*, *Cavia porcellus*, *Chinchilla lanigera* and Cephalomyidae indet, whereas it is less than one-quarter in *Neoe. acrensis*, *D. minuscula*, and other extant taxa. Linear measurements were not provided for the endocasts described in Piñero et al. (2021). Cerebellar fissures are present in *D. minuscula* (Dozo 1997a), *Chinchilla lanigera* and *Phyllomys dasythrix* (see supplementary figures from Ferreira et al. 2020) and also in *Metacaremys primitiva* comb. nov. and extant Octodontidae, *Abrocoma*, and Echimyidae (See Fig. 2 in Piñero et al. 2021). The fossa for the pituitary gland is visible in nearly all extant taxa, *Neor. australis* and *Neoe. acrensis* (Ferreira et al. 2020) but not always well demarcated on the endocranial surface. The fossa is not visible (despite good preservation) in extant Octodontidae, *Abrocoma*, and Echimyidae (See Fig. 2 in Piñero et al. 2021). Because of lack of preservation, it is unclear if the fossa was present in *Metacaremys primitiva* comb. nov. (See Fig. 2 in Piñero et al. 2021).

16.3.2 Spaces Associated with Cranial Nerves and Blood Supply

Various casts of the openings for the cranial nerves are present and similarly positioned on the ventral surface of the endocasts of the sampled specimens (Fig. 16.3). The optic foramina, through which the optic nerves (II) exit, are positioned rostroventrally. The passageway for the trigeminal nerve (V) and its three branches are located behind the optic foramina. The maxillary nerve V_2 exits through the

foramen rotundum, whereas the ophthalmic V_1 exits through the sphenorbital fissure with the ophthalmic veins and cranial nerves III (oculomotor), IV (trochlear), and VI (abducens) in all taxa except for *I. typus*, *M. paniensis*, *Pros. relictus*, *Neor. australis*, *N. acrensis* and extant caviomorphs. In those taxa, the foramen rotundum cannot be distinguished from the sphenorbital fissure and is presumably absent (Fig. 16.3d; see supplementary figures in Ferreira et al. 2020; Piñero et al. 2021). The foramen rotundum and sphenorbital fissure are conjoined but represent distinct openings in almost all other Sciuroidea and Ischyromyidae specimens that preserve this region (Wahlert 1974; Bertrand et al. 2017, 2018; Ferreira et al. 2020), as is the primitive condition for eutherians (Novacek 1986). In *A. rufa*, the foramen rotundum is separated from the sphenorbital fissure (Bertrand et al. 2018). The mandibular nerve (V_3) would have passed through both the foramen ovale and foramen ovale accessorius in *Ra. atramontis*, *I. typus*, *Pros. relictus*, *Prot. cf. rachelae*, and *C. wilsoni*. In contrast, *M. paniensis*, *A. rufa* and the genera *Paramys* and *Pseudotomus* lack this configuration, so V_3 would have passed through the foramen ovale only (Wahlert 1974; Bertrand et al. 2018, 2019). Both conditions are present in extant squirrels (see supplementary table from Bertrand et al. 2018). In all rodents sampled, two foramina transmit two branches of the mandibular nerve (V_3): the masseteric and the buccinator nerves (Fig. 16.3c; Wahlert 1974), except for *I. typus* in which distinct foramina for these nerves are absent (Bertrand and Silcox 2016; Bertrand et al. 2018). The foramina for the masseteric and buccinator nerves remain separated in all Ischyromyidae, *M. paniensis*, and *A. rufa*. The passageways for these nerves are confluent in *Pros. relictus*, *Prot. cf. rachelae*, *C. wilsoni* and in all extant squirrels except *Heliosciurus rufobrachium* and *Pteromys volans* in which the passage for each branch remains separated from one another and lead to two separate foramina (Bertrand et al. 2017, 2018). The condition for the configuration of V_3 and associated branches is uncertain for extant and fossil caviomorphs. The masseteric and buccinator branch casts appear absent in all caviomorphs (see Ferreira et al. 2020; Piñero et al. 2021). Caudal to these foramina, casts of the internal auditory meatus, with passageways for cranial nerves VII (facial) and VIII (vestibulocochlear), are located rostro-ventral to the petrosal lobules in all specimens (Fig. 16.3d). The cast of the jugular foramen, which corresponds to the passageway of the internal jugular vein and cranial nerves IX (glossopharyngeal), X (vagus), XI (accessory), is positioned ventral to the caudal end of the petrosal lobules in all taxa. One hypoglossal foramen, through which passed the hypoglossal nerve (XII), is present on each side of the brainstem in all sampled specimens (Fig. 16.3d). In *I. typus*, *Ps. oweni*, *A. rufa* and several extant squirrels, two pairs of foramina are present (Bertrand et al. 2016a, 2018, 2019). Based on the published virtual endocasts of extinct and extant caviomorph rodents, it is unclear if one or more foramina are present on each side.

The intracranial dural sinus system of the rodents sampled is typical of therian mammals (Wible and Rougier 2000). With regards to the venous system, the superior sagittal sinus is visible and continuous with the transverse and sigmoid sinuses, which then connect with the jugular foramina in specimens that preserve those structures. The cast for the internal jugular vein is also continuous with the cast of

the inferior petrosal sinus in all specimens (Bertrand et al. 2018; Fig. 16.3c, d). The postglenoid foramen transmits the postglenoid vein that branches off the external jugular vein (Novacek 1986; Meng et al. 2003) and is positioned dorsally from the casts of the internal auditory meatus in all taxa (Fig. 16.3b). The condition for this feature is not known for extinct and extant caviomorphs and was not studied by Ferreira et al. (2020) or Piñero et al. (2021).

Regarding the arterial system, a trace of the passage for the main internal carotid artery is visible on the ventral surface of the endocast near the proximal part of the inferior petrosal sinus of *Paramys*, *Pseudotomus* and *Rapamys* but is not preserved in *Ischyromys*, Reithroparamyinae and extant and extinct Sciuroidea (Fig. 16.3c). The stapedia artery, a branch of the internal carotid artery (Bugge 1985), enters the endocranial cavity through the stapedia foramen (Wible and Shelley 2020) in rodents and the distal stapedia artery cast can be traced (see terminology in Wible and Shelley 2020) in almost all Ischyromyidae and Sciuroidea (Fig. 16.3f). This cast is not visible despite good preservation of the area in *I. typus*, *M. paniensis*, *A. rufa*, and two extant flying squirrels *Pteromyscus pulverulentus* and *Petinomys setosus* (Bertrand and Silcox 2016; Bertrand et al. 2018, 2019). The distal stapedia artery and the facial nerve (VII) appear to have occupied a common canal for a short distance in fossil Sciuroidea, several extant squirrels and Ischyromyidae except for *Paramys* in which they remained separated (Bertrand et al. 2016a; Wible and Shelley 2020). Some extant squirrels show another condition in which the passage of the stapedia artery and the facial nerve are separated by a thin plate of bone (Bertrand et al. 2017). The distal stapedia artery divides into the ramus superior and ramus inferior in rodents (Wible and Shelley 2020). The presence of a branch of the ramus superior, the ramus temporalis, is a primitive feature for eutherians (Wible 1987). All extant and extinct rodents sampled have at least one ramus temporalis with the exception of *I. typus*, *Prot. cf. rachelae*, *A. rufa* and three extant squirrels (*Petinomys setosus*, *Tamias minimus*, and *Protoxerus stangeri*) for which this vessel is absent (Bertrand and Silcox 2016; Bertrand et al. 2017). *Paramys*, *Pseudotomus* and *M. paniensis* have two rami temporales whereas the remaining taxa only have one on each side (Bertrand et al. 2018; Fig. 16.3e). The condition for the internal carotid artery system has not been studied using endocasts of caviomorph rodents.

16.4 Brain Evolution and Paleobiological Inferences Based on Endocast Morphology

16.4.1 Morphological Brain Diversity

Based on the knowledge that we have gathered from the various endocasts, we can start making some inferences about brain evolution from early ischyromyid rodents to more derived Sciuroidea. Because of the limited amount of available material for Caviomorpha, we will not make morphological evolutionary deductions. The

endocasts of Ischyromyidae share likely ancestral features also present in other fossil members of Euarchontoglires such as the gliroid *R. turpanensis*, plesiadapiform primates, apatemyids and stem lagomorphs (Meng et al. 2003; Silcox et al. 2009, 2010, 2011; López-Torres et al. 2020). All these taxa have pedunculated olfactory bulbs, a circular fissure not covered by the frontal lobes, and a midbrain not covered by the caudal region of the cerebrum. These features were presumably present in the ancestor of Euarchontoglires as they are also visible in other early members of the group (see Silcox et al. this volume).

The tectum of the midbrain (dorsal part) consists of the tectal lamina, which consists of the superior and inferior colliculi. The superior colliculi play a role in visual reflexes and the inferior colliculi in acoustic reflexes (Christensen and Evans 1979). The presence of visible colliculi in the midbrain area might be related to preservation but could also be due to other factors. The exposure of the inferior colliculi in Reithroparamyinae could represent a primitive condition, associated with a short cerebrum that simply does not cover these structures. However, it is worth noting that Paramyinae do not have visible colliculi but do have a midbrain that is exposed between the cerebrum and cerebellum (Bertrand et al. 2019). Edinger (1964) cautioned against viewing exposed inferior colliculi as a primitive trait in mammals and suggested that ‘extensive’ midbrain exposure (with visible inferior colliculi) could be a derived feature linked to increase in auditory acuity. The Oligocene *I. typus* variably exhibits exposed inferior colliculi, which may reflect a lack of expansion of the neocortex but could alternatively be associated with enlargement of these structures. A parallel conclusion could be drawn for the superior colliculi (possibly visible in one specimen of *Ra. atramontis*; Bertrand et al. 2019), which are associated with visual reflexes (Christensen and Evans 1979).

There are fundamental morphological changes occurring from basal Ischyromyidae to more derived Sciuroidea. Ischyromyidae exhibit olfactory bulbs that are above the M2 and M1, whereas in extant and extinct sciuroids they are above the P4, P4/P3 and/or the diastema (Bertrand et al. 2018). These differences might stem from changes in the proportions of the cranium among Ischyromyidae and Sciuroidea, suggesting that the endocranial cavity is proportionally becoming bigger compared to the rest of the cranium in Sciuroidea. Additionally, the rostrum may have also shortened in the transition from Ischyromyidae to Sciuroidea. In contrast to Ischyromyidae, the frontal lobes and caudal region of the cerebrum cover the circular fissure and midbrain respectively at least partially in fossil sciuroids. The position of the orbitotemporal canal is also more ventral, located below the temporal fossa, in extant and extinct Sciuroidea compared to Ischyromyidae, suggesting an overall expansion of the neocortex. The Miocene aplodontid *M. panienensis* and extant *A. rufa* display a different pattern and in some ways more closely resemble ischyromyid rodents in having an uncovered circular fissure and an orbitotemporal canal positioned dorsal to the temporal fossa. This would suggest a reduction in the size of the neocortex.

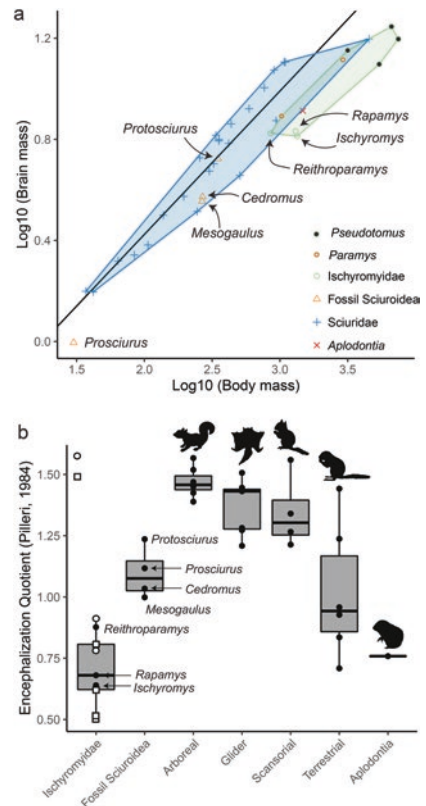
Parallel fissures on the cerebellum are only visible on the surface of the endocast of extant and extinct squirrels (Fig. 16.3b) and are absent in Ischyromyidae and Aplodontidae, suggesting an increase in the complexity of this region in the

Sciuridae. An increase in cerebellar complexity (i.e., more fissures) leads to information being processed faster and an increase in functional specialization (Sillitoe et al. 2005). The cerebellum is partly responsible for eye and head movements as well as balance, posture and limb control (Cerminara and Apps 2011). Therefore, these functions may have been enhanced in early squirrels. Alternatively, the absence of these fissures could be due to preservation.

16.4.2 Brain-Size Evolution and Encephalization Quotient

Quantitative volumetric data on extant and extinct rodent endocasts have been published for Ischyromyidae, Sciuroidea and Caviomorpha. To make meaningful comparisons among brain volumes of different species, it is necessary to take body mass into consideration (Fig. 16.4a). The encephalization quotient (EQ), has been used for decades for this specific purpose. However, it has become clear that the original equation conceived by Jerison (1973) might be problematic due to the low sample size upon which it was based. Indeed, some recent work showed that phylogeny has

Fig. 16.4 Relationship between brain and body mass for Sciuridae, Aplodontidae and Ischyromyidae, and encephalization quotients for Ischyromyidae, Sciuridae and Aplodontidae. (a), bivariate plot of \log_{10} (endocranial volume) vs \log_{10} (body mass). The regression line corresponds to extant Sciuridae; (b), boxplot of EQs based on Pilleri et al.'s (1984) equation. Volumes are in mm^3 and body mass in grams. Data used for generating the plots are presented in Appendix 1



an impact on the scaling of the brain relative to body size (Burger et al. 2019), suggesting that an ordinal specific equation might be more appropriate for comparisons within an order. Pilleri et al. (1984) created an equation specifically designed for rodents, which is therefore more appropriate for examining relative brain size variation within our sample than the original Jerison (1973) equation. As mentioned above, body mass is part of the equation that determines EQ; therefore, its estimation will have a great impact on the results for fossil taxa. Equations based on cranial dimensions have been produced for rodents using a sample of 203 specimens from all three clades (Bertrand et al. 2016b). The advantage of using cranial dimensions is that the body mass estimate derives from the specimen for which the EQ is to be determined. The best estimator of body mass in rodents appears to be cranial length ($r^2 = 0.96$) and so that variable was used to obtain EQs for the majority of Ischyromyidae and Sciuroidea (e.g. Bertrand et al. 2016a, 2017, 2019). When cranial length was not available, cheek-tooth area was used instead ($r^2 = 0.94$; Bertrand et al. 2016b).

An increase in EQ through time has been shown to occur in several mammalian orders (Jerison 1973; Radinsky 1976; Gurche 1982; Silcox et al. 2010; Orliac and Gilissen 2012; Yao et al. 2012) but recent studies on rodent brain evolution have suggested that this pattern was not consistently present in Rodentia (i.e. some older specimens have higher EQs than some younger specimens; Bertrand and Silcox 2016; Bertrand et al. 2016a, 2017). For example, the early Eocene *Pa. copei* had a higher EQ compared to the late middle Eocene *Ps. petersoni*. A regression showing EQ through time using Ischyromyidae, *C. wilsoni* and extant members of the Squirrel-related clade, revealed a weak, but statistically significant relationship between EQ and time ($r^2 = 0.22$; Bertrand et al. 2019). This analysis was based on a very limited sample and this issue should be reassessed with fossil members of all rodent groups.

Pilleri et al. (1984) obtained the EQ for 269 rodents from all rodent clades except Anomaluromorpha and found a relationship between ecological parameters and EQ. For example, members of the Squirrel-related clade with a low EQ are usually terrestrial, gregarious and/or nocturnal animals, whereas those with a high EQ are arboreal, solitary and/or diurnal. More generally, rodents with higher EQ are arboreal, taxa with medium EQ are terrestrial or semiaquatic, whereas fossorial species have a lower EQ (Pilleri et al. 1984). Other studies have made a similar conclusion that EQ may vary as a function of locomotion in extant rodents (e.g. Mace et al. 1981; Roth and Thorington 1982; Meier 1983; Bertrand et al. 2021).

So far, there are some indications that EQ varies with locomotion in fossil taxa, although the interpretation of this signal is complicated by the possible temporal effect on brain size. *Paramys copei* has the highest EQ among fossil ischyromyids, which could be related to its scansorial adaptations (Wood 1962; Rose and Chinnery 2004; Prufrock et al. 2021). *Pseudotomus* and *I. typus* have been reconstructed as fossorial (Scott et al. 1937; Dunn and Rasmussen 2007) and have EQs lower than calculated for the arboreal fossil squirrel *C. wilsoni*, and extant sampled squirrels (Fig. 16.4b). The early and late Oligocene fossil squirrels *C. wilsoni* and *Prot. cf. rachelae* have higher EQs compared to the early Oligocene fossorial *I. typus*. No

postcrania have been published for *C. wilsoni*, but its semicircular canals are similar in relative size to those of arboreal species, which means that *C. wilsoni* may have lived a comparable lifestyle (Bhagat et al. 2021). *Protosciurus* cf. *rachelae* is considered to be arboreal (Emry and Thorington 1982; Steppan et al. 2004; Korth and Samuels 2015; Rocha et al. 2016) and the postcranial elements of *Prot.* cf. *rachelae* appear to be very similar to those of the fossil *Douglassciurus jeffersoni* and the extant *Sciurus*, both known for displaying arboreal adaptations (Korth and Samuels 2015). It is worth noting that the semicircular canals of *Prot.* cf. *rachelae* indicate that the specimen was as agile as *C. wilsoni* and *Sciurus carolinensis* (Bhagat et al. 2021). This would suggest that high EQ might be related to arboreality in fossil and modern squirrels. A similar conclusion was obtained by Bertrand et al. (2021) who used the phylogenetic encephalization quotient (PEQ; Ni et al. 2019) that takes phylogenetic relationships into account. The fact that fossil arboreal squirrels have not reached the EQ of related modern arboreal taxa could be due to a temporal effect on EQ (Fig. 16.4b; Bertrand et al. 2021). Based on these results, EQ is likely to be influenced by both temporal and ecological factors.

A different pattern emerges with respect to EQ temporal variation in aplodontids. A decrease in relative brain size occurred from *Pros. relictus* to the later-occurring *M. paniensis* (Bertrand et al. 2018). Results from the semicircular canals show that *Pros. relictus* was very agile and therefore may have been arboreal (Bhagat et al. 2021). *Mesogaulus paniensis* has been reconstructed as highly specialized for fossorial life, in contrast to early members of the group showing more squirrel-like lifestyles (Hopkins 2005, 2008). The low EQ of *M. paniensis* could be associated with its more fossorial locomotion compared to *Pros. relictus* (Bertrand et al. 2018). Using ancestral state reconstruction (ASR) methods, Bertrand et al. (2021) showed that PEQ started to increase at the Sciuroidea node and that this shift may be related to arboreality.

A recent study noted that the late Miocene caviomorph *Neoe. acrensis* exhibited a relatively small brain compared to its body size (Ferreira et al. 2020). The authors speculated that it could be related to the fact that this species and other giant rodents evolved in isolation when South America was separated from the other continents (Pascual et al. 1990). During this time, large predators were absent, which may have allowed the evolution of large mammals such as rodents with relatively small brains (Ferreira et al. 2020), as large brains are expensive to maintain, and high computational power might not be required in the absence of predators.

16.4.3 Sensory Evolution: Vestibular Sense, Vision, Hearing, Olfaction, Taste, etc.

Variation in EQ might be related to proportional changes in different regions of the endocast. The relative size of three distinct parts of the endocast can be estimated: the olfactory bulb volume, the petrosal lobule volume, and the neocortical surface

area. The size of the neocortex and the petrosal lobules have not been systematically quantified for any rodent groups other than sciuroids and ischyromyids.

The neocortical surface area ratio is higher in fossil squirrels (Fig. 16.5a), and the caudal part of the neocortex where the visual cortex is located (Krubitzer et al. 2011) is expanded in the early arboreal sciuroids *Pros. aff. saskatchewaensis*, *C. wilsoni* and *Prot. cf. rachelae* compared to the fossorial *I. typus* from the same epoch (Bertrand and Silcox 2016; Bertrand et al. 2017, 2018). Only a very short portion of the midbrain is visible in fossil Sciuroidea, which would suggest that expansion of the cerebrum occurred from Ischyromyidae to Sciuroidea (Bertrand et al. 2018, 2019) and that early squirrels and early apodontids may have had enhanced vision compared to their ischyromyid ancestors (Bertrand et al. 2017, 2018). However, Bertrand et al. (2021) showed that neocortical expansion started before the

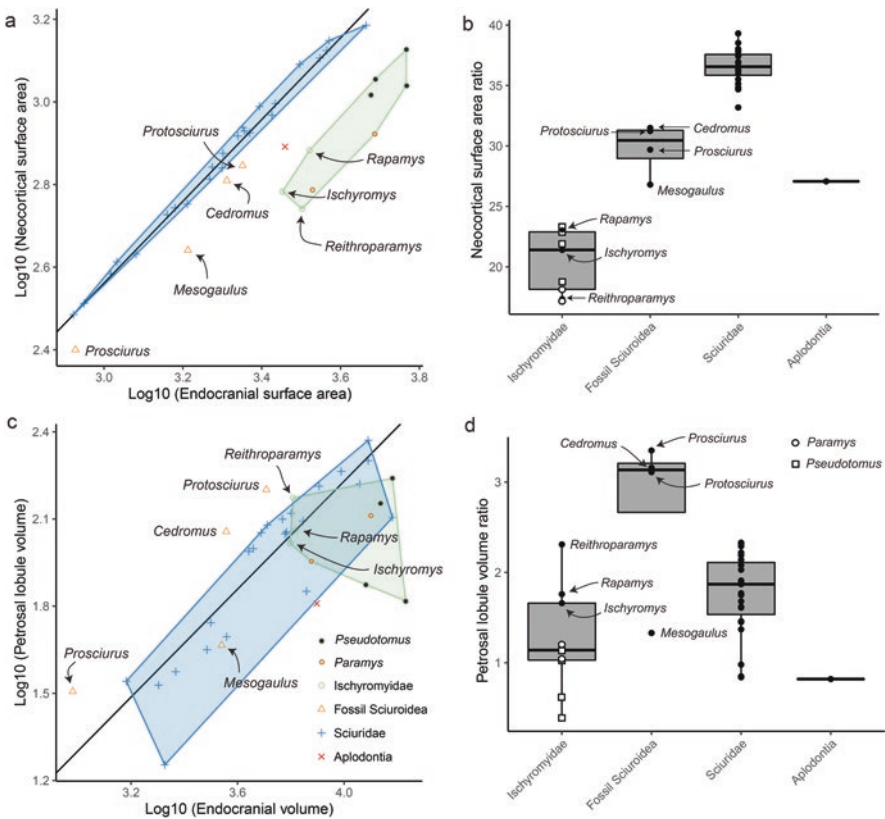


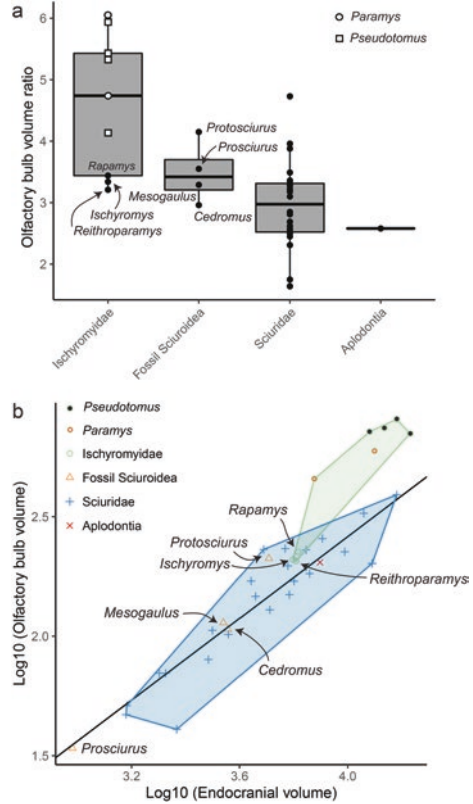
Fig. 16.5 Endocranial changes in Ischyromyidae and Sciuroidea. (a), bivariate plot of \log_{10} (neocortical surface area) vs \log_{10} (endocranial surface area); (b), boxplot of the neocortical surface area percentage ratio; (c), bivariate plot of \log_{10} (petrosal lobule volume) vs \log_{10} (endocranial volume); (d), boxplot of the petrosal lobule volume percentage ratio. The regression line corresponds to extant Sciuridae. Volumes are in mm^3 and surface areas in mm^2 . Data used for generating the plots are in Appendix 1

Sciuroidea node in their ASR analyses. This would suggest that neocortical expansion could have facilitated the transition to arboreal life in early sciuroid rodents as better vision may be critical in the complex 3D environment of the trees (Bertrand et al. 2017). In Aplodontidae, a different pattern emerges with neocortical size decreasing through time. A reduction in the relative size of the caudal part of the cerebrum, where the visual cortex is located, is apparent in *M. paniensis* compared to *Pros. aff. saskatchewaensis*, *Prot. cf. rachelae*, *C. wilsoni* and modern squirrels. This could be the result of a specialization to a more fossorial life as vision might be less crucial when living underground rather than in the trees (Fig. 16.5a; Bertrand et al. 2018, 2021).

The petrosal lobules play a role in head coordination (vestibulo-ocular reflex) and the stabilization of eye position and movement when tracking an object (smooth pursuit; Rambold et al. 2002; Voogd and Wylie 2004; Waespe et al. 1983). The petrosal lobules of Ischyromyidae are smaller compared to those of Oligocene fossil Sciuroidea and an expansion in the relative size of these structures may have occurred in early Sciuroidea (Fig. 16.5c, d; Bertrand et al. 2017, 2018, 2019). Based on the ASR of the petrosal lobule volume ratio, Bertrand et al. (2021) showed a similar pattern to the neocortex with an increase occurring before the Sciuroidea node, suggesting that petrosal lobule expansion may have had a role in the transition to a life in trees, providing advantageous enhanced vision to these early tree dwellers (Bertrand et al. 2017). In more derived aplodontids, the petrosal lobules decreased in relative size (Fig. 16.5c, d), which could be related to becoming fossorial, as less balance and eye movement coordination may be required when living underground (Bertrand et al. 2018, 2021). Although this would seem to contradict the findings of a recent study, which found a lack of relationship between the size of the subarcuate fossa (=petrosal lobule) and locomotion in birds and mammals (Ferreira-Cardoso et al. 2017), this analysis was very limited in the number of species analyzed per order (e.g. 11 rodents). In another study, it was deduced that the relatively small petrosal lobules (=subarcuate fossa) in the octodontid *Ctenomys* could be related to subterranean specialization where high agility and mobility are not required. In contrast, the semi-aquatic *Myocastor* has large petrosal lobules that might be associated with the fact that it lives in a more complex environment (Arnaudo et al. 2020). A more recent study that limited their sample to Sciuroidea found that arboreal and scansorial taxa had larger petrosal lobules compared to fossorial species (Bertrand et al. 2021). Therefore, results suggest that it is possible to identify evolutionary changes associated with ecology in the relative size of the petrosal lobules when examined in the context of the evolutionary trajectories within a particular group.

The volume of the olfactory bulbs has been quantified for Sciuroidea, Ischyromyidae and some caviomorph rodents (Bertrand et al. 2017; Bertrand et al. 2018, 2019; Ferreira et al. 2020). A decrease in the relative size of the olfactory bulbs has been observed through time in Ischyromyidae and Sciuroidea (Fig. 16.6a). However, this relative decrease is probably a reflection of neocortical expansion through time in extant squirrels, suggesting that the olfactory bulb volume may have

Fig. 16.6 Relationship between the olfactory bulbs and endocranial volume for Sciuroidea and Ischyromyidae. **(a)**, boxplot of the olfactory bulb percentage ratio; **(b)**, bivariate plot of \log_{10} (olfactory bulb volume) vs \log_{10} (endocranial volume). The regression line corresponds to extant Sciuridae. Volumes are in mm^3 . Data used for generating the plots are in Appendix 1



stayed stable through time but represents a smaller proportion of the brain in extant squirrels (Bertrand et al. 2018).

The semicircular canals of the bony labyrinth are located in the petrosal bone and surround the petrosal lobules (when present). Previous studies have focused on the relationship between the semicircular canal size and locomotor agility because of their role in detecting angular acceleration of the head (Spor and Zonneveld 1995). A recent study using a wide range of linear and angular measurements on the semicircular canals of extant mammals found that fossorial taxa had a higher vestibular sensitivity compared to flying and gliding species. The authors suggested that the nervous system of gliding squirrels might be flooded with less sensory information to prevent overstimulation of the vestibular system (Pfaff et al. 2015). More recently, Bhagat et al. (2021) used the radius of curvature dimensions to investigate the locomotor behaviour of fossil sciuroid and ischyromyid rodents. Ischyromyinae (*Ischyromys*) and Paramyinae (*Paramys* and *Pseudotomus*) are reconstructed as slower compared to Reithroparamyinae (*Rapamys* and *Reithroparamys*). The fossil squirrels *Cedromus*, *Protosciurus* and the early aplodontid rodent *Prosciurus* have

higher agility scores, in the range of extant arboreal squirrels, while the later aplodontid taxon *Mesogaulus* and the extant *Aplodontia* have semicircular canal dimensions consistent with slower locomotion. These results are consistent with previous work using postcranial data to determine locomotor mode (e.g. Korth and Samuels 2015; Hopkins 2005; Wood 1962; Rose and Chinnery 2004; Dunn and Rasmussen 2007).

Concerning the cochlea, this portion of the inner ear has been identified as less coiled in the fossil caviomorph *Prospaniomys* compared to extant taxa. Arnaudo et al. (2020) deduced that it might be because of its Miocene age, suggesting that the cochlea may have become more coiled through time in caviomorphs. However, data from more fossil taxa will be necessary to test this hypothesis. The length of the basilar membrane (=length of the cochlea) has been used to explore the frequency hearing range of mammals (West 1985). Two extant taxa, *Abrocoma* and *Ctenomys*, both have long basilar membranes suggesting enhanced low-frequency hearing that might be related to living in arid or underground environments respectively (Arnaudo et al. 2020).

Turbinial bones have been used to estimate olfactory, heat and water conservation capabilities (Van Valkenburgh et al. 2014). Rodents that feed on worms have a tendency to display larger and more elaborated olfactory turbinates compared to other dietary categories (i.e. carnivores and omnivores). Vermivorous species that have this olfactory specialization also exhibit a decrease in the size of the respiratory turbinates, which may indicate reduced heat and water conservation abilities (Martinez et al. 2018). Other mammals show the opposite pattern. Another study investigated how the aquatic environment may have influenced the evolution of turbinates in small mammals including rodents. The authors confirmed that amphibious species have reduced olfactory but expanded respiratory turbinates, which enable them to more efficiently regulate their temperature during respiration while being under water (Martinez et al. 2020).

16.5 Future Directions: Outstanding Questions and Perspectives

Many questions remain to be answered about rodent brain evolution. Only a limited sample of specimens has been studied so far in comparison to the dazzling diversity of living rodents.

A recent study using geometric morphometrics showed that different families of rodents (Sciuridae, Aplodontidae, Gliridae, Ischyromyidae) each shared certain commonalities in terms of shape, suggesting that phylogeny had an impact on overall endocranial morphology in the sampled taxa (Bertrand et al. 2019). The same study showed that locomotor behavior may also have impacted endocranial shape. Indeed, fossorial aplodontids converged with Ischyromyidae in some aspects of endocranial shape (i.e. leading them to occupy a similar position in the

phyломorphospace) and were more similar to this group than to their closest relatives, the squirrels. This line of research could be expanded to other rodent clades to investigate whether or not these results are characteristic of rodents in general or are specific to certain groups.

The relationship between locomotor behavior and different regions of the brain has only been explored in Sciuroidea and Ischyromyidae (Bertrand et al. 2018). The relative size of different areas of the brain has not been systematically estimated when endocasts of rodents have been published. For example, only the volume of the olfactory bulbs (and not of the petrosal lobules or the neocortical surface area) were reported for caviomorph rodents (Ferreira et al. 2020). In the future, gathering these data will be crucial to test the hypotheses emerging from the study of Sciuroidea and Ischyromyidae in other groups to see whether these findings can be generalized to Rodentia.

Another factor that will need to be investigated is the relationship between diet and endocranial size. Hypotheses have been formulated for extant Primates, with data supporting the inference that frugivorous species tend to have relatively larger brains compared to folivorous taxa (DeCasien et al. 2017), whereas in fossil primates, frugivores exhibits a higher neocortical ratio than folivores (Long et al. 2015). We know virtually nothing about the diet of Ischyromyidae and fossil Sciuroidea, or about the presence or absence of an effect of a specific diet on the brain evolution of rodents. First and foremost, a modern sample will be required to establish the relationship between diet and dental topography in rodents, as has been done to deduce the diets of fossil primates (Boyer 2008; Bunn et al. 2011).

Inner ear data have been published for some rodents including some fossils (Bhagat et al. 2021), and in particular for the semicircular canals, which provide information about the agility of an animal. Quantification of functional aspects of the cochlea are lacking and we have no knowledge of the hearing range capacity of extinct rodents. Additionally, a previous study has shown that the 3D shape of the inner ear may be influenced by phylogeny and ecology in musteloid carnivores (Grohé et al. 2016). This hypothesis would be interesting to test considering the relationship found between locomotion and brain shape in Ischyromyidae and the Squirrel-related clade (Bertrand et al. 2019).

Finally, we still have very little knowledge of the earliest representatives of Rodentia in Asia and more taxa should be sampled such as the ctenodactyloid rodent *E. mini* (Wible et al. 2005), and *C. lingchaensis* (Li et al. 1989) to have a better representation of the primitive condition for rodents. Ultimately, a major problem that we are facing is the fact that the oldest cranial material available for rodents is early Eocene in age; specifically the oldest endocast known currently is for the ischyromyid *N. costilloi*, which is too flattened to obtain any quantitative data (Bertrand et al. 2019). Rodents appear in the fossil record during the late Paleocene in North America (Dawson 2015) but no three-dimensionally preserved crania have been described so far. The study of Paleocene fossil mammals (Napoli et al. 2018; Cameron et al. 2019; Bertrand et al. 2020, 2022) outside of Euarchontoglires may provide clues to what the condition of the ancestor of Euarchontoglires and other crown groups may have been.

16.6 Concluding Remarks

The hypotheses that researchers could formulate in the 1960's and 1970's about fossil rodents from the study of natural endocasts were very limited. In recent years, with the increase in availability of CT scanning, virtual endocasts for rodents have finally been generated, and this expanded record has improved considerably our understanding of the evolution of the brain in this group. The study of the virtual endocasts of rodents showed that, as in other early members of Euarchothoglires, ischyromyids have a relatively simple endocranial anatomy with relatively large olfactory bulbs, uncovered midbrain, and a small neocortex. There is only a weak relationship between the encephalization quotient and time in rodents, unlike the stronger relationship observed in Primates (Bertrand et al. 2019). Moreover, the encephalization quotient appears to be influenced by different factors including ecology, at least in rodents (Pilleri et al. 1984). Through geological time, and from Ischyromyidae to more derived early Sciuroidea, the neocortex expanded and the proportion of the olfactory bulbs decreased as observed for Primates (Silcox et al. 2010; Long et al. 2015). More importantly, the neocortical and petrosal lobule expansion observed in early Sciuroidea could be related to becoming arboreal (Bertrand et al. 2018). Specialization for a fossorial lifestyle appears to have influenced endocranial evolution, and fossil aplodontids inferred to have been fossorial show a size reduction of the neocortex and petrosal lobules compared to their tree-dwelling ancestors (Bertrand et al. 2018).

Although these conclusions represent a major step forward in terms of our knowledge of brain evolution in Rodentia, the Order has been understudied, even though museum collections include a vast number of crania for extant and extinct species. Thus, there is considerable potential for future insights into the degree to which these conclusions apply more broadly to rodents.

Appendix

Data used to make figures 16.4–16.6. Endocranial volume were converted to brain mass by multiplying the endocranial volume by 1.036 following Stephan et al. (1981). References for locomotor modes can be found in Bertrand et al. (2021)

Group	Species	Collection number	Body mass (g)	Endocranial volume (cm ³)	Brain mass (g)	EQ (Pilleri, 1984)	Endocranial volume (mm ³)	Brain surface (mm ²)	Neocortex surface (mm ²)	Olfactory bulb volume (mm ³)	Petrosal lobe volume (mm ³)	Neocortical surface area percentage (%)	Petrosal lobe volume percentage (%)	Olfactory bulb volume percentage (%)	Locomotion
Paramyinae	<i>Paramys copei</i>	AMNH 4756	1029.89	7.53	7.8	0.91	7526.65	3378.48	612.69	455.45	89.99	18.14	1.2	6.05	Scansorial
Paramyinae	<i>Paramys delicatus</i>	AMNH 12506	2913.82	12.57	13.02	0.78	12565.4	4864.86	836.31	595.51	129.3	17.19	1.03	4.74	Scansorial
Paramyinae	<i>Pseudotomus horribilis</i>	USNM 17159	7466.7	15.19	15.73	0.52	15188.2	5842.8	1095.61	808.92	173.8	18.75	1.14	5.33	Fossorial
Paramyinae	<i>Pseudotomus oweni</i>	USNM 17161	5396	12.06	12.5	0.50	12063	4744.38	1038.73	717.06	74.8	21.89	0.62	5.94	Fossorial
Paramyinae	<i>Pseudotomus petersoni</i>	AMNH 2018	6644.56	17.01	17.63	0.62	17014.9	5843.7	1337.58	704.34	65.8	22.89	0.39	4.14	Fossorial
Paramyinae	<i>Pseudotomus litans</i>	AMNH 5025	3153.5	13.68	14.17	0.81	13679.1	4878.63	1136.08	743.2	142.4	23.29	1.04	5.43	Fossorial
Reithro paramyinae	<i>Reithroparamys delicatissimus</i>	AMNH 12561	856.23	6.43	6.67	0.88	6433.98	3178.9	550.88	206.31	148.86	17.33	2.31	3.21	Scansorial
Reithro paramyinae	<i>Rapamys atramentis</i>	AMNH 128706; AMNH 128704	1307.61	6.56	6.79	0.68	6558.22	3321.41	763.65	225.34	115.56	22.99	1.76	3.44	Scansorial
Ischyromyinae	<i>Ischyromys typus</i>	ROMV 1007; AMNH 12252; AMNH F:AM 144638	1342.23	6.26	6.49	0.64	6263.18	2835.36	606.72	209.22	103.85	21.4	1.66	3.34	Fossorial
Cedromurinae	<i>Cedromus wilsoni</i>	USNM 256584	268.89	3.61	3.74	1.03	3609.87	2048.7	645.15	106.97	113.96	31.49	3.16	2.96	Arboreal

Group	Species	Collection number	Body mass (g)	Endocranial volume (cm ³)	Brain mass (g)	EQ (Pilleri, 1984)	Endocranial volume (mm ³)	Brain surface (mm ²)	Neocortex surface (mm ²)	Olfactory bulb volume (mm ³)	Petrosal lobe volume (mm ³)	Neocortical surface area percentage (%)	Petrosal lobe volume percentage (%)	Olfactory bulb volume percentage (%)	Locomotion
Sciurini	<i>Protoosciurus rachelae</i>	YPM 14736; YPM 14737	349.62	5.1	5.29	1.24	5102.89	2245.8	701.39	211.55	158.93	31.23	3.11	4.15	Arboreal
Sciurini	<i>Sciurus carolinensis</i>	AMNH 258346	592.55	8.05	8.34	1.39	8052.59	2720.59	990.64	255.92	163.26	36.41	2.03	3.18	Arboreal
Sciurini	<i>Sciurus grantiensis</i>	USNM 441999	336.99	6.32	6.55	1.57	6323.66	2340.36	841.62	169.88	131.63	35.96	2.08	2.69	Arboreal
Sciurini	<i>Tamiasciurus hudsonicus</i>	USNM 549146	256.61	5.15	5.33	1.52	5146.7	2003.97	751.24	128.89	120.02	37.49	2.33	2.5	Arboreal
Xerinae	<i>Tamias minimus</i>	USNM 298500	37.05	1.52	1.58	1.56	1521.59	890.54	325.31	51.19	34.8	36.53	2.29	3.36	Scansorial
Xerinae	<i>Famisciurus pyropus</i>	USNM 294865	301.15	4.55	4.72	1.21	4554.13	1881.42	695.25	146.78	99.54	36.95	2.19	3.22	Scansorial
Xerinae	<i>Heliosciurus rufobrachium</i>	USNM 378091	354.98	6.08	6.3	1.46	6076.64	2271.66	850.16	149.15	113.61	37.42	1.87	2.45	Arboreal
Xerinae	<i>Paraxerus cepapi</i>	USNM 367956	138.13	3.05	3.16	1.34	3053.3	1445.98	533.37	79.88	44.66	36.89	1.46	2.62	Scansorial
Xerinae	<i>Protoxerus stangeri</i>	USNM 435027	767.23	9.75	10.1	1.42	9746.91	3138.06	1233.5	225.57	183.74	39.31	1.89	2.31	Arboreal
Xerinae	<i>Xerus rutilus</i>	AMNH 179092	353.9	6	6.22	1.44	6001.83	2249.69	866.66	196.97	111.95	38.52	1.87	3.28	Terrestrial
Xerinae	<i>Marmota marmota</i>	AMNH 146619	4546.97	15.2	15.74	0.71	15195.8	4622.4	1533.62	390.88	127.4	33.18	0.84	2.57	Terrestrial
Xerinae	<i>Cynomys ludovicianus</i>	AMNH 114522	938.7	7.22	7.48	0.93	7220.3	2666.16	928.61	182.73	70.97	34.83	0.98	2.53	Terrestrial
Xerinae	<i>Urociellus richardsonii</i>	AMNH 15062	245.78	3.16	3.27	0.96	3157.99	1514.13	553.66	105.75	55.33	36.57	1.75	3.35	Terrestrial
Pteromyini	<i>Aeromys tephromelas</i>	USNM 481190	904.59	11.46	11.87	1.51	11461.5	3528.53	1276.75	326.77	166.1	36.18	1.45	2.85	Glider

Group	Species	Collection number	Body mass (g)	Endocranial volume (cm ³)	Brain mass (g)	EQ (Pilleri, 1984)	Endocranial volume (mm ³)	Brain surface (mm ²)	Neocortex surface (mm ²)	Olfactory bulb volume (mm ³)	Petrosal lobe volume (mm ³)	Neocortical surface area percentage (%)	Petrosal lobe volume percentage (%)	Olfactory bulb volume percentage (%)	Locomotion
Pteromyiini	<i>Glaucomys volans</i>	AMNH 240290	63.97	2.01	2.08	1.45	2010.43	1040.25	383.61	70.08	33.73	36.88	1.68	3.49	Glider
Pteromyiini	<i>Petaurista petaurista</i>	USNM 589079	1096.65	12.32	12.76	1.43	12317.7	3673.24	1331.61	201.76	199.9	36.25	1.62	1.64	Glider
Pteromyiini	<i>Hypopetes spadiceus</i>	USNM 488639	84.22	2.12	2.2	1.28	2120.74	1078.4	410.01	69.95	17.93	38.02	0.85	3.3	Glider
Pteromyiini	<i>Petinomys setosus</i>	USNM 488674	41.86	1.51	1.57	1.43	1512.53	836.52	305.69	46.96	NA	36.54	NA	3.1	Glider
Pteromyiini	<i>Pteromyscus pulverulentus</i>	USNM 481178	195.44	3.62	3.75	1.27	3621.04	1627.4	565.88	101.74	49.5	34.77	1.37	2.81	Glider
Pteromyiini	<i>Pteromys volans</i>	USNM 172622	106.37	2.33	2.41	1.21	2330.8	1205.34	427.98	40.79	37.53	35.51	1.61	1.75	Glider
Callosciurinae	<i>Rhinosciurus laticaudatus</i>	USNM 488511	507.38	4.38	4.54	0.84	4383.6	1851.63	650.59	170.11	97.36	35.14	2.22	3.88	Terrestrial
Callosciurinae	<i>Callosciurus</i> sp.	USNM 294865	437.35	7.01	7.26	1.47	7007.94	2479.31	974.42	229.77	123.91	39.3	1.77	3.28	Arboreal
Callosciurinae	<i>Lariscus insignis</i>	USNM 488570	324.71	4.88	5.05	1.24	4878.57	1993.8	691.54	230.63	113	34.68	2.32	4.73	Terrestrial
Callosciurinae	<i>Dremomys rufigenis</i>	USNM 488602	418.43	5.87	6.08	1.27	5866.09	2185.23	826.93	232.42	125.71	37.84	2.14	3.96	Scansorial
Ratufinae	<i>Ratufa affinis</i>	USNM 488104	1074.27	12.31	12.76	1.45	12313.7	3725.22	1407.87	201.44	234.9	37.79	1.91	1.64	Arboreal
Aplodontinae	<i>Aplodontia rufa</i>	AMNH 42389	1475.86	7.89	8.18	0.76	7894.92	2878.28	779.01	203.71	64.41	27.07	0.82	2.58	Fossorial
Mylagaulinae	<i>Mesogaulus panitensis</i>	AMNH F:AM 65511	266.48	3.47	3.59	1.00	3467.99	1632.28	437.51	113.99	46.27	26.8	1.33	3.29	Fossorial
Prosciurinae	<i>Prosciurus relictus</i>	USNM 437793	30.07	0.96	0.99	1.12	957.45	845.9	251.16	34	32.08	29.69	3.35	3.55	Arboreal
Prosciurinae	<i>Prosciurus relictus</i>	USNM 437793	30.07	0.96	0.99	1.12	957.45	845.9	251.16	34	32.08	29.69	3.35	3.55	Arboreal

Acknowledgments This work was funded by a Marie Skłodowska-Curie Actions: Individual Fellowship (H2020-MSCA-IF-2018-2020; No. 792611) to OCB; an NSERC Discovery Grant to MTS.

References

- Anderson D (2008) Ischyromyidae. In: Janis C, Scott K, Jacobs L (eds) Evolution of tertiary mammals of North America: small mammals, xenarthrans, and marine mammals, vol 2. Cambridge University Press, Cambridge, pp 311–325
- Antoine PO, Marivaux L, Croft DA et al (2012) Middle Eocene rodents from Peruvian Amazonia reveal the pattern and timing of caviomorph origins and biogeography. *Proc R Soc B* 279:1319–1326. <https://doi.org/10.1098/rspb.2011.1732>
- Arnaudo ME, Arnal M, Ekdale EG (2020) The auditory region of a caviomorph rodent (Hystricognathi) from the early Miocene of Patagonia (South America) and evolutionary considerations. *J Vertebr Paleontol* 40:e1777557. <https://doi.org/10.1080/02724634.2020.1777557>
- Asher RJ, Smith MR, Rankin A et al (2019) Congruence, fossils and the evolutionary tree of rodents and lagomorphs. *R Soc Open Sci* 6:190387. <https://doi.org/10.1098/rsos.190387>
- Bertrand OC, Silcox MT (2016) First virtual endocasts of a fossil rodent: *Ischyromys typus* (Ischyromyidae, Oligocene) and brain evolution in rodents. *J Vertebr Paleontol* 36:e1095762. <https://doi.org/10.1080/02724634.2016.1095762>
- Bertrand OC, Flynn JJ, Croft DA et al (2012) Two new taxa (Caviomorpha, Rodentia) from the Early Oligocene Tinguiririca Fauna (Chile). *Am Mus Novit* 3750:1–36
- Bertrand OC, Amador-Mughal F, Silcox MT (2016a) Virtual endocasts of Eocene *Paramys* (Paramyinae): oldest endocranial record for Rodentia and early brain evolution in Euarchontoglires. *Proc R Soc B* 283(1823):20152316. <https://doi.org/10.1098/rspb.2015.2316>
- Bertrand OC, Schillaci MA, Silcox MT (2016b) Cranial dimensions as estimators of body mass and locomotor habits in extant and fossil rodents. *J Vertebr Paleontol* 36:e1014905. <https://doi.org/10.1080/02724634.2015.1014905>
- Bertrand OC, Amador-Mughal F, Silcox MT (2017) Virtual endocast of the early Oligocene *Cedromus wilsoni* (Cedromurinae) and brain evolution in squirrels. *J Anat* 230:128–151. <https://doi.org/10.1111/joa.12537>
- Bertrand OC, Amador-Mughal F, Lang MM et al (2018) Virtual endocasts of fossil Sciuroidea: brain size reduction in the evolution of fossoriality. *Palaeontology* 61:919–948. <https://doi.org/10.1111/pala.12378>
- Bertrand OC, Amador-Mughal F, Lang MM et al (2019) New virtual endocasts of Eocene Ischyromyidae and their relevance in evaluating neurological changes occurring through time in Rodentia. *J Mamm Evol* 26:345–371. <https://doi.org/10.1007/s10914-017-9425-6>
- Bertrand OC, Shelley SL, Wible JR et al (2020) Virtual endocranial and inner ear endocasts of the Paleocene ‘condylarth’ *Chriacus*: new insight into the neurosensory system and evolution of early placental mammals. *J Anat* 236:21–49. <https://doi.org/10.1111/joa.13084>
- Bertrand OC, Püschel HP, Schwab JA et al (2021) The impact of locomotion on the brain evolution of squirrels and close relatives. *Commun Biol* 4(460):1–15. <https://doi.org/10.1038/s42003-021-01887-8>
- Bertrand OC, Shelley SL, Williamson TE, Wible JR, Chester SGB, Flynn JJ, Holbrook LT, Lyson TR, Meng J, Miller IM, Püschel Hans P, Smith T, Spaulding M, Tseng ZJ, Brusatte SL (2022) Brawn before brains in placental mammals after the end-Cretaceous extinction. *Science* 376(6588):80–85
- Bhagat R, Bertrand OC, Silcox MT (2021) Evolution of arboreality and fossoriality in squirrels and aplodontid rodents: insights from the semicircular canals of fossil rodents. *J Anat* 238:96–112. <https://doi.org/10.1111/joa.13296>

- Blanga-Kanfi S, Miranda H, Penn O et al (2009) Rodent phylogeny revised: analysis of six nuclear genes from all major rodent clades. *BMC Evol Biol* 9:71. <https://doi.org/10.1186/1471-2148-9-71>
- Boyer DM (2008) Relief index of second mandibular molars is a correlate of diet among prosimian primates and other euarchontan mammals. *J Hum Evol* 55:1118–1137. <https://doi.org/10.1016/j.jhevol.2008.08.002>
- Bugge J (1985) Systematic value of the carotid arterial pattern in rodents. In: Luckett WP, Hartenberger J-L (eds) *Evolutionary relationships among rodents, a multidisciplinary approach*. Springer US, Boston, pp 355–379
- Bunn JM, Boyer DM, Lipman Y et al (2011) Comparing Dirichlet normal surface energy of tooth crowns, a new technique of molar shape quantification for dietary inference, with previous methods in isolation and in combination. *Amer J Phys Anthropol* 145:247–261. <https://doi.org/10.1002/ajpa.21489>
- Burger JR, George MA Jr, Leadbetter C et al (2019) The allometry of brain size in mammals. *J Mammal* 100:276–283. <https://doi.org/10.1093/jmammal/gyz043>
- Burgin CJ, Colella JP, Kahn PL et al (2018) How many species of mammals are there? *J Mammal* 99:1–14. <https://doi.org/10.1093/jmammal/gyx147>
- Cameron J, Shelley SL, Williamson TE et al (2019) The brain and inner ear of the early Paleocene “Condylarth” *Carsiptychus coarctatus*: implications for early placental mammal neurosensory biology and behavior. *Anat Rec* 302:306–324. <https://doi.org/10.1002/ar.23903>
- Cerminara NL, Apps R (2011) Behavioural significance of cerebellar modules. *Cerebellum* 10:484–494. <https://doi.org/10.1007/s12311-010-0209-2>
- Christensen GC, Evans HE (1979) *Miller’s anatomy of the dog*. W.B. Saunders, Philadelphia, Pennsylvania
- Chuan-Kuei L, Wilson RW, Dawson MR et al (1987) The origin of rodents and lagomorphs. In: Genoways HH (ed) *Current mammalogy*. Springer US, Boston, pp 97–108. https://doi.org/10.1007/978-1-4757-9909-5_3
- Churakov G, Sadasivuni MK, Rosenbloom KR et al (2010) Rodent evolution: back to the root. *Mol Biol Evol* 27:1315–1326. <https://doi.org/10.1093/molbev/msq019>
- Dawson MR (2003) Paleogene rodents of Eurasia. *Deinsea* 10:97–126
- Dawson MR (2015) Emerging perspectives on some Paleogene sciurognath rodents in Laurasia: the fossil record and its interpretation. In: Hautier L, Cox PG (eds) *Evolution of the rodents: advances in phylogeny, functional morphology and development*, Cambridge studies in morphology and molecules: new paradigms in evolutionary bio, vol 5. Cambridge University Press, Cambridge, pp 70–86. <https://doi.org/10.1017/CBO9781107360150.004>
- Dawson MR, Li C-K, Qi T (1984) Eocene ctenodactyloid rodents (Mammalia) of eastern and Central Asia. *Spec publ- Carnegie Mus Nat Hist* 9:138–150
- DeCasien AR, Williams SA, Higham JP (2017) Primate brain size is predicted by diet but not sociality. *Nat Ecol Evol* 1:0112. <https://doi.org/10.1038/s41559-017-0112>
- Dechaseaux C (1958) Encéphales de Simplicidentés fossiles. In *Traité de paléontologie: L’origine des mammifères et les aspects fondamentaux de leur évolution*. 2. v (ed Piveteau J), pp. 819–821. Masson
- Douzery EJ, Delsuc F, Stanhope MJ et al (2003) Local molecular clocks in three nuclear genes: divergence times for rodents and other mammals and incompatibility among fossil calibrations. *J Mol Evol* 57:S201–S213. <https://doi.org/10.1007/s00239-003-0028-x>
- Dozo MT (1997a) Paleoneurología de *Dolicavia minuscula* (Rodentia, Caviidae) y *Paedotherium insigne* (Notoungulata, Hegetotheriidae) del Plioceno de Buenos Aires, Argentina. *Ameghiniana* 34:427–435
- Dozo MT (1997b) Primer estudio paleoneurológico de un roedor caviomorfo (Cephalomyidae) y sus posibles implicancias filogenéticas. *Mastozool Neotrop* 4:89–96
- Dozo MT, Vucetich MG, Candela AM (2004) Skull anatomy and neuromorphology of *Hypsosteiomys*, a Colhuehuapian erethizontid rodent from Argentina. *J Vertebr Paleontol* 24:228–234. <https://doi.org/10.1671/18.1>

- Dunn RH, Rasmussen DT (2007) Skeletal morphology and locomotor behavior of *Pseudotomus eugenei* (Rodentia, Paramyinae) from the Uinta Formation, Utah. *J Vertebr Paleontol* 27:987–1006. [https://doi.org/10.1671/0272-4634\(2007\)27\[987:Smalbo\]2.0.Co;2](https://doi.org/10.1671/0272-4634(2007)27[987:Smalbo]2.0.Co;2)
- Edinger T (1964) Midbrain exposure and overlap in mammals. *Am Zool* 4:5–19
- Emry RJ, Thorington RW (1982) Descriptive and comparative osteology of the oldest fossil squirrel, *Protosciurus* (Rodentia: Sciuridae). *Smithson Contrib Paleobiol* 47:1–35
- Fabre P-H, Hautier L, Dimitrov D et al (2012) A glimpse on the pattern of rodent diversification: a phylogenetic approach. *BMC Evol Biol* 12:88. <https://doi.org/10.1186/1471-2148-12-88>
- Fabre P-H, Jönsson KA, Douzery EJP (2013) Jumping and gliding rodents: mitogenomic affinities of Pedetidae and Anomaluridae deduced from an RNA-Seq approach. *Gene* 531:388–397. <https://doi.org/10.1016/j.gene.2013.07.059>
- Fabre P-H, Hautier L, Douzery EJP (2015) A synopsis of rodent molecular phylogenetics, systematics and biogeography. In: Hautier L, Cox PG (eds) *Evolution of the rodents: advances in phylogeny, functional morphology and development*, Cambridge studies in morphology and molecules: new paradigms in evolutionary bio, vol 5. Cambridge University Press, Cambridge, pp 19–69. <https://doi.org/10.1017/CBO9781107360150.003>
- Ferreira JD, Negri FR, Sánchez-Villagra MR et al (2020) Small within the largest: brain size and anatomy of the extinct *Neoepiblema acrensis*, a giant rodent from the Neotropics. *Biol Lett* 16:20190914. <https://doi.org/10.1098/rsbl.2019.0914>
- Ferreira JD, Dozo MT, de Moura Bubadué J, Kerber L (2022) Morphology and postnatal ontogeny of the cranial endocast and paranasal sinuses of capybara (*Hydrochoerus hydrochaeris*), the largest living rodent. *J Morphol* 283: 66–90
- Ferreira-Cardoso S, Araújo R, Martins NE et al (2017) Floccular fossa size is not a reliable proxy of ecology and behaviour in vertebrates. *Sci Rep* 7:2005. <https://doi.org/10.1038/s41598-017-01981-0>
- Flynn LJ, Jacobs LL, Cheema IU (1986) Baluchimyinae, a new ctenodactyloid rodent subfamily from the Miocene of Baluchistan. *Am Mus Novit* 2841:1–58
- Graur D, Hide WA, Li W-H (1991) Is the guinea-pig a rodent? *Nature* 351:649–652. <https://doi.org/10.1038/351649a0>
- Grohé C, Tseng ZJ, Lebrun R et al (2016) Bony labyrinth shape variation in extant Carnivora: a case study of Musteloidea. *J Anat* 228:366–383. <https://doi.org/10.1111/joa.12421>
- Gurche JA (1982) Early primate brain evolution. In: Armstrong E, Falk D (eds) *Primate brain evolution: methods and concepts*. Springer US, Boston, pp 227–246. https://doi.org/10.1007/978-1-4684-4148-2_15
- Hartenberger J (1980) Données et hypothèses sur la radiation initiale des rongeurs. *Palaeovertebrata*, Mémoire jubilaire en hommage à René Lavocat:285–301
- Holden M (2005) Family Gliridae, Order Rodentia. In: *Mammal species of the world: a taxonomic and geographic reference*, 3rd edn. John Hopkins University Press, Baltimore, pp 819–841
- Hopkins SS (2005) The evolution of fossoriality and the adaptive role of horns in the Mylagaulidae (Mammalia: Rodentia). *Proc R Soc B* 272:1705–1713. <https://doi.org/10.1098/rspb.2005.3171>
- Hopkins SS (2008) Phylogeny and evolutionary history of the Aplodontioidea (Mammalia: Rodentia). *Zool J Linn Soc* 153:769–838. <https://doi.org/10.1111/j.1096-3642.2008.00399.x>
- Houle A (1999) The origin of platyrrhines: an evaluation of the Antarctic scenario and the floating island model. *Amer J Phys Anthropol* 109:541–559
- Huchon D, Douzery EJ (2001) From the Old World to the New World: a molecular chronicle of the phylogeny and biogeography of hystricognath rodents. *Mol Phylogenetics Evol* 20:238–251. <https://doi.org/10.1006/mpev.2001.0961>
- Huchon D, Catzeflis FM, Douzery EJ (1999) Molecular evolution of the nuclear von Willebrand factor gene in mammals and the phylogeny of rodents. *Mol Biol Evol* 16:577–589. <https://doi.org/10.1093/oxfordjournals.molbev.a026140>
- Huchon D, Catzeflis FM, Douzery EJP (2000) Variance of molecular datings, evolution of rodents and the phylogenetic affinities between Ctenodactylidae and Hystricognathi. *Proc R Soc B* 267:393–402. <https://doi.org/10.1098/rspb.2000.1014>

- Huchon D, Madsen O, Sibbald MJJB et al (2002) Rodent phylogeny and a timescale for the evolution of Glires: evidence from an extensive taxon sampling using three nuclear genes. *Mol Biol Evol* 19:1053–1065. <https://doi.org/10.1093/oxfordjournals.molbev.a004164>
- Jerison HJ (1973) Evolution of the brain and intelligence. Academic, New York
- Kerber L, Negri FR, Ferigolo J, Mayer EL, Ribeiro AM (2017) Modifications on fossils of neopiblemids and other South American rodents. *Lethaia*, 50:149–161
- Korth WW (1984) Earliest Tertiary evolution and radiation of rodents in North America. *Bull Carnegie Mus* 24:1–71
- Korth WW (1994) The Tertiary record of rodents in North America. Plenum Press, New York
- Korth WW, Emry RJ (1991) The skull of *Cedromus* and a review of the Cedromurinae (Rodentia, Sciuridae). *J Paleontol* 65:984–994. <https://doi.org/10.1017/S002233600033291>
- Korth WW, Samuels JX (2015) New rodent material from the John Day Formation (Arikareean, Middle Oligocene to Early Miocene) of Oregon. *Ann Carnegie Mus* 83:19–84. <https://doi.org/10.2992/007.083.0102>
- Krubitzer L, Campi KL, Cooke DF (2011) All rodents are not the same: a modern synthesis of cortical organization. *Brain Behav Evol* 78:51–93. <https://doi.org/10.1159/000327320>
- Lavocat R (1973) Les Rongeurs du Miocene D’Afrique Orientale. Miocene Inferieur. Institut de Montpellier de l’ecole Pratique des Hautes Etudes, Montpellier
- Lavocat R, Parent J-P (1985) Phylogenetic Analysis of Middle Ear Features in Fossil and Living Rodents. In *Evolutionary Relationships among Rodents* (eds Lockett WP, Hartenberger J-L). Springer US, Boston, pp. 333–354
- Li CK, Zheng JJ, Ting SY (1989) The skull of *Cocomys lingchaensis*, an early Eocene ctenodactyloid rodent of Asia. In: Black CC, Dawson MR (eds) *Papers on fossil rodents in honour of Albert Elmer Wood*, Natural history museum of Los Angeles County science series, vol 33, pp 179–192
- Long A, Bloch JI, Silcox MT (2015) Quantification of neocortical ratios in stem primates. *Amer J Phys Anthropol* 157:363–373. <https://doi.org/10.1002/ajpa.22724>
- López-Torres S, Bertrand OC, Lang MM et al (2020) Cranial endocast of the stem lagomorph *Megalagus* and brain structure of basal Euarchontoglires. *Proc R Soc B* 287:20200665. <https://doi.org/10.1098/rspb.2020.0665>
- Lockett WP, Hartenberger JL (1985) *Evolutionary relationships among rodents: a multidisciplinary analysis*. Plenum Press, New York
- Mace GM, Harvey PH, Clutton-Brock TH (1981) Brain size and ecology in small mammals. *J Zool* 193:333–354. <https://doi.org/10.1111/j.1469-7998.1981.tb03449.x>
- Macrini TE, Rougier GW, Rowe T (2007) Description of a cranial endocast from the fossil mammal *Vincelestes neuquenianus* (Theriiiformes) and its relevance to the evolution of endocranial characters in therians. *Anat Rec* 290:875–892. <https://doi.org/10.1002/ar.20551>
- Marivaux L, Vianey-Liaud M, Jaeger JJ (2004) High-level phylogeny of early Tertiary rodents: dental evidence. *Zool J Linnean Soc* 142:105–134. <https://doi.org/10.1111/j.1096-3642.2004.00131.x>
- Martin RD (1990) *Primate origins and evolution. A phylogenetic reconstruction*. Princeton University Press, Princeton
- Martinez Q, Lebrun R, Achmadi AS et al (2018) Convergent evolution of an extreme dietary specialisation, the olfactory system of worm-eating rodents. *Sci Rep* 8:17806. <https://doi.org/10.1038/s41598-018-35827-0>
- Martinez Q, Clavel J, Esselstyn JA et al (2020) Convergent evolution of olfactory and thermoregulatory capacities in small amphibious mammals. *PNAS* 117:8958–8965. <https://doi.org/10.1073/pnas.1917836117>
- Matthew W (1910) On the osteology and relationships of *Paramys*, and the affinities of the Ischyromyidae. *Bull Am Mus Nat Hist* 28:1–72
- McKenna MC, Bell SK (1997) *Classification of mammals: above the species level*. Columbia University Press, New York
- Meier PT (1983) Relative brain size within the North American Sciuridae. *J Mammal* 64:642–647. <https://doi.org/10.2307/1380520>

- Meng J (1990) The auditory region of *Reithroparamys delicatissimus* (Mammalia, Rodentia) and its systematic implications. *Am Mus Novit* 2972:1–35
- Meng J (2004) Phylogeny and divergence of basal Glires. *Bull Am Mus Nat Hist* 285:93–109
- Meng J, Hu Y, Li C (2003) The osteology of *Rhombomylus* (Mammalia, Glires): implications for phylogeny and evolution of Glires. *Bull Am Mus Nat Hist* 275:1–247
- Mercer JM, Roth VL (2003) The effects of Cenozoic global change on squirrel phylogeny. *Science* 299:1568–1572. <https://doi.org/10.1126/science.1079705>
- Meredith RW, Janečka JE, Gatesy J et al (2011) Impacts of the Cretaceous terrestrial revolution and KPg extinction on mammal diversification. *Science* 334:521–524. <https://doi.org/10.1126/science.1211028>
- Michaux J (1968) Les Paramyidae (Rodentia) de l'éocène inférieur du bassin de Paris. *Palaeovertebrata* 1:135–193
- Montgelard C, Forty E, Arnal V et al (2008) Suprafamilial relationships among Rodentia and the phylogenetic effect of removing fast-evolving nucleotides in mitochondrial, exon and intron fragments. *BMC Evol Biol* 8:321. <https://doi.org/10.1186/1471-2148-8-321>
- Murphy WJ, Eizirik E, Johnson WE et al (2001a) Molecular phylogenetics and the origins of placental mammals. *Nature* 409:614–618. <https://doi.org/10.1038/35054550>
- Murphy WJ, Eizirik E, O'Brien SJ et al (2001b) Resolution of the early placental mammal radiation using Bayesian phylogenetics. *Science* 294:2348–2351. <https://doi.org/10.1126/science.1067179>
- Napoli JG, Williamson TE, Shelley SL et al (2018) A digital endocranial cast of the Early Paleocene (Puercan) 'archaic' mammal *Onychodectes tisonensis* (Eutheria: Taeniodonta). *J Mamm Evol* 25:179–195. <https://doi.org/10.1007/s10914-017-9381-1>
- Ni X, Flynn JJ, Wyss AR et al (2019) Cranial endocast of a stem platyrrhine primate and ancestral brain conditions in anthropoids. *Sci Adv* 5:eaav7913. <https://doi.org/10.1126/sciadv.aav7913>
- Novacek MJ (1986) The skull of leptictid insectivorans and the higher-level classification of eutherian mammals. *Bull Am Mus Nat Hist* 183:1–112
- Nowak MM (1999) Walker's mammals of the world, vol 2. Johns Hopkins University, Baltimore
- O'Leary MA, Bloch JI, Flynn JJ et al (2013) The placental mammal ancestor and the post-K-Pg radiation of placentals. *Science* 339:662–667. <https://doi.org/10.1126/science.1229237>
- Orliac MJ, Gilissen E (2012) Virtual endocranial cast of earliest Eocene *Diacodexis* (Artiodactyla, Mammalia) and morphological diversity of early artiodactyl brains. *Proc R Soc B* 279:3670–3677. <https://doi.org/10.1098/rspb.2012.1156>
- Pascual R, Vucetich M, Scillato-Yané G (1990) Extinct and Recent South American and Caribbean edentates and rodents: outstanding examples of isolation. *Biogeographical aspects of insularity Atti Convegno Lincei* 87:627–640
- Patterson BD, Upham NS (2014) A newly recognized family from the Horn of Africa, the Heterocephalidae (Rodentia: Ctenohystrica). *Zool J Linn Soc* 172:942–963. <https://doi.org/10.1111/zoj.12201>
- Pérez ME, Vallejo-Pareja MC, Carrillo JD, Jaramillo C (2017) A new Pliocene capybara (Rodentia, Caviidae) from Northern South America (Guajira, Colombia), and its implications for the great American biotic interchange. *J Mamm Evol* 24:111–125
- Pfaff C, Martin T, Ruf I (2015) Bony labyrinth morphometry indicates locomotor adaptations in the squirrel-related clade (Rodentia, Mammalia). *Proc R Soc B* 282:20150744. <https://doi.org/10.1098/rspb.2015.0744>
- Pilleri G, Gihl M, Kraus C (1984) Cephalization in rodents with particular reference to the Canadian beaver (*Castor canadensis*). In: *Investigations on beavers*, vol 2. Institute of Brain Anatomy, Berne
- Piñero P, Verzi DH, Olivares AI et al (2021) Evolutionary pattern of *Metacaremys* gen. nov. (Rodentia, Octodontidae) and its biochronological implications for the late Miocene and early Pliocene of southern South America. *Pap Palaeontol* 7:1895–1917. <https://doi.org/10.1002/spp2.1368>
- Poux C, Chevret P, Huchon D et al (2006) Arrival and diversification of caviomorph rodents and platyrrhine primates in South America. *Syst Biol* 55:228–244. <https://doi.org/10.1080/10635150500481390>

- Prufrock KA, Ruff CB, Rose KD (2021) Locomotor behavior and body mass of *Paramys delicatus* (Ischyromyidae, Rodentia) and commentary on other early North American paramyines. *J Mamm Evol* 28:435–456. <https://doi.org/10.1007/s10914-020-09523-8>
- Radinsky L (1976) Oldest horse brains: more advanced than previously realized. *Science* 194:626–627. <https://doi.org/10.1126/science.790567>
- Rambold H, Churchland A, Selig Y et al (2002) Partial ablations of the flocculus and ventral paraflocculus in monkeys cause linked deficits in smooth pursuit eye movements and adaptive modification of the VOR. *J Neurophysiol* 87:912–924. <https://doi.org/10.1152/jn.00768.2000>
- Rasia LL, Candela AM (2019) Upper molar morphology, homologies and evolutionary patterns of chinchilloid rodents (Mammalia, Caviomorpha). *J Anat* 234:50–65
- Rensberger JM (1981) Evolution in a late Oligocene–early Miocene succession of meniscomyine rodents in the Deep River Formation, Montana. *J Vertebr Paleontol* 1:185–209. <https://doi.org/10.1080/02724634.1981.10011891>
- Rensberger JM (1983) Successions of meniscomyine and allomyine rodents (Aplodontidae) in the Oligo-Miocene John Day Formation, Oregon, vol 124. University of California Press, Berkeley
- Rinderknecht A, Blanco RE (2008) The largest fossil rodent. *Proc R Soc B* 275:923–928. <https://doi.org/10.1098/rspb.2007.1645>
- Rocha RG, Leite YLR, Costa LP et al (2016) Independent reversals to terrestriality in squirrels (Rodentia: Sciuridae) support ecologically mediated modes of adaptation. *J Evol Biol* 29:2471–2479. <https://doi.org/10.1111/jeb.12975>
- Rose KD (2006) The beginning of the age of mammals. Johns Hopkins University Press, Baltimore
- Rose KD, Chinnery BJ (2004) The postcranial skeleton of Early Eocene rodents. *Bull Carnegie Mus* 36:211–244. [https://doi.org/10.2992/0145-9058\(2004\)36\[211:Tpsoe\]2.0.Co;2](https://doi.org/10.2992/0145-9058(2004)36[211:Tpsoe]2.0.Co;2)
- Roth VL, Thorington RW (1982) Relative brain size among African squirrels. *J Mammal* 63:168–173. <https://doi.org/10.2307/1380690>
- Scott WB, Osborn HF (1887) Preliminary report on the vertebrate fossils of the Uinta Formation, collected by the Princeton Expedition of 1886. *Proc Am Phil Soc* 24(126):255–264
- Scott WB, Osborn HF (1890) The Mammalia of the Uinta Formation. *Trans Am Philos Soc* 16:461–572. <https://doi.org/10.2307/1005400>
- Scott WB, Jepsen GL, Wood AE (1937) The mammalian fauna of the White River Oligocene: Part II. Rodentia. *Trans Am Philos Soc* 28:155–269. <https://doi.org/10.2307/1005501>
- Silcox MT, Dalmyrn CK, Bloch JI (2009) Virtual endocast of *Ignacius graybullianus* (Paromomyidae, Primates) and brain evolution in early primates. *PNAS* 106:10987–10992. <https://doi.org/10.1073/pnas.0812140106>
- Silcox MT, Benham AE, Bloch JI (2010) Endocasts of *Microsypops* (Microsypopidae, Primates) and the evolution of the brain in primitive primates. *J Hum Evol* 58:505–521. <https://doi.org/10.1016/j.jhevol.2010.03.008>
- Silcox MT, Dalmyrn CK, Hrenchuk A et al (2011) Endocranial morphology of *Labidolemur kayi* (Apatemyidae, Apatotheria) and its relevance to the study of brain evolution in Euarchontoglires. *J Vertebr Paleontol* 31:1314–1325. <https://doi.org/10.1080/02724634.2011.609574>
- Sillitoe RV, Marzban H, Larouche M et al (2005) Conservation of the architecture of the anterior lobe vermis of the cerebellum across mammalian species. *Prog Brain Res* 148:283–297. [https://doi.org/10.1016/S0079-6123\(04\)48022-4](https://doi.org/10.1016/S0079-6123(04)48022-4)
- Simpson GG (1945) The principles of classification and a classification of mammals. *Bull Am Mus Nat Hist* 85:1–350
- Spoor F, Zonneveld F (1995) Morphometry of the primate bony labyrinth: a new method based on high-resolution computed tomography. *J Anat* 186:271–286
- Steppan SJ, Storz BL, Hoffmann RS (2004) Nuclear DNA phylogeny of the squirrels (Mammalia: Rodentia) and the evolution of arboreality from c-myc and RAG1. *Mol Phylogenetics Evol* 30:703–719. [https://doi.org/10.1016/s1055-7903\(03\)00204-5](https://doi.org/10.1016/s1055-7903(03)00204-5)
- Thorington RW, Koprowski JL, Steele MA et al (2012) Squirrels of the world. Johns Hopkins University Press, Baltimore. <https://doi.org/10.1644/13-mamm-r-075.1>

- Ting S, Meng J, McKenna MC et al (2002) The osteology of *Matutinia* (Simplicidentata, Mammalia) and its relationship to *Rhombomylus*. *Am Mus Novit* 3371:1–33
- Tullberg T (1899) Ueber das System der Nagethiere: eine phylogenetische Studie. *Nova Acta Regiae Soc Sci Upsal* 18:1–514
- Upham N, Patterson B (2015) Evolution of caviomorph rodents: a complete phylogeny and timetree for living genera. In: Vassallo A, Antenucci D (eds) *Biology of caviomorph rodents: diversity and evolution*. Sociedad Argentina para el estudio de los Mamíferos, Buenos Aires, pp 63–120
- Van Valkenburgh B, Smith TD, Craven BA (2014) Tour of a labyrinth: exploring the vertebrate nose. *Anat Rec* 297:1975–1984. <https://doi.org/10.1002/ar.23021>
- Vianey-Liaud M, Rodrigues HG, Marivaux L (2013) Early adaptive radiations of Aplodontoidea (Rodentia, Mammalia) on the Holarctic region: systematics, and phylogenetic and paleobiogeographic implications. *Palaontol Z* 87:83–120
- Voogd J, Wylie DR (2004) Functional and anatomical organization of floccular zones: a preserved feature in vertebrates. *J Comp Neurol* 470:107–112
- Vucetich M, Arnal M, Deschamps C et al (2015) A brief history of caviomorph rodents as told by the fossil record. In: Vassallo A, Antonucci D (eds) *Biology of caviomorph rodents: diversity and evolution*. Sociedad Argentina para el estudio de los Mamíferos, Buenos Aires, pp 11–62
- Waespe W, Cohen B, Raphan T (1983) Role of the flocculus and paraflocculus in optokinetic nystagmus and visual-vestibular interactions: effects of lesions. *Exp Brain Res* 50:9–33
- Wahlert JH (1974) The cranial foramina of protrogomorphous rodents: an anatomical and phylogenetic study. *Bull Mus Comp Zool* 146:363–410
- West CD (1985) The relationship of the spiral turns of the cochlea and the length of the basilar membrane to the range of audible frequencies in ground dwelling mammals. *J Acoust Soc Am* 77:1091–1101. <https://doi.org/10.1121/1.392227>
- Wible JR (1987) The eutherian stapedial artery: character analysis and implications for superordinal relationships. *Zool J Linnean Soc* 91:107–135. <https://doi.org/10.1111/j.1096-3642.1987.tb01725.x>
- Wible JR (2005) Cranial anatomy and relationships of a new ctenodactyloid (Mammalia, Rodentia) from the early Eocene of Hubei Province, China. *Ann Carnegie Museum* 74:91–151
- Wible JR, Rougier GW (2000) Cranial anatomy of *Kryptobaatar dazhzevegi* (Mammalia, Multituberculata), and its bearing on the evolution of mammalian characters. *Bull Am Mus Nat Hist* 247:1–120. [https://doi.org/10.1206/0003-0090\(2000\)247<0001:CAOKDM>2.0.CO;2](https://doi.org/10.1206/0003-0090(2000)247<0001:CAOKDM>2.0.CO;2)
- Wible JR, Shelley SL (2020) Anatomy of the petrosal and middle ear of the brown rat, *Rattus norvegicus* (Berkenhout, 1769) (Rodentia, Muridae). *Ann Carnegie Mus* 86:1–35. <https://doi.org/10.2992/007.086.0101>
- Wible JR, Wang Y, Li C et al (2005) Cranial anatomy and relationships of a new ctenodactyloid (Mammalia, Rodentia) from the early Eocene of Hubei Province, China. *Ann Carnegie Mus* 74:91–151. [https://doi.org/10.2992/0097-4463\(2005\)74\[91:CAAROA\]2.0.CO;2](https://doi.org/10.2992/0097-4463(2005)74[91:CAAROA]2.0.CO;2)
- Wilson RW (1949) Additional Eocene rodent material from southern California. *Carnegie Instit Wash Pub* 584:1–25
- Wilson DE, Reeder DAM (2005) *Mammal species of the world: a taxonomic and geographic reference*, vol 1. Johns Hopkins University Press, Baltimore
- Wood AE (1955) A revised classification of the rodents. *J Mammal* 36:165–187. <https://doi.org/10.2307/1375874>
- Wood AE (1962) The early Tertiary rodents of the family Paramyidae. *Trans Am Philos Soc* 52:3–261
- Wood AE (1976) The paramyid rodent *Ailuravus* from the middle and late Eocene of Europe, and its relationships. *Palaeovertebrata* 7:117–149
- Wood AE (1974) Early Tertiary vertebrate faunas Vieja Group Trans-Pecos Texas : Rodentia, University of Texas at Austin, Austin
- Yao L, Brown JP, Stapanoni M et al (2012) Evolutionary change in the brain size of bats. *Brain Behav Evol* 80:15–25. <https://doi.org/10.1159/000338324>

Chapter 17

Paleoneurology of Carnivora



George A. Lyras, Alexandra A. E. van der Geer, and Lars Werdelin

Institutional Abbreviations

AMNH American Museum of Natural History, New York, USA
FAM Frick collection, American Museum
FMNH Field Museum of Natural History, Chicago, USA
MNHN Muséum National d'Histoire Naturelle, Paris, France

17.1 Systematic and Phylogenetic Context

The order Carnivora (whose members are here denoted carnivorans) is one of the most species-rich mammalian groups of the modern world. Although there is no consensus regarding the number of extant species, it can be estimated at more than 280, to which can be added well over 1000 known fossil species. Confusingly, not all members of the Carnivora are carnivores (i.e. animals that require substantial amounts of animal protein in their diet), nor are all carnivores members of the Carnivora. Among extant species of Carnivora, several, e.g. the giant panda, feed

G. A. Lyras (✉)

Department of Geology and Geoenvironment, National and Kapodistrian University of Athens, Athens, Greece

e-mail: glyras@geol.uoa.gr

A. A. E. van der Geer

Vertebrate Evolution, Development and Ecology, Naturalis Biodiversity Center, Leiden, The Netherlands

e-mail: alexandra.vandergeer@naturalis.nl

L. Werdelin

Department of Palaeobiology, Swedish Museum of Natural History, Stockholm, Sweden

e-mail: lars.werdelin@nrm.se

nearly exclusively on plant matter, and conversely, there are groups of animals, such as the marsupial *Sarcophilus*, that are as carnivorous as any extant carnivoran. Among fossil groups, one in particular is of importance, the order Hyaenodonta (sometimes united with Oxyaenida into the order Creodonta). Herein, we focus exclusively on Carnivora, the endocrania of which are by far the better known in the fossil record.

Carnivora originated in the early Paleocene, ca 65 million years ago. They diversified rapidly and spread across the Northern Hemisphere in the late Paleocene and early Eocene, with a long stem lineage that included widespread taxa such as *Viverravus* and *Vulpavus*, as well as the sister-taxon to all living carnivorans, *Quercygale* (Wesley-Hunt and Werdelin 2005; Spaulding and Flynn 2012; but see Tomiya et al. 2021). These early forms are all small, and larger-sized carnivorans did not appear until the mid-early Eocene with the common ancestor of all extant carnivorans (Carnivora *sensu stricto*). This coincided with a separation of Carnivora into two major groups, the Caniformia (canids, mustelids, ursids, ailurids, procyonids, mephitids, amphicyonids, odobenids, otariids, phocids) and the Feliformia (felids, hyaenids, percrocotids, herpestids, euplerids, prionodontids, viverrids, nandiniids, nimravids, barbourfelids). These two groups have had distinct evolutionary trajectories, with Caniformia being less carnivorous and primarily distributed in North America and Feliformia more carnivorous and primarily distributed in Eurasia. It was not until the late Miocene that carnivoran faunas were fully homogenized with the dispersal of canids into Eurasia. Therefore, during the majority of their evolutionary history, Carnivora in North America and Eurasia existed in very different competitive regimes, a circumstance that must have been important to the evolution of their cognitive systems. In addition, carnivorans were in competition with the Hyaenodonta during the first 40 million years of the Cenozoic, which also would have influenced the evolution of their cognitive systems in ways that have yet to be explored.

Similar considerations apply to the relationship between carnivorans and their prey. This would have been affected by bottom-up forces originating with climate change, especially the global cooling following the early Eocene climatic optimum some 52 million years ago and the formation of permanent Antarctic ice sheets at the end of the Eocene (Wright 2009). Climate change would have affected vegetation and habitats and these in turn the composition of the herbivore communities, which may have been the driver of the gradually increasing brain complexity and cognitive abilities of carnivorans during the Paleocene to late Miocene (see below).

17.2 Historical Background

The earliest detailed descriptions of endocranial casts of fossil carnivorans are those by the French naturalist Paul Gervais of the Miocene nimravid ('false saber-toothed cat') *Sansanosmilus*, attributed to *Pseudaelurus quadridentatus* (but see Radinsky 1975a), and a *Canis* from a Neolithic cave site, both from France (Gervais 1870). A

few years later, Gervais (1872) described an endocast of the amphicyonid *Cynelos rugosidens* (as *Cephalogale geoffroyi*) from the early Miocene of Saint-Gérard-le-Puy (France). Since then several authors have provided detailed descriptions of endocasts of fossil carnivorans. Roy Moodie, one of the founders of paleopathology, described a natural endocast of the Oligocene nimravid *Hoplophoneus* from the Badlands of South Dakota, USA (Moodie 1922). In the same paper, he also described artificial endocasts of two Pleistocene species, the dire wolf (*Canis dirus*) (Fig. 17.1a) and the saber-toothed cat *Smilodon fatalis*, from the tar pits of Rancho la Brea in Los Angeles. John Merriam and Chester Stock (1932) also described an endocast of *Smilodon fatalis*, as well as two endocasts of the American lion (*Panthera atrox*). Jean Piveteau (1931, 1950, 1951, 1961, 1962) described endocasts of early fossil carnivorans from France, including *Eusmilus* (1931), *Plesictis* (1950, 1951), *Potamotherium* (1950, 1951), *Pachycynodon* (1951), *Herpestes* (1961), *Cynelos* (1961) and *Quercygale* (1962). Piveteau (1961) also wrote an overview, where he described carnivoran brain evolution as a series of evolutionary ‘steps’ using several figures of endocasts. Jury Orlov (1948) described the brain of *Eomellivora ursogulo* and Robert Savage (1957) described the brain of *Potamotherium*. Edward Mitchell and Richard Tedford (1973) described natural endocasts of the basal pinniped *Pinnarctidion bishopi* from California (as *Enaliarctos*). Later, Charles Repenning and Tedford (1977) depicted a partly exposed natural endocast of the otariid *Thalassoleon macnallyae*. Czyżewska (1981a, b) studied the carnivorans from the early Pliocene site Węże, near Działoszyń in Poland, and described natural endocasts of a mustelid and a canid. The latter was re-described as *Nyctereutes* by Ivanoff et al. (2014). Mödden and Wolsan (2000) described endocasts of the early procyonid *Bavarictis* and compared it to endocasts of other early carnivorans. Lyras and van der Geer (2003) and Lyras (2009) described the external brain morphology of canids from a phylogenetic point of view. Iurino et al. (2015) and Lyras et al. (2019) described endocasts of fossil felids. Apart from these works, there are several studies that provide comments or brief descriptions of endocranial casts from fossil carnivorans. A comprehensive summary of the earlier literature is provided by Edinger (1977).

The scientist who most extensively studied the brain anatomy of fossil carnivorans is undoubtedly the American paleontologist Leonard Radinsky. He applied an improved non-destructive technique to make endocranial casts with latex rubber (Radinsky 1968a; Murril and Wallace 1971). Skulls that had their braincase filled with relatively soft sediments were cleaned either directly through the foramen magnum or through a small window opened for this purpose in the walls of the braincase (Fig. 17.1b). When the braincase was filled with hard sediment, he chipped away part of the braincase wall to reveal a natural endocast (Fig. 17.1d). Using phylogenetic data from other works, he reconstructed the evolutionary history of the brain in several carnivoran groups, including otters (Radinsky 1968b), canids (Radinsky 1969, 1973a), felids (Radinsky 1969, 1975a) and amphicyonids (Radinsky 1980). He also analysed the comparative neuroanatomy of living groups, including mustelids and mephitids (Radinsky 1973b) and viverrids (Radinsky

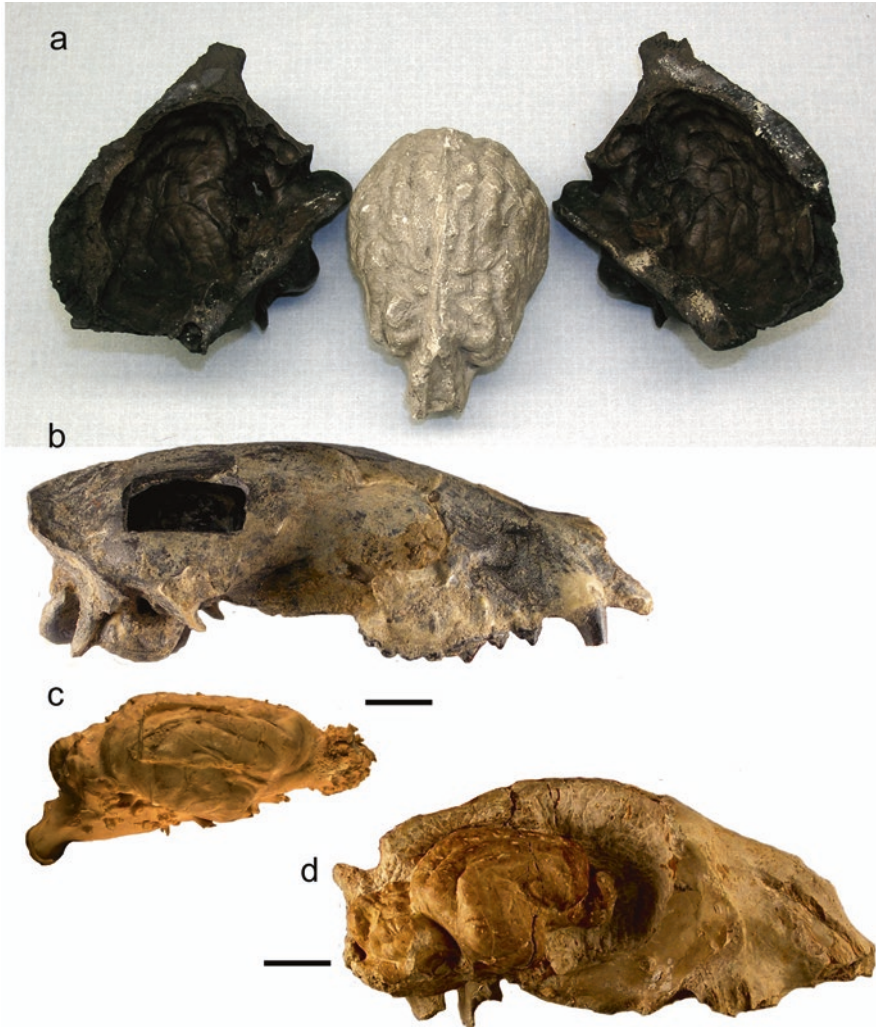


Fig. 17.1 Types of endocasts. (a) Plaster endocast of *Canis dirus* (FMNH PM 394) used by Moodie (1922). The brain case was split in two halves that were used as a mould for building the plaster brain cast. (b) Skull of *Paracynarctus sinclairi* (FAM 61009) with a small window opened for cleaning the sediment in the braincase. (c) Latex endocast of *Paracynarctus sinclairi* (FMNH PM 58973) made by Radinsky (1973a) from FAM 61009. (d) Skull of *Hoplophoneus* sp. (AMNH 460) whose braincase wall has been partly chipped away to reveal a natural endocast. Scale bar 1 cm

1975b). He further developed museum kits with endocasts of fossil carnivores (Radinsky 1978b, c).

More recently, the endocranial morphology of fossil carnivores has been studied using computed tomography (CT) technology (García et al. [2006, 2007] and

Koufos et al. [2017] on ursine bears; Dong [2008] on the oldest giant panda *Ailuropoda microta*; Vinuesa et al. [2015a, b] and Petrovič et al. [2018] on hyaenids; Dong et al. [2007] and Cuff et al. [2016] on felids; Geraads and Spassov [2016] on mephitids; Paterson et al. [2020] on mustelids, Moscarella et al. [2020] on canids), providing detailed insight into the brain anatomy of these taxa without the need for a physical endocast.

17.3 Overview of General and Comparative Anatomy

17.3.1 Characterization of Cranial Endocast Morphology of Living Taxa

In lateral aspect the cerebrum of all living carnivorans consists of convolutions arranged in concentric arcs around the Sylvian sulcus and progressively increasing in length (Fig. 17.2). In dorsal aspect, the lateral gyrus abuts the longitudinal fissure. Anteriorly it is continuous with the sigmoid gyrus, a convolution that surrounds the cruciate sulcus. The cruciate sulcus is a distinctive carnivoran feature. Nearly all extant carnivoran genera display such a sulcus. Exceptions to this are most viverrids, the Asiatic linsang *Prionodon* and the African palm civet *Nandinia* (Radinsky 1975b).

The exact shape and extent of individual gyri differ among taxa. For example, Fig. 17.3 demonstrates the differences in the ectosylvian, coronal and sigmoid gyri among various living taxa.

The domestic dog and cat have served as experimental models in neuroscience for centuries. Consequently, there is a large body of literature on various aspects of their neuroanatomy. The literature on wild taxa, on the other hand, is mostly limited to their external brain anatomy. Differences in cortical folding patterns distinguish various families of extant carnivorans (e.g. Gervais 1870; Krueg 1880; Mivart 1885; Klatt 1928; Smith 1933; Davis 1964; Pilleri 1960, Thiede 1966; Atkins 1970; England 1973; Radinsky 1973a, b, 1975a, b; Kamiya and Pirlot 1988; Lyras and van der Geer 2003; Sienkiewicz et al. 2019). The most important features of the external brain anatomy of living carnivorans are briefly described below.

Felidae The brains of living felids are strikingly similar to each other in their external morphology. The cerebrum is rather spherical with a well-developed temporal region. The Sylvian sulcus extends caudad. In most species the ectosylvian sulcus is interrupted dorsally and thus is divided into an anterior and a posterior limb (Fig. 17.2a). The coronal sulcus is located rather anteriorly. The overall shape of their brain is the same across most members of the family, although most lynx species (*Lynx*) and to a lesser degree the cheetah (*Acinonyx*), have relatively more globose brains than other felids (Radinsky 1975a). The two most apparent differences among living felid species are the degree of gyrification of the cerebral cortex and the protrusion of the olfactory bulbs. Both features are size-related. Although large-

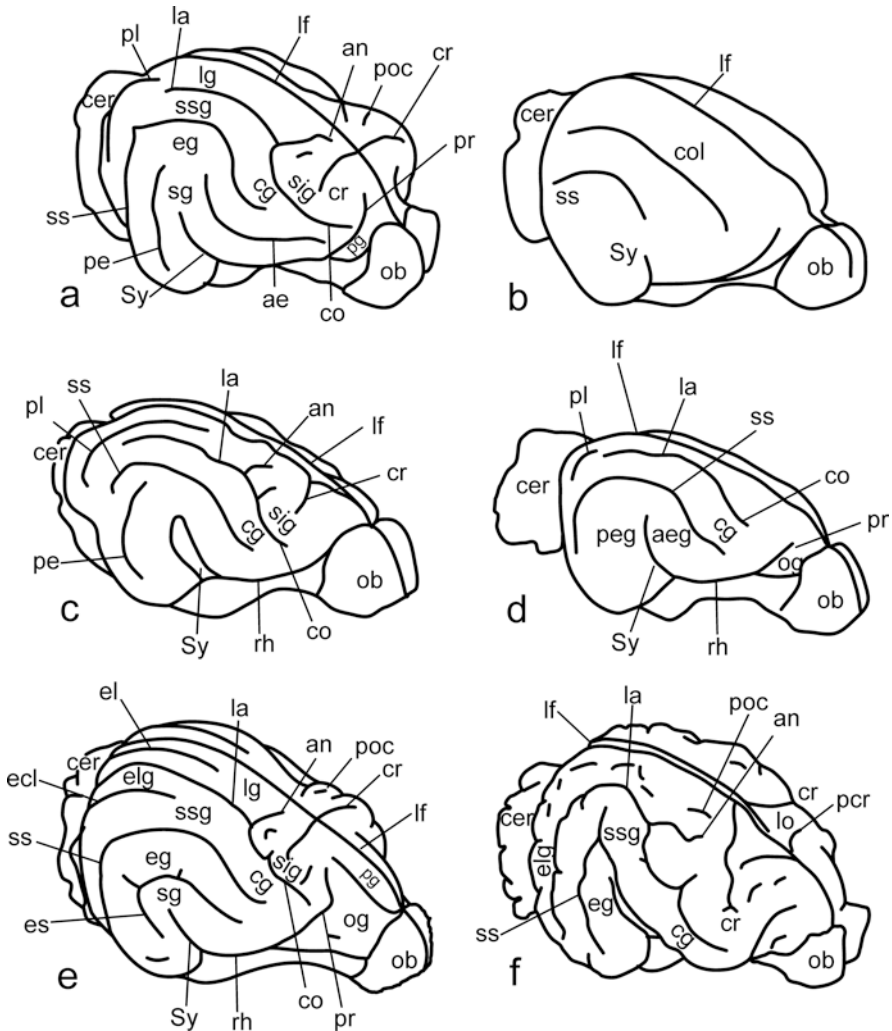


Fig. 17.2 Endocrasts of modern carnivores to illustrate the sulcal and gyral terminology used in this work. **(a)** *Leopardus*, **(b)** *Prionodon*, **(c)** *Herpestes*, **(d)** *Genetta*, **(e)** *Canis*, **(f)** *Tremarctos*. Abbreviations: *ae* anterior ectosylvian sulcus, *aeg* anterior ectosylvian gyrus, *an* ansate sulcus, *cer* cerebellum, *cg* coronal gyrus, *co* coronal sulcus, *col* coronolateral sulcus, *cr* cruciate sulcus, *ecl* ectolateral sulcus, *eg* ectosylvian gyrus, *el* endolateral sulcus, *elg* ectolateral gyrus, *es* ectosylvian sulcus, *la* lateral sulcus, *lf* longitudinal fissure, *lg* lateral gyrus, *lo* ursine lozenge area, *ob* olfactory bulb, *og* orbital gyrus, *pe* posterior ectosylvian sulcus, *peg* posterior ectosylvian gyrus, *pg* prorean gyrus, *poc* postcruciate sulcus, *pr* presylvian sulcus, *prc* precruciate sulcus, *rh* rhinal fissure, *sg* sylvian gyrus, *ss* suprasylvian sulcus, *ssg* suprasylvian gyrus, *Sy* Sylvian sulcus. Note that the Sylvian sulcus is also called the pseudosylvian fissure. **(a)** has been redrawn from Radinsky (1975a), **(c)** and **(d)** from Radinsky (1977), **(e)** from Lyras (2009) and **(f)** from Radinsky (1971). All endocrasts are depicted with the same anteroposterior length

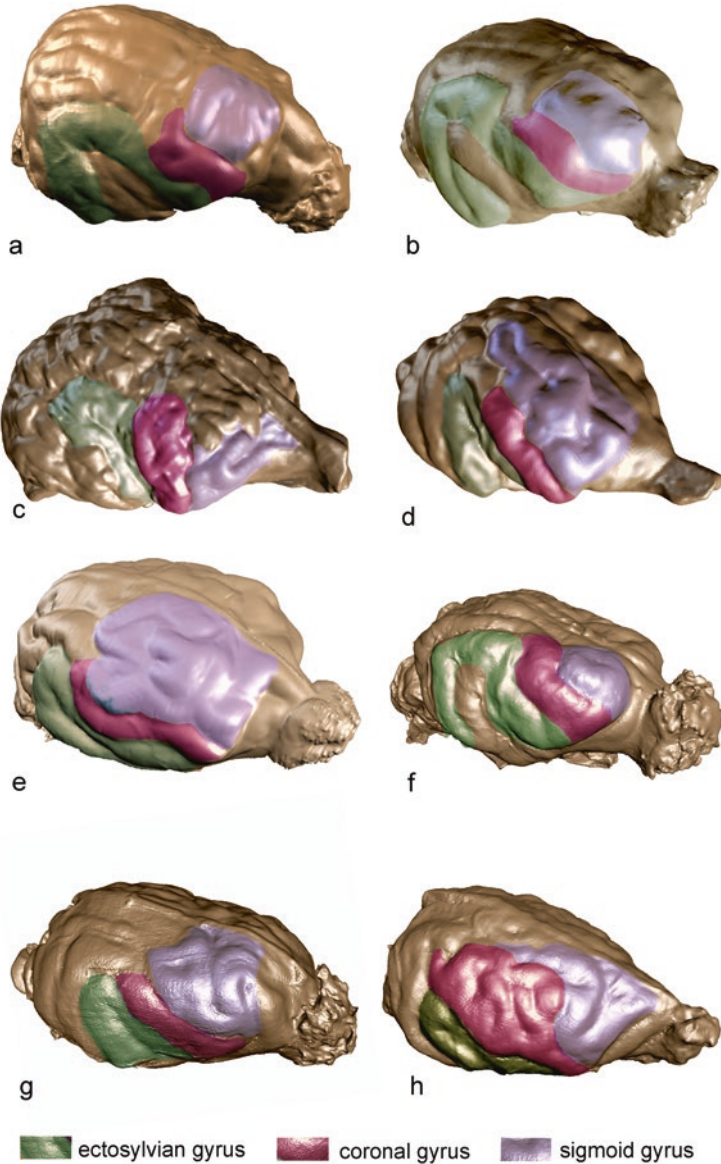


Fig. 17.3 Anterodorsolateral view of endocranial casts of modern carnivores. Different colors mark the extent of the ectosylvian, coronal and sigmoid gyri. (a) *Cuon alpinus* (FMNH 146298); (b) *Neofelis nebulosa* (FMNH 146480); (c) *Otaria flavescens* (MNHN); (d) *Ailuropoda melanoleuca* (MNHN); (e) *Procyon lotor* (FMNH 147619); (f) *Hyaena hyaena* (FMNH 31122); (g) *Martes pennanti* (FMNH 81486); (h) *Lutra lutra* (FMNH 75863). All endocrasts are depicted with the same anteroposterior length

sized species show similar sulcal patterns to small-sized species, they exhibit a higher level of gyrification, with numerous additional small gyri separated by small sulci, spurs, and dimples (Welker 1990). Small-sized species also have less projecting olfactory bulbs (Radinsky 1975a) and their brains tend to be somewhat more spherical (Radinsky 1978c). Despite this uniformity, there are some differences. According to Radinsky (1975a), the predominant condition among the smaller species is that the posterolateral sulcus is continuous with the lateral sulcus, while in the larger felids, it usually overlaps the lateral sulcus medially, and divides the lateral gyrus for a variable part of its length. The ectosylvian sulcus is divided into an anterior and a posterior limb, although according to Sakai et al. (2016) a single-arched ectosylvian sulcus is variably present in lions (*Panthera leo*) and cougars (*Puma concolor*). The cheetah (*Acinonyx jubatus*) lacks a postcruciate sulcus.

Prionodontidae This family is represented today by the single genus *Prionodon*. The external brain anatomy of the spotted linsang (*Prionodon pardicolor*) was described by Radinsky (1975b). Its brain has two major sulci, the coronolateral and suprasylvian (Fig. 17.2b). It also has a small presylvian sulcus and a small Sylvian sulcus. Its cerebellum is widely exposed. *Prionodon pardicolor* is one of the few living carnivorans that lack a cruciate sulcus, a trait that is shared only with viverrids (see below).

Viverridae The external brain anatomy of viverrids was described by Radinsky (1975b). Many viverrid species lack a cruciate sulcus (Fig. 17.2d). This sulcus, if present, tends to extend in an anterolateral direction across the dorsal surface of the cerebrum. Most genets (*Genetta*) are examples of species without a cruciate sulcus. Here, the coronal sulci diverge rostrally with incipient ansate or postcruciate sulci between them. Some *Genetta* specimens show what appears to be an incipient development of a second sulcus, presumably a posterior ectosylvian sulcus, caudal to the Sylvian sulcus. A short cruciate sulcus is present in the aquatic genet (*Genetta piscivora*) despite the fact that its coronal sulcus is less laterally divergent than in other *Genetta* species. *Arctictis binturong* has two major sulci, the coronolateral and the suprasylvian. The cruciate sulcus is absent.

Nandiniidae The brain of the African palm civet, *Nandinia binotata* (Nandiniidae) has been briefly described by Carlsson (1900) and Radinsky (1975b). Its brain is similar to that of *Arctictis* (see above). It differs from the latter in that the coronal sulci do not bow out laterally (Radinsky 1975b).

Hyaenidae The cerebrum of living hyaenids is ovate in shape. The temporal lobe is not as expanded as it is in felids. The Sylvian gyrus consists of only a posterior arm and the ectosylvian gyrus is arcuate to quadrate shape. The lateral gyrus is narrow. In the aardwolf (*Proteles*) the ventral extension of the temporal lobe is limited, thus leaving a larger portion of the pyriform lobe exposed. The cruciate sulcus of the aardwolf is short. In *Hyaena* and *Crocuta* the cruciate sulcus is much wider (England 1973).

Herpestidae The brain of mongooses is characterized by the presence of a cruciate sulcus, a short Sylvian sulcus and a short or no presylvian sulcus (Carlsson 1911). The orbital gyrus is missing in most species (Radinsky 1975b). The Sylvian sulcus ranges from moderately open in most genera to practically closed in *Bdeogale*. A short presylvian sulcus is present in *Bdeogale*, *Ichneumia*, *Cynictis*, *Paracynictis* and some *Atilax*. The posterolateral sulcus overlaps the lateral sulcus medially in most mongooses, which Radinsky (1975b) considered suggestive of a visual specialization. The postlateral sulcus often extends rostrally as an entolateral sulcus. The mongooses with the largest brains (e.g. *Atilax*, *Herpestes urva*) also have the most complex sulcal pattern with an ansate sulcus, a postcruciate sulcus and a third sulcus extending medially from the coronal sulcus between the postcruciate and cruciate sulci (Radinsky 1975b).

Eupleridae Radinsky (1975b) described the brain of Malagasy euplerids in much detail. The brain of the fossa (*Cryptoprocta ferox*) has a short, well-developed cruciate sulcus, shared with most carnivorans but not with viverrids, the family to which they were originally attributed. It further has a short presylvian sulcus, an open Sylvian sulcus and a posterior ectosylvian sulcus. The posterior cerebellar vermis is twisted. The brain of the falanouc (*Eupleres*) has an enlarged orbital gyrus with a depression in its anteroventral part. The presylvian sulcus is branched at its medial end and, unlike in other carnivorans, it is not connected to the anterior rhinal fissure at the lateral end. Variably developed secondary sulci are present in the expanded cortex medial to the coronal sulci. A shallow depression, isolated dimples or a short transverse sulcus are found instead of a cruciate sulcus. The brain has an open Sylvian sulcus and lacks a posterior ectosylvian sulcus. The posterior cerebellar vermis is straight.

Canidae Brains of living canids differ from those of living felids in having an ectolateral sulcus, a complete rather than divided ectosylvian sulcus, a relatively wider and more dorsally expanded prorean gyrus (Fig. 17.2e), a more overlapped cerebellum, and differently shaped olfactory bulbs (Radinsky 1969, 1973a). In living canids, the neocortical expansion is most marked in the frontal region, with the anterior and posterior sigmoid gyri bulging out around the cruciate sulcus and the prorean gyrus (Radinsky 1969). Lyras and van der Geer (2003) elaborated on these two features and noted the different sulcal patterns formed on the cortex medial to the coronal sulci and the shape and relative size of the prorean gyrus.

Procyonidae The overall shape of the cerebrum varies between genera. There is no ectolateral gyrus and the Sylvian gyrus is not visible on the external cerebrum surface. In *Procyon lotor* the sigmoid gyrus, and in particular the posterior arm of this gyrus, is greatly expanded (Welker and Seidenstein 1959). In other procyonids the sigmoid gyrus is moderately broad (Welker and Campos 1963; Welker et al. 1964).

Ailuridae The family is represented today by the single species, the red panda (*Ailurus fulgens*). Its brain is subspherical in overall shape. The Sylvian sulcus forms an inverted U and subdivides the posterior arm of the ectosylvian gyrus (England 1973). The posterior sigmoid gyrus is broad and subdivided by subfissures; it does not, however, reach the width and fissuration seen in *Procyon* (Welker and Campos 1963).

Mustelidae In most mustelids only three arcuate gyri are present (England 1973). The Sylvian gyrus is always lacking, and in most species the ectolateral gyrus is lacking as well. In a few extant mustelid species (such as *Eira barbara*, *Galictis vittatus*, *Martes flavigula*) an ectolateral gyrus is present (Radinsky 1973b, 1980). The otters have expanded coronal and posterior sigmoid gyri. *Lutra* and *Pteronura* have an enlarged coronal gyrus with secondary sulci within it. *Amblonyx*, *Aonyx* and *Enhydra* have a moderate elaboration of the coronal gyrus but in addition to this, there is a major cortical expansion of the lateral part of the posterior sigmoid gyrus (Radinsky 1968b).

Mephitidae *Mephitis*, *Mydaus*, *Conepatus* and *Spinogale* have a relatively unexpanded neocortex, particularly in the region of the temporal and occipital lobes (Thiede 1966; Radinsky 1973b). The rhinal fissure is high, the Sylvian sulcus is short and suprasylvian and lateral sulci are only slightly arched (Radinsky 1973b; England 1973).

Ursidae The brain of living bears has been described by several authors (e.g. Krueg 1880; Klatt 1928; Smith 1933; Davis 1964; Kamiya and Pirlot 1988; Sienkiewicz et al. 2019). The cerebrum of modern bears is highly convoluted, with the major sulci frequently divided by secondary sulci (Fig. 17.2f). The ectosylvian gyrus covers the complete Sylvian gyrus and consequently only two arcuate gyri are seen on the surface of the cerebral hemispheres: the ectosylvian and the suprasylvian. The ectolateral gyrus is positioned as a vertical convolution. The sigmoid gyrus is rather broad and there is a well-developed postcruciate sulcus. Anterior to the cruciate sulcus there is a precruciate sulcus. The area between the cruciate and the precruciate sulcus is known as the lozenge area. Due to the great development of the sigmoid gyri, the coronal sulcus is displaced downwards.

Pinnipedia The brain surface of extant pinnipeds is highly convoluted. Their cerebrum appears complex due to extensive subfissuring. Gyrals and sulcal maps of living pinnipeds have been published by several authors including England (1973), Sawyer et al. (2016) and Turner et al. (2017). The Sylvian gyrus is buried within the pseudosylvian fossa. The posterior arm of the ectosylvian gyrus is broader than its anterior arm. The coronal sulcus is nearly perpendicular to the ventral border of the brain. The sigmoid gyri are located extremely rostrally and the prorean gyrus is ventrad in most species. In earless, or true, seals (Phocidae) the coronal sulcus is situated far caudally and lies close to the Sylvian sulcus. According to England (1973) the coronal sulcus fuses with the median arm of the ectosylvian gyrus. The

lateral gyrus is subdivided by one or two longitudinal fissures. In the elephant seal (*Mirounga angustirostris*) the endolateral sulcus runs close to the primary fissure of the cerebellum. The walruses (*Odobenus*, Odobenidae) have rather spherical brains. The exposed anterior arm of the ectosylvian gyrus is very narrow, whereas its posterior arm is, on the contrary, very wide. The coronal gyrus contains a number of small sulci. The brain of eared seals (Otariidae) is wedged-shaped with a rounded posterior end of the cerebrum. The coronal gyrus overlies a larger part of the anterior part of the ectosylvian gyrus. The suprasylvian is oriented almost vertically.

17.3.2 Sensory Evolution

During the evolutionary history of mammals, the cortical areas of the brain evolved local elaboration, diversification and better separation, in association with the development of specialized functions, as suggested by Uylings and van Eden (1990). Comparative studies on extant mammals indicate that the cortex has fewer subdivisions in small-brained mammals with little neocortex. Based on this observation, Molnár et al. (2014) hypothesized that the neocortex of early mammals should have had a simpler organization as well. Fossils of early carnivorans display a small cerebral cortex with limited gyrification (see Sect. 17.4), confirming the idea that the early forms had a simpler cortical organization. During the evolutionary history of carnivorans a trend towards increasing cortical size and gyrification can be observed (Lyras et al. 2016), leading to the complex cortical organization seen in the living carnivoran species.

The extant raccoon (*Procyon lotor*) has an enormously enlarged cortical forepaw projection lobule. Its five hand digits are represented on the cerebral cortex on distinct, separate gyri, with sulci and fissures separating the cortical representation of each digit individually. The coatimundi (*Nasua narica*) has a relatively large somatosensory representation of the contralateral rhinarium on the crown of the coronal gyrus (Welker and Seidenstein 1959; Welker and Campos 1963). The kinkajou (*Potos*) and the ring-tailed cat (*Bassaricyon*) seem to lack such somatosensory specializations or obvious correlations between external brain morphology and behavior.

The external brain anatomy of otters was studied by Radinsky (1968b). The coronal gyrus is enlarged in all otter genera relative to that of terrestrial mustelids. In addition, a major expansion of the lateral part of the posterior sigmoid gyrus on the cortex is present in the small-clawed otter (*Amblonyx*), the clawless otter (*Aonyx*) and the sea otter (*Enhydra*). To our knowledge, no electrophysiological mapping studies exist for otters. However, electrophysiological mapping of the coronal gyrus in canids, felids and procyonids (Woolsey 1958; Welker and Seidenstein 1959; Welker and Campos 1963; Welker et al. 1964) shows that somatosensory input from the head is received by this cortical region. Similarly, that from the forelimb is received by the posterocruciate gyrus (Woolsey 1958; Welker and Seidenstein 1959; Welker and Campos 1963; Welker et al. 1964). Since an unequal expansion of a

particular region of the neocortex may indicate a specialization of function, Radinsky thus (1968b) concluded that the sulcal patterns of *Lutra* and *Pteronura* are suggestive of highly developed receptor fields on the head, whereas those of *Amblonyx*, *Aonyx* and *Enhydra* suggest greatly increased forelimb sensitivity, in addition to mildly increased head sensitivity. The unequal expansion of the somatosensory regions of the coronal gyrus may be explained by a similar expansion of the number of nerves innervating tactile hairs (vibrissae), or whiskers, as proposed by Marshall et al. (2014). Living pinnipeds have distinctive mystacial vibrissae, which they use to explore their environment. Hydrodynamic trail following has only been shown in the harbour seal (*Phoca vitulina*) and sea lion (*Zalophus californianus*) (Wieskotten et al. 2010; Gläser et al. 2011). Sea lions and seals have been shown to be able use their whiskers to differentiate objects by their size and shape, and to perform complex sensorimotor tasks (Dehnhardt et al. 1998; Wieskotten et al. 2011; Milne and Grant 2014). Electrophysiological mapping of the cortex of the northern fur seal (*Callorhinus ursinus*) indicated that the projection area of the head occupies the greatest part, and within it, the greatest area is occupied by the region of the superior labial vibrissae (Ladygina et al. 1985). On the same level, the expanded coronal gyrus in some viverrids, specifically Hose's palm civet (*Diplogale hosei*) and the otter civet (*Cynogale bennetti*), is also suggestive of increased facial tactile sensitivity, likely through an elaboration of whiskers (Radinsky 1975b).

17.3.3 Cellular Composition

Jardim-Messeder et al. (2017) analyzed the cellular composition of the brain of eight carnivoran species (ferret, banded mongoose, raccoon, domestic cat, domestic dog, striped hyena, lion, and brown bear). They found that the dog (*Canis familiaris*) and raccoon (*Procyon lotor*) have significantly higher numbers of neurons in their cerebral cortex than the other six carnivoran species studied. They further noted that the brain of the brown bear (*Ursus arctos*), despite being the largest carnivoran brain in their sample, had far fewer cortical neurons than expected: about as many as the cat and almost 50% fewer than the raccoon. On the other hand, carnivorans have the same relationship between the number of non-neuronal cells and brain mass as other mammals do.

Jardim-Messeder et al. (2017) also found that with increasing absolute brain size, the thickness of the cerebral cortex of carnivorans increases slower than cortical surface area. In this respect also, the brown bear is a clear outlier, with a cortex that is too thin for its surface area when following the general trendline for carnivorans.

17.4 Brain Evolution and Paleobiological Inferences Based on Endocast Morphology

17.4.1 Morphological Brain Diversity Through Time

Most living carnivorans share the same general pattern of neocortical convolutions, in particular a pattern of arcuate folds arranged concentrically around the Sylvian sulcus and a sigmoid gyrus wrapped around the cruciate sulcus (Fig. 17.3). This pattern evolved independently multiple times during the evolutionary history of carnivorans (Radinsky 1971). This parallel evolution in unrelated carnivoran lineages is probably best explained by constraints on folding patterns inherent to the ancestral pattern of thalamocortical connections, as present in the Eocene common ancestor of extant carnivorans (Radinsky 1980).

Eocene Carnivorans

The ancestors of the extant carnivorans are found among archaic, fox-sized members of early carnivorans. The endocasts from three species of primitive carnivorans (Carnivoramorpha), ranging from Paleocene to Eocene, show a progressive cortical expansion. The earliest is *Viverravus politus* from the Late Paleocene of Wyoming (USA) (described as *Didymictis* by Radinsky 1977). *Viverravus politus* has a widely exposed midbrain, which indicates a low degree of cortical expansion. The second is *Vulpavus palustris* (Fig. 17.4a) from the Eocene of Wyoming (USA). The cerebral cortex of this species is more expanded than that of *Viverravus*. The posterior lobe of the cerebrum overlaps the midbrain, but leaves the cerebellum completely uncovered. The rhinal sulcus is high and there are two short cortical folds: the coronolateral, which runs almost parallel to the longitudinal fissure, and the suprasylvian, which forms a wide vertical arch on the lateral side of the brain. The third endocast is *Quercygale angustidens* from the Late Eocene of Quercy (France). The specimen has been described as *Viverravus*, *Humbertia* and *Procynodictis* (by Piveteau 1962; Radinsky 1976, 1977, respectively). Increased expansion of the neocortex relative to the condition seen in *Vulpavus* is indicated by a greater area of contact between the cerebrum and the cerebellum, lengthening and arching of the two sulci, mainly the coronolateral, expansion of the cortex in the temporal region and expansion of the frontal pole up to the olfactory bulbs. The advanced brain of *Quercygale* is consistent with its hypothesized phylogenetic position. According to Wesley-Hunt and Werdelin (2005) and Spaulding and Flynn (2012) (but see Tomiya et al. 2021) *Quercygale* is the most derived of the stem group 'Miacidae' and the sister taxon to Nimravidae and crown-group Carnivora.

The earliest known endocasts of crown-group Carnivora are two partially exposed natural endocasts from the late Eocene of Texas (USA). The first belongs to *Prohesperocyon wilsoni*, which is considered to be the most primitive stem canid (Wang 1994). The rhinal sulcus is much lower than in *Vulpavus* and there are two

cortical folds, the coronolateral and the suprasylvian, which are much longer than those of *Vulpavus*. The overlap of the cerebellum by the cerebrum is small, leaving almost the entire vermis exposed. The second belongs to *Gustafsonia cognita*, a basal member of Amphicyonidae (Tomiya and Tseng 2016). This partially exposed natural endocast suggests that its brain was comparable to that of *Prohesperocyon*.

Oligocene Carnivorans

Endocasts from Oligocene canids, amphicyonids, nimravids, ursids and mustelids are known from several localities in North America and Europe.

Canidae The first canid, *Hesperocyon*, appeared in North America during the late Eocene – early Oligocene. The genus gave rise to three main evolutionary clades, the Hesperocyoninae, Borophaginae (both extinct subfamilies), and Caninae, to which all living canids belong. There are several natural endocasts of *Hesperocyon* known from Oligocene localities in the USA. Their anatomy has been described in detail by Scott (1895, 1898), Tilney (1931), Scott and Jepsen (1936), Radinsky (1969, 1971, 1973a) and Lyras (2009). The endocast of *Hesperocyon* (Fig. 17.4b, c) was in many ways similar to that of the late Eocene carnivorans, including *Prohesperocyon*; for example, its cerebral cortex had only two sulci, the coronolateral and the suprasylvian. Its brain is slightly more globular than that of *Prohesperocyon*. The rhinal sulcus is considerably lower than that of *Vulpavus* and the olfactory bulbs are large and not covered by the cerebral hemispheres.

The Oligocene was a critical period for Canidae, a time during which many new forms appeared, and the family reached its maximum species richness. One major lineage of Hesperocyoninae is the *Mesocyon* – *Enhydrocyon* clade. The lineage is characterized by an increasing trend towards hypercarnivory. Endocranial material is known from three genera: *Mesocyon*, *Cynodesmus* and *Enhydrocyon* (described by Radinsky 1973a and Lyras 2009). Their brains have a more expanded cerebral cortex than in *Hesperocyon*. The brain of *Mesocyon* is slightly more advanced than that of *Cynodesmus*. An evolutionary advance over *Hesperocyon* is that *Mesocyon* has a short ectolateral and an ectosylvian sulcus in addition to the coronolateral and suprasylvian sulci (Fig. 17.6i, f). *Cynodesmus* lacks the ectolateral sulcus and instead of the ectosylvian sulcus only a series of variable depressions is present. However, *Cynodesmus* does have a presylvian sulcus. The brain of *Enhydrocyon* has four neocortical sulci (coronolateral, suprasylvian, ectosylvian and presylvian). The most important difference between *Enhydrocyon* and its ancestor (*Cynodesmus*) is that its brain has very high frontal lobes, a feature that is related to its short rostrum (Lyras 2009).

The oldest Borophaginae had brains similar in size, lobation and fissuration to that of *Hesperocyon*. The brain anatomy of early Borophaginae is known for *Otarocyon*, *Archaeocyon* and *Rhizocyon* (described by Radinsky 1973a and Lyras 2009). The differences between *Archaeocyon*, *Rhizocyon* and *Hesperocyon* are small. On the other hand, *Otarocyon* differs by having a neocortex with very small

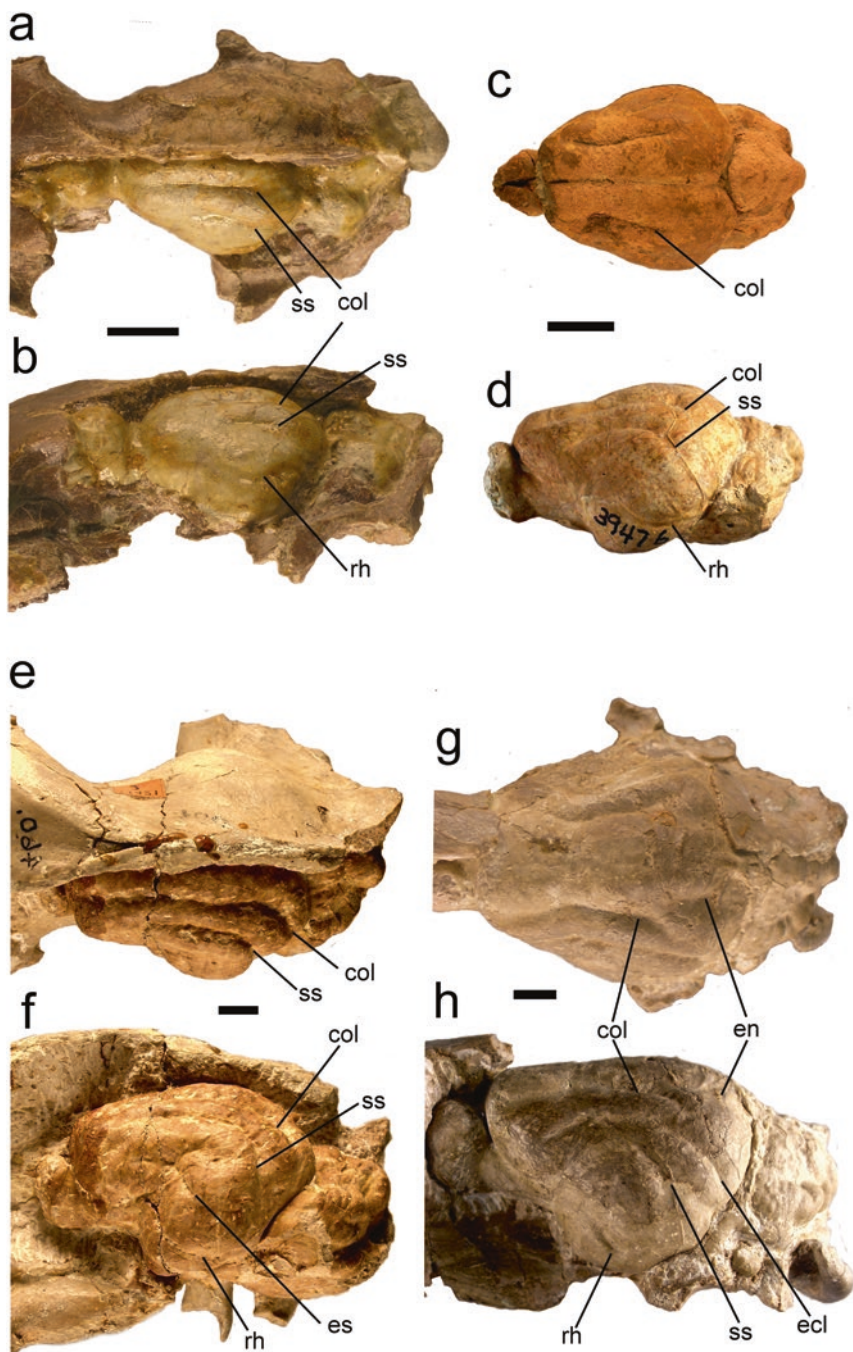


Fig. 17.4 Natural endocasts of Eocene and Oligocene carnivoramorphans. (a) Dorsal and (b) lateral views of *Vulpavus palustris* (AMNH 1900); (c) dorsal view of *Hesperocyon* sp. (AMNH 9766) and (d) lateral view of *Hesperocyon* sp. (AMNH 39476); (e) dorsal and (f) lateral views of *Hoplophoneus* sp. (AMNH 460; mirrored from the right side); (g) dorsal and (h) lateral views of *Daphoenus hartshorianus* (AMNH 9757). Abbreviations for sulcal terminology as in Fig. 17.2. Scale bar 1 cm

expansion: the rhinal sulcus is very high, and the coronolateral and suprasylvian sulci are very short. The simplicity of its brain stands in sharp contrast to its rather derived cranial anatomy (Lyras 2009). The skull of *Otarocyon* has many derived characters and is morphologically similar to the living fennec fox of Africa and Arabia (*Vulpes zerda*) (Wang et al. 1999). Its brain, on the other hand, is not only simpler than that of *V. zerda*, but is the simplest of all borophagines (Lyras 2009).

Amphicyonidae The brains of Oligocene amphicyonids, or bear dogs, are represented by endocasts of *Daphoenus hartshorianus* (Fig. 17.4h), known by several endocasts in the USA (described by Scott and Jepsen 1936 and Radinsky 1980) and *Pseudocyonopsis ambiguus* from the French Quercy Phosphorites (described as *Amphicyon ambiguus* by de Beaumont in 1964). The brain of *Daphoenus* had four neocortical sulci, a relatively straight coronolateral sulcus, a gently arched suprasylvian sulcus, an ectolateral sulcus and a short endolateral (or posterolateral) sulcus. The brain of *Pseudocyonopsis* is slightly more advanced than that of *Daphoenus*. It has a longer entolateral sulcus, a more arched suprasylvian sulcus, a more strongly developed ectosylvian sulcus, a presylvian sulcus and a notch at the junction between the anterior and posterior limbs of the rhinal sulcus.

Nimravidae Some of the most specialized predators of the Late Eocene- Oligocene were the Nimravidae, sometimes referred to as ‘false saber-toothed cats’. Endocasts of Oligocene nimravids (*Hoplophoneus* and *Eusmilus*) have been described by several authors (e.g. Bruce 1883; Moodie 1922; Piveteau 1931; Radinsky 1969, 1971, 1975a, 1978c). In both *Hoplophoneus* and *Eusmilus* the posterior vermis of the cerebellum is straight and the overlap of the cerebellum by the cerebrum is smaller than in living felids. There are only three neocortical sulci: the coronolateral, the suprasylvian and the ectosylvian (Fig. 17.4e, f). The ectosylvian sulcus is more tightly arched in *Eusmilus* than in *Hoplophoneus*. The olfactory bulbs are relatively small in both genera.

Ursidae An endocast of *Phoberogale minor* (Quercy, France) was illustrated by Radinsky (1971; as *Cephalogale minor*). The most notable feature of *Phoberogale* is the presence of a well-developed cruciate sulcus (Fig. 17.5a). In contrast, the canids, nimravids and amphicyonids of the same geological period had not yet evolved a clear cruciate sulcus.

Mustelidae Three early mustelids, *Corumictis wolsani* (described by Paterson et al. 2020), *Mustelictis piveteaui* and *Plesictis branssatensis* (described by Mödden and Wolsan 2000) also have well-developed cruciate sulci (Fig. 17.5d).

Another Oligocene carnivoran of North America is *Palaeogale lagopus*, a weasel-sized carnivoran of unresolved phylogenetic position (*incertae sedis*; Baskin 1998b). Its brain is known from two endocasts, both described by Radinsky (1977). Neocortical expansion is less than that of other Oligocene carnivorans: the rhinal sulcus is higher, there is no angle between the posterior and anterior rhinal sulcus, there is only a short sulcus and the cerebrum only just covers the midbrain.

Early and Middle Miocene Carnivorans

Canidae The last surviving member of the Hesperocyoninae is the genus *Osbornodon*. The brain of *Osbornodon fricki*, the last species, was in terms of external brain anatomy far more derived than that of the Oligocene hesperocyonines. In addition to the sulci seen in the Oligocene *Cynodesmus*, it has a large orbital gyrus, a small Sylvian sulcus, a complete ectosylvian sulcus and a large cruciate depression. The rostral parts of the coronolateral sulci bow out laterally, indicating a separation between the coronal and lateral parts, and the first appearance of the sigmoid gyri (Lyras 2009).

During the Miocene a major diversification of Borophaginae took place. Several endocasts of Miocene Borophagine were described in detail by Radinsky (1973a) and Lyras (2009). Two early Miocene Borophaginae are *Phlaocyon* and *Desmocyon*. The brain of the former has three main sulci (coronolateral, ectolateral and ectosylvian). Additionally, the rostral part of the coronolateral gyrus widens and in the middle of this area an incipient cruciate sulcus is present. Although this is an advanced feature, in this particular case it is unrelated to the cruciate sulcus of the other borophagines. *Desmocyon*, the genus from which all later borophagines evolved, has no indication of a cruciate sulcus. Since later borophagines have a cruciate sulcus, this structure must have evolved independently twice within the subfamily (Lyras 2009). The evolutionary history of later borophagines comprises three major paths, the Cynarctina, Aelurodontina and Borophagina. The latter two show a tendency to increase in body and brain size over time. The evolution of their brain is characterized by the expansion of the occipital and temporal lobes, and of the cortex medial to the coronal sulci (Fig. 17.6). The expansion of the cortex of the occipital lobe is recognized by a larger overlap of the cerebellum, while that of the temporal lobe resulted in an elongation of the Sylvian sulcus. The cortex medial to the coronal sulci expanded by arching out of the coronal sulci, and by the development of the cruciate and postcruciate sulci. The development of the sigmoid gyri took place independently in the two lineages. This area expanded independently several times in carnivoran evolution.

Amphicyonidae Several endocasts of three early Miocene Amphicyonidae species are known: *Adilophontes brachykolos*, *Mammacyon ferocior* (described as *Daphoenodon superbus* and *Temnocyon* by Radinsky 1980) and *Cynelos rugosidens* (described by Gervais 1872; Edinger 1929; Piveteau 1961; de Beaumont 1962, 1964; Radinsky 1980). The brain of *Adilophontes brachykolos* had an incipient Sylvian sulcus and a well-developed ectosylvian sulcus, a relatively long and arched suprasylvian sulcus, a presylvian sulcus and an early stage of the expansion of the sigmoid gyri. The ectolateral sulcus did not contact the suprasylvian sulcus. Furthermore, there is a transversely oriented depression within the sigmoid gyrus, which according to Radinsky (1980) may represent incipient development of the cruciate sulcus. The brain of *Mammacyon ferocior* was morphologically similar to that of *Daphoenodon*. It had a short sulcus, which probably represented the cruciate sulcus. The middle Miocene *Cynelos rugosidens* had a slightly more advanced brain

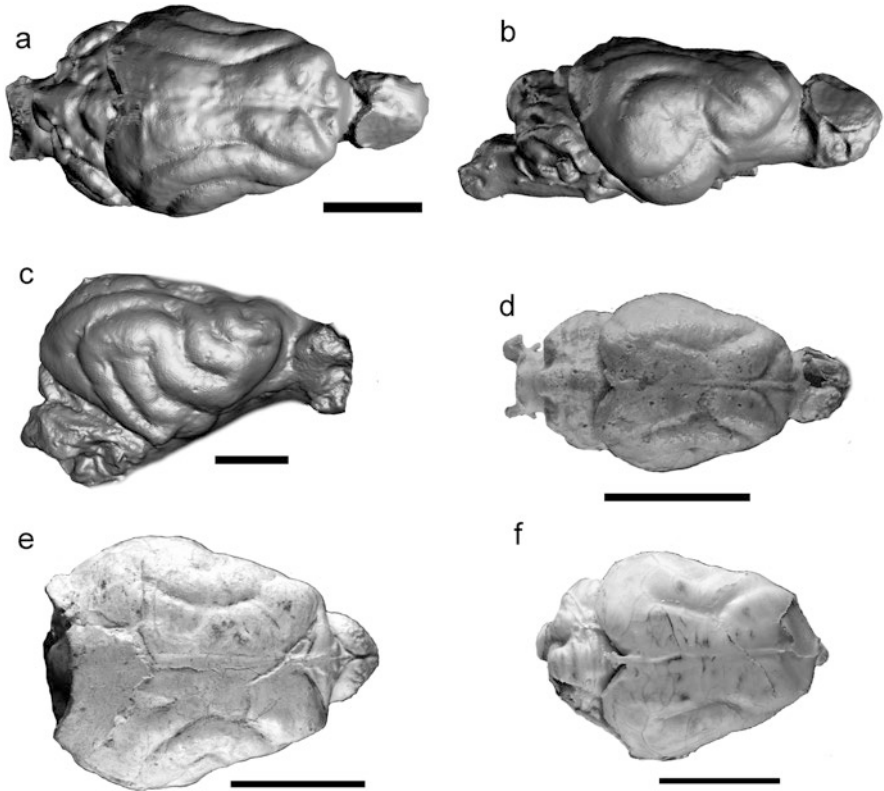


Fig. 17.5 (a) Dorsal and (b) lateral views of *Phoberogale minor* (FMNH PM 59026); (c) lateral view of *Ictitherium viverrinum* (AMNH 20696); (d) dorsal view of *Plesictis branssatensis* (FMNH PM 57182); (e) dorsal view of *Promartes* sp. (FMNH PM 25233); (f) dorsal view of *Probassariscus matthewi* (FMNH PM 57177). Scale bar 2 cm

than *Adilophontes*. It had more expanded sigmoid and orbital gyri (Radinsky 1980). The sigmoid gyrus had variably developed dimples. An endocast from the middle Miocene *Pliocyon medius* from Nebraska (USA) was described by Radinsky (1980). Its brain was further advanced over that of the earlier amphicyonids in having a more expanded frontal lobe, as indicated by the bowed out coronal sulci, the presence of an ansate sulcus and a laterally extending cruciate sulcus.

The typical amphicyonid sulcal pattern consists of a long ectolateral that usually extended to contact the suprasylvian sulcus, a short sulcus between the caudal ends of the ectolateral and suprasylvian sulci, and an ectosylvian sulcus that was an unbroken arch and remained unopercularized on the lateral surface of the brain (Radinsky 1980).

Mustelidae An early mustelid representative is *Promartes*, which is known from the late Oligocene, but its earliest known endocasts date to the early Miocene.

Radinsky (1971) and Mödden and Wolsan (2000) depict such endocasts. The brain of *Promartes* had clearly developed cruciate, postcruciate and Sylvian sulci and a slightly less developed endolateral sulcus. Another Miocene mustelid is the lutrine *Mionictis*. The endocast of a *Mionictis* from the middle Miocene of Texas was described by Radinsky (1968b). Its brain, although more primitive than that of modern otters, already had an expanded coronal gyrus, a feature that is present in all modern otters.

Pinnipedia Natural endocasts of a stem pinnipediform, *Pinnarctidion bishopi* (early Miocene, California, USA), were described under the name *Enaliarctos mealsi* by Mitchell and Tedford (1973). Its brain had a well-formed Sylvian sulcus. The cruciate sulcus and sigmoid gyrus are located extremely rostrally. The most interesting feature of its brain was the large expansion of the coronal gyrus. It is broad, nearly vertically oriented and partly overlapping the anterior arm of the ectosylvian gyrus. Although the *Pinnarctidion* brain was rather convoluted, its gyrification was not as high as in later pinnipeds (Lyras et al. 2016).

Procyonidae During the middle Miocene, procyonids appeared in North America (Baskin 1998a). One of the earlier forms is *Probassariscus*. Although important neuroanatomical features like the cruciate sulci are present in the brain of *Probassariscus*, its sulcal pattern lacks the complexity seen in the living forms (this study, Fig. 17.5f).

Felidae The earliest felids are from the early Oligocene of Europe. Their first representative is *Proailurus lemanensis* (Fig. 17.6m). The brain of these early cats resembles that of living viverrids more than that of living felids. It has a significantly less expanded neocortex, with undeveloped temporal and frontal lobes, and only three main cortical sulci (see descriptions in Radinsky 1975a and Lyras et al. 2019). The brain of the earliest North American felid (an as yet unnamed felid from Ginn Quarry, Nebraska, USA) has many similarities to that of *Proailurus* (Lyras et al. 2019). A later North American felid is the genus *Hyperailurictis* (Fig. 17.6l). Its brain has an even more expanded neocortex, with the rostral part of the coronal sulci diverging laterally, thus creating a wider space for the cortex medial to them (see descriptions in Radinsky 1975a and Lyras et al. 2019). This cortex expansion represents the initial stages of appearance of the cruciate sulcus.

Late Miocene and Plio-Pleistocene Carnivorans

Canidae At the end of the Miocene Borophaginae diversity dropped even further and during the Pliocene *Borophagus* was the only surviving member of the subfamily. The coronal sulci bow out more in *Borophagus* than in earlier borophagines. The late Miocene to Pleistocene was a period of diversification in Caninae. The brain of a late Miocene *Leptocyon* has a more overlapped cerebellum and a more twisted cerebellar vermis than any canid of that time or earlier. Its sulcal pattern is, in

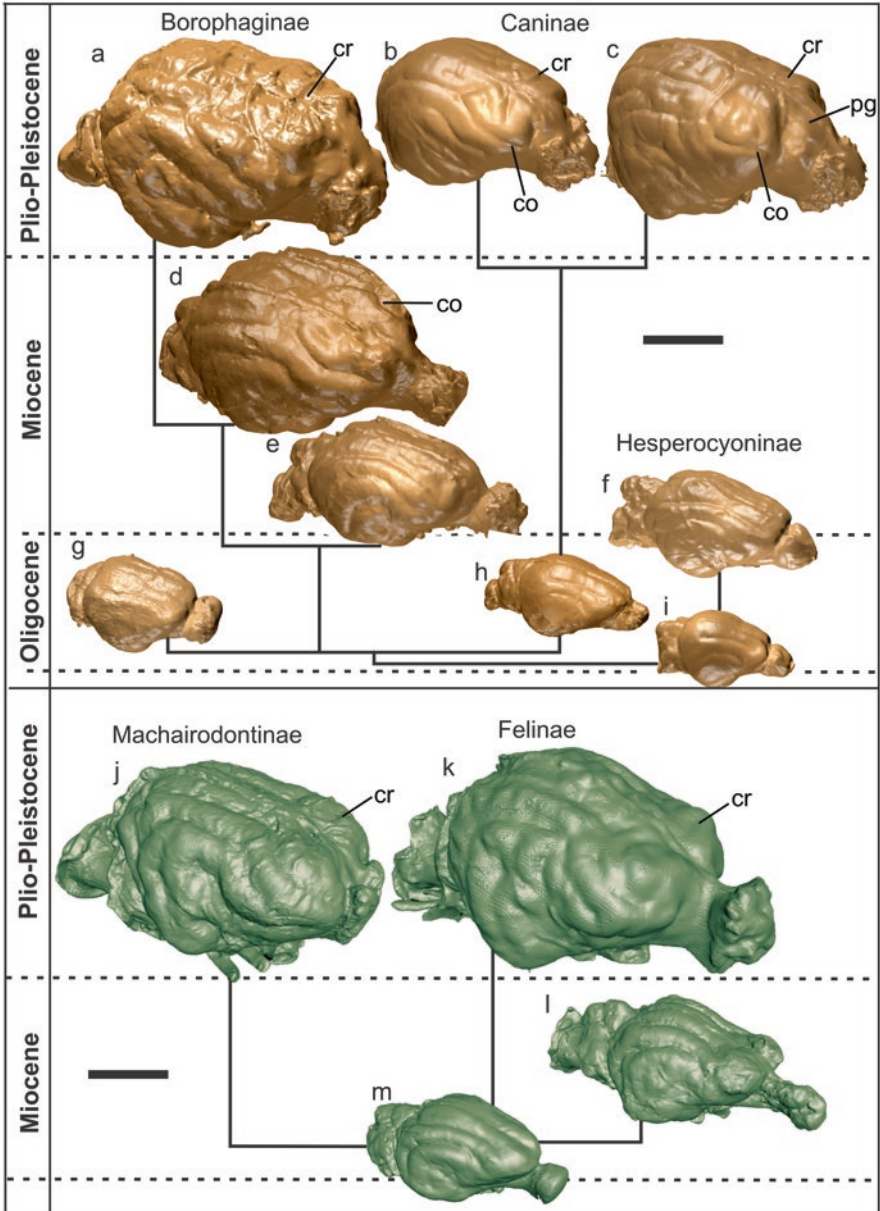


Fig. 17.6 Outline of canid and felid brain evolution. (a) *Borophagus secundus* (FMNH PM 58954); (b) *Vulpes vulpes* (FMNH 67413); (c) *Cuon alpinus* (FMNH 146298); (d) *Carpocyon webbi* (FMNH PM 58964); (e) *Paracynarctus sinclairi* (FMNH PM 58973); (f) *Mesocyon* sp. (FMNH PM 58979); (g) *Otarocyon cooki* (FMNH PM 58987); (h) *Leptocyon gregorii* (FMNH PM 58961); (i) *Hesperocyon gregarius* (FMNH PM 57170); (j) *Smilodon fatalis* (FMNH PM 12140); (k) *Panthera tigris* (FMNH 39459); (l) *Hyperailurictis validus* (FMNH PM 58870); (m) *Proailurus lemanensis* (FMNH PM 58876). Abbreviations for sulcal terminology as in Fig. 17.2. Scale bar 3 cm

general, similar to that of extant Caninae. The most important distinction from later Caninae is the very narrow region medial to the coronal sulci (Lyras 2009). The major diversification of Caninae started during the late Miocene and Pliocene. During this period the evolution of the cerebrum took place mainly in the region medial to the coronal sulci, in the form of different sulcal patterns, and in the region rostral to the presylvian sulcus, in the shape and relative size of the prorean gyrus. One early branch of the Mio-Pliocene Caninae diversification was the fox genus *Vulpes*. Its earliest known species, *Vulpes stenognathus*, has a brain comparable to that of living species of *Vulpes*. In all living *Vulpes* species, the coronal sulci form a pentagonal outline on the dorsal surface of the cerebrum and the prorean gyrus is short. Another outcome of the canid radiation was the dog-like species (Canini). The brain of their earliest representative, *Eucyon davisi*, is more primitive than that of *Canis* and in some respects comparable to that of *Vulpes* (Lyras and van der Geer 2003). The prorean gyrus is bilaterally constricted, but it is shorter than in similar-sized living *Canis*. The cerebral hemispheres of all *Canis*-like species (members of *Canis*, *Cuon*, *Cynotherium*, *Lycaon* and *Xenocyon*) expand abruptly behind the presylvian sulcus. The prorean gyrus is long and bilaterally constricted, more so than in any other canid group (Fig. 17.6c). Additionally, in these species the sigmoid gyri expand very abruptly. This creates an orthogonal or oblong outline of the ansate and coronal sulci on the dorsal surface of the cerebrum. The external brain anatomy of *Cynotherium sardous*, the insular dwarf species of Sardinia-Corsica, is comparable to that of its mainland relative *Xenocyon lycaonoides* (Lyras et al. 2006). Furthermore, despite being on an island, it did not undergo brain size reduction as many insular species do (Lyras 2018).

Amphicyonidae The external brain anatomy of late Miocene amphicyonids is known from endocasts of *Amphicyon*. Its brain had proportionally longer ectosylvian and suprasylvian sulci, which were more tightly arched, and a narrow lateral gyrus than in earlier amphicyonids. The entolateral sulcus was absent. The sigmoid gyrus had variably developed dimples, suggesting incipient subdivisions (Radinsky 1980).

Barbourofelidae *Barbourofelis* came to North America during the late Miocene, as an immigrant from Eurasia. *Barbourofelis*, despite its derived craniodental adaptations, had a brain that was comparable to that of the Oligocene nimravids, from which it may have descended (Wang et al. 2020). Its brain had relatively narrow anterior lobes compared with living felids, and the highest point of the cerebrum is situated more caudally (Radinsky 1975a; Lyras et al. 2019).

Mustelidae *Brachypsalis* is a Miocene mustelid from North America. It is a medium- to large-sized mustelid that is phylogenetically related to *Promartes* (see Baskin 1998b). Although its cerebral cortex is rather convoluted, particularly in comparison to contemporary Borophaginae, it is less convoluted than the brain of living mustelids (Lyras et al. 2016). The brain of the late Miocene mustelid

Eomellivora ursogulo has been described by Orlov (1948 as *Perunium ursogulo*). Its brain had all the main gyri seen in modern terrestrial mustelids.

Felidae The felid brain reached its present configuration during the late Miocene. An endocranial cast of a late Miocene “*Felis*” *attica* (now *Pristifelis*) from China (see description in Radinsky 1975a) already shows the morphology of living, similarly sized felids. Thus, from the late Miocene to the present, the brain of Felinae (modern cats with conical canines) has not undergone much change and there are only a few differences between the brains of Plio-Pleistocene and living species (Radinsky 1975a). A very interesting case is the brain of the Pleistocene saber-toothed cat *Smilodon*. Several *Smilodon* endocasts are known from Rancho La Brea tar pits of California (Radinsky 1975a). *Smilodon* is one of the most specialized carnivorans that ever lived. However, its brain is the least derived of all Pleistocene felids: it has very small cerebral hemispheres and a small overlap of the cerebellum. Its temporal lobe is considerably smaller than that of modern felids and its frontal lobe is compressed rostrally. Interestingly, other saber-toothed felids, like *Homotherium*, had derived brains, comparable to those of living members of the family (Radinsky 1975a).

Hyaenidae The brain of the early, small-sized late Miocene hyena *Ictitherium* (Fig. 17.5c) has the basic arrangement of that of modern hyenas including a well-developed cruciate sulcus. In the late Miocene *Adcrocuta eximia*, one of the earliest bone-cracking hyenas, the cruciate sulcus is situated more anteriorly than in extant bone-cracking hyenas and more closely approaches the condition of the insectivorous *Proteles* (Vinuesa et al. 2014). The brain morphology and sulcal pattern of the Plio-Pleistocene *Pliocrocota perrieri* was similar to modern *Hyaena hyaena* and *Parahyaena brunnea* (Vinuesa et al. 2015b). However, *Pliocrocota* was less encephalized than the highly-social modern *Crocota crocuta* and had a relatively smaller anterior cerebrum (the part of the cerebrum anterior to the cruciate sulcus) than in all extant bone-cracking hyenas (Vinuesa et al. 2015b). The Pleistocene *Crocota spelaea* and *C. ultima* had a lesser development of the anterior brain than the modern *C. crocuta* (Vinuesa et al. 2015a). According to the same authors the greater anterior brain development of modern *C. crocuta* is a derived and recently-acquired trait, and the extinct species of *Crocota* displayed less developed social abilities.

17.4.2 The Evolution of Gyrification in Carnivorans

Gyral folding can enlarge the cortical surface by increasing either the height or the number of gyri. These increases must evolve simultaneously, because an increase of only the height or only the number of gyri has functional disadvantages (Prothero and Sundsten 1984). Cortical features are correlated, due to the way the cerebral cortex folds and fissures. For example, gyral length and total cortical surface area

are strongly correlated in mammals as a whole, as noted by Elias and Schwartz (1971). Similarly, Zilles et al. (1989) observed a correlation between sulcal length and degree of folding in primates. Since the relative length of the superficially exposed gyri and sulci is correlated with the degree of folding, the evolutionary history of cortical folding can be followed through simple length measurements (Zilles et al. 1989), as was applied to carnivorans by Lyras et al. (2016). They found that the relative length of the superficially exposed gyri differs among extant carnivorans. Living viverrids as a group have a relatively lower degree of gyrification than other carnivorans (Lyras et al. 2016). Extant felids, canids, and mustelids share a more or less similar degree of gyrification. Among mustelids, otters have the highest values. This agrees with the comparative observations mentioned above, as the cortex of otters has an enlarged somatic sensory area (Radinsky 1968b; Marshall et al. 2014).

The reconstruction of the evolutionary history of gyrification using statistical tools and ancestral state reconstructions estimated that the first carnivorans should have had brains as convoluted as those of the living forms (Lewitus et al. 2014). The reconstruction of evolutionary patterns in deep geological time based solely on living species may, however, be flawed, as living species may be limited proxies of the actual evolutionary history of the clade they belong to (Finarelli and Goswami 2013). Indeed, Lyras et al. (2016) demonstrated that, in contrast to the estimates of Lewitus et al. (2014), the fossil record indicates that contemporary carnivorans have significantly more convoluted brains than their early representatives.

Another surface variable that can be measured using endocranial casts is the size of the exposed cerebral cortex area. According to Lyras et al. (2016), the relative surface area of the outer cortex has increased by approximately 50% from the first carnivorans some 40 million years ago to the present day. This trend of increasing cortical surface is not limited to carnivorans, but evolved in other mammalian groups as well. Hofman (2014) suggests that neocortical expansion was driven by an increasing environmental pressure for more complex cognitive abilities. Evolutionary time played a crucial role in this process. Overall, as well as within each family independently, the cortical surface and the degree of cortical folding progressively increased through time. However, this evolution is relatively slow, as each family required millions of years of evolution to achieve its present-day configuration of cortical folding (Lyras et al. 2016).

17.4.3 Brain-Size Evolution

Finarelli and Flynn (2009) explored the evolutionary history of encephalization across terrestrial carnivorans using a large data set of living and fossil taxa. They documented clade-specific evolutionary transformations in encephalization allometries among different carnivoran families. Felidae are significantly larger-brained than basal Carnivora. The larger-bodied felids have low encephalization, however, comparable to those of basal carnivorans, while the smaller felid taxa exhibit higher

encephalization. In Amphicyonidae the larger species exhibit lower encephalization as well. In Ursidae, Caninae and Musteloidea, Finarelli and Flynn (2009) noted an allometric increase of brain size with increasing body size. They further noted that these encephalization increases were independent of each other.

Several authors have presented hypotheses regarding the biological significance of brain size in carnivorans. In an early work, Jerison (1970) postulated that at any given geological time carnivorans (including creodonts) had relatively larger brains than their ungulate contemporaries. Later, Radinsky (1978a) re-evaluated the available data and concluded that there is no evidence for or against Jerison's model. Recently Smaers et al. (2021) demonstrated that shifts in relative brain size are often primarily characterized by marked changes in body size. For example large modern pinnipeds attained a low brain to body size ratio because of strong selection for larger body size. Thus, according to the same authors, relative brain size may not always be a valid proxy of cognition.

Mammalian brain size seems to be correlated to maternal basal metabolic rate (Martin 1981). Finarelli (2010) could not find evidence for such a correlation within Carnivora, however. Instead, Finarelli (2010) found that taxa with higher encephalization tend to have fewer, larger offspring. This observation demonstrates the importance of maternal investment on shaping adult encephalization in their offspring.

Another factor previously considered to be important in neural evolution among mammalian carnivorans is social complexity. This hypothesis postulates that the degree of encephalization should increase with increasing complexity of the intra-specific social environment. Such a relationship was initially suggested to be present in carnivorans by Gittleman (1986). However, Finarelli and Flynn (2009) demonstrated that the association of increased encephalization and highly social behaviour appears to be restricted to the Canidae among extant Carnivora and cannot be generalized to the entire order. Similarly, Swanson et al. (2012), who investigated the importance of social complexity in neural evolution among contemporary carnivorans, did not find support for the social brain hypothesis when they examined overall brain volume. They did, however, identify a positive relationship between relative cerebrum volume and sociality. The cerebrum is the only region of the brain that might be critical for social cognition. Another study (Benson-Amram et al. 2016) investigated the idea that brain size predicts cognitive abilities in carnivorans. They examined performance of captive individuals of 39 species from nine families housed in zoos and reported that problem-solving capabilities indeed corresponded with larger relative brain size.

Other works have focused on within-family comparisons. Sakai et al. (2016) investigated the relationship between relative brain size and regional brain volumes and sociality in contemporary felids. They found that sociality does not correspond with larger relative brain size, but instead seems to be predicted by anterior cerebrum volume. They noted however, that the lion, a species with a highly complex group structure, has the largest relative anterior brain, while the cheetah, a species with solitary females, has the smallest. Similarly, the anterior cerebrum of wolves (*Canis lupus*) is larger than that of coyotes (*C. latrans*) (Sakai et al. 2018). Arsznov

et al. (2010) found that the volume of the anterior cerebrum relative to that of the total brain is larger in the spotted hyaena (*Crocuta crocuta*) than in the other three living hyaena species. Furthermore, they found that the volume of the frontal cortex in the aardwolf (*Proteles cristata*), which is the least social living hyaena, is the smallest among all living hyaenid species.

17.5 Concluding Remarks

The cerebrum of all living carnivorans in lateral aspect consists of convolutions arranged in concentric arcs arranged around the Sylvian sulcus and progressively increasing in length. The lateral gyrus abuts the longitudinal fissure in dorsal view, whereas anteriorly it is continuous with the sigmoid gyrus, a convolution that surrounds the cruciate sulcus. The cruciate sulcus is a common landmark in living carnivorans, except for most viverrids, the African palm civet and the linsang. This pattern evolved independently multiple times during the evolutionary history of carnivorans.

The evolution of the carnivoran brain follows a general tendency of cortical expansion and increased folding, starting from the archaic, fox-sized earliest members of the late Paleocene. Contemporary carnivorans have significantly more convoluted brains than their early representatives. This expansion followed the same general pattern of neocortical convolutions in all carnivoran groups. However, each group evolved distinctive sulcal patterns.

The felid brain reached its present configuration already during the late Miocene. Extant felids, canids, and mustelids share a similar degree of gyrification. Within mustelids, otters have the highest degree of gyrification, in agreement with their enlarged somatic sensory area on the cortex. Living viverrids have a relatively lower degree of gyrification compared to other carnivorans.

Acknowledgments We thank Larry Heaney, William Simpson, and the late Bill Stanley (Field Museum of Natural History, Chicago, USA), John Flynn, Jin Meng and Judy Galkin (American Museum of Natural History, New York, USA), Christine Argot and Christine Lefèvre (Muséum National d'Histoire Naturelle, Paris, France) and Natasja den Ouden (Naturalis Biodiversity Center, Leiden, the Netherlands) for providing access to collections under their charge. We are indebted to Bartholomeus van der Geer for his assistance with the raw data collection. We also thank the reviewer and the editors for making constructive suggestions to improve the manuscript.

References

- Arsznov BM, Lundrigan BL, Holekamp KE et al (2010) Sex and the frontal cortex: a developmental study in the spotted hyena. *Brain Behav Evol* 76:185–197
- Atkins DL (1970) Comparative morphology and evolution of the cerebellum in the mammalian order Carnivora. Unpublished PhD thesis, Texas A&M University

- Baskin JA (1998a) Procyonidae. In: Janis CM, Scott KM, Jacobs LL (eds) Evolution of tertiary mammals of North America, Vol. 1. Terrestrial carnivores, ungulates and ungulate-like mammals. Cambridge University Press, Cambridge, pp 144–151
- Baskin JA (1998b) Mustelidae. In: Janis CM, Scott KM, Jacobs LL (eds) Evolution of tertiary mammals of North America, Vol. 1. Terrestrial carnivores, ungulates and ungulate-like mammals. Cambridge University Press, Cambridge, pp 152–173
- Benson-Amram S, Dantzer D, Stricker G et al (2016) Brain size predicts problem – solving ability in mammalian carnivores. *Proc Natl Acad Sci U S A* 113:2532–2537
- Bruce AT (1883) Observations upon the brain casts of Tertiary mammals. Contributions from the E.M. Museum of Geology and Archeology of Princeton College 3(iii):36–45
- Carlsson A (1900) Ueber die systematische Stellung der *Nandina binotata*. *Zool Jahrb Abt Syst* 13:509–528
- Carlsson A (1911) Über *Cryptoprocta ferox*. *Zool Jahrb Abt Syst* 30:419
- Cuff AR, Stockey C, Goswami A (2016) Endocranial morphology of the extinct North American lion (*Panthera atrox*). *Brain Behav Evol* 88:213–221
- Czyzewska T (1981a) Natural endocranial casts of the Canidae from Wéze I, near Działosyn (Poland). *Acta Zool Cracov* 25:251–260
- Czyzewska T (1981b) Natural endocranial casts of the Mustelinae from Wéze I near Działosyn (Poland). *Acta Zool Cracov* 25:261–270
- Davis DD (1964) The giant panda: a morphological study of evolutionary mechanisms. *Fieldiana Zool Memoir* 2:1–339
- De Beaumont G (1962) Observations sur l' ostéologie crânienne et la position systématique des petits «*Amphicyon*» de l' oligocène européen. *Bull Soc Vaud sc nat* 68:81–92
- De Beaumont G (1964) Un crane d'*Amphicyon ambiguus* (Filhol) (Carnivora) des Phosphorites du Quercy. *Arch Sci (Genève)* 17:331–339
- Dehnhardt G, Mauck B, Bleckmann H (1998) Seal whiskers detect water movements. *Nature* 394:235–236
- Dong W (2008) Virtual cranial endocast of the oldest giant panda (*Ailuropoda microta*) reveals great similarity to that of its extant relative. *Naturwissenschaften* 95:1079–1083
- Dong W, Hou X, Liu J et al (2007) 3D virtual reconstruction of the Pleistocene cheetah skull from the Tangshan, Nanjing, China. *Prog Nat Sci* 17:74–79
- Edinger T (1929) Die fossilen Gehirne. *Ergebn Anat Entwickl* 28:1–249
- Edinger T (1977) Paleoneurology 1804–1966: an annotated bibliography. *Adv Anat Embryol Cell* 49(1–6):1–258
- Elias H, Schwartz D (1971) Cerebral-cortical surface areas, volumes, lengths of gyri and their interdependence in mammals, including man. *Z Säugetierkunde* 36:147–163
- England DR (1973) The phylogeny of the order Carnivora based on the cerebral structure. Unpublished PhD thesis, Texas A&M University, College Station
- Finarelli JA (2010) Does encephalization correlate with life history or metabolic rate in Carnivora? *Biol Lett* 6:350–353
- Finarelli JA, Flynn JJ (2009) Brain-size evolution and sociality in Carnivora. *Proc Natl Acad Sci U S A* 106:9345–9349
- Finarelli JA, Goswami A (2013) Potential pitfalls of reconstructing deep time evolutionary history with only extant data, a case study using the Canidae (Mammalia, Carnivora). *Evolution* 67:3678–3685
- García N, Santos E, Arsuaga JL et al (2006) High-resolution X-ray computed tomography applied to the study of some endocranial traits in cave and brown bears. *Scientific Annals, School of Geology Aristotle University of Thessaloniki. Special vol* 98, pp 141–146
- García N, Santos E, Arsuaga JL et al (2007) Endocranial morphology of *Ursus deningeri* Von Reichenau, 1904, from the Sima de Los Huesos (Sierra de Atapuerca) Middle Pleistocene site. *J Vertebr Paleontol* 27:1007–1017
- Geraards D, Spassov N (2016) Musteloid carnivores from the upper Miocene of South-Western Bulgaria, and the phylogeny of the Mephitidae. *Geodiversitas* 38:543–558

- Gervais P (1870) Mémoire sur les formes cérébrales propres aux Carnivores vivants et fossiles. *Archs Mus Hist nat Paris* 6:103–162
- Gervais P (1872) Formes cérébrale du *Cephalogale geoffroyi*. *J Zool* 1:131–133
- Gittleman JL (1986) Carnivore brain size, behavioral ecology, and phylogeny. *J Mammal* 67:23–36
- Gläser N, Wieskotten S, Otter C et al (2011) Hydrodynamic trail following in a California sea lion (*Zalophus californianus*). *J Comp Physiol A* 197:141–151
- Hofman M (2014) Evolution of the human brain: when bigger is better. *Front Neuroanat* 8. <https://doi.org/10.3389/fnana.2014.00015>
- Iurino DA, Profico A, Cherin M et al (2015) A lynx natural brain endocast from Ingarano (Southern Italy; Late Pleistocene): Taphonomic, morphometric and phylogenetic approaches. *Hystrix* 26:110–117
- Ivanoff DV, Wolsan M, Marciszak A (2014) Brainy stuff of long-gone dogs: a reappraisal of the supposed *Canis* endocranial cast from the Pliocene of Poland. *Naturwissenschaften* 101:645–651
- Jardim-Messeder D, Lambert K, Noctor S et al (2017) Dogs have the most neurons, though not the largest brain: trade-off between body mass and number of neurons in the cerebral cortex of large carnivoran species. *Front Neuroanat* 11. <https://doi.org/10.3389/fnana.2017.00118>
- Jerison HJ (1970) Brain evolution: new light on old principles. *Science* 170:1224–1225
- Kamiya T, Pirlot P (1988) The brain of the Malayan bear (*Helarctos malayanus*). *Z Zool Syst Evol* 26:225–235
- Klatt B (1928) Vergleichende untersuchungen an Caniden und Procyoniden. *Zool Jb* 45:217–292
- Koufos GD, Konidaris GE, Harvati K (2017) Revisiting *Ursus etruscus* (Carnivora, Mammalia) from the Early Pleistocene of Greece with description of new material. *Quat Int* 497:222–239
- Krueg J (1880) Über die Furchen auf der Grosshirnrinde der zonoplacentalen Säugethiere. *Z Wiss Zool* 33:595–648
- Ladygina TF, Popov VV, Supin AY (1985) Topical organization of somatic projections in the fur seal cerebral cortex. *Neurophysiology* 17:246–252
- Lewitus E, Kelava I, Kalinka AT et al (2014) An adaptive threshold in mammalian neocortical evolution. *PLoS Biol* 12:e1002000
- Lyras GA (2009) The evolution of the brain in Canidae (Mammalia: Carnivora). *Scr Geol* 139:1–93
- Lyras GA (2018) Brain changes during phyletic dwarfing in elephants and hippos. *Brain Behav Evol* 92:167–181
- Lyras GA, van der Geer AAE (2003) External brain anatomy in relation to phylogeny of Caninae (Carnivora: Canidae). *Zool J Linn Soc Lond* 138:505–522
- Lyras GA, van der Geer AAE, Dermitzakis MD et al (2006) *Cynotherium sardous*, an insular canid (Mammalia: Carnivora) from the Pleistocene of Sardinia (Italy), and its origin. *J Vertebr Paleontol* 26:735–745
- Lyras GA, Giannakopoulou A, Kouvari M et al (2016) Evolution of gyrification in carnivores. *Brain Behav Evol* 88:187–203
- Lyras GA, Giannakopoulou A, Werdelin L (2019) The brain anatomy of an early Miocene felid from Ginn Quarry (Nebraska, USA). *Palaeontol Z* 93:345–355
- Marshall CD, Rozas K, Kot B et al (2014) Innervation patterns of sea otter (*Enhydra lutris*) mystacial follicle-sinus complexes: support for a specialized somatosensory system. *Front Neuroanat*. <https://doi.org/10.3389/fnana.2014.00121>
- Martin RD (1981) Relative brain size and basal metabolic-rate in terrestrial vertebrates. *Nature* 293:57–60
- Merriam JC, Stock C (1932) The Felidae of Rancho La Brea. Carnegie Institution of Washington, Washington, DC
- Milne AO, Grant RA (2014) Characterisation of whisker control in the California sea lion (*Zalophus californianus*) during a complex, dynamic sensorimotor task. *J Comp Physiol A* 200:871–879
- Mitchell E, Tedford RH (1973) The Enaliarctinae: a new group of extinct aquatic Carnivora and a consideration of the origin of the Otariidae. *Bull Am Mus Nat Hist* 151:203–284

- Mivart SG (1885) Notes on the cerebral convolutions of the Carnivora. *J Linn Soc Lond Zool* 19:1–25
- Mödden C, Wolsan M (2000) External brain morphology of the late Oligocene musteloid carnivoran *Bavarictis gaimersheimensis*. *Acta Palaeontol Pol* 45:301–310
- Molnár Z, Kaas JH, de Carlos JA et al (2014) Evolution and development of the mammalian cerebral cortex. *Brain Behav Evol* 83:126–139
- Moodie R (1922) On the endocranial anatomy of some Oligocene and Pleistocene mammals. *J Comp Neurol* 34:342–379
- Moscarella A, Iannucci A, Iurino DA et al (2020) The wolf from Grotta Romanelli: new insights from brain morphology. *Fossilia* 2020:45–46
- Murrill RI, Wallace DT (1971) A method for making an endocranial cast through the foramen magnum of an intact skull. *Am J Phys Anthropol* 34:441–446
- Orlov JA (1948) *Perunium ursogulo* Orlov, a new gigantic extinct mustelid: a contribution to the morphology of the skull and brain and to the phylogeny of Mustelidae. *Acta Zool* 29:63–105
- Paterson R, Samuels JX, Rybczynski N et al (2020) The earliest mustelid in North America. *Zool J Linn Soc* 188:1318–1339
- Petrovič V, Sabol M, Šurka J et al (2018) External brain morphology of juvenile cave hyena (*Crocota crocuta spelaea*) from the Jasovská jaskyňa Cave (Slovakia) revealed by X-ray computed tomography. *Acta Geol Slovaca* 10:133–142
- Pilleri G (1960) Das Gehirn von *Mustela vison* und *Mephitis mephitis* (Carnivora, Mustelidae). *Rev Suisse Zool* 67:141–158
- Piveteau J (1931) Les chats des Phosphorites du Quercy. *Ann Paleontol* 20:107–163
- Piveteau J (1950) Note sur l'encéphale d'un mustelidé Oligocene. *Bull Soc hist nat Toulouse* 85:263–265
- Piveteau J (1951) Recherches sur l'évolution de l'encéphale chez les Carnivores fossils. *Ann Paléontol* 37:133–152
- Piveteau J (1961) Encéphales de carnivores fossiles. *Traité de Paléontologie* 6:806–820
- Piveteau J (1962) L'encéphale de *Viverravus angustidens*, Miocène des Phosphorites de Quercy. *Ann Paléontol* 48:163–175
- Prothero J, Sundsten J (1984) Folding of the cerebral cortex in mammals: a scaling model. *Brain Behav Evol* 24:152–167
- Radinsky LB (1968a) A new approach to mammalian cranial analysis, illustrated by examples of prosimian primates. *J Mammal* 124:167–179
- Radinsky LB (1968b) Evolution of somatic sensory specialization in otter brains. *J Comp Neurol* 134:495–505
- Radinsky LB (1969) Outlines of canid and felid brain evolution. *Ann N Y Acad Sci* 167:277–288
- Radinsky L (1971) An example of parallelism in carnivore brain evolution. *Evolution* 25:518–522
- Radinsky L (1973a) Evolution of the canid brain. *Brain Behav Evol* 7:169–202
- Radinsky L (1973b) Are stink badgers skunks? Implications of neuroanatomy for mustelid phylogeny. *J Mammal* 54:585–593
- Radinsky L (1975a) Evolution of the felid brain. *Brain Behav Evol* 11:214–254
- Radinsky L (1975b) Viverrid neuroanatomy: phylogenetic and behavioral implications. *J Mammal* 56:130–150
- Radinsky L (1976) The brain of *Mesonyx*, a Middle Eocene condylarth. *Fieldiana Geol* 13:323–337
- Radinsky L (1977) Brains of early carnivores. *Paleobiology* 3:333–349
- Radinsky L (1978a) Evolution of brain size in carnivores and ungulates. *Am Nat* 112:815–831
- Radinsky LB (1978b) The evolutionary history of dog brains. *Museologia* 10:25–29
- Radinsky LB (1978c) The evolutionary history of cat brains. *Museologia* 11:35–41
- Radinsky L (1980) Endocasts of amphicyonid carnivorans. *Am Mus Novit* 2694:1–11
- Repenning CA, Tedford RH (1977) Otarioid seals of the Neogene. *U.S. Geol Surv Prof Pap* 992:1–93

- Sakai ST, Arsznov BM, Hristova AE et al (2016) Big cat coalitions: a comparative analysis of regional brain volumes in Felidae. *Front Neuroanat* 10:99. <https://doi.org/10.3389/fnana.2016.00099>
- Sakai ST, Whitt B, Arsznov BM et al (2018) Endocranial development in the coyote (*Canis latrans*) and gray wolf (*Canis lupus*): a computed tomographic study. *Brain Behav Evol* 91:65–81
- Savage RJG (1957) The anatomy of *Potamotherium* an Oligocene latrine. *Proc Zool Soc London* 129:151–244
- Sawyer EK, Turner EC, Kaas JH (2016) Somatosensory brainstem, thalamus, and cortex of the California sea lion (*Zalophus californianus*). *J Comp Neurol* 524:1957–1975
- Scott WB (1895) The Mammalia of the deep river beds. *Trans Am Philos Soc (ns)* 18:55–185
- Scott WB (1898) Notes on the Canidae of the White River Oligocene. *Trans Am Philos Soc (ns)* 19:325–415
- Scott W, Jepsen G (1936) The mammalian fauna of the White River Oligocene. I. Insectivora and Carnivora. *Trans Am Philos Soc (ns)* 28:1–153
- Sienkiewicz T, Sergiel A, Huber D et al (2019) The brain anatomy of the brown bear (Carnivora, *Ursus arctos* L., 1758) compared to that of other carnivorans: a cross-sectional study using MRI. *Front Neuroanat* 13:79. <https://doi.org/10.3389/fnana.2019.00079>
- Smaers B, Rothman RS, Hudson DR et al (2021) The evolution of mammalian brain size. *Sci Adv* 7(18):eabe2101
- Smith WK (1933) Cerebral hemispheres of the American black bear (*Ursus americanus*). Morphological and phylogenetic characteristics. *Arch Neurol Psychiatr* 30:14–39
- Spaulding M, Flynn JJ (2012) Phylogeny of the Carnivoramorpha: the impact of postcranial characters. *J Syst Palaeontol* 10:653–677
- Swanson EM, Holekamp KE, Lundrigan BL et al (2012) Multiple determinants of whole and regional brain volume among terrestrial carnivorans. *PLoS One* 7:e38447
- Thiede U (1966) Zur Evolution von Hirneigenschaften mitteleuropäischer und südamerikanischer Musteliden. *Z Zool Syst Evol* 4:318–377
- Tilney F (1931) Fossil brains from some early Tertiary mammals of North America. *Bull Neurol Inst NY* 1930:24–50
- Tomiya S, Tseng ZJ (2016) Whence the beardogs? Reappraisal of the Middle to Late Eocene ‘*Miacis*’ from Texas, USA, and the origin of Amphicyonidae (Mammalia, Carnivora). *R Soc Open Sci* 3:160518. <https://doi.org/10.1098/rsos.160518>
- Tomiya S, Zack SP, Spaulding M et al (2021) Carnivorous mammals from the middle Eocene Washakie Formation, Wyoming, USA, and their diversity trajectory in a post-warming world. *J Paleontol* 95(S82):1–115
- Turner EC, Sawyer EK, Kaas JH (2017) Optic nerve, superior colliculus, visual thalamus, and primary visual cortex of the Tomiya northern elephant seal (*Mirounga angustirostris*) and California sea lion (*Zalophus californianus*). *J Comp Neurol* 525:2109–2132
- Uylings HBM, van Eden CG (1990) Qualitative and quantitative comparison of the prefrontal cortex in rats and primates, including humans. *Prog Brain Res* 85:31–62
- Vinuesa V, Madurell-Malapeira J, Ansón M et al (2014) New cranial remains of *Pliocrocota perrieri* (Carnivora, Hyaenidae) from the Villafranchian of the Iberian Peninsula. *Boll Soc Paleontol Ital* 53:39–47
- Vinuesa V, Iurino DA, Madurell-Malapeira J et al (2015a) Inferences of social behavior in bone-cracking hyaenids (Carnivora, Hyaenidae) based on digital paleoneurological techniques: implications for human–carnivoran interactions in the Pleistocene. *Q Int* 413(B):7–14
- Vinuesa V, Madurell-Malapeira J, Fortuny J et al (2015b) The endocranial morphology of the Plio-Pleistocene bone-cracking hyena *Pliocrocota perrieri*: behavioral implications. *J Mamm Evol* 22:421–434
- Wang X (1994) Phylogenetic systematics of the Hesperocyoninae (Carnivora: Canidae). *Bull Am Mus Nat Hist* 221:1–1207
- Wang X, Tedford RH, Taylor BE (1999) Phylogenetic systematics of the Borophaginae (Carnivora: Canidae). *Bull Am Mus Nat Hist* 278:147–162

- Wang X, White SC, Guan J (2020) A new genus and species of sabretooth, *Oriensmilus liupanensis* (Barbourfelinae, Nimravidae, Carnivora), from the middle Miocene of China suggests barbourfelines are nimravids, not felids. *J Syst Palaeontol* 18:783–803
- Welker W (1990) Why does cerebral cortex fissure and fold? In: Jones EG, Peters A (eds) *Cerebral cortex*, vol 8B. Springer, Boston, pp 3–136
- Welker W, Campos G (1963) Physiological significance of sulci in somatic sensory cerebral cortex in mammals of the family Procyonidae. *J Comp Neurol* 120:19–36
- Welker WI, Seidenstein S (1959) Somatic sensory representation in the cerebral cortex of the raccoon (*Procyon lotor*). *J Comp Neurol* 111:469–501
- Welker WI, Johnson JI Jr, Pubols BH Jr (1964) Some morphological and physiological characteristics of the somatic sensory system in raccoons. *Am Zool* 4:75–96
- Wesley-Hunt GD, Werdelin L (2005) Basicranial morphology and phylogenetic position of the upper Eocene carnivoramorph *Quercygale*. *Acta Palaeontol Pol* 50:837–846
- Wieskotten S, Dehnhardt G, Mauck B et al (2010) The impact of glide phases on the trackability of hydrodynamic trails in harbour seals (*Phoca vitulina*). *J Exp Biol* 213:3734–3740
- Wieskotten S, Mauck B, Miersch L et al (2011) Hydrodynamic discrimination of wakes caused by objects of different size or shape in a harbour seal (*Phoca vitulina*). *J Exp Biol* 214:1922–1930
- Woolsey CN (1958) Organization of somatic sensory and motor areas of the cerebral cortex. In: Harlow HF, Woolsey CN (eds) *Biological and biochemical bases of behavior*. University of Wisconsin Press, Madison, pp 63–81
- Wright JD (2009) Cenozoic climate change. In: Gornitz V (ed) *Encyclopedia of paleoclimatology and ancient environments*. Springer, Dordrecht, pp 148–155
- Zilles K, Armstrong E, Moser K et al (1989) Gyrification in the cerebral cortex of primates. *Brain Behav Evol* 34:143–150

Chapter 18

Paleoneurology of Extinct Cingulates and Insights into Their Inner Ear Anatomy



P. Sebastián Tambusso, Flávio Góis, Jorge Felipe Moura, Chiara Villa, and Roberta Veronese do Amaral

18.1 Systematic and Phylogenetic Context

Cingulata is one of the two orders within the Superorder Xenarthra. The classic morphological systematic scheme of Cingulata comprises two main clades: Dasypodoidea, consisting of living and extinct armadillos, and Glyptodontoidea, a monophyletic group that includes the extinct glyptodonts and pampatheres (McKenna and Bell 1997). Glyptodonts are one of the most bizarre groups of mammals known. Like all cingulates, they bear a carapace composed of a mosaic of dermal scutes, although, unlike the other cingulates, their carapace is immobile. There is a complete fusion of thoracic and lumbar vertebrae to form the dorsal tube (Lydekker 1894; Gillette and Ray 1981). In addition, the presence of a dermal

P. S. Tambusso (✉)

Departamento de Paleontología, Facultad de Ciencias, Universidad de la República, Montevideo, Uruguay

Servicio Académico Universitario y Centro de Estudio Paleontológicos (SAUCE-P), Departamento de Canelones, Universidad de la República, Montevideo, Uruguay
e-mail: stambusso@fcien.edu.uy

F. Góis

Laboratorio de Paleontología de Vertebrados, Centro de Investigación Científica y de Transferencia Tecnológica a la Producción, Diamante, Entre Ríos, Argentina

J. F. Moura

Laboratório de Paleocologia e Paleoicnologia, Departamento de Ecologia e Biologia Evolutiva (DEBE), Universidade Federal de São Carlos (UFSCar), São Carlos, SP, Brazil

C. Villa

Laboratory of Advanced Imaging and 3D Modeling, Section of Forensic Pathology, Department of Forensic Medicine, University of Copenhagen, Copenhagen, Denmark

R. V. do Amaral

Departamento de Geologia e Paleontologia, Setor de Paleovertebrados, Museu Nacional/ Universidade Federal do Rio de Janeiro, Rio de Janeiro, Brazil

caudal tube is characteristic of glyptodonts with the exception of the clades Propalaeohoplophoridae and Glyptodontinae (Fericola and Porpino 2012); in some species (e.g. *Doedicurus clavicaudatus*), a large tail club is present that may have been adapted for antagonistic behavior (Fariña 1995; Alexander et al. 1999; Blanco et al. 2009). The singular position of the masticatory apparatus in glyptodonts, in which the toothrow extends to or posterior to the mandibular glenoid/jaw joint, is a unique feature among mammals (Fariña and Parietti 1983; Fariña 1985, 1988; Fariña and Vizcaíno 2001), with the exception of vermilinguan anteaters, in which the palate extends posterior to the ear region (Patterson et al. 1992).

The allocation of Pamphathiidae to the classic (but out-of-date) systematic groups dasypodoids or glyptodontoids has been controversial historically, as they have morphological characters that can be associated with either group. They resemble Dasypodoidea in having a carapace divided into three regions (scapular buckler, movable bands and pelvic buckler), and in the anatomy of the limbs and certain cranial characters (e.g., the length of the snout) (Simpson 1930; Hoffstetter 1958; Paula Couto 1979). However, they resemble Glyptodontoidea in characters of the auditory region (petrosal with a narrow and triangular promontory), cranial robustness, the morphology and function of the masticatory apparatus (e.g. the ascending ramus of the mandible anteriorly inclined, the elevation of the mandibular notch well above the dental series and lobate teeth, bilobate in pamphathes and trilobate in glyptodonts), and the elevation of the basicranial axis relative to the palate (De Iuliis et al. 2000; Vizcaíno 2009; Góis et al. 2012, 2015; Góis 2013; Fericola et al. 2017; Gaudin and Lyon 2017). Recent morphological phylogenetic analyses placed pamphathes as the sister group of glyptodonts (Gaudin and Wible 2006; Billet et al. 2011) (Fig. 18.1).

Armadillos comprise approximately 21 extant species, and recent molecular analysis (Delsuc et al. 2012; Gibb et al. 2016) divide them into two families: Dasypodidae with a single extant subfamily (Dasypodinae); and Chlamyphoridae with three extant subfamilies (Chlamyphorinae, Euphractinae and Tolypeutinae; but see below). According to Gaudin and Lyon (2017) this reordering at the family level diversity among cingulates does not adequately reflect the age, morphological disparity, and taxonomic diversity encompassed by cingulates in general, and the Chlamyphoridae in particular (see below). In fact, the Dasypodinae, one of the long-recognized subfamilies of armadillos (and indeed the smallest subfamily in terms of generic level diversity), is being accorded family level status, while the other three extant armadillo subfamilies are lumped together into a single, very large, taxonomically, morphologically and ecologically diverse family (Gaudin and Lyon 2017). Morphological phylogenetic analyses have considered armadillos a paraphyletic group and have suggested a close relationship between glyptodonts and the armadillo subfamily Euphractinae (Billet et al. 2011; Gaudin and Wible 2006). However, two recent molecular analyses (Delsuc et al. 2016; Mitchell et al. 2016) support a close relationship between glyptodonts and a clade composed of the extant subfamilies Chlamyphorinae (fairy armadillos) and Tolypeutinae (three-banded, naked-tailed and giant armadillos) (Fig. 18.1). Mitchell et al. (2016) based on a complementary morphological analysis with a molecular backbone constraint

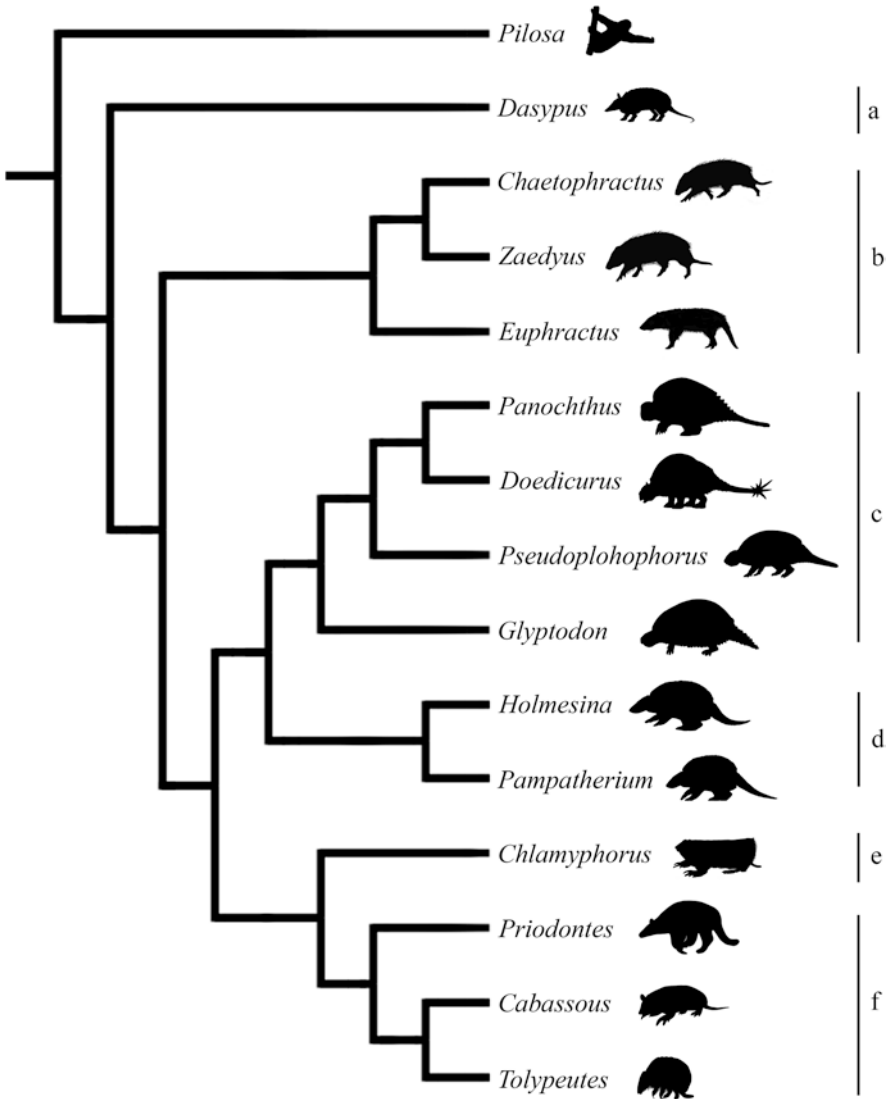


Fig. 18.1 Non-calibrated phylogeny of Cingulata (Modified from Delsuc et al. 2016 and Cuadrelli et al. 2020). (a) Daypodinae, (b) Euphractinae, (c) Glyptodontinae, (d) Pamphaterinae, (e) Chlamyphorinae, (f) Tolypeutinae

propose a close relationship with the extant armadillo subfamily Chlamyphorinae, which was also supported by a morphological complementary analysis by Delsuc et al. (2016). This grouping is surprising since they are among the most derived cingulates. Moreover, Pleistocene glyptodonts were generally large-bodied and heavily armored, as reflected in the graviportal modifications of the limbs, whereas fairy armadillos are the smallest armadillos and are highly adapted for burrowing

(Mitchell et al. 2016). So far, there are no molecular data for pampatheres. Therefore, it remains to be determined whether their phylogenetic relationships will remain based on the morphological characters, or will be modified as happened with glyptodonts based on the results of molecular analysis.

18.2 Historical Background

18.2.1 *The Record of Endocranial Morphology of Fossil Cingulates*

A considerable number of paleoneurological studies on the South American Cenozoic mammal fauna, many of which focused on xenarthrans, were carried out in the nineteenth and twentieth centuries (Serres 1865; Gervais 1869; Dechaseaux 1958; Dozo 1987, 1989, 1994, 1998). These works were based on both natural endocranial casts and artificial casts constructed with latex or silicone rubber. Some of these historical studies involved glyptodonts as well (Serres 1865; Gervais 1869; Dechaseaux 1958, Dozo 1989), but the paleoneurology of the pampatheres was not studied until recently.

The first researchers to study the brain of Pleistocene glyptodonts noted that they had a lissencephalic condition and that, in absolute terms, this was a small organ relative to the body size of these animals (Serres 1865; Gervais 1869). This observation is even more noticeable when compared with other mammals of similar size, in particular, other large xenarthrans. Serres (1865: 458) noted this particular character based on an endocranial cast of a specimen of *Glyptodon clavipes*: “*La cavité crânienne offre quelques particularités qu’il peut être intéressant de signaler ici: sa face inférieure présente un plan à peu près horizontal. Elle est terminée, à la partie antérieure, par deux cavités de taille à peu près à loger une noisette et qui étaient remplies par les lobes olfactifs. Plus en arrière, les hémisphères cérébraux mesurent environ 55 millimètres de long et 40 millimètres de large en moyenne.*” (The cranial cavity offers some peculiarities that it may be interesting to point out here: its underside presents a more or less horizontal plane. It is terminated, at the anterior part, by two cavities of size approximately to lodge a hazelnut and which were filled by the olfactory lobes. Further back, the cerebral hemispheres are about 55 millimeters long and 40 millimeters wide on average). This characteristic is also mentioned by Gervais (1869: 45): “*...le cerveau des Glyptodontes ... rentre assez bien, sous ce rapport, dans le type général des Dasypides [sic], mais il a évidemment les hémisphères de petite dimension eu égard à la taille gigantesque de l’animal.*” (...the brain of the Glyptodonts... fits quite well, in this respect, in the general type of the Dasypids [sic], but it obviously has the hemispheres of small dimension with regard to the gigantic size of the animal). Subsequently, he refers to the lissencephalic condition of glyptodonts: “*Il est également digne de remarque qu’appartenant à des mammifères d’aussi grande dimension, le cerveau des Glyptodontes soit aussi*

pauvre en replis entérioriformes, et l'on ne saurait douter que ce curieux groupe d'Edentés n'ait eu une intelligence plus bornée que le Scélidothérium, le Mylodon ou le Mégathérium." (It is also worth noting that, belonging to mammals of such large size, the brain of Glyptodonts is also poor in enteriform folds, and we cannot doubt that this curious group of Edentates had a more limited intelligence than *Scelidotherium*, *Mylodon* or *Megatherium*).

The doctoral thesis of Dozo (1989) represents the first exhaustive analysis of the brain in extant and extinct xenarthrans in order to evaluate their neurological evolution. Regarding the neocortical morphology of cingulates, her results show that it represents the simplest model within xenarthrans, with two primary variants that are consistent with the traditional classifications of cingulates: Dasydopoidea and Glyptodontoidea, with the Dasydopoidea presenting greater variability in their neocortical patterning, which would coincide with the disparity of the group. It should be noted that, although several species of extinct armadillos were included in the work of Dozo (1989), there were only two species of glyptodonts: *Glyptodon* and *Propalaeophlophorus*, and in the latter, the casts were not complete.

More recently, the use of computed tomography (CT) scanning on fossil materials has allowed us to increase our knowledge of xenarthran paleoneurology; from CT images is possible to obtain more accurate details of the internal structures, such as braincase or inner ear structures. In the case of cingulates, it has been possible to qualitatively and quantitatively analyze the brain of Miocene and Pleistocene glyptodonts (Tambusso and Fariña 2015a), as well as to describe the brain of a pamphateres (Tambusso and Fariña 2015b). The CT scanning method has also allowed the access to other structures within the skull such as the anatomy of the ear region of xenarthrans, which has been an important source of information for phylogenetic analyses (Patterson et al. 1989, 1992; Gaudin 1995, 2004; Gaudin and Wible 2006), as well as for some aspects of their paleobiology (Blanco and Rinderknecht 2008, 2012). This method has provided access to a new set of morphological data not otherwise accessible, such as the inner ear bony labyrinth. The inner ear anatomy of extant xenarthrans has recently been examined, showing that it is possible to find correlations with aspects of their locomotion, as well as with their phylogenetic history (Billet et al. 2012, 2015; Coutier et al. 2017). In the case of extant cingulates, Billet et al. (2015) observe that the morphological study of the bony labyrinth shows its morphology is largely congruent with phylogenetic relationships based on molecular analyses (Delsuc et al. 2012; Gibb et al. 2016). Studies of the inner ear of extinct xenarthrans are limited and had mostly been carried out in folivorans (Billet et al. 2013; Boscaini et al. 2018) until recently, when Tambusso et al. (2021) described the inner ear anatomy of extinct cingulates (glyptodonts and pamphateres).

18.2.2 Problematics

In their work on the brain of *Glossotherium*, Boscaini et al. (2018) observed that there are many similarities between the endocranial cast of this ground sloth and the extant sloth *Choloepus*, particularly regarding the pattern of sulci and convolutions, whereas the extant sloth *Bradypus* has more similarities with the Miocene sloths *Hapalops* and *Eucholoeops*. Boscaini et al. (2020) interpreted these similarities based on the phylogenetic scenarios with the best evidence up to that time (Gaudin 2004), which placed *Bradypus* as the most basally diverging sloth, and *Choloepus* within the clade Megalonychidae. However, the most recent molecular analyses (Delsuc et al. 2019; Presslee et al. 2019) ally *Choloepus* with the mylodont clade, so it would be more closely related to *Glossotherium*, whereas *Bradypus* is placed within the megatherioid clade, and is therefore possibly more closely related to *Hapalops* and *Eucholoeops*. These new phylogenetic analyzes are congruent with the observations on the endocast morphology of sloths studied by Boscaini et al. (2020).

These results show that xenarthran neuromorphology could provide additional information on the phylogenetic relationships within this group. Although it does not replace the evidence from molecular analyses, they can be a complementary aid in clades or taxa where it is not possible to extract genetic material due either to the quality of preservation or the (geological) age of the specimen. Therefore, the analysis of the brain and other endocasts structures (such as the bony labyrinth) of extinct cingulates can complement or improve the phylogenetic information obtained from other analyses, for example, helping to evaluate whether glyptodonts are more closely related to Chlamyphorinae or to another cingulate clade.

This work summarizes the results of these recent investigations on the brain and inner ear of fossil cingulates, as well as presenting brain endocast data from two new specimens, the glyptodont *Glyptodon* (ZMK 1-1845-9250) and the pampathere *Holmesina* (LPP-PV-002), providing an overview of the brain endocast diversity and evolution in cingulates in general.

18.3 Overview of General and Comparative Anatomy

18.3.1 Characterization of Cranial Endocast Morphology

Armadillos

Some aspects of the endocranial morphology of extant armadillos deserve further attention to compare with and to better assess the brain morphology of fossil cingulates. Extant armadillos show variation in brain morphology among the different species, although several characteristics are common to all (Dozo 1989, 1998). The olfactory bulbs have a triangular shape, they are very close to each other, and the

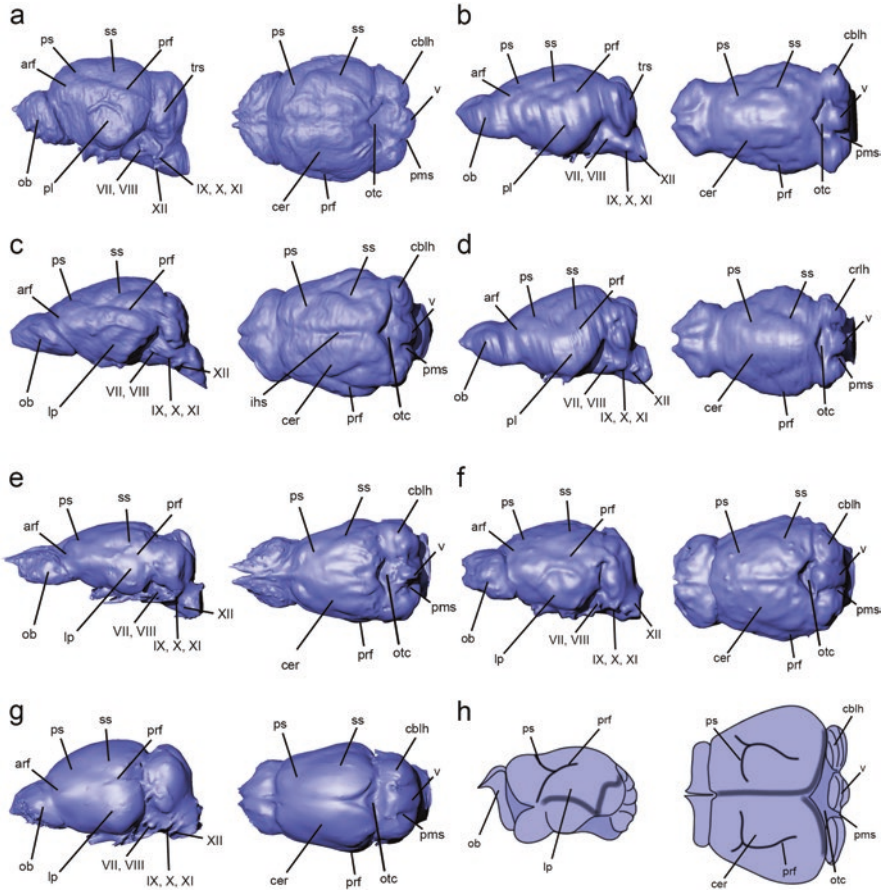


Fig. 18.2 Digital endocast of extant armadillos: (a) *Dasypos* in left lateral and dorsal view, (b) *Chaetophractus* in left lateral and dorsal view, (c) *Zaedyus* in left lateral and dorsal view, (d) *Euphractus* in left lateral and dorsal view, (e) *Priodontes* in left lateral and dorsal view, (f) *Cabassous* in left lateral and dorsal view, (g) *Tolypeutes* in left lateral and dorsal view, (h) schematic representation of the endocast of *Chlamyphorus* in left lateral and dorsal view (Modified from Dozo 1989). Abbreviations: *arf*, anterior rhinal fissure; *cblh*, cerebellar hemisphere; *cer*, cerebrum; *ihs*, interhemispheric sulcus; *ob*, olfactory bulb; *otc*, ossified tentorium cerebelli; *pl*, pyriform lobe; *pms*, paramedian sulcus; *prf*, posterior rhinal fissure; *ps*, presylvian sulcus; *ss*, suprasylvian sulcus; *v*, vermis; VII–XII, cranial nerves

olfactory peduncles are covered by the brain, so the bulbs are considered sessile (Fig. 18.2). The relative size of the bulbs are quite large occupying close to 10% of the total endocranial cast.

The cerebrum presents differences in its shape that largely corresponds to the division into two families of extant armadillos (Delsuc et al. 2012; Gibb et al. 2016). In Dasypodidae, the cerebrum has an ovoid shape (Fig. 18.2a), while in Chlamyphoridae the shape is rather triangular both in dorsal and lateral views

(Fig. 18.2b–h). Within Chlamyphoridae, the most notable difference is presented in *Chlamyphorus* (Chlamyphorinae), since the brain has a strong antero-posterior flattening causing the cerebral hemispheres to have a transverse measurement greater than the length, as well as the olfactory bulbs and the cerebellum are flattened against them (Dozo 1989). All extant armadillos have a rather simple cortical sulcus pattern, represented by the suprasylvian sulcus in the temporal lobe and the presylvian sulcus, which extends anterodorsally in the frontal lobe. This sulcus pattern exists with some variability in all extant armadillos (Dozo 1989), but it may differ in fossil armadillos, as in *Utaetus buccatus* (from the Eocene) which possesses a sulcus that is interpreted as the union of the presylvian and suprasylvian sulci (Dozo 1998). There is a great development of the piriform lobe, as indicated by a high position of the rhinal fissure, which has an anterior and a posterior branch. The cerebellum is separated from the cerebrum by a low posteromedially ossified tentorium cerebelli. The cerebellar hemispheres are separated from the vermis by two deep paramedian sulci. The cerebellum also shows significant development, comprising between 18% and 25% of the total endocranial cast. These cerebellar size values are some of the highest values in relation to total size of the brain known among mammals (Clark et al. 2001).

Glyptodonts

The general outline of the digital endocasts of both Pleistocene and Miocene glyptodonts is triangular or trapezoidal in dorsal view (Fig. 18.3). The olfactory bulbs are large, with an oval cross-sectional shape. Unlike armadillos, the olfactory peduncles are not covered by the cerebrum, so they are clearly present in dorsal and lateral view. There is some variation among glyptodonts, since *Doedicurus* has a very short peduncle, while in *Panochthus* it is much more elongated. The olfactory bulbs diverge from each other, with *Pseudoplohophorus* showing the lowest angle at 37.5° , and *Panochthus* the highest 73° (measured at the ventral margin of the bulbs).

The shape of the cerebrum is triangular in dorsal view, as in extant Chlamyphorid armadillos, although in lateral view, unlike these, it is rather globose. In the genus *Glyptodon* it is possible to observe that in the new specimen analyzed here (ZMK 1-1845-9250) the cerebral hemispheres are a bit more flattened than the previously studied specimens described by Tambusso and Fariña (2015a). Besides this intraspecific variation, some interspecific variation is also observed (Fig. 18.3) with *Panochthus* showing a slightly more globose shape, being shorter and taller than the other glyptodonts. Unlike extant armadillos, in glyptodonts the rhinal fissure is not divided into anterior and posterior branches (Dozo 1998), but appears as a continuous groove with a slightly inclined path in the antero-ventral direction that can be observed in both lateral and dorsal views (Fig. 18.3). In *Panochthus* the rhinal fissure is shorter than in other glyptodonts. Ventrally, the rhinal fissure delimits a prominent piriform lobe, whose lateral expansion marks the maximum transverse width of the brain. As in extant armadillos, the neocortical sulcus pattern of glyptodonts is not very complex: the suprasylvian sulcus is observed in both lateral and

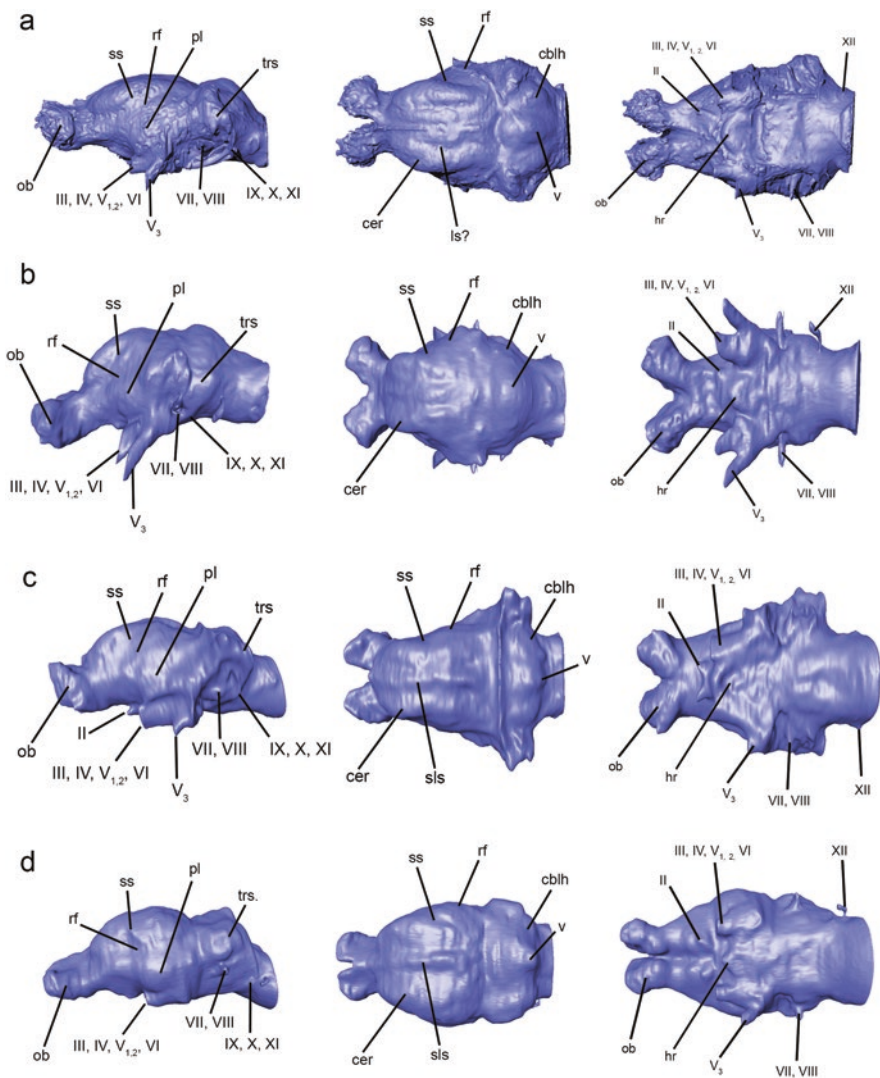


Fig. 18.3 Endocast of (a) *Glyptodon* in lateral, dorsal, and ventral views, (b) *Panochthus* in lateral, dorsal and ventral views, (c) *Doedicurus* in lateral, dorsal and ventral views, (d) *Pseudoplohophorus*, in lateral, dorsal and ventral views. Abbreviations: *cblh*, cerebellar hemisphere; *cer*, cerebrum; *ls?*, lateral sulcus; *ob*, olfactory bulb; *otc*, ossified tentorium cerebelli; *pl*, pyriform lobe; *rf*, rhinal fissure; *sls*, superior longitudinal sinus; *ss*, suprasylvian sulcus; *trs*, transverse sinus; *v*, vermis; II–XII, cranial nerves. Scale bars: 5 cm

dorsal views, following an oblique path in the postero-dorsal direction above the rhinal fissure. In the specimens of *Glyptodon* and *Pseudoplohophorus*, the suprasylvian sulcus is located towards the temporal lobe of the cerebral hemispheres, while in *Doedicurus* and most notably in *Panochthus* it is displaced towards the frontal

lobe (Fig. 18.3). In the new specimen of *Glyptodon* (ZMK 1-1845-9250), a second sulcus is evident (Fig. 18.3a), located between the midline and the suprasylvian sulcus, and following an anteroposterior path. This sulcus would seem to be present in the specimen Mpa 11-04 as well (Tambusso and Fariña 2015a), as both Dozo (1989) and Gervais (1869) mention that a depression in the same region could represent a second sulcus. This second sulcus is not clearly present in the other glyptodonts, although, in *Panochthus* there is a small depression in the region that may correspond to it. There is no evidence for the presence of a presylvian sulcus in any glyptodont endocast.

The cerebellum of glyptodonts is large, with a volume between 26.5% and 30.0% of the endocast (Tambusso and Fariña 2015a), a slightly larger proportion than in extant armadillos. There is no evidence of an ossified cerebellar tentorium, instead a transverse groove is observed in *Glyptodon*, *Pseudoplohophorus* and *Panochthus* (less marked in this one). In *Doedicurus*, a ridge-like structure can be seen above the groove that separates the cerebrum from the cerebellum (Fig. 18.3c). The cerebellum is transversally slightly narrower than the brain. Both Serres (1865) and Gervais (1869) mention that the maximum width of the cerebellum exceeds that of the brain; however, this measurement can be misleading due to the presence of other structures, such as venous sinuses that create the appearance of a wider cerebellum. Tambusso and Fariña (2015a) showed that the maximum width of the cerebellum is smaller than the maximum width of the cerebrum in all glyptodonts. The cerebellum maximum length/cerebrum maximum length ratio of glyptodonts is between 0.39 (*Pseudoplohophorus*) and 0.44 (*Panochthus*). This ratio is larger than that of extant euphractines (0.24–0.33) and smaller than of dasypodines (0.52–0.55), but is comparable to that of tolypeutines (0.44–0.48). The vermis and cerebellar hemispheres are clearly visible. As in extant armadillos, the vermis is more dorsally expanded than the cerebellar hemispheres, so that in lateral view it projects considerably over their dorsal surfaces. In *Pseudoplohophorus* this projection is more noticeable than in the other glyptodonts, and similar to that observed in the extant giant armadillo *Priodontes*.

On the ventral surface of the endocast it is possible to observe most of the cranial nerves (CN) (Fig. 18.3). The roots and trajectories of these nerves show little variation between the different species of glyptodonts and they are very similar to that of extant armadillos. The most notable differences among glyptodonts are that in *Panochthus* the roots of CN III, IV, V1,2 and VI are oriented more anteroventrally compared to the other species. In *Doedicurus* the root of CN V3 is not so close to the preceding roots (III, IV, V1,2 and VI), but attaches instead much further posterior, and in *Pseudoplohophorus* the internal auditory meatus (for CN VII and VIII) occupies a more dorsal position than in Pleistocene glyptodonts. The relative size of the roots of CN III, IV, V1-2, VI and V3 are much larger in glyptodonts than that of extant armadillos. Lastly, the hypophyseal fossa in glyptodonts is located more anteriorly, i.e. closer to the root of CN II, than in armadillos.

Regarding the cranial vasculature, the best represented vessels are the superior longitudinal sinus, clearly seen along the entire dorsal median surface of the brain, and the transverse sinus, represented by the rounded ridge observed between the

brain and cerebellum (although this latter one is not clearly observed in *Pseudoplohophorus*). In *Glyptodon*, above the pyriform lobes, a large vessel that originates in the transverse sinus and has an antero-ventral path could correspond to the middle cerebral artery. Part of the path of the internal carotid artery can be distinguished lateral to the hypophyseal region in *Glyptodon* and *Pseudoplohophorus* (Fig. 18.3).

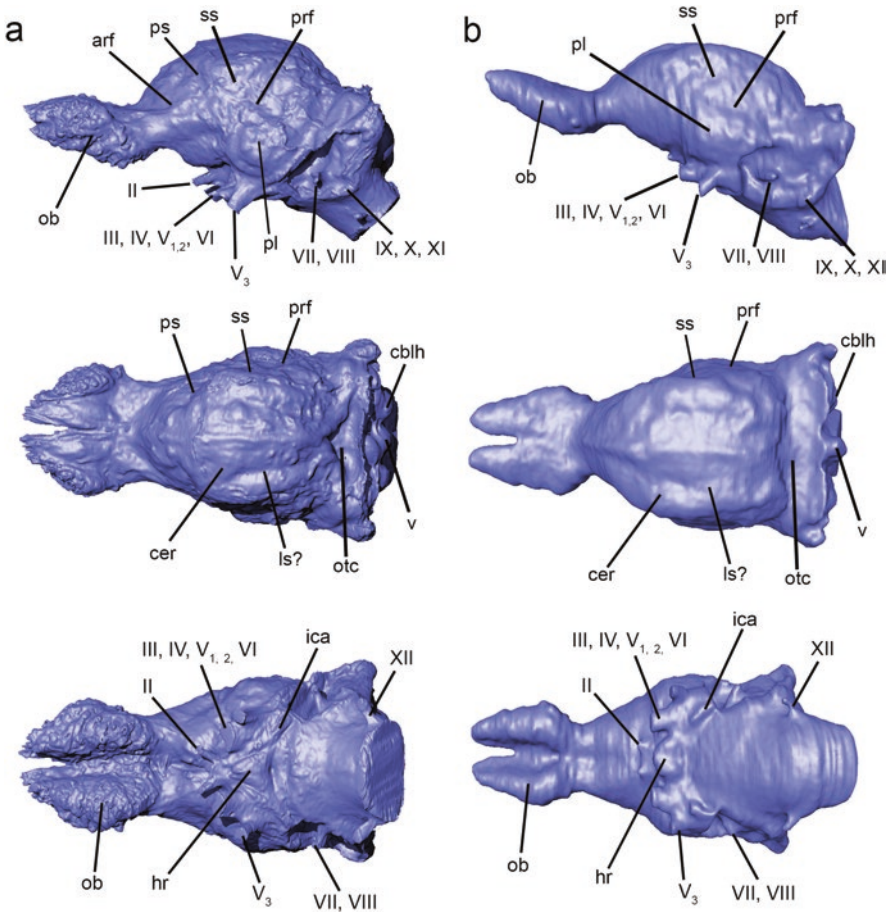


Fig. 18.4 Endocast of (a) *Holmesina* in lateral, dorsal and ventral views, (b) *Pamphaterium* in lateral, dorsal and ventral views. Abbreviations: *arf*, anterior rhinal fissure; *cblh*, cerebellar hemisphere; *cer*, cerebrum; *ls?*, lateral sulcus?; *ob*, olfactory bulb; *otc*, ossified tentorium cerebelli; *pl*, pyriform lobe; *prf*, posterior rhinal fissure; *ps*, presylvian sulcus; *ss*, suprasylvian sulcus; *v*, vermis; II–XII, cranial nerves

Pampatheres

One of the most notable differences that distinguish pampatheres with glyptodonts and armadillos is found in the olfactory bulbs (Fig. 18.4). These are pedunculated, large, very elongated in the anteroposterior direction and with the anteriormost ends dorsally displaced. They are not divergent from each other as in glyptodonts, and remain close to each other along their entire length as in armadillos. The bulbs of *Pampatharium* appear to be thinner than in *Holmesina*, although this may be the result of a better quality in the reconstruction of the endocast of the latter. The olfactory peduncles are relatively short compared to the total size of the bulbs but allow a clear separation between them and the brain.

The cerebrum is elongated in an anteroposterior direction. Its maximum transverse width is in the middle region of the endocast, mainly due to the lateral widening of the paleocortex. In *Pampatharium*, it is slightly dorsoventrally compressed, while in *Holmesina* it is more globose in lateral view. The rhinal fissure of *Pampatharium* appears to be continuous with a slightly sinuous and anterodorsal inclined trajectory. However, in *Holmesina* the presence of an anterior and posterior branch is evident, as in extant armadillos, as well as a presylvian sulcus (Fig. 18.4a). The suprasylvian sulcus emerges from the posterior branch of the rhinal fissure. A second sulcus with an anteroposterior path is located between the midline and the suprasylvian sulcus, similar to that observed in *Glyptodon* ZMK 1-1845-9250. This sulcus is very evident in *Holmesina*, while in *Pampatharium* it is observed more tenuously.

The cerebellum is a large structure in which it is possible to distinguish the vermis and laterally, separated by two prominent paramedian sulci, the cerebellar hemispheres (Fig. 18.4). Unlike glyptodonts, the size of the vermis is not much larger than that of the cerebellar hemispheres, resembling armadillos in this respect. In *Holmesina* a deep posteromedially ossified cerebellar tentorium similar to that observed in extant armadillos separates the brain and the cerebellum. While in *Pampatharium*, the tentorium appears to span the entire width of the endocast, almost completely separating the cerebrum from cerebellum at the dorsal level of the endocast. As in glyptodonts the maximum transverse width of the cerebellum is slightly less than the maximum width of the brain. However, the cerebellum/cerebrum length ratio (0.23–0.25) is less than in glyptodonts, and more comparable to that of extant euphractines.

The location, size and orientation of the cranial nerves do not differ from the general conditions observed in glyptodonts. In ventral view, the greatest difference is in the hypophyseal fossa of *Holmesina*, which is more elongated with a sub triangular shape, than is present in *Pampatharium* and glyptodonts.

18.3.2 Inner Ear Endocast Anatomy

The first comprehensive analyses of the inner ear diversity of extant xenarthrans demonstrated a strong phylogenetic signal in the morphology of the bony labyrinth (Billet et al. 2012, 2015). In cingulates, the geometric morphometric analysis of both the semicircular canals and the cochlea show that *Chlamyphorus* deviates from the pattern present in the rest of the armadillos (Billet et al. 2015). However, the analysis of discrete characters from the inner ear show support for the molecular results that ally the Chlamyphorinae to the Tolypeutinae, as well as for many traditional nodes. In fossil xenarthrans, the first studies of the inner ear were carried out in the sloths *Megatherium* and *Glossotherium* (Billet et al. 2013; Boscaini et al. 2018). Regarding cingulates, Tambusso et al. (2021) conducted the first morphological description of the bony labyrinth in the glyptodonts *Glyptodon*, *Panochthus*, *Doedicurus* and *Pseudoplohophorus*, and the pampathere *Holmesina* (Fig. 18.5).

The inner ear of glyptodonts and the pampathere are relatively small compared to skull size, as in the fossil sloths *Megatherium* and *Glossotherium* (Billet et al. 2013; Boscaini et al. 2018). Although Tambusso et al. (2021) did not perform a 3D geometric morphometric analysis similar to that of Billet et al. (2015) and Boscaini et al. (2018), the anatomical and morphometric comparison shows that there is relatively little variation among different glyptodonts, which mainly involves the semicircular canals, and more specifically, their size, shape, and the angles among the canals. Moreover, Tambusso et al.'s (2021) results also show that the inner ear of glyptodonts is largely similar to that of modern armadillos, and in particular, shares many similarities with *Chlamyphorus*. Whereas in the pampathere *Holmesina*, the inner ear is, in some aspects, similar to that of glyptodonts, but it also presents some characteristics that more closely resemble that of extant armadillos. The shared characters of glyptodonts with *Chlamyphorus* includes the small size of the semicircular canals (a character also observed in extant sloths, Billet et al. 2015), as well as the elongated shape of the lateral semicircular canal (lsc; shared also by tolpeutines, Billet et al. 2015). A rounded shape of the posterior semicircular canal (psc) is observed in glyptodonts and *Chlamyphorus*, whereas in most extant armadillos the psc is quite elongated. Both glyptodonts and *Chlamyphorus* have a reduced secondary common crus (the union of the posterior portion of the lsc and the ventral portion of the psc, distal to the posterior ampulla, Billet et al. 2015). The cochlea also has similarities, such as having fewer than two coils, a characteristic observed also in *Myrmecophaga* and *Glossotherium* (Billet et al. 2015; Boscaini et al. 2018). The secondary bony (basilar) lamina sulcus of the cochlea is indistinct or not observable in glyptodonts and *Chlamyphorus* (a condition also observed in sloths and *Myrmecophaga*, Billet et al. 2015; Boscaini et al. 2018). The cochlea is substantially smaller than in extant armadillos, and presents a large gap between the poorly coiled proximal part and the more tightly coiled distal part (Billet et al. 2015; Tambusso et al. 2021). *Holmesina* shares with glyptodonts the small size of the semicircular canals, the elongated shape of the lsc and the rounded shape of the asc (a condition similar to that observed in extant anteaters, Billet et al. 2015). The

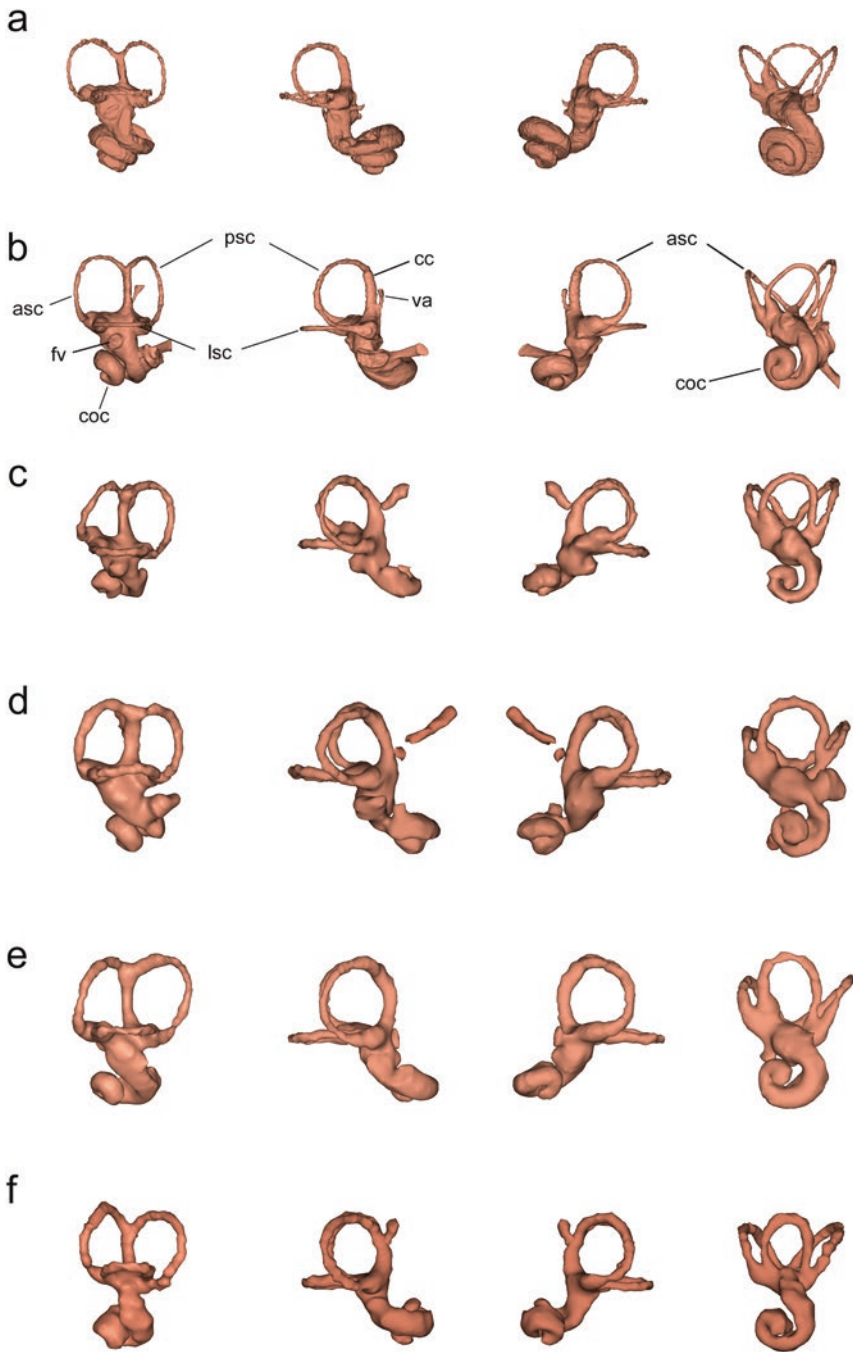


Fig. 18.5 Left inner ear of (a) *Dasypus*, in lateral, posterior, anterior and ventral view, (b) *Holmesina*, in lateral, posterior, anterior and ventral view, (c) *Glyptodon*, in lateral, posterior, anterior and ventral view, (d) *Panochthus*, in lateral, posterior, anterior and ventral view, (e) *Doedicurus*, in lateral, posterior, anterior and ventral view, (f) *Pseudoplohophorus*, in lateral, posterior, anterior and ventral view. Abbreviations: *asc*, anterior semicircular canal; *cc*, crus commune; *coc*, cochlea; *fv*, fenestra vestibuli; *lsc*, lateral semicircular canal; *psc*, posterior semicircular canal; *va*, vestibular aqueduct

relative size of the fenestra vestibuli in glyptodonts and *Holmesina* is slightly smaller than that of most extant armadillos (with the exception of tolypeutines) a condition shared by sloths and anteaters (Billet et al. 2015). The cochlea of *Holmesina* also has fewer than two coils. However, the gap between the proximal and distal parts is more reduced than in glyptodonts and it is not as tightly coiled as in extant armadillos, and as in them, a secondary bony (basilar) lamina sulcus appears to be distinct but reduced in extent. A secondary common crus is absent in *Holmesina*, as in *Dasypus*, and the semicircular canals are thinner than those of glyptodonts, more similar to those in most extant armadillos (Billet et al. 2015).

The lateral semicircular canal in glyptodonts is strongly tilted relative to the basicranial plane, with a lsc-basisphenoid angle that ranges between 49.8 and 54.1°; in *Holmesina*, this angle is equal to 41.4° (Tambusso et al. 2021). These values are higher than those observed for extant armadillos with the exception of *Dasypus kappleri* and *Zaedyus pichiy* (Coutier et al. 2017). The observations of Coutier et al. (2017) on head posture in living xenarthrans in comparison with the lsc orientation shows a good correspondence between the lsc-basisphenoid angle and head posture in cingulates. Therefore, the lsc-basisphenoid angles observed for glyptodonts and pampatheres imply that they would have held a strong nose-down head posture if the lsc were oriented horizontally, as proposed for their rest and/or usual head posture (Coutier et al. 2017). According to Benoit et al. (2020) this head posture could be related to the dietary habits (e.g. grazing ungulates have to keep their head low while foraging on grass), which would be in agreement with the grazing diet proposed for most large glyptodonts and pampatheres (Vizcaíno et al. 2004, 2011). Although this snout down head posture also may result from a strong phylogenetic correlation, since in most extant Cingulata, which have an insectivorous to omnivorous diet, a snout down posture was also observed (Coutier et al. 2017).

18.4 Brain Evolution and Paleobiological Inferences Based on Endocast Morphology

18.4.1 Morphological Brain Diversity

The endocranial casts of the four genera of Pleistocene glyptodonts examined here and in previous publications are fairly similar in their general morphology, and are also similar with the first casts analyzed by Serres (1865) and Gervais (1869). Some morphological variations can be observed but, as in extant armadillos, many general features are held in common among these species. The olfactory bulbs are large although, relative to the total volume of the cast, they comprise a somewhat smaller proportion than that of extant armadillos (Tambusso and Fariña 2015a). The cerebellum constitutes a large portion of the endocranial cast (26–30%) in glyptodonts, even larger than in extant armadillos, whereas the cerebrum is less developed than in that clade (Tambusso and Fariña 2015a). These results are consistent with the

observations made by Gervais (1869) about the small size of the brain of glyptodonts and their relatively larger cerebellum compared to the cerebrum.

Like extant armadillos, glyptodonts in general possessed a fairly primitive brain. As already mentioned, in most specimens analyzed only one neocortical sulcus can be distinguished, which, due to its position and orientation, is homologized with the suprasylvian sulcus. Gervais (1869: 45) described this sulcus, which according to him, delimits the Sylvian convolution in glyptodonts. This author mentions a possible second oblique sulcus in *G. clavipes*, and Dozo (1989) mentioned the presence of a depression in the cast of *Glyptodon* that could be homologized with the lateral sulcus of sloths. As mentioned before, a second sulcus is clearly observed in the cast of *Glyptodon* ZMK 1-1845-9250 and possibly in Mpa 11-04, which would confirm the presence of this sulcus in this genus. It is possible that this sulcus may be present in *Panochthus*, although it is not as clearly marked as in *G. clavipes*.

The endocranial cast of pampatheres represented by *Pampatherium* and *Holmesina* shows a combination of both unique characteristics and some others shared with glyptodonts and armadillos. The most peculiar feature of their endocast is the very antero-posteriorly elongated olfactory bulbs, a feature that is not shared by either glyptodonts or armadillos. The presence of a rhinal fissure with an anterior and posterior branch and a presylvian sulcus (observed in *Holmesina*) is shared with extant armadillos. Tambusso and Fariña (2015b) only observed the suprasylvian sulcus in *Pampatherium*; however, in the endocast of *Holmesina* described here, besides the presylvian sulcus, it is possible to observe another sulcus that can be homologized with the oblique sulcus observed in *Glyptodon*. This difference in the neocortical sulcal pattern between the two pampathere specimens may be due to the lower resolution of the computed tomography performed in *Pampatherium* (Tambusso and Fariña 2015b) than the one performed for *Holmesina*, which could have resulted in the lack of an observable presylvian and lateral sulcus in *Pampatherium*.

Dozo (1989) observed the presence of a sulcus located between the midline and the suprasylvian sulcus in the endocast of some extant and extinct armadillos (*Chaetophractus*, *Euphractus*, *Scagliatus*, *Epipeltephilus*, *Propalaeohoplophorus*). According to its location and size, this sulcus appears to be homologous with the oblique sulcus observed here in *Glyptodon* and *Holmesina*. Dozo (1989) named this groove “sulcus Z”, and mentions that it could be homologized with the lateral sulcus observed in extant and extinct sloths. One difference that glyptodonts exhibit relative to extant armadillos is a slightly greater development of the frontal region of the cerebrum. Dozo (1989) already noted that characteristic in *Glyptodon*, and attributes it to allometry or to its specialization for a grazing diet. This later hypothesis was based on Radinsky (1976) who noted that in ungulates the expansion of the frontal region could be related to the development of masticatory specializations. Similarly, the greater expansion of the frontal region in glyptodonts would be related to their masticatory adaptations for an herbivorous diet including the deepening of the maxillae for the hypselodont dentition (Vizcaíno et al. 2004, 2011). The endocast of pampatheres also shows this frontal expansion. Since their body size is much smaller than that of the large Pleistocene glyptodonts, but still much larger than

most extant armadillos, it can not be ruled out that it is due to an allometric effect. Moreover, as this group also presents specializations for a grazing diet (Vizcaíno et al. 2004), this hypothesis can not be ruled out either.

18.4.2 Brain-Size Evolution and Encephalization Quotient

The very small brain size relative to body mass of glyptodonts, already observed by Gervais (1869), is further substantiated when their encephalization quotient (EQ) is compared with those of other mammals. Tambusso and Fariña (2015a, b) evaluated the EQ of 796 extant mammals (included in 26 orders) and compared them with that of fossil xenarthrans. They showed that glyptodonts and ground sloths have very low EQs compared to other mammals. However, significant differences were also demonstrated in the allometric relationship of brain volume and body mass in the different orders. Due to the differences in the allometric relationship of brain volume and body mass in the several orders of mammals, the analysis of the EQ of extant and fossil cingulates was evaluated using the regression values for the order *Xenarthra* only, resulting in an expected brain volume of $E_c = 0.123 m^{0.606}$ (Tambusso and Fariña 2015a, b). This represents a lower slope compared to the equation for all other mammals of 0.751, and lower than most mammal orders with the exception of Afrosoricida, Artiodactyla and Cetacea (0.564, 0.585 and 0.516 respectively).

The EQ calculated from the equation for xenarthrans shows that extant and fossil cingulates present the lowest values among xenarthrans, with ranges between 0.39 and 0.94. The only exception is the armadillo *Cabassous* that has an EQ of 1.44, which places it in the range of extant and fossil sloths (Tambusso and Fariña 2015a). Within cingulates, Pleistocene glyptodonts have the lowest EQ values (0.39–0.61), whereas the Miocene glyptodont *Pseudoplohophorus* has an EQ in the range of extant armadillos (0.84). Pampatheres show EQ values of 0.69 (*Pampatherium*) and 0.84 (*Holmesina*), which are within the range of extant armadillos.

These results are interesting since, within xenarthrans, the Cingulata show a tendency to have smaller than expected brains relative to the entire clade, and this is independent of whether they are extant or extinct. Various explanations have been offered for variations in relative brain size including the hypothesis that the metabolic rate of individuals may play an important role (Isler and Van Schaik 2006). Extant Cingulata and Pilosa are two of the eutherian orders that possess the lowest basal metabolic rates (1.83 kJ/h and 2.05 kJ/h on average, respectively), the third order being Pholidota (1.81 kJ/h) (McNab 2008). In these mammals the low metabolic rate would be associated mainly with their highly specialized diets (tree leaves, insects, termites, ants) as well as the fact that they can be fossorial or arboreal (McNab 1986, 2008). However, this alone might not be sufficient to explain the differences of relative brain sizes between cingulates and pilosans, both extant and fossil. In particular, many of the extinct species (as well as some extant armadillos) have not had specialized diets, being able to be grazers, browsers, frugivores and even scavengers (Vizcaíno et al. 2004; Vizcaíno 2009).

A possible cause for the difference in brain size between Pilosa and Cingulata could be the presence of the carapace in cingulates. The carapace imposes certain restrictions on the biology and ecology of armored mammals, such as in locomotion (Lovegrove 2001) and thermoregulation (Superina and Loughry 2012). On the other hand, a possible benefit of the carapace is protection against predators (Superina and Loughry 2012). It is possible that cingulates can expend less energy on an expensive organ such as the brain, because of a reduced need for vigilance against predation that the carapace could allow when running to escape was not an option. In glyptodonts, the carapace and the large body size could have been a passive defense, and they would not have required high neuronal processing for the development of escape or defense strategies against predators. A small relative brain size associated with passive defense strategies is also observed in some ornithischian dinosaurs, such as the armored ankylosaurs, which had a low EQ in comparison with non-armored dinosaurs (except sauropods, Hopson 1977). Likewise, there are many convergences between glyptodonts and ankylosaurs, among the most noticeable of which is the tail club (Alexander et al. 1999; Blanco et al. 2009; Arbour and Zanno 2020), and due to the potential tail club's impact on locomotion, it would be possible that this convergence was also reflected in brain size.

The smaller brain size in Pleistocene glyptodonts compared to other cingulates could be due to biomechanical constraints. The carapace restricts the development of the cervical musculature that supports the skull, as reflected in the fusion of the cervical series. An increase in the size of the skull normally accompanies an increase in body size; therefore, the allometric scaling of the skull implies a proportionately stronger neck musculature to keep it in position. Since the skull weight increases in cubed proportions while the muscle strength grows in squared proportions, the neck musculature would have to increase in size to a point in which the covering by the carapace would restrict its increase. Telescoping the masticatory apparatus underneath the braincase reduces the moment arm of the skull (Fariña and Vizcaíno 2001), and the same holds true for a reduced brain size, perhaps compensating for the restricted cervical musculature. *Pseudoplohophorus* from the Miocene had a lower body mass (about 200 kg Tambusso and Fariña 2015a) and a less telescoped skull than the large Pleistocene glyptodonts, and its relative brain size (0.84) is the largest among the glyptodonts. In pampatheres, the same combination is observed. A poorly telescoped skull and lower body mass are accompanied by relative brain sizes similar to those of extant armadillos. This possible reduction in brain size in large glyptodonts can be observed in the position of the inner ear relative to the brain; in Pleistocene glyptodonts the inner ear appears laterally displaced, and separated by a gap from the brain, whereas in armadillos, pampatheres and *Pseudoplohophorus*, the inner ear is located very close to the brain. This lateral displacement can be compared with the orientation of the vestibular aqueduct, which shows clear differences between large glyptodonts in comparison to pampatheres and *Pseudoplohophorus* (Tambusso et al. 2021). In large ground sloths, this gap between the ear and the brain does not appear to be present (Boscaini et al. 2018; Billet et al. 2015). The small size of the brain in glyptodonts could be the result of a combination of factors that include life history, low metabolic rate, a

passive defense against predators, and the need to reduce skull weight. The relative small size of the brain might be also caused by some allometric effects: the large contribution of the carapace to cingulate body mass would make them heavier relative to body length when compared to other mammals, and this in turn could cause the EQ to skew lower.

18.4.3 Sensory Evolution: Vestibular Sense

The morphology of the inner ear of fossil cingulates shows that there is relatively little variation among glyptodonts. The existing variation is mainly concentrated in the semicircular canals, which exhibit a certain degree of difference in their size, shape and in the angles between the canals. The morphometric analysis of Tambusso et al. (2021) shows that the inner ear of glyptodonts is largely similar to that of modern armadillos, but they have many particular similarities to *Chlamyphorus*. This result is interesting because it is congruent with recent molecular analyses that show a close phylogenetic relationship between glyptodonts and the clade formed by Chlamyphorinae/Tolypeutinae (Delsuc et al. 2016), as well as in the constrained morphological analysis of Mitchell et al. (2016) to the Chlamyphorinae. The inner ear of pampatheres, (represented by *Holmesina*) is very similar to that of glyptodonts, but it also presents some characteristics that resemble extant armadillos more closely, in particular the thinner semicircular canals, the orientation of the vestibular aqueduct, the development of the secondary bony (basilar) lamina sulcus, and the presence of a reduced gap in the coiled cochlea.

Billet et al. (2015) performed a 3D geometric morphometric analysis on the bony labyrinth of the three orders of xenarthrans, that showed a well-defined discrimination of sloths, anteaters, and armadillos in their morphospace. The only exceptions are *Chlamyphorus*, which is closer to sloths, and *Megatherium*, which came out being closer to armadillos. This pattern is largely similar when only the three semicircular canals were analyzed, and, to a lesser extent, when only the cochlea was analyzed. Their results shows that *Chlamyphorus* is separated from the rest of extant armadillos mainly by having smaller and less rounded semicircular canals, and an irregular and poorly coiled cochlea. The analyses of Billet et al. (2015) show in general that *Dasybus* and euphractines are well differentiated, while tolpeutines have more distinct morphologies.

Tambusso et al. (2021) performed a functional analysis of the bony labyrinth following the methodology of Spoor et al. (2007) and Silcox et al. (2009) in order to evaluate the agility levels of extant and fossil cingulates. It should be noted that these methodologies have been criticized by several authors (see Boscaini et al. 2018) since they could suffer from great uncertainties. Spoor et al. (2007) assigned six agility categories (from extra slow to fast) to a large sample of extant mammals and evaluated the SC radii of curvature relative to body size, showing that agile mammals have relatively larger semicircular canals than slow ones. However, according to Malinzak et al. (2012), these a priori agility categories correspond to

subjective impressions. Spoor et al. (2007) used the mean SC radii of curvature, while Silcox et al. (2009) showed that the lateral SC (lsc) could be a better predictor of agility level. However, Billet et al. (2013) and Ruf et al. (2016) demonstrated the difficulty of using these later equations for extremely large and small-sized taxa. For this reason, the results obtained from these methodologies should be taken with caution. Tambusso et al. (2021) analyzed the \log_{10} LSCR (logarithm of lateral SC radius) vs. \log_{10} BM (logarithm of body mass) and performed phylogenetic generalized linear regressions (PGLS) in order to account for non-independence in biological data due to phylogenetic relationship. Also, following Malinzak et al. (2012) and Ruf et al. (2016), they evaluated the variance from 90° (90var) of the ipsilateral semicircular canals, that is, the deviations from orthogonality of the canals, which are correlated with sensitivity and angular head velocity, and consequently with locomotor agility.

The results of Tambusso et al. (2021) showed a significant correlation of the PGLS of \log_{10} LSCR vs \log_{10} Body Mass, consistent with previous results (Spoor et al. 2007). The analysis of the residuals of the lateral SC radius in relation to body mass and agility levels shows that xenarthrans' agility falls in the range of medium to extra slow. Taking into account the previous cautions about this methodology, the large Pleistocene glyptodonts would fall within the range of slow to medium-slow agility levels, along with most extant armadillos and *Glossotherium*. While *Holmesina* would fall in the range of medium-slow to medium agility levels, along with extant anteaters and *Megatherium*. Among glyptodonts, *Glyptodon* shows a relatively smaller LSC size, which could be explained by the fact that this genus does not have a caudal tube like *Pseudoplohophorus*, *Doedicurus* and *Panochthus*. These last two genera could have used their tails for defense or antagonistic behavior (Fariña 1995; Alexander et al. 1999, Blanco et al. 2009), which would require greater coordination, so this could be reflected in the size of the lsc. *Holmesina* has a relatively large lsc for its body size, which is similar to the condition in the armadillo *Priodontes*, and the anteaters *Tamandua* and *Myrmecophaga*, so it appears likely that it had higher levels of agility than glyptodonts.

The \log_{10} 90var analysis of Tambusso et al. (2021) shows that glyptodonts exhibit large variance in the angles of semicircular canals. *Pseudoplohophorus* and *Holmesina* produce the smallest values, with a \log_{10} 90var of 2.15 and 2.16, respectively; whereas, the remaining glyptodonts have higher values: *Glyptodon*, 2.32; *Panochthus*, 2.41; and *Doedicurus*, 2.55. This range of variance is consistent with that observed in most extant cingulates (from 2.12 to 2.49), with the exception of *Chlamyphorus* and *Chaetophractus* in which the \log_{10} 90var are considerably lower (1.72 and 1.62, respectively).

These functional aspects of the bony labyrinth show that the extinct cingulates would have been mostly slow animals, with agility similar to extant armadillos. Although it is possible to observe variation among glyptodonts and *Holmesina* that could be related to locomotor habits, intraspecific variation may represent an important source of variation, as observed in the extant xenarthrans' data (Billet et al. 2015). The results of Tambusso et al. (2021) represent a first approximation that can

be further improved with the inclusion of new specimens and species in future research.

18.5 Future Directions: Outstanding Questions and Perspectives

It is interesting that both the brain and the inner ear of the pampatheres show characteristics similar to glyptodonts and to extant armadillos, and in some cases, they are more similar to the latter. This would be consistent with the old hypothesis that pampatheres were not the sister group of the glyptodonts, but rather of some group of extinct or extant armadillos (Simpson 1930; Hoffstetter 1958; Paula Couto 1979). In such a case, it remains unclear which armadillo clade would be a good candidate as a sister group of pampatheres. It should be mentioned that some of the morphological characters that unite pampatheres most closely with glyptodonts come from the masticatory apparatus, and these could be the result of convergence due to similar adaptations to a grazing diet. A phylogenetic analysis by Tambusso et al. (2021) performed on a set of 16 characters defined by Billet et al. (2015) from the inner ear of extant and fossil xenarthrans resulted in groupings among the extant species that are congruent with the most recent molecular analysis of the armadillo subfamilial relationships (Gibb et al. 2016). Although it showed some differences in the species relationships within each subfamily. Glyptodonts grouped together with *Chlamyphorus* in a very consistent manner, which is partly congruent with the results from molecular phylogenetic analyses (Delsuc et al. 2016; Mitchell et al. 2016), and differ with the results of other morphological analyses in which all groups of cingulates were analyzed (e.g. Gaudin and Wible 2006). *Holmesina*, appeared as the sister taxon of the clade formed by *Chlamyphorus* and the glyptodonts, which is partially consistent with previous morphological phylogenies that placed it as the sister clade of the glyptodonts. The use of only these characters for a cladistics analysis has several limitations: fewer characters than taxa, the approach used for their definition in some cases, and the limited coverage regarding the region of the skeleton (Billet et al. 2015) which can lead to the phylogenetic inferences not being robust. Although this result is not conclusive, it shows that the inner ear morphology could potentially be phylogenetically informative, since it is apparently less variable than other character systems. For example, the osteoderms, which have been one of the main characters used to evaluate the taxonomy of glyptodonts, present variations in the different regions of the carapace of each individual, as well as morphological variations at ontogenetic, population and taphonomic levels (Zurita et al. 2011; Gillette et al. 2016), which has led to nomenclatural problems and taxonomic overestimates. Furthermore, as mentioned before, the brain endocast of *Holmesina* shows a neocortical sulcal pattern that resembles that of extant armadillos, in particular due to the presence of a presylvian sulcus, that is not evident in *Pampatherium* due, most likely, to the low resolution of the CT scans performed on

that genus. Considering this, it would be very interesting to encode characters from the brain to add to other morphological characters from the ear region and elsewhere, in order to analyze their possible implications for systematic relationships.

New molecular analyses have shaken the phylogenetic tree of sloths (Delsuc et al. 2019; Presslee et al. 2019), but some signs of these newly proposed relationships had already been observed in their endocast morphology (Boscaini et al. 2018). Similarly, the cingulate tree was also shaken by molecular analyses that included data from a glyptodont (Delsuc et al. 2016; Mitchell et al. 2016), and, as shown by Tambusso et al. (2021), the morphological data of the inner ear might be congruent with these new relationships. Therefore, until we have molecular data from pamphateres, it would be interesting to re-evaluate their phylogenetic relationships by adding new traits from the inner ear and, if possible, from the brain endocast.

The presence of convergent characters between glyptodonts and ankylosaurs could be another topic interesting to investigate. As mentioned above, these two clades are convergent in terms of being armored and having a tail club, but they also present convergences in the morphological evolution of these traits, i.e. the order of trait appearance in both clades evolved in a statistically similar pattern (Arbour and Zanno 2020). Given the restrictions and advantages that these characteristics confer on these clades, it would be interesting to evaluate whether some of the sensory systems, the brain and the inner ear, also present convergences.

18.6 Final Considerations

Although the brain of fossil cingulates such as glyptodonts has been known since the mid-nineteenth century thanks to the preservation of natural endocranial casts or the preparation of artificial casts, recent technological advances have made it possible to delve deeper into the study of its morphology, and how it relates to the evolutionary history and functional aspects of these animals.

In this way, it has been possible to observe some intrageneric variability in the endocasts of the genus *Glyptodon* thanks to the study of several specimens. The analysis of genera older and smaller than the giants of the late Pleistocene, such as *Pseudoplohophorus* from the late Miocene, will provide a more complete picture of the evolution of the brain in this group of mammals. However, more specimens, as well as new species, still need to be analyzed to better understand intraspecific variation, as well as the evolutionary and functional patterns in this group.

The description of the *Holmesina* endocast corroborated the observations that the brain of pamphateres presents some very important differences from both glyptodonts and extant armadillos. However, it also allowed us to observe characteristics that had not been observed in the *Pampatherium* endocast, such as the presence of a presylvian sulcus, which is characteristic of extant armadillos but is absent in glyptodonts.

In the case of the inner ear, the functional aspects of the bony labyrinth have shown that the extinct cingulates would have been mostly slow animals at least with agility similar to that of extant armadillos. The inner ear anatomy of glyptodonts is largely similar to that of modern armadillos, particularly with that of *Chlamyphorus*, which is congruent with recent molecular analyses. The inner ear of *Holmesina*, in contrast, presents some characteristics similar to glyptodonts and others more similar to extant armadillos, as it was the case for their brain anatomy. Therefore, the inclusion of traits from the inner ear and brain endocast would be highly interesting in any re-evaluation of their phylogenetic relationships.

Acknowledgments We would like to thank the technical staff of Hospital Mautone (Uruguay) for their assistance in the CT scans of *G. reticulatus*, *P. absolutus*, *D. clavicaudatus*, and *P. tuberculatus* skulls, and Prof. H.E.D. Zaher and A.B. Carvalho (MZUSP, Brazil) for allowing and performing the CT scanning of the *H. crypatae* skull. We also thank the Zoological Museum of Denmark for access to the specimen of *G. reticulatus* (ZMK 1-1845-9250). We are grateful to the reviewers Guillaume Billet and Timothy Gaudin for careful reading, comments and corrections that greatly improved the manuscript and to H. Greg McDonald for improving the English text. Finally, thanks to the editorial team, Ariana Paulina-Carabajal, Thomas E. Macrini, Stig Walsh and María Teresa Dozo, for the invitation to prepare in this chapter.

References

- Alexander RM, Fariña RA, Vizcaíno SF (1999) Tail blow energy and carapace fractures in a large glyptodont (Mammalia, Xenarthra). *Zool J Linnean Soc* 126:41–49
- Arbour VM, Zanno LE (2020) Tail weaponry in ankylosaurs and glyptodonts: An example of a rare but strongly convergent phenotype. *Anat Rec* 303(4):988–998
- Benoit J, Legendre LJ, Farke AA et al (2020) A test of the lateral semicircular canal correlation to head posture, diet and other biological traits in “ungulate” mammals. *Sci Rep* 10(1):1–22
- Billet G, Hautier L, de Muizon C et al (2011) Oldest cingulate skulls provide congruence between morphological and molecular scenarios of armadillo evolution. *Proc R Soc B Biol Sci* 278(1719):2791–2797
- Billet G, Hautier L, Asher RJ et al (2012) High morphological variation of vestibular system accompanies slow and infrequent locomotion in three-toed sloths. *Proc R Soc B Biol Sci* 279:3932–3939
- Billet G, Germain D, Ruf I et al (2013) The inner ear of *Megatherium* and the evolution of the vestibular system in sloths. *J Anat* 223(6):557–567
- Billet G, Hautier L, Lebrun R (2015) Morphological diversity of the bony labyrinth (inner ear) in extant xenarthrans and its relation to phylogeny. *J Mammal* 96(4):658–672
- Blanco RE, Rinderknecht A (2008) Estimation of hearing capabilities of Pleistocene ground sloths (Mammalia, Xenarthra) from middle-ear anatomy. *J Vertebr Paleontol* 28(1):274–276
- Blanco RE, Rinderknecht A (2012) Fossil evidence of frequency range of hearing independent of body size in South American Pleistocene ground sloths (Mammalia, Xenarthra). *C R Palevol* 11(8):549–554
- Blanco RE, Jones WW, Rinderknecht A (2009) The sweet spot of a biological hammer: the centre of percussion of glyptodont (Mammalia: Xenarthra) tail clubs. *Proc R Soc B Biol Sci* 276:3971–3978

- Boscaini A, Iurino DA, Billet G et al (2018) Phylogenetic and functional implications of the ear region anatomy of *Glossotherium robustum* (Xenarthra, Mylodontidae) from the Late Pleistocene of Argentina. *Sci Nat* 105:28. <https://doi.org/10.1007/s00114-018-1548-y>
- Boscaini A, Iurino DA, Sardella R et al (2020) Digital cranial endocasts of the extinct sloth *Glossotherium robustum* (Xenarthra, Mylodontidae) from the Late Pleistocene of Argentina: Description and comparison with the extant sloths. *J Mammal Evol* 27:55–71
- Clark DA, Mitra PP, Wang SS-H (2001) Scalable architecture in mammalian brains. *Nature* 411:189–193
- Coutier F, Hautier L, Cornette R et al (2017) Orientation of the lateral semicircular canal in Xenarthra and its links with head posture and phylogeny. *J Morph* 278:704–717
- Cuadrelli F, Zurita AE, Toriño P et al (2020) A new species of glyptodontine (Mammalia, Xenarthra, Glyptodontidae) from the Quaternary of the Eastern Cordillera, Bolivia: phylogeny and palaeobiogeography. *J Sys Palaeontol* 18(18):1543–1566
- De Iuliis G, Bargo SM, Vizcaíno SF (2000) Variation in skull morphology and mastication in the fossil giant armadillos *Pampatherium* spp. and allied genera (Mammalia: Xenarthra: Pampatheriidae), with comments on their systematics and distribution. *J Vertbr Paleontol* 20:743–754
- Dechaseaux C (1958) Encéphales de xénarthres fossiles. In: Piveteau J (ed) *Traité de paléontologie*. Masson, Paris, pp 637–640
- Delsuc F, Superina M, Tilak MK et al (2012) Molecular phylogenetics unveils the ancient evolutionary origins of the enigmatic fairy armadillos. *Mol Phylogenet Evol* 62:673–668
- Delsuc F, Gibb GC, Kuch M et al (2016) The phylogenetic affinities of the extinct glyptodonts. *Curr Biol* 26:R155–R156
- Delsuc F, Kuch M, Gibb GC et al (2019) Ancient mitogenomes shed light on the evolutionary history and biogeography of sloths. *Curr Biol* 29(12):2031–2042
- Dozo MT (1987) The endocranial cast of an early Miocene Edentate, *Hapalops indifferens* Ameghino (Mammalia, Edentata, Tardigrada, Megatheriidae). Comparative study with brains of recent sloths. *J Hirnforsch* 28:397–406
- Dozo MT (1989) Estudios correlativos paleo-neoneurológicos en edentados xenartros (Mammalia, Edentata, Xenarthra): Neuroevolución. Dissertation, Universidad Nacional de La Plata
- Dozo MT (1994) Interpretación del molde endocraneano de *Eucholoeops fronto*, un Megalonychidae (Mammalia, Xenarthra, Tardigrada) del Mioceno temprano de Patagonia (Argentina). *Ameghiniana* 31:317–329
- Dozo MT (1998) Neuromorfología de *Utaetus buccatus* (Xenarthra, Dasypodidae): un armadillo del Eoceno temprano de la Provincia del Chubut, Argentina. *Ameghiniana* 35:285–289
- Fariña RA (1985) Some functional aspects of mastication in Glyptodontidae. *Forts Zool* 30:277–280
- Fariña RA (1988) Observaciones adicionales sobre la biomecánica masticatoria en Glyptodontidae. *Bol Soc Zool Uru* 4:5–9
- Fariña RA (1995) Limb bone strength and habits in large glyptodonts. *Lethaia* 28:189–196
- Fariña RA, Parietti M (1983) Uso del método R.F.T.R.A. en la comparación de la morfología craneana en Edentata (Mammalia). *Res Com Jorn C Nat* 3:106–108
- Fariña RA, Vizcaíno SF (2001) Carved teeth and strange jaws: how glyptodonts masticated. *Acta Paleontol Pol* 46:219–234
- Fernicola JC, Porpino KO (2012) Exoskeleton and systematics: A historical problem in the classification of glyptodonts. *J Mamm Evol* 19:171–183
- Fernicola JC, Rinderknecht A, Jones W et al (2017) A new species of *Neoglyptatelus* (Mammalia, Xenarthra, Cingulata) from the late Miocene of Uruguay provides new insights on the evolution of the dorsal armor in cingulates. *Ameghiniana* 55(3):233–252
- Gaudin TJ (1995) The ear region of edentates and the phylogeny of the Tardigrada (Mammalia, Xenarthra). *J Vertebr Paleontol* 15(3):672–705
- Gaudin TJ (2004) Phylogenetic relationships among sloths (Mammalia, Xenarthra, Tardigrada): the craniodental evidence. *Zool J Linnean Soc* 140(2):255–305

- Gaudin TJ, Lyon LM (2017) Cranial osteology of the pampathere *Holmesina floridanus* (Xenarthra: Cingulata; Blancan NALMA), including a description of an isolated petrosal bone. Peer J 5:e4022. <https://doi.org/10.7717/peerj.4022>
- Gaudin TJ, Wible JR (2006) The phylogeny of living and extinct armadillos (Mammalia, Xenarthra, Cingulata): a craniodontal analysis. In: Carrano MT, Gaudin TJ, Blob RW et al (eds) Amniote paleobiology: perspectives on the evolution of mammals, birds and reptiles. University of Chicago Press, Chicago, pp 153–198
- Gervais P (1869) Mémoire sur les formes cérébrales propres aux édentés vivants et fossiles: précédé de remarques sur quelques points de la structure anatomique de ces animaux et sur leur classification. Nouvelles archives du Musée d'Histoire naturelle 5. Paris
- Gibb GC, Condamine FL, Kuch M et al (2016) Shotgun mitogenomics provides a reference phylogenetic framework and timescale for living xenarthrans. Mol Biol Evol 33(3):621–642
- Gillette DD, Ray CE (1981) Glyptodonts of North America. Smithson Contrib Paleobiol 40:1–255
- Gillette DD, Carranza-Castañeda Ó, White RS et al (2016) Ontogeny and sexual dimorphism of *Glyptotherium texanum* (Xenarthra, Cingulata) from the Pliocene and Pleistocene (Blancan and Irvingtonian NALMA) of Arizona, New Mexico, and Mexico. J Mamm Evol 23(2):133–154
- Góis F (2013) Análisis morfológico y afinidades de los Pampatheriidae (Mammalia, Xenarthra). Dissertation, Universidad Nacional de La Plata
- Góis F, Scillato-Yané GJ, Carlini AA et al (2012) Una nueva especie de *Holmesina* Simpson (Xenarthra, Cingulata, Pampatheriidae) del Pleistoceno de Rondônia, Sudoeste de la Amazonia, Brasil. Rev Bras Paleontol 15:211–227
- Góis F, González Ruiz LR, Scillato-Yané GJ et al (2015) A peculiar new Pampatheriidae (Mammalia: Xenarthra: Cingulata) from the Pleistocene of Argentina and comments on Pampatheriidae diversity. PLoS One 10(6):e0128296. <https://doi.org/10.1371/journal.pone.0128296>
- Hoffstetter R (1958) Xenarthra. In: Piveteau J (ed) Traité de Paléontologie. Masson, Paris, pp 535–636
- Hopson JA (1977) Relative brain size and behavior in archosaurian reptiles. Ann Rev Ecol Syst 8:429–448
- Isler K, van Schaik CP (2006) Metabolic costs of brain size evolution. Biol Lett 2:557–560
- Lovegrove BG (2001) The evolution of body armor in mammals: Plantigrade constraints of large body size. Evolution 55:1464–1473
- Lydekker R (1894) Contributions to a knowledge of the fossil vertebrates of Argentina, parte 2, Extinct Edentates of Argentina. An Mus La Plata:1–61
- Malinzak MD, Kay RF, Hullar TE (2012) Locomotor head movements and semicircular canal morphology in primates. Proc Natl Acad Sci Unit States Am 109(44):17914–17919
- McKenna MC, Bell SK (1997) Classification of mammals above the species level. Columbia University Press, New York
- McNab BK (1986) The influence of food habits on the energetics of eutherian mammals. Ecol Monogr 56:1–19
- McNab BK (2008) An analysis of the factors that influence the level and scaling of mammalian BMR. Comp Biochem Physiol Part A 151:5–28
- Mitchell KJ, Scanferla A, Soibelzon E et al (2016) Ancient DNA from the extinct South American giant glyptodont *Doedicurus* sp. (Xenarthra: Glyptodontidae) reveals that glyptodonts evolved from Eocene armadillos. Mol Ecol 25(14):3499–3508
- Patterson B, Segall W, Turnbull WD (1989) The ear region in xenarthrans (= Edentata: Mammalia). Part I. Cingulates. Fieldiana Geol 18:1–46
- Patterson B, Turnbull WD, Segall W, Gaudin TJ (1992) The ear region in xenarthrans (= Edentata: Mammalia). Part II. Pilosa (sloths, anteaters), palaeonodonts, and a miscellany. Fieldiana Geol 24:1–78
- Paula Couto C (1979) Tratado de Paleomastozoologia. Academia Brasileira de Ciências, Rio de Janeiro
- Presslee S, Slater GJ, Pujos F et al (2019) Palaeoproteomics resolves sloth relationships. Nat Ecol Evol 3(7):1121–1130

- Radinsky L (1976) New evidence on ungulate brain evolution. *Amer Zool* 16(2):207
- Ruf I, Volpato V, Rose KD et al (2016) Digital reconstruction of the inner ear of *Leptictidium auderiense* (Leptictida, Mammalia) and North American leptictids reveals new insight into leptictidan locomotor agility. *PalZ* 90(1):153–171
- Serres M (1865) Deuxième note sur le squelette du Glyptodon clavipes. *C R Acad Sci Paris* 61:457–466
- Silcox MT, Bloch JI, Boyer DM et al (2009) Semicircular canal system in early primates. *J Hum Evol* 56(3):315–327
- Simpson GG (1930) *Holmesina septentrionalis*, extinct giant armadillo of Florida. *Am Mus Novit* 422:1–10
- Spoor F, Garland T, Krovitz G et al (2007) The primate semicircular canal system and locomotion. *Proc Natl Acad Sci U S A* 104(26):10808–10812
- Superina M, Loughry WJ (2012) Life on the half-shell: Consequences of a carapace in the evolution of armadillos (Xenarthra: Cingulata). *J Mamm Evol* 19:217–224
- Tambusso PS, Fariña RA (2015a) Digital cranial endocast of *Pseudoplohophorus absolutus* (Xenarthra, Cingulata) and its systematic and evolutionary implications. *J Vertebr Paleontol* 35(5):e967853. <https://doi.org/10.1080/02724634.2015.967853>
- Tambusso PS, Fariña RA (2015b) Digital endocranial cast of *Pampatherium humboldtii* (Xenarthra, Cingulata) from the Late Pleistocene of Uruguay. *Swiss J Palaeontol* 134(1):109–116
- Tambusso PS, Varela L, Góis F et al (2021) The inner ear anatomy of glyptodonts and pampatheres (Xenarthra, Cingulata): functional and phylogenetic implications. *J S Am Earth Sci* 108:103189. <https://doi.org/10.1016/j.jsames.2021.103189>
- Vizcaíno SF (2009) The teeth of the “toothless”: novelties and key innovations in the evolution of xenarthrans (Mammalia, Xenarthra). *Paleobiology* 35:343–366
- Vizcaíno SF, Fariña RA, Bargo MS et al (2004) Functional and phylogenetical assessment of the masticatory adaptations in Cingulata (Mammalia, Xenarthra). *Ameghiniana* 41:651–664
- Vizcaíno SF, Cassini GH, Fernicola JC et al (2011) Evaluating habitats and feeding habits through ecomorphological features in glyptodonts (Mammalia, Xenarthra). *Ameghiniana* 48(3):305–319
- Zurita AE, Oliveira EV, Torino P et al (2011) On the taxonomic status of some Glyptodontidae (Mammalia, Xenarthra, Cingulata) from the Pleistocene of South America. *Ann Paleontol* 97(1–2):63–83

Chapter 19

The Endocranial Cavities of Sloths (Xenarthra, Folivora): Insights from the Brain Endocast, Bony Labyrinth, and Cranial Sinuses



Alberto Boscaini, Dawid A. Iurino, Raffaele Sardella, Timothy J. Gaudin,
and François Pujos

19.1 Systematic and Phylogenetic Context

Xenarthra are composed of Cingulata (armadillos, glyptodonts, and pampatheres), and Pilosa, which includes Folivora (sloths) and Vermilingua (anteaters), and together constitute an “assemblage unlike anything that evolved elsewhere in the world” (Patterson and Pascual 1968: p. 422). Xenarthrans originated in South America by at least the early Eocene (Bergqvist et al. 2004; Gelfo et al. 2009; Gaudin and Croft 2015), but several clades expanded across the entire American continent later in the Cenozoic (e.g. Pascual 2006; Woodburne 2010). The earliest

A. Boscaini (✉)

Instituto de Ecología, Genética y Evolución de Buenos Aires (IEGEBA – CONICET),
Departamento de Ecología, Genética y Evolución, Facultad de Ciencias Exactas y Naturales,
Universidad de Buenos Aires, Ciudad Autónoma de Buenos Aires, Argentina
e-mail: aboscaini@ege.fcen.uba.ar

D. A. Iurino

PaleoFactory, Sapienza Università di Roma, Rome, Italy
e-mail: dawid.iurino@uniroma1.it

R. Sardella

PaleoFactory, Sapienza Università di Roma, Rome, Italy

Dipartimento di Scienze della Terra, Sapienza Università di Roma, Rome, Italy

e-mail: raffaele.sardella@uniroma1.it

T. J. Gaudin

Department of Biology, Geology, and Environmental Sciences, University of Tennessee at
Chattanooga, Chattanooga, TN, USA

e-mail: Timothy-Gaudin@utc.edu

F. Pujos

Instituto Argentino de Nivología, Glaciología y Ciencias Ambientales (IANIGLA), CCT-
CONICET-Mendoza, Mendoza, Argentina

e-mail: fpujos@mendoza-conicet.gob.ar

record of pilosans is that of *Pseudoglyptodon*, an enigmatic sloth from the late Eocene–early Oligocene of Chile and Argentina (McKenna et al. 2006), whereas the earliest undisputable fossil of an anteater is from the late Oligocene–early Miocene of the Argentinian Atlantic coast (Carlini et al. 1992). However, it is not until the early Miocene that well-preserved, nearly complete pilosan skulls become available, reflecting the extreme paucity of data on early cranial morphology in the clade (Gaudin and Croft 2015).

The three extant anteater genera (i.e. *Cyclopes*, *Myrmecophaga*, and *Tamandua*) currently inhabit the tropical forests and open grasslands of Central and South America. They are terrestrial/arboreal mammals that display a remarkable set of anatomical adaptations to myrmecophagy (Naples 1999; McDonald et al. 2008). Similarly, the fossil record of Vermilingua comprises two undoubted genera (i.e. *Protamandua* and *Palaeomyrmidon*) and a probable third genus, *Neotamandua* (Gaudin and Branham 1998; Casali et al. 2020), known from cranial remains, all of which display the same specialist feeding habits (McDonald et al. 2008; Bargo et al. 2012). The scanty nature of their fossil record and the lack of detail in several of the known fossil skulls (Bargo et al. 2012; Gaudin and Croft 2015) are surely some of the main factors that have impeded a paleoneurological exploration of the clade Vermilingua. However, this limitation is not present in their sister group, Folivora.

Extant sloths are represented by only two genera, the three-toed *Bradypus*, and the two-toed *Choloepus*, both restricted to modern tropical rain forests of Central and South America (Nowak 1999). They are folivorous, almost exclusively arboreal mammals, with distinctive upside-down posture and suspensory behavior (Hayssen 2010, 2011; Nyakatura 2012). The sloth fossil record is characterized by much greater richness, incorporating more than 90 extinct genera from all over the American continent, including the West Indies (McKenna and Bell 1997). Not only was the taxonomic diversity of extinct Folivora greater than today, but also its morphological disparity. In fact, remarkable variation has been observed in aspects ranging from general body size (spanning a few kilograms to 3–4 tons; Raj Pant et al. 2014; Toledo et al. 2017) to morphologies associated with differing feeding habits (including grazers, browsers, and mixed feeders; Bargo et al. 2006; Bargo and Vizcaíno 2008; Pujos et al. 2012) and locomotory modes (including arboreal and semiarboreal taxa, facultative bipeds, obligate quadrupeds, and even some swimming taxa; Pujos et al. 2012; Amson et al. 2014; Toledo 2016).

Despite the strong similarity in feeding habits and locomotion between *Bradypus* and *Choloepus*, the diphyletic origin of the two extant sloth genera is almost universally accepted, although a consensus on their phylogenetic relationships is still far from being achieved (e.g. Engelmann 1985; Gaudin 1995, 2004; Clack et al. 2012; Slater et al. 2016; Varela et al. 2019; Delsuc et al. 2019; Presslee et al. 2019). Phylogenetic analyses based on osteological characters consider *Bradypus* the only representative of Bradypodidae and the sister taxon to the other main clades (Gaudin 1995, 2004; Varela et al. 2019). *Choloepus* is considered the sole living member of Megalonychidae and is deeply nested in a group composed of extinct species from the Antillean islands (Gaudin 1995, 2004; Varela et al. 2019). The other three major extinct sloth clades are the Nothrotheriidae, the Megatheriidae, and the Mylodontidae

(e.g. Engelmann 1985; Gaudin 2004; McDonald and De Iuliis 2008). The enigmatic *Pseudoglyptodon* is currently considered the oldest and perhaps most primitive sloth – it has not been assigned to any of these groups (Boscaini et al. 2019; Varela et al. 2019). In contrast, recent phylogenetic analyses based on ancient DNA and collagen sequences recovered *Bradypus* among the extinct megatherioids and *Choloepus* among the extinct mylodontid sloths (Delsuc et al. 2019; Presslee et al. 2019). In this revolutionary scenario, the extinct Antillean taxa still constitute a monophyletic group (i.e. Megalocnidae), but positioned as the sister clade to all other extant and extinct sloths (Delsuc et al. 2019; Presslee et al. 2019).

Giving this context, a reappraisal of folivoran morphology-based phylogenetic analyses is an urgent need. At the same time, a further exploration of poorly known morphologies, such as the digitally reconstructed skull endocasts of modern and fossil taxa, assumes greater importance. In fact, new morphological information has the potential not only to reveal hidden phylogenetic signatures, but also to shed new light on the paleobiology of extinct sloths and their peculiar adaptations.

19.2 Historical Background

19.2.1 *The Record of Endocranial Morphology of Fossil Sloths*

The first information on the endocranial anatomy of an extinct folivoran, and the corresponding paleobiological inferences, dates back to an 1856 publication of Richard Owen (1804–1892) on the giant megatheriine sloth *Megatherium americanum*. In this work, the famed British paleontologist noted the extensive cranial sinuses and the relatively small size of the brain cavity, which “must have been less, by nearly one half, than that of the Elephant”, and suggested that “*Megatherium* was a beast of less intelligence, and with the command of fewer resources, or less varied instincts, than the Elephant” (Owen 1856: pp. 574–575).

A few years later, the first solid 3D model of an extinct sloth brain cavity, that of the mylodontine *Mylodon robustus* (= *Glossotherium robustum*) was produced, presumably as a plaster cast taken from a naturally or intentionally broken skull, although the author does not specify his methodology (Pouchet 1868–1869; Fig. 19.1). It appeared, together with those of other extant and extinct xenarthrans, in a publication of Charles Henri Georges Pouchet (1833–1894). In this work, the French anatomist suggested that the complexity of the brain of this extinct sloth appeared to be higher than that of the surviving forms, casting doubt on the “*marche progressive et ascendante du développement de l’encéphale chez des espèces immédiatement dérivées les unes des autres à travers le temps*” (progressive and ascending march of the development of the encephalon in species immediately derived from each other over time) (Pouchet 1868–1869: p. 359), an established paradigm of the nineteenth century. The same endocast of *Glossotherium robustum* is also described in a second and more comprehensive study by François Luis Paul Gervais

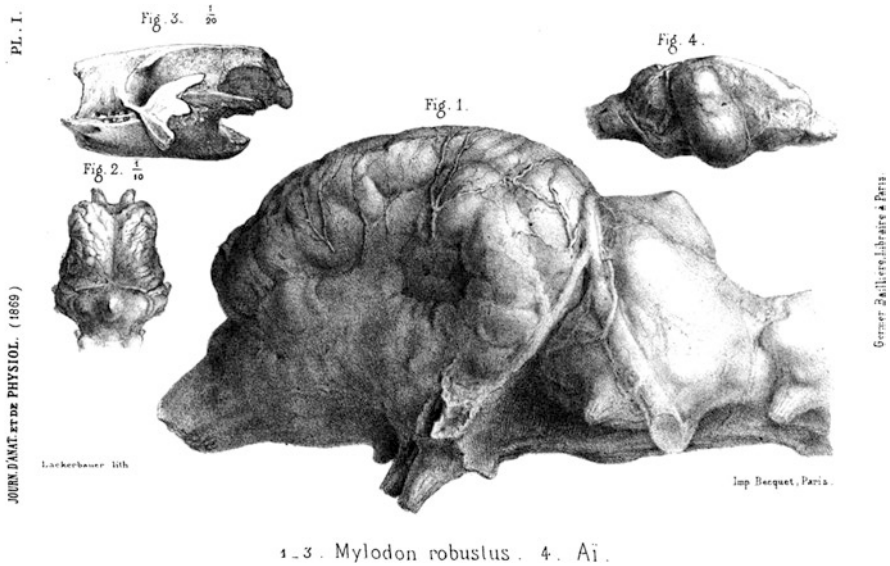


Fig. 19.1 First published illustration of a three-dimensional model of an extinct sloth brain endocast (i.e., *Glossotherium robustum*) and its comparison with the brain endocast of the three-toed sloth. (Modified from Pouchet 1868–1869)

(1816–1879). In this extended comparative work, Gervais (1869) figured for the first time other solid endocasts from extinct sloths, including those of the giant megathere *Megatherium americanum* and the mylodontid *Scelidotherium leptcephalum*. Gervais (1869) also identified a general similarity among the brain endocasts of extinct and extant sloths, in both their general shape and their convolution patterns, providing additional morphological support for the earlier attribution of *Megatherium americanum* to the folivoran clade (Cuvier 1796). At the end of the nineteenth century, after the discovery of the iconic “Cueva del Milodón” in southern Patagonia, several works were dedicated to the study of an extinct mylodontid sloth found in an exceptional state of preservation. These include a study by the British paleontologist Arthur Smith Woodward (1864–1944) who described, in Woodward (1900), the plaster cast of the brain cavity of *Grypotherium* (*Neomylodon*) *listai* (= *Mylodon darwini*).

With the dawn of a new century, comparative paleoneurological studies on extant and extinct South American mammals finally commenced in the southern hemisphere. Remarkable efforts were made by the German neurobiologist Christfried Jakob (1866–1956; Fig. 19.2a) and the Italian zoologist Clemente Onelli (1864–1924; Fig. 19.2b), who both adopted Argentina as their country of vocation (Triarhou and del Cerro 2006; Brinkman and Vizcaíno 2014). Their collaboration took place in the first decade of the twentieth century and their first results were presented in 1910 in two important scientific events held in conjunction with celebrations for the centennial of the Argentinian May Revolution (Jakob and Onelli

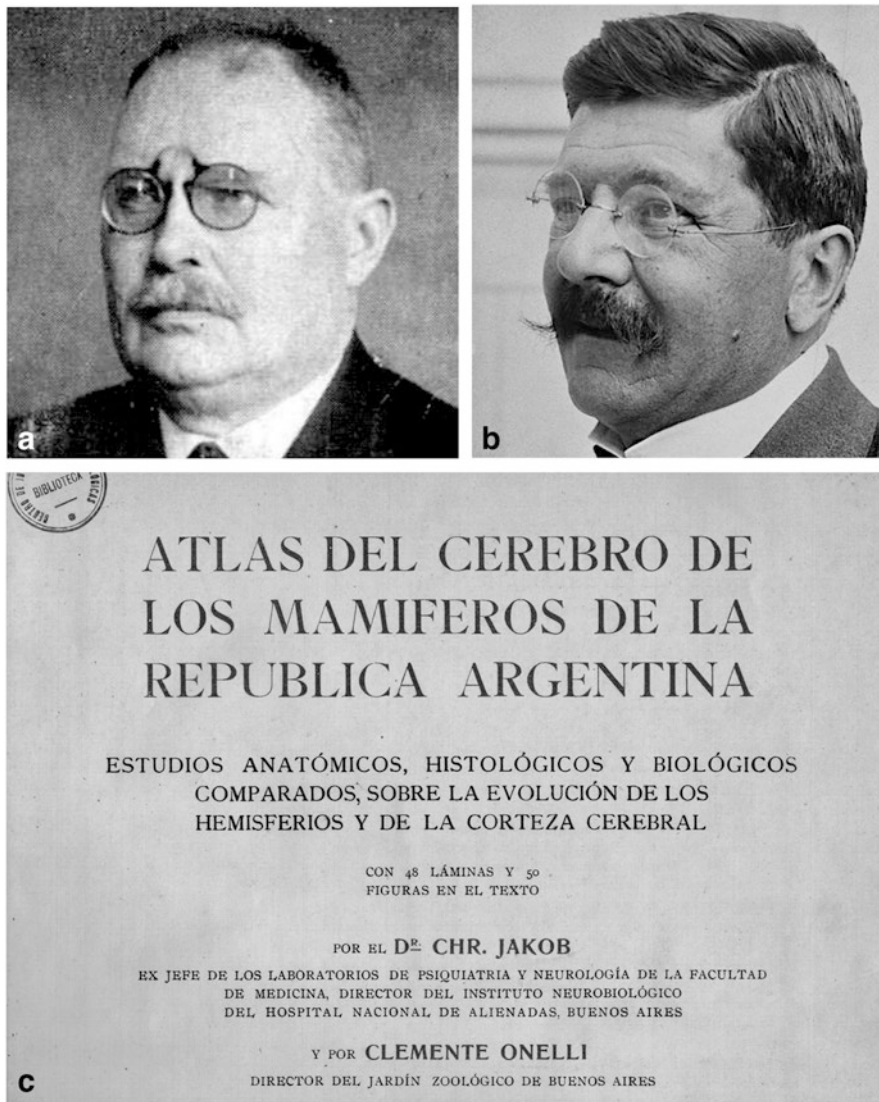


Fig. 19.2 Christfried Jakob (a), Clemente Onelli (b), and the frontispiece of their 1913 atlas on the brains of some mammalian species from Argentina (c). (Modified from Triarhou and del Cerro 2006 and Brinkman and Vizcaíno 2014)

1910; Jakob 1912). Analyzing the convolution pattern of their brains, Jakob (1912) noticed a certain similarity between *Megatherium* and the extant *Bradypus*, whereas the morphology of the large mylodontines *Lestodon* and *Grypotherium* (= *Mylodon*) were thought to compare favorably with the living anteater *Myrmecophaga* and the cingulate *Dasybus*, respectively.

The neuroanatomical studies of Jakob and Onelli were published in German (Jakob and Onelli 1911) and Spanish (Jakob and Onelli 1913). The 1913 Argentinian edition of their atlas (Fig. 19.2c) represents the first treatment of this subject in South America, combining phylogenetic and ontogenetic approaches (Triarhou and del Cerro 2006). They analyzed brains from 40 extant South American mammals, including modern cingulates and pilosans, as well as brain endocasts of some extinct notoungulates and xenarthrans. Among them, casts of the giant sloths *Grypotherium* (= *Myiodon*), *Megatherium*, and *Lestodon* were figured (Jakob and Onelli 1913).

Soon thereafter, Lull (1915) illustrated a partial reconstruction of the brain endocast of *Myiodon harlani* (= *Paramyiodon harlani*) from the Pleistocene of North America, stressing the striking similarities between its convolutions and those of the extant two-toed sloths. A more complete brain endocast of *Paramyiodon harlani* was later obtained by Stock (1925), together with those of other extinct taxa, specifically the stem megatherioid *Hapalops* sp. and the Pleistocene nothrothere *Nothrotherium shastense* (= *Nothrotheriops shastensis*) (Stock, 1925: Plate 3). Stock (1925) also noted that the pattern of convolutions was more complex in larger sized species than in smaller ones.

In the second half of the twentieth century, additional studies on brain endocasts of extinct folivores were conducted by Colette Dechaseaux, with a reappraisal of previous studies (Gervais 1869; Jakob and Onelli 1913; Stock 1925) and a re-description of some specimens (Dechaseaux 1958, 1962a, b). A few years later, Dechaseaux (1971) described a new endocranial cast belonging to the mylodontine *Oreomyiodon wegneri* (= *Glossotherium wegneri*, following De Iuliis et al. 2020) from the Pleistocene of Ecuador, and produced the first exhaustive study of the endocranial anatomy of an extinct sloth. In this detailed study, she confirmed the general conservatism of brain morphology in extant and extinct sloths, but stressed some peculiar traits of the early Miocene *Hapalops* sp. from the Santa Cruz Formation of Argentinian Patagonia. This taxon, similar to the extant genus *Bradypus*, exhibits a brain endocast with a less globose aspect and fewer sulci than that of other extant and extinct forms (Dechaseaux 1971). A similar morphology is also present in other early Miocene specimens from Santa Cruz, such as those of *Hapalops indifferens* and the stem-megalonychid *Eucholoeops fronto* (Dozo 1987, 1994).

Currently, a greater worldwide access to new techniques such as CT scanning and digital 3D reconstruction has enabled large-scale, non-destructive access to the internal cranial features of both extinct and extant vertebrates. This approach allows the exploration of brain endocasts in greater detail, but also allows access to other cavities within skulls, such as the bony labyrinth and cranial sinuses. These high-resolution scans can in some cases also recover important details related to the trajectories of cranial nerves and blood vessels. The applications of these new techniques to extant and extinct Folivora started less than a decade ago, and are now undergoing a rapid increase (e.g. Billet et al. 2012, 2013, 2015; Coutier et al. 2017; Amson et al. 2018; Boscaini et al. 2018, 2020a, b). In these works, the sloth endocranial cavities that have been more intensively analyzed are: (i) the brain cavity and cranial nerves, (ii) the bony labyrinth of the inner ear, and (iii) the cranial sinuses.

The present study summarizes the main results of these most recent investigations, and explores possible future directions of research.

19.3 Overview of General and Comparative Anatomy

19.3.1 Brain Cavity and Cranial Nerves

Brain Cavity

Like the early brain endocasts produced in the nineteenth century, the first extinct sloth species whose neuroanatomy was studied in detail using digital methods was *Glossotherium robustum* (Boscaini et al. 2020a; Fig. 19.3a–c).

The brain endocast of this species was compared to that of the modern arboreal forms *Bradypus variegatus* (Fig. 19.3j–l) and *Choloepus hoffmanni* (Boscaini et al. 2020a; Fig. 19.3g–i), and subsequently, to that of another extinct mylodontid sloth, the scelidotheriine *Catonyx tarijensis* (Boscaini et al. 2020b; Fig. 19.3d–f).

In accordance with the first paleoneurological studies of extant and extinct sloths, a general resemblance in brain anatomy among folivorans was also evident when analyzing digital models (Boscaini et al. 2020a, b; Fig. 3). This similarity applied not only to the general shape of the brain, but also to its pattern of convolutions. This suggests that the brain morphology of the clade has remained quite conservative during the last ~16-million-years, independently of body size variations (e.g. Dozo 1987, 1994; Boscaini et al. 2020a). However, some important differences have been detected among these taxa regarding the anatomy of the olfactory bulbs, cerebral hemispheres, and cerebellum.

In dorsal view, the olfactory bulbs are divergent and display a horizontal anterior margin in *Glossotherium*, *Catonyx*, and *Choloepus* (Fig. 19.3a, d, g), whereas they are closer to each other and pointed at their anterior tip in *Bradypus* (Fig. 19.3j). The ventral margin of the olfactory bulbs is inclined more anterodorsally in *Glossotherium*, *Catonyx*, and *Choloepus* (Fig. 19.3b, e, h) in lateral view, whereas the margin is almost horizontal in *Bradypus* (Fig. 19.3k).

The convolution pattern of the cerebral hemispheres is simpler in *Bradypus* than in all the other sloths analyzed (Boscaini et al. 2020a, b). In fact, in dorsal view, only the lateral sulcus is observable in *Bradypus*, running anteroposteriorly along almost the entire length of the cerebral hemisphere (Fig. 19.3j). In contrast, *Glossotherium*, *Catonyx*, and *Choloepus* also exhibit a detached entolateral sulcus on the dorsal side of their brain endocast (Fig. 19.3a, d, g). In these latter genera, the entolateral sulcus is shorter and placed more medially than the lateral sulcus (Boscaini et al. 2020a, b). Similarly, the convolution pattern in *Bradypus* is quite peculiar in lateral view, with the presence of marked tuberosities at the level of the temporal lobe and the anterior portion of the suprasylvian gyrus (Fig. 19.3k). These are less pronounced in other sloth taxa (Fig. 19.3b, e, h).

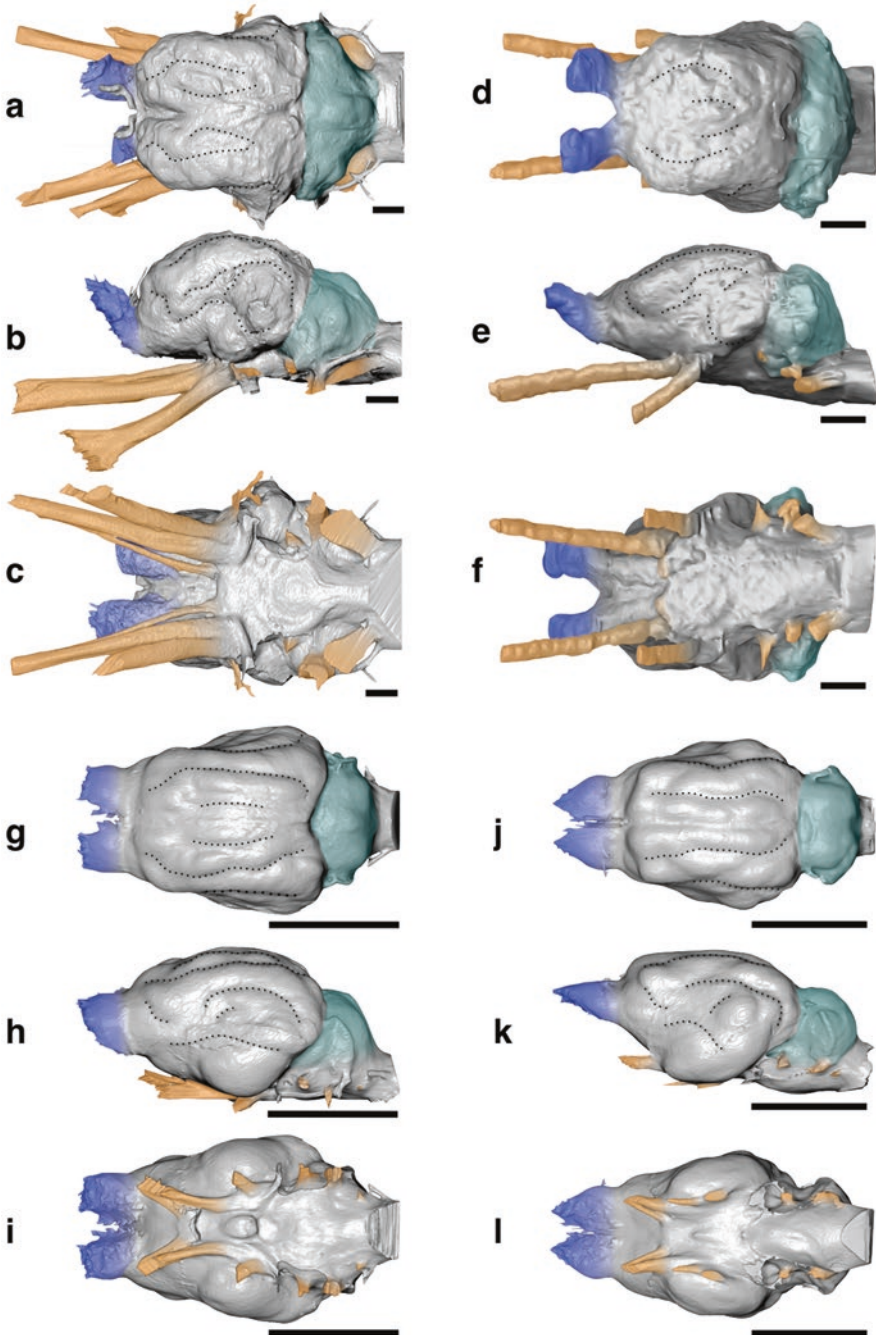


Fig. 19.3 Brain endocasts of *Glossotherium robustum* (a–c), *Catonyx tarijensis* (d–f), *Choloepus hoffmanni* (g–i), and *Bradypos variegatus* (j–l), in dorsal (a, d, g, j), lateral (b, e, h, k), and ventral (c, f, i, l) views. Colors indicate: blue, olfactory bulbs; grey, cerebrum; orange, neurovascular connections; turquoise, cerebellum. Scale bars equal 2 cm. (Modified from Boscaini et al. 2020a, b)

In *Glossotherium* and *Catonyx*, the cerebellum is greatly enlarged mediolaterally in dorsal view (Fig. 19.3a, d). The cerebellum appears less broad transversely in *Choloepus* (Fig. 19.3g), whereas *Bradypus* (Fig. 19.3j) shows the narrowest condition (Boscaini et al. 2020a, b). A well-defined vermis, located in the middle of the cerebellar hemispheres in dorsal view, is visible in *Glossotherium*, *Catonyx*, and *Choloepus* (Fig. 19.3a, d, g), whereas it is absent in *Bradypus* (Fig. 19.3j).

Cranial Nerves

Digital models allow the reconstruction of the trajectories of the main cranial nerves emerging from the brain cavity with a consistently higher resolution than previous non-digital models (Boscaini et al. 2020a, b). Based on these models, it is evident that in the extinct giant sloths *Glossotherium* and *Catonyx*, the grooves for the sphenorbital fissure, the foramen ovale, and the hypoglossal foramen are relatively larger than other foramina transmitting cranial nerves. In contrast, more uniformity in the relative size of the nerve-transmitting foramina is observed in *Bradypus* and *Choloepus* (Boscaini et al. 2020a, b; Fig. 3).

According to the available data, another difference in the organization of the cranial nerves ramifications is present. In *Bradypus* (Fig. 19.3l), the maxillary division of the trigeminal nerve (V_2) extends into the foramen rotundum independently (Boscaini et al. 2020a). In contrast, in *Glossotherium* (Fig. 19.3c), *Catonyx* (Fig. 19.3f), and some *Choloepus* specimens (Fig. 19.3i), both the ophthalmic (V_1) and maxillary (V_2) divisions of the trigeminal nerve pass through the sphenorbital fissure (Gaudin 2004, 2011; Boscaini et al. 2020a, b).

19.3.2 Bony Labyrinth

The first digitally reconstructed models of the bony labyrinth in sloths are those of the extant sloth genera *Bradypus* and *Choloepus* (Billet et al. 2012). These analyses demonstrated a peculiar shape for the semicircular canals in extant sloths. The canals appear particularly thick and possess a reduced radius of curvature compared to those of other xenarthrans and of mammals in general (Billet et al. 2012, 2015; Fig. 19.4c, d).

Additionally, the semicircular canals of living sloths show an unusual amount of intraspecific variation in their shape, angles, and relative size - this variable configuration is more evident in *Bradypus* than *Choloepus* (Billet et al. 2012). The configuration of the semicircular canals in the extinct giant sloths *Glossotherium robustum* (Boscaini et al. 2018; Fig. 19.4a) and *Megatherium americanum* (Billet et al. 2013; Fig. 19.4b) are, like those of anteaters and cingulates, thinner with a larger radius of curvature, therefore contrasting with the morphology of the extant sloths. These two extinct sloth genera also exhibit a strongly oblique orientation of the lateral semicircular canal relative to the cranial base (Billet et al. 2013; Boscaini et al. 2018), a

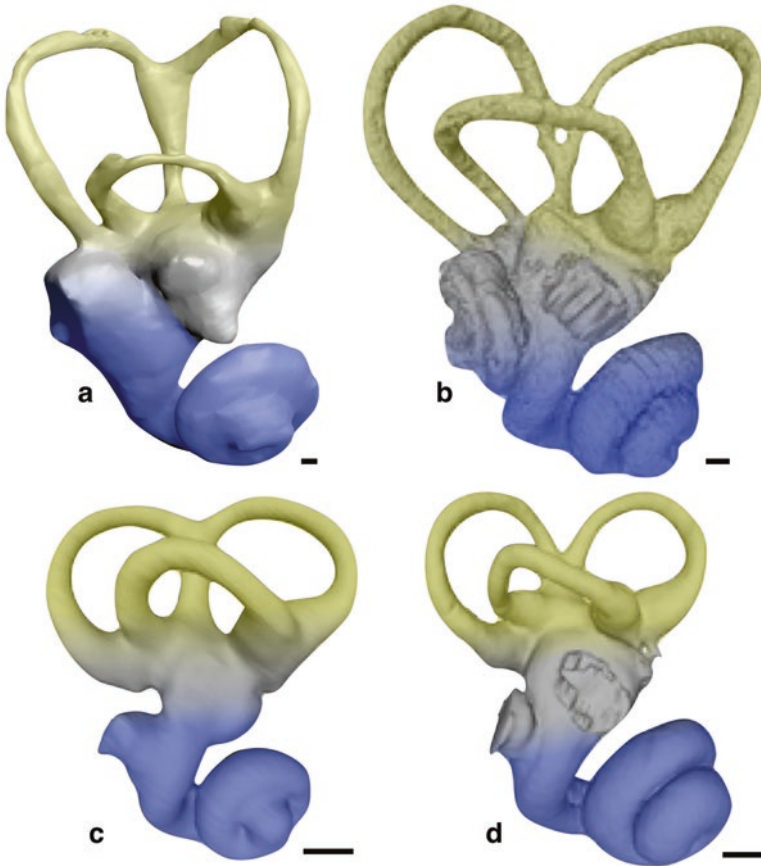


Fig. 19.4 Lateral view of the bony labyrinth of *Glossotherium robustum* (a), *Megatherium* sp. (b), *Choloepus hoffmanni* (c), and *Bradypus variegatus* (d). Colors indicate: yellow, semicircular canals and utricle region; blue, cochlea. Scale bars equal 1 mm. (Modified from Billet et al. 2015; Boscaini et al. 2018)

feature also observed in the extinct sloth *Pelecodyon* (Coutier et al. 2017). In contrast, the lateral semicircular canal in *Bradypus* and *Choloepus* is weakly inclined compared to the ventral surface of the basicranium, a feature that is probably related with head posture (Coutier et al. 2017).

Despite a general resemblance between the bony labyrinths of the two extinct sloths, some important differences have been detected. For instance, in *Glossotherium* the posterior root of the lateral semicircular canal is located at the level of the ampullar entrance of the posterior semicircular canal, whereas in *Megatherium* it is situated more dorsally (Fig. 19.4a, b). *Glossotherium* and *Megatherium* also differ in the torsion of the lateral semicircular canal, which is much more pronounced in the latter than in the former taxon (Boscaini et al. 2018; Fig. 19.4a, b). Moreover, *Glossotherium* and *Megatherium* differ in the shape and position of their anterior

and posterior semicircular canals, the canals being more dorsoventrally elongated and oriented at an acute angle to one another in *Glossotherium*, whereas they are more rounded and disposed at an obtuse angle in *Megatherium* (Billet et al. 2013; Boscaini et al. 2018; Fig. 19.4a, b). The differences in the shape and orientation of the semicircular canals in *Glossotherium* and *Megatherium* are the main reason for the similarity of the former to extant anteaters and the latter to extant cingulates (Boscaini et al. 2018).

An examination of cochlear morphology reveals a general conservatism in shape among xenarthrans, as compared to the variability in shape of the semicircular canals (Billet et al. 2015; Fig. 19.4). Only the extinct sloth *Glossotherium* (Fig. 19.4a) and the extant anteater *Myrmecophaga* (Billet et al. 2015; Boscaini et al. 2018) possess a shorter cochlear canal with less than two complete coils. A cochlear feature common to both extant and extinct sloths and the pink fairy armadillo *Chlamyphorus* is the absence of the secondary bony (basilar) lamina sulcus on the cochlear endocast (Billet et al. 2015; Boscaini et al. 2018).

19.3.3 Cranial Sinuses

The first digital models of the paranasal and paratympanic sinuses of extant and extinct sloths have also been published recently (Boscaini et al. 2020a, b). As was the case for brain endocasts, the digital three-dimensional models of cranial sinuses reconstructed so far are those of *Glossotherium robustum* (Fig. 19.5a–b), *Catonyx tarijensis* (Fig. 19.5c–d), *Choloepus hoffmanni* (Fig. 19.5e–f), and *Bradypus variegatus* (Fig. 19.5g–h).

Due to lack of preservation of the nasal cavity region in the fossil specimens, the maxillary sinuses/recesses, as well as the anteriormost portions of the frontal sinuses, have not yet been properly characterized for all taxa. However, the other paranasal sinuses (i.e. the sphenoidal and posterior portions of the frontal sinuses, *sensu* Moore 1981) have been reconstructed for all the previously listed taxa (Boscaini et al. 2020a, b). Digital models of the paratympanic cavities of the living sloths have also been recovered (Boscaini et al. 2020a).

Among the taxa analyzed, the extant three-toed sloth *Bradypus variegatus* (Fig. 19.5g–h) presents the simplest arrangement of paranasal pneumatization, with well-developed and individualized frontal and sphenoidal sinuses (Boscaini et al. 2020a). More posteriorly, paratympanic pneumatization is also recognizable: the epitympanic sinus, which communicates with the tympanic cavity, invades the squamosal at the level of the posterior portion of the zygomatic process (Fig. 19.5g–h). In *Bradypus torquatus*, an additional pneumatized area, corresponding to the pterygoid sinus, is also observed (e.g. Guth 1961; Wetzel 1985).

The two-toed sloth shows a consistently more pneumatized skull (Boscaini et al. 2020a). When compared to *Bradypus variegatus*, the frontal and sphenoid bones appear more heavily pneumatized in *Choloepus hoffmanni*. In addition, other elements are invaded by sinuses, such as the palatine and pterygoid (Fig. 19.5e–f). In

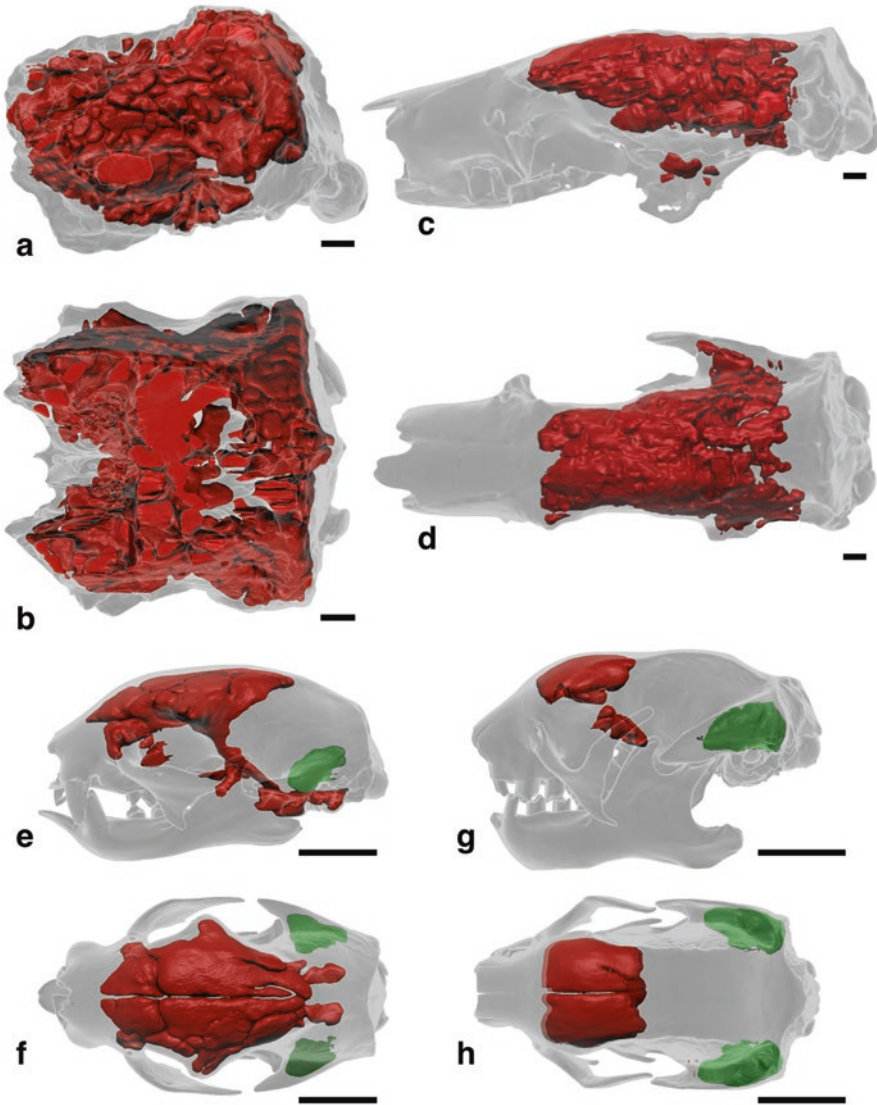


Fig. 19.5 Cranial sinuses of *Glossotherium robustum* (a–b), *Catonyx tarijensis* (c–d), *Choloepus hoffmanni* (e–f), and *Bradypus variegatus* (g–h), in lateral (a, c, e, g), and dorsal (b, d, f, h) views. Colors indicate: red, paranasal pneumatization; green, paratympanic pneumatization. Scale bars equal 2 cm. (Modified from Boscaini et al. 2020a, b)

this way, the sinuses of the cranial vault and base are interconnected in the middle cranial region (Boscaini et al. 2020a). Paratympanic pneumatization is also present at the base of the zygomatic process of the squamosal (Fig. 19.5e–f), but the epitympanic sinus is relatively smaller than that of *Bradypus variegatus* (Fig. 19.5g–h).

A similar arrangement of the paranasal sinuses is observed in *Catonyx tarijensis*, in which the pneumatization of the middle cranial area is even more extensive than in the two-toed sloth (Boscaini et al. 2020b; Fig. 19.5c–d). As in *Choloepus*, the posterior portion of the frontal sinuses extends partially into the parietal, but unlike the living form, it displays much greater ventral development, reaching the anterior-most portion of the squamosal (Boscaini et al. 2020b; Fig. 19.5c–d).

The extinct mylodontine *Glossotherium robustum* shows the greatest extent of cranial pneumatization described so far among sloths (Boscaini et al. 2020a; Fig. 19.5a–b). In fact, in this species, sinuses invade almost every bone of the braincase, even extending into the occipital posteriorly. The only sinus-free areas are those in the vicinity of the stylohyal fossa and the foramen magnum (Boscaini et al. 2020a; Fig. 19.5a–b). Both *Catonyx* and *Glossotherium* lack paratympanic pneumatization: the epitympanic sinus observed in *Bradypus* and *Choloepus* is absent in extinct mylodontid sloths (Gaudin 1995; Fig. 19.5).

19.4 Evolutionary Inferences Based on Endocast Morphology

19.4.1 Brain Cavity and Cranial Nerves

Brain Cavity

The conservative nature of brain endocast morphology among extant and extinct sloths was first observed based on solid models by Gervais (1869), and was subsequently confirmed in more recent works implementing the same technique (e.g. Dechaseaux 1971; Dozo 1987, 1994).

This neuroanatomical uniformity is also recognizable in digital models (Fig. 19.3), where a similar brain morphology has been recognized in the small-sized suspensory lineages of *Choloepus* and *Bradypus*, and giant terrestrial taxa like *Glossotherium* and *Catonyx* (Boscaini et al. 2020a, b). However, among the taxa digitally reconstructed so far, *Bradypus* (Fig. 19.3j–l) shows the most disparate morphology, with distinct differences from other sloths in the pattern of sulci and gyri and in the shape of the olfactory bulbs and the cerebellum (Boscaini et al. 2020a). Given its body-size and locomotory similarities to the two-toed sloth, these peculiar features are probably not related to function, but are more likely indicative of a distinct phylogenetic history. In fact, even if morphological and molecular phylogenies contrast in several aspects, the diphyletic origin of the two extant lineages is commonly accepted (e.g. Gaudin 2004; Delsuc et al. 2019; Presslee et al. 2019). The endocranial morphology of sloths appears to be conservative even for those taxa which show the most remarkable adaptive changes, such as *Thalassocnus* (de Muizon and McDonald 1995). In this form, which is characterized by several anatomical adaptations to aquatic lifestyle (e.g. Amson et al. 2014, 2015), preliminary observations on its brain cavity features did not highlight peculiar characteristics

(Amson et al. 2018). In fact, the olfactory bulbs of *Thalassocnus*, when compared to those of the living sloths, do not show the reduction observed in other mammalian lineages secondarily adapted to aquatic environments, such as cetaceans (Berta et al. 2014), sirenians (Orihuela et al. 2019), aquatic otters, and pinnipeds (Gittleman 1991; Bininda-Emonds et al. 2001).

Studies dedicated to the correlation between the cerebral convolution pattern of sloths and their possible functional aspects are scarce (Goffart 1971; Saraiva and Magalhães-Castro 1975). A sensory and motor mapping of the cerebral cortex of the living three-toed sloth was conducted by Saraiva and Magalhães-Castro (1975). According to this study, the anteriormost portion of the suprasylvian gyrus appears to be devoted to the representation of the forelimb, especially to the claws of the forepaw. A similar cortical representation of the forelimb was observed in other manually dexterous mammals such as raccoons and primates (Welker and Seidenstein 1959). This portion of the cortex appears well-developed in all the extant and extinct sloth taxa observed so far (Boscaini et al. 2020a, b). The strong development of this area results in brain endocasts that are mediolaterally wider in dorsal view than those in cingulates (Tambusso and Fariña 2015a, b). This morphology may be correlated with a higher degree of specialization achieved by sloths in the autopodia, relative to cingulates. In sloths, the use of the forelimb is especially important because, during their long evolutionary history, forelimbs were devoted to several critical tasks, such as feeding, digging, climbing, swimming, and suspensory arboreal locomotion (e.g. Pujos et al. 2012).

Cranial Nerves

Variation among sloths in features associated with the cranial nerves are also likely attributable to phylogenetic and functional influences. The independent trajectory of the maxillary division of the trigeminal nerve (V_2) through the foramen rotundum is, to date, invariably observed in *Bradypus*, whereas in *Catonyx*, *Glossotherium*, and some *Choloepus* specimens, this nerve branch passes through the sphenorbital fissure (Gaudin 2004, 2011; Boscaini et al. 2020a, b; Fig. 19.3). This is in part related to the confluence/separation of the foramen rotundum and the sphenorbital fissure observed on the external surface of the skull, thereby constituting a phylogenetically informative character (Gaudin 2004: char. 159). In *Catonyx* and *Glossotherium* (Fig. 19.3a–f), the diameter of the canals for the sphenorbital fissure, the foramen ovale, and the hypoglossal foramen are enlarged relative to other nerve-transmitting canals, contrasting with the condition in living sloths (Boscaini et al. 2020a, b). This was probably related to a greater development of the trigeminal and hypoglossal nerves in the two extinct mylodontids, reflecting heightened sensory input coming from their enlarged rostrum and nasal cavity, as well as the need for increased motor output due to their larger tongue and jaw muscles (Boscaini et al. 2020a). However, minor differences between *Catonyx* and *Glossotherium* can be also detected in the relative size of the hypoglossal canal (Fig. 19.3a–f). In the former taxon, the smaller diameter of the hypoglossal canal, coupled with the robust

morphology of the hyoid elements, suggest a more limited tongue protrusion than in the latter genus. All these characteristics are indicative of different feeding behaviors, with scelidotheriines being more browsers/mixed feeders, whereas the mylodontines were predominately grazers (Bargo et al. 2006; Pujos et al. 2012, Boscaini et al. 2020b).

19.4.2 Bony Labyrinth

In mammals, the morphology of the bony labyrinth is strongly influenced by both phylogeny and function. The vestibule and semicircular canals are associated with the sense of balance and equilibrium, whereas the cochlea is strongly linked to the sense of hearing (Ekdale 2013, 2016). Among Xenarthra, detailed studies of inner ear morphology have been conducted on its extant representatives, with particular emphasis on living sloths and with the recent addition of some fossil specimens to the dataset (Billet et al. 2012, 2015; Boscaini et al. 2018). These first analyses have revealed important characteristics that have the potential to be phylogenetically informative (Billet et al. 2015; Boscaini et al. 2018). For example, the absence of the secondary bony (basilar) lamina sulcus on the cochlear endocast is a feature shared by all the sloth bony labyrinths examined so far (Billet et al. 2015; Boscaini et al. 2018).

Among extant xenarthrans, three-dimensional geometric morphometric analyses revealed a strong phylogenetic imprint on labyrinthine morphology (Billet et al. 2013, 2015; Boscaini et al. 2018). In fact, the general xenarthran morphology of the inner ear clusters largely into three well-defined groups, coinciding with the main phylogenetic subdivisions (i.e. sloths, anteaters, and cingulates), with the unique exception of the pink fairy armadillo, which shows some unusual morphologies (Billet et al. 2013, 2015; Boscaini et al. 2018). However, when the bony labyrinths of some extinct sloths are taken into consideration, this scenario appears more complicated. In fact, the morphology of the inner ear of *Megatherium* and *Glossotherium* approaches that of extant armadillos and anteaters, respectively, disrupting the previously identified phylogenetic pattern (Billet et al. 2015; Boscaini et al. 2018). This resemblance appears to be more significantly driven by the morphology of the semicircular canals than the cochlea. More precisely, extant cingulates and anteaters, together with the extinct *Megatherium* and *Glossotherium*, share semicircular canals that are longer (i.e. with a larger radius of curvature) than those of the extant sloths *Bradypus* and *Choloepus* (Fig. 19.4). In other mammals, differences in shape, size, and orientation of the semicircular canals have been correlated with body mass and agility (Spoor et al. 2007; Silcox et al. 2009) and vestibular sensitivity (Malinzak et al. 2012; Berlin et al. 2013). In accordance with these general observations, it is highly probable that the paleobiology of the large terrestrial *Megatherium* and *Glossotherium*, which is doubtless quite distinct from the biology of the smaller, suspensory living forms, is primarily responsible for the observed disparity in semicircular canal anatomy among sloths (Billet et al. 2015; Boscaini et al. 2018).

Whether the folivoran semicircular canal morphology is more strongly related to differences in body size, agility levels, or locomotor styles will require further study, including the addition of new taxa to the geometric morphometric analyses. For the time being, the available data is consistent with the hypothesis that the similarities in the semicircular canals of extant sloths (Fig. 19.4) are due to convergence, probably linked to their independent acquisition of slow suspensory arboreal locomotion (e.g. Gaudin 2004; Nyakatura 2012).

The association of *Megatherium* with cingulates and *Glossotherium* with anteaters, rather than with extant sloths, is also observed in their cochlear morphology, even if the signal is consistently weaker than in the semicircular canal dataset (Boscaini et al. 2018). Considering the diverse habitats occupied by extant and extinct xenarthrans (from open temperate areas to closed tropical forests, and their accompanying differences in sound frequency transmission), particular cochlear morphologies may also correlate with environmental factors (Boscaini et al. 2018).

19.4.3 Cranial Sinuses

Similar to the other endocranial regions discussed so far, the cranial pneumatization of Folivora, and more generally among Pilosa, displays a strong correlation with phylogeny. Among sloth cranial bones, the frontal usually shows the greatest levels of pneumatization (Boscaini et al. 2020a, b; Fig. 19.5). Frontal sinuses, however, are not present in anteaters (Storch and Habersetzer 1991; Gaudin 2004: char. 174). The presence of frontal sinuses is considered a folivoran synapomorphy, albeit with different degrees of expression (Gaudin 2004). Among the extant and extinct sloths digitally reconstructed so far, *Bradypus* possesses the smallest frontal sinuses. The sinus in this genus is restricted to the frontal bone, without invading the parietal bone posteriorly (Naples 1982; Boscaini et al. 2020a; Fig. 19.5g–h). Conspicuously larger frontal sinuses, partially invading the parietals posteriorly, are observed in *Choloepus* (Fig. 19.5e–f) and *Catonyx* (Fig. 19.5c–d), whereas the greatest degree of cranial pneumatization is observed in large-sized mylodontines such as *Glossotherium* (Fig. 19.5a–b) and *Paramylodon* (Stock 1925; Boscaini et al. 2020a, b). These preliminary observations agree with morphology-based phylogenies (e.g. Gaudin 2004; Varela et al. 2019) but also fit with the most recent phylogenetic scenarios based on molecular evidence (i.e. Delsuc et al. 2019; Presslee et al. 2019). A probable functional correlation, i.e. the presence of more extensive sinuses in larger-sized taxa to reduce the weight of the head, is likely also at least partly responsible for the difference. Indeed, living sloths are remarkably small when compared to *Glossotherium* and *Catonyx*, and they also show the smallest extent of pneumatization. However, despite their size similarity, the level of pneumatization of *Choloepus* (Fig. 19.5e–f) is consistently higher than that of *Bradypus* (Fig. 19.5g–h). Furthermore, paranasal pneumatization in *Catonyx* (Fig. 19.5c–d) is more reduced than in *Glossotherium* (Fig. 19.5a–b), even though its estimated body mass is somewhat higher (Boscaini et al. 2020b). All this evidence suggests that, in sloths, sinus

organization could be driven primarily by phylogeny and only secondarily by body size. Similar observations have been reported in other herbivorous mammalian clades, such as bovids, which show analogous levels of size disparity (Farke 2010).

Regarding the epitympanic pneumatization, detached epitympanic sinuses have been reconstructed for the extant *Bradypus* and *Choloepus* (Fig. 19.5e–h). This sinus appears to be larger in the three-toed sloth (Fig. 19.5g–h) than in the two-toed sloth (Fig. 19.5e–f), again reflecting the strong influence of phylogeny on pneumatization. In fact, epitympanic sinuses are invariably present in anteaters, and are therefore considered primitive for *Pilosa* (Storch and Habersetzer 1991; Gaudin 1995, 2004). These sinuses were probably secondarily lost in mylodontids, such as *Glossotherium* and *Catonyx* (Gaudin 1995, 2004; Boscaini et al. 2020a, b; Fig. 19.5a–d). Consequently, the presence of epitympanic sinuses in *Choloepus* is apparently inconsistent with its recent inclusion among mylodontids based on molecular data (Delsuc et al. 2019; Presslee et al. 2019).

19.5 Open Problems and Future Directions: Outstanding Questions and Perspectives

The first studies of the internal cavities in folivoran skulls date back to the nineteenth century, but such studies are currently experiencing a rapid increase. The main reason of the proliferation of these studies is the greater worldwide availability of CT-scanning facilities, as well as the recent spread of powerful computational software and hardware to process the large 3D data files produced by such scans. The availability of clinical and micro-CT scans in proximity to fossil collections, and the reduction of computational times needed for digital reconstructions, have substantially increased the opportunities for applying these non-destructive techniques to fossil sloths. Thus, the decade 2010–2020 marked the beginning of anatomical study on sloth digital endocranial casts, including aspects such as the brain cavity, bony labyrinth, and cranial sinuses (e.g. Billet et al. 2012, 2013, 2015; Boscaini et al. 2018, 2020a, b; Amaral et al. 2021).

As stated previously, reconstructions of the morphology of the brain cavity were also possible in the past using plaster-silicone casts. However, these methods were partially or largely destructive of the fossil material studied, and ultimately retained anatomical traits in less detail than modern digital techniques. In contrast, a reliable three-dimensional reconstruction of the inner ear and the cranial sinuses has only been possible through CT-scanning and digital imaging techniques (e.g. Billet et al. 2012, 2013, 2015; Boscaini et al. 2018, 2020a, b). The studies published so far represent a first approach to the reconstruction of the morphologies of the internal cavities of sloth skulls using digital methods. These analyses served in many cases as initial anatomical characterizations, using extant sloths as a comparative framework, and opening the way for the inclusion of extinct taxa (e.g. Billet et al. 2012, 2015; Boscaini et al. 2018, 2020a, b). However, considering the high taxonomic

richness of extinct sloths, the data published to date is still far from reliably covering all the main cranial morphologies associated with the major folivoran clades. Broader-scale datasets are now being processed, and their analysis will be the objective of some of our future studies. A preliminary morphometric study of xenarthran brain endocasts, including three extinct sloth genera, was recently conducted by Amaral et al. (2021), who confirmed the conservative pattern of xenarthran brain anatomy, with lesser influences on morphology probably related to locomotion. These first analyses have demonstrated the potential of endocranial information for shedding light on important aspects of the evolutionary history of the sloth clade, allowing us to outline some preliminary conclusions.

Overall, the morphology of the endocranial structures observed in the extant and extinct sloths analyzed so far appear to be more strongly influenced by phylogenetic relationships than functional/paleobiological factors. This is true for several features pertaining to the brain cavity and cranial nerves (Fig. 19.3), but is also reflected in the morphology of the bony labyrinth (Fig. 19.4) and cranial sinuses (Fig. 19.5). At the moment, the influence of the phylogeny appears strong, regardless of the phylogenetic hypothesis used as a reference for evolutionary relationships. In fact, for the taxa reconstructed so far, many anatomical observations agree with phylogenetic relationships based on both morphological (e.g. Gaudin 2004; Boscaini et al. 2019; Varela et al. 2019) and molecular (Delsuc et al., 2019; Presslee et al., 2019) characters. However, some features such as the presence/absence of the epitympanic sinuses (Fig. 19.5), seem to support morphology-based phylogenies (Gaudin 2004; Varela et al. 2019). In this sense, the digital endocranial analysis of new taxa has the potential to provide useful information for elucidating the relationships among extant and extinct sloths.

To a lesser degree, some aspects of cranial pneumatization patterns and the anatomy of the bony labyrinth, brain cavity, and cranial nerves, could be correlated with biological factors such as body size, locomotory mode, and feeding habits. For example, the extent of the sinus development and the size of the semicircular canals of the inner ear seem to be related to body size and agility/locomotion, whereas the different proportions among cranial nerves could reflect distinct diets. As was the case for *Catonyx tarijensis*, the study of the internal cavities of fossil skulls offers new indirect evidence that can provide a useful anatomical basis for paleobiological inferences, especially if coupled with observations of external skull traits (Boscaini et al. 2020b). Future large-scale studies on endocranial structures in extinct sloths may reflect the disparity already observed in their exterior skull surfaces and post-cranial anatomies, and add information on the diversity of past ecological adaptations.

Another important source of morphological diversity in the endocranial cavities is intraspecific variation, although this aspect can only be easily evaluated for extant taxa. Even though living sloth species only constitute a restricted fraction of the total diversity attained by the group (Vizcaíno et al. 2018), they offer the unique opportunity to analyze large intraspecific samples for each endocranial structure. To date, intraspecific variation has been properly evaluated only for the morphology of the bony labyrinth of inner ear, where uncommonly high variability in the form of

the semicircular canals, especially in *Bradypus*, was recorded (Billet et al. 2012). This may be correlated with a reduced functional demand for rapid postural adjustments due to the remarkable slow locomotory style of extant sloths (Billet et al. 2012; Perier et al. 2016). It has been observed that the structure of the mammalian inner ear is mostly complete in the early prefetal period, and that its final size is achieved before the inner ear is functional (Ekdale 2010; Solntseva 2010). Therefore, the morphology of the bony labyrinth does not change much during ontogeny, whereas the opposite has been observed for other endocranial areas, such as paranasal pneumatization (Farke 2010). For this reason, with the exception of the bony labyrinth, comparisons among equivalent ontogenetic stages are necessary for interspecific comparisons of endocranial cavities to properly avoid development-related transformations.

In the last decade, new technologies constituted an important step for facilitating the comprehension of endocranial anatomy in extant and extinct sloths, allowing access to previously unknown morphologies in a non-destructive way. These methods also allow information to be shared easily among scholars based in different countries, facilitating collaboration. In fact, the cranial remains of extant and extinct sloths are housed in numerous collections, mainly in America and Europe. New collaborative efforts and large-scale quantitative studies, such as 3D geometric morphometrics and volumetric calculations, will be essential for revealing evolutionary trends in the whole clade and represent promising directions for future research.

19.6 Concluding Remarks

The first studies on the endocranial cavities of extinct sloths date back to the nineteenth century, but currently they are rapidly increasing in number thanks to the widespread availability of CT-scans and digital technologies. Today, highly detailed digital images of endocranial structures in and around the brain cavity, as well as the bony labyrinth and cranial sinuses, are relatively easy to reconstruct in a non-destructive way. The analyses published in the last decade have focused on the extant lineages and a few well-preserved, recently extinct taxa, though an increasingly larger number of fossil specimens are being considered. The first comparisons among the taxa reconstructed so far (i.e. *Bradypus*, *Choloepus*, *Catonyx*, *Glossotherium*, and *Megatherium*) show that the observed morphologies can best be explained by phylogeny and only secondarily by paleobiological factors such as body size, locomotory modes, and possible feeding habits.

The general form of the brain cavity appears to be conservative among sloths, with some peculiar characteristics in the olfactory bulbs, convolution pattern and cerebellum observed in *Bradypus*. In contrast, the morphology of the inner ear, and particularly that of the semicircular canals, appears different among the extant sloths *Bradypus* and *Choloepus* and the extinct giant sloths *Glossotherium* and *Megatherium*. Also, the pattern of cranial pneumatization appears to be driven primarily by phylogeny, and only secondarily related to body size. In the future,

large-scale analyses of the morphology of the brain cavity, inner ear, and cranial sinuses can provide valuable, phylogenetically-informative characters and may be helpful in resolving the controversial phylogenetic relationships within Folivora. These same anatomical regions can also yield important functional insights and have the potential for elucidating the remarkable adaptations of extinct sloths.

Acknowledgments We are grateful to Prof. Lazaros C. Triarhou (University of Macedonia, Greece) for providing us bibliographic information on the publications of Christfried Jakob and Clemente Onelli. We also thank the MAECI (Ministry of Foreign Affairs and International Cooperation, Italy) for funding that greatly facilitated scientific collaboration between CONICET (Argentina) and Sapienza Università di Roma (Italy). This manuscript greatly benefited from the careful revisions by two anonymous referees.

References

- Amaral RV, Oliveira JA, Carvalho LB (2021) Comparative multivariate analysis of 3-D reconstructed encephalon in extant and fossil Folivora (Pilosa) and other representatives Xenarthra. *Hist Biol*. <https://doi.org/10.1080/08912963.2021.1891418>
- Amson E, de Muizon C, Laurin M et al (2014) Gradual adaptation of bone structure to aquatic lifestyle in extinct sloths from Peru. *Proc R Soc B* 281:20140192. <https://doi.org/10.1098/rspb.2018.0270>
- Amson E, Argot C, McDonald HG et al (2015) Osteology and functional morphology of the forelimb of the marine sloth *Thalassocnus* (Mammalia, Tardigrada). *J Mammal Evol* 22(2):169–242. <https://doi.org/10.1007/s10914-014-9268-3>
- Amson E, Billet G, de Muizon C (2018) Evolutionary adaptation to aquatic lifestyle in extinct sloths can lead to systemic alteration of bone structure. *Proc R Soc B* 285(1878):20180270. <https://doi.org/10.1098/rspb.2018.0270>
- Bargo MS, Vizcaíno SF (2008) Paleobiology of Pleistocene ground sloths (Xenarthra, Tardigrada): biomechanics, morphogeometry and ecomorphology applied to the masticatory apparatus. *Ameghiniana* 45(1):175–196
- Bargo MS, Toledo N, Vizcaíno SF (2006) Muzzle of South American Pleistocene ground sloths (Xenarthra, Tardigrada). *J Morphol* 267(2):248–263. <https://doi.org/10.1002/jmor.10399>
- Bargo MS, Toledo N, Vizcaíno SF (2012) Paleobiology of the Santacrucian sloths and anteaters (Xenarthra, Pilosa). In: Vizcaíno SF, Kay RF, Bargo MS (eds) *Early miocene paleobiology in patagonia. High-latitude paleocommunities of the santa cruz formation*. Cambridge University Press, Cambridge, pp 216–242. <https://doi.org/10.1017/CBO9780511667381.014>
- Bergqvist LP, Abrantes EAL, Avilla LS (2004) The Xenarthra (Mammalia) of São José de Itaboraí Basin (Upper Paleocene, Itaboraian), Rio de Janeiro. *Brazil Geodiversitas* 26(2):323–337
- Berlin JC, Kirk EC, Rowe TB (2013) Functional implications of ubiquitous semicircular canal non-orthogonality in mammals. *PLoS One* 8(11):e79585. <https://doi.org/10.1371/journal.pone.0079585>
- Berta A, Ekdale EG, Cranford TW (2014) Review of the cetacean nose: form, function, and evolution. *Anat Rec* 297(11):2205–2215. <https://doi.org/10.1002/ar.23034>
- Billet G, Hautier L, Asher RJ et al (2012) High morphological variation of vestibular system accompanies slow and infrequent locomotion in three-toed sloths. *Proc R Soc B* 279:3932–3939. <https://doi.org/10.1098/rspb.2012.1212>
- Billet G, Germain D, Ruf I et al (2013) The inner ear of *Megatherium* and the evolution of the vestibular system in sloths. *J Anat* 223(6):557–567. <https://doi.org/10.1111/joa.12114>

- Billet G, Hautier L, Lebrun R (2015) Morphological diversity of the bony labyrinth (inner ear) in extant xenarthrans and its relation to phylogeny. *J Mammal* 96(4):658–672. <https://doi.org/10.1093/jmammal/gyv074>
- Bininda-Emonds ORP, Gittleman JL, Kelly CK (2001) Flippers versus feet: comparative trends in aquatic and non-aquatic carnivores. *J Anim Ecol* 70(3):386–400. <https://doi.org/10.1046/j.1365-2656.2001.00499.x>
- Boscaini A, Iurino DA, Billet G et al (2018) Phylogenetic and functional implications of the ear region anatomy of *Glossotherium robustum* (Xenarthra, Mylodontidae) from the late Pleistocene of Argentina. *Sci Nat* 105:28. <https://doi.org/10.1007/s00114-018-1548-y>
- Boscaini A, Pujos F, Gaudin TJ (2019) A reappraisal of the phylogeny of Mylodontidae (Mammalia, Xenarthra) and the divergence of mylodontine and lestodontine sloths. *Zool Scr* 48:691–710. <https://doi.org/10.1111/zsc.12376>
- Boscaini A, Iurino DA, Sardella R et al (2020a) Digital cranial endocasts of the extinct sloth *Glossotherium robustum* (Xenarthra, Mylodontidae) from the late Pleistocene of Argentina: description and comparison with the extant sloths. *J Mammal Evol* 27:55–71. <https://doi.org/10.1007/s10914-018-9441-1>
- Boscaini A, Iurino DA, Mamani Quispe B et al (2020b) Cranial anatomy and paleoneurology of the extinct sloth *Catonyx tarijensis* (Xenarthra, Mylodontidae) from the Late Pleistocene of Oruro, southwestern Bolivia. *Front Ecol Evol* 8:69. <https://doi.org/10.3389/fevo.2020.00069>
- Brinkman PD, Vizcaíno SF (2014) Clemente Onelli's sketch map and his first-hand, retrospective account of an early fossil-hunting expedition along the Río Santa Cruz, southern Patagonia, 1888–1889. *Arch Natural Hist* 41(2):326–337. <https://doi.org/10.3366/anh.2014.0251>
- Carlini AA, Scillato-Yané GJ, Vizcaíno SF et al (1992) Un singular Myrmecophagidae (Xenarthra, Vermilingua) de Edad Colhuehuapense (Oligoceno tardío, Mioceno temprano) de Patagonia. *Argentina Ameghiniana* 29(2):176
- Casali DM, Santos Júnior JE, Miranda FR et al (2020) Total-evidence phylogeny and divergence times of Vermilingua (Mammalia: Pilosa). *Syst Biodivers* 18(3):216–227. <https://doi.org/10.1080/14772000.2020.1729894>
- Clack AA, MacPhee RDE, Poinar HN (2012) *Myiodon darwini* DNA sequences from ancient fecal hair shafts. *Ann Anat* 194:26–30. <https://doi.org/10.1016/j.aanat.2011.05.001>
- Coutier F, Hautier L, Cornette R et al (2017) Orientation of the lateral semicircular canal in Xenarthra and its links with head posture and phylogeny. *J Morphol* 278(5):704–717. <https://doi.org/10.1002/jmor.20665>
- Cuvier G (1796) Notice sur le squelette d'une très grande espèce de quadrupède inconnue jusqu'à présent, trouvé au Paraguay, et déposé au cabinet d'histoire naturelle de Madrid. *Mag Encycl* 1:303–310
- De Iuliis G, Boscaini A, Pujos F, McAfee RK, Cartelle C, Tsuji LJS, Rook L (2020) On the status of the giant mylodontine sloth *Glossotherium wegneri* (Spillmann, 1931) (Xenarthra, Folivora) from the late Pleistocene of Ecuador. *Comptes Rendus Palevol* 19(12):215–232. <https://doi.org/10.5852/cr-palevol2020v19a12>
- de Muizon C, McDonald HG (1995) An aquatic sloth from the Pliocene of Peru. *Nature* 375:224–227. <https://doi.org/10.1038/375224a0>
- Dechaseaux C (1958) Encéphales de xénarthres fossiles. In: Piveteau J (ed) *Traité de Paléontologie*. Masson and Cie, Paris, pp 637–640
- Dechaseaux C (1962a) Encéfalos de Notungulados y de Desdentados Xenarthros Fósiles. *Ameghiniana* 2(11):193–209
- Dechaseaux C (1962b) Singularités de l'encéphale de *Lestodon*, mammifère édenté géant du Pléistocène d'Amérique du Sud. *C R Acad Sci* 254:1470–1471
- Dechaseaux C (1971) *Oreomyiodon wegneri*, édenté gravigrade du Pléistocène de l'Équateur – Crâne et moulage endocrânien. *Ann Paleontol* 57(2):243–285
- Delsuc F, Kuch M, Gibb GC et al (2019) Ancient mitogenomes reveal the evolutionary history and biogeography of sloths. *Curr Biol* 29(2):2031–2042. <https://doi.org/10.1016/j.cub.2019.05.043>

- Dozo MT (1987) The endocranial cast of an early Miocene edentate, *Hapalops indifferens* Ameghino (Mammalia, Edentata, Tardigrada, Megatheriidae). Comparative study with brains of recent sloths. *J Hirnforsch* 28(4):397–406
- Dozo MT (1994) Interpretación del molde endocraneano de *Euchloeops fronto*, un Megalonychidae (Mammalia, Xenarthra, Tardigrada) del Mioceno temprano de Patagonia (Argentina). *Ameghiniana* 31(4):317–329
- Ekdale EG (2010) Ontogenetic variation in the bony labyrinth of *Monodelphis domestica* (Mammalia: Marsupialia) following ossification of the inner ear cavities. *Anat Rec* 293:1896–1912. <https://doi.org/10.1002/ar.21234>
- Ekdale EG (2013) Comparative anatomy of the bony labyrinth (inner ear) of placental mammals. *PLoS One* 8(6):e66624. <https://doi.org/10.1371/journal.pone.0066624>
- Ekdale EG (2016) Form and function of the mammalian inner ear. *J Anat* 228(2):324–337. <https://doi.org/10.1111/joa.12308>
- Engelmann GF (1985) The phylogeny of the Xenarthra. In: Montgomery GG (ed) *The ecology and evolution of armadillos, sloths, and vermilings*. Smithsonian Institution Press, Washington, DC, pp 51–64
- Farke AA (2010) Evolution and functional morphology of the frontal sinuses in Bovidae (Mammalia: Artiodactyla), and implications for the evolution of cranial pneumaticity. *Zool J Linnean Soc* 159(4):988–1014. <https://doi.org/10.1111/j.1096-3642.2009.00586.x>
- Gaudin TJ (1995) The ear region of edentates and the phylogeny of the Tardigrada (Mammalia, Xenarthra). *J Vertebr Paleontol* 15(3):672–705. <https://doi.org/10.1080/02724634.1995.10011255>
- Gaudin TJ (2004) Phylogenetic relationships among sloths (Mammalia, Xenarthra, Tardigrada): the craniodental evidence. *Zool J Linnean Soc* 140:255–305. <https://doi.org/10.1111/j.1096-3642.2003.00100.x>
- Gaudin TJ (2011) On the osteology of the auditory region and orbital wall in the extinct West Indian sloth genus *Neocnus* Arredondo, 1961 (Placentalia, Xenarthra, Megalonychidae). *Ann Carnegie Mus* 80(1):5–28. <https://doi.org/10.2992/007.080.0102>
- Gaudin TJ, Branham DG (1998) The phylogeny of the Myrmecophagidae (Mammalia, Xenarthra, Vermilingua) and the relationship of *Eurotamandua* to the Vermilingua. *J Mammal Evol* 5(3):237–265. <https://doi.org/10.1023/A:1020512529767>
- Gaudin TJ, Croft DA (2015) Paleogene Xenarthra and the evolution of south American mammals. *J Mammal* 96(4):622–634. <https://doi.org/10.1093/jmammal/gyv073>
- Gelfo JN, Reguero MA, López GM et al (2009) Eocene mammals and continental strata from Patagonia and Antarctic Peninsula. *Mus North Ariz Bull* 65:567–592
- Gervais P (1869) Mémoire sur les formes cérébrales propres aux édentés vivants et fossiles. *Nouv Arch du Mus Hist Nat Paris* 5:1–56
- Gittleman JL (1991) Carnivore olfactory bulb size: allometry, phylogeny and ecology. *J Zool* 225(2):253–272. <https://doi.org/10.1111/j.1469-7998.1991.tb03815.x>
- Goffart M (1971) Function and form in the sloth, International series of monographs in pure and applied biology. Modern trends in physiological sciences, vol 34. Pergamon Press, Oxford
- Guth C (1961) La région temporale des Edentés. Dissertation, Université de Paris
- Hayssen V (2010) *Bradypus variegatus* (Pilosa: Bradypodidae). *Mamm Species* 42(850):19–32. <https://doi.org/10.1644/850.1>
- Hayssen V (2011) *Choloepus hoffmanni* (Pilosa: Megalonychidae). *Mamm Species* 43(873):37–55. <https://doi.org/10.1644/873.1>
- Jakob C (1912) Sobre cerebros fósiles de la fauna argentina, con presentación del material Actas del XVII° Congreso Internacional de Americanistas, 134–142 Buenos Aires, 17–23 May 1910
- Jakob C, Onelli C (1910) Anatomía comparada del encéfalo de los mamíferos de la República Argentina, atlas y planchas. In: Barabino SE, Besio Moreno N (eds) Congreso Científico Internacional Americano, Relación general del funcionamiento del Congreso, vol 1. Coni Hermanos, Buenos Aires, pp 455–456

- Jakob C, Onelli C (1911) Vom Tierhirn zum Menschenhirn: Vergleichend Morphologische, Histologische und Biologische Studien zur Entwicklung der Grosshirnhemisphären und ihrer Rinde. JF Lehmann's Verlag, München
- Jakob C, Onelli C (1913) Atlas del cerebro de los mamíferos de la República Argentina. Estudios anatómicos, histológicos y biológicos comparados sobre la evolución de los hemisferios y de la corteza cerebral. Imprenta de Guillermo Kraft, Buenos Aires
- Lull RS (1915) A Pleistocene ground sloth, *Myiodon harlani*, from Rock Creek. Texas Am Jour Sci 39(232):327–385. <https://doi.org/10.2475/ajs.s4-39.232.327>
- Malinzak MD, Kay RF, Hullar TE (2012) Locomotor head movements and semicircular canal morphology in primates. Proc Natl Acad Sci U S A 109(44):17914–17919. <https://doi.org/10.1073/pnas.1206139109>
- McDonald HG, De Iuliis G (2008) Fossil history of sloths. In: Vizcaíno SF, Loughry WJ (eds) The biology of the Xenarthra. University Press of Florida, Gainesville, pp 39–55
- McDonald HG, Vizcaíno SF, Bargo MS (2008) Skeletal anatomy and the fossil history of the Vermilingua. In: Vizcaíno SF, Loughry WJ (eds) The biology of the Xenarthra. University Press of Florida, Gainesville, pp 64–78
- McKenna MC, Bell SK (1997) Classification of mammals above the species level. Columbia University Press, New York
- McKenna MC, Wyss AR, Flynn JJ (2006) Paleogene Pseudoglyptodont Xenarthrans from Central Chile and Central Patagonia. Am Mus Nov 3536:1–18. [https://doi.org/10.1206/0003-0082\(2006\)3536\[1:PPXFCC\]2.0.CO;2](https://doi.org/10.1206/0003-0082(2006)3536[1:PPXFCC]2.0.CO;2)
- Moore WJ (1981) The mammalian skull. Cambridge University Press, Cambridge
- Naples VL (1982) Cranial osteology and function in the tree sloths, *Bradypus* and *Choloepus*. Am Mus Nov 2739:1–41
- Naples VL (1999) Morphology, evolution and function of feeding in the giant anteater (*Myrmecophaga tridactyla*). J Zool 249:19–41. <https://doi.org/10.1111/j.1469-7998.1999.tb01057.x>
- Nowak RM (1999) Walker's mammals of the world. The Johns Hopkins University Press, Baltimore/London
- Nyakatura JA (2012) The convergent evolution of suspensory posture and locomotion in tree sloths. J Mammal Evol 19(3):225–234. <https://doi.org/10.1007/s10914-011-9174-x>
- Orihuela J, Viñola López LW, Macrini TE (2019) First cranial endocasts of early Miocene sirenians (Dugongidae) from the West Indies. J Vertebr Paleontol 39(2):e1584565. <https://doi.org/10.1080/02724634.2019.1584565>
- Owen R (1856) On the *Megatherium* (*Megatherium americanum*, Cuvier and Blumenbach). Part III. – the skull. Phil Trans R Soc London 146:571–589. <https://doi.org/10.1098/rstl.1856.0028>
- Pascual R (2006) Evolution and geography: the biogeographic history of South American land mammals. Ann Mo Bot Gard 93:209–230. [https://doi.org/10.3417/0026-6493\(2006\)93\[209:EAGTBH\]2.0.CO;2](https://doi.org/10.3417/0026-6493(2006)93[209:EAGTBH]2.0.CO;2)
- Patterson B, Pascual R (1968) The fossil mammal fauna of South America. Q Rev Biol 43(4):409–451. <https://doi.org/10.1086/405916>
- Perier A, Lebrun R, Marivaux L (2016) Different level of intraspecific variation of the bony labyrinth morphology in slow- versus fast-moving primates. J Mammal Evol 23(4):353–368. <https://doi.org/10.1007/s10914-016-9323-3>
- Pouchet G (1868–1869) Mémoire sur l'encéphale des Édentés. J Anat et Physiol 5:658–675; 6:1–18, 147–162, 349–363
- Presslee S, Slater GJ, Pujos F et al (2019) Palaeoproteomics resolves sloth relationships. Nat Ecol Evol 3:1121–1130. <https://doi.org/10.1038/s41559-019-0909-z>
- Pujos F, Gaudin TJ, De Iuliis G et al (2012) Recent advances on variability, morpho-functional adaptations, dental terminology, and evolution of sloths. J Mammal Evol 19(3):159–169. <https://doi.org/10.1007/s10914-012-9189-y>
- Raj Pant S, Goswami A, Finarelli JA (2014) Complex body size trends in the evolution of sloths (Xenarthra: Pilosa). BMC Evol Biol 14:184. <https://doi.org/10.1186/s12862-014-0184-1>

- Saraiva PES, Magalhães-Castro B (1975) Sensory and motor representation in the cerebral cortex of the three-toed sloth (*Bradypus tridactylus*). *Brain Res* 90(2):181–193. [https://doi.org/10.1016/0006-8993\(75\)90300-5](https://doi.org/10.1016/0006-8993(75)90300-5)
- Silcox MT, Bloch JI, Boyer DM et al (2009) Semicircular canal system in early primates. *J Hum Evol* 56(3):315–327. <https://doi.org/10.1016/j.jhevol.2008.10.007>
- Slater GJ, Cui P, Forasiepi AM et al (2016) Evolutionary relationships among extinct and extant sloths: the evidence of mitogenomes and retroviruses. *Genome Biol Evol* 8(3):607–621. <https://doi.org/10.1093/gbe/evw023>
- Solntseva GN (2010) Morphology of the inner ear of mammals in ontogeny. *Russ J Dev Biol* 41(2):94–110. <https://doi.org/10.1134/S1062360410020062>
- Spoor F, Garland T, Krovitz G et al (2007) The primate semicircular canal system and locomotion. *Proc Natl Acad Sci U S A* 104(26):10808–10812. <https://doi.org/10.1073/pnas.0704250104>
- Stock C (1925) Cenozoic gravigrade edentates of western North America. *Publ Carnegie Instit Wash* 331:1–206
- Storch G, Habersetzer J (1991) Rückverlagerte Choanen und akzessorische Bulla tympanica bei rezenten Vermilingua und *Eurotamandua* aus dem Eozän von Messel (Mammalia: Xenarthra). *Z Säugetierk* 56:257–271
- Tambusso PS, Fariña RA (2015a) Digital cranial endocast of *Pseudoplohophorus absolutus* (Xenarthra, Cingulata) and its systematic and evolutionary implications. *J Vertebr Paleontol* 35:5. <https://doi.org/10.1080/02724634.2015.967853>
- Tambusso PS, Fariña RA (2015b) Digital endocranial cast of *Pampatherium humboldtii* (Xenarthra, Cingulata) from the Late Pleistocene of Uruguay. *Swiss J Palaeontol* 134:109–116. <https://doi.org/10.1007/s13358-015-0070-5>
- Toledo N (2016) Paleobiological integration of Santacrucian sloths (Early Miocene of Patagonia). *Ameghiniana* 53(2):100–141. <https://doi.org/10.5710/AMGH.07.10.2015.2891>
- Toledo N, Bargo MS, Vizcaíno S et al (2017) Evolution of body size in anteaters and sloths (Xenarthra, Pilosa): phylogeny, metabolism, diet and substrate preferences. *Earth Environ Sci Trans R Soc Edinb* 106(4):289–301. <https://doi.org/10.1017/S1755691016000177>
- Triarhou LC, del Cerro M (2006) Semicentennial tribute to the ingenious neurobiologist Christfried Jakob (1866–1956). 1. Works from Germany and the first Argentina period, 1891–1913. *Eur Neurol* 56:176–188. <https://doi.org/10.1159/000096424>
- Varela L, Tambusso PS, McDonald HG et al (2019) Phylogeny, macroevolutionary trends and historical biogeography of sloths: insights from a Bayesian morphological clock analysis. *Syst Biol* 68(2):204–218. <https://doi.org/10.1093/sysbio/syy058>
- Vizcaíno SF, Toledo N, Bargo MS (2018) Advantages and limitations in the use of extant xenarthrans (Mammalia) as morphological models for paleobiological reconstruction. *J Mammal Evol* 25:495–505. <https://doi.org/10.1007/s10914-017-9400-2>
- Welker WI, Seidenstein S (1959) Somatic sensory representation in the cerebral cortex of the racoon (*Procyon lotor*). *J Comp Neurol* 111(3):469–501. <https://doi.org/10.1002/cne.901110306>
- Wetzel RM (1985) The identification and distribution of recent Xenarthra (= Edentata). In: Montgomery GG (ed) *The ecology and evolution of armadillos, sloths, and Vermilinguas*. Smithsonian Institution Press, Washington, DC, pp 5–21
- Woodburne MO (2010) The great american biotic interchange: dispersals, tectonics, climate, sea level and holding pens. *J Mammal Evol* 17:245–264. <https://doi.org/10.1007/s10914-010-9144-8>
- Woodward AS (1900) On some remains of *Grypotherium (Neomyiodon) listai* and associated mammals from a cavern near Consuelo Cove, Last Hope Inlet, Patagonia. *Proc Zool Soc London* 69:64–79. <https://doi.org/10.1111/j.1096-3642.1890.tb01704.x>

Chapter 20

Endocranial Morphology and Paleoneurology in Notoungulates: Braincast, Auditory Region and Adjacent Intracranial Spaces



Gastón Martínez, Thomas E. Macrini, María Teresa Dozo, Bárbara Vera, and Javier N. Gelfo

20.1 Systematic and Phylogenetic Context

20.1.1 *South American Native Ungulates*

The South American native ungulates (SANUs) are extinct mammals that evolved within the context of South America geographic isolation, which lasted most of the Cenozoic. They include approximately 280 genera grouped into at least five

G. Martínez (✉)

Museo de Paleontología, Facultad de Ciencias Exactas, Físicas y Naturales, Universidad Nacional de Córdoba, Córdoba, Argentina
e-mail: gmartinez@unc.edu.ar

T. E. Macrini

Department of Biological Sciences, St. Mary's University, San Antonio, TX, USA
e-mail: tmacrini@stmarytx.edu

M. T. Dozo

Consejo Nacional de Investigaciones Científicas y Técnicas (CONICET), CABA, Argentina

Instituto Patagónico de Geología y Paleontología, CCT CONICET-CENPAT,

Puerto Madryn, Argentina

e-mail: dozo@cenpat-conicet.gob.ar

B. Vera

Consejo Nacional de Investigaciones Científicas y Técnicas (CONICET), CABA, Argentina

Centro de Investigación Esquel de Montaña y Estepa Patagónica, CONICET–Universidad Nacional de la Patagonia ‘San Juan Bosco’, Esquel, Argentina

e-mail: barbara.vera@comahue-conicet.gob.ar

J. N. Gelfo

Consejo Nacional de Investigaciones Científicas y Técnicas (CONICET), CABA, Argentina

División Paleontología Vertebrados, Museo de La Plata, Facultad de Ciencias Naturales y Museo, Universidad Nacional de La Plata, La Plata, Argentina

e-mail: jgelfo@fcnym.unlp.edu.ar

© Springer Nature Switzerland AG 2023

M. T. Dozo et al. (eds.), *Paleoneurology of Amniotes*,
https://doi.org/10.1007/978-3-031-13983-3_20

well-accepted major groups: Astrapotheria, Litopterna, Notoungulata, Pyrotheria and Xenungulata. Among them, Astrapotheria and Litopterna have been also recorded in Antarctica (Gelfo et al. 2019) and, in the case of Notoungulata, some toxodontid remains have been reported for Central and North America (Lundelius et al. 2013). SANUs ranged from <1 kg to several tons in mass and evolved into a variety of primarily herbivorous diets and locomotor adaptations. Many authors (Simpson 1934, 1945, 1980; Cifelli 1993; Muizon and Cifelli 2000) suggested SANUs descended from one or more groups of Laurasian condylarths (which includes the probable ancestors of perissodactyls and artiodactyls), others placed them either closer to the uniquely South American xenarthrans (anteaters, armadillos and sloths) or to the Afrotherians (e.g. elephants and hyraxes), and others even suggested a polyphyletic origin for SANUs (Croft et al. 2020, and references therein).

McKenna (1975) erected the mirorder Meridiungulata to include all the SANUs originated from a hypothetical condylarth (didolodont-like) ancestor present in South America before the end of the Cretaceous. This interpretation was reformulated by Soria (1988), who considered two main lineages derived from an ancestral arctocyonid stock. One of them would be related to the origin of Didolodontidae + Litopterna, and the other to the rest of the SANUs. Muizon and Cifelli (2000) questioned the monophyly of Meridiungulata and proposed, instead, the order Panameriungulata to include the North American Mioclaenidae and the South American Didolodontidae and Litopterna, which implied a separate origin and no close relationships with other SANUs (Astrapotheria, Notoungulata, Pyrotheria and Xenungulata). On the other hand, affinities of xenungulates and pyrotheres with Dinocerata (Uintatheriomorpha) were also proposed (Schoch and Lucas 1985).

Alternatively, Astrapotheria, Notoungulata, Pyrotheria, and Xenungulata have been linked to Afrotheria based on some controversial interpretations of Agnolín and Chimento (2011; but see Billet and Martin 2011; Kramarz and Bond 2014). Meanwhile, Notoungulata and Xenungulata, were also included within Afrotheria based on a phylogenetic analysis (phenomic and genomic data) performed by O'Leary et al. (2013). In contrast, proteomic derived data placed together *Macrauchenia patachonica* (Litopterna), *Toxodon platensis* (Notoungulata) and Perissodactyla (Buckley 2015). Similar results were obtained by Welker et al. (2015), who proposed the name Panperissodactyla for the clade (Fig. 20.1a). In partial agreement, mitogenomic data place *Macrauchenia* (Litopterna) as the sister taxon to crown Perissodactyla, with an estimated divergence time of ~66 Ma (Welker et al. 2015). In a combined phylogenetic analysis (DNA, collagen, and morphological data), *Thomashuxleya* (Notoungulata) was recovered either within Afrotheria (if no-constrained maximum parsimony analysis is performed) or within Laurasiatheria (stem to Euungulata) if notoungulates + litopterns monophyly is forced based on proteomic data (Carrillo and Asher 2017).

A recent study by Avilla and Mothé (2021) dismisses previous molecular phylogenetic analyses and, based on morphological data, defined the new clade Sudamericungulata, which includes Astrapotheria, Notoungulata, Pyrotheria and Xenungulata. According to these authors, this would be a new lineage within

20.1.2 *Notoungulata*

The taxon name Notoungulata was introduced by Roth (1903), who recognized the peculiarity of this group by a unique configuration of the temporal region of the skull noted in toxodonts (e.g. *Toxodon*) and tyotheres (e.g. “*Tyotherium*”). Universally accepted as a natural group, Notoungulata constitute the most successful and diverse group of SANUs with more than 140 genera distributed in about 13 families, spanning the Paleocene-Holocene time range. Together with Litopterna, Notoungulata were the only SANUs that survived beyond the Great American Biotic Interchange (GABI) event, with the most recent fossils being found in association with human remains (Croft et al. 2020, and references therein). Only a single genus, *Mixotoxodon*, dispersed from South America and reached the south of North America during the Late Pleistocene (Lundelius et al. 2013; Hernández Jasso and Piñon 2020).

Cifelli (1993) performed one of the first cladistic analyses of Notoungulata, obtaining several synapomorphies for this clade and supporting the monophyly of the two traditional suborders, Tyotheria (including Archaeohyracidae, Archaeopithecidae, Hegetotheriidae, Interatheriidae, Mesotheriidae and Oldfieldthomasiidae) and Toxodontia *sensu lato* (including Homalodotheriidae, Isotemnidae, Leontiniidae, Notohippidae, and Toxodontidae). However, no synapomorphies were recovered to support “Notioprogenia”, an early diverging lineage previously proposed by Simpson (1934) which includes Arctostylopidae, Henricosborniidae and Notostylopidae. Later contributions provided new evidence for the monophyly of Notoungulata including Notostylopidae and Henricosborniidae but leaving Arctostylopidae as a separate order (Cifelli et al. 1989; Missiaen et al. 2012). The similarities in the auditory region between Notoungulata and Pyrotheria (Patterson 1977), particularly between *Notostylops* and *Pyrotherium*, led to the inclusion of pyrotheres within notoungulates (Fig. 20.1b; Billet 2010, 2011). However, a phylogenetic analysis at higher level (Muizon et al. 2015) and the particularities of the enamel structure in *Pyrotherium* (Koenigswald et al. 2015) seem to reinforce previous hypotheses (Simpson 1978) against the abovementioned notoungulate-pyrothere affinity. Subsequently, the traditional concepts of notoungulate families have been challenged during the last decades. Several phylogenetic revisions resulted in new hypotheses, such as considering Notopithecidae as a clade separated from the Interatheriidae *sensu stricto*, or the recognition of Henricosborniidae, Archaeohyracidae, Oldfieldthomasiidae, Isotemnidae and Notohippidae as non-monophyletic assemblages (Fig. 20.1b; Cifelli 1993; Shockey 1997; Marani 2005; Cerdeño and Vera 2010; Reguero and Prevosti 2010; Billet 2011; Cerdeño et al. 2012, 2018; García-López and Babot 2015; Vera 2015; García-López et al. 2018b; Martínez et al. 2021). In turn, the monophyly of Toxodontidae, Homalodotheriidae, Leontiniidae, Hegetotheriidae, Mesotheriidae and Interatheriidae Interatheriinae is broadly accepted (Cifelli 1993; Reguero and Prevosti 2010; Billet 2011; Shockey et al. 2012; Cerdeño and Vera 2015; Deraco and García-López 2016; Vera et al. 2017, 2019; Seoane and Cerdeño 2019;

Hernández del Pino et al. 2019; Bauzá et al. 2019). From here and throughout the text, the use of quotation marks indicates non-monophyletic groups.

From a paleobiological standpoint, body masses of notoungulates ranged from less than a kilogram to several tons. Among henricosborniids and notostylopids shown in Fig. 20.1b (thought to be early diverging representatives, but see Bauzá et al. (2020)), *Simpsonotus praecursor* and *S. major* (“Henricosborniidae”) would have weighed ~1 and ~3–4 kg, respectively, whereas *Notostylops murinus* (Notostylopidae) likely weighed between 5 and 13 kg (Croft 2016; Lorente et al. 2019; Croft et al. 2020). Morphofunctional indices and interpretations of the skeleton of *N. murinus* indicate locomotor faculties expected for terrestrial (unspecialized), semifossorial or even fossorial animals (Lorente et al. 2019), the latter being the ancestral condition hypothesized for notoungulates (Croft and Anderson 2008).

Toxodonts are usually compared to extant hippos or rhinos (in appearance, ecological role, molar crown patterns, etc.), although this assertion only seems to apply well for Toxodontidae (Fig. 20.1b). They were medium to very large herbivores (their body masses ranged from ~50 to more than 1000 kg (Cassini et al. 2012a, b; Elissamburu 2012)) with long and high skulls, high crowned cheek teeth, lateral tusk-like incisors and robust skeletons (MacFadden 2005; Croft et al. 2020).

Other toxodonts (e.g. “Isotemnidae”), ranging from ~50 to ~350 kg, were plantigrades (not adapted for agile locomotion), have crouching posture and/or scratch-digging capabilities (Shockey and Flynn 2007; Shockey and Anaya 2008; Elissamburu 2012; Carrillo and Asher 2017; Croft et al. 2020), whereas others (e.g. “Notohippidae”), ranging from ~20 to ~130 kg, were digitigrades or semidigitigrades and, at least some representatives (e.g. *Eurygenium pacegnum*, *Rhynchippus equinus* and *R. pumilus*) would have been subcursorial generalists (Shockey 1997; Elissamburu 2012; Shockey et al. 2012; Croft et al. 2020). Some members of Leontiniidae and Homalodotheriidae (Fig. 20.1b) developed very large body sizes (comparable to that of toxodontids or even larger) and showed quite interesting skeletal features, such as the relatively long neck of *Scarrittia canquelensis* (Chaffee 1952) and the Neogene Eurasian chalicotheriid-like appearance (forelimbs longer than hindlimbs and claws instead of hooves) of *Homalodotherium* (Scott 1930; Riggs 1937; Coombs 1983; Elissamburu 2010) mentioned by Croft et al. (2020).

There were also medium to small representatives (<20 kg), as the early diverging toxodonts *Puelia* sp. (MLP 67-II-27-27) and *Pampahippus* spp. (Giannini and García-López 2014; Deraco and García-López 2016; Croft 2016; García-López et al. 2018a; Martínez et al. 2019). From the late Oligocene onward (and following the general pattern observed in notoungulates as a whole), toxodonts developed hypsodont or hypselodont cheekteeth, probably associated with an increasingly abrasive diet (Madden 2015, and references therein; Croft et al. 2020; Domingo et al. 2020; Solórzano and Núñez-Flores 2021).

The other major group within Notoungulata, Typotheria (Fig. 20.1b), occupied small- to medium-sized herbivore niches. They included forms that weighed from less than 1 kg (e.g. middle Eocene Notopithecidae, see Vera (2015, 2017)) to nearly 200 kg (e.g. the Pleistocene Mesotheriidae *Mesotherium cristatum*). Early Paleogene representatives (e.g. Notopithecidae and representatives of “Oldfieldthomasidae”

included in Fig. 20.1b) showed generalized features such as low-crowned and rooted teeth and mostly plantigrade or semidigitigrade posture, which is indicative of terrestrial or semifossorial lifestyles and browsing feeding behavior (Croft 1999; Bergqvist and Fortes Bastos 2009). In turn, late diverging forms were specialized grazers with ever-growing high crowned cheek-teeth and gracile postcranial skeletons (Croft 1999; Croft and Anderson 2008; Cassini et al. 2012a; Croft et al. 2020; Solórzano and Núñez-Flores 2021).

Based solely on the skull morphology, tyotheres are described as rodent-like notoungulates, but a wider spectrum of morphotypes is presumed based on the post-cranium. Clear-cut examples are the morpho-functional differences observed between representatives of Mesotheriidae (which probably resemble extant capybaras) and Intertheriidae (likely comparable to hyraxes), or between any of them and some members of Hegetotheriidae, for which a lagomorph-like appearance is inferred. As expected, such diversity implies a wide range of locomotor behaviors involving cursorial (or functionally cursorial (Croft and Lorente 2021)), fossorial, semi-fossorial, occasional digging or arboreal adaptations (Croft 1999; Croft et al. 2004, 2020; Shockey et al. 2007; Croft and Anderson 2008; Cassini et al. 2012a, b; Lorente et al. 2019; Croft and Lorente 2021).

20.2 The Study of Notoungulates Braincast and Auditory Region over the Years

20.2.1 Braincast

The first descriptions of notoungulate braincast date back to the nineteenth century (Serres 1867; Gervais 1872) and correspond to *Mesotherium* (Mesotheriidae) and *Toxodon* (Toxodontidae), two well-known representatives of Typotheria and Toxodontia, respectively. Since then, and many years before the advent of computed tomography X-ray technology, a series of contributions produced valuable data based on natural or artificial casts of endocranial cavities of several notoungulates. Here, we will mention some classical contributions that followed the first insights of Serres and Gervais and laid the foundations for subsequent research.

In 1932, Simpson described the skulls and natural endocasts of *Notostylops* and *Oldfieldthomasia*, two early diverging notoungulates from the middle Eocene (Casamayoran South American Land Mammal age [SALMA]), noting their resemblance with the endocast of *Mesotherium* figured by Gervais (1872). In the case of *Notostylops*, Simpson (1932: 6) described its endocast as “strikingly primitive” and similar, to some extent, to condylarths but also to rodents (a rodent-like “primitive” notoungulate). A year later, Simpson (1933a) provided new data (e.g. descriptions of lateral and ventral surfaces, detail on some lateral vascular elements and cranial nerves) and much better illustrations of the endocast of *Notostylops*, and also made useful comparisons with *Rhyphodon* (“Isotemnidae”) and the archaic ungulate

Phenacodus (“Condylarthra”). Although the author recognized differences between them (e.g. concerning the olfactory bulbs, cerebellar relative size, piriform lobe shape, cortical design, exit of some cranial nerves and vessels; see later in Sect. 20.4), he mentioned that *Notostylops* and *Phenacodus* were remarkably similar, and that *Rhyphodon* showed the same “primitive developmental level” of *Notostylops*.

Shortly after, Simpson (1933b) described the endocast of two derived typotheres (*Hegetotherium* [Hegetotheriidae] and *Protypotherium* [Interatheriidae]) and the litoptern *Tetramerorhinus* (Ameghino 1894, *sensu* Soria 2001) and compared them with *Notostylops* and *Phenacodus*. According to Simpson, the cranial endocast of *Hegetotherium* was shorter, wider and deeper than that of *Notostylops*, and he also mentioned that it was “advanced” in “effective brain size” (Simpson 1933b: 1), having great reduction of the olfactory bulbs, expanded neopallium (which retains its triangular contour), and a “more definite and perhaps more complex” convolution pattern (Simpson 1933b: 3). No structural differences were mentioned about cranial nerves and associated major vascular elements, except for some considerations regarding the entocarotid (=internal carotid artery).

Patterson (1934b) described the exit of some cranial nerves of the endocast of *Trachytherus spegazzinianus* (Mesotheriidae). In addition, he discussed similarities and differences in the arrangement of the brain and cerebellum between *T. spegazzinianus*, *Hegetotherium*, *Protypotherium* and *Notostylops*. The endocast of *T. spegazzinianus* was previously described by Loomis (1914), who mentioned that the large size of the endocast (especially the frontal lobes) and other features were “highly specialized” and led him to doubt about a close relationship with the “Archaeohyracidae” *Archaeohyrax*.

Patterson (1937) provided new data for the toxodonts by describing the endocasts of *Rhynchippus* (“Notohippidae”), *Adinotherium* and *Nesodon* (Toxodontidae), *Homalodotherium* (Homalodotheriidae), and the typothere *Typtotheriopsis* (Mesotheriidae). Although he mentioned a couple of shared features between *Rhynchippus* and *Hegetotherium*, and between *Rhynchippus* and *Rhyphodon*, similarities in the general vascular pattern and the auditory region between *Rhynchippus*, *Nesodon* and *Adinotherium* led the author to reinforce his previous proposal of a close relationship between “Notohippidae” and Toxodontidae (Patterson 1936). In the case of *Homalodotherium*, Patterson (1937) described the endocast as resembling the morphological “toxodontid-notohippid” pattern in which the olfactory bulbs are expanded and widely separated, and also noted similarities in the lateral and anterior petrosal venous sinuses. As for the endocast of *Typtotheriopsis*, it was described as shallower and slightly less flexed than that of *Hegetotherium*, with a well-developed rhinencephalon and a general morphology closer to other typotheres such as the Mesotheriidae *Trachytherus* and the Interatheriidae *Protypotherium* and *Interatherium*.

Dechaseaux (1956, 1958, 1962) provided updated descriptions of the endocasts of *Pachyrukhos* (Hegetotheriidae) and that of the abovementioned *Notostylops* (Notostylopidae), *Protypotherium* and *Mesotherium* (typotheres), and *Rhynchippus* and *Toxodon* (toxodonts), adding interesting comments on the neopallium fissuration. She concluded (mainly based on *Mesotherium* and *Toxodon*) that the sulci on

the Sylvian region were not homologous to the Sylvian complex or the pseudosylvian sulcus observed in other eutherians. Furthermore, Dechaseaux (1962) concluded that despite *Toxodon* being a late-diverging notoungulate, it had a primitive brain based on its serial disposition of the ventral elements and suggested that the well-developed cerebral hemispheres (which would indicate an “evolved” brain) could have resulted from the development of the white matter. Regardless of the arguments themselves, Dechaseaux (1962) pertinently highlighted how difficult is to propose homologies of cranial endocast structures between notoungulates and other eutherians.

Radinsky (1981) inferred the location of some neocortical areas in notoungulates based on the sulci observed in *Hegetotherium* and *Protypotherium*. As noted by the author, the general shape of the endocast and the sulcal pattern of these taxa resemble that of some hystricomorph rodents for which cortical mapping studies had been previously performed (see Campos and Welker 1976). Even though the location of the auditory, primary motor, primary somatic and visual cortices were extrapolated (Radinsky 1981: fig. 8), this author mentioned that it was not possible to be sure about the homology of the sulci and gyri that delimitate these areas. In this context, Radinsky (1981) suggested that if they were homologous, the bulging temporal lobe observed in tytopheres could indicate an expanded auditory cortex. In agreement, Dozo (1997) noted the striking similarities in general shape and location of the sulci between the endocasts of *Paedotherium insigne* (Notoungulata, Hegetotheriidae) and *Dolicavia minuscula* (Rodentia, Caviidae) and provided a comparative description of both species.

20.2.2 Auditory Region

Other endocranial spaces of notoungulates such as the tympanic cavity proper and adjacent spaces (e.g. the characteristic epitympanic sinuses and auditory bullae) received special attention from Patterson (1932, 1934a, 1936) and Simpson (1936), being Patterson's (1936) and Simpson's (1936) pivotal contributions in this regard. Patterson (1936) thoroughly described the internal structure of the auditory region (i.e. middle ear) of several tytopheres (*Hegetotherium*, *Interatherium*, *Pachyrukhos*, *Protypotherium* and *Pseudotypotherium*) and toxodonts (*Adinotherium*, *Ancylocoelus*, *Homalodotherium*, *Nesodon* and *Rhynchippus*), and recognized some traits that seemed to be common to all notoungulates and others that were distinctive of different groups within the order (e.g. Hegetotheriidae, Interatheriidae, Mesotheriidae, and Toxodontia).

Simpson (1936) described and figured the auditory region (tympanic cavity, auditory bullae and epitympanic sinuses) of *Oldfieldthomasia debilitata* based on external features and parasagittal serial sections of the specimen AMNH FM 28600. This method allowed him to identify contacts between bones and tentatively map them on the surface of the skull in areas where sutures were not so evident. This analysis provided new data on the course of the entocarotid artery (=internal carotid

artery [ICA]), the apertures surrounding the auditory bullae, and the periotic. Additionally, Simpson (1936: 26) mentioned that the general plan of the endocranial cavity in *O. debilitata* was identical to that of *Notostylops*, and made valuable comments on vascular elements observed on the internal surface of the skull and diploe. Following Patterson and Simpson's contributions, it was not until the current century that the auditory region of notoungulates was actively studied again, strongly aided by the application of CT or Micro-CT scanning techniques.

Gabbert (2004) redescribed the basicranium of the Toxodontia based on representatives of "Isotemnidae" (*Pleurostylodon* sp., *Periphragnis* sp.), "Notohippidae" (*Puelia* sp., *Rhynchippus equinus*), Leontiniidae (*Leontinia gaudryi*, *Ancylocoelus frequens*, and *Scarrittia canquelensis*), Homalodotheriidae (*Homalodotherium segoviae*) and Toxodontidae (*Adinotherium* spp., *Nesodon imbricatus*). She focused on the auditory bullae (bone composition and surrounding foramina) and concluded that the internal crests identified on the bullar wall should not be interpreted as evidence for a compound bullae made of ento- and ectotympanic, as stated by Patterson (1934a, 1936) for tytopheres and toxodonts. Instead, Gabbert (2004: fig. 14.3) suggested that, at least in toxodonts, the crest could be the medial margin of the ectotympanic that curves on itself due to its own ventromedial inflation during ontogeny. As for the ICA (internal carotid artery), she could not find the posterior carotid foramen mentioned by Patterson (1936), which led her to challenge Patterson's assertion about an intratympanic course of this artery.

20.2.3 Advances in Recent Years

The advent of CT scanning techniques stimulated new research in almost all the aforementioned topics. A series of contributions provided valuable data on the inner ear of *Notostylops murinus* (Macrini et al. 2010) and the tytopheres *Altitypotherium chucalensis* (Mesotheriidae), *Pachyrukhos moyani* (Hegetotheriidae) and *Cochilius* sp. (Intertheriidae) (Macrini et al. 2013). Billet and Muizon (2013) described not only the internal but also the external morphology of an early Eocene isolated petrosal bone (Notoungulata indet.) and identified imprints of the ICA and the stapedia system. MacPhee (2014) provided a thorough revision of the posterior skull of the Tytopheria based on several representatives of "Oldfieldthomasiidae", Intertheriidae, Mesotheriidae and Hegetotheriidae.

More recently, Fernández-Monescillo et al. (2019) described the brain endocasts of the mesotheriids *Eutytopherium superans*, *Plesiotypotherium achirense*, *Trachytherus alloxus*, *Pseudotypotherium* sp. (see comment in Table 20.1) and *M. cristatum* (they also included *T. spegazzinianus*, although based on a natural endocast). MacPhee et al. (2021) provided new data on *Cochilius volvens*, whereas Perini et al. (2022) did the same with *Notostylops murinus*.

The main endocranial spaces and posterior cranial morphology of toxodonts were studied by means of CT scanning in *Homalodotherium* sp. (Homalodotheriidae), *Rhynchippus equinus*, *Eurygenium latirostris*, *Mendozahippus fierensis*

(“Notohippidae”) and *Gualta cuyana* (Leontiniidae) (Dozo and Martínez 2016; Martínez et al. 2016, 2020; MacPhee et al. 2021). García-López et al. (2018b) described a late middle Eocene Toxodontia indet. with emphasis on the auditory region, and Hernández Del Pino (2018) provided 3D digital models (including braincast and bony labyrinth reconstructions) of the toxodontids *Proadinotherium muensteri*, *Adinotherium ovinum*, *Nesodon imbricatus*, and *N. tawaretus*. Recently, MacPhee and Forasiepi (2022) re-evaluated the cranial pathway of the ICA in notoungulates based in representatives of both toxodonts and typtotheres. Some of these contributions are mentioned in detail throughout the text.

In this context, the aim of this chapter is to provide a brief but updated review of the current knowledge about the endocranial spaces in notoungulates with focus on contributions of the last two decades, and to add new observations on some taxa (Table 20.1). However, it is worth mentioning that classical contributions of the past century are still sources of valuable data (measurements, EQs, drawings, etc.), which is an indication of how much work needs to be done by means of CT imaging techniques, volume rendering, and multidimensional shape analysis.

Table 20.1 Taxa, specimens and data source

Taxa		Specimen(s) and data source
Notoungulata indet.	–	MNHN-F-BRD 23* (Billet and Muizon 2013)
Notostylopidae	<i>Notostylops murinus</i>	AMNH FM 28614 (Simpson 1933a) FMNH-P 13319* (Macrini et al. 2013; Perini et al. 2022)
Toxodontia indet.	–	IBIGEO-P 12 (García-López et al. 2018b)
“Isotemnidae” (Toxodontia)	<i>Rhyphodon</i> sp. <i>Periphragnis</i> sp.	AMNH FM 29414 (Simpson 1933a) MPEF-PV 1026***
Homalodotheriidae (Toxodontia)	<i>Homalodotherium</i> sp.	FMNH-P 13092 (Patterson 1937), MPM PV 17490* (Hernández del Pino 2018; MacPhee et al. 2021)
Leontiniidae (Toxodontia)	<i>Gualta cuyana</i> <i>Leontinia gaudryi</i>	MCNAM-PV 3951* (Martínez et al. 2020) FMNH-P 13285 (Radinsky 1981)
“Notohippidae” (Toxodontia)	<i>Rhynchippus equinus</i> <i>Rhynchippus pumilus</i> <i>Eurygenium latirostris</i> <i>Mendozahippus fierensis</i>	FMNH-P 13420 (Patterson 1937), MPEF-PV 695* (Dozo and Martínez 2016; Martínez et al. 2016, 2020) MACN-A 52-61* (Martínez 2018) UNPSJB-PV 60* (Dozo and Martínez 2016) MCNAM-PV 4004* (Martínez et al. 2020)
Toxodontidae (Toxodontia)	<i>Nesodon imbricatus</i>	MPEF-PV 1323***b

(continued)

Table 20.1 (continued)

Taxa		Specimen(s) and data source
Mesotheriidae (Typotheria)	<i>Trachytherus spgazzinianus</i>	UNPSJB-PV 112* (Fernández-Monescillo et al. 2019)
	<i>Trachytherus alloxus</i>	MNHN-Bol-V 6355* (Fernández-Monescillo et al. 2019)
	<i>Eutypotherium superans</i>	MACN-A 11079* (Fernández-Monescillo et al. 2019)
	<i>Plesiotypotherium achirense</i>	MNHN-Bol-V 12664*, MNHN-Bol-V 8507*, MNHN.F.ACH 26* (Fernández-Monescillo et al. 2019)
	<i>Mesotherium cristatum</i>	MNHN.F.PAM 2* (Fernández-Monescillo et al. 2019)
	<i>Pseudotypotherium</i> sp.	MACN-Pv 2925* ^c , MACN-Pv 1111* ^c (Fernández-Monescillo et al. 2019)
	<i>Altiypotherium chucalensis</i>	SGOPV 4100* (Macrini et al. 2013)
Hegetotheriidae (Typotheria)	<i>Pachyrukhos moyani</i>	FMNH-P 13051* (Macrini et al. 2013)
Interatheriidae (Typotheria)	<i>Cochilius volvens</i>	AMNH FM 29651* (MacPhee et al. 2021)
	<i>Cochilius</i> sp.	SGOPV 3774* (Macrini et al. 2013; Perini et al. 2022)

*CT or micro CT data previously reported

**CT data first reported in this chapter (CT scanning performed at Instituto de Diagnóstico del Este del Chubut, Puerto Madryn, Argentina). Series exported in DICOM format (image resolution of 512 × 512 pixels). Reslicing, resampling, segmentation and volumetric reconstructions performed using 3D Slicer 4.10.2 (Fedorov et al. 2012)

^aPixel size of 0.516 mm, interslice spacing of 2.5 mm (resampled to get isotropic voxels)

^bPixel size of 0.410 mm, interslice spacing of 1 mm (resampled to get isotropic voxels)

^cOriginally referred to *M. maendrum*, but currently under taxonomic review and considered *Pseudotypotherium* sp. by M. Fernández-Monescillo (pers. comm)

Institutional abbreviations: *AMNH FM* American Museum of Natural History, Fossil Mammal Collection, New York, USA, *FMNH-P* Field Museum of Natural History, Paleontological Collection, Chicago, USA, *IBIGEO-P* Colección Paleontología Instituto de Bio y Geociencias del Noroeste Argentino, Rosario de Lerma, Argentina, *MACN-A -Pv*, Museo Argentino de Ciencias Naturales Bernardino Rivadavia, Ameghino and Paleovertebrate Collections, respectively, Buenos Aires, Argentina, *MCNAM-PV* Museo de Ciencias Naturales y Antropológicas “J. C. Moyano”, Vertebrate Paleontology Collection, Mendoza, Argentina, *MNHN-F-BRD -PAM, -ACH*, Muséum National d’Histoire Naturelle, Brazil, Pampean and Achiri Fossil Collections, respectively, Paris, France, *MNHN-Bol* Museo Nacional de Historia Nacional de Bolivia, La Paz, Bolivia, *MPEF-PV* Museo Paleontológico Egidio Feruglio, Vertebrate Paleontology Collection, Trelew, Argentina, *MPM-PV* Museo Regional Provincial Padre M. Jesús Molina, Vertebrate Paleontology Collection, Río Gallegos, Argentina, *SGOPV* Museo Nacional de Historia Natural de Santiago, Vertebrate Paleontology Collection, Santiago, Chile, *UNPSJB-PV* Repositorio Científico y Didáctico de la Facultad de Ciencias Naturales de la Universidad Nacional de la Patagonia San Juan Bosco, Comodoro Rivadavia, Argentina

20.3 Overview of the Endocranial Morphology

20.3.1 Characterization of Notoungulate Braincast

Three major regions can be recognized (and potentially described based on endocasts) in a generic mammalian brain: the forebrain (paleocortex and neocortex), the midbrain (sometimes dorsally covered by the forebrain), and the hindbrain (cerebellum, pons, and medulla oblongata). Additionally, the cast of the main cranial nerves and the hypophyseal region (closely integrated to the brain) are usually distinguishable on the midventral surface of the endocasts.

Despite the morphological diversity observed within notoungulates (see Sect. 20.4.1), the general neocortical gyrification and the position of the orbitotemporal canal relative to both the piriform lobes and the rhinal fissure seem to be useful traits to tentatively differentiate notoungulates from litopterns and astrapotheres. The sulci on the neocortex of notoungulates show a typically well-marked oblique sulcus (here interpreted as the suprasylvian sulcus) that separates the frontal lobe from the temporal lobe (Figs. 20.2 and 20.3), different from the parallel longitudinal sulci observed in litopterns (Radinsky 1981; this book, Chap. 21). Conversely, astrapotheres show almost completely lissencephalic cerebral hemispheres, and only a blurred oblique sulcus has been mentioned for *Astrapotherium magnum* (Radinsky 1981: fig. 4; MacPhee et al. 2021: fig. 8).

The cast of the orbitotemporal canal (= cranioorbital canal sensu MacPhee et al. (2021)) seems to be another relatively noticeable difference. It is very close to (or even conceals) the rhinal fissure in notoungulates (Figs. 20.2 and 20.3), whereas it is placed very low (relative to the piriform lobes) and well below the rhinal fissure in litopterns (Forasiepi et al. 2016: figs. 22, 23; this book, Chap. 21). In astrapotheres, the orbitotemporal canal is visible at mid-height on the piriform lobes, and the rhinal fissure appears to be even more dorsally shifted than in litopterns (MacPhee et al. 2021: fig. 8).

In contrast, it is not possible to recognize a notoungulate pattern based on the midbrain and hindbrain regions. Early diverging representatives generally show a more dorsoventrally compressed brain and posteriorly projected hindbrain (Fig. 20.2a; Perini et al. 2022: fig 3a), whereas later diverging representatives (especially toxodonts) show brains with a greater dorsoventral development and less posteriorly projected hindbrain (Table 20.2 and Fig. 20.3a, b). The midbrain seems to be dorsally exposed in *Notostylops* (Simpson 1933a; Radinsky 1981), even though the colliculi of the corpora quadrigemina (probably concealed by non-nervous tissue) are not distinguishable (Simpson 1933a; but see Perini et al. 2022). The casts of the hypophyseal fossa and main cranial nerves (observed on the midventral surface) also show some differences among notoungulates, especially between early and late diverging representatives (see Sect. 20.4.1).

At this point, it is worth noting the absence of data on endocasts of other SANUs such as Pyrotheria and Xenungulata, which is a major limitation for comparative descriptions at high taxonomic levels. No endocasts have been figured or described

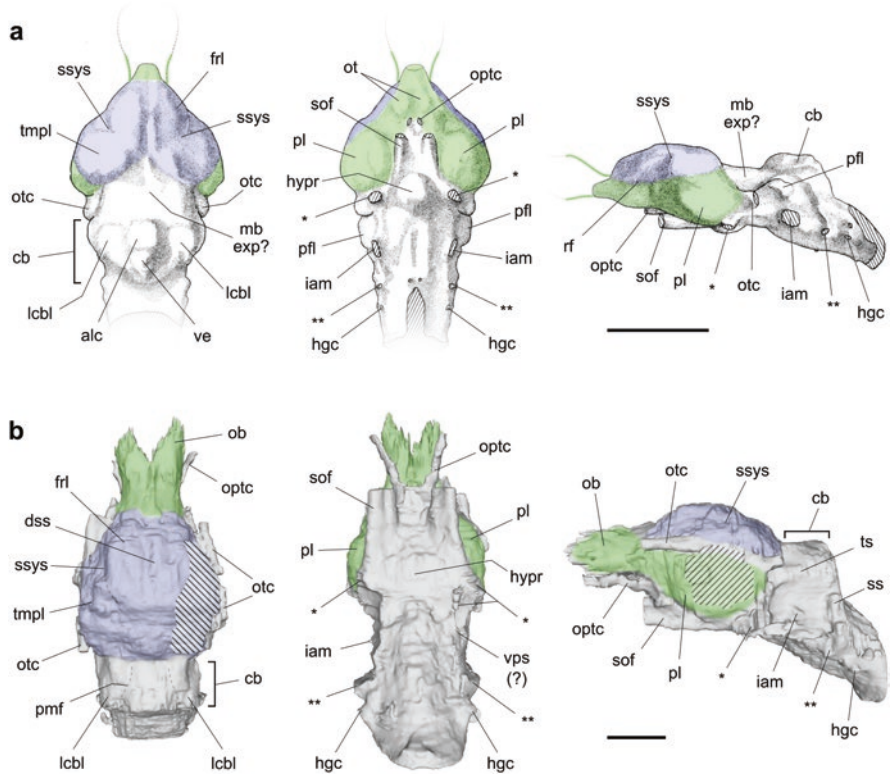


Fig. 20.2 Drawing and digital rendering of endocranials of *Notostylops murinus* (AMNH FM 28614, adapted from Simpson (1933a: fig. 2)) (a) and *Periphragnis* sp. (MPEF-PV 1026)(b) in dorsal (left), ventral (center) and lateral (right) views. Neocortex and paleocortex colored in blue and green, respectively. Lateral view in “a” corresponds to the specular image of the right side. Dashed areas in “b” indicate unpreserved surfaces. Asterisk and double asterisk indicate the rostral and jugular portions of the basicapsular fenestra respectively. Abbreviations: *alc* anterior lobe of the cerebellum, *cb* cerebellum, *dss* dorsal sagittal sinus, *fri* frontal lobe, *hgc* hypoglossal canal, *hypr* hypophyseal region, *iam* internal auditory meatus, *lcbi* lateral lobe of the cerebellum, *ls* lateral sulcus, *mb exp* midbrain exposure, *ob* olfactory bulb, *optc* optical canal, *ot* olfactory tubercle, *otc* orbitotemporal canal (=cranioorbital canal), *pfl* parafloroculus, *pl* piriform lobe, *pmf* paramedial fissure, *rf* rhinal fissure, *sof* sphenorbital fissure, *ss* sigmoid sinus, *ssys* suprasylvian sulcus, *tmpl* temporal lobe, *ts* temporal sinus, *ve* vermis, *vps* ventral petrosal sinus. Scale bars = 20 mm

for pyrotheres even though the fossil record includes specimens probably suitable for this purpose. Conversely, skull remains of xenungulates, other than mandibular and maxillary fragments, are virtually unknown.

Notwithstanding, before focusing on the cranial endocast regions themselves, a brief mention of some spaces associated with intracranial blood supply and the auditory region is pertinent, either because they are potentially informative for phylogenetic purposes, or because they allow some physiological and morphofunctional inferences. The spaces associated with intracranial blood supply includes not

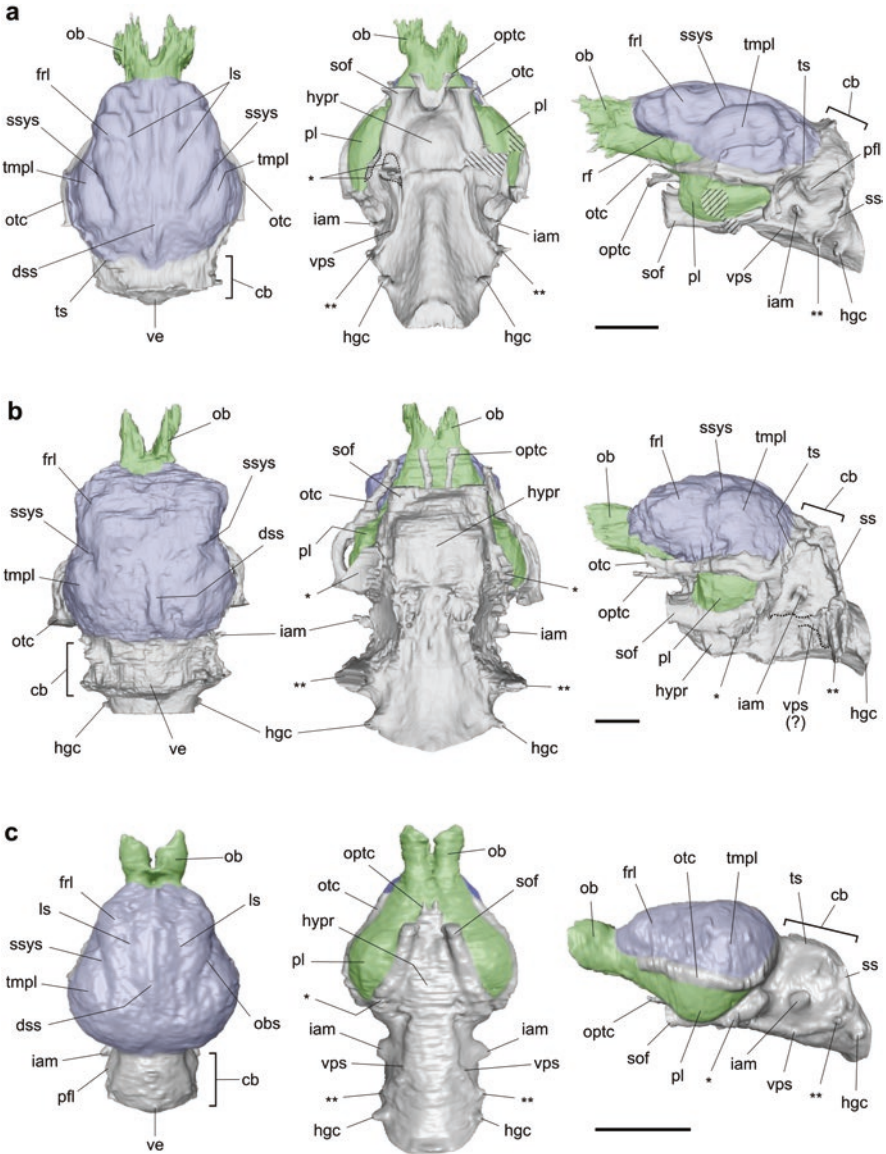


Fig. 20.3 Digital endocasts of *Rhynchippus equinus* (MPEF-PV 695) (a), *Nesodon imbricatus* (MPEF-PV 1323) (b), and *Pseudotyotherium* sp. (MACN-Pv 2925, see comment in Table 20.1) (c), in dorsal (left), ventral (center) and lateral (right) views. Neocortex and paleocortex are colored in blue and green, respectively. Dashed areas in “a” indicate unpreserved surfaces. Asterisk and double asterisk indicate the rostral and jugular portions of the basicapsular fenestra respectively. Abbreviations: as for Fig. 20.2. Scale bars = 20 mm

Table 20.2 Cranial endocast measurements for *Periphragnis* sp. (MPEF-PV 1026) and *Nesodon imbricatus* (MPEF-PV 1323)

Dimension (mm)/ratio	<i>Periphragnis</i> sp.	<i>Nesodon imbricatus</i>
cbl	13.8	16.3
cbw	31.7	50.7
crh	43.7	81.6
crl	45.4	75.3
crw	45.7	71.2
el	86.2	110.0
el-ob	64.0	93.5
frw	21.4	61.2
hbh	37.5	70.3
obh	15.7	22.0
obl	21.3	17.2
obw	20.4	23.4
pld	34.8	47.6
frw/crw ratio	1/2.24	1/1.16
obw/frw ratio	1/1.05	1/3.56
el-ob/cbl ratio	1/0.21	1/0.17
el-ob/crh ratio	1/0.68	1/0.87
eflex	24°	55°

Abbreviations: *cbl* maximum length of cerebellar cast, *cbw* maximum width of cerebellar cast, *crh* maximum height of cerebral cast, *crl* maximum length of cerebral cast exclusive of olfactory bulbs, *crw* maximum width of cerebral cast, *eflex* encephalic flexure angle, *el* maximum length of endocast, *el-ob* maximum length of endocast exclusive of olfactory bulbs, *frw* maximum width of frontal region, *hbh* maximum height of hindbrain cast, *obh* maximum height of olfactory bulb casts, *obl* maximum length of olfactory bulb casts, *obw* maximum combined width of olfactory bulb casts, *pld* maximum distance between ventral edges of piriform lobes. Linear measurements expressed in millimeters. See Macrini et al. (2007: fig. 2) and Dozo and Martínez (2016: fig. 2) for details on how measurements were taken. See Martínez et al. (2020: table 1) for comparison with other toxodonts, and Fernández-Monescillo et al. (2019: table 1) for comparison with tytopheres. Linear measurements obtained from virtual cranial endocasts in 3D Slicer 4.10.2 (Fedorov et al. 2012).

only the main dural venous sinuses, but also some foramina and canals related to the internal carotid artery and the stapodial system. The endocranial spaces of the auditory region comprise both the middle ear (tympanic cavity and epitympanic sinuses) and the inner ear (bony labyrinth of the petrosal).

20.3.2 Spaces Associated with Intracranial Blood Supply

The cast of main dural venous sinuses are variably distinguishable among the order. In some small to medium-sized notoungulates (e.g. tytopheres and small toxodonts as the “Notohippidae”), the dorsal sagittal sinus is generally recognizable on the cranial endocast when viewed dorsally, whereas it is often totally or partially

obscured by the meninges in large-sized representatives (e.g. large toxodonts as Leontiniidae). As expected for a therian mammal, the sagittal sinus runs dorsally on the sagittal plane and is connected to the transverse sinuses (Butler 1967). As its name suggests, the transverse sinuses (which generally leave less noticeable imprints than the sagittal sinus) run transversally and bifurcate into the temporal (anteriorly) and the sigmoid (posteriorly) sinuses (Wible and Zeller 1994).

Enlarged intradiploic spaces related to the transverse sinuses (observed in a variety of mammals) have been also described for some notoungulates (*Cochilius* [Interatheriidae], *Homalodotherium* [Holodotheriidae], *Nesodon* [Toxodontidae], and *Periphragnis* ["Isotemnidae"]) and the astropothere *Trigonostylops* (Fig. 20.4; MacPhee et al. 2021: figs. 7–9, 16). They are placed in the supraoccipital, parietal, and interparietal bones, and are grouped together as "accessory lacunae of the transverse sinuses" (MacPhee et al. 2021). Among notoungulates, *Cochilius*, *Periphragnis*, and *Nesodon* show the typical condition consisting of a series of small canals connected to larger networks that lead to the transverse sinuses (Fig. 20.4; MacPhee et al. 2021: figs. 9, 16). However, *Homalodotherium* sp. (MPM PV 17490) shows a particular morphology in which accessory lacunae of the transverse sinuses are in the shape of an elaborated structure capping the dorsal surface of the cerebellum, highly vermiculated, continuous with sulci for dural sinuses, and with large canals extending into the bone (MacPhee et al. 2021: fig. 7). Additionally, the presence of a sinus communicans (a transversal canal linked to the sagittal and the transverse sinuses) was mentioned for *Homalodotherium* sp. and *Cochilius volvens* (MacPhee et al. 2021: figs. 7, 16). In *Mendozahippus fierensis* ["Notohippidae"], there is a thick canal that resembles the sinus communicans (Martínez et al. 2020: fig. 9), but further discussion is needed since no connection between this canal and the sagittal sinus is clearly distinguishable in the studied specimen (MCNAM-PV 4004).

The temporal sinus (=petrosquamus sinus) occupies the petrosquamosal canal, between the dorsal edge of the petrosal and the squamosal (Fig. 20.4a–e). In the "Notohippidae" *M. fierensis* (MCNAM-PV 4004) and *Rhynchippus equinus* (MPEF-PV 695), the canal is enclosed and only partially visible when viewed endocranially (Martínez et al. 2016: fig. 11, 2020: fig. 6). In the case of the leontiniid *Gualta cuyana* (MCNAM-PV 3951), the petrosquamosal canal is wider and deeper than in other notoungulates, indicating a conspicuous dilatation at level of the temporal sinus or at the junction of the transverse and temporal sinuses (Martínez et al. 2020: fig. 6). Regardless of their massiveness, paired emissary veins (variable in number) branch from the temporal and transverse sinuses in all notoungulates for which this region is known. The emissary veins pass (probably together with the accompanying arteries) through the temporal foramina (external apertures of the parietosquamosal canals) observed on the squamosal, the parietal, and/or the parieto-occipital suture (Fig. 20.4a, b, d–f). Anteriorly, the temporal sinus is connected to the cranioorbital sinus (=orbitotemporal vein) and is also linked to the external jugular vein by the retroarticular emissary vein (=capsuloparietal emissary vein; postglenoid vein), which exits the skull through the retroarticular (=postglenoid) canal (Fig. 20.4).

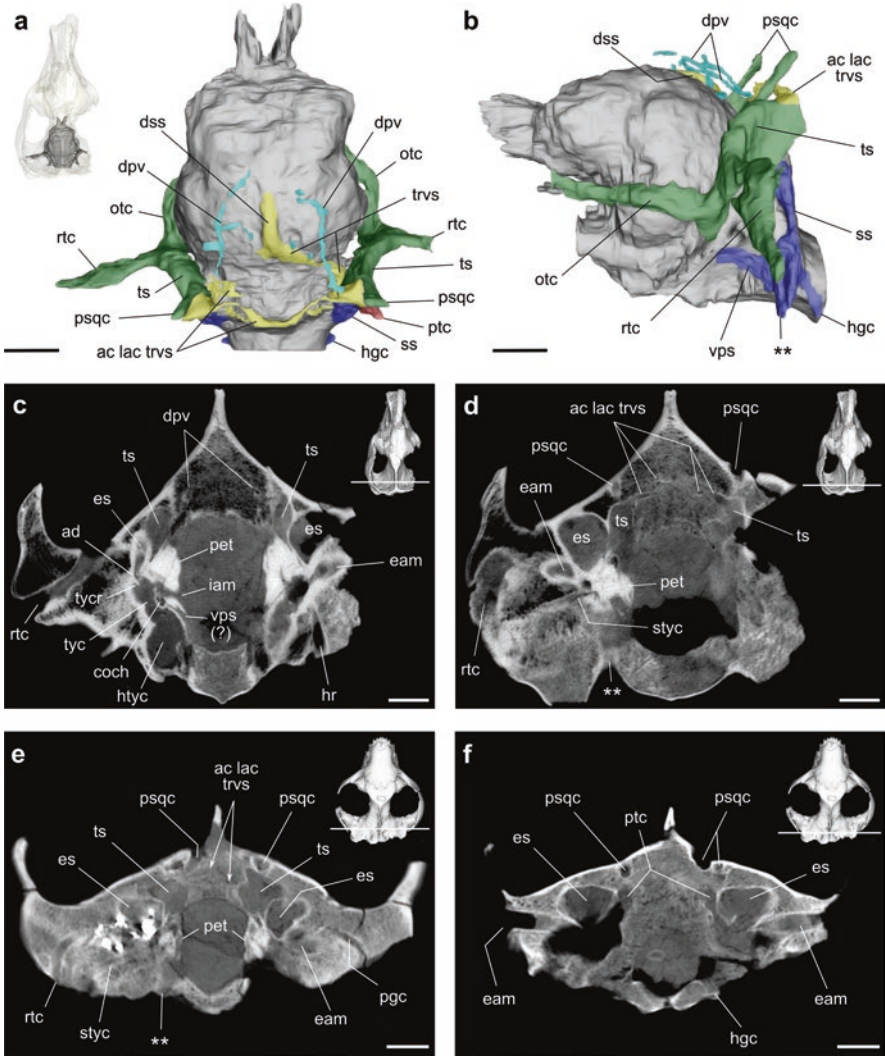


Fig. 20.4 Digital brain endocast and caudodorsal vasculature of *Nesodon imbricatus* (a, b), and CT-slices at level of the caudal cranium of *Nesodon imbricatus* (c, d) and *Periphragnis* sp. (e, f): a–d MPEF-PV 1323; e, f MPEF-PV 1026. Abbreviations: *ac lac trvs* accessory lacunae of the transverse sinus, *ad* aditus, *coch* cochlea, *dpv* diploic vein, *dss* dorsal sagittal sinus, *eam* external auditory meatus, *es* epitympanic sinus, *hgc* hypoglossal canal, *hr* hyoid recess, *htyc* hypotympanic cavity (interior of bullae), *iam* internal auditory meatus, *otc* obitotemporal canal (=cranioorbital canal), *pet* petrosal bone, *psqc* parietosquamosal canal, *ptc* posttemporal canal, *rtc* retroarticular canal, *ss* sigmoid sinus, *styc* stylomastoid canal, *trvs* transverse sinus, *ts* temporal sinus, *tyc* tympanic cavity, *tycr* tympanic crest, *vps* ventral petrosal sinus. Double asterisk indicates the jugular portion of the basicapsular fenestra. Scale bars = 20 mm

The second main sinus that branches from the transverse sinus is the sigmoid sinus, which accommodates between the pars mastoidea of the petrosal and the occipital. It joins the ventral petrosal sinus (=inferior petrosal sinus) and empties in the internal jugular vein (Figs. 20.2, 20.3, and 20.4). It is well distinguishable in some notoungulates (e.g. *Homalodotherium* (MacPhee et al. 2021: fig. 7), *Nesodon* and seemingly *Periphragnis* (Figs. 20.2b and 20.3b)), but it is less marked in others (e.g., *Cochilius* (MacPhee et al. 2021: fig. 9), *Notostylops*, *Rhynchippus*, *Pseudotyotherium* (Figs. 20.2a and 20.3a, c), among others). The variable development of the sigmoid sinus (and the internal jugular vein) could be related to the proportional role of this system in the endocranial venous return in comparison to other intracranial routes (as the retroarticular emissary vein) or to an extracranial pathway associated to the vertebral venous system (MacPhee et al. 2021).

The course of the internal carotid artery is probably the most debated issue in notoungulates. Patterson (1936) suggested that it could be intratympanic (at least in toxodonts and some tyotheres), which means that the internal carotid artery would travel through the tympanic cavity before entering the main endocranial cavity. Patterson (1936) based this proposal on the presence of a posterior carotid foramen (=caudal carotid foramen) that would transmit the internal carotid artery into the tympanic cavity. Although Gabbert (2004) could not corroborate this when describing the basicranial and auditory region of the Toxodontia, an alleged posterior carotid foramen near the jugular area has been reported for *Pleurostylodon*, *Homalodotherium*, *Rhynchippus*, *Mendozahippus*, *Gualta*, *Nesodon* and *Posnaskytherium* (Patterson 1932, 1936; Billet and Muizon 2013; Martínez et al. 2016, 2020), and in the tyotheres *Oldfieldthomasia*, *Argyrohyrax*, *Interatherium* and *Pseudotyotherium* (Patterson 1932, 1936; Simpson 1936; Billet and Muizon 2013). However, MacPhee et al. (2021) and MacPhee and Forasiepi (2022) have recently challenged this hypothesis based on their observations on representatives of Notoungulata (*Cochilius volvens*, *Hegetotherium mirabile*, *Homalodotherium* sp., *Mesotherium pachygnathum*, *Paedotherium bonaerense*, *Piauhytherium* sp., *Rhynchippus equinus*, and *Toxodon* sp.), Astrapotheria, Litopterna, Perissodactyla, and the condylarth *Meniscotherium chamense*. As part of a thorough revision that involved the whole caudodorsal and basicranial vasculature, MacPhee et al. (2021) and MacPhee and Forasiepi (2022) reinterpreted the alleged caudal carotid foramen observed in some of the abovementioned notoungulates as the canal for the tympanic nerve. This possibility, combined with the absence of other indicia (e.g. sulci on the promontorium), led MacPhee et al. (2021) to consider that the reported evidence supporting an intratympanic course of the internal carotid artery is inconclusive. In this regard, MacPhee and Forasiepi (2022) proposed an extratympanic route, either enclosed within a canal along the basicranial kneel (tentatively corroborated in hegetotheriids and probably also applicable to archaeohyracids) or unenclosed (i.e. the internal carotid artery would entered the piriform fenestra freely), the later seemingly applicable to most notoungulate clades.

A functional proximal stapedia artery arising from the internal carotid artery (if present) was inferred in notoungulates based on a groove and a canal that pierces the tegmen tympani of an isolated petrosal (Notoungulata indet. from the Eocene of

Brazil; Billet and Muizon 2013: fig. 8). The authors interpreted these structures as the passage for the superior ramus of the stapedia artery. A similar condition was mentioned for *Mendozahippus fierensis* (Martínez et al. 2020), but MacPhee et al. (2021) and MacPhee and Forasiepi (2022) have recently proposed that such canal could be the tympanic aperture of the prootic canal, for a retained lateral head vein or remnant prootic sinus.

Finally, the presence of the arteria diploëtica magna (a connection between the stapedia system -or remnants- and the occipital artery) is also unresolved in notoungulates. It was explicitly mentioned for the isolated petrosal of the Notoungulata indet. described by Billet and Muizon (2013) and for *R. equinus* and *M. fierensis* (Martínez et al. 2016, 2020) based on the presence of a posttemporal canal/foramen, but MacPhee et al. (2021) argued that the sole existence of a posttemporal canal should not be interpreted as conclusive evidence of a functional arteria diploëtica magna (the canal could transmit the arteria, the vena, or both). In fact, the authors considered that the morphology observed in *Cochilius* (AMNH FM 29651), *Toxodon* (MACN-PV 16615) and *Homalodotherium* sp. (MPM PV 17490) is suggestive of venous circulation only or strongly predominant (MacPhee et al. 2021: table 6).

20.3.3 Spaces Associated with the Middle and Inner Ear

Notoungulates have a highly pneumatized middle ear composed of the tympanic cavity proper and well-developed auditory bullae. Externally, the size and form of the auditory bullae ranged from ovoid and well inflated to roughly triangular in ventral view and moderately inflated. Furthermore, all but a few early representatives of the order possess large paratympanic spaces (the epitympanic sinuses) situated posterodorsally on the lateral sidewalls of the skull (squamosal).

The tympanic bone forms the floor and ventrolateral wall of the tympanic cavity. In notoungulates (as in other groups of mammals), the tympanic is ventrally inflated, resulting in well-developed auditory bullae that enlarge the tympanic cavity (e.g. *Nesodon imbricatus* in Fig. 20.4c). Internally, auditory bullae are partially divided by bullar septa that seem to vary among different representatives regarding orientation (vertical vs. horizontal), osteological interpretation (whether or not it implies a compound bulla made of ento and ectotympanic), and ontogenetic inferences (developmental and bone remodeling processes). Such an intricate issue is beyond the scope of this chapter, but see Patterson (1936, 1977), Gabbert (2004), García-López (2011), MacPhee (2014) and MacPhee et al. (2021) for details in this regard.

In most notoungulates, the tympanic cavity dorsally communicates with the abovementioned epitympanic sinus (thought to be a derivative of the epitympanic recess) through the aditus (= foramen pneumaticum; Fig. 20.4c). Based on this communication, a hearing-related function has been proposed for the sinuses. The epitympanic sinus lies more dorsocaudally in the squamosal bone in pachyrhines and mesotheriids (MacPhee et al. 2021). However, some Paleogene notoungulates such as *Simpsonotus* (“Henricosborniidae”) and *Colbertia* (“Oldfieldthomasiidae”)

do not show conspicuous epitympanic sinuses (Pascual et al. 1978; García-López 2011). As pointed out by MacPhee (2014), no evidence of an aditus is observed in the Eocene isolated petrosal (Notoungulata indet.) described by Billet and Muizon (2013), suggesting that the epitympanic sinuses as paratympanic spaces would be absent in the earliest representatives of the group. An exception is the Eocene *Toxodontia* indet. IBIGEO-P 12, for which prominent epitympanic sinuses connected to the tympanic cavity were described (García-López et al. 2018b).

The inner ear of notoungulates has been exclusively studied based on CT-imagery in a relatively limited number of taxa. Throughout the rest of the section, references to these taxa are based on Macrini et al. (2010, 2013) for *Notostylops murinus* (FMNH-P 13319, Notostylopidae), *Altityotherium chucalensis* (SGOPV 4100, Mesotheriidae), *Pachyrukhos moyani* (FMNH P13051, Hegetotheriidae) and *Cochilius* sp. (SGOPV 3774, Intertheriidae), and Billet and Muizon (2013) for the early Eocene Notoungulata indet. MNHN-F-BRD 23. Additionally, data on *Cochilius volvens* (AMNH-FM 29651) provided by MacPhee et al. (2021) and incipient new observations on the holotype of the toxodont *Rhynchippus pumilus* (MACN-A 52-61, “Notohippidae”) are included.

Notoungulates show the general mammalian pattern in which the cochlear canal (housing the membranous cochlea) is placed anteriorly, followed by the vestibule (cavity for the membranous sacculus and utriculus) and semicircular canals (Figs. 20.5 and 20.6). The cochlear canal occupies most of the total bony labyrinth volume, ranging from ~53% to ~70% (reported for *Cochilius* sp. and *P. moyani*, respectively), with a value of ~66 in the case of *N. murinus*. The cochlear turns ranged from 2.0 (e.g., *P. moyani*, *Cochilius* sp., and *A. chucalensis*) to 2.75 (reported for the Notoungulata indet. MNHN-F-BRD 23), whereas the cochlea consists of 2.25 turns in *N. murinus*. Interestingly, MacPhee et al. (2021) reported 3.5 cochlear turns for *Cochilius volvens*, a striking difference that needs further discussion. Both the primary and secondary osseous spiral laminae are distinguishable in notoungulates if CT-imagery resolution is appropriate (Fig. 20.5a, c).

The fenestra vestibuli (associated to the footplate of the stapes) lies at about the vestibulo-cochlear boundary. It varies from roughly rounded to clearly elliptical (with the major diameter in an anteroventral to posterodorsal orientation). In *N. murinus* and MNHN-F-BRD 23 (Notoungulata indet.) the stapedia ratio values (1.6 and 1.7 respectively) are among the lowest values recorded for a eutherian and similar to that of metatherians (Segall 1970). This is not the case of the mesotheriid *Altityotherium chucalensis*, whose stapedia ratio (2.0) is comparable to that of other eutherians (generally >1.8). No values were reported for toxodonts. The fenestra cochleae (for the secondary tympanic membrane) lies posterior and slightly ventral to the fenestra vestibuli and faces posterolaterally. It is notably larger than the fenestra vestibuli in *N. murinus* and MNHN-F-BRD 23, opposite to the condition observed in the known tyotheres. The cast of the aqueductus cochleae (=cochlear canaliculus, canal for the perilymphatic duct that communicates the inner ear with the subarachnoid space of the endocranial cavity) was reconstructed in MNHN-F-BRD 23, *N. murinus* and *P. moyani* (Fig. 20.5a, c; Billet and Muizon 2013: fig. 5c). The posterior end of the canal extends beyond the posterior

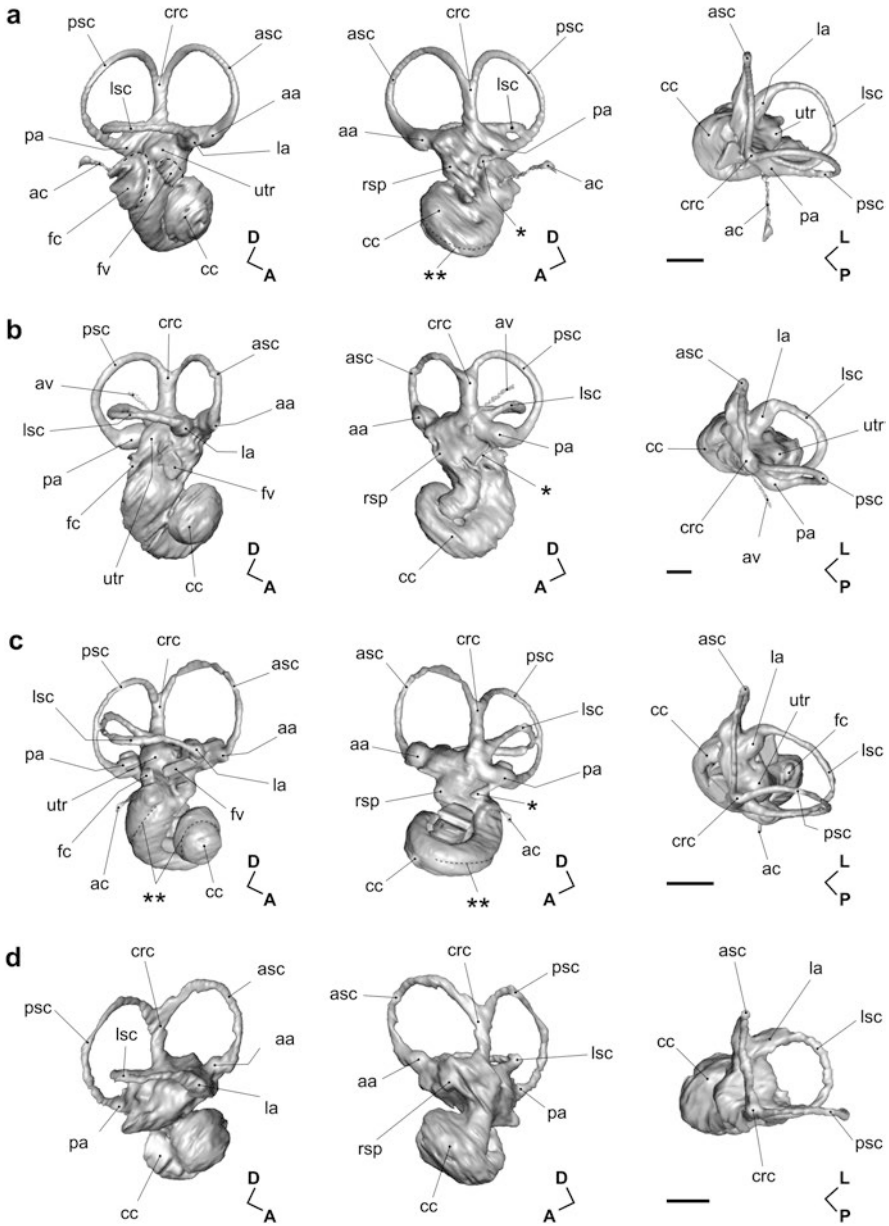


Fig. 20.5 Digital renderings of inner ear of distinct notoungulates in lateral (left), medial (center), and dorsal (right) views: **(a)** left inner ear (reversed for comparison) of *Notostylops murinus* (FMNH-P 13319); **(b)** left inner ear (reversed for comparison) of *Altitypothierium chucalensis* (SGOPV 4100); **(c)** right inner ear of *Pachyrukhos moyani* (FMNH-P 13051); **(d)** right inner ear of *Cochillius* sp. (SGOPV 3774). Abbreviations: *aa* anterior ampulla, *ac* aqueduct cochleae, *asc* anterior semicircular canal, *av* aqueduct vestibuli, *cc* cochlear canal, *crc* crus commune, *fc* fenestra cochleae, *fv* fenestra vestibuli, *la* lateral ampulla, *lsc* lateral semicircular canal, *pa* posterior ampulla, *psc* posterior semicircular canal, *rsp* recessus sphericus, *utr* utricle. Asterisk indicates the canal for the nervus ampullaris. Double asterisk indicates the secondary osseous spiral laminae. Capital letters (A, P, D and L) indicate anterior, posterior, dorsal and lateral, respectively. Scale bars = 2 mm

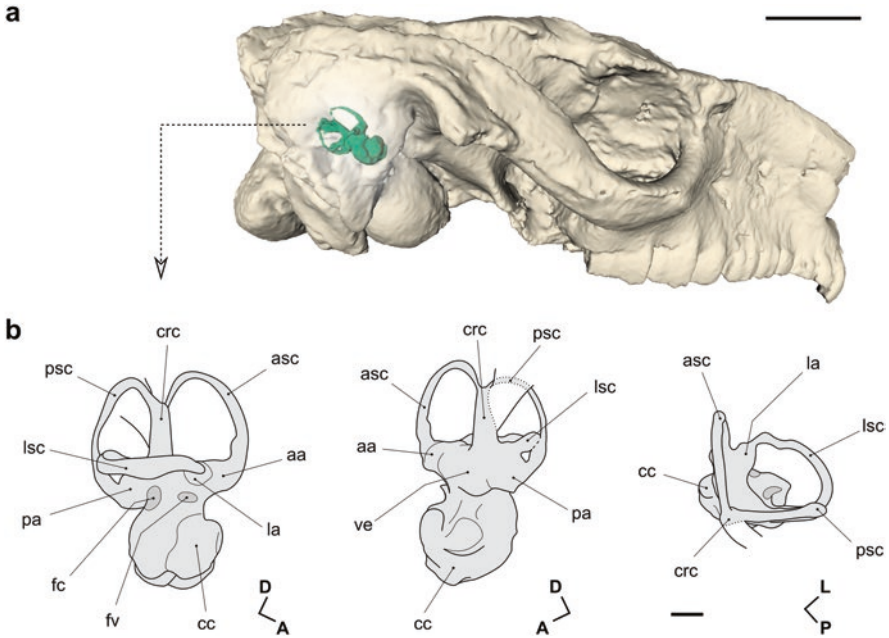


Fig. 20.6 Digital rendering and drawing of the skull and inner ear of *Rhynchippus pumilus* (MACN-A 52-61): (a) skull, partially rendered in transparency to see inner ear endocast *in situ*; (b) right inner ear in lateral (left), medial (center), and dorsal (right) views (drawn from the digital rendering shown in (a)). Abbreviations: as for Fig. 20.5. Capital letters (A, P, D and L) indicate anterior, posterior, dorsal and lateral, respectively. Scale bars = 20 mm (a) and 2 mm (b)

semicircular canal in *N. murinus* and MNHN-F-BRD 23, whereas it is less projected posteriorly in *P. moyani*.

The vestibule is also easily distinguishable in notoungulates and both the cast of the smaller recessus sphericus (which houses the membranous saccule) and the larger utricular cavity (for the membranous utricule) are visible in the abovementioned typotheres and *N. murinus*. However, in *N. murinus* the utricular cavity is located more anteriorly than in *A. chucalensis* and *P. moyani* (Fig. 20.5a–c). The cast of a canal for the nervus ampullaris is distinguishable in almost all of the abovementioned inner ear endocasts, except for that of *Cochilius* sp., probably because of preservation issues. The CT scan resolution did not allow this feature to be evaluated in *R. pumilus*. The canal extends from the posterior ampulla to the foramen singulare and appears to vary in thickness among taxa (it is thinner than the semicircular canals in *A. chucalensis* and *N. murinus*, but roughly equal in *P. moyani*). In MNHN-F-BRD 23 (Notoungulata indet.), FMNH P13319 (*N. murinus*), SGOPV 4100 (*A. chucalensis*) and MACN-A 52-61 (*R. pumilus*), the cast of the aqueductus vestibuli (canal for the endolymphatic duct) is also distinguishable.

The semicircular canals (SCs) are the most conspicuous canals of the pars mastoidea. The overall morphology varies from roughly rounded to slightly elliptical

arches (Figs. 20.5 and 20.6). In MNHN-F-BRD 23, the anterior, posterior and lateral semicircular canals (ASC, PSC and LSC respectively) are nearly circular, whereas in *N. murinus* both the LSC and (especially) the ASC are elliptical in contour. The opposite condition is observed in *A. chucalensis*, in which the roundest canal is the ACS, followed by the LSC and PSC. In SGOPV 3774 (*Cochilius* sp.), the LSC is the roundest of the three canals (Fig. 20.5d), whereas in *R. pumilus* the same canal is the most elliptical (Fig. 20.6), suggesting that there is not a unique pattern in notoungulates. In MNHN-F-BRD 23 and *N. murinus* (early diverging taxa), the SCs stay in their respective planes along their entire course. Conversely, the LSC (and sometimes the PSC) undulate or bend in the known tyotheres (and probably in *R. pumilus*, although it should be considered with caution due to the lack of resolution). Additionally, the PSC (in *P. moyani*) or both the ASC and PSC (in *Cochilius* sp.) are bowed when viewed dorsally. In the same view, the posterolateralmost point of the PSC slightly exceeds the LSC in SGOPV 3774 (*Cochilius* sp.).

Each canal abruptly thickens and forms an ampulla at one of their junctions with the vestibule (Figs. 20.5 and 20.6), a generalized condition among mammals. In MNHN-F-BRD 23 (Notoungulata indet.), the lateral ampulla attaches slightly ventral to the anterior ampulla, whereas in *N. murinus*, the toxodont *R. pumilus* (barely observed because of CT resolution) and the tyotheres *A. chucalensis*, *P. moyani* and *Cochilius* sp., the anterior and lateral ampulla attach at approximately the same horizontal plane and above that of the posterior ampulla. As expected for mammals, the posterior end of the ASC and the anterior end of the PSC join to form the crus commune before reaching the vestibule. A secondary crus commune (junction of the posterior end of the LSC and PSC) seems to be present in MNHN-F-BRD 23, contrary to *N. murinus*, the tyotheres *A. chucalensis*, *P. moyani* and *Cochilius* sp., and the toxodont *R. pumilus*, in which the posterior end of LSC does not join the posterior ampulla.

Several of the inner ear characters mentioned above were shown to be phylogenetically informative at different taxonomic levels (therians, eutherians and notoungulates). For detailed descriptions and thorough morphological and phylogenetic discussions, see Macrini et al. (2010, 2013), Billet and Muizon (2013), Billet et al. (2015), and MacPhee et al. (2021).

20.4 Brain Evolution and Paleobiological Inferences Based on Endocast Morphology

20.4.1 Morphological Brain Diversity

General Morphology Pending a comprehensive morphometric analysis to evaluate and quantify the morphological variability within notoungulates, some incipient observations are worth mentioning here. We also mention findings from a recent phylogenetic analysis of notoungulates that incorporated endocast characters and

found the suprasylvian sulcus of the cerebrum to be a synapomorphy of notoungulates (Perini et al. 2022).

One of the most obvious differences is the general brain arrangement and endocast flexure angle. The *Notostylops* specimen figured by Simpson (1933a: fig. 2) shows a low endocast flexure (taken after Macrini et al. (2007: fig. 2)), which results in olfactory bulbs, hypophyseal region and foramen magnum roughly aligned (Fig. 20.2a). A low endocast flexure is also observed in condylarths (e.g., Simpson 1933a: fig. 1; Orliac et al. 2012: fig. 3), some toxodonts (e.g. *Mendozahippus*, *Periphragnis* and *Homalodotherium*) and tyotheres (e.g. *Trachytherus* and *Cochilius*) (Figs. 20.2 and 20.3; Fernández-Monescillo et al. 2019: fig. 1; MacPhee et al. 2021: fig. 9; Perini et al. 2022: fig. 3). Conversely, the toxodonts *Leontinia*, *Gualta*, *Rhynchippus*, *Nesodon* and *Adinotherium*, and the tyotheres *Mesotherium* and *Pseudotyotherium* (Table 20.2 and Fig. 20.3; Hernández del Pino 2018; Fernández-Monescillo et al. 2019; Martínez et al. 2020; MacPhee et al. 2021) show more flexed cranial endocasts ($\geq 30^\circ$).

Perini et al. (2022) reported an endocast flexure of 34° for the specimen FMNH-P 13319 (*Notostylops murinus*), comparable to the abovementioned toxodonts. However, it must be noted that if an endocast is dorsoventrally or anteroposteriorly compressed, the endocast flexure angle will probably be distorted. In this context, differences in endocast flexure angle between the specimens AMNH FM 28614 (Simpson 1933a: fig. 2) and FMNH-P 13319 (Perini et al. 2022: fig. 3) could be attributed to *post mortem* deformation, and should not be overrated until further comparisons are performed.

A second difference in gross morphology concerns the telencephalic outline in dorsal view. Excluding the olfactory bulbs, *Notostylops* shows a heart-shaped telencephalic contour, which is not observed in later diverging notoungulates. Among toxodonts, the early diverging taxa *Rhyphodon* (Simpson 1933a: fig. 3) and, to a lesser extent, *Periphragnis* (Fig. 20.2b), show a triangular telencephalic contour different from the roughly elliptical or rhomboidal contour observed in the Oligocene and Miocene representatives such as *Homalodotherium* sp. (MacPhee et al. 2021: fig. 7), *Gualta cuyana* (Martínez et al. 2020: fig. 2), *Leontinia gaudryi* (Radinsky 1981: fig. 4), *Mendozahippus fierensis* (Martínez et al. 2020: fig. 2), *Rhynchippus equinus*, *Eurygenium latirostris* (Dozo and Martínez 2016: fig. 5, 7, respectively) and *Nesodon* sp. (Fig. 20.3b). Furthermore, the Oligocene and Miocene representatives display some variability concerning the anterior curvature of the telencephalon, which is proportionally wider in *L. gaudryi*, *G. cuyana*, *Homalodotherium* sp. and *Nesodon imbricatus* than in *R. equinus*, *M. fierensis* or *E. latirostris*, also denoted by the maximum width of the frontal region relative to the maximum width of cerebral cast (frw/crw ratio) (Table 20.2; Martínez et al. 2020: table 1). Regarding tyotheres, *Oldfieldthomasia* shows a heart-shaped telencephalic contour that resembles *Notostylops* (Simpson 1932: fig. 5), whereas a roughly triangular contour is observed in some later diverging taxa, in which the maximum cerebral width is shifted posteriorly when compared to the Oligocene or Miocene toxodonts (Fig. 20.3c; Simpson 1933b: fig. 1, 2; Patterson 1937: fig. 80; Radinsky 1981: fig.

5; Fernández-Monescillo et al. 2019: fig. 1–4; MacPhee et al. 2021: *Cochilius* in fig. 9).

Neocortical Development Both qualitative and quantitative data show an increase in the relative neocortical area through time in notoungulates (Figs. 20.2, 20.3, 20.7b, and Table 20.3), a process that has occurred independently in several mammalian clades (Jerison 1973, 2012; Smaers et al. 2021). In early diverging representatives such as *Notostylops* or *Rhyphodon* (Simpson 1933a: figs. 2–3), the rhinal fissure (which represents the limit between the neocortex and paleocortex (Jerison 1973; Long et al. 2015)) is located relatively high in lateral view (Fig. 20.2). This implies a proportionally reduced neocortical surface, differing from the more ventral position observed in later representatives (Fig. 20.3), also measurable by the neocortical ratio (NR in Table 20.3).

Furthermore, the pattern of increased gyrification through time observed especially in Toxodontia also denotes the expansion of the neocortex. In early diverging representatives such as *Notostylops* (Fig. 20.2a) only an oblique sulcus (tentatively identified as the suprasylvian sulcus) is distinguishable, which is similar to the condition observed in the Eocene toxodonts *Rhyphodon* (Simpson 1933a: fig. 3) and *Periphragnis* (Fig. 20.2b). Conversely, lateral sulci (parallel to the median sulcus) and additional sulci on both frontal and lateral lobes are recognizable in later diverging taxa such as the “Notohippidae” *Rhynchippus equinus* (Dozo and Martínez 2016: fig. 5), *Mendozahippus fierensis*, (Martínez et al. 2020: fig. 2) or the Toxodontidae *Nesodon imbricatus* (Fig. 20.3b). Even though the meninges attenuate imprints of sulci and convolutions in some large taxa as the Leontiniidae *Gualta cuyana* (Martínez et al. 2020: fig. 2) and *Leontinia gaudryi* (Radinsky 1981: fig. 4), the symmetrical bulges and depressions observed on their endocasts suggest an underlying neocortical gyrification as complex as in *Rhynchippus* and *Mendozahippus*. In tyotheres (Fig. 20.2c), only the lateral (other than the suprasylvian) sulci are distinguishable in representatives of Mesotheriidae, Intertheriidae, and Hegetotheriidae (Simpson 1933b: fig. 1, 2; Patterson 1937: fig. 80; Radinsky 1981: fig. 3; Fernández-Monescillo et al. 2019: fig. 1–4; MacPhee et al. 2021: see *Cochilius* in fig. 9; but see Dechaseaux 1962).

Rhinencephalon Cast Although hard to quantify in terms of volume, the rhinencephalon (well developed in notoungulates) can be inferred from the position of the rhinal fissure, under which conspicuous piriform lobes are distinguishable. This is especially noticeable in some early diverging taxa such as *Notostylops* (Fig. 20.2a), *Rhyphodon* (Simpson 1933a: fig. 3) or *Periphragnis* (Fig. 20.2b). The olfactory bulbs, which receive input from the olfactory epithelium and the vomeronasal organ, are invariably well developed and generally separated from the rest of the forebrain by thick olfactory peduncles. According to Perini et al. (2022), the presence of olfactory bulbs that are wider than deep would be a synapomorphy of Toxodontidae, whereas the divergence of the olfactory bulb from each other near their posterior union with the rest of the cerebrum (just anterior to the circular fissure) appears to be a synapomorphy of Toxodontia. The especially large and anteriorly projected

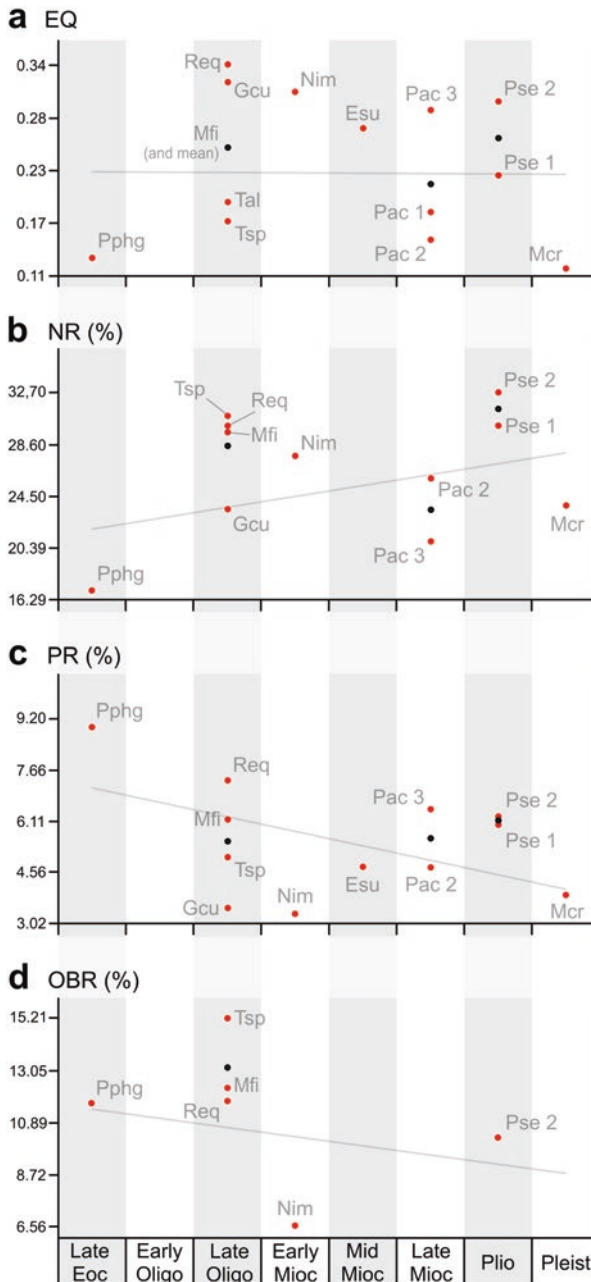


Fig. 20.7 Scatter plot and best fit line of some dimensions shown in Table 20.3: (a) encephalization quotient; (b) neocortical ratio; (c), piriform ratio, (d), olfactory bulb ratio. Abbreviations: *Esu* *Eutyotherium superans* (MACN-A 11079), *Gcu* *Gualta cuyana* (MCNAM-PV 3841), *Mcr* *Mesotherium cristatum* (MNHN.F.PAM 2), *Mfi* *Mendozahippus fierensis* (MCNAM-PV 4004),

olfactory bulbs observed in the above-mentioned early diverging taxa are consistent with the well-developed piriform lobes of *Periphragnis* sp. and the high PR (piriform ratio) showed in Fig. 20.7c (see below in Sect. 20.4.3). Having especially large piriform lobes (i.e. visible in dorsal view of the endocast) is a feature seen in *Rhyphodon* (Simpson 1933a), *Cochilius* (Perini et al. 2022), *Notostylops* (Simpson 1932, 1933a; Perini et al. 2022) (“Isotemnidae”, Interatheriidae and Notostylopidae, respectively), and the condylarths *Phenacodus* (Simpson 1933a) and *Hyopsodus* (Orliac et al. 2012).

Other representatives show relatively smaller (but still well-developed) and/or less divergent olfactory bulbs, such as toxodontids (Fig. 20.3c) and *Homalodotherium* (MacPhee et al. 2021: fig. 7). In general, neither the lateral olfactory tract nor the olfactory tubercles are clearly distinguishable on the endocasts of notoungulates, except for the specimens of *Notostylops* and *Hegetotherium* figured by Simpson (1933a: fig. 2, b: fig. 1) for which he mentioned the presence of olfactory tubercles.

Midbrain and Cerebellum Contrary to Simpson (1933a) and Radinsky (1981), Perini et al. (2022) stated that there was no dorsal exposure of the midbrain in *Notostylops murinus* (based on the specimen FMNH-P 13319). However, a more cautious approach is here preferred until further comparisons are available. Although no cast of the corpora quadrigemina are observed neither in Simpson’s (1933a) drawings nor in Perini et al.’s (2022) figures, a dorsally exposed midbrain (likely obscured by meninges and sinuses) is not dismissed for *Notostylops*. Our cautious position is based on the large separation between the posterior extent of the cerebral hemispheres and the anterior lobe of the cerebellum, especially noticeable in the specimen AMNH FM 28614 (Fig. 20.2a; Simpson 1933a: fig. 2).

To a lesser extent, a similar condition is observed in the toxodont *Rhyphodon* (Simpson 1933a: fig. 2, 3). Unfortunately, this region is poorly preserved in the specimen of *Periphragnis* sp. examined here (Fig. 20.2b), preventing the assessment of this trait in this taxon closely related to *Rhyphodon*. Despite these examples, the derived and prevalent condition in notoungulates is a non-dorsally exposed midbrain (Fig. 20.3), as observed in a variety of toxodonts and tyotheres (Simpson 1933b: fig. 1–2; Patterson 1937: fig. 77, 79; Dechaseaux 1962: fig. 1–3; Radinsky 1981: fig. 3–5; Dozo and Martínez 2016: fig. 4, 5, 8; Fernández-Monescillo et al. 2019: fig. 1–4; Martínez et al. 2020: fig. 2, 10; MacPhee et al. 2021: fig. 7, 9). This scenario is consistent with the abovementioned neocortical expansion and the consequent caudal overlapping of the cerebral hemispheres upon the midbrain, as is the case in many other groups of mammals (Macrini et al. 2007; Rowe et al. 2011).



Fig. 20.7 (continued) *Nim Nesodon imbricatus* (MPEF-PV 1323), *Pac 1 Plesiotyotherium achirens* (MNHN-Bol-V 12664), *Pac 2 Plesiotyotherium achirens* (MNHN-Bol-V 8507), *Pac 3 Plesiotyotherium achirens* (MNHN.F.ACH 26), *Pphg Periphragnis* sp. (MPEF-PV 1026), *Pse 1 Pseudotyotherium* sp. (MACN-Pv 1111), *Pse 2 Pseudotyotherium* sp. (MACN-Pv 2925), *Tal Trachytherus alloxus* (MNHN-Bol-V 6355), *Tsp Trachytherus spegazzinianus* (UNPSJB-PV 112). Black dots are the mean value when more than one datum is available for the same time lapse

Table 20.3 Estimated body mass and non-linear endocast dimensions and ratios of representatives of Toxodontia and Typotheria

Taxon	Epoch	BM (Kg)	EV (cm ³)	EQ1 EQ2 EQ mean	EA (mm ²)	EA-NA (mm ²)	EA-OBA (mm ²)	NA (mm ²)	PCA (mm ²)	NR (%)	PR (%)	OBR (%)
<i>Periphragmus</i> sp. (MPEF-PV 1026)	Late Eocene	357	88.87	0.141 0.126 0.1335	15504	13127	13972	2377	1246	17.01	8.92	11.67
<i>Gualta ciyana</i> (MCNAM-PV 3841)	Late Oligocene	404	235.04	0.343 0.303 0.323	–	–	25358	5970	886	23.54	3.49	–
<i>Rhynchippus equinus</i> (MPEF-PV 695)	Late Oligocene	85	82.53	0.342 0.337 0.3395	13541	9821	12385	3720	907	30.04	7.32	11.77
<i>Eurygenium latirostris</i> (UNPSJB-PV 60)	Late Oligocene	119	*77.57	0.256* 0.247** 0.2515**	–	–	–	3404	966	–	–	–
<i>Mendozhippus fierensis</i> (MCNAM-PV 4004)	Late Oligocene	82	59.44	0.251 0.248 0.2495	12467	9113	11349	3354	696	29.56	6.14	12.28
<i>Nesodon imbricatus</i> (MPEF-PV 1323)	Early Miocene	581	292.00	0.334 0.288 0.311	43998	32420	41871	11579	1383	27.65	3.30	6.56
<i>Trachylherus spegazzinianus</i> (UNPSJB-PV 112)	Oligocene Deseadan	145 ^a	60.41 ^b	0.175 0.166 0.1705	10441 ^b	7518	9288 ^b	2860 ^b	467 ^b	30.79	5.03 ^b	15.21
<i>Trachylherus alloxus</i> (MNHN-Bol-V 6355)	Oligocene Deseadan	48 ^a	30.89 ^b	0.188 0.193 0.1905	6062 ^b	–	–	–	–	–	–	–
<i>Eurytherium superans</i> (MACN-A 11079)	Middle Miocene	55 ^a	47.36 ^b	0.263 0.267 0.265	–	–	8944 ^b	–	425 ^b	–	4.75 ^b	–

Taxon	Epoch	BM (Kg)	EV (cm ³)	EQ1 EQ2 EQ mean	EA (mm ²)	EA-NA (mm ²)	EA-OBA (mm ²)	NA (mm ²)	PCA (mm ²)	NR (%)	PR (%)	OBR (%)
<i>Plesiotypotherium achirense</i> (MNHN-Bol-V 12664)	Late Miocene	52 ^a	30.46 ^b	0.176 0.179 0.1775	–	–	–	1948 ^b	463 ^b	–	–	–
<i>Plesiotypotherium achirense</i> (MNHN-Bol-V 8507)	Late Miocene	89 ^a	38.72 ^b	0.156 0.153 0.1545	–	–	8703 ^b	2255 ^b	409 ^b	25.91	4.70 ^b	–
<i>Plesiotypotherium achirense</i> (MNHN.F.ACH 26)	Late Miocene	89 ^a	72.42 ^b	0.291 0.286 0.2885	–	–	11136 ^b	2334 ^b	719 ^b	20.96	6.45 ^b	–
<i>Pseudotypotherium</i> sp. (MACN-Pv 1111) ^c	Pliocene	114 ^a	65.34 ^b	0.223 0.215 0.219	–	–	9777 ^b	2940 ^b	585 ^b	30.07	5.98 ^b	–
<i>Pseudotypotherium</i> sp. (MACN-Pv 2925) ^c	Pliocene	124 ^a	93.25 ^b	0.302 0.290 0.296	13608 ^b	9475	12641 ^b	4133 ^b	789 ^b	32.70	6.24 ^b	10.21
<i>Mesotherium cristatum</i> (MNHN.F.PAM 2)	Pleistocene	194 ^a	54.23 ^b	0.129 0.120 0.1245	–	–	9319 ^b	2210 ^b	360 ^b	23.71	3.86 ^b	–

^aProbably lower than the actual value due to the poor preservation of the occipital region

^bCalculated with cranial and dental measurements taken from Fernández-Monescillo et al. (2019: table 4 in online resource 2)

^cTaken from Fernández-Monescillo et al. (2019: table 2)

^dSee comment in Table 20.1

Abbreviations: *BM* estimated body mass using algorithm 4.1 from Mendoza et al. (2006), *EA* endocranial total area, *EA-NA* endocranial area exclusive of neocortical area, *EA-OBA* endocranial area exclusive of olfactory bulbs, *EQ 1* neocortical quotient following Jerison (1973), *EQ 2* encephalization quotient following Eisenberg (1981), *EV* endocranial volume, *NA* neocortical area, *NR* neocortical ratio (percentage of the endocranial area [exclusive of olfactory bulbs] that corresponds to the neocortex), *OBR* olfactory bulb ratio (percentage of the endocranial area exclusive of neocortical area [EA-NA] that corresponds to the olfactory bulbs), *PCA* piriform cortex area, *PR* piriform ratio, (percentage of the endocranial area exclusive of olfactory bulbs [EA-OBA] that corresponds to the piriform cortex area). Area measurements for toxodonts were obtained from surface models in MorphoDig 1.6.1 (Lebrun 2018)

The cerebellum is relatively longer in *Rhyphodon* than in the other notoungulates considered here (Fig. 20.2; Simpson 1933a: fig. 2, 3; Perini et al. 2022: fig. 3), even considering the aforementioned differences concerning the cranial endocast general morphology. In dorsal view, the vermis and the cerebellar hemispheres are distinct and separated by weak paramedian fissures (sometimes subtle depressions) in *Notostylops* and *Rhyphodon* (Fig. 20.2; Simpson 1933a: fig. 2, 3; Perini et al. 2022: fig. 3). Conversely, only the vermis is roughly visible in later diverging toxodonts and tyotheres.

In lateral view, the cast of the paraflocculus (the cerebellar lobe that occupies the subarcuate fossa of the petrosal) is distinguishable on most notoungulate cranial endocasts (Perini et al. 2022), with exceptions being *Nesodon* (Patterson 1937; Radinsky 1981), *Toxodon* (Dechaseaux 1962), and *Leontinia* (Radinsky 1981). Among specimens examined here, we were also unable to identify the paraflaccular lobe (at least conspicuously) in *Periphragnis* sp. (MPEF-PV 1026). Most notoungulates have broad and rounded paraflocculi similar to what is seen in *Notostylops* (Fig. 20.2a; Perini et al. 2022), but some taxa exhibit a cone-shaped paraflocculi, such as *Hegetotherium* (Simpson 1933b), *Protypotherium* (Simpson 1933b; Radinsky 1981), *Cochilius* (Perini et al. 2022), and *Pachyrhinos* (Dechaseaux 1962; Radinsky 1981; Perini et al. 2022). Having a cone-shaped paraflocculus was proposed as an equivocal synapomorphy for Hegetotheriidae (Perini et al. 2022: character #15, modified from Macrini et al. (2007: character #16)).

Cranial Nerves and Midventral Surface Several structures of the ventral aspect of the braincast such as the hypophyseal region, exit of cranial nerves and medulla oblongata are visible in notoungulates. The cast of the hypophyseal fossa (if present) is typically placed between or slightly posterior to the cast of the sphenorbital fissure, approximately at level of the piriform lobes. In *Notostylops*, however, the cast of the hypophyseal fossa is placed further back (Fig. 20.2a; Simpson 1933a: fig. 2; Perini et al. 2022: fig. 3), although data about other taxa is required to evaluate whether this is a generalized condition for early diverging notoungulates. A large and rounded hypophyseal fossa is present in the toxodonts *Rhynchippus* and *Nesodon* (Fig. 20.3; Patterson 1937: fig. 75; Dozo and Martínez 2016: fig. 5), differing from the smaller and teardrop-shaped cast observed in *Mendozahippus fierensis* (Martínez et al. 2020: fig. 2). Interestingly, the rostral cerebral artery was tentatively identified anterolaterally to the cast of the hypophyseal fossa in *Homalodotherium* (MacPhee et al. 2021: fig. 7). Until then, no imprints of the vasculature surrounding the hypophyseal region had been reported. In other toxodonts (e.g. *Periphragnis* or *Gualta*), the cast of the hypophyseal region cannot be accurately demarcated either because there is no hypophyseal fossa or because it is very shallow (Fig. 20.2b; Martínez et al. 2020: fig. 5).

Absence of hypophyseal fossa or, if present, shallow and fuzzy, is also observed in some tyotheres, as in the mesotheriids *Plesiotypotherium*, *Pseudotypotherium* and *Mesotherium*, or the hegetotheriid *Hegetotherium* (Fig. 20.3c; Simpson 1933b: fig. 1; Dechaseaux 1962: fig. 8; Fernández-Monescillo et al. 2019: fig. 2–4). In the case of *Trachytherus spagazzinianus*, the cast of a large hypophyseal fossa is

distinguishable in the specimen UNPSJB-PV 112 (Fernández-Monescillo et al. 2019: fig. 1), and a relatively small but well-marked fossa can be inferred from the endocast of *Cochilius volvens* (MacPhee et al. 2021: fig. 9). An approximately equal hypophyseal fossa length and width was proposed as an equivocal synapomorphy for Interatheriidae (Perini et al. 2022).

The cast of the sphenorbital fissure (exit of the oculomotor [III], trochlear [IV], ophthalmic [V₁] and maxillary [V₂] branches of the trigeminal nerve, and abducens [VI] cranial nerves) is clearly visible anterolaterally (anteriorly in the case of *Notostylops*) to the hypophyseal region (Figs. 20.2 and 20.3) when viewed in ventral view. These paired openings (in the form of thick canals) show an interesting variability within notoungulates, concerning thickness, divergence, and separation from the sagittal plane. In *Notostylops*, the sphenorbital canals originate close to each other, they run roughly parallel and are relatively thin (Fig. 20.2a; Perini et al. 2022: fig. 3). In tyotheres (e.g. *Plesiotyotherium achirense*, *Pseudotyotherium* sp., *Mesotherium cristatum* and *Hegetotherium mirabile*), the canals originate relatively close to the sagittal plane, but they are markedly convergent (Simpson 1933b: fig. 1; Fernández-Monescillo et al. 2019: fig. 2–4). In turn, in some toxodonts (e.g. *Periphragnis* sp., *Gualta cuyana*, *Mendozahippus fierensis*, *Rhynchippus equinus*, *Eurygenium latirostris* and *Nesodon imbricatus*), the casts of the sphenorbital canals are well separated from each other and converge less abruptly than in the above-mentioned tyotheres (Figs. 20.2 and 20.3; Patterson 1937: fig. 75; Dozo and Martínez 2016: fig. 5; Martínez et al. 2020: fig. 5, 7). Finally, the sphenorbital canals originate well separated from each other and run parallel (or even diverge) in *Homalodotherium*, similar, to some extent, to the condition observed in the astrapotheres *Trigonostylops* and *Astrapotherium* (MacPhee et al. 2021: fig. 7–8). Anterovertrally, the cast of the optic chiasm and the exits of the optic nerves (the later only distinguishable in the best-preserved specimens) are generally visible (Figs. 20.2 and 20.3).

The pons (a structure of the hindbrain that is posterior to the hypophyseal region) is typically not clearly visible on endocasts of mammals. However, the cast of the pons is present on the cranial endocasts of *Homalodotherium* and *Rhyphodon* (Simpson 1933a; Patterson 1937; Perini et al. 2022). Laterally (posterolaterally to the hypophyseal region), the cast of the basicapsular fenestra (= sphenotympanic fissure sensu Gabbert 2004) is distinguishable (Figs. 20.2 and 20.3). In notoungulates, the rostral area is usually observed in the form of a large opening that transmits several vascular and neural elements, including the mandibular branch of the trigeminal nerve (V₃). Although a separate foramen ovale has been individualized in some representatives (MacPhee 2014: fig. 13; Martínez et al. 2016: fig. 6, 2020: fig. 8), these interpretations should be taken with caution considering how difficult it is to identify subdivisions or incisures on the rostral area of the fenestra (see MacPhee et al. (2021) and MacPhee and Forasiepi (2022) for additional details on this regard). The cast of the jugular area of the basicapsular fenestra (exit for the glossopharyngeal [IX], vagus [X], and spinal accessory [XI] cranial nerves) is observed in most of the endocasts (Figs. 20.2 and 20.3). Posteriorly and laterally, the cast of the internal auditory meatus (passage of the facial [VII] and the vestibulocochlear [VIII]

cranial nerves) is well distinguishable in the center of the petrosal imprint. Finally, the cast of the hypoglossal foramen (transmitting the hypoglossal [XII] cranial nerve) is visible laterally at the base of the medulla oblongata (Figs. 20.2 and 20.3).

20.4.2 *Relative Brain Size Evolution: A Challenging Task in Notoungulates*

Notoungulates are thought to have had relatively small brains in comparison to coeval Holarctic mammals that presumably occupied similar ecological niches (Jerison 1973; Perini et al. 2022; but see Radinsky 1981). Following the idea that predation pressure is positively related to the brain size of the prey (Jerison 1973; Shultz and Finlayson 2010), the general smaller relative brain size of notoungulates has been explained by the absence of “large-brained” predators during most of the Cenozoic in South America (Jerison 1973; Fernández-Monescillo et al. 2019; Perini et al. 2022). At less inclusive taxonomic levels, however, only Fernández-Monescillo et al. (2019) have proposed relationships between the relative brain size and specific ecological traits inferred for representatives of Mesotheriidae. According to the authors, mesotheriids would have small brains even in the context of notoungulates (but see Perini et al. 2022) and, based on an extrapolation of what is seen in rodents (Pilleri et al. 1984; Bertrand and Silcox 2016; see also Bertrand et al. 2021), Fernández-Monescillo et al. (2019) attributed this to the probably semifossorial lifestyle of the examined taxa.

In parallel to the abovementioned ecomorphological hypothesis, there are methodological issues concerning how the relative brain size is assessed and quantified that also need to be discussed. It is well known that the brain size scales allometrically with body size (both ontogenetically and evolutionary) in vertebrates, which precludes direct comparisons between taxa by means of simple brains size/body size ratios (Burger et al. 2019). Jerison (1970, 1973) modeled this relationship by means of an exponential function whose parameters were empirically determined based on a variety of living mammals. As a result, he obtained an allometric equation to find expected brain sizes given a body size. The ratio between the observed value (i.e. the measured brain size) and the expected value (according to the body size) results in the broadly known encephalization quotient (EQ). Since then, the EQ (either following Jerison’s proposal or Eisenberg’s (1981) modified version) becomes one of the most employed methods to quantify the encephalization and make comparisons between taxa (see below Eqs. 20.1 and 20.2, abbreviations in Table 20.3).

$$EQ1 = EV / 0.12(BM)^{0.67} \text{ (Jerison1973)} \quad (20.1)$$

$$EQ2 = EV / 0.055(BM)^{0.74} \text{ (Eisenberg1981)} \quad (20.2)$$

Interestingly, the taxonomic sample considered by Jerison (1973) included SANUs. He observed that the relative brain sizes obtained for the representatives of the group (most of them notoungulates) did not increase over time, unlike what he observed in the Holarctic ungulates. However, and contrary to Jerison, Radinsky (1981: table 1) found that the relative brain size did increase in both SANUs and Holarctic ungulates. As explained by Radinsky, such differences were due to some criteria adopted by the authors concerning the body mass (BM) estimation method.

In an attempt to correct some values, Jerison (1973) double the BM estimates obtained for those taxa considered robust or “bulky”, which provoked a marked drop in their EQs. Conversely, Radinsky (1981) not only dismissed Jerison’s correction but also estimated BMs by means of an equation derived from a sample of living mammals including carnivores. This explains why BM estimates obtained by Radinsky (1981) are generally much lower than those provided by other authors (see Elissamburu 2012: table 2). It is beyond the scope of this review to discuss which of these subjective decisions were the most appropriate or best supported, but instead we highlight how important is to consider the BM estimation method if comparisons are to be made with previously reported data. In addition, Fernández-Monescillo et al. (2019) mentioned that biases related to intraspecific variation would also be of major impact (even more significant than that associated to BM estimation methods) and they suggested that EQs based on a single specimen should be considered with caution.

Recent contributions have provided the EQs for *Notostylops* and representatives of mesotheriids, intertheriids, hegetotheriids (Typotheria), leontiniids, “notohippids” and toxodontids (Toxodontia) for which BMs were estimated by means of a variety of methods (e.g. Dozo and Martínez 2016; Fernández-Monescillo et al. 2019: online resource 2; Martínez et al. 2020; Perini et al. 2022). In order to minimize biases associated to BM estimation method, we only considered here taxa whose BMs were obtained following Mendoza et al. (2006: table 2, algorithm 4.1), plus new data on *Periphragnis* and *Nesodon* (Table 20.3). The algorithm 4.1 returns ln-transformed BM estimates from a set of ln-transformed cranial measurements (muzzle width, palatal width, length of the posterior portion of skull, depth of face under the orbit, second upper molar length and second upper molar width). We opted for this equation because it has the lowest prediction error (13.5–17.5%) among those applicable to our fossil sample considering the measurements required.

Alternative BM predictions based on geometric morphometrics (using the centroid size as the predictor) have been applied in a handful of notoungulates (Cassini et al. 2012b). However, these authors reported that BMs based on the centroid size were higher and lower, respectively, than those based on dental and craniomandibular measurements (Cassini et al. 2012b: table 6), which led us not to consider those estimates for EQ calculation. It is worth noting that this decision is based exclusively on consistency (i.e. not including estimates obtained by different methods), but does not imply preference for a particular BM estimation method.

However, the challenges of assessing the relative brain size in notoungulates are not restricted merely to discrepancies in BM estimates. Smaers et al. (2021) evaluated the brain size evolution in several mammalian lineages and found evidence to

suggest that brain size/body size allometry should not be assumed equal and stable across mammals. Based on the brain size and body size (ln-transformed values) from more than 1400 species, they identified 30 different grades of allometry (Smaers et al. 2021: table 1, fig. 2), each of them characterized by statistically significant differences in the slope and/or the intercept of the phylogenetic general least-squares regressions. As pointed out by the authors, comparisons of relative brain size (and therefore EQ) would be valid only if they involve groups with similar regression parameters. In this context, the EQs provided here only allow to conclude that the relative brain size (based on deviations from a stable and generalized allometric slope) does not show clear trends across our sample of taxa composed of Eocene to Pleistocene notoungulates (Table 20.3 and Fig. 20.7a). However, this should be considered extremely cautiously given the small sample size, as a result of using exclusively Mendoza et al.'s (2006) algorithm 4.1 as BM estimation method.

Recently, and based on EQs and the PEQs (phylogenetic encephalization quotient) Perini et al. (2022) concluded that both tyotheres and toxodonts show an increase in EQ (and also PEQ) values if compared with the ancestral condition inferred for notoungulates but increases and decreases seem to have occurred independently within these groups (Perini et al. 2022: fig. 7). Despite a homogenous methodological-based discrepancy between EQ values obtained here and those of Perini et al. (2022: table 3), both analyses coincide in that the highest EQ values do not correspond to the latest representatives of each lineage, which suggests that the straightforward idea of a generalized EQ increase throughout time should not be assumed for the whole order (i.e. there is at least partial independence in EQ variations among clades). However, forthcoming contributions should provide specific allometric parameters for notoungulates, which would allow better-supported comparisons and more solid inferences about the major forces driving the brain size evolution of the group.

20.4.3 *Inferred Sensory and Locomotor Capabilities: Olfaction, Hearing and Vestibular Sense*

Olfactory Capabilities The well-developed olfactory bulbs and piriform lobes observed in both early diverging and late diverging notoungulates suggest high reliance on olfaction. Enlarged olfactory bulbs are especially noticeable in *Notostylops* (Notostylopidae) and in the earliest diverging toxodonts considered here (*Rhyphodon* and *Periphragnis*), which also show large piriform lobes. The olfactory bulbs of these taxa are comparable or slightly smaller than that of some condylarths such as *Chriacus*, *Meniscotherium*, *Hyopsodus*, *Cebochoerus* or *Alcidedorbignya* (Orliac et al. 2012: fig. 5; Muizon et al. 2015: fig. 54; Bertrand et al. 2020: fig. 5), a condition considered “archaic” or plesiomorphic among mammals (Orliac et al. 2012).

Mendozahippus, *Rhynchippus* and *Eurygenium* (included within the paraphyletic notohippids) also show large olfactory bulbs and piriform lobes. The piriform ratio

(PR) is lower in *M. fierensis* and *R. equinus* (the data is not available for *E. latirostris*) than in *Periphragnis* sp., although the fact that both notoungulates and *Periphragnis* sp. have similar olfactory bulb ratio (OBR) suggests that decrease in the PR could be explained by the expansion of the neocortex (i.e. increase in neocortical ratio [NR]). Conversely, the OBR is lower in *N. imbricatus* than in the above-mentioned taxa, which could indicate less reliance on olfaction (Table 20.3, Figs. 20.2, and 20.3, see also NR, PR and OBR in Fig. 20.7b, c, d). The olfactory bulbs could not be reconstructed in the leontiniid *Gualta cuyana* (MCNAM-PV 3951), but a low PR (the lowest for the late Oligocene representatives) in co-occurrence with a low NR is suggestive of less reliance in olfaction. In *Leontinia gaudryi* (based on the specimen FMNH-P 13285 and in data provided by Radinsky (1981: fig. 5)), the olfactory bulbs (roughly parallel and rounded in dorsal view) seem slightly smaller and less divergent than in coeval toxodonts. In the case of *Homalodotherium* (Patterson 1937: fig. 79; MacPhee et al. 2021: fig. 7), they are laterally compressed and do not diverge, although functional implications related to these morphological differences are uncertain.

Among tyotheres, olfactory bulbs can be entirely appreciated only in *Hegetotherium* (Simpson 1933b: fig. 1), *Mesotherium* (Dechaseaux 1962: fig. 7), *Trachytherus* (Fernández-Monescillo et al. 2019: fig. 1), *Pseudotyotherium* (Fig. 20.3c; Fernández-Monescillo et al. 2019: fig. 3 [referred to *Mesotherium*, but later revised]) and *Cochilius* (MacPhee et al. 2021: fig. 9; Perini et al. 2022: fig. 2), although the olfactory bulb ratio (OBR) is only available for *Pseudotyotherium* and *Trachytherus* (Table 20.3 and Fig. 20.7d). Based on both qualitative and quantitative data, a roughly similar olfactory acuity to that of *Periphragnis*, *Mendozahippus*, *Rhynchippus* and *Eurygenium* could be expected for *Pseudotyotherium* sp. In the case of *Trachytherus spegazzinianus*, the OBR is higher than in any other taxa here considered, but the preservation of the specimen from which measurements were taken led us to avoid inferences until new data is provided. An interesting question also arises from the olfactory tubercles mentioned by Simpson (1933b: fig. 1) for *Hegetotherium mirabile*, which are not present (at least conspicuously) in any other tyotheres. Additional observations are needed to confirm its presence (as evidence of a more acute olfaction) in this taxon.

More precise interpretations are not possible without further comprehensive approaches. Unlike other regions of the brain, the olfactory bulbs are not (or seem less) subjected to the developmental constrain of a conserved neurogenetic scheduling (Carlisle et al. 2017) and their size do not scale to the rest of the brain as predictably as other structures. The olfactory spatial theory proposed by Jacobs (2012), according to which the olfactory bulbs of vertebrates would be involved not only in odorant discrimination but also (and mainly) in the ability to map odorants in space, provides a useful example. The theory integrates (among others) previous ideas that relate the olfactory bulb development with other structures of the limbic system (especially the hippocampus) (Jacobs 2012), the absolute size of the neocortex (Reep et al. 2007) and the home range size (Gittleman 1991). Some of these data seem unattainable in fossil taxa, but highlight how complex could be the processes underlying the olfactory bulbs developmental pattern.

Hearing As mentioned in Sect. 20.2, Radinsky (1981) argued that the bulged temporal lobe of notoungulates could reflect the expansion of the auditory cortex. He based his argument on the resemblance in gross brain anatomy between some typotheres and hystricomorph rodents. Indeed, the location of the auditory cortex seems relatively constant among mammals, and the well-developed temporal lobe observed in notoungulates could imply the expansion of this cortical area. Radinsky (1981) interpreted such condition as consistent with the enlarged and elaborated middle ear chamber typical of notoungulates, although this assumption lacks morpho-functional support (an elaborated middle ear chamber does not necessary imply a complex sensory input).

The well-developed epitympanic sinuses observed in notoungulates could be indicative of an enhanced low-frequency audition, although, as mentioned by MacPhee (2014), this relationship has yet to be demonstrated. In this regard, some data were provided based on the inner ear. Macrini et al. (2013) estimated the low-frequency hearing limit (at 60 dB) from the ratio of the cochlear apical and basal turns radii ($\text{Radius}_{\text{BASE}}/\text{Radius}_{\text{APICAL}}$) in some notoungulates. Following the methodology proposed by Manoussaki et al. (2008), Macrini et al. (2013) estimated 15 Hz for *Notostylops murinus*, 92 Hz for *Altitypotherium chucalensis*, 149 Hz for *Pachyrukhos moyani*, and 84 Hz for *Cochilius* sp. These results (though lacking representatives of important groups such as toxodonts) are consistent with the idea that notoungulates would have been capable of hearing low-frequency sounds (extremely low in the case of *Notostylops*). Further research would be desirable to assess if low-frequency limit (or any other parameter of the frequency map) co-vary with any morphological dimension of the middle ear in mammals.

Vestibular Sense In vertebrates, the vestibular system is essentially involved in movement coordination, balance and spatial orientation. In particular, the semicircular canals (SC) sense the rotational acceleration and play a critical role in gaze stabilization during locomotion and head movements in general (Spoor 2003; Spoor et al. 2007, and references therein). Of particular interest were the results obtained by Spoor et al. (2007), who studied the radius of curvature of the canals in 210 species (91 primates and 191 other mammals) and found that agile animals (i.e. those with fast and jerky locomotion) have significantly larger canals (relative to body mass) than those with a leisurely and less dizzying locomotion. Spoor et al. (2007) used behavioral observations of extant mammals to quantify agility for these species by means of a score that ranged from 1 (the less agile) to 6 (the most agile). This methodology is somewhat controversial because of the degree of subjectivity to which agility scores were assigned (see discussions in Macrini et al. 2010, 2013). Nonetheless, Silcox et al. (2009) analyzed the relationship between measures of semicircular canals (e.g. semicircular canal radius of curvature) and the agility scores, and derived predictive equations based on the dataset of Spoor et al. (2007). The author concluded that the locomotor agility inferred from the semicircular canal radii generally conforms to the postcranium-based interpretations in Paleocene and Eocene fossil primates (except for “plesiadapiforms”, to whom semicircular canal radii did not reflect fine scale differences in agility).

Macrini et al. (2010, 2013) used the equations derived by Silcox et al. (2009) to calculate the agility scores for *N. murinus* (3.4–3.9), *A. chucalensis* (3.2–4.0), *P. moyani* (4.4–5.5) and *Cochilius* sp. (3.2–4.1), with the purpose of hypothesizing their locomotor capabilities. It is important to point out that locomotor capabilities inferred from agility scores are merely hypotheses that require rigorous testing with morpho-functional analyses of available postcranial remains. Except for *N. murinus* (for which postcranial remains were not described at the time of Macrini et al.'s contributions), the agility scores obtained for the typotheres are consistent with postcranial-based inference on these (or closely related) taxa.

Macrini et al. (2010) were particularly cautious when interpreting the locomotor agility score obtained for the *N. murinus*, which was tentatively regarded as a generalized terrestrial mammal with cursorial tendencies. Recently, Lorente et al. (2019) provided detailed descriptions of postcranial remains of *Notostylops* and suggested that it would be plantigrade, robust and capable of fully supination, all indicative of unspecialized terrestrial, semifossorial or fossorial adaptations. Here (Table 20.4), we recalculated the agility score for *Notostylops* with the estimated BM range provided by Lorente et al. (2019) and obtained scores between 3.1 and 3.6 (when calculated with 5.02 kg, the lower value of the range), and between 2.7 and 3.1 (when calculated with 13.56 kg, the higher value of the range). These scores (especially those obtained with the highest values of the BM range) are closer to (or fall within) the 2–3 interval of living scratch-diggers (Spoor et al. 2007: supporting information), which is more consistent with Lorente et al.'s (2019) behavioral inferences.

Finally, only a brief mention is possible concerning toxodonts since no agility scores were previously reported for the group. Here (Table 20.4), we calculated the agility score for *Rhynchippus pumilus* (“Notohippidae”) and *Gualta cuyana* (Leontiniidae) based on measurements obtained from relatively low-quality SC reconstructions (Table 20.5). The values obtained for *R. pumilus* (with an estimated BM of 21.83 kg (Elissamburu 2012)) ranged from 3.2 to 3.5. Although similar scores were reported for living mammals with a variety of locomotor behaviors (Spoor et al. 2007: supporting information), some postcranial traits observed in *R. pumilus* and *R. equinus* (e.g. the ventrally directed olecranon, digit reduction, and tight and parallel metacarpals/metatarsals) are suggestive of an erect stance and some degree of cursoriality (Loomis 1914; Chaffee 1952; Shockey et al. 2012). In this context, though poorly informative, the agility scores obtained for *R. pumilus* are consistent with the postcranium-based evidence.

In *Gualta cuyana*, only the posterior SC was reconstructed, and therefore the agility score (2.2) is based solely on this canal (Tables 20.4 and 20.5). This value is expectable for a large notoungulate with an estimated BM of 404 kg. (Martínez et al. 2020). Although more slender than other large sized notoungulates (e.g. toxodontids), *G. cuyana* is thought to be robust and hardly cursorial, which is consistent with an agility score suggestive of a slow-moving animal. However, these incipient observations should be compared with inner ear-based data from other toxodonts and integrated with further postcranium-based inference.

Table 20.4 Agility scores calculated for *Notostylops murinus* (FMNH-P 13319), *Rhynchippus pumilus* (MACN-A 52-61) and *Gualta cuyana* (MCNAM-PV 3951). AGIL_{ASCR}, AGIL_{PSCR}, AGIL_{LSCR}, and AGIL_{SCR} are the agility scores calculated from the anterior, posterior, lateral and average semicircular canal radius of curvature respectively. Agility scores calculated following Silcox et al. (2009)

	Body mass (kg)	AGIL _{ASCR}	AGIL _{PSCR}	AGIL _{LSCR}	AGIL _{SCR}
<i>N. murinus</i> ^a	3.12	3.4	3.6	3.9	3.7
<i>N. murinus</i> ^b	5.02	3.1	3.4	3.6	3.4
<i>N. murinus</i> ^c	13.56	2.7	2.9	3.1	2.9
<i>R. pumilus</i> ^d	21.69	3.2	3.2	3.5	3.4
<i>G. cuyana</i> ^d	404.00	–	2.2	–	–

^aAgility scores calculated with same body mass estimate as in Macrini et al. (2013)

^bAgility scores calculated with the lowest value of the estimated body mass range provided by Lorente et al. (2019)

^cAgility scores calculated with the highest value of the estimated body mass range provided by Lorente et al. (2019)

^dAgility scores calculated with SC radius of curvature provided in Table 20.5

Table 20.5 Semicircular canal measurements and radius of curvature obtained for *Rhynchippus pumilus* (MACN-A 52-61) and *Gualta cuyana* (MCNAM-PV 3951)

Measurements (mm) and radius of curvature	<i>Rhynchippus pumilus</i>	<i>Gualta cuyana</i>
ASCL	5.6	–
ASCW	5.9	–
ASCR	2.875	–
PSCL	5.6	5.2
PSCW	4.6	6.2
PSCR	2.55	2.85
LSCL	5.2	–
LSCW	4.1	–
LSCR	2.325	–

Abbreviations: ASCL anterior semicircular canal length, ASCR anterior semicircular canal radius of curvature, ASCW anterior semicircular canal width, LSCL lateral semicircular canal length, LSCR lateral semicircular canal radius of curvature, LSCW lateral semicircular canal width, PSCL posterior semicircular canal length, PSCR posterior semicircular canal radius of curvature, PSCW posterior semicircular canal width. Radius of curvature calculated following Spoor and Zonneveld (1998)

20.5 Final Considerations: Conclusions, Outstanding Questions and Perspectives

The endocranial spaces of notoungulates (especially the endocranial casts) have been of special interest since the pioneer contributions of Serres (1867) and Gervais (1872). Despite a couple of features shared by notoungulates that differentiate their braincasts from that of others SANUs (e.g. presence of a suprasylvian sulcus, a well-developed temporal lobe, and the orbitotemporal canal being close to, or even concealing, the rhinal fissure), there is an interesting morphological diversity within

the order. Such diversity ranges from almost lissencephalic and anteriorly narrow braincasts with cerebellum projecting posteriorly (e.g. *Notostylops murinus*) that grossly resemble that of some condylarths, to anteriorly wide and dorsoventrally developed braincasts showing a well-developed neocortex and a relatively complex gyrification pattern (e.g. later diverging toxodonts). Other endocranial spaces have also been extensively studied, such as the tympanic cavity proper, the hypotympanic cavity (quite conspicuous in several representatives with large auditory bullae), and the epitympanic sinuses (posterodorsally located on the lateral sidewalls of the skull in all but some early diverging representatives). These spaces configure a heavily pneumatized middle ear, although morphofunctional interpretations concerning this condition have been scarcely addressed in the literature.

The relative brain size (quantified by means of the EQ) does not seem to increase or decrease according to our data. However, methodological artifact (e.g. those derived from body mass estimation methods or from an oversimplification of the allometry) or biases (e.g. single specimen estimates) led us to be cautious on this assertion. Forthcoming contributions should provide brain size/body size allometric parameters specific for notoungulates and take into consideration the phylogenetic signal. This would allow better-supported comparisons and more solid inferences about the major forces driving the brain size evolution of the group.

The advent of computed tomography technology not only revitalized the study of the above-mentioned issues but also stimulated research on other areas, such as the caudodorsal and basicranial vasculature. Of special interest is the presence and course of the internal carotid artery. Although an intratympanic course was first proposed (and later followed by some researchers), recently reported data suggest that the prevailing condition among notoungulates would be the opposite (i.e. an extratympanic course). As for the venous vasculature, the relative development of the transverse, temporal and sigmoid sinuses (and their emissary veins and connectors) show that, despite a shared general pattern, there are some differences within notoungulates, even between relatively close related representatives. Such variability deserves to be addressed taking advantage of a growing sample of taxa for which data is available.

Regarding the inferred sensory and locomotor capabilities, the well-developed olfactory bulbs and large piriform lobes observed in most notoungulates suggest high reliance on olfaction. On the contrary, inferences about auditory capabilities are not straightforward. Although bulged temporal lobes could reflect the expansion of the auditory cortex, the inability to perform cortical mapping studies precludes strongly supported assertions. An elaborated middle ear chamber composed of tympanic and paratympanic spaces could be associated to a hearing-related function, but such relationship needs yet to be demonstrated. The only morphofunctional-based inference about notoungulate auditory capabilities is based on cochlear measurements that suggest low-frequency hearing limits for *Notostylops*, *Altitypothierium*, *Pachyrukhos* and *Cochilius*. Finally, the locomotion capabilities derived from the vestibular system dimensions (reported for a handful of notoungulates) is consistent with the postcranial-based inference. However, it is important to highlight that inner ear-based inferences must be considered as a complementary approach, avoiding conclusions based solely on this evidence (i.e. when no postcranial data is available).

As might be expected, there is a plethora of though-provoking questions arising from any of the above-mentioned research lines. They are not new ideas (some of them date back to the last century), but the technical facilities for data acquisition and the methodological procedures for shape analysis and comparison, represent a promising opportunity to make substantial contributions. As mentioned earlier in the chapter, classical publications remain as the only source of data for some representatives of the order, which underlines the need for new data on such an iconic group of SANUs.

Acknowledgments The authors thank Marcos Fernández-Monescillo (Museo de Paleontología, Universidad Nacional de Córdoba) for providing captures of the virtual endocast of MACN-Pv 2925 and for comments on some taxonomic assignments, and CT technologist Alejandro Panes (Instituto de Diagnóstico del Este del Chubut) for general assistance and CT scanner operation. We also thank Eduardo Ruigómez and María Encarnación Pérez (Museo Paleontológico Egidio Feruglio), Alejandro Kramarz (Museo Argentino de Ciencias Naturales Bernardino Rivadavia), Stella Maris Álvarez (former technician curator at the Museo Argentino de Ciencias Naturales Bernardino Rivadavia), Ruth O’Leary, Jin Meng and Judy Galkin (American Museum of Natural History), and Bill Simpson (Field Museum of Natural History) for providing access to the collections under their care. Finally, the authors acknowledge Ornella Bertrand and an anonymous reviewer for their pertinent corrections, comments and suggestions, which greatly improved the quality of the final version of the chapter. This research was partially funded by CONICET PIP 11220150100113 (to MTD) and PUE-IPGP 22920200100014 (CONICET 2020 Executing Units Project awarded to the Patagonian Institute of Geology and Paleontology). TEM was supported by the Biaggini Research Fund in the Department of Biological Sciences at St. Mary’s University.

References

- Agnolín FL, Chimento NR (2011) Afrotherian affinities for endemic South American “ungulates”. *Mamm Biol* 76:101–108. <https://doi.org/10.1016/j.mambio.2010.12.001>
- Ameghino F (1894) Énumération synoptique des espèces de mammifères fossiles des formations éocènes de Patagonie. *Bol Acad Nac Cienc/Córdoba* 13:259–452
- Avilla LS, Mothé D (2021) Out of Africa: a new Afrotheria lineage rises from extinct South American mammals. *Front Ecol Evol* 9:654302. <https://doi.org/10.3389/fevo.2021.654302>
- Bauzá N, Gelfo JN, López GM (2019) Early steps in the radiation of notoungulate mammals in southern South America: a new henricosbornioid from the Eocene of Patagonia. *Acta Palaeontol Pol* 64(3):597–607. <https://doi.org/10.4202/app.00565.2018>
- Bauzá N, Gelfo JN, López GM (2020) Phylogenetic implications of dental characters in Henricosborniidae (Mammalia, Notoungulata). *Ameghiniana* 57:90–102. <https://doi.org/10.5710/AMGH.18.01.2020.3304>
- Bergqvist LP, Fortes Bastos AC (2009) A postura locomotora de *Colbertia magellanica* (Mammalia, Notoungulata) da Bacia de São José de Itaboraí (Paleoceno superior), Rio de Janeiro. *Rev Bras Paleontol* 12:83–89. <https://doi.org/10.4072/rbp.2009.1.08>
- Bertrand OC, Silcox MT (2016) First virtual endocasts of a fossil rodent: *Ischyromys typus* (Ischyromyidae, Oligocene) and brain evolution in rodents. *J Vertebr Paleontol* 36(3):e1095762. <https://doi.org/10.1080/02724634.2016.1095762>
- Bertrand OC, Shelley SL, Wible JR et al (2020) Virtual endocranial and inner ear endocasts of the Paleocene ‘condylarth’ *Chriacus*: new insight into the neurosensory system and evolution of early placental mammals. *J Anat* 236:21–49. <https://doi.org/10.1111/joa.13084>

- Bertrand OC, Püschel HP, Schwab JA et al (2021) The impact of locomotion on the brain evolution of squirrels and close relatives. *Commun Biol* 4:460. <https://doi.org/10.1038/s42003-021-01887-8>
- Billet G (2010) New observations on the skull of *Pyrotherium* (Pyrotheria, Mammalia) and new phylogenetic hypotheses on South American ungulates. *J Mamm Evol* 17:21–59. <https://doi.org/10.1007/s10914-009-9123-0>
- Billet G (2011) Phylogeny of the Notoungulata (Mammalia) based on cranial and dental characters. *J Syst Palaeontol* 9:481–497. <https://doi.org/10.1080/14772019.2010.528456>
- Billet G, Martin T (2011) No evidence for an afrotherian-like delayed dental eruption in South American notoungulates. *Naturwissenschaften* 98:509–517. <https://doi.org/10.1007/s00114-011-0795-y>
- Billet G, Muizon CD (2013) External and internal anatomy of a petrosal from the late Paleocene of Itaboraí, Brazil, referred to Notoungulata (Placentalia). *J Vertebr Paleontol* 33(2):455–469. <https://doi.org/10.1080/02724634.2013.722153>
- Billet G, Muizon CD, Schellhorn R et al (2015) Petrosal and inner ear anatomy and allometry amongst specimens referred to Litopterna (Placentalia). *Zool J Linn Soc* 173:956–987. <https://doi.org/10.1111/zoj.12219>
- Buckley M (2015) Ancient collagen reveals evolutionary history of the endemic South American ‘ungulates’. *Proc R Soc B Biol Sci* 282:20142671. <https://doi.org/10.1098/rspb.2014.2671>
- Burger JR, George MA, Leadbetter C et al (2019) The allometry of brain size in mammals. *J Mammal* 100:276–283. <https://doi.org/10.1093/jmammal/gyz043>
- Butler H (1967) The development of mammalian dural venous sinuses with especial reference to the post-glenoid vein. *J Anat* 102(1):33–56
- Campos GB, Welker WI (1976) Comparisons between brains of a large and a small hystricomorph rodent: *Capybara*, *Hydrochoerus* and Guinea pig, *Cavia*; neocortical projection regions and measurements of brain subdivisions. *Brain Behav Evol* 13(4):243–266. <https://doi.org/10.1159/000123814>
- Carlisle A, Selwood L, Hinds LA et al (2017) Testing hypotheses of developmental constraints on mammalian brain partition evolution, using marsupials. *Sci Rep* 7:4241. <https://doi.org/10.1038/s41598-017-02726-9>
- Carrillo JD, Asher RJ (2017) An exceptionally well-preserved skeleton of *Thomashuxleya externa* (Mammalia, Notoungulata), from the Eocene of Patagonia, Argentina. *Palaeontol Electron* 20.2(34A):1–33. <https://doi.org/10.26879/759>
- Cassini GH, Cerdeño E, Villafañe A et al (2012a) Paleobiology of Santacrucian native ungulates (Meridiungulata: Astrapotheria, Litopterna, and Notoungulata). In: Vizcaíno SF, Kay RF, Bargo MS (eds) Early miocene paleobiology in Patagonia: high-latitude paleocommunities of the Santa Cruz formation. Cambridge University Press, Cambridge, pp 243–286. <https://doi.org/10.1017/CBO9780511667381.015>
- Cassini GH, Vizcaíno SF, Bargo MS (2012b) Body mass estimation in Early Miocene native South American ungulates: a predictive equation based on 3D landmarks. *J Zool* 287:53–64. <https://doi.org/10.1111/j.1469-7998.2011.00886.x>
- Cerdeño E, Vera B (2010) *Mendozahippus fierensis* gen. et sp. nov., new Notohippidae (Notoungulata) from the late Oligocene of Mendoza (Argentina). *J Vertebr Paleontol* 30(6):1805–1817. <https://doi.org/10.1080/02724634.2010.520781>
- Cerdeño E, Vera B (2015) A new Leontiniidae (Notoungulata) from the late Oligocene beds of Mendoza Province, Argentina. *J Syst Palaeontol* 13:943–962. <https://doi.org/10.1080/14772019.2014.982727>
- Cerdeño E, Vera B, Schmidt GI et al (2012) An almost complete skeleton of a new Mesotheriidae (Notoungulata) from the late Miocene of Casira, Bolivia. *J Syst Palaeontol* 10:341–360. <https://doi.org/10.1080/14772019.2011.569576>
- Cerdeño E, Vera B, Combina AM (2018) A new early Miocene Mesotheriidae (Notoungulata) from the Mariño Formation (Argentina): taxonomic and biostratigraphic implications. *J S Am Earth Sci* 88:118–131. <https://doi.org/10.1016/j.jsames.2018.06.016>

- Chaffee RG (1952) The Deseadan vertebrate fauna of the Scarritt Pocket, Patagonia. *Bull Am Mus Nat Hist* 98(6):509–562
- Cifelli RL (1993) The phylogeny of the native South American ungulates. In: Szalay FS, Novacek MJ, McKenna MC (eds) *Mammal phylogeny, volume 2: placentals*. Springer, New York, pp 195–216
- Cifelli R, Schaff CR, McKenna MC (1989) Relationships of the Arctostylopidae (Mammalia). *Bull Mus Comp Zool* 152:1–44
- Coombs MC (1983) Large mammalian clawed herbivores: a comparative study. *Trans Am Philos Soc* 73:1–96
- Croft DA (1999) Placentals: endemic South American ungulates. In: Singer R (ed) *The encyclopedia of paleontology*. Fitzroy-Dearborn, Chicago, pp 890–906
- Croft DA (2016) *Horned armadillos and rafting monkeys: the fascinating fossil mammals of South America*. Indiana University Press, Bloomington
- Croft DA, Anderson LC (2008) Locomotion in the extinct notoungulate *Protypotherium*. *Palaeontol Electron* 11.1.1A:1–20
- Croft DA, Lorente M (2021) No evidence for parallel evolution of cursorial limb adaptations among Neogene South American native ungulates (SANUs). *PLoS ONE* 16(8):e0256371. <https://doi.org/10.1371/journal.pone.0256371>
- Croft DA, Flynn JJ, Wyss AR (2004) Notoungulata and Litopterna of the early Miocene Chucal Fauna, northern Chile. *Fieldiana Geol* 50:1–52. [https://doi.org/10.3158/0096-2651\(2004\)50\[1:NALOTE\]2.0.CO;2](https://doi.org/10.3158/0096-2651(2004)50[1:NALOTE]2.0.CO;2)
- Croft DA, Gelfo JN, López GM (2020) Splendid innovation: the extinct South American native ungulates. *Annu Rev Earth Planet Sci* 48:259–290. <https://doi.org/10.1146/annurev-earth-072619-060126>
- de Muizon C, Cifelli RL (2000) The “condylarths” (archaic Ungulata, Mammalia) from the early Palaeocene of Tiupampa (Bolivia): implications on the origin of the South American ungulates. *Geodiversitas* 22(1):47–150
- de Muizon C, Billet G, Argot C et al (2015) *Alcidedorbignya inopinata*, a basal pantodont (Placentalia, Mammalia) from the early Palaeocene of Bolivia: anatomy, phylogeny and palaeobiology. *Geodiversitas* 37(4):397–634. <https://doi.org/10.5252/g2015n4a1>
- Dechaseaux C (1956) L'encéphale de *Protypotherium*, mammifère miocène d'Amérique du Sud. *C R Hebd Seances Acad Sci* 242(13):1753–1755
- Dechaseaux C (1958) Encéphales de Notungulés. In: Piveteau J (ed) *Traité de Paléontologie*. Masson et Cie, Paris, pp 121–129
- Dechaseaux C (1962) Encéfalos de notungulados y de desdentados xenartros fósiles. *Ameghiniana* 2(11):193–209
- Deraco MV, García-López DA (2016) A new Eocene Toxodontia (Mammalia Notoungulata) from northwestern Argentina. *J Vertebr Paleontol* 36:e1037884. <https://doi.org/10.1080/02724634.2015.1037884>
- Domingo L, Tomassini RL, Montalvo CI et al (2020) The Great American Biotic interchange revisited: a new perspective from the stable isotope record of Argentine pampas fossil mammals. *Sci Rep* 10:1608. <https://doi.org/10.1038/s41598-020-58575-6>
- Dozo MT (1997) Paleoneurología de *Dolicavia minuscula* (Rodentia, Caviidae) y *Paedotherium insigne* (Notoungulata, Hegetotheriidae) del Plioceno de Buenos Aires, Argentina. *Ameghiniana* 34(4):427–435
- Dozo MT, Martínez G (2016) First digital cranial endocasts of late Oligocene Notohippidae (Notoungulata): implications for endemic South American ungulates brain evolution. *J Mamm Evol* 23(1):1–16. <https://doi.org/10.1007/s10914-015-9298-5>
- Eisenberg JF (1981) *The mammalian radiations: an analysis of trends in evolution, adaptation and behavior*. University of Chicago Press, Chicago
- Elissamburu A (2010) Estudio biomecánico y morfofuncional del esqueleto apendicular de *Homalodotherium* Flower 1873 (Mammalia, Notoungulata). *Ameghiniana* 47(1):25–43

- Elissamburu A (2012) Estimación de la masa corporal en géneros del Orden Notoungulata. *Estud Geol* 68:91–111. <https://doi.org/10.3989/egeol.40336.133>
- Ezcurra MD, Agnolin FL (2012) A new global palaeobiogeographical model for the late mesozoic and early tertiary. *Syst Biol* 61:553–566. <https://doi.org/10.1093/sysbio/syr115>
- Fedorov A, Beichel R, Kalpathy-Cramer J et al (2012) 3D Slicer as an image computing platform for the quantitative imaging network. *Magn Reson Imaging* 30(9):1323–1341. <https://doi.org/10.1016/j.mri.2012.05.001>
- Fernández-Monescillo M, Antoine PO, Pujos F et al (2019) Virtual endocast morphology of Mesotheriidae (Mammalia, Notoungulata, Typotheria): new insights and implications on notoungulate encephalization and brain evolution. *J Mamm Evol* 26(1):85–100. <https://doi.org/10.1007/s10914-017-9416-7>
- Forasiepi AM, MacPhee RDE, Hernández del Pino S, et al (2016) Exceptional skull of *Huayqueriana* (Mammalia, Litopterna, Macrauchenidae) from the Late Miocene of Argentina: anatomy, systematics, and paleobiological implications. *B Am Mus Nat Hist* 404:1–76. <https://doi.org/10.1206/0003-0090-404.1.1>
- Gabbert SL (2004) The basicranial and posterior cranial anatomy of the families of Toxodontia. *Bull Am Mus Nat Hist* 285:177–190. [https://doi.org/10.1206/0003-0090\(2004\)285<0177:C>2.0.CO;2](https://doi.org/10.1206/0003-0090(2004)285<0177:C>2.0.CO;2)
- García-López D (2011) Basicranial osteology of *Colbertia lumbrense* Bond, 1981 (Mammalia: Notoungulata). *Ameghiniana* 48(1):3–12. [https://doi.org/10.5710/AMGH.v48i1\(262\)](https://doi.org/10.5710/AMGH.v48i1(262))
- García-López DA, Babot MJ (2015) Notoungulate faunas of north-western Argentina: new findings of early-diverging forms from the Eocene Geste Formation. *J Syst Palaeontol* 13(7):557–579. <https://doi.org/10.1080/14772019.2014.930527>
- García-López DA, Deraco V, Del Papa C (2018a) Fossil mammals of the Quebrada de los Colorados Formation (late middle Eocene) at the locality of La Poma, Salta Province, Argentina. *Hist Biol* 30(4):507–517. <https://doi.org/10.1080/08912963.2017.1299150>
- García-López DA, Babot J, González R et al (2018b) Cranial anatomy of an Eocene notoungulate mammal from northwestern Argentina with special reference on the ear region. *Hist Biol* 30(7):957–975. <https://doi.org/10.1080/08912963.2017.1326112>
- Gelfo JN, Goin FJ, Bauzá N et al (2019) The fossil record of Antarctic land mammals: commented review and hypotheses for future research. *Adv Polar Sci* 30(3):274–292. <https://doi.org/10.13679/j.advps.2019.0021>
- Gervais P (1872) Mémoire sur les formes cérébrales propres à différents groupes de Mammifères. *J Zool* 1:425–469
- Giannini PG, García-López DA (2014) Ecomorphology of mammalian fossil lineages: identifying morphotypes in a case study of endemic South American ungulates. *J Mamm Evol* 21:195–212. <https://doi.org/10.1007/s10914-013-9233-6>
- Gittleman JL (1991) Carnivore olfactory bulb size: allometry, phylogeny and ecology. *J Zool (Lond)* 225:253–272. <https://doi.org/10.1111/j.1469-7998.1991.tb03815.x>
- Hernández del Pino S (2018) Anatomía y Sistemática de los Toxodontidae (Notoungulata) de la Formación Santa Cruz, Mioceno Temprano, Argentina. Dissertation, Universidad Nacional de La Plata
- Hernández del Pino S, Fernández M, Cerdeño E et al (2019) Anatomy and systematics of *Notohippus toxodontoides* Ameghino, 1891 (Mammalia, Notoungulata), from the Miocene of Santa Cruz Province, Argentina. *J Vertebr Paleontol* 39(1):e1577870. <https://doi.org/10.1080/002724634.2019.1577870>
- Hernández Jasso RM, Piñon AB (2020) Late Pleistocene toxodont remains of Tamaulipas, Mexico. Confirmation of the occurrence of *Mixotoxodon larensis* (Van Frank, 1957) and an analysis of sexual dimorphism. *J S Am Earth Sci* 104:102849. <https://doi.org/10.1016/j.jsames.2020.102849>
- Jacobs LF (2012) From chemotaxis to the cognitive map: the function of olfaction. *Proc Natl Acad Sci USA* 109(1):10693–10700. <https://doi.org/10.1073/pnas.1201880109>

- Jerison HJ (1970) Brain evolution: new light on old principles. *Science* 170:1224–1225. <https://www.science.org/doi/10.1126/science.170.3963.1224>
- Jerison HJ (1973) Evolution of the brain and intelligence. Academic Press, New York
- Jerison HJ (2012) Digitized fossil brains: neocorticalization. *Biolinguistics* 6(3–4):383–392
- Kramarz A, Bond M (2014) Critical revision of the alleged delayed dental eruption in South American “ungulates”. *Mamm Biol* 79(3):170–175. <https://doi.org/10.1016/j.mambio.2013.11.001>
- Lebrun R (2018) MorphoDig, an open-source 3d freeware dedicated to biology. In: Abstracts of the 5th International Paleontological Congress, Paris, 9–13 July 2018
- Long A, Bloch JI, Silcox MT (2015) Quantification of neocortical ratios in stem primates. *Am J Phys Anthropol* 157:363–373. <https://doi.org/10.1002/ajpa.22724>
- Loomis (1914) The Deseado Formation of Patagonia. Rumford Press, Concord
- Lorente M, Gelfo JN, López GM (2019) First skeleton of the notoungulate mammal *Notostylops murinus* and palaeobiology of Eocene Notostylopidae. *Lethaia* 52(2):244–259. <https://doi.org/10.1111/let.12310>
- Lundelius EL Jr, Vaughn MB, Mandel R et al (2013) The first occurrence of a toxodont (Mammalia, Notoungulata) in the United States. *J Vertebr Paleontol* 33(1):229–232. <https://doi.org/10.1080/00272463.2012.711405>
- MacFadden BJ (2005) Diet and habitat of toxodont megaherbivores (Mammalia, Notoungulata) from the late Quaternary of South and Central America. *Quat Res* 64(2):113–124. <https://doi.org/10.1016/j.yqres.2005.05.003>
- MacPhee RDE (2014) The serialis bone, interparietals, “X” elements, entotympanics, and the composition of the notoungulate caudal cranium. *Bull Am Mus Nat Hist* 384:1–69. <https://doi.org/10.1206/384.1>
- MacPhee RDE, Forasiepi AM (2022) Re-evaluating cranial pathways of the internal carotid artery in Notoungulata (Mammalia, Panperissodactyla). *Ameghiniana* 59(2):141–161. <https://doi.org/10.5710/AMGH.06.12.2021.3465>
- MacPhee RDE, Hernández del Pino S, Kramarz A et al (2021) Cranial morphology and phylogenetic relationships of *Trigonostylops wortmani*, an Eocene South American native ungulate. *Bull Am Mus Nat Hist* 449:1–183. <https://doi.org/10.1206/0003-0090.449.1.1>
- Macrini TE, Rougier GW, Rowe T (2007) Description of a cranial endocast from the fossil mammal *Vincelestes neuquenianus* (Theriiiformes) and its relevance to the evolution of endocranial characters in therians. *Anat Rec* 290:875–892. <https://doi.org/10.1002/ar.20551>
- Macrini TE, Flynn JJ, Croft DA et al (2010) Inner ear of a notoungulate placental mammal: anatomical description and examination of potentially phylogenetically informative characters. *J Anat* 216(5):600–610. <https://doi.org/10.1111/j.1469-7580.2010.01224.x>
- Macrini TE, Flynn JJ, Ni X et al (2013) Comparative study of notoungulate (Placentalia, Mammalia) bony labyrinths and new phylogenetically informative inner ear characters. *J Anat* 223(5):442–461. <https://doi.org/10.1111/joa.12108>
- Madden RH (2015) Hypsodonty in mammals: evolution, geomorphology, and the role of earth surface processes. Cambridge University Press, Cambridge
- Manoussaki D, Chadwick RS, Ketten DR et al (2008) The influence of cochlear shape on low-frequency hearing. *Proc Natl Acad Sci USA* 105(16):6162–6166. <https://doi.org/10.1073/pnas.0710037105>
- Marani HA (2005) Los Rhynchippinae (Mammalia, Notoungulata: Toxodontia: Notohippidae) de la edad Deseadense de Cabeza Blanca (Chubut, Argentina): revisión sistemática y filogenia. Dissertation, Universidad Nacional de la Patagonia San Juan Bosco
- Martínez G (2018) Evolución de los “Notohippidae” (Mammalia, Notoungulata, Toxodontia): sistemática, filogenia y paleobiología. Dissertation, Universidad Nacional de Córdoba
- Martínez G, Dozo MT, Gelfo JN et al (2016) Cranial morphology of the late Oligocene patagonian Notohippid *Rhynchippus equinus* Ameghino, 1897 (Mammalia, Notoungulata) with emphases in basicranial and auditory region. *PLoS ONE* 11(5):e0156558. <https://doi.org/10.1371/journal.pone.0156558>

- Martínez G, González-José R, Dozo MT et al (2019) Estimación de masa corporal en los “Notohippidae” (Mammalia, Panperissodactyla, Notoungulata) en base al tamaño del centroide. In: 33th Jornadas Argentinas de Paleontología de Vertebrados, abstract. 33as Jornadas Argentinas de Paleontología, Córdoba, May 2019. Abstract. PE-APA, Buenos Aires, p R23
- Martínez G, Dozo MT, Vera B et al (2020) Paleoneurology, auditory region, and associated soft tissue inference in the late Oligocene notoungulates *Mendozahippus fierensis* and *Gualta cuyana* (Toxodontia) from central-western Argentina. *J Vertebr Paleontol* 39(6):e1725531. <https://doi.org/10.1080/02724634.2019.1725531>
- Martínez G, Dozo MT, Gelfo JN et al (2021) A new toxodont (Mammalia, Panperissodactyla, Notoungulata) from the Oligocene of Patagonia, Argentina, and systematic considerations on the paraphyletic ‘Notohippidae’. *J Syst Palaeontol* 18(24):1995–2013. <https://doi.org/10.1080/01472019.2021.1872723>
- McKenna MC (1975) Toward a phylogenetic classification of mammals. In: Luckett WP, Szalay FS (eds) *Phylogeny of the primates*. Plenum Press, New York, pp 21–46. https://doi.org/10.1007/978-1-4684-2166-8_2
- Mendoza M, Janis CM, Palmqvist P (2006) Estimating the body mass of extinct ungulates: a study on the use of multiple regression. *J Zool* 270(1):90–101. <https://doi.org/10.1111/j.1469-7998.2006.00094.x>
- Missiaen P, Escarguel G, Hartenberger JL, Smith T (2012) A large new collection of *Palaeostylops* from the Paleocene of the Flaming Cliffs area (Ulan-Nur Basin, Gobi Desert, Mongolia), and an evaluation of the phylogenetic affinities of Arctostylopidae (Mammalia, Gliriformes). *Geobios* 45(3):311–322. <https://doi.org/10.1016/j.geobios.2011.10.004>
- O’Leary MA, Bloch JJ, Flynn JJ et al (2013) The placental mammal ancestor and the post-K-Pg radiation of placentals. *Science* 339(6120):662–667. <https://www.science.org/doi/10.1126/science.1229237>
- Oliveira FB, Cassola Molina E, Marroig G (2009) Paleogeography of the South Atlantic: a route for primates and rodents into the New-World? In: Garber PA, Estrada A, Bicca-Marques JC et al (eds) *South American primates, developments in primatology: progress and prospects*. Springer, New York, pp 55–68
- Orliac MJ, Argot C, Gilissen E (2012) Digital cranial endocast of *Hyopsodus* (Mammalia, “Condylarthra”): a case of Paleogene terrestrial echolocation? *PLoS ONE* 7(2):e30000. <https://doi.org/10.1371/journal.pone.0030000>
- Pascual R, Vucetich MG, Fernández J (1978) Los primeros mamíferos (Notoungulata, Henricosborniidae) de la Formación Mealla (Grupo Salta, subgrupo Santa Bárbara): sus implicancias filogenéticas, taxonómicas y cronológicas. *Ameghiniana* 15(3–4):366–390
- Patterson B (1932) The auditory region of the Toxodontia. *Field Mus Nat Hist Geol Ser* 6(1):1–27. <https://doi.org/10.5962/bhl.title.6626>
- Patterson B (1934a) The auditory region of an Upper Pliocene typotherid. *Geol Ser Field Mus Nat Hist* 6(5):83–89. <https://doi.org/10.5962/bhl.title.63156>
- Patterson B (1934b) *Trachytherus*, a typotherid from the Deseado beds of Patagonia. *Geol Ser Field Mus Nat Hist* 6:119–139
- Patterson B (1936) The internal structure of the ear in some notoungulates. *Geol Ser Field Mus Nat Hist* 6(15):199–227. <https://doi.org/10.5962/bhl.title.5312>
- Patterson B (1937) Some notoungulate braincasts. *Geol Ser Field Mus Nat Hist* 6(19):273–301. <https://doi.org/10.5962/bhl.title.5197>
- Patterson B (1977) A primitive pyrothere (Mammalia, Notoungulata) from the early Tertiary of northwestern Venezuela. *Fieldiana Geol* 33(22):397–422. <https://doi.org/10.5962/bhl.title.5225>
- Perini FA, Macrini TE, Flynn JJ et al (2022) Comparative endocranial anatomy, encephalization, and phylogeny of Notoungulata (Placentalia, Mammalia). *J Mamm Evol* 29:369–394. <https://doi.org/10.1007/s10914-021-09583-4>
- Pilleri G, Gihl M, Kraus C (1984) Cephalization in rodents with particular reference to the Canadian beaver (*Castor canadensis*). In: Pilleri G (ed) *Investigations beavers. Brain Anatomy Institute, Berne*, pp 11–102

- Radinsky L (1981) Brain evolution in extinct South American ungulates. *Brain Behav Evol* 18:169–187. <https://doi.org/10.1159/000121785>
- Reep RL, Finlay BL, Darlington RB (2007) The limbic system in mammalian brain evolution. *Brain Behav Evol* 70:57–70. <https://doi.org/10.1159/000101491>
- Reguero MA, Prevosti FJ (2010) Rodent-like notoungulates: tyotheria. Phylogeny and systematics. In: Madden R, Carlini AA, Vucetich MG et al (eds) *The paleontology of Gran Barranca: evolution and environmental change through the Middle Cenozoic of Patagonia*. Cambridge University Press, Cambridge, pp 148–165
- Riggs ES (1937) Mounted skeleton of *Homalodotherium*. *Geol Ser Field Mus Nat Hist* 6(17):233–243
- Roth S (1903) Los ungulados sudamericanos. *Anales del Museo La Plata, Paleontología Argentina* 5:1–36. <https://doi.org/10.5962/bhl.title.155433>
- Rowe T, Macrini TE, Luo Z-X (2011) Fossil evidence on origin of the mammalian brain. *Science* 332(6032):955–957. <https://doi.org/10.1126/science.1203117>
- Schoch RM, Lucas SG (1985) The phylogeny and classification of the Dinocerata (Mammalia, Eutheria). *Bull Geol Inst Univ Upsala* 11:31–57
- Scott WB (1930) A partial skeleton of *Homalodontotherium* from the Santa Cruz beds of Patagonia. *Memoirs of the Field Museum of Natural History* 50:1–39
- Segall W (1970) Morphological parallelisms of the bulla and auditory ossicles in some insectivores and marsupials. *Fieldiana Zool* 51:169–205
- Seoane F, Cerdeño E (2019) Systematic revision of *Hegetotherium* and *Pachyrukhos* (Hegetotheriidae, Notoungulata) and a new phylogenetic analysis of Hegetotheriidae. *J Syst Palaeontol* 17(19):1635–1663. <https://doi.org/10.1080/14772019.2018.1545146>
- Serres ÉRA (1867) De l'ostéographie du *Mesotherium* et de ses affinités zoologiques. *C R Hebd Seances Acad Sci* 65:140–148
- Shockey BJ (1997) Two new notoungulates (Family Notohippidae) from the Salla Beds of Bolivia (Deseadan: late Oligocene): systematics and functional morphology. *J Vertebr Paleontol* 17(3):584–599. <https://doi.org/10.1080/02724634.1997.10011005>
- Shockey BJ, Anaya F (2008) Postcranial osteology of mammals from Salla, Bolivia (late Oligocene): form, function, and phylogenetic implications. In: Sargis EJ, Dagosto M (eds) *Mammalian evolutionary morphology: a tribute to Frederick S. Szalay*. Springer, Dordrecht, pp 135–157. https://doi.org/10.1007/978-1-4020-6997-0_7
- Shockey BJ, Flynn JJ (2007) Morphological diversity in the postcranial skeleton of Casamayoran (?middle to late Eocene) Notoungulata and foot posture in notoungulates. *Am Mus Novit* 3601:1–26. [https://doi.org/10.1206/0003-0082\(2007\)3601\[1:MDITPS\]2.0.CO;2](https://doi.org/10.1206/0003-0082(2007)3601[1:MDITPS]2.0.CO;2)
- Shockey BJ, Croft DA, Anaya F (2007) Analysis of function in the absence of extant functional homologues: a case study using mesotheriid notoungulates (Mammalia). *Paleobiology* 33:227–247. <https://doi.org/10.1666/05052.1>
- Shockey BJ, Flynn JJ, Croft DA et al (2012) New leontiniid Notoungulata (Mammalia) from Chile and Argentina: comparative anatomy, character analysis, and phylogenetic hypotheses. *Am Mus Novit* 3737:1–64. <https://doi.org/10.1206/3737.2>
- Shultz S, Finlayson LV (2010) Large body and small brain and group sizes are associated with predator preferences for mammalian prey. *Behav Ecol* 21:1073–1079. <https://doi.org/10.1093/beheco/arq108>
- Silcox MT, Bloch JI, Boyer DM et al (2009) Semicircular canalsystem in early primates. *J Hum Evol* 56(3):315–327. <https://doi.org/10.1016/j.jhevol.2008.10.007>
- Simpson GG (1932) Skulls and brains of some mammals from the *Notostylops* beds of Patagonia. *Am Mus Novit* 578:1–11
- Simpson GG (1933a) Braincasts of *Phenacodus*, *Notostylops*, and *Rhyphodon*. *Am Mus Novit* 622:1–19
- Simpson GG (1933b) Braincasts of two tyotheres and a litoptern. *Am Mus Novit* 629:1–18
- Simpson GG (1934) Provisional classification of extinct South American hoofed mammals. *Am Mus Novit* 750:1–21
- Simpson GG (1936) Structure of a primitive notoungulate cranium. *Am Mus Novit* 824:1–31

- Simpson GG (1945) The principles of classification and a classification of mammals. *Bull Am Mus Nat Hist* 85:1–350
- Simpson GG (1978) Early mammals in South America: fact, controversy, and mystery. *Proc Am Phil Soc* 122(5):318–328
- Simpson GG (1980) Splendid isolation: the curious history of South American mammals. Yale University Press, New Haven
- Smaers JB, Rothman RS, Hudson DR et al (2021) The evolution of mammalian brain size. *Sci Adv* 7(18):eabe2101. <https://www.science.org/doi/10.1126/sciadv.abe2101>
- Solórzano A, Núñez-Flores M (2021) Evolutionary trends of body size and hypsodonty in notoungulates and their probable drivers. *Palaeogeogr Palaeoclimatol Palaeoecol* 568:110306. <https://doi.org/10.1016/j.palaeo.2021.110306>
- Soria MF (1988) Notopterna: un nuevo orden de mamíferos ungulados eógenos de América de Sur. Parte II. *Notonychops powelli* gen. et sp. nov. (Notonychopidae nov.) de la Formación Río Loro (Paleoceno medio), provincia de Tucumán, Argentina. *Ameghiniana* 25(3):259–272
- Soria MF (2001) Los Protheroheriidae (Mammalia, Litopterna): sistemática, origen y filogenia. *Monografías del Museo Argentino de Ciencias Naturales “Bernardino Rivadavia”* 1:1–167
- Spoor F (2003) The semicircular canal system and locomotor behaviour, with special reference to hominin evolution. *Cour Forsch-Inst Senckenberg* 243:93–104
- Spoor F, Zonneveld F (1998) Comparative review of the human bony labyrinth. *Yearb Phys Anthropol* 41(S27):211–251. [https://doi.org/10.1002/\(SICI\)1096-8644\(1998\)107:27<211::AID-AJPA8>3.0.CO;2-V](https://doi.org/10.1002/(SICI)1096-8644(1998)107:27<211::AID-AJPA8>3.0.CO;2-V)
- Spoor F, Garland T, Krovitz G et al (2007) The primate semicircular canal system and locomotion. *Proc Natl Acad Sci USA* 104(26):10808–10812. <https://doi.org/10.1073/pnas.0704250104>
- Vera B (2015) Phylogenetic revision of the South American notopithecines (Mammalia, Notoungulata). *J Syst Palaeontol* 14(6):461–480. <https://doi.org/10.1080/14772019.2015.1066454>
- Vera B (2017) Patagonian Eocene Archaeopithecidae Ameghino, 1897 (Notoungulata): systematic revision, phylogeny and biostratigraphy. *J Paleontol* 91(6):1272–1295. <https://doi.org/10.1017/jpa.2017.53>
- Vera B, Reguero MA, González-Ruiz L (2017) The Intertheriinae (Notoungulata) from the Collón Curá Formation (middle Miocene), Argentina. *Acta Palaeontol Pol* 62(4):845–863. <https://doi.org/10.4202/app.00373.2017>
- Vera B, González Ruiz L, Novo N et al (2019) The Intertheriinae (Mammalia, Notoungulata) of the Friasian *sensu stricto* and Mayoan (middle to late Miocene) and the fossils from Cerro Zeballos, Patagonia, Argentina. *J Syst Palaeontol* 17(13):923–943. <https://doi.org/10.1080/14772019.2018.1511387>
- von Koenigswald W, Martin T, Billet G (2015) Enamel microstructure and mastication in *Pyrotherium romeroi* (Pyrotheria, Mammalia). *Paläontol Z* 89:593–609. <https://doi.org/10.1007/s12542-014-0241-5>
- Welker F, Collins MJ, Thomas JA et al (2015) Ancient proteins resolve the evolutionary history of Darwin’s South American ungulates. *Nature* 522:81–84. <https://doi.org/10.1038/nature14249>
- Wible JR, Zeller U (1994) Cranial circulation of the pen-tailed tree shrew *Ptilocercus lowii* and relationships of Scandentia. *J Mamm Evol* 2:209–230. <https://doi.org/10.1007/BF01464275>

Chapter 21

Paleoneurology of Litopterna: Digital and Natural Endocranial Casts of Macraucheniidae



María Teresa Dozo, Gastón Martínez, and Javier N. Gelfo

Institutional Abbreviations

AMNH	American Museum of Natural History, New York, USA
CNP-ME	Colección de Moldes endocraneanos, Centro Nacional Patagónico, Puerto Madryn, Chubut, Argentina
IANIGLA-PV	Instituto Argentino de Nivología, Glaciología y Ciencias Ambientales, Paleontología de Vertebrados, Mendoza, Argentina
IDECH	Instituto de Diagnóstico del Este del Chubut, Argentina
MACN-PV	División Paleontología de Vertebrados, Museo Argentino de Ciencias Naturales Bernardino Rivadavia, Buenos Aires, Argentina
MLP	Museo de la Plata, La Plata, Argentina
MPEF-PV	Museo Paleontológico Egidio Feruglio, Colección de Paleontología de Vertebrados, Trelew, Argentina

M. T. Dozo (✉)

Consejo Nacional de Investigaciones Científicas y Técnicas (CONICET), Caba, Argentina

Instituto Patagónico de Geología y Paleontología, CCT CONICET-CENPAT,
Puerto Madryn, Argentina

e-mail: dozo@cenpat-conicet.gob.ar

G. Martínez

Museo de Paleontología, Facultad de Ciencias Exactas, Físicas y Naturales, Universidad Nacional de Córdoba, Córdoba, Argentina

e-mail: gmartinez@unc.edu.ar

J. N. Gelfo

Consejo Nacional de Investigaciones Científicas y Técnicas (CONICET), Caba, Argentina

División Paleontología Vertebrados, Museo de La Plata, Facultad de Ciencias Naturales y Museo, Universidad Nacional de La Plata, La Plata, Argentina

e-mail: jgelfo@fcnym.unlp.edu.ar

© Springer Nature Switzerland AG 2023

M. T. Dozo et al. (eds.), *Paleoneurology of Amniotes*,
https://doi.org/10.1007/978-3-031-13983-3_21

UNPSJB-PV Repositorio Científico y Didáctico de la Facultad de Ciencias Naturales de la Universidad Nacional de la Patagonia San Juan Bosco, Comodoro Rivadavia, Chubut, Argentina

21.1 Systematic and Phylogenetic Context

The Litopterna Ameghino 1889, is the second largest group of South American native ungulates in abundance and diversity after Notoungulata. They are recorded from the early Paleocene, Peligran South American Land Mammal Age (SALMA) to the Pleistocene, Lujanian SALMA in South America, and also from the Eocene in West Antarctica (Gelfo et al. 2019). Phylogenetic inferences based on molecular evidence suggest that they share a common ancestor with Notoungulata, and both, are closer to Perissodactyla than to any other group with extant relatives (Buckley 2015; Welker et al. 2015; Westbury et al. 2017). Like notoungulates and perissodactyls, litopterns kept mesoaxonic limbs with odd toes, with different kinds of digit reductions. Many of them had hooves remarkably similar to those of living horses, rhinos, or pigs (Gelfo et al. 2016; Croft et al. 2020). Through their evolutionary history, litopterns experienced a tachytelic rhythm in the locomotor system, generating very early, limb specializations as a digitigrade posture, knee-locking mechanism, or even a complete digit reduction, which predates that developed by horses (Gelfo et al. 2016; Croft et al. 2020). Most litopterns retain primitive brachyodont teeth, and in some groups, a small degree of hypsodonty is observed. They are characterized by a complete dentition, but some may display a reduction in the number of incisors and upper canines. They developed different types of occlusal morphology (bunodont, bunoselenodont, or lophoselenodont), which clearly contrast to the more specialized dental morphology developed among notoungulates.

Taxonomic proposals for litopterns recognized nine families (Gelfo et al. 2016: Table 1; Croft et al. 2020), among which Proterotheriidae Ameghino 1887, and Macraucheniidae Huxley 1871, were the more conservative and stable through more than a century of studies, the more diversified in time, and the best-known representatives of the order. The status of the remnant groups rests contentious and according to different author opinions, it is possible to recognize some variations in the systematics. Adianthidae Ameghino 1891, similar to Eocene up to early Miocene forms, showed a trend towards selenodont dentition. They include some Paleogene taxa, considered either, as a separate group within litopterns, the Indaleciidae Cifelli and Soria (1983), or as part of a different order: Notopterna (Soria 1989a, b). This last order neither followed by later authors nor completely tested as phylogenetic hypothesis (but see Bonaparte and Morales 1997), also includes two other litoptern families: the Paleocene Notonychopidae Soria, 1989b and the Eocene Amilnedwarsiidae Soria 1989a. The Paleogene stock of proterotheriids was also separated in the Anisolambdidae Soria 2001, but from a cladistic perspective, they are paraphyletic and most probably belong to the stem group of Proterotheriidae. The

Eocene Sparnotheriodontidae Soria 1980, were considered as part of the “Condylarthra” (Cifelli 1983), but since these archaic ungulates are not a natural group, most authors just keep them with Litopterna because of their dental features. The Protolipternidae Cifelli 1983, which supposedly merged two exclusively bunodont litopterns, is also considered as a junior synonym of the classic condylarths Didolodontidae Scott 1913, which was moved to Litopterna (Gelfo et al. 2020).

The origin and evolutionary history of Macrauchiinae litopterns are unknown, even though proteomic and ancient DNA analyses of *Macrauchenia* reveal that litopterns are close allies to the Laurasiatheria, Perissodactyla (Buckley 2015; Welker et al. 2015; Westbury et al. 2017). They were not very abundant in the fossil record, and they had been particularly scarce before the late Oligocene, Deseadan SALMA (Dozo and Vera 2010). Since *Polymorphis lechei* (Roth 1899), from the late Eocene (Mustersan SALMA) of Patagonia, is the only known pre-Deseadan taxon of this family (Cifelli 1983), the possible phylogenetic relationships among Macrauchiinae and other litopterns such as Proterotheriidae and Adiantidae, or with the stem-group Didolodontidae, remains uncertain (Muizon and Cifelli 2000; Gelfo 2006).

As mentioned above, Macrauchiinae and Proterotheriidae are the best-known families among litopterns and also have the best skull material available. The first remains assigned to Macrauchiinae, all postcranial elements, were collected by Charles Darwin in Puerto San Julian (Santa Cruz, Argentina) in 1834 and described by Owen (1840), under the name of *Macrauchenia patachonica*. Macrauchiinae is known from the late Eocene (following Cifelli [1983], the Eocene genus *Polymorphis* is considered a macrauchenid) up to the late Pleistocene/early Holocene. Sensu Soria (1981), they are represented by Cramauchiinae (including Theosodontinae) and Macrauchiinae (Cifelli 1983; Bond 1999; Soria 2001; Schmidt and Ferrero 2014). According to the most recent phylogenetic analysis (McGrath et al. 2018) by paraphyletic Cramauchiinae and monophyletic Macrauchiinae.

Macrauchiinae comprise medium to large-sized forms. McGrath et al. (2020) recognized three size classes that correspond temporally to Eocene (small *Polymorphis* sp.), Miocene–Pliocene (medium sized cramauchiinae as *Theosodon* and early macrauchiinae as *Promacrauchenia*), and Pleistocene (large macrauchiinae as *Macrauchenia*) representatives. Macrauchiinae have three functional toes on each foot, and never evolved large gaps in their dentition or enlarged incisors or canines. A well-documented nostrils migration (from terminal to dorsal) is observed in this group, remarkably evident in the last known genera, the Pleistocene *Macrauchenia*, in which the external bony nostrils were positioned completely dorsal in the skull, between the orbits (Lobo 2020; Croft et al. 2020).

Proterotheriidae, on the other hand, developed small- to medium-sized cursorial forms, with brachyodont dentitions. Its temporal range spans from the Oligocene to Late Pleistocene (but note that the biochrone is subjected to whether *P. lechei* is regarded as Proterotheriidae or Macrauchiinae). Proterotheriidae is divided into two subfamilies (Soria, 2001); the bunodont and less diverse Megadolodinae, restricted to the Miocene of Venezuela and Colombia (Carlini et al. 2006) and the

Protheroetheriinae. The latter was characterized by several dental modifications such as the second upper and the third lower incisors transformed in defenses, the loss of canines, and the reduction of nasal bones (although it is not even close to the reduction observed in Macraucheniiinae). Protheroetheriinae developed remarkable specializations in their limbs, losing the first and fifth toes, and keeping the third one as the only truly functional digit. Basal forms such as *Notodiaphorus* preserved strongly reduced second and the fourth toes, which are totally reduced in derived taxa, such as *Thoatherium* (Soria 2001).

21.2 Historical Background

21.2.1 *The Record of Endocranial Morphology and Any Other Paleoneurological Approaches in Litopterna*

The evolutionary history of the litoptern brain started with studies on Protheroetheriidae carried out by George Gaylord Simpson (1933). He described the cranial endocast of a specimen, from now on, *Tetramerorhinus lucarius* AMNH 9245 (Ameghino 1894; sensu Soria 2001) of the Santacrucian SALMA (early middle Miocene of Santa Cruz province, Argentina). It consists of a plaster endocast prepared from a complete endocranial cavity with some deformation and some part of the olfactory bulbs missing. The neocortical region was well preserved. Simpson considered that the brain of *Tetramerorhinus lucarius* was relatively large, with small olfactory bulbs, and an expanded neocortex with many convolutions. The cerebellum was large and complex. He described the rhinal fissure and four (lateral, ectolateral, suprasylvian, and ectosylvian) longitudinal neocortical sulci. He emphasized that the sylvian region was not very developed and mentioned that the suprasylvian and lateral sulci unites anteriorly in a way that resembles the coronal sulcus or coronal and ansate sulci in the frontal region, although it is highly probable that these sulci do not have any real homologues in any other mammalian order. Simpson (1933: 13) compared the brain of these South American extinct ungulates with extinct ungulates from the Northern Hemisphere stating: “It has no special resemblance to any Perissodactyla brain known to me, and perhaps least of all to the early horses (*Mesohippus* has been compared)”.

Jerison (1973) in his book “*Evolution of the Brain and Intelligence*” devoted an entire chapter (Chap. 14) to extinct South American native ungulates (SANUs) that flourished in South America for most of the Cenozoic. He analyzed relative brain size in SANUs with his encephalization quotient (EQ) that allows comparisons between species considering the allometric component that prevents direct comparisons by means of brain weight/body weight ratios but he includes only one Litopterna (*Protheosodon*) in these analyses.

Radinsky (1981) carried out studies on the brain of litopterns in the context of brain evolution in extinct SANUs. He described the endocasts of protheroetheriids

Diadiaphorus and *Thoatherium*, and he cited the same specimen (AMNH 9245) studied by Simpson (1933). Radinsky (1981) described the hemispheres and the olfactory bulbs, with special emphasis in the neocortex. He mentioned three important longitudinal sulci, the most lateral of them curved medially at its anterior end delimiting a small “frontal” lobe. This lobe shows a longitudinal sulcus in *Tetramerorhinus* and *Thoatherium* and a transversal sulcus in *Diadiaphorus*, which would be lost in the middle sulcus. The olfactory bulbs are larger than those described by Simpson (1933). Radinsky (1981) postulated that in the endocast of *Tetramerorhinus* the bulbar filling is partial. Finally, he compared the endocasts of proteroterids with those of the Holarctic perissodactyl *Hyrachyus* and the artiodactyl *Merycoidodon*, with respect to longitudinal neocortical sulci. Radinsky (1981: 177) also referred to an endocranial cast from *Promacrauchenia*, probably from late Miocene (Huayquerian SALMA), the only one from a macraucheniid but without references, or figures, or collection number.

Quiroga (1988) mentioned the endocast of specimen AMNH 9245 too and described an exceptional natural endocast of another specimen of Proterotheriidae from Buenos Aires Province. The provenance was not precise, but the author assigned the specimen to a time between the late Miocene and Pliocene. In this work, he mentioned that the neocortex of both Proterotheriidae showed a clear sulcus pattern of an ungulate mammal (Quiroga 1988: 80).

Forasiepi et al. (2016) provided the first paleoneurological study on Macraucheniidae based on 3D reconstructions from micro-CT (computed tomography) from an exceptionally preserved skull of *Huayqueriana* cf. *H. cristata* (IANIGLA-PV 29) from the late Miocene Huayquerías Formation, Mendoza, Argentina. This new research on the neurocranium allowed the 3D reconstruction of the endocast, petrosal, and inner ear, and revealed the presence of several derived features that will provide information for phylogenetic analyses.

Recently, Fernández-Monescillo (2020), in a special publication about the Kamac Mayu locality in Calama (Chile), provided the 3D reconstruction from CT from two skulls of *Macrauchenia patachonica*. The locality is characterized by its valuable Quaternary megafauna, where *Macrauchenia patachonica* constitutes the most abundant specimens found there. This preliminary paleoneurological study provides a quantitative analysis of the encephalization quotient, although the descriptions of the endocasts are approached only from a general perspective.

21.2.2 Problematics

The aims of this chapter are: (1) to perform an update of the macraucheniids endocasts (Cramaucheniinae and Macraucheniinae), particularly to provide key information to the understanding of endocranial spaces closely associated with the brain and frontal sinuses and (2) to compare neuromorphological characters of macraucheniids with those from extinct South American native ungulates, particularly litopterns proteroteriids and notungulates, and with those from living and extinct

Euungulata evolved in the Northern Hemispheres, such as Perissodactyla (the closest living relatives), and others that could be considered as ecological convergents (e.g. some representatives of Artiodactyla).

In addition, the study will include the description of a natural endocranial cast assigned, presumably, to a litoptern and its importance in the fossil record of mammals.

21.3 Overview of General and Comparative Anatomy

21.3.1 Characterization of Endocranial Cast Morphology

CT Scanning and Endocast Acquisition

This study used high-resolution X-ray computed tomography data to provide the descriptions of digital endocasts, based on the well-preserved skulls of the following Macraucheniidae (Fig. 21.1): *Cramauchenia normalis* (MPEF-PV 2524) from Deseadan SALMA (late Oligocene) of Cabeza Blanca, Chubut, Argentina (Dozo and Vera 2010); *Theosodon* cf. *T. gracilis* (MLP 12–1123) from Miocene of Río

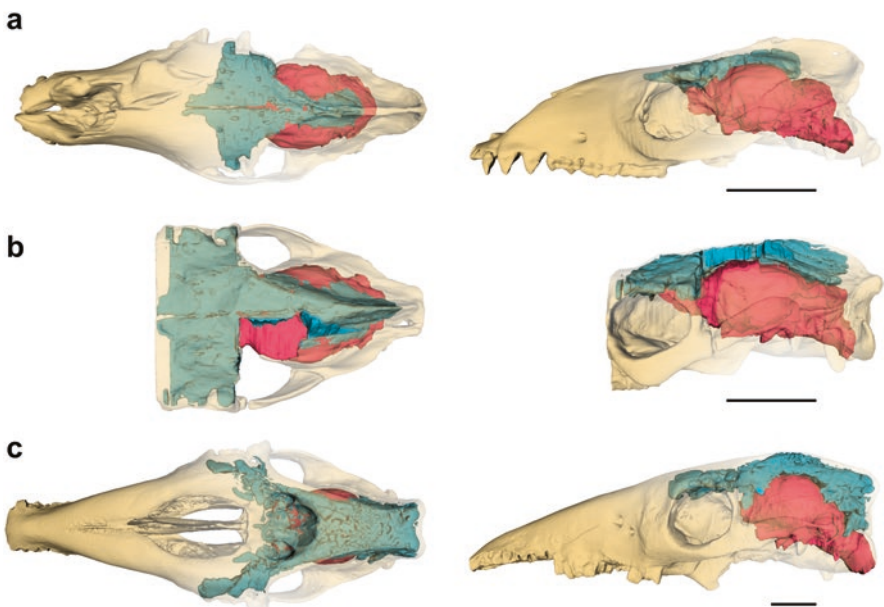


Fig. 21.1 (a) *Cramauchenia normalis* (MPEF-PV 2524), (b) *Theosodon* cf. *T. gracilis* (MLP 12–1123), and (c) *Macrauchenia patachonica* (MACN-PV 2). Translucent digital renderings of skulls to show the extent of the dorsal pneumatization (light blue) and braincast (red). Dorsal and lateral views on the left and right sides, respectively. Scale bars = 5 cm

Frías locality, Chubut, Argentina; and *Macrauchenia patachonica* (MACN-PV 2) from Pleistocene of Salto locality, Buenos Aires, Argentina. The CT scanning was performed at IDECH, Chubut, Argentina (MPEF-PV 2524; MLP 12–1123), and at Clínica “Sagrada Familia” Buenos Aires, Argentina (MACN-PV 2). Reslicing, visualization, segmentation, and volumetric reconstruction were performed using the free (open source) software 3D Slicer 4.10.2 (Fedorov et al. 2012).

Criteria for Neuromorphological Interpretation

Following classical organizational criteria, the cranial endocast is described by regions (rhinencephalon, neopallium, midbrain, and cerebellum), including the exit of cranial nerves and the description of spaces associated with cranial sinuses (Martínez et al. 2020).

The co-occurrence of neuroanatomical, skeletal, and/or behavioral convergence in different mammalian clades (De Winter and Oxnard 2001; Ahrens 2014; Aristide et al. 2016) shows a close relationship between endocast morphology (as a proxy for brain morphology) and some complex paleobiological issues such as sensory system development, motor functions, and (to some extent) ecological traits. In this context for neocortical sulci identification, we follow the topographic criteria (sulci located at similar positions are tentatively considered homologous) and the neuroanatomical interpretation based on Artiodactyla and Perissodactyla (Euungulata, according to Asher and Helgen 2010) detailed in Dozo and Martínez (2016, Fig. 1). The recent communications (Buckley 2015; Welker et al. 2015; Westbury et al. 2017) on molecular analysis of *Macrauchenia* reveals that litopterns (and notoungulates) are close allies of Euungulata, particularly Perissodactyla.

Description of the Digital Endocranial Casts and Neuromorphological Interpretation (Figs. 21.1, 21.2, 21.3 and 21.4)

The digital cranial endocasts of *Cramauchenia normalis* (MPEF-PV 2524), *Theosodon* cf. *T. gracilis* (MLP 12–1123), and *Macrauchenia patachonica* (MACN-PV 2) represent a rendering of the complete brain, allowing for the identification of the cerebral hemispheres, the olfactory bulbs, the ventral surface, and the hindbrain region (cerebellum and brain stem) (Figs. 21.2, 21.3, 21.4 and Table 21.1).

At first glance, the endocasts of *C. normalis* and *T. cf. T. gracilis* show elongated cerebral hemispheres (Figs. 21.2a–d and 21.4a–b), with elliptical outlines in lateral and dorsal views, which resemble those of *Huayqueriana* cf. *H. cristata* (IANIGLA-PV 29, Forasiepi et al. 2016). This is a clear difference from the roughly spherical condition exhibited by the cerebral hemispheres of *M. patachonica* (Figs. 21.3a and 21.4c).

Rhinencephalon Cast (Figs. 21.2b–c, e–f and 21.3b–c) – The digital cranial endocasts show a developed rhinencephalon. The olfactory bulbs (ob), the most anterior

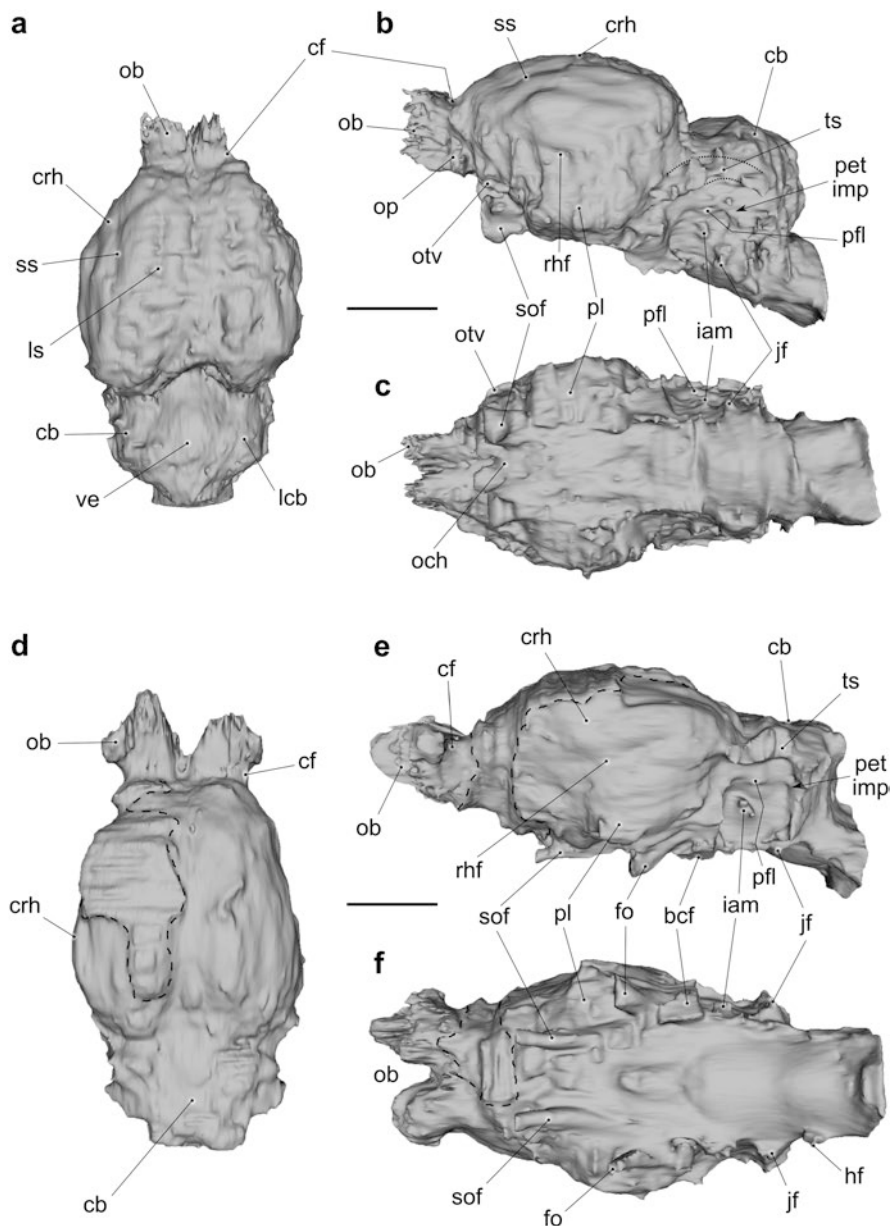


Fig. 21.2 Digital renderings of endocasts of Cramaucheniinae: *Cramauchenia normalis* (MPEF-PV 2524) and *Theosodon* cf. *T. gracilis* (MLP 12–1123). *C. normalis* in (a) dorsal, (b) lateral and (c) ventral views, *T. cf. T. gracilis* in (d) dorsal, (e) lateral and (f) ventral views. Dashed lines (in d, e, and f) indicate unpreserved surfaces. Abbreviations (it also apply for Figs. 21.3, 21.4, and 21.5): *as* ansate sulcus, *bcf* cast of basicapsular fenestra, *cb* cerebellum, *cs* coronal sulcus, *c-as* coronal-ansate sulcus, *cf* circular fissure, *crh* cerebral hemispheres, *ds* diagonal sulcus, *fo* cast of foramen ovale (exit of the mandibular (V3) branch of the trigeminal nerve), *hf* cast of hypoglossal foramen (exit of cranial nerve XII), *hr* hypophyseal region, *iam* cast of internal auditory meatus (exit of cranial nerves VII, VIII), *jf* cast of jugular foramen (exit of cranial nerves IX, X, XI), *lcb* lateral lobe of the cerebellum, *ls* lateral sulcus, *och* optic chiasm, *ob* olfactory bulbs, *op* olfactory peduncles, *otv* cast of orbitotemporal vessels, *pet imp* imprint of the cerebellar aspect of the petrosal, *pfl* paraflocculus, *pl* piriform lobe, *rhf* rhinal fissure, *sof* cast of sphenorbital fissure (exit of cranial nerves III, IV, V1 and V2, VI), *ss* suprasylvian sulcus, *sss* superior sagittal sinus, *ts* temporal sinus, *ve* vermis. Scale bars = 2 cm

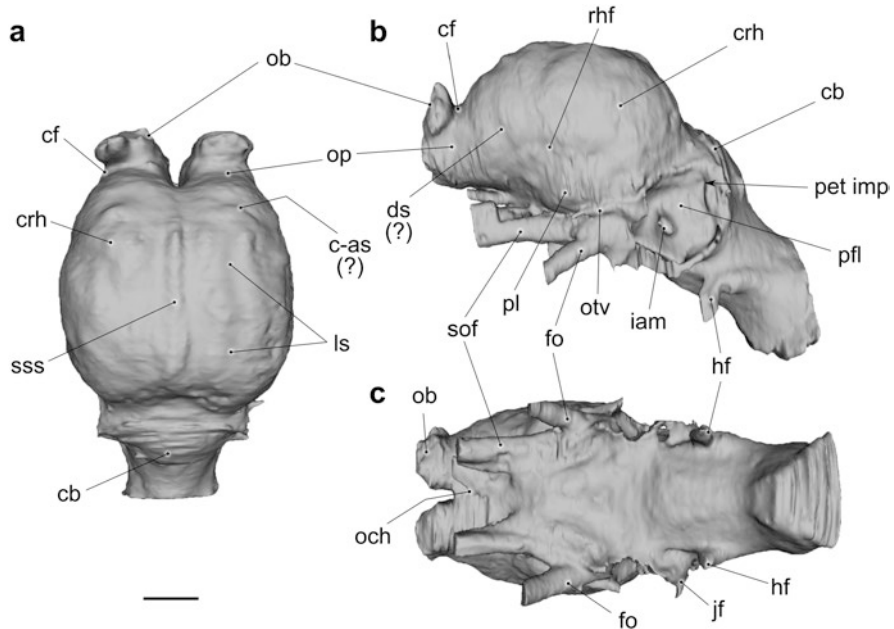


Fig. 21.3 Digital rendering of endocranium of *Macrauchenia patachonica* (MACN-PV 2) in (a) dorsal, (b) lateral, and (c) ventral views. Scale bar = 2 cm. Abbreviations as in Fig. 21.2

structures of the endocranium, are complete and probably reflect their morphology on the brain. They are not overlapped by the cerebral hemispheres and are connected to the frontal pole by short olfactory peduncles (op). These bulbs, like those of IANIGLA-PV 29, are subspherical, anteriorly diverging, and slightly shorter than the width of the frontal region. The circular fissure (cf), that separates the olfactory bulbs from the cerebral hemispheres, is deep and relatively wide. The paleocortex (or paleopallium) is also represented by the piriform lobes (pl). They are similar in size to the temporo-occipital region of the neocortex. The impressions of the lateral olfactory tract and the olfactory tubercle cannot be distinguished. The rhinal fissure (rhf), marking the division between the paleocortex and the neocortex, is visible in the endocranium as a weak sulcus. It runs longitudinally on both sides and is better distinguishable in the caudal portion. The cast of the orbitotemporal vessel (otv) is clearly distinguishable on the lateral side of endocranium of *M. patachonica* and, to a lesser extent, in *C. normalis*.

Neocortical Region (Figs. 21.2a–b, d–e, 21.3a–b and 21.4) – The neocortical (= isocortical) region, which is dorsal to the rhinal fissure, is more expanded than the ventral paleocortex. Only in *M. patachonica* the superior sagittal sinus (sss) or longitudinal sinus is visible on the sagittal line between the cerebral hemispheres. This sinus is more easily distinguishable on the posterior portion of the endocranium. With

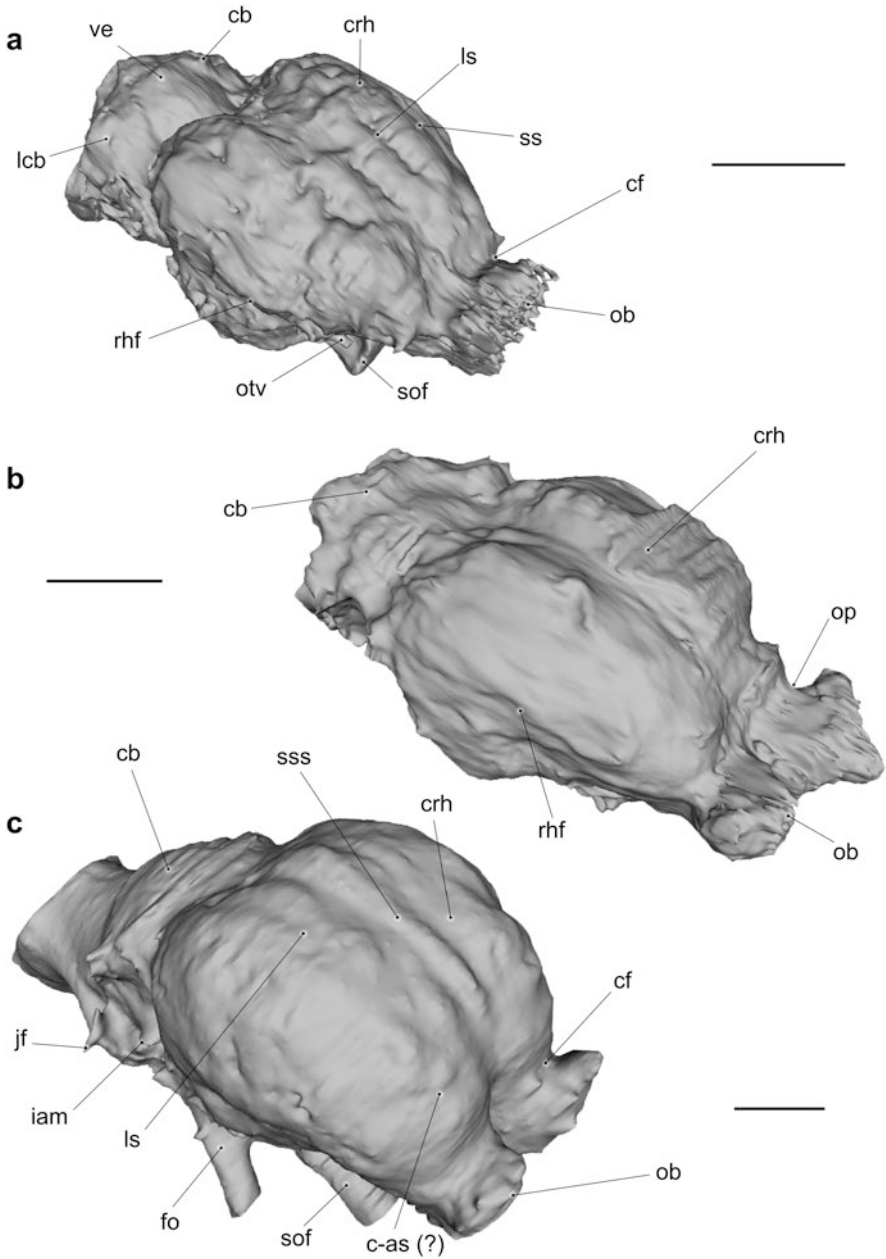


Fig. 21.4 Digital renderings of endocasts of (a) *Cramauchenia normalis* (MPEF-PV 2524), (b) *Theosodon* cf. *T. gracilis* (MLP 12–1123), and (c) *Macrauchenia patachonica* (MACN-PV 2) from right anterodorsolateral view. Scale bars = 2 cm. Abbreviations as in Fig. 21.2

Table 21.1 Measurements for natural endocast (CNP-ME 149), and digital endocasts from *Cramauchenia normalis* (MPEF-PV 2524), *Theosodon* cf. *T. gracilis* (MLP 12–1123) and *Macrauchenia patachonica* (MACN-PV 2)

(in mm)	CNP-ME 149	Digital endocast of <i>C. normalis</i>	Digital endocast of <i>T. cf. T. gracilis</i>	Digital endocast of <i>M. patachonica</i>
EL	–	98.6 ^a	110.0	124.0
EL-OB	78.78 ^a	82.5	93.5	109.0
CRL	50.32 ^a	53.8	64.8	87.1
CRW	51.65	54.0	58.2	84.6
FRW	36.17 ^a	41.7	47.5	72.6
CRH	39.71	45.8	45.1	82.3
OBL	–	–	17.0	15.0
OBW	–	19.3 ^a	39.3	56.9
OBH	–	18.5 ^a	19.6	35.1
PLD	32.55	31.3	41.7	46.5
CBL	16.51	28.7	28.7	21.9
CBW	35.84 ^a	37.7	43.5	59.0
HBH	35.97	44.0	35.4	64.5
HPL	16.28	–	–	–
HPW	14.71	–	–	–

Measurements following Macrini (2009, Fig. 2) and Dozo and Martínez (2016, Fig. 2). Abbreviations: *CBL* maximum length of cerebellar cast, *CBW* maximum width of cerebellar cast, *CRH* maximum height of cerebral cast, *CRL* maximum length of cerebral cast exclusive of olfactory bulbs, *CRW* maximum width of cerebral cast, *EL* maximum length of endocast, *EL-OB* maximum length of endocast exclusive of olfactory bulbs, *FRW* maximum width of frontal region, *HBH* maximum height of hindbrain cast, *HPL* maximum length of hypophysis cast, *HPW* maximum transverse width of hypophysis cast, *OBH* maximum height of olfactory bulb casts, *OBL* maximum length of olfactory bulb casts, *OBW* maximum combined width of olfactory bulb casts, *PLD* maximum distance between ventral edges of piriform lobes

^aApproximated values due to the poor preservation of anterior and posterior regions of the natural endocast and anterior region of the digital endocast

respect to the bifurcation at the caudal end into two transverse sinus, these structures are not conserved. As in IANIGLA-PV 29 (*Huayqueriana* cf. *H. cristata*), the well-developed telencephalic hemispheres and convoluted pattern seems relatively complex, suggested by the conspicuous bulges observed on the endocasts surface. The meninges, cisterns, and venous sinuses preclude identifying clear imprints of sulci and convolutions in *T. cf. T. gracilis*, but a few sulci are distinguishable in *C. normalis* and *M. patachonica*. In the former, weakly marked lateral (ls) and suprasylvian (ss) sulci lie subparallel to the midline and they are curved when viewed laterally. In *M. patachonica*, only the lateral sulcus can be distinguished. In both species, the Sylvian region is somewhat developed (more accentuated in *M. patachonica*). This is a difference when compared to the proteroterid *Tetramerorhinus lucarius* described by Simpson (1933) based on the specimen AMNH 9245, which shows subparallel dorsal sulci but lacks a developed Sylvian region.

In contrast to *C. normalis* and *T. cf. T. gracilis*, the frontal region in *M. patachonica* is apparently more developed (similar to that of *H. cf. H. cristata*) and impressions of a couple of sulci can be distinguished. A transversal sulcus could be treated as homologous to the ansate sulcus or to the coronal-ansate sulcus (c-as), which has been described for some euungulates (Dozo and Martínez 2016). Additionally, on the antero-lateral aspect, a wide sulcus (almost a depression) could be interpreted as the diagonal sulcus (ds).

Midbrain and Cerebellar Cast (Figs. 21.2a–b, d–e and 21.3a–b) – When viewed dorsally, it was not possible to identify any structures that suggest the dorsal exposure of the midbrain on the endocasts. Therefore, it is inferred that the mesencephalon is covered by the neocortex. Posteriorly, the cerebellum (cb) is well represented in the endocasts. The depression that separates the cerebrum from the cerebellum (probably associated to the base of the osseous tentorium cerebelli) is shallower in *M. patachonica* and *T. cf. T. gracilis* than in *C. normalis*. As in IANIGLA-PV 29 (*H. cf. H. cristata*), the cerebellar casts are narrower than the maximum width of the cerebral casts. The casts of the central vermis (ve) and the lateral cerebellar hemispheres (lcb) are distinguishable only in *C. normalis*. A small and weak lobule is seen on the lateral side of the cerebellar cast of *T. cf. T. gracilis* (almost undistinguishable in *C. normalis* and *M. patachonica*). It lies on the subarcuate fossa of the petrosal bone and is interpreted as the cast of paraflocculus (pfl).

Cranial Nerve Casts and Midventral Surface (Figs. 21.2c–f and 21.3c) – The ventral surface of the endocasts between the olfactory bulbs and the base of the sphenorbital fissure is poorly preserved in the three specimens. However, the casts of the optic chiasm (och) are roughly distinguishable in *C. normalis* and *M. patachonica*. The hypophyseal region is not clearly demarcated, but it seems concave rather than convex on the endocast.

Anterolaterally to the hypophyseal region, the cast of the sphenorbital fissure (sof, exit of the ophthalmic [V₁] and maxillary [V₂] branches of the trigeminal nerve, oculomotor [III], trochlear [IV], and abducens [VI] cranial nerves) is observed. In the case of *T. cf. T. gracilis* and *M. patachonica*, the cast of the foramen ovale (fo, exit for the mandibular [V₃] branch of the trigeminal nerve) is also well visible posterolaterally to the sphenorbital fissure. In *T. cf. T. gracilis*, a large opening is observed posteriorly to the cast of the foramen ovale. Following MacPhee et al. (2021) it is here identified as the basicapsular fenestra (bcf).

In lateral view, a well-marked depression (imprint of the cerebellar aspect of the petrosal) is observed. Within such depression, the cast of the internal auditory meatus (iam) is visible (for passage of the facial [VII] and the vestibulocochlear [VIII] cranial nerves). The casts of the jugular foramen (jf, exit for the glossopharyngeal [IX], vagus [X], and spinal accessory [XI] cranial nerves) are also distinguishable. Finally, the cast of the hypoglossal foramen (hf, exit of cranial nerve [XII]) is distinguishable on the side of the medulla oblongata (posterior and slightly ventral to the jugular foramen) in *T. cf. T. gracilis* and *M. patachonica*.

Endocranial Spaces Associated with Pneumatization of the Cranial Roof

Besides the braincast, the casts of the endocranial spaces associated with the dorsal pneumatic sinuses (Fig. 21.1) were obtained for *Cramauchenia normalis* (MPEF-PV 2524), *Theosodon* cf. *T. gracilis* (MLP 12–1123), and *Macrauchenia patachonica* (MACN-PV 2). In the case of *Cramauchenia normalis* (Fig. 21.1a), the sinuses as a whole have a kite shape, with a sharp rostral end at the anterior part of the frontals. Posteriorly, they extend into the parietals until the middle part of these bones, without reaching the sagittal crest. In lateral view, the sinuses gradually increase in size towards the posterior portion of the frontals and extend laterally surrounding the anteriormost portion of the frontal lobes of the brain/endocast, after the region of the olfactory bulbs. At the level of the parietal bones, the sinuses are restricted to the dorsal portion, ending at the mid-level of the cerebellum roof, which coincides with the highest point of the sagittal crest.

In *Theosodon* cf. *T. gracilis* (Fig. 21.1b), due to less development of the nasal bones, a greater lateral expansion of the frontal sinuses is observed, which are “T-shaped”. Towards the back, the frontal sinuses invade the parietals even more than in *C. normalis*, almost reaching the posterior end of the neurocranium. They have numerous internal trabeculae, although they do not divide the frontal sinuses into smaller cavities. In lateral view, the frontal sinuses maintain a similar height for most of their length, ending above the cerebellar region.

In *Macrauchenia patachonica* (Fig. 21.1c), due to posterodorsal position of the nasal opening and the reduction of nasal bones, the frontal sinuses have a “Y” shape in dorsal view, covering the frontal, parietal, and occipital bones. In many areas, small air chambers surrounded by delicate bone are observed.

21.3.2 Natural Endocranial Cast (or Natural Brain Endocast)

A natural endocranial cast is a brain replica obtained by the lithification of the sediment inside the brain cavity, a process that occurs only under specific sedimentary conditions. It has preserved in detail the general endocranial morphology. The integrity of such a cast and the quality of its morphological details depends on multiple factors as the type and granulometry of the sediment, the amount of filling material, and the presence of percolation waters depositing calcium (Dozo 2009; Iurino et al. 2020).

Natural endocranial casts of mammals are rare in the fossil record. However, they are known for several groups of mammals of the Miocene of Santa Cruz Province, such as edentates (Dasypodidae, Glyptodontidae, Megatheriidae), litopterns (Protheroheriidae), notoungulates (Hegetotheriidae), and rodents (Dasyproctidae) (Dozo 2009). Another example is the large sample of natural endocasts assigned to *Bathygenys reevesi* (Merycoidodontidae) collected from an Eocene locality in West Texas, USA, (Macrini 2009) and a natural brain endocast of a late middle Pleistocene Rhinocerotinae from Melpignano, Apulia, Italy (Iurino et al.

2020). Natural endocranial casts are not only important for paleoneurology (since in extinct mammals they are the only source of information to extract data on the nervous system and deduce functional, behavioral, and phylogenetic aspects), but they also constitute a valuable source of data to assess, albeit indirectly, the presence of certain taxa in a paleontological locality, at least at high taxonomic levels (Dozo 2009).

In Cabeza Blanca (Escalante Department, SE of Chubut), the paleontological works carried out in the last 15 years have allowed us to expand the knowledge on various groups of Patagonian mammals of the Deseadan SALMA (late Oligocene). The discovery of complete skulls has generated new anatomical and paleoneurological studies, and new approaches to clarify the systematics and phylogeny, especially of notoungulates (notohippids, hegetoteriids) and litopterns (macrauchenids) (Reguero et al. 2007; Marani and Dozo 2008; Dozo and Vera 2010; Dozo and Martínez 2016; Martínez et al. 2016).

Recently, a concretion, whose morphology resembles a three-dimensional representation of the internal cavity of a skull, was found in Deseadan levels of the Sarmiento Formation that outcrops in Cabeza Blanca (Dozo and Vera 2010). This sedimentary structure was interpreted as a partial natural endocranial cast (CNP-ME 149) of an extinct mammal (Fig. 21.5a). An interesting antecedent for this locality is the natural endocast described by Loomis (1914) and referred to *Eutrachytherus spegazzinianus*. However, Patterson (1937) considered that the specimen unquestionably belongs to a “Notohippidae” (Notoungulata). Unlike the endocast collected by Loomis, the braincast described here shows litoptern affinities, and represents the first natural braincast tentatively assigned to the order.

Description The cast (CNP-ME 149) (Fig. 21.5a), formed by cemented sediment, consists of a natural endocranial cast that shows the partial morphology of the endocranial cavity, but the braincase bones that enclosed the endocranial cavity are missing. Considering the quality of preservation, only the general morphology of most of the telencephalon and much of the cerebellum are appreciable. The olfactory bulbs and the anterior portion of the frontal lobes are not preserved. Also, it is possible to identify some morphological details of the blood vessels and nerves.

Both cerebral hemispheres (crh) are largely preserved and seem gyrencephalic, that is, with evidence of the sulci and convolutions (Fig. 21.5a). The rhinal fissure is visible as a weak sulcus that runs longitudinally on both sides of the natural endocasts (rhf). The neocortical (=isocortical) region is more expanded than the ventral paleocortex and the convoluted pattern seems relatively complex. A few sulci are visible on each side of the cerebral hemispheres cast. From medial to lateral, they are identified as the lateral (ls) and suprasylvian sulci (ss). The lateral sulcus lies parallel to the median sulcus. The suprasylvian sulcus, external to the lateral sulcus, runs antero-posteriorly and is curved when viewed laterally. On the anterodorsal side, although partially broken, the frontal region seems developed, and a small depression is observed (coronal sulcus?) (cs).

The cerebellum (cb) is partially preserved. It is heavily damaged on the right side, but it is clearly narrower than the maximum width of the cerebral cast. A

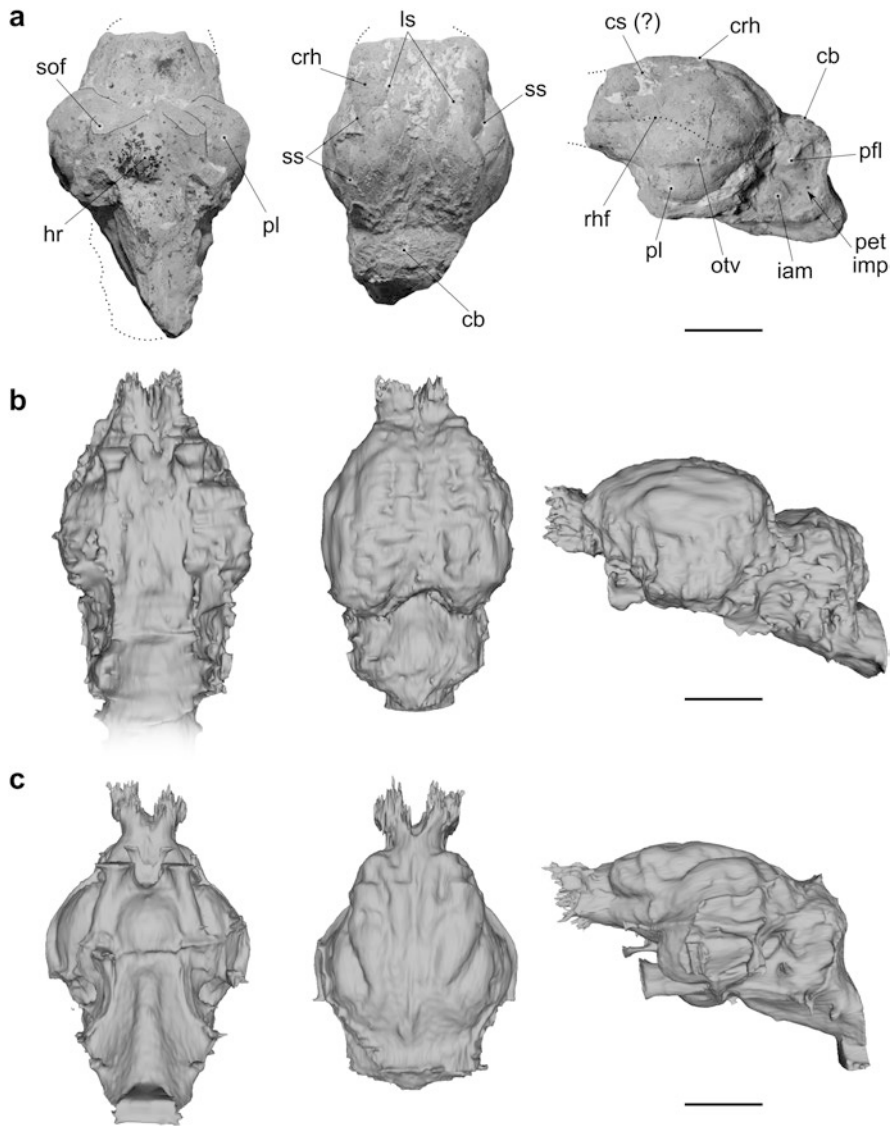


Fig. 21.5 Comparisons between natural braincast tentatively assigned to (a) *Macraucheniiidae* indet. (CNP-ME 149), (b) digital cranial endocasts of *Cramauchenia normalis* (MPEF-PV 2524), and (c) *Rhynchippus equinus* (MPEF-PV 695). Ventral, dorsal and lateral views on the left, middle and right sides, respectively. Scale bars = 2 cm. Abbreviations as in Fig. 21.2

depression that separates the cerebrum and cerebellum is well distinguishable, representing the cast of the osseous tentorium cerebelli. Because of preservation and segmentation issues, neither the cast of the central vermis nor the lateral cerebellar hemispheres are clearly identified. A subtle protuberance (which may represent the parafloccular cast) is observed on the lateral left surface of the cerebellum (pfl).

In the ventral view, the brain cast is quite impaired. However, the hypophyseal region is clearly demarcated, with a relevant and convex region on the endocast (hr). Also, anterolaterally to the hypophyseal region, the cast of the sphenorbital fissure (exit of the ophthalmic [V₁] and maxillary [V₂] branches of the trigeminal nerve, oculomotor [III], trochlear [IV], and abducens [VI] cranial nerves) is well preserved (sof).

Comparative Study In order to establish the mammalian affinities of this natural endocast, a comparative neuroanatomical study (Fig. 21.5b–c) was carried out with three digital endocranial casts of specimens corresponding to notoungulates “Notohippidae” (*Rhynchippus equinus*, MPEF-PV 695; *Eurygenium latirostris*, UNPSJB-PV 60) (Dozo and Martínez 2016), and a litoptern Macraucheniiidae (*Cramauchenia normalis*, MPEF-PV 2524) also found in Deseadan (late Oligocene) levels of Cabeza Blanca, Chubut, Argentina. Unlike the notoungulates “Notohippidae” (Dozo and Martínez 2016; Martínez et al. 2020) (Fig. 23.5c), the telencephalic flexure is not pronounced in the natural endocast here described. Its general morphology, particularly that of the telencephalon (with conspicuous sulci), is similar to that observed in the digital endocast of *C. normalis*, but better represented than in the digital endocast (Fig. 21.5b).

In summary, characters such as the elongated cerebral hemispheres, with a rounded outline, the disposition of the rhinal fissure, the weak telencephalic flexion, the relatively poor development of the Sylvian region, and the impression of longitudinal neocortical sulci in the neocortex, suggests this specimen would be more likely related to a litoptern than to any other South American native ungulate. Moreover, the possibility of being attributed to *Cramauchenia normalis* should not be dismissed, given that both the species and the natural braincast occur in the same locality and stratigraphic levels. However, the absence of craniodental remains associated to the endocast prevents a precise taxonomic assignment. Until more information is available, the specimen should be referred to a Macraucheniiidae indet.

21.4 Brain Evolution and Paleobiological Inferences Based on Endocast Morphology

21.4.1 Morphological Endocranial Cast Diversity

Comparative Neuromorphology with Extinct South American Native Ungulates and Living and Extinct Euungulata

The three-dimensional virtual reconstructions of the internal cavity of Macraucheniiidae skulls from high-resolution computed tomography images have allowed visualization of the corresponding digital endocranial casts. These endocasts are not exact copies of the brain (because the internal bones show molds of meninges, sinuses, and cisterns), however, they conform to the topography of the

brain, making it possible to reproduce the external morphology in some detail (Dozo and Martínez 2016).

There are obvious differences in cranial morphology between the Macraucheniidae studied here. Probably the most evident is the abovementioned nostril migration, which are positioned completely dorsal (between the orbits) in the skull of *Macrauchenia* (Lobo 2020; Croft et al. 2020). Such morphological variation is also observed in the endocranial casts. The endocasts of *Cramauchenia normalis* and *Theosodon* cf. *T. gracilis*, with elongated cerebral hemispheres and rounded outline, resemble more closely that of *Huayqueriana* cf. *H. cristata* (IANIGLA-PV 29, Forasiepi et al. 2016), but differ from the spherical form exhibited by the cerebral hemispheres of *Macrauchenia patachonica*.

When compared with Proterotheriidae and despite the limited knowledge on these extinct forms (Simpson 1933; Radinsky 1981; Quiroga 1988), it is possible to observe some interesting differences, especially regarding the telencephalic morphology. The endocranial casts of *Tetramerorhinus*, *Thoatherium*, and *Diadiaphorus* are characterized by a rectangular cerebrum in dorsal view (Radinsky 1981; Quiroga 1988). There is no oblique Sylvian sulcus, no bulging temporal lobe, and the neocortex is well-developed and divided by a series of parallel longitudinal sulci that extend for most of the length of the cerebrum. In contrast, macraucheniids show the Sylvian region slightly developed. Although the neocortical sulci are partially obscured by meninges, cisterns, and venous sinuses, the endocast seems relatively complex and as gyrencephalic as that of proterotheriids.

When compared with notoungulates, the endocasts of macraucheniids (just like proterotheriids), are quite different from the morphology described for representatives of Toxodontia and Typotheria (Dozo and Martínez 2016; Martínez et al. 2020). In these notoungulates, a pronounced telencephalic flexure, a prominent oblique sulcus (the Sylvian or suprasylvian sulcus), and a bulging temporal lobe are features that characterize the notoungulate neuromorphology and were regarded by Madden (1990) as diagnostic traits for Notoungulata.

In living Euungulata (Perissodactyla and Artiodactyla), the forebrain flexure is not pronounced, the sylvian region is poorly developed, and the neocortex is expanded and bears mostly longitudinal sulci (Kuhlenbeck 1978; Johnson 1990; Welker 1990). Likewise, this pattern is similar to the brains that Radinsky (1981) described for Oligocene and Miocene perissodactyls (e.g. the equid *Mesohippus*) and artiodactyls (e.g. the camelids *Poebrotherium* and *Oxidactylus*) from the Northern Hemisphere and Miocene Proterotheriidae in South America. However, the absence of clearly identifiable sulci on the neocortex of the Macraucheniidae studied here prevents close comparisons to living Euungulata.

Frontal Sinuses

The cranial sinuses, air spaces that optimize the combination of strength and being light (Sharp 2016), are highly variable in shape and development among mammals. Using CT-scan data, the cranial sinuses (and their origins) have been described in

several taxa (Witmer 1997; Rossie 2006; Ferretti 2007; Farke 2008, 2010a, b; Black et al. 2010; Black and Hand 2010; Badlangana et al. 2011; Siliceo et al. 2011; Sharp 2016). The most accepted hypothesis suggests that they originate from the expansion of the mucosa of the epithelial tissue of the nasopharyngeal cavity into different cranial bones that are close to the nasal cavity and rich in osteoclasts, (Witmer 1997; Smith et al. 2005). For example, the frontal sinuses are variable among mammals and can be restricted to the frontals or invade nearby bones where they are not originally present (García et al. 2007).

In general, cranial pneumatization is thought to be related to physiology or the architecture, development, and biomechanics of the skull. Typical examples are weight reduction, increasing surface area for the olfactory mucosa, humidifying, and warming the inspired air, thermoregulation of the brain, etc. (Siliceo et al. 2011). For some species, it has been proposed that frontal sinuses could play an indirect biomechanical role by removing bone to optimize dissipation of stress during feeding and combat. In other groups of mammals (specifically in arctoid carnivores), skull shape disparity is related to variables (skull size, ecology, and diet) that also have implications in frontal sinus development (e.g. species with the largest skulls tended to have the largest frontal sinuses) (Curtis et al. 2015).

In some living artiodactyls, the frontal sinuses show variable morphology, too. According to Farke (2007), the frontal sinuses of bovids (sheep, goats, cattle, and antelope) display a great deal of diversity attributed to both phylogeny and function. He observed that, at least in the hartebeest (*Alcelaphus buselaphus*, a large African antelope), the frontal sinuses are tightly associated to the frontal shape and size, and not necessarily to the overall skull size or horn size. Farke (2007) also mentioned that, contrary to many others bovids, the horncores are never extensively pneumatized in the hartebeest.

The pneumatization of the cranial vault and basicranium of litopterns is also notable, at least in some macraucheniiids. It probably reached a maximum in *M. patachonica*, in which the pneumatization involves the tables of the cranial vault, the central stem, pterygoids, and alisphenoids (Forasiepi et al. 2016). *Huayqueriana* also shows marked pneumatization affecting the entire dorsum of the skull, which is characterized by large frontal sinuses separated by a sagittal septum along its entire length. A similar condition is observed in *Equus* and probably other perissodactyls (Forasiepi et al. 2016).

Here, the three-dimensional reconstructions show different morphologies of the frontal sinuses between *Cramauchenia normalis* (MPEF-PV 2524), *Theosodon* cf. *T. gracilis* (MLP 12-1123), and *Macrauchenia patachonica* (MACN-PV 2) (Fig. 21.1a-c). Such differences are mainly related to the retraction of the nasal aperture and the relocation of the nasal bones, particularly marked in *Macrauchenia* and, to a lesser degree, in *Theosodon*. This posterior repositioning of the nasal aperture may indicate the presence of a proboscis or a similar structure, but there is no detailed anatomical study supporting this inference (Forasiepi et al. 2016). To assess the morphofunctional implications of cranial pneumatization in Macraucheniiidae would require a broadly comparative, anatomical, and comprehensive quantitative analysis involving a more representative sample of macraucheniiids and other groups

of Litopterna (i.e. Protheroheriidae). Also, the data should be examined within a phylogenetic context, which exceeds the aim of the present contribution.

21.4.2 *Brain-Size Evolution and Encephalization Quotient*

Across vertebrates, brain and body size are allometrically coupled. Therefore, evaluating encephalization and comparisons between different taxa is notoriously contentious if allometry is not properly considered (Burger et al. 2019). Jerison, in 1973, introduced the encephalization quotient (EQ), which provided a quantitative value to describe and compare relative brain mass across a wide range of species of varying body mass.

Encephalization or evolutionary changes in brain size is defined as a higher-than-expected brain mass relative to total body mass, and it is often hypothesized that deviations from this brain-body allometric relationship may correlate with cognitive abilities (Boddy et al. 2012; Peñaherrera Aguirre et al. 2017). Some mammalian taxa show strong macroevolutionary evidence for an increase in brain size, whereas others do not show a clear pattern. As mentioned by Schultz and Dunbar (2010) these findings challenge the long-term assumption that encephalization is a general trend across mammals.

The meaning of the level of encephalization, as we said at the beginning, is a complex and problematic issue. Several groups of mammals show an increase in encephalization from the basal to derived forms (Orliac and Gilissen 2012). On the other hand, small brains can be related to evolutionary processes such as fossoriality, changes in social behavior, domestication, and insularism, processes that are associated with the absence/reduction of predators and low competition (Ferreira et al. 2020).

By last, there are few studies that could explain the encephalization pattern in mammals during the Cenozoic in South America, in the long history of isolated evolution (Ferreira et al. 2020; Fontoura et al. 2020). A priori, it could be considered that the relatively low levels of encephalization in notoungulates and litopterns, which have no living representatives, could be due to the fact that the predatory pressures exerted on the fossil ungulates of South America were very different due to the absence of placental carnivores which are more active predators (Marshall 1977; Croft 2006; Kay et al. 2012; Croft et al. 2018). However, this should be carefully considered, since despite the Carnivora absence almost up to the late Miocene (Huayquerian SALMA), most of their ecological niches, were partially fulfilled by marsupials and specialized aves. These so-called terror birds (phorusrhacids) ranged in height from ca. 60 cm to nearly 3 m making them large and swift enough to prey on smaller notoungulates and litopterns (Croft and Lorente 2021).

Here, the relative brain size was evaluated by the means of the encephalization quotient (EQ) as calculated by Jerison (1973) ($EQ1 = EV/0.12[BM]^{0.67}$) and Eisenberg (1981) ($EQ2 = EV/0.055 [BM]^{0.74}$). The latter was based on a regression analysis including a large sample of extant placental mammals according to which

the widely accepted brain size to body size scaling exponent of about 0.75 is confirmed (Orliac et al. 2012). However, the reasons to explain why brain size scales to the 3/4 power to body size across mammals is unknown (Burger et al. 2019).

These methods for EQ calculation are widely employed and allow comparison with EQ values provided by other authors (Jerison 1973; Radinsky 1981; Dozo and Martínez 2016; Fernández-Monescillo et al. 2019). The input data for both equations included the endocranial volume (EV), which was obtained directly from the 3D model by means of the software 3D Slicer 4.10.2 (Fedorov et al. 2012), and body mass (BM), which was estimated from the algorithm 4.1 proposed by Mendoza et al. (2006) by calculating BM from cranial and upper molar measurements. The EV, BM and EQ values of the macrauchenids are presented in Table 21.2 and Fig. 21.6.

In addition, Fernández-Monescillo et al. (2019) calculated the EQ values for the macraucheniid *Huayqueriana* cf. *H. cristata* (see Forasiepi et al. 2016) based on the mean of two BM methods, EQ1 = 0.46 (following Mendoza et al. 2006) and EQ2 = 0.41 (Cassini et al. 2012). These values are slightly different from those obtained here for this taxon EQ1 = 0.43 and EQ2 = 0.40 (Table 21.2) since we used in the equations the BM of 250 kg (see Forasiepi et al. 2016 for a discussion of the BM values). Despite these differences all the values for macrauchenids fall within an interval of 0.43 and 0.69 for EQ1 and 0.40 and 0.60 for EQ2.

The EQ values for basal macrauchenids fluctuate between a 0.40 and 0.53 but could be considered stable. This suggests that despite the increase in BM observed in the phylogeny through *Cramauchenia normalis*, *Theosodon* cf. *T. gracilis*, and *Huayqueriana* cf. *H. cristata*, the variations in EV are not considerable. However, in the case of the terminal taxon *Macrauchenia patachonica*, EQ1 and EQ2 values (0.69–0.60 respectively) increase substantially (i.e., it is higher than what could be expected following the trend observed in the abovementioned basal taxa depicted in Fig. 21.6). Interestingly, such EQ increase or “jump” occurs in a representative that shows notable cranial particularities related to the posterior migration of the nasal

Table 21.2 Data for relative brain size of digital endocasts

	<i>Cramauchenia normalis</i>	<i>Theosodon</i> cf. <i>T. gracilis</i>	<i>Huayqueriana</i> cf. <i>H. cristata</i>	<i>Macrauchenia patachonica</i>
EBM (kg)	80.25	106.45	250	458.39
EV (cm ³)	111.72	153.66	217.29	514.64
EQ 1	0.48	0.54	0.43	0.69
EQ 2	0.47	0.53	0.40	0.60

From *Cramauchenia normalis* (MPEF-PV 2524); *Theosodon* cf. *T. gracilis* (MLP 12–1123); *Huayqueriana* cf. *H. cristata* (IANIGLA-PV 29); *Macrauchenia patachonica* (MACN-PV 2). Abbreviations: EBM, estimated body mass; EV, endocast volume; EQ1, encephalization quotient using Jerison’s equation (1973); EQ2, encephalization quotient using Eisenberg’s equation (1981) EBM obtained using algorithm 4.1 from Mendoza et al. (2006). EV obtained from virtual endocasts in 3D Slicer 4.10.2 (Fedorov et al. 2012). EBM and EV for IANIGLA-PV 29 taken from Forasiepi et al. (2016)

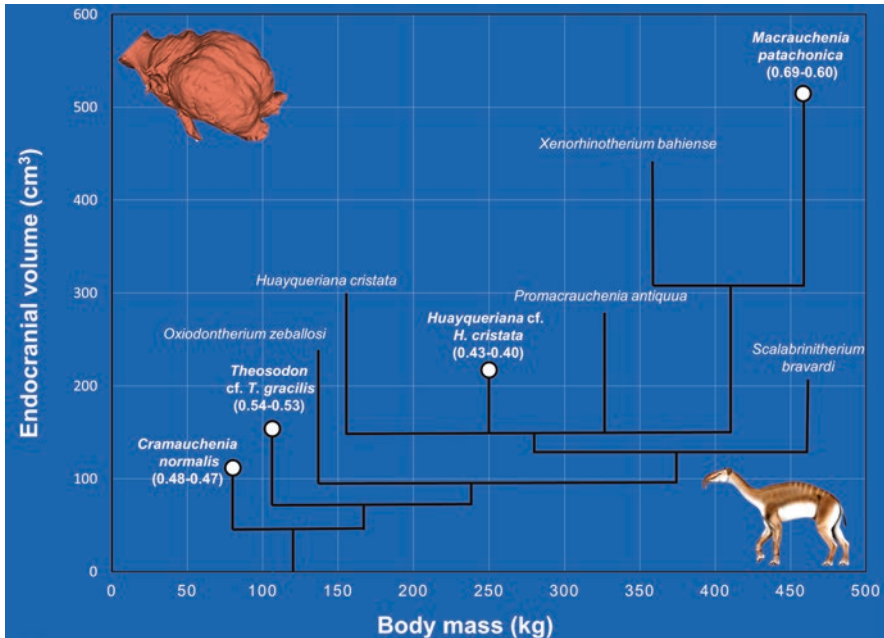


Fig. 21.6 Endocranial volume versus body mass of *Craumauchenia normalis* (MPEF-PV 2524), *Theosodon* cf. *T. gracilis* (MLP 12–1123), *Huayqueriana* cf. *H. cristata* (IANIGLA-PV 29), and *Macrauchenia patachonica* (MACN-PV 2), plotted over the strict consensus cladogram obtained by Forasiepi et al. (2016). The EQ1 and EQ2 values for these taxa are mentioned between brackets, respectively

openings (and the possible presence of a muscular proboscis associated with it) and an extremely pneumatized cranial roof.

However, would it be possible to associate the “EQ jump” observed in *M. patachonica* to an artifact derived from a low body mass estimation? Previous body masses reported for *M. patachonica* show that, while limb bone dimensions generate overestimations, craniodental proxies tend to underestimate them (Fariña et al. 1998). Here, all body masses were calculated with craniodental proxies (algorithm 4.1 from Mendoza et al. 2006), except for *Huayqueriana* cf. *H. cristata*, whose value (taken from Forasiepi et al. [2016]) was estimated using the centroid size of a 3D configuration of cranial landmarks following Cassini et al. (2012). In this context, if all body mass estimations included in Table 21.2 would have been derived from limb bones or averages from the same proxies (instead of cranial or craniodental dimensions), we could expect a homogeneous overestimation across the entire sample that would drag the EQ values to the right of the Fig. 21.6, but would not disappear the “EQ jump”. Further considerations about encephalization in *M. patachonica* should be made taking this putative constraint into account and based on a larger taxon sample of macraucheniiids.

Regarding comparisons with other coeval SANUs and Holartic ungulates, the EQ values of the Oligocene macraucheniid *Cramauchenia normalis* (0.48–0.47) are higher than EQ values reported for the Oligocene toxodonts (Notoungulata) *Rhynchippus equinus* (0.34), *Eurygenium latirostris* (0.25), *Mendozahippus fierensis* (0.25), and *Gualta cuyana* (0.31; Dozo and Martínez 2016; Martínez et al. 2020). Conversely, the EQ obtained for *C. normalis* is below that of the late Oligocene perissodactyl *Mesohippus* (EQ = 0.88) and near the values obtained for the artiodactyl *Poebrotherium* (EQ = 0.36 to 0.42; Jerison 1973), which could be regarded as ecological analogues. Finally, at higher taxonomic levels, the mean EQ calculated for extant perissodactyls and cetartiodactyls (Boddy et al. 2012: Table 1) were 1 and 1.42, respectively. These values are significantly higher than those of macrauchenids, notoungulates, and extinct euungulates. It is interesting to comment that *Mesohippus* has a higher EQ than *Poebrotherium*, but modern cetartiodactyls have higher values than modern perissodactyls. However, this is relative considering that, within Cetartiodactyla, Odontoceti (mean EQ = 3.10) was solely responsible for such a peak in EQ, and differs significantly from that of Rumiantia (mean EQ = 0.86) (Boddy et al. 2012).

After 40 years, the words of Leonard Radinsky (1981) are still valid: “*The question of the significance of relative brain size is a fascinating one, all the more so because our own species has such an unusually large brain: the answer, however, still remains an enigma.*”

21.5 Future Directions: Outstanding Questions and Perspectives

Few data are available to understand the morphological endocranial cast diversity and brain evolution in the second largest group of South American native ungulates in abundance and diversity, the Litopterna. They are scarce in Macrauchenidae, and there are no studies based on digital endocranial casts with an emphasis on Proterotheriidae. As stated above, endocranial studies of proterotheriids are based on a single known plaster-silicone cast (Simpson 1933; Radinsky 1981; Quiroga 1988), except for 3D reconstructions (of *Tetramerorhinus lucarius*) provided by Forasiepi et al. (2016) and MacPhee et al. (2021) in the context of specific research focused on other taxa or specific features. Regarding Macrauchenidae, only Forasiepi et al. (2016) and Fernández-Monescillo (2020) performed paleoneurological studies on Macrauchenidae based on 3D reconstructions obtained from micro-CT. They provided 3D reconstructions of the endocranium, petrosal, and inner ear for *Huayqueriana* cf. *H. cristata* and quantitative analysis of the encephalization quotient accompanying a brief description of the endocrania for *Macrauchenia patachonica*.

In the present study, three additional endocranial casts of the macrauchenids (representatives of Cramaucheniinae and Macraucheninae) are disclosed. Although we focused strictly on describing and understanding the endocranial spaces

associated with the brain and frontal sinuses, the new morphological data could be potentially valuable for phylogenetic analyses.

In the future, in-deep research on the interaction between the endocranial morphology and skull shape will hopefully contribute to filling the gap in such an interesting issue concerning litopterns, one of the most emblematic groups of South American native ungulates that inhabited the continent since the beginning of the Cenozoic. These studies merit further discussion and should include not only macraucheniiids but also proteroteriids, and must be carried out in a phylogenetic framework that allow a better understanding of the brain evolution and morphological change in litopterns.

21.6 Conclusions

The digital endocasts of *Cramauchenia normalis*, *Theosodon* cf. *T. gracilis*, and *Macrauchenia patachonica* described herein provide an interesting perspective to begin understanding litoptern brain evolution, particularly to improve our understanding of evolution within the Macraucheniiidae.

The endocasts of *Cramauchenia normalis* and *Theosodon* cf. *T. gracilis*, with elongated cerebral hemispheres that are rounded in outline, resemble more closely those of *Huayqueriana* cf. *H. cristata* (IANIGLA-PV 29, Forasiepi et al. 2016) and differ from the more spherical form exhibited by the cerebral hemispheres of *Macrauchenia patachonica*. When compared with Proterotheriidae, the most notable difference is the slightly (but present) development of the Sylvian region.

The endocasts of macraucheniiids and proteroteriids (without pronounced telencephalic flexure, lacking a prominent Sylvian or suprasylvian sulcus, and lacking bulging temporal lobes) contrast to the neocortical morphological pattern described for notoungulates (Toxodontia and Typotheria).

Also, the three-dimensional reconstructions show different morphologies of the dorsal pneumatic sinuses (not only restricted to the frontals but also invading the surrounding bones) between *Cramauchenia normalis*, *Theosodon* cf. *T. gracilis*, and *Macrauchenia patachonica*. Differences are mainly attributed to the retraction of the nasal aperture and the relocation of the nasal bones, particularly in *Macrauchenia* and, to a lesser degree, in *Theosodon*.

Regarding the relative brain size, the EQ values obtained for the Oligocene *Cramauchenia normalis* are higher than those of the coeval notoungulates “notohippids” *Rhynchippus equinus*, *Eurygenium latirostris*, *Mendozahippus fierensis*, and the leontinid *Gualta cuyana*.

When compared to similar-sized Holarctic ungulates from the late Oligocene, the EQ of *Cramauchenia normalis* is below that of the perissodactyl *Mesohippus* and around the values obtained for the artiodactyl *Poebrotherium*.

The EQ values of *Macrauchenia patachonica* could indicate the highest point in the encephalization process among macraucheniiids and coincides with a notable skull specialization (Lobo 2020). How strongly related are encephalization

(represented by the “EQ jump” hypothesis) and general skull specialization in *M. patachonica* is an interesting, and still pending, question.

Finally, a concretion recovered from the Deseadan levels of the Sarmiento Formation that outcrops in Cabeza Blanca locality (Chubut), was interpreted as a partial natural endocranial cast. This natural endocast represents the first natural braincast assigned to a litoptern (potentially referable to Macrauchenidae).

Acknowledgments We express our gratitude to M. R. Ciancio, F. Busker, L. Cheme Arriaga for collaboration during fieldwork, S. Bessone, who found the natural endocranial cast, for professional assistance during fieldwork and fossil preparation, CT technologist A. Panes (IDECH) for guidance and help during the scanning process and to A. Venter and family (Estancia El Molino owners) for their hospitality. Fieldwork was conducted with permission of the Secretaría de Cultura, Chubut Province. This research was funded by CONICET PIP 11220150100113 (to MTD) and PUE-IPGP 22920200100014 (CONICET 2020 Executing Units Project awarded to the Patagonian Institute of Geology and Paleontology).

References

- Ahrens HE (2014) Morphometric study of phylogenetic and ecologic signals in procyonid (Mammalia: Carnivora) endocasts. *Anat Rec* 297:2318–2330
- Ameghino F (1887) Enumeración sistemática de las especies de mamíferos fósiles coleccionados por Carlos Ameghino en los terrenos eocenos de Patagonia austral y depositados en el Museo de La Plata. *Bol Mus La Plata* 1:1–26
- Ameghino F (1889) Contribución al conocimiento de los mamíferos fósiles de la República Argentina. *Actas Acad Nac Cienc Córdoba* 6:1–1027
- Ameghino F (1891) Mamíferos y Aves fósiles argentinas. Especies nuevas, adiciones y correcciones. *Rev Argentina Hist Nat* 1:240–259
- Ameghino F (1894) Énumération synoptique des espèces de mammifères fossiles des formations éocènes de Patagonie. *Actas Acad Nac Cienc Córdoba* 13:259–445
- Aristide L, Furtado DRS, Machado AC et al (2016) Brain shape convergence in the adaptive radiation of New World monkeys. *P Natl Acad Sci USA* 113:2158–2163
- Asher RJ, Helgen KM (2010) Nomenclature and placental mammal phylogeny. *BMC Evol Biol* 10(102):1–9
- Badlangana NL, Adams JW, Manger PR (2011) A comparative assessment of the size of the frontal air sinus in the giraffe (*Giraffa camelopardalis*). *Anat Rec* 294:931–940
- Black KH, Archer M, Hand SJ et al (2010) First comprehensive analysis of the cranial ontogeny in a fossil marsupial - from a 15-million-year-old cave deposit in northern Australia. *J Vertebr Paleontol* 30:993–1011
- Black KH, Hand SJ (2010) First crania and assessment of species boundaries in *Nimbadon* (Marsupialia: Diprotodontidae) from the Middle Miocene of Australia. *Am Mus Novit* 3678:1–60
- Boddy AM, McGowen MR, Sherwood CC et al (2012) Comparative analysis of encephalization in mammals reveals relaxed constraints on anthropoid primate and cetacean brain scaling. *J Evol Biol* 25:981–994
- Bonaparte JF, Morales J (1997) Un primitivo Notonychopidae (Litopterna) del Paleoceno inferior de Punta Peligro, Chubut, Argentina. *Est Geol* 53(5-6):263–274
- Bond M (1999) Quaternary native ungulates of Southern South America. A synthesis. In: Tonni EP, Cione AL (eds) Quaternary Vertebrate Paleontology in South America, Quaternary of South America and Antarctic Peninsula. Special Volume, vol 12, pp 177–205

- Buckley M (2015) Ancient collagen reveals evolutionary history of the endemic South American 'ungulates'. *Proc R Soc B: Biol Sci* 282:20142671
- Burger JR, George MA, Leadbetter C et al (2019) The allometry of brain size in mammals. *J Mammal* 100:276–283. <https://doi.org/10.1093/jmammal/gyz043>
- Carlini AA, Gelfo JN, Sánchez R (2006) A new Megadolodinae (Mammalia, Litopterna, Protherotheriidae) from the Urumaco Formation (Late Miocene) of Venezuela. *J Syst Palaeontol* 4:279–284
- Cassini GH, Vizcaíno SF, Bargo MS (2012) Body mass estimation in early Miocene native South American ungulates: a predictive equation based on 3D landmarks. *J Zool* 287:53–64
- Cifelli RL (1983) The origin and affinities of the South American Condylarthra and early Tertiary Litopterna (Mammalia). *Am Mus Novit* 2772:1–49
- Cifelli RL, Soria MF (1983) Systematics of the Adianthidae (Litopterna, Mammalia). *Am Mus Novit* 2771:1–25
- Croft DA (2006) Do marsupials make good predators? Insights from predator-prey diversity ratios. *Evol Ecol Res* 8(7):1193–1214
- Croft DA, Engelman RK, Dolgushina T, Wesley G (2018) Diversity and disparity of sparassodonts (Metatheria) reveal non-analogue nature of ancient South American mammalian carnivore guilds. *Proc R Soc B Biol Sci* 285(1870):20172012. <https://doi.org/10.1098/rspb.2017.2012>
- Croft DA, Gelfo JN, López GM (2020) Splendid innovation: the extinct South American native ungulates. *Annu Rev Earth Pl Sc* 48:259–290
- Croft DA, Lorente M (2021) No evidence for parallel evolution of cursorial limb adaptations among Neogene South American native ungulates (SANUs). *PLoS ONE* 16(8):e0256371. <https://doi.org/10.1371/journal.pone.0256371>
- Curtis AA, Lai G, Wei F et al (2015) Repeated loss of frontal sinuses in arctoid carnivorans. *J Morphol* 276:22–32
- De Winter W, Oxnard CE (2001) Evolutionary radiations and convergences in the structural organization of mammalian brains. *Nature* 409:710–714
- Dozo MT (2009) Paleoneurología de Mamíferos de Edad Santacrucense. In: Mirelman S (ed) Estado actual de las Investigaciones realizadas sobre Patrimonio Cultural en Santa Cruz. Patrimonio Cultural, Provincia de Santa Cruz, pp 93–102
- Dozo MT, Martínez G (2016) First digital cranial endocasts of late Oligocene Notohippidae (Notoungulata): implications for endemic South American Ungulates brain evolution. *J Mamm Evol* 23:1–16. <https://doi.org/10.1007/s10914-015-9298-5>
- Dozo MT, Vera B (2010) First skull and associated postcranial bones of Macraucheniiidae (Mammalia, Litopterna) from the Deseadan SALMA (late Oligocene) of Cabeza Blanca (Chubut, Argentina). *J Vertebr Paleontol* 30:1818–1826. <https://doi.org/10.1080/02724634.2010.521534>
- Eisenberg JF (1981) The mammalian radiations: an analysis of trends in evolution, adaptation and behavior. University of Chicago Press, Chicago
- Fariña RA, Vizcaíno SF, Bargo MS (1998) Body mass estimations in Lujanian (late Pleistocene - early Holocene of South America) mammal megafauna. *Mastozool Neotrop* 5(2):87–108
- Farke AA (2007) Morphology, constraints, and scaling of frontal sinuses in the hartebeest, *Alcelaphus buselaphus* (Mammalia: Artiodactyla, Bovidae). *J Morphol* 268:243–253
- Farke AA (2008) Frontal sinuses and head-butting in goats: a finite element analysis. *J Exp Biol* 211:3085–3094
- Farke AA (2010a) Evolution and functional morphology of the frontal sinuses in Bovidae (Mammalia: Artiodactyla), and implications for the evolution of cranial pneumaticity. *Zool Journal Linn Soc-Lond* 159:988–1014
- Farke AA (2010b) Evolution, homology, and function of the supracranial sinuses in ceratopsian dinosaurs. *J Vertebr Paleontol* 30:1486–1500
- Fedorov A, Beichel R, Kalpathy-Cramer J et al (2012) 3D Slicer as an image computing platform for the Quantitative Imaging Network. *Magn Reson Imaging* 30:1323–1341

- Fernández-Monescillo M (2020) Reconstrucción digital de la cavidad endocraneal de *Macrauchenia patachonica*. In: Rojas Mondaca I (ed) Martínez Rivera I. Un enigmático animal extinto de la Cuenca de Calama. Publicación Especial del Museo de Historia Natural y Cultural del Desierto de Atacama, Macrauchenia, pp 39–47
- Fernández-Monescillo M, Antoine PO, Pujos F et al (2019) Virtual endocast morphology of Mesotheriidae (Mammalia, Notoungulata, Typotheria): new insights and implications on notoungulate encephalization and brain evolution. *J Mamm Evol* 26:85–100
- Ferreira JD, Negri FR, Sánchez-Villagra M et al (2020) Small within the largest: brain size and anatomy of the extinct *Neoeopiblema acrensis*, a giant rodent from the Neotropics. *Biol Lett* 16:20190914
- Ferretti MP (2007) Evolution of bone-cracking adaptations in hyaenids (Mammalia, Carnivora). *Swiss J Geosci* 100:41–52
- Fontoura E, Ferreira JD, Bubadué J et al (2020) Virtual brain endocast of *Antifer* (Mammalia: Cervidae), an extinct large cervid from South America. *J Morphol* 281(10):1223–1240
- Forasiepi A, Macphee R, Hernández del Pino S et al (2016) Exceptional skull of *Huayqueriana* (Mammalia, Litopterna, Macraucheniiidae) from the Late Miocene of Argentina: anatomy, systematics, and paleobiological implications. *B Am Mus Nat Hist* 404:1–76
- García N, Santos E, Arsuaga JL et al (2007) Endocranial morphology of the *Ursus deningeri* Von Reichenau 1904 from the Sima de Los Huesos (Sierra de Atapuerca) Middle Pleistocene site. *J Vertebr Paleontol* 27:1007–1017
- Gelfo JN (2006) Los Didolodontidae (Mammalia: Ungulatomorpha) del Terciario Sudamericano. Sistemática, origen y evolución. PhD Thesis, Univ. Nacional de La Plata
- Gelfo JN, Alonso RN, Madden RH et al (2020) An Eocene bunodont South American native ungulate (Didolodontidae) from the Lumbrera Formation, Salta Province, Argentina. *Ameghiniana* 57:132–145
- Gelfo JN, Goin FJ, Bauzá N et al (2019) The fossil record of Antarctic land mammals: commented review and hypotheses for future research. *Adv Polar Sci* 30:274–292
- Gelfo JN, López GM, Lorente M (2016) Los ungulados arcaicos de América del Sur: Condylarthra y Litopterna. *Contrib MACN* 6:285–291
- Huxley TH (1871) A manual of the anatomy vertebrated animals. J A Churchill, London
- Iurino DA, Conti J, Mecozzi B et al (2020) Braincase with natural endocast of a juvenile Rhinocerotinae from the Late Middle Pleistocene site of Melpignano (Apulia, Southern Italy). *Front Earth Sci* 09:1–14. <https://doi.org/10.3389/feart.2020.00094>
- Jerison HJ (1973) Evolution of the brain and intelligence. Academic Press, New York
- Johnson JI (1990) Comparative development of somatic sensory cortex. In: Jones EG, Peters A (eds) *Cerebral Cortex*, vol 8B. Plenum Press, New York, pp 335–449
- Kay RF, Vizcaíno SF, Bargo MS (2012) A review of the paleoenvironment and paleoecology of the Miocene Santa Cruz Formation. In: Vizcaíno SF, Kay RF, Bargo MS (eds) *Early Miocene Paleobiology in Patagonia: High-Latitude Paleocommunities of the Santa Cruz Formation*. Cambridge University Press, Cambridge, pp 331–365
- Kuhlenbeck H (1978) The central nervous system of vertebrates. Mammalian telencephalon: surface morphology and central cortex. *The Vertebrate Neuraxis as a Whole*. Vol. 5, Part II. S. Karger, Basel
- Lobo LS (2020) Evolução dos Macraucheniiidae (Mammalia, Litopterna): Taxonomia, Filogenia e Diversificação Craniana. Universidade Federal do Rio de Janeiro, Tese de Doutorado
- Loomis FB (1914) The Deseado Formation of Patagonia. Rumford, Concord
- MacPhee RDE, Hernández del Pino S, Kramarz A et al (2021) Cranial morphology and phylogenetic relationships of *Trigonostylops wortmani*, an Eocene South American native ungulate. *B Am Mus Nat Hist* 449:1–183
- Macrini TE (2009) Description of a digital cranial endocast of *Bathygenys reevesi* (Merycoiodontidae; Oreadontoidea) and implications for apomorphy-based diagnosis of isolated, natural endocasts. *J Vertebr Paleontol* 24:1199–1211

- Madden RH (1990) Miocene Toxodontidae (Notoungulata, Mammalia) from Colombia. Dissertation, Duke University, Durham, Ecuador and Chile
- Marani H, Dozo MT (2008) El cráneo más completo de *Eurygenium latirostris* Ameghino, 1895 (Mammalia, Notoungulata), un Notohippidae del Deseadense (Oligoceno Tardío) de la Patagonia, Argentina. *Ameghiniana* 45:619–626
- Marshall LG (1977) Evolution of the carnivorous adaptive zone in South America. In: Hecht MK, Goody PC, Hecht BM (eds) *Major Patterns in Vertebrate Evolution*. Plenum Press, New York, pp 709–721
- Martínez G, Dozo MT, Gelfo JN et al (2016) Cranial morphology of the Late Oligocene Patagonian notohippid *Rhynchippus equinus* Ameghino, 1897 (Mammalia, Notoungulata) with emphases in basicranial and auditory region. *Plos One* 11:e0156558
- Martínez G, Dozo MT, Vera B et al (2020) Paleoneurology, auditory region, and associated soft tissue inferences in the late Oligocene notoungulates *Mendozahippus fierensis* and *Gualta cuyana* (Toxodontia, Notoungulata) from central-western Argentina. *J Vertebr Paleontol* 39(6):e1725531. <https://doi.org/10.1080/02724634.2019.1725531>
- McGrath AJ, Anaya F, Croft DA (2018) Two new macraucheniiids (Mammalia: Litopterna) from the late middle Miocene (Laventan South American Land Mammal Age) of Quebrada Honda, Bolivia. *J Vertebr Paleontol* 38(3):e1461632. <https://doi.org/10.1080/02724634.2018.1461632>
- McGrath AJ, Anaya F, Croft DA (2020) New proterotheriids (Litopterna, Mammalia) from the middle Miocene of Quebrada Honda, Bolivia, and trends in diversity and body size of proterotheriid and macraucheniid litopterns. *Ameghiniana* 52(2):159–188. <https://doi.org/10.5710/AMGH.03.03.2020.3268>
- Mendoza M, Janis C, Palmqvist P (2006) Estimating the body mass of extinct ungulates: a study on the use of multiple regression. *J Zool* 270:90–101
- de Muizon C, Cifelli RL (2000) The condylarths (archaic Ungulata, Mammalia) from the early Palaeocene of Tiupampa (Bolivia): implications on the origin of the South American ungulates. *Geodiversitas* 22:47–150
- Orliac MJ, Argot C, Gilissen E (2012) Digital cranial endocast of *Hyopsodus* (Mammalia, Condylarthra): a case of Paleogene terrestrial echolocation? *PLoS ONE* 7(e30000):1–10
- Orliac MJ, Gilissen E (2012) Virtual endocranial cast of earliest Eocene *Diacodexis* (Artiodactyla, Mammalia) and morphological diversity of early artiodactyl brains. *Proc R Soc B* 279:3670–3677. <https://doi.org/10.1098/rspb.2012.1156>
- Owen R (1840) The zoology of the voyage of H. M. S. Beagle under the command of Captain Fitzroy, R. N., during the years 1832 to 1836. Fossil Mammalia. Part I. Edited and Superintended by Charles Darwin, London
- Patterson B (1937) Some notoungulates braincasts. *Field Mus Nat Hist Geol Ser* 6:273–301
- Peñaherrera Aguirre M, Fernandes HBF, Woodley of Menie MA (2017) Relative brain size, encephalization quotient. In: Shackelford T, Weekes-Shackelford V (eds) *Encyclopedia of evolutionary psychological science*. Springer, Cham. https://doi.org/10.1007/978-3-319-16999-6_3098-2
- Quiroga JC (1988) Cuantificación de la corteza cerebral en moldes endocraneanos de mamíferos girencéfalos. Procedimiento y aplicación en tres mamíferos extinguidos. *Ameghiniana* 25:67–84
- Radinsky L (1981) Brain evolution in extinct South American ungulates. *Brain Behav Evol* 18:169–187
- Reguero M, Dozo MT, Cerdeño E (2007) A poorly known rodentlike mammal (Pachyrukhinae, Hegetotheriidae, Notoungulata) from the Deseadan (Late Oligocene) of Argentina. Paleogeography, biogeography and radiation of the rodentlike ungulates in South America. *J Paleontol* 81:1301–1307
- Rossie JB (2006) Ontogeny and homology of the paranasal sinuses in Platyrrhini (Mammalia: Primates). *J Morphol* 267:1–40
- Roth S (1899) Aviso preliminar sobre mamíferos mesozoicos encontrados en Patagonia. *Revista Mus La Plata* 9:381–388

- Schmidt GI, Ferrero BS (2014) Taxonomic reinterpretation of *Theosodon hystatus* Cabrera and Kraglievich, 1931 (Litopterna, Macraucheniiidae) and phylogenetic relationships of the family. *J Vertebr Paleontol* 34:1231–1238
- Schultz S, Dunbar R (2010) Encephalization is not a universal macroevolutionary phenomenon in mammals but is associated with sociality. *PNAS* 107:21582–21586
- Scott WB (1913) A history of land mammals in the Western Hemisphere. The Mc Millan Co, New York
- Sharp AC (2016) A quantitative comparative analysis of the size of the frontoparietal sinuses and brain in vombatiform marsupials. *Mem Mus Vic* 74:331–342
- Siliceo G, Salesa MJ, Antón M et al (2011) Comparative anatomy of the frontal sinuses in the primitive sabre-toothed felid *Promegantereon ogygia* (Felidae, Machairodontinae) and similarly sized extant felines. *Estud Geol-Madrid* 67:277–290
- Simpson GG (1933) Braincasts of two tyotheres and a litoptern. *Am Mus Novitates* 629:1–18
- Smith TD, Rossie JB, Cooper GM et al (2005) Secondary pneumatization of the maxillary sinus in callitrichid primates: insights from immunohistochemistry and bone cell distribution. *Anat Rec* 285:677–689
- Soria MF (1980) Una nueva y problemática forma de ungulado del Casamayorensis. *Actas II Congr Argent Paleontol Bioestratigr I Congr Latinoam Paleontol* 3:193–203
- Soria MF (1981) Los Litopterna del Colhuehuapense (Oligoceno tardío) de la Argentina. *Rev Mus Argent Cienc Nat* 3:1–54
- Soria MF (1989a) Notopterna; un nuevo orden de mamíferos ungulados Eógenos de America del Sur; Parte I, Los Amilnedwardsidae. *Ameghiniana* 25:245–258
- Soria MF (1989b) Notopterna; un nuevo orden de mamíferos ungulados eógenos de América de Sur. Parte II. *Notonychops powelli* gen. et sp. nov. (Notonychopidae nov.) de la Formación Río Loro (Paleoceno medio), provincia de Tucumán, Argentina. *Ameghiniana* 25:259–272
- Soria MF (2001) Los Proterotheriidae (Mammalia, Litopterna), sistemática, origen y filogenia. *Monograf Museo Argent Cienc Nat* 1:1–167
- Welker WI (1990) Why does cerebral cortex fissure and fold? A review of determinants of gyri and sulci. In: Jones EG, Peters A (eds) *Cerebral Cortex*, vol 8B. Plenum Press, New York, pp 3–136
- Welker F, Collins MJ, Thomas JA et al (2015) Ancient proteins resolve the evolutionary history of Darwin's South American ungulates. *Nature* 522:81–84
- Westbury M, Baleka S, Barlow A et al (2017) A mitogenomic time tree for Darwin's enigmatic South American mammal *Macrauchenia patachonica*. *Nat Commun* 8:1–8
- Witmer LM (1997) The evolution of the antorbital cavity of archosaurs: a study in soft-tissue reconstruction in the fossil record with an analysis of the function of pneumaticity. *J Vertebr Paleontol* 17:1–76

Index

A

Adapoids, 462–464, 475–479, 482, 483, 485, 488–490, 493, 494
Amniote, 1, 2, 4, 5, 15, 19, 56, 79, 94, 99, 107, 110, 111, 146, 225, 229, 231, 248, 285, 292, 367–369, 371–387, 399, 403, 405, 407, 409, 410, 431, 444
Archosauria, 180, 181, 200, 267
Armadillos, 717

B

Behavior, 5, 58, 60, 103, 107, 125, 152, 154, 161, 164, 183, 201, 286, 288, 295, 302, 305, 306, 311, 316, 317, 333, 342, 348, 349, 352, 356, 370, 374, 379, 383, 389, 393, 395, 406, 407, 409, 443, 444, 487, 490, 491, 496, 580, 595–597, 668, 669, 691, 712, 730, 738, 751, 766, 797, 827
Bony labyrinth, 61, 140, 230, 238, 338, 348, 430, 446, 448, 561, 571, 573, 600, 607–631, 667, 715, 716, 723, 729, 730, 733, 737–756, 770, 775, 780
Brain, 1–5, 11–19, 22, 23, 46, 47, 54–58, 63, 79–113, 125–126, 131, 146–158, 160, 164, 218, 225–227, 229, 230, 232–247, 251–256, 272–274, 280–288, 290, 291, 293, 295, 298–307, 309–311, 313–317, 423–450, 457–496, 507–545, 557–574, 580–631
Braincase, 3, 12–18, 20, 23, 35–37, 39, 42, 46, 47, 51, 53, 55, 80, 81, 83, 85, 86, 89, 91–99, 101, 102, 109, 113,

124–145, 147, 148, 150–152, 154, 155, 157, 163, 164, 183–185, 187–191, 193–195, 197–199, 201, 203, 218, 226, 229, 234, 235, 238, 247, 248, 250, 256, 271, 273, 274, 280–284, 287, 289, 292, 296, 297, 299, 300, 305, 306, 313, 316, 370, 371, 381, 389, 390, 395, 406, 407, 440, 449, 514, 527, 531, 561, 580, 587, 589, 599, 600, 602, 630, 683, 684, 715, 728, 749, 822
Braincase endocast, 13, 37, 92–96, 98, 99, 602
Brain endocast, 46, 82, 83, 94, 101, 111, 156, 164, 189, 286, 306, 335, 429, 580–631, 716, 731–733, 737–756, 769, 777, 821, 822, 824
Brain evolution, 1, 4, 15–23, 54–61, 101–112, 164, 200–203, 283, 285, 295, 303, 315, 354, 357, 390, 395, 404, 426, 428, 439–448, 457–460, 462, 463, 480–493, 495, 496, 516, 527, 530, 534–545, 567–573, 581, 645–670, 683, 693–705, 711–733, 783–794, 812, 824–827, 830, 831
Brain size, 1, 4, 12, 18, 55, 56, 85, 93, 94, 101–104, 146, 154, 274, 283, 285, 303, 309, 313, 314, 344–346, 353, 355, 356, 384, 426, 427, 438, 441, 443–449, 463, 469, 470, 477, 478, 481–488, 493, 495, 496, 508, 510, 516, 526, 531, 537, 539–545, 568, 569, 573, 574, 581–587, 589–594, 600, 606, 630, 662–664, 692, 697, 701, 703–705, 727, 728, 767, 792–794, 799, 812, 827, 828, 830, 831

- Brain size evolution, 1, 18, 55, 56, 101–104, 146, 285, 309, 314, 443–449, 481–486, 537, 539, 568, 569
- Brain tissue, 83, 85, 88, 92–95, 101, 154, 227, 357, 441, 443, 537, 586, 594, 607
- C**
- Carotid circulation, 11
- Caviomorpha, 647–649, 651, 652, 657, 658, 660, 662
- Cenozoic, 3, 127, 132, 140, 144, 217, 282, 334, 390, 409, 541, 542, 580, 581, 682, 714, 737, 761, 763, 792, 812, 827, 831
- Cerebral cortex, 494, 595, 596, 598, 606, 685, 691–694, 701–703, 750
- Cetacea, 508, 510, 514–517, 531–535, 537, 539–545, 592, 727
- Cingulata, 711
- Climate change, 682
- Cranial endocast, 13, 35, 37–51, 55, 56, 63, 124, 132, 152–163, 191, 194, 195, 197, 200, 218, 220–232, 234, 235, 237–246, 254, 255, 273, 274, 281–287, 289–313, 317, 429–440, 447–450, 471–475, 514, 516–533, 558–565, 567, 570, 572–574, 652–658, 685, 716, 718, 767, 768, 773, 775, 784, 790, 791, 812, 815, 823
- Cranial nerves, 3, 11, 14, 17, 19, 35, 41, 49–51, 87–91, 125, 126, 129, 131, 146, 154, 156, 160, 184, 185, 187, 188, 191, 194–200, 220, 229, 231, 233–235, 240, 246–253, 282, 288, 289, 292, 295–297, 306, 339, 340, 343, 376, 435, 438, 447, 561, 563, 564, 658–660, 717, 719–722, 742–745, 749–751, 754, 766, 767, 772, 790–792, 815, 816, 820, 824
- Cranial sinuses, 737–756, 815, 825
- Crocodylomorpha, 2, 5, 217–256
- CT imaging, 231, 770
- CT-scan, 37, 85, 128, 145, 187, 190, 197, 231, 282, 335, 429, 479, 510, 512, 516, 533, 544, 581, 584, 613, 623, 650, 782, 825
- D**
- Diapsida, 5, 10, 23, 63
- Dinosauria, 2, 3, 5, 267–269, 303
- Disparity, 62, 83, 139, 156, 202, 204, 239, 245, 271, 333, 341–343, 356, 426, 520, 712, 715, 738, 751, 753, 754, 826
- Dugong, 557, 561, 563, 566, 567, 569–572
- E**
- Elephants, 297, 458, 558, 572, 580, 581, 585–587, 590–598, 600–603, 605–613, 615, 619, 621, 623, 627, 630, 691, 739, 762
- Encephalization Quotient (EQ), 4, 5, 18, 55, 56, 102, 155, 192, 200, 274, 312–314, 344, 346, 371, 389, 395, 396, 400, 403, 404, 443–448, 460, 469, 470, 480–486, 488, 508, 537, 539–544, 568–570, 582–584, 586–589, 591, 592, 630, 631, 648, 662–664, 670, 727–729, 786–789, 792–794, 799, 812, 813, 827–832
- Endocast, 2–5, 11–13, 15–18, 22, 23, 35–37, 42–50, 54–63, 80–83, 85, 86, 89, 92–99, 101–113, 128, 131, 133, 137, 145, 152–156, 158–160, 162, 183–185, 187–195, 197–200, 203, 236, 244, 252, 254, 273, 274, 281–311, 313, 315–317, 333–357, 369–373, 378, 381, 384, 389, 390, 395–404, 408, 429–432, 434–449, 460, 462–469, 471–495, 508–521, 524–545, 559–564, 566–573, 581, 584, 585, 587–589, 595–602, 605–607, 632, 648–650, 652–658, 660–670, 683–687, 693–705, 716–723, 725–732, 739, 740, 747, 749–753, 766–769, 772–775, 782–794, 812–822, 824–832
- Endocranial cast, 81, 152, 154, 155, 157, 164, 183, 187, 189, 196, 203, 508–514, 518, 520, 525–527, 531, 532, 545, 561, 580–581, 585, 587, 590, 592, 598–607, 630, 682, 683, 687, 702, 703, 714, 716–718, 725, 726, 732, 742, 753, 798, 810–832
- Endocranium, 3, 38, 56, 289, 300, 335, 353, 478
- Euprimates, 462, 463, 466, 470, 472, 474–477, 479–482, 484, 487–490, 492, 493, 495, 496
- Evolution, 1, 5, 11, 12, 15, 18, 22, 23, 36, 41, 54–59, 63, 79–113, 140, 146, 155, 184, 201–203, 231, 254, 270, 285, 290, 292, 300, 303, 305, 309, 310, 313–316, 333–357, 367–411, 423–450, 457–496, 507–545, 557–574, 581–632, 652, 662–664, 666–668, 670, 682, 691–693, 697, 701–705, 715, 716, 732, 793, 794, 799, 812, 827, 831

G

- Glyptodont, 711–716, 718, 720, 722, 723, 725–733, 737
 Gyrfication, 438, 449, 495, 527, 529, 581, 606–607, 685, 688, 691, 699, 702, 703, 705, 772, 785, 799

I

- Ichthyopterygia, 2, 5, 30–64
 Infraorbital foramen, 399, 602, 603, 605
 Infrasound, 595, 598, 612, 630
 Inner ear, 3, 11, 12, 15, 19–21, 45, 82, 105, 107, 108, 112, 124, 128, 132, 137, 140, 145, 153, 156–158, 160–162, 187–189, 191, 193–195, 198, 199, 220, 230–246, 249, 254, 256, 279, 280, 295, 297, 302, 304, 307, 338–340, 347–349, 355, 356, 379, 387, 388, 402, 430, 431, 445, 446, 448, 490, 570, 573, 574, 615, 630, 631, 668, 669, 711–733, 742, 751, 753–756, 769, 775, 779–783, 796, 813, 830
 Ischyromyidae, 520, 646–656, 659–663, 665–670

L

- Litopterna, 2, 5, 762, 764, 778, 810–832

M

- Macraucheniiidae, 810–832
 Mammalia, 5, 367–369, 371, 378–380, 382–384, 387, 389, 390, 392–395, 397, 399, 400, 402–407, 409–411, 458–460, 538, 540, 580–631
 Marsupial, 376, 382, 395, 423–432, 434–450, 573, 682, 827
 Mesozoic, 3, 30, 63, 123, 126, 143, 183, 217, 268, 270, 316, 354, 356, 390, 601
 Metatheria, 2, 5, 423, 429, 568
 Miocene, 127, 355, 424, 429, 430, 462, 511–515, 528, 529, 532, 538, 542, 559, 561, 564, 566–568, 570, 572, 583, 589, 593, 594, 601, 605, 649, 651, 661, 664, 668, 682, 683, 697–699, 701, 702, 705, 715, 716, 718, 727, 728, 732, 738, 742, 784, 788, 789, 810–814, 821, 825, 827

N

- Native Ungulates, 761–763, 810, 812, 813, 824, 830, 831

- Neocortex, 367, 370, 382, 394, 395, 399, 401, 403, 405, 408–411, 458, 460, 468, 474, 476, 480, 481, 486, 487, 536, 563, 650, 654, 658, 661, 665, 666, 670, 690–694, 699, 772–774, 785, 789, 795, 799, 812, 813, 817, 820, 824, 825

- Neopallium, 509, 510, 512, 516–520, 522, 524–532, 534–538, 544, 545, 572, 599, 767, 815

- Neornithes, 334–336, 340, 342, 345, 346, 353

- Neuroanatomy, 3, 15, 81–83, 92, 112, 126, 146–154, 158, 164, 183, 184, 204, 217–256, 286, 296, 303, 304, 307, 309, 310, 313–316, 429, 488, 491, 580, 595–598, 683, 685, 743

- Neurosensory evolution, 316, 367, 384, 410

- Notoungulata, 762

O

- Olfaction, 22, 57, 59, 110–112, 192, 203, 247, 252, 273, 286, 287, 302, 347, 352, 353, 376, 385–387, 393, 396, 408, 409, 411, 445–447, 486–491, 570–572, 597, 664, 666–668, 794–797, 799

- Olfactory genome, 411

- Omomyoids, 462–464, 475, 476, 478, 479, 482, 484, 488–490, 493

- Operculization, 517–519, 521, 524–527, 529, 530, 535–537, 539

P

- Paleobiology, 15, 24, 96, 111, 185, 251, 348, 369, 715, 739, 751

- Paleoneurology, 1–5, 9–23, 30–64, 125, 130, 145, 153–162, 164, 180–204, 217–225, 228, 267–317, 335, 369, 375, 429, 431, 449, 462, 507–545, 561, 563, 573, 580–631, 681–705, 711–733, 761–800, 810–832

- Pampathere, 711, 712, 714–716, 722, 723, 725–729, 731, 732, 737

- Parareptilia, 9

- Petrosal lobule, 475, 477, 479, 492, 650, 654, 656, 658, 659, 664–667, 669, 670

- Pleistocene, 3, 513, 526, 528, 589, 590, 612, 683, 699, 702, 713–715, 718, 720, 725–728, 730, 732, 742, 764, 765, 789, 794, 810, 811, 815, 821

- Plesiadapiforms, 460, 461, 463, 464, 470–482, 489, 492, 493, 496, 661, 796

Pneumatization, 336, 604, 747–749, 752–755,
814, 821, 826
Proboscis, 110, 297, 602–605, 826, 829

R

Reptilia, 184, 274, 368, 369, 384
Rhinchocephalia, 123, 126, 129–132, 146

S

Sauropterygia, 5, 30–64
Sciuroidea, 646, 647, 650, 655, 656, 659–667,
669, 670
Sea cow, 557
Secondarily aquatic, 11, 30–64
Sensorial organs, 110, 183, 186, 203
Sensory capabilities, 56, 57, 286, 490
Sirenians, 557–561, 563–574, 587, 598, 600,
607, 613–615, 619, 621, 623, 750
Sloths, 606, 716, 723, 725–729, 732,
737–756, 762
South America, 9, 180–182, 267, 268, 280,
300, 309, 423, 424, 426, 449, 557,
561, 647, 649, 651, 664, 737, 738,
742, 761–764, 792, 810, 812,
825, 827
Squamata, 123–128, 132–145, 148–153
Stem marsupials, 428, 429, 432, 438, 440,
445, 448–450

Sulcal pattern, 516–517, 526, 536, 544, 572,
606, 607, 688, 689, 692, 698, 699,
701, 702, 705, 726, 731, 768

T

Terrestriality, 9–11, 15, 19, 23, 32, 61, 63, 99,
107, 108, 111, 150, 156, 161, 180,
182, 199, 201, 217–219, 221, 244,
251, 253, 254, 256, 267, 333,
373–376, 379, 383, 388, 411, 516,
532, 533, 535, 568, 572, 581, 586,
595, 596, 599, 612, 663, 672, 673,
691, 702, 703, 749, 751, 765,
766, 797
3D modelling, 335
Tympanic hearing, 19, 21

V

Virtual endocast, 11, 14, 22, 45, 297, 336, 345,
460, 464–466, 469–472, 475, 477,
479, 493, 495, 510, 646, 649–652,
655, 657, 659, 670, 800, 828

X

Xenarthra, 711, 727, 737–756